WOODS HOLE OCEANOGRAPHIC INSTITUTION

COLLECTED REPRINTS

1955

PART I

OCT 1956
LIBRARY
POFI
FISH & WILDLIFE
SERVICE

JULY, 1956

PERIODICAL

Woods Hole
Oceanogr.
Institution

Collected
Reprints

1955

Part 1

PERIODICAL
Woods Hole
Oceanogr.
Institution
Collected
Reprints
1955
Part 1

DATE OF MAGAZINE	BORROWER'S NAME	TIME DU

LIBRARY
BUREAU OF COMMERCIAL FISHERIES
U. S. FISH AND WILDLIFE SERVICE
P. O. BOX 3830
HONOLULU 12, HAWAII

WOODS HOLE OCEANOGRAPHIC INSTITUTION

COLLECTED REPRINTS

1955

PART I

1799

JULY, 1956

LIBRARY
BUREAU OF COMMER[illegible] FIS
U. S. FISH AND W[illegible] SERV
P. O. BOX [illegible]
[illegible]NOLULU 12, HAWAII

This volume contains contributions from the WOODS HOLE OCEANOGRAPHIC INSTITUTION which were published in 1955; also the Annual Report of the Director for the year 1955. Other contributions from the Institution are included in Part II of *Collected Reprints* issued also as "*Papers in Marine Biology and Oceanography*," dedicated to Dr. Henry Bryant Bigelow, published as supplement to Volume 3 of *Deep Sea Research.*

TABLE OF CONTENTS

Contribution No.

BARLOW, JOHN P.
Physical and Biological Processes Determining the Distribution of Zooplankton in a Tidal Estuary 753

BARRETT, EARL and GUNNAR |BRODIN
The Acidity of Scandinavian Precipitation 785

BIGELOW, HENRY B. and WILLIAM C. SCHROEDER
Occurrence off the Middle and North Atlantic United States of the Offshore Hake *Merluccius albidus* (Mitchill) 1818, and of the Blue Whiting *Gadus (Micromesistius) poutassou* (Risso) 1826 732

BIGELOW, HENRY B., WILLIAM C. SCHROEDER and STEWART SPRINGER
Three New Shark Records from the Gulf of Mexico 787

BLANCHARD DUNCAN C.
Electrified Droplets from the Bursting of Bubbles at an Air-Sea Water Interface 747

BUMPUS, DEAN F.
The Circulation over the Continental Shelf South of Cape Hatteras 788

BUNKER, ANDREW F.
Turbulence and Shearing Stresses Measured over the North Atlantic Ocean by an Airplane-Acceleration Technique 740

CHASE, JOSEPH
Winds and Temperatures in Relation to the Brood-Strength of Georges Bank Haddock 735

CREITZ, GRACE I. and FRANCIS A RICHARDS
The Estimation and Characterization of Plankton Populations by Pigment Analysis. III. A Note on the use of "Millipore" Membrane Filters in the Estimation of Plankton Pigments 736

DOW, WILLARD
Underwater Telemetering 729

EDGERTON, HAROLD E. and LLOYD D. HOADLEY
Cameras and Lights for Underwater Use 817

ESSAPIAN, FRANK S.
Speed-Induced Skin Folds in the Bottle-Nosed Porpoise, *Tursiops truncatus* . . 751

FARMER, H. G., W. MARKS, R. G. WALDEN and G. G. WHITNEY, JR.
A Technique for Ocean Wave Measurements 746

FUGLISTER, F. C.
Alternative Analyses of Current Surveys 749

GEALY, BETTY LEE
Topography of the Continental Slope in Northwest Gulf of Mexico . . . 650

Contribution No.

GORDON, MALCOLM S.
Summer Ecology of Oceanic Birds off Southern New England 742

GOREAU, T. F. and V. T. BOWEN
Calcium Uptake by a Coral 786

KANWISHER, J. W.
Freezing in Intertidal Animals 778

KANWISHER, J. W. and GORDON VOLKMANN
A Scattering Layer Observation 744

KETCHUM, BOSTWICK H.
Distribution of Coliform Bacteria and other Pollutants in Tidal Estuaries . . 772

KETCHUM, BOSTWICK H., NATHANIEL CORWIN and D. JEAN KEEN
The Significance of Organic Phosphorus Determinations in Ocean Waters . . 759

MACHLUP, STEFAN and J. B. HERSEY
Analysis of Sound-Scattering Observations from Non-Uniform Distributions of Scatterers in the Ocean 771

MALKUS, JOANNE STARR
On the Formation and Structure of Downdrafts in Cumulus Clouds 726
The Effect of a Large Island upon the Trade-Wind Air Stream . . . 727

MALKUS, JOANNE STARR and R. S. SCORER
The Erosion of Cumulus Towers 706

MARKS, WILBUR and F. CLAUDE RONNE
Aerial Stereo-Photography and Ocean Waves 741

METCALF, WILLIAM G.
On the Formation of Bottom Water in the Norwegian Basin 739

MOORE, HILARY B.
Variations in Temperature and Light Response within a Plankton Population 756

MOULTON, JAMES M. and RICHARD H. BACKUS
Annotated References Concerning the Effects of Man-Made Sounds on the Movements of Fishes 802

OFFICER, CHARLES B.
Southwest Pacific Crustal Structure 724
A Deep-Sea Seismic Reflection Profile 731
Geologic Interpretation of a Series of Seismic Reflection Profiles from Bermuda to the Continental Margins 743

RICHARDS, FRANCIS A. and ALFRED C. REDFIELD
Oxygen-Density Relationships in the Western North Atlantic 688

ROSSBY, C.-G. and H. EGNÉR
On the Chemical Climate and its Variation with Atmospheric Circulation Pattern 770

Contribution No.

RYTHER, JOHN H.
Ecology of Autotrophic Marine Dinoflagellates with Reference to Red Water Conditions 712
The Ratio of Photosynthesis to Respiration in Marine Plankton Algae and its Effect upon the Measurement of Productivity 733

SCHOLANDER, P. F.
Evolution of Climatic Adaptation in Homeotherms 755
Hydrostatic Pressure in Coconuts 822

SCHOLANDER, P. F. and WILLIAM E. SCHEVILL
Counter-Current Vascular Heat Exchange in the Fins of Whales 807

SCHOLANDER, P. F., L. VAN DAM, C. LLOYD CLAFF and J. W. KANWISHER
Micro Gasometric Determination of Dissolved Oxygen and Nitrogen . . . 795

SCHOLANDER, P. F., L. VAN DAM and SUSAN I. SCHOLANDER
Gas Exchange in the Roots of Mangroves 710

SCHOLANDER, SUSAN I.
Land Birds over the Western North Atlantic 773

SCOTT, GEORGE T. and HUGH R. HAYWOOD
Sodium and Potassium Regulations in *Ulva lactuca* and *Valonia macrophysa* . 597

SOULE, FLOYD M., A. J. BUSH and J. E. MURRAY
Physical Oceanography of the Grand Banks Region and the Labrador Sea in 1953 675

SOULE, FLOYD M., and J. E. MURRAY
Physical Oceanography of the Grand Banks Region and the Labrador Sea in 1954 758

STEEMANN NIELSEN, E.
The Interaction of Photosynthesis and Respiration and its Importance for the Determination of ^{14}C-Discrimination in Photosynthesis 808

STOMMEL, HENRY
Lateral Eddy Viscosity in the Gulf Stream System 796

THORNDIKE, EDWARD M.
Hydroscopes 767

TURNER, HARRY J., JR.
How Clam Drills Capture Razor Clams 777

TURNER, HARRY J., JR. and STANLEY SCHER
Seventh Report on Investigations of the Shellfisheries of Massachusetts (Dated 1954) 783

VINE, ALLYN C.
Oceanographic Instrumentation 806

VON ARX, WILLIAM S. and W. S. RICHARDSON
On the Fine-Structure of the Gulf Stream Front 794

Contribution No.

VOSS, GILBERT L.
The Cephalopoda Obtained by the Harvard-Havana Expedition off the Coast of Cuba in 1938–39 750

WILSON, K. G. and A. B. ARONS
Osmotic Pressures of Sea Water Solutions Computed from Experimental Vapor Pressure Lowering 725

WOODCOCK, A. H.
Bursting Bubbles and Air Pollution 761

WOODCOCK, A. H. and D. C. BLANCHARD
Tests of Salt-Nuclei Hypothesis of Rain Formation 768

WOODCOCK, A. H. and W. A. MORDY
Salt Nuclei, Wind and Daily Rainfall in Hawaii 757

WORTHINGTON, L. V.
A New Theory of Caribbean Bottom-Water Formation 791

THE WOODS HOLE OCEANOGRAPHIC INSTITUTION
Report for the Year 1955

LIST OF CONTRIBUTIONS

The following contributions, published in 1955, are not included in this volume.

FISH, CHARLES J.
Preliminary Observations on the Biology of Boreo-Arctic and Subtropical Oceanic Zooplankton Populations 737

SCHOLANDER, P. F., WARNER E. LOVE and J. W. KANWISHER
The Rise of Sap in Tall Grapevines 709

The following contributions, published in 1955, are among the papers included in Part II of Collected Reprints.

BUMPUS, DEAN F. and E. LOWE PIERCE
The Hydrography and the Distribution of Chaetognaths over the Continental Shelf off North Carolina 760

EDMONDSON, W. T.
Factors Affecting Productivity in Fertilized Water 781

GRIFFIN, DONALD R.
Hearing and Acoustic Orientation in Marine Animals 789

ISELIN, C. O'D.
Coastal Currents and the Fisheries 792

Contribution No.

KETCHUM, BOSTWICK H. and D. JEAN KEEN
The Accumulation of River Water over the Continental Shelf between Cape Cod and Chesapeake Bay 775

REDFIELD, ALFRED C.
The Hydrography of the Gulf of Venezuela 776

RILEY, GORDON A.
Review of the Oceanography of Long Island Sound 762

SCHROEDER, WILLIAM C.
Report on the Results of Exploratory Otter-Trawling along the Continental Shelf and Slope between Nova Scotia and Virginia during the Summers of 1952 and 1953 790

STEEMAN NIELSEN, E.
The Production of Antibiotics by Plankton Algae and its Effect upon Bacterial Activities in the Sea 780

STETSON, HENRY C.
Patterns of Deposition at the Continental Margin 782

TURNER, RUTH D.
Scaphopods of the Atlantis Dredgings in the Western Atlantic with a Catalogue of the Scaphopod Types in the Museum of Comparative Zoology 779

WATERMAN, TALBOT H.
Polarization of Scattered Sunlight in Deep Water 763

Digitized by the Internet Archive
in 2025

https://archive.org/details/collected-reprints-woods-hole-oceanographic-institution_1955_part-1

Contribution No. 597

Reprinted from Electrolytes in Biological Systems
1955

Sodium and Potassium Regulation in Ulva Lactuca and Valonia Macrophysa[1] [2] [3]

GEORGE T. SCOTT AND HUGH R. HAYWOOD[4]

Oberlin College, Oberlin, Ohio, The Marine Biological Laboratory, The Bermuda Biological Station, and the Woods Hole Oceanographic Institution, Woods Hole, Massachusetts

A MAJOR PROBLEM of all living systems is the maintenance within the cell of a chemical composition which differs both quantitatively and qualitatively from that of the external environment. Such regularity of cellular composition is essential to life. The maintenance of a high intracellular potassium ion concentration and low sodium ion concentration, contrasted with a bathing medium high in sodium and low in potassium, such as blood and sea water, is a basic characteristic of cells living in these environments. This uneven distribution of sodium and potassium between living cells and their environments has long attracted the interest of a large number of physiologists.

Of paramount significance in stimulating interest in this field is the work of Dr. W. J. V. Osterhout and his co-workers, who were foremost in an attempt to understand the potassium-accumulating mechanism. One form which early attracted the attention of Dr. Osterhout was the large coenocytic alga *Valonia macrophysa*. As a result of investigations on this interesting organism Dr. Osterhout suggested one of the first theories of potassium accumulation, namely, that potassium was accumulated owing to the activity product (K) (OH) being greater outside than inside because of the pH difference between sap and sea water (28, 29).

More recently evidence obtained on erythrocytes (12) and muscle (43) has been interpreted in terms of a primary sodium secretion of the cell and secondarily of an absorption of potassium within the cell as electro-chemical neutrality is maintained. Such a theory presupposes an active transport of sodium out of the cell and a passive accumulation of potassium within. A third view-point has been proposed by Ling (22) who maintains that the distribution of sodium and potassium between muscle cells and plasma is to be accounted for on the

---

[1] Contribution No. 217 of the Bermuda Biological Station.

[2] Contribution No. 597 of the Woods Hole Oceanographic Institution.

[3] This research was conducted under Contract No. AT(11-1)-181 between the U. S. Atomic Energy Commission and Oberlin College.

[4] Present address: University of Rochester, School of Medicine and Dentistry, Rochester, N. Y.

basis of differences in coulombic forces between the cations and fixed negative binding sites within the cell. According to his hypothesis an active transport mechanism is not only unnecessary but indeed impossible.

The results of the present investigations on *Ulva* and *Valonia* suggest strongly that two independent mechanisms are operative in regulating cellular sodium and potassium concentrations.

At the present time certain important findings are cogent to this general problem. The presence of a dynamic equilibrium between the cell and its environment has been indicated by the use of radioactive potassium and sodium as tracers.

Such investigations have revealed that a large fraction, if not all the potassium and sodium in those cells studied, is constantly exchanging with environmental cations (14–16, 22). Potassium and sodium ions are continuously diffusing across the cell membrane with their concentration gradients, outward and inward respectively. But the ionic composition of a particular type of cell is relatively constant; hence there must be cellular mechanisms which compensate for this continual flux of ions across the cell surface. These mechanisms are apparently energetically coupled with carbohydrate metabolism, for carbohydrate metabolism has been found to be of great importance in the maintenance of potassium and sodium balance in a large variety of cells (8, 10, 16, 25, 33, 38, 39).

This paper represents a summary of our investigations of the general problem of sodium and potassium balance in the cells of the marine alga *Ulva lactuca* var. *latissima*. In addition, certain studies carried out by the senior author on *Valonia macrophysa* during the spring of 1954 at Bermuda are included for comparative purposes.

Evidence will be presented which indicates the following: *a*) an influence of metabolism on the exchange rate of potassium ion in *Ulva*; *b*) an association of carbohydrate metabolism with cation-regulating mechanisms; *c*) an active transport of cations; *d*) the presence of independent mechanisms for the transport of sodium and potassium in *Ulva*.

The green alga *Ulva lactuca*, like most cells living in a high-sodium, low-potassium environment, normally accumulates potassium and partially excludes sodium. Consisting of large membranous fronds two cell layers in thickness, thus presenting a large surface area for interchange with the environment, this alga is particularly well suited for investigations of this nature. Furthermore, it is possible to prepare the material for analysis in such a way as to remove completely contamination with electrolytes in the extracellular fluid. Evidence for this will be discussed in the next section.

Valonia has the unique distinction of great cell size, as much as 1 cc. in volume. The cell consists of a thin peripheral layer of protoplasm, several microns in thickness, surrounding a very large central vacuole, several millimeters in diameter, and filled with a clear, watery sap. Within this fluid potassium is concentrated to the extent of forty times the concentration in sea water, while sodium is maintained at one third the sea-water level.

The green plant cell offers a further advantage for studying metabolic factors in cation regulation: the ease of turning on or shutting off a normal metabolic process, photosynthesis, by merely illuminating the cells or eliminating light from their environment. Thus, important carbohydrate intermediates are made available to the cell by photosynthetic reduction of carbon dioxide, either for assimilation into stored carbohydrates or for metabolic degradation through the glycolytic cycle.

METHODS

Ulva. The methods employed have been described in detail elsewhere (35, 37, 38). In brief, samples of *Ulva* 4 or 5 inches square, previously cut from a single frond, were removed at time intervals, rinsed 30 seconds in isotonic sucrose to remove sea-water contamination and blotted consistently in absorbent tissue to remove the sucrose. Analyses of tissue extracts were accomplished by flame photometry. As shown in the graphs, samples were removed in triplicate. Values in the tables represent averages of at least three samples each, in which the variation was of the same order of magnitude as in the graphs. In the data to be presented, potassium concentration is expressed as mEq/100 gm cell water, while sodium values are calculated as mEq/100 gm dry weight, for reasons to be discussed below.

Valonia. In order to ensure uniformity of material a large amount of algae was collected at once, the clumps of cells separated and allowed to condition under illumination in the laboratory two or more weeks before use. The experiments were carried out in liter beakers containing about 100 cells in 500 ml of sea water. The weight of the cells used varied from 0.15 to 0.3 gm. At various time intervals approximately 10 cells were removed and drained on paper tissue for one minute, placed on cheese cloth which was drawn across a finger bowl, then lowered in distilled water for 10 seconds and again drained on cheese cloth for one minute after which wet weights were recorded. Since samples removed after 20 and 30 seconds are not significantly different in sodium and potassium content from those removed after 5 and 10 seconds, it is unlikely that the distilled-water rinse removes any significant amount of intracellular cation. Preparation for flame photometry followed essentially the same procedure as employed on *Ulva*.

RESULTS

Extracellular Space in Ulva

In order to obtain valid values for the sodium and potassium concentrations in the cells it is essential to determine what fraction of the electrolytes in the samples as they are analyzed is due to contamination by the sea water which might be in the interstitial spaces. To this end several experiments were carried out to determine the extracellular space in the tissue under the conditions employed in preparation of the samples for analysis.

In one set of experiments samples were placed in sea water containing 1% inulin for several hours,[5] then transferred to exactly 100 ml of fresh sea water. Immediately before transfer some of the samples were dipped very briefly (1–2 sec.) into fresh sea water to remove adhering inulin solution; the other samples were rinsed for 30 seconds in fresh sea water, then blotted three times in absorbent tissue (same procedure used in preparation for sodium and potassium analyses) and then transferred. 'Inulin space' was measured under these conditions by determination of the inulin in the final solution a few hours after transfer. At the end of an experiment the samples were removed, blotted and weighed. Results of a typical experiment, indicating that the combination of the 30-second rinse plus the triple-blot are sufficient to reduce the inulin space to almost zero, are presented in table 1A.

TABLE 1. EFFECTS OF RINSING AND BLOTTING ON INULIN AND SUCROSE 'SPACES' IN ULVA

	1- to 3-Sec. Rinse, No Blot	30-Sec. Rinse, Triple Blot	1- to 2-Sec. Rinse, No Blot	1- to 2-Sec. Rinse, Triple Blot
	A. Rinsing and Blotting		*B. Blotting*	
Inulin space	19–21%	0–1%	20–22%	2–3%
Sucrose space	20–21%	0–1%	20–21%	2–3%

In the same manner sucrose was used as an indicator of extracellular space. Representative data, which agree very well with the inulin values, are also shown in table 1A.

To verify these results other experiments were designed to determine the effects of rinsing procedure and the blotting technic alone on the extracellular space. Samples were soaked in inulin-sea water as before and rinsed for 1 to 2 seconds in fresh sea water. One set was then transferred directly to fresh sea water, while the other was first blotted according to the standard procedure. Typical results are shown in table 1B, where it is seen that blotting alone reduces the extracellular space from about 20% to about 2 to 3%. A similar experiment was done using sucrose as the indicator of extracellular space.

Finally sodium and potassium determinations were run on samples removed from sea water under the following conditions: all samples were rinsed for 2 to

---

[5] The time course for diffusion of inulin into the tissue indicates that equilibrium was established within 1–2 hours.

3 seconds in isotonic sucrose; one set was blotted three times according to the standard procedure while the surfaces of the other samples were brushed lightly with absorbent tissue to remove grossly the adherent sucrose only from the surface. In this second group, then, the extracellular space has not been blotted out of the tissue. The samples were weighed, dried, extracted and analyzed. Average sodium and potassium values are presented in table 2. It can be seen that the lightly blotted samples actually have less sodium than the triple-blotted samples. Since as shown above the triple blotting almost completely removes the inulin space, these data clearly indicate that the smaller solutes in the extracellular space very rapidly diffuse from this space (1–3 sec. here) in isotonic sucrose. Further, it can be seen that the relative difference in sodium concentration between the two sets of samples is exactly equal to the relative potassium difference (*row d*). Since the potassium concentration in sea water and in the isotonic sucrose is so small relative to the total amount of potassium in the cells, this difference in potassium content is probably almost exclusively due to weight differences: that is, the lightly blotted samples will be heavier because of the sucrose solution which was not blotted in these samples. Hence there will appear to be less potassium (and sodium) per unit weight in the lightly blotted samples. Since the percentage sodium difference is identical with the percentage potassium difference, it is presumably to be accounted for by the same explanation. Sodium and potassium ions, then, diffuse very rapidly from the extracellular space of the samples after they are transferred from sea water to isotonic sucrose.

TABLE 2. POTASSIUM AND SODIUM VALUES FOR SAMPLES OF ULVA REMOVED FROM SEA WATER

	K	Na
a. Very light blot	21.8	13.5
b. 'Triple-blot'	31.0	19.2
c. $b-a$	9.2	5.7
d. $c/a \times 100$	42.2%	42.1%

All samples rinsed 1–2 seconds in isotonic sucrose. Some were brushed to remove sucrose from surface (*a*), while the rest were 'triple-blotted' (*b*). Values are expressed as mEq/100 gm cell water.

The possibility that the sucrose rinse washes out some of the electrolytes from within the cell is remote, since samples removed after 30 and 60 seconds in sucrose are not appreciably different in sodium and potassium content from those removed after only 1 to 3 seconds.

These experiments indicate that the 30-second rinse in sucrose plus the blotting procedure remove essentially all of the extracellular sodium and potassium and essentially none of the intracellular fractions of these cations. Hence the data presented represent true cellular sodium and potassium concentrations.

Influence of Metabolism on Exchange Rate of Potassium Ion

In studying the mechanisms of cation regulation in living cells it is desirable to determine the rate and extent of exchange of the ions in question between the cell and its environment. The use of radioactive potassium has demonstrated that a dynamic equilibrium normally prevails between the potassium of a variety of living cells and that of their environments. According to the studies of Raker *et al.* (32) on the human erythrocyte and Fenn *et al.* (11) on muscle, all the potassium of these cells appears to be exchangeable.

Ulva lactuca is well suited for such investigations because of the ready interchange possible between the cells and the surrounding sea water. Accordingly K^{42} was used to determine the influence of illumination and temperature on the rate and extent of potassium ion exchange (37).

TABLE 3. EFFECT OF ILLUMINATION AND TEMPERATURE ON RATE OF POTASSIUM ION EXCHANGE IN ULVA LACTUCA

Conditions	Time for 75% exchange hr.
Light 30°C	0.4
Dark 30°C	1.8
Light 20°C	2.2
Dark 20°C	3.2

The specific activities were calculated according to the following equation:

$$\text{Specific Activity} = \frac{\text{counts/min} \times 100 \text{ mg}}{\text{mEq K/100 gm}}$$

The rate of exchange, as indicated by the time required for the cellular specific activity to reach 75% that of the sea water (75% exchange), was much faster in the illuminated samples and those at the higher temperature (table 3). Since under all of these conditions the algal specific activity, K^{42} cellular/K^{39} cellular, reaches equality with that of the sea water K^{42} sea water/K^{39} sea water the complete exchangeability of the cellular potassium is indicated. It may be noted that the rate of exchange of potassium in illuminated *Ulva* is many times more rapid than in human erythrocytes and slowly fermenting yeast and not too different from strongly fermenting yeast (32, 19).

Role of Metabolism in Cation Regulation

In the following section evidence will be discussed which indicates an energetic coupling of cation regulation to metabolism and the presence of separate mechanisms for the active transport of both Na and K cations against their concentration gradients. In order to modify the prevailing cellular metabolism the following agents were used: *1*) light and dark, *2*) the metabolic inhibitors monoiodoacetate, phenylurethane and 4,6-dinitro-o-cresol, *3*) the addition along with iodoacetate of carbohydrate intermediates, the normal production of which is prevented by this inhibitor, *4)* low temperatures. In addition, experiments were carried out in which the effect of external sodium concentration on potassium reaccumulation was studied.

An examination of a large body of data indicates a close correlation between potassium content and calculated cell water in *Ulva*, while sodium content is most consistent on a dry weight basis. For these reasons the potassium and sodium are expressed as indicated although essentially the same results appear when the data for each ion are expressed on either basis.

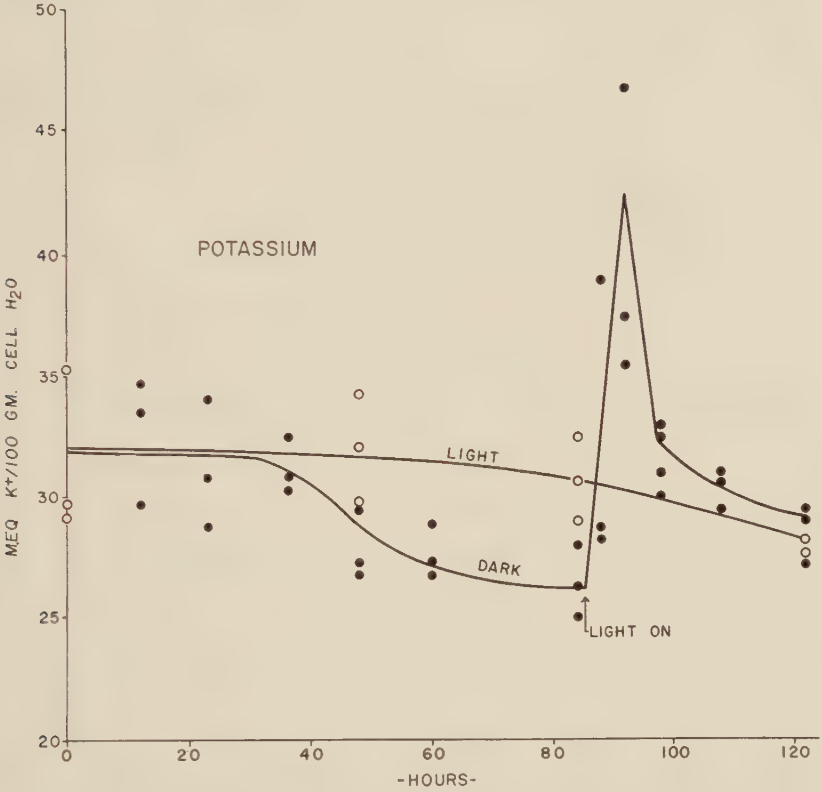

FIG. 1. Influence of illumination and darkness on the potassium content of *Ulva lactuca.*

The variation in ion contents in these experiments cannot be a reflection of changing cell volume, since although the percentage dry weight varied between the limits of 25 and 33 there was no trend correlating with any variation in ion contents.

Influence of Light and Dark. In these experiments two groups of algae were used, the one being maintained in the light throughout the experiment and the other being kept in the dark for a period and then illuminated. Samples were removed at intervals and analyzed for sodium and potassium; representative data are presented in figures 1 and 2. After a latency of approximately 30 hours a progressive loss of potassium occurs, amounting to 20% of the original potassium content of the cell in 82 hours. Upon illumination there occurs an abrupt accumulation of potassium which, for a short time, remains considerably above the level of the illuminated controls, then returns to this concentration level (fig. 1).

The sodium content of the cells gradually increases over the course of the experiment, 72 hours, in the dark. On illumination the sodium content is reduced in a period of 20 hours to the level of the controls, while that of the illuminated controls remains essentially constant (fig. 2).

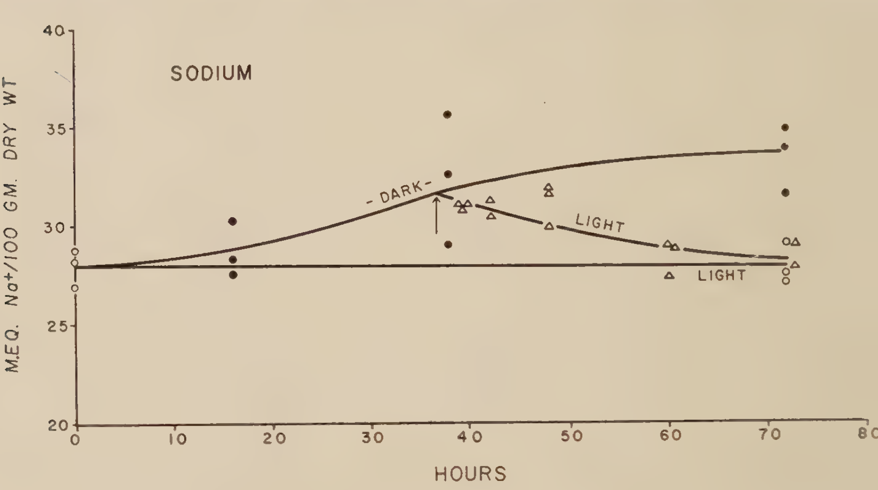

Fig. 2. Influence of illumination and darkness on the sodium content of *Ulva lactuca.*

The data indicate a marked influence of photosynthesis on the maintenance of the normal distribution of potassium and sodium in the cells of *Ulva.* The condition of darkness is sufficient to cause a loss of potassium and gain of sodium, presumably because the cell is using up its carbohydrate reserves or intermediates. The reexcretion of sodium and reaccumulation of potassium when light is admitted to fronds previously maintained in the dark lend further support to this interpretation, for under conditions of illumination the important glycolytic intermediate, phosphoglyceric acid, is made available to cellular metabolism by photosynthesis (3, 13). The influence of light on the uptake of electrolytes in algae has been previously observed by Hoagland and Davis (20) and Jacques and Osterhout (15). The latter authors interpret the uptake of potassium on more intense illumination in terms of an increase in the pH of the medium caused by photosynthesis and hence an increase in the activity product (K)(OH) outside the cell. In the above experiments the samples were maintained in freely running sea water so that changes in external pH would be insignificant.

Influence of Iodoacetate in the Light and the Dark: Ulva. The relationship of carbohydrate metabolism to cation regulation was further explored by use of the glycolytic inhibitor monoiodoacetate.

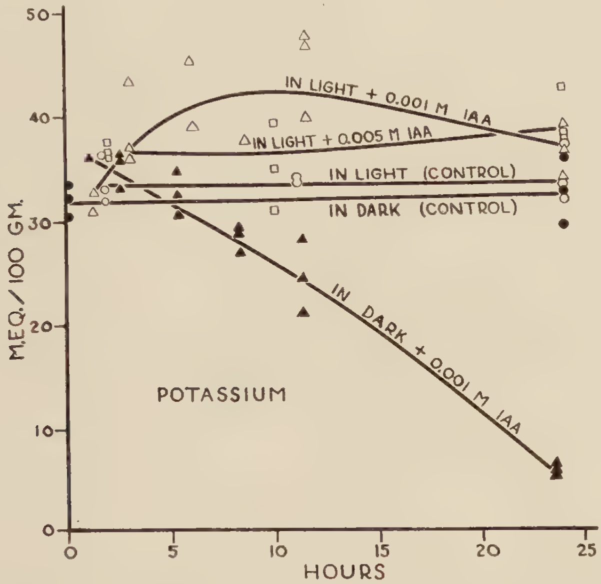

FIG. 3. Influence of 0.001 M/l. iodoacetate on the potassium content of *Ulva lactuca* in the light and in the dark. Potassium is expressed in terms of cell water.

The presence of the inhibitor in a concentration of 0.001 M/l. results in a marked loss of potassium from the cells over a period of 24 hours in the dark. Control samples taken at the beginning and end of this period were essentially constant in potassium content (fig. 3). In the presence of light the inhibitor is completely ineffective in causing the loss of potassium. Rather, the potassium content of the experimentals temporarily increases over that of the controls.

To evaluate further the influence of light on the prevention of the iodoacetate effect, the concentration of the inhibitor was raised to 0.005 M/l. Again light prevented the loss of potassium.

Concomitant with the potassium loss caused by the 0.001 M/l. iodoacetate in the dark, the cellular sodium increases over that of the controls although the condition of darkness alone is sufficient to cause some sodium increase. Illumination again prevents this action of the inhibitor, and sodium is actually somewhat reduced compared to the controls (fig. 4). Light also prevents an increase in sodium when the inhibitor concentration is raised to 0.005 M/l.

Influence of iodoacetate in the light and the dark: Valonia. The presence of the inhibitor at a concentration of 0.001 M/l. causes no significant change in the potassium and sodium content of cells placed in the light and dark for a period of at least 300 hours. When the concentration of iodoacetate is raised to 0.01 M/l., however, a marked loss of potassium and gain of sodium ion occurs for a period of 250 hours, changes which do not occur in the controls in light and dark without the inhibitor. In the presence of light the inhibitor is completely ineffective (fig. 5). Similar experiments in which the concentration of inhibitor was raised to 0.02 and 0.03 M/l. respectively gave essentially similar results with the potassium-loss and sodium-gain curves displaced slightly to the left. In all three experiments light prevented the iodoacetate effect; in fact, in the illuminated samples with the inhibitor the potassium was somewhat higher than in the controls. The similarity between *Ulva* and *Valonia* in this experiment is striking.

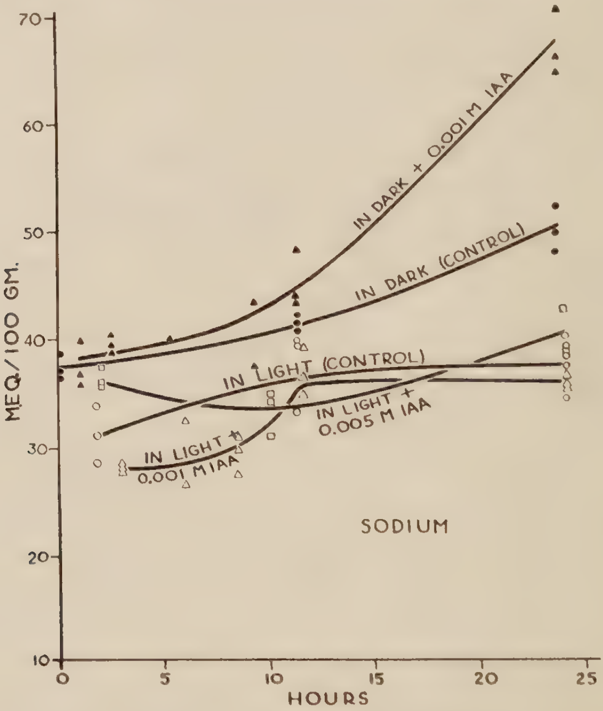

FIG. 4. Influence of iodoacetate on the sodium content of *Ulva lactuca* in the light and in the dark. Sodium is expressed in terms of dry weight.

A logical explanation of the action of iodoacetate in the dark is that the glycolytic breakdown of carbohydrate is blocked at the level of phosphoglyceraldehyde dehydrogenase, the principal site of attack of this inhibitor (14). Accordingly, metabolic energy apparently required for cation regulation is no longer supplied; potassium is lost and sodium gained by the cell.

The prevention of these ions shifts by light further supports this hypothesis, since phosphoglyceric acid, the compound which is formed by the action of phosphoglyceraldehyde dehydrogenase, has been shown to be the first stable product formed in the photosynthetic reduction of carbon dioxide (3, 13).

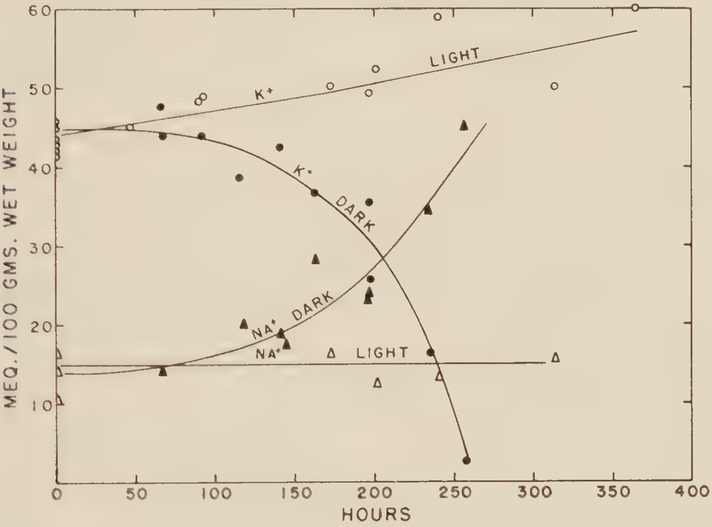

FIG. 5. Influence of 0.01 M/l. iodoacetate on the potassium and sodium content of *Valonia macrophysa* in the light and dark.

Hence, in the light, even in the presence of the inhibitor, which prevents the glycolytic formation of phosphoglyceric acid, this intermediate is made available to cellular metabolism by photosynthesis.

The postulated reactions are summarized in figure 21.

In the interpretation of the prevention by light of the iodoacetate effect it is essential to know whether or not the cell when illuminated is permeable to the inhibitor. In order to examine this problem the inhibitor was added to samples of *Ulva* in the light and maintained for 12 hours. At this time samples were transferred to sea water without the inhibitor and placed in the dark. Typical results are presented in figures 6 and 7, indicating a marked loss of potassium and gain of sodium after transfer to the inhibitor-free medium in the dark.

Washing-out of the iodoacetate effect. It is of interest to determine whether or not the ion shifts caused by iodoacetate in the dark are permanent or whether, after removal of the inhibitor from the environment, the cell can tend to restore the normal levels of sodium and potassium. To elucidate this point, samples of

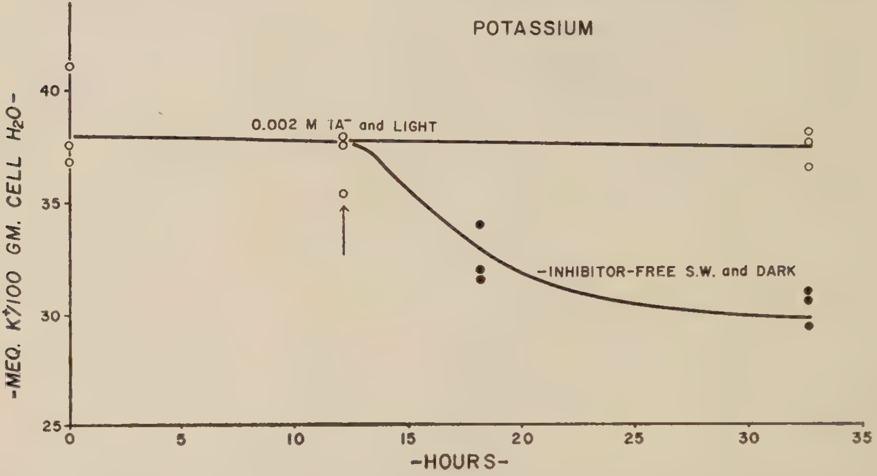

Fig. 6. Loss of potassium in the dark from *Ulva* previously treated with 0.002 M/l. iodoacetate in the light. The arrow indicates time of transfer of six samples to inhibitor-free sea water and darkness.

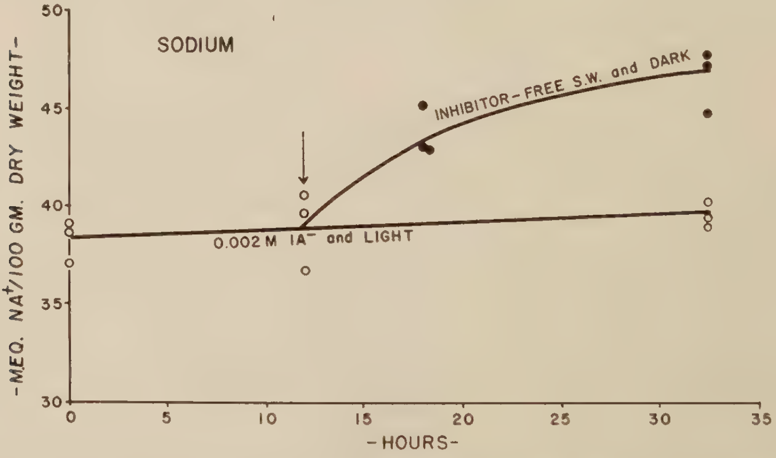

Fig. 7. Gain of sodium in the dark from *Ulva* previously treated with 0.002 M/l. iodoacetate in the light. The arrow indicates the time of transfer of six samples to inhibitor-free sea water and darkness.

Ulva were maintained in 0.001 M/l. iodoacetate in the dark for 16 hours, then placed in running sea water (no inhibitor) in the light.

After 16 hours in the iodoacetate, approximately 30% of the cellular potassium is lost, and a progressive loss, amounting to an additional 50% of the original concentration, continues in running sea water in the light for about 2 hours. At this point a gradual but definite and reproducible re-accumulation begins, the full extent of which could not be measured because of termination of the experiments (fig. 8).

The cellular sodium concentration after 16 hours in 0.001 M/l. iodoacetate in the dark is increased to 30% above the control level. In contrast to the potassium, the net movement of sodium against its concentration gradient begins immediately when the cells are returned to light and running sea water, and restoration of the normal level reaches completion in about 4 hours (fig. 9).

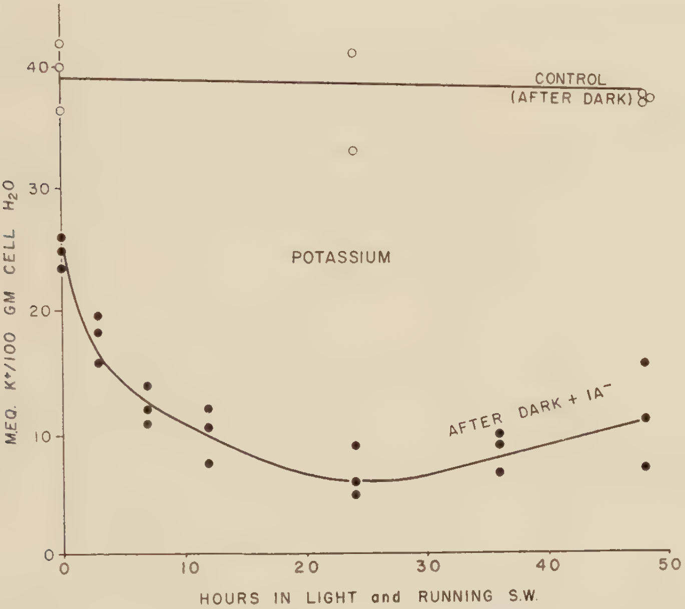

FIG. 8. Influence of light and running sea water on the potassium content of *Ulva* previously maintained for 16 hours in sea water containing 0.001 M/l. iodoacetate in the dark. Zero time on the graph represents time of transfer to running sea water and light. Control samples were illuminated after 16 hours in the dark.

These experiments indicate that although the iodoacetate causes a marked loss of potassium and gain of sodium by the cell, this effect of iodoacetate can apparently be 'washed out' of the cell in running sea water in the presence of light. Potassium loss ceases whereas sodium ion is secreted out of the cells against its concentration gradient. Attention is directed to the differential behavior of the cell as regards sodium and potassium movements in these experiments; i.e. although potassium is progressively lost from the cell for 25 hours sodium is excreted to the normal level within 4 hours.

Influence of Arsenate on Ion Shifts Caused by Iodoacetate. Two types of experiments were done involving iodoacetate and arsenate. In the one the cells were exposed to the two agents simultaneously in the dark, while in the other

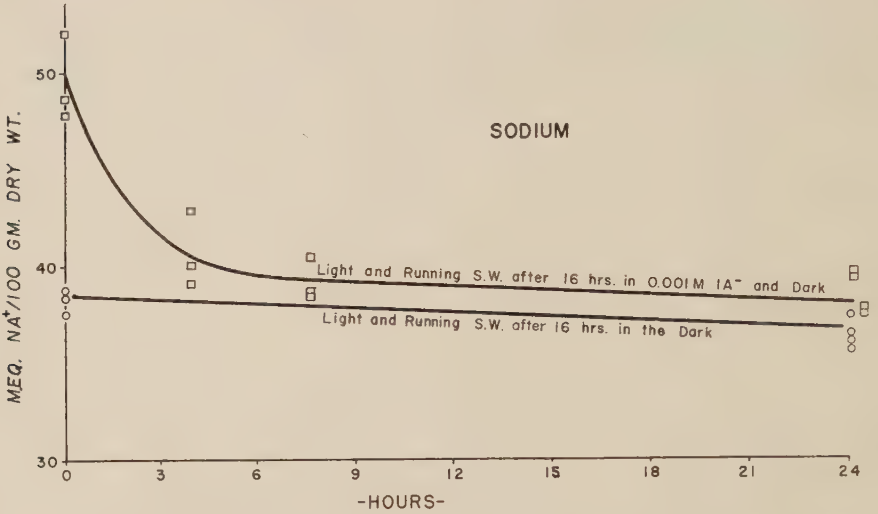

FIG. 9. Influence of light and running sea water on the sodium content of *Ulva* previously maintained for 16 hours in sea water containing 0.001 M/l. iodoacetate in the dark. Zero time on the graph represents time of transfer to running sea water and light. Control samples were illuminated after 16 hours in the dark.

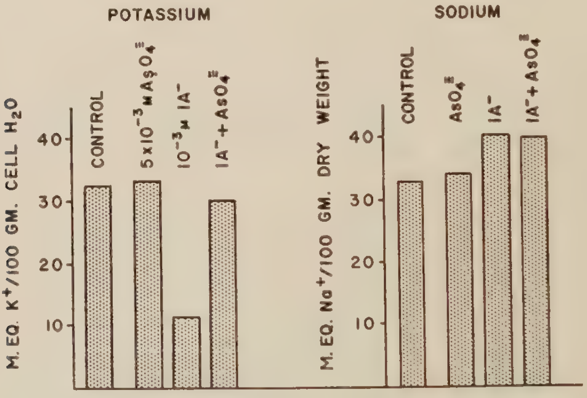

FIG. 10. Protection by arsenate against the potassium loss caused by iodoacetate in the dark. Triplicate samples were removed after 13 hours under the conditions described on the graph (*Ulva*).

arsenate was added to algae which had been exposed to iodoacetate in the dark for 18 to 20 hours. The results are shown in figures 10 and 12. In figure 10 it is seen that arsenate alone under the conditions employed had no effect on either the potassium or sodium contents, while iodoacetate caused a marked fall in potassium and a smaller rise in sodium. The effect of arsenate given with iodoacetate was to prevent almost completely (95%) the potassium loss with essentially no effect on the sodium increase.

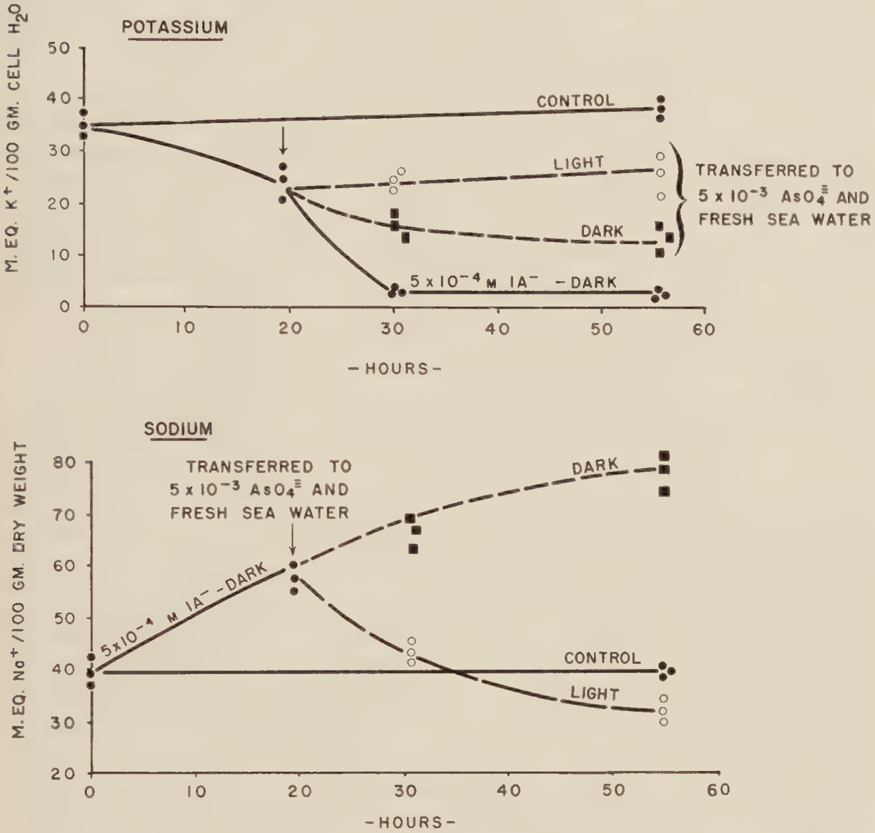

FIGS. 11 (*top*) and 12. Influence of arsenate after iodoacetate. Samples were maintained in the dark in 5×10^{-4}M/l. iodoacetate. At 20 hours (arrow) some samples were transferred to 5×10^{-3} M/l. Na_2HAsO_4 in sea water; some were illuminated (light), the others maintained in darkness (*Ulva*).

In the experiment described by figures 11 and 12 the samples were maintained in 10^{-3} M/l. iodoacetate for 20 hours. At this time 12 samples were transferred to fresh sea water (no iodoacetate) containing 5×10^{-3} M/l. Na_2HAsO_4; 6 were maintained under illumination, the rest placed in the dark. As seen in figure 11 the arsenate in the dark, although some further loss of potassium continued, offered significant protection against the loss as compared to the samples maintained in iodoacetate in the dark throughout the experiment. In the light no further potassium loss occurred with arsenate.

It is to be noted that the sodium movements in these cells are of a distinctly different nature from those of potassium. Thus in the dark arsenate affords no protection against continued sodium entry resulting from the iodoacetate, while in the light a dramatic secretion of sodium to the control level occurs within several hours.

The action of arsenate in these experiments is presumably to be explained by a mechanism proposed by Warburg and Christian (46); that is, arsenolysis at the level of 3-phosphoglyceraldehyde dehydrogenase, with the formation of 1-arseno, 3-phosphoglyceric acid, and subsequent spontaneous decomposition of this to 3-phosphoglyceric acid. It has been observed in yeast (17) that arsenate offers complete protection against the loss of potassium and gain of sodium usually observed aerobically with iodoacetate. It was proposed, then, that arsenate allows the metabolic pattern to circumvent the site of iodoacetate inhibition and that the 3-phosphoglyceric acid formed is further metabolized via the usual Embden-Meyerhof scheme.

Several features of the experiment described by figure 10 should be pointed out. First, it is apparent that, so far as the potassium-regulating mechanism is concerned, 3-phosphoglyceraldehyde dehydrogenase is the only enzyme blocked by iodoacetate. Since arsenate is effective when given after iodoacetate (figs. 11 and 12), the possibility that arsenate acts by preventing the iodoacetate from attacking the enzyme in the first place is not tenable. The most plausible explanation, then, is the one outlined above. The fact that arsenate does not protect against the sodium increase with iodoacetate suggests that the iodoacetate may be acting on another sulfhydryl enzyme—one which would be essential for an effective sodium pump in the dark, and not necessary for potassium accumulation—at a site where this special relief by arsenate is not possible. In accordance with this hypothesis is the observation that added phosphoglycerate in the presence of iodoacetate resulted in no protection against sodium gain but did allow protection against potassium loss.

Such an interpretation is consistent with the data shown in figures 11 and 12. Again the arsenate relieves the potassium loss resulting from iodoacetate. It is important to note that this relief is almost certainly in no part due to a washing out of the inhibitor since profound potassium loss occurs for many hours after transfer from iodoacetate to light and running sea water as already described. Furthermore, as mentioned above, iodoacetate inhibition is essentially irreversible. The protection in the dark after transfer to arsenate would be, according to the hypothesis, a measure of arsenolysis of cellular carbohydrate reserves. The additional protection in the light (to the extent of an actual slight reaccumulation) would be the result of additional phosphoglycerate formed in the cells during photosynthesis (3, 13, 35). It should be noted that these samples in the light were actively photosynthesizing, as judged by the formation of gas bubbles on the under surfaces of the samples.

In the complementary study of sodium movements in these same samples quite different behavior was observed. As in the experiment when arsenate and iodoacetate were given simultaneously, the arsenate added after iodoacetate (fig. 12) offered no protection in the dark. In the light, on the other hand, a fairly rapid active resecretion of sodium occurred so that it reached the control level in several hours. A similar resecretion of sodium was observed when samples were transferred to light and running sea water, without arsenate (35). The presence of arsenate, then, as regards the sodium secretion in the light appears to be quite incidental. The fact that sodium is not resecreted in the dark is further evidence that the procedures employed involved no 'washing out' of the inhibitor.

It is probable that this effect of light on the sodium pump is quite apart from the generation of carbohydrate intermediates through photosynthesis (which appears to be the chief effect of light as regards the potassium-pumping mechanism), since under these conditions light and darkness have a much greater effect on sodium than on potassium—the difference between no protection and complete resecretion. From the existing data it is not possible to postulate the exact nature of this effect, but it might be suggested, since the reducing properties of light are well known, that it is associated with a redox mechanism of some sort. In this connection it should be mentioned that Conway (5, 6) has postulated a redox pump for potassium in the yeast cell and Lundegardh (24) a redox mechanism for anion absorption in plant roots.

These experiments with arsenate serve to indicate that iodoacetate acts on the potassium mechanism in the same manner as already proposed (8, 14, 16, 35, 39) (i.e. inhibition of 3-phosphoglyceraldehyde dehydrogenase with a resulting stoppage of energy-yielding reactions in the cell), that it acts on the sodium pump in a different manner, and that light, perhaps through its reducing power, has a primary action on the sodium-pumping mechanism (fig. 21).

Synergistic Effects of Iodoacetate and Phenyl Urethane. Iodoacetate causes a loss of potassium and a gain of sodium in *Ulva* in the dark, but fails to do so in the light (35, 36). This protection by light was interpreted as resulting from the photosynthetic production of phosphoglyceric acid (product of the reaction inhibited by iodoacetate) in the light, but not in the dark. To evaluate this interpretation iodoacetate and phenyl urethane, a photosynthetic as well as a metabolic inhibitor, were added together to samples in the light. Results of a typical experiment are shown in table 4. Thus 10^{-3} M/l. iodoacetate has no appreciable effect on cellular sodium and potassium concentrations. Phenyl urethane in 10^{-3} M/l. concentration alone causes some potassium loss and sodium gain, but iodoacetate and phenyl urethane together cause considerably greater ion shifts. An examination of the kinetics of potassium loss and sodium gain caused by the addition of 10^{-3} M/l. iodoacetate to samples previously maintained in 10^{-3} M/l. phenyl urethane in the light reveals a difference in potassium and sodium movements subsequent to the addition of iodoacetate (38).

The experiments with iodoacetate and phenylurethane support the conclusion that iodoacetate penetrates the cells in the light. Phenyl urethane was selected as the agent to inhibit photosynthesis in these experiments since the margin of safety between 50% inhibition of photosynthesis and 50% inhibition of respiration was shown to be largest of a series of urethanes studied by Warburg (45). In actual practice, however, it was impossible to find a concentration which effectively blocked photosynthesis which did not at the same time cause some loss of potassium and gain of sodium presumably from some inhibition of cell respiration. These ion movements cannot be the result of stopping photosynthesis, since, although darkness causes some net ion changes, these occur only after a relatively long period of time and are not nearly so large as those with phenyl urethane. At any rate, iodoacetate markedly enhances the potassium loss immediately after addition to samples in phenyl urethane for 11.5 hours, and, after several hours, increases the sodium uptake.

TABLE 4. COMBINED EFFECTS OF 10^{-3} M/L. IODOACETATE AND 10^{-3} M/L. PHENYL URETHANE ON POTASSIUM AND SODIUM CONTENTS

	K mEq. % cell water	Na mEq. % dry weight
Control	40.3	38.9
10^{-3} M/l. iodoacetate	40.0	38.6
10^{-3} M/l. phenyl urethane	27.4	60.3
10^{-3} M/l. iodoacetate plus 10^{-3} M/l. phenyl urethane	16.1	71.1

Experiment run for 22 hr. in the light (*Ulva*).

Another possible interpretation of the action of iodoacetate is that light produces sulfhydryl groups which prevent the inhibitor from reacting with the enzyme. Three pieces of evidence, however, support the first interpretation: *1*) the higher potassium and lower sodium in illuminated iodoacetate-samples than in controls, as already discussed. *2*) The experiments reported in which potassium and sodium immediately begin to move with their chemical gradients when samples were transferred to inhibitor-free sea water in the dark after 12 hours in the light with 2×10^{-3} M/l. iodoacetate. Had the iodoacetate not been tied up by the enzyme but rather by other sulfhydryl groups within the cell, these ion shifts would not have been observed, since the reaction between iodoacetate and sulfhydryl groups (alkylation) is essentially irreversible (2, 9). *3*) Finally, the experiments discussed above, in which iodoacetate is effective in the light in the presence of an inhibitor of photosynthesis, phenyl urethane.

Exogenous Phosphoglycerate and Pyruvate Given With Iodoacetate. To evaluate further the interpretation of the action of iodoacetate (in the dark) experiments were carried out in which either phosphoglycerate or pyruvate were added to *Ulva* in the dark along with the inhibitor. These intermediates are, of course, normal components of the glycolytic cycle occurring below the level of 3-phosphoglyceraldehyde dehydrogenase, the site of action of iodoacetate. Representative data are presented in table 5.

Thus pyruvate affords the cell 100% protection against the sodium increase caused by iodoacetate in the dark, while it protects against potassium loss only to a much smaller extent. Phosphoglycerate, on the other hand, offers essentially no protection against sodium increase but allows a very significant protection against potassium loss.

TABLE 5. PROTECTIVE INFLUENCE OF PYRUVATE AND PHOSPHOGLYCERATE WHEN GIVEN WITH IODOACETATE

	K mEq. % all water	Na mEq. % dry weight
*A. Pyruvate**		
Control	38.6	35.6
2×10^{-3} M/l. iodoacetate	28.9	44.7
2×10^{-3} M/l. iodocate plus 50 mg % pyruvate simultaneously, with 25 mg % pyruvate at 4 hours	31.5	35.7
B. Phosphoglycerate†		
Control	28.9	45.9
2×10^{-3} M/l. iodoacetate	9.4	49.4
2×10^{-3} M/l. iodoacetate plus 50 mg. % phosphoglycerate	19.0	49.3

* Experiment run for 5 hr. in the dark (*Ulva*).

† Experiment run for 6 hr. in the dark (*Ulva*).

It might be suggested from the experiments with exogenous pyruvate and phosphoglycerate that the two transport mechanisms are energetically coupled to metabolism at different points in the glycolytic and/or respiratory cycles. Indeed, such a possibility is in line with some of the other experimental results presented here. But to define precisely where these points of coupling are (and there is no good reason at present to believe that there may not be more than one for each 'pump') is not possible on the basis of the existing data. We might say that energy for the 'potassium pump' seems to come from below the level of phosphoglycerate, while the 'sodium pump' seems to be coupled to the metabolism of pyruvate or a product of its metabolic degradation.

Action of 4,6-Dinitro-o-Cresol. Since energy apparently is necessary to accomplish potassium accumulation and sodium secretion and since the high energy phosphate bond may be the principal type of energy currency the cell uses, the action of 4,6-dinitro-o-cresol (DNC) was investigated. This agent, like related substituted phenols, effectively dissociates aerobic respiration from the generation of high energy phosphate bonds (4, 23). Figures 13 and 14 indicate the net movements of potassium and sodium in *Ulva* treated with 3.3×10^{-5} M/l. DNC in the dark over a period of 48 hours. Again it is to be

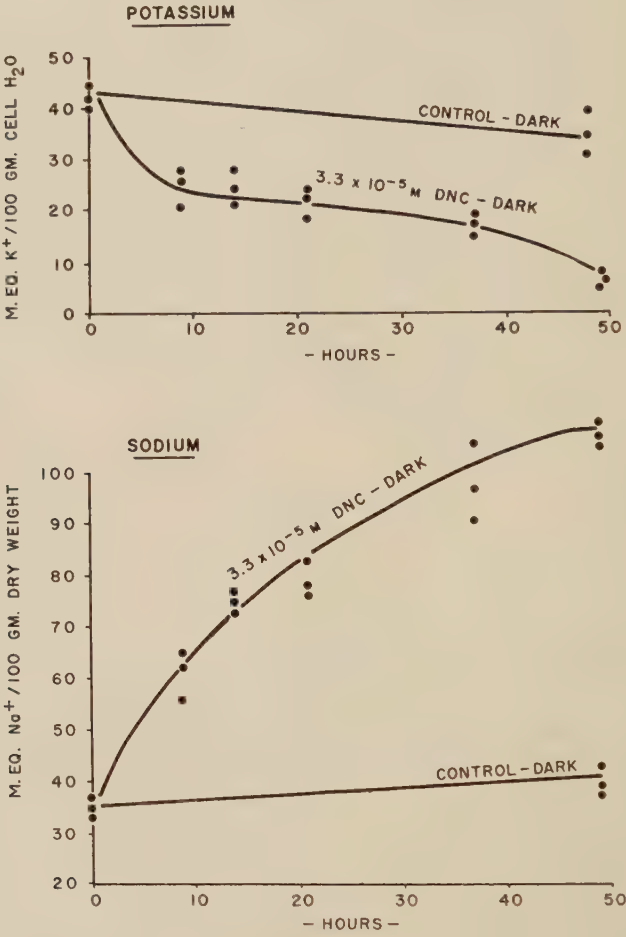

FIGS. 13 (*top*) and 14. Influence of 4,6-dinitro-o-cresol (DNC) on the potassium and sodium contents of *Ulva lactuca*.

noted that the kinetics of potassium loss are distinctly different from those of sodium uptake in the presence of this 'decoupling agent'. It should be pointed out that these experiments were carried out in the dark not because DNC does not cause these ion shifts in the light (as is the case with iodoacetate) but rather because DNC is an effective inhibitor of photosynthesis. Thus the experiment is more easily controlled in the dark, since darkness alone causes some ion shifts.

Protection by ATP Against Ion Shifts Caused by Iodoacetate. Since DNC caused a loss of potassium and a gain of sodium by *Ulva*, presumably by dissociating respiration from the production of energy-rich phosphate bonds, the possibility of some degree of protection by exogenous ATP against the ion shifts caused by iodoacetate was investigated. In these experiments ATP was added in small amounts at 2- to 3-hour intervals to samples maintained in iodoacetate in the dark. The data in table 6 represent one such experiment. Thus, over a 26-hour period the higher concentration of ATP afforded about 25% protection against the potassium loss by iodoacetate. However, the ATP offered no protection against the sodium influx resulting from iodoacetate, but rather the iodoacetate-ATP samples showed a higher sodium than the iodoacetate samples.

TABLE 6. PROTECTIVE INFLUENCE OF ATP AGAINST POTASSIUM LOSS OBSERVED WITH 10^{-3} M/L. IODOACETATE IN THE DARK

	K mEq. % cell water	Na mEq. % dry weight
Control	37.9	38.7
10^{-3} M/l. iodoacetate	17.6	48.3
10^{-3} M/l. iodoacetate plus 3×10^{-5} M/l. ATP	19.9	54.2
10^{-3} M/l. iodoacetate plus 10^{-4} M/l. ATP	23.5	58.7

The experimental period covered here is 26 hr. The ATP was added in the concentrations shown at 2 to 3 hr. intervals throughout this period (*Ulva*).

The difficulties described below in experiments with exogenous ATP may well apply to experiments with any exogenous metabolite. Because of the metabolic complexities of any biological system, any attempt to localize precisely the sites of coupling between ion transports and metabolism is beset with difficulties. Nonetheless, these experiments do show that while added phosphoglycerate is more effective in protecting against potassium loss with iodoacetate, pyruvate effectively maintains the sodium-pumping mechanism in the presence of the inhibitor.

The experiments with ATP, while they did not show a complete protection by ATP against the potassium disturbances caused by iodoacetate, did nevertheless demonstrate a significant protection for potassium. It would probably be an unjustified extrapolation to conclude on the basis of these few experiments that the sodium-pumping mechanism is not energized at one stage or another by ATP. Certainly the decoupling agent employed, DNC, caused a markedly rapid increase in cellular sodium.

There are certain inherent difficulties in experiments with exogenous ATP. One problem is the penetration of this relatively large molecule into the cell, and to overcome this difficulty presumably a high concentration in the external medium would be advantageous. But on the other hand, too high an outside concentration of a normally occurring intracellular component might have detrimental effects on the cell. Thus the ideal situation probably represents a balance between these two opposing factors. In the experiments described here a compromise was attempted by adding the ATP in small amounts at short intervals. Since the potassium and sodium regulating mechanisms responded differently in the other experiments it should not be surprising that they behave differently here.

Action of Phenyl Urethane and its Reversibility: Ulva. The presence of 10^{-3} M/l. phenyl urethane in the sea water around the cells caused a marked progressive loss of potassium and gain of sodium over a 48-hour period (figs. 15 and 16). At 36 hours, when the cellular sodium was 275% of the original value and the potassium 38%, some samples were transferred to running sea water to determine the reversibility of these ion shifts. At 48 hours, when these samples were removed, the cellular sodium concentration had been restored to the normal level, while 78% of the potassium which had been lost was reaccumulated. In other experiments, where potassium reaccumulation was followed over a longer period, it was observed to be complete (to the control level).

The precise mechanism of action of the urethane series of narcotics has not yet been clearly defined. Cornman (7) has recently reviewed the effects of these narcotics with special reference to cell-division inhibition. Lamanna and Campbell (21) have presented data which indicate that urethane inhibits yeast-cell respiration by a surface action. But since these agents do inhibit cell respiration the action of phenyl urethane was investigated here. The most striking feature of this disturbance of cation regularity is its *complete reversibility*. Experiments with metabolic inhibitors frequently are not shown to be completely reversible as regards electrolyte disturbances; hence such experiments are open to the criticism that the potassium loss and or sodium gain observed with inhibitors represents merely a general deterioration of the cell with a resulting non-specific movement of cations with their concentration gradients. The experiments presented here allow no such interpretation, for certainly some active process must be involved in the restoration of potassium and sodium to normal values after removal of the inhibitor.

Influence of phenyl urethane: Valonia. The presence of 10^{-3} M l. phenyl urethane in the sea water in the dark results in a loss of potassium and gain of sodium. In 75 hours the cells have lost approximately 50% of their potassium whereas the sodium content has increased 60%. At the time the cells are transferred to light and running sea water a gradual reaccumulation of potassium and secretion of sodium out of the cells begins and continues for approximately 75 hours, after which time the cells have reestablished essentially their normal composition with respect to these cations. If the experiment is carried beyond 75 hours in the presence of phenyl urethane the influence of the inhibitor is not

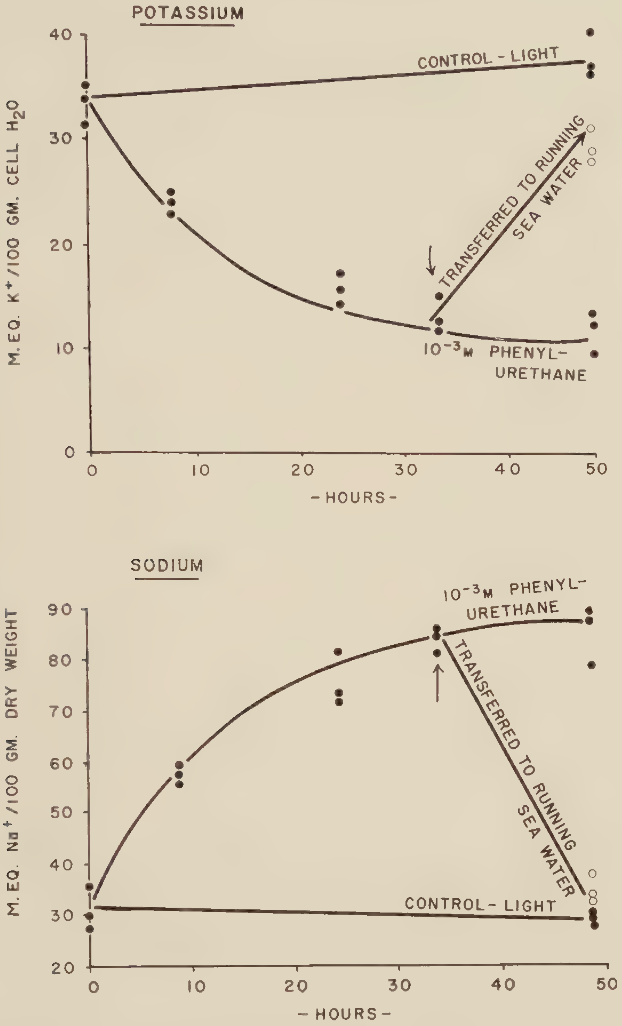

FIGS. 15 (*top*) and 16. Loss of potassium and gain of sodium in *Ulva* resulting from 0.001 M/l. phenyl urethane. At the arrow 3 samples were transferred to running sea water.

reversible on restoration to light and running sea water (fig. 17). As in *Ulva* an active process must be postulated for cation regulation. The possibility of passive accumulation of potassium in the sap does not exist, since, as pointed out by Osterhout, the concentration of diffusible anion in the sap is not low enough to account for the observed ratio of internal to external potassium and the Donnan principle cannot apply (28).

Influence of Cold on Ulva and Valonia. One of the first suggestions that there was a close association of metabolism with cation regulation was made by Harris (16) on observing a reaccumulation of potassium by human erythrocytes after the cells had been kept in the cold and were then returned to 38°C. A study of the Q_{10} for potassium exchange by Ponder (31), Sheppard and Martin (41) and Raker *et al.* (32) further supported the idea of a direct influence of carbohydrate metabolism on electrolyte balance.

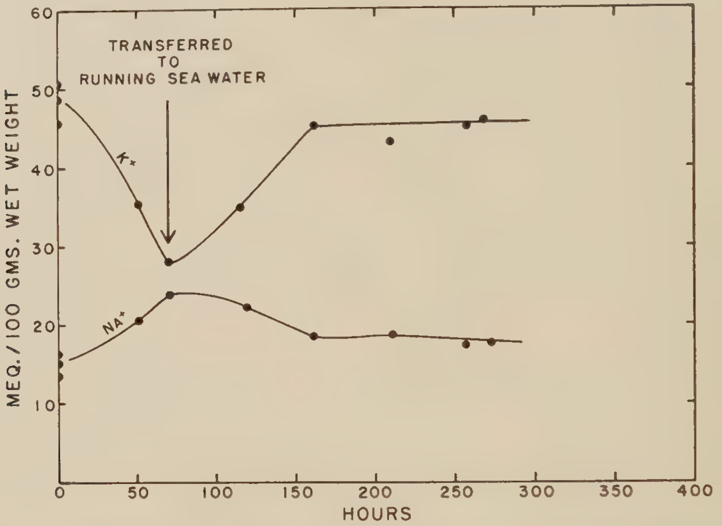

FIG. 17. Loss of potassium and gain of sodium in *Valonia macrophysa* resulting from 0.001 M/l. phenyl urethane. At the time indicated by the arrow the cells were transferred to running sea water without the inhibitor.

Attempts to demonstrate an influence of temperature on sodium and potassium balance in *Ulva* have not been too successful since these cations in *Ulva* undergo no significant change when the alga is maintained at 2°C for 24 hours. It is possible that mechanisms operate to reduce the permeability of the cells to cations so that even though the rate of metabolism (and likewise transport mechanisms) is reduced, the cell maintains its normal composition at least for 24 hours.

In the case of *Valonia*, however, when the cells are maintained at 2 to 5°C for approximately 75 hours, a slight loss of potassium and gain of sodium occurs. On return to a temperature of 18°C a further and striking loss of potassium and gain of sodium takes place. After 75 hours at the higher temperature a reaccumulation of potassium and a secretion of sodium begin and continue for about 250 hours. Within this time the cells have restored nearly the normal potassium and sodium levels (fig. 18).

Effect of External Sodium on Potassium Accumulation in Ulva. It is of considerable importance to determine whether or not the potassium-accumulating mechanism is passive, dependent upon and secondary to the sodium-secreting mechanism, or whether it is active and independent of sodium secretion. To this end the following type of experiment was carried out. Samples of *Ulva* fronds were repeatedly suspended in isotonic sucrose for 2 to 3 hours, at which time the cells had lost about 85% of their sodium and potassium (figs. 19 and 20). At this time half the samples were transferred to complete natural sea water, while the others were placed in sodium-free Allen's artificial sea water, isotonicity maintained by the addition of sucrose. Potassium reaccumulation was followed in the two groups by removing samples at various times over a 24-hour period. Two features of the data are outstanding: *1*) the potassium reaccumulation is, within experimental error, linear; and *2*) the presence of sodium in the external fluid made no measurable difference in the rate of potassium reaccumulation. It is noteworthy that in other experiments the potassium reaccumulation was complete to the control level. The sodium concentration in those samples returned to complete sea water is seen to have reached the control level within the time at which the first samples of this series were removed; the curve for re-entry of sodium, then, is probably steeper than the one shown here and need not be linear.

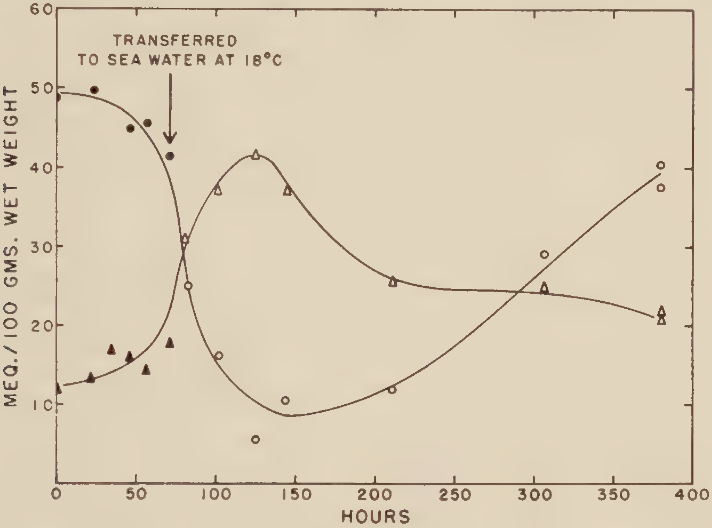

FIG. 18. Influence of cold (2–5°C) on the potassium and sodium content of *Valonia macrophysa*. At the time indicated by the arrow the cells were transferred to running sea water at 18°C in the light.

The results of these experiments indicate a mechanism for potassium uptake which is independent of sodium secretion. Further, since the kinetics of potassium reaccumulation under these conditions are described by a straight line,

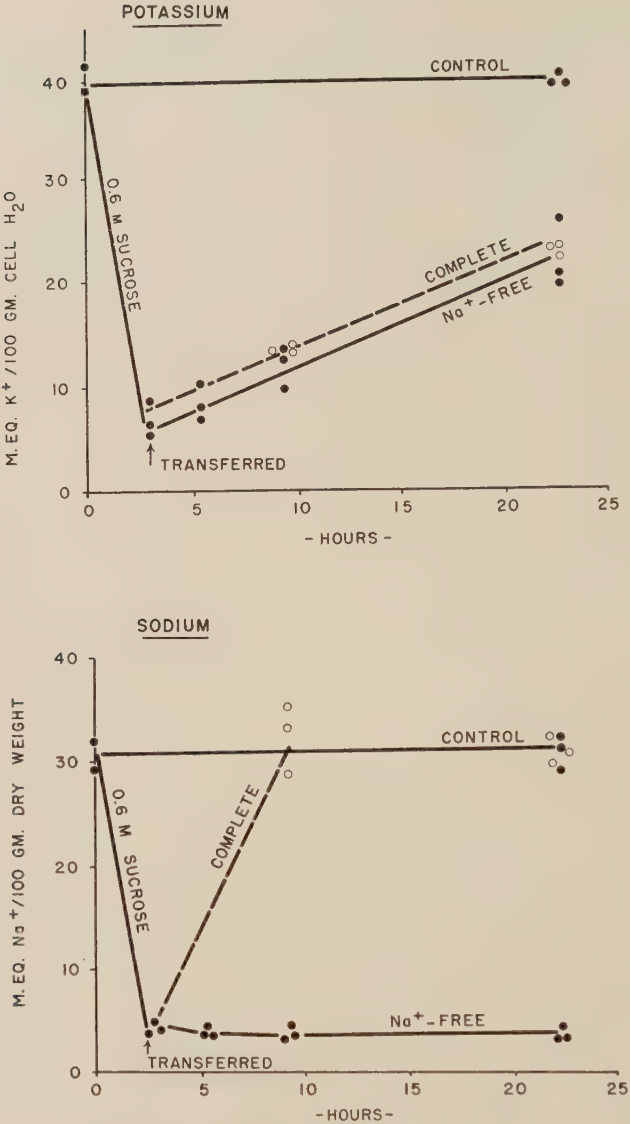

FIGS. 19 (*top*) and 20. Effect of external sodium on potassium accumulation. The minerals were 'leached' from the samples by repeated washing in isotonic sucrose solution for three hours. At this time (arrow) some were transferred to complete natural sea water ('complete') and the rest to sodium-free Allen's artificial sea water ('Na-free') (*Ulva*).

the mechanism appears to have a limited capacity. A transport system for potassium, such as the carrier hypothesis first proposed by Osterhout (30), would seem to fit the data best. Mudge (27) has recently described experiments on rabbit kidney slices in which the turnover of potassium as measured with K^{42} was not affected by variation in extracellular sodium concentration from 78-234 mEq/liter. The interpretation of our data is consistent with his findings.

Recent studies were carried out in relation to an observed variation in the potassium content of *Ulva* collected from the brackish water of Perch Pond, near Falmouth, Massachusetts, the salinity of which was found to be from 65 to 70% that of ocean water. *Ulva* from this source contained significantly less potassium than material from the Eel Pond in Woods Hole, where the salinity is closer to that of ocean water.

Accordingly, the following experiment was performed: sea water was diluted to 70% with distilled water, and calcium, magnesium, sulfate, and bicarbonate ions were restored to full strength according to Allen's formula for artificial sea water (1). Four solutions were prepared from this as follows: *a*) no additions; *b*) KCl added to restore normal K content of sea water; *c*) NaCl added to restore normal Na content of sea water; *d*) both K and Na restored to normal.

TABLE 7. ALTERATION OF CELLULAR CATIONS AS A RESPONSE TO CHANGES IN ENVIRONMENTAL SODIUM AND POTASSIUM

	K^+ mEq/100 gm cell H_2O	Na^+ mEq/100 gm dry wt.	Dry wt. %
a. '70% S.W.'	31.3	46.9	31.5
b. '70% S.W.' KCl	32.8	37.3	30.1
c. '70% S.W.' NaCl	37.3	47.7	31.4
d. '70% S.W.' KCl, NaCl	37.0	47.1	31.4

'70% S.W.' denotes the dilution of sea water by 30% with distilled water and the addition of salts of $CaCl_2$, $MgCl_2$, $MgSO_4$, and $NaHCO_3$ to the full natural concentrations. In (*b*) K^+ was restored to normal concentration (9.73 mEq/l.), in (*c*) Na^+ was restored (423 mEq/l.), and in (*d*) both salts were added. The time was 15 hr. and the samples were maintained in the dark (*Ulva*).

Thus (*c*) and (*d*) have essentially the same osmotic pressure, whereas the osmotic pressures of (*a*) and (*b*) are approximately 30% lower. The potassium contents of fronds in (*c*) and (*d*) were observed to be higher than those of (*a*) and (*b*) (table 7). Since the percentage dry weights of samples from all four solutions were constant, the potassium increment in (*c*) and (*d*) cannot be the result of a concentration by water loss. Apparently the cell has adjusted its potassium concentration with respect to the change in external salinity in order to maintain osmotic regulation. In the previous section in which potassium accumulation was shown to be independent of external sodium concentration in artificial sea water, osmotic pressure was maintained constant by the addition of sucrose. In both cases, therefore, one major function of intracellular potassium is to contribute to the internal osmotic pressure.

DISCUSSION

Concerning the experiments on *Ulva*, the most tenable interpretation of the data presented is that mechanisms are operative in *Ulva* for the accumulation of potassium and the secretion of sodium, that these mechanisms are independent of each other, and that they are energized by the metabolic degradation of carbohydrate (fig. 21).

Any comparison between *Ulva* and *Valonia* must take cognizance of the morphological differences between the cells of the two organisms. In the relatively small cells of *Ulva* the cytoplasmic mass is large relative to the amount of fluid in the vacuole, while in *Valonia* cells the opposite situation pertains, i.e. by far the greater portion of the mass is vacuole with the cytoplasm contributing only a very small part. There are three obvious consequences of these relationships which must be considered in comparing the two forms. First, in *Ulva* one analyzes largely the cytoplasmic fluid, while in *Valonia* the cytoplasm contributes little to whole-cell analyses. Secondly, in *Valonia* the major fraction of the analyzed ions has passed through two living membranes. Finally, the ratio of total exterior surface to total mass is much greater in *Ulva* than in *Valonia*. These last two factors are important in kinetic studies and may probably be at least partly responsible for the rather sluggish responses of *Valonia* to metabolic inhibitors contrasted with the more rapid responses in *Ulva*. There also exists the possibility that the *Valonia* membranes are less permeable to ions of sodium and potassium than is the *Ulva* membrane.

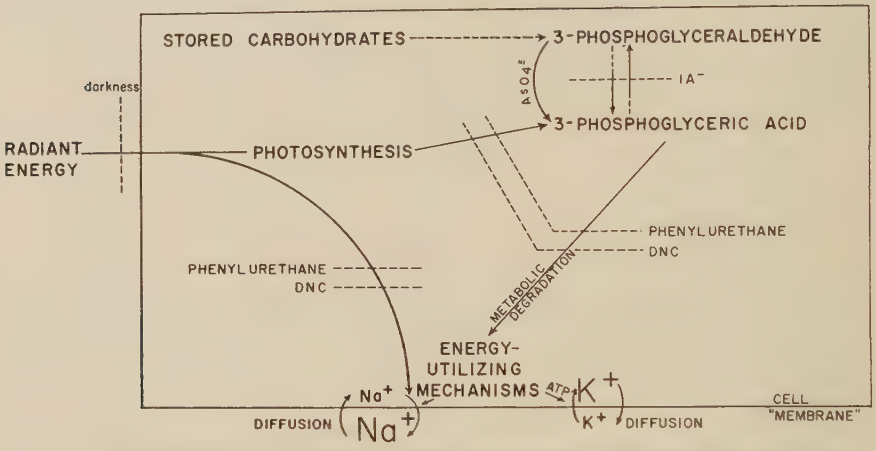
STORED CARBOHYDRATES
3-PHOSPHOGLYCERALDEHYDE
ASO4=
IA⁻
3-PHOSPHOGLYCERIC ACID
darkness
RADIANT ENERGY
PHOTOSYNTHESIS
PHENYLURETHANE
DNC
PHENYLURETHANE
DNC
METABOLIC DEGRADATION
ENERGY-UTILIZING MECHANISMS
ATP
Na+
Na+
K+
K+
DIFFUSION
DIFFUSION
CELL "MEMBRANE"

FIG. 21. Diagrammatic representation of the interpretation of the data presented above.

Regardless of the differences in the time scales, the striking feature of this comparison is the similarity of the two organisms as regards sodium and potassium movements in response to inhibition by iodoacetate and phenyl urethane. Although the data presented do not serve to separate the mechanisms regulating potassium and sodium in *Valonia*, since the organism behaves in other respects so much like *Ulva*, where separate mechanisms must be postulated, it is probable that independent potassium- and sodium-regulating mechanisms do exist in *Valonia* as well.

In spite of the large variety of cells in which this problem has been studied, a general pattern is emerging with relatively minor variations. These variations are appropriate to the specific environment of a cell and to its specialized function.

REFERENCES

1. Allen. *Allen's Artificial Sea Water* In: Marine Biological Laboratory *Formillae and Methods*, 1952, vol. 4.
2. Barron, E. S. G. and T. P. Singer. Studies on biological oxidations: XIX sulfhydryl enzymes in carbohydrate metabolism. *J. Biol. Chem.* 157: 221, 1945.
3. Calvin, M. and A. A. Benson. The path of carbon in photosynthesis IV: The identity and sequence of the intermediates in sucrose synthesis. *Science* 109: 140, 1949.
4. Clowes, G. H. A., A. K. Keltch, C. F. Strittmatter and C. P. Walters. Action of nitro and halophenols upon oxygen consumption and phosphorylation by a cell-free particulate system from *Arbacia* eggs. *J. Gen. Physiol.* 33: 555, 1950.
5. Conway, E. J. Biological interlinkage of acid-alkali formation with ion transport and synthetic reduction. *Irish J. M. Sc.* 288: 787, 1949.
6. Conway, E. J., T. G. Brady and E. Carton. Biological production of acid and alkali; 2. A redox theory for the process in yeast with application to the production of gastric acidity. *Biochem. J.* 47: 369, 1950.
7. Cornmann, I. Urethan in relation to mitosis. *Internat. Rev. Cytol.* In press.
8. Dean, R. B. Anaerobic loss of potassium from frog muscle. *J. Cell. & Comp. Physiol.* 15: 189, 1940.
9. Dickens, F. Interaction of halogenacetates and -SH compounds. *Biochem. J.* 27: 1141, 1933.
10. Dixon, K. C. Anaerobic leakage of potassium from brain. *Biochem. J.* 44: 187, 1949.
11. Fenn, W. O., T. R. Noonan, L. J. Mullins and L. Haege. Exchange of radioactive potassium with body potassium. *Am. J. Physiol.* 135: 149, 1941.
12. Flynn, F. and M. Maizels. Cation control in human erythrocytes. *J. Physiol.* 110: 301, 1949.
13. Gaffron, H., E. W. Fager and J. L. Rosenberg. Intermediates in photosynthesis: formation and transformation of phosphoglyceric acid. *Symp. Soc. Exper. Biol.* (Great Britain) 5: 262, 1951.
14. Green, D. E., D. M. Needham and J. G. Dewan. Dismutations and oxidoreductions. *Biochem. J.* 31: 2327, 1937.
15. Jacques, A. G. and W. J. V. Osterhout. The accumulation of electrolytes VI. The effect of External pH. *J. Gen. Physiol.* 17: 727, 1934.
16. Harris, J. E. The influence of the metabolism of human erythrocytes on their potassium content. *J. Biol. Chem.* 141: 579, 1941.
17. Hayward, H. R. Unpublished observations.
18. Hayward, H. R. and G. T. Scott. Evidence for independent mechanisms regulating potassium accumulation and sodium secretion in *Ulva lactuca*. *Biol. Bull.* 105: 366, 1953.
19. Hevesy, G. and N. Nielsen. Potassium interchange in yeast cells. *Acta physiol. scandinav.* 2: 347, 1941.
20. Hoagland, D. R. and A. R. Davis. Further experiments on the absorption of ions by plants including observations on the effect of light. *J. Gen. Physiol.* 6: 47, 1923.
21. Lamanna, C. and J. R. Campbell. Surface activity as the cause of the anomalous behaviour of urethane as an inhibitor of yeast respiration. *J. Bacteriol.* 65: 596, 1953.
22. Ling, G. N. The role of phosphate in the maintenance of the resting potential and selective ionic accumulation in frog muscle cells in: *Phosphorous Metabolism, A Symposium on the*

Role of Phosphorous in Plants and Animals, edited by W. D. McElroy and B. Glass. Baltimore: John Hopkins Press, 1952. vol. 2, p. 748.

23. Loomis, W. F. and F. J. Lipmann. Reversible inhibition of the coupling between phosphorylation and oxidation. *J. Biol. Chem.* 173: 807, 1948.
24. Lundegardh, H. Spectroscopic evidence of the participation of the cytochrome—cytochrome oxidase system in the active transport of salts. *Arkiv. Kemi. Mineral. Geol.* 3: 69, 1951.
25. Maizels, M. Factors in the active transport of cations. *J. Physiol.* 112: 59, 1951.
26. Mudge, G. H. Electrolyte and water metabolism of rabbit kidney slices: effect of metabolic inhibitors. *Am. J. Physiol.* 167: 206, 1951.
27. Mudge, G. H. Electrolyte metabolism of rabbit-kidney slices: studies with radioactive potassium and sodium. *Am. J. Physiol.* 173: 511, 1953.
28. Osterhout, W. J. V. The accumulation of electrolytes. II. Suggestions as to the nature of accumulation in *Valonia. J. Gen. Physiol.* 14: 285, 1930.
29. Osterhout, W. J. V. and S. E. Kamerling. The accumulation of electrolytes. VIII. The accumulation of KCl in models. *J. Gen. Physiol.* 19: 167, 1935.
30. Osterhout, W. J. V. Some models of protoplasmic surfaces. *Cold Spring Harbor Symp. Quant. Biol.* 8: 51, 1940.
31. Ponder, E. Accumulation of potassium by human red cells. *J. Gen. Physiol.* 33: 745, 1950.
32. Raker, J. W., I. M. Taylor, J. M. Weller and A. B. Hastings. Rate of potassium exchange of the human erythrocyte. *J. Gen. Physiol.* 33: 691, 1950.
33. Roberts, R. B., I. Z. Roberts and D. B. Cowie. Potassium metabolism in *Escherichia coli*. II, metabolism in the presence of carbohydrates and their metabolic derivatives. *J. Cell. & Comp. Physiol.* 34: 259, 1949.
34. Rothenberg, M. A. Studies on permeability in relation to nerve function. II. Ionic movements across axonal membranes. *Biochim. et biophys. acta.* 4: 96, 1950.
35. Scott, G. T. and H. R. Hayward. Metabolic factors influencing the sodium and potassium distribution in *Ulva lactuca. J. Gen. Physiol.* 36: 659, 1953.
36. Scott, G. T. and H. R. Hayward. The influence of iodoacetate on the sodium and potassium content of *Ulva lactuca* and the prevention of its influence by light. *Science* 117: 719, 1953.
37. Scott, G. T. and H. R. Hayward. The influence of temperature and illumination on the exchange of potassium ion in *Ulva lactuca. Biochim. et biophys. acta.* 12: 401, 1953.
38. Scott, G. T. and H. R. Hayward. Evidence for the presence of separate mechanisms regulating potassium and sodium distribution in *Ulva lactuca. J. Gen. Physiol.* 37: 601, 1954.
39. Scott, G. T., M. Jacobson and M. E. Rice. The influence of glycolytic factors on the potassium and sodium content of *Saccharomyces cerevisiae. Arch. Biochem.* 30: 282, 1951.
40. Sheppard, C. W. New developments in potassium and cell physiology: 1940–1950. *Science* 114: 85, 1951.
41. Sheppard, C. W. and W. R. Martin. Cation exchange between cells and plasma of mammalian blood. I. Methods and application to potassium exchange in human blood. *J. Gen. Physiol.* 33: 703, 1950.
42. Steinbach, H. B. Permeability. *Ann. Rev. Physiol.* 13: 21, 1951.
43. Steinbach, H. B. On the sodium and potassium balance of isolated frog muscles. *Proc. Nat. Acad. Sc.* 38: 451, 1952.
44. Ussing, H. H. Transport of ions across cellular membranes. *Physiol. Rev.* 29: 127, 1949.
45. Warburg, O. Über die Geschwindigkeit der photochemischen Kohlensäurezersetzung in lebenden Zellen. *Biochem. Ztschr.* 103: 188, 1920.
46. Warburg, O. and W. Christian. Isolierung und Kristallisation des Proteins des oxydierenden Garungsferments. *Biochem. Ztschr.* 303: 40, 1940.

Contribution No. 650

BULLETIN OF THE GEOLOGICAL SOCIETY OF AMERICA
VOL. 66, PP. 203-228, 7 FIGS., 3 PLS. FEBRUARY 1955

TOPOGRAPHY OF THE CONTINENTAL SLOPE IN NORTHWEST GULF OF MEXICO

BY BETTY LEE GEALY

ABSTRACT

Topographic charts of the continental slope in the northwest Gulf of Mexico were constructed largely from soundings from unpublished hydrographic surveys of the U. S. Coast and Geodetic Survey. The configuration of the slope and the nature of its sediments suggest a genetic interpretation for its varied topography and high relief.

Twenty-one profiles show that the break in slope at the edge of the continental shelf is marked only by a gradual steepening. A hummocky zone on the upper part of the slope shows features resembling landslide scars and deposits, sediment-flow scars, and surface expressions of faults. These features indicate that the upper part of the slope is underlain by a mass of relatively unstable sediments, probably deposited during the Pleistocene when sea level was near the present 75-fathom curve.

Steep slopes and a lack of hummocks on the lower part of the slope indicate that most of the underlying sediments are relatively stable. Many steep-sided troughs cut this portion of the slope. Their position and configuration suggest a history which may involve (1) subaerial erosion, (2) submergence and tilting, (3) masking of the upper part of the slope by Pleistocene sediments, and (4) extensive modification by the failure of sediment under the stress of gravity.

The Sigsbee Scarp, at the base of the slope, is at least 340 miles long and as high as 4800 feet. It may represent one of a series of large faults surrounding the Gulf of Mexico and downthrown toward the Sigsbee Deep.

The Sigsbee Deep is a basin of gentle slopes and subdued relief extending from the base of the Sigsbee Scarp, at 1700 fathoms, to a maximum depth of about 2200 fathoms.

Although salt domes may underlie a number of features of low relief on and near the edge of the continental shelf, there is no evidence which indicates they have been an important geomorphic factor on the continental slope.

The topography and sediments suggest that in the northwest Gulf of Mexico there is a large mass of sediment under the stress of gravity and failing by landslides, faults, creep, sediment flows, and intermediate types of failure.

CONTENTS

TEXT

Page
Introduction 204
Acknowledgments 204
Construction of topographic charts 205
  Location and extent 205
  Sources of data 205
  Contouring technique 205
  Sources of error 207
    Positional control 207
    Depth control 207
    Frequency of observations 207
Topography 207
  Continental Shelf 207
  Sigsbee Deep 210
  Continental Slope 211
    General 211
    Sigsbee scarp 211
    Trough zone 211
    Hummocky zone 214
    Mississippi Trough 214
Origin of topography on continental slope 214
  General 214
  Crustal faulting 214
  Salt domes 215
  Subaerial erosion 215
    Topographic evidence of subaerial erosion 215
    Effects of Pleistocene lowering of sea level 215
    Submergence by downwarping 216
  Failure of sediment under stress of gravity 216
    General 216
    Sources of stress 217
    Sediments 217
    Types of failure 219
Conclusions 224
Appendix 226
References cited 226

ILLUSTRATIONS

Figure Page
1.—Map of Sigsbee Scarp.................. 206
2.—Profiles across break in slope (A–G)...... 208
3.—Profiles across break in slope (H–N)...... 209
4.—Profiles across break in slope (O–U)...... 210
5.—Fathograms across Sigsbee Scarp.... 212–213
6.—Sedimentary profile across continental shelf, continental slope, and into Sigsbee Deep.............................. 218
7.—Profiles across alignments resembling faults.............................. 221

Plate Facing page
1.—Submarine topography in the northwest quarter of the Gulf of Mexico, western part.............................. 203
2.—Submarine topography in the northwest quarter of the Gulf of Mexico, eastern part.............................. 214
3.—Physiographic features on the continental slope in the northwest Gulf of Mexico... 228

TABLE

Table Page
1.—Hydrographic surveys of U. S. Coast and Geodetic Survey used in preparing Plates 1 and 2........................ 205

Introduction

The topography of the continental slope in the northwest Gulf of Mexico has remained virtually unknown until recent years, and neither adequate topographic charts of the region nor accurate descriptions of the topography are available. In 1949 the writer began: (1) to compile and contour the most accurate soundings available in the region, (2) to study the factors which may have influenced the development of the topography on the continental slope, and (3) to seek a genetic interpretation of the topography.

The U. S. Coast and Geodetic Survey completed a series of hydrographic surveys in 1940 using echo-sounding devices and good positional control. A few of the data obtained on these surveys were published on U. S. Coast and Geodetic Survey Charts numbers 1116 (1943) and 1117 (1941) (scale approximately 1:500, 000). Random soundings taken from the hydrographic surveys are shown on these charts numerically, and 100-fathom curves are shown on the continental slope to a maximum depth of 500 fathoms. However, most of the data obtained on these surveys remains unpublished on file in the offices of the Survey in Washington, D. C. While mechanisms have been devised recently which permit even more precise depth and positional control than that obtained on these surveys, this region probably will not be resurveyed in detail with these new devices for many years. Echo-sounding records made since 1945 aboard the Research Vessel Atlantis of Woods Hole Oceanographic Institution and aboard surveying vessels of the Hydrographic Office of the U. S. Navy have provided additional unpublished soundings.

The continental slope has been found to have a varied topography of high relief which does not resemble the topography on the continental slopes of either the Atlantic or Pacific coast of North America. The topography, the agencies operating in the Gulf, and the sediments underlying the region suggest several working hypotheses concerning the origin of the topography.

Acknowledgments

The writer is grateful to Mr. H. C. Stetson for encouragement and advice throughout the preparation of the accompanying topographic charts and manuscript.

Woods Hole Oceanographic Institution has given financial assistance to the writer during the summers of 1949–1952, and has provided necessary equipment and paid expenses throughout the project.

The National Science Foundation has furnished financial assistance through a Predoctoral Fellowship for the academic year 1952–1953.

The writer is indebted to members of the U. S. Coast and Geodetic Survey for their enthusiastic co-operation in the preparation of the topographic charts. Copies of the original unpublished hydrographic surveys, on file in the offices of the Survey, as well as detailed information concerning the positional control of those surveys were made available to the writer. Members of the Survey spent much time discussing the problems and limitations of marine surveying and methods of compiling and correcting data. In addition, members read the section of the manuscript entitled "Construction of Topographic Charts" and offered a

number of helpful suggestions. Adm. L. O. Colbert, Adm. Robert W. Knox, Mr. H. R. Edmonston, Comdr. F. B. Quinn, and Mr. R. H. Carstens were especially helpful.

The Hydrographic Office of the U. S. Navy provided echo-sounding records taken in the northwest Gulf of Mexico prior to 1948. The U. S. Geological Survey provided a Salzman Projector which was used to reduce and compile base charts. Dr. W. H. Bradley and Mr. K. P. Cartrette were of particular assistance.

Dr. S. D. Wilson has read the portions of the manuscript dealing with the behavior of sediments under stress and has suggested revisions. Dr. M. P. Billings, Dr. Francis Birch, Dr. L. D. Leet, Dr. Charles E. Stearns, and Dr. P. D. Trask have read the manuscript and offered many helpful suggestions. Discussions with the late Mr. M. G. Cheney, Dr. H. N. Fisk, Dr. F. P. Shepard, and Adm. Paul A. Smith have helped the writer in the formation of ideas. Miss Jean Stilwell constructed the profiles used in Figures 2, 3, and 4.

CONSTRUCTION OF TOPOGRAPHIC CHARTS

Location and Extent

Topographic charts of the continental slope in the northwest Gulf of Mexico have been constructed (Pls. 1, 2). The contoured area is bounded on the north and west by the edge of the continental shelf at about the 75-fathom curve, on the south by the southern limit of the hydrographic surveys of the U. S. Coast and Geodetic Survey in the northwest Gulf of Mexico, and on the east by the Mississippi Trough southwest of the Southwest Pass of the Mississippi River. The area extends nearly 400 miles[1] from east to west and more than 75 miles from north to south. The shoreward margin of the contoured area is about 45 miles from the mouth of the Rio Grande, 120 miles from the mouth of the Sabine River, and 50 miles from shore west of Southwest Pass.

Sources of Data

Most soundings used in contouring the area were taken from original unpublished hydrographic surveys of the U. S. Coast and Geodetic Survey. Photostats or bromide copies of these surveys can be obtained at cost from the office of the Survey in Washington, D. C. by those interested in seeing the original material. The hydrographic surveys used in constructing the charts are given in Table 1. Copies of the hydrographic surveys were photographed on a common scale of 1:120,000 and were used as base maps for contouring.

TABLE 1.—HYDROGRAPHIC SURVEYS OF THE U. S. COAST AND GEODETIC SURVEY USED IN PREPARING PLATES 1 AND 2

Survey number	Original scale	Date of survey
H-5768	1:120,000	1934
H-6184	1:80,000	1936
H-6185	1:80,000	1936
H-6292	1:80,000	1937
H-6293	1:80,000	1937
H-6499-A	1:240,000	1939
H-6499-B	1:80,000	1939
H-6501	1:120,000	1939
H-6502	1:120,000	1940
H-6546	1:120,000	1940
H-6547	1:160,000	1940

In addition to the above soundings, echo-sounding records made aboard the Research Vessel ATLANTIS of Woods Hole Oceanographic Institution, and aboard surveying vessels of the Hydrographic Office of the U. S. Navy were available. However, as positional control is relatively poor for these records, the soundings from them were used only to validate the existence of large topographic features in areas not covered adequately by U. S. Coast and Geodetic Survey soundings. These records also were used to outline what the writer has termed the Sigsbee Scarp (Fig. 1).

Construction of the charts was completed in September 1950, and data acquired since then have not been incorporated.

Contouring Technique

The techniques and limitations of contouring submarine soundings have been discussed thoroughly by Veatch and Smith (1939), who state (p. 84), "In any approach, the fundamental problem is to fit a type of topography to the facts—the soundings," and (p. 83), "... the stream erosion type as delineated is, in the light of our present knowledge of the continental shelf, the most satisfactory topography possible." Thus, where soundings are scanty, Veatch and Smith have superimposed a detailed subaerial erosion pattern even where it is not indicated clearly.

---

[1] Throughout, the term miles refers to nautical miles.

On Plates 1 and 2 detailed topography is omitted except where soundings are dense. As a result, topographic features are drawn smoother and more regular than they probably are. Preconceived topographic types have been avoided as much as possible as the origin of some submarine topographic features is still under study, and charts like these are used in such studies. One disadvantage of this technique is that the topography appears to differ in complexity from place to place whereas this is due only to variation in concentrations of soundings.

Areas shoaler than 250 fathoms were contoured originally with a 5-fathom contour interval, and those deeper than 250 fathoms with a 25-fathom interval.

The separate base maps were compiled, re-

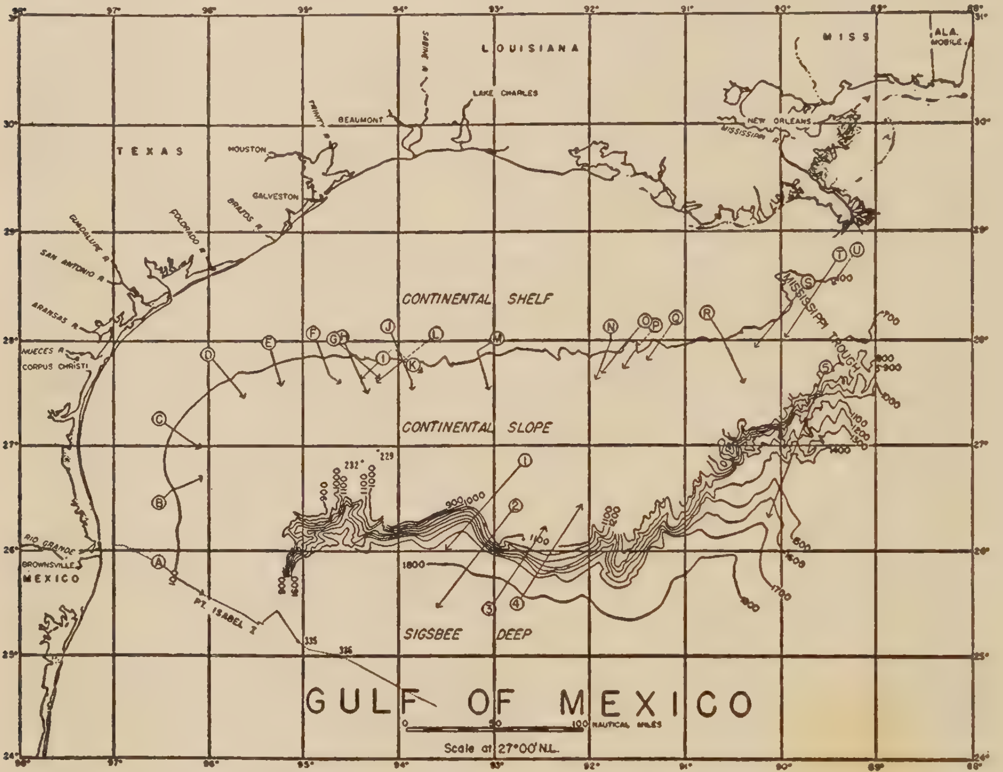
LOUISIANA
TEXAS
MISS
ALA.
MOBILE
MEXICO
LAKE CHARLES
BEAUMONT
HOUSTON
GALVESTON
NEW ORLEANS
MISSISSIPPI R.
SABINE R.
TRINITY R.
BRAZOS R.
COLORADO R.
GUADALUPE R.
SAN ANTONIO R.
ARANSAS R.
NUECES R.
CORPUS CHRISTI
RIO GRANDE
BROWNSVILLE
PT. ISABEL I.
CONTINENTAL SHELF
CONTINENTAL SLOPE
MISSISSIPPI TROUGH
SIGSBEE DEEP
GULF OF MEXICO
Scale at 27°00'N.L.
NAUTICAL MILES
0
50
100
1800
335
336
229
232
98°
97°
96°
95°
94°
93°
92°
91°
90°
89°
88°
31°
30°
29°
28°
27°
26°
25°
24°

FIGURE 1.—MAP OF SIGSBEE SCARP

Depths in Fathoms. Contour interval 100 fathoms.

Location and extent of Sigsbee Scarp indicated by contour lines from 700 fathoms to 1800 fathoms.

Lines *A* through *U* are locations of profiles across break in slope shown on Figures 2, 3, and 4. Arrows point to right end of profiles. Sources of echo-sounding records used in constructing profiles given in Appendix 1. Dotted portions taken from Plates 1 and 2.

Lines *1* through *5* are locations of echo-sounding records' crossing Sigsbee Scarp shown on Figure 5. Arrows point to right end of echo-sounding records.

Dotted line shows location of Port Isabel I. sedimentary profile shown on Figure 6. Traverse made by ATLANTIS in 1947.

Long cores 335 and 336 were taken by ATLANTIS in 1947 and include a sand. Cores 229 and 232 taken in submarine trough by ATLANTIS in 1951.

duced, and transferred onto a Mercator Projection with a scale of 1:250,000 at 27°30′ N. Lat. A contour interval of 25 fathoms was used throughout. This single chart was then reduced 50 per cent and reproduced as Plates 1 and 2.

Sources of Error

Positional control.—Positional control on the hydrographic surveys of the U. S. Coast and Geodetic Survey on the continental shelf is excellent. Sono-radio buoys were used, and the precise distances between buoys was established in many cases by taut-wire surveys. On charts having a scale of 1:500,000 (Pls. 1, 2), no error should be evident.

Positional control on the continental slope is less accurate. Sono-radio buoys were established on shoals at about the 75-fathom curve, and, under the most favorable conditions, positions accurate to one part in 200 can be obtained up to 100 miles from the buoys. Beyond the range of the buoys, lines were fixed only by dead reckoning and celestial navigation.

Crossings of sounding lines are checks on the positional control, and some sounding lines were adjusted slightly to make the soundings at the crossings match. Even on the deepest part of the continental slope mapped, the maximum error in the position of a sounding probably is no greater than 1 mile. Throughout most of the map, the error is less than half a mile which is small for marine navigation.

Depth control.—The U. S. Coast and Geodetic Survey soundings were taken with visually read echo soundings which in some cases are less reliable than those automatically recorded, but which are infinitely more accurate than the older wire soundings. These soundings were corrected for temperature, salinity, and pressure, but no corrections for the slope of the ocean bottom were made. It can be assumed that all slopes are slightly steeper and that all valleys are somewhat deeper than indicated on the charts, although, at the published scale, these errors should be small.

Frequency of observations.—As time must be allowed for the return of the echo, fewer soundings per minute can be taken in deep water than in shallow. Thus, assuming the speed of the ship is 12 knots, and the speed of sound in water is 800 fathoms per second, a maximum of 1200 soundings per mile can be recorded at 100 fathoms, 120 soundings per mile at 1000 fathoms, and 60 soundings per mile at 2000 fathoms. However, as these soundings had to be read visually, only about 6 soundings per mile were recorded at 100 fathoms, and 2 soundings per mile between 1000 and 2000 fathoms. From the point of view of the cartographer it is regrettable that most sounding lines are perpendicular to the edge of the continental shelf and that few are parallel to the edge of the shelf. This plan has influenced the accuracy of the contour lines considerably and, in some cases, has been the sole reason for placing an area in the third category of accuracy (Pls. 1, 2).

On the continental shelf, the sounding lines are 2–5 miles apart and on deeper parts of the continental slope the lines are 5–10 miles apart.

TOPOGRAPHY

Continental Shelf

The continental shelf (Fig. 1) in the northwest Gulf of Mexico extends from shore to the break in slope at a depth of about 75 fathoms. Off the mouth of the Rio Grande the shelf is about 45 miles wide and has an average gradient of about 2 fathoms per mile (1:500); at 93° 30′ W. Long. it is 120 miles wide and has an average gradient of less than 1 fathom per mile (1:1000). West of the Mississippi Trough (Fig. 1) the shelf is about 60 miles wide and has an average gradient of about 1.5 fathoms per mile (1:700). Topographic irregularities on the shelf have a relief of only a few feet or tens of feet, whereas those on the continental slope have a relief of hundreds or thousands of feet.

The break in slope at the edge of the continental shelf must be chosen arbitrarily as it is marked only by a gradual increase in gradient in most areas. In some cases topographic irregularities, such as bioherms, further obscure the break. Profiles have been made from the available echo-sounding records that cross the 100-fathom curve at nearly right angles. The profiles are shown on Figures 2, 3, and 4, and the locations of the profiles on Figure 1. The "abrupt shelf-break" in the northwest

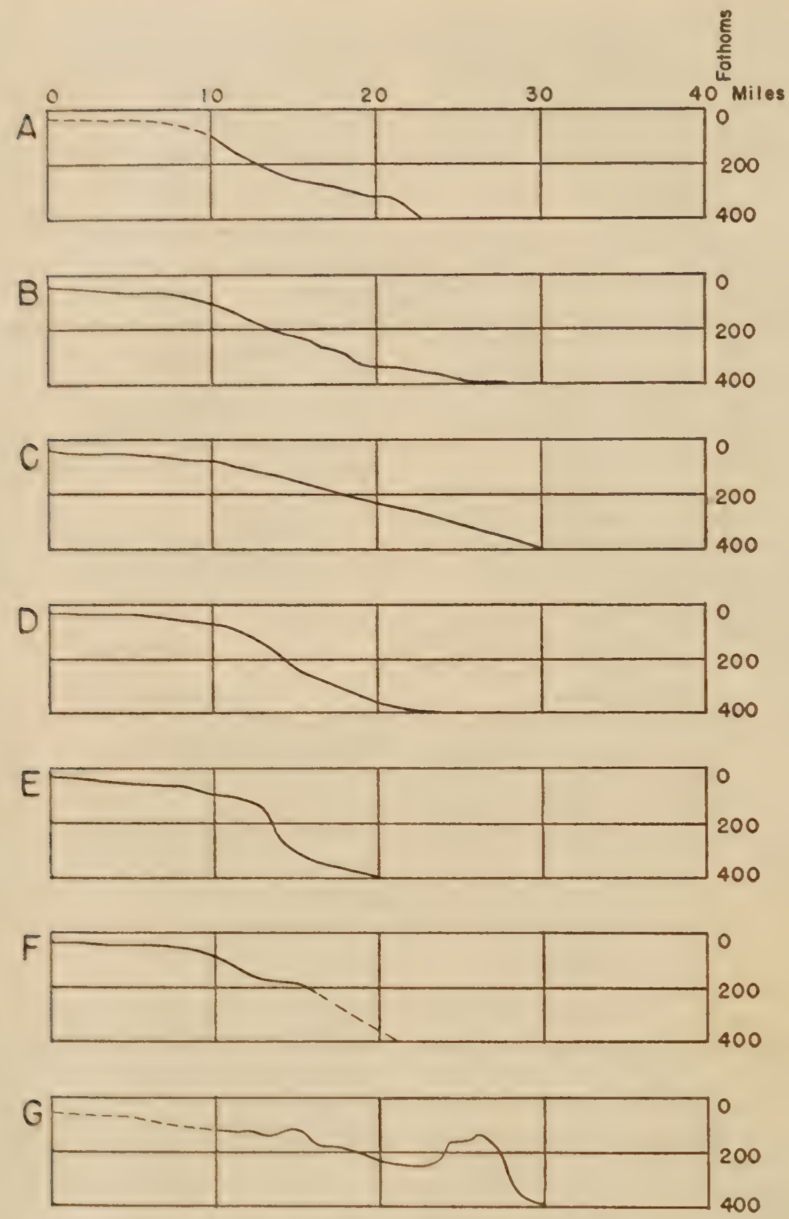

FIGURE 2.—PROFILES ACROSS BREAK IN SLOPE (A–G)

Locations shown on Figure 1. Solid portions of profiles taken from fathograms. Dotted portions taken from Plates 1 and 2. Sources of fathograms given in Appendix I. Vertical exaggeration × 17.

Gulf of Mexico described by Dietz and Menard (1951) and Dietz (1952, p. 1815) is evident on few of these profiles, even at the great vertical exaggeration of × 17.

If the break in slope is assumed to be a line along which the gradient increases to 10 fathoms per mile, the line is variable in depth. Off the mouth of the Rio Grande south of 26°40′ N. Lat. and in the vicinity of the Mississippi Trough, the line is at a depth of about 50 fathoms. Throughout most of the rest of the contoured area, it is near the 75-fathom curve

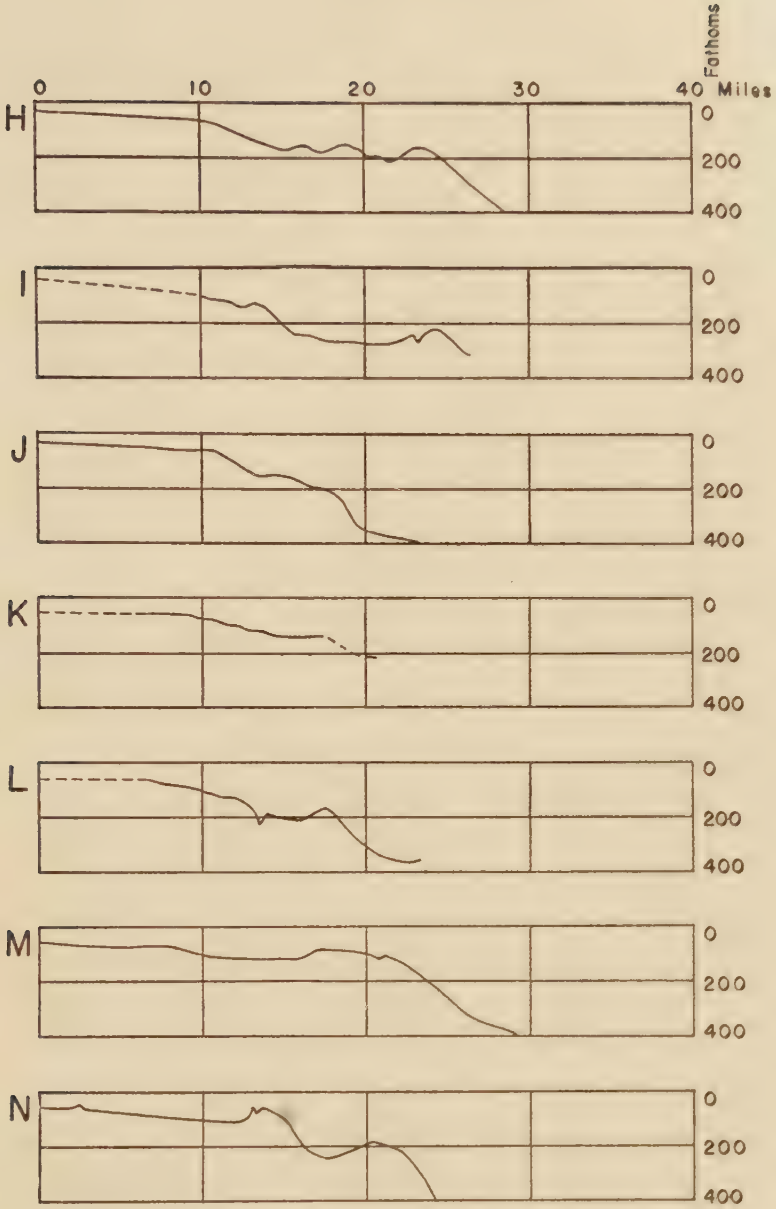

FIGURE 3.—PROFILES ACROSS BREAK IN SLOPE (H–N)

Locations shown on Figure 1. Solid portions of profiles taken from fathograms. Dotted portions taken from Plates 1 and 2. Sources of fathograms given in Appendix I. Vertical exaggeration × 17.

although locally it is deeper than 100 fathoms.

Many bioherms, described by Stetson (1953), rise to within a few fathoms of the surface near the break in slope between 90°00′ W.Long. and 95°00′ W.Long. The flat tops of the bioherms are covered with living corals and calcareous algae, and their steep flanks are covered with calcareous debris which grades into the surrounding fine-grained clastics. Many of these bioherms can be seen on Plates 1 and 2, and more would be indicated if a smaller contour interval had been used.

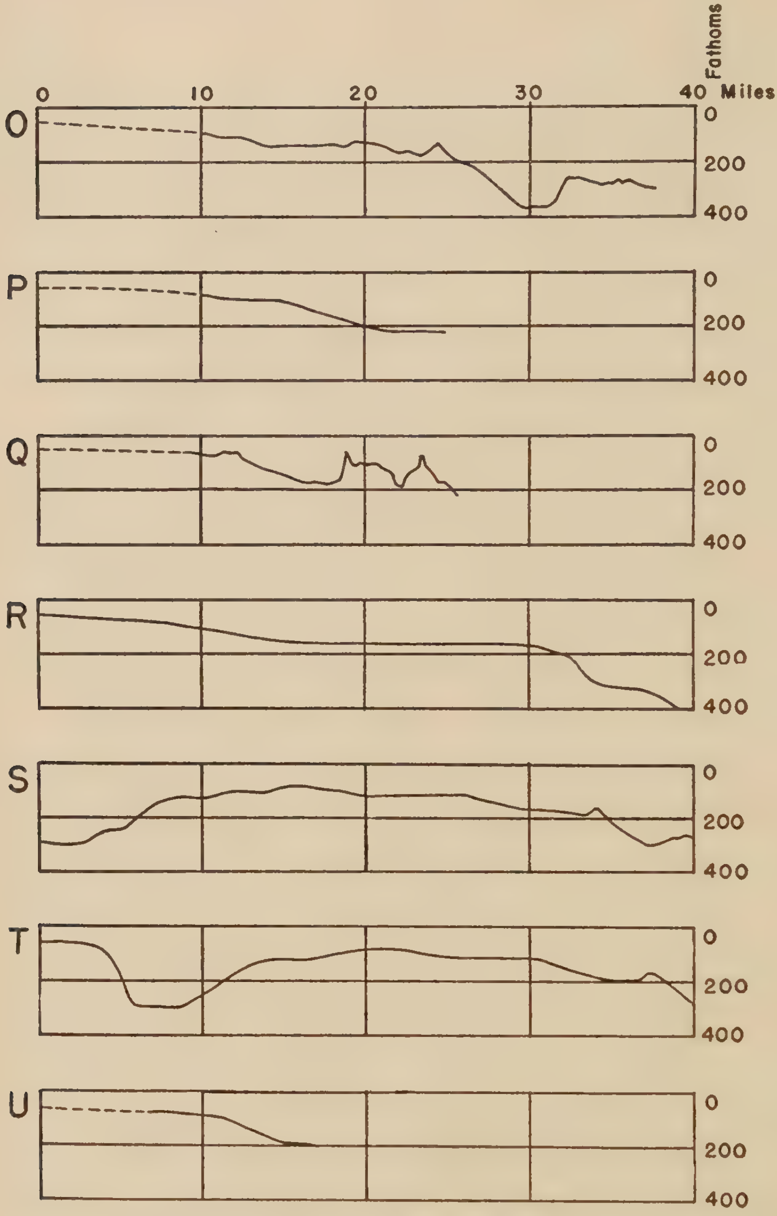

Figure 4.—Profiles Across Break in Slope (O–U)

Locations shown on Figure 1. Solid portions of profiles taken from fathograms. Dotted portions taken from Plates 1 and 2. Sources of fathograms given in Appendix I. Vertical exaggeration × 17.

Sigsbee Deep

The Sigsbee Deep (Fig. 1) is a basin in the western Gulf of Mexico which extends from the base of the continental slope at about 1700 fathoms to a maximum depth of about 2200 fathoms. The basin has not been surveyed in detail, but available information indicates that slopes are gentle and relief subdued.

Continental Slope

General.—The continental slope (Fig. 1) in the northwest Gulf or Mexico extends from the edge of the continental shelf to the edge of the Sigsbee Deep. Between the 75- and 1700-fathom curves the slope is about 70 miles wide off the mouth of the Rio Grande, 135 miles wide at 92°00′ W.Long., and 70 miles wide west of the Mississippi Trough. The average gradient of the slope ranges between about 12 and 25 fathoms per mile, but these figures are not significant because of the varied topography of high relief on the continental slope. Locally, gradients exceed 500 fathoms per mile. The continental slope can be divided into four parts: (1) the Sigsbee Scarp, (2) the Trough Zone, (3) the Hummocky Zone, and (4) the Mississippi Trough.

Sigsbee Scarp.—An abrupt scarp, which the writer has termed the Sigsbee Scarp, is at the base of the continental slope (Fig. 1). The curves on the scarp were made from echo-sounding records taken by the Research Vessel ATLANTIS and surveying vessels of the Hydrographic Office of the U. S. Navy (Fig. 5). As positional control was relatively poor, the location is only approximate, and it can be assumed that topographic details are inaccurate. For instance, a greater concentration of lines of soundings permits more topographic detail to be shown northeast of 90°30′ W.Long. than between 93°00′ W.Long. and 94°00′ W.Long., although there is no evidence indicating smoother topography in either area. Also, it can be assumed that the scarp is steeper than shown.

The scarp is shown on Plate 1 between 95°10′ W.Long. and 94°10′ W.Long. at the lower edge of the contoured area; it is incised by a submarine trough at 94°30′. The scarp is shown also on Plate 2 trending northeast from the lower edge of the contoured area at 90°30′ W.Long. until it disappears at its junction with the Mississippi Trough.

The Sigsbee Scarp is comparable in size and relief to the fault scarp on the west side of the Wasatch Range, Utah, although the Wasatch Scarp is only about half as long as the Sigsbee Scarp.[2] That part of the Sigsbee Scarp shown on Figure 1 is more than 340 miles long, and it extends an unknown distance south off the east coast of Mexico. The scarp trends east from 95°10′ W.Long. to 91°40′ W.Long. where it turns abruptly northeast. It is 4800 feet high and has an average gradient of at least 200 fathoms per mile (1:5) at its western end. It decreases both in height and steepness to the east. The scarp is incised in places by troughs.

Another abrupt scarp about 350 miles long and trending roughly northwest occurs in the east Gulf of Mexico off the coast of Florida. The northwestern 150 miles of the scarp has been mapped and described by Jordan (1951); he found that it was about 7200 feet high and had an average gradient of about 500 fathoms per mile at 27°30′ N.Lat. and 85°30′ W.Long. The northwesternmost part forms the east flank of the lower part of the DeSoto Canyon, 125 miles east of the Mississippi Trough and beyond the limits of Figure 1. Between the DeSoto Canyon and the Mississippi Trough the continental slope trends northeast paralleling the strike of the easternmost part of the Sigsbee Scarp. The continental slope in this area has gentler gradients than those found on the Sigsbee Scarp, but they are steeper than the average gradient of the continental slope in the northwestern Gulf. The steepest slope in the area is about 60 fathoms per mile (1:17). The area is not considered part of the Sigsbee Scarp although it may be an extension of the same structure. Near the lower part of the DeSoto Canyon, the Florida Scarp turns north and intersects this northeast extension of the Sigsbee Scarp trend at about 60°.

Trough zone.—Above the Sigsbee Scarp a zone about 50 miles wide extends the length of the continental slope (shown in part on Pls. 1, 2). The zone consists of a surface of relatively low relief, typically illustrated in the area about

---

[2] Information concerning the Wasatch Range was taken from U. S. Geological Survey topographic sheets of the Timpanagos Cave, Orem, Aspen Grove, and Bridal Veil Falls quadrangles, Utah. The Wasatch Range is about 150 miles long and 7000 feet high from the base of the range at 5000 feet above sea level to the highest peaks at about 12,000 feet high. Average gradients on the scarp are as high as 3200 feet per mile but average less than 2300 feet per mile.

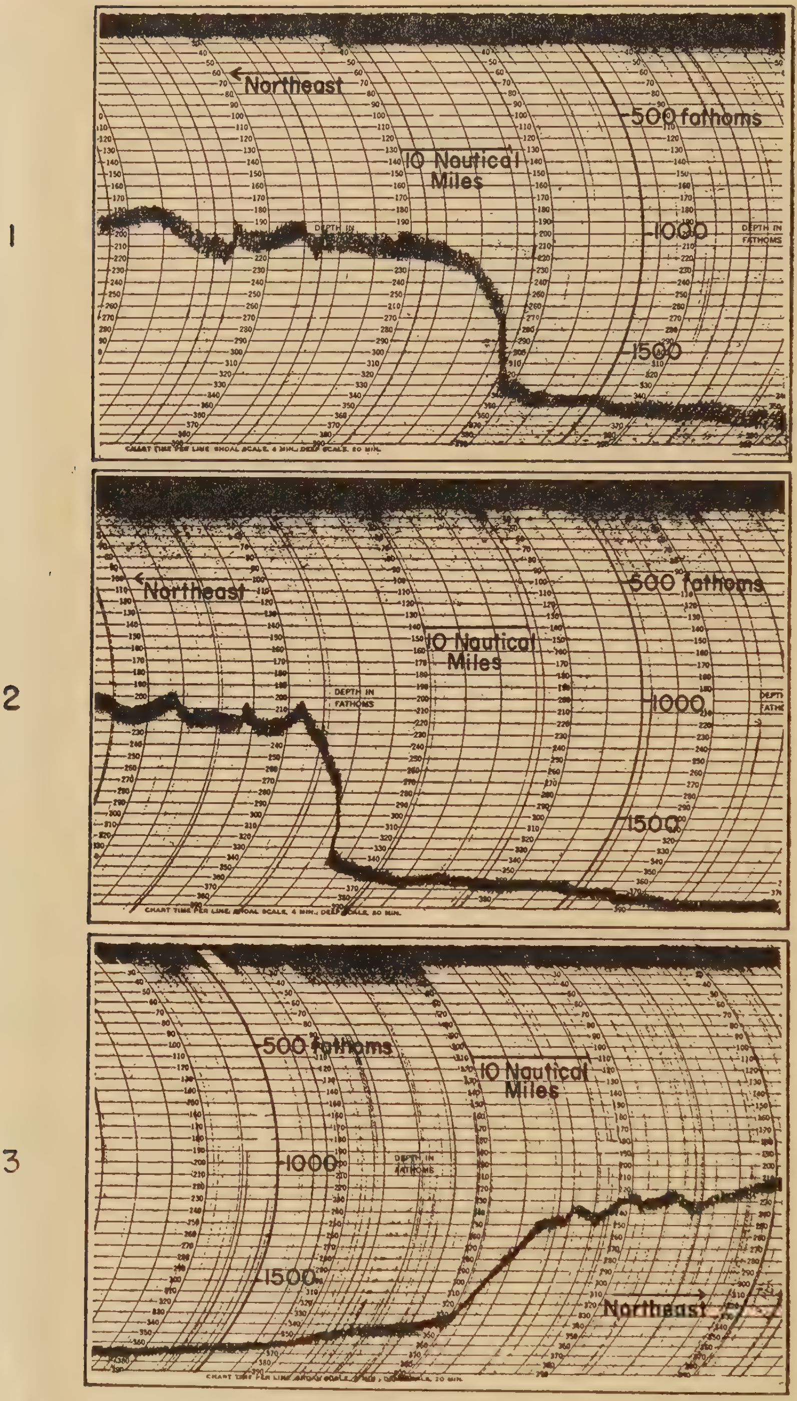
1
2
3
Northeast
500 fathoms
10 Nautical Miles
1000
1500
DEPTH IN FATHOMS
CHART TIME PER LINE SHOAL SCALE 4 MIN., DEEP SCALE 20 MIN.

FIGURE 5 (1–3)

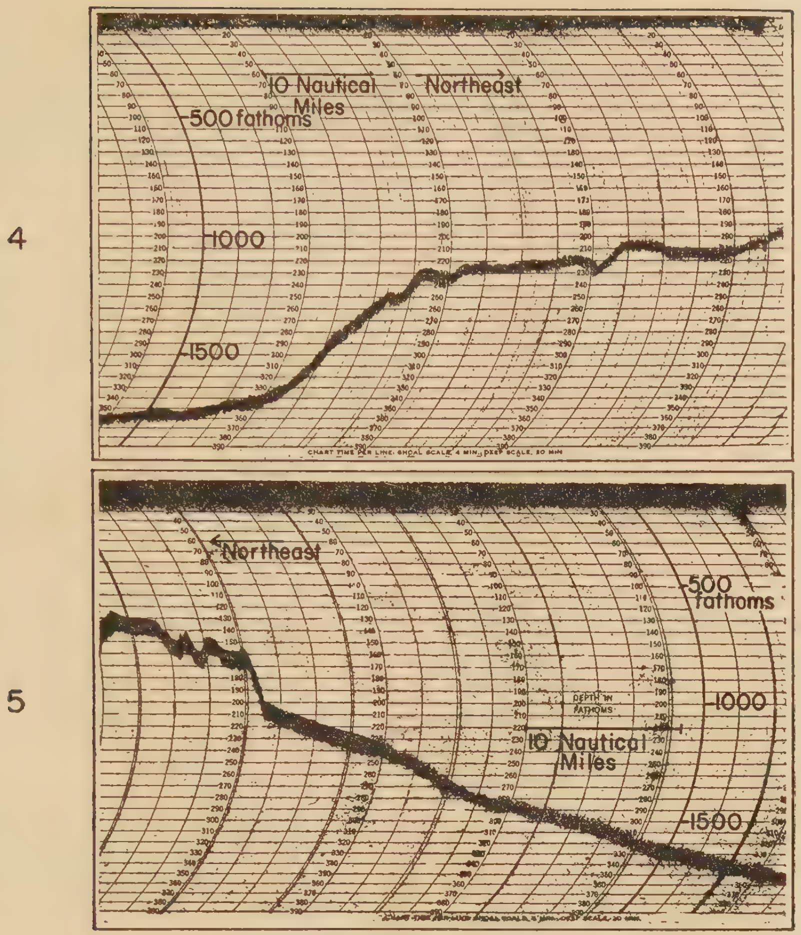

FIGURE 5 (4–5)

FIGURE 5.—FATHOGRAMS ACROSS SIGSBEE SCARP

Locations of profiles shown on Figure 1. All fathograms taken by surveying vessels of Hydrographic Office, U. S. Navy. (Vertical exaggeration = × 20 approximately)

(1) March 3, 1949; Book 91, Roll 37. Approximate position of base of scarp: 26° 11′ N. Lat., 93° 20′ W. Long.

(2) March 3, 1949; Book 85, Roll 30. Approximate position of base of scarp: 26° 01′ N. Lat., 93° 08′ W. Long.

(3) February 15–16, 1949; Book 61–62, Roll 24. Approximate position of base of scarp: 25° 53′ N. Lat., 92° 44′ W. Long.

(4) November 23, 1947; Book 53, Roll 30. Approximate position of base of scarp: 25° 45′ N. Lat., 92° 37′ W. Long.

(5) April 3–4, 1947; Book 16, Roll 20. Approximate position of base of scarp: 27° 27′ N. Lat., 89° 38′ W. Long.

95°10′ W.Long., 26°40′ N.Lat., and into which are cut many deep steep-sided troughs. These troughs extend down the slope and into the Sigsbee Deep and cut across the Sigsbee Scarp.

One complete trough is shown on Plate 2 at 94°20′ W.Long. In March 1951 a resurvey by the Research Vessel ATLANTIS corroborated the existence of the trough although additional data indicate that the location and shape indicated here are somewhat inaccurate. It is evident, however, that the trough is about 80 miles long, 3000 feet deep, and about 5 miles wide from rim to rim. The walls have average gradients of at least 3000 feet per mile (1:2), and locally some of the slopes may be nearly vertical. The trough is comparable to Yosemite Valley, California, in both size and shape.[3] The heads of other troughs are shown at the southern edge of the contoured area east of this trough (Pls. 1, 2). Fathograms taken by the Research Vessel ATLANTIS and surveying vessels of the Hydrographic Office show a number of troughs in the unsurveyed area north of the Sigsbee Scarp. Presumably these troughs join the heads shown on Plates 1 and 2. More closely spaced soundings with better positional control are necessary to determine their exact shape, size, and location. However, available information suggests that some are more than 3000 feet deep and that the slopes of their sides may exceed 3000 feet per mile (1:2). Some of the troughs have nearly flat bottoms such as the one at 91°00′ W.Long. at the southern edge of the contoured area on Plate 2; some are V-shaped such as the one that trends north-northwest from the southern edge of the contoured area at 92°20′ W.Long. (Pl. 2). From available soundings, many troughs cannot be contoured without depressions, the deepest being 1500 feet. The presence of depressions in submarine troughs is not uncommon, but proof of the existence of any of this magnitude must await further data.

Hummocky zone.—Between the break in slope at about the 75-fathom curve and the zone with troughs is a hummocky zone dominated by small hills and closed depressions, many of which are in areas of closely spaced soundings and excellent positional control. Although some troughs extend into this zone, they are not so plentiful or so striking. Two types of topographic patterns may be present in this zone:

Several topographic alignments are shown on Plate 3, and profiles across them are shown on Figure 7. Some depressions appear to be aligned with the troughs below them. Possibly the troughs formerly extended into the upper part of the slope and have been filled partially and irregularly by masses of sediment.

Mississippi Trough.—The Mississippi Trough (Pl. 2) cuts into the continental shelf and extends across the other three zones of the slope. It is about 20 miles wide and 1800 feet deep where it cuts across the break in slope at the edge of the continental shelf. The trough widens considerably in deeper water.

ORIGIN OF TOPOGRAPHY ON CONTINENTAL SLOPE

General

The topography on the continental slope of the northwest Gulf of Mexico may have been developed by crustal faulting, salt domes, subaerial erosion, and the failure of sediment under the stress of gravity.

Crustal Faulting

The Sigsbee Deep is bounded by scarps of such great extent and relief that only large crustal faults can explain them. The term "crustal fault" is used in contrast to smaller faults in sediments on the continental slope. The Florida Scarp off the west coast of Florida is about 350 miles long and at least 7200 feet high (Jordan, 1951). The Florida Straits are bounded by abrupt scarps probably formed by large normal faults (Pressler, 1947). The north and west sides of the Campeche Bank are bounded by scarps up to 8000 feet high (U. S. Coast and Geodetic Survey Chart No. 1007, Gulf of Mexico, 1927). The Sigsbee Scarp may represent a fault downthrown toward the Sigsbee Deep. In the northwest Gulf of Mexico the height of the continental slope may be increasing owing to continued movement of this fault.

---

[3] Information concerning Yosemite Valley was taken from the U. S. Geological Survey Topographic map of Yosemite, California, 1938 edition. Yosemite Valley is about 2 miles wide from rim to rim and 2500 to 3500 feet deep. The valley floor is about three quarters of a mile wide. The walls of the valley are locally vertical, but average gradients range from 3000 to 8000 feet per mile.

As the height of the Sigsbee Scarp is greater toward its western end, the throw of the fault may diminish progressively eastward. The fault may merge with a flexure between the Mississippi Trough (Fig. 1) and the DeSoto Canyon, 125 miles east of the Trough. However, because of the proximity of the Mississippi River, sedimentation may be more rapid on the eastern end of the scarp and the scarp partially masked by sediment. Two small troughs that cross the Sigsbee Scarp at 89°50′ W.Long. and 90°25′ W.Long. resemble hanging valleys. If they are hanging valleys, at least part of the faulting may postdate the cutting of the troughs. Otherwise, they may have been cut by an agency that does not necessarily produce accordant junctions.

The lower part of the DeSoto Canyon appears to have been formed by the junction of two major structural trends: the steep continental slope northeast of the Mississippi Trough, and the northern end of the Florida Scarp.

Salt Domes

There are a number of topographic features of very low relief on the continental shelf (R. A. Geyer, personal communication) which may indicate underlying salt domes. The features are roughly oval or circular and have diameters of a few miles to less than a mile. Also, the bioherms at the edge of the continental shelf may overlie other domes.

On the continental slope salt domes may have influenced some of the topography but there is no evidence that they have been an important geomorphic factor. The great size, high relief, and topographic form of most of the major features indicate that they were formed primarily by faulting, the failure of sediment under the stress of gravity, and, possibly, subaerial erosion.

Subaerial Erosion

Topographic evidence of subaerial erosion.—To test the theory of the subaerial erosion of the topography on the continental slope of the northwest Gulf of Mexico, Plate 3 was constructed showing "streams" in the valley bottoms and depressions filled with "lakes." The depths of the depressions from the sill depth to the deepest point are shown to the nearest 25 fathoms. This "stream-lake" pattern is used only as an aid in analyzing the topography and it is not presumed that streams and lakes ever existed on this surface as indicated.

Throughout most of the region troughs can be joined and tend to merge downhill as do subaerial valleys. In some areas, such as west of 94°30′ W. Long., the stream pattern is dendritic and resembles some subaerial stream erosion patterns. In other areas, such as between 94°00′ W. Long. and 93°00′ W. Long., the pattern suggests structural control.

Major streams shown by the technique have gradients of tens or hundreds of feet per mile. Most subaerial valleys of comparable size have gradients of a few inches or feet per mile. If these submarine troughs are the result of subaerial erosion their gradients must have been increased by: (1) a rate of sedimentation greater on the upper part of the continental slope than on the lower part, (2) tilting of the whole continental slope toward the Sigsbee Deep, (3) faulting, landslides, and folding producing local high gradients, and/or (4) submarine erosion.

Some of the submarine troughs contain depressions 250 fathoms deep, considerably deeper than depressions in most subaerial stream valleys. However, these submarine depressions can be explained by the unequal filling of pre-existing troughs or by large-scale faulting or folding.

Effects of Pleistocene lowering of sea level.—Authorities estimate that, during the maximum extent of glaciers during the Pleistocene, sea level was lowered from about 350 to 400 feet less an uncalculated amount attributable to isostatic adjustment (Flint, 1947, p. 437). Fisk (1944) has concluded, largely on the basis of the buried trenches of Pleistocene rivers on the Gulf Coastal Plain, that sea level was lowered about 450 feet. If sea level were lowered 450 feet, the shore line would have been near the present 75-fathom curve.

That Pleistocene rivers cut valleys on the continental shelf is implied by the fact that all the rivers entering the northwest Gulf of Mexico except the Rio Grande and Mississippi have estuaries, and by the fact that an entrenched Pleistocene Mississippi valley system is buried beneath Recent sediments (Fisk, 1944). However, the Mississippi Trough is the only topographic evidence of such valleys. Fisk (1944) finds that the bottom of the Late Wisconsin Mississippi Valley is between 400 and 450 feet below sea level in areas that show no evidence of recent warping or faulting. The valley is filled with sediment; the lower layers are gravel, and the upper levels finer material. Seismic surveys show that this valley continues offshore and trends in the direction of the Mississippi Trough (Carsey, 1950, p. 372).

The obvious conclusion is that the Mississippi Trough was cut by subaerial erosion during the Pleistocene when sea level was lowered. However, the present Mississippi Trough cuts the edge of the continental shelf to a depth of about 1800 feet, and it can be traced across the continental slope to at least the 1000-fathom curve. If sea level were lowered only 450 feet, the depth and extent of the trough implies either that the trough and buried valley system were eroded during lowered sea level of the Pleistocene or earlier and that the slope has been downwarped subsequently, or that at least that part of the Trough deeper than 75 fathoms was cut by submarine erosion.

Some indentations in the 100-fathom contour, such as those at 93°30′ W.Long., 92°18′ W. Long., and 91°35′ W.Long., may be related to other river valleys which crossed the continental shelf during lowered sea level of the Pleistocene but which subsequently have been filled with sediment.

During Pleistocene lowering of sea level great quantities of sediment would have been deposited near the edge of the continental shelf from: (1) material eroded from the continental shelf, (2) material removed when Pleistocene river valleys on the Gulf Coastal Plain were deepened, and (3) material normally transported by those rivers. Deposits of this material may be thick on the upper part of the continental slope, and the hummocky zone may be the surface of those deposits. These sediments should be thinner on the lower part of the continental slope and in the Sigsbee Deep. They should consist of weak unconsolidated and semiconsolidated material which would tend to move down the continental slope. Also, the mass should increase the gradient of the whole continental slope and make the slope less stable.

Submergence by downwarping.—The northwest Gulf of Mexico and the adjacent Coastal Plain are tectonically unstable. Nettleton (1952) reports about 40,000 feet of upper Jurassic and post-Jurassic sediments at the coast line. Wells drilled near the edge of the continental shelf have penetrated 16,000+ feet of upper Cenozoic sediment with shallow-water characteristics (Fisk, 1953). Near the Mississippi delta, Quaternary depoits are about 4000 feet thick, and post-Wisconsin sediments are more than 600 feet thick (Fisk, 1944). This indicates subsidence throughout the Cenozoic.

Geophysical and geological data are too meager to indicate the location, nature, or even the existence of the southern limb of the proposed Gulf Coast geosyncline. Well control in all cases is limited to on-shore and near-shore areas and to depths of less than 20,000 feet. Fisk (1953) has presented subsurface information indicating seaward thinning of several major stratigraphic units; he concludes that the axis of a geosyncline lies south of Houston, Texas, and near New Orleans, Louisiana. He claims that gravity relationships support this. Nettleton (1952) concludes from geophysical evidence that the regional dip of the basement underlying upper Jurassic and post-Jurassic sediments extends to the coast line without any indications of a synclinal axis at or immediately beyond the coast. At present it is not conclusive that the rate of post-Jurassic downwarp has been either greater or less under the continental slope than under the shore line.

Available evidence does not preclude that the continental slope could have subsided from above sea level to its present depth during the Cenozoic; much of the subsidence could have taken place during the Quaternary. The rate of subsidence could have been greater on the lower part of the continental slope, thus causing tilting toward the Sigsbee Deep. Irregular subsidence could have contributed to the irregularity of the topography on the continental slope.

Failure of Sediment under Stress of Gravity

General.—Under the northwest Gulf of Mexico a large, thick mass of unstable sediment is under shearing stress. There is evidence in the topography and sediments that the continental slope in this region is being modified by the failure of these sediments under stress.

The discussion of the behavior of sediments is based largely on literature in soil mechanics (Baver, 1948; Terzaghi and Peck, 1948; Knight, 1948). In addition, S. D. Wilson of the Division of Applied Science, Harvard University, has offered many suggestions.

Throughout the discussion the terms sand, silt, and clay refer only to size. The Wentworth grade scale is used where the term sand includes sediment with median diameters between 1 and $\frac{1}{16}$ mm, silt between $\frac{1}{16}$ and $\frac{1}{256}$ mm, and clay less than $\frac{1}{256}$ mm. "Clay minerals" refer to members of the illite, montmorillonite, kaolinite, and other hydrous silicate groups which are abundant in most clays and do not refer to grain size. This usage contrasts with that in the field of soil mechanics where all sediments consisting largely of clay minerals and possessing plasticity would be termed clay regardless of their grain size. Sediments with median diameters of clay would be called silt if they did not exhibit such plasticity, as their behavior under stress would correspond to that of silt.

Sources of stress.—Shearing stresses on the sediments under the northwest Gulf of Mexico result from several conditions: (1) An accumulation of sediment of uniform thickness on the continental shelf and slope, and on the floor of the Sigsbee Deep will tend both to increase the shearing stresses on the sediment and to consolidate and increase the shearing resistance of the underlying sediment. If consolidation does not take place before the shearing resistance is exceeded by the shearing stresses, the material will fail. (2) Sedimentation is probably not uniform over the whole area but is greater on the continental shelf and the upper part of the slope. This will increase the gradient of the continental slope and increase shearing stresses on the underlying sediment even more than an accumulation of uniform thickness. (3) The height of the continental slope is probably being increased by continued movement along a fault represented by the Sigsbee Scarp. As the height is increased, shearing stresses on the underlying material are increased. (4) Continued downwarping of the lower part of the continental slope may be increasing the angle of the slope. (5) While strong older sediments underlying the continental slope may maintain slopes of a given height and gradient, weak younger sediment being deposited on that slope may fail after reaching a critical thickness.

Sediments.—The sediments underlying the northwest Gulf of Mexico may be the largest mass of unstable sediment in the world. As the behavior of this sediment under shearing stress depends on the type of material involved, a summary of information concerning the sediments follows.

SURFACE AND NEAR-SURFACE SEDIMENTS: Recent surface and near-surface sediments, on the whole, are fine-grained, have low sorting coefficients and high water contents, and are unconsolidated. The upper 3 meters has been sampled during two cruises of the Research Vessel ATLANTIS of Woods Hole Oceanographic Institution. A reconnaissance survey of sedimentary conditions in the region was made in 1947 (Phleger, 1951a; Stetson, 1953; Trask, 1953). A critical area on the continental slope was surveyed in detail in 1951, and the data are being studied by the writer.

From 550 surface samples of sediment taken on the 1947 cruise of the ATLANTIS, Stetson (1953) has found that the continental shelf and slope in the northwest Gulf of Mexico is covered with silts, sands, and clays (Fig. 6). On the shelf, median diameters and the sorting coefficients of the sediments vary considerably. Sands as coarse as 0.1 mm are found in water as deep as 100 fathoms, and some clays are found in very shallow water. Below the 100-fathom curve the sediments are more uniformly distributed and consist of a fine, well-sorted clay (average median diameter: 0.0012 mm; average Trask sorting coefficient: 2.9).[4]

The 100 3-meter cores taken on the 1947 cruise of the ATLANTIS are being studied by H. C. Stetson, and the 15 3-meter cores taken on the 1951 cruise are being studied by the writer. Most of these cores can be correlated and show an upper zone of brown clay 5-60 cm thick with abundant globigerina. Beneath this clay is a mottled gray clay with some color banding. At a depth of 2 m the clay has a porosity greater than 30 per cent and as great as 70 per cent in some places. Mrs. Constance F. Klebba determined the water contents, and the writer converted them to approximate porosities. This sequence accumulated by normal particle sedimentation.

---

[4] The Trask sorting coefficient is based on the ratio between the first and third quartiles: So = $\sqrt{Q_1/Q_3}$ where 75 per cent by weight of the sample consists of particles with diameters smaller than Q_1 and 25 per cent consists of particles smaller than Q_3 (Krumbein and Pettijohn, 1938, p. 230).

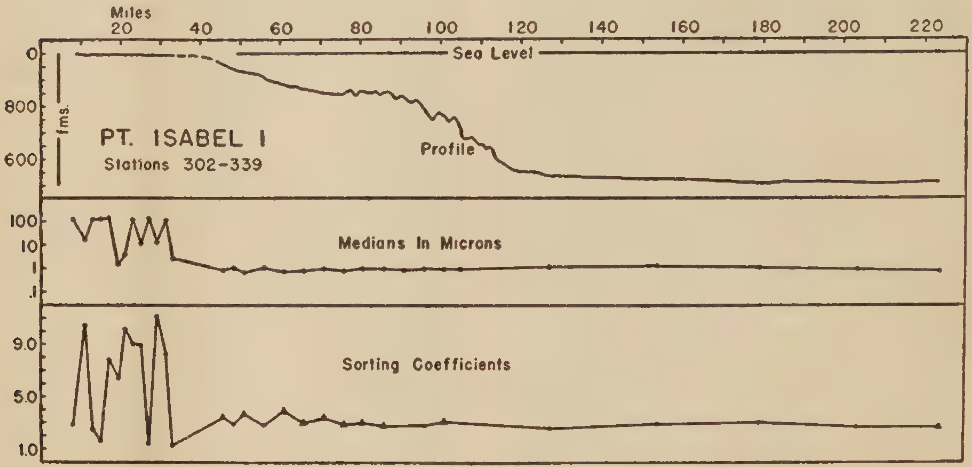

Figure 6.—Sedimentary Profile Across Continental Shelf, Continental Slope, and into Sigsbee Deep

Traverse was made by Atlantis in 1951. Sedimentary analyses made by H. C. Stetson (1953). Location of profile shown on Figure 1. Vertical exaggeration on topographic profile × 17. (After H. C. Stetson)

SEDIMENTS AT DEPTH: There are no data concerning the sediments under the outer continental shelf, continental slope, and the Sigsbee Deep beneath the upper 3 meters, and the nature of these sediments must be postulated. Petroleum exploration programs have provided detailed information on Gulf Coastal Plain sediments to depths greater than 15,000 feet. Under the Gulf Coastal Plain, post-Paleocene sediments generally dip and thicken toward the present coast line; older beds dip more steeply than younger beds. The updip portions of the sediments consist largely of continental sandy and lignitic facies with some interbedded near-shore marine sands and clays (King, 1951, p. 169–174). Downdip these continental deposits interfinger with and grade into brackish-water and near-shore marine facies farther downdip. Near the coast, wells have not been drilled deep enough to penetrate Oligocene beds, but the upper Miocene and post-Miocene section consists largely of marine shales with minor amounts of sand. The sediments are highly consolidated but retain relatively high porosities. R. J. Granberry (Personal communication) says that Miocene montmorillonite shales in South Texas at depths greater than 17,000 feet have porosities as high as 25 per cent in places although most voids probably are filled with adsorbed water rather than free water. It is not uncommon to find sands with porosities of 25 per cent at this depth.

Under the outer continental shelf and slope sediments at depth probably resemble those found under the coast, but should be finer, on the whole, than their updip equivalents. However, at times of lowered sea level, as during the Pleistocene, coarse material may have been deposited far out into the Gulf. The sediments probably consist largely of clays and silts, with minor amounts of fine sand, and are highly consolidated. They should be much stronger than the near-surface sediments but probably are unstable under some conditions.

ANGLE OF REPOSE: The angle of repose of sediments underlying the continental slope in the northwest Gulf of Mexico depends on (1) the characteristics of the sediments, (2) the rate at which the slope increases, and (3) the mass of the sediments subject to failure.

The behavior of the whole mass of sediments underlying the continental slope should be dominated by the behavior of silts and clays, for coarser sediments probably constitute only a small fraction. At depth the sediments may be highly consolidated and strong although they may retain relatively high porosities.

Consolidated fine sediment on the continental slope can form steeper slopes than unconsolidated or remolded sediment. If the overburden is removed from consolidated sediment by landslides or other agencies, this sediment will maintain steeper slopes than the adjacent unconsolidated surface material. However, removal of the overburden and exposure to water may cause the consolidated material to lose its original strength. Thixotropic effects will cause older unconsolidated sediment to have a higher angle of repose than younger material. Cross-bedding may increase the strength of a mass of sediment. However, failure may result from the inclusion of a single unstable layer in otherwise stable material.

If a slope is steepened slowly enough to permit complete drainage in the sediment, a steeper angle of repose can be acquired than if the slope is steepened suddenly and little drainage can occur. Thus, the rate of faulting or tilting will influence the angle of response of the sediments. A steeper angle of repose can be acquired if sediment accumulates slowly on the upper part of a slope than if it is deposited suddenly by a landslide.

Although vertical slopes a few feet high may be stable, slopes several hundred feet high in the same material may be unstable, because the total stresses tending to produce failure increase as the mass of the sediments increases.

Thus, the angle of repose is not constant for a given sediment but varies with the height of the slope and the rate at which the slope increases.

Types of failure.—When the angle of repose of the sediments underlying the continental slope is exceeded, the slope will fail by the downslope displacement of sediments. This displacement may be along a single shearing or fault plane, along several planes, or along so many planes that the failure would be termed plastic deformation or flow. The type of displacement depends on (1) the grain size, sorting coefficient, and mineralogy of the sediment; (2) the internal structure of the sediment resulting from its deposition, consolidation, and disturbance history; (3) the mass of the sediments involved; (4) the pressure under which the sediments are confined; and (5) the rate of stress application and the accompanying drainage conditions.

The terminology used for the types of failure in sediments depends on the presence of a well-defined shearing plane, the amount of mixing in the transported mass, the size of the failure, and the rate of movement. If a single shearing plane is present and if internal mixing in the transported mass is not great enough to destroy bedding and other internal structures, the failures commonly are called faults, if large, and landslides or slumps, if small. Confusion arises because fault is the term used for a surface of displacement, but landslide is the term used for the displaced material. If no single shearing plane is dominant and if the movement is relatively slow, the failure may be called creep and some features commonly called landslides or slumps are formed by creep. In either case, if the movement of the transported mass is dominated by flow characteristics and is relatively rapid, the failure may be called a sediment flow and would include mud flows and turbidity currents.

Divisions between these methods of transfer of sediment are arbitrary, and many failures may be intermediate ones. The amount of internal mixing is probably gradational between the stable transported masses of some faults and the most turbulent sediment flows. The transported mass may break into many large chunks which remain intact during movement but which are carried in a matrix of mixed sediment. A mass of sediment may move along an arcuate shearing plane at the upper end of the failure zone but may move by plastic failure or creep at the lower end of the failure zone. The transported mass may be so weakened during movement that, although the failure began as a fault, it may proceed as a sediment flow.

LANDSLIDES: Many smaller topographic features in the hummocky zone probably are due to landslides or small faults (Pl. 3, symbol no. 5). Downslope from some of the features are small hills which may represent the landslide deposits, indicating that the slides took place in relatively stable sediments. The absence of hills downslope from other features may imply that the landslide material, perhaps liquid, was transported a considerable distance down the slope.

These landslide features are confined to the hummocky zone on the upper part of the slope where relatively weak Pleistocene sediments should be thickest.

These features closely resemble the scars and deposits of many subaerial landslides. Landslides typically take place along narrow shearing zones or planes. The plane is usually curved, the radius of curvature being least at the upper end, greatest in the middle, and intermediate at the lower end. Commonly, a depression is formed at the upper end of the failure as the mass moves away from the slump scarp and down the slope under its own weight. The lower part fails passively owing to the thrust of the upper part, and the landslide deposit may be folded or faulted by thrusting. In layers of alternately weak and strong beds, failure is most likely along a weak stratum, and the shearing plane will not be a simple arc.

FAULTS: A number of topographic features on the continental slope may have been formed by faults (Pl. 3, symbol no. 3). Perhaps the most convincing feature is the scarp which trends due north from the southern edge of the map at 95°40′ W.Long. The scarp is over 3600 feet high, and a low area parallels the fault trace. The scarp is shown for over 20 miles, and it may extend beyond the southern limit of the map. The other topographic alingnments show no pronounced scarp, but only a steepened area on the upthrown side of the fault. The trace is marked by a line of low areas and depressions. Several profiles across these features are shown on Figure 7.

These features closely resemble structure-contour maps across some faults in Gulf Coastal Plain sediments. Faults are common throughout the western part of the Gulf Coastal Plain, and many of those not associated with salt domes have characteristic patterns. They tend to be concentric with the present coast and downthrown toward it (Kidd, 1939; King, 1951, p. 178). Beds on the downthrown side of these faults are bent down toward the fault plane in reverse drag, and a contour map of any stratigraphic horizon which crosses the fault shows a line of depressions, equivalent to sag ponds, next to the fault trace. In some cases, smaller antithetic faults parallel the major fault and are downthrown toward it on the downdip side, forming grabens (Cooper, 1937).

Many fault movements in the Gulf Coast were contemporaneous with deposition as some downthrown beds are thicker than their upthrown equivalents, and the two segments may consist of different facies (Kidd, 1939; Pool, 1940; Storm, 1945). Because of the contemporaneous deposition, the Gulf Coast faults may have an indistinct surface expression or disappear before reaching the upper beds, even though the maximum vertical displacement of a horizon at depth may amount to many hundreds of feet (Kidd, 1939; Pool, 1940). As faulting in the Gulf Coast apparently took place under conditions similar to those now existing in the northwest Gulf of Mexico, it is reasonable to expect faulting in the Gulf of Mexico.

Faults on the continental slope in the northwest Gulf of Mexico and many faults in the Gulf Coastal Plain may be the upper parts of large landslides. Geologists (Sheets, 1947; Storm, 1945) have noted the similarity between Gulf Coastal Plain faults and landslide features. In the Gulf Coastal Plain some fault planes decrease in dip with depth. In some cases, the vertical displacement diminishes not only upward, but also with depth as the dip of the fault plane decreases. These faults may be the upper parts of large landslides, the downthrown blocks moving along typical arcuate surfaces, steepest at their upper ends. The depth at which vertical displacement diminishes should be that depth at which movement of the block has a relatively large horizontal component. Only the upper part of the fault plane is commonly observed, and the middle and lower parts may not be recognizable from oil-well data. The failure plane may interesect the surface at its lower end, or the transported mass may be accomodated by plastic deformation.

CREEP: While creep may not produce effects recognizable in the topography, it may be of major importance in quantities of sediment transported over long periods of time. Creep is the movement of sediment down slopes by plastic failure where no single shearing plane is dominant. Sediments near the surface generally are least consolidated and least resistant to failure, but the stresses tending to produce failure increase with depth, so the rate of creep may not be greatest at the surface, as it is on subaerial slopes.

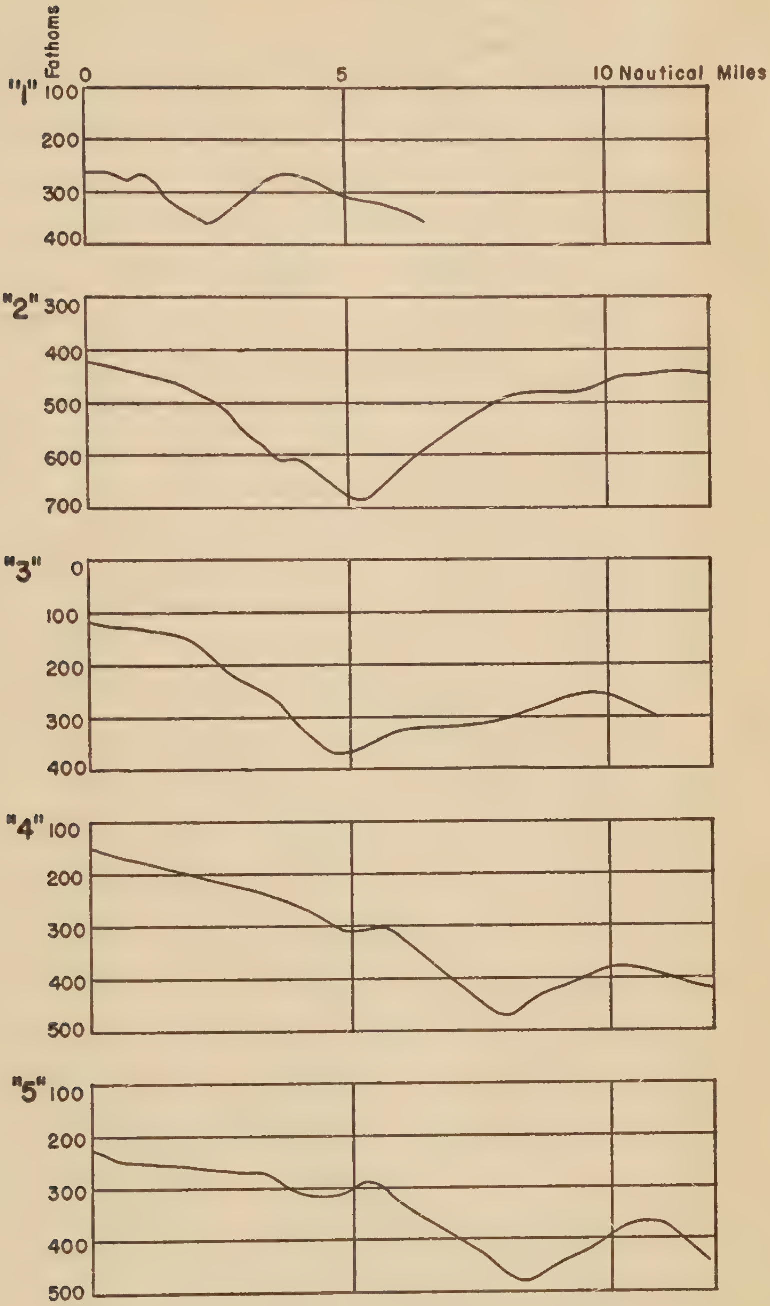

FIGURE 7.—PROFILES ACROSS ALIGNMENTS RESEMBLING FAULTS
Locations of profiles shown on Plate 3. Vertical exaggeration × 10.

SEDIMENT FLOWS: A sediment flow is a relatively rapid movement of sediment dominated by flow characteristics. It may be a viscous lamellar flow, a dilute turbulent flow, or any type between the two. A turbidity current is a sediment flow and may result from the failure of unstable sediments. Dietz (1952, p. 1807) suggests that the transition between a turbidity flow and a mud flow is where an increase in the density of the flow results in a decrease in velocity. Kuenen (1950), in his flume experiments on turbidity flows, found that suspensions with densities as high as 2.2 (about 30 per cent porosity) could be made to flow down slopes. Denser suspensions moved by sliding. The change from sliding to turbulent flow was abrupt, and the density at which it occurred was a function of the slope, volume of the transported mass, and the grain-size distribution of the sediment. For convenience the term turbidity flow is confined to those sediment flows characterized by turbulence rather than to a change in density or a change in velocity, either of which may be more difficult to observe. Sediment flows may be made up largely of chunks of relatively intact sediment carried in a matrix of liquefied sediment. If a layer of unstable sediment is buried, the sediment may liquefy and act as a gliding plane. Thus, some landslides and faults may result from the liquefaction of sediment at depth.

Saturated loose sands, unconsolidated clays with high water contents, consolidated quick-clays with high water contents, and silts may be transformed into suspensions or semiliquids which can flow down gentle slopes for great distances. These sediments can flow without increasing the water content. However, subsequent dilution may take place after flow has begun, and the distance of the flow may be increased thereby.

In the hummocky zone a number of amphitheaterlike depressions with narrow outlets closely resemble bottleneck scars characteristic of flow failures. An excellent example of such a scar is one 35 meters deep left by the 1893 landslide in Vaerdalen, Norway. A mass of quick-clay over a large area was transformed into a semiliquid which flowed through a narrow outlet into the valley below (Holmsen, 1953).

The steep headwalls of many of the troughs in the northwest Gulf of Mexico suggest that the troughs may have been enlarged and lengthened by landslide-sediment flow mechanisms, and some of the troughs may have been formed completely by them. Landslides moving along arcuate surfaces leave relatively steep slump scarps. If the transported mass is removed from the area by flow the scarp remains unsupported and may be a site for subsequent landslides. Many of the troughs off the Atlantic coast of North America also have steep headwalls. The writer considers this landslide-sediment flow mechanism the most effective submarine erosion agency yet proposed for the formation of submarine troughs.

The topographic form of most of the submarine troughs in the northwest Gulf of Mexico indicates that they have been formed predominantly through erosion, but the topography does not indicate whether the erosion was subaerial or submarine. Once in motion, submarine sediment flows may erode the surface over which they move. That subaerial sediment flows can erode is well known. Crandell (1952) described what he termed an earth-flow in South Dakota which began as a landslide in the upper part of a valley, left a slump scarp, and moved 350 feet down the valley. The transported mass consisted of debris with a high sorting coeffecient and was 10–20 feet thick and 85 feet long. The moving mass gouged extensive slickensides along the walls of the gully, indicating that the flow actually eroded the surface over which it moved. Blackwelder (1928) describes a mud flow which moved down a canyon on the west side of the Wasatch Range, Utah, and left the walls of the canyon torn and scarred. Submarine sediment flows may move more slowly and be less effective agencies of erosion than either subaerial sediment flows or normal streams. However, that the troughs in the northwest Gulf of Mexico were eroded by submarine sediment flows remains a possibility.

Sediment flows are depositional agencies, but some beds deposited by them are difficult to distinguish from those deposited by normal particle sedimentation. Graded beds may be deposited under several conditions (Kuenen, 1950) including deposition by sediment flows. However, not all beds deposited by sediment flows will be graded. A graded bed requires that the sediment have a high sorting coefficient and that it be mixed, and that the flow have a viscosity low enough to permit differential settling. If the sediment has a low sorting coefficient and remains uncontaminated, grading may not be apparent in the resulting deposit. If the sediment has a high sorting coefficient, if it is thoroughly mixed during flow, and if the viscosity of the flow is high, the resulting deposit should consist of a homogeneous mass of material with a high sorting coefficient.

The presence of a chronological sequence of layers is not proof that the sequence was not deposited by a sediment flow for sediments may flow without vertical mixing. In 1938 a large section of the upstream face of the Fort Peck Dam, Montana, and the underlying material moved downslope about 1400 feet in about 3 minutes. Because of the speed and distance of the movement and because the resulting deposit had a nearly level surface, some engineers believe that the material must have been liquid during movement and that movement was by flow (Middlebrooks, 1942; Casagrande, 1950). The stratigraphic sequence in the dam material and the underlying sediment was preserved during flow and was present in the resulting deposit, although the thicknesses and horizontal extent of the beds had been altered. The implication is that the flow was lamellar. Therefore, sections of layered sediment may move down slopes for great distances and still retain the original stratigraphic sequence.

In the northwest Gulf of Mexico, sediments believed to have been deposited by sediment flows have been found in two localities. The first is in the bottom of a steep-sided submarine trough where cores 229 and 232 were taken by the ATLANTIS in 1951 (Fig. 1). The cores were taken 7 miles apart, 135 miles from the coast, and at a depth of 1050 fathoms. The trough has a flat bottom in contrast to other V-shaped troughs in the region. Both cores consist of many layers from less than 1 mm to about 20 cm thick, but they cannot be correlated lithologically. The layers consist of sand, silt, and clay which contain Foraminifera, pteropod, and fish fragments. Sorting coefficients are high in some layers, low in others. Some of the layers contain clay balls. The sequences in these two cores are radically different from those in cores not taken in submarine troughs. The layers differ so much in grain size, sorting, and fossil content that, if they were not deposited by sediment flows, sedimentary conditions must have changed more radically and frequently than is believed possible in such deep water so far from the coast. It is unlikely that these are older sediments into which the trough has been cut because the sediments are as unconsolidated as other sediments known to be late Pleistocene-Recent by their Foraminifera content. The trough is about 3000 feet deep, and, even if the height of the walls has been increased by sedimentation while the bottom has been kept clear by sediment flows, the trough probably was cut into consolidated sediment. The U shape of the trough is considered to be due to partial filling of the trough by debris deposited by less viscous sediment flows. Similar layers of debris may be expected in other U-shaped troughs in the region, but not in the V-shaped troughs.

The second locality in which sediments believed to have been deposited by a sediment flow have been found is in the Sigsbee Deep. During the 1947 cruise of the ATLANTIS to the northwest Gulf of Mexico, cores 335 and 336 (Fig. 1) were taken 30 miles apart, 120 miles from the mouth of the Rio Grande, at a depth of 1900 fathoms. The cores have been described in part by Phleger (1951b) and consist of three layers: (1) an upper clay, (2) a middle sand, and (3) a lower clay. The upper clay is about 1.5 m thick, and Phleger (1951b, p. 71) reports benthonic Foraminifera which are predominantly deep-water types and planktonic Foraminifera characteristic of warm water. The Foraminifera and grain size of the upper clay are both characteristic of the locality and depth at which they are found. The middle sand is 32 cm thick in core 335 and 86 cm thick in core 336. The sand has a median diameter of 0.1 mm and a Trask sorting coefficient of 1.3. No graded bedding is apparent. Phleger (1951b, p. 72) says that the benthonic Foraminifera in the sand consist of a few deep-water types, some intermediate types, and many types characteristic of water shoaler than 50 fathoms. The planktonic Foraminifera are those characteristic of cold water; the sand is probably equivalent to the last glacial period. The lower clay was recovered in core 336 only.

Sands as coarse as this are found as surface sediment only in water shoaler than 100 fathoms and in most cases shoaler than 50 fathoms. Considering the grain size and Foraminifera content, the sand must either have been submerged to its present depth by downwarp of the ocean floor or by rising sea level, or have been transported to its present position. As a post-Wisconsin submergence of 11,000 feet seems unlikely, transportation of the sand to its present site seems a preferable theory. Since sea level was probably near the present 75-fathom curve during late Pleistocene time the site of accumulation need not have been farther inland than the edge of the continental shelf. A surface deposit of loose sand near the edge of the shelf may have liquefied and flowed down the steep continental slope. Such a flow could have moved down the large submarine trough north of the present position of the sand.

Phleger (1951b, p. 74) says that the inclusion in the sand of fauna characteristic of intermediate and deep water in addition to shallow water must be attributed to one of three conditions: (1) the sand moved down the slope in stages, being repopulated with fauna characteristic of the depth at each resting place; (2) the supply of sand came from several sources and depths; or (3) the sediment was mixed during one movement. If Foraminifera characteristic of all depths were mixed with or added to the original sand, finer sediment characteristic of those depths must also have been mixed with or added to the original sand. The fact that the present sand has a sorting coefficient lower than most beach sand indicates that sorting by grain size took place during movement and that fractions finer than the sand were carried beyond cores 335 and 336.

Conclusions

Several hypotheses concerning the origin of the topography on the continental slope in the northwest Gulf of Mexico present themselves when the agencies which may be operating in the Gulf and the sediments underlying the region are considered:

(1) A number of features of low relief on the continental shelf and the bioherms at the edge of the continental shelf have topographic forms and dimensions suggesting they overlie salt domes. On the continental slope salt domes may have influenced some of the topography, but there is no evidence which indicates that they have been an important geomorphic factor.

(2) The Sigsbee Deep is bounded by scarps of such great extent and relief that large crustal faults are the only reasonable explanation of them. The Sigsbee Scarp probably represents a fault downthrown toward the Sigsbee Deep. The height and gradient of the scarp indicate that faulting is greatest at the western end of the scarp, diminishes near the Mississippi Trough, and merges into a flexure between the Mississippi Trough and the DeSoto Canyon. Hanging valleys indicate either that at least part of the faulting took place after the troughs on the continental slope were cut, or that the troughs were cut by submarine agencies which produce hanging valleys as a normal process of erosion. The northeast side of the Sigsbee Deep is shoaler than the northwest side, owing either to heavier sedimentation in the east or greater downfaulting in the west.

(3) In the northwest Gulf of Mexico a large mass of unstable sediments is under stress. Evidence in the topography and sediments indicates that this mass is failing by landslides, faults, creep, and sediment flows. Divisions among these types of failure are arbitrary, and many failures may be intermediate. Most of the topographic features on the continental slope probably have been formed completely or modified extensively by the failure of these sediments under the stress of gravity.

(4) The sand beneath a meter of clay in the Sigsbee Deep may have accumulated near the edge of the continental shelf during lowered sea level of the late Pleistocene and transported down the continental slope to its present position. As the sand contains benthonic Foraminifera characteristic of shallow, intermediate, and deep water, those forms must have been mixed with the sediment during movement. As the finer sediments characteristic of intermediate and deep water are not present in the sand, it is assumed the sediment was sorted during movement and the fine fractions carried beyond the sand.

(5) The topographic form of most of the submarine troughs in the northwest Gulf of Mexico indicates they were formed predominantly by erosion. The topography does not indicate conclusively what agencies were primarily responsible for that erosion. The writer believes the most reasonable hypothesis for the formation of these troughs is a composite one involving four phases:

(a) The original troughs were formed by

subaerial erosion prior to the formation of the Gulf of Mexico. Although the landslide-sediment flow mechanism is considered by the writer the most effective submarine erosion agency yet proposed for the formation of submarine troughs, she is hesitant to ascribe the formation of troughs 60 miles long and 3000 feet deep to this mechanism.

(b) After the troughs were formed the continental slope was submerged and tilted. The basement at the coast of the northwest Gulf of Mexico has been downwarped about 40,000 feet since the Jurassic, and the basement under the continental slope may have been downwarped an equal amount. Thick Pleistocene and Recent sediments under the coast line indicate that the basement is still subsiding. The continental slope could have subsided from above sea level to its present depth during the Cenozoic, and much of the subsidence could have taken place during the Quaternary.

(c) The upper parts of the troughs were masked by sediments deposited when sea level was lowered during the Pleistocene. The hummocky zone on the upper part of the continental slope represents the surface of these sediments. Few troughs extend into this zone; those present are more shallow, and their form is more irregular than those on the lower part at the slope.

(d) The troughs were modified extensively, largely by the failure of sediments under stress. The troughs may have been enlarged and lengthened after submergence by landslide-sediment flow mechanisms, and some troughs or parts of troughs may have been formed completely by them. The relatively unconsolidated Pleistocene sediments on the upper part of the slope should furnish an ample source of supply for the sediment flows. Although submarine sediment flows probably are less effective agencies of erosion than either subaerial sediment flows or normal streams, some part of the troughs could have been deepened by them.

The deep depressions in the troughs could have been formed during or after submergence by faults which cross the troughs, partial and irregular filling of the troughs by landslide debris and viscous sediment flows, or folding accompanying irregular subsidence.

Those troughs with flat bottoms have been filled partially with many thin layers of sediment, and it is presumed that this fill is absent in V-shaped troughs. The thin layers of sediment probably have been deposited by less viscous sediment flows.

Some aspects of this composite hypothesis for the origin of submarine troughs resembles a hypothesis presented by Shepard (1951a; 1951b; 1952).

(6) The upper part of the Mississippi Trough may be related to the Pleistocene Mississippi River Valley, including the buried off-shore extension of the Valley on the continental shelf. The upper part of the Mississippi Trough and a buried extension on the continental shelf could have been eroded subaerially during lowered sea level of the Pleistocene. If that part of the Mississippi Trough deeper than the 75-fathom curve were eroded subaerially, it must have been downwarped subsequently to its present depth. At least the lower part of the Mississippi Trough may be the same age as other troughs on the continental slope, and the upper part could have been re-opened by subaerial erosion during the Pleistocene.

Some of the indentations in the 100-fathom cruve may be related to other Pleistocene river valleys which crossed the continental shelf and which have been filled with sediment.

(7) On the upper part of the continental slope is a hummocky zone which probably represents the surface of thick Pleistocene sediments deposited when sea level was near the present 75-fathom curve. The presence of many topographic features which resemble landslide scars, landslide deposits, and sediment-flow scars indicates that this mass of sediments is relatively unconsolidated and weak and that the stresses tending to produce failure have increased rapidly. These relatively weak sediments are probably the source of many sediment flows which move down the troughs below the zone into the Sigsbee Deep.

The absence of a hummocky topography and the presence of relatively steep slopes on the lower part of the continental slope indicate that sediments underlying this region are more stable and less subject to failure than are those on the upper part. Pleistocene sediments may be thin on the lower part of the slope, and older more consolidated sediments may be near the surface.

As only a few submarine troughs of modified form are found in this upper zone, probably the troughs are older than these Pleistocene sediments and the sediments have filled the upper parts of the troughs. Some depressions in the hummocky zone are aligned with troughs below them, indicating that the upper parts of the troughs have been partially and irregularly filled with sediment.

(8) The red lines shown on Plate 3 follow a series of depressions and low areas which may correspond to sagponds near fault traces. Above the lines are steep slopes which may be fault scarps. These faults are probably large arcuate shear planes along which large masses of sediment have failed. These alignments may indicate only a few of the many faults still active on the continental shelf and slope. Other faults may leave less pronounced topographic expressions or may be masked or obliterated by sedimentation.

Appendix I

Sources of fathograms used in constructing profiles across break in slope (Figs. 2, 3, 4). Locations of profiles shown on Figure 1.

"A"—Atlantis, 1947. Port Isabel I, stations 314–324
"B"—Atlantis, 1947. Port Isabel II, stations 276–286
"C"—Atlantis, 1947. Aransas, stations 256–269
"D"—Atlantis, 1947. Matagorda II, stations 169–179
"E"—Atlantis, 1947. Brazos I, stations 117–119
"F"—Atlantis, 1947. Brazos II, stations 66–74
"G"—Atlantis, 1951. March 7, 1300–1534
"H"—Atlantis, 1947. Galveston, stations 346–364
"I"—Atlantis, 1951. March 9, 0118–0318
"J"—Atlantis, 1947. Heald Bank, stations 25–37
"K"—Atlantis, 1951. March 8, 0537–0656
"L"—Atlantis, 1951. March 8, 0326–0537
"M"—Atlantis, 1947. Trinity Shoal I, stations 436–450
"N"—Atlantis, 1947. Trinity Shoal II, stations 485–492
"O"—Hydrographic Office A. March 11, 1949; Book 91, Roll 43, 0708–0947
"P"—Hydrographic Office E. February 16, 1949; Book 84, Roll 35, 1122–1300
"Q"—Hydrographic Office G. February 16, 1949; Book 62, Roll 24, 1200–1410
"R"—Atlantis, 1947. Ship Shoal, stations 525–534
"S"—Hydrographic Office K. January 5, 1949; Book 38, Roll 19, 1900–2400
"T"—Hydrographic Office O. February 11, 1947; Book 9, Roll 20, 0930–1400
"U"—Hydrographic Office N. March 7, 1949; Book 63, Roll 25, 2249–2310

References Cited

Baver, L. D., 1948, Soil physics: N. Y., John Wiley and Sons, 398 pages.

Blackwelder, Eliot, 1928, Mudflow as a geologic agent in semi-arid mountains: Geol. Soc. America Bull., v. 39, p. 465–484.

Carsey, J. Ben, 1950, Geology of Gulf Coastal area and Continental Shelf: Am. Assoc. Petroleum Geologists Bull., v. 34, p. 361–385.

Casagrande, Arthur, 1950, Notes on the design of earth dams: Boston Soc. Civil Eng. Jour., v. 37, p. 417–423.

Colle, Jack, Cookes, W. F., Jr., Denham, R. L., Ferguson, H. C., McGuirt, J. H., Reedy, Frank, Jr., and Weaver, Paul, 1952, Sedimentary volumes in Gulf Coastal Plain of United States and Mexico, part IV, volume of Mesozoic and Cenozoic sediments in Western Gulf Coastal Plain: Geol. Soc. America Bull., v. 63, p. 1193–1200.

Cooper, Herschel H., 1937, Occurrence and accumulation of oil in Laredo district, Texas: Am. Assoc. Petroleum Geologists Bull., v. 21, p. 1422–1438.

Crandell, Dwight R., 1952, Landslides and rapid-flowage phenomena near Pierre, South Dakota: Econ. Geology, v. 47, p. 548.

Dietz, Robert S., 1952, Geomorphic evolutions of Continental Slope terrace (Continental Shelf and Slope): Am. Assoc. Petroleum Geologists Bull., v. 36, p. 1802–1819.

Dietz, Robert S., and Menard, Henry W., 1951, Origin of abrupt change in slope at Continental Shelf margin: Am. Assoc. Petroleum Geologists Bull., v. 35, p. 1994–2016.

Fisk, Harold N., 1944, Geological investigation of the alluvial valley of the lower Mississippi River: War Dept., Corps Engineers, U. S. Army, Miss. River Comm., Vicksburg, Miss., 78 pages.

—— 1953, Setting of Gulf Coast geosyncline: Am. Assoc. Petroleum Geologists Bull., v. 37, p. 1129.

Flint, Richard Foster, 1947, Glacial geology and the Pleistocene epoch: N. Y., John Wiley and Sons, 589 pages.

Holmsen, Per, 1953, Landslips in Norwegian quick-clays: Inst. Civil Engineers, Geotechnique, v. III, p. 187–194.

Jordan, G. F., 1951, Continental Slope off Apalachicola River, Florida: Am. Assoc. Petroleum Geologists Bull., v. 35, p. 1978–1993.

Kidd, Gentry, 1939, Developments in South Texas, 1938–1939: Am. Assoc. Petroleum Geologists Bull., v. 23, p. 860–870.

King, Philip B., 1951, The tectonics of middle North America: Princeton, N. J., Princeton Univ. Press, 203 pages.

Knight, B. H., 1948, Soil mechanics for civil engineers: London, E. Arnold and Co., 255 p.

Koppejan, A. W., Wamelen, B. M., and Weinberg, L. J. H., 1948, Coastal flow slides in the Dutch Province of Zeeland: Rotterdam, Proc. 2nd Internat. Conf. Soil Mech. and Found. Engineering, v. 5, p. 89–96.

Krumbein, W. C., and Pettijohn, F. J., 1938, Manual of sedimentary petrography: N. Y., Appleton-Century-Crofts, Inc., 549 pages.

Kuenen, Ph. H., and Migliorini, C. I., 1950, Turbidity currents as a cause of graded bedding: Jour. Geology, v. 58, p. 91–127.

Middlebrooks, T. A., 1942, Fort Peck slide: Am. Soc. Civil Engineers Trans., Paper no. 2144, v. 68, p. 723–764. Discussions by Jacob Feld, Joel D. Justin, William Gerig, Alfred J. Ryan, Glennon Gilboy, Frank E. Falquist, Irving B. Crosby, and T. A. Middlebrooks.

Nettleton, L. L., 1952, Sedimentary volumes in Gulf Coastal Plain of United States and Mexico, part VI, Geophysical aspects: Geol. Soc. America Bull., v. 63, p. 1221–1228.

Phleger, Fred B, 1951a, Ecology of Foraminifera, Northwest Gulf of Mexico, part I: Foraminifera distribution: Geol. Soc. America Mem. 46, p. 1–88.

—— 1951b, Displaced Foraminifera faunas, in turbidity currents and the transportation of coarse sediments to deep water, a symposium: Soc. Econ. Paleontologists and Mineralogists, Special Pub. no. 2, p. 66–75.

Pool, J. C., 1940, Saxet oil and gas field, Nueces County, Texas: Am. Assoc. Petroleum Geologists Bull., v. 24, p. 1805–1835.

Pressler, E. D., 1947, Geology and occurrence of oil in Florida: Am. Assoc. Petroleum Geologists Bull., v. 31, p. 1851–1862.

Rosenqvist, I. Th., 1953, Considerations on the sensitivity of Norwegian quick-clays: Inst. Civil Engineers, Geotechnology, v. III, p. 195–200.

Sebring, Louie Jr., 1948, Slick-Wilcox field, DeWitt and Goliad Counties, Texas: Am. Assoc. Petroleum Geologists Bull., v. 32, p. 228–251.

Sheets, Martin, 1947, Diastrophism during historic time in Gulf Coastal Plain: Am. Assoc. Petroleum Geologists Bull., v. 31, p. 201–226.

Shepard, Francis (1951a), Submarine canyons: A joint product of rivers and submarine processes: Science, v. 114, no. 2949, p. 7–9.

—— (1951b), Submarine erosion, a discussion of recent papers: Geol. Soc. America Bull., v. 62, p. 1413–1418.

—— (1952), Composite origin of submarine canyons; Jour. Geology, v. 60, p. 84–96.

Stetson, Henry C., 1953, The continental terrace of the Western Gulf of Mexico: its surface sediments, origin and development: Mass. Inst. Technology and Woods Hole Oceanographic Inst., Papers in Physical Oceanography and Meteorology, v. 12, no. 4, pt. I, p. 1–45.

Storm, L. W., 1945, Résumé of facts and opinions on sedimentation in Gulf Coast region of Texas and Louisiana: Am. Assoc. Petroleum Geologists Bull., v. 29, p. 1304–1335.

Terzaghi, K., and Peck, Ralph B., 1948, Soil mechanics in engineering practice: N. Y., John Wiley and Sons, 566 p.

Trask, Parker D., 1953, Chemical studies of sediments in the Northwest Gulf of Mexico: Mass. Inst. Technology and Woods Hole Oceanographic Inst., Papers in Physical Oceanography and Meteorology, v. 12, no. 4, pt. II, p. 47–120.

Veatch, A. C., and Smith, Paul A., 1939, Atlantic submarine valleys of the United States and the Congo submarine valley: Geol. Soc. America Special Papers, no. 7, 101 p.

221 OHIO ST., CORPUS CHRISTI, TEXAS

MANUSCRIPT RECEIVED BY THE SECRETARY OF THE SOCIETY, JULY 2, 1953
WOODS HOLE OCEANOGRAPHIC INSTITUTION CONTRIBUTION NUMBER 650

PHYSICAL OCEANOGRAPHY OF THE GRAND BANKS REGION AND THE LABRADOR SEA IN 1953[1]

By Floyd M. Soule, A. J. Bush, and J. E. Murray, U. S. Coast Guard

The 180-foot tender-class cutter USCGC *Evergreen* again served in 1953 as the oceanographic vessel of the ice patrol. The only major change affecting the oceanographic work was the installation on the starboard side of the fantail of a davit and cradle to handle and hold a new instrument known as a deep electronic bathythermograph. As the instrument traces a curve of temperature against depth it will be be referred to by the abbreviated title TD in a subsequent description of it and the work done with it.

The oceanographic survey work of the 1953 ice patrol season began with the departure of the *Evergreen* from Argentia on the evening of 1 April. Because of the rapid movement of a couple of early season bergs along the eastern slope of the Grand Banks to and somewhat westward of the southern end of the banks the first survey was planned to include a small area just west of the Tail of the Banks and extending around the southern end of the banks and northward along the eastern slope of the banks to about the 46th parallel.

The work of collection of data began at the southwestern corner of the survey on the early morning of 3 April and was completed without interruption from the weather on the early afternoon of 14 April, 66 stations having been occupied. A course was then laid for Argentia where the *Evergreen* arrived on the morning of 16 April.

On the evening of 26 April the *Evergreen* departed Argentia for the purpose of making a second survey, this time of the waters over and immediately seaward of the northeastern and eastern slopes of the Grand Banks north of about 45° N., and west of about 45° W. The survey began on the morning of 28 April at the northwestern edge of the area and progressed southward. The survey work was interrupted on the evening of 28 April after completing station 5063 to search the area of probable drift of a berg reported at 47°55′ N., 47°40′ W., at 1430 G. C. T., on the 27th. Current fixes were obtained once an hour with the von Arx current meter (GEK) and, following arrival at the reported position at 0730 G. C. T., on 29 April, the ship proceeded downstream as indicated by the GEK for 33 miles after which a ladder search, beginning 6 miles farther downstream, was undertaken back

"Extract from U. S. Coast Guard Bulletin No. 39"

toward the reported position. Two radar targets found in the area were identified as vessels. The *Evergreen* then returned to the position of station 5064 and resumed oceanographic work on the late evening of 29 April. No further interruptions occurred and the survey, comprised of 81 stations was completed on the early morning of 9 May. Course was then laid for the vicinity of station 5130 where earlier measurements indicated the presence of surface water of approximately the desired salinity for use as substandard water. The location was reached on the late afternoon of 9 May and a carboy of water was collected for use during subsequent surveys. The *Evergreen* then proceeded toward Argentia and after searching the area in the vicinity of Cape Race and westward for bergs Argentia was reached on the evening of 11 May.

---

[1] To be reprinted as Contribution No. 675 in the Collected Reprints of the Woods Hole Oceanographic Institution.

A third survey was begun with the departure of the *Evergreen* from Argentia on the afternoon of 26 May. This survey consisted of the occupation of the Bonavista triangle beginning and ending at the offshore corner. The work of collection of data began late on 27 May. Work progressed counterclockwise around the triangle without incident until the early morning of 29 May when the Wenner salinity bridge developed a derangement in its measuring circuits. Tests indicated the existence of a ground inside the tank containing the constant temperature oil bath. On completion of station 5155 the ship was hove to on the easiest possible heading while the bridge was completely dismantled, the grounded circuit remedied, and the bridge reassembled. Operations were then resumed after a delay of about 14 hours. No further interruptions occurred and the last of the 30 stations comprising the survey was completed on the early morning of 31 May. The *Evergreen* then proceeded to Argentia arriving there about noon on 1 June.

At midday on 5 June the *Evergreen* departed Argentia to begin a fourth survey. The area to be covered was similar in location to that of the first survey but extending northward to the latitude of Flemish Cap and omitting the area westward of the southern end of the Grand Banks. Work began at the northern end of the area on the afternoon of 6 June and was completed, after the occupation of 78 stations, on the early morning of 17 June. As the International Ice Patrol had been discontinued for the 1953 season during the progress of the survey the *Evergreen* proceeded to Boston to await the beginning of the postseason cruise.

On the afternoon of 7 July the *Evergreen* departed Boston to begin the postseason observations reaching the offshore corner of the Bonavista triangle on 11 July. Proceeding counterclockwise around the triangle the last of the 30 stations was completed on the afternoon of 14 July. From this point the *Evergreen* proceeded to South Wolf Island where, on the early morning of 16 July, a section across the Labrador Sea to Cape Farewell, Greenland, was begun. Just seaward of the Labrador continental shelf it was necessary for the first and only time during the 1953 operations, to heave to because of boisterous weather. After a delay of approximately 18 hours progress was resumed. A coastal belt of ice off Cape Farewell, combined with darkness and low visibility forced the termination of the section, the last of 22 stations being completed 14½ miles off Cape Farewell late on the evening of 20 July. The *Evergreen* then proceeded via Argentia to Woods Hole where the field work for 1953 was concluded with the unloading on 27 July of oceanographic equipment and personnel.

The oceanographic work was under the supervision of Oceanographer Floyd M. Soule who was assisted by LCDR Armand J. Bush and LT John E. Murray. Other assistants in the observational work were Francis N. Brown, yeoman first class; Lewis M. Lawday, aerographer's mate second class; Hugh R. McCartney, Jr., aerographer's mate second class; Donald Zacher, aerographer's mate third class; and Joseph R. Stefanick, seaman.

Of the 306 stations occupied during the season and postseason cruises, the 22 stations comprising the section across the Labrador Sea were occupied from the surface to as near bottom as was practicable, and at the remaining 284 stations the observations extended to a depth of about 1,500 meters where the depth of water permitted. As in previous years the intended depths of observation, in meters, were 0, 25, 50, 75, 100, 150, 200, 300, 400, 600, 800, 1,000, and thence by 500-meter intervals. The dynamic heights have been referred to the 1,000-decibar surface, except for the section across the Labrador Sea where the 1,500-decibar surface was used as the reference surface.

In addition to the usual measurements of temperature and salinity, 261 samples were taken during the occupation of the South Wolf Island-Cape Farewell section for ultimate determination of total phosphorus concentration.

Temperatures were measured with deep sea reversing thermometers. Most of the protected thermometers were of Richter and Wiese manufacture but a small percentage were manufactured by Negretti and Zambra, G. M. Manufacturing Co., and the Kahl Scientific Instrument Corp. The depths of observation were based on unprotected thermometers made by Richter and Wiese and by Kahl. The thermometers were used in pairs and a program of intercomparison of protected thermometers was carried out by periodically changing the individual thermometers comprising the pairs. In all 2,042 comparisons were made. After eliminating constant corrections these comparisons gave a probable difference between the corrected readings of a pair of thermometers of 0.011° C. As many of the thermometers had recent laboratory comparisons with thermometers tested by the National Bureau of Standards, and as in most cases the temperatures are the means of the corrected readings of a pair of thermometers, it is considered that the observed temperatures listed

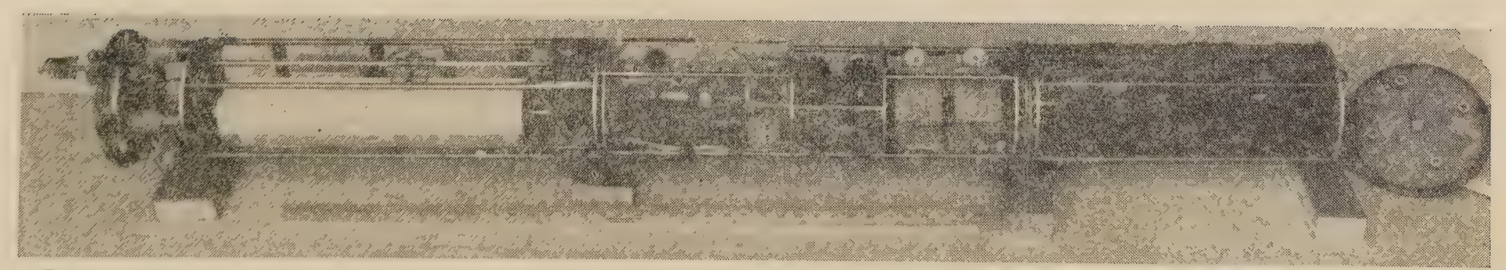

FIGURE 12.—Interior sections (upper, center, and lower) of deep electronic bathythermograph assembled outside of pressure case.

in the table of oceanographic data have a probable error of about ±0.01° C.

The new TD mentioned above is a self-contained instrument of rapid response which traces a continuous curve of temperature against depth on a scale of approximately 11.2 mm. per degree C and 13.6 mm. per 100 meters. The temperature scale accommodates 35 centigrade degrees and the depth range is limited to 1,800 meters. The temperature element is an electrical resistance thermometer which controls the axial position of the pencil carriage. The depth element is a helical Bourdon tube which controls the angular position of the drum holding the record chart. The movements of pencil and drum are the electronically magnified changes in balance of the alternating current thermometer bridge and of the changes in shape of the Bourdon tube followed up by means of a linear differential transformer (Schaevitz). A frequency of 400 cycles is used in the servo balancing systems and a 12 volt lead nonspill battery is the primary power source.

The instrument is made up in 3 sections which are assembled in a steel pressure case 6 feet long and having an outside diameter of 8 inches and a wall thickness of three-eighths of an inch. The assembled instrument weighs 337 pounds in air and about 200 pounds in water. The forward or lower section contains the battery which must be removed periodically for charging. The rear or upper section contains the recording drum and must be removed, at least partially, to change the record chart. The center or control section need be removed only infrequently. Figure 12 shows the three sections assembled outside the pressure case. A block diagram of the instrument is shown in figure 13. A more detailed description is contained in Woods Hole Oceanographic Institution's unpublished report of February 1953 "The Deep Electronic Bathythermograph" by Karl E. Schleicher (Reference No. 53–10).

In use the TD was shackled, in lieu of a sinker, to the lower end of the oceanographic wire rope to which the Nansen bottles and reversing thermometers were attached. As the instrument had been used on only a small number of lowerings previously, no standard handling procedure had been developed. Because of its weight and size the TD was very difficult to control in launching it from and returning it to its cradle on deck. On numerous occasions the side of the case hit the side of the ship with varying degrees of impact resulting in displacements of the atmospheric pressure position of the Shaevitz transformer core. On one occasion the thermal element hit the A frame and this probably was responsible for the eventual failure of the instrument when it filled with water through the thermal element. In all, 26 casts were made. Many of these were trials after unsuccessful attempts to remedy faults. As a result 14 traces were obtained

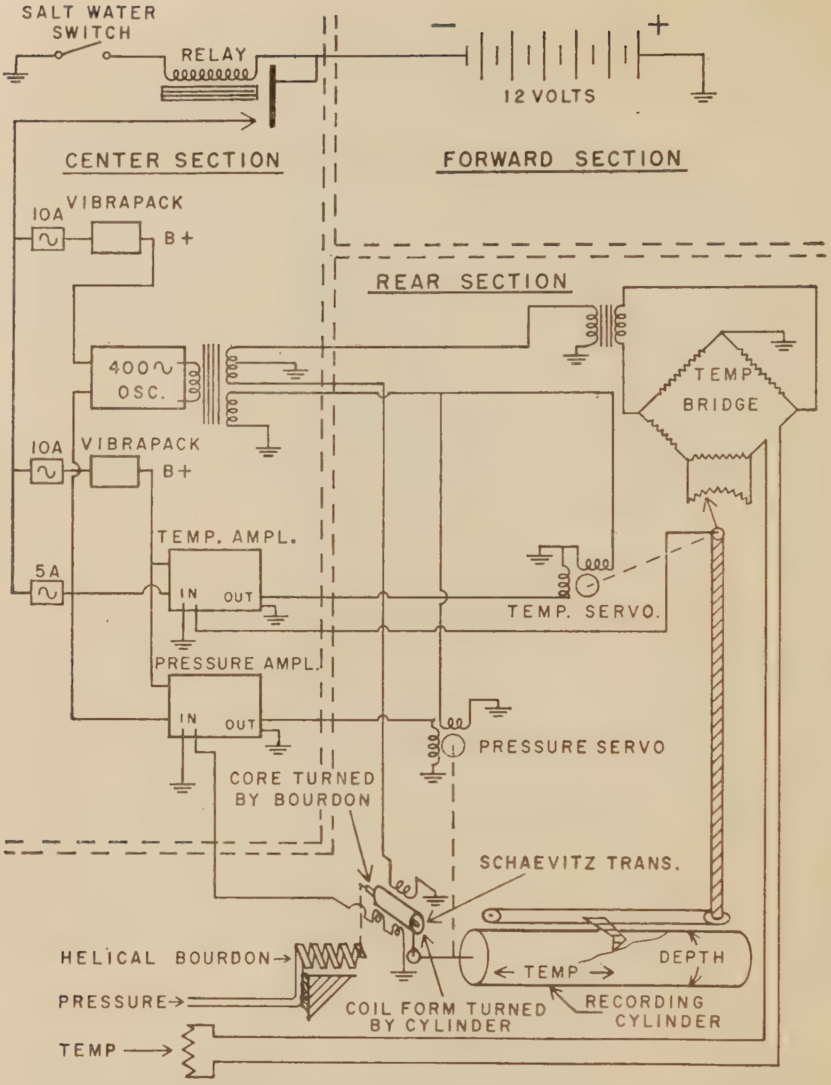
SALT WATER SWITCH
RELAY
12 VOLTS
CENTER SECTION
FORWARD SECTION
10A
VIBRAPACK
B+
REAR SECTION
TEMP BRIDGE
400~ OSC.
10A
VIBRAPACK
B+
TEMP. AMPL.
5A
IN
OUT
TEMP. SERVO.
PRESSURE AMPL.
IN
OUT
PRESSURE SERVO
CORE TURNED BY BOURDON
SCHAEVITZ TRANS.
HELICAL BOURDON
DEPTH
TEMP
PRESSURE
COIL FORM TURNED BY CYLINDER
RECORDING CYLINDER
TEMP

FIGURE 13.—Block diagram of deep electronic bathythermograph.

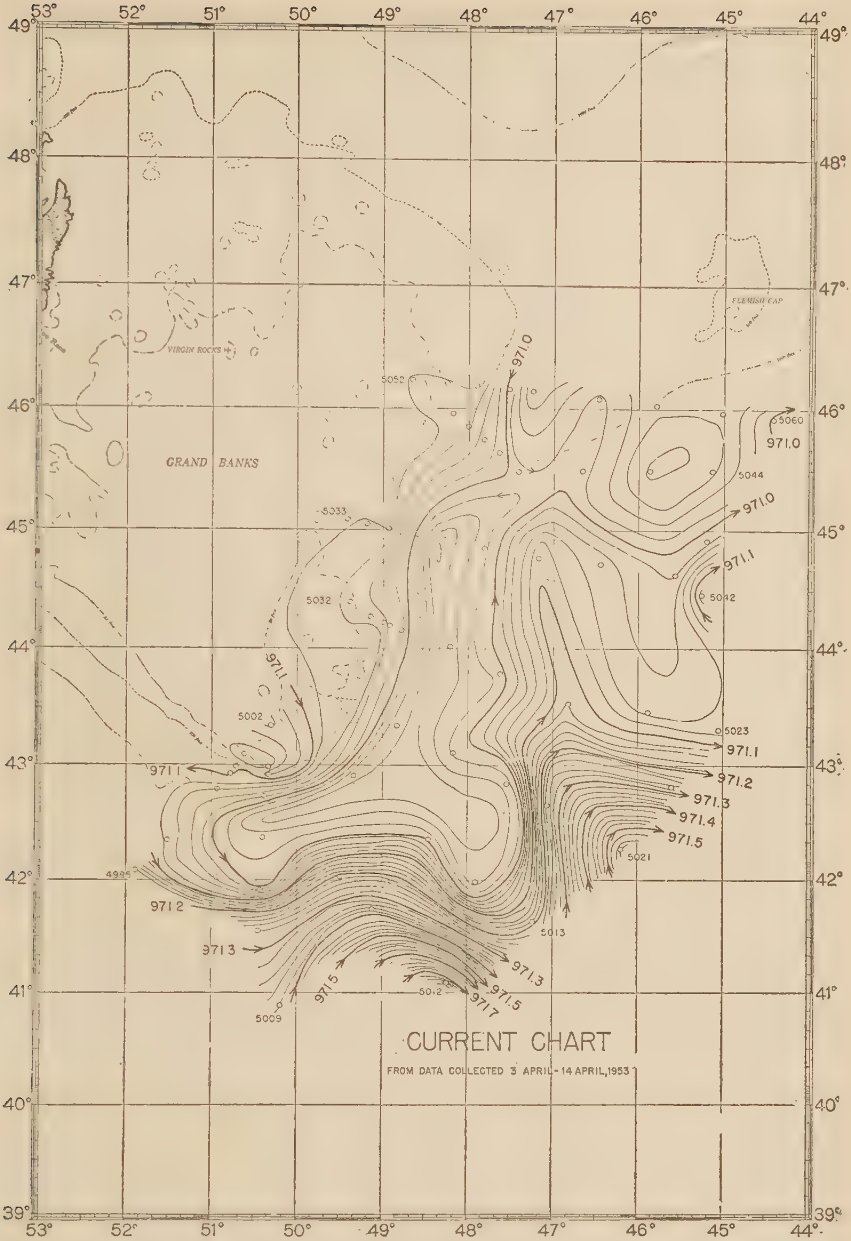
53°
52°
51°
50°
49°
48°
47°
46°
45°
44°
49°
48°
47°
46°
45°
44°
43°
42°
41°
40°
39°
FLEMISH CAP
VIRGIN ROCKS
GRAND BANKS
971.0
5052
5060
971.0
5044
971.0
5033
971.1
5042
5032
971.1
5002
5023
971.1
971.1
971.2
971.3
971.4
971.5
5021
4995
971.2
5013
971.3
971.3
971.5
971.5
971.7
5012
5009
CURRENT CHART
FROM DATA COLLECTED 3 APRIL - 14 APRIL,1953

FIGURE 14.—Dynamic topography of the sea surface relative to the 1,000-decibar surface from data collected 3–14 April 1953. Oceanographic station positions are indicated and the station numbers given at turning points.

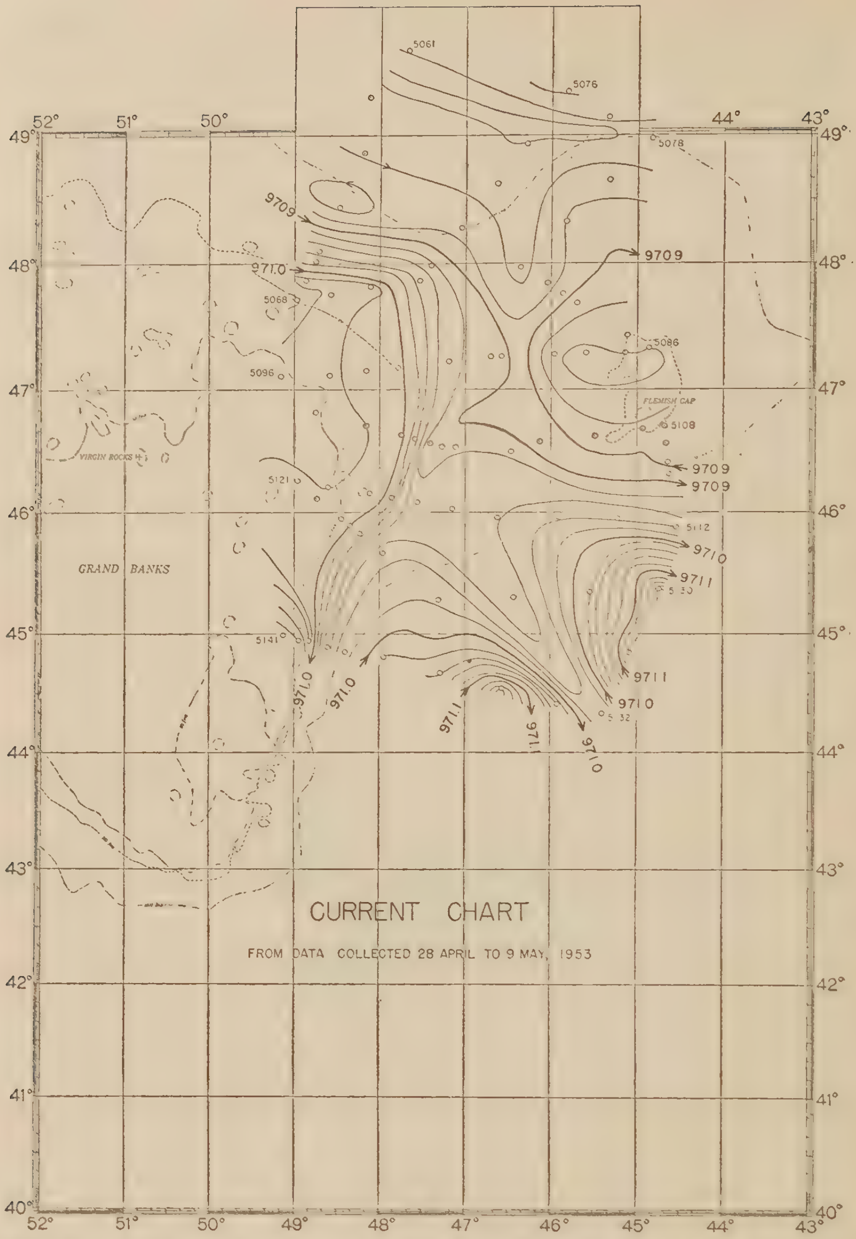
CURRENT CHART
FROM DATA COLLECTED 28 APRIL TO 9 MAY, 1953
GRAND BANKS
VIRGIN ROCKS
FLEMISH CAP
9709
971.0
9710
9711
971.1
5061
5076
5078
5068
5096
5086
5108
5121
5112
5130
5141
5132
52°
51°
50°
49°
48°
47°
46°
45°
44°
43°
42°
41°
40°

FIGURE 15.—Dynamic topography of the sea surface relative to the 1,000-decibar surface from data collected 28 April–9 May 1953. Oceanographic station positions are indicated and the station numbers given at turning points.

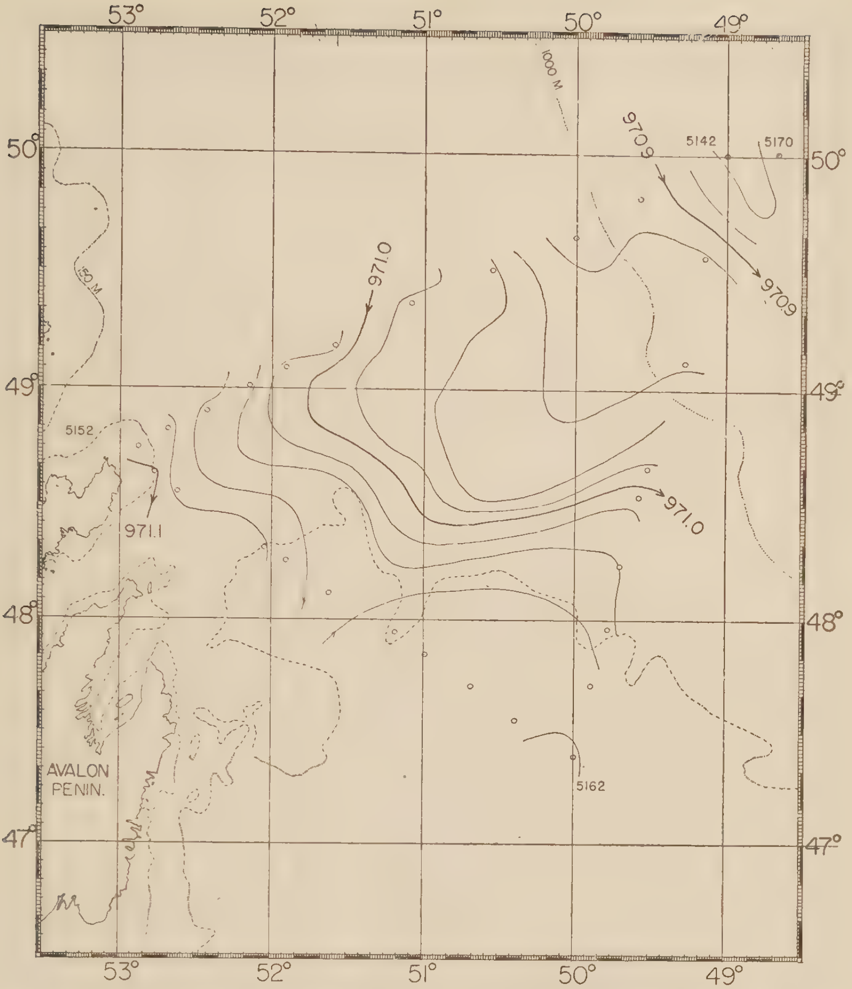
53°
52°
51°
50°
49°
1000 M
9709
5142
5170
50°
971.0
150 M
49°
5152
971.1
971.0
48°
5162
AVALON PENIN.
47°

FIGURE 16.—Dynamic topography of the sea surface relative to the 1,000-decibar surface from data collected 27–31 May 1953. Oceanographic station positions are indicated and the station numbers given at turning points.

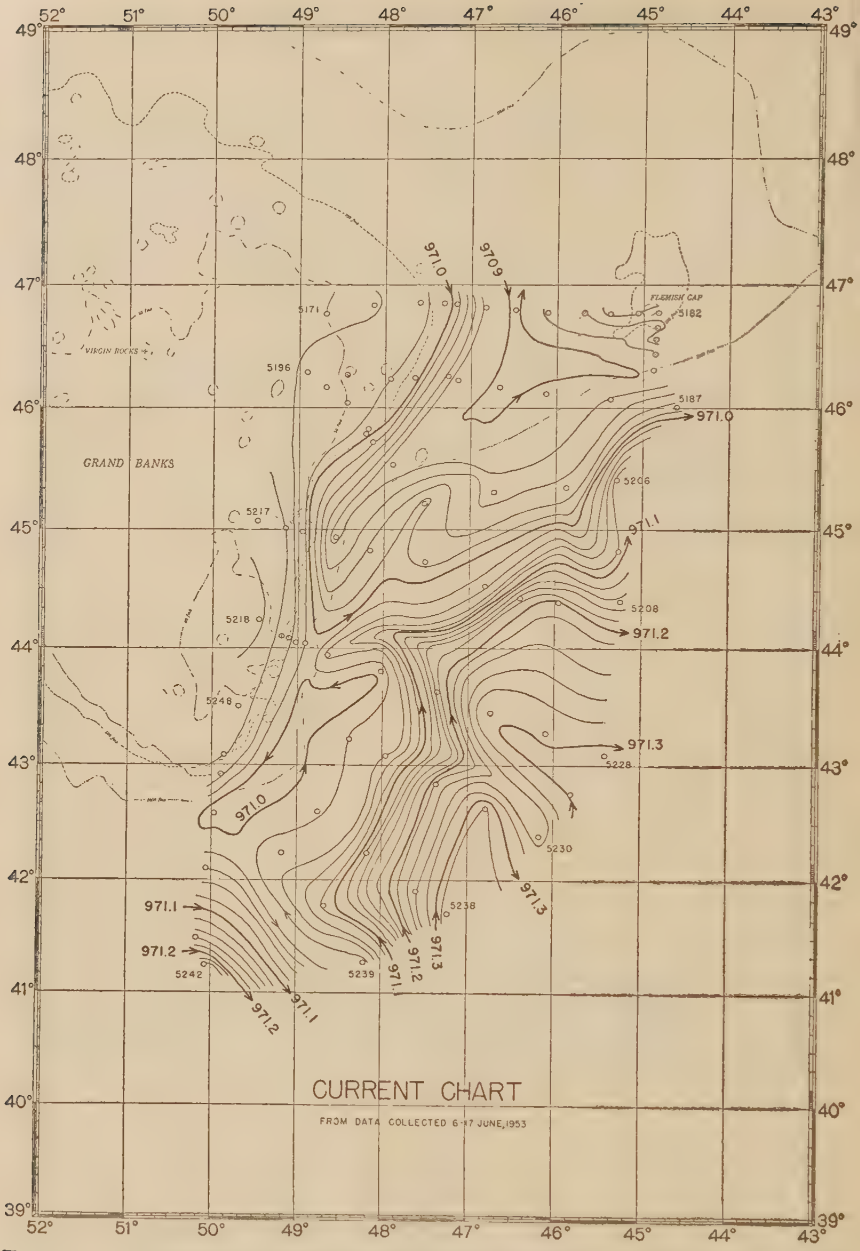
52°
51°
50°
49°
48°
47°
46°
45°
44°
43°
49°
48°
47°
46°
45°
44°
43°
42°
41°
40°
39°
VIRGIN ROCKS
FLEMISH CAP
GRAND BANKS
971.0
9709
5171
5182
5196
5187
971.0
5206
5217
971.1
5218
5208
971.2
5248
971.3
5228
971.0
5230
971.3
971.1
5238
971.2
5242
5239
971.1
971.2
971.3
971.1
971.2
CURRENT CHART
FROM DATA COLLECTED 6-17 JUNE, 1953

FIGURE 17.—Dynamic topography of the sea surface relative to the 1,000-decibar surface from data collected 6–17 June 1953. Oceanographic station positions are indicated and the station numbers given at turning points.

and of these 12 are regarded as useable in comparing the TD measurements with reversing thermometers.

As in previous years routine salinity determinations were made with a Wenner salinity bridge. Standardizations were made with water from an oil-sealed carboy of sea water and at least twice during each run a sample of Copenhagen standard water of the batch P17 was measured as an unknown. At the end of each survey these measurements of Copenhagen water were used to correct all the salinities measured during the survey. For each of the surveys, including the postseason cruise, these indicated corrections were less than 0.005°/₀₀ and so no corrections have been made.

Figures 14 through 17 show, in chronological order, the dynamic topography of the sea surface found during the four surveys made during the season. Figure 14 shows the Labrador Current along the eastern edge of the Grand Banks.to have had a subnormal surface speed but increasing to swifter than usual at the Tail of the Banks. Bergs entering this pattern from the north might reach the Tail of the Banks and drift thence westward to longitudes of between 50°30′ W., and 51°50′ W., thence southward to about 42° N., and thence easterly. There was little liklihood of bergs reaching farther south than about 41°45′ N. At the southern edge of the surveyed area the Atlantic Current was flowing with considerable strength and the height of 971.776 dynamic meters at station 5012 is probably the highest that has been found by the ice patrol in the area covered by this survey. An associated feature of figure 14 is that the pool of cold mixed water, which has frequently been found extending southeasterward from the Tail of the Banks, was of smaller extent than usual. Bergs entering the area from the north and crossing the 46th parallel between about 47° W., and 47°30′ W., could have been taken in a southeasterly direction to positions of potential hazard to the North Atlantic Track Agreement tracks between about 45° N., and 46° N.

The areas covered by the first and second surveys overlap between about 44°30′ N., and 46° N., but this is insufficient to permit following particular meanders with certainty. In the Labrador Current shown in figure 15 the southward path to the Tail of the Banks apparently remained unobstructed for those bergs which might have passed the 47th parallel between longitudes of about 47°15′ W., and 48°00′ W. As in the first survey, figure 15 shows the possibility of bergs entering the area from the north proceeding in a general southeasterly direction to menace the Track Agreement tracks between about 45° N., and 46° N. In fact a weak clockwise eddy centered over the northern part of Flemish Cap appeared to be the only obstruction to the eastward branching of the Labrador Current between latitudes 46° N., and 49° N. Cold mixed water covered all of the area except those margins in the southeastern part of the surveyed area where the dynamic heights were greater than about 971.1 dynamic meters.

Figure 16 shows the dynamic topography found during the third survey. It should be borne in mind that in surveys of the Bonavista triangle the middle part of the triangle is too distant from oceanographic stations to permit of accurately estimating the details of the dynamic topography there. In this particular survey there is also some uncertainty as to the longitude of the southeastern section of the triangle. Just prior to this occupation of the triangle an intense low barometric pressure system persisted for several days in the area of the triangle. It was anticipated that its effect would be to weaken the eastern branch of the Labrador Current and strengthen the western branch. Figure 16 verifies this in part. However, this portion of the current which was diverted westward toward Cape Bonavista seemingly did not continue southward along the Avalon Peninsula but recurved eastward along the northern slope of the Grand Banks.

Only 6 days separated the last station of the third survey and the first station of the fourth survey. Figures 16 and 17, therefore, are more nearly two parts of the same synoptic picture than is usually the case with two successive surveys. Comparison of figures 15 and 17 in the area between 45° N., and 47° N., shows the changes taking place during the approximately 1-month interval. The contour lines took on a more regular shape in the later survey and the meanders in this area seem to be less noticeable although many of the features, somewhat displaced, are recognizable in each figure. At about 44° N., figure 17 shows a westward incursion of Atlantic Current water which accompanied the northeastward recurvature of a major part of the Labrador Current north of this latitude. South of 44° N., the cold mixed water pool was considerably reduced in area compared to the first survey although it extended southward very nearly to 41° N. The dynamic heights in margins of the Atlantic Current in the southeastern edge of the surveyed area were not as high as usual.

The volume of flow, mean temperature, and heat transport of the Labrador Current have been determined for each of 19 sections occupied during the 1953 season and postseason cruises. Some of these sections have been occupied in other years, and in the case of sections T, U, and W, numerous occupations have provided the data for determining rough approximations to normal seasonal variation curves. These have been published in bulletin number 36 of this series. Less is known of the seasonal variation in the Labrador

Current at the Bonavista triangle. However, 12 occupations of this triangle during the 6-year period 1948–53 are now available and the results are summarized in table 1. In this table as well as in subsequent tables, figures, and discussion the units are as follows: volume of flow, 1 million cubic meters per second; mean temperature and minimum observed temperature, degrees Centigrade; heat transport, 1 million cubic meter degrees C per second. In table 1 some of the 1950 values appear in parentheses to indicate a greater than usual amount of estimation. In the first 1950 occupation a large change occurred during the occupation of the southeast section of the triangle. In the second 1950 occupation the southeast section was not occupied and the values were derived by difference. In the third 1950 occupation the southwest section was not occupied but it is estimated from the other two sections that none of the Labrador Current was following the western branch.

The northwest section is considered to include the total Labrador Current off Cape Bonavista, the southwest section including the western branch and the southeast section including the eastern branch. Thus the volume and heat transports are determined twice for any occupation of the triangle, once on entering the triangle (northwest side) and once on leaving the triangle (tne sum of the southwest and southeast sides). The values under the heading "mean triangle" are the means of these two determinations for volume and heat transport, while the mean temperature is derived as the mean heat transport divided by the mean volume transport.

In figure 18 the individual values given in table 1 have been plotted against time of year and identified by the last two digits of the year of observation. In all years where more than one occupation occurred the rate of change was computed. Giving each year equal weight, mean values, assumed to apply at the mean date and adjusted by the mean rate, were taken as approximate seasonal normals. The inconsistencies appearing in table 1 and figure 18 may be taken as an indication of the limitations of the observations and the methods employed in their reduction.

These seasonal normals have been used for comparison with the 1953 occupations of the Bonavista triangle. In the case of the South Wolf Island section across the Labrador Current, although there have been 16 occupations in as many different years from 1928 to 1953, nearly all have been made at about the same time of year and no attempt has been made to derive seasonal variation curves. Instead the 1953 results have been compared with average values. For the section F (between the Grand Banks and Flemish Cap) and the sections

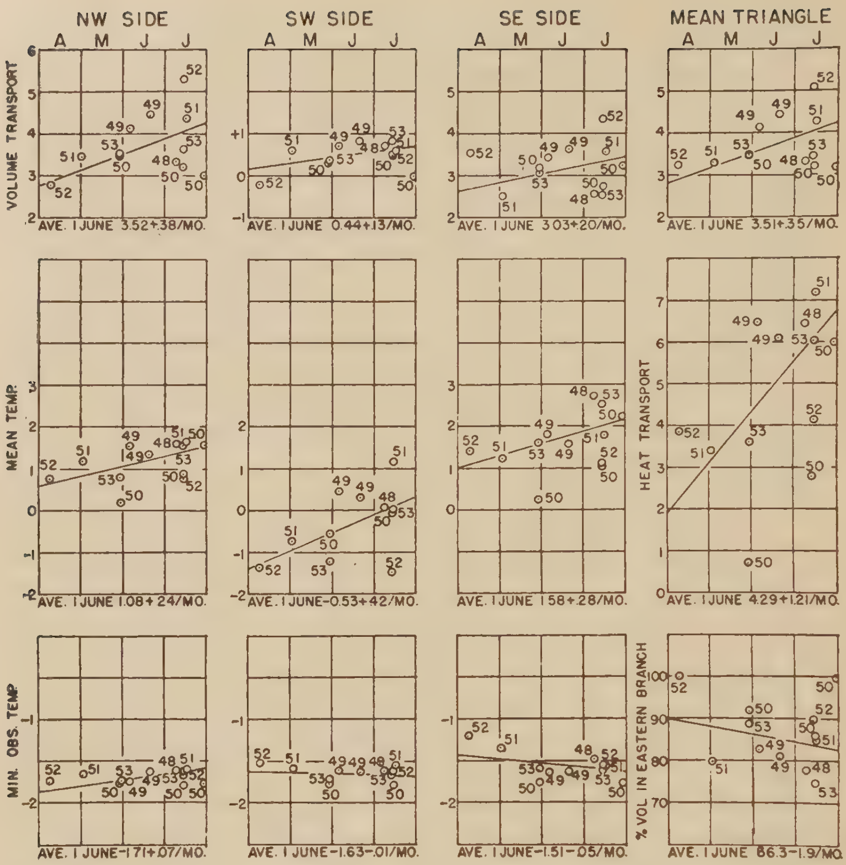

Figure 18.—Seasonal variations in the elements of the Bonavista triangle.

G and H (between section F and the Bonavista triangle) too few occupations have been made even to derive average values. Table 2 presents a summary of the velocity sections across the Labrador Current occupied in 1953 and comparisons with normal values where available. Sections T, U, and W are located as follows: T extending southeasterly from about 46°20′ N., 49°00′ W.; U extending eastward from the Grand Banks at about 45° N.; W extending southward from the Grand Banks at about 50° W.

Table 1.—SUMMARY OF VELOCITY SECTIONS AT BONAVISTA TRIANGLE

	1948	1949		1950			1951		1952		1953	
NW section:												
Volume	3.35	4.13	4.44	3.47	3.21	3.01	3.48	4.39	2.77	5.31	3.58	3.63
Mean Temperature	1.60	1.54	1.38	0.21	0.87	1.56	1.19	1.67	0.78	0.76	0.79	1.57
Heat	5.36	6.35	6.13	0.71	2.80	4.70	4.15	7.33	2.16	4.03	2.84	5.71
Minimum Temperature	−1.59	−1.73	−1.62	−1.76	−1.78	−1.76	−1.64	−1.58	−1.73	−1.63	−1.73	−1.65
SW section:												
Volume	0.73	0.72	0.84	0.29	0.46	(0.00)	0.61	0.61	*−0.20	0.48	0.39	0.83
Mean Temperature	0.07	0.47	0.30	−0.58	−0.05		−0.71	1.17	−1.34	−1.47	−1.27	0.00
Heat	0.51	0.34	0.26	−0.17	−0.02		−0.43	0.72	−0.26	−0.70	−0.49	0.00
Minimum Temperature	−1.61	−1.61	−1.62	−1.77	−1.78		−1.58	−1.56	−1.52	−1.61	−1.70	−1.67
SE section:												
Volume	2.55	3.46	3.63	(3.18)	(2.75)	3.26	2.52	3.55	3.56	4.36	3.02	2.52
Mean Temperature	2.75	1.82	1.60	(0.28)	(1.03)	2.24	1.23	1.79	1.42	1.12	1.62	2.52
Heat	7.01	6.30	5.81	(0.88)	(2.82)	7.30	3.09	6.35	5.08	4.90	4.89	6.34
Minimum Temperature	−1.47	−1.63	−1.61	−1.75		−1.75	−1.33	−1.57	−1.20	−1.54	−1.59	−1.62
Mean triangle:												
Volume	3.32	4.15	4.46	(3.47)	(3.21)	(3.14)	3.30	4.28	3.26	5.08	3.50	3.49
Heat	6.44	6.50	6.10	(0.71)	(2.80)	(6.00)	3.40	7.20	3.85	4.12	3.62	6.02
Mean Temperature	1.94	1.57	1.37	(0.21)	(0.87)	(1.91)	1.03	1.68	1.18	0.81	1.03	1.72
Percent in E. Branch	78	83	81	92	86	100	80	85	100	90	89	75

*0.20 northeast.

Table 2.—SUMMARY OF VELOCITY SECTIONS ACROSS LABRADOR CURRENT OCCUPIED IN 1953

Section	Volume transport			Mean temperature			Minimum observed temperature			Heat transport		
	1953	Normal	Anomaly	1953	Normal	Anomaly	1953	Normal	Anomaly	1953	Normal	Anomaly
First survey:												
T	1.28	3.35	−2.07	0.81	1.95	−1.14	−1.55	−1.40	−0.15	1.04	6.53	−5.49
U	2.96	5.28	−2.32	0.92	1.53	−0.61	−1.36	−1.21	−0.15	2.72	8.08	−5.36
W	6.06	4.25	+1.81	2.06	2.07	−0.01	−0.86	−0.51	−0.35	12.48	8.80	+3.68
Second survey:												
H	2.86			0.86			−1.54			2.46		
G	3.15			1.53			−1.61			4.82		
F	1.43			1.71			−1.33			2.44		
T	0.65	3.38	−2.73	0.76	1.82	−1.06	−1.44	−1.38	−0.06	0.49	6.15	−5.66
U	3.29	4.55	−1.26	1.38	2.10	−0.72	−1.26	−1.18	−0.08	4.55	9.56	−5.01
Third survey:												
NW	3.58	3.50	+0.08	0.79	1.07	−0.28	−1.73	−1.71	−0.02	2.84	3.75	−0.91
SW	0.39	0.43	−0.04	−1.27	−0.56	−0.71	−1.70	−1.63	−0.07	−0.49	−0.24	−0.25
SE	3.02	3.02	0.00	1.62	1.56	+0.06	−1.59	−1.51	−0.08	4.89	4.71	+0.18
Fourth survey:												
F	2.74			2.85			−1.18			7.80		
T	1.61	2.67	−1.06	1.88	1.83	+0.05	−0.67	−1.55	+0.88	3.02	4.89	−1.87
U	3.73	3.54	+0.19	1.97	2.22	−0.25	−0.41	−1.22	+0.81	7.36	7.86	−0.50
W	2.81	4.16	−1.35	4.10	3.45	+0.65	0.74	−0.50	+1.24	11.55	14.35	−2.80
Postseason:												
NW	3.63	4.06	−0.43	1.57	1.42	+0.15	−1.65	−1.61	−0.04	5.71	5.76	−0.05
SW	0.83	0.62	+0.21	0.00	0.07	−0.07	−1.67	−1.64	−0.03	0.00	0.04	−0.04
SE	2.52	3.31	−0.79	2.52	1.98	+0.54	−1.62	−1.58	−0.04	6.34	6.55	−0.21
South Wolf Island	5.02	4.45	+0.57	2.43	2.48	−0.05	−1.21	−1.47	+0.26	12.19	11.60	+0.59

Table 2 shows the volume of flow of the Labrador Current to have been decidedly subnormal at sections T and U during the first survey. During the second survey, while both sections were still below normal, section U had begun to recover and by the fourth survey was about normal. The fourth survey also showed partial recovery at section T. The unusually large volume at section W in the first survey is considered to be made up partly of recirculating mixed water some of which was also present at section U.

The volume transport was close to normal at each of the sections of the Bonavista triangle during the third survey but did not follow the normal seasonal increase so that during the postseason cruise the volume at the triangle was subnormal. The significance of the positive anomaly at the southwest section during this occupation is that a smaller than normal proportion of the current was following the eastern branch. The dynamic topography at the sea surface found at the Bonavista triangle during the postseason cruise is shown in figure 19.

Of the other sections in the Grand Banks region only section F was occupied more than once. The increase in volume at this section between the second survey and the fourth survey is interpreted as meaning that part of the Labrador Current continued farther south before recurving to the northeast during the fourth survey than was the case during the second survey.

The mean temperatures were below normal at sections T and U during the first two surveys and near normal at the time of the fourth survey. At section W the mean temperature was near normal at the first survey and above normal during the fourth survey. The mean temperature at the Bonavista triangle was below normal during the third survey and above normal at the time of the postseason cruise. An exception to these general statements is that it will be noted that the mean temperature at the southeast section of the triangle during the third survey was about normal as was section T during the fourth survey. It will be remembered that the southeast section of the triangle represents the eastern branch and that the third and fourth surveys were close together in time of occupation. It is considered that the subnormal temperatures and volumes and their recoveries indicate an initial but decreasing deficiency in that component of the Labrador Current which is supplied by the West Greenland Current.

The minimum observed temperatures were slightly colder than but near normal during the first three surveys. The higher than normal minimum temperatures observed during the fourth survey at sections T, U, and W are looked upon as being the result of northeastward recurvature of Labrador Current water although this is not so clearly indicated by the volume transports. During the postseason cruise the minimum observed temperatures at the Bonavista triangle were close to normal. The circulation deduced from data in table 2 has

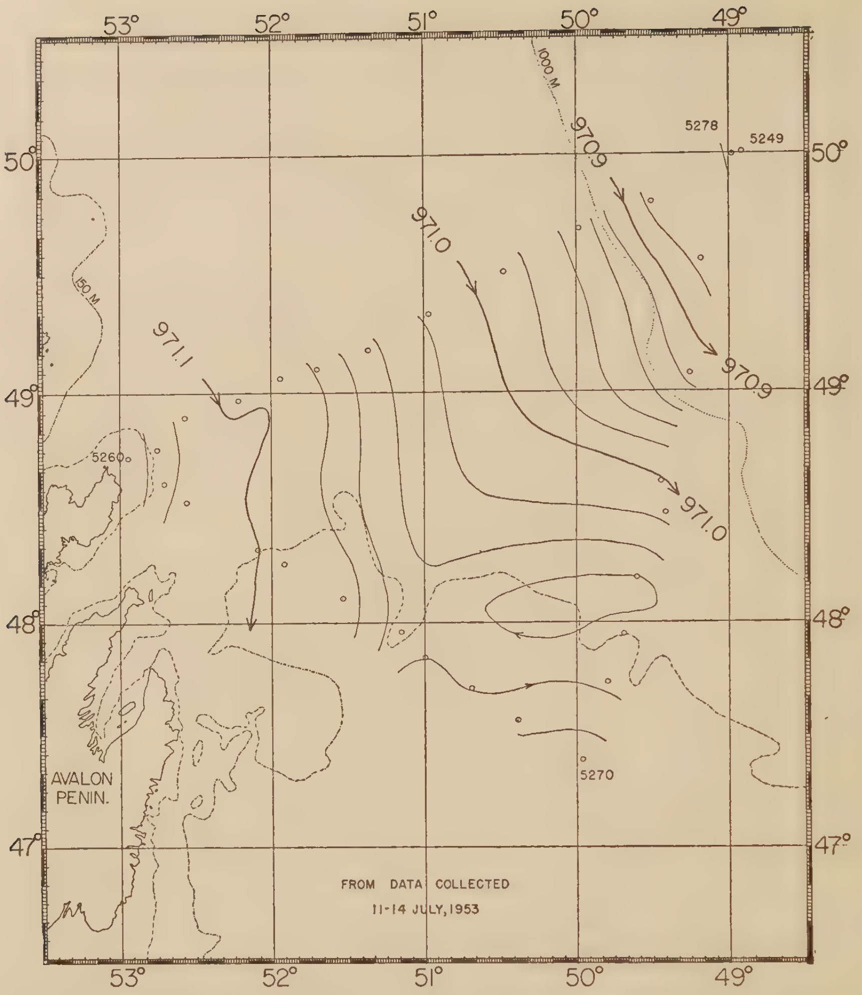
53°
52°
51°
50°
49°
50°
49°
48°
47°
1000 M.
970.9
5278
5249
971.0
150 M.
971.1
970.9
5260
971.0
AVALON
PENIN.
5270
FROM DATA COLLECTED
11-14 JULY, 1953

Figure 19.—Dynamic topography of the sea surface relative to the 1,000-decibar surface from data collected 11–14 July 1953. Oceanographic station positions are indicated and the station numbers given at turning points.

been shown schematically in figure 20. This figure will be referred to subsequently after consideration of the velocity section across the West Greenland Current off Cape Farewell.

Table 2 shows the Labrador Current off South Wolf Island during the postseason cruises to have been above average in volume and close to average in mean temperature. It is noted that not only was the minimum observed temperature about a quarter of a degree warmer than average, but it was 0.46° warmer than that at the Bonavista triangle occupied a few days earlier. An examination of the records shows that 1953 was not the only year during which the post-season cruise data included colder minima at the triangle than at the South Wolf Island section. Temperature minima and their cor-

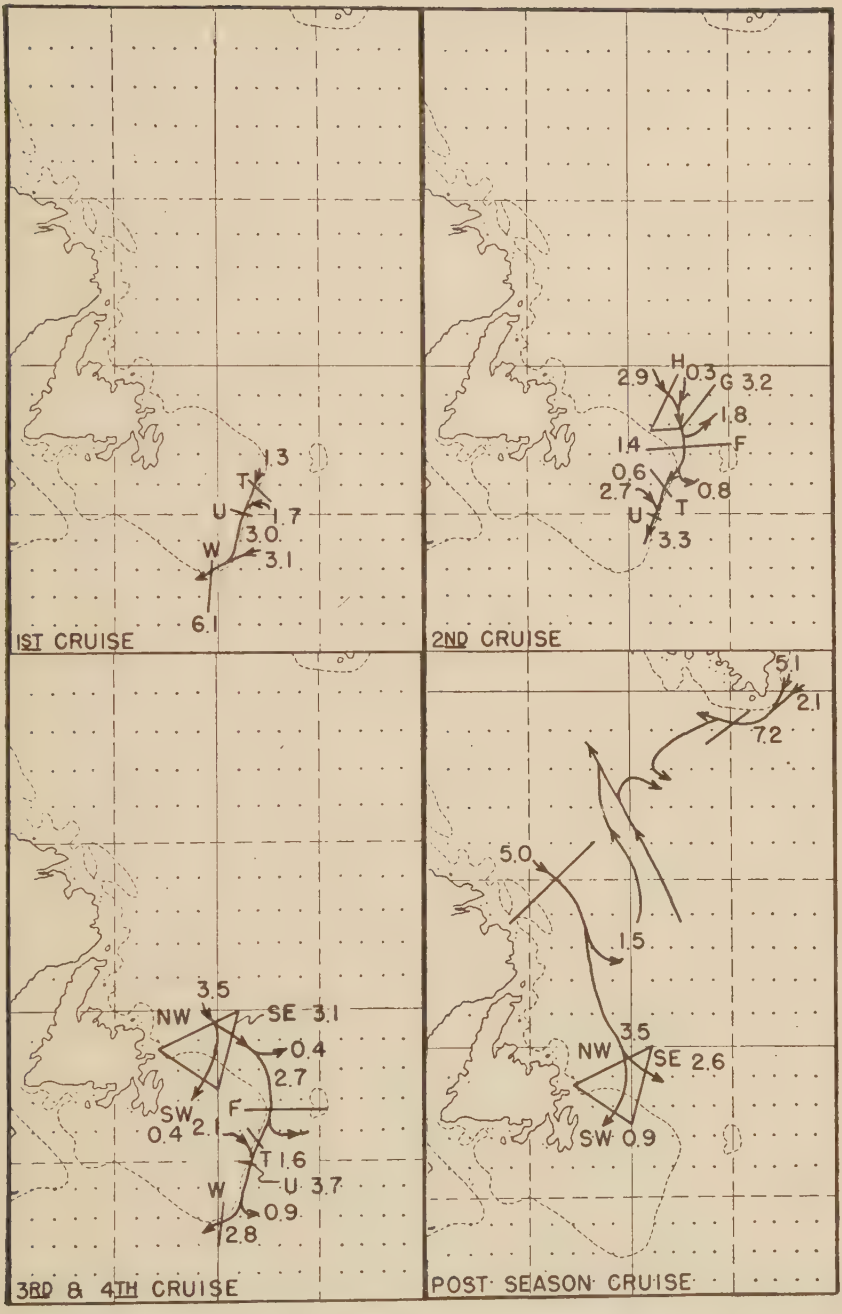
1.3
T
U
1.7
3.0
W
3.1
6.1
1ST CRUISE
2.9
H
0.3
G 3.2
1.8
1.4
F
0.6
2.7
0.8
T
U
3.3
2ND CRUISE
3.5
NW
SE 3.1
0.4
2.7
SW
0.4
2.1
F
T 1.6
U 3.7
W
0.9
2.8
3RD & 4TH CRUISE
5.1
2.1
7.2
5.0
1.5
3.5
NW
SE 2.6
SW 0.9
POST SEASON CRUISE

Figure 20.—Schematic representation of circulation deduced from sections occupied during 1953. Numerals indicate volume transport in units of cu.m/sec. × 10^{-6}.

responding observed salinities are tabulated below for all the years during which observations were made:

Year	South Wolf Island		Bonavista Triangle	
	Temperature	Salinity	Temperature	Salinity
1948	−1.55	32.72	−1.61	33.17
1949	−1.70	32.98	−1.62	33.28
1950	−1.68	32.82	−1.76	33.16
1951	−1.34	32.66	−1.58	33.00
1952	−1.68	32.78	−1.63	33.13
1953	−1.21	32.88	−1.67	33.06
Average	−1.53	32.81	−1.64	33.13

These years were not especially warm years, as the average minimum observed temperature for all 16 years during which the South Wolf Island section has been occupied is −1.47°. At both the South Wolf Island section and the Bonavista triangle the coldest water is found not far from the beach and at a depth of about 75 meters in the summer time. At such a depth there is no direct warming from the surface and certainly at the more southerly sections T and U in the Grand Banks region the normal minimum temperatures is essentially constant (±0.05°) from 1 April to 1 July. The great stability of the upper layers in summer time makes it improbable that the temperature minimum is much affected by the stirring of recent gales.

The summer time salinity distribution in a section across the Labrador Current with the isohalines inclined downward toward the beach indicates the seaward spreading of the realtively fresh coastal water at the surface and the compensating shoreward movement of the saltier deeper water. This screwing motion, with its associated upwelling along the beach must be decidedly affected (increased or decreased) by the occurrence of protracted periods of offshore or onshore winds.[2]) It is not known whether the process ever proceeds at such a rate that the disturbed isopycnals result in a north-flowing or counter current along the beach. In any case the transverse movements in themselves have little direct effect on the temperature minimum layer since the transverse movements take place above and below it. They might introduce saltier surface water and, by reducing the vertical salinity gradient and the stability, facilitate wind stirring to the depth of the summer time temperature minimum earlier in the fall with warmer temperatures.

Such an explanation would require that the salinities at the temperature minima be greater at the section with the warmer temperature minima. This, however, is not in accord with the observations. The above tabulation shows the average salinity at the temperature minimum at the South Wolf Island section to be about 1 percent less than at the Bonavista triangle. This suggests that the water found in the temperature minima at the South Wolf Island section in summer time were formed with the onset of cold weather in the autumn and the water at the temperature minima found at the Bonavista triangle in summer time were formed later in the winter after concentration of the salt through freezing and removal of about 75 to 100 cm. of ice. The reconcilliation of the two essential parts of such a mechanism (mixing or stirring to a depth of some 75 meters or more and the formation of an ice cover which would prevent wind stirring) is not difficult when it is remembered that the ice covering is frequently opened by storms through rafting and by the ice being blown seaward. Almost certainly such a mechanism would produce different minimum temperatures in different years and would probably produce different minimum temperatures in different geographical parts of the area of formation during the same year. Such irregularities are in accord with observations in the Grand Banks region. Assuming that the season during which such a mechanism would be operating would be limited to about 5 months of the year, September to April, the explanation leaves much to be desired in accounting for what happens in the other 7 months and would seem to require a seasonal variation in volume transport or that the area in which such stirring occurs extend over more than the distance traveled in a single year.

---

[2] In Trinity Bay, Newfoundland, it is understood to have sufficient effect on bottom temperatures to require adjustments in transatlantic cable operations.

From table 1 the mean heat transport at the Bonavista triangle just prior to the occupation of the South Wolf Island section was 5.98 and the mean volume transport was 3.96 for the 6 years 1948–53. During the same years at the South Wolf Island section the mean heat transport was 12.83 and the mean volume transport 5.13. By difference the mean heat and volume transports of that part of the Labrador Current which branches eastward between the South Wolf Island section and the Bonavista triangle are 6.85 and 1.17 which give a mean temperature of about 5.8°. It is considered that this mean temperature is too high but it emphasizes that it is the warmer offshore part of the current which is diverted from the Grand Banks by such branching.

Not all of the eastern branch of the Labrador Current as it leaves the Bonavista triangle passes through the valley between the Grand Banks and Flemish Cap, but part of it recurves northeastward. This recurvature is of considerable practical importance in determining the degree to which bergs endanger the steamer tracks passing southeastward of Flemish Cap. It has been noted qualitatively that as the ice season advances a larger proportion of bergs fail to move southward between the Grand Banks and Flemish Cap. The area of this recurvature, northward of Flemish Cap and the northeastern slope of the Grand Banks is one from which comparitively few data are available. Hence, even though the approximate normals for the Bonavista triangle as derived above and the approximate normals for section T are on very shaky foundations it is of interest to consider the difference between the normals for the volume transports of the eastern branch at the Bonavista triangle and at section T as an indicator of the seasonal change in the volume of the recurving current northward of the valley between the Grand Banks and Flemish Cap. The accuracy with which the two normals are known is too doubtful for the derived volume of recurvature to be considered reliable. The derived recurvature has been computed for each of 4 months, however, and the points plotted in figure 21. They show an increase of about a million cubic meters per second from the first half of the season to the second half. The negative sign of the early season points (meaning an additional contribution from the Labrador Sea), may not be real.

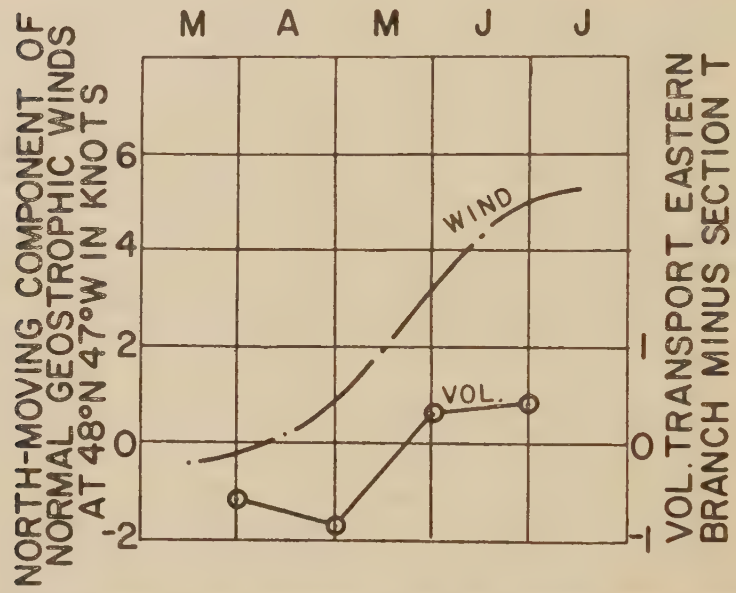

Figure 21.—Derived volume transport of part of Labrador Current recurving northeastward northward of Flemish Cap and north-moving component of normal geostrophic wind at 48° N., 47° W.

The explanation usually offered in the past for the presumed seasonal increase in this northeastward recurvature was the seasonal change in wind direction into the southwest. An examination of the monthly mean normal barometric pressure distribution shows not only a shift in direction but also an increase in gradient as the Iceland low moves westward and the Azores high moves northward. The geostrophic wind has been scaled from these normal charts at 48° N., 47° W., and the south (north-moving) component has been plotted in figure 21. Although in the case of the Labrador Current factors directly effecting density distribution are of greater relative importance than in many ocean areas where the winds play a dominant part in determining the currents, the wind does have an important effect in modifying the Labrador Current. The magnitude of the component of the goestrophic wind shown in figure 21 is not spectacular but its seasonal increase is in qualitative agreement with the northeastward diversion of a part of the Labrador Current and with the observed behavior of late-season bergs.

The 14 usable traces obtained from the TD and mentioned earlier in the description of instruments and methods are reproduced in figures 22 to 35. Superimposed on the traces are the temperatures obtained with reversing thermometers attached to the wire during the TD cast. The reversing thermometer temperatures are connected by broken lines. The solid lines are drawn through values of σ_t computed from the observed salinities and the reversing thermometer temperatures. While there has accumulated a considerable mass of data from bathythermograph casts and although the BT is a rapid response instrument it is not very stable and to date has been limited in depth range to about 275 meters. It is considered doubtful that the BT is reliable to the desired precision of 0.1° but we are hopeful that even with the experimental model of the TD used such a precision was attained. Figures 22 to 35, then, represent the first reliable subsurface temperature data obtained with a rapid response instrument between depths of 275 and 1,500 meters and probably between the surface and 1,500 meters. The precision with which the TD recorded depth was not as satisfactory, not because of any inherent weakness in design but simply because the windings of the Schaevitz transformer were mounted on a shaft with a press fit instead of being rigidly pinned and the friction was not sufficient to prevent accidental rotation of the windings with respect to the instrument thus producing fortuitous shifts of the atmospheric pressure position of the drum carrying the trace.

The traces can be grouped as coming from four general geographical areas: figures 22–24 are from the area southwest of the Tail of the Banks; figures 25–28 are from the area near the offshore corner of the Bonavista triangle; figures 29 and 30 are from south of Flemish Cap; and figures 31–35 are centered around the 45th parallel east of the eastern slope of the Grand Banks. The first group involve multiple lowerings: to approximately 100, 300, and 1,500 meters wire length in the case of figure 22; to 300, 500, 1,170, and 1,596 in the case of figure 23; and to 300, 1,506 and 300 in the case of figure 24. Thus there should be in figure 22 for example, 6 traces in the upper 100 meters, 4 traces from 100 to 300 meters and 2 traces from 300 to 1,500 meters. In the other figures there are only the downtrace and the uptrace except for figure 25 where various lowerings were made preliminary to

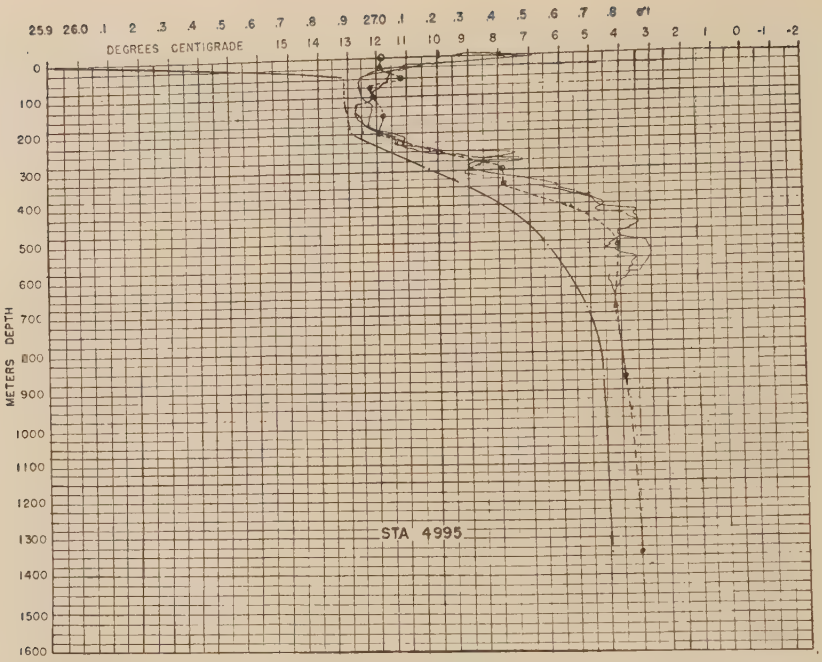

FIGURE 22.—Temperature trace of TD at station 4995; 3 April 1953; 42°04.5′ N., 51°53′ W. In figures 22–35 the temperatures by reversing thermometers have been superimposed and connected by a broken line. The solid lines connect values of σ_t computed from reversing thermometer temperatures.

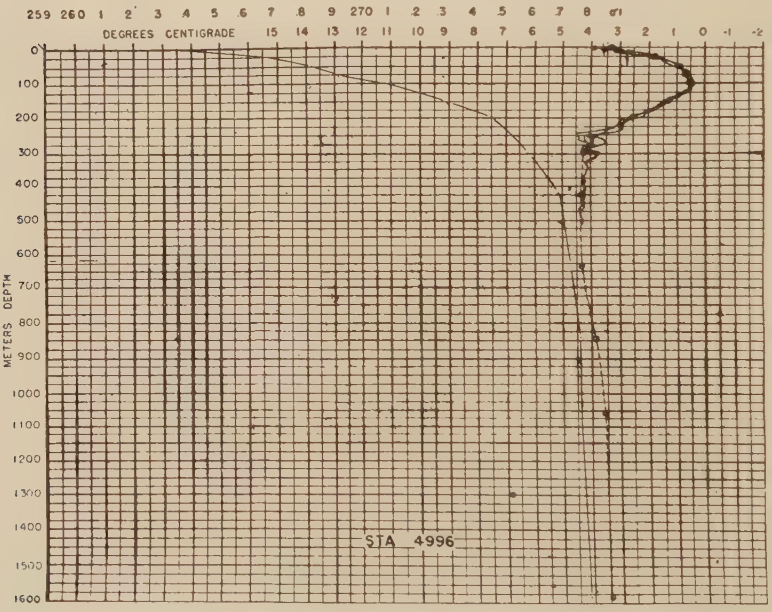

FIGURE 23.—Temperature trace of TD at station 4996; 3 April 1953; 42°01′ N., 50°57′ W.

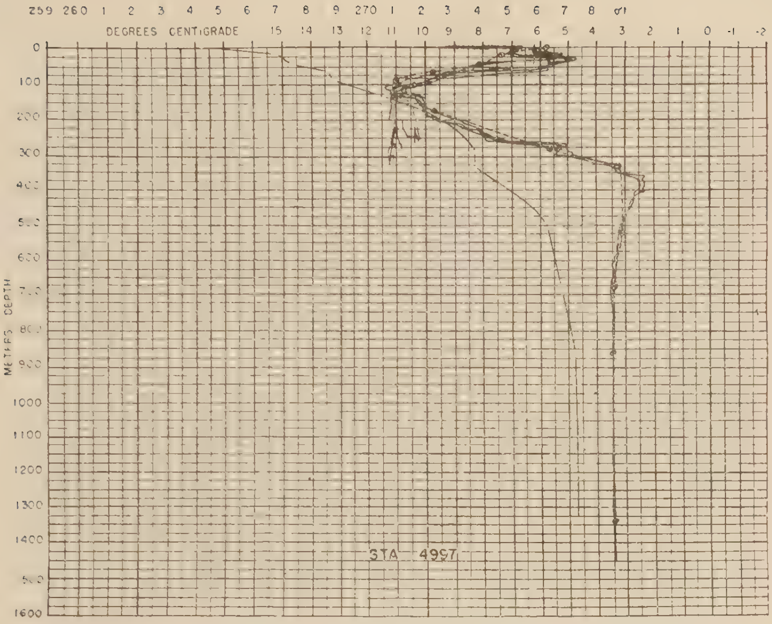

Figure 24.—Temperature trace of TD at station 4997; 3 April 1953; 42°21′ N., 51°31′ W.

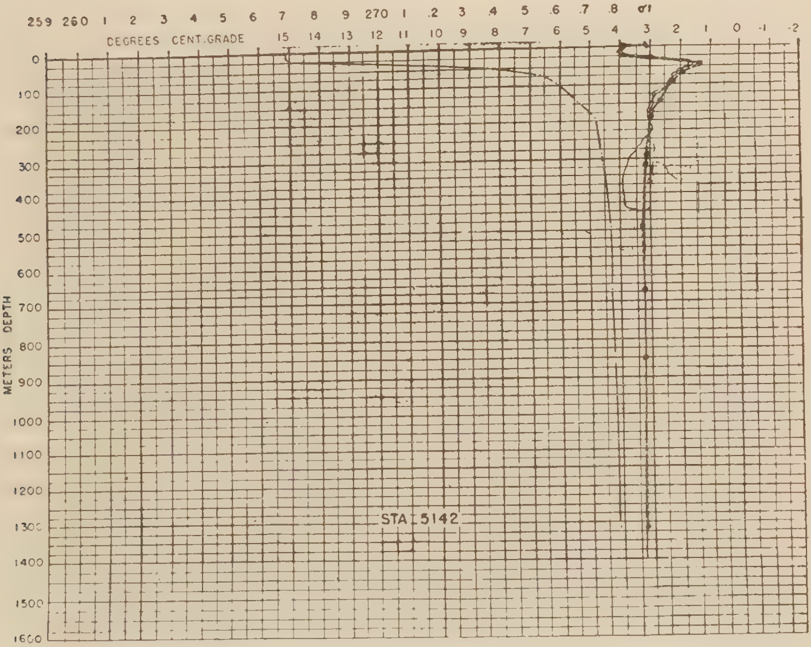

Figure 25.—Temperature trace of TD at station 5142; 27 May 1953; 50°00′ N., 49°00′ W.

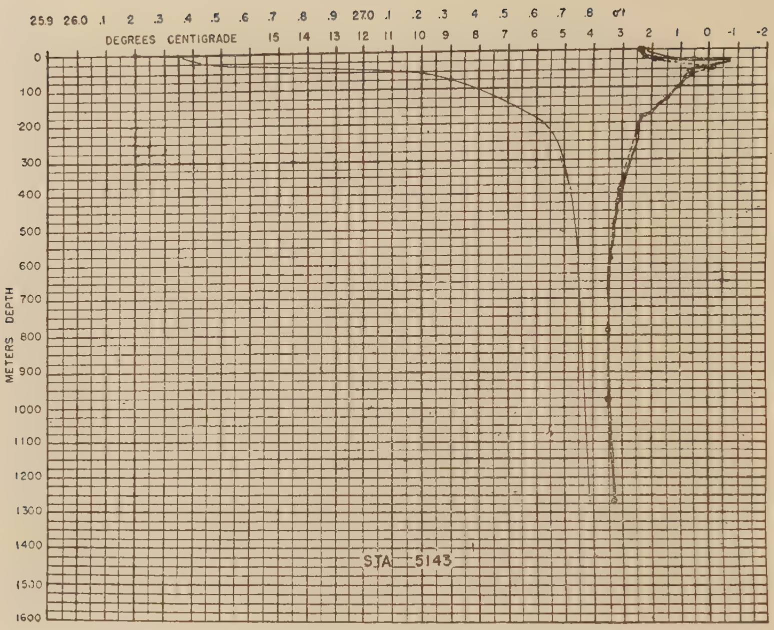

Figure 26.—Temperature trace of TD at station 5143; 28 May 1953; 49°49′ N., 49°34′ W.

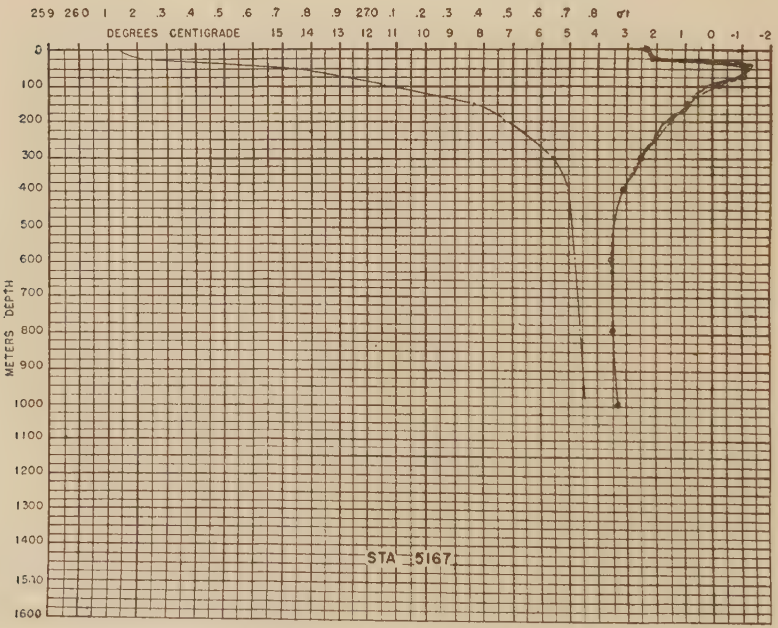

Figure 27.—Temperature trace of TD at station 5167; 30 May 1953; 48°40′ N., 49°31′ W.

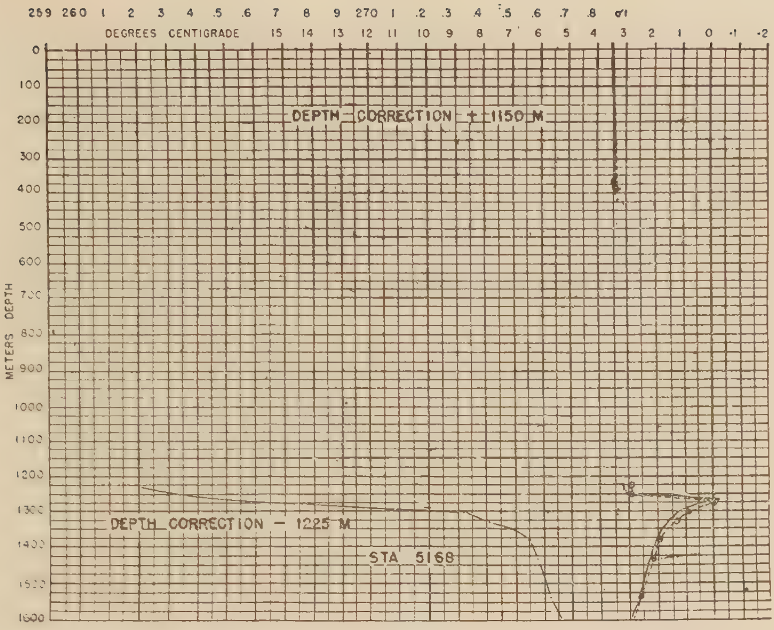

FIGURE 28.—Temperature trace of TD at station 5168; 30 May 1953; 49°07′ N., 49°16′ W.

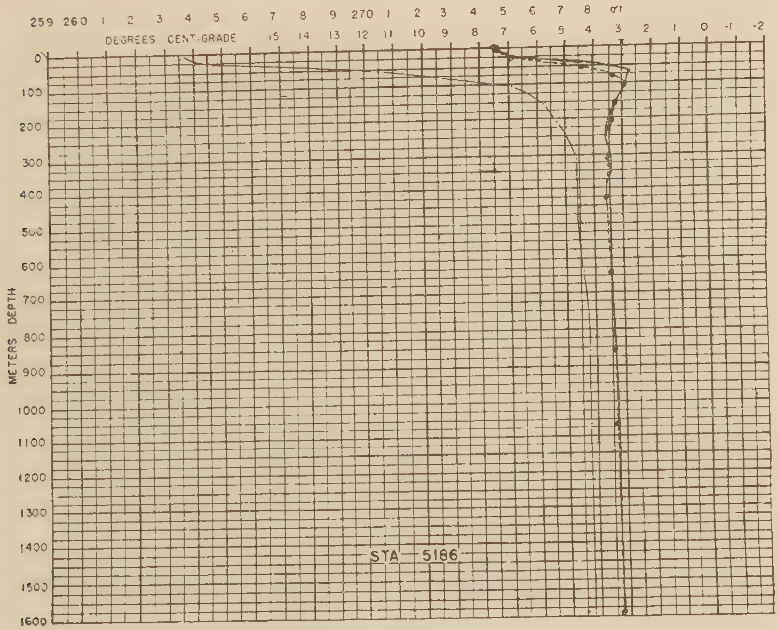

FIGURE 29.—Temperature trace of TD at station 5186; 7 June 1953; 46°19.5′ N., 44°54′ W.

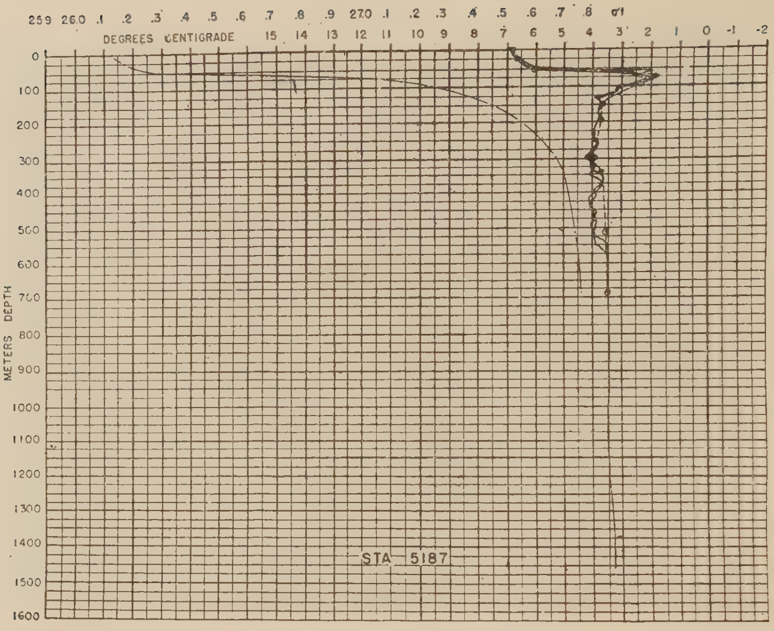

FIGURE 30.—Temperature trace of TD at station 5187; 7 June 1953; 46°01′ N., 44°37′ W.

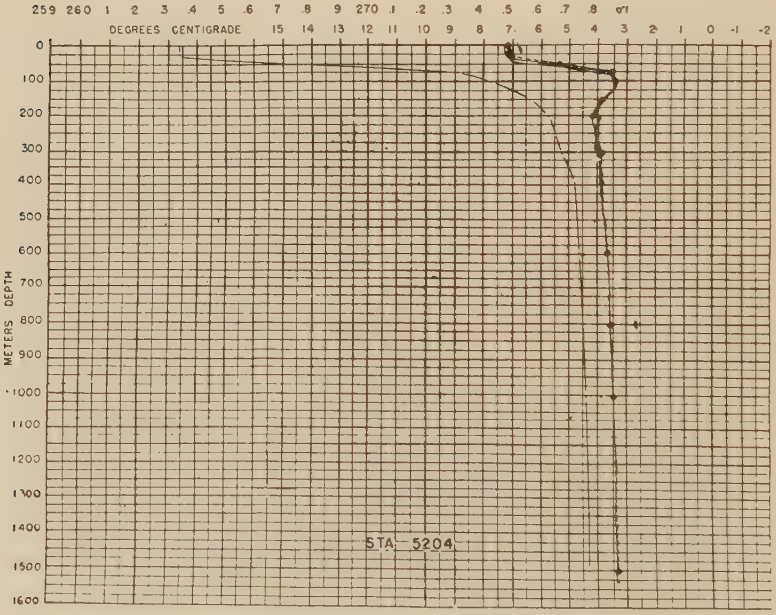

FIGURE 31.—Temperature trace of TD at station 5204; 9 June 1953; 45°19′ N., 46°44′ W.

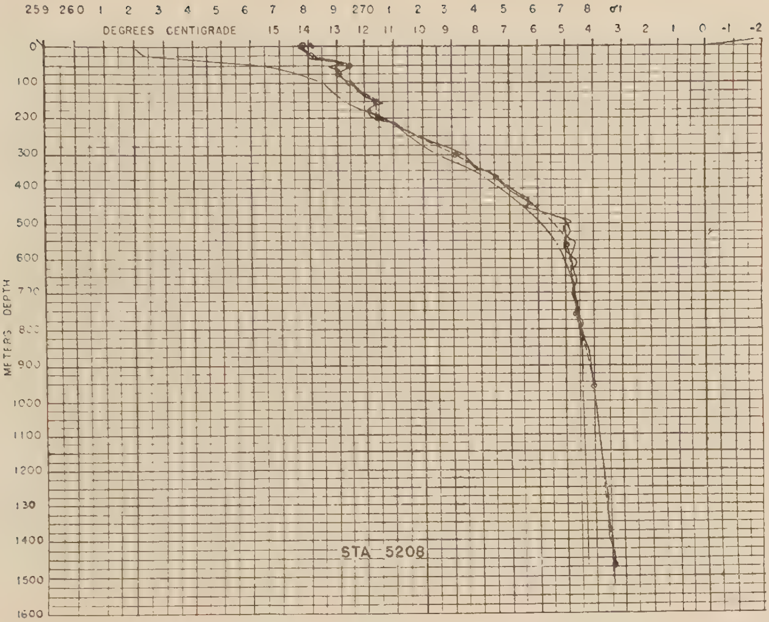

FIGURE 32.—Temperature trace of TD at station 5208; 10 June 1953; 44°24.5 N., 45°15′ W.

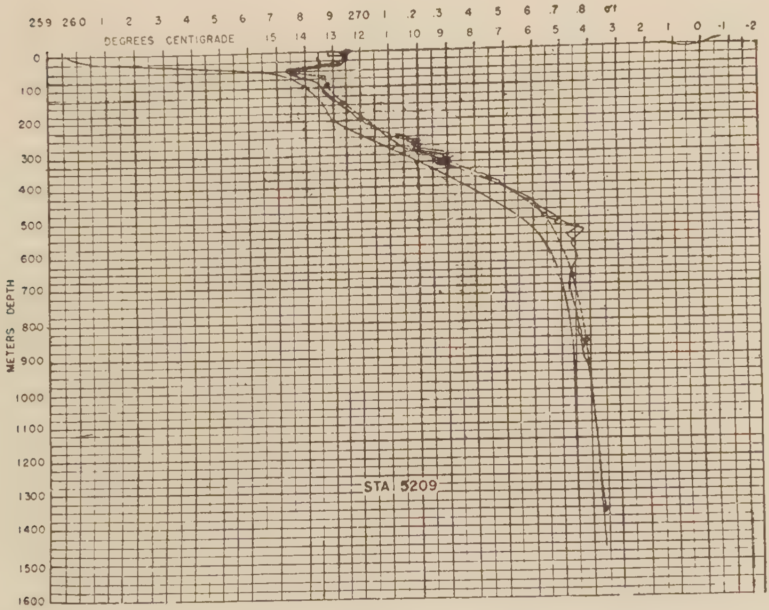

FIGURE 33.—Temperature trace of TD at station 5209; 10 June 1953; 44°24′ N., 45°58′ W.

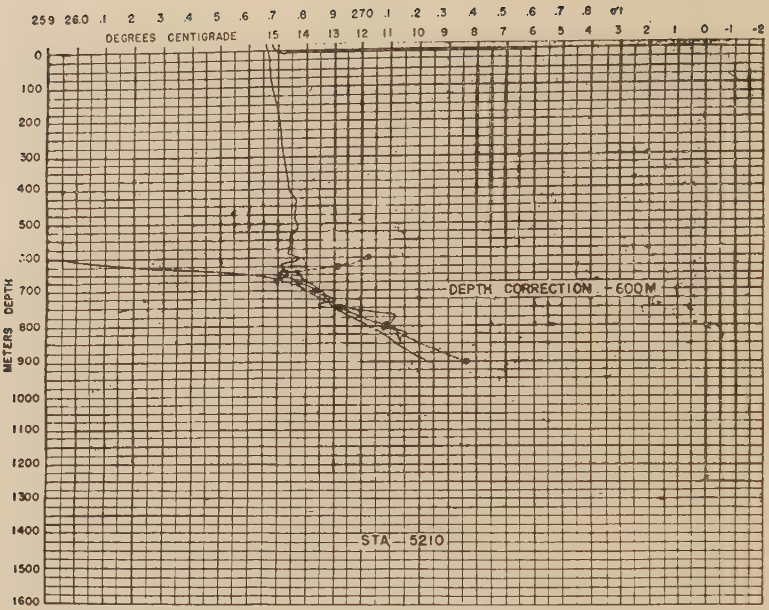

FIGURE 34.—Temperature trace of TD at station 5210; 10–11 June 1953: 44°26′ N., 46°24′ W.

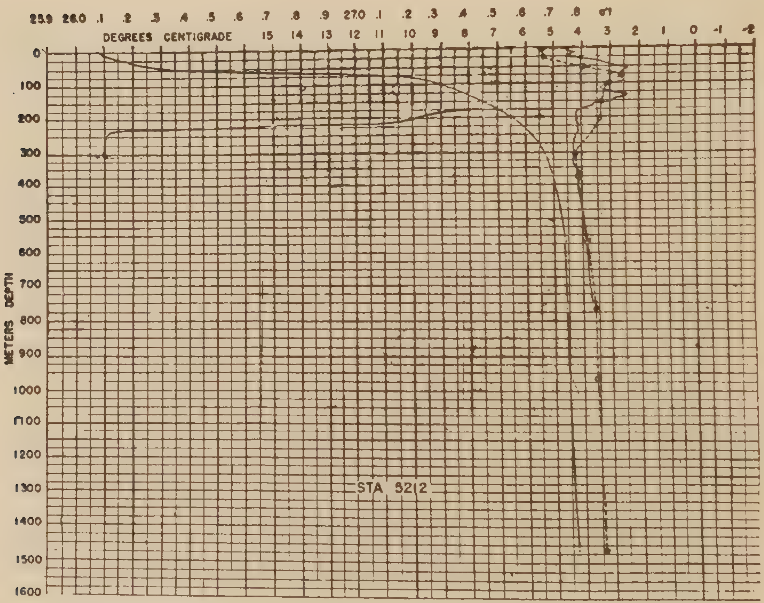

FIGURE 35.—Temperature trace of TD at station 5212; 11 June 1953; 44°43.5′ N., 47°32′ W.

the cast with the reversing thermometers; in figure 35 where the record is interpreted as indicating failure to extend the downtrace after reaching about 750 meters with no uptrace; and in figure 32 where the trace cannot be followed beyond about 230 meters on the downtrace.

Where the uptrace and downtrace are similar in shape but do not coincide such as at the secondary minimum and maximum at 250 and 325 meters in figure 22 the reason may be time lag in the instrument (slow response) or time variation in the temperature of the water. However, if it were due to slow response of the instrument the uptrace and downtrace would not coincide as they do at such abrupt changes as the temperature minimum at about 65 meters in figure 29. Also such temperature differences as are shown by the two traces in figure 24 at the temperature minimum at 375 meters cannot be explained by slow response of the instrument. As the area of operation is one of great contrasts possibly some of the discrepancies are the recording of geographical (horizontal) differences. Most of the differences between the uptraces and downtraces, however, are considered to be the result of time variations such as would be produced by internal waves since there are numerous cases in which the uptrace and the downtrace are both higher or both lower than the temperature indicated by reversing thermometer. As the reversing thermometer is a slow response instrument which gives a reading depending on the average temperature of its surroundings for the several minutes prior to its reversal, cases in which the temperature by reversing thermometer is not included between the traces are indicative of short period internal waves where the period is of the order of magnitude of the length of time required for the reversing thermometer to attain equilibrium. Where the reversing thermometer temperature is included between the traces there is no indication as to the length of period of the internal waves involved.

The temperature differences between the uptraces and downtraces and the reversing thermometer readings are small in the deeper water. Geographically, it would seem that the large variations extend deeper at stations in the margins of the Atlantic Current than at stations in Labrador Current water with intermediate depths at stations in mixed water. This apparent difference may not be real, however, since the vertical temperature gradient at a given depth is greater in Atlantic Current water than in Labrador Current water and for a given amplitude of vertical movement the temperature changes would be greater.

Inasmuch as the internal wave involves a periodic vertical displacement of water the result is not only a fluctuation in temperature at a particular point but presumably also a fluctuation in salinity and density with a resulting undulation of the dynamic topography of the sea surface and of the assumed motionless surface to which it is referred. The work of Fjeldstad, Defant, and others[3] indicates that an unlimited number of internal waves of differing phase, period and order may be present in the usual sea condition of continuous vertical density gradient. Such analyses as have been made emphasize the waves of longer period, of the order of magnitude of several hours. This may be because of the sampling methods which so far have been available. Figures 22 to 35 indicate that much shorter period waves, of the order of magnitude of several minutes, also are present. For the study of such waves a rapid response water sampler or salinity measuring device is necessary. The Nansen type water bottle is not a rapid flushing bottle but instead requires somewhat more than 6 minutes to trap a sample representative of its surroundings.[4] Evidently then it cannot be used with a rapid response thermometer such as the TD. However, just as the reversing thermometer averages the temperature over the several minutes prior to its reversal, so also does the Nansen type water bottle and the two together eliminate many of the uncertainties in dynamic topography which might otherwise arise from short period internal waves. The undulations with periods of several hours, of course, remain in the topography developed from measurements made with the reversing thermometer-Nansen type bottle methods and may be the cause of some of the peculiarities in our topographic charts which have been difficult to explain. While remembering that the dynamic topographic charts have been in sufficiently good accord with observed drifts of bergs to be of great practical use, the degree of reliance which may be placed on such computations as volume and heat transport and mean temperature derived from such observations is in doubt.

It has been found that in the Grand Banks region Labrador Current water and Atlantic Current water are present as water masses having characteristic temperature-salinity relationships and in addition the mixed water formed from these parent water masses is usually present in sufficiently uniform proportions of each of its components so that it may be regarded as a virtual water mass. Of the data collected during 1953, those from the first and fourth surveys were from the same area which has been the source of the T-S data in the past and so provide a good basis for comparison. Except for its southern end, the area covered by the second survey, which included the northeastern slope of the Grand Banks, is north of the area from which earlier data have been considered. The third survey was comprised of the Bonavista triangle only and was not analyzed for

---

[3] As summarized by Sverdrup, Johnson, and Fleming in "The Oceans" pp. 585-602 (1942), Prentice-Hall, New York.

[4] See R. L. I. Fjarlie "A seawater sampling bottle" Pacific Oceanographic Group, Joint Committee on Oceanography P. O. G. file N7-7 (15 Aug 1952) Nanaimo, B.C., wherein the author describes the performance of a new bottle designed to flush rapidly. He compared the new bottle with other types of bottles at 0, 2, 4, and 6 meters. The salinity at 2 meters was essentially the same as at the surface. A replot of his data for only the 4 and 6 meter levels shows the Nansen type bottle to require about 6 minutes to trap samples of the same salinity trapped by the new bottle under the existing sea conditions (not stated).

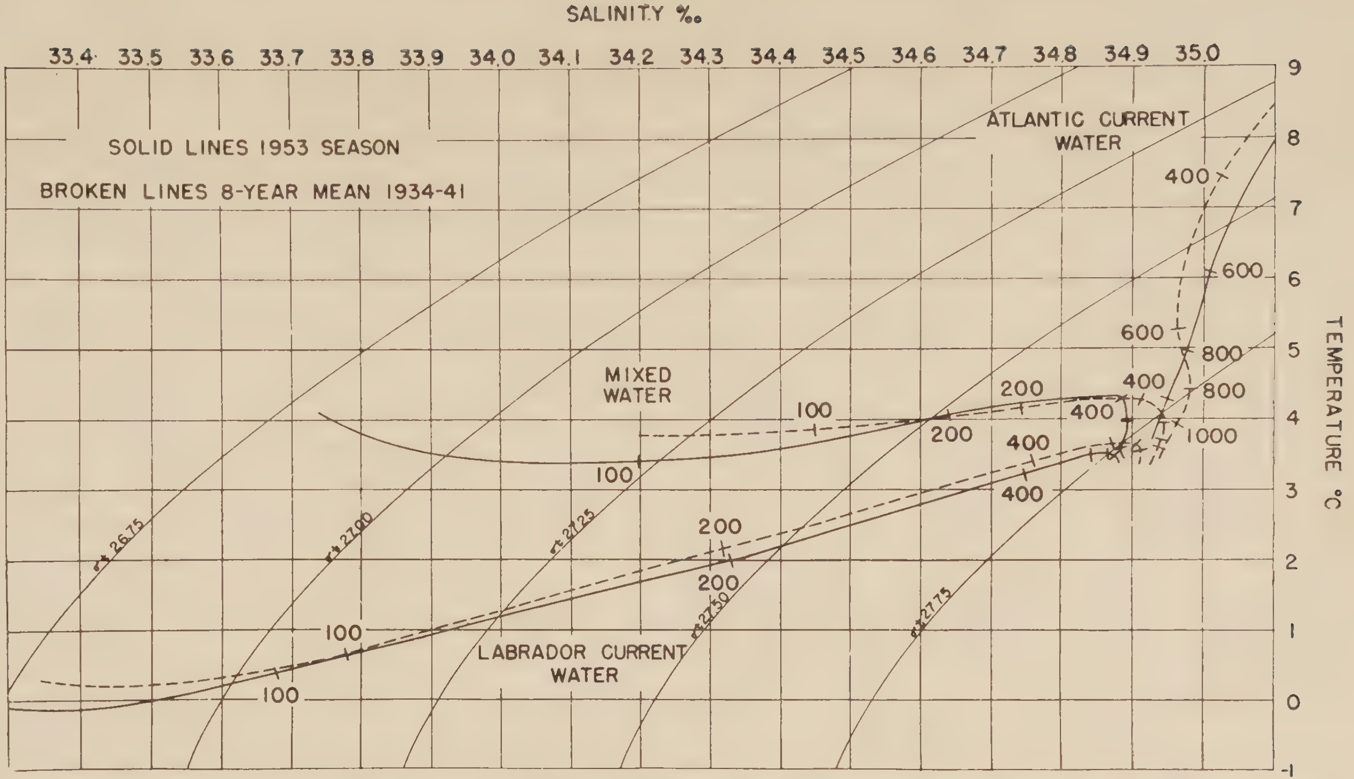

FIGURE 36.—Temperature-salinity relationships for Labrador Current water, Atlantic Current water, and mixed water found in the Grand Banks region. Solid lines show conditions during the 1953 season and broken lines represent the 8-year mean for the period 1934–41. An approximate depth scale in meters is given.

T-S relationships as being probably too far removed from the source of the other data for direct comparison. The results of the first, second, and fourth surveys were examined separately and it was found that while there were differences from survey to survey these differences were small. However, because of geographical differences only the Atlantic Current water stations of the second survey were included in the average values for 1953. These T-S relationships for the three water masses are shown in figure 36 as solid lines in comparison with the averages for the 8-year period 1934–41 which are shown as broken lines.

The Labrador Current water was somewhat fresher from 50 to 100 meters, somewhat colder from 100 to 400 meters, and both colder and fresher below 400 meters than the 8-year mean. The mixed water was fresher than the 8-year mean at all levels. The Atlantic Current water appeared to be warmer and saltier above about 800 meters, and warmer and fresher below that level, than the 8-year mean. Again in 1953 the salinity minimum at a temperature of about 6° was not apparent in the mean for the year although some individual station curves exhibited it. If this minimum is the result of mixing and is, as has been assumed, a characteristic of the outer margins of the Atlantic Current water mass, the minimum may have disappeared from the yearly average because of a larger number of stations taken farther into the Atlantic Current water mass.

The number of atypical stations, that is, stations which do not definitely fall into one of the water mass categories, was larger than usual. In the first survey there were 6 stations between Atlantic Current water and mixed water characteristics and 9 such stations in the fourth survey. In addition there were evidences that boundaries between water masses were not vertical, with one water mass over a different water mass at each of several stations. The Labrador Current water (for which more stations were available than for other water masses) was saltier during the second survey than either the first or fourth surveys and except for the 50-meter level it was fresher during the first survey than during the fourth. The differences were small enough to be of doubtful significance.

As a check on whether the mixed water was or was not a virtual water mass, the probable departures of temperature and salinity at a given level at an individual station, from the temperature and salinity at that leval on the T-S curves for 1953 shown in figure 36 were computed for each level for each water mass. These probable departures were then used as the axes of elipses of uncertainty constructed with their centers at the appropriate points on the T-S curves. Level for level the elipses for Labrador Current water and mixed water did not overlap except at 600 meters and below; and for mixed water and Atlantic Current water they did not overlap except at the 1,500 meter level.

Some interest has been expressed as to whether there has been any progressive change in the salinity of the North Atlantic eddy over the years. Small consistent differential changes would have a marked effect on circulation. For the postwar years 1948–53 the T-S points representing the year's mean have been plotted for each year and each level for each of the three water masses found in the Grand Banks region. Such a period of 6 years is too short to reveal any gradual shift in a particular T-S point as the annual excursions of the point are greater than any anticipated permanent shift of the point.

In each water mass the excursions were greatest in the upper levels and decreased with increasing depth. In the Labrador Current water the major axis of the excursion pattern was parallel to the characteristic T-S curve of the water mass down to about 200 meters, indicating changes in density for a specific level in this depth range. Below about 200 meters the fluctuations were more nearly isopycnal. No such regularity was apparent in the plots for the mixed water, In the Atlantic Current water the major axis of the excursion pattern was roughly parallel to the characteristic T-S curve down to about 800 meters but below that depth there was no pronounced major axis in the pattern. Caution must be used in interpreting these measurements made in Atlantic Current water because, unlike the measurements in the other two water masses, these sample only the outer part of the North Atlantic eddy and so must contain a varying proportion of marginal stations from year to year. Thus while the geographical distribution of the sampling is roughly the same from year to year, the fluctuations recorded may represent fluctuations in geographical position of the margins of the North Atlantic eddy rather than fluctuations in its T-S characteristics.

In comparison with the 8-year mean for the period 1934–41, the postwar observations in the Labrador Current water were fresher and slightly colder in the upper 200 meters and fresher below 400 meters. The mixed water was fresher at all levels and the Atlantic Current water was warmer and fresher below about 800 meters.

In earlier Bulletins of this series attempts have been made to describe numerically the fluctuations in the position of the cold wall and to relate these fluctuations to other phenomena. As the cold wall is not vertical the outer margin of Atlantic Current water has been used. This has been defined as the horizontal projection of the line along which a temperature of 6° corresponds to a salinity of 34.95°/₀₀. This border is serpentine in shape and its position has been characterized by measuring the area northwestward of it between the border and fixed rumb lines (the 45th parallel, the 49th meridian from 45° N., to 43° N., and a line from 43° N., 49° W., through 42° N., 47° W.). Thus, as the border moves toward the Grand Banks the area decreases. It was assumed that the position taken up by the border was determined partly by forces associated with the Labrador Current and partly by forces associated with the North Atlantic eddy. It was assumed that the area would be increased by 10,000 square kilometers for each million cubic meters per second volume of flow of the Labrador Current entering the area past section U. After subtracting such an amount from the area to obtain an adjusted area, A, this adjusted area was considered to represent the effects of causes associated with the Gulf Stream system. Assuming that these causes were related to the difference in sea level between Bermuda and Charleston, S. C., the fluctuations in A would be related to the fluctuations in this sea level difference. If sea level at Charleston minus the departure from average sea level at Bermuda, expressed in feet, is H and A, expressed in units of 10,000 square kilometers, is the adjusted area 13½ months later, 27 surveys made during the ice patrol seasons 1934–41 give the expression

$$A=6.8\ (H-5.07)+1.34$$

No surveys were made during the years 1942–47. Ten surveys made during 1948–52 did not agree with the above relationship but followed approximately the same relationship if a time lag of 11½ months were used. Combining all 37 surveys and using the phase difference of 13½ months for the prewar data and 11½ months for the postwar data the expression became

$$A=6.97(H-5.07)+1.67$$

However, the correlation was much poorer and it is evident that the full explanation involves more than has so far been considered.

In 1953, the first survey gave a gross area of 9.63 with an adjusted area A of 6.67 and in the fourth survey the gross area measured 6.95 for an adjusted area of 3.22, both of which are widely different from the values of A computed with either of the above formulae. The phase difference could have been either 11½ months or 13½ months during 1953.

The postwar data now include 12 surveys with 4 each made during April, May and June. The means of these actual values of A plotted on the curve of postwar averages of the Charleston minus Bermuda departure show the following possible time lag correlations: 1 month negative; 2½ months positive; 4 months negative; 6 months positive; 9½ months negative; 11½ months positive; 13 months negative; and 14½ months positive. Examining each year, survey by survey, shows only one of these (11½ months positive) to have no years where the sign of the correlation was contradictory. The quantity (H–5.07) has continued to have low values whereas the actual value of A has remained high. A decreasing value of (H–5.07) is interpreted to mean an increasing activity in the North Atlantic eddy. If the adjusted area A remains high it may be because of an anomalous failure of the Labrador Current to increase. Another possible interpretation is that the Atlantic Current water has decreased in salinity in its T-S

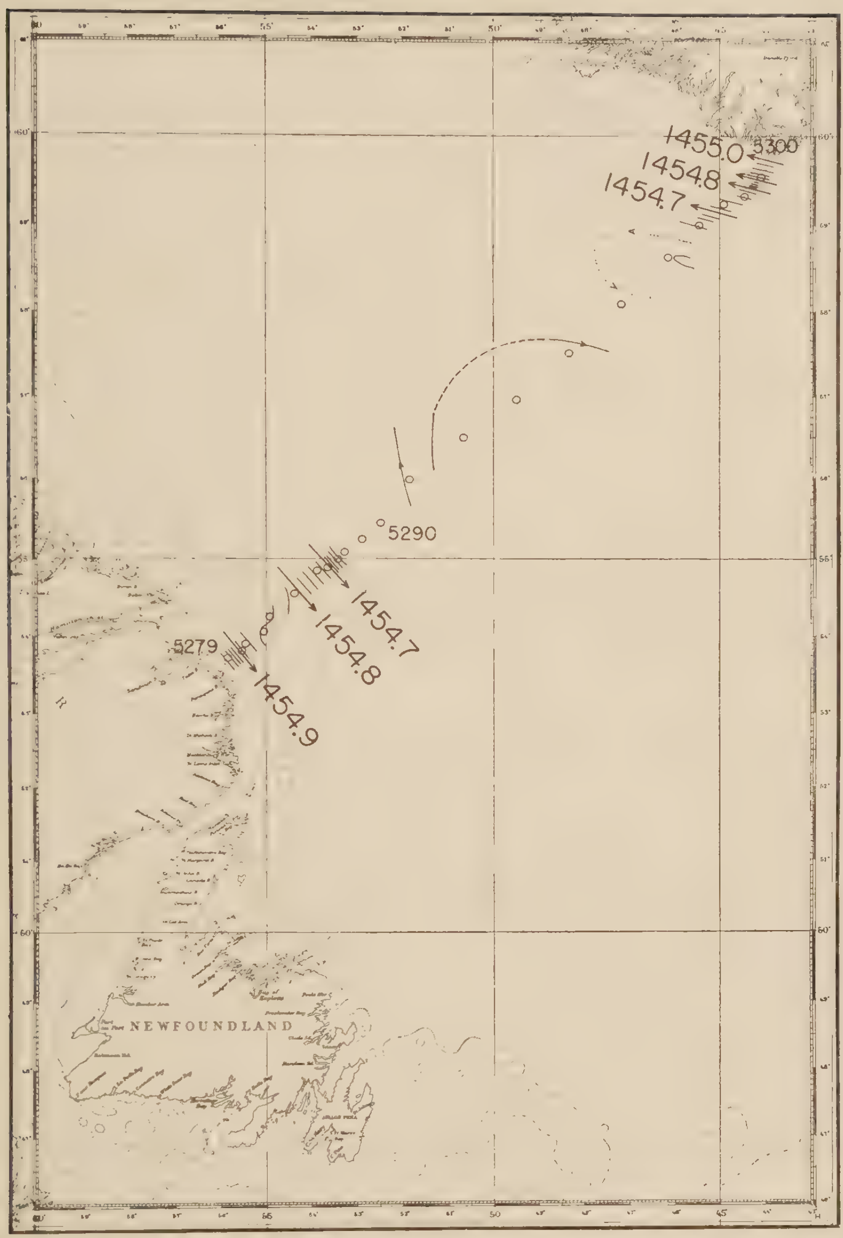
1455.0
5300
1454.8
1454.7
5290
1454.7
1454.8
5279
1454.9
NEWFOUNDLAND
60°
55
50
45

FIGURE 37.—Dynamic topography of the sea surface relative to the 1,500-decibar surface from data collected 16–20 July 1953. Oceanographic station positions are indicated and the station numbers given at turning points.

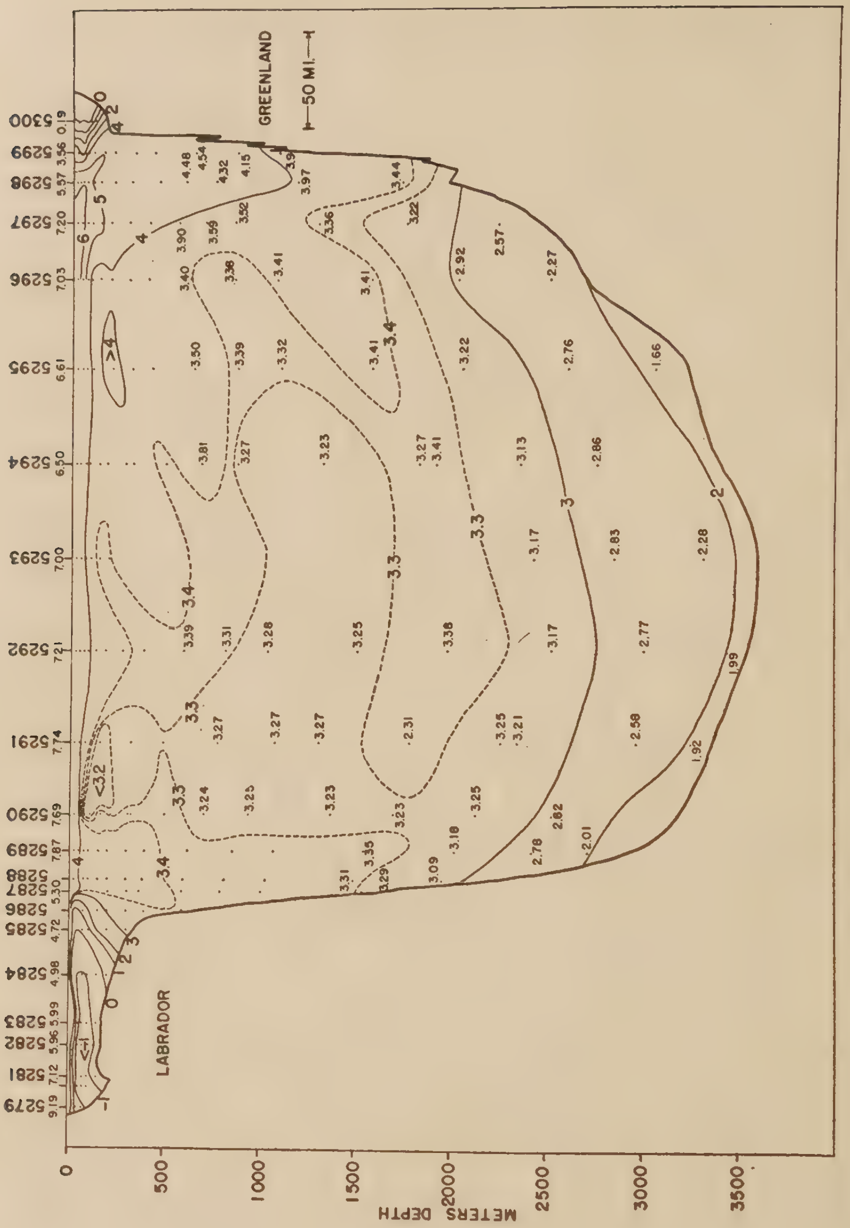

FIGURE 38.—Temperature distribution between South Wolf Island, Labrador, and Cape Farewell, Greenland, 16–20 July 1953.

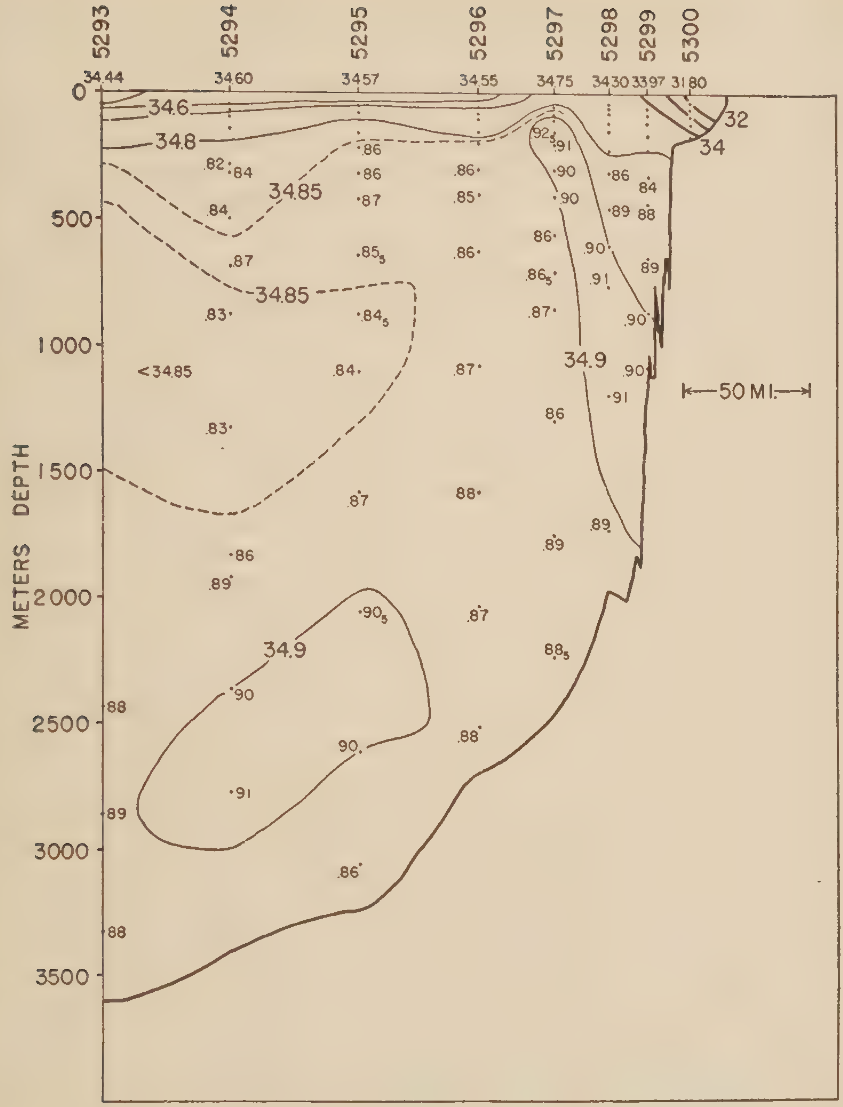

Figure 39.—Salinity distribution off Cape Farewell, Greenland, 19–20 July 1953.

relationship so that one must get farther into the North Atlantic eddy to find the boundary criterion of 34.95°/₀₀ at 6°.

Figure 20, presented earlier in illustration of the interpretation of the volume transports found at various sections of the Labrador Current, also shows schematically the circulation in part of the Labrador Sea as deduced from the observations made during the postseason cruise. Figure 37 shows the dynamic topography of the sea surface during the 1953 postseason cruise, in the vicinity of the section from South Wolf Island, Labrador, to Cape Farewell, Greenland. Figure 38 shows the temperature distribution along this section and figure 39 shows the salinity distribution along the Greenland end of this section.

The dynamic topography shown in figure 37 has a pattern similar to that found in 1952, with the Labrador Current having two bands separated by the shoal off Hamilton Inlet, and with the possibility of a cyclonic eddy offshore of the outermost band and located between it and what appears to be the northwestwardmost margins of the North Atlantic eddy. As the water in the margin of the North Atlantic eddy moved eastward it again was joined on the Greenland side by water recurving from the West Greenland Current.

Inspection of figure 38 gives some verification of this interpretation of the circulation. The temperature minimum at about 150 meters at stations 5290 and 5291 is an indication that this northward moving water was associated with the Labrador Current and has recurved somewhere southeastward of this section. Farther seaward the warmer temperatures at station 5292 support the identification of this water as being the northwestern margin of the North Atlantic eddy. At station 5295 the temperature maximum of more than 4° indicates that this water has recurved from the warm West Greenland Current somewhere northwestward of this section. Elsewhere in figure 38 the frigid part of the Labrador Current is to be seen over the shelf and the warmer offshore part of the Labrador Current, derived from the West Greenland Current, is defined by the 3.4° isotherm at stations 5287 and 5288. The temperature minimum in the intermediate water in the central part of the section, with a temperature of about 3.25°, was about the mean of the warmer years. During the 7 years 1934–39 and 1950 this minimum was about 3.17° and during the 7 years 1940–41, 1948–49, and 1951–53 the minimum was about 0.10° to 0.15° warmer. The gap in the observations 1942–47 makes it difficult to compare the 8-year series of prewar observations with the 6-year postwar series. In figure 38 the temperature maximum below this minimum is defined by the 3.3° and 3.4° isotherms at about the 2,000-meter level. It is interesting to note that the intermediate minimum and the underlying maximum are still present when the temperatures in situ are converted to potential temperatures. Within the West Greenland Current the cross sectional area with a temperature greater than 4° is somewhat greater in figure 38 than was found in 1952. The area within the 5° isotherm is about the same as in 1952.

Using temperature as an indicator of the relative magnitude of the contributions of the Irminger Current and the East Greenland Current this increase in the cross sectional area within the 4° isotherm would mean an increase in the Irminger Current component of the West Greenland Current. Figure 39, however, contradicts this and shows no salinity that is even as much as 34.95‰. The salinity maximum found in 1953 was 34.925‰ which is the lowest value found since 1949 when the Irminger Current component of the West Greenland Current disappeared from this vicinity. On the basis of temperature alone and assuming that the West Greenland Current off Cape Farewell is made up exclusively of an East Greenland Current component of constant mean temperature of 3.2° and an Irminger Current component of constant mean temperature of 5.5° the observed volume transport of the West Greenland Current of 7.23 with a heat transport of 27.92 and a mean temperature of 3.86 may be broken down into an East Greenland Current component of 5.15 volume of flow (compared with a seasonal normal of 1.57) and an Irminger Current component of 2.08 (compared with a seasonal normal volume of 2.95), as shown in figure 20. The low salinity maximum, however, indicates that the warm water involved is not Irminger Current water but more probably is a direct contribution of water from the outer margins of the North Atlantic eddy.

As mentioned earlier, 1,500 decibars was used as the reference surface in this section across the Labrador Sea in order to make the resulting dynamic topography, velocities, and transports comparable with the results of earlier work. Examination of the complete velocity section shows that using this reference surface the net volume transport across the section from South Wolf Island to Cape Farewell is 3.67 northwesterly. There is normally a small net contribution into the Baffin Bay-Labrador Sea system through the northern openings and it is not reasonable to account for such a large northwesterly transport by sinking and outflow below the reference surface. Analysis of the computations shows the net northwesterly transport to be present at all levels with the maximum rate occurring in the upper 300 meters and decreasing with increasing depth to the reference surface. A deeper surface was suggested as being more nearly motionless. The volume of flow was recomputed using for reference the 2,000-decibar surface, which gave 3.13 net northwesterly and again using for reference the 2,500-decibar surface which gave 1.77 net southeasterly. Although the motionless surface was probably undulatory the most nearly motionless surface seems to have been between 2,000 and 2,500 meters.

Using the 2,500-decibar surface produces little change in the computed values of the West Greenland Current, giving a value of 7.35

instead of 7.23 for the volume transport (divided on the basis of temperature as 5.31 East Greenland Current and 2.04 Irminger Current) 3.84 instead of 3.86 for the mean temperature and 28.22 instead of 27.92 for the heat transport. A greater change is produced in the computed values for the Labrador Current, however, giving 6.41 instead of 5.02 for the volume transport, 2.64 instead of 2.43 for the mean temperature, and 16.94 instead of 12.19 for the heat transport. These values, using 2,500 decibars as the reference surface, are very close to the values obtained in 1952 when 1,500 decibars was used as the reference surface and are considered to be more nearly the true values than those derived in reference to the 1,500-decibar surface.

Phosphorus in the sea forms an important part of the nutrient salts and its concentration in that form is subject to alteration, as it passes through the life cycle, with fluctuations in the activity of marine life. The concentration of total phosphorus, however, should be a reasonably conservative property of sea water. Until recent years comparatively little work has been done on total phosphorus. Ocean-wide differences have been known to exist. For instance, that there is a lower concentration in the Atlantic than in the Pacific. There seemed to be a possibility of using total phosphorus as a tracer which might be of use in identifying the water in the high salinity core of the West Greenland Current as being water supplied from the North Atlantic eddy by the Irminger Current or as water recirculated from the south central Labrador Sea. If total phosphorus could be used as a tracer then the three water masses found in the Grand Banks region, or at least the Atlantic Current water and the Labrador Current water, were expected to show characteristic differences in total phosphorus. Accordingly during the May survey of the Grand Banks region in 1952, samples were taken from all levels at most of the stations and during July 1952, samples were taken from all levels at all stations comprising the section from South Wolf Island, Labrador to Cape Farewell, Greenland. Similar sampling also was carried out during the 1953 occupation of this section across the Labrador Sea. The results of the determinations of total phosphorus concentration in the samples (carried out by personnel of the Woods Hole Oceanographic Instituition [5]) are tabulated at the end of the usual table of oceanographic data.

The stations in the Grand Banks survey were classified as to water mass according to their temperature-salinity characteristics. As there is very little overlap between Labrador Current water and Atlantic Current water in either salinity or temperature it was considered that a more illuminating plot would result if phosphorus

---

[5] With only minor modifications, methods and procedures were as reported by Harvey, H. W., in "The estimation of phosphate and of total phosphorus in sea waters," Journ. Mar. Biol. Assoc., vol. XXVII, pp. 337-359 (1948), Plymouth, England. Recent work at the Woods Hole Oceanographic Institution (unpublished) indicates the probable error in the determinations to be about ±10 percent.

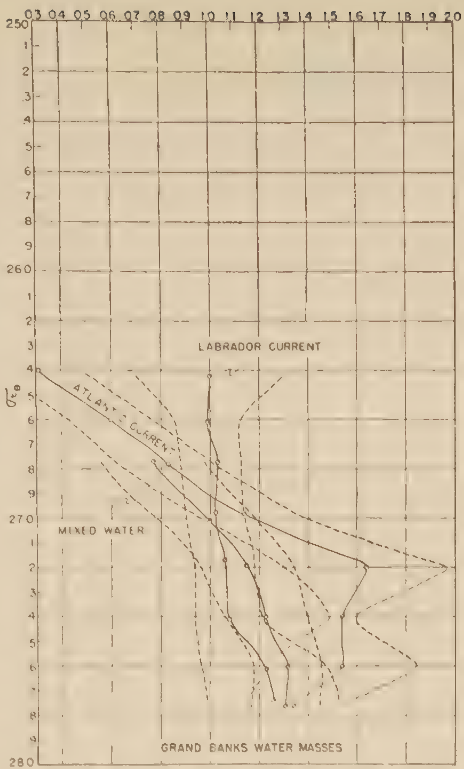

FIGURE 40.—Characteristic phosphorus-density curves for water masses found in the Grand Banks region in May 1952.

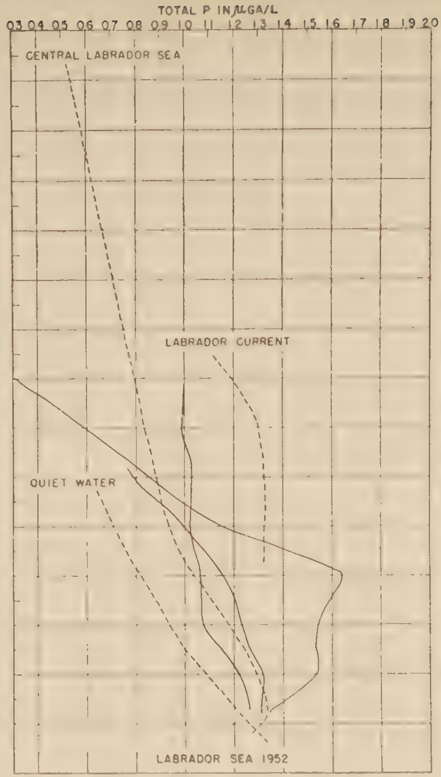

FIGURE 41.—Mean curves showing the relationship between total phosphorus and potential density found in the South Wolf Island-Cape Farewell section 17–20 July 1952, compared with the characteristic Grand Banks water mass curves.

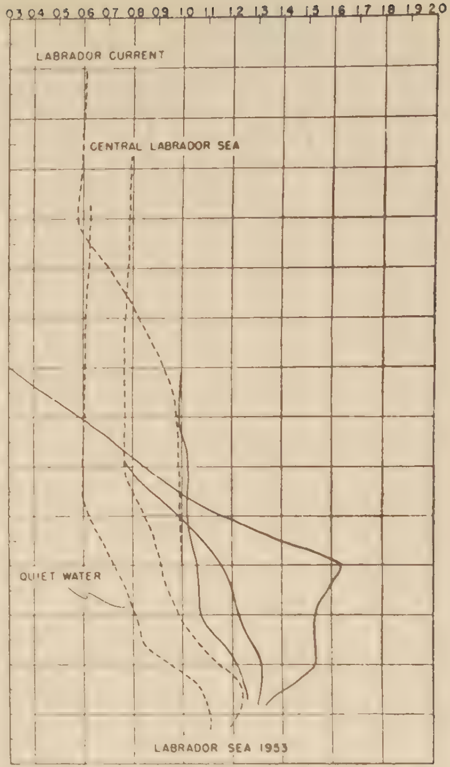

FIGURE 42.—Mean curves showing the relationship between total phosphorus and potential density found in the South Wolf Island-Cape Farewell section 16–20 July 1953, compared with the characteristic Grand Banks water mass curves.

were plotted as a function of some property more uniformly common to all water masses. Considering the possiblity of changes in depth as the water moved from one geographical location to another, potential density [6] was chosen as the property against which to plot the phosphorus concentration. The individual station curves did seem to have shapes characteristic of the water masses. Average curves for each of the water masses were then drawn and the probable departure of individual observations from the average curve computed. The average curves are shown in figure 40 as solid lines bracketed by broken lines indicating the probable departure. Thus the Labrador Current water had a practically constant concentration of total phosphorus of about 1.0 to 1.1 microgram-atoms per liter down to intermediate depths below which there was an increase to about 1.25 microgram-atoms per liter in the deep water. The Atlantic Current water had much lower values near the surface, increased to an intermediate maximum of more than 1.5 μga/L, and then decreased approaching in deep water the values in the Labrador Current water. The mixed water showed a relationship roughly intermediate between the Atlantic Current water and the Labrador Current water, and, like the T-S characteristic, closer to the curve of Labrador Current water than the curve of Atlantic Current water.

Thus the concentration of total phosphorus was shown to be a water mass tracer in the Grand Banks region, but not a very good tracer. The data for the 1952 occupation of the section across the Labrador Sea were then plotted and the stations fell into three groups. Stations on the Labrador shelf formed one group in which the phosphorus concentration was constant but about 0.3 μga/L higher than the Labrador Current water in the Grand Banks region. The stations in the central Labrador Sea and West Greenland Current formed a second group similar to but slightly lower in concentration than the mixed water of the Grand Banks region. Four stations, two on each side of the central Labrador Sea, formed a third group in which the concentration was the lowest of the entire section. Figure 41 shows average curves representing these groups along with the Grand Banks curves for comparison. The data for the 1953 occupation of the section across the Labrador Sea have been similarly treated and the results shown in figure 42. Each of the three groups showed lower concentrations in 1953 than in 1952 but the greatest change was in the Labrador Current water.[7] In 1952

---

[6] $\sigma_{t\theta}$ where t_θ is the temperature a water particle would have if the particle were adiabatically reduced to atmospheric pressure, and where $\sigma_{t\theta}$ is 1,000 (density−1) at atmospheric pressure and temperature t_θ.

[7] The decided differences in the concentration of total phosphorus in the Labrador Current between the Labrador coast and the Grand Banks region the same year (July and May) and between 1952 and 1953 in the same location off South Wolf Island at the same time of year brings up additional unanswered questions as to variations with time and the mechanisms by which the concentration is altered. Remembering that the samples from the Grand Banks region were taken from locations distant from land and that those off South Wolf Island were taken from locations relatively near the beach it is suggested that the phosphorus concentration may be increased locally by fecal products from birds being washed into the sea from adjacent rookeries and from seals which whelp on the ice over the shelf.

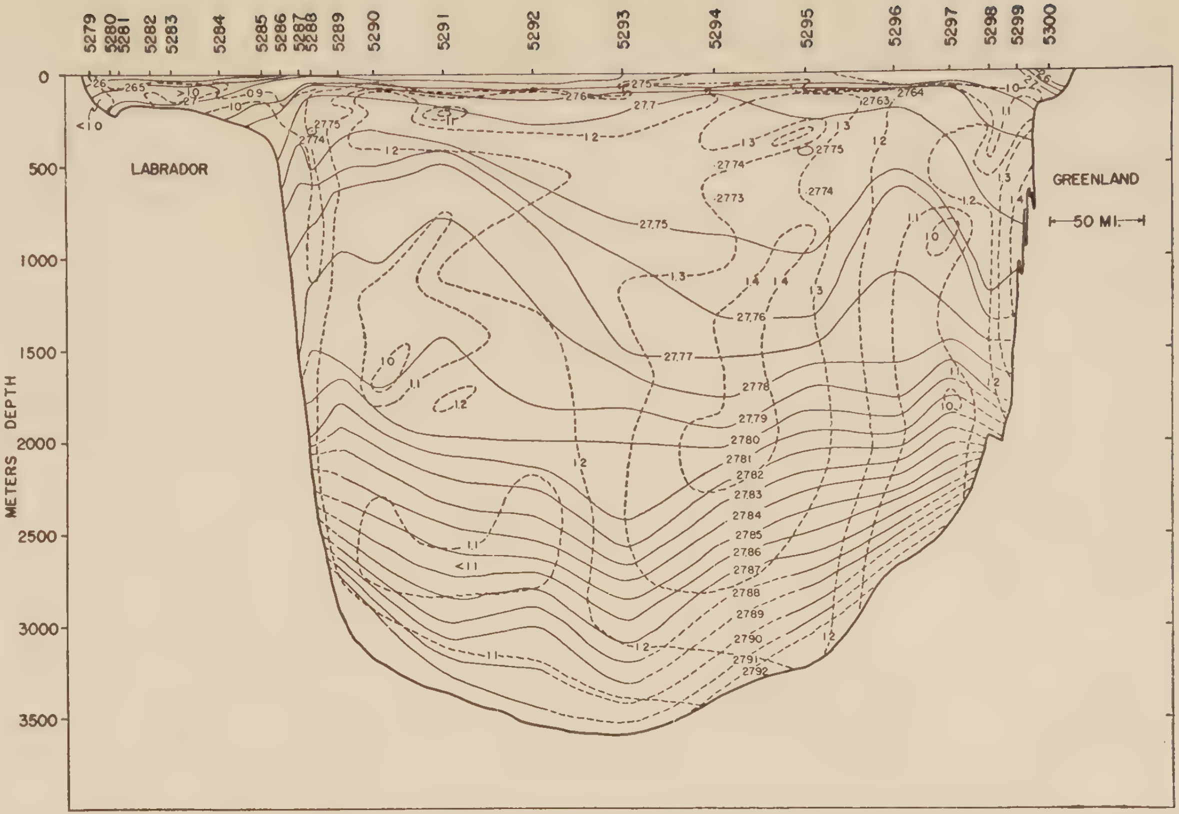

FIGURE 44.—Distribution of total phosphorus between South Wolf Island, Labrador, and Cape Farewell, Greenland, 16–20 July 1953. Concentration is given in microgram-atoms per liter. Solid lines show isentropic surfaces of equal σ_{t_θ}.

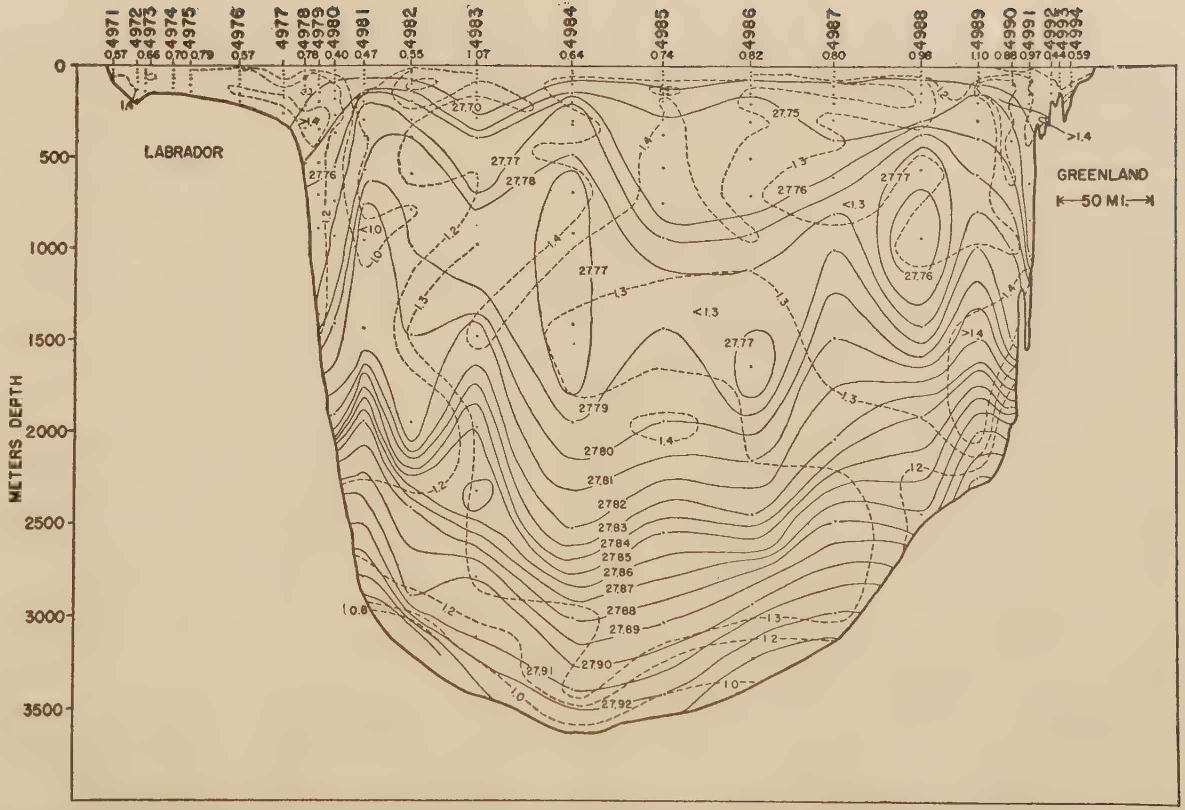

FIGURE 43.—Distribution of total phosphorus between South Wolf Island, Labrador, and Cape Farewell, Greenland, 17–20 July 1952. Concentration is given in microgram-atoms per liter. Solid lines show isentropic surfaces of equal $\sigma_{t\theta}$.

the station containing the salinity maximum in the West Greenland Current was indistinguishable from the others in the group from the Central Labrador Sea and West Greenland Current. In 1953 the station containing the salinity maximum was lower in phosphorus than the group from the central Labrador Sea and West Greenland Current and close to but somewhat higher than the low phosphorus group.

From the observations available, and on the basis of the characteristic curves shown in figure 40, it is not possible to identify the high salinity core of the West Greenland Current off Cape Farewell in either 1952 or 1953 as having been contributed by the Irminger Current. Whether this is because of a change in the characteristic total phosphorus distribution which takes place during the long journey from the Grand Banks to Cape Farewell by way of Iceland, or because the salinity maximum was not contributed by the Irminger Current, cannot be stated from the information now available.

The distribution of total phosphorus concentration along the section across the Labrador Sea found in 1952 and 1953 is shown in figures 43 and 44. Lines of equal phosphorus are shown broken and the isentropic surfaces of equal $\sigma_{t\theta}$ are shown as solid lines. While, as noted above, the concentration was less in general in 1953 than in 1952, figures 43 and 44 display some features of distribution in common. There is a maximum in the central part of the section in the intermediate water which grades to lower values at the bottom and to minima on each side. These minima reach to the surface near the offshore boundaries of the swifter horizontal circulation. Shoreward of these minima there are maxima near the continental slopes. A considerably smaller concentration is present in the upper 50 meters.

SUMMARY

1. The surface circulation in the Grand Banks region during the ice patrol season of 1953 has been discussed on the basis of four dynamic topographic surveys which indicated the presence of currents adequate to transport bergs to areas of potential hazard to the steamer lanes if bergs had entered the surveyed area from the north.

2. The circulation in the upper 1,000 meters in the Grand Banks region has been considered in greater detail by presentation of the volume and heat transports, mean temperature and minimum temperature observed in 1953 during 19 occupations of 10 selected sections across the Labrador Current. These have been compared with seasonal normal values where such normals are available and the figures for the 1953 deficiency in volume and heat transport have been given.

3. The 12 occupations of the Bonavista triangle made during the past 5 years have been summarized as to volume of flow, mean temper-

ature, minimum observed temperature, and heat transport for each of the three sides and approximate normal seasonal variation relationships developed for these functions and for the percentage of the volume transport following the eastern branch of the Labrador Current.

4. A new self-contained rapid response subsurface thermograph, which records temperature against depth down to 1,800 meters, has been described and the results of field tests have been discussed. Fourteen traces obtained before accidental destruction of the instrument have been shown with corresponding observations by reversing thermometers. The results indicate the presence of short period internal waves which are averaged out in the reversing thermometer-Nansen water bottle technic.

5. The temperature-salinity characteristics of the Labrador Current water mixed water and Atlantic Current water found in the Grand Banks region in 1953 have been compared with the 8-year mean for the period 1934–41. The year-to-year changes in the position of the T-S points for several levels in each of the 3 water masses were investigated for the 6 postwar years 1948–53 but any steady trend which may be present was masked by the large year-to-year excursions of the points. Some slight freshening in the deeper levels, compared to prewar observations, was noted.

6. Two more surveys in 1953 were added to the study of the relationship which is presumed to exist between the location of the northern boundary of Atlantic Current water in the Grand Banks region, the strength of the Labrador Current and the strength of the North Atlantic eddy as indicated by the difference in sea level between Bermuda and Charleston. As with all the postwar observations, the 1953 measurements gave a poor agreement with the relationship developed for the prewar observations.

7. The 1953 repetition of the section from South Wolf Island, Labrador, to Cape Farewell, Greenland, has been examined and the results presented. The abnormally vigorous circulation in the Labrador Sea which has characterized the last few years continued in 1953. The temperature minimum of the intermediate water was found to be warmer than during the period 1934–39. In this respect 1953 was like 1940–41 and all the postwar years except 1950. On the basis of the salinity maximum in the West Greenland Current the Irminger Current contribution to that current was judged to be negligibly small in 1953. The temperature of this portion of the West Greenland Current, however, remained fairly warm, so that on the basis of heat transport and assumed constant mean temperatures of the contributary currents the Irminger Current contribution was about two-thirds of its normal volume transport.

8. From measurements made on samples collected in the Grand Banks region in 1952 and from the section across the Labrador Sea in 1952 and 1953 it is concluded that the concentration of total phosphorous is roughly characteristic of water masses though of doubtful utility as a tracer of water masses. The distribution of phosphorous found in the southern Labrador Sea has been described.

TABLE OF OCEANOGRAPHIC DATA

The data collected during 1953 are tabulated below. The individual station headings give the station number, date, geographical position, depth of water, and the dynamic height of the sea surface used in the construction of the dynamic topographic charts shown in figures 14, 15, 16, 17, 19, and 37. The depths of water are rough approximations, being uncorrected sonic soundings based on a sounding velocity of 800 fathoms per second and containing an additional mechanical speed error of about $1/60$. Where the depths of scaled values are enclosed in parentheses, the data are based on extrapolated vertical distribution curves of temperature or salinity or both. Asterisks appearing before observed temperatures indicate that these temperatures were determined from the depth of reversal and the corrected reading of an unprotected thermometer. The symbol σ_t signifies 1,000 (density−1) at atmospheric pressure and temperature t.

Table of Oceanographic Data

STATIONS OCCUPIED IN 1953

Station 4995; Apr. 3; latitude 42°04.5′ N., longitude 51°53′ W.; depth 3,658 meters; dynamic height 971.171

Observed values			Scaled values			
Depth, meters	Temperature, ° C.	Salinity, °/oo	Depth, meters	Temperature, ° C.	Salinity, °/oo	σ_t
0	11.83	34.05	0	11.83	34.05	25.91
25	11.88	34.88	25	11.88	34.88	26.54
50	11.17	35.16	50	11.17	35.16	26.89
75	12.23	35.42	75	12.23	35.42	26.89
99	12.15	35.40	100	12.15	35.40	26.89
149	11.80	35.32	150	11.80	35.32	26.90
199	11.90	35.36	200	11.90	35.36	26.91
298	7.88	34.82	300	7.85	34.82	27.18
342	7.84	34.95	400	6.45	34.86	27.40
513	4.03	34.70	600	4.10	34.80	27.64
684	4.17	34.88	800	4.00	34.90	27.73
866	3.90	34.90	1,000	3.75	34.90	27.75
1,341	3.50	34.88				

Station 4996; Apr. 3; latitude 42°01′ N., longitude 50°57′ W.; depth 3,292 meters; dynamic height 971.039

Observed values			Scaled values			
Depth, meters	Temperature, ° C.	Salinity, °/oo	Depth, meters	Temperature, ° C.	Salinity, °/oo	σ_t
0	3.33	33.10	0	3.33	33.10	26.35
25	1.65	33.31	25	1.65	33.31	26.66
50	0.90	33.44	50	0.90	33.44	26.82
75	0.72	33.54	75	0.72	33.54	26.91
100	0.52	33.74	100	0.52	33.74	27.08
150	1.33	34.06	150	1.33	34.06	27.29
199	2.56	34.37	200	2.60	34.37	27.44
299	4.26	34.75	300	4.30	34.75	27.58
423	*4.33	34.90	400	4.35	34.79	27.60
634	4.30	34.95	600	4.30	34.84	27.65
845	3.87	34.92	800	3.95	34.83	27.67
1,057	3.54	34.89	1,000	3.60	34.80	27.69
1,585	3.46	34.91				

Table of Oceanographic Data—Continued

STATIONS OCCUPIED IN 1953—Continued

Observed values			Scaled values			
Depth, meters	Temperature, ° C.	Salinity, °/oo	Depth, meters	Temperature, ° C.	Salinity, °/oo	σ_t
Station 4997; Apr. 3; latitude 42°21′ N., longitude 51°31′ W.; depth 2,926 meters; dynamic height 971.079						
0	5.79	33.56	0	5.79	33.56	26.46
22	7.29	34.09	25	7.40	34.12	26.69
43	8.12	34.32	50	8.50	34.43	26.77
65	9.72	34.80	75	10.45	34.95	26.85
87	11.00	35.11	100	11.05	35.22	26.95
130	11.06	35.35	150	10.50	35.30	27.12
173	9.65	35.20	200	8.65	35.08	27.25
280	5.59	34.68	300	4.55	34.57	27.41
328	*3.34	34.44	400	3.20	34.52	27.51
500	3.12	34.66	600	3.30	34.74	27.67
679	3.45	34.78	800	3.50	34.81	27.71
862	3.50	34.82	1,000	3.50	34.83	27.72
1,340	3.48	34.84				
Station 4998; Apr. 3–4; latitude 42°48.5′ N., longitude 50°54′ W.; depth 1,326 meters; dynamic height 971.078						
0	0.92	33.00	0	0.92	33.00	26.47
22	−0.13	33.22	25	−0.15	33.24	26.72
43	−0.23	33.31	50	−0.20	33.35	26.80
64	0.06	33.45	75	0.05	33.51	26.93
85	0.07	33.55	100	0.10	33.58	26.97
129	0.22	33.62	150	0.35	33.68	27.04
172	0.52	-------	100	0.75	33.86	27.17
257	1.23	34.11	300	1.15	34.16	27.38
320	*1.11	34.18	400	1.95	34.38	27.50
485	2.79	34.56	600	3.20	34.74	27.68
653	3.36	34.78	800	3.50	34.80	27.70
850	3.48	34.80	(1,000)	3.50	34.81	27.71
Station 4999; Apr. 4; latitude 42°56′ N., longitude 50°46′ W.; depth 586 meters; dynamic height 971.106						
0	1.17	32.92	0	1.17	32.92	26.39
23	−0.04	33.12	25	−0.15	33.13	26.63
45	−0.48	33.20	50	−0.50	33.21	26.71
68	−0.56	33.24	75	−0.60	33.24	26.73
90	−0.69	33.24	100	−0.65	33.26	26.75
136	−0.14	33.46	150	0.05	33.53	26.94
182	0.36	33.70	200	0.45	33.76	27.10
272	0.78	33.96	300	1.00	34.05	27.30
312	*1.15	34.10	400	2.05	34.37	27.49
477	2.89	34.60				
Station 5000; Apr. 4; latitude 42°59′ N., longitude 50°42′ W.; depth 163 meters; dynamic height 971.109						
0	1.10	32.97	0	1.10	32.97	26.43
25	0.20	33.14	25	0.20	33.14	26.62
49	−0.44	33.22	50	−0.45	33.22	26.71
74	−0.55	33.26	75	−0.55	33.26	26.74
99	−0.41	33.32	100	−0.40	33.32	26.79
148	0.34	33.55	150	0.35	33.55	26.94
Station 5001; Apr. 4; latitude 43°06′ N., longitude 50°36′ W.; depth 89 meters; dynamic height 971.088						
0	0.03	33.26	0	0.03	33.26	26.72
25	0.32	33.45	25	0.32	33.45	26.86
50	0.65	-------	50	0.65	33.48	26.86
75	−0.16	33.42	75	−0.16	33.42	26.87
Station 5002; Apr. 4; latitude 43°20.5′ N., longitude 50°18′W.; depth 60 meters, dynamic height 971.141						
0	3.58	32.30	0	3.58	32.30	25.70
24	2.95	32.46	25	2.90	32.46	25.89
48	1.91	32.65	50	1.85	32.66	26.13
Station 5003; Apr. 4; latitude 42°59.5′ N., longitude 50°20′ W.; depth 86 meters; dynamic height 971.094						
0	2.76	32.50	0	2.76	32.50	25.93
26	−0.18	33.26	25	−0.20	33.25	26.72
52	0.23	33.46	50	0.20	33.45	26.87
78	0.02	33.48	75	0.05	33.48	26.90
Station 5004; Apr. 4; latitude 42°54.5′ N., longitude 50°20′ W.; depth 322 meters; dynamic height 971.121						
0	0.13	33.06	0	0.13	33.06	26.56
25	−0.26	33.07	25	−0.26	33.07	26.58
50	−0.58	33.07	50	−0.58	33.07	26.59
74	−0.86	33.13	75	−0.85	33.13	26.65
99	−0.82	33.17	100	−0.80	33.17	26.68
149	−0.52	33.34	150	−0.50	33.35	26.82
198	0.64	33.87	200	0.65	33.88	27.18
297	1.94	34.36	300	1.95	34.37	27.50
Station 5005; Apr. 4; latitude 42°44.5′ N., longitude 50°21′ W.; depth 1386 meters; dynamic height 971.028						
0	4.26	33.25	0	4.26	33.25	26.38
24	2.75	33.22	25	2.70	33.22	26.51
49	−0.25	33.18	50	−0.25	33.18	26.67
73	−0.22	33.33	75	−0.20	33.35	26.80
97	2.12	33.64	100	2.10	33.66	26.91
146	1.04	33.87	150	1.05	33.88	27.16
195	1.12	34.08	200	1.20	34.10	27.33
292	2.45	34.49	300	2.50	34.50	27.55
389	2.84	34.62	400	2.85	34.63	27.62
584	3.37	34.79	600	3.35	34.80	27.71
781	3.48	34.85	800	3.50	34.85	27.74
977	3.51	34.88	1,000	3.50	34.88	27.76

Table of Oceanographic Data—Continued

STATIONS OCCUPIED IN 1953—Continued

Station 5006; Apr. 4; latitude 42°22′ N., longitude 50°24′ W.; depth 2,743 meters; dynamic height 970.965

Observed values			Scaled values			
Depth, meters	Temperature, ° C.	Salinity, ‰	Depth, meters	Temperature, ° C.	Salinity, ‰	σ_t
0	3.93	33.23	0	3.93	33.23	26.41
24	3.31	33.26	25	3.25	33.26	26.49
49	1.99	33.33	50	2.00	33.33	26.66
73	1.03	33.53	75	1.05	33.54	26.89
97	1.31	33.80	100	1.35	33.84	27.11
146	2.66	34.38	150	2.70	34.39	27.44
326	3.84	34.82	200	3.30	34.54	27.51
489	3.83	34.90	300	3.85	34.76	27.63
652	3.78	34.89	400	3.85	34.88	27.72
830	3.53	34.89	600	3.80	34.90	27.75
1,302	3.45	34.88	800	3.55	34.89	27.76
			1,000	3.50	34.89	27.77

Station 5007; Apr. 4; latitude 41°54.5′ N., longitude 50°25′ W.; depth 3,567 meters; dynamic height 971.003

Observed values			Scaled values			
Depth, meters	Temperature, ° C.	Salinity, ‰	Depth, meters	Temperature, ° C.	Salinity, ‰	σ_t
0	3.10	33.00	0	3.10	33.00	26.31
22	2.03	33.23	25	2.00	33.25	26.60
44	1.73	33.38	50	1.20	33.39	26.76
66	−0.09	33.42	75	−0.10	33.44	26.87
88	−0.02	33.48	100	0.25	33.54	26.94
133	1.06	33.83	150	1.50	33.98	27.21
177	2.31	34.22	200	2.95	34.38	27.41
265	4.16	34.71	300	4.15	34.76	27.60
460	4.03	34.86	400	4.10	34.84	27.67
688	3.73	34.88	600	3.85	34.88	27.72
915	*3.51	34.89	800	3.60	34.89	27.76
1,142	3.55	34.88	1,000	3.50	34.88	27.76
1,709	3.52	34.94				

Station 5008; Apr. 5; latitude 41°33′ N., longitude 50°27′ W.; depth 3,658 meters; dynamic height 971.279

Observed values			Scaled values			
Depth, meters	Temperature, ° C.	Salinity, ‰	Depth, meters	Temperature, ° C.	Salinity, ‰	σ_t
0	15.47	35.92	0	15.47	35.92	26.59
26	15.37	35.92	25	15.35	35.92	26.62
52	14.92	35.90	50	14.95	35.90	26.69
78	14.45	35.80	75	14.50	35.82	26.73
104	13.53	35.65	100	13.70	35.67	26.79
157	13.13	35.58	150	13.20	35.59	26.82
209	12.01	35.36	200	12.25	35.40	26.87
313	9.10	34.86	300	9.40	34.90	26.99
438	9.25	35.18	400	9.20	35.08	27.16
664	5.85	35.00	600	6.60	35.04	27.52
894	4.82	35.02	800	5.15	35.01	27.69
1,117	4.19	34.96	1,000	4.50	35.00	27.75
1,668	3.70	34.95				

Station 5009; Apr. 5; latitude 40°52.5′ N., longitude 50°11′ W.; depth 3,475 meters; dynamic height 971.374

Observed values			Scaled values			
Depth, meters	Temperature, ° C.	Salinity, ‰	Depth, meters	Temperature, ° C.	Salinity, ‰	σ_t
0	19.61	36.28	0	19.61	36.28	25.86
25	19.64	36.28	25	19.64	36.28	25.86
49	19.56	36.27	50	19.50	36.27	25.88
74	16.88	35.93	75	16.85	35.93	26.28
99	15.75	35.81	100	15.75	35.81	26.44
147	13.92	35.64	150	13.85	35.63	26.72
196	13.23	35.56	200	13.20	35.56	26.80
295	12.79	35.63	300	12.70	35.62	26.95
372	10.75	35.38	400	10.25	35.31	27.17
566	7.74	35.06	600	7.20	35.04	27.44
766	*5.00	34.98	800	4.75	34.98	27.70
962	4.02	34.96	1,000	4.00	34.96	27.78
1,459	3.88	34.95				

Station 5010; Apr. 5; latitude 42°01.5′ N., longitude 49°30′ W.; depth 3,109 meters; dynamic height 971.211

Observed values			Scaled values			
Depth, meters	Temperature, ° C.	Salinity, ‰	Depth, meters	Temperature, ° C.	Salinity, ‰	σ_t
0	15.69	35.90	0	15.69	35.90	26.52
27	15.55	36.01	25	15.55	36.01	26.65
54	15.24	35.96	50	15.25	35.96	26.67
80	15.15	35.95	75	15.20	35.95	26.67
107	14.73	35.84	100	14.85	35.87	26.69
160	14.52	35.82	150	14.60	35.83	26.71
214	13.19	35.65	200	13.55	35.70	26.84
321	10.06	35.26	300	10.70	35.34	27.11
397	7.93	35.08	400	7.85	35.08	27.38
595	5.56	35.02	600	5.50	35.02	27.65
792	4.65	34.99	800	4.60	34.99	27.73
996	4.11	34.95	1,000	4.10	34.95	27.76
1,516	3.73	34.94				

Station 5011; Apr. 5; latitude 41°45′ N., longitude 49°07′ W.; depth 3,475 meters; dynamic height 971.358

Observed values			Scaled values			
Depth, meters	Temperature, ° C.	Salinity, ‰	Depth, meters	Temperature, ° C.	Salinity, ‰	σ_t
0	18.80	36.16	0	18.80	36.16	25.97
26	18.50	35.12	25	18.50	36.12	26.02
52	16.50	35.85	50	16.65	35.86	26.27
78	16.02	36.03	75	16.10	36.02	26.53
104	15.82	36.05	100	15.85	36.05	26.60
155	14.48	35.82	150	14.60	35.85	26.73
207	13.07	35.55	200	13.15	35.57	26.82
311	12.81	35.62	300	12.90	35.62	26.91
408	10.06	35.27	400	10.30	35.30	27.15
615	6.42	35.00	600	7.20	35.00	27.41
			(800)	4.85	35.01	27.72
			(1,000)	4.40	35.00	27.76

Table of Oceanographic Data—Continued

STATIONS OCCUPIED IN 1953—Continued

Station 5012; Apr. 6; latitude 41°07.5′ N., longitude 48°15′ W.; depth 3,621 meters; dynamic height 971.776

Observed values			Scaled values			
Depth, meters	Temperature, ° C.	Salinity, °/oo	Depth, meters	Temperature, ° C.	Salinity, °/oo	σ_t
0	18.48	36.34	0	18.48	36.34	26.20
25	18.42	36.36	25	18.42	36.36	26.24
49	17.64	36.43	50	17.65	36.43	26.47
74	17.62	36.44	75	17.65	36.44	26.48
98	17.61	36.44	100	17.65	36.44	26.48
146	17.60	36.44	150	17.60	36.44	26.49
196	17.57	36.45	200	17.55	36.45	26.51
294	17.36	--------	300	17.35	36.41	26.53
373	*16.89	36.38	400	16.55	36.32	26.65
571	13.72	35.78	600	13.30	35.70	26.89
819	10.27	35.16	800	10.60	35.20	27.02
976	6.07	35.03	1,000	5.70	35.03	27.63
1,458	4.17	34.985				

Station 5013; Apr. 6; latitude 41°37′ N., longitude 47°14′ W.; depth 4,207 meters; dynamic height 971.180

Observed values			Scaled values			
Depth, meters	Temperature, ° C.	Salinity, °/oo	Depth, meters	Temperature, ° C.	Salinity, °/oo	σ_t
0	6.88	33.83	0	6.88	33.83	26.54
27	12.80	35.40	25	12.40	35.38	26.82
53	10.07	34.85	50	10.45	34.91	26.82
80	8.17	34.46	75	8.35	34.51	26.86
106	10.90	35.09	100	10.40	35.00	26.90
159	9.75	34.90	150	9.95	34.93	26.92
212	8.81	34.72	200	8.90	34.75	26.96
318	9.65	35.16	300	9.55	35.10	27.12
412	6.43	34.78	400	6.80	34.82	27.33
615	4.46	34.85	600	4.50	34.84	27.62
818	4.36	34.935	800	4.40	34.93	27.70
1,025	3.54	34.90	1,000	3.60	34.90	27.77
1,547	3.57	34.90				

Station 5014; Apr. 6; latitude 41°59′ N., longitude 47°54′ W.; depth 3,749 meters; dynamic height 970.955

Observed values			Scaled values			
Depth, meters	Temperature, ° C.	Salinity, °/oo	Depth, meters	Temperature, ° C.	Salinity, °/oo	σ_t
0	5.60	33.30	0	5.60	33.30	26.27
26	2.18	33.53	25	2.15	33.52	26.81
52	5.30	34 28	50	5.15	34.23	27.06
78	5.73	34.47	75	5.70	34.47	27.20
104	3.10	34.24	100	3.20	34.27	27.31
154	4.86	34.62	150	4.80	34.59	27.39
206	4.77	34.75	200	4.80	34.73	27.50
310	-------	34.90	300	4.60	34.89	27.65
423	4.43	34.90	400	4.45	34.90	27.68
634	4.25	34.95	600	4.25	34.94	27.73
848	3.75	34.90	800	3.85	34.91	27.75
1,059	3.58	34.87	1,000	3.60	34.87	27.75
1,584	3.44	34.90				

Station 5015; Apr. 7; latitude 42°21.5′ N., longitude 48°28′ W.; depth 3,182 meters; dynamic height 971.000

Observed values			Scaled values			
Depth, meters	Temperature, ° C.	Salinity, °/oo	Depth, meters	Temperature, ° C.	Salinity, °/oo	σ_t
0	5.62	33.21	0	5.62	33.21	26.22
26	4.50	33.53	25	4.55	33.52	26.58
51	2.38	33.40	50	2.45	33.40	26.68
77	0.10	33.42	75	0.15	33.42	26.85
102	2.30	33.91	100	2.10	33.85	27.06
152	3.46	34.38	150	3.40	34.35	27.35
203	5.06	34.74	200	5.05	34.72	27.47
305	4.98	34.90	300	5.00	34.89	27.61
405	4.78	34.935	400	4.80	34.93	27.66
607	4.02	34.90	600	4.00	34.90	27.73
810	3.76	34.87	800	3.75	34.87	27.73
1,016	3.61	34.89	1,000	3.65	34.89	27.75
1,535	3.45	34.90				

Station 5016; Apr. 7; latitude 42°54′ N., longitude 49°20′ W.; depth 1,829 meters; dynamic height 970.943

Observed values			Scaled values			
Depth, meters	Temperature, ° C.	Salinity, °/oo	Depth, meters	Temperature, ° C.	Salinity, °/oo	σ_t
0	4.38	33.40	0	4.38	33.40	26.50
24	3.07	33.55	25	3.00	33.50	26.71
49	0.81	33.68	50	0.80	33.69	27.02
73	0.29	33.84	75	0.30	33.85	27.18
97	0.55	33.94	100	0.55	33.95	27.25
146	0.44	34.23	150	0.45	34.24	27.48
194	1.82	34.34	200	2.00	34.36	27.48
291	4.19	34.80	300	4.15	34.81	27.64
349	3.82	34.83	400	3.60	34.83	27.71
527	3.42	34.82	600	3.45	34.83	27.72
708	3.51	34.86	800	3.50	34.87	27.76
893	3.51	34.87	1,000	3.50	34.87	27.76
1,368	3.39	34.88				

Station 5017; Apr. 7; latitude 43°21′ N., longitude 48°50′ W.; depth 1,701 meters; dynamic height 970.950

Observed values			Scaled values			
Depth, meters	Temperature, ° C.	Salinity, °/oo	Depth, meters	Temperature, ° C.	Salinity, °/oo	σ_t
0	5.57	33.36	0	5.57	33.36	26.33
25	3.18	33.57	25	3.18	33.57	26.75
50	2.84	33.84	50	2.84	33.84	26.99
75	3.23	34.08	75	3.23	34.08	27.14
99	3.25	34.26	100	3.25	34.26	27.29
149	3.33	34.44	150	3.35	34.44	27.42
199	3.83	34.61	200	3.85	34.61	27.51
298	4.26	34.83	300	4.30	34.83	27.64
401	4.25	34.90	400	4.30	34.90	27.69
599	3.74	34.88	600	3.75	34.88	27.73
795	3.63	34.89	800	3.60	34.89	27.76
995	3.52	34.88	1,000	3.50	34.88	27.76
1,494	3.41	34.88				

STATIONS OCCUPIED IN 1953—Continued

Station 5018; Apr. 7; latitude 43°07′ N., longitude 48°10′ W.; depth 3,109 meters; dynamic height 970.982

Observed values			Scaled values			
Depth, meters	Temperature, ° C.	Salinity, °/oo	Depth, meters	Temperature, ° C.	Salinity, °/oo	σt
0	6.92	33.68	0	6.92	33.68	26.41
24	------	34.83	25	9.35	34.82	26.94
49	7.88	34.57	50	7.85	34.56	26.97
73	7.44	34.52	75	7.45	34.52	27.00
97	7.95	34.83	100	8.00	34.84	27.17
146	8.42	35.05	150	8.40	35.04	27.26
194	4.66	34.55	200	4.55	34.55	27.39
291	4.09	34.74	300	4.15	34.76	27.60
350	4.82	34.91	400	4.70	34.93	27.67
530	4.29	34.94	600	4.20	34.93	27.73
714	4.04	34.92	800	3.85	34.91	27.75
900	3.75	34.90	1,000	3.70	34.90	27.76
1,379	3.54	34.91				

Station 5019; Apr. 7–8; latitude 42°50.5′ N., longitude 47°33′ W.; depth 3,658 meters; dynamic height 970.961

Observed values			Scaled values			
Depth, meters	Temperature, ° C.	Salinity, °/oo	Depth, meters	Temperature, ° C.	Salinity, °/oo	σt
0	6.35	33.36	0	6.35	33.36	26.23
26	5.12	34.02	25	5.10	34.00	26.89
52	5.10	34.19	50	5.10	34.18	27.03
78	5.26	34.30	75	5.25	34.29	27.10
103	2.36	34.06	100	2.45	34.08	27.21
154	2.83	34.36	150	2.85	34.34	27.39
206	3.14	34.50	200	3.10	34.48	27.48
309	4.99	34.945	300	4.95	34.92	27.64
411	4.23	34.89	400	4.30	34.89	27.68
617	4.50	34.97	600	4.50	34.97	27.73
822	3.65	34.88	800	3.70	34.89	27.75
1,028	3.46	34.86	1,000	3.45	34.86	27.75
1,541	3.43	34.89				

Station 5020; Apr. 8; latitude 42°40′ N., longitude 47°07′ W.; depth 4,024 meters; dynamic height 971.229

Observed values			Scaled values			
Depth, meters	Temperature, ° C.	Salinity, °/oo	Depth, meters	Temperature, ° C.	Salinity, °/oo	σt
0	16.24	36.04	0	16.24	36.04	26.50
24	15.92	36.07	25	15.90	36.07	26.60
49	15.56	36.02	50	15.55	36.01	26.65
73	14.92	35.89	75	14.90	35.89	26.69
97	14.57	35.82	100	14.55	35.82	26.72
145	13.92	35.73	150	13.85	35.71	26.79
194	12.74	35.54	200	12.60	35.52	26.89
291	11.20	35.41	300	10.40	35.27	27.11
265	11.13	35.36	400	5.45	34.60	27.32
399	5.50	34.60	600	4.85	34.86	27.60
534	4.48	34.72	800	4.85	34.98	27.69
679	5.15	34.98	1,000	4.50	34.98	27.73
1,062	4.41	34.98				

Station 5021; Apr. 8; latitude 42°15.5′ N., longitude 46°12′ W.; depth 4,481 meters; dynamic height 971.561

Observed values			Scaled values			
Depth, meters	Temperature, ° C.	Salinity, °/oo	Depth, meters	Temperature, ° C.	Salinity, °/oo	σt
0	17.33	36.35	0	17.33	36.35	26.48
25	17.13	36.33	25	17.13	36.33	26.53
50	16.72	36.28	50	16.72	36.28	26.58
75	16.71	36.28	75	16.71	36.28	26.58
100	16.63	36.28	100	16.63	36.28	26.60
149	16.64	36.29	150	16.65	36.29	26.61
199	16.66	36.30	200	16.65	36.30	26.61
299	16.56	36.26	300	16.50	36.26	26.61
318	15.81	36.12	400	14.55	35.90	26.78
508	12.81	35.66	600	11.00	35.45	27.14
687	9.23	35.28	800	7.70	35.22	27.51
886	6.90	35.19	1,000	5.90	35.11	27.67
1,296	4.34	34.96				

Station 5022; Apr. 9; latitude 42°48.5′ N., longitude 45°36′ W.; depth 4,755 meters; dynamic height 971.271

Observed values			Scaled values			
Depth, meters	Temperature, ° C.	Salinity, °/oo	Depth, meters	Temperature, ° C.	Salinity, °/oo	σt
0	16.12	36.02	0	16.12	36.02	26.52
26	16.17	36.04	25	16.15	36.04	26.52
51	15.68	36.05	50	15.70	36.05	26.64
77	15.30	35.97	75	15.35	35.98	26.66
102	14.68	35.84	100	14.75	35.85	26.70
153	13.98	35.76	150	14.05	35.77	26.79
204	12.04	35.34	200	12.25	35.37	26.85
306	9.61	34.95	300	9.70	34.97	27.00
333	9.28	35.02	400	8.10	34.94	27.23
533	5.87	34.84	600	5.35	34.86	27.54
724	4.83	34.90	800	4.55	34.92	27.69
927	4.24	34.93	1,000	4.15	34.93	27.73
1,336	3.69	34.91				

Station 5023; Apr. 9; latitude 43°19′ N., longitude 45°04′ W.; depth 4,755 meters; dynamic height 971.070

Observed values			Scaled values			
Depth, meters	Temperature, ° C.	Salinity, °/oo	Depth, meters	Temperature, ° C.	Salinity, °/oo	σt
0	9.86	34.35	0	9.86	34.35	26.49
25	9.64	34.61	25	9.64	34.61	26.74
50	9.33	34.73	50	9.33	34.73	26.86
76	9.21	34.74	75	9.20	34.74	26.90
101	8.74	34.70	100	8.75	34.70	26.94
151	8.52	34.73	150	8.55	34.73	26.99
201	7.11	34.75	200	7.15	34.75	27.22
302	5.85	34.84	300	5.90	34.84	27.46
338	5.55	34.83	400	5.15	34.85	27.56
555	4.49	34.91	600	4.40	34.92	27.70
767	4.24	34.93	800	4.20	34.93	27.73
981	4.07	34.93	1,000	4.05	34.93	27.74
1,410	3.68	34.88				

Station 5024; Apr. 9; latitude 43°28′ N., longitude 45°55′ W.; depth 4,572 meters; dynamic height 971.052

Observed values			Scaled values			
Depth, meters	Temperature, ° C.	Salinity, °/oo	Depth, meters	Temperature, ° C.	Salinity, °/oo	σt
0	9.50	34.26	0	9.50	34.26	26.48
25	8.98	34.55	25	8.98	34.55	26.79
51	9.64	34.80	50	9.60	34.80	26.88
76	9.42	34.80	75	9.45	34.80	26.91
102	9.65	34.95	100	9.65	34.94	26.98
153	9.19	35.04	150	9.25	35.04	27.13
203	7.51	34.89	200	7.60	34.90	27.27
305	5.97	34.81	300	6.05	34.81	27.42
352	5.62	34.86	400	5.30	34.88	27.56
576	4.43	34.91	600	4.40	34.91	27.69
794	4.33	-------	800	4.30	34.99	27.76
1,013	3.67	34.92	1,000	3.70	34.92	27.78
1,447	3.61	34.92				

Station 5025; Apr. 9; latitude 43°32′ N., longitude 46°50′ W.; depth 4,079 meters; dynamic height 971.119

Observed values			Scaled values			
Depth, meters	Temperature, ° C.	Salinity, °/oo	Depth, meters	Temperature, ° C.	Salinity, °/oo	σt
0	10.89	34.70	0	10.89	34.70	26.58
25	10.14	34.73	25	10.14	34.73	26.74
50	9.74	34.83	50	9.74	34.83	26.88
75	7.77	34.51	75	7.77	34.51	26.94
100	7.31	34.43	100	7.31	34.43	26.94
150	9.17	34.84	150	9.17	34.84	26.98
199	7.80	34.64	200	7.75	34.64	27.05
299	------	34.55	300	6.00	34.55	27.22
357	6.73	34.915	400	6.25	34.91	27.46
578	4.24	34.89	600	4.25	34.89	27.69
794	4.34	34.95	800	4.30	34.95	27.73
1,013	3.91	34.92	1,000	3.95	34.92	27.75
1,449	3.53	34.89				

Table of Oceanographic Data—Continued

STATIONS OCCUPIED IN 1953—Continued

Station 5026; Apr. 9; latitude 43°46.5′ N., longitude 47°38′ W.; depth 3,932 meters; dynamic height 970.984

Observed values			Scaled values			
Depth, meters	Temperature, ° C.	Salinity, °/oo	Depth, meters	Temperature, ° C.	Salinity, °/oo	σ_t
0	6.79	33.19	0	6.79	33.19	26.05
25	3.98	33.47	25	3.98	33.47	26.60
50	2.33	33.56	50	2.33	33.56	26.82
75	1.43	33.70	75	1.43	33.70	26.99
100	1.77	33.88	100	1.77	33.88	27.10
150	2.36	34.26	150	2.36	34.26	27.37
199	3.30	34.56	200	3.30	34.56	27.53
299	3.65	34.74	300	3.70	34.74	27.63
349	4.47	34.90	400	4.35	34.89	27.68
571	3.96	34.86	600	3.90	34.86	27.71
788	3.84	34.89	800	3.80	34.89	27.74
1,006	3.61	34.88	1,000	3.60	34.88	27.75
1,442	3.41	34.88				

Station 5027; Apr. 10; latitude 44°01′ N., longitude 48°13′ W.; depth 3,383 meters; dynamic height 970.955

Observed values			Scaled values			
Depth, meters	Temperature, ° C.	Salinity, °/oo	Depth, meters	Temperature, ° C.	Salinity, °/oo	σ_t
0	6.65	33.24	0	6.65	33.24	26.11
25	4.05	33.60	25	4.05	33.60	26.69
50	2.06	33.65	50	2.06	33.65	26.92
75	3.07	34.01	75	3.07	34.01	27.11
100	4.43	34.40	100	4.43	34.40	27.28
150	3.83	34.50	150	3.83	34.50	27.42
199	5.12	34.81	200	5.10	34.81	27.54
299	4.35	34.82	300	4.35	34.82	27.63
343	4.33	34.87	400	4.30	34.89	27.68
563	4.08	34.92	600	4.00	31.92	27.75
781	3.69	34.90	800	3.70	34.90	27.76
998	3.57	34.89	1,000	3.55	34.89	27.76
1,434	3.40	35.89				

Station 5028; Apr. 10; latitude 44°09′ N., longitude 48°47′ W.; depth 1,792 meters; dynamic height 971.024

Observed values			Scaled values			
Depth, meters	Temperature, ° C.	Salinity, °/oo	Depth, meters	Temperature, ° C.	Salinity, °/oo	σ_t
0	0.62	32.81	0	0.62	32.81	26.34
23	−0.03	32.92	25	−0.10	32.89	26.42
45	−1.16	32.96	50	−1.15	32.99	26.55
68	−0.78	33.15	75	−0.50	33.23	26.72
90	0.51	33.44	100	0.65	33.52	26.90
135	1.11	33.81	150	1.90	34.00	27.20
180	3.78	34.38	200	3.95	34.53	27.43
270	3.27	34.58	300	3.30	34.61	27.57
214	*4.03	34.57	400	3.35	34.73	27.65
352	3.31	34.67	600	3.55	34.84	27.72
490	3.48	34.82	800	3.60	34.86	27.74
643	3.59	34.84	1,000	3.60	34.88	27.75
972	3.57	34.88				

Station 5029; Apr. 10; latitude 44°12′ N., longitude 48°55′ W.; depth 622 meters; dynamic height 971.037

Observed values			Scaled values			
Depth, meters	Temperature, ° C.	Salinity, °/oo	Depth, meters	Temperature, ° C.	Salinity, °/oo	σ_t
0	0.93	32.78	0	0.93	32.78	26.29
25	−0.52	32.88	25	−0.52	32.88	26.44
49	−1.04	32.97	50	−1.05	32.98	26.54
74	−1.06	33.10	75	−1.05	33.11	26.64
97	0.33	33.46	100	0.35	33.49	26.89
146	0.68	33.77	150	0.70	33.79	27.11
194	1.25	34.15	200	1.30	34.18	27.38
291	2.20	34.45	300	2.25	34.47	27.55
388	2.66	34.60	400	2.70	34.62	27.63
558	3.45	34.80	(600)	3.55	34.84	27.72

Station 5030; Apr. 10; latitude 44°14′ N., longitude 48°59′ W.; depth 137 meters; dynamic height 971.056

Observed values			Scaled values			
Depth, meters	Temperature, ° C.	Salinity, °/oo	Depth, meters	Temperature, ° C.	Salinity, °/oo	σ_t
0	0.91	32.81	0	0.91	32.81	26.32
26	−0.04	32.88	25	0.00	32.88	26.42
51	−1.35	32.99	50	−1.35	32.98	26.55
77	−0.97	33.11	75	−1.00	33.10	26.63
102	−0.65	33.20	100	−0.65	33.19	26.70
128	−0.29	33.35				

Station 5031; Apr. 10; latitude 44°17′ N., longitude 49°08′ W.; depth 75 meters; dynamic height 971.050

Observed values			Scaled values			
Depth, meters	Temperature, ° C.	Salinity, °/oo	Depth, meters	Temperature, ° C.	Salinity, °/oo	σ_t
0	0.32	32.87	0	0.32	32.87	26.40
26	−.051	33.04	25	−0.50	33.03	26.51
52	2.62	33.32	50	2.60	33.32	26.60
67	2.21	33.35	(75)	1.95	33.36	26.68

Station 5032; Apr. 10; latitude 44°24′ N., longitude 49°23′ W.; depth 48 meters; dynamic height 971.050

Observed values			Scaled values			
Depth, meters	Temperature, ° C.	Salinity, °/oo	Depth, meters	Temperature, ° C.	Salinity, °/oo	σ_t
0	3.00	32.98	0	3.00	32.98	26.30
25	0.18	33.07	25	0.18	33.07	26.56
40	0.18	33.07	(50)	0.20	33.07	26.56

Station 5033; Apr. 10; latitude 45°06′ N., longitude 49°25′ W.; depth 59 meters; dynamic height 971.086

Observed values			Scaled values			
Depth, meters	Temperature, ° C.	Salinity, °/oo	Depth, meters	Temperature, ° C.	Salinity, °/oo	σ_t
0	1.96	32.92	0	1.96	32.92	26.33
26	−0.14	32.92	25	−0.10	32.92	26.45
52	−0.88	33.00	50	−0.85	32.99	26.54

Station 5034; Apr. 10; latitude 45°04′ N., longitude 49°11′ W.; depth 81 meters; dynamic height 971.077

Observed values			Scaled values			
Depth, meters	Temperature, ° C.	Salinity, °/oo	Depth, meters	Temperature, ° C.	Salinity, °/oo	σ_t
0	1.78	32.70	0	1.78	32.70	26.16
27	0.58	33.27	25	0.60	33.24	26.68
54	1.93	33.43	50	1.80	33.41	26.74
65	1.88	33.46	(75)	1.80	33.48	26.79

Station 5035; Apr. 10; latitude 45°01′ N., longitude 48°56′ W.; depth 714 meters; dynamic height 971.091

Observed values			Scaled values			
Depth, meters	Temperature, ° C.	Salinity, °/oo	Depth, meters	Temperature, ° C.	Salinity, °/oo	σ_t
0	2.11	32.60	0	2.11	32.60	26.07
24	−0.47	32.72	25	−0.55	32.72	26.31
48	−1.36	32.94	50	−1.35	32.95	26.52
72	−1.20	33.01	75	−1.20	33.02	26.58
97	−0.93	33.10	100	−0.90	33.12	26.65
145	0.01	33.40	150	0.15	33.42	26.85
193	0.75	33.58	200	0.85	33.65	26.99
290	3.11	34.51	300	3.15	34.53	27.51
325	----	34.57	400	3.30	34.69	27.63
516	3.40	34.81	(600)	3.45	34.84	27.73

Table of Oceanographic Data—Continued

STATIONS OCCUPIED IN 1953—Continued

Station 5036; Apr. 10; latitude 44°58′ N., longitude 48°36′ W.; depth 1,499 meters; dynamic height 970.993

Observed values			Scaled values			
Depth, meters	Temperature, °C.	Salinity, ‰	Depth, meters	Temperature, °C.	Salinity, ‰	σ_t
0	1.02	32.84	0	1.02	32.84	26.31
25	−0.43	33.04	25	−0.43	33.04	26.57
50	0.99	33.26	50	0.99	33.26	26.67
75	−0.46	33.34	75	−0.46	33.34	26.81
100	0.00	33.51	100	0.00	33.51	26.93
150	0.98	33.84	150	0.98	33.84	27.13
200	1.63	34.26	200	1.63	34.26	27.43
300	3.21	34.71	300	3.21	34.71	27.66
358	3.33	34.79	400	3.40	34.81	27.72
582	3.48	34.83	600	3.50	34.83	27.72
798	3.50	34.88	800	3.50	34.88	27.76
1,018	3.54	34.88	1,000	3.50	34.89	27.76
1,455	3.40	34.89				

Station 5037; Apr. 11; latitude 44°55′ N., longitude 48°18′ W.; depth 2,065 meters; dynamic height 970.923

Observed values			Scaled values			
Depth, meters	Temperature, °C.	Salinity, ‰	Depth, meters	Temperature, °C.	Salinity, ‰	σ_t
0	5.19	33.67	0	5.19	33.67	26.63
23	4.50	33.70	25	4.35	33.70	26.74
46	2.39	33.78	50	2.30	33.80	27.01
68	1.75	33.93	75	1.55	33.91	27.15
91	1.14	34.06	100	1.20	34.11	27.34
137	1.69	34.36	150	1.80	34.40	27.53
182	2.18	34.47	200	2.35	34.50	27.56
273	2.98	34.67	300	4.05	34.88	27.70
306	4.18	34.90	400	4.15	34.91	27.72
510	3.95	34.91	600	3.75	34.90	27.75
718	3.67	34.88	800	3.65	34.89	27.75
925	3.68	34.90	1,000	3.65	34.90	27.76
1,346	3.51	34.90				

Station 5038; Apr. 11; latitude 44°51′ N., longitude 47°49′ W.; depth 3,567 meters; dynamic height 970.970

Observed values			Scaled values			
Depth, meters	Temperature, °C.	Salinity, ‰	Depth, meters	Temperature, °C.	Salinity, ‰	σ_t
0	6.62	33.29	0	6.62	33.29	26.14
24	4.79	33.47	25	4.75	33.47	26.52
49	4.61	33.74	50	4.60	33.75	26.75
73	5.05	34.06	75	5.05	34.06	26.95
98	3.06	34.06	100	2.90	34.06	27.17
147	1.39	34.18	150	1.40	34.20	27.40
195	4.10	34.64	200	4.10	34.66	27.53
293	4.27	34.83	300	4.25	34.83	27.65
476	3.50	34.82	400	3.75	34.82	27.69
667	3.71	34.90	600	3.65	34.88	27.74
865	3.48	34.87	800	3.55	34.88	27.75
1,278	3.43	34.89	1,000	3.45	34.88	27.76

Station 5039; Apr. 11; latitude 44°46′ N., longitude 47°11′ W.; depth 3,475 meters; dynamic height 971.095

Observed values			Scaled values			
Depth, meters	Temperature, °C.	Salinity, ‰	Depth, meters	Temperature, °C.	Salinity, ‰	σ_t
0	9.89	34.67	0	9.89	34.67	26.73
25	9.83	34.84	25	9.83	34.84	26.87
48	10.25	35.12	50	10.25	35.02	26.94
73	10.33	35.14	75	10.30	35.04	26.95
97	10.27	35.13	100	10.25	35.03	26.95
146	10.35	35.14	150	10.30	35.04	26.95
194	10.45	35.16	200	10.40	35.06	26.95
291	5.81	34.73	300	5.80	34.74	27.39
229	6.76	34.64	400	5.45	34.86	27.53
378	5.55	34.84	600	4.55	34.93	27.69
526	4.77	34.91	800	4.20	34.93	27.73
703	4.35	34.94	1,000	3.90	34.91	27.75
1,097	3.72	34.90				

Station 5040; Apr. 11; latitude 44°42′ N., longitude 46°26′ W.; depth 3,603 meters; dynamic height 971.048

Observed values			Scaled values			
Depth, meters	Temperature, °C.	Salinity, ‰	Depth, meters	Temperature, °C.	Salinity, ‰	σ_t
0	9.71	34.52	0	9.71	34.52	26.65
23	9.57	34.56	25	9.55	34.58	26.72
34	10.22	34.97	50	10.20	34.96	26.91
68	9.90	34.93	75	9.45	34.85	26.94
90	8.15	34.60	100	8.30	34.63	26.95
135	9.15	34.85	150	9.20	34.91	27.04
180	9.16	35.00	200	8.05	34.90	27.21
270	5.52	34.68	300	5.40	34.73	27.43
244	5.60	34.67	400	4.95	34.89	27.61
407	4.90	34.90	600	4.25	34.92	27.72
574	4.32	34.92	800	3.90	34.91	27.75
748	3.96	34.91	1,000	3.70	34.90	27.76
1,118	3.59	34.89				

Station 5041; Apr. 11; latitude 44°37′ N., longitude 45°34′ W.; depth 4,024 meters; dynamic height 971.020

Observed values			Scaled values			
Depth, meters	Temperature, °C.	Salinity, ‰	Depth, meters	Temperature, °C.	Salinity, ‰	σ_t
0	8.71	34.10	0	8.71	34.10	26.48
24	7.95	34.04	25	7.70	34.03	26.57
46	4.15	33.71	50	4.10	33.71	26.78
70	3.98	33.86	75	4.00	33.97	26.99
93	6.87	34.46	100	6.80	34.46	27.04
140	5.81	34.48	150	5.95	34.54	27.21
186	6.54	34.80	200	6.50	34.80	27.35
279	4.55	34.75	300	4.60	34.77	27.56
222	6.21	34.80	400	4.85	34.90	27.63
376	4.85	34.88	600	4.50	34.94	27.70
537	4.65	34.95	800	3.90	34.91	27.75
711	4.15	34.92	1,000	3.55	34.90	27.77
1,092	3.47	34.89				

Station 5042; Apr. 12; latitude 44°28′ N., longitude 45°15′ W.; depth 4,024 meters; dynamic height 971.124

Observed values			Scaled values			
Depth, meters	Temperature, °C.	Salinity, ‰	Depth, meters	Temperature, °C.	Salinity, ‰	σ_t
0	11.76	34.90	0	11.76	34.90	26.58
25	11.62	34.92	25	11.62	34.92	26.63
50	10.33	34.96	50	10.33	34.96	26.88
75	9.02	34.74	75	9.02	34.74	26.93
99	8.90	34.76	100	8.90	34.76	26.97
150	8.81	34.80	150	8.85	34.80	27.01
200	9.54	35.05	200	9.55	35.05	27.08
299	8.15	35.04	300	8.15	35.04	27.30
221	8.72	34.98	400	6.75	34.98	27.45
365	7.27	35.01	600	4.90	34.94	27.66
511	5.26	34.93	800	4.40	34.94	27.71
679	4.69	34.95	1,000	3.90	34.92	27.76
1,046	3.80	34.92				

Station 5043; Apr. 12; latitude 44°54′ N., longitude 45°11′ W.; depth 3,987 meters; dynamic height 971.013

Observed values			Scaled values			
Depth, meters	Temperature, °C.	Salinity, ‰	Depth, meters	Temperature, °C.	Salinity, ‰	σ_t
0	7.20	33.69	0	7.20	33.69	26.38
25	6.40	33.76	25	6.40	33.76	26.55
50	9.47	34.84	50	9.47	34.84	26.94
75	8.95	34.68	75	8.95	34.84	27.02
100	8.89	34.84	100	8.89	34.84	27.03
151	8.40	34.94	150	8.45	34.94	27.18
201	7.02	34.90	200	7.10	34.91	27.36
301	4.49	34.70	300	4.50	34.70	27.51
245	5.36	34.70	400	4.80	34.90	27.64
387	4.78	34.89	600	4.30	34.94	27.72
518	4.58	34.96	800	3.80	34.92	27.77
680	4.01	34.92	1,000	3.60	34.91	27.78
1,025	3.61	34.91				

Table of Oceanographic Data—Continued

STATIONS OCCUPIED IN 1953—Continued

Station 5044; Apr. 12; latitude 45°30′ N., longitude 45°08′ W.; depth 3,914 meters; dynamic height 970.935

Observed values			Scaled values			
Depth, meters	Temperature, ° C.	Salinity, °/oo	Depth, meters	Temperature, ° C.	Salinity, °/oo	σ_t
0	6.22	33.69	0	6.22	33.69	26.51
26	4.57	33.88	25	4.55	33.88	26.85
50	3.51	33.96	50	3.50	33.96	27.03
76	3.73	34.16	75	3.70	34.16	27.17
100	4.05	34.35	100	4.05	34.35	27.29
152	4.27	34.58	150	4.30	34.57	27.44
202	4.19	34.68	200	4.20	34.67	27.53
302	4.30	34.86	300	4.30	34.86	27.66
278	4.24	34.84	400	4.20	34.91	27.72
461	4.11	34.92	600	3.90	34.91	27.75
645	3.83	34.90	800	3.55	34.88	27.75
842	3.50	34.87	1,000	3.45	34.88	27.76
1,259	3.43	34.90				

Station 5045; Apr. 12; latitude 45°30′ N.; longitude 45°52′ W.; depth 3,475 meters; dynamic height 970.917

Observed values			Scaled values			
Depth, meters	Temperature, ° C.	Salinity, °/oo	Depth, meters	Temperature, ° C.	Salinity, °/oo	σ_t
0	6.36	33.71	0	6.36	33.71	26.51
23	6.16	33.75	25	6.10	33.75	26.58
47	5.22	33.99	50	4.85	34.02	26.94
70	3.02	34.20	75	2.90	34.22	27.30
93	2.69	34.26	100	2.75	34.29	27.36
140	4.06	34.58	150	4.10	34.61	27.49
187	4.15	34.72	200	4.15	34.75	27.59
280	4.12	34.87	300	4.20	34.89	27.70
290	4.21	34.90	400	4.10	34.92	27.74
483	3.98	34.92	600	3.85	34.92	27.76
678	3.74	34.91	800	3.60	34.90	27.77
879	3.55	34.89	1,000	3.55	34.90	27.77
1,303	3.55	34.91				

Station 5046; Apr. 12; latitude 45°30′ N.; longitude 46°39′ W.; depth 2,195 meters; dynamic height 970.989

Observed values			Scaled values			
Depth, meters	Temperature, ° C.	Salinity, °/oo	Depth, meters	Temperature, ° C.	Salinity, °/oo	σ_t
0	5.50	33.71	0	5.50	33.71	26.62
26	5.15	33.76	25	5.20	33.76	26.70
51	4.02	33.78	50	4.05	33.78	26.82
77	3.79	33.78	75	3.80	33.78	26.86
102	3.80	33.94	100	3.80	33.92	26.97
154	4.57	34.42	150	4.50	34.38	27.26
205	4.90	34.68	200	4.90	34.66	27.44
307	4.75	34.88	300	4.90	34.87	27.61
305	4.93	34.88	400	4.60	34.90	27.66
510	4.13	34.91	600	3.90	34.91	27.75
721	3.73	34.90	800	3.70	34.90	27.76
928	3.62	34.89	1,000	3.55	34.89	27.76
1,348	3.41	34.89				

Station 5047; Apr. 12; latitude 45°30′ N.; longitude 47°24′ W.; depth 1,582 meters; dynamic height 970.990

Observed values			Scaled values			
Depth, meters	Temperature, ° C.	Salinity, °/oo	Depth, meters	Temperature, ° C.	Salinity, °/oo	σ_t
0	6.29	33.56	0	6.29	33.56	26.40
24	6.11	33.59	25	6.10	33.59	26.45
47	4.71	33.86	50	4.60	33.86	26.84
71	4.19	33.84	75	4.20	33.85	26.87
94	4.38	33.95	100	4.30	33.98	26.96
141	3.50	34.22	150	3.60	34.29	27.28
189	4.13	34.60	200	4.20	34.64	27.50
283	4.40	34.82	300	4.40	34.84	27.63
485	4.11	34.90	400	4.25	34.89	27.69
684	3.55	34.84	600	3.80	34.87	27.73
886	3.52	34.86	800	3.50	34.85	27.74
1,303	3.44	34.88	1,000	3.50	34.87	27.76

Station 5048; Apr. 13; latitude 45°38.5′ N., longitude 47°38′ W.; depth 1,257 meters; dynamic height 971.016

Observed values			Scaled values			
Depth, meters	Temperature, ° C.	Salinity, °/oo	Depth, meters	Temperature, ° C.	Salinity, °/oo	σ_t
0	0.44	32.72	0	0.44	32.72	26.27
20	0.47	32.73	25	0.00	32.78	26.34
40	−1.55	33.00	50	−1.45	33.08	26.63
60	−1.29	33.15	75	−0.70	33.29	26.77
81	−0.42	33.34	100	0.25	33.52	26.93
121	0.75	33.72	150	0.80	33.85	27.15
161	0.84	33.92	200	2.50	34.26	27.36
242	3.83	34.64	300	4.20	34.80	27.63
379	4.29	34.88	400	4.20	34.88	27.69
543	3.59	34.84	600	3.55	34.85	27.73
712	3.53	34.86	800	3.55	34.86	27.74
929	3.51	34.87	(1,000)	3.50	34.88	27.76

Station 5049; Apr. 13; latitude 45°45′ N., longitude 47°49′ W.; depth 691 meters; dynamic height 971.035

Observed values			Scaled values			
Depth, meters	Temperature, ° C.	Salinity, °/oo	Depth, meters	Temperature, ° C.	Salinity, °/oo	σ_t
0	0.44	32.62	0	0.44	32.62	26.19
20	0.43	32.62	25	0.20	32.62	26.20
41	−1.20	32.94	50	−1.25	33.02	26.58
61	−1.24	33.11	75	−1.00	33.22	26.73
81	−0.87	33.26	100	−0.37	33.40	26.85
122	0.15	33.59	150	0.80	33.84	27.14
163	1.02	33.94	200	1.20	34.09	27.32
244	1.43	34.23	300	2.10	34.44	27.53
412	3.46	34.80	400	3.40	34.78	27.69
650	3.46	34.84	600	3.45	34.83	27.72

Station 5050; Apr. 13; latitude 45°51′ N., longitude 48°00′ W.; depth 174 meters; dynamic height 971.063

Observed values			Scaled values			
Depth, meters	Temperature, ° C.	Salinity, °/oo	Depth, meters	Temperature, ° C.	Salinity, °/oo	σ_t
0	0.46	32.58	0	0.46	32.58	26.16
29	−0.21	32.74	25	−0.10	32.72	26.29
60	−1.37	32.94	50	−1.10	32.87	26.45
90	−0.18	33.28	75	−0.90	33.11	26.64
150	0.56	33.61	100	0.00	33.35	26.80
			150	0.55	33.61	26.98

Station 5051; Apr. 13; latitude 45°57.5′ N., longitude 48°11′ W.; depth 116 meters; dynamic height 971.075

Observed values			Scaled values			
Depth, meters	Temperature, ° C.	Salinity, °/oo	Depth, meters	Temperature, ° C.	Salinity, °/oo	σ_t
0	0.70	32.60	0	0.70	32.60	26.17
25	0.66	32.62	25	0.66	32.62	26.18
50	−0.70	32.84	50	−0.70	32.84	26.42
75	−1.32	32.91	75	−1.32	32.91	26.49
100	−1.30	33.04	100	−1.30	33.04	26.59

Station 5052; Apr. 13; latitude 46°14′ N., longitude 48°39′ W.; depth 94 meters; dynamic height 971.072

Observed values			Scaled values			
Depth, meters	Temperature, ° C.	Salinity, °/oo	Depth, meters	Temperature, ° C.	Salinity, °/oo	σ_t
0	0.91	32.74	0	0.91	32.74	26.26
25	0.86	32.74	25	0.86	32.74	26.27
50	−0.57	32.88	50	−0.57	32.88	26.44
75	−0.72	32.94	75	−0.72	32.94	26.50

STATIONS OCCUPIED IN 1953—Continued

Station 5053; Apr. 13; latitude 46°13′ N., longitude 48°14′ W.; depth 114 meters; dynamic height 971.072

Observed values			Scaled values			
Depth, meters	Temperature, °C.	Salinity, °/oo	Depth, meters	Temperature, °C.	Salinity, °/oo	σ_t
0	0.75	32.66	0	0.75	32.66	26.20
25	0.43	32.65	25	0.43	32.65	26.22
51	−1.19	32.88	50	−1.15	32.86	26.44
76	−1.23	33.05	75	−1.25	33.04	26.59
102	−0.38	33.24	100	−0.50	33.22	26.71

Station 5054; Apr. 13; latitude 46°12′ N., longitude 47°54′ W.; depth 179 meters; dynamic height 971.091

Observed values			Scaled values			
Depth, meters	Temperature, °C.	Salinity, °/oo	Depth, meters	Temperature, °C.	Salinity, °/oo	σ_t
0	0.26	32.64	0	0.26	32.64	26.22
25	0.22	32.65	25	0.22	32.65	26.22
50	−0.86	32.69	50	−0.86	32.69	26.29
75	−1.35	32.92	75	−1.35	32.92	26.50
100	−0.83	33.13	100	−0.83	33.13	26.65
150	−0.06	33.45	150	−0.06	33.45	26.88

Station 5055; Apr. 13; latitude 46°10′ N., longitude 47°31′ W.; depth 686 meters; dynamic height 970.998

Observed values			Scaled values			
Depth, meters	Temperature, °C.	Salinity, °/oo	Depth, meters	Temperature, °C.	Salinity, °/oo	σ_t
0	0.42	32.62	0	0.42	32.62	26.19
25	0.41	32.62	25	0.41	32.62	26.19
50	−0.84	33.12	50	−0.84	33.12	26.64
74	−0.12	33.46	75	−0.15	33.47	26.91
99	0.81	33.86	100	0.80	33.87	27.17
149	1.28	34.02	150	1.30	34.02	27.26
198	1.06	34.12	200	1.05	34.13	27.36
297	2.22	34.47	300	2.25	34.48	27.55
374	2.92	34.66	400	3.15	34.72	27.67
564	3.49	34.86	(600)	3.50	34.87	27.76

Station 5056; Apr. 13; latitude 46°09′ N., longitude 47°14′ W.; depth 1,518 meters; dynamic height 970.923

Observed values			Scaled values			
Depth, meters	Temperature, °C.	Salinity, °/oo	Depth, meters	Temperature, °C.	Salinity, °/oo	σ_t
0	0.96	32.76	0	0.96	32.76	26.27
26	3.33	33.59	25	3.30	33.57	26.74
50	1.31	33.94	50	1.30	33.95	27.20
76	2.51	34.20	75	2.50	34.20	27.31
101	1.31	34.18	100	1.30	34.18	27.38
152	1.85	34.32	150	1.80	34.32	27.47
202	1.62	34.37	200	1.60	34.37	27.52
303	3.14	34.72	300	3.10	34.71	27.67
282	2.94	34.67	400	3.50	34.81	27.71
467	3.54	34.84	600	3.55	34.87	27.75
653	3.51	34.87	800	3.50	34.86	27.75
847	3.49	34.86	1,000	3.45	34.87	27.76
1,253	3.47	34.88				

Station 5057; Apr. 13; latitude 46°05′ N., longitude 46°28′ W.; depth 622 meters; dynamic height 970.985

Observed values			Scaled values			
Depth, meters	Temperature, °C.	Salinity, °/oo	Depth, meters	Temperature, °C.	Salinity, °/oo	σ_t
0	5.46	33.71	0	5.46	33.71	26.63
26	5.46	33.71	25	5.45	33.71	26.63
51	4.17	33.78	50	4.15	33.78	26.82
76	5.29	34.00	75	5.30	34.00	26.87
101	3.97	33.91	100	3.95	33.91	26.94
152	5.41	34.59	150	5.40	34.56	27.35
203	4.95	34.70	200	4.95	34.69	27.45
304	4.63	34.83	300	4.60	34.82	27.60
326	4.51	34.85	400	4.35	34.89	27.68
507	4.08	34.90	(600)	3.90	34.90	27.74

Station 5058; Apr. 14; latitude 46°02′ N., longitude 45°47′ W.; depth 2,579 meters; dynamic height 970.943

Observed values			Scaled values			
Depth, meters	Temperature, °C.	Salinity, °/oo	Depth, meters	Temperature, °C.	Salinity, °/oo	σ_t
0	6.47	33.76	0	6.47	33.76	26.53
27	6.49	33.76	25	6.50	33.76	26.53
53	5.48	34.07	50	5.60	34.01	26.84
79	4.95	34.40	75	5.00	34.35	27.18
105	4.14	34.42	100	4.25	34.42	27.32
159	4.07	34.62	150	4.05	34.59	27.47
211	4.48	34.76	200	4.40	34.73	27.54
316	4.69	34.93	300	4.70	34.92	27.67
349	4.09	34.87	400	3.85	34.86	27.71
565	3.55	34.86	600	3.55	34.86	27.74
772	3.58	34.88	800	3.55	34.88	27.75
988	3.51	34.89	1,000	3.50	34.89	27.77
1,426	3.39	34.88				

Station 5059; Apr. 14; latitude 45°58′ N., longitude 45°01′ W.; depth 3,621 meters; dynamic height 970.947

Observed values			Scaled values			
Depth, meters	Temperature, °C.	Salinity, °/oo	Depth, meters	Temperature, °C.	Salinity, °/oo	σ_t
0	6.38	33.65	0	6.38	33.67	26.48
27	5.04	33.76	25	5.05	33.79	26.73
53	5.94	34.12	50	5.90	34.08	26.86
81	5.59	34.43	75	5.65	34.39	27.13
107	5.62	34.53	100	5.60	34.50	27.23
161	4.84	34.68	150	4.90	34.65	27.43
215	5.07	34.85	200	5.00	34.82	27.56
322	4.63	34.92	300	4.75	34.92	27.66
334	4.64	34.94	400	4.40	34.93	27.70
551	3.95	34.92	600	3.85	34.91	27.75
767	3.57	34.88	800	3.55	34.88	27.75
			(1,000)	3.55	34.89	27.76

Station 5060; Apr. 14; latitude 45°55′ N., longitude 44°25′ W.; depth 3,841 meters; dynamic height 971.005

Observed values			Scaled values			
Depth, meters	Temperature, °C.	Salinity, °/oo	Depth, meters	Temperature, °C.	Salinity, °/oo	σ_t
0	6.27	33.54	0	6.27	33.54	26.39
24	6.15	33.52	25	6.15	33.52	26.39
49	4.64	33.76	50	4.65	33.76	26.75
73	6.88	34.30	75	6.85	34.30	26.91
97	4.74	34.10	100	4.65	34.10	27.02
146	3.99	34.30	150	3.95	34.31	27.27
194	3.69	34.47	200	3.70	34.49	27.43
291	4.42	34.76	300	4.45	34.77	27.58
321	4.44	34.80	400	4.40	34.87	27.66
528	4.26	34.93	600	4.15	34.93	27.73
734	3.95	34.92	800	3.90	34.92	27.76
943	3.81	34.91	1,000	3.75	34.91	27.76
1,367	3.41	34.87				

Station 5061; Apr. 28; latitude 49°40′ N., longitude 47°40′ W.; depth 2,561 meters; dynamic height 970.881

Observed values			Scaled values			
Depth, meters	Temperature, °C.	Salinity, °/oo	Depth, meters	Temperature, °C.	Salinity, °/oo	σ_t
0	6.04	34.35	0	6.04	34.35	27.05
25	5.87	34.34	25	5.87	34.34	27.07
49	4.65	34.45	50	4.65	34.45	27.30
74	4.26	34.52	75	4.25	34.52	27.40
98	3.99	34.55	100	4.00	34.55	27.45
148	4.41	34.79	150	4.40	34.79	27.59
197	3.93	34.80	200	3.90	34.80	27.66
295	3.26	34.80	300	3.25	34.80	27.72
383	3.21	34.80	400	3.25	34.80	27.72
575	3.40	34.85	600	3.45	34.85	27.74
766	3.49	34.87	800	3.55	34.87	27.75
962	3.46	34.88	1,000	3.45	34.88	27.76
1,457	3.37	34.90				

Table of Oceanographic Data—Continued

STATIONS OCCUPIED IN 1953—Continued

Station 5062; Apr. 28; latitude 49°18′ N., longitude 48°09′ W.; depth 2,323 meters; dynamic height 970.849

Observed values			Scaled values			
Depth, meters	Temperature, ° C.	Salinity, ‰	Depth, meters	Temperature, ° C.	Salinity, ‰	σ_t
0	4.44	34.41	0	4.44	34.41	27.29
24	4.31	34.41	25	4.30	34.41	27.31
47	4.20	34.50	50	4.15	34.51	27.40
71	3.46	34.56	75	3.45	34.58	27.52
95	3.65	34.71	100	3.65	34.72	27.62
142	3.48	34.78	150	3.45	34.78	27.68
189	3.31	34.78	200	3.30	34.78	27.70
284	3.38	34.80	300	3.30	34.79	27.71
326	3.04	34.78	400	3.15	34.80	27.73
487	3.26	34.83	600	3.35	34.85	27.75
647	3.37	34.86	800	3.50	34.87	27.76
			1,000	3.50	34.88	27.76

Station 5063; Apr. 28; latitude 48°53′ N., longitude 48°11′ W.; depth 2,265 meters; dynamic height 970.858

Observed values			Scaled values			
Depth, meters	Temperature, ° C.	Salinity, ‰	Depth, meters	Temperature, ° C.	Salinity, ‰	σ_t
0	3.94	34.20	0	3.94	34.20	27.18
23	4.21	34.33	25	4.20	34.34	27.26
47	4.23	34.46	50	4.20	34.47	27.37
70	3.34	34.54	75	3.15	34.56	27.54
94	2.60	34.61	100	2.60	34.62	27.64
141	2.71	34.64	150	2.75	34.66	27.66
187	2.92	34.74	200	2.95	34.74	27.70
281	3.03	34.77	300	3.10	34.78	27.72
315	3.13	34.78	400	3.25	34.80	27.72
482	3.34	34.82	600	3.40	34.83	27.73
658	*3.32	34.84	800	3.45	34.86	27.75
841	3.45	34.86	1,000	3.40	34.86	27.76
1,327	3.34	34.86				

Station 5064; Apr. 29-30; latitude 48°28′ N., longitude 48°28′ W.; depth 1,866 meters; dynamic height 970.850

Observed values			Scaled values			
Depth, meters	Temperature, ° C.	Salinity, ‰	Depth, meters	Temperature, ° C.	Salinity, ‰	σ_t
0	2.38	33.63	0	2.38	33.63	26.86
19	2.49	33.87	25	2.30	34.03	27.19
38	1.94	34.46	50	2.05	34.49	27.58
58	2.11	34.51	75	2.25	34.55	27.61
77	2.24	34.56	100	2.40	34.60	27.64
115	2.52	34.63	150	2.70	34.67	27.67
153	2.74	34.68	200	3.00	34.71	27.68
230	3.16	34.73	300	3.40	34.82	27.73
294	3.36	34.81	400	3.50	34.85	27.74
450	3.51	34.86	600	3.55	34.86	27.74
610	3.48	34.86	800	3.50	34.87	27.76
764	3.50	34.87	1,000	3.40	34.88	27.77
1,148	3.33	34.88				

Station 5065; Apr. 30; latitude 48°07.5′ N., longitude 48°42′ W.; depth 732 meters; dynamic height 970.950

Observed values			Scaled values			
Depth, meters	Temperature, ° C.	Salinity, ‰	Depth, meters	Temperature, ° C.	Salinity, ‰	σ_t
0	1.15	32.97	0	1.15	32.97	26.43
24	0.13	33.22	25	0.15	33.23	26.69
47	0.41	33.78	50	0.40	33.79	27.13
71	0.54	33.88	75	0.55	33.90	27.21
94	0.63	34.01	100	0.65	34.03	27.30
140	1.03	34.15	150	1.10	34.17	27.40
187	1.29	34.26	200	1.40	34.29	27.47
281	2.13	34.51	300	2.30	34.54	27.60
298	------	34.53	400	2.80	34.68	27.66
454	3.07	34.74	(600)	3.50	34.84	27.73

Station 5066; Apr. 30; latitude 48°02.5′ N., longitude 48°45′ W.; depth 315 meters; dynamic height 970.964

Observed values			Scaled values			
Depth, meters	Temperature, ° C.	Salinity, ‰	Depth, meters	Temperature, ° C.	Salinity, ‰	σ_t
0	1.05	32.82	0	1.05	32.82	26.32
25	0.66	33.04	25	0.66	33.04	26.51
50	0.13	33.68	50	0.13	33.68	27.05
74	0.29	33.87	75	0.30	33.88	27.20
99	0.49	34.00	100	0.50	34.00	27.29
148	1.01	34.18	150	1.05	34.19	27.41
197	1.46	34.30	200	1.50	34.30	27.47
286	2.29	34.51	(300)	2.45	34.55	27.59

Station 5067; Apr. 30; latitude 47°53′ N., longitude 48°53′ W.; depth 215 meters; dynamic height 971.028

Observed values			Scaled values			
Depth, meters	Temperature, ° C.	Salinity, ‰	Depth, meters	Temperature, ° C.	Salinity, ‰	σ_t
0	0.33	32.43	0	0.33	32.43	26.04
24	0.33	32.43	25	0.30	32.43	26.04
48	−1.54	33.10	50	−1.55	33.12	26.67
72	−1.50	33.26	75	−1.45	33.27	26.78
97	−0.60	33.42	100	−0.55	33.45	26.90
145	0.43	33.85	150	0.50	33.88	27.19
193	1.10	34.09	200	1.20	34.12	27.35

Station 5068: Apr. 30; latitude 47°53.5′ N., longitude 48°58′ W.; depth 180 meters; dynamic height 971.064

Observed values			Scaled values			
Depth, meters	Temperature, ° C.	Salinity, ‰	Depth, meters	Temperature, ° C.	Salinity, ‰	σ_t
0	1.33	32.54	0	1.33	32.54	26.08
25	1.28	32.55	25	1.28	32.55	26.08
49	−0.57	32.66	50	−0.60	32.67	26.27
74	−1.44	32.98	75	−1.45	32.99	26.56
99	−1.21	33.12	100	−1.20	33.12	26.66
148	0.37	33.54	150	0.50	33.57	26.95

Station 5069; Apr. 30; latitude 47°46′ N., longitude 48°35′ W.; depth 220 meters; dynamic height 971.029

Observed values			Scaled values			
Depth, meters	Temperature, ° C.	Salinity, ‰	Depth, meters	Temperature, ° C.	Salinity, ‰	σ_t
3	0.45	32.42	0	0.45	32.42	26.03
25	0.42	32.43	25	0.42	32.43	26.04
47	−1.44	33.10	50	−1.55	33.12	26.67
68	−1.61	33.22	75	−1.60	33.24	26.76
90	−1.31	33.29	100	−0.85	33.38	26.85
133	0.72	33.80	150	0.90	33.90	27.19
177	*1.07	34.02	(200)	1.20	34.09	27.32

Station 5070; Apr. 30; latitude 47°49′ N., longitude 48°06′ W.; depth 283 meters; dynamic height 971.034

Observed values			Scaled values			
Depth, meters	Temperature, ° C.	Salinity, ‰	Depth, meters	Temperature, ° C.	Salinity, ‰	σ_t
0	0.53	32.40	0	0.53	32.40	26.01
23	0.51	32.40	25	0.50	32.40	26.02
45	−1.28	32.86	50	−1.35	32.95	26.52
68	−1.39	33.15	75	−1.30	33.20	26.72
91	−0.81	33.32	100	−0.55	33.39	26.85
136	0.36	33.72	150	0.40	33.80	27.14
182	0.54	33.98	200	0.90	34.08	27.33
250	1.89	34.37				

STATIONS OCCUPIED IN 1953—Continued

Station 5071; Apr. 30; latitude 47°53′ N., longitude 47°32′ W.; depth 352 meters; dynamic height 970.950.

Observed values			Scaled values			
Depth, meters	Temperature, ° C.	Salinity, °/oo	Depth, meters	Temperature, ° C.	Salinity, °/oo	σ_t
0	1.21	32.52	0	1.21	32.52	26.07
26	0.44	32.91	25	0.45	32.90	26.41
51	0.26	33.70	50	0.25	33.67	27.05
77	0.49	33.85	75	0.45	33.84	27.16
102	0.89	34.08	100	0.85	34.06	27.32
155	1.42	34.28	150	1.35	34.26	27.45
206	2.07	34.46	200	2.00	34.43	27.53
308	2.59	34.62	300	2.55	34.61	27.64

Station 5072; Apr. 30; latitude 48°00′ N., longitude 47°24′ W.; depth 439 meters; dynamic height 970.923.

Observed values			Scaled values			
Depth, meters	Temperature, ° C.	Salinity, °/oo	Depth, meters	Temperature, ° C.	Salinity, °/oo	σ_t
0	1.39	32.84	0	1.39	32.84	26.32
26	1.61	33.04	25	1.60	33.04	26.46
50	1.74	33.90	50	1.75	33.90	27.13
76	2.78	34.34	75	2.80	34.33	27.39
101	2.00	34.45	100	2.00	34.29	27.42
152	2.20	34.46	150	2.20	34.45	27.54
202	2.43	34.58	200	2.40	34.57	27.62
303	2.91	34.68	300	2.90	34.67	27 66
405	3.39	34.80	400	3.40	34.80	27.71

Station 5073; Apr. 30–May 1; latitude 48°18′ N., longitude 47°02′ W.; depth 1,500 meters; dynamic height 970.870.

Observed values			Scaled values			
Depth, meters	Temperature, ° C.	Salinity, °/oo	Depth, meters	Temperature, ° C.	Salinity, °/oo	σ_t
0	2.20	33.44	0	2.20	33.44	26.73
24	2.20	33.47	25	2.20	33.47	26.76
48	1.93	34.14	50	1.95	34.20	27.36
72	2.17	34.50	75	2.20	34.51	27.59
96	2.44	34.58	100	2.50	34.59	27.62
145	2.62	34.63	150	2.65	34.64	27.65
193	2.94	34.73	200	3.00	34.74	27.70
289	3.36	34.82	300	3.45	34.82	27.72
313	3.50	34.83	400	3.55	34.86	27.74
474	3.57	34.87	600	3.60	34.88	27.75
639	3.57	34.88	800	3.55	34.87	27.75
809	3.53	34.87	1,000	3.45	34.88	27.76
1,149	3.37	34.88				

Station 5074; May 1; latitude 48°38′ N., longitude 46°38′ W;. depth 2,225 meters; dynamic height 970.853.

Observed values			Scaled values			
Depth, meters	Temperature, ° C.	Salinity, °/oo	Depth, meters	Temperature, ° C.	Salinity, °/oo	σ_t
0	3.29	33.84	0	3.29	33.84	26.95
24	3.30	33.85	25	3.30	33.85	26.96
47	3.98	34.46	50	3.15	34.47	27.47
71	3.02	34.58	75	3.00	34.59	27.58
94	2.86	34.62	100	2.85	34.62	27.62
142	2.72	34.65	150	2.75	34.66	27.66
189	2.98	34.75	200	3.00	34.76	27.72
283	3.39	34.84	300	3.35	34.83	27.73
292	3.35	34.81	400	3.50	34.86	27.75
451	3.52	34.87	600	3.55	34.88	27.75
621	3.50	34.88	800	3.50	34.88	27.76
800	3.48	34.88	1,000	3.40	34.88	27.77
1,290	3.32	34.88				

Station 5075; May 1; latitude 48°57′ N., longitude 46°16′ W.; depth 2,616 meters; dynamic height 970.841.

Observed values			Scaled values			
Depth, meters	Temperature, ° C.	Salinity, °/oo	Depth, meters	Temperature, ° C.	Salinity, °/oo	σ_t
0	4.45	34.40	0	4.45	34.40	27.28
24	4.46	34.40	25	4.45	34.40	27.28
47	4.46	34.41	50	4.45	34.42	27.30
71	3.13	34.64	75	3.05	34.65	27.62
95	2.98	34.70	100	3.00	34.70	27.67
143	3.02	34.74	150	3.00	34.74	27.70
190	2.87	34.74	200	2.85	34.74	27.71
285	3.02	34.78	300	3.10	34.79	27.73
357	3.44	34.85	400	3.45	34.85	27.74
536	3.34	34.855	600	3.40	34.86	27.76
717	3.43	34.87	800	3.45	34.88	27.76
899	3.43	34.88	1,000	3.40	34.88	27.77
1,356	3.36	34.88				

Station 5076; May 1; latitude 49°19.5′ N., longitude 45°49′ W.; depth 3,017 meters; dynamic height 970.883.

Observed values			Scaled values			
Depth, meters	Temperature, ° C.	Salinity, °/oo	Depth, meters	Temperature, ° C.	Salinity, °/oo	σ_t
0	5.28	34.20	0	5.28	34.20	27.03
26	5.27	34.22	25	5.30	34.22	27.05
52	5.06	34.24	50	5.10	34.24	27.08
78	3.82	34.50	75	3.95	34.48	27.40
103	3.54	34.56	100	3.55	34.55	27.49
156	2.94	34.62	150	2.95	34.61	27.60
207	4.00	34.85	200	3.95	34.84	27.68
310	3.60	34.84	300	3.65	34.84	27.71
397	3.46	34.82	400	3.45	34.82	27.72
599	3.52	34.86	600	3.55	34.86	27.74
805	3.47	34.88	800	3.50	34.88	27.76
1,015	3.41	34.88	1,000	3.40	34.88	27.77
1,551	3.39	34.91				

Station 5077; May 1; latitude 49°10′ N., longitude 45°21′ W.; depth 2,378 meters; dynamic height 970.872.

Observed values			Scaled values			
Depth, meters	Temperature, ° C.	Salinity, °/oo	Depth, meters	Temperature, ° C.	Salinity, °/oo	σ_t
0	5.58	34.32	0	5.58	34.32	27.09
27	5.58	34.32	25	5.60	34.32	27.09
52	5.17	34.31	50	5.30	34.31	27.12
79	3.30	34.52	75	3.60	34.50	27.45
105	3.11	34.59	100	3.10	34.57	27.56
158	3.26	34.71	150	3.25	34.69	27.63
210	3.43	34.79	200	3.40	34.78	27.69
315	3.56	34.82	300	3.55	34.83	27.71
345	3.54	34.84	400	3.55	34.84	27.72
546	3.50	34.86	600	3.50	34.86	27.75
768	3.48	34.87	800	3.50	34.87	27.76
976	3.37	34.87	1,000	3.35	34.87	27.77
1,525	3.33	34.90				

Station 5078; May 1; latitude 48°59′ N., longitude 44°49′ W.; depth 1,884 meters; dynamic height 970.844.

Observed values			Scaled values			
Depth, meters	Temperature, ° C.	Salinity, °/oo	Depth, meters	Temperature, ° C.	Salinity, °/oo	σ_t
0	4.77	34.28	0	4.77	34.28	27.15
26	4.78	34.31	25	4.75	34.30	27.17
51	3.57	34.50	50	3.60	34.50	27.45
77	3.15	34.57	75	3.15	34.56	27.54
103	3.21	34.68	100	3.20	34.67	27.63
153	3.19	34.74	150	3.20	34.73	27.67
205	3.47	34.82	200	3.45	34.81	27.71
308	3.36	34.84	300	3.35	34.84	27.74
414	3.35	------	400	3.35	34.85	27.75
621	3.48	34.88	600	3.50	34.88	27.76
1,037	3.34	34.87	800	3.45	34.88	27.76
1,561	3.28	34.88	1,000	3.35	34.87	27.77

STATIONS OCCUPIED IN 1953—Continued

Station 5079; May 2; latitude 48°40′ N., longitude 45°19′ W.; depth 1,097 meters; dynamic height 970.872

Observed values			Scaled values			
Depth, meters	Temperature, ° C.	Salinity, ‰	Depth, meters	Temperature, ° C.	Salinity, ‰	σ_t
0	4.12	33.91	0	4.12	33.91	26.93
24	4.15	34.04	25	4.15	34.04	27.03
49	3.30	34.18	50	3.25	34.19	27.23
73	2.10	34.42	75	2.10	34.42	27.52
97	2.08	34.43	100	2.10	34.43	27.52
145	2.53	34.56	150	2.55	34.58	27.61
194	2.89	34.69	200	2.95	34.70	27.67
291	3.49	34.82	300	3.50	34.81	27.71
339	3.59	34.82	400	3.60	34.86	27.74
514	3.58	34.89	600	3.60	34.88	27.75
691	3.52	34.87	800	3.45	34.88	27.76
873	3.45	34.89	(1,000)	3.35	34.88	27.77

Station 5080; May 2; latitude 48°20.5′ N., longitude 45°49′ W.; depth 951 meters; dynamic height 970.881

Observed values			Scaled values			
Depth, meters	Temperature, ° C.	Salinity, ‰	Depth, meters	Temperature, ° C.	Salinity, ‰	σ_t
0	3.88	33.72	0	3.88	33.72	26.80
25	3.86	33.73	25	3.86	33.73	26.81
50	2.23	34.14	50	2.23	34.14	27.28
74	2.13	34.35	75	2.15	34.35	27.46
99	2.08	34.40	100	2.10	34.40	27.50
148	2.62	34.56	150	2.65	34.57	27.60
198	3.51	34.75	200	3.50	34.73	27.66
297	3.56	34.84	300	3.55	34.83	27.71
342	3.55	34.84	400	3.55	34.85	27.73
532	3.50	34.86	600	3.50	34.86	27.75
736	3.41	34.86	800	3.40	34.86	27.76

Station 5081; May 2; latitude 47°59.5′ N., longitude 46°21′ W.; depth, 1,170 meters; dynamic height 970.855

Observed values			Scaled values			
Depth, meters	Temperature, ° C.	Salinity, ‰	Depth, meters	Temperature, ° C.	Salinity, ‰	σ_t
0	3.37	33.72	0	3.37	33.72	26.85
25	3.46	33.87	25	3.46	33.87	26.96
50	2.06	34.39	50	2.06	34.39	27.50
75	2.28	34.51	75	2.28	34.51	27.58
100	2.36	34.56	100	2.36	34.56	27.61
150	2.86	34.66	150	2.86	34.66	27.65
200	3.54	34.80	200	3.54	34.80	27.69
300	3.54	34.85	300	3.54	34.85	27.73
375	3.58	34.88	400	3.55	34.88	27.75
563	3.48	34.87	600	3.50	34.87	27.76
753	3.44	34.88	800	3.45	34.88	27.76
978	3.38	34.87	1,000	3.40	34.87	27.77

Station 5082; May 2; latitude 47°51.5′ N., longitude 46°03′ W.; depth 604 meters; dynamic height 970.873

Observed values			Scaled values			
Depth, meters	Temperature, ° C.	Salinity, ‰	Depth, meters	Temperature, ° C.	Salinity, ‰	σ_t
0	3.35	33.42	0	3.35	33.42	26.62
25	3.43	33.60	25	3.43	33.60	26.75
50	2.23	34.16	50	2.23	34.16	27.30
75	1.92	34.40	75	1.92	34.40	27.52
100	1.93	34.46	100	1.93	34.46	27.57
150	2.69	34.62	150	2.69	34.62	27.63
201	3.03	34.71	200	3.05	34.71	27.67
301	3.51	34.82	300	3.50	34.82	27.72
403	3.56	34.875	400	3.55	34.87	27.75
506	3.50	34.88	(600)	3.50	34.88	27.76

Station 5083; May 2; latitude 47°47′ N., longitude 45°52′ W.; depth 353 meters; dynamic height 970,883

Observed values			Scaled values			
Depth, meters	Temperature, ° C.	Salinity, ‰	Depth, meters	Temperature, ° C.	Salinity, ‰	σ_t
0	2.90	33.47	0	2.90	33.47	26.70
24	3.09	33.54	25	3.10	33.55	26.74
49	0.85	34.03	50	0.85	34.04	27.30
73	1.22	34.16	75	1.25	34.18	27.39
97	1.99	34.36	100	2.00	34.37	27.49
145	2.42	34.56	150	2.45	34.57	27.61
194	2.52	34.62	200	2.55	34.63	27.65
291	3.65	34.85	300	3.65	34.85	27.72
357	3.73	34.86				

Station 5084; May 2; latitude 47°42.5′ N., longitude 45°42′ W.; depth 293 meters; dynamic height 970.917

Observed values			Scaled values			
Depth, meters	Temperature, ° C.	Salinity, ‰	Depth, meters	Temperature, ° C.	Salinity, ‰	σ_t
0	3.81	33.32	0	3.81	33.32	26.49
24	3.57	33.45	25	3.60	33.46	26.63
48	3.59	34.02	50	3.55	34.04	27.09
72	3.12	34.19	75	3.05	34.21	27.27
96	2.72	34.28	100	2.60	34.28	27.36
144	1.59	34.27	150	1.75	34.28	27.43
191	4.33	34.73	200	4.30	34.74	27.57
278	4.00	34.83				

Station 5085; May 2; latitude 47°27′ N., longitude 45°07′ W.; depth 225 meters; dynamic height 970.938

Observed values			Scaled values			
Depth, meters	Temperature, ° C.	Salinity, ‰	Depth, meters	Temperature, ° C.	Salinity, ‰	σ_t
0	5.62	33.71	0	5.62	33.71	26.61
27	5.45	33.74	25	5.50	33.73	26.63
54	3.75	33.86	50	4.10	33.83	26.86
81	2.89	34.07	75	3.00	34.03	27.13
107	2.82	34.16	100	2.85	34.13	27.22
162	3.93	34.54	150	3.75	34.46	27.40
216	4.18	34.66	200	4.15	34.63	27.49

Station 5086; May 2; latitude 47°21′ N., longitude 44°51′ W.; depth 157 meters; dynamic height 970.940

Observed values			Scaled values			
Depth, meters	Temperature, ° C.	Salinity, ‰	Depth, meters	Temperature, ° C.	Salinity, ‰	σ_t
0	5.56	33.72	0	5.56	33.72	26.62
27	5.42	33.74	25	5.45	33.73	26.64
53	3.24	33.94	50	3.60	33.92	26.99
80	2.98	33.98	75	3.00	33.97	27.09
107	2.94	34.03	100	2.95	34.01	27.12
156	3.60	34.36	150	3.50	34.31	27.31

Station 5087; May 2; latitude 47°19′ N., longitude 45°08′ W.; depth 200 meters; dynamic height 970.939

Observed values			Scaled values			
Depth, meters	Temperature, ° C.	Salinity, ‰	Depth, meters	Temperature, ° C.	Salinity, ‰	σ_t
0	5.50	33.78	0	5.50	33.78	26.67
25	5.48	33.80	25	5.48	33.80	26.69
51	5.21	33.82	50	5.25	33.81	26.73
76	3.12	33.97	75	3.15	33.96	27.06
101	2.93	34.10	100	2.95	34.09	27.18
152	3.83	34.43	150	3.80	34.42	27.37
182	4.01	34.64	(200)	4.10	34.76	27.61

STATIONS OCCUPIED IN 1953—Continued

Observed values			Scaled values			
Depth, meters	Temperature, ° C.	Salinity, °/oo	Depth, meters	Temperature, ° C.	Salinity, °/oo	σ_t
Station 5088; May 2–3; latitude 47°18′ N., longitude 45°34′ W.; depth 266 meters; dynamic height 970.946						
0	5.36	33.65	0	5.36	33.65	26.59
25	5.30	33.65	25	5.30	33.65	26.59
50	4.72	33.74	50	4.72	33.74	26.73
75	2.82	33.91	75	2.82	33.91	27.06
100	2.68	34.08	100	2.68	34.08	27.19
150	3.84	34.45	150	3.84	34.45	27.39
200	4.20	34.66	200	4.20	34.66	27.52
250	4.25	34.79				
Station 5089; May 3; latitude 47°17.5′ N., longitude 45°57′ W.; depth 322 meters; dynamic height 970.936						
0	4.35	33.32	0	4.35	33.32	26.43
25	5.46	33.73	25	5.46	33.73	26.64
49	3.49	33.91	50	3.50	33.91	26.99
74	3.27	34.11	75	3.25	34.11	27.17
98	2.95	34.17	100	2.95	34.17	27.25
147	3.17	34.40	150	3.20	34.41	27.42
197	3.93	34.62	200	3.95	34.62	27.51
295	4.16	34.88	300	4.15	34.88	27.69
Station 5090; May 3; latitude 47°16.5′N., longitude 46°34′ W.; depth 732 meters; dynamic height 970.906						
0	4.26	33.32	0	4.26	33.32	26.44
24	4.32	33.37	25	4.30	33.37	26.48
49	1.39	34.04	50	1.40	34.05	27.28
73	1.83	34.20	75	1.85	34.21	27.37
97	2.46	34.34	100	2.45	34.34	27.42
146	2.07	34.40	150	2.10	34.41	27.51
195	2.58	34.57	200	2.65	34.59	27.61
292	4.12	34.88	300	4.10	34.88	27.70
373	3.94	34.89	400	3.85	34.89	27.73
564	3.55	34.88	600	3.55	34.87	27.75
687	3.46	34.86				
Station 5091; May 3; latitude 47°16.5′ N., longitude 46°41′ W.; depth 1,152 meters; dynamic height 970.912						
0	3.77	33.20	0	3.77	33.20	26.40
25	4.29	33.36	25	4.29	33.36	26.47
49	2.88	34.17	50	2.90	34.18	27.26
74	2.95	34.30	75	2.95	34.30	27.35
99	2.75	34.34	100	2.75	34.34	27.40
148	3.16	34.50	150	3.15	34.50	27.49
197	3.16	34.66	200	3.15	34.66	27.62
296	3.50	34.79	300	3.50	34.79	27.69
390	3.53	34.85	400	3.50	34.85	27.74
587	3.52	34.85	600	3.50	34.85	27.74
785	3.46	34.88	800	3.50	34.88	27.76
986	3.38	34.87	1,000	3.40	34.87	27.77
Station 5092; May 3; latitude 47°14.5′ N., longitude 47°11′ W.; depth 1,005 meters; dynamic height 970.924						
0	4.06	33.23	0	4.06	33.23	26.39
23	4.12	33.23	25	4.10	33.24	26.40
46	1.78	33.86	50	1.65	33.91	27.14
69	1.43	34.11	75	1.35	34.13	27.34
92	1.26	34.17	100	1.25	34.18	27.39
138	1.75	34.23	150	1.85	34.29	27.43
184	2.04	34.48	200	2.10	34.51	27.59
276	2.43	34.61	300	2.60	34.66	27.67
341	3.02	34.74	400	3.35	34.80	27.71
523	3.56	34.87	600	3.55	34.87	27.75
714	3.47	34.86	(800)	3.50	34.87	27.76
Station 5093; May 3; latitude 47°11′ N., longitude 47°47′ W.; depth 220 meters; dynamic height 971.003						
0	0.76	32.39	0	0.76	32.39	25.99
22	0.75	32.40	25	0.75	32.41	26.01
43	−1.29	32.98	50	−1.25	33.03	26.58
65	−0.99	33.12	75	−1.00	33.16	26.68
87	−1.05	33.22	100	−0.70	33.32	26.80
131	0.47	33.63	150	0.85	33.87	27.17
174	1.29	34.20	(200)	1.70	34.53	27.63
Station 5094; May 3; latitude 47°09.5′ N., longitude 48°09′ W.; depth 169 meters; dynamic height 971.004						
0	1.17	32.46	0	1.17	32.46	26.02
23	1.15	32.48	25	1.15	32.49	26.04
45	−1.32	32.88	50	−1.30	32.93	26.50
68	−1.31	33.06	75	−1.30	33.09	26.63
90	−1.33	33.19	100	−1.05	33.29	26.78
136	0.52	33.67	(150)	0.95	33.90	27.18
Station 5095; May 3; latitude 47°07′ N., longitude 48°36′ W.; depth 115 meters; dynamic height 971.028						
0	2.52	32.56	0	2.52	32.56	26.00
24	2.52	32.58	25	2.50	32.58	26.02
47	1.69	32.63	50	1.40	32.64	26.15
71	−0.16	32.73	75	−0.30	32.79	26.36
94	−0.66	33.04	100	−0.70	33.12	26.64
Station 5096; May 3; latitude 47°07′ N., longitude 49°09′ W.; depth 91 meters; dynamic height 971.032						
0	2.80	32.54	0	2.80	32.54	25.96
27	2.83	32.57	25	2.80	32.56	25.97
53	1.16	32.75	50	1.35	32.74	26.23
80	−0.27	32.91	75	−0.05	32.89	26.42
Station 5097; May 3; latitude 46°49′ N., longitude 48°45′ W.; depth 96 meters; dynamic height 971.028						
0	2.54	32.65	0	2.54	32.65	26.07
27	2.54	32.65	25	2.55	32.65	26.07
52	0.71	32.75	50	0.90	32.74	26.26
79	−0.56	32.92	75	−0.35	32.90	26.44

STATIONS OCCUPIED IN 1953—Continued

Observed values			Scaled values			
Depth, meters	Temperature, ° C.	Salinity, ‰	Depth, meters	Temperature, ° C.	Salinity, ‰	σ_t
Station 5098; May 4; latitude 46°43′ N., longitude 48°09′ W.; depth 127 meters; dynamic height 971.020						
0	1.86	32.56	0	1.86	32.56	26.05
25	1.87	32.55	25	1.87	32.55	26.04
50	−1.05	32.82	50	−1.05	32.82	26.41
75	−1.17	33.02	75	−1.17	33.02	26.58
100	−0.75	33.20	100	−0.75	33.20	26.71
Station 5099; May 4; latitude 46°38.5′ N., longitude 47°45′ W.; depth 179 meters; dynamic height 971.016						
0	1.00	32.50	0	1.00	32.50	26.06
22	1.00	32.50	25	1.00	32.50	26.06
43	−0.21	32.67	50	−0.65	32.79	26.38
66	−1.27	33.07	75	−1.15	33.14	26.67
87	−0.85	33.24	100	−0.55	33.35	26.82
127	0.11	33.64	(150)	0.70	33.88	27.18
Station 5100; May 4; latitude 46°36.5′ N., longitude 47°35′ W.; depth 329 meters; dynamic height 970.962						
0	1.07	32.51	0	1.07	32.51	26.06
20	0.10	32.98	25	−0.25	32.97	26.50
41	−1.08	32.92	50	−0.80	33.10	26.62
61	−0.35	33.42	75	−0.10	33.57	26.98
82	−0.02	33.64	100	0.25	33.80	27.15
122	0.59	33.99	150	0.95	34.12	27.36
162	1.09	34.18	200	1.55	34.32	27.48
244	2.11	34.49	(300)	2.75	34.68	27.67
Station 5101; May 4; latitude 46°34′ N., longitude 47°24′ W.; depth 640 meters; dynamic height 970.910						
0	2.04	32.94	0	2.04	32.94	26.35
26	2.45	33.05	25	2.40	33.04	26.40
51	0.86	33.81	50	0.85	33.79	27.10
77	1.01	34.11	75	1.00	34.09	27.33
102	1.18	34.21	100	1.15	34.20	27.41
153	1.74	34.38	150	1.70	34.37	27.51
204	2.24	34.53	200	2.20	34.51	27.59
306	2.95	34.74	300	2.90	34.73	27.70
419	3.50	34.88	400	3.45	34.87	27.76
			(600)	3.60	34.89	27.76
Station 5102; May 4; latitude 46°33′ N., longitude 47°16′ W.; depth 1,097 meters; dynamic height 970.913						
0	2.66	32.99	0	2.66	32.99	26.34
28	3.39	33.22	25	3.35	33.17	26.41
55	2.25	34.08	50	2.35	33.94	27.11
83	2.50	34.35	75	2.40	34.30	27.40
110	2.70	34.41	100	2.70	34.38	27.43
166	2.03	34.48	150	2.20	34.46	27.55
222	2.42	34.60	200	2.25	34.55	27.61
332	3.29	34.77	300	3.05	34.73	27.68
444	3.55	34.84	400	3.50	34.82	27.72
663	3.50	34.88	600	3.50	34.88	27.76
881	3.49	34.88	800	3.50	34.88	27.76
1,039	3.48	34.88	1,000	3.50	34.88	27.76

Observed values			Scaled values			
Depth, meters	Temperature, ° C.	Salinity, ‰	Depth, meters	Temperature, ° C.	Salinity, ‰	σ_t
Station 5103; May 4; latitude 46°32′ N., longitude 47°07′ W.; depth 723 meters; dynamic height 970.919						
0	2.39	32.98	0	2.39	32.98	26.35
23	2.41	33.00	25	2.40	33.08	26.43
47	1.67	33.86	50	1.55	33.88	27.12
70	0.82	33.98	75	0.85	34.01	27.28
94	1.23	34.18	100	1.30	34.22	27.42
141	1.87	34.42	150	1.95	34.44	27.55
187	2.16	34.51	200	2.30	34.53	27.59
281	3.08	34.72	300	3.20	34.75	27.69
362	3.49	34.81	400	3.50	34.82	27.72
559	3.51	34.88	(600)	3.55	34.88	27.75
Station 5104; May 4; latitude 46°30′ N., longitude 48°28′ W.; depth 914 meters; dynamic height 970.919						
0	3.29	33.21	0	3.29	33.21	26.46
23	3.23	33.25	25	3.15	33.27	26.51
47	1.81	34.01	50	1.75	34.02	27.23
70	1.21	34.15	75	1.20	34.17	27.39
94	1.55	34.24	100	1.60	34.25	27.42
140	1.77	34.41	150	2.00	34.44	27.54
186	2.66	34.57	200	2.85	34.61	27.61
280	3.62	34.80	300	3.65	34.81	27.69
263	3.54	34.78	400	3.65	34.83	27.70
427	3.62	34.84	600	3.55	34.84	27.72
615	3.50	34.84	(800)	3.50	34.86	27.75
Station 5105; May 4; latitude 46°35′ N., longitude 47°08′ W.; depth 423 meters; dynamic height 970.888						
0	5.61	33.91	0	5.61	33.91	26.77
22	5.61	33.91	25	5.50	33.92	26.78
44	3.81	34.10	50	3.40	34.13	27.17
66	2.86	34.20	75	2.90	34.24	27.31
88	3.15	34.33	100	3.30	34.40	27.40
133	3.61	34.55	150	3.70	34.61	27.53
177	3.78	34.68	200	3.80	34.71	27.60
265	3.87	34.78	300	3.80	34.81	27.68
372	3.69	34.86	(400)	3.60	34.88	27.75
Station 5106; May 4; latitude 46°38′ N., longitude 45°29′ W.; depth 218 meters; dynamic height 970.910						
0	5.31	33.82	0	5.31	33.82	26.73
23	5.30	33.82	25	5.30	33.82	26.73
46	4.66	33.92	50	4.45	33.95	26.92
70	3.25	34.10	75	3.05	34.12	27.20
92	2.67	34.18	100	2.65	34.20	27.30
139	2.68	34.34	150	2.85	34.39	27.43
185	3.87	34.65	(200)	4.10	34.75	27.60
Station 5107; May 4; latitude 46°41′ N., longitude 44°56′ W.; depth 194 meters; dynamic height 970.918						
0	5.36	33.84	0	5.36	33.84	26.74
26	5.35	33.84	25	5.35	33.84	26.74
52	5.01	33.805	50	5.10	33.81	26.75
78	2.68	34.04	75	2.85	34.00	27.12
104	2.74	34.22	100	2.70	34.19	27.28
156	3.39	34.47	150	3.30	34.44	27.43

Table of Oceanographic Data—Continued

STATIONS OCCUPIED IN 1953—Continued

Station 5108; May 4; latitude 46°42′ N., longitude 44°40′ W.; depth 183 meters; dynamic height 970.909

Observed values			Scaled values			
Depth, meters	Temperature, ° C.	Salinity, °/oo	Depth, meters	Temperature, ° C.	Salinity, °/oo	σ_t
0	5.35	33.87	0	5.35	33.87	26.77
28	5.34	33.88	25	5.35	33.87	26.77
55	2.81	34.08	50	3.15	34.04	27.12
83	2.70	34.18	75	2.70	34.15	27.25
110	2.73	34.26	100	2.70	34.22	27.31
165	3.84	34.60	150	3.50	34.50	27.46

Station 5109; May 4; latitude 46°34′ N., longitude 44°40′ W.; depth 277 meters; dynamic height 970.918

Observed values			Scaled values			
Depth, meters	Temperature, ° C.	Salinity, °/oo	Depth, meters	Temperature, ° C.	Salinity, °/oo	σ_t
0	5.04	33.64	0	5.04	33.64	26.61
25	5.03	33.64	25	5.03	33.64	26.61
50	3.24	34.00	50	3.24	34.00	27.08
75	2.70	34.14	75	2.70	34.14	27.24
100	2.77	34.26	100	2.77	34.26	27.34
150	2.70	34.46	150	2.70	34.46	27.50
200	3.97	34.72	200	3.97	34.72	27.59

Station 5110; May 5; latitude 46°25.5′ N., longitude 44°39′ W.; depth 605 meters; dymanic height 970.906

Observed values			Scaled values			
Depth, meters	Temperature, ° C.	Salinity, °/oo	Depth, meters	Temperature, ° C.	Salinity, °/oo	σ_t
0	4.58	33.54	0	4.58	33.54	26.58
22	4.51	33.57	25	4.50	33.59	26.64
43	3.16	33.90	50	2.85	33.95	27.08
64	2.46	34.06	75	2.55	34.18	27.29
85	2.69	34.27	100	2.60	34.33	27.40
128	2.49	34.43	150	3.05	34.56	27.55
171	3.57	34.66	200	3.75	34.76	27.64
256	3.64	34.84	300	3.65	34.85	27.72
218	3.84	34.80	(400)	3.60	34.86	27.74
374	3.62	34.86	(600)	3.55	34.87	27.75

Station 5111; May 5; latitude 46°19′ N., longitude 44°38′ W.; depth 2,140 meters; dynamic height 970.889

Observed values			Scaled values			
Depth, meters	Temperature, ° C.	Salinity, °/oo	Depth, meters	Temperature, ° C.	Salinity, °/oo	σ_t
0	4.55	33.52	0	4.55	33.52	26.58
23	4.65	33.57	25	4.65	33.61	26.64
45	3.81	34.31	50	3.65	34.33	27.31
68	3.17	34.43	75	3.05	34.45	27.46
91	2.88	34.52	100	2.90	34.54	27.55
137	3.10	34.59	150	3.25	34.65	27.60
182	3.57	34.79	200	3.65	34.80	27.68
273	3.72	34.85	300	3.75	34.85	27.71
252	3.64	34.82	400	3.75	34.88	27.73
376	3.74	34.88	600	3.60	34.88	27.75
500	3.63	34.89	800	3.55	34.88	27.75
648	3.58	34.88	1,000	3.50	34.88	27.76
1,058	3.45	34.88				

Station 5112; May 5; latitude 45°53′ N., longitude 44°36′ W.; depth 3,841 meters; dynamic height 970.962

Observed values			Scaled values			
Depth, meters	Temperature, ° C.	Salinity, °/oo	Depth, meters	Temperature, ° C.	Salinity, °/oo	σ_t
0	5.59	33.61	0	5.59	33.61	26.53
22	5.60	33.70	25	5.60	33.71	26.61
44	5.38	33.75	50	5.00	33.79	26.74
66	3.89	33.96	75	3.70	34.03	27.06
87	3.61	34.12	100	3.65	34.22	27.23
131	4.17	34.44	150	4.05	34.48	27.39
175	3.90	34.54	200	3.70	34.59	27.51
262	3.47	34.72	300	3.55	34.75	27.65
415	3.88	34.82	400	3.85	34.81	27.67
616	3.75	34.90	600	3.75	34.89	27.74
814	3.75	34.89	800	3.65	34.88	27.74
1,022	3.53	34.88	1,000	3.55	34.88	27.75
1,549	3.36	34.88				

Station 5113; May 5; latitude 45°57.5′ N., longitude 45°12′ W.; depth 3,146 meters; dynamic height 970.951

Observed values			Scaled values			
Depth, meters	Temperature, ° C.	Salinity, °/oo	Depth, meters	Temperature, ° C.	Salinity, °/oo	σ_t
0	5.63	33.43	0	5.63	33.43	26.37
25	5.69	33.49	25	5.69	33.49	26.42
50	4.04	33.97	50	4.04	33.97	26.98
75	3.52	34.19	75	3.52	34.19	27.21
100	3.66	34.34	100	3.66	34.34	27.32
150	3.89	34.54	150	3.89	34.54	27.45
200	5.03	34.84	200	5.03	34.84	27.56
300	4.27	34.85	300	4.27	34.85	27.66
350	4.09	34.85	400	4.05	34.86	27.69
525	4.06	34.91	600	4.00	34.91	27.74
701	3.78	34.91	800	3.75	34.90	27.75
886	3.67	34.89	1,000	3.65	34.89	27.75
1,366	3.55	34.90				

Station 5114; May 5; latitude 45°58′ N., longitude 45°54′ W.; depth 2,177 meters; dynamic height 970.959

Observed values			Scaled values			
Depth, meters	Temperature, ° C.	Salinity, °/oo	Depth, meters	Temperature, ° C.	Salinity, °/oo	σ_t
0	6.47	33.63	0	6.47	33.63	26.43
23	6.25	33.64	25	6.20	33.64	26.47
46	5.02	33.77	50	4.75	33.81	26.78
68	3.76	34.06	75	3.60	34.11	27.14
91	3.43	34.19	100	3.30	34.22	27.26
136	2.98	34.32	150	3.25	34.41	27.41
181	4.11	34.64	200	4.05	34.67	27.54
272	3.30	34.68	300	3.75	34.76	27.64
289	4.30	34.82	400	3.60	34.81	27.70
425	3.59	34.82	600	3.55	34.86	27.74
554	4.24	34.86	800	3.55	34.86	27.74
728	3.55	34.86	1,000	3.50	34.86	27.75
1,226	3.39	34.86				

Station 5115; May 5; latitude 45°58′ N., longitude 46°37′ W.; depth 549 meters; dynamic height 970.939

Observed values			Scaled values			
Depth, meters	Temperature, ° C.	Salinity, °/oo	Depth, meters	Temperature, ° C.	Salinity, °/oo	σ_t
0	2.39	32.76	0	2.39	32.76	26.17
27	2.52	33.15	25	2.55	33.11	26.43
54	1.72	33.76	50	1.85	33.66	26.93
82	0.76	33.94	75	0.85	33.89	27.18
109	1.43	34.13	100	1.10	34.06	27.31
163	3.85	34.59	150	3.30	34.49	27.47
217	4.17	34.75	200	4.10	34.71	27.57
326	3.74	34.78	300	3.80	34.77	27.65
398	4.18	34.91	400	4.15	34.91	27.72
527	3.69	34.89				

Table of Oceanographic Data—Continued

STATIONS OCCUPIED IN 1953—Continued

Station 5116; May 6; latitude 46°02′ N., longitude 47°08′ W.; depth 1,490 meters; dynamic height 970.926

Observed values			Scaled values			
Depth, meters	Temperature, ° C.	Salinity, °/oo	Depth, meters	Temperature, ° C.	Salinity, °/oo	σ_t
0	3.64	33.06	0	3.64	33.06	26.29
23	3.37	33.17	25	3.30	33.18	26.43
45	1.92	33.77	50	1.75	33.87	27.11
68	1.36	34.13	75	1.40	34.17	27.38
90	1.69	34.28	100	1.85	34.23	27.38
135	2.42	34.49	150	2.50	34.51	27.56
180	2.66	34.56	200	2.80	34.60	27.60
270	3.38	34.77	300	3.45	34.79	27.69
305	3.47	34.79	400	3.50	34.80	27.70
457	3.53	34.80	600	3.80	34.88	27.73
609	3.76	34.88	800	3.50	34.86	27.75
783	3.49	34.86	1,000	3.45	34.87	27.76
1,153	3.43	34.88				

Station 5117; May 6; latitude 46°05.5′ N., longitude 47°33′ W.; depth 695 meters; dynamic height 970.928

Observed values			Scaled values			
Depth, meters	Temperature, ° C.	Salinity, °/oo	Depth, meters	Temperature, ° C.	Salinity, °/oo	σ_t
0	2.07	32.86	0	2.07	32.86	26.28
23	2.03	32.97	25	2.05	33.00	26.40
46	1.02	33.56	50	0.95	33.65	26.98
70	0.87	33.93	75	0.90	33.98	27.25
93	1.06	34.11	100	1.10	34.13	27.36
139	1.38	34.27	150	1.50	34.31	27.48
185	1.92	34.42	200	2.05	34.45	27.55
278	2.41	34.59	300	2.55	34.62	27.65
393	3.13	34.76	400	3.15	34.77	27.71
560	3.49	34.86	(600)	3.50	34.87	27.76

Station 5118; May 6; latitude 46°08′ N., longitude 47°51′ W.; depth 176 meters; dynamic height 970.995

Observed values			Scaled values			
Depth, meters	Temperature, ° C.	Salinity, °/oo	Depth, meters	Temperature, ° C.	Salinity, °/oo	σ_t
0	1.24	32.48	0	1.24	32.48	26.03
24	−0.13	32.64	25	−0.15	32.65	26.24
47	−1.05	33.08	50	−1.05	33.11	26.64
71	−0.81	33.30	75	−0.70	33.35	26.82
95	0.15	33.54	100	0.25	33.57	26.97
142	0.62	33.82	(150)	0.70	33.85	27.16

Station 5119; May 6; latitude 46°10′ N., longitude 48°06′ W.; depth 119 meters; dynamic height 971.013

Observed values			Scaled values			
Depth, meters	Temperature, ° C.	Salinity, °/oo	Depth, meters	Temperature, ° C.	Salinity, °/oo	σ_t
0	1.99	32.55	0	1.99	32.55	26.04
24	1.56	32.56	25	1.50	32.56	26.08
48	−1.12	32.90	50	−1.15	32.93	26.50
73	−1.05	33.13	75	−1.00	33.14	26.67
			(100)	−0.40	33.33	26.80

Station 5120; May 6; latitude 46°13.5′ N., longitude 48°35′ W.; depth 93 meters; dynamic height 971.022

Observed values			Scaled values			
Depth, meters	Temperature, ° C.	Salinity, °/oo	Depth, meters	Temperature, ° C.	Salinity, °/oo	σ_t
0	2.64	32.66	0	2.64	32.66	26.07
24	2.51	32.66	25	2.50	32.66	26.08
48	0.49	32.78	50	0.30	32.79	26.33
73	−0.74	33.00	75	−0.80	33.01	26.56

Station 5121; May 6; latitude 46°16′ N., longitude 48°58′ W.; depth 73 meters; dynamic height 971.019

Observed values			Scaled values			
Depth, meters	Temperature, ° C.	Salinity, °/oo	Depth, meters	Temperature, ° C.	Salinity, °/oo	σ_t
0	3.03	32.68	0	3.03	32.68	26.06
26	1.96	32.72	25	2.00	32.72	26.17
51	−0.42	32.90	50	−0.40	32.89	26.44

Station 5122; May 6; latitude 46°08′ N., longitude 48°44′ W.; depth 91 meters; dynamic height 971.025

Observed values			Scaled values			
Depth, meters	Temperature, ° C.	Salinity, °/oo	Depth, meters	Temperature, ° C.	Salinity, °/oo	σ_t
0	2.51	32.66	0	2.51	32.66	26.08
26	2.47	32.66	25	2.50	32.66	26.08
52	−0.18	32.82	50	−0.05	32.81	26.37
78	−0.47	33.01	75	−0.45	32.98	26.52

Station 5123; May 6; latitude 45°57′ N., longitude 48°26′ W.; depth 115 meters; dynamic height 971.012

Observed values			Scaled values			
Depth, meters	Temperature, ° C.	Salinity, °/oo	Depth, meters	Temperature, ° C.	Salinity, °/oo	σ_t
0	1.39	32.53	0	1.39	32.53	26.06
26	0.91	32.57	25	0.95	32.57	26.12
51	−1.44	32.99	50	−1.40	32.98	26.55
76	−1.40	33.22	75	−1.40	33.21	26.74
101	−0.16	33.49	100	−0.25	33.48	26.91

Station 5124; May 6; latitude 45°54.5′ N., longitude 48°21′ W.; depth 190 meters; dynamic height 971.001

Observed values			Scaled values			
Depth, meters	Temperature, ° C.	Salinity, °/oo	Depth, meters	Temperature, ° C.	Salinity, °/oo	σ_t
0	1.61	32.53	0	1.61	32.53	26.04
25	0.28	32.68	25	0.28	32.68	26.25
50	−0.83	33.11	50	−0.83	33.11	26.63
75	−0.34	33.39	75	−0.34	33.39	26.84
99	0.31	33.70	100	0.30	33.70	27.06
150	0.54	33.82	150	0.55	33.82	27.15

Station 5125; May 6; latitude 45°50′ N., longitude 48°14′ W.; depth 732 meters; dynamic height 970.963

Observed values			Scaled values			
Depth, meters	Temperature, ° C.	Salinity, °/oo	Depth, meters	Temperature, ° C.	Salinity, °/oo	σ_t
0	1.59	32.56	0	1.59	32.56	26.07
23	1.80	32.80	25	1.80	32.84	26.28
47	0.37	33.42	50	0.40	33.47	26.88
70	0.49	33.77	75	0.65	33.83	27.14
93	1.18	34.02	100	1.20	34.05	27.29
140	1.32	34.21	150	1.45	34.25	27.43
186	2.00	34.42	200	2.05	34.45	27.55
279	2.33	34.57	300	2.45	34.60	27.63
373	2.94	34.70	400	3.05	34.73	27.68
561	*3.44	34.86	(600)	3.50	34.87	27.76

STATIONS OCCUPIED IN 1953—Continued

Station 5126; May 6; latitude 45°40′ N., longitude 47°58′ W.; depth 1,353 meters; dynamic height 970.957

Observed values			Scaled values			
Depth, meters	Temperature, ° C.	Salinity, ‰	Depth, meters	Temperature, ° C.	Salinity, ‰	σ_t
0	2.53	32.72	0	2.53	32.72	26.13
23	2.49	32.76	25	2.45	32.84	26.23
47	0.84	33.73	50	0.85	33.77	27.09
70	1.25	34.02	75	1.30	34.04	27.27
94	1.38	34.13	100	1.40	34.14	27.35
140	1.56	34.27	150	1.65	34.30	27.46
186	2.09	34.43	200	2.30	34.48	27.55
280	3.36	34.72	300	3.55	34.77	27.67
331	3.73	34.82	400	3.70	34.83	27.70
500	3.60	34.84	600	3.55	34.83	27.71
670	3.50	34.83	800	3.50	34.83	27.72
844	3.48	34.83	1,000	3.40	34.85	27.75
1,109	3.38	34.85				

Station 5127; May 6; latitude 45°17′ N., longitude 47°18′ W.; depth 2,999 meters; dynamic height 970.979

Observed values			Scaled values			
Depth, meters	Temperature, ° C.	Salinity, ‰	Depth, meters	Temperature, ° C.	Salinity, ‰	σ_t
0	2.67	32.68	0	2.67	32.68	26.09
24	3.62	33.42	25	3.60	33.44	26.61
48	3.40	33.74	50	3.35	33.74	26.87
73	2.52	33.76	75	2.50	33.78	26.97
97	3.40	34.11	100	3.50	34.13	27.16
144	4.15	34.48	150	4.15	34.49	27.38
193	3 92	34.59	200	3.90	34.60	27.50
290	4.00	34.76	300	4.00	34.77	27.63
378	3.81	34.81	400	3.80	34.82	27.69
566	3.77	34.85	600	3.75	34.85	27.71
753	3.57	34.86	800	3.55	34.86	27.74
938	3.50	34.86	1,000	3.50	34.86	27.75
1,400	3.37	34.89				

Station 5128; May 7; latitude 45°19′ N., longitude 46°25′ W.; depth 2,438 meters; dynamic height 970.934

Observed values			Scaled values			
Depth, meters	Temperature, ° C.	Salinity, ‰	Depth, meters	Temperature, ° C.	Salinity, ‰	σ_t
0	6.53	33.62	0	6.53	33.62	26.42
24	5.97	33.66	25	5.90	33.66	26.53
49	4.15	34.00	50	4.10	34.00	27.00
73	3.36	34.16	75	3.35	34.17	27.21
98	3.35	34.32	100	3.35	34.33	27.33
146	3.66	34.51	150	3.70	34.53	27.46
194	4.14	34.72	200	4.20	34.74	27.58
292	4.49	34.91	300	4.50	34.91	27.68
380	4.07	34.89	400	3.95	34.89	27.72
569	3.68	34.89	600	3.65	34.89	27.75
756	3.55	34.88	800	3.55	34.88	27.75
946	3.50	34.87	1,000	3.50	34.87	27.76
1,425	3.40	34.89				

Station 5129; May 7; latitude 45°21′ N., longitude 45°33′ W.; depth 3,823 meters; dynamic height 971.015

Observed values			Scaled values			
Depth, meters	Temperature, ° C.	Salinity, ‰	Depth, meters	Temperature, ° C.	Salinity, ‰	σ_t
0	6.49	33.38	0	6.49	33.38	26.22
24	6.54	33.59	25	6.55	33.62	26.42
47	6.56	34.22	50	6.55	34.25	26.91
71	7.16	34.45	75	7.35	34.50	27.00
94	8.34	34.72	100	8.20	34.70	27.03
141	5.92	34.49	150	5.45	34.45	27.21
189	3.88	34.38	200	3.95	34.40	27.34
283	5.14	34.83	300	4.75	34 81	27.58
324	4.28	34.78	400	4.25	34.85	27.66
489	4.22	34.90	600	4.10	34.90	27.72
656	4.00	34.90	800	3.85	34.90	27.74
825	3.78	34.90	1,000	3.70	34.90	27.76
1,256	3.52	34.90				

Station 5130; May 7; latitude 45°23′ N., longitude 44°44′ W.; depth 4,298 meters; dynamic height 971.178

Observed values			Scaled values			
Depth, meters	Temperature, ° C.	Salinity, ‰	Depth, meters	Temperature, ° C.	Salinity, ‰	σ_t
0	13.45	35.39	0	13.45	35.39	26.62
23	13.52	35.43	25	13.60	35.48	26.66
45	14.88	35.89	50	14.90	35.90	26.70
68	14.88	35.91	75	14.25	35.77	26.75
91	12.29	35.34	100	12.05	35.30	26.83
136	11.47	35.23	150	11.35	35.22	26.90
191	10.95	35.19	200	10.85	35.19	26.97
272	10.00	35.23	300	9.35	35.17	27.21
358	7.82	35.01	400	7.25	35.01	27.41
542	5.94	35.00	600	5.50	34.99	27.62
729	4.85	34.97	800	4.60	34.96	27.71
912	4.31	34.95	1,000	4.20	34.94	27.74
1,369	3.69	34.92				

Station 5131; May 7; latitude 44°51′ N., longitude 45°05′ W.; depth 4,295 meters; dynamic height 971.146

Observed values			Scaled values			
Depth, meters	Temperature, ° C.	Salinity, ‰	Depth, meters	Temperature, ° C.	Salinity, ‰	σ_t
0	12.32	35.46	0	13.30	35.46	26.71
24	14.34	35.72	25	14.35	35.74	26.70
48	15.00	36.00	50	15.00	36.00	26.76
73	15.00	36.01	75	15.00	36.00	26.76
97	14.26	35.83	100	14.15	35.81	26.80
145	12.78	35.55	150	12.70	35.54	26.89
193	11.53	35.37	200	11.35	35.35	27.00
290	8.96	35.09	300	8.60	35.06	27.25
372	6.28	34.84	400	6.00	34.85	27.46
564	4.92	34.91	600	4.80	34.92	27.66
760	4.34	34.94	800	4.25	34.94	27.73
951	4.03	34.94	1,000	4.00	34.94	27.76
1,429	*3.59	34.90				

Station 5132; May 7; latitude 44°20′ N., longitude 45°24′ W.; depth 4,262 meters; dynamic height 970.969

Observed values			Scaled values			
Depth, meters	Temperature, ° C.	Salinity, ‰	Depth, meters	Temperature, ° C.	Salinity, ‰	σ_t
0	7.71	33.51	0	7.71	33.51	26.17
24	7.00	33.66	25	6.95	33.66	26.40
48	5.09	33.83	50	4.95	33.84	26.78
72	4.01	33.98	75	3.90	33.99	27.01
96	3.58	34.13	100	3.60	34.15	27.17
144	3.73	34.42	150	3.80	34.44	27.38
191	3.88	34.57	200	3.90	34.59	27.49
287	4.19	34.82	300	4.20	34.84	27.66
368	4.14	34.89	400	4.15	34.90	27.71
559	3.95	34.91	600	3.90	34.91	27.75
755	3.69	34.89	800	3.65	34.89	27.75
945	3.60	34.90	1,000	3.60	34.90	27.77
1,419	3.42	34.88				

Table of Oceanographic Data—Continued

STATIONS OCCUPIED IN 1953—Continued

Station 5133; May 7; latitude 44°25.5′ N., longitude 45°55′ W.; depth 3,841 meters; dynamic height 971.043

Observed values			Scaled values			
Depth, meters	Temperature, ° C.	Salinity, °/oo	Depth, meters	Temperature, ° C.	Salinity, °/oo	σ_t
0	6.45	33.33	0	6.45	33.33	26.19
24	6.47	33.50	25	6.50	33.55	26.36
48	9.70	34.90	50	9.65	34.89	26.94
72	8.84	34.79	75	8.85	34.80	27.01
96	9.04	34.91	100	9.05	34.91	27.06
144	8.43	34.94	150	8,30	34.93	27.19
191	6.82	34.79	200	6.65	34.78	27.31
287	5.42	34.77	300	5.30	34.77	27.48
362	4.78	34.82	400	4.70	34.85	27.61
545	4.45	34.92	600	4.35	34.92	27.71
729	4.14	34.92	800	4.00	34.91	27.74
913	3.81	34.90	1,000	3.75	34.90	27.75
1,379	3.46	34.88				

Station 5134; May 8; latitude 44°32.5′ N., longitude 46°34′ W.; depth 3,695 meters; dynamic height 971.165

Observed values			Scaled values			
Depth, meters	Temperature, ° C.	Salinity, °/oo	Depth, meters	Temperature, ° C.	Salinity, °/oo	σ_t
0	8.59	33.86	0	8.59	33.86	26.31
23	14.20	35.65	25	14.20	35.65	26.66
47	13.94	35.63	50	13.85	35.62	26.72
70	13.45	35.60	75	13.35	35.59	26.79
93	13.12	35.54	100	13.10	35.54	26.81
140	12.90	35.54	150	12.35	35.43	26.87
187	9.75	34.91	200	9.75	34.94	26.96
280	9.84	35.21	300	9.10	35.11	27.21
363	6.06	34.74	400	5.90	34.78	27.41
550	5.25	34.94	600	5.00	34.94	27.65
740	4.41	34.92	800	4.20	34.92	27.73
925	4.14	34.93	1,000	4.05	34.93	27.74
1,390	3.53	34.89				

Station 5135; May 8; latitude 44°40.5′·N., longtitude 47°17′ W.; depth 3,841 meters; dynmaic height 971.043

Observed values			Scaled values			
Depth, meters	Temperature, ° C.	Salinity, °/oo	Depth, meters	Temperature, ° C.	Salinity, °/oo	σ_t
0	7.58	33.56	0	7.58	33.56	26.23
18	8.42	33.99	25	9.00	34.30	26.59
36	9.66	34.76	50	7.25	34.44	26.96
54	6.78	34.36	75	7.55	34.55	27.00
72	7.53	34.55	100	7.30	34.56	27.05
109	7.21	34.57	150	7.85	34.84	27.19
145	7.92	34.85	200	5.65	34.62	27.32
217	5.00	34.56	300	6.05	34.89	27.48
314	6.19	34.94	400	5.10	34.88	27.59
481	4.37	34.83	600	4.40	34.91	27.69
656	4.44	34.94	800	4.20	34.94	27.74
831	4.16	34.94	1,000	3.95	34.93	27.75
1,288	3.58	34.90				

Station 5136; May 8; latitude 44°48.5′ N., longitude 47°58′ W.; depth 3,365 meters; dynamic height 971.022

Observed values			Scaled values			
Depth, meters	Temperature, ° C.	Salinity, °/oo	Depth, meters	Temperature, ° C.	Salinity, °/oo	σ_t
0	3.99	32.70	0	3.99	32.70	25.98
25	5.36	33.78	25	5.36	33.78	26.69
49	7.89	34.57	50	7.90	34.57	26.97
74	7.24	34.53	75	7.25	34.53	27.03
98	7.54	34.66	100	7.60	34.67	27.10
148	8.07	34.99	150	8.10	34.99	27.27
196	5.47	34.64	200	5.45	34.64	27.35
294	5.40	34.84	300	5.45	34.84	27.51
376	5.11	34.88	400	5.05	34.89	27.60
569	4.39	34.92	600	4.30	34.92	27.71
766	4.06	34.94	800	4.00	34.93	27.75
959	3.71	34.905	1,000	3.70	34.90	27.76
1,445	3.40	34.88				

Station 5137; May 8; latitude 44°51.5′ N., longitude 48°24′ W.; depth 2,661 meters; dynamic height 970.972

Observed values			Scaled values			
Depth, meters	Temperature, ° C.	Salinity, °/oo	Depth, meters	Temperature, ° C.	Salinity, °/oo	σ_t
0	2.35	32.49	0	2.35	32.49	25.95
26	0.47	32.68	25	0.50	32.67	26.23
51	−0.13	33.28	50	−0.10	33.26	26.72
78	2.48	33.83	75	2.15	33.77	27.00
413	3.97	34.89	100	3.15	34.14	27.20
629	3.75	34.86	150	3.80	34.48	27.41
853	3.70	34.91	200	4.15	34.69	27.54
1,064	3.43	34.88	300	4.25	34.89	27.69
1,586	3.39	34.88	400	4.05	34.89	27.71
			600	3.75	34.86	27.72
			800	3.70	34.90	27.76
			1,000	3.50	34.89	27.77

Station 5138; May 8; latitude 44°53′ N., longitude 48°36′ W.; depth 2,286 meters; dynamic height 970.930

Observed values			Scaled values			
Depth, meters	Temperature, ° C.	Salinity, °/oo	Depth, meters	Temperature, ° C.	Salinity, °/oo	σ_t
0	2.66	32.52	0	2.66	32.52	25.96
25	1.62	32.80	25	1.62	32.80	26.27
50	1.23	33.68	50	1.23	33.68	26.98
75	1.06	34.04	75	1.06	34.04	27.29
100	1.22	34.18	100	1.22	34.18	27.39
150	2.08	34.46	150	2.08	34.46	27.55
199	2.72	34.60	200	2.75	34.60	27.61
299	3.43	34.80	300	3.45	34.80	27.70
395	3.89	34.89	400	3.95	34.89	27.72
595	3.72	34.89	600	3.70	34.89	27.75
797	3.56	34.88	800	3.55	34.88	27.75
995	3.46	34.87	1,000	3.45	34.87	27.76
1,486	3.38	34.89				

Station 5139; May 8; latitude 44°56′ N., longitude 48°50′ W.; depth 1,054 meters; dynamic height 971.059.

Observed values			Scaled values			
Depth, meters	Temperature, ° C.	Salinity, °/oo	Depth, meters	Temperature, ° C.	Salinity, °/oo	σ_t
0	1.51	32.42	0	1.51	32.42	25.97
25	−1.26	32.90	25	−1.26	32.90	26.48
50	−0.77	33.12	50	−0.77	33.12	26.64
74	−0.12	33.33	75	−0.15	33.33	26.79
99	−0.08	33.52	100	−0.05	33.53	26.94
149	0.48	33.80	150	0.50	33.90	27.21
198	0.80	33.96	200	0.80	33.97	27.25
297	1.56	34.24	300	1.60	34.25	27.42
400	*2.35	34.53	400	2.35	34.53	27.58
604	3.48	34.80	600	3.45	34.80	27.70
800	3.54	34.85	800	3.55	34.85	27.73
954	3.49	34.845	(1,000)	3.50	34.85	27.74

Station 5140; May 8; latitude 44°57′ N., longitude 48°56′ W.; depth 842 meters; dynamic height 971.080.

Observed values			Scaled values			
Depth, meters	Temperature, ° C.	Salinity, °/oo	Depth, meters	Temperature, ° C.	Salinity, °/oo	σ_t
0	2.82	32.60	0	2.82	32.60	26.01
25	−0.90	32.89	25	−0.90	32.89	26.46
50	−0.89	33.06	50	−0.89	33.06	26.60
75	−0.77	33.10	75	−0.77	33.10	26.62
99	−0.50	33.20	100	−0.50	33.20	26.70
149	−0.52	33.36	150	−0.50	33.36	26.82
199	0.93	33.96	200	0.95	33.96	27.23
298	1.74	34.30	300	1.80	34.30	27.45
50	*−0.85	33.06	400	2.70	34.59	27.60
252	1.23	34.18	(600)	3.50	34.85	27.74
399	2.67	34.59	(800)	3.45	34.85	27.74

Table of Oceanographic Data—Continued

STATIONS OCCUPIED IN 1953—Continued

Station 5141; May 9; latitude 45°00′ N., longitude 49°08′ W.; depth 132 meters; dynamic height 971.097.

Observed values			Scaled values			
Depth, meters	Temperature, ° C.	Salinity, ‰	Depth, meters	Temperature, ° C.	Salinity, ‰	σ_t
0	3.57	32.68	0	3.57	32.68	26.01
25	2.43	32.68	25	2.43	32.68	26.10
50	0.35	32.80	50	0.35	32.80	26.34
76	−0.50	32.92	75	−0.45	32.92	26.47
111	−0.94	32.98	100	−0.85	32.97	26.52

Station 5142; May 27; latitude 50°00′ N., longitude 49°00′ W.; depth 1,884 meters; dynamic height 970.852.

Observed values			Scaled values			
Depth, meters	Temperature, ° C.	Salinity, ‰	Depth, meters	Temperature, ° C.	Salinity, ‰	σ_t
0	3.91	33.58	0	3.91	33.58	26.69
24	3.94	33.60	25	3.90	33.60	26.71
48	1.42	34.16	50	1.40	34.20	27.40
72	1.95	34.43	75	2.00	34.44	27.54
96	2.24	34.52	100	2.25	34.52	27.59
144	2.62	34.65	150	2.65	34.66	27.67
192	2.99	34.76	200	3.00	34.77	27.73
288	3.12	34.81	300	3.15	34.81	27.74
322	3.15	34.82	400	3.25	34.84	27.75
493	3.29	34.86	600	3.25	34.86	27.77
672	3.26	34.86	800	3.25	34.87	27.78
851	3.27	34.88	1,000	3.25	34.88	27.78
1,317	3.28	34.89				

Station 5143; May 28; latitude 49°49′ N., longitude 49°34′ W.; depth 1,353 meters; dynamic height 970.915.

Observed values			Scaled values			
Depth, meters	Temperature, ° C.	Salinity, ‰	Depth, meters	Temperature, ° C.	Salinity, ‰	σ_t
0	2.42	32.98	0	2.42	32.98	26.34
25	1.89	33.06	25	1.89	33.06	26.45
49	−0.18	33.75	50	0.15	33.77	27.13
386	3.09	34.78	75	0.75	34.02	27.30
583	3.45	34.86	100	1.15	34.18	27.39
783	3.52	34.88	150	1.80	34.40	27.53
979	3.51	34.88	200	2.20	34.55	27.62
1,272	3.33	34.90	300	2.70	34.70	27.69
			400	3.20	34.79	27.72
			600	3.45	34.86	27.75
			800	3.50	34.88	27.76
			1,000	3.50	34.88	27.76

Station 5144; May 28; latitude 49°39′ N., longitude 50°00′ W.; depth 640 meters; dynamic height 970.911.

Observed values			Scaled values			
Depth, meters	Temperature, ° C.	Salinity, ‰	Depth, meters	Temperature, ° C.	Salinity, ‰	σ_t
0	2.55	32.84	0	2.55	32.84	26.22
23	2.42	32.85	25	2.35	32.85	26.24
47	0.47	33.68	50	0.45	33.70	27.05
70	0.60	33.96	75	0.70	34.00	27.28
93	1.18	34.18	100	1.30	34.23	27.43
140	1.94	34.46	150	2.00	34.48	27.57
186	2.25	34.56	200	2.35	34.58	27.62
279	2.78	34.70	300	2.90	34.73	27.70
368	3.25	34.80	400	3.35	34.83	27.73
572	3.46	34.89	(600)	3.45	34.89	27.77

Station 5145; May 28; latitude 49°31′ N., longitude 50°33′ W.; depth 331 meters; dynamic height 970.963.

Observed values			Scaled values			
Depth, meters	Temperature, ° C.	Salinity, ‰	Depth, meters	Temperature, ° C.	Salinity, ‰	σ_t
0	2.21	32.89	0	2.21	32.89	26.28
24	2.02	32.90	25	2.00	32.90	26.31
47	1.85	32.90	50	1.80	32.90	26.32
71	−0.22	33.52	75	−0.20	33.56	26.98
94	0.00	33.73	100	0.05	33.76	27.13
141	0.45	34.02	150	0.65	34.08	27.34
188	1.53	34.34	200	1.70	34.40	27.53
282	2.74	34.69	(300)	2.90	34.73	27.70

Station 5146; May 28; latitude 49°22′ N., longitude 51°05′ W.; depth 340 meters; dynamic height 970.977.

Observed values			Scaled values			
Depth, meters	Temperature, ° C.	Salinity, ‰	Depth, meters	Temperature, ° C.	Salinity, ‰	σ_t
0	2.32	32.84	0	2.32	32.84	26.24
24	2.27	32.90	25	2.25	32.91	26.30
47	0.72	33.01	50	0.55	33.03	26.51
71	−1.26	33.34	75	−1.20	33.39	26.88
94	−0.36	33.58	100	−0.25	33.62	27.03
141	0.41	33.90	150	0.55	33.96	27.26
188	1.35	34.22	200	1.55	34.28	27.44
282	2.54	34.62	(300)	2.70	34.67	27.67

Station 5147; May 28, latitude 49°10.5′ N., longitude 51°34′ W.; depth 318 meters; dynamic height 971.025

Observed values			Scaled values			
Depth, meters	Temperature, ° C.	Salinity, ‰	Depth, meters	Temperature, ° C.	Salinity, ‰	σ_t
0	1.47	32.65	0	1.47	32.65	26.15
21	1.46	32.65	25	1.40	32.65	26.16
42	0.33	32.74	50	−0.45	32.87	26.43
62	−1.64	33.22	75	−1.60	33.27	26.79
83	−1.54	33.29	100	−1.45	33.34	26.84
125	−1.12	33.43	150	−0.45	33.60	27.02
167	0.04	33.74	200	0.50	33.92	27.23
250	1.12	34.16	(300)	1.60	34.40	27.54

Station 5148; May 28; latitude 49°05.5′ N., longitude 51°54′ W.; depth 293 meters; dynamic height 971.012

Observed values			Scaled values			
Depth, meters	Temperature, ° C.	Salinity, ‰	Depth, meters	Temperature, ° C.	Salinity, ‰	σ_t
0	2.20	32.77	0	2.20	32.77	26.19
21	2.00	32.81	25	1.85	32.82	26.26
42	0.57	32.96	50	−0.25	33.02	26.54
63	−1.63	33.11	75	−1.70	33.15	26.70
84	−1.73	33.18	100	−1.70	33.22	26.75
126	−1.60	33.28	150	−0.65	33.54	26.98
168	0.16	33.77	200	1.05	34.12	27.36
229	1.74	34.36				

Station 5149; May 28; latitude 49°01′ N., longitude 52°08′ W.; depth 293 meters; dynamic height 971.046

Observed values			Scaled values			
Depth, meters	Temperature, ° C.	Salinity, ‰	Depth, meters	Temperature, ° C.	Salinity, ‰	σ_t
0	1.60	32.24	0	1.60	32.24	25.81
23	1.54	32.24	25	1.50	32.24	25.82
44	0.02	32.86	50	−0.45	32.94	26.49
67	−1.41	33.12	75	−1.60	33.15	26.69
89	−1.73	33.18	100	−1.70	33.21	26.75
134	−0.96	33.42	150	−0.70	33.51	26.96
178	−0.10	33.68	200	0.35	33.83	27.16
243	1.38	34.15				

STATIONS OCCUPIED IN 1953—Continued

Observed values			Scaled values			
Depth, meters	Temperature, ° C.	Salinity, °/oo	Depth, meters	Temperature, ° C.	Salinity, °/oo	σ_t
Station 5150; May 28; latitude 48°54.5′ N., longitude 52°25′ W.; depth 348 meters; dynamic height 971.058						
0	1.70	32.32	0	1.70	32.32	25.87
25	1.69	32.33	25	1.69	32.33	25.88
49	−1.36	33.05	50	−1.40	33.06	26.61
74	−1.73	33.17	75	−1.70	33.17	26.71
98	−1.63	33.22	100	−1.60	33.22	26.75
148	−1.36	33.36	150	−1.35	33.37	26.86
197	−0.16	33.68	200	−0.10	33.70	27.08
295	1.64	34.30	300	1.70	34.32	27.47
Station 5151; May 28; latitude 48°50′ N., longitude 52°40′ W.; depth 220 meters; dynamic height 971.087						
0	1.35	31.99	0	1.35	31.99	25.63
26	1.71	32.49	25	1.70	32.47	25.99
52	−1.73	33.03	50	−1.70	33.01	26.58
78	−1.71	33.13	75	−1.70	33.12	26.67
104	−1.65	33.18	100	−1.65	33.17	26.71
157	−1.39	33.27	150	−1.45	33.26	26.77
209	0.01	-------	(200)	−0.40	33.55	26.94
Station 5152; May 28; latitude 48°45′ N., longitude 52°52′ W.; depth 114 meters; dynamic height 971.087						
0	1.86	31.75	0	1.86	31.75	25.40
26	−1.35	32.91	25	−1.35	32.88	26.46
53	−1.40	32.91	50	−1.40	32.91	26.49
80	−1.59	33.07	75	−1.55	33.03	26.59
106	−1.58	33.11	100	−1.60	33.10	26.65
Station 5153; May 28–29; latitude 48°39′ N., longitude 52°46′ W.; depth 117 meters; dynamic height 971.105						
0	1.64	31.91	0	1.64	31.91	25.55
26	1.15	32.08	25	1.20	32.07	25.71
52	−1.44	32.90	50	−1.40	32.83	26.43
79	−1.54	33.04	75	−1.50	33.02	26.58
105	−1.53	33.10	100	−1.55	33.09	26.64
Station 5154; May 29; latitude 48°34′ N., longitude 52°36′ W.; depth 256 meters; dynamic height 971.075						
0	1.02	32.50	0	1.02	32.50	26.06
26	0.95	32.52	25	0.95	32.52	26.08
52	−1.30	33.01	50	−1.20	32.97	26.54
78	−1.70	33.12	75	−1.65	33.11	26.66
104	−1.68	33.16	100	−1.70	33.15	26.70
156	−1.39	33.24	150	−1.45	33.23	26.75
208	−1.02	33.42	200	−1.10	33.37	26.85
239	0.15	33.72				

Observed values			Scaled values			
Depth, meters	Temperature, ° C.	Salinity, °/oo	Depth, meters	Temperature, ° C.	Salinity, °/oo	σ_t
Station 5155; May 29; latitude 48°19.5′ N., longitude 52°02′ W.; depth 176 meters; dynamic height 971.081						
0	2.38	32.19	0	2.38	32.19	25.71
24	2.31	32.26	25	2.30	32.27	25.79
49	−1.18	32.96	50	−1.20	32.97	26.54
73	−1.44	33.12	75	−1.45	33.12	26.66
97	−1.63	33.18	100	−1.65	33.18	26.71
146	−1.49	33.27	150	−1.50	33.28	26.79
Station 5156; May 29; latitude 48°16′ N., longitude 51°54′ W.; depth 183 meters; dynamic height 971.066						
0	2.85	32.31	0	2.85	32.31	25.77
25	2.06	32.59	25	2.06	32.59	26.07
49	−0.26	32.96	50	−0.40	32.96	26.50
74	−1.64	33.20	75	−1.65	33.20	26.73
99	−1.55	33.27	100	−1.55	33.27	26.79
148	−1.06	33.40	150	−1.05	33.40	26.88
Station 5157; May 29; latitude 48°07.5′ N., longitude 51°37′ W.; depth 187 meters; dynamic height 971.059						
0	2.94	32.25	0	2.94	32.25	25.72
25	2.47	32.46	25	2.47	32.46	25.92
50	−1.08	32.96	50	−1.08	32.96	26.52
76	−1.58	33.23	75	−1.60	33.22	26.75
100	−0.56	33.39	100	−0.55	33.39	26.85
151	0.36	33.70	150	0.30	33.69	27.05
Station 5158; May 29; latitude 47°57′ N., longitude 51°11′ W.; depth 157 meters; dynamic height 971.066						
0	2.97	32.04	0	2.97	32.04	25.56
25	2.73	32.11	25	2.73	32.11	25.62
49	−1.33	33.00	50	−1.35	33.01	26.58
74	−1.60	33.19	75	−1.60	33.19	26.72
99	−1.57	33.26	100	−1.55	33.26	26.78
138	0.09	33.64	(150)	0.45	33.76	27.10
Station 5159; May 30; latitude 47°51′ N., longitude 50°59′ W.; depth 119 meters; dynamic height 971.067						
0	2.88	32.12	0	2.88	32.12	25.63
26	2.84	32.13	25	2.85	32.13	25.64
52	−1.14	33.00	50	−1.10	32.96	26.52
78	−0.56	33.22	75	−0.60	33.21	26.71
104	−0.34	33.32	100	−0.40	33.30	26.77
Station 5160; May 30; latitude 47°43′ N., longitude 50°41′ W.; depth 108 meters; dynamic height 971.071						
0	3.09	32.09	0	3.09	32.09	25.58
26	2.36	32.28	25	2.45	32.27	25.77
52	−1.04	32.83	50	−0.95	32.80	26.39
77	−1.21	33.02	75	−1.20	33.01	26.57
98	−0.37	33.28	100	−0.20	33.31	26.77

STATIONS OCCUPIED IN 1953—Continued

Station 5161; May 30; latitude 47°34′ N., longitude 50°24′ W.; depth 119 meters; dynamic height 971.077

Observed values			Scaled values			
Depth, meters	Temperature, ° C.	Salinity, °/oo	Depth, meters	Temperature, ° C.	Salinity, °/oo	σ_t
0	3.18	32.25	0	3.18	32.25	25.70
25	2.98	32.30	25	2.98	32.30	25.75
50	−0.15	32.62	50	−0.15	32.62	26.22
74	−0.79	32.92	75	−0.70	32.93	26.49
99	−0.35	33.24	100	−0.30	33.25	26.72

Station 5162; May 30; latitude 47°24.5′ N., longitude 50°00′ W.; depth 71 meters; dynamic height 971.082

Observed values			Scaled values			
Depth, meters	Temperature, ° C.	Salinity, °/oo	Depth, meters	Temperature, ° C.	Salinity, °/oo	σ_t
0	3.49	32.35	0	3.49	32.35	25.74
20	3.38	32.40	25	3.20	32.42	25.83
45	1.78	32.55	50	0.80	32.63	26.18
60	−0.80	32.83				

Station 5163; May 30; latitude 47°43′ N., longitude 49°53′ W.; depth 115 meters; dynamic height 971.072

Observed values			Scaled values			
Depth, meters	Temperature, ° C.	Salinity, °/oo	Depth, meters	Temperature, ° C.	Salinity, °/oo	σ_t
0	3.09	32.36	0	3.09	32.36	25.79
25	2.90	32.39	25	2.90	32.39	25.84
51	−0.46	32.69	50	−0.45	32.68	26.28
76	−0.65	32.95	75	−0.65	32.94	26.50
102	−0.48	33.09	100	−0.50	33.08	26.60

Station 5164; May 30; latitude 47°58′ N., longitude 49°47′ W.; depth 169 meters; dynamic height 971.044

Observed values			Scaled values			
Depth, meters	Temperature, ° C.	Salinity, °/oo	Depth, meters	Temperature, ° C.	Salinity, °/oo	σ_t
0	2.86	32.27	0	2.86	32.27	25.74
26	2.62	32.34	25	2.65	32.34	25.82
51	−1.16	33.11	50	−1.15	33.10	26.64
77	−1.09	33.30	75	−1.10	33.29	26.78
103	−0.61	33.49	100	−0.65	33.47	26.93
154	0.48	33.81	150	0.40	33.79	27.13

Station 5165; May 30; latitude 48°14.5′ N., longitude 49°42′ W.; depth 220 meters; dynamic height 971.040

Observed values			Scaled values			
Depth, meters	Temperature, ° C.	Salinity, °/oo	Depth, meters	Temperature, ° C.	Salinity, °/oo	σ_t
0	2.64	32.43	0	2.64	32.43	25.89
25	2.26	32.53	25	2.26	32.53	26.00
50	−1.48	33.14	50	−1.48	33.14	26.68
75	−1.59	33.24	75	−1.59	33.24	26.76
100	−1.32	33.34	100	−1.32	33.35	26.84
151	0.54	33.80	150	0.50	33.79	27.12
201	2.13	34.48	200	2.10	34.47	27.56

Station 5166; May 30; latitude 48°33′ N., longitude 49°34′ W.; depth 622 meters; dynamic height 971.013

Observed values			Scaled values			
Depth, meters	Temperature, ° C.	Salinity, °/oo	Depth, meters	Temperature, ° C.	Salinity, °/oo	σ_t
0	2.75	32.74	0	2.75	32.74	26.13
25	2.59	32.77	25	2.59	32.77	26.16
49	−0.68	33.23	50	−0.70	33.24	26.74
74	−0.93	33.42	75	−0.95	33.43	26.90
98	−0.57	33.60	100	−0.55	33.61	27.03
147	0.39	33.97	150	0.40	33.98	27.28
196	0.71	34.09	200	0.75	34.10	27.36
294	2.22	34.50	300	2.25	34.51	27.58
388	2.75	34.66	400	2.80	34.67	27.66
594	3.42	34.81	600	3.40	34.81	27.72

Station 5167; May 30; latitude 48°40′ N., longitude 49°31′ W.; depth 1,060 meters; dynamic height 970.984

Observed values			Scaled values			
Depth, meters	Temperature, ° C.	Salinity, °/oo	Depth, meters	Temperature, ° C.	Salinity, °/oo	σ_t
0	2.34	32.72	0	2.34	32.72	26.14
25	2.16	32.80	25	2.16	32.80	26.23
49	−1.14	33.23	50	−1.15	33.23	26.74
74	−1.02	33.44	75	−1.00	33.45	26.92
99	−0.20	33.66	100	−0.10	33.67	27.06
147	0.87	34.13	150	0.90	34.14	27.38
196	1.50	34.30	200	1.55	34.31	27.47
295	2.50	34.61	300	2.55	34.62	27.65
391	3.10	34.75	400	3.20	34.76	27.70
590	3.54	34.84	600	3.50	34.84	27.73
792	3.50	34.85	800	3.50	34.85	27.74
997	3.36	34.86	1,000	3.35	34.86	27.76

Station 5168; May 30; latitude 49°07′ N., longitude 49°16′ W.; depth 1,628 meters; dynamic height 970.938

Observed values			Scaled values			
Depth, meters	Temperature, ° C.	Salinity, °/oo	Depth, meters	Temperature, ° C.	Salinity, °/oo	σ_t
0	2.95	32.84	0	2.95	32.84	26.19
26	2.92	33.02	25	2.95	33.00	26.32
52	−0.05	33.80	50	−0.05	33.76	27.13
78	0.89	34.06	75	0.75	34.04	27.31
104	1.36	34.21	100	1.30	34.18	27.38
156	1.96	34.44	150	1.90	34.42	27.54
208	2.16	34.50	200	2.15	34.49	27.57
312	2.58	34.60	300	2.50	34.58	27.61
405	2.98	34.71	400	3.00	34.70	27.67
610	3.34	34.84	600	3.30	34.84	27.75
818	3.43	-------	800	3.45	34.86	27.75
1,024	3.52	-------	1,000	3.50	34.87	27.76
1,538	3.34	34.89				

Station 5169; May 30–31; latitude 49°34′ N., longitude 49°08′ W.; depth, 1,719 meters; dynamic height 970.924

Observed values			Scaled values			
Depth, meters	Temperature, ° C.	Salinity, °/oo	Depth, meters	Temperature, ° C.	Salinity, °/oo	σ_t
0	2.51	32.90	0	2.51	32.90	26.27
20	2.11	33.09	25	1.65	33.23	26.60
40	0.35	33.76	50	0.25	33.86	27.20
60	0.25	33.94	75	0.55	34.04	27.32
80	0.70	34.07	100	1.25	34.18	27.39
121	1.76	34.30	150	2.35	34.42	27.50
161	2.51	34.47	200	2.70	34.55	27.57
241	2.84	34.63	300	3.00	34.70	27.67
370	3.09	34.77	400	3.15	34.78	27.71
560	3.26	34.82	600	3.25	34.82	27.74
755	3.35	34.84	800	3.35	34.84	27.74
950	3.35	34.85	1,000	3.35	34.85	27.75
1,450	3.29	34.88				

Station 5170; May 31; latitude 50°01′ N., longitude 48°40′ W.; depth 2,103 meters; dynamic height 970.864

Observed values			Scaled values			
Depth, meters	Temperature, ° C.	Salinity, °/oo	Depth, meters	Temperature, ° C.	Salinity, °/oo	σ_t
0	3.71	33.44	0	3.71	33.44	26.60
25	2.47	33.88	25	2.47	33.88	27.05
49	3.02	34.40	50	3.05	34.41	27.43
74	4.07	34.66	75	4.05	34.66	27.53
08	2.99	34.62	100	3.00	34.62	27.61
147	3.21	34.73	150	3.20	34.73	27.67
196	3.32	34.78	200	3.35	34.78	27.69
294	3.33	34.81	300	3.40	34.81	27.72
307	3.43	34.81	400	3.35	34.83	27.73
481	3.35	34.84	600	3.35	34.85	27.75
669	3.33	34.85	800	3.25	34.84	27.75
857	3.26	34.84	1,000	3.30	34.85	27.76
1,362	3.35	34.87				

Table of Oceanographic Data—Continued

STATIONS OCCUPIED IN 1953—Continued

Station 5171; June 6; latitude 46°46′ N., longitude 48°43′ W.; depth 89 meters; dynamic height 971.046

Observed values			Scaled values			
Depth, meters	Temperature, ° C.	Salinity, °/oo	Depth, meters	Temperature, ° C.	Salinity, °/oo	σ_t
0	4.27	32.59	0	4.27	32.59	25.87
26	3.57	32.59	25	3.60	32.59	25.94
51	3.24	32.60	50	3.25	32.59	25.97
77	−0.25	32.96	75	0.05	32.93	26.46

Station 5172; June 6; latitude 46°50′ N., longitude 48°10′ W.; depth 117 meters; dynamic height 971.042

Observed values			Scaled values			
Depth, meters	Temperature, ° C.	Salinity, °/oo	Depth, meters	Temperature, ° C.	Salinity, °/oo	σ_t
0	3.78	32.50	0	3.78	32.50	25.84
25	3.09	32.50	25	3.09	32.50	25.90
49	2.26	32.64	50	2.25	32.65	26.10
74	−1.08	33.01	75	−1.10	33.02	26.57
98	−0.55	33.24	100	−0.50	33.25	26.74

Station 5173; June 6 latitude 46°51′ N., longitude 47°38′ W.; depth 183 meters; dynamic height 971.028

Observed values			Scaled values			
Depth, meters	Temperature, ° C.	Salinity, °/oo	Depth, meters	Temperature, ° C.	Salinity, °/oo	σ_t
0	3.37	32.53	0	3.37	32.53	25.91
25	2.66	32.55	25	2.66	32.55	25.98
51	−0.36	32.92	50	−0.30	32.91	26.45
76	−1.18	33.22	75	−1.20	33.21	26.73
101	−0.75	33.39	100	−0.80	33.38	26.85
152	0.59	33.87	150	0.55	33.86	27.18

Station 5174; June 6; latitude 46°51′ N., longitude 47°20′ W.; depth 344 meters; dynamic height 971.009

Observed values			Scaled values			
Depth, meters	Temperature, ° C.	Salinity, °/oo	Depth, meters	Temperature, ° C.	Salinity, °/oo	σ_t
0	2.66	32.69	0	2.66	32.69	26.09
25	2.27	32.72	25	2.27	32.72	26.15
50	0.80	32.99	50	0.80	32.99	26.47
75	−0.27	33.55	75	−0.27	33.55	26.97
100	0.19	33.77	100	0.19	33.77	27.13
150	0.96	34.07	150	0.96	34.07	27.32
201	1.52	34.29	200	1.50	34.28	27.45
301	2.01	34.43	300	2.00	34.43	27.53

Station 5175; June 6; latitude 46°50.5′ N., longitude 47°12′ W.; depth 695 meters; dynamic height 970.995

Observed values			Scaled values			
Depth, meters	Temperature, ° C.	Salinity, °/oo	Depth, meters	Temperature, ° C.	Salinity, °/oo	σ_t
0	2.58	32.72	0	2.58	32.72	26.12
25	2.14	32.72	25	2.14	32.72	26.16
50	1.37	32.89	50	1.37	32.89	26.34
75	0.39	33.55	75	0.39	33.55	26.94
101	0.75	33.80	100	0.70	33.79	27.11
151	1.39	34.22	150	1.40	34.21	27.41
201	2.03	34.42	200	2.00	34.41	27.52
302	2.56	34.62	300	2.55	34.61	27.64
426	3.17	34.76	400	3.10	34.74	27.69
643	3.46	34.81	600	3.45	34.80	27.70

Station 5176; June 6–7; latitude 46°49′ N., longitude 46°52′ W.; depth 1,197 meters; dynamic height 970.919

Observed values			Scaled values			
Depth, meters	Temperature, ° C.	Salinity, °/oo	Depth, meters	Temperature, ° C.	Salinity, °/oo	σ_t
0	4.32	33.21	0	4.32	33.21	26.36
25	4.21	33.37	25	4.21	33.37	26.49
49	4.29	33.66	50	4.30	33.68	26.73
74	3.23	34.16	75	3.20	34.16	27.22
98	2.83	34.44	100	2.80	34.44	27.47
147	2.48	34.58	150	2.50	34.58	27.61
196	2.87	34.66	200	2.90	34.67	27.66
294	3.61	34.80	300	3.65	34.81	27.69
344	3.65	34.84	400	3.65	34.85	27.72
523	3.63	34.86	600	3.55	34.86	27.74
707	3.44	34.86	800	3.40	34.86	27.76
891	3.41	34.86	1,000	3.35	34.87	27.77
1,030	3.34	34.88				

Station 5177; June 7; latitude 46°48′ N., longitude 46°31′ W.; depth 604 meters; dynamic height 970.900

Observed values			Scaled values			
Depth, meters	Temperature, ° C.	Salinity, °/oo	Depth, meters	Temperature, ° C.	Salinity, °/oo	σ_t
0	5.07	33.53	0	5.07	33.53	26.52
23	4.92	33.54	25	4.90	33.54	26.55
47	3.00	33.74	50	3.00	33.79	26.94
70	2.98	34.35	75	2.95	34.36	27.40
93	2.58	34.39	100	2.60	34.42	27.48
140	3.09	34.55	150	3.10	34.57	27.56
186	3 09	34.63	200	3.15	34.65	27.61
279	3.60	34.81	300	3.65	34.82	27.70
332	3.67	34.84	400	3.60	34.86	27.74
524	3.50	34.87	(600)	3.45	34.87	27.76

Station 5178; June 7; latitude 46°47′ N., longitude 46°08′ W.; depth 300 meters; dynamic height 970.922

Observed values			Scaled values			
Depth, meters	Temperature, ° C.	Salinity, °/oo	Depth, meters	Temperature, ° C.	Salinity, °/oo	σ_t
0	6.29	33.84	0	6.29	33.84	26.62
21	6.28	33.86	25	6.25	33.87	26.66
42	4.95	33.89	50	4.70	33.93	26.88
63	4.31	34.04	75	3.70	34 10	27.12
83	3.38	34.14	100	3.00	34.21	27.28
125	2.67	34.32	150	3.25	34.49	27.47
167	3.71	34.58	200	3.75	34.64	27.54
250	3.74	34.72	(300)	3.70	34.80	27.68

Station 5179; June 7; latitude 46°46′ N., longitude 45°42′ W.; depth 260 meters; dynamic height 970.939

Observed values			Scaled values			
Depth, meters	Temperature, ° C.	Salinity, °/oo	Depth, meters	Temperature, ° C.	Salinity, °/oo	σ_t
0	6.78	33.72	0	6.78	33.72	26.46
20	6.67	33.73	25	6.50	33.73	26.50
40	5.72	33.76	50	4.55	33.84	26.82
60	3.26	33.94	75	2.90	34.01	27.13
80	2.82	34.03	100	2.55	34.08	27.21
121	2.36	34.15	150	3.05	34.36	27.39
161	3.29	34.42	200	3.20	34.53	27.51
201	3.18	34.53				

STATIONS OCCUPIED IN 1953—Continued

Observed values			Scaled values			
Depth, meters	Temperature, ° C.	Salinity, °/oo	Depth, meters	Temperature, ° C.	Salinity, °/oo	σ_t
Station 5180; June 7; latitude 46°46′ N., longitude 45°24′ W.; depth 220 meters; dynamic height 970.967						
0	7.11	33.60	0	7.11	33.60	26.33
25	7.02	33.60	25	7.02	33.60	26.33
49	6.08	33.67	50	6.00	33.68	26.53
74	3.68	33.87	75	3.65	33.88	26.94
98	2.99	33.97	100	2.95	33.98	27.09
148	2.84	34.24	150	2.85	34.25	27.32
197	3.57	34.48	200	3.55	34.49	27.44
Station 5181; June 7; latitude 46°46.5′ N., longitude 45°05′ W.; depth 169 meters; dynamic height 970.960						
0	7.26	33.64	0	7.26	33.64	26.34
28	7.11	33.65	25	7.10	33.65	26.36
55	4.96	33.78	50	5.35	33.75	26.67
82	3.10	33.94	75	3.40	33.90	26.99
109	2.78	34.09	100	2.85	34.04	27.15
165	3.08	34.31	150	2.95	34.26	27.32
Station 5182; June 7; latitude 46°46′ N., longitude 44°51′ W.; depth 141 meters; dynamic height 970.946						
0	7.29	33.64	0	7.29	33.64	26.33
25	7.17	33.64	25	7.17	33.64	26.35
50	4.06	33.84	50	4.06	33.84	26.87
76	2.96	34.06	75	2.95	34.05	27.15
101	2.94	34.23	100	2.95	34.23	27.29
131	2.93	34.25				
Station 5183; June 7; latitude 46°40′ N., longitude 44°51′ W.; depth 170 meters; dynamic height 970.933						
0	7.52	33.62	0	7.52	33.62	26.29
26	5.94	33.74	25	6.05	33.73	26.56
52	3.13	33.95	50	3.20	33.94	27.04
78	2.93	34.07	75	2.95	34.05	27.15
104	3.07	34.28	100	3.05	34.26	27.31
155	3.74	34.49	150	3.65	34.47	27.42
Station 5184; June 7; latitude 46°34′ N., longitude 44°52′ W.; depth 220 meters; dynamic height 970.956						
0	7.56	33.64	0	7.56	33.64	26.29
24	7.31	33.65	25	7.25	33.65	26.35
47	5.47	33.73	50	5.20	33.74	26.68
71	3.22	33.90	75	3.15	33.93	27.03
94	2.94	34.05	100	2.95	34.08	27.17
141	2.97	34.28	150	3.05	34.33	27.36
188	3.95	34.60	(200)	4.00	34.69	27.56

Observed values			Scaled values			
Depth, meters	Temperature, ° C.	Salinity, °/oo	Depth, meters	Temperature, ° C.	Salinity, °/oo	σ_t
Station 5185; June 7; latitude 46°27′ N., longitude 44°52′ W.; depth 677 meters; dynamic height 970.916						
0	7.34	33.64	0	7.34	33.64	26.32
25	7.06	33.66	25	7.06	33.66	26.38
49	3.79	34.17	50	3.70	34.17	27.18
74	3.00	34.28	75	3.00	34.28	27.33
98	3.06	34.36	100	3.05	34.36	27.39
147	2.85	34.52	150	2.85	34.53	27.54
197	3.45	34.68	200	3.50	34.68	27.60
295	3.58	34.81	300	3.60	34.81	27.70
368	3.55	34.83	400	3.55	34.84	27.72
568	3.48	34.86	(600)	3.45	34.86	27.75
Station 5186; June 7; latitude 46°19.5′ N., longitude 44°54′ W.; depth 2,103 meters; dynamic height 970.907						
0	7.45	33.70	0	7.45	33.70	26.36
26	6.92	33.73	25	6.95	33.73	26.45
53	4.39	34.10	50	4.60	34.05	26.99
79	3.37	34.23	75	3.50	34.20	27.22
105	2.93	34.50	100	2.95	34.46	27.48
157	3.27	34.67	150	3.20	34.65	27.61
209	3.44	34.76	200	3.45	34.74	27.65
314	3.52	34.85	300	3.55	34.84	27.72
426	*3.60	34.86	400	3.60	34.86	27.74
641	3.51	34.875	600	3.50	34.87	27.76
858	3.47	34.89	800	3.50	34.88	27.76
1,068	3.39	34.89	1,000	3.45	34.89	27.77
1,590	3.36	34.89				
Station 5187; June 7; latitude 46°01′ N., longitude 44°37′ W.; depth 3,292 meters; dynamic height 970.973						
0	6.81	33.30	0	6.81	33.30	26.13
25	6.65	33.33	25	6.65	33.33	26.17
50	6.03	33.38	50	6.03	33.38	26.28
75	1.86	33.83	75	1.86	33.83	27.06
99	2.37	34.10	100	2.40	34.12	27.26
149	3.71	34.51	150	3.70	34.51	27.45
199	3.75	34.65	200	3.75	34.65	27.55
298	4.17	34.85	300	4.20	34.85	27.67
344	3.70	34.825	400	3.65	34.84	27.71
517	3.59	34.86	600	3.55	34.86	27.74
689	3.51	-------	(800)	3.50	34.87	27.76
			(1,000)	3.45	34.88	27.76
Station 5188; June 8; latitude 46°05′ N., longitude 45°23′ W.; depth 2,561 meters; dynamic height 970.921						
0	7.07	33.81	0	7.07	33.81	26.49
25	6.90	33.80	25	6.90	33.80	26.51
49	4.26	34.08	50	4.25	34.08	27.05
74	2.56	34.17	75	2.55	34.18	27.29
98	3.41	34.46	100	3.45	34.47	27.44
147	3.94	34.70	150	3.95	34.70	27.57
196	3.85	34.77	200	3.85	34.77	27.64
294	3.94	34.84	300	3.95	34.84	27.68
377	4.09	34.90	400	4.10	34.90	27.72
568	3.89	34.90	600	3.85	34.90	27.74
760	*3.74	34.89	800	3.70	34.89	27.75
954	3.56	34.88	1,000	3.55	34.88	27.75
1,446	3.38	34.86				

STATIONS OCCUPIED IN 1953—Continued

Station 5189; June 8; latitude 46°07.5′ N., longitude 46°08′ W.; depth 1,719 meters; dynamic height 970.902

Observed values			Scaled values			
Depth, meters	Temperature, ° C.	Salinity, ‰	Depth, meters	Temperature, ° C.	Salinity, ‰	σ_t
0	7.36	33.72	0	7.36	33.72	26.39
24	6.88	33.73	25	6.80	33.73	26.47
48	3.78	34.10	50	3.75	34.11	27.13
72	3.10	34.33	75	3.10	34.34	27.37
96	3.32	34.47	100	3.30	34.48	27.46
144	3.20	34.62	150	3.25	34.64	27.59
192	3.80	34.78	200	3.85	34.80	27.66
288	3.97	34.89	300	3.90	34.88	27.72
323	3.77	34.865	400	3.70	34.87	27.74
494	3.62	34.875	600	3.55	34.88	27.75
672	3.55	34.89	800	3.50	34.88	27.76
852	3.49	34.88	1,000	3.45	34.88	27.76
1,325	3.35	34.88				

Station 5190; June 8; latitude 46°10.5′ N., longitude 46°41′ W.; depth 1,097 meters; dynamic height 970.898

Observed values			Scaled values			
Depth, meters	Temperature, ° C.	Salinity, ‰	Depth, meters	Temperature, ° C.	Salinity, ‰	σ_t
0	5.21	33.30	0	5.21	33.30	26.32
24	4.57	33.38	25	4.50	33.39	26.47
49	2.12	34.04	50	2.05	34.06	27.24
73	1.65	34.26	75	1.65	34.27	27.44
97	2.04	34.37	100	2.05	34.38	27.49
145	2.65	34.56	150	2.70	34.57	27.59
194	3.32	34.72	200	3.35	34.73	27.65
291	3.58	34.83	300	3.60	34.84	27.72
362	3.99	34.91	400	3.95	34.91	27.74
551	3.67	34.88	600	3.55	34.88	27.75
740	3.47	34.87	800	3.45	34.88	27.76
934	3.42	34.89	(1,000)	3.40	34.89	27.78

Station 5191; June 8; latitude 46°14′ N., longitude 47°10′ W.; depth 1,051 meters; dynamic height 970.908

Observed values			Scaled values			
Depth, meters	Temperature, ° C.	Salinity, ‰	Depth, meters	Temperature, ° C.	Salinity, ‰	σ_t
0	3.91	33.18	0	3.91	33.18	26.37
26	3.40	33.31	25	3.40	33.31	26.52
51	3.56	33.60	50	3.55	33.57	26.72
77	2.49	34.43	75	2.50	34.35	27.43
102	2.67	34.49	100	2.65	34.48	27.52
155	2.43	34.58	150	2.45	34.57	27.61
206	2.72	34.66	200	2.70	34.65	27.65
308	3.40	34.82	300	3.35	34.81	27.72
394	3.52	34.84	400	3.55	34.84	27.72
596	3.56	34.88	600	3.55	34.88	27.75
803	3.48	34.88	800	3.50	34.88	27.76
1,000	3.50	34.89	1,000	3.50	34.89	27.77

Station 5192; June 8; latitude 46°16′ N., longitude 47°17′ W.; depth 595 meters; dynamic height 970.938

Observed values			Scaled values			
Depth, meters	Temperature, ° C.	Salinity, ‰	Depth, meters	Temperature, ° C.	Salinity, ‰	σ_t
0	2.89	32.90	0	2.89	32.90	26.24
24	1.70	32.95	25	1.65	32.95	26.38
49	0.64	33.39	50	0.65	33.10	26.56
73	0.61	33.83	75	0.65	33.89	27.19
98	1.22	34.17	100	1.25	34.18	27.39
147	1.82	34.39	150	1.85	34.40	27.52
195	2.27	34.54	200	2.30	34.55	27.61
293	2.72	34.67	300	2.75	34 68	27.67
374	3.27	34.80	400	3.30	34.81	27.73
577	3.44	34.85				

Station 5193; June 8; latitude 46°15.5′ N., longitude 47°40′ W.; depth 172 meters; dynamic height 971.010

Observed values			Scaled values			
Depth, meters	Temperature, ° C.	Salinity, ‰	Depth, meters	Temperature, ° C.	Salinity, ‰	σ_t
0	2.81	32.68	0	2.81	32.68	26.07
26	1.97	32.76	25	2.00	32.76	26.20
52	0.55	32.98	50	0.60	32.97	26.46
78	−0.45	33.24	75	−0.40	33.22	26.71
103	−0.30	33.56	100	−0.35	33.53	26.95
156	0.50	33.84	150	0.45	33.81	27.14

Station 5194; June 8; latitude 46° 14′ N., longitude 47°57′ W.; depth 117 meters; dynamic height 971.020

Observed values			Scaled values			
Depth, meters	Temperature, ° C.	Salinity, ‰	Depth, meters	Temperature, ° C.	Salinity, ‰	σ_t
0	3.20	32.50	0	3.20	32.50	25.89
25	2.86	32.56	25	2.86	32.56	25.97
48	0.82	32.76	50	0.65	32.79	26.32
73	−1.26	33.21	75	−1.25	33.24	26.75
97	−0.43	33.41	100	−0.35	33.43	26.87

Station 5195; June 8; latitude 46°16′ N., longitude 48°28′ W.; depth 91 meters; dynamic height 971.032

Observed values			Scaled values			
Depth, meters	Temperature, ° C.	Salinity, ‰	Depth, meters	Temperature, ° C.	Salinity, ‰	σ_t
0	4.44	32.59	0	4.44	32.59	25.85
22	4.44	32.60	25	4.40	32.60	25.87
45	3.49	32.61	50	2.30	32.62	26.07
67	−0.47	32.93	(75)	−0.95	33.09	26.62

Station 5196; June 9; latitude 46°18′ N., longitude 48°56′ W.; depth 68 meters; dynamic height 971.033

Observed values			Scaled values			
Depth, meters	Temperature, ° C.	Salinity, ‰	Depth, meters	Temperature, ° C.	Salinity, ‰	σ_t
0	4.25	32.59	0	4.25	32.59	25.87
15	4.24	32.59	25	4.20	32.59	25.88
41	3.99	32.61	50	2.65	32.70	26.10
56	0.63	32.80				

Station 5197; June 9; latitude 46°10′ N., longitude 48°42′ W.; depth 82 meters; dynamic height 971.034

Observed values			Scaled values			
Depth, meters	Temperature, ° C.	Salinity, ‰	Depth, meters	Temperature, ° C.	Salinity, ‰	σ_t
0	4.52	32.58	0	4.52	32.58	25.84
23	4.51	32.58	25	4.50	32.58	25.84
47	3.84	32.60	50	3.00	32.63	26.02
61	−0.56	32.92	(75)	−1.00	33.15	26.68

Station 5198; June 9; latitude 46°02′ N., longitude 48°27′ W.; depth 89 meters; dynamic height 971.034

Observed values			Scaled values			
Depth, meters	Temperature, ° C.	Salinity, ‰	Depth, meters	Temperature, ° C.	Salinity, ‰	σ_t
0	3.42	32.53	0	3.42	32.53	25.90
25	3.40	32.53	25	3.40	32.53	25.90
49	2.44	32.62	50	2.30	32.63	26.08
74	−0.67	32.97	75	−0.75	32.98	26.53

STATIONS OCCUPIED IN 1953—Continued

Station 5199; June 9; latitude 45°49′ N., longitude 48°12′ W.; depth 115 meters; dynamic height 971.015

Observed values			Scaled values			
Depth, meters	Temperature, ° C.	Salinity, ‰	Depth, meters	Temperature, ° C.	Salinity, ‰	σt
0	3.00	32.52	0	3.00	32.52	25.93
23	2.97	32.53	25	2.95	32.54	25.95
46	0.42	32.91	50	0.15	32.98	26.49
69	−0.55	33.24	75	−0.55	33.34	26.81
92	0.03	33.65	100	0.25	33.82	27.17

Station 5200; June 9; latitude 45°47′ N., longitude 48°14′ W.; depth 179 meters; dynamic height 971.019

Observed values			Scaled values			
Depth, meters	Temperature, ° C.	Salinity, ‰	Depth, meters	Temperature, ° C.	Salinity, ‰	σt
0	2.79	32.61	0	2.79	32.61	26.02
23	2.57	32.67	25	2.50	32.68	26.10
46	1.03	33.02	50	0.80	33.08	26.54
69	0.07	33.34	75	0.05	33.41	26.85
93	0.11	33.63	100	0.15	33.68	27.05
139	0.65	33.90	(150)	0.80	33.96	27.24

Station 5201; June 9; latitude 45°43′ N., longitude 48°10′ W.; depth 685 meters; dynamic height 970.985

Observed values			Scaled values			
Depth, meters	Temperature, ° C.	Salinity, ‰	Depth, meters	Temperature, ° C.	Salinity, ‰	σt
0	2.60	32.74	0	2.60	32.74	26.14
26	2.44	32.78	25	2.45	32.78	26.18
51	1.11	33.26	50	1.15	33.24	26.65
77	0.66	33.60	75	0.65	33.57	26.94
102	0.91	34.03	100	0.90	34.01	27.28
152	1.42	34.24	150	1.40	34.23	27.42
203	1.72	34.35	200	1.70	34.34	27.48
305	2.10	34.47	300	2.10	34.46	27.55
350	2.48	34.60	400	2.80	34.67	27.66
539	3.26	34.78	(600)	3.30	34.81	27.73

Station 5202; June 9; latitude 45°31.5′ N., longitude 47°56′ W.; depth 1,335 meters; dynamic height 970.910

Observed values			Scaled values			
Depth, meters	Temperature, ° C.	Salinity, ‰	Depth, meters	Temperature, ° C.	Salinity, ‰	σt
0	3.89	33.08	0	3.89	33.08	26.29
27	3.52	33.16	25	3.55	33.15	26.38
53	1.97	34.13	50	2.15	34.00	27.18
80	1.59	34.30	75	1.60	34.28	27.44
105	1.89	34.40	100	1.80	34.38	27.51
159	2.25	34.52	150	2.20	34.50	27.58
212	2.72	34.65	200	2.60	34.62	27.64
317	3.36	34.80	300	3.25	34.78	27.70
387	3.87	34.88	400	3.85	34.88	27.72
585	3.56	34.86	600	3.55	34.86	27.74
788	3.53	34.89	800	3.55	34.89	27.76
990	3.49	34.89	1,000	3.50	34.89	27.77
1,293	3.39	34.88				

Station 5203; June 9; latitude 45°12.5′ N., longitude 47°33′ W.; depth 2,944 meters; dynamic height 970.985

Observed values			Scaled values			
Depth, meters	Temperature, ° C.	Salinity, ‰	Depth, meters	Temperature, ° C.	Salinity, ‰	σt
0	6.20	33.30	0	6.20	33.30	26.20
25	5.99	33.30	25	5.99	33.30	26.23
49	4.70	33.50	50	4.65	33.52	26.57
74	2.57	33.87	75	2.55	33.88	27.05
99	2.88	34.10	100	2.90	34.10	27.20
147	3.16	34.33	150	3.20	34.35	27.37
196	3.63	34.58	200	3.65	34.60	27.52
295	4.82	34.90	300	4.85	34.90	27.63
368	4.71	34.93	400	4.60	34.93	27.68
563	4.14	34.93	600	4.05	34.93	27.74
764	3.87	34.92	800	3.80	34.91	27.76
960	3.67	34.90	1,000	3.70	34.90	27.76
1,459	3.53	34.92				

Station 5204; June 9; latitude 45°19′ N., longitude 46°44′ W.; depth 3,292 meters; dynamic height 970.935

Observed values			Scaled values			
Depth, meters	Temperature, ° C.	Salinity, ‰	Depth, meters	Temperature, ° C.	Salinity, ‰	σt
0	7.13	33.62	0	7.13	33.62	26.34
25	7.12	33.62	25	7.12	33.62	26.34
51	5.37	33.89	50	5.55	33.88	26.74
76	3.54	34.32	75	3.55	34.31	27.30
101	3.44	34.46	100	3.45	34.45	27.42
151	3.85	34.68	150	3.85	34.68	27.56
202	4.13	34.79	200	4.10	34.78	27.62
303	3.85	34.82	300	3.85	34.82	27.68
394	3.86	34.87	400	3.85	34.87	27.72
597	3.66	34.87	600	3.65	34.87	27.74
802	3.57	34.88	800	3.55	34.88	27.75
1,002	3.49	34.88	1,000	3.55	34.88	27.75
1,502	3.37	34.87				

Station 5205; June 10; latitude 45°21′ N., longitude 45°54′ W.; depth 3,438 meters; dynamic height 970.949

Observed values			Scaled values			
Depth, meters	Temperature, ° C.	Salinity, ‰	Depth, meters	Temperature, ° C.	Salinity, ‰	σt
0	6.07	33.36	0	6.07	33.36	26.27
23	6.00	33.36	25	6.00	33.36	26.28
45	5.04	33.73	50	4.75	33.83	26.79
68	3.48	34.15	75	3.35	34.22	27.25
90	3.29	34.32	100	3.30	34.36	27.37
135	3.35	34.49	150	3.55	34.56	27.50
180	4.00	34.70	200	4.10	34.74	27.59
270	4.20	34.85	300	4.20	34.86	27.68
292	4.21	34.86	400	4.05	34.87	27.70
451	3.96	34.87	600	3.80	34.88	27.73
620	3.80	34.88	800	3.60	34.88	27.75
796	3.56	34.88	1,000	3.50	34.88	27.76
1,274	3.42	34.88				

Table of Oceanographic Data—Continued

STATIONS OCCUPIED IN 1953—Continued

Station 5206; June 10; latitude 45°25′ N., longitude 45°19′ W.; depth 4,207 meters; dynamic height 971.092

Observed values			Scaled values			
Depth, meters	Temperature, ° C.	Salinity, °/oo	Depth, meters	Temperature, ° C.	Salinity, °/oo	σ_t
0	6.90	33.25	0	6.90	33.25	26.08
27	10.50	34.39	25	10.25	34.33	26.40
53	11.55	34.84	50	11.45	34.81	26.57
79	11.72	35.03	75	11.70	35.01	26.68
105	11.32	35.10	100	11.45	35.09	26.78
159	8.92	-------	150	9.35	34.93	27.02
211	7.11	34.79	200	7.45	34.80	27.22
316	5.69	34.80	300	5.90	34.80	27.43
422	4.62	34.84	400	4.80	34.83	27.58
631	4.41	34.94	600	4.45	34.93	27.70
840	3.84	34.90	800	3.90	34.91	27.75
1,048	3.65	34.90	1,000	3.70	34.90	27.76
1,563	3.40	34.88				

Station 5207; June 10; latitude 44°50′ N., longitude 45°16′ W.; depth 4,134 meters; dynamic height 971.083

Observed values			Scaled values			
Depth, meters	Temperature, ° C.	Salinity, °/oo	Depth, meters	Temperature, ° C.	Salinity, °/oo	σ_t
0	4.17	32.73	0	4.17	32.73	25.99
26	10.56	34.34	25	10.40	34.25	26.32
51	11.72	34.73	50	11.70	34.72	26.45
78	11.98	35.25	75	12.00	35.23	26.79
103	10.95	35.15	100	11.20	35.16	26.88
155	6.59	34.54	150	6.70	34.60	27.16
206	7.26	34.87	200	7.25	34.83	27.27
309	6.84	35.02	300	6.85	35.00	27.46
341	6.95	35.10	400	6.20	35.04	27.58
519	4.75	34.92	600	4.40	34.92	27.70
703	4.18	34.92	800	4.05	34.92	27.74
893	3.99	34.92	1,000	3.90	34.92	27.76
1,393	3.60	34.90				

Station 5208; June 10; latitude 44°24.5′ N., longitude 45°15′ W.; depth 3,942 meters; dynamic height 971.150

Observed values			Scaled values			
Depth, meters	Temperature, ° C.	Salinity, °/oo	Depth, meters	Temperature, ° C.	Salinity, °/oo	σ_t
0	14.17	35.04	0	14.17	35.04	26.21
25	13.96	35.04	25	13.96	35.04	26.25
50	12.51	35.17	50	12.51	35.17	26.65
75	12.94	35.49	75	12.94	35.49	26.80
100	12.54	35.45	100	12.54	35.45	26.85
150	11.68	35.34	150	11.68	35.34	26.93
200	11.55	35.47	200	11.55	35.47	27.05
300	*8.89	35.12	300	8.89	35.12	27.25
370	7.47	35.06	400	6.95	35.04	27.48
563	4.94	34.96	600	4.85	34.96	27.68
762	4.67	35.00	800	4.55	34.99	27.74
961	4.01	34.94	1,000	3.95	34.94	27.76
1,471	3.40	34.88				

Station 5209; June 10; latitude 44°24′ N., longitude 45°58′ W.; depth 3,841 meters; dynamic height 971.209

Observed values			Scaled values			
Depth, meters	Temperature, ° C.	Salinity, °/oo	Depth, meters	Temperature, ° C.	Salinity, °/oo	σ_t
0	12.44	34.28	0	12.44	34.28	25.96
24	12.53	34.44	25	12.55	34.48	26.09
48	14.54	35.67	50	14.55	35.66	26.59
72	13.37	35.53	75	13.35	35.53	26.75
95	13.24	35.56	100	13.20	35.56	26.80
144	12.63	35.48	150	12.55	35.46	26.86
191	11.99	35.36	200	11.90	35.34	26.89
286	10.40	35.27	300	9.85	35.18	27.13
325	*9.00	35.08	400	7.25	35.03	27.42
497	5.57	34.90	600	4.90	34.93	27.65
676	4.59	34.94	800	4.30	34.93	27.71
863	4.14	34.93	1,000	4.00	34.92	27.75
1,360	3.60	34.88				

Station 5210; June 10–11; latitude 44°26′ N., longitude 46°24′ W.; depth 3,749 meters; dynamic height 971.171

Observed values			Scaled values			
Depth, meters	Temperature, ° C.	Salinity, °/oo	Depth, meters	Temperature, ° C.	Salinity, °/oo	σ_t
0	11.79	34.10	0	11.79	34.10	25.95
25	12.92	34.70	25	12.92	34.70	26.20
50	14.83	35.76	50	14.83	35.76	26.61
76	14.25	35.75	75	14.25	35.75	26.73
100	13.64	35.67	100	13.60	35.67	26.81
151	12.80	35.57	150	12.80	35.57	26.90
201	11.13	35.33	200	11.15	35.33	27.02
301	8.33	34.98	300	8.35	34.98	27.22
322	7.43	34.94	400	5.55	34.81	27.48
491	4.21	34.72	600	4.45	34.85	27.64
666	4.53	34.92	800	4.20	34.92	27.73
844	4.11	34.92	1,000	3.90	34.91	27.75
1,306	3.55	34.885				

Station 5211; June 11; latitude 44°31′ N., longitude 46°50′ W.; depth 3,603 meters; dynamic height 971.036

Observed values			Scaled values			
Depth, meters	Temperature, ° C.	Salinity, °/oo	Depth, meters	Temperature, ° C.	Salinity, °/oo	σ_t
0	3.95	32.77	0	3.95	32.77	26.04
23	2.68	32.71	25	2.60	32.71	26.11
46	0.61	33.03	50	0.30	33.09	26.57
69	−0.52	33.37	75	−0.55	33.44	26.89
91	−0.48	33.62	100	−0.05	33.73	27.10
138	3.21	34.19	150	2.85	34.17	27.26
184	1.47	34.11	200	1.65	34.16	27.35
275	3.11	34.54	300	3.40	34.61	27.56
289	3.05	34.53	400	4.50	34.88	27.65
440	4.71	34.94	600	4.30	34.94	27.72
596	4.34	34.94	800	3.95	34.91	27.74
762	4.00	34.91	1,000	3.70	34.89	27.75
1,207	3.46	34.88				

Table of Oceanographic Data—Continued

STATIONS OCCUPIED IN 1953—Continued

Station 5212; June 11; latitude 44°43.5′ N., longitude 47°32′ W.; depth 3,841 meters; dynamic height 970.974

Observed values			Scaled values			
Depth, meters	Temperature, ° C.	Salinity, ‰	Depth, meters	Temperature, ° C.	Salinity, ‰	σ_t
0	5.44	33.02	0	5.44	33.02	26.08
26	5.38	33.13	25	5.40	33.13	26.17
51	3.98	33.22	50	4.15	33.22	26.37
77	2.53	34.03	75	2.65	33.95	27.10
102	3.13	34.27	100	3.10	34.26	27.31
153	3.33	34.48	150	3.30	34.47	27.46
204	3.45	34.62	200	3.45	34.61	27.55
306	4.24	34.86	300	4.25	34.84	27.65
376	4.19	34.89	400	4.15	34.89	27.70
570	3.84	34.90	600	3.80	34.90	27.75
768	3.62	34.87	800	3.60	34.87	27.75
965	3.58	34.88	1,000	3.55	34.88	27.75
1,468	3.40	34.88				

Station 5213; June 11; latitude 44°49.5′ N., longitude 48°11′ W.; depth 2,834 meters; dynamic height 970.966

Observed values			Scaled values			
Depth, meters	Temperature, ° C.	Salinity, ‰	Depth, meters	Temperature, ° C.	Salinity, ‰	σ_t
0	5.69	33.14	0	5.69	33.14	26.15
22	5.77	33.15	25	5.75	33.16	26.15
42	4.36	33.54	50	3.85	33.71	26.80
64	3.25	33.97	75	2.90	34.10	27.20
85	2.68	34.20	100	2.85	34.26	27.33
128	3.27	-------	150	3.60	34.47	27.43
170	3.93	34.54	200	4.10	34.63	27.50
255	4.14	34.80	300	4.15	34.83	27.65
361	4.11	34.86	400	4.05	34.87	27.70
549	3.72	34.88	600	3.70	34.88	27.74
744	3.60	34.87	800	3.55	34.87	27.75
942	3.48	34.88	1,000	3.50	34.88	27.76
1,457	3.50	34.88				

Station 5214; June 11; latitude 44°56′ N., longitude 48°34′ W.; depth 1,939 meters; dynamic height 970.916

Observed values			Scaled values			
Depth, meters	Temperature, ° C.	Salinity, ‰	Depth, meters	Temperature, ° C.	Salinity, ‰	σ_t
0	3.08	32.96	0	3.08	32.96	26.27
24	2.78	33.02	25	2.80	33.02	26.36
47	3.38	33.55	50	3.30	33.64	26.79
71	1.73	34.21	75	1.75	34.26	27.42
94	2.08	34.38	100	2.10	34.40	27.50
141	2.29	34.52	150	2.30	34.53	27.59
188	2.50	34.59	200	2.60	34.61	27.63
282	3.58	34.82	300	3.55	34.82	27.71
393	3.53	34.83	400	3.55	34.83	27.72
591	3.52	34.87	600	3.50	34.87	27.76
791	3.48	-------	800	3.50	34.87	27.76
987	3.48	-------	1,000	3.50	34.88	27.76
1,476	3.39	34.89				

Station 5215; June 11; latitude 44°58′ N., longitude 48°58′ W.; depth 869 meters; dynamic height 971.026

Observed values			Scaled values			
Depth, meters	Temperature, ° C.	Salinity, ‰	Depth, meters	Temperature, ° C.	Salinity, ‰	σ_t
0	3.50	32.49	0	3.50	32.49	25.85
26	2.20	32.88	25	2.30	32.88	26.28
51	0.71	33.21	50	0.80	33.19	26.63
77	0.30	33.48	75	0.30	33.45	26.86
102	0.42	33.83	100	0.35	33.79	27.13
154	1.22	34.14	150	1.20	34.12	27.35
205	1.45	34.24	200	1.45	34.23	27.41
307	1.83	34.38	300	1.80	34.37	27.51
425	*2.56	34.61	400	2.35	34.56	27.61
637	3.38	34.81	600	3.30	34.78	27.70

Station 5216; June 11; latitude 45°00′ N., longitude 49°10′ W.; depth 70 meters; dynamic height 971.061

Observed values			Scaled values			
Depth, meters	Temperature, ° C.	Salinity, ‰	Depth, meters	Temperature, ° C.	Salinity, ‰	σ_t
0	4.53	-------	0	4.53	32.49	25.75
25	2.10	32.72	25	2.10	32.72	26.16
50	−0.41	32.98	50	−0.41	32.98	26.52
60	−0.40	33.01				
75	−0.33	33.03				

Station 5217; June 12; latitude 45°03.5′ N., longitude 49°30′ W.; depth 66 meters; dynamic height 971.071

Observed values			Scaled values			
Depth, meters	Temperature, ° C.	Salinity, ‰	Depth, meters	Temperature, ° C.	Salinity, ‰	σ_t
0	4.54	32.49	0	4.54	32.49	25.75
26	3.49	32.57	25	3.50	32.56	25.91
52	0.25	32.84	50	0.35	32.82	26.36

Station 5218; June 12; latitude 44°14′ N., longitude 49°28′ W.; depth 50 meters; dynamic height 971.088

Observed values			Scaled values			
Depth, meters	Temperature, ° C.	Salinity, ‰	Depth, meters	Temperature, ° C.	Salinity, ‰	σ_t
0	6.79	31.94	0	6.79	31.94	25.06
28	3.91	32.62	25	4.25	32.55	25.84
44	3.47	32.66	(50)	3.40	32.67	26.01

Station 5219; June 12; latitude 44°06′ N., longitude 49°12′ W.; depth 100 meters; dynamic height 971.056

Observed values			Scaled values			
Depth, meters	Temperature, ° C.	Salinity, ‰	Depth, meters	Temperature, ° C.	Salinity, ‰	σ_t
0	5.37	32.40	0	5.37	32.40	25.61
26	2.52	32.72	25	2.60	32.71	26.11
53	0.31	32.98	50	0.50	32.95	26.44
79	0.04	33.18	75	0.10	33.14	26.63

Station 5220; June 12; latitude 44°05′ N., longitude 49°06′ W.; depth 320 meters; dynamic height 971.046

Observed values			Scaled values			
Depth, meters	Temperature, ° C.	Salinity, ‰	Depth, meters	Temperature, ° C.	Salinity, ‰	σ_t
0	4.10	32.44	0	4.10	32.44	25.77
25	1.81	32.76	25	1.81	32.76	26.21
50	0.13	33.03	50	0.13	33.03	26.53
75	−0.40	33.34	75	−0.40	33.34	26.81
100	−0.26	33.50	100	−0.26	33.50	26.93
151	0.42	33.83	150	0.40	33.83	27.16
201	0.97	34.03	200	0.95	34.02	27.28
251	1.18	34.13				

Station 5221; June 12; latitude 44°03′ N., longitude 49°02′ W.; depth 951 meters; dynamic height 971.038

Observed values			Scaled values			
Depth, meters	Temperature, ° C.	Salinity, ‰	Depth, meters	Temperature, ° C.	Salinity, ‰	σ_t
0	3.46	32.43	0	3.46	32.43	25.82
25	2.22	32.73	25	2.22	32.73	26.16
50	0.27	33.01	50	0.27	33.01	26.52
75	−0.52	33.28	75	−0.52	33.28	26.76
100	−0.22	33.48	100	−0.22	33.48	26.91
150	0.56	33.90	150	0.56	33.90	27.21
200	1.20	34.12	200	1.20	34.12	27.35
300	2.93	34.59	300	2.93	34.59	27.58
401	2.79	34.64	400	2.80	34.64	27.63
596	3.38	34.81	600	3.40	34.81	27.72
			(800)	3.45	34.85	27.74

STATIONS OCCUPIED IN 1953—Continued

Station 5222; June 12; latitude 44°02′ N., longitude 48°56′ W.; depth 1,646 meters; dynamic height 971.023

Observed values			Scaled values			
Depth, meters	Temperature, ° C.	Salinity, °/oo	Depth, meters	Temperature, ° C.	Salinity, °/oo	σ_t
0	3.73	32.25	0	3.73	32.25	25.64
25	2.91	32.68	25	2.91	32.68	26.07
50	1.78	32.80	50	1.78	32.80	26.25
75	0.73	33.21	75	0.73	33.21	26.65
100	0.36	33.68	100	0.36	33.68	27.04
150	2.11	34.24	150	2.11	34.24	27.37
200	2.11	34.37	200	2.11	34.37	27.48
300	2.35	34.54	300	2.35	34.54	27.59
394	2.92	34.70	400	2.95	34.71	27.68
593	3.48	34.83	600	3.45	34.83	27.72
793	3.51	34.85	800	3.50	34.85	27.74
990	3.51	34.86	1,000	3.50	34.86	27.75
1,479	3.44	34.86				

Station 5223; June 12; latitude 43°56′ N., longitude 48°40′ W.; depth 3,120 meters; dynamic height 971.022

Observed values			Scaled values			
Depth, meters	Temperature, ° C.	Salinity, °/oo	Depth, meters	Temperature, ° C.	Salinity, °/oo	σ_t
0	9.38	32.91	0	9.38	32.91	25.44
24	8.31	33.18	25	8.10	33.20	25.88
49	3.16	33.63	50	3.20	33.65	26.81
73	6.58	34.42	75	6.70	34.45	27.05
98	7.48	34.73	100	7.50	34.74	27.16
147	6.93	34.86	150	6.85	34.85	27.34
195	4.85	34.62	200	4.90	34.62	27.41
293	6.14	35.03	300	6.20	35.05	27.59
374	6.38	35.16	400	6.15	35.13	27.65
561	4.12	34.93	600	4.05	34.92	27.74
748	3.88	34.91	800	3.85	34.90	27.74
933	3.70	34.90	1,000	3.70	34.90	27.76
1,391	3.53	34.91				

Station 5224; June 12; latitude 43°48′ N., longitude 48°02′ W.; depth 3,566 meters; dynamic height 971.003

Observed values			Scaled values			
Depth, meters	Temperature, ° C.	Salinity, °/oo	Depth, meters	Temperature, ° C.	Salinity, °/oo	σ_t
0	6.87	33.00	0	6.87	33.00	25.89
25	4.82	33.08	25	4.82	33.08	26.20
49	3.51	33.24	50	3.45	33.25	26.46
74	1.80	33.62	75	1.75	33.63	26.91
99	1.48	33.90	100	1.50	33.91	27.16
148	2.04	34.26	150	2.05	34.26	27.40
197	1.90	34.38	200	1.95	34.39	27.51
296	3.63	34.73	300	3.65	34.74	27.63
381	4.50	34.91	400	4.50	34.91	27.68
576	3.99	34.88	600	3.95	34.88	27.71
775	3.69	-------	800	3.70	34.88	27.74
968	3.57	34.88	1,000	3.55	34.88	27.75
1,450	3.39					

Station 5225; June 12-13; latitude 43°37′ N., longitude 47°23′ W.; depth 3,932 meters; dynamic height 971.161

Observed values			Scaled values			
Depth, meters	Temperature, ° C.	Salinity, °/oo	Depth, meters	Temperature, ° C.	Salinity, °/oo	σ_t
0	10.26	32.98	0	10.26	32.98	25.36
25	11.69	34.16	25	11.69	34.16	26.02
50	11.84	35.18	50	11.84	35.18	26.78
74	13.12	35.53	75	13.10	35.53	26.80
99	12.47	35.40	100	12.40	35.40	26.84
149	11.42	35.26	150	11.40	35.26	26.93
198	9.82	35.10	200	9.80	35.10	27.08
297	6.40	34.73	300	6.75	34.78	27.30
302	7.03	34.83	(400)	5.50	34.81	27.49
			(600)	4.25	34.87	27.68
			(800)	3.95	34.87	27.71
			(1,000)	3.85	34.88	27.72

Station 5226; June 13; latitude 43°27′ N., longitude 46°44′ W.; depth 4,298 meters; dynamic height 971.299

Observed values			Scaled values			
Depth, meters	Temperature, ° C.	Salinity, °/oo	Depth, meters	Temperature, ° C.	Salinity, °/oo	σ_t
0	14.32	34.13	0	14.32	34.13	25.46
25	15.23	35.11	25	15.23	35.11	26.02
49	15.55	35.46	50	15.55	35.47	26.22
74	14.95	35.68	75	14.90	35.68	26.53
98	14.55	35.79	100	14.50	35.79	26.70
147	13.63	35.66	150	13.60	35.65	26.79
197	12.80	35.55	200	12.80	35.54	26.87
295	10.95	35.35	300	10.95	35.35	27.08
315	*10.68	35.33	400	8.85	35.14	27.27
500	6.84	34.96	600	5.75	34.95	27.56
688	5.13	34.95	800	4.60	34.93	27.68
868	4.36	34.92	1,000	4.15	34.92	27.73
1,337	3.76	34.93				

Station 5227; June 13; latitude 43°17′ N., longitude 46°06′ W.; depth 4,663 meters; dynamic height 971.295

Observed values			Scaled values			
Depth, meters	Temperature, ° C.	Salinity, °/oo	Depth, meters	Temperature, ° C.	Salinity, °/oo	σ_t
0	14.46	34.76	0	14.46	34.76	25.93
25	12.91	34.78	25	12.91	34.78	26.26
50	12.89	34.91	50	12.89	34.91	26.37
74	12.52	34.98	75	12.50	34.98	26.50
99	12.85	35.27	100	12.85	35.28	26.66
149	12.80	35.47	150	12.80	35.47	26.82
198	12.15	35.38	200	12.15	35.37	26.87
403	8.29	34.92	300	10.45	35.14	27.00
620	5.02	34.87	400	8.40	34.92	27.17
841	4.67	34.98	600	5.15	34.87	27.58
1,044	4.18	34.93	800	4.75	34.96	27.69
1,553	3.61	34.91	1,000	4.25	34.94	27.73

Station 5228; June 13; latitude 43°06′ N., longitude 45°25′ W.; depth 4,609 meters; dynamic height 971.310

Observed values			Scaled values			
Depth, meters	Temperature, ° C.	Salinity, °/oo	Depth, meters	Temperature, ° C.	Salinity, °/oo	σ_t
0	15.52	35.04	0	15.52	35.04	25.90
25	15.42	35.42	25	15.42	35.42	26.22
50	15.44	35.62	50	15.44	35.62	26.37
74	15.03	35.75	75	15.00	35.75	26.56
99	14.13	35.68	100	14.10	35.68	26.71
149	13.48	35.64	150	13.50	35.64	26.80
198	13.18	35.62	200	13.20	35.62	26.85
297	10.62	35.18	300	10.55	35.17	27.01
406	8.28	34.90	400	8.40	34.90	27.15
615	5.61	34.91	600	5.75	34.91	27.54
810	4.92	34.98	800	4.95	34.98	27.68
1,016	4.33	34.95	1,000	4.35	34.95	27.73
1,537	3.63	34.91				

Station 5229; June 13; latitude 42°45′ N., longitude 45°47′ W.; depth 4,572 meters; dynamic height 971.300

Observed values			Scaled values			
Depth, meters	Temperature, ° C.	Salinity, °/oo	Depth, meters	Temperature, ° C.	Salinity, °/oo	σ_t
0	16.30	34.87	0	16.30	34.87	25.59
25	16.50	35.28	25	16.50	35.28	25.87
50	15.76	35.41	50	15.76	35.41	26.14
74	15.51	35.50	75	15.50	35.50	26.26
99	14.73	35.59	100	14.70	35.59	26.51
149	13.66	35.58	150	13.65	35.58	26.73
198	12.77	35.54	200	12.75	35.54	26.88
297	11.29	35.44	300	11.20	35.43	27.09
381	8.87	35.14	400	8.45	35.13	27.32
595	6.34	35.07	600	6.30	35.07	27.59
800	4.88	34.97	800	4.90	34.97	27.69
1,001	4.25	34.94	1,000	4.25	34.94	27.73
1,504	3.60	34.90				

STATIONS OCCUPIED IN 1953—Continued

Station 5230; June 13; latitude 42°23.5′ N., longitude 46°09′ W.; depth 4,755 meters; dynamic height 971.252

Observed values			Scaled values			
Depth, meters	Temperature, ° C.	Salinity, °/oo	Depth, meters	Temperature, ° C.	Salinity, °/oo	σ_t
0	16.65	35.20	0	16.65	35.20	25.77
23	16.56	35.22	25	16.50	35.22	25.82
47	15.91	35.31	50	15.80	35.32	26.05
70	15.08	35.38	75	14.80	35.38	26.33
93	13.54	35.36	100	13.30	35.34	26.61
140	11.59	35.19	150	11.25	35.15	26.87
187	9.66	34.99	200	9.50	34.99	27.04
280	8.83	35.05	300	8.70	35.06	27.23
325	8.49	35.07	400	7.65	35.04	27.37
497	6.51	35.00	600	5.70	34.99	27.60
660	5.32	34.98	800	4.85	34.98	27.69
838	4.77	34.98	1,000	4.45	34.96	27.73
1,306	3.87	34.92				

Station 5231; June 14; latitude 42°37.5′ N., longitude 46°48′ W.; depth 3,932 meters; dynamic height 971.320

Observed values			Scaled values			
Depth, meters	Temperature, ° C.	Salinity, °/oo	Depth, meters	Temperature, ° C.	Salinity, °/oo	σ_t
0	16.11	35.18	0	16.11	35.18	25.88
24	16.29	35.55	25	16.25	35.55	26.13
49	15.56	35.66	50	15.50	35.66	26.39
73	14.77	35.73	75	14.75	35.73	26.60
98	14.53	35.75	100	14.50	35.75	26.68
147	13.55	35.63	150	13.50	35.63	26.79
195	13.05	35.56	200	13.00	35.56	26.84
293	11.71	35.46	300	11.60	35.45	27.03
366	10.63	35.34	400	10.05	35.29	27.18
569	7.36	35.11	600	6.95	35.09	27.52
752	5.48	35.02	800	5.25	35.01	27.68
946	4.71	34.99	1,000	4.60	34.98	27.72
1,440	3.85	34.90				

Station 5232; June 14; latitude 42°50.5′ N., longitude 47°22′ W.; depth 3,658 meters; dynamic height 971.226

Observed values			Scaled values			
Depth, meters	Temperature, ° C.	Salinity, °/oo	Depth, meters	Temperature, ° C.	Salinity, °/oo	σ_t
0	13.82	33.81	0	13.82	33.81	25.32
23	15.44	35.46	25	15.40	35.50	26.28
46	14.68	35.63	50	14.55	35.63	26.57
69	14.15	35.62	75	14.05	35.61	26.67
92	13.71	35.60	100	13.60	35.59	26.74
138	13.15	35.55	150	13.15	35.58	26.83
184	13.24	35.68	200	12.75	35.62	26.94
276	10.41	35.28	300	9.95	35.21	27.15
289	10.13	35.22	400	8.40	35.17	27.37
441	7.84	35.15	600	5.40	34.99	27.64
581	5.50	34.99	800	4.65	34.97	27.72
728	4.87	34.99	1,000	4.15	34.94	27.74
1,092	3.91	34.93				

Station 5233; June 14; latitude 43°05′ N., longitude 47°58′ W.; depth 3,566 meters; dynamic height 971.037

Observed values			Scaled values			
Depth, meters	Temperature, ° C.	Salinity, °/oo	Depth, meters	Temperature, ° C.	Salinity, °/oo	σ_t
0	10.24	33.03	0	10.24	33.03	25.40
20	9.65	33.13	25	8.60	33.15	25.75
40	5.86	33.33	50	6.10	33.80	26.62
60	6.35	34.29	75	6.55	34.43	27.05
80	6.55	34.46	100	6.40	34.53	27.15
120	6.18	34.59	150	6.25	34.69	27.29
159	6.24	34.72	200	5.85	34.78	27.41
239	5.46	34.83	300	5.20	34.88	27.57
400	4.81	34.96	400	4.80	34.96	27.69
			(600)	5.20	35.05	27.71
			(800)	3.70	34.87	27.74
			(1,000)	3.55	34.87	27.75

Station 5234; June 14; latitude 43°14′ N., longitude 48°23′ W.; depth 3,109 meters; dynamic height 971.020

Observed values			Scaled values			
Depth, meters	Temperature, ° C.	Salinity, °/oo	Depth, meters	Temperature, ° C.	Salinity, °/oo	σ_t
0	9.01	32.91	0	9.01	32.91	25.49
23	6.30	32.98	25	6.10	32.98	25.97
45	4.46	33.06	50	4.10	33.10	26.28
68	2.68	33.35	75	2.40	33.45	26.72
90	2.08	33.72	100	2.10	33.82	27.04
135	2.35	34.12	150	2.85	34.25	27.32
181	3.58	34.48	200	3.75	34.55	27.47
271	4.08	34.70	300	3.80	34.72	27.61
325	3.64	34.74	400	3.65	34.80	27.68
512	3.62	34.86	600	3.60	34.87	27.75
700	3.53	34.88	800	3.50	34.88	27.76
887	3.48	34.88	1,000	3.45	34.88	27.76
1,375	3.31	34.89				

Station 5235; June 14; latitude 42° 35.5′ N., longitude 48°44′ W.; depth 2,433 meters; dynamic height 971.017

Observed values			Scaled values			
Depth, meters	Temperature, ° C.	Salinity, °/oo	Depth, meters	Temperature, ° C.	Salinity, °/oo	σ_t
0	9.00	33.06	0	9.00	33.06	25.62
25	6.72	33.02	25	6.72	33.02	25.92
50	5.06	33.45	50	5.06	33.45	26.46
75	3.98	33.90	75	3.98	33.90	26.93
99	4.36	34.26	100	4.35	34.26	27.18
149	4.04	34.45	150	4.05	34.45	27.36
199	5.09	34.78	200	5.10	34.78	27.51
298	4.26	34.79	300	4.25	34.79	27.61
410	4.30	34.88	400	4.30	34.87	27.67
632	3.93	34.895	600	3.95	34.89	27.72
836	3.64	34.88	800	3.65	34.88	27.74
1,045	3.57	34.88	1,000	3.60	34.88	27.75
1,569	3.40	34.89				

Station 5236; June 15; latitude 42°14′ N., longitude 48°10′ W.; depth 3,402 meters; dynamic height 971.119

Observed values			Scaled values			
Depth, meters	Temperature, ° C.	Salinity, °/oo	Depth, meters	Temperature, ° C.	Salinity, °/oo	σ_t
0	12.71	33.34	0	12.71	33.34	25.18
24	11.35	34.43	25	11.30	34.46	26.32
48	10.77	34.89	50	10.80	34.95	26.79
72	11.87	35.24	75	11.90	35.25	26.82
96	11.76	35.26	100	11.75	35.25	26.85
144	9.41	34.87	150	9.40	34.89	26.98
192	9.65	35.10	200	9.50	35.09	27.12
288	7.03	34.89	300	6.40	34.83	27.38
261	7.09	34.82	400	4.60	34.80	27.58
403	4.58	34.80	600	4.60	34.94	27.69
537	4.66	34.93	800	4.35	34.94	27.72
689	4.51	34.95	1,000	4.00	34.92	27.75
1,102	3.84	34.91				

Station 5237; June 15; latitude 41°54′ N., longitude 47°35′ W.; depth 3,658 meters; dynamic height 971.262

Observed values			Scaled values			
Depth, meters	Temperature, ° C.	Salinity, °/oo	Depth, meters	Temperature, ° C.	Salinity, °/oo	σ_t
0	13.82	33.16	0	13.82	33.16	24.82
22	11.70	33.73	25	11.70	33.83	25.76
45	12.09	34.64	50	12.25	34.80	26.41
67	12.84	35.36	75	12.80	35.37	26.74
90	12.63	35.38	100	12.65	35.40	26.79
135	12.90	35.50	150	12.70	35.47	26.84
179	12.14	35.38	200	11.75	35.32	26.91
269	9.99	35.16	300	9.45	35.11	27.15
359	8.47	35.06	400	7.95	35.05	27.34
561	6.09	35.01	600	5.80	35.00	27.60
753	4.93	34.96	800	4.70	34.95	27.69
950	4.11	34.92	1,000	4.05	34.92	27.74
1,455	3.68	34.90				

Table of Oceanographic Data—Continued

STATIONS OCCUPIED IN 1953—Continued

Station 5238; June 15; latitude 41°42′ N., longitude 47°14′ W.; depth 4,298 meters; dynamic height 971.332

Observed values			Scaled values			
Depth, meters	Temperature, ° C.	Salinity, °/oo	Depth, meters	Temperature, ° C.	Salinity, °/oo	σ_t
0	15.46	33.74	0	15.46	33.74	24.82
24	14.79	34.91	25	14.75	34.92	25.99
48	14.40	35.28	50	14.40	35.35	26.39
71	15.20	35.80	75	15.10	35.80	26.58
95	14.10	35.62	100	14.05	35.63	26.68
143	14.05	35.72	150	13.90	35.70	26.76
191	13.13	35.56	200	13.00	35.55	26.84
286	12.01	35.50	300	11.75	35.47	27.02
392	9.88	35.26	400	9.75	35.25	27.20
605	7.02	35.14	600	7.10	35.14	27.53
803	4.48	34.89	800	4.50	34.89	27.66
1,008	4.31	34.95	1,000	4.30	34.95	27.73
1,521	3.67	34.91				

Station 5239; June 15; latitude 41°16.5′ N., longitude 48°12′ W.; depth 3,731 meters; dynamic height 971.012

Observed values			Scaled values			
Depth, meters	Temperature, ° C.	Salinity, °/oo	Depth, meters	Temperature, ° C.	Salinity, °/oo	σ_t
0	14.09	32.92	0	14.09	32.92	24.57
25	4.33	33.40	25	4.33	33.40	26.60
51	5.10	34.07	50	5.00	34.04	26.93
76	7.32	34.62	75	7.25	34.60	27.09
101	8.00	34.88	100	8.00	34.88	27.20
152	6.29	34.76	150	6.35	34.76	27.34
203	4.81	34.69	200	4.85	34.69	27.47
304	6.10	35.04	300	6.10	35.03	27.58
424	5.41	35.02	400	5.55	35.02	27.65
649	4.58	35.00	600	4.75	35.00	27.72
855	4.04	34.93	800	4.15	34.95	27.75
1,066	3.51	34.87	1,000	3.60	34.88	27.75
1,586	3.60	34.94				

Station 5240; June 15; latitude 41°46′ N., longitude 48°41′ W.; depth 3,475 meters; dynamic height 971.085

Observed values			Scaled values			
Depth, meters	Temperature, ° C.	Salinity, °/oo	Depth, meters	Temperature, ° C.	Salinity, °/oo	σ_t
0	14.30	32.81	0	14.30	32.81	24.45
23	8.80	33.18	25	8.60	33.19	25.78
47	7.15	33.25	50	6.60	33.27	26.13
70	3.32	33.51	75	3.60	33.61	26.75
93	5.45	34.14	100	5.35	34.20	27.02
140	4.79	34.42	150	4.60	34.41	27.27
186	3.89	34.38	200	4.00	34.45	27.37
279	5.29	34.86	300	5.70	34.96	27.58
347	6.61	35.15	400	6.10	35.09	27.63
538	4.67	34.95	600	4.35	34.93	27.71
719	4.08	34.92	800	4.15	34.93	27.73
909	4.18	34.96	1,000	4.05	34.95	27.76
1,401	3.47	34.88				

Station 5241; June 16; latitude 42°13.5′ N.; longitude 49°10′ W.; depth 2,853 meters; dynamic height 971.025

Observed values			Scaled values			
Depth, meters	Temperature, ° C.	Salinity, °/oo	Depth, meters	Temperature, ° C.	Salinity, °/oo	σ_t
0	10.08	32.66	0	10.08	32.66	25.13
23	2.60	32.90	25	2.50	32.92	26.29
46	1.56	33.30	50	1.70	33.39	26.73
70	3.47	33.86	75	3.60	33.95	27.01
93	4.32	34.26	100	4.70	34.36	27.22
139	7.47	34.96	150	7.20	34.93	27.35
185	6.13	34.82	200	5.75	34.79	27.44
278	4.39	34.74	300	4.60	34.79	27.57
352	5.09	34.94	400	4.95	34.95	27.66
544	4.58	34.96	600	4.40	34.94	27.71
722	4.07	34.91	800	3.95	34.89	27.72
913	3.74	34.88	1,000	3.65	34.88	27.74
1,410	3.45	34.88				

Station 5242; June 16; latitude 41°15′ N., longitude 49°58′ W.; depth 3,036 meters; dynamic height 971.242

Observed values			Scaled values			
Depth, meters	Temperature, ° C.	Salinity, °/oo	Depth, meters	Temperature, ° C.	Salinity, °/oo	σ_t
0	19.66	35.35	0	19.66	35.35	25.13
25	17.29	35.50	25	17.29	35.50	25.85
48	16.20	35.58	50	16.15	35.59	26.18
73	15.32	35.76	75	15.20	35.76	26.53
97	14.18	35.65	100	14.10	35.64	26.68
146	13.22	35.55	150	13.20	35.55	26.80
195	13.11	35.65	200	13.00	35.65	26.91
292	10.13	35.40	300	10.00	35.37	27.26
362	8.83	35.14	400	8.15	35.10	27.35
507	6.24	35.00	600	4.90	34.92	27.65
624	4.67	34.91	800	4.15	34.91	27.72
773	4.18	34.91	1,000	3.85	34.90	27.74
1,160	3.65	34.90				

Station 5243; June 16; latitude 41°27′ N., longitude 50°11′ W.; depth 3,566 meters; dynamic height 971.161

Observed values			Scaled values			
Depth, meters	Temperature, ° C.	Salinity, °/oo	Depth, meters	Temperature, ° C.	Salinity, °/oo	σ_t
0	14.12	33.28	0	14.12	33.28	24.84
27	11.91	34.42	25	11.95	34.32	26.09
53	11.84	34.93	50	11.85	34.89	26.55
80	11.64	35.13	75	11.70	35.12	26.76
106	11.07	35.05	100	11.20	35.06	26.81
160	11.33	35.27	150	11.30	35.23	26.92
212	9.19	35.02	200	9.55	35.07	27.10
318	7.66	35.01	300	8.00	35.01	27.30
500	4.46	34.86	400	6.25	34.95	27.50
713	4.59	34.96	600	4.50	34.91	27.68
908	4.13	34.95	800	4.35	34.96	27.74
1,112	3.93	34.95	1,000	4.00	34.94	27.76
1,621	3.67	34.94				

Station 5244; June 16; latitude 42°06′ N., longitude 50°04′ W.; depth 3,109 meters; dyanmic height 971.039

Observed values			Scaled values			
Depth, meters	Temperature, ° C.	Salinity, °/oo	Depth, meters	Temperature, ° C.	Salinity, °/oo	σ_t
0	11.83	32.75	0	11.83	32.75	24.90
24	3.41	32.94	25	3.15	32.95	26.26
49	1.20	33.18	50	1.20	33.21	26.63
73	5.38	34.14	75	5.40	34.14	26.97
97	4.65	34.12	100	4.60	34.13	27.05
146	4.09	34.32	150	4.05	34.33	27.27
195	3.50	34.38	200	3.50	34.39	27.37
292	3.90	34.68	300	4.00	34.70	27.57
387	5.10	34.98	400	5.10	34.98	27.66
598	4.52	34.94	600	4.50	34.94	27.70
795	4.11	34.95	800	4.10	34.95	27.76
996	3.80	34.91	1,000	3.80	34.91	27.76
1,504	3.44	34.90				

Station 5245; June 16; latitude 42°34′ N., longitude 49°58′ W.; depth 1,920 meters; dynamic height 970.987

Observed values			Scaled values			
Depth, meters	Temperature, ° C.	Salinity, °/oo	Depth, meters	Temperature, ° C.	Salinity, °/oo	σ_t
0	10.51	33.06	0	10.51	33.06	25.37
24	5.93	33.10	25	5.70	33.10	26.11
48	3.03	33.34	50	2.90	33.36	26.61
72	2.11	33.73	75	2.10	33.75	26.98
96	2.01	34.03	100	2.00	34.06	27.24
144	2.39	34.33	150	2.50	34.35	27.43
192	3.22	34.54	200	3.20	34.55	27.53
288	3.10	34.66	300	3.10	34.67	27.64
394	3.53	34.80	400	3.55	34.81	27.70
607	3.83	34.89	600	3.80	34.89	27.74
804	3.66	34.89	800	3.65	34.89	27.75
1,011	3.59	34.88	1,000	3.60	34.88	27.75
1,533	3.41	34.86				

Table of Oceanographic Data—Continued

STATIONS OCCUPIED IN 1953—Continued

Station 5246; June 17; latitude 42°54′ N., longitude 49°54′ W.; depth 448 meters; dynamic height 971.044

Observed values			Scaled values			
Depth, meters	Temperature, ° C.	Salinity, ‰	Depth, meters	Temperature, ° C.	Salinity, ‰	σ_t
0	8.32	32.50	0	8.32	32.50	25.28
25	3.64	33.01	25	3.64	33.01	26.26
50	0.74	33.50	50	0.74	33.50	26.88
75	3.85	34.13	75	3.85	34.13	27.13
100	7.64	34.74	100	7.64	34.74	27.14
150	6.18	34.66	150	6.18	34.66	27.28
199	6.36	34.76	200	6.35	34.76	27.34
299	4.22	34.63	300	4.20	34.63	27.49

Station 5247: June 17; latitude 43°05′ N., longitude 49°52′ W.; depth 75 meters; dynamic height 971.063

Observed values			Scaled values			
Depth, meters	Temperature, ° C.	Salinity, ‰	Depth, meters	Temperature, ° C.	Salinity, ‰	σ_t
0	9.38	32.44	0	9.38	32.44	25.07
26	5.39	33.04	25	5.40	32.99	26.06
51	7.48	34.32	50	7.45	34.20	26.74
77	5.31	34.17	75	5.50	34.18	26.98

Station 5248; June 17; latitude 43°30′ N., longitude 49°47′ W.; depth 55 meters; dynamic height 971.072

Observed values			Scaled values			
Depth, meters	Temperature, ° C.	Salinity, ‰	Depth, meters	Temperature, ° C.	Salinity, ‰	σ_t
0	9.01	32.42	0	9.01	32.42	25.12
26	3.80	32.67	25	4.10	32.66	25.94
47	1.57	33.07	50	1.45	33.12	26.53

Station 5249; July 11; latitude 50°00′ N., longitude 48°55′ W.; depth 1,920 meters; dynamic height 970.844.

Observed values			Scaled values			
Depth, meters	Temperature, ° C.	Salinity, ‰	Depth, meters	Temperature, ° C.	Salinity, ‰	σ_t
0	7.29	33.91	0	7.29	33.91	26.55
25	4.74	33.92	25	4.74	33.92	26.87
50	3.18	34.34	50	3.18	34.34	27.36
75	2.85	34.60	75	2.85	34.60	27.60
100	3.02	34.69	100	3.02	34.69	27.66
150	3.25	34.80	150	3.25	34.80	27.72
199	3.45	34.84	200	3.45	34.84	27.73
299	3.41	34.86	300	3.40	34.86	27.76
405	3.42	34.86	400	3.40	34.86	27.76
624	3.32	34.86	600	3.30	34.86	27.77
828	3.28	34.87	800	3.30	34.87	27.78
1,038	3.24	34.88	1,000	3.25	34.88	27.78
1,567	3.32	34.90				

Station 5250; July 11; latitude 49°48′ N., longitude 49°30′ W.; depth 1,371 meters; dynamic height 970.876.

Observed values			Scaled values			
Depth, meters	Temperature, ° C.	Salinity, ‰	Depth, meters	Temperature, ° C.	Salinity, ‰	σ_t
0	6.25	32.95	0	6.25	32.95	25.92
25	2.87	33.79	25	2.87	33.79	26.95
50	0.79	34.06	50	0.79	34.06	27.32
75	1.26	34.20	75	1.26	34.20	27.41
99	1.68	34.35	100	1.70	34.35	27.49
149	2.40	34.56	150	2.40	34.56	27.61
199	2.84	34.69	200	2.85	34.69	27.67
298	3.24	34.80	300	3.25	34.80	27.72
383	3.22	34.82	400	3.20	34.82	27.75
580	3.33	34.86	600	3.30	34.86	27.77
780	3.25	34.86	800	3.25	34.86	27.77
979	3.25	34.86	1,000	3.25	34.86	27.77
1,210	3.26	34.87				

Station 5251; July 11; latitude 49°41.5′ N., longitude 49°59′ W.; depth 659 meters; dynamic height 970.951.

Observed values			Scaled values			
Depth, meters	Temperature, ° C.	Salinity, ‰	Depth, meters	Temperature, ° C.	Salinity, ‰	σ_t
0	5.83	32.76	0	5.83	32.76	25.83
23	3.89	32.86	25	3.65	32.92	26.19
46	1.36	33.54	50	1.10	33.58	26.91
68	−0.13	33.75	75	0.00	33.80	27.16
91	0.36	33.92	100	0.50	33.97	27.27
137	1.14	34.16	150	1.35	34.22	27.42
183	1.78	34.36	200	2.00	34.43	27.53
274	2.76	34.66	300	2.90	34.70	27.68
327	3.00	34.74	400	3.15	34.78	27.71
520	3.23	34.82	(600)	3.25	34.84	27.75

Station 5252; July 11–12; latitude 49°30.5′ N., longitude 50°28′ W.; depth 329 meters; dynamic height 970.989.

Observed values			Scaled values			
Depth, meters	Temperature, ° C.	Salinity, ‰	Depth, meters	Temperature, ° C.	Salinity, ‰	σ_t
0	6.81	32.78	0	6.81	32.78	25.72
24	2.93	32.83	25	2.80	32.84	26.21
47	−1.24	33.24	50	−1.25	33.26	26.77
71	−1.09	33.41	75	−1.00	33.45	26.92
94	−0.50	33.63	100	−0.35	33.68	27.07
141	0.72	33.94	150	0.85	33.98	27.25
189	1.21	34.16	200	1.35	34.20	27.40
283	2.27	34.52	(300)	2.40	34.59	27.63

Station 5253; July 12; latitude 49°19.5′ N., longitude 50°58′ W.; depth 327 meters; dynamic height 971.018.

Observed values			Scaled values			
Depth, meters	Temperature, ° C.	Salinity, ‰	Depth, meters	Temperature, ° C.	Salinity, ‰	σ_t
0	7.15	32.73	0	7.15	32.73	25.64
25	4.45	32.74	25	4.45	32.74	25.97
50	1.81	32.86	50	1.81	32.86	26.29
75	−1.16	33.29	75	−1.16	33.29	26.79
100	−0.79	33.52	100	−0.79	33.52	26.97
150	0.35	33.90	150	0.35	33.90	27.22
199	1.20	34.19	200	1.25	34.19	27.40
299	2.46	34.52	300	2.50	34.52	27.57

Station 5254; July 12; latitude 49°11′ N., longitude 51°22′ W.; depth 333 meters; dynamic height 971.042.

Observed values			Scaled values			
Depth, meters	Temperature, ° C.	Salinity, ‰	Depth, meters	Temperature, ° C.	Salinity, ‰	σ_t
0	7.16	32.51	0	7.16	32.51	25.46
25	4.63	32.72	25	4.63	32.72	25.93
50	1.81	32.85	50	1.81	32.85	26.28
75	−1.23	33.21	75	−1.23	33.21	26.73
99	−0.92	33.41	100	−0.90	33.42	26.90
149	0.12	33.74	150	0.15	33.75	27.11
199	0.87	34.02	200	0.90	34.02	27.29
298	2.10	34.45	300	2.15	34.46	27.55

Station 5255; July 12; latitude 49°06′ N., longitude 51°42′ W.; depth 274 meters; dynamic height 971.078.

Observed values			Scaled values			
Depth, meters	Temperature, ° C.	Salinity, ‰	Depth, meters	Temperature, ° C.	Salinity, ‰	σ_t
0	8.28	32.31	0	8.28	32.31	25.15
25	1.96	32.39	25	1.96	32.39	25.91
50	−1.41	32.89	50	−1.41	32.89	26.47
75	−1.62	33.06	75	−1.62	33.06	26.62
100	−1.50	33.16	100	−1.50	33.16	26.69
151	−1.01	33.36	150	−1.00	33.36	26.84
201	−0.37	33.61	200	−0.40	33.61	27.03
256	1.69	34.27				

STATIONS OCCUPIED IN 1953—Continued

Observed values			Scaled values			
Depth, meters	Temperature, ° C.	Salinity, °/oo	Depth, meters	Temperature, ° C.	Salinity, °/oo	σ_t
Station 5256; July 12; latitude 49°04′ N., longitude 51°56′ W.; depth 298 meters; dynamic height 971.094						
0	8.61	32.18	0	8.61	32.18	24.99
24	3.14	32.48	25	2.75	32.50	25.93
48	−1.04	32.94	50	−1.15	32.96	26.52
71	−1.64	33.06	75	−1.65	33.07	26.63
95	−1.64	33.11	100	−1.65	33.12	26.67
143	−1.54	33.21	150	−1.50	33.23	26.75
190	−0.98	33.44	200	−0.75	33.50	26.95
271	1.27	34.15				
Station 5257; July 12; latitude 48°58.5′ N., longitude 52°13′ W.; depth 292 meters; dynamic height 971.091.						
0	8.83	32.27	0	8.83	32.27	25.03
25	4.03	32.41	25	4.03	32.41	25.75
49	−0.12	32.82	50	−0.15	32.83	26.39
74	−1.65	33.07	75	−1.65	33.07	26.63
99	−1.60	33.14	100	−1.60	33.14	26.68
148	−1.22	33.33	150	−1.20	33.33	26.83
197	−0.67	33.58	200	−0.60	33.59	27.01
266	1.45	34.22				
Station 5258; July 12; latitude 48°54′ N., longitude 52°34′ W.; depth 224 meters; dynamic height 971.112.						
0	9.78	32.18	0	9.78	32.18	24.80
25	3.91	32.53	25	3.91	32.53	25.86
50	1.88	32.67	50	1.88	32.67	26.14
74	−1.08	32.97	75	−1.15	32.98	26.54
99	−1.53	33.14	100	−1.55	33.15	26.69
149	−1.19	33.32	150	−1.20	33.32	26.82
198	−1.03	33.37	200	−1.00	33.37	26.85
Station 5259; July 12; latitude 48°46′ N., longitude 52°45′ W.; depth 169 meters; dynamic height 971.132.						
0	11.33	31.36	0	11.33	31.36	23.92
25	3.76	32.42	25	3.76	32.42	25.78
49	0.54	32.70	50	0.45	32.70	26.25
74	−1.48	32.97	75	−1.50	32.98	26.55
99	−1.61	33.10	100	−1.60	33.10	26.65
148	−1.60	33.12	150	−1.60	33.12	26.67
Station 5260; July 12; latitude 48°43.5′ N., longitude 52°57′ W.; depth 100 meters; dynamic height 971.150						
0	12.09	31.09	0	12.09	31.09	23.57
27	1.90	32.35	25	2.65	32.26	25.75
53	0.11	32.60	50	0.25	32.58	26.17
80	−1.09	32.79	75	−0.90	32.75	26.35
			(100)	−1.60	32.91	26.50
Station 5261; July 12; latitude 48°37′ N., longitude 52°43′ W.; depth 272 meters; dynamic height 971.131						
0	10.76	31.50	0	10.76	31.50	24.12
24	3.49	32.34	25	3.20	32.35	25.78
48	−0.73	32.74	50	−0.85	32.75	26.34
72	−1.40	32.92	75	−1.45	32.94	26.52
96	−1.61	33.02	100	−1.60	33.03	26.59
145	−1.63	33.08	150	−1.65	33.09	26.64
193	−1.58	33.11	200	−1.55	33.11	26.66
Station 5262; July 12; latitude 48°32′ N., longitude 52°34′ W.; depth 222 meters; dynamic height 971.108						
0	10.27	31.48	0	10.27	31.48	24.19
23	3.77	32.45	25	3.40	32.50	25.87
46	0.26	32.84	50	−0.10	32,87	26.41
69	−1.28	32.96	75	−1.50	32.99	26.56
92	−1.67	33.06	100	−1.65	33.08	26.63
138	−1.62	33.14	150	−1.55	33.18	26.71
183	−1.28	33.31	200	−1.05	33.40	26.88
211	−0.85	33.46				
Station 5263; July 12–13; latitude 48°20′ N., longitude 52°06′ W.; depth 187 meters; dynamic height 971.101						
0	9.81	31.62	0	9.81	31.62	24.37
24	6.05	32.00	25	5.90	32.03	25.25
48	0.95	32.79	50	0.70	32.82	26.33
72	−1.33	33.10	75	−1.40	33.11	26.65
96	−1.57	33.19	100	−1.55	33.21	26.74
144	−0.77	33.42	150	−0.65	33.45	26.91
Station 5264; July 13; latitude 48°16′ N., longitude 51°55′ W.; depth 201 meters; dynamic height 971.096						
0	10.28	31.68	0	10.28	31.68	24.34
25	3.97	32.25	25	3.97	32.25	25.62
49	−1.45	33.01	50	−1.45	33.01	26.58
74	−1.59	33.08	75	−1.60	33.08	26.63
99	−1.63	33.13	100	−1.65	33.13	26.67
148	−1.25	33.30	150	−1.20	33.30	26.80
Station 5265; July 13; latitude 48°07′ N., longitude 51°32′ W.; depth 192 meters; dynamic height 971.092						
0	10.00	31.87	0	10.00	31.87	24.54
25	5.76	32.06	25	5.76	32.06	25.29
50	−0.74	32.97	50	−0.74	32.97	26.52
75	−1.61	33.16	75	−1.61	33.16	26.70
101	−1.46	33.17	100	−1.45	33.17	26.70
151	−0.35	33.59	150	−0.35	33.58	26.99
Station 5266; July 13; latitude 47°58′ N., longitude 51°09′ W.; depth 167 meters; dynamic height 971.045						
0	9.68	32.01	0	9.68	32.01	24.70
21	5.69	32.28	25	4.40	32.41	25.72
41	0.32	32.90	50	−0.95	33.06	26.60
62	−1.41	33.19	75	−1.30	33.27	26.78
82	−1.13	33.31	100	−0.55	33.47	26.92
119	0.07	33.68	(150)	1.15	34.05	27.29
Station 5267; July 13; latitude 47°51′ N., longitude 51°00′ W.; depth 121 meters; dynamic height 971.060						
0	9.56	31.94	0	9.56	31.94	24.66
25	5.43	32.26	25	5.43	32.26	25.48
50	−0.43	33.00	50	−0.43	33.00	26.54
76	−1.61	33.19	75	−1.60	33.19	26.72
101	−1.23	33.34	100	−1.25	33.34	26.84

Table of Oceanographic Data—Continued

STATIONS OCCUPIED IN 1953—Continued

Station 5268; July 13; latitude 47°43′ N., longitude 50°42′ W.; depth 117 meters; dynamic height—971.057

Observed values			Scaled values			
Depth, meters	Temperature, ° C.	Salinity, ‰	Depth, meters	Temperature, ° C.	Salinity, ‰	σ_t
0	10.09	31.87	0	10.09	31.87	24.52
25	3.63	32.21	25	3.63	32.21	25.63
49	−0.46	32.90	50	−0.50	32.91	26.46
74	−1.12	33.18	75	−1.10	33.19	26.71
98	−0.35	33.50	100	−0.25	33.54	26.96

Station 5269; July 13; latitude 47°34′ N., longitude 50°23′ W.; depth 114 meters; dynamic height 971.074

0	10.69	31.66	0	10.69	31.66	24.26
25	4.68	32.24	25	4.68	32.24	25.54
50	−0.73	32.79	50	−0.73	32.79	26.38
76	−0.89	33.11	75	−0.90	33.10	26.63
101	−0.55	33.36	100	−0.55	33.35	26.82

Station 5270; July 13; latitude 47°24′ N., longitude 49°58′ W.; depth 93 meters; dynamic height 971.092

0	10.87	31.80	0	10.87	31.80	24.33
25	6.16	32.09	25	6.16	32.09	25.26
50	2.76	32.46	50	2.76	32.46	25.90
75	−0.06	32.94	75	−0.06	32.94	26.47

Station 5271; July 13; latitude 47°45′ N., longitude 49°48′ W.; depth 115 meters; dynamic height 971.057

0	10.08	32.02	0	10.08	32.02	24.64
25	4.20	32.26	25	4.20	32.26	25.61
50	−0.15	32.83	50	−0.15	32.83	26.39
75	−0.42	33.28	75	−0.42	33.28	26.76
100	−0.28	33.42	100	−0.28	33.42	26.87

Station 5272; July 13; latitude 47°57.5′ N., longitude 49°42′ W.; depth 169 meters; dynamic height 971.055

0	9.76	32.10	0	9.76	32.10	24.75
25	3.77	32.44	25	3.77	32.44	25.80
50	0.83	32.86	50	0.83	32.86	26.36
75	−1.08	33.18	75	−1.08	33.18	26.70
101	−1.15	33.36	100	−1.15	33.36	26.85
151	0.33	33.80	150	0.30	33.79	27.13

Station 5273; July 13; latitude 48°12′ N., longitude 49°36′ W.; depth 220 meters; dynamic height 971.060

0	9.09	32.25	0	9.09	32.25	24.97
25	3.43	32.58	25	3.43	32.58	25.94
50	−1.47	33.01	50	−1.47	33.01	26.58
75	−1.62	33.14	75	−1.62	33.14	26.68
100	−1.31	33.27	100	−1.31	33.27	26.78
151	−0.74	33.51	150	−0.75	33.51	26.96
201	0.16	33.78	200	0.15	33.78	27.13

Station 5274; July 13-14; latitude 48°29.5′ N., longitude 49°25′ W.; depth 622 meters; dynamic height 971.013

Observed values			Scaled values			
Depth, meters	Temperature, ° C.	Salinity, ‰	Depth, meters	Temperature, ° C.	Salinity, ‰	σ_t
0	7.66	32.75	0	7.66	32.75	25.58
25	4.32	32.80	25	4.32	32.80	26.04
50	0.98	33.08	50	0.98	33.08	26.53
75	−0.26	33.38	75	−0.26	33.38	26.83
100	0.06	33.62	100	0.06	33.62	27.02
150	0.29	33.90	150	0.29	33.90	27.22
201	1.00	34.12	200	1.00	34.12	27.36
301	2.48	34.58	300	2.50	34.58	27.61
393	3.16	34.74	400	3.15	34.75	27.69
597	3.36	34.84	600	3.35	34.84	27.74

Station 5275; July 14; latitude 48°37′ N., longitude 49°27′ W.; depth 1,079 meters; dynamic height 971.003

0	8.22	32.70	0	8.22	32.70	25.45
25	3.92	32.78	25	3.92	32.78	26.06
50	−1.52	33.13	50	−1.52	33.13	26.67
75	−1.31	33.29	75	−1.31	33.29	26.79
100	−0.77	33.52	100	−0.77	33.52	26.97
150	0.79	34.02	150	0.79	34.02	27.29
200	1.68	34.31	200	1.68	34.31	27.46
300	2.45	34.58	300	2.45	34.58	27.61
424	3.03	34.76	400	2.95	34.73	27.69
644	3.37	34.85	600	3.35	34.84	27.74
846	3.35	34.875	800	3.35	34.87	27.77
998	3.28	34.87	1,000	3.30	34.87	27.78

Station 5276; July 14; latitude 49°04.5′ N., longitude 49°15′ W.; depth 1,646 meters; dynamic height 970.915

0	6.98	32.84	0	6.98	32.84	25.74
25	−0.51	33.40	25	−0.51	33.40	26.86
51	−0.10	33.74	50	−0.10	33.74	27.11
76	0.89	34.03	75	0.85	34.03	27.29
101	1.60	34.29	100	1.55	34.28	27.44
152	2.16	34.46	150	2.15	34.45	27.54
203	2.59	34.62	200	2.55	34.61	27.64
304	3.12	34.76	300	3.10	34.76	27.71
395	3.32	34.80	400	3.30	34.80	27.72
595	3.31	34.82	600	3.30	34.82	27.74
794	3.31	34.80	800	3.30	34.82	27.74
996	3.28	34.825	1,000	3.30	34.83	27.74
1,503	3.29	34.83				

Station 5277; July 14; latitude 49°33′ N., longitude 49°11′ W.; depth 1,609 meters; dynamic height 970.876

0	8.00	33.58	0	8.00	33.58	26.18
25	3.73	33.91	25	3.73	33.91	26.96
51	2.72	34.32	50	2.70	34.31	27.38
76	2.68	34.54	75	2.70	34.53	27.55
101	2.82	34.64	100	2.80	34.64	27.63
152	3.19	34.74	150	3.20	34.74	27.68
203	3.21	34.78	200	3.20	34.78	27.71
304	3.29	34.80	300	3.30	34.80	27.72
416	3.34	34.82	400	3.35	34.82	27.73
642	3.36	34.82	600	3.35	34.82	27.73
853	3.27	34.85	800	3.30	34.83	27.74
1,066	3.23	34.83	1,000	3.25	34.83	27.74
1,600	3.29	34.84				

Table of Oceanographic Data—Continued

STATIONS OCCUPIED IN 1953—Continued

Station 5278; July 14; latitude 49°59′ N., longitude 48°58′ W.; depth 1,829 meters; dynamic height 970.866

Observed values			Scaled values			
Depth, meters	Temperature, ° C.	Salinity, °/oo	Depth, meters	Temperature, ° C.	Salinity, °/oo	σ_t
0	9.07	33.70	0	9.07	33.70	26.10
25	6.21	33.99	25	6.21	33.99	26.75
50	3.39	34.37	50	3.39	34.37	27.37
75	2.90	34.65	75	2.90	34.65	27.64
100	3.03	34.74	100	3.08	34.74	27.69
150	3.25	34.79	150	3.25	34.79	27.71
201	3.33	-------	200	3.35	34.82	27.73
301	3.42	34.84	300	3.40	34.84	27.74
406	3.39	34.83	400	3.40	34.84	27.74
625	3.27	34.84	600	3.30	34.84	27.75
830	3.28	34.83	800	3.30	34.84	27.75
1,041	3 25	34.835	1,000	3.25	34.84	27.75
1,570	3.31	34.83				

Station 5279; July 16; latitude 53°43′ N., longitude 55°48′ W.; depth 112 meters; dynamic height 1454.972

Observed values			Scaled values			
Depth, meters	Temperature, ° C.	Salinity, °/oo	Depth, meters	Temperature, ° C.	Salinity, °/oo	σ_t
0	9.19	26.33	0	9.19	26.33	20.35
26	0.63	32.07	25	0.95	31.85	25.54
51	−0.25	32.37	50	−0.20	32.36	26.01
77	−0.81	32.50	75	−0.80	32.49	26.13
97	−1.00	32.55	100	−1.00	32.55	26.20

Station 5280; July 16; latitude 53°49.5 N., longitude 55°32′ W.; depth 218 meters; dynamic height 1454.881

Observed values			Scaled values			
Depth, meters	Temperature, ° C.	Salinity, °/oo	Depth, meters	Temperature, ° C.	Salinity, °/oo	σ_t
0	7.12	30.99	0	7.12	30.99	24.26
26	1.27	32.34	25	1.50	32.29	25.85
52	−1.12	32.71	50	−1.10	32.70	26.31
78	−1.19	32.90	75	−1.20	32.88	26.46
104	−1.20	33.02	100	−1.20	33.00	26.56
156	−1.14	33.26	150	−1.15	33.23	26.74
198	−0.79	33.56	200	−0.75	33.57	27.01

Station 5281; July 16; latitude 53°53′ N., longitude 55°26′ W.; depth 181 meters; dynamic height 1454.862

Observed values			Scaled values			
Depth, meters	Temperature, ° C.	Salinity, °/oo	Depth, meters	Temperature, ° C.	Salinity, °/oo	σ_t
0	7.12	31.08	0	7.12	31.08	24.34
25	0.57	32.33	25	0.57	32.33	25.94
51	−0.92	32.70	50	−0.95	32.69	26.30
76	−1.17	32.91	75	−1.15	32.91	26.48
101	−1.14	33.10	100	−1.15	33.10	26.64
152	−0.83	33.56	150	−0.85	33.54	26.98

Station 5282; July 16; latitude 54°03′ N., longitude 55°04′ W.; depth 161 meters; dynamic height 1454.842

Observed values			Scaled values			
Depth, meters	Temperature, ° C.	Salinity, °/oo	Depth, meters	Temperature, ° C.	Salinity, °/oo	σ_t
0	5.96	31.95	0	5.96	31.95	25.17
26	1.03	32.44	25	1.25	32.42	25.98
51	−1.21	32.88	50	−1.20	32.86	26.45
77	−1.15	33.04	75	−1.15	33.03	26.58
103	−1.14	33.22	100	−1.15	33.20	26.72
144	−1.00	33.46	150	−1.00	33.49	26.95

Station 5283; July 16; latitude 54°14′ N., longitude 54°56′ W.; depth 174 meters; dynamic height 1454.850

Observed values			Scaled values			
Depth, meters	Temperature, ° C.	Salinity, °/oo	Depth, meters	Temperature, ° C.	Salinity, °/oo	σ_t
0	5.99	32.04	0	5.99	32.04	25.24
25	2.68	32.18	25	2.68	32.18	25.68
51	−0.56	32.82	50	−0.50	32.81	26.39
76	−1.17	32.99	75	−1.15	32.98	26.54
101	−1.15	33.19	100	−1.15	33.19	26.71
152	−0.88	33.52	150	−0.90	33.51	26.97

Station 5284; July 16; latitude 54°31′ N., longitude 54°24′ W.; depth 225 meters; dynamic height 1454.810

Observed values			Scaled values			
Depth, meters	Temperature, ° C.	Salinity, °/oo	Depth, meters	Temperature, ° C.	Salinity, °/oo	σ_t
0	4.98	31.88	0	4.98	31.88	25.23
25	−0.69	32.72	25	−0.69	32.72	26.32
50	−1.00	33.03	50	−1.00	33.03	26.57
76	−1.06	33.21	75	−1.05	33.21	26.73
101	−1.00	33.42	100	−1.00	33.42	26.90
151	−0.44	33.70	150	−0.45	33.70	27.10
202	0.17	33.92	200	0.15	33.91	27.24

Station 5285; July 16; latitude 54°48′ N., longitude 53°54′ W.; depth 327 meters; dynamic height 1454.730

Observed values			Scaled values			
Depth, meters	Temperature, ° C.	Salinity, °/oo	Depth, meters	Temperature, ° C.	Salinity, °/oo	σ_t
0	4.72	31.61	0	4.72	31.61	25.04
25	0.67	33.24	25	0.67	33.24	26.67
50	0.03	33.73	50	0.03	33.73	27.10
75	0.48	33.96	75	0.48	33.96	27.26
101	0.76	34.04	100	0.75	34.04	27.31
151	2.05	34.40	150	2.05	34.40	27.51
201	2.29	34.49	200	2.30	34.49	27.56
302	3.10	34.72	300	3.10	34.72	27.68

Station 5286; July 16; latitude 54°53′ N., longitude 53°40′ W.; depth 631 meters; dynamic height 1454.702

Observed values			Scaled values			
Depth, meters	Temperature, ° C.	Salinity, °/oo	Depth, meters	Temperature, ° C.	Salinity, °/oo	σ_t
0	4.27	32.44	0	4.27	32.44	25.75
25	0.53	33.77	25	0.53	33.77	27.11
50	0.87	33.97	50	0.87	33.97	27.25
75	1.66	34.18	75	1.66	34.18	27.36
100	1.84	34.28	100	1.84	34.28	27.42
150	2.85	34.48	150	2.85	34.48	27.50
201	3.02	34.60	200	3.00	34.60	27.59
301	3.25	34.72	300	3.25	34.72	27.66
393	3.35	34.77	400	3.35	34.77	27.69
595	3.39	34.80	600	3.40	34.80	27.71

Station 5287; July 16; latitude 54°59′ N., longitude 53°26′ W.; depth 1,582 meters; dynamic height 1454.625

Observed values			Scaled values			
Depth, meters	Temperature, ° C.	Salinity, °/oo	Depth, meters	Temperature, ° C.	Salinity, °/oo	σ_t
0	5.30	33.92	0	5.30	33.92	26.81
25	5.83	34.37	25	5.83	34.37	27.10
51	4.34	34.55	50	4.40	34.55	27.41
76	3.29	34.61	75	3.30	34.61	27.57
102	3.31	34.67	100	3.30	34.66	27.61
153	3.42	34.75	150	3,40	34.74	27.66
204	3.45	34.80	200	3.45	34.79	27.69
306	3.51	34.85	300	3.50	34.85	27.74
369	3.47	34.86	400	3.45	34.86	27.75
590	3.39	34.86	600	3.40	34.86	27.76
798	3.34	34.86	800	3.35	34.86	27.76
1,010	3.32	34.86	1,000	3.30	34.86	27.77
1,542	3.29	34.86	1,500	3.30	34.86	27.77

Table of Oceanographic Data—Continued

STATIONS OCCUPIED IN 1953—Continued

Station 5288; July 16; latitude 55°04′ N., longitude 53°17′ W.; depth 2,195 meters; dynamic height 1454.607

Observed values			Scaled values			
Depth, meters	Temperature, ° C.	Salinity, ‰	Depth, meters	Temperature, ° C.	Salinity, ‰	σ_t
0	7.58	34.38	0	7.58	34.38	26.86
25	5.54	34.56	25	5.54	34.56	27.28
50	3.88	34.72	50	3.88	34.72	27.60
74	3.62	34.74	75	3.60	34.74	27.64
99	3.53	34.80	100	3.55	34.80	27.69
149	3.63	34.84	150	3.65	34.84	27.71
198	3.58	34.85	200	3.60	34.85	27.73
297	3.49	34.86	300	3.50	34.86	27.75
382	3.44	34.85	400	3.45	34.86	27.75
597	3.37	34.86	600	3.35	34.86	27.76
812	3.36	34.86	800	3.35	34.86	27.76
1,031	3.34	-------	1,000	3.35	34.86	27.76
1,495	3.31	34.88	1,500	3.30	34.88	27.78
1,963	3.09	34.87	2,000	3.10	34.87	27.80

Station 5289; July 17; latitude 55°12.5′ N., longitude 52°56′ W.; depth 2,926 meters; dynamic height 1454.606

Observed values			Scaled values			
Depth, meters	Temperature, ° C.	Salinity, ‰	Depth, meters	Temperature, ° C.	Salinity, ‰	σ_t
0	7.87	34.50	0	7.87	34.50	26.92
25	6.49	34.64	25	6.49	34.64	27.22
50	4.57	34.71	50	4.57	34.71	27.51
75	3.68	34.76	75	3.68	34.76	27.65
99	3.57	34.79	100	3.55	34.79	27.68
149	3.44	34.82	150	3.45	34.82	27.72
199	3.46	34.84	200	3.50	34.84	27.73
298	3.46	34.86	300	3.45	34.86	27.75
397	3.44	34.86	400	3.45	34.86	27.75
621	3.34	34.86	600	3.35	34.86	27.76
859	3.33	34.88	800	3.35	34.88	27.77
1,074	3.33	34.88	1,000	3.35	34.88	27.77
1,551	3.35	34.88	1,500	3.35	34.88	27.77
2,029	3.18	34.91	2,000	3.20	34.91	27.82
2,431	2.78	34.90	2,500	2.65	34.90	27.86
2,730	2.01	34.88				

Station 5290; July 17; latitude 55°26′ N., longitude 52°30′ W.; depth 3,182 meters; dynamic height 1454.611

Observed values			Scaled values			
Depth, meters	Temperature, ° C.	Salinity, ‰	Depth, meters	Temperature, ° C.	Salinity, ‰	σ_t
0	7.69	34.22	0	7.69	34.22	26.73
27	6.08	34.32	25	6.20	34.31	27.00
53	3.54	34.56	50	3.75	34.53	27.45
80	3.19	34.68	75	3.25	34.66	27.61
106	3.18	34.74	100	3.20	34.73	27.67
161	3.35	34.81	150	3.30	34.80	27.72
214	3.26	34.82	200	3.30	34.82	27.74
320	3.29	34.83	300	3.35	34.84	27.74
308	3.42	34.86	400	3.35	34.86	27.76
497	3.36	34.86	600	3.30	34.86	27.77
706	3.24	34.86	800	3.25	34.86	27.77
940	3.25	34.86	1,000	3.25	34.86	27.77
1,374	3.23	34.86	1,500	3.25	34.86	27.77
1,836	3.36	-------	2,000	3.25	34.90	27.80
1,706	3.23	34.86	2,500	2.90	34.90	27.84
2,136	3.25	34.91	(3,000)	1.60	34.86	27.91
2,537	2.82	34.90				

Station 5291; July 17–18; latitude 55°58′ N., longitude 51°52′ W.; depth 3,365 meters; dynamic height 1454.621

Observed values			Scaled values			
Depth, meters	Temperature, ° C.	Salinity, ‰	Depth, meters	Temperature, ° C.	Salinity, ‰	σ_t
0	7.74	34.32	0	7.74	34.32	26.80
27	7.73	34.32	25	7.75	34.32	26.80
53	4.13	34.52	50	4.45	34.50	27.36
80	3.57	34.60	75	3.65	34.59	27.51
106	3.44	34.68	100	3.45	34.67	27.60
160	3.10	34.72	150	3.10	34.71	27.67
214	3.21	34.80	200	3.20	34.78	27.71
320	3.28	34.83	300	3.30	34.82	27.74
490	3.30	34.86	400	3.30	34.85	27.76
776	3.27	34.86	600	3.30	34.86	27.77
1,080	3.27	34.87	800	3.25	34.86	27.77
1,310	3.27	34.87	1,000	3.25	34.87	27.78
1,789	3.31	34.88	1,500	3.30	34.88	27.78
2,270	3.25	34.91	2,000	3.30	34.90	27.80
2,354	3.21	34.91	2,500	3.10	34.91	27.83
2,979	2.58	34.89	3,000	2.55	34.89	27.86
3,264	1.92	34.86				

Station 5292; July 18; latitude 56°29′ N., longitude 50°42′ W.; depth 3,548 meters; dynamic height 1454.655

Observed values			Scaled values			
Depth, meters	Temperature, ° C.	Salinity, ‰	Depth, meters	Temperature, ° C.	Salinity, ‰	σ_t
0	7.21	34.36	0	7.21	34.36	26.91
23	7.22	34.38	25	7.20	34.38	26.92
45	7.22	34.39	50	7.00	34.40	26.97
68	5.78	34.52	75	5.25	34.58	27.33
90	4.44	34.68	100	4.15	34.68	27.53
135	3.59	34.67	150	3.50	34.68	27.60
181	3.44	34.72	200	3.45	34.74	27.65
271	3.43	34.80	300	3.40	34.81	27.72
381	3.38	34.84	400	3.40	34.84	27.74
598	3.39	34.85	600	3.40	34.85	27.75
819	3.31	34.86	800	3.30	34.86	27.77
1,042	3.28	34.86	1,000	3.30	34.86	27.77
1,511	3.25	34.86	1,500	3.25	34.86	27.77
1,987	3.38	34.89	2,000	3.40	34.89	27.78
2,536	3.17	34.91	2,500	3.20	34.91	27.82
3,012	2.77	34.92	3,000	2.80	34.92	27.86
3,450	1.99	34.87	(3,500)	1.85	34.86	27.89

Station 5293; July 19; latitude 56°57.5′ N., longitude 49°33′ W.; depth 3,603 meters; dynamic height 1454.650

Observed values			Scaled values			
Depth, meters	Temperature, ° C.	Salinity, ‰	Depth, meters	Temperature, ° C.	Salinity, ‰	σ_t
0	7.00	34.44	0	7.00	34.44	27.00
25	7.01	34.44	25	7.01	34.44	27.00
50	6.48	34.49	50	6.48	34.49	27.10
75	3.90	34.66	75	3.90	34.66	27.55
100	3.60	34.67	100	3.60	34.67	27.59
148	3.31	34.74	150	3.30	34.74	27.67
198	3.35	34.78	200	3.40	34.78	27.69
298	3.60	34.86	300	3.60	34.86	27.74
2,436	3.17	34.88	400	3.60	34.86	27.74
2,859	2.83	34.89	600	3.40	34.835	27.74
3,325	2.28	34.88	800	3.30	34.83	27.74
			1,000	3.25	34.835	27.75
			1,500	3.25	34.85	27.76
			2,000	3.20	34.87	27.79
			2,500	3.15	34.88	27.79
			3,000	2.70	34.91	27.86
			(3,500)	1.95	34.86	27.89

STATIONS OCCUPIED IN 1953—Continued

Station 5294; July 19; latitude 57°30′ N., longitude 48°23′ W.; depth 3,402 meters; dynamic height 1454.642

Observed values			Scaled values			
Depth, meters	Temperature ° C.	Salinity, ‰	Depth, meters	Temperature ° C.	Salinity, ‰	σ_t
0	6.50	34.60	0	6.50	34.60	27.19
24	6.33	34.60	25	6.30	34.60	27.22
47	6.30	34.60	50	6.30	34.60	27.22
71	5.18	34.67	75	4.90	34.68	27.45
94	3.81	34.72	100	3.80	34.73	27.61
142	3.73	34.78	150	3.75	34.78	27.65
189	3.81	--------	200	3.80	34.80	27.67
283	3.48	34.82	300	3.50	34.83	27.72
321	3.50	34.84	400	3.45	34.84	27.73
499	3.35	34.84	600	3.65	34.86	27.73
685	3.81	34.87	800	3.45	34.84	27.73
874	3.27	34.83	1,000	3.25	34.83	27.74
1,328	3.23	34.83	1,500	3.25	34.84	27.75
1,837	3.27	34.86	2,000	3.30	34.88	27.78
1,922	3.41	34.89	2,500	3.05	34.90	27.82
2,363	3.13	34.90	(3,000)	2.60	34.90	27.86
2,770	2.86	34.91				

Station 5295; July 19; latitude 58°05′ N., longitude 47°14′ W.; depth 3,237 meters; dynamic height 1454.634

Observed values			Scaled values			
Depth, meters	Temperature ° C.	Salinity, ‰	Depth, meters	Temperature ° C.	Salinity, ‰	σ_t
0	6.61	34.57	0	6.61	34.57	27.16
27	6.30	34.56	25	6.30	34.56	27.19
53	5.05	34.74	50	5.20	34.73	27.45
80	4.38	34.77	75	4.45	34.76	27.57
106	3.93	34.80	100	4.00	34.79	27.64
160	4.01	34.84	150	4.00	34.83	27.67
213	4.08	34.86	200	4.10	34.85	27.68
319	3.78	34.86	300	3.85	34.86	27.71
423	3.60	34.87	400	3.60	34.87	27.75
647	3.50	34.855	600	3.50	34.86	27.75
875	3.39	34.845	800	3.40	34.85	27.75
1,103	3.32	34.84	1,000	3.35	34.845	27.75
1,582	3.41	34.87	1,500	3.40	34.86	27.76
2,060	3.22	34.905	2,000	3.25	34.90	27.80
2,615	2.76	34.90	2,500	2.90	34.90	27.84
3,063	1.66	34.86	3,000	1.90	34.87	27.90

Station 5296; July 20; latitude 58°39′ N., longitude 46°12′ W.; depth 2,698 meters; dynamic height 1454.626

Observed values			Scaled values			
Depth, meters	Temperature ° C.	Salinity, ‰	Depth, meters	Temperature ° C.	Salinity, ‰	σ_t
0	7.03	34.55	0	7.03	34.55	27.08
25	6.72	34.58	25	6.72	34.58	27.15
50	5.88	34.66	50	5.88	34.66	27.32
75	4.85	34.75	75	4.85	34.75	27.52
100	3.81	34.76	100	3.81	34.76	27.64
150	3.68	34.74	150	3.68	34.75	27.64
200	3.84	34.86	200	3.84	34.86	27.71
300	3.58	34.86	300	3.58	34.86	27.74
400	3.44	34.85	400	3.44	34.85	27.74
625	3.40	34.86	600	3.40	34.86	27.76
854	3.38	--------	800	3.35	34.86	27.76
1,080	3.41	34.87	1,000	3.40	34.87	27.77
1,581	3.41	34.88	1,500	3.40	34.88	27.77
2,038	2.92	34.87	2,000	3.00	34.87	27.81
2,517	2.27	34.88	2,500	2.30	34.88	27.87

Station 5297; July 20; latitude 58°59.5′ N., longitude 45°31′ W.; depth 2,469 meters; dynamic height 1454.646

Observed values			Scaled values			
Depth, meters	Temperature ° C.	Salinity, ‰	Depth, meters	Temperature ° C.	Salinity, ‰	σ_t
0	7.20	34.75	0	7.20	34.75	27.21
25	6.91	34.73	25	6.91	34.73	27.24
50	6.48	34.83	50	6.48	34.83	27.37
76	5.31	34.86	75	5.30	34.86	27.55
101	5.12	34.925	100	5.15	34.92	27.62
151	5.04	34.925	150	5.05	34.92	27.63
201	4.63	34.91	200	4.65	34.91	27.67
302	4.39	34.90	300	4.40	34.90	27.68
403	4.18	34.90	400	4.20	34.90	27.71
560	3.90	34.86	600	3.80	34.86	27.72
704	3.59	34.865	800	3.50	34.87	27.76
855	3.52	34.87	1,000	3.45	34.87	27.76
1,294	3.36	34.86	1,500	3.30	34.88	27.78
1,753	3.22	34.89	2,000	3.00	34.89	27.82
2,238	2.57	34.885				

Station 5298; July 20; latitude 59°13′ N., longitude 44°58′ W.; depth 1,975 meters; dynamic height 1454.733

Observed values			Scaled values			
Depth, meters	Temperature ° C.	Salinity, ‰	Depth, meters	Temperature ° C.	Salinity, ‰	σ_t
0	5.57	34.30	0	5.57	34.30	27.07
19	5.55	34.37	25	5.55	34.40	27.15
37	5.62	34.48	50	5.85	34.65	27.32
56	5.96	34.73	75	5.10	34.68	27.43
74	5.15	34.68	100	5.00	34.75	27.50
111	4.89	34.77	150	4.30	34.72	27.56
148	4.28	34.72	200	4.35	34.76	27.58
222	4.45	34.78	300	4.85	34.85	27.59
311	4.89	34.86	400	4.65	34.88	27.64
456	4.59	34.89	600	4.50	34.90	27.67
600	4.48	34.90	800	4.30	34.91	27.70
758	4.32	34.91	1,000	4.10	34.91	27.73
1,190	3.97	34.91	1,500	3.65	34.90	27.76
1,731	3.44	34.89				

Station 5299; July 20; latitude 59°19.5′ N., longitude 44°30′ W.; depth 1,188 meters; dynamic height 1454.763

Observed values			Scaled values			
Depth, meters	Temperature ° C.	Salinity, ‰	Depth, meters	Temperature ° C.	Salinity, ‰	σ_t
0	3.56	33.97	0	3.56	33.97	27.03
28	3.15	34.01	25	3.20	34.00	27.09
55	2.76	34.15	50	2.80	34.10	27.21
82	4.28	34.48	75	3.80	34.38	27.33
109	4.75	34.58	100	4.65	34.55	27.38
165	4.98	34.73	150	4.95	34.70	27.46
219	4.95	34.80	200	4.95	34.78	27.52
328	4.83	34.84	300	4.85	34.83	27.57
432	4.73	34.88	400	4.75	34.87	27.62
649	4.54	34.89	600	4.60	34.89	27.65
868	4.15	34.90	800	4.25	34.90	27.70
1,087	3.90	34.90	1,000	4.00	34.90	27.73

Station 5300; July 20; latitude 59°33′ N., longitude 44°07′ W.; depth 171 meters; dynamic height 1454.923

Observed values			Scaled values			
Depth, meters	Temperature ° C.	Salinity, ‰	Depth, meters	Temperature ° C.	Salinity, ‰	σ_t
0	0.19	31.80	0	0.19	31.80	25.54
29	−0.03	31.98	25	0.00	31.95	25.67
58	0.07	32.26	50	0.05	32.16	25.84
87	−0.16	32.87	75	−0.05	32.59	26.19
115	1.18	33.54	100	0.35	33.19	26.65
173	3.84	34.36	150	2.95	34.06	27.16

In the following table the potential density is represented by σ_{t_θ} which signifies 1,000 (density−1) at atmospheric pressure and potential temperature t_θ. The concentration of total phosphorus is given in microgram-atoms per liter.

TOTAL PHOSPHORUS DATA COLLECTED IN 1952

Station 4741; Apr. 29; latitude 47°16′ N., longitude 49°14′ W.; depth 91 meters

Depth meters	σ_{t_θ}	Total P µga/L
0	26. 30	0. 63
26	26. 34	0. 70
52	26. 37	0. 76
78	26. 71	0. 92

Station 4742; Apr. 29; latitude 47°22′ N., longitude 48°47′ W.; depth 139 meters

Depth meters	σ_{t_θ}	Total P µga/L
0	26. 34	0. 59
25	26. 40	0. 70
49	26. 41	0. 68
74	26. 70	0. 88
98	----------	0. 73
128	26. 93	1. 05

Station 4743; Apr. 29; latitude 47°28.5′ N., longitude 48°26′ W.; depth 174 meters

Depth meters	σ_{t_θ}	Total P µga/L
0	26. 37	0. 63
25	26. 42	0. 77
50	26. 48	0. 90
75	26. 73	1. 08
99	26. 84	1. 09
149	27. 10	1. 01

Station 4744; Apr. 29; latitude 47°34′ N., longitude 48°04′ W.; depth 218 meters

Depth meters	σ_{t_θ}	Total P µga/L
0	26. 43	0. 71
25	26. 51	0. 88
50	26. 68	1. 09
75	26. 76	0. 88
100	26. 87	0. 95
201	27. 33	1. 10

Station 4745; Apr. 29; latitude 47°41.5′ N., longitude 47°32′ W. depth 315 meters

Depth meters	σ_{t_θ}	Total P µga/L
0	26. 75	0. 91
25	26. 90	0. 91
49	26. 94	0. 91
74	27. 10	0. 96
99	27. 18	1. 09
148	27. 35	1. 08
197	27. 47	0. 94
286	27. 54	1. 08

Station 4746; Apr. 30; latitude 47°48.5′ N., longitude 46°54′ W.; depth 646 meters

Depth meters	σ_{t_θ}	Total P µga/L
0	27. 26	0. 92
22	27. 32	0. 99
43	27. 35	0. 93
65	27. 36	0. 93
86	27. 41	0. 94
129	27. 50	1. 06
173	27. 57	1. 07
259	27. 67	1. 17
350	27. 71	1. 09
532	27. 75	1. 08

Station 4747; Apr. 30; latitude 47°59.5′ N., longitude 46°21′ W.; depth 1,171 meters

Depth meters	σ_{t_θ}	Total P µga/L
0	27. 21	1. 22
25	27. 34	1. 27
50	27. 40	1. 36
76	27. 46	1. 39
100	27. 51	1. 44
151	27. 60	1. 40
201	27. 66	1. 77
301	27. 70	1. 56
330	27. 71	1. 44
507	27. 72	1. 68
692	27. 75	1. 41
896	27. 77	1. 67

Station 4748; Apr. 30; latitude 47°55.5′ N., longitude 46°10′ W. depth 1,060 meters

Depth meters	σ_{t_θ}	Total P µga/L
0	27. 13	0. 84
26	27. 20	0. 89
51	27. 23	0. 82
77	27. 47	0. 87
102	27. 55	0. 87
152	27. 62	0. 86
203	27. 66	0. 94
305	27. 71	0. 82
415	27. 72	0. 95
614	27. 74	0. 93
821	27. 77	1. 02
1,028	27. 79	1. 16

Station 4749; Apr. 30; latitude 47°47′ N., longitude 45°50′ W.; depth 436 meters

Depth meters	σ_{t_θ}	Total P µga/L
0	27. 02	0. 93
21	27. 10	0. 94
43	27. 26	0. 87
64	27. 32	1. 07
86	27. 42	1. 14
128	27. 53	1. 35
170	27. 59	1. 19
256	27. 67	1. 13
341	27. 70	1. 15

Station 4750; Apr. 30; latitude 47°43′ N., longitude 45°40′ W.; depth 306 meters

Depth meters	σ_{t_θ}	Total P µga/L
0	27. 03	0. 91
23	27. 18	0. 96
47	27. 26	1. 06
70	27. 31	1. 31
94	27. 38	1. 15
141	27. 46	1. 20
187	27. 55	1. 20
253	27. 67	1. 33

Station 4751; Apr. 30; latitude 47°29′ N., longitude 45°04′ W.; depth 224 meters

Depth meters	σ_{t_θ}	Total P µga/L
0	26. 72	0. 63
24	26. 73	0. 67
49	26. 74	0. 60
73	26. 74	0. 62
97	26. 89	0. 65
146	----------	1. 37
194	27. 48	1. 00

Station 4752; Apr. 30; latitude 47°22′ N., longitude 45°00′ W.; depth 188 meters

Depth meters	σ_{t_θ}	Total P µga/L
0	26. 70	0. 64
26	26. 73	0. 64
51	26. 73	0. 54
77	26. 75	0. 91
101	27. 04	0. 68
153	27. 40	1. 00

Station 4753; Apr. 30; latitude 47°23′ N., longitude 45°13′ W.; depth 220 meters

Depth meters	σ_{t_θ}	Total P µga/L
0	26. 73	0. 62
23	26. 73	0. 55
47	26. 72	0. 66
70	26. 73	0. 58
93	26. 79	0. 70
140	27. 31	0. 89
186	27. 50	0. 95

Station 4754; Apr. 30; latitude 47°22′ N., longitude 45°35′ W.; depth 265 meters

Depth meters	σ_{t_θ}	Total P µga/L
0	26. 73	0. 61
26	26. 73	0. 66
51	26. 74	0. 64
77	26. 75	0. 60
102	27. 20	0. 89
153	27. 46	0. 97
204	27. 59	1. 10

TOTAL PHOSPHORUS DATA COLLECTED IN 1952—Continued

Station 4755; Apr. 30; latitude 47°22′ N., longitude 45°53′ W.; depth 318 meters

Depth meters	$\sigma_{t\theta}$	Total P µga/L
0	26.73	0.53
25	26.75	0.65
49	27.04	0.78
74	27.08	0.77
98	27.20	1.70
147	27.36	1.04
197	27.59	0.97
295	27.69	1.02

Station 4756; Apr. 30; latitude 47°22′ N., longitude 46°14′ W.; depth 635 meters

Depth meters	$\sigma_{t\theta}$	Total P µga/L
0	27.02	0.72
25	27.04	0.76
50	27.20	0.88
75	27.30	0.95
100	27.36	1.12
150	27.47	1.13
200	27.54	1.14
300	27.67	1.15
376	27.69	0.88
570	----------	0.87

Station 4757; May 1; latitude 47°19′ N., longitude 47°06′ W.; depth 558 meters

Depth meters	$\sigma_{t\theta}$	Total P µga/L
0	26.52	1.36
25	26.81	1.32
51	27.01	1.40
77	27.17	1.23
103	27.25	1.32
153	27.44	1.35
204	27.54	1.44
307	27.63	1.67
411	27.69	1.43

Station 4758; May 1; latitude 47°16.5′ N., longitude 47°16′ W.; depth 330 meters

Depth meters	$\sigma_{t\theta}$	Total P µga/L
0	26.54	0.91
22	26.56	0.91
45	26.76	1.14
67	26.95	0.92
89	27.04	1.07
133	27.28	1.09
178	27.45	1.00
267	27.60	1.16

Station 4759; May 1; latitude 47°11.5′ N., longitude 47°32′ W.; depth 227 meters

Depth meters	$\sigma_{t\theta}$	Total P µga/L
0	26.36	0.73
25	26.52	0.84
51	26.68	0.94
76	26.83	0.95
101	26.93	1.07
152	27.14	0.95
203	27.32	1.14

Station 4760; May 1; latitude 47°05.5′ N., longitude 47°49′ W.; depth 174 meters

Depth meters	$\sigma_{t\theta}$	Total P µga/L
0	26.34	0.74
21	26.40	0.76
42	26.57	0.87
63	26.76	0.92
84	26.81	0.86
168	27.01	1.05

Station 4761; May 1; latitude 46°59′ N., longitude 48°10′ W.; depth 134 meters

Depth meters	$\sigma_{t\theta}$	Total P µga/L
0	26.31	0.65
30	26.39	0 98
58	26.46	1.36
88	26.76	1.02
116	26.93	1.04

Station 4762; May 1; latitude 46°48′ N., longitude 48°43′ W.; depth 102 meters

Depth meters	$\sigma_{t\theta}$	Total P µga/L
0	26.26	0.69
24	26.32	0.63
49	26.33	0.82
73	26.60	1.16

Station 4793; May 4; latitude 45°34.5′ N., longitude 47°52′ W.; depth 1,439 meters

Depth meters	$\sigma_{t\theta}$	Total P µga/L
24	26.83	0.90
48	27.07	1.06
72	27.30	0.96
96	27.43	1.32
144	27.51	1.26
192	27.59	1.26
992	27.76	1.17
1,341	27.77	1.14

Station 4794; May 4; latitude 45°20′ N., longitude 47°23′ W.; depth 2,509 meters

Depth meters	$\sigma_{t\theta}$	Total P µga/L
76	27.11	1.02
101	27.27	1.21
151	27.42	1.27
201	27.51	1.31
302	27.64	1.32
979	27.77	1.24
1,474	----------	1.14

Station 4795; May 4; latitude 45°24′ N., longitude 46°40′ W.; depth 3,011 meters

Depth meters	$\sigma_{t\theta}$	Total P µga/L
0	26.37	0.86
50	26.55	0.59
75	26.84	0.81
101	27.03	1.01
150	27.20	1.27
200	27.41	1.44
301	27.54	1.48
395	27.63	1.28
602	27.74	1.23
809	27.76	1.28
1,015	27.77	1.21
1,538	27.82	1.30

Station 4796; May 5; latitude 45°27′ N., longitude 46°00′ W., depth 3,402 meters

Depth meters	$\sigma_{t\theta}$	Total P µga/L
0	26.55	0.61
25	26.59	0.64
49	26.66	0.60
74	26.90	0.79
98	27.05	1.01
147	27.21	1.24
196	27.34	1.21
294	27.52	1.24
336	27.55	1.32
535	27.72	1.27
734	27.73	1.27
929	27.76	1.27
1,434	----------	1.34

Station 4797; May 5; latitude 45°30′ N., longitude 45°25′ W.; depth 3,658 meters

Depth meters	$\sigma_{t\theta}$	Total P µga/L
0	26.26	0.52
25	26.65	0.59
50	26.78	0.67
75	26.84	0.67
100	26.86	0.70
150	26.98	1.03
200	27.16	1.21
300	27.43	1.69
411	27.57	1.40
618	27.71	1.28
825	27.77	1.25
1,032	27.77	1.19
1,550	27.82	1.10

Station 4798; May 5; latitude 44°45.5′ N., longitude 45°23′ W.; depth 3,896 meters

Depth meters	$\sigma_{t\theta}$	Total P µga/L
0	26.62	0.49
26	26.70	0.48
53	26.71	0.49
79	26.73	0.58
105	26.73	0.55
157	26.78	0.67
209	26.86	0.75
314	27.13	1.26
474	27.45	1.45
646	27.65	1.29
825	27.73	1.50
1,306	27.78	1.15

Station 4799; May 5; latitude 44°18.5′ N., longitude 45°15′ W.; depth 4,115 meters

Depth meters	$\sigma_{t\theta}$	Total P µga/L
0	26.49	0.51
25	26.66	0.50
51	26.68	0.47
76	26.70	0.65
102	26.72	0.74
151	26.76	0.70
202	26.81	0.75
304	27.01	1.36
426	27.28	1.46
639	27.62	1.32
854	27.71	1.45
1,069	27.75	1.14
1,608	27.83	1.31

TOTAL PHOSPHORUS DATA COLLECTED IN 1952—Continued

Depth meters	$\sigma_{t\theta}$	Total P µga/L
Station 4,800; May 5; latitude 44°26.5′ N., longitude 45°54′ W.; depth 3,658 meters		
0	26.17	0.51
19	26.42	0.48
38	26.65	0.64
58	26.65	0.49
76	26.76	0.77
115	26.93	1.20
154	26.91	1.35
230	27.19	1.13
260	27.09	1.33
388	27.49	1.42
515	27.64	1.46
658	27.72	1.45
1,038	27.76	1.48
Station 4801; May 5; latitude 44°36.5′ N., longitude 46°40′ W.; depth 3,749 meters		
0	26.20	0.72
28	26.46	0.77
55	26.64	0.73
84	27.04	0.99
111	27.18	1.07
167	27.42	1.40
223	27.51	1.42
334	27.64	1.43
404	27.67	1.32
632	27.74	1.34
877	27.77	1.22
1,098	27.78	1.28
1,654	27.80	1.53
Station 4802; May 6; latitude 44°44′ N., longitude 47°18′ W.; depth 3,658 meters		
0	26.34	0.94
24	26.55	1.02
49	26.57	1.04
72	26.76	1.21
97	27.12	1.26
145	27.39	1.41
193	27.57	1.58
290	27.64	1.62
376	27.71	1.50
560	27.71	1.50
742	27.76	1.48
932	27.76	1.54
1,422	27.78	1.49
Station 4803; May 6; latitude 44°52.5′ N., longitude 48°04′ W.; depth 2 834 meters.		
0	26.56	0.94
24	26.82	1.41
49	27.03	1.33
73	27.25	1.21
98	27.39	1.49
146	27.46	1.35
195	27.57	1.38
293	27.66	1.44
389	27.71	1.42
584	27.74	1.66
778	27.76	1.42
991	27.78	1.35
1,560	27.80	1.66
Station 4804; May 6; latitude 44°56′ N., longitude 48°32′ W.; depth 1,518 meters		
0	26.62	0.74
24	26.71	0.78
49	27.21	1.66
97	27.45	1.48
146	27.50	1.41
195	27.60	1.55
292	27.67	1.58
338	27.71	1.73
513	27.74	1.50
690	27.77	1.55
880	27.78	1.58
1,385	27.79	1.64
Station 4805; May 6; latitude 44°57′ N., longitude 48°45′ W.; depth 1,371 meters		
0	26.55	0.80
27	26.80	1.10
52	26.97	1.46
79	27.04	1.00
104	27.10	0.93
157	27.29	0.98
210	27.46	1.09
314	27.58	1.01
442	27.70	1.07
658	27.74	0.97
871	27.75	1.18
1,092	----------	1.14
Station 4806; May 6; latitude 44°58.5′ N., longitude 48°59′ W.; depth 604 meters		
0	26.32	0.73
24	26.38	0.59
48	26.63	1.04
72	26.75	1.38
96	26.82	1.46
144	26.98	0.93
193	27.17	1.23
289	27.44	0.93
391	27.60	1.27
583	27.68	1.07
Station 4807; May 6; latitude 44°59.5′ N., longitude 49°08′ W.; depth 77 meters		
0	26.17	0.76
23	26.38	1.00
47	26.65	1.03
70	----------	1.24
Station 4808; May 6; latitude 44°59′ N., longitude 49°24′ W.; depth 70 meters		
0	26.20	0.61
25	26.22	0.70
50	26.43	1.41
Station 4809; May 6; latitude 44°16′ N., longitude 49°29′ W.; depth 53 meters		
0	26.17	0.72
26	26.42	1.10
46	26.46	1.43
Station 4810; May 7; latitude 44°14′ N., longitude 49°23′ W.; depth 93 meters		
0	26.26	0.72
25	26.46	1.08
51	26.54	1.00
76	26.72	0.93
Station 4811; May 7; latitude 44°13.5′ N., longitude 49°19′ W.; depth 201 meters		
0	26.25	0.71
25	26.44	0.68
49	26.52	0.99
74	26.70	0.94
98	26.81	0.95
147	27.04	0.86
Station 4812; May 7; latitude 44°12′ N., longitude 49°15′ W.; depth 713 meters		
0	26.28	0.73
25	26.54	0.94
51	26.73	1.07
76	26.92	0.97
101	26.98	0.99
152	27.10	0.93
203	27.13	0.99
304	27.38	0.97
399	27.58	1.06
593	27.71	0.97
Station 4813; May 7; latitude 44°10′ N., longitude 49°07′ W.; depth 1,582 meters		
0	26.27	0.66
25	26.56	0.97
50	26.77	1.07
75	26.92	0.96
99	27.04	1.02
149	27.10	1.03
199	27.22	1.06
298	27.44	1.02
404	27.62	1.00
600	27.71	1.24
792	27.74	1.12
990	27.76	1.17
1,484	27.77	1.16
Station 4814; May 7; latitude 44°07′ N., longitude 48°52′ W.; depth 2,615 meters		
0	26.27	0.59
24	26.56	0.95
48	26.77	1.08
72	26.93	1.08
96	27.02	0.96
144	27.14	1.01
193	27.36	1.14
289	27.53	1.12
368	27.65	1.30
554	27.71	1.25
741	27.75	1.27
934	27.77	1.22
1,429	27.79	1.14

Station 4815; May 7; latitude 43°58′ N., longitude 48°21′ W.; depth 3,475 meters

Depth meters	$\sigma_{t\theta}$	Total P µga/L
0	26.22	0.59
25	26.54	0.62
51	26.94	0.93
76	27.15	1.00
102	27.26	1.04
152	27.44	1.13
204	27.53	1.10
306	27.65	1.27
412	27.70	1.24
615	27.74	1.13
816	27.76	1.11
1,022	27.78	1.15
1,544	27.80	1.21

Station 4816; May 7; latitude 43°48′ N., longitude 47°43′ W.; depth 3,841 meters

Depth meters	$\sigma_{t\theta}$	Total P µga/L
0	26.13	0.54
22	26.71	0.60
43	26.78	0.58
65	26.83	0.69
87	26.84	0.65
130	26.85	0.67
173	27.12	1.13
260	27.35	1.33
296	27.40	1.36
451	27.61	1.33
610	27.71	1.27
777	27.75	1.26
1,219	27.77	1.21

Station 4817; May 7; latitude 43°36.5′ N., longitude 46°59′ W.; depth 4,490 meters

Depth meters	$\sigma_{t\theta}$	Total P µga/L
0	26.27	0.53
25	26.40	0.67
50	26.63	0.66
75	26.86	0.90
99	27.01	0.95
150	----------	0.85
200	27.26	1.37
299	27.45	1.40
302	27.47	1.42
499	27.65	1.27
698	27.73	1.18
903	27.75	1.38
1,433	27.77	1.41

Station 4818; May 8; latitude 43°28′ N., longitude 46°14′ W.; depth 4,572 meters

Depth meters	$\sigma_{t\theta}$	Total P µga/L
0	26.01	0.52
24	26.24	0.59
48	26.49	0.67
71	26.61	0.83
95	26.96	0.98
142	27.19	0.95
190	27.41	1.25
285	27.56	1.31
316	27.60	1.42
486	27.68	1.31
663	27.72	1.35
849	27.76	1.21
1,349	27.79	1.28

Station 4819; May 8; latitude 43°20.5′ N., longitude 45°33′ W.; depth 4,572 meters

Depth meters	$\sigma_{t\theta}$	Total P µga/L
0	26.30	0.43
28	26.30	0.39
56	26.39	0.41
84	26.67	0.67
111	26.74	0.68
167	----------	0.55
223	----------	0.94
334	27.33	1.39
400	27.45	1.42
584	27.65	1.12
756	27.72	1.25
954	27.76	1.22
1,467	27.80	1.25

Station 4820; May 8; latitude 42°52.5′ N., longitude 45°53′ W.; depth 4,663 meters

Depth meters	$\sigma_{t\theta}$	Total P µga/L
0	26.01	0.43
26	26.03	0.53
52	26.49	0.44
78	26.57	0.56
104	26.58	0.49
156	26.59	0.54
208	26.60	0.48
311	----------	0.86
415	26.73	1.17
625	27.24	2.27
836	27.56	2.04
1,046	27.70	1.86
1,572	27.78	1.79

Station 4821; May 8; latitude 42°28′ N., longitude 46°09′ W.; depth 4,572 meters

Depth meters	$\sigma_{t\theta}$	Total P µga/L
0	26.01	0.35
26	26.06	0.38
52	----------	0.36
78	26.42	0.36
103	26.46	0.38
156	26.53	0.51
207	26.64	0.57
310	26.78	0.68
421	26.96	0.97
630	27.32	1.49

Station 4822; May 8; latitude 42°47.5′ N., longitude 46°40′ W.; depth 4,207 meters

Depth meters	$\sigma_{t\theta}$	Total P µga/L
0	25.97	0.49
26	26.21	0.51
52	26.42	0.59
78	26.49	0.68
104	26.54	0.83
157	26.69	1.00
208	26.82	1.23
312	26.93	1.47
278	26.83	1.20
456	27.29	2.21
660	27.56	2.20
844	27.70	1.78
1,336	27.78	1.66

Station 4823; May 9; latitude 42°58.5′ N., longitude 47°21′ W.; depth 3,731 meters

Depth meters	$\sigma_{t\theta}$	Total P µga/L
0	26.24	0.47
26	26.24	0.39
51	26.47	0.39
77	26.66	0.59
103	26.75	0.73
153	26.83	0.83
205	26.90	0.79
308	27.18	1.50
365	27.26	1.51
549	27.56	1.41
737	27.71	1.31
937	27.75	1.29
1,462	27.78	1.18

Station 4824; May 9; latitude 43°09.5′ N., longitude 48°05′ W.; depth 3, 292 meters

Depth meters	$\sigma_{t\theta}$	Total P µga/L
0	25.90	0.49
27	26.75	0.65
53	26.84	0.73
80	26.89	0.82
105	27.05	1.09
159	27.22	0.84
212	27.37	1.40
317	27.57	1.08
404	27.63	1.25
606	27.72	1.26
811	27.76	1.28
1,017	27.76	1.25
1,540	27.81	1.29

Station 4825; May 9; latitude 43°20′ N., longitude 48°50′ W.; depth 1,920 meters

Depth meters	$\sigma_{t\theta}$	Total P µga/L
0	26.23	0.66
24	26.46	0.66
50	26.97	1.00
74	27.25	1.10
99	27.32	1.19
148	27.47	1.25
198	27.55	1.17
297	27.64	1.10
393	27.68	1.21
588	27.71	1.17
781	27.74	1.19
979	27.75	1.14
1,483	27.78	1.20

Station 4826; May 9; latitude 42°37.5′ N., longitude 49°01′ W.; depth 2,286 meters

Depth meters	$\sigma_{t\theta}$	Total P µga/L
0	26.22	0.54
24	26.57	0.78
49	26.85	0.93
73	27.12	1.00
98	27.19	0.92
145	27.34	1.04
194	27.49	1.09
292	27.59	1.17
353	27.63	1.26
529	27.69	1.64
703	27.72	1.13
889	27.74	1.27
1,370	27.77	1.24

TOTAL PHOSPHORUS DATA COLLECTED IN 1952—Continued

Station 4827; May 9; latitude 42°24.5′ N., longitude 48°33′ W.; depth 3,109 meters

Depth meters	$\sigma_{t\theta}$	Total P µga/L
0	25.68	0.80
27	26.79	0.79
53	27.00	1.39
81	27.11	1.28
107	27.16	1.24
161	27.26	1.33
215	27.35	1.42
322	27.56	1.50
257	27.47	1.41
408	27.67	1.40
576	27.72	1.26
755	27.76	1.34
1,265	27.75	1.28

Station 4828; May 10; latitude 41°59.5′ N., longitude 48°02′ W.; depth 3,658 meters

Depth meters	$\sigma_{t\theta}$	Total P µga/L
0	25.63	0.61
25	26.28	0.65
50	26.72	0.88
75	26.94	0.93
101	27.11	1.00
150	27.26	1.17
200	27.37	1.32
301	27.55	1.39
392	27.63	1.36
589	27.72	1.35
788	27.76	1.22
986	27.78	1.18
1,480	27.80	1.17

Station 4829; May 10; latitude 41°34.5′ N., longitude 47°14′ W.; depth 4,207 meters

Depth meters	$\sigma_{t\theta}$	Total P µga/L
0	25.95	0.62
25	26.54	0.70
50	26.65	0.86
75	26.71	1.12
99	26.78	0.79
149	26.86	0.91
199	27.00	1.07
298	27.19	1.65
284	27.16	1.71
443	27.52	1.68
612	27.68	1.53
787	27.73	1.50
1,265	27.78	1.39

Station 4830; May 10; latitude 40°59′ N., longitude 48°28′ W.; depth 3,011 meters

Depth meters	$\sigma_{t\theta}$	Total P µga/L
0	26.18	1.03
54	26.54	0.78
81	26.79	0.76
108	26.84	0.93
163	26.94	1.15
217	27.09	1.21
325	27.36	1.42
417	27.50	1.65
621	27.68	1.36
823	27.73	1.22
1,030	27.78	1.29
1,550	27.81	1.25

Station 4831; May 10; latitude 41°31′ N., longitude 48°54′ W.; depth 3,200 meters

Depth meters	$\sigma_{t\theta}$	Total P µga/L
0	25.54	0.52
27	26.38	0.69
53	26.73	1.06
80	26.98	1.07
105	27.18	1.09
159	27.36	1.23
212	27.48	1.40
317	27.60	1.31
402	27.65	1.38
599	27.73	1.34
795	27.77	1.26
998	27.77	1.22
1,511	27.79	1.22

Station 4832; May 11; latitude 42°00′ N., longitude 49°27′ W.; depth 3,011 meters

Depth meters	$\sigma_{t\theta}$	Total P µga/L
0	----------	0.52
23	26.14	0.81
45	26.88	0.89
68	26.97	0.94
89	27.13	1.05
134	27.26	1.24
179	27.35	1.31
268	27.53	1.41
305	27.55	1.39
515	27.68	1.32
722	27.74	1.35
930	27.77	1.09
1,452	27.79	1.05

Station 4833; May 11; latitude 40°59′ N., longitude 50°15′ W.; depth 3,603 meters

Depth meters	$\sigma_{t\theta}$	Total P µga/L
0	24.25	0.22
25	25.82	0.14
49	26.16	0.18
74	26.31	0.10
98	26.36	0.16
148	26.38	0.16
197	26.40	0.23
296	26.43	0.22
307	26.42	0.32
464	----------	0.78
624	27.10	1.34
782	27.47	1.59
1,180	27.77	1.28

Station 4834; May 11; latitude 41°30′ N., longitude 50°09′ W.; depth 3,779 meters

Depth meters	$\sigma_{t\theta}$	Total P µga/L
0	25.69	0.14
26	25.92	0.24
51	26.13	0.30
76	26.35	0.47
102	26.57	0.45
152	26.70	0.73
203	26.81	0.86
305	26.98	1.07
401	27.15	1.47
595	27.51	1.32
787	27.69	1.35
996	27.75	1.28
1,540	27.78	1.24

Station 4835; May 11; latitude 42°02′ N., longitude 50°13′ W.; depth 3,564 meters

Depth meters	$\sigma_{t\theta}$	Total P µga/L
0	25.65	0.12
23	26.35	0.66
46	26.54	0.98
69	26.89	1.00
92	27.01	1.04
137	27.19	1.14
182	27.35	1.29
274	27.55	1.39
345	27.57	1.40
527	27.67	1.35
716	27.72	1.31
907	27.76	1.24
1,402	27.78	1.24

Station 4836; May 11; latitude 42°25.5′ N., longitude 50°10′ W.; depth 1.929 meters

Depth meters	$\sigma_{t\theta}$	Total P µga/L
0	26.14	1.44
25	26.62	0.78
50	26.86	1.23
75	26.99	1.12
99	27.08	1.12
148	27.25	1.16
198	27.37	1.25
297	27.57	1.43
369	27.60	1.43
555	27.67	1.29
743	27.73	1.35
938	27.75	1.34
1,441	27.77	1.38

Station 4837; May 11–12; latitude 42°45.5′ N., longitude 50°09′ W.; depth 732 meters

Depth meters	$\sigma_{t\theta}$	Total P µga/L
0	26.27	0.51
25	26.39	0.60
49	26.59	0.67
74	26.70	1.01
98	26.80	1.07
146	27.01	1.03
196	27.17	1.08
294	27.38	1.05
375	27.47	1.15
576	27.71	1.11

Station 4838; May 12; latitude 42°49.5′ N., longitude 50°10′ W.; depth 287 meters

Depth meters	$\sigma_{t\theta}$	Total P µga/L
0	26.16	0.59
24	26.20	0.62
49	26.52	0.92
73	26.69	1.11
97	26.81	1.09
146	26.96	1.00
194	27.18	1.15
243	27.26	1.20

Station 4839; May 12; latitude 42°58′ N., longitude 50°11′ W.; depth 88 meters

Depth meters	$\sigma_{t\theta}$	Total P µga/L
0	26.00	0.66
21	26.24	0.66
43	26.46	1.02
64	26.64	1.06

TOTAL PHOSPHORUS DATA COLLECTED IN 1952—Continued

Depth meters	$\sigma_{t\theta}$	Total P µga/L
Station 4840; May 12; latitude 43°11.5′ N., longitude 50°17′ W.; depth 68 meters		
0	25.45	0.87
22	25.57	0.89
43	26.27	1.31
Station 4970; July 15; latitude 50°00′ N., longitude 49°00′ W.; depth 1,847 meters		
0	25.13	0.55
25	27.47	1.07
50	27.63	1.42
76	27.67	1.37
101	27.71	1.38
151	27.72	1.17
202	27.73	1.38
303	27.76	1.38
403	27.76	1.37
604	27.77	1.43
803	27.78	1.48
1,004	27.77	1.49
1,508	27.80	1.43
Station 4971; July 17; latitude 53°43′ N. longitude 55°48′ W.; depth 110 meters		
0	21.66	0.57
25	25.74	0.79
49	26.35	1.27
74	26.39	1.41
98	26.43	1.43
Station 4972; July 17; 53°52′ N., longitude 55°32′ W.; depth 215 meters		
23	26.18	0.87
47	26.44	1.28
70	26.53	1.30
93	26.58	1.27
140	26.86	1.38
177	27.26	1.31
Station 4973; July 17; latitude 53°55.5′ N., longitude 55°26′ W.; depth 170 meters		
0	24.70	0.66
25	26.25	0.88
49	26.54	1.40
74	26.72	1.40
98	26.89	1.21
147	27.16	1.21
Station 4974; July 17; latitude 54°05.5′ N., longitude 55°07′ W.; depth 165 meters		
0	24.58	0.70
25	26.35	0.99
51	26.77	1.38
76	26.91	1.32
101	27.03	1.24
147	27.13	1.39
Station 4975; July 17; latitude 54°11′ N., longitude 54°55′ W.; depth 165 meters		
0	24.60	0.73
25	26.46	0.91
50	26.65	1.31
75	26.84	1.26
101	27.04	1.30
151	27.31	1.34
Station 4976; July 17; latitude 54°30.5′ N., longitude 54°22′ W.; depth 224 meters		
0	24.61	0.57
25	26.47	1.38
50	26.65	1.21
76	26.77	1.32
101	26.89	1.35
151	27.10	1.47
202	27.29	1.28
Station 4977; July 17; latitude 54°45′ N., longitude 53°51′ W.; depth 320 meters		
0	25.74	1.84
23	26.75	0.89
45	27.07	0.84
68	27.25	0.95
90	27.34	1.09
135	27.48	1.33
180	27.50	1.44
270	27.55	1.23
Station 4978; July 17; latitude 54°51′ N., longitude 53°34′ W.; depth 619 meters		
0	26.07	0.78
18	27.18	0.90
37	27.39	1.21
55	27.44	1.12
74	27.51	1.27
111	27.57	1.39
147	27.62	1.09
221	27.72	1.35
342	27.73	1.45
533	27.75	1.29
Station 4979; July 17; latitude 54°55′ N., longitude 53°23′ W., depth 1,463 meters		
0	26.37	0.82
25	27.19	0.96
51	27.45	1.20
76	27.61	1.31
102	27.65	1.33
152	27.72	1.38
203	27.71	1.34
305	27.74	1.46
352	27.75	1.42
532	27.75	1.55
713	27.77	1.54
897	27.76	1.22
1,370	27.77	1.23
Station 4980; July 17; latitude 55°00′ N., longitude 53°11′ W.; depth, 2,067 meters		
0	26.40	0.48
23	27.00	0.55
46	27.54	1.10
69	27.67	1.04
92	27.73	1.15
138	27.73	1.28
184	27.74	1.21
276	27.75	1.26
370	27.75	1.10
557	27.76	1.08
746	27.76	1.09
935	27.78	1.17
1,419	27.79	1.17
1.916	27.82	0.95
Station 4981; July 17–18; latitude 55°10.5′ N., longitude 52°51′ W.; depth 2,871 meters		
0	26.67	0.47
25	26.88	0.43
50	27.57	0.90
74	27.70	0.94
99	27.70	0.98
149	27.76	1.03
198	27.77	1.13
297	27.77	1.13
379	27.77	0.98
571	27.78	1.03
762	27.80	1.01
956	27.80	0.99
1,446	27.80	1.06
1,945	27.87	1.10
2,504	27.91	1.30
2,792	27.93	1.17
Station 4982; July 18; latitude 55°30′ N., longitude 52°19′ W.; depth 3,200 meters		
0	26.64	0.55
25	27.28	1.17
49	27.64	1.26
74	27.70	1.37
98	27.73	1.52
147	27.75	1.38
197	27.76	1.22
295	27.77	1.18
394	27.78	1.22
592	27.78	1.31
790	27.77	0.98
989	27.79	1.13
1,475	27.80	1.34
1,954	27.80	1.08
2,416	27.88	1.23
2,893	27.90	1.19
3,038	27.94	0.66

TOTAL PHOSPHORUS DATA COLLECTED IN 1952—Continued

Station 4983 July 18; latitude 55°55.5′ N., longitude 51°34′ W.; depth 3,402 meters

Depth meters	$\sigma_{t\theta}$	Total P µga/L
0	26.59	1.07
25	26.76	0.69
49	27.29	1.00
74	27.42	1.25
99	27.48	1.16
148	27.59	1.16
197	27.62	1.28
296	27.72	1.34
398	27.76	1.33
596	27.76	1.20
792	27.78	1.21
988	27.78	1.30
1,486	27.81	1.42
1,987	27.85	1.31
2,335	27.84	1.32
2,801	27.90	1.32
3,126	27.91	1.18

Station 4984; July 18; latitude 56°30.5′ N., longitude 50°25′ W.; depth 3,530 meters

Depth meters	$\sigma_{t\theta}$	Total P µga/L
0	26.84	0.64
26	27.12	1.02
51	27.56	1.30
77	27.71	1.44
103	27.71	1.44
153	27.76	1.48
204	27.77	1.47
307	27.78	1.25
310	27.77	1.35
495	27.78	1.45
700	27.77	1.36
924	27.77	1.41
1,427	27.77	1.25
1,956	27.79	1.32
2,532	27.82	1.34
3,016	27.88	1.27
3,405	27.91	1.32

Station 4985; July 19; latitude 57°02′ N., longitude 49°02′ W.; depth 3,475 meters

Depth meters	$\sigma_{t\theta}$	Total P µga/L
0	26.67	0.74
24	27.03	0.85
49	27.46	1.23
74	27.65	1.34
99	27.67	1.52
148	27.71	1.85
197	27.72	1.39
296	27.75	1.40
379	27.75	1.34
568	27.75	1.38
758	27.75	1.38
948	27.77	1.36
1,442	27.79	1.20
1,948	27.80	1.42
2,552	27.85	1.38
3,040	27.89	1.40
3,429	27.92	0.99

Station 4986; July 19; latitude 57°34.5′ N., longitude 48°04′ W.; depth 3,347 meters

Depth meters	$\sigma_{t\theta}$	Total P µga/L
0	26.89	0.82
25	27.25	0.80
52	27.65	1.13
77	27.72	1.42
104	27.71	1.41
154	27.75	1.34
206	27.76	1.34
310	27.75	1.42
513	27.75	1.38
719	27.75	1.31
924	27.77	1.41
1,129	27.78	1.30
1,646	27.77	1.26
2,164	27.81	1.30
2,453	27.83	1.37
2,937	27.90	1.34
3,227	27.93	1.09

Station 4987; July 19; latitude 58°05.5′ N., longitude 47°01′ W.; depth 3,054 meters

Depth meters	$\sigma_{t\theta}$	Total P µga/L
0	26.94	0.80
25	27.14	0.91
50	27.34	0.95
75	27.68	1.31
100	27.71	1.48
150	27.73	1.47
199	27.73	1.34
299	27.74	1.27
406	27.75	1.32
609	27.76	1.20
812	27.78	1.28
1,015	27.79	1.37
1,494	27.81	1.37
2,044	27.83	1.28
2,490	27.88	1.37
2,986	27.92	1.33

Station 4988; July 20; latitude 58°37.5′ N., longitude 45°57′ W.; depth 2,505 meters

Depth meters	$\sigma_{t\theta}$	Total P µga/L
0	27.06	0.98
25	27.32	1.02
51	27.50	1.16
76	27.71	1.27
101	27.72	1.39
152	27.74	1.35
203	27.74	1.39
304	27.75	1.36
376	27.77	1.24
565	27.77	1.44
755	---	1.30
946	---	1.29
1,431	27.78	1.33
1,926	27.84	1.30
2,448	27.87	1.18

Station 4989; July 20; latitude 59°00′ N., longitude 45°16′ W.; depth 2,286 meters

Depth meters	$\sigma_{t\theta}$	Total P µga/L
0	27.15	1.10
25	27.34	1.05
49	27.53	1.16
74	27.65	1.31
98	27.71	1.49
147	27.75	1.36
196	27.75	1.27
294	27.74	1.26
393	27.76	1.25
591	27.77	1.29
789	27.78	1.29
988	27.79	1.31
1,492	27.82	1.47
2,002	27.88	1.47
2,253	27.90	1.17

Station 4990; July 20; latitude 59°14.5′ N., longitude 44°54′ W.; depth 1,957 meters

Depth meters	$\sigma_{t\theta}$	Total P µga/L
0	27.09	0.88
25	27.16	1.01
50	27.54	1.27
76	27.63	1.39
101	27.67	1.47
151	27.70	1.49
202	27.71	1.35
303	27.75	1.42
404	27.74	1.26
605	27.76	1.45
806	27.77	1.36
1,005	27.78	1.27
1,506	27.79	1.47
1,862	27.85	1.02

Station 4991; July 20; latitude 59°21.5′ N., longitude 44°41′ W.; depth 1,097 meters

Depth meters	$\sigma_{t\theta}$	Total P µga/L
0	26.91	0.97
24	27.22	1.14
49	27.38	1.12
74	27.49	1.51
99	27.57	1.18
148	27.69	1.30
197	27.69	1.27
296	---	1.18
429	27.71	1.20
635	27.72	1.23
838	27.74	1.34
1,036	27.76	1.35

Station 4992; July 20; latitude 59°31.5′ N., longitude 44°31′ W.; depth 179 meters

Depth meters	$\sigma_{t\theta}$	Total P µga/L
0	24.90	0.44
23	25.14	0.58
47	26.19	0.71
70	26.84	1.15
94	27.21	1.04
140	27.51	1.10
159	27.60	1.09

TOTAL PHOSPHORUS DATA COLLECTED IN 1952—Continued

Depth meters	$\sigma_{t\theta}$	Total P µga/L	Depth meters	$\sigma_{t\theta}$	Total P µga/L	Depth meters	$\sigma_{t\theta}$	Total P µga/L
Station 4993; July 20; latitude 59°34.5′ N., longitude 44°23′ W.; depth 153 meters			Station 4994; July 20; latitude 59°36′ N., longitude 44°11′ W.; depth 165 meters					
0	25.09	0.40	0	25.03	0.59			
25	25.42	0.49	25	25.22	0.63			
51	26.42	0.74	51	25.95	0.76			
76	26.65	0.95	76	26.45	0.99			
101	27.01	0.93	101	26.91	1.02			
147	27.19	1.10	152	27.41	1.42			

TOTAL PHOSPHORUS DATA COLLECTED IN 1953

Depth meters	$\sigma_t\theta$	Total P μga/L
Station 5279; July 16; latitude 53°43′ N., longitude 55°48′ W.; depth 112 meters		
0	20.35	1.11
26	25.74	0.66
51	26.02	0.66
77	26.14	0.83
97	26.20	0.92
Station 5280; July 16; latitude 53°49.5′ N., longitude 55°32′ W.; depth 218 meters		
0	24.26	0.49
26	25.92	0.59
52	26.32	0.92
78	26.48	1.01
104	26.58	1.01
156	26.77	0.95
198	27.00	1.06
Station 5281; July 16; latitude 53°53′ N., longitude 55°26′ W.; depth 181 meters		
0	24.34	0.47
25	25.95	0.53
51	26.31	0.88
76	26.48	1.08
101	26.64	1.05
152	27.00	1.14
Station 5282; July 16; latitude 54°03′ N., longitude 55°04′ W.; depth 161 meters		
0	25.17	0.60
26	26.02	0.68
51	26.46	1.06
77	26.59	1.01
103	26.74	0.76
144	26.93	1.00
Station 5283; July 16; latitude 54°14′ N., longitude 54°56′ W.; depth 174 meters		
0	25.24	0.58
25	25.68	0.55
51	26.39	0.64
76	26.55	1.05
101	26.71	1.05
152	26.97	1.00
Station 5284; July 16; latitude 54°31′ N., longitude 54°24′ W.; depth 225 meters		
0	25.24	0.66
25	26.32	0.80
50	26.57	0.98
76	26.73	1.00
101	26.90	0.87
151	27.10	0.94
202	27.25	1.07
Station 5285; July 16; latitude 54°48′ N., longitude 53°54′ W.; depth 327 meters		
0	25.04	0.69
25	26.67	0.68
50	27.10	0.99
75	27.26	0.87
101	27.31	0.94
151	27.51	1.01
201	27.56	1.02
302	27.68	1.01
Station 5286; July 16; latitude 54°53′ N., longitude 53°40′ W.; depth 631 meters		
0	25.75	0.63
25	27.11	0.79
50	27.25	0.82
75	27.36	0.88
100	27.43	0.88
150	27.50	0.88
201	27.59	0.91
301	27.66	1.05
393	27.69	1.04
595	27.71	1.06
Station 5287; July 16; latitude 54°59′ N., longitude 53°26′ W.; depth 1,582 meters		
0	26.81	0.58
25	27.10	0.53
51	27.41	0.64
76	27.57	0.82
102	27.61	0.93
153	27.67	0.95
204	27.70	0.95
306	27.74	0.99
369	27.75	1.06
590	27.76	1.03
798	27.77	1.08
1,010	27.77	1.06
1,542	27.78	1.03
Station 5288; July 16; latitude 55°04′ N., longitude 53°17′ W.; depth 2,195 meters		
0	26.87	0.47
25	27.28	0.52
50	27.60	0.71
74	27.64	0.77
99	27.69	1.00
149	27.72	1.02
198	27.73	1.01
297	27.75	1.05
382	27.74	1.00
597	27.76	1.00
812	27.77	0.95
1,031	----------	0.98
1,495	27.79	1.07
1,963	27.81	1.09
Station 5289; July 17; latitude 55°12.5′ N., longitude 52°56′ W.; depth 2,926 meters		
0	26.92	0.67
25	27.22	0.68
50	27.51	0.85
75	27.65	1.00
99	27.68	1.04
149	27.72	1.14
199	27.73	1.05
298	27.75	1.15
397	27.75	1.17
621	27.77	1.10
859	27.78	1.15
1,074	27.78	1.14
1,551	27.79	1.22
2,029	27.83	1.16
2,431	27.86	1.16
2,730	27.91	1.11
Station 5290; July 17; latitude 55°26′ N., longitude 52°30′ W.; depth 3,182 meters		
0	26.73	0.74
27	27.03	0.58
53	27.50	1.05
80	27.63	1.11
106	27.68	1.29
161	27.72	1.29
214	27.74	1.21
320	27.74	1.28
308	27.75	1.30
497	27.76	1.12
706	27.78	1.20
940	27.78	1.15
1,374	27.78	1.06
1,836	----------	1.12
1,706	27.79	0.98
2,136	27.83	1.13
2,537	27.86	1.04

TOTAL PHOSPHORUS DATA COLLECTED IN 1952—Continued

Depth meters	$\sigma_t\theta$	Total P µga/L
Station 5291; July 17–18; latitude 55°58′ N., longitude 51°52′ W.; depth 3,365 meters		
0	26.80	0.60
27	26.80	0.54
53	27.41	0.83
80	27.53	0.97
106	27.61	1.03
160	27.68	1.18
214	27.73	0.98
320	27.74	1.24
490	27.77	1.15
776	27.78	1.09
1,080	27.79	1.24
1,310	27.79	1.02
1,789	27.79	1.22
2,270	27.83	1.13
2,354	27.83	1.20
2,979	27.88	1.14
3,264	27.91	1.06
Station 5292; July 18; latitude 56°29′ N., longitude 50°42′ W.; depth 3,548 meters		
0	26.91	0.70
23	26.92	0.73
45	26.93	0.97
68	27.22	0.90
90	27.51	1.10
135	27.59	1.18
181	27.64	1.19
271	27.70	1.17
381	27.74	1.26
598	27.75	1.16
819	27.77	1.24
1,042	27.78	1.24
1,511	27.78	1.16
1,987	27.80	1.14
2,536	27.84	1.03
3,012	27.89	1.13
3,450	27.91	1.05
Station 5293; July 19; latitude 56°57.5′ N., longitude 49°33′ W.; depth 3,603 meters		
0	27.00	0.67
25	27.00	0.66
50	27.11	0.79
75	27.55	1.11
100	27.59	0.80
148	27.67	1.15
198	27.69	1.12
298	27.74	1.17
2,436	27.81	1.30
2,859	27.85	1.29
3,325	27.89	1.13
Station 5294; July 19; latitude 57°30′ N., longitude 48°23′ W.; depth 3,402 meters		
0	27.19	1.02
24	27.21	1.08
47	27.22	1.10
71	27.41	1.15
94	27.60	1.27
142	27.66	1.18
189	----------	1.23
283	27.72	1.39
321	27.73	1.34
499	27.74	1.29
685	27.73	1.34
874	27.75	1.24
1,328	27.76	1.40
1,837	27.78	1.36
1,922	27.79	1.49
2,363	27.83	1.38
2,770	27.87	1.31
Station 5295; July 19; latitude 58°05′ N., longitude 47°14′ W.; depth 3,237 meters		
0	27.15	1.06
27	27.19	1.04
53	27.48	1.14
80	27.58	1.04
106	27.65	1.35
160	27.68	1.36
213	27.69	1.35
319	27.72	1.17
423	27.75	1.31
647	27.74	1.27
875	27.75	1.46
1,103	27.75	1.32
1,582	27.78	1.33
2,060	27.82	1.35
2,615	27.87	1.29
3,063	27.92	1.25
Station 5296; July 20; latitude 58°39′ N., longitude 46°12′ W.; depth 2,698 meters		
0	27.08	0.84
25	27.15	0.87
50	27.32	0.90
75	27.52	1.01
100	27.64	1.23
150	27.63	1.19
200	27.71	1.18
300	27.74	1.19
400	27.74	1.16
625	27.76	1.15
854	----------	1.12
1,080	27.77	1.10
1,581	27.78	1.10
2,038	27.82	1.14
2,517	27.89	1.03
Station 5297; July 20; latitude 58°59.5′ N., longitude 45°31′ W.; depth 2,469 meters		
0	27.21	0.82
25	27.24	0.82
50	27.38	0.87
76	27.55	0.95
101	27.62	1.22
151	27.63	1.18
201	27.67	1.13
302	27.68	1.15
403	27.71	1.29
560	27.71	1.25
704	27.74	1.18
855	27.76	0.92
1,294	27.77	1.20
1,753	27.81	0.97
2,238	27.87	1.04
Station 5298; July 20; latitude 59°13′ N., longitude 44°58′ W.; depth 1,975 meters		
0	27.08	0.87
19	27.13	0.91
37	27.21	0.87
56	27.36	0.94
74	27.42	0.96
111	27.53	1.00
148	27.56	1.05
222	27.58	1.12
311	27.60	1.19
456	27.65	1.09
600	27.68	1.24
758	27.71	1.19
1,190	27.75	1.18
1,731	27.79	1.19
Station 5299; July 20; latitude 59°19.5′ N., longitude 44°30′ W.; depth 1,188 meters		
0	27.03	0.90
28	27.10	0.82
55	27.25	0.80
82	27.36	0.97
109	27.39	1.01
165	27.49	1.11
219	27.54	1.17
328	27.59	1.14
432	27.63	1.33
649	27.66	1.37
868	27.72	1.44
1,087	27.75	1.46
Station 5300; July 20; latitude 59°33′ N., longitude 44°07′ W.; depth 171 meters		
0	25.54	0.87
29	25.69	0.79
58	25.92	0.80
87	26.42	0.80
115	26.88	0.95
173	27.32	0.90

U. S. GOVERNMENT PRINTING OFFICE: 1955

Contribution No. 688

Deep-Sea Research, 1955, Vol. 2, pp. 182 to 199. Pergamon Press Ltd., London.

Oxygen-density relationships in the western North Atlantic

F. A. RICHARDS and A. C. REDFIELD*[†]

(*Recieved January* 1955)

Summary—A distinctive correlation between oxygen content and sigma-*t* has been shown to exist in the Sargasso Sea. Waters of the Caribbean Sea, Yucatan Channel and Straits of Florida are anomalously lower in oxygen. Similar oxygen anomalies along the supposed course of the Gulf Stream can be used to delineate its right-hand boundary and to trace water of southern origins to as far as 43°W. longitude. The distribution of oxygen anomalies across the Gulf Stream shows that water of southern origins is present in highly variable amounts, that it is present in the various currents and counter-currents, and that these currents are materially related and do not represent merely the transfer of momentum from southern sources.

SALINITY-temperature correlations distinguish the Gulf Stream from Slope water, but not from the Sargasso Sea, and in the past either inferred or measured motion has been used to dilineate the right hand limit of the Gulf Stream. No method of tracing the physical continuity of the actual moving water has been available. The oxygen content of the upper layers in the Gulf Stream is characteristically less than that of Sargasso Sea water of the same density, and can be used to trace its continuity from the Caribbean to at least 61°W. longitude.

ROSSBY (1936), showed that the oxygen-salinity correlation in the Sargasso Sea is different from that in the Yucatan Channel-Florida Straits region, and that this difference is distinct for some distance along the course of the Gulf Stream. He showed that the lowest oxygen concentrations emanate from the Straits of Florida, and that a secondary tongue in which the minimum values are somewhat higher enters the system from the Antilles Current[‡]. We have found that the oxygen content of the shallower layers is more distinctive of Caribbean waters than is that of the oxygen minimum layer, with which ROSSBY's treatment was concerned.

In order to use the oxygen content to distinguish the water masses in question, the correlation between the oxygen concentration and sigma-*t* of Sargasso Sea water has been defined, and anomalies from this correlation have been examined. Sigma-*t* was chosen as a correlative because surfaces of equal sigma-*t* are of approximately constant potential density, and thus identify the paths of free movement by lateral mixing or flow. Sigma-*t* values have the advantage over salinity of increasing continuously with depth, and thus a certain ambiguity is avoided in identifying the layer from which a sample is collected.

OXYGEN-DENSITY CORRELATION OF SARGASSO SEA WATER

To define the oxygen-sigma-*t* correlation of the Sargasso Sea, 2,759 samples from

---

*Contribution No. 688 from the Woods Hole Oceanographic Institution.

[†] Part of this research was sponsored by the Office of Naval Research under Contracts Nonr 27701 and 769 (00).

[‡] ICHIYE (1954) has recently employed oxygen-chlorinity correlations to distinguish the types of water present in the seas adjacent to Japan and to recognise the sources of the waters which result from their admixture.

175 hydrographic stations occupied in the area between 30 and 40°N. latitude, west of 40°W. longitude, and east of the " Gulf Stream " were considered. In order, to eliminate water of Gulf Stream or other origin, all samples from stations showing salinities less than 36‰ at depths less than 500 metres were excluded.

The correlation between the oxygen content and sigma-*t* of these samples from the Sargasso Sea is shown in Fig. 1. The oxygen content gradually increases with density until sigma-*t* values of 26·0 are reached, and then decreases rather rapidly until minimum values are encountered at about 27·3, in good agreement with Seiwell's (1937) finding that the statistical value of sigma-*t* at the oxygen minimum is 27·23 in the western basin of the North Atlantic. At greater densities, the oxygen

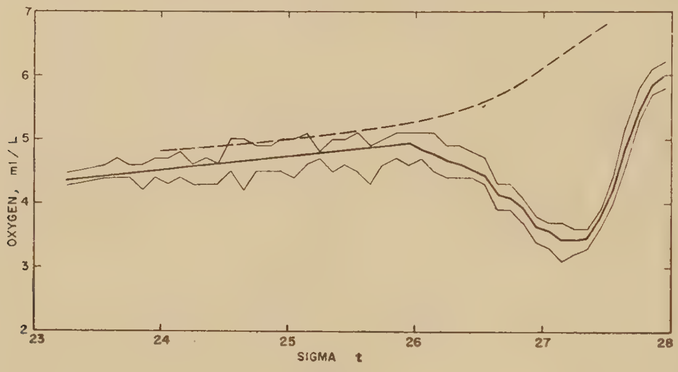

Fig. 1.

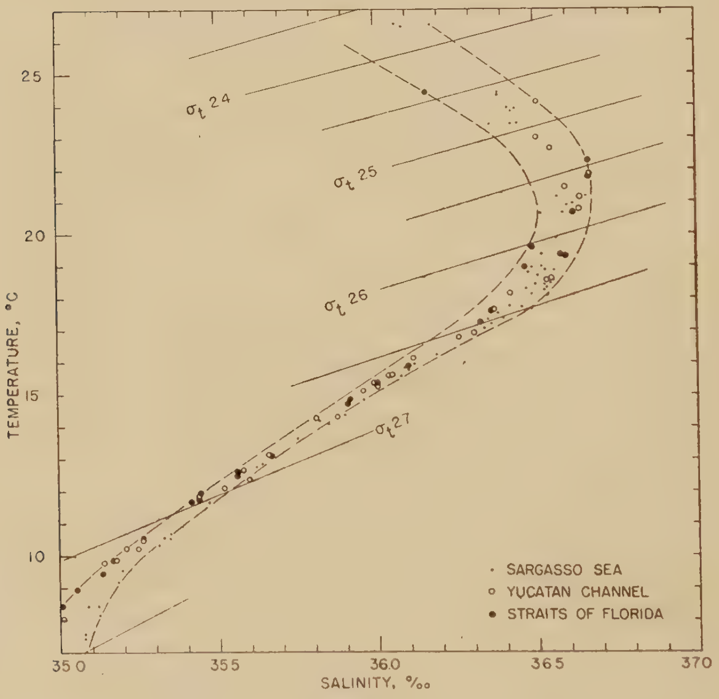

Fig. 2.

content increases to concentrations of about 6·0 ml./litre at sigma-*t* values slightly less than 28·00. In this range, below the oxygen minimum, there is rather wide scatter in the values, owing at least in part to the steepness of the curve.

Between σ_t — 23·5 and 25·95, the correlation is the linear least squares regression, in which the standard error of estimate is ± 0·29 ml./litre. The layer in which these densities are found is thin and shallow, and the number of observations in water having these densities is small, ranging from 10 to 70 samples in each 0·1 sigma-*t* unit span. In the denser waters, the correlation is the arithmetic average of all observations made within 0·1 sigma-*t* unit ranges. The envelope shown on Fig. 1 contains half of all the observations.

The dashed line in Fig. 1 shows the concentration of oxygen in fully saturated waters having the salinity-temperature characteristics of Sargasso Sea water (see Fig. 2). The linear part of the oxygen-sigma-*t* correlation (between $\sigma_t = 23{\cdot}5$ and 25·95) is practically parallel to the saturation curve, but everywhere falls somewhat below saturation. In the denser layers, typical Sargasso water is well under-saturated.

OXYGEN SIGMA-*t* CORRELATIONS AND ANOMALIES

The correlations between oxygen and sigma-*t* have been examined in sections across the Yucatan Channel from Cuba to the Yucatan Peninsula, across the Florida Straits from Key West to Havana, seaward from Onslow Bay, North Carolina, and in six sections across the Gulf Stream between Cape Hatteras and Nova Scotia (Figs. 3 and 4). It is evident from Fig. 4 that these sections contain waters with considerably less oxygen than Sargasso Sea water of the same sigma-*t*. In treating the data, oxygen anomalies were estimated by subtracting the oxygen content of Sargasso water of

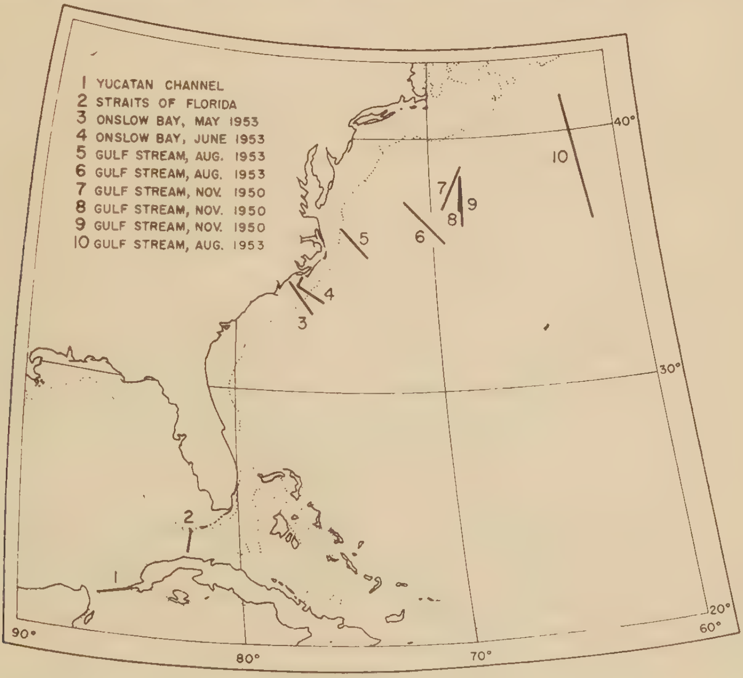
1 YUCATAN CHANNEL
2 STRAITS OF FLORIDA
3 ONSLOW BAY, MAY 1953
4 ONSLOW BAY, JUNE 1953
5 GULF STREAM, AUG. 1953
6 GULF STREAM, AUG. 1953
7 GULF STREAM, NOV. 1950
8 GULF STREAM, NOV. 1950
9 GULF STREAM, NOV. 1950
10 GULF STREAM, AUG. 1953
10
7
9
8
5
6
4
3
2
1
40°
30°
20°
60°
70°
80°
90°

Fig. 3.

Table I

Sections showing the distribution of negative oxygen anomalies of more than — 0·50 ML/L.

No.	*Section*	*Station numbers*	*Dates*	*Positions at ends*	*Range of depths (metres)*	*Largest anomaly observed. (ml./l.)*	*References*
1	Yucatan Channel	1604- 1610	4 V '33- 5 V '33	21°36′N. 86°26′W 21°51′N. 85°00′W	60-620	— 1·41	Seiwell, 1938 Rakestraw, *et al.*, 1937 Bull. Hydro., 1934
2	Straits of Florida	2003- 2007	4 III '34- 4 III '34	23°15′N. 82°16′W 24°18′N. 82°11′W	55-610	— 2·12	Seiwell, 1938 Bull. Hydro., 1935
3	Onslow Bay, May	C-172- C-182	12 V '53- 14 V '53	33°01′N. 76°06′W 34°27′N. 77°27·5′W	54-444	— 1·63	—
4	Onslow Bay, June	C-183- C-192	8 VI '53- 10 VI '53	33°25′N. 75°41′W 34°31′N. 76°44′W	100-700	— 1·73	—
8	Gulf Stream	4842- 4853	20 X '50- 22 X '50	37°03′N. 68°29′W 38°36′N. 68°22′W	40-610	— 1·49	Worthington, 1954
9	Gulf Stream	4853- 4867	22 X '50- 26 X '50	38°36′N. 68°22′W 36°33′N. 68°33′W	50-600	— 1·46	Worthington, 1954
7	Gulf Stream	4868- 4882	30 X '50- 2 XI '50	38°56′N. 68°17′W 37°06′N. 69°19′W	60-650	— 1·22	Worthington, 1954
5	Gulf Stream	5084- 5094	10 VIII '53 12 VIII '53	36°20′N. 74°37′W 35°11′N. 73°19′W	38-365	— 1·43	—
6	Gulf Stream	5095- 5106	19 VIII '53 21 VIII '53	37°28′N. 71°12·W 35°50′N. 69°25′W	83-312	— 1·53	—
10	Gulf Stream	5107- 5122	26 VIII '53 29 VIII '53	36°25′N. 61°59′W 41°21′N. 62°48·W	90-580	— 0·83	—

All stations occupied by *Atlantis* except *Caryn* stations C–172 to C–192 the same sigma-t value, as obtained from the correlation curve shown in Fig. 1, from the observed oxygen content of the sample, and these anomalies have been plotted in the diagrams of the sections (Table I and Figs. 5-14).

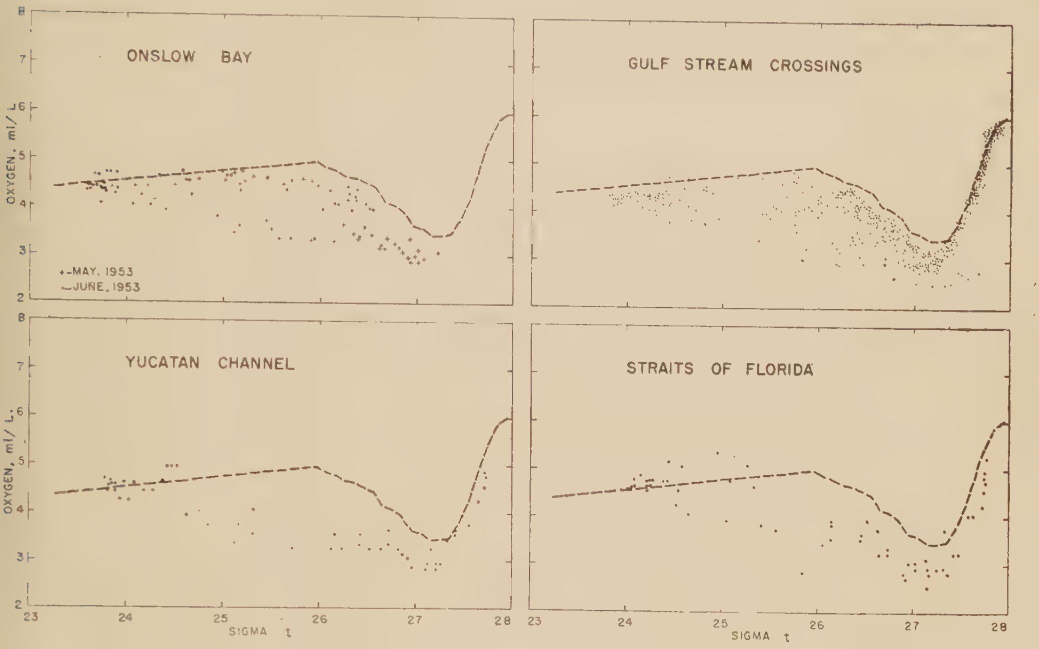

Fig. 4.

In order to eliminate slope water and waters of coastal origin, a diagram showing the salinity-temperature correlation of all samples from the Yucatan Channel and Florida Straits sections, and from the most southerly stations in the six Gulf Stream crossings, was prepared (Fig. 2)*. Samples which were significantly less saline, for the correlated temperature, than the left hand envelope shown in Fig. 2 were excluded as being of neither Caribbean nor Sargasso Sea origin.

Anomalies smaller than ± 0·5 ml./litre have not been considered significant.

YUCATAN CHANNEL AND STRAITS OF FLORIDA—SECTIONS 1 AND 2

Negative anomalies of at least 0·5 ml./litre were present in quantity in the upper 600 metres of these sections (Figs. 5 and 6). The most deficient water lay between sigma-t values of about 25·00 and 26·50, where anomalies up to − 1·41 ml./litre occur in the Yucatan Channel and − 2·12 ml./litre in the Straits of Florida.

Anomalies of more than − 0·5 ml./litre were found in both sections in a separate zone below the 27·50 sigma-t surface. These are related to the extremely low oxygen minima noted by ROSSBY (1936, p. 37), who pointed out that these low oxygen concentrations, unlike those of the upper layers, cannot be traced through the Florida Straits.

---

*This salinity-temperature correlation represents waters slightly fresher, at any temperature, than ISELIN's (1936) correlation for Central Atlantic water between Chesapeake Bay and Bermuda.

ONSLOW BAY, MAY AND JUNE, 1953—SECTIONS 3 AND 4

In May (Fig. 7), negative anomalies were limited to the upper 500 metres, but they extended to greater depths in June (Fig. 8). It appears that the Florida Current was hugging the shore more closely in June than May. This is shown by the more inshore location of the 26·50 isopycnal, which was also steeper and correspondingly deeper in June.

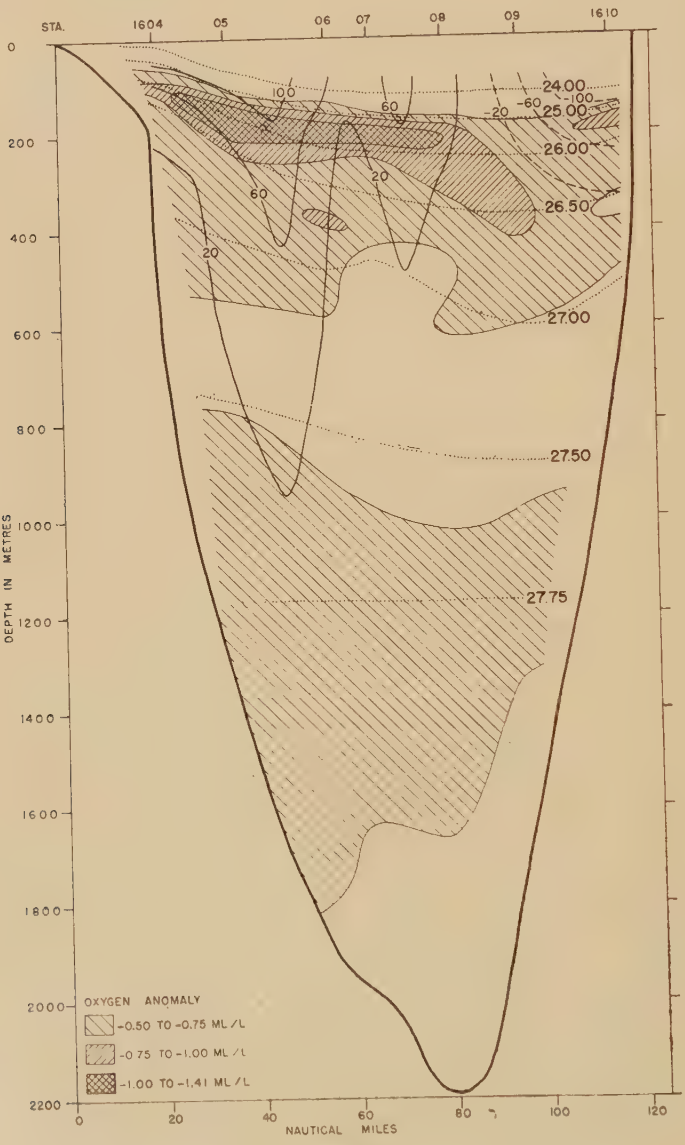

Fig. 5.

The oxygen anomalies were centered around $\sigma_t = 26{\cdot}00$ in May, but in June, most of them were in denser waters, and they appeared in two discrete portions;

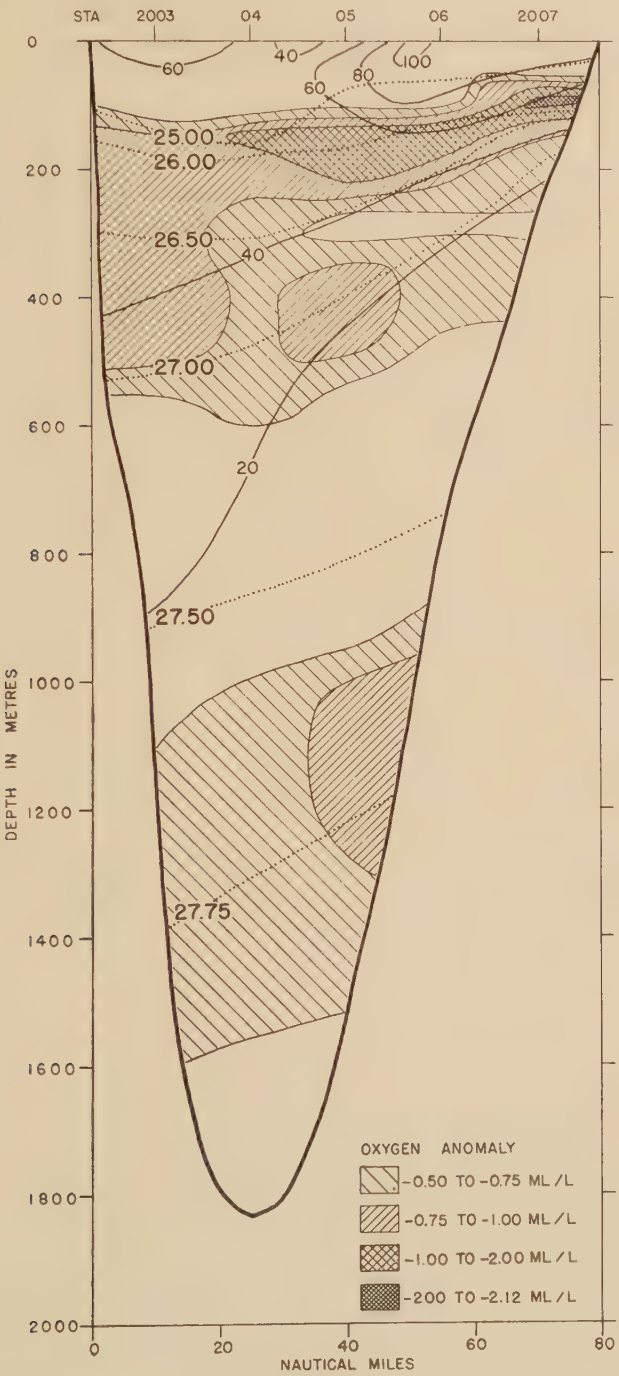
STA
2003
04
05
06
2007
0
200
400
600
800
1000
1200
1400
1600
1800
2000
DEPTH IN METRES
0
20
40
60
80
NAUTICAL MILES
60
40
60
80
100
25.00
26.00
26.50
40
27.00
20
27.50
27.75
OXYGEN ANOMALY
-0.50 TO -0.75 ML/L
-0.75 TO -1.00 ML/L
-1.00 TO -2.00 ML/L
-200 TO -2.12 ML/L

Fig. 6.

the main body was close inshore, but a separate portion was observed between 100 and 200 metres at Stations 183 and 184, suggesting a filamentous dichotomy in waters of Caribbean (or other southerly) origin at these latitudes. This discontinuous distribution of the oxygen anomaly will be shown in other sections.

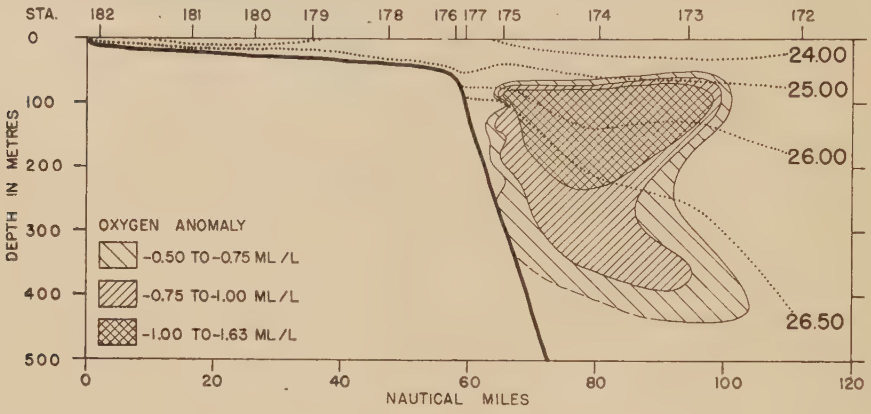

Fig. 7.

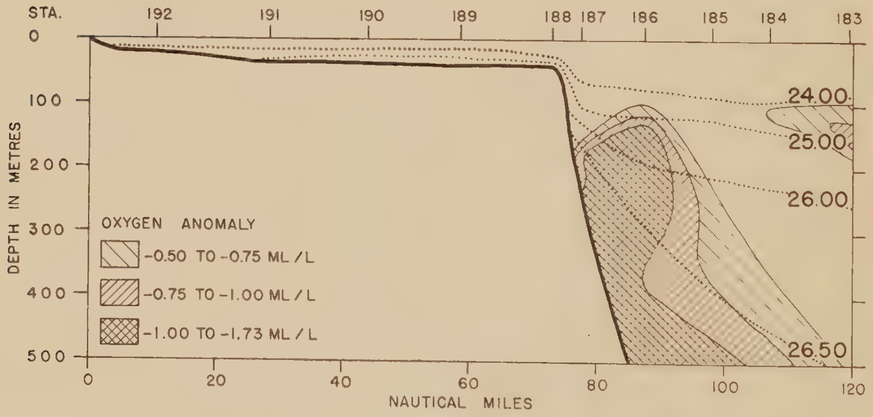

Fig. 8.

THE GULF STREAM—SECTIONS 5 THROUGH 10

Three sections across the Gulf Stream were occupied in October and November, 1950 (Figs. 9, 10 and 11). In all three, anomalies of at least − 0·5 ml./litre were found extending between something less than 100 to about 600 metres. The greatest deficiencies were centred at sigma-*t* values of about 26·00. In many cases the lines of equal anomaly can and have been drawn approximately parallel to isopycnals in order to suggest isentropic mixing with adjacent water masses of equal density.

Three additional sections across the Gulf Stream were occupied in August, 1953 in an attempt to make observations of oxygen anomalies along the course of the stream as nearly synoptically as possible from one ship. These sections (Figs. 12, 13 and 14) show remarkable contrasts with the sections occupied in 1950. Water anomalously low in oxygen was present in much smaller amounts, and was shallower in 1953 than in 1950. With one exception it was confined to the upper 300 metres in 1953, compared with 600 metres in the previous sections. The highest anomalies were found at sigma-*t* values between 25 and 26 in Sections 5 and 6, and at about 26·5 in Section 10 as well as in the 1950 sections. The maximum anomalies in Sections 5 and 6 were about the same as in the 1950 sections (— 1·43 and — 1·53 ml./litre in 1953 compared with — 1·49, — 1·46, and — 1·22 in 1950) but in Section 10, the maximum anomaly was only — 0·83 ml./litre.

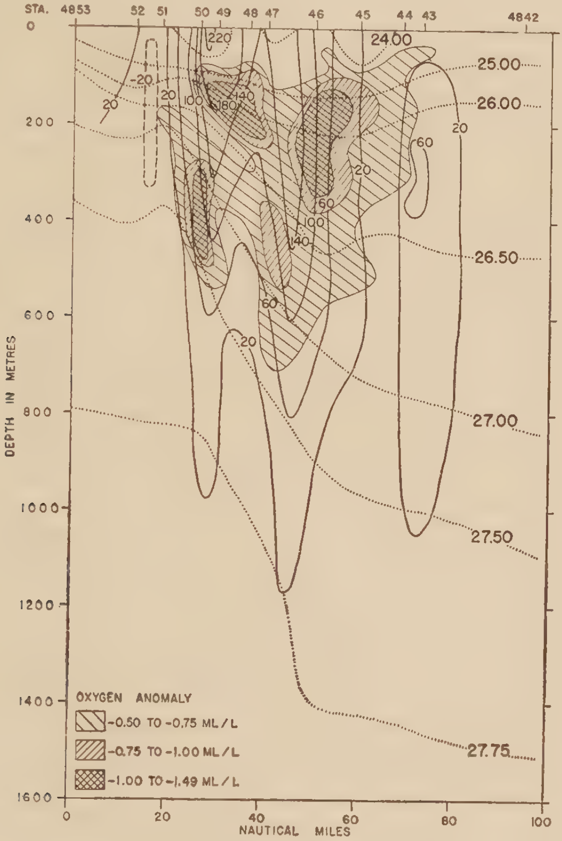

Fig. 9.

OBSERVATIONS EAST OF 61°W LONGITUDE

Water which meets both the oxygen and salinity anomaly criteria for Caribbean water has been observed by *Atlantis* in at least three stations (Table II) east of the area covered by Gulf Stream Section 10. These data are too scanty to draw any conclusions regarding the distribution of Caribbean water in this region, but Station 4811, occupied at 41°23′N. and 43°23′W., shows that Caribbean water can be identified in this region by the oxygen-sigma-*t* relationship.

RELATIONS BETWEEN OXYGEN ANOMALIES AND CURRENTS IN THE GULF STREAM SYSTEM

In all three of the Gulf Stream sections occupied in 1950 (Nos. 7, 8 and 9, Figs. 9

10 and 11) the largest anomalies were found below the maximum current velocities* This suggests that the swiftest moving water retains its characteristic anomaly for the greatest distance, except in the surface layers, where reoxygenation by vertical turbulence would be expected to be most rapid. The highest anomalies are displaced slightly to the south (right) of the maximum velocities suggesting that isentropic mixing is most effective along the north side of the current (to the left, facing downstream). Below the surface layers, the time factor appears to have had the least effect in mixing and reoxygenation of the swiftest waters. This last effect is particularly evident in Section 6, Fig. 13, occupied in August, 1953. The small mass of anomalous water is found below the highest velocity observed in any of the six sections between Cape Hatteras and Nova Scotia, and contains the most highly anomalous (– 1·52 ml./litre) water observed in the region.

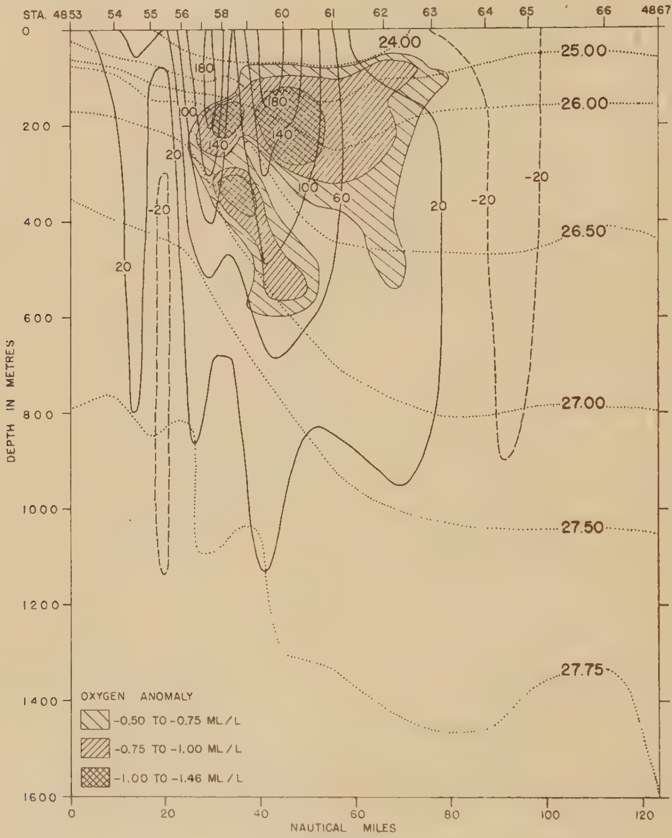

Fig. 10.

The envelope of – 0·5 ml./litre anomalies is continuous but deeply lobed and otherwise irregular in Gulf Stream Sections 5, 7, 8 and 9 and is broken into three discrete portions in Section 6 and into four in Section 10. Worthington (1954) commented on the irregularities in the velocity profiles of Section 7, 8 and 9 and pointed out that these irregularities did not appear in the corresponding G.E.K. current measurements at the surface and at 100 metres. The irregularities and discontinuities which appear in the oxygen anomaly profiles are evidently related to corresponding irregularities in the velocity profiles. This appears to substantiate the velocity structures obtained by dynamic computations and perhaps to emphasize the tendency of G.E.K. observations to smooth and integrate velocity gradients.

---

*The velocity structure and other physical characteristics of these sections, and the hydrographic methods used have been described by Worthington (1954).

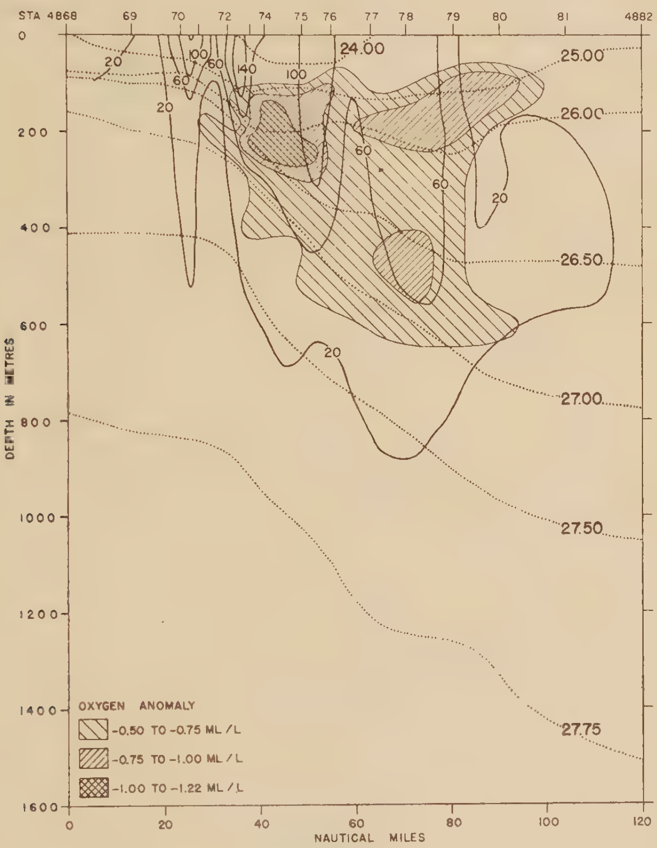

Fig. 11.

Anomalies were found in counter-currents in all three of the 1953 sections (5, 6 and 10), and appear to extend continuously from the east-setting current to the counter-current. Between Stations 5112 and 5115 in Section 6*. It is tempting to associate this with an eddy or loop, but the observations are inadequate to test the possibility. The thin stratum of low oxygen water lying along the 26·50 sigma-*t* surface between

---

*The geostrophic velocity profiles of these 1953 sections were computed by the methods Worthington (1954) used, assuming a level of no motion at 2,000 metres. Attempts to make the crossings at right angles to the main course of the stream were based on bathythermograph observations of the so-called inshore front, which is marked by abrupt and distinct temperature changes. Section 6 contains the highest velocities yet found from dynamic computations in the Gulf Stream. These high velocities were confirmed by drift on station and set while underway as observed by frequent Loran fixes and dead reckoning.

Stations 5116 and 5122 is associated with the steepest thermal gradient at the 200 metre surface.

Section 6 is of some special interest, since it appears to demonstrate a rapidly moving jet-like structure, in which the main moving mass has retained its original characteristics, but in which the peripheral water has mixed so completely as to be no longer recognizable by its oxygen content. On the other hand, Section 10 represents a condition further downstream in which the currents are slower and more diffuse, and the oxygen anomalies have been maintained, although they are less intense than in the upstream sections, the waters being partially reoxygenated.

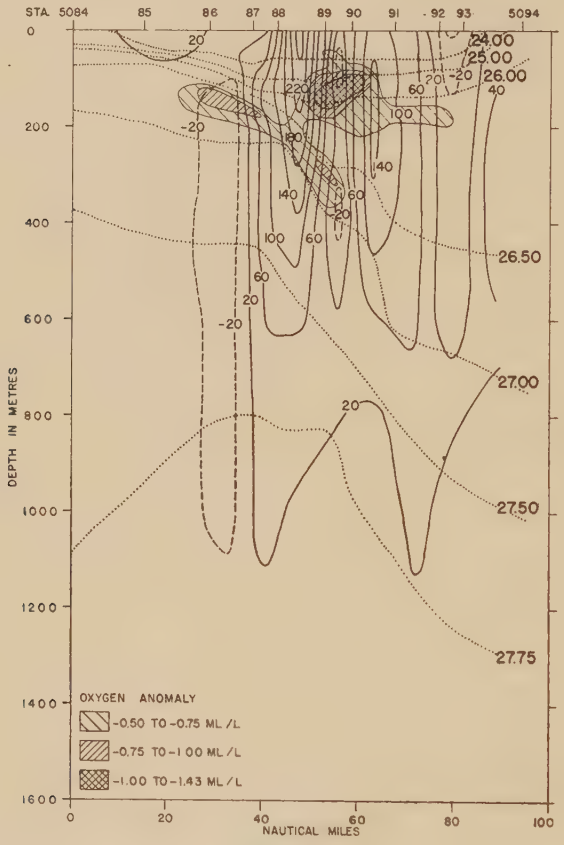

Fig. 12.

RELATION OF ANOMALIES TO TRANSPORTS

The transport of water, recognizable as of Caribbean origin by its oxygen content, across the sections can be computed by multiplying the planimetered area of the water having anomalies greater than — 0·5 ml./litre. *Oxygen deficits* can be estimated by multiplying these transports by the average anomalies. Deficits thus computed represent the difference in the oxygen content of the Caribbean water passing through a section in a unit of time and that of an equal volume of Sargasso Sea water. Thus, the deficits are related to the transport, and are expressed in litres of oxygen per second. The computed transports and deficits of the sections are shown in Table III.

There is more than a four-fold variation in the transports, and nearly a five-fold variation in the oxygen deficits in the sections between Cape Hatteras and Delaware Bay (Sections 5 through 9). These amounts bracket the transports and deficits computed for the Yucatan Channel and Straits of Florida sections. It is known that the transport through the Straits of Florida varies widely at different times. Montgomery (1941) computed the transport in four sections off Havana and found that it varied between 26·0 and 30·3 × 10^6 cubic metres per second, and Wertheim (1954), computing the transport from the electric potential between Key West and Havana, found that it varied between 14 and 39 × 10^6 cubic metres per second during the period between August, 1952 and July, 1953. The total mass transport in the Straits of Florida Section (No. 2) was computed by Montgomery to be 26·0 cubic metres per second, which is very close to the average mass transport estimated by Wertheim

Table II

Additional Atlantis stations where both salinity and oxygen anomalies indicate the presence of Caribbean water.

Sta. No.	*Position*	*Date occupied*	*Depth*	*Oxygen anomaly ml./l.*	*Salinity anomaly*
1047	37° 16′N.	19 VIII '31	87 m	– 1·37	*
	57° 54′W.		173	– 0·32	*
4762	38° 54′N.	13 VII '49	91	– 0·47	*
	60° 35′W.		135	– 1·02	*
			179	– 1·94	*
			261	– 1·00	– 4
			416	– 0·67	– 7
4811	41° 23′N.	19 VIII '49	97	– 1·07	*
	43° 23′W.		194	– 0·36	– 7

* Salinity-temperature falls within envelope on Fig. 2.

Table III

Transport of Caribbean water (anomalies of at least – ·5 ml./l.) and oxygen deficits in the section.

Section	*No.*	*Transport (10^6 m^3/sec.)*		*Oxygen Deficit (10^6 litres/sec.)*	
		Current	*Counter-current*	*Current*	*Counter-current*
Yucatan Channel	1	1·72	0·41	1·32	0·32
Straits of Florida	2	2·09	—	1·79	—
Gulf Stream	7	2·83	—	2·13	—
,, ,,	8	2·46	—	2·20	—
,, ,,	9	2·69	—	2·31	—
,, ,,	5	0·67	0·02	0·47	0·01
,, ,,	6	0·83	0·002	0·90	0·001
,, ,,	10	0·58	0·17	0·39	0·11

(27×10^6 m^3/sec). Proportionately, the transport of Caribbean water (with anomalies greater than $-0{\cdot}5$ mlO$_2$/litre) could be expected to vary between 1·08 and 3·02 million cubic metres per second and the oxygen deficit to vary between 0·92 and 2·58 million litres per second. The ranges of these quantities observed in Sections 5 through 9 are quite close to the above ranges, but the degree to which the waters have been reoxygenated by mixing cannot be estimated without better information on the distribution of oxygen and velocity across the Straits of Florida at the times corresponding to the departure of these waters from that region.

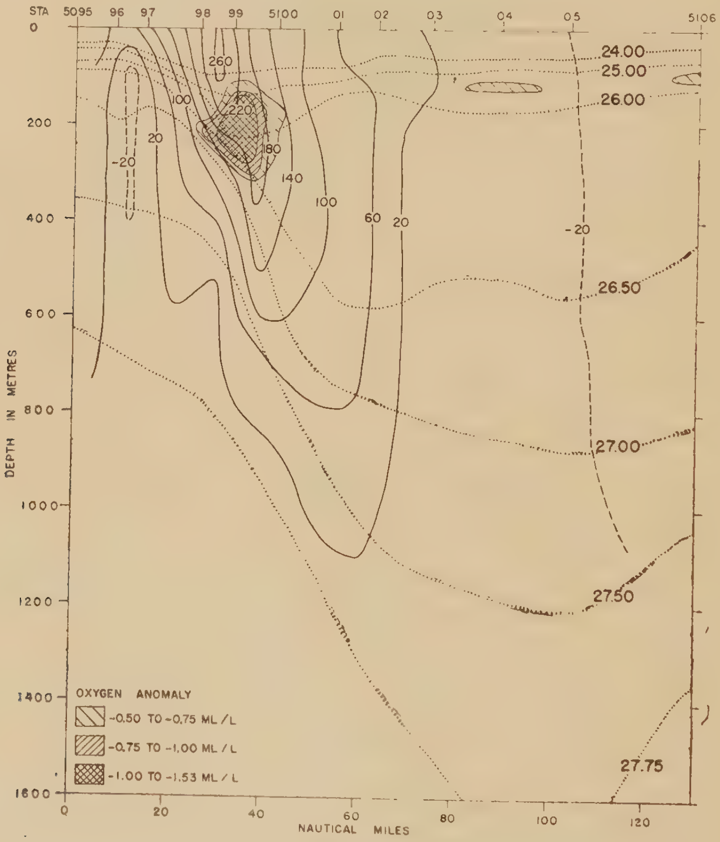

Fig. 13.

ISELIN (1940) computed that the mass transport of the Gulf Stream between Montauk Point and Bermuda varied between 93 and 76 × 10^6 cubic metres per second in 13 sections occupied between June, 1937, and January, 1940. It is apparent that the transports we have computed are smaller than ISELIN'S, but ours are limited to water which is clearly marked as of Caribbean origin by its oxygen content, and the velocity structures show that more water than this is in motion relative to the 2,000 metre level.

A further point of interest lies in comparison of Sections 5 and 6, in which both the transports and the anomalies are larger in the downstream section (No. 6)

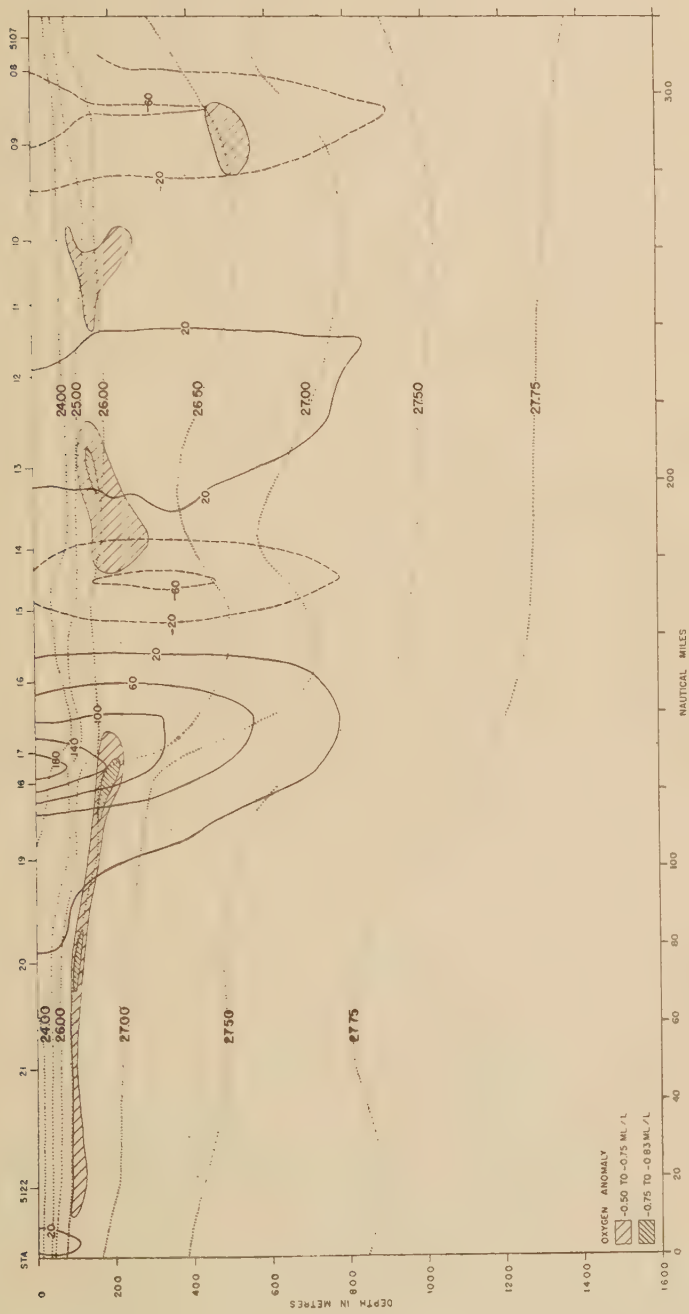
STA
5107
08
09
10
11
12
13
14
15
16
17
18
19
20
21
5122
0
200
400
600
800
1000
1200
1400
1600
DEPTH IN METRES
0
20
40
60
80
100
200
300
NAUTICAL MILES
24.00
25.00
26.00
26.50
27.00
27.50
27.75
20
60
100
140
180
-20
-60
OXYGEN ANOMALY
-0.50 TO -0.75 ML/L
-0.75 TO -0.83 ML/L

Fig. 14.

suggesting that a large decrease took place in the transport through the Straits of Florida, between the times of the emergence of these two water masses.

DISCUSSION

Negative oxygen anomalies are characteristic of the Caribbean, where they are present in quantity as shown by *Atlantis* observation of 1933 and 1934 (PARR, 1937 ; RAKESTRAW and SMITH, 1937 ; SEIWELL, 1938, Bulletin Hydrographique, 1934, 1935). The possibility that there are substantial increments of water of this type to the Gulf Stream *via* the Antilles Current has not been eliminated, and sufficient data are not now at hand to examine this possibility fully. SEIWELL'S section C (SEIWELL, 1934) from Bermuda to Hispaniola is not in sufficient detail, particularly in the upper 200 metres, to answer this question; examination of other stations occupied by *Atlantis* in the Bermuda-Hispaniola-Bimini Triangle indicate that waters meeting the oxygen and salinity criteria for Caribbean water are present, but in quite small amounts.

The Straits of Florida section may give the order of magnitude of the amounts of oxygen-low water which are available from the Caribbean to the Gulf Stream. It would have to be assumed that only a portion of the oxygen deficit emerging from the Straits of Florida will still exist at any point downstream, because of reoxygenation by vertical and isentropic mixing. According to RILEY'S (1951) estimates, it can be safely assumed that neither photosynthesis nor respiration will appreciably change the oxygen concentrations in this water mass during the time it remains unmixed in the area between Florida and Nova Scotia. RILEY estimated that consumption of oxygen in the Atlantic proceeds at the average rate of 0·21 ml./litre/year at the sigma-*t* 26·5 surface, and that the rate decreases to 0·15 ml./litre/year at the sigma-*t* 26·9 surface. Thus, except for aeration from the surface, the oxygen content should be conservative throughout the area, and it should be possible to estimate vertical and isentropic mixing coefficients from the downstream decrease of oxygen anomalies. However, this is made difficult by fluctuations in the increments of water of southern origins to the Gulf Stream system.

It is probable that variations in the flow of the Florida Current out of the Straits of Florida can account for the wide variations in the transports and oxygen deficits observed north of Cape Hatteras. If there are increments of this oxygen-low water *via* the Antilles Current, variations in this contribution might augment or dampen the effects of variation in the Florida Current. The causes of these latter variations are beyond the scope of this paper, but they may include (a) periodic fluctuations associated with the tides in the North Atlantic Ocean, the Gulf of Mexico, and possibly the Caribbean Sea (VON ARX, BUMPUS and RICHARDSON, 1954), (b) non-periodic fluctuations related to the Atlantic wind system (*op. cit.*, WERTHEIM, 1953 ; CHASE, 1954 ; STOMMEL, private communication), and (c) seasonal variations. The discontinuous observations of the oxygen anomaly at hand are insufficient to establish correlations with any of these factors. However, WERTHEIM and VON ARX *et al.*, have established that there are major fluctuations in the structure and transport of the Florida Current off Havana and off the North Carolina coast; in the latter locality it has been shown that these can occur within very short time intervals (hours). ISELIN (1940) observed that there was a seasonal periodicity in the fluctuations in the transport of the Gulf Stream between Montauk Point and Bermuda between June, 1937 and January, 1940.

The discontinuous distribution of oxygen anomalies appears to afford some confirmation of Fuglister's (1951) multiple current Gulf Stream theory. Fuglister pointed out that this multiple stream system extends at least as far southwest as Cape Hatteras. The distribution of the oxygen anomalies in the June, 1953, Onslow Bay section, as well as von Arx and Richardson's (1953) airborne observations of a discontinuous feature in the surface temperatures of the Florida Current and the Gulf Stream, suggest that the multiple current system may exist and have its genesis south of Hatteras. The discontinuous distribution of oxygen anomalies in Gulf Stream Sections 5 and 6, and their appearance in the counter-currents in Sections 4, 5 and 6, show that these waters are materially related to waters of southern origin and that the several currents and counter-currents observed contain southern water, not merely momentum transferred from southern sources.

CONCLUSIONS

1. The oxygen-sigma-*t* correlation provides a means of identifying water of southern origins in the Gulf Stream and of delineating the Stream's right-hand boundary. The relationship is especially useful in the temperature range 10 to 18 °C, where Florida Current-Caribbean Sea waters cannot easily be distinguished from Sargasso Sea waters by temperature and salinity.

2. The oxygen-sigma-*t* correlation in the Caribbean Sea, the Yucatan Channel, and the Straits of Florida shows that the Caribbean is the primary source of Gulf Stream water, although the possiblity that there are increments from the Antilles Current has not been eliminated.

3. Oxygen anomalies in two sections seaward from Onslow Bay support other observations that there are significant fluctuations and discontinuities in the Florida Current south of Cape Hatteras.

4. Wide variations in the amount of Caribbean water detectable in the Gulf Stream by the oxygen anomaly are observed between Cape Hatteras and Nova Scotia, confirming the occurrence of major fluctuations in the mass transport of the Gulf Stream.

5. Discontinuities in the oxygen anomaly in Gulf Stream sections downstream from Cape Hatteras tend to confirm Fuglister's multiple stream theory.

6. The presence of water marked by oxygen anomalies in the separate filaments of the current and in the counter-currents of the Gulf Stream shows that these currents are materially related and do not represent merely the transfer of momentum from southern sources.

ACKNOWLEDGMENT

The authors wish to acknowledge the aid of Mr. Arnold Clarke in a preliminary study of the sigma-*t*-oxygen correlations.

Without the collaboration of L. V. Worthington, the 1950 Gulf Stream sections could not have been successfully investigated. The authors wish also to acknowledge the many helpful suggestions of F. C. FUGLISTER, HENRY STOMMEL, B. H. KETCHUM, W. S. VON ARX, C. O'D. ISELIN, and D. F. BUMPUS, and the technical assistance of R. A. GESSNER and GALE PASLEY.

REFERENCES

CHASE, JOSEPH (1954), A comparison of certain North Atlantic wind, tide gauge and current data. *J. Mar. Res.*, **13** (1), 22-31.

Conseil Permanent pour l'Exploration de la Mer (1932), Bulletin Hydrographique pour l'annee 1931, 1, 2.

——————(1934), *Ibid.*, 1933, 48, 103, 104.

—————— (1935), *Ibid.*, 1934, 45, 111.

FUGLISTER, F. C. (1951), Multiple currents in the Gulf Stream system. *Tellus*, **3** (4), 230-233.

ICHIYE, T. (1954), On the distribution of oxygen and their seasonal variations in the adjacent seas of Japan (11). *Ocean Mag., Tokyo*, **6** (2), 67-100.

ISELIN, C. O'D. (1936), A study of the circulation of the western North Atlantic. *Pap. Phys. Oceanogr. Meteor.*, **4** (4), 1-101.

ISELIN, C. O'D. (1940), Preliminary report on long-period variations in the transport of the Gulf Stream system. *Ibid.*, **8** (1), 1-40.

MONTGOMERY, R. B. (1941), Transport of the Florida Current off Havana. *J. Mar. Res.* **4** (3), 198-220.

PARR, A. E. (1937), A contribution to the hydrography of the Caribbean and Cayman Seas. *Bull. Bingham Oceanogr. Coll.*, **5** (4), 1-110.

RAKESTRAW, N. W. and SMITH, H. P. (1937), A contribution to the chemistry of the Caribbean and Cayman Seas. *Bull. Bingham Oceanogr. Coll.*, **6** (1), 1-41.

RILEY, GORDON A. (1951), Oxygen, phosphate and nitrate in the Atlantic Ocean. *Bull. Bingham Oceanogr. Coll.*, **13** (1), 1-26.

ROSSBY, C.-G. (1936), Dynamics of steady ocean currents in the light of experimental fluid mechanics. *Pap. Phys. Oceanogr. Meteor.*, **5** (1), 1-43.

SEIWELL, H. R. (1934), The distribution of oxygen in the western basin of the North Atlantic *Pap. Phys. Oceanogr. Meteor.*, **3** (1), 1-86, 43 pp.

SEIWELL, H. R. (1937), The minimum oxygen concentration in the western basin of the North Atlantic. *Ibid.*, **5** (3), 1-24.

SEIWELL, H. R. (1938), Application of the distribution of oxygen to the physical oceanography of the Caribbean sea region. *Ibid.*, **6** (1), 1-60.

WERTHEIM, G. (1954), Studies of the electric potential between Key West, Florida and Havana. *Trans. Amer. Geophys. Union*, **35** (6), 872-882.

WORTHINGTON, L. V. (1954), Three detailed cross-sections of the Gulf Stream. *Tellus*, **6** (2), 116-123.

VON ARX, W. S. and RICHARDSON, W. S. (1953), The surface outcrop of the Gulf Stream front. *Woods Hole Oceanographic Institution Ref.* 53-24, 1-4. Unpublished Manuscript.

VON ARX, W. S., BUMPUS, D. F. and RICHARDSON, W. S. (1954), Short term fluctuations in the structure and transport of the Gulf Stream system. *Woods Hole Oceanographic Institution. Ref.* 54-76, 1-23. Unpublished Manuscript.

Printed in Great Britain by The Salisbury Press Ltd., Publicity House, Wilton Road, Salisbury, Wilts. (89856)

Contribution No. 706

THE EROSION OF CUMULUS TOWERS

By Joanne Starr Malkus

Woods Hole Oceanographic Institution [1,2]

and R. S. Scorer

Imperial College, University of London

(Manuscript received 5 April 1954)

ABSTRACT

A differential equation is formulated for the rate of rise of isolated buoyant elements in the atmosphere, based in part on analogy with the work of Davies and Taylor (1950) who studied the ascent of air bubbles in liquid. The equation involves a drag force which is proportional to the ascent velocity squared and which depends upon a linear dimension of the buoyant element, such as the radius of curvature of its upper surface. To eliminate this dimension from the differential equation, a law for the erosion, or rate of decrease in size of these buoyant air bubbles has been proposed. The basic assumptions are that the elements erode sufficiently slowly so that the flow around them is nearly the same as if they were in equilibrium, and that they retain their shape. From combination of the erosion law and the equation of motion, an erosion parameter, E, is derived, which to the extent that the laws are valid should be constant for all isolated cloudy bubbles, regardless of air mass or location. The erosion constant has been expressed in terms of the bubble's upward velocity, acceleration, and its buoyancy. The theory is thus subject to test in the case of cumulus towers, by simple measurements from time-lapse motion pictures and an environmental temperature sounding.

Observations of twelve relatively isolated cumulus bubbles, selected from both the trade-wind region and middle latitudes, show that E is indeed constant within the limits of measurement. A case of the aggregation of several small bubbles into a larger one is also studied, and the applicability to it of the same erosion and drag laws is established. The interaction of bubbles with one another, and with the environment to form large cumulus clouds, is discussed qualitatively.

1. Introduction

Much of the recent work on convective clouds has concentrated attention on the model of the steady-state, homogeneous, entraining updraft. This model [reviewed by Malkus (1952a)] has been extremely useful in finding and relating the orders of magnitude of many of the important parameters controlling the behavior of updrafts; and by use of ideas of entrainment, many observed features of cumulus clouds were clarified that were completely ignored in the concept of the non-interacting parcel. The assumption of a steady state, however, has so far precluded inquiry into the time dependence or life cycle of a cloud, and the actual mechanism of the entrainment has been circumvented by considering a homogeneous chimney of air whose properties differ by a discontinuous jump from those of the surroundings.

Recently an approach was suggested by Scorer and Ludlam (1953) which focuses attention on the individual buoyant elements, or bubbles, which go together to compose an updraft. If this approach can be made quantitative, it offers hope of at least partially surmounting the foregoing difficulties, simultaneously introducing time dependence and providing a mechanism for the entrainment process. The new model envisages a cumulus cloud as an aggregate of these buoyant bubbles of saturated air, which interact both temporally and spatially. The buoyancy of an individual bubble is nearly balanced by the drag caused by the deflection and flow of air around its spherical cap, so that its velocity of ascent is prevented from approaching anywhere near that of a freely accelerating parcel. The model further envisages that the bubble continuously sheds its outer skin as it rises, while maintaining the shape of its upper surface, until finally its life cycle ends when it has been completely wasted away by erosion.

Behind the flattened bubble cap is formed a turbulent wake, which is composed of a mixture of the saturated air shed from the bubble and air from the surroundings, which has been incorporated or entrained into the wake. The eddy stresses within the wake transform the potential energy released by the bubble's ascent into turbulent energy in the wake behind it. The wake thus consists of rough, slowly ascending buoyant air, with properties somewhere between those of the undiluted bubble cap and those of the surroundings. It thus consistutes a preferred region for the ascent of succeeding bubbles, protecting them from erosion by the environment.

The model further hypothesizes that large cloud

---

[1] Contribution No. 706 from the Woods Hole Oceanographic Institution.

[2] The work discussed in this article was carried out in large part under Contract N6onr-27702 (NR-082-021) between the Office of Naval Research and the Woods Hole Oceanographic Institution.

bubbles (see Ludlam and Scorer, 1953) are formed by aggregation of smaller ones and their wakes, and that a cloud which penetrates to great heights generally does so by the successive release of single bubbles. These emerge beyond the region of protection by surrounding cloud mass as isolated towers. The initial formation and maintenance of a cumulus may occur in different ways, depending on location and external conditions. A succession of bubbles may enter through the cloud base, originating from thermals in the subcloud layer; or the cloud-scale bubbles may form entirely within the cloud layer, usually at any level up to that where the environment lapse-rate becomes more stable than moist adiabatic, called the "tectonic limit" by Scorer and Ludlam (1953).

Many features of this model are supported qualitatively by observations already existing; among these are the growth of large cumuli by successive tower production (Byers and Battan, 1949), the aggregation of smaller cloud elements to form larger ones (Malkus, 1954), and others such as the rounded tops of growing cumuli which are common visual observations.

Perhaps the most promising feature of the bubble model is, however, that it points to the unit or "proton" of convection, the mechanics and life cycle of which may possibly be described analytically. If so, the way is paved for building up a cumulus by a series of interacting bubbles. The primary purpose of the present article is to formulate the laws governing the rise and erosion of a single, isolated, saturated bubble, and to test these by observations upon individual cumulus towers. It is assumed here that the erosion of isolated bubbles depends simply on a few parameters and is, to first order, independent of properties of the environment other than lapse rate. The role of the environment is held critical in the interaction of bubbles to constitute a cloud. Preliminary steps toward the aggregation of smaller bubbles into larger ones are taken in later sections.

2. Mathematical description of an isolated rising bubble

Basic structure of the model.—Many of the essential features of an isolated bubble are illustrated schematically in fig. 1. A cloud tower is considered to be composed of one or more of these elements. Each element consists of a buoyant cap with a rounded or nearly rounded upper surface. R is the radius of curvature, and D is the diameter of the cap. Two of the basic assumptions of the work are (a) that during the life of each bubble the ratio of D to R remains nearly constant (that is to say, the bubble retains its shape and aperture angle θ_m), (b) that all isolated bubbles are geometrically similar and thus may be described by fig. 1.

The interaction between each bubble and its surroundings is not ignored, but is considered paramount and is believed to have two important results: the first result is a drag upon the bubble produced by the deflection and flow of the outside air around the cap; the second is the erosion or shedding of the surface layers of the cap into the wake behind. It is with the quantitative formulation of these two effects that this section is concerned. A drag law, and thence a differential equation for the rate of rise of the bubble cap, may be developed either by use of work in turbulent hydrodynamics concerning flow around objects or by analogy with work on air bubbles in liquid by Davies and Taylor (1950). The erosion law is one of the basic assumptions of the present paper, and its justification lies primarily in the observations.

Once a visible cloud bubble is formed, it ascends through a stable environment which we assume to contain no motion left over from the ascent of previous bubbles which have evaporated completely. The surface layers of the bubble are continuously diluted by mixing and sink relatively, so that they are swept back into the wake. Undiluted air from the interior of the cap rises to the surface and maintains the large density gradient over the upper surface. The wake continues to be diluted and may often acquire negative buoyancy if evaporation takes place.

The bubble cap thus continuously decreases in size (while retaining its shape) until it is completely eroded, and at this moment undiluted air of the bubble ceases to appear at the top. The outline therefore loses its shape and becomes diffuse, while the rate of ascent becomes almost zero. At this instant, the life cycle of the element is considered ended.

During its ascent, the bubble cap follows a wet adiabat (with due allowance for the weight of accumulated water); thus, its buoyancy may be deduced

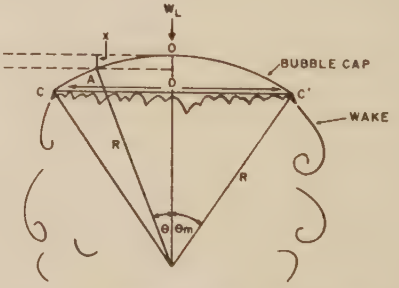

FIG. 1. Schematic diagram showing spherical upper surface *CAOC'* of buoyant bubble of radius of curvature R. Coordinates are shifted, so that bubble is at rest and surrounding fluid has undisturbed velocity w_L equal and opposite to bubble's rate of rise. Point O is stagnation point, and A is any point at angle θ from axis of symmetry. Vertical distance between A and O is x. Radius of curvature R and cap diameter D are related by equation, $\sin\theta_m = D/2R$, where θ_m is one-half total angular aperture of bubble cap.

from its level of origin and a sounding made in the surrounding clear air. The rate of rise of cumulus towers can be measured, and it is our purpose to derive as simple a law as possible to describe the dependence of the height covered by the bubble, and its time derivatives, upon the buoyancy and dimensions.

The drag law.—Since at high Reynolds numbers no properties of the surrounding fluid, such as viscosity, play a part in determining the flow, we follow practice in the aerodynamics of large bodies and assume the velocity of rise to be determined solely by the buoyancy, gB (B being the percentage excess of the outside density over that inside the bubble) and a linear dimension of the bubble, r. The limiting velocity, w_L, for a bubble that has constant B and r must then, by dimensional argument, be given by

$$w_L = k(gBr)^{\frac{1}{2}}. \tag{1}$$

If the shape and velocity are assumed unchanging, the constant of proportionality, k, is determined by the shape and by the specification of r.

Davies and Taylor (1950) showed that, for bubbles of air rising through liquid, the upper surface of the bubble is very nearly spherical. Reference may again be made to fig. 1 to clarify their work, where the frame of reference has been shifted so that the bubble's constant rate of rise w_L has been imparted to the surrounding fluid. The velocity normal to the surface of the bubble decreases away from the stagnation point O, so that the dynamic pressure decreases; at the same time, the hydrostatic pressure increases. If the bubble cap is to be in equilibrium and rising at a uniform rate (*i.e.*, w_L = constant), the dynamic pressure decrease must exactly cancel the hydrostatic increase. If the flow around the upper cap is the same as potential flow around that portion of a complete sphere, this condition is very nearly satisfied up to angles of well over 30 deg on either side of the flow axis. Thus, at any point A at an angle θ ($\leq 30°$) from the flow axis, the decrease in dynamic pressure under potential flow conditions is just balanced by the increase in static pressure due to the increment of height x. Therefore, a bubble with a spherical upper surface is a possible shape, and one that Davies and Taylor experimentally found their bubbles to maintain. At large angles, this equilibrium is no longer possible, and the spherical shape must break down.

For the bubbles studied by Davies and Taylor, $B \approx 1$; and if r is taken as the radius of curvature, R, of the bubble, they showed, using the equations for potential flow, that

$$w_L = (2/3)(gR)^{\frac{1}{2}}. \tag{2}$$

And so, if we suppose that bubbles in the atmosphere are more or less the same shape, we deduce that

$$w_L = (2/3)(gBR)^{\frac{1}{2}}, \tag{3}$$

or

$$gB = \frac{9}{4R} w_L^2. \tag{3a}$$

This indicates, as did (1), that for a given bubble the limiting velocity is proportional to $(gB)^{\frac{1}{2}}$. Since at the limiting velocity the total buoyancy acceleration is equal and opposite to the drag force per unit mass [as expressed in (3a)], the drag must be proportional to w^2, in accordance with the normal behavior of large bodies. If K is the constant of proportionality between w_L^2 and the drag force per unit mass, we find by (3) and (3a) that

$$K = \frac{gB}{w_L^2} = \frac{9}{4R}, \tag{4}$$

or, using (1) without drawing upon the work of Davies and Taylor, we have

$$K = (gB/w_L^2) = (1/k^2 r). \tag{4a}$$

A differential equation for the rise of bubbles of decreasing size.—If R is decreasing with time, as will be the case if the bubble is eroding, (3) tells us that w_L will be decreasing with time. Thus, at any instant, the bubble will be rising at a rate greater than w_L and decelerating due to an excess of drag over buoyancy. A differential equation for its rise is thus required, which may be shown to be

$$\alpha \dot{w} = -Kw^2 + gB, \tag{5}$$

where $\dot{w} = dw/dt$, and w is the actual ascent velocity. α is a number, probably between 1 and 3/2, which indicates that, in accelerating a body immersed in a fluid, some of the fluid must also be accelerated, so that the body possesses an apparent mass greater than its own.

Equation (5) states that the vertical acceleration of the bubble cap is equal to the resultant of the forces (per unit mass) acting upon it, namely the buoyancy minus the drag. Its applicability to cloudy bubbles depends only upon the assumption that the drag upon an eroding bubble is the same as that which would obtain if the bubble were not eroding, but in equilibrium. The flow around an eroding bubble will approach that around an equilibrium bubble, the slower the erosion and the nearer the actual velocity, w, to w_L. That the cloud towers studied possessed rates of rise very near that of equilibrium will be demonstrated in the observations to follow.

If (4) for K may be substituted into (5), we have

$$\alpha \dot{w} + \frac{9}{4R} w^2 = gB. \tag{5a}$$

We can proceed further with (5a) in application to cloud towers only if R may somehow be specified as a function of time. This involves the formulation of an erosion law, which is discussed in the following paragraphs.

The erosion law.—The model suggests that the rate of erosion depends mainly upon the density difference between the bubble and its surroundings. The relationship suggested first was that the rate of decrease of bubble volume depended on the buoyancy and the exposed area. Thus,

$$dR^3/dt = -3EgBR^2, \tag{6}$$

where E is a coefficient to be determined. Carrying out the differentiation on the left side of (6), we obtain

$$dR/dt = -EgB, \tag{7}$$

in which E has the dimensions of time. It is not clear how a coefficient with such dimensions can arise from the conditions of the problem, and it might be more natural to expect a relationship of the form

$$dR/dt = -E'(gBR)^{\frac{1}{2}}; \tag{8}$$

but this makes the erosion very nearly proportional to the velocity (for w is not very different from w_L) and, as described below, does not fit the observations well.

If we suppose the more general law,

$$dR/dt = -E(gB)^{m+n}R^n, \tag{9}$$

then, if B is constant, or the environment lapse rate is moist adiabatic,

$$R^{1-n} = (1-n)E(gB)^{m+n}(-t), \tag{10}$$

if we measure time backwards from the moment of exhaustion of the bubble. Upon substituting (10) into (5a) and rearranging, we obtain

$$\frac{9}{4}\{(1-n)E\}^{-1/(1-n)} = \frac{gB^{(m+n)/(1-n)}(gB - \alpha\dot{w})(-t)^{1/(1-n)}}{w^2}. \tag{11}$$

If we choose first that early part of the bubble's ascent in which $gB \gg \dot{w}$, we have

$$(-t)^{1/(1-n)} = \text{const} \times w^2, \tag{12}$$

and the observations to be described satisfy this well if $n = 0$. This determination of n does not depend on the actual value of B, but only upon the assumption that B is constant, which was the case in those observations used.

To determine m, we again consider only the early part of the ascents in which the $\dot{w}$ term may be ignored in comparison to gB. We first took a few of the most accurately measured bubbles with different buoyancies, B, and found an m that gives the same value of E for all bubbles. Secondly, we took several cases[3] where gB changes as a function of time and applied a similar test. With the observations presently available, $m = 1$ gives the best fit. For only a small part of the ascent is $\dot{w}$ comparable to gB, and the observations are not sensitive enough for us to determine α. Furthermore, the shedding of mass from the bubble into the wake acts to compensate the excess apparent mass. Since both effects may be shown to be small, we therefore put $\alpha = 1$ and obtain

$$G \equiv \tfrac{3}{2}E^{-\frac{1}{2}} = \frac{(-t)^{\frac{1}{2}}gB(1 - \dot{w}/gB)^{\frac{1}{2}}}{w}. \tag{13}$$

The equation is solved for a constant proportional to E, to test its validity with observations; as a differential equation for w as a function of time it is of a nonlinear type which cannot be readily solved. The right-hand side of (13) can be determined from observations of buoyancy and rate of rise of a bubble; and if the theory is correct, E and thus G should be constant both throughout the life of a single bubble (even when $\dot{w}/gB \to 1$), and from one bubble to the next regardless of air mass and surroundings.

Furthermore, if $n = 0$ and $m = 1$, (9) becomes identical with (7), and if the buoyancy is constant may be integrated to give

$$R = EgB(-t). \tag{14}$$

Equation (13) could have been obtained by substitution of (14) into (5a) and rearrangement.

It must be emphasized that the observational testing of (13) would be no different had (4a) been used for K in the differential equation (5), provided only that the linear dimension r obeys an equation like (14). If the analogous equation to (14) is

$$r = E''gB(-t), \tag{14a}$$

using (4a) and (5) we get, with $\alpha = 1$,

$$G'' \equiv \frac{1}{k}(E'')^{-\frac{1}{2}} = \frac{(-t)^{\frac{1}{2}}gB(1 - \dot{w}/gB)^{\frac{1}{2}}}{w}, \tag{13a}$$

the observational testing of which would differ in no way from that of (13) which follows. Thus, the entire theoretical model used could have been constructed without drawing upon the work on bubbles by Davies and Taylor (1950) and without assuming that cloud towers possess spherical upper surfaces. The only assumptions upon which (13a) depends are a slow decrease of linear dimension of the form (14a), and little or no change in shape of the elements during their lifetime. The model of Davies and Taylor and the bubble approach suggested here, however, are felt to contribute to visualization of mechanism, both concerning the maintenance of shape and the production of a wake, and seem justifiable in view of the common observation that active cumulus towers are generally rounded on top.

---

[3] These cases will appear in a forthcmoing paper in *Tellus*, "On the structure of some cumulonimbus clouds which penetrated the high tropical troposphere" by Joanne Starr Malkus and Claude Ronne. Unpublished manuscript at present on file at the Woods Hole Oceanographic Institution.

Variable buoyancy.—In general, the lapse rate of the bubble's environment may differ from moist adiabatic, and B will change with time as the bubble rises. If B is specified as a function of time, (7) may be integrated and the effect of a variation of B along the path of the bubble may be investigated.

If, for a simple example, we put

$$B = B_0 e^{\gamma t}, \tag{15}$$

we find that $(-t)^{1/2}$ in (13) is replaced by $[(e^{-\gamma t}-1)/\gamma]^{1/2}$, which is equal to $(-t+\frac{1}{2}\gamma t^2-\cdots)^{1/2}$, while the rest of the formula remains unchanged. If the buoyancy increases by one third in 100 sec, $\gamma t \approx 0.3$, and the error in G caused by writing $(-t)^{1/2}$ in the formula is less than 10 per cent. This is a much larger change in buoyancy than is usually observed, and so we will use (13) unchanged but will write in the actual (variable) value of B. Only three of the twelve observational cases to follow exhibited variable buoyancy, but in these cases (13) proved equally satisfactory as in the others.

A similar conclusion is arrived at by using any simple expression for B as a function of time. If a sudden large change in B occurred during the ascent of the bubble, the formula would apply to the two parts of the ascent only if a different origin were used for t for the two parts of the ascent; but this has not occurred in our observations.

The effect of wind shear.—If the bubble ascends through a shearing wind field, it will acquire a horizontal velocity relative to its surroundings, as well as its upward motion. If u is this relative horizontal velocity of the bubble, the total vector drag-force per unit mass is $K(u^2+w^2)$. If the horizontal velocity of the environment is U, a function of z, the horizontal acceleration of the bubble (relative to a fixed x-axis chosen in the direction of U) is $d(U+u)/dt$. The relative horizontal velocity u is only large near the beginning of the bubble's life cycle, when it is only slowly varying with time. Under these conditions, when the shear is constant,

$$du/dt \ll dU/dt = w\,dU/dz, \tag{16}$$

and

$$d(U+u)/dt \approx w\,dU/dz. \tag{17}$$

If the bubble reached its limiting velocity, the buoyancy, the total vector drag, and the total acceleration would be balanced, and so

$$K(u_L^2+w_L^2) = [g^2B^2 + w_L^2(dU/dz)^2]^{1/2}. \tag{18}$$

By (3),

$$(u_L^2+w_L^2)^{1/2} = (2/3)\{[g^2B^2 + w_L^2(dU/dz)^2]^{1/2}R\}^{1/2}. \tag{19}$$

Equations (18) and (19) give $K = 9/4R$ as before; but if the drag were proportional to any other power of the velocity than the square, K would depend upon B and dU/dz. In fact, however, this result means that the bubble is unaltered in shape although its axis is inclined to the vertical at an angle β, where β is $\sin^{-1}[u/(u^2+w^2)^{1/2}]$.

The vertical component of the drag, therefore, becomes

$$(\cos\beta)K(u^2+w^2) = [w/(u^2+w^2)^{1/2}]K(u^2+w^2), \tag{20}$$

so that (13) is altered to

$$G \equiv \tfrac{3}{2}E^{-1/2} = \frac{(-t)^{1/2}gB(1-\dot{w}/gB)^{1/2}}{[w(u^2+w^2)^{1/2}]^{1/2}}. \tag{21}$$

The equation for the horizontal motion of the bubble near the beginning of its life is thus

$$w\frac{dU}{dz} \approx -\frac{u}{(u^2+w^2)^{1/2}}\frac{9}{4R}(u^2+w^2). \tag{22}$$

so that

$$\frac{u}{w} \approx \frac{4R\,dU/dz}{9(u^2+w^2)^{1/2}}. \tag{23}$$

In the case of the highest wind shear presented in this article, namely 5 (m/sec)/km on 14 August 1950, we find that, when $R = 5 \times 10^4$ cm, $u/w \approx 1/4$. Later in the ascent, this ratio decreases as R decreases. Then $(u^2+w^2)^{1/2} \approx 1.03\,w$, and the error in setting this equal to w is much less than that of the buoyancy determination in the present work. The wind-shear effect only becomes significant for shears of about 20 (m/sec)/km.

The importance of this conclusion is that it is not at present possible to measure u accurately, while a large shear is desirable because it isolates a bubble from others and makes it readily observable for testing (13).

3. Observations on isolated cumulus towers

The primary purpose of the observational work is to test the constancy of E in (13) over the total lifetime of numerous bubbles of varying size and surroundings. A superficial examination of time-lapse photographs reveals many cumulus towers sufficiently isolated for the equation to be applicable to them. It was envisaged (by Scorer and Ludlam), however, that each bubble or tower would be composed by aggregation of several smaller ones. This process has been observed in the trade-wind region and described qualitatively by Malkus (1954). The composite nature of the large bubbles used in the present study was apparent from the time-lapse films. In general, the uppermost visible part of a rising tower ascends somewhat irregularly, while the upper limit of a smoothed outline ascends with a more slowly varying speed. It is sometimes possible to make measurements both on the bubble as a whole and on the individual ones of which it is composed, if at any time they emerge from the top long enough to make an ascent alone in the clear air. It is significant that (13) has been applied successfully both to composite and to individual bubbles, and this strengthens the contention that the theory describes a real process, and that not only are cloudy bubbles built up from several smaller ones, but that we may treat the composite ones just like the individuals. After discussion of the measurements on several cases of isolated single bubbles, a case of aggregation of several of these individuals into a composite bubble will be considered.

The time-lapse motion pictures used were made on field programs of cumulus studies by the marine meteorology group of the Woods Hole Oceanographic Institution. A group of films was used from the Nantucket program of the summer of 1950 (see Malkus and Bunker, 1952; Malkus, 1952b; Malkus and Stern, 1953), and another group from the Caribbean expeditions of 1952 and 1953 [described in part by Malkus (1954)]. The measurements were made by projecting the films in a microfilm reader. The height of the cloud base was known from airplane observations (usually of the same clouds being photographed, while the photography was in progress) and the cloud-top height was derived from the height of it and the base above the horizon. Errors due to the earth's curvature and to the height of the camera above sea level were found to be negligible. The height of each tower was plotted against time (the camera shutter was automatically tripped at a fixed interval), and a curve was drawn to smooth out the irregularities produced by the knobby surface of the tower.

The vertical velocity was drawn to be reduced to zero at the end of each ascent; but since we are concerned with the velocity relative to the air, and the air may have been ascending slowly above the buoyant wake, it is likely that the deceleration of the bubble in its final stages has been overestimated, though the velocity would not be seriously affected. This would lead to an overestimation of G in the last second or so, which is indeed observed in many cases.

Altogether, twelve cases of individual bubbles were studied; in nine of these, the environment lapse-rate was such that a constant value of buoyancy could be used. Estimation of the bubble buoyancy, gB, from the clear-air sounding was the most difficult and uncertain of the evaluations from the observations in the testing of (13). Although the bubble caps rise along moist adiabats, the choice of the proper moist adiabat in each case requires knowledge of the temperature excess of the bubble at its level of origin. The formula $gB = g(T_v - T_v')/T_v'$ was used in all the buoyancy calculations, where T_v is the virtual temperature of the bubble, obtained from the appropriate adiabat, and T_v' is the virtual temperature of the environment, calculated from the sounding curve. However, in several of the cases a sizeable negative correction to the buoyancy must be expected from the presence of liquid droplets suspended in the cap. Fortunately, three of the twelve bubbles (see in table 3 the two bubbles on 18 March 1953 and the one of 2 April 1953) were trade-wind bubbles which originated at or very near cloud base and could be shown to have a negligible (<15 per cent) correction to gB due to liquid water. Since it has been demonstrated by other work (Bunker *et al*, 1949; Malkus, 1954) that at cloud base the only excess buoyancy of trade cumuli is due to water-vapor content, in these cases the moist adiabat intersecting the actual sounding at cloud base could be picked with confidence and gB for each bubble estimated therefrom. In these cases, G averaged about 0.20 ± 15 per cent, giving E, the erosion constant, as 50 sec ± 23 per cent, or 50 ± 12 sec. In evaluation of the remaining cases, gB was estimated from the soundings with this average value of G in mind, and it was determined whether the consequent liquid-water content and excess buoyancy at bubble origin were consistent and reasonable. This procedure is illustrated in detail in succeeding paragraphs. Eight of the twelve cloud towers studied appeared over Nantucket Island, Massachusetts, and four were towers from oceanic trade cumuli in the Caribbean. A typical case from each of these two groups will be presented in detail, and those remaining will be briefly summarized.

Case of 14 August 1950, Nantucket.—On this occasion, vast amounts of supplementary data were available. The cloud studied is shown in fig. 2, which was obtained by tracing one of the frames from the time-lapse film. The entire sequence of photographs has been reproduced in an earlier study of the slopes of

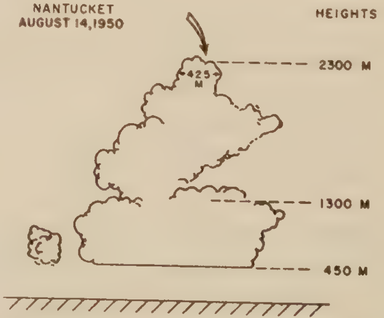

Fig. 2. Tracing, from time-lapse film for 14 August 1950, of cloud over Nantucket Island [see Malkus (1952b, fig. 6) for actual film sequence]. Bubble studied is indicated by arrow. Tracing made at frame corresponding to starred observation in table 1.

TABLE 1. Bubble of 14 August 1950, Nantucket. Height range studied: 2200 to 2600 m. Cloud base: 450 m. $gB = 8.2$ cm/sec² = constant. $\bar{G} = 0.200$. $\Delta = 20$ per cent.

Observation number	$-t$ (sec)	$(-t)^{\frac{1}{2}}$ (sec$^{\frac{1}{2}}$)	w (cm/sec)	$\dot{w}$ (cm/sec²)	$\dot{w}/gB$	G (sec$^{-\frac{1}{2}}$)	R_{scale} (m)	w_L (cm/sec)	$\frac{w-w_L}{w_L}$	$(1-\dot{w}/gB)^{\frac{1}{2}}-1$
1	108	10.4	428	−0.82	−0.091	0.21	445	400	0.07	0.05
2*	96	9.8	410	−0.82	−0.091	0.20	390	380	0.08	0.05
3	84	9.2	395	−0.98	−0.119	0.20	345	352	0.12	0.06
4	72	8.5	378	−1.15	−0.140	0.20	295	326	0.16	0.07
5	60	7.8	355	−1.30	−0.159	0.19	245	300	0.18	0.08
6	48	6.9	326	−1.64	−0.200	0.19	195	268	0.22	0.09
7	36	6.0	306	−2.80	−0.342	0.19	150	232	0.32	0.16
8	24	4.9	276	−5.43	−0.661	0.19	100	187	0.47	0.29
9	12	3.5	197	−11.80	−1.44	0.23	50	133	0.48	0.57

* Diameter of bubble measured on film at this frame to be 425 m.

these clouds by Malkus (1952b, fig. 6) [see also Malkus and Bunker (1952) and Malkus and Stern (1953)]. The bubble selected is the topmost forming the cloud turret and is indicated by the arrow. The wind shear on this day was so high [5(m/sec)/km] that successive bubbles were unable to interact, and the cloud tower disappeared at a height where the environment lapse-rate still exceeded moist adiabatic.

The measurements from the time-lapse films are shown in fig. 3. The points give the height of the bubble cap at each frame (3 sec apart), beginning when the bubble emerges from the cloud, until it reached nearly its maximum height and the film showed its edges becoming fuzzy. At this frame, as nearly as it could be specified, t was set equal to zero. A smooth curve is drawn through these points on fig. 3, and observations were read off every fourth point, or 12 sec apart. Velocities were found by taking first differences of these heights, and accelerations by taking second differences. These second differences are indicated by x's in the inset graph of fig. 3, converted into centimeters per second per second, and a smooth curve is drawn through them. The accelerations used in table 1 are taken from the smoothed curve, and the velocities are usually smoothed in a similar manner. If the buoyancy gB is taken as a constant equal to 8.2 cm/sec² (to be discussed presently), the value of G comes out for each observation as shown in table 1.

The buoyancy acceleration of the bubble of 8.2 cm/sec², which was chosen to give an average G of approximately 0.20, was checked from a clear-air sounding (fig. 4) made very near the clouds, according to the following procedure. The level of bubble origin was estimated from the time-lapse films to be about 1300 m. At this level, also a visible transition from main cloud body to "turret" appeared to take place, thus indicating the tectonic limit. This division is discernible in fig. 2. If the left-hand dotted adiabat in fig. 4 is chosen for the bubble — *i.e.*, if it had no excess temperature over the surroundings at its level of origin — a buoyancy averaging 8.2 cm/sec² and only increasing slightly upward is obtained. This, however, ignores the presence of liquid water which, as the sounding shows, may attain a value as high as 2 g/m³ near the top of the bubble's height range. The negative buoyancy contributed by this weight of liquid water is about 23 per cent of the net buoyancy in the table. If, however, the bubble starts with an

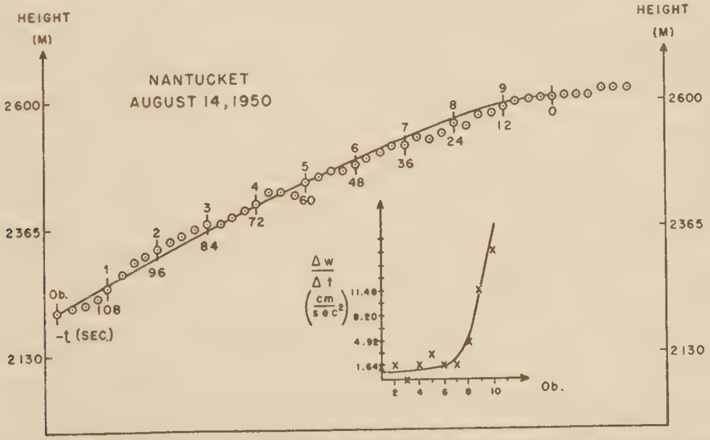

FIG. 3. Main curve shows height as function of time for bubble indicated in fig. 2. Points correspond to each frame on film (3 sec apart), and tabulations (table 1) were made every fourth point (12 sec apart). Vertical velocities were obtained from smoothed curve of first differences of these heights, and accelerations from smoothed curve of second differences. Latter curve is shown in inset graph, with units converted to c.g.s. Negative of acceleration is plotted for convenience.

excess temperature of 0.5C relative to its surroundings and follows the solid adiabat on fig. 4, the buoyancy corrected for weight of liquid water comes out very nearly (within 10 per cent) a constant figure of 8.2 cm/sec² throughout the height range studied. The bubble's increasing virtual-temperature excess toward the top may be shown to be closely compensated by the rate of accumulation of water if no precipitation is occurring, as was the case. The moist adiabat originating from the sounding at cloud base is shown, for reference, by the right-hand dashed curve on fig. 4. These large bubbles are believed to be formed by an aggregation of smaller saturated bubbles and more dilute wake material. The degree of dilution represented by a 0.5C temperature excess of cloudy over clear air at 1300 m may be shown very plausible from entrainment calculations made in a previous study of these same clouds (Malkus, 1952b), and also from actual airplane-made temperature cross-sections through the clouds.[4]

Thus, by the use of supportable assumptions concerning the buoyancy acceleration of the bubble, an average value of G, called $\bar{G}$ in the caption of table 1, of 0.20 is found. Furthermore, the percentage spread in G (called Δ) throughout this bubble's life is only 20 per cent, or not in excess of observational error.

Now the last four columns in the table may be discussed. To test the internal consistency of the bubble model, and especially the assumption that w did not greatly exceed w_L, R may be calculated from (14) with use of $E = 50$ sec. The limiting velocity, w_L, is then calculated from (3) with use of this value of R. The actual w is seen always slightly to exceed this calculated w_L. The fraction by which w exceeds w_L is calculated in the next-to-last column. It is possible to make an independent check computation of this fraction by solving (5a) for w, and subtracting w_L from the numerator and dividing by it. This gives, after substitution of (3),

$$(w - w_L)/w_L = (1 - \dot{w}/gB)^{\frac{1}{2}} - 1. \tag{24}$$

The last column shows the fractional departure of w from w_L found by use of this method. Since a 1 m/sec error in measuring w may give an error in this quantity of 100 to 200 per cent, the agreement between the two methods may be considered very satisfactory. The angular half-aperture of the bubble may be calculated from the relation (see fig. 1)

$$\sin\theta_m = \tfrac{1}{2}D/R. \tag{25}$$

With use of the measured value of D at the second observation and the corresponding R, θ_m comes out as 33 deg, which is on the small end of the range studied by Davies and Taylor (1950).

Next, a trade-cumulus bubble is considered.

Case of 30 June 1952, St. Croix.—The largest bubble of the twelve, and also the one which penetrated to greatest altitude, was photographed on this day from the island of St. Croix, Virgin Islands. Although the films lacked sufficient contrast for reproduction, one of the frames is traced in fig. 5, which shows the dimensions and appearance of the bubble studied. This case was particularly important because it was the only one permitting a direct check of the erosion law. The same calculations as made for the preceding bubble are presented in table 2. The frames

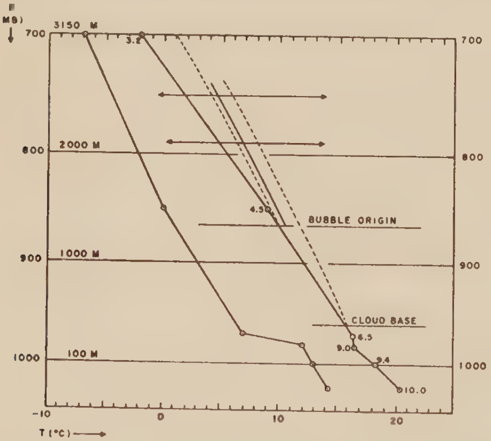

FIG. 4. Radiosonde observation made in clear air over Nantucket Island, 1500 *GCT* 14 August 1950. Right-hand solid curve is temperature; Left-hand curve is dew point. Mixing ratios (g/kg) are entered next to temperature curve. Remaining three curves are moist adiabats; central one is hypothesized to be curve followed by cloudy bubble (see text). Height range studied in table 1 is delimited by horizontal arrows.

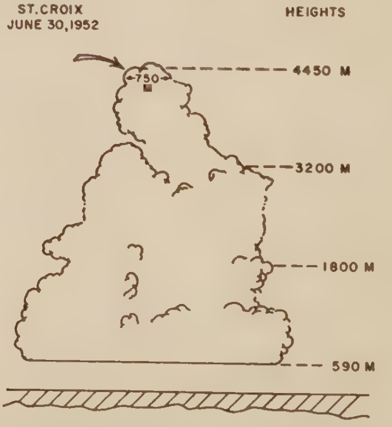

FIG. 5. Tracing from time-lapse film taken from St. Croix, 30 June 1952. Arrow indicates cloud bubble studied. Tracing made from frame corresponding to starred observation in table 2. Height and distance scales determined from film and simultaneous airplane determination of cloud-base height. Camera was pointed almost due south, and wind blew from east (left to right).

---

[4] Unpublished data, on file at the Woods Hole Oceanographic Institution, taken in connection with an observational study of the air flow over a heated island by Malkus and Bunker (1952).

Table 2. Bubble of 30 June 1952, St. Croix. Height range studied: 2900 to 4950 m. Cloud base: 590 m. $gB = 10.0$ cm/sec² ≈ constant. $\bar{G} = 0.204$. $\Delta = 15$ per cent.

Observation number	$-t$ (sec)	$(-t)^{\frac{1}{2}}$ (sec$^{\frac{1}{2}}$)	w (cm/sec)	$\dot{w}$ (cm/sec²)	$\dot{w}/gB$	G (sec$^{-\frac{1}{2}}$)	R_{calc} (m)	w_L (cm/sec)	$\frac{w-w_L}{w_L}$	$(1-\dot{w}/gB)^{\frac{1}{2}}-1$
1	297	17.2	860	−0.38	−0.038	0.20	1500	820	0.05	0.02
2	273	16.6	846	−0.63	−0.063	0.20	1380	785	0.08	0.03
3	249	15.8	846	−0.87	−0.087	0.20	1260	750	0.13	0.05
4	225	15.0	830	−1.20	−0.120	0.19	1135	710	0.17	0.06
5	201	14.2	795	−1.64	−0.164	0.19	1015	670	0.19	0.08
6	177	13.3	755	−2.08	−0.208	0.19	895	635	0.19	0.10
7	153	12.4	710	−2.52	−0.252	0.20	770	585	0.21	0.12
8*	129	11.3	634	−2.96	−0.296	0.20	650	540	0.17	0.14
9	105	10.3	550	−3.34	−0.334	0.22	530	485	0.13	0.15
10	81	9.0	483	−3.53	−0.353	0.22	410	428	0.13	0.16
11	57	7.5	400	−3.93	−0.393	0.22	285	358	0.12	0.18
12	33	5.7	320	−4.72	−0.472	0.22	165	273	0.17	0.21
13	9	3.0	196	−6.30	−0.630	0.20	45	141	0.39	0.28

* Diameter measured as 750 m.

were 6 sec apart, and measurements were made every fourth frame.

A constant buoyancy of 10.0 cm/sec² was taken, to give the average value of G shown. The support of this choice from the sounding is shown in fig. 6. On this occasion, not only did the films indicate that the large bubbles were forming at about 1800 m, but the sounding showed that the external lapse rate exceeded moist adiabatic up to that level, above which it became moist adiabatic, thus clearly indicating the tectonic limit. If the bubble started at this level with no excess temperature over the clear-air surrounding, it would follow the left-hand dashed adiabat in fig. 6. If no correction for liquid water is required, this adiabat gives an average buoyancy of 10.0 cm/sec², which, however, increases markedly near the top. The sounding indicates, however, that the liquid-water content near the top of the bubble's height range may be 4 to 6 g/m³. Since clouds even smaller than this size were found by the aircraft to be precipitating internally, the smaller figure of 4 g/m³ is chosen. This would mean a negative buoyancy of about 4.0 cm/sec². The negative buoyancy due to liquid water may be just balanced, however, and a nearly constant net buoyancy of 10 cm/sec² arrived at, if the bubble follows up the solid adiabat in fig. 6. This implies a temperature excess at the tectonic limit of 1.1C, which is consistent with the rather small entrainment rate which might be expected on this day of weak wind shear. Airplane cross-sections[5] through several somewhat smaller clouds in the area at 1800-m heights gave average temperature excesses within cloud ranging from 0.8 to 1.0C.

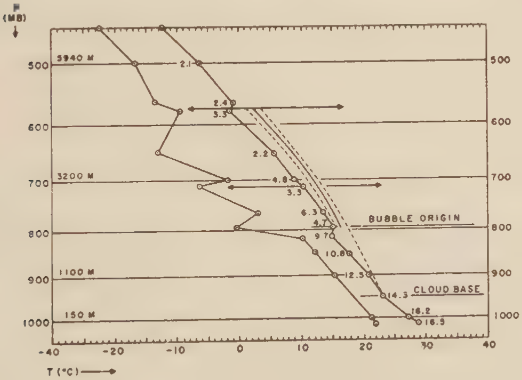

Fig. 6. Clear-air sounding in vicinity of St. Croix, 30 June 1952 (combination airplane sounding at low levels and San Juan radiosonde at upper levels). Right-hand solid curve is temperature; Left-hand curve is dew point. Mixing ratios (g/kg) are entered next to temperature curve. Remaining three curves are moist adiabats; Central one is hypothesized to be curve followed by cloud bubble (see text). Height range studied in table 2 is delimited by horizontal arrows.

Thus, again with the use of supportable assumptions concerning gB, table 2 shows a $\bar{G}$ in this case which is nearly identical to that for the Nantucket cloud previously studied, despite an entirely different air mass and location, and far weaker wind shear. The percentage variation in G during this bubble's life (Δ) is smaller than previously and does not exceed the error of the observations.

This bubble was so isolated on the film, and maintained such a smooth spherical cap, that it was possible

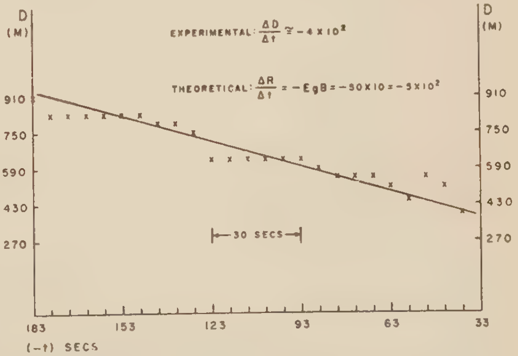

Fig. 7. Diameter of bubble as function of time, St. Croix, 30 June 1952. Times correspond to those in table 2, with $t = 0$ at bubble's demise.

---

[5] Unpublished data on file at the Woods Hole Oceanographic Institution.

TABLE 3. Radius and w_L calculation for each bubble, and comparison of values of $\bar{G}$. (T denotes trade-wind clouds; remainder formed over Nantucket Island.) $\bar{\bar{G}} = 0.20 \approx 0.2$. $\bar{\Delta} = 15$ per cent.

Bubble (Date and number)	Δ (%)	D (measured) (m)	R (calc. from E) (m)	w_L (calc.) (cm/sec)	$\frac{w - w_L}{w_L}$ at $(-t)$*	$(1 - \dot{w}/gB)^{\frac{1}{2}} - 1$ at $(-t)$*	$\bar{G}$ ($\mathrm{sec}^{-\frac{1}{2}}$)
14 Aug.	20	425	390	380	0.08	0.05	0.20
T 30 June	15	750	650	540	0.17	0.14	0.20
T #1, 18 March	25	160	145	220	0.27	0.07	0.20
T #2, 18 March	20	340*	345	350	0.09	0.04	0.19
T 2 April	20	290	240	250	0.11	0.07	0.19
#4, 8 Aug.	29	250	230	260	0.27	0.12	0.21
#5, 8 Aug.	29	250	270	355	0.20	0.09	0.21
#6, 8 Aug.	32	250*	240	356	0.22	0	0.21
#7, 8 Aug.	45	dimension too difficult to measure	260	285	0.16	0.10	0.22
#8, 8 Aug.	70	280	250	280	0	−0.14	0.20
#9, 8 Aug.	21	310	300	370	0.19	0.06	0.19
#10, 8 Aug.	5	390	465	455	0.10	0.08	0.21

* Very rough measurement.

to measure the cap diameter with some confidence from $t = -183$ to $t = -33$ sec. The results are plotted in fig. 7. A straight line was fitted to these points; it has a slope $\Delta D/\Delta t = -4 \times 10^2$ cm/sec. Since the diameter of a bubble, according to the model, should be proportional to the radius of curvature, and they are shown in examples below to be about equal, $\Delta D/\Delta t$ should equal $\Delta R/\Delta t$. When $\Delta R/\Delta t$ is calculated from (7), it comes out as $\Delta R/\Delta t = -EgB = -50 \times 10 = -5 \times 10^2$ cm/sec. Thus, the observed slope departs from the theoretical by only 20 per cent (about the accuracy with which the measured values of D adhere to the straight line in fig. 7), and we may consider that the erosion law has been directly checked in this one case. The half-aperture θ_m was calculated for $t = -129$ sec to be 35.5 deg; and since the bubble was seen to retain its shape throughout the times represented in fig. 7, it may be deduced that this angle remained very nearly constant throughout its lifetime.

Summary of observations of individual bubbles.—The calculations of $\bar{G}$ for the remaining bubbles were carried out essentially in the same manner as for the two cases just presented, and the results are summarized in table 3. In none of the remaining ten bubbles did the buoyancy correction due to liquid water amount to as much as 15 per cent of the net buoyancy; thus, it was ignored. The determination of gB for 18 March and 2 April 1953, was straightforward and has already been discussed earlier in this section. The case of 8 August will be described in section 4, below.

The table shows that the average value of $\bar{G}$, called $\bar{\bar{G}}$, for all the bubbles is just slightly greater than 0.2 $\mathrm{sec}^{-\frac{1}{2}}$. With use of $\bar{\bar{G}}$ in (13), the average value of E comes out to be 54 sec; it will henceforth be taken as 50 ± 10 sec, since the accuracy of the observations is such that only the first figure is significant. The total percentage spread in $\bar{G}$, called $\bar{\Delta}$, is 15 per cent, which is within the accuracy of the measurements. Within the lifetime of each single bubble, the percentage scatter in G is given by the column marked Δ (see tables 1 and 2). Only in the cases of bubbles 7 and 8, on 8 August 1950, is the variation in G large within the life of a single bubble. On this occasion, bubbles were followed very closely in one another's wakes and were readily combining to form larger cloud towers. The ascent velocities fluctuated widely and were frequently higher than expected. It appears that the laws for isolated elements only hold rather poorly when bubbles are being pushed upward by neighbors or wakes, or are perhaps also being protected by them from erosion.

The average angular half-aperture θ_m of the bubbles may be estimated by comparing values of the bubble diameter D, measured from one frame on the film for each bubble (the starred observation in tables 1 and 2), and the corresponding radius of curvature R, calculated from (14), $R = -EgBt$. Comparison of columns three and four in table 3 shows that the average ratio D/R is approximately one, giving an average θ_m of 30 deg. The few cases where it was possible to measure D fairly accurately (14 August and 30 June) indicate that that θ_m probably should be a few degrees larger than this. The next column in table 3 gives w_L at the same frame, calculated with use of the values of R in (3). The fractional departure of the measured w from w_L is also given in the table and should be equal to $(1 - \dot{w}/gB)^{\frac{1}{2}} - 1$, which is presented beside it [see (24)]. Although the departures between these two sets of results are within observational error, it will be noted that the one calculated from accelerations is systematically smaller than the other. This may perhaps be an indication that α should have been chosen greater than one in (5a). It may only indicate that the method of measuring $\dot{w}$ from the films, using smoothed second differences in heights, gives results which are systematically too small. There is no apparent theoretical way of arriving at any factor α greater than one to be multiplied by the inertial term in (5a); even if there were,

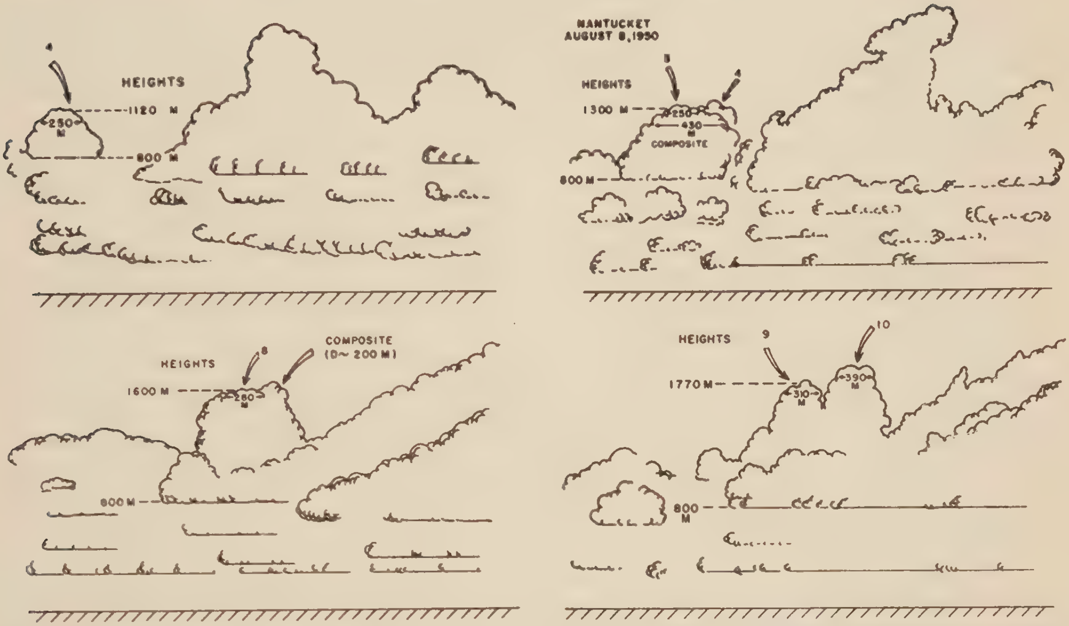

Fig. 8. Selected tracings, from time-lapse film for 8 August 1950, of clouds formed over Nantucket Island [see Malkus (1952b, fig. 8) for actual film sequence]. Bubbles studied are indicated by arrows. Frames shown are separated by approximately following time intervals: top left to top right, 1½ min; top right to bottom left, 2 min; bottom left to bottom right, 2½ min.

no way exists at present of testing it observationally. Therefore, nothing will be done here to complicate the model, which has worked out quite satisfactorily.

Thus it may be concluded that, for relatively isolated cloud bubbles, the proposed force and erosion laws are applicable. The importance of this conclusion lies in the simplicity of the laws and the independence of the bubble's life cycle from government by vast numbers of environmental parameters. To progress from a single bubble to a cumulus, however, we must consider the interaction of many bubbles with one another and with their environment, and we must eventually attempt to study the process of wake formation. As a first step in the direction of this building process, the interaction of several bubbles to produce a larger one may be considered, since information on this point is at present available.

4. Formation and life cycle of a composite bubble

In the foregoing work, bubbles ranging in diameter from 100 m to about 1 km were studied. Some of the larger ones were visibly composed of bubbles of a

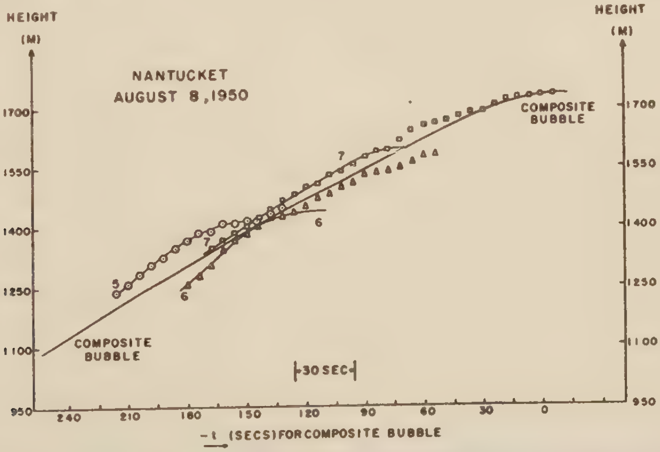

Fig. 9. Height-time curves for bubbles 5, 6 and 7, 8 August 1950, and for composite bubble formed by these individuals. Curve for composite bubble was drawn using points on this figure, and was checked on film by tracking smoothed upper outline of large tower dominating upper right part of fig. 8b, which was in fact composite bubble.

TABLE 4. Composite bubble of 8 August 1950, Nantucket, consisting of individuals 5, 6 and 7. Height range studied: 1090 to 1730 m. Cloud base: 800 m, $gB = 4.5$ cm/sec² = constant. $\bar{G} = 0.192$. $\Delta = 37$ per cent.

Observation number	$-t$ (sec)	$(-t)^{\frac{1}{2}}$ ($\text{sec}^{\frac{1}{2}}$)	w (cm/sec)	$\dot{w}$ (cm/sec²)	$\dot{w}/gB$	$(1-\dot{w}/gB)^{\frac{1}{2}}$	G ($\text{sec}^{-\frac{1}{2}}$)
1*	240	15.5	314	−0.28	−0.062	1.03	0.23
2	225	15.0	304	−0.28	−0.062	1.03	0.23
3	210	14.5	304	−0.28	−0.062	1.03	0.22
4	195	14.0	304	−0.28	−0.062	1.03	0.21
5	180	13.5	294	−0.28	−0.062	1.03	0.21
6	165	12.8	294	−0.28	−0.062	1.03	0.20
7	150	12.2	282	−0.28	−0.062	1.03	0.20
8	135	11.6	282	−0.28	−0.062	1.03	0.19
9	120	11.0	272	−0.28	−0.062	1.03	0.19
10	105	10.3	272	−0.28	−0.062	1.03	0.18
11	90	9.5	262	−0.28	−0.062	1.03	0.17
12	75	8.7	248	−0.35	−0.078	1.04	0.16
13	60	7.8	238	−0.49	−0.109	1.06	0.16
14	45	6.7	228	−1.75	−0.390	1.18	0.16
15	30	5.5	198	−3.08	−0.685	1.30	0.16
16	15	3.8	126	−4.90	−1.09	1.45	0.20

* Diameter measured as 500 m.

smaller size, which often made themselves apparent as the bumpy nodules at the top. On 8 August 1950, the process of amalgamation of several small bubbles into a larger one took place before the eyes of the observers, bubbles 5, 6 and 7 joining together to constitute a single large tower [the photographs have been previously published by Malkus (1952b, fig. 8)]. Most of the individual bubbles studied on this day are illustrated in selected tracings from the time-lapse films shown in fig. 8. The composite bubble is shown in the upper right and lower left portions of the figure, which illustrate how the smaller, numbered bubbles continue to be identified as protrusions from the top of this composite bubble, exhausting at different levels as each executes its own life cycle. Fig. 9 shows the height-time curve for each of these individuals and for the composite formed by them. The resulting calculation of G for the composite bubble is presented in table 4.

As shown earlier in table 3, some of the smaller numbered bubbles, particularly 8, were hardly sufficiently isolated to be treated individually. Fig. 8 illustrates this point more clearly. Fig. 10 indicates the manner in which the buoyancies were chosen for these numbered bubbles. On this day, the appropriate values of gB were again obtained by working backward, since the approximate value of G was known from the other bubbles studied. The correction due to liquid water was negligible. It was concluded, from many pieces of evidence, that the bubbles constituting the clouds on 8 August had risen all the way from the ground, or nearly from the ground. Among the evidence was the fact that bubbles appeared again and again over preferred positions [see Malkus and Bunker (1952, p. 11)]. Also, the lapse rate above cloud base was more stable than moist adiabatic; thus, the tectonic limit must have been at cloud base (800 m). Therefore the small bubbles were assumed to have risen dry adiabatically up to cloud base, and from thence moist adiabatically, the moist adiabat being chosen in such a way as to give $\bar{G}$ somewhere in the previously determined range. It is interesting to note that the maximum temperature required by a bubble leaving the ground (numbers 9 and 10) only exceeds the observed maximum temperature at Nantucket airport by 0.2C.

The composite bubble was believed to have formed at cloud base, from an amalgamation of individual bubbles and their wakes, and from thence to have risen moist adiabatically. Its buoyancy was determined merely by choosing that moist adiabat which gave a G in the range obtained for the other bubbles studied. The adiabat so chosen gives a value of $gB = 4.5$ cm/sec² ≈ constant. This implies a virtual temperature excess for the bubble of 1.3C, or an actual temperature difference of 1.0C and an increment due to excess water vapor of 0.3C. The excess virtual temperature of 1.3C is to be compared to corresponding

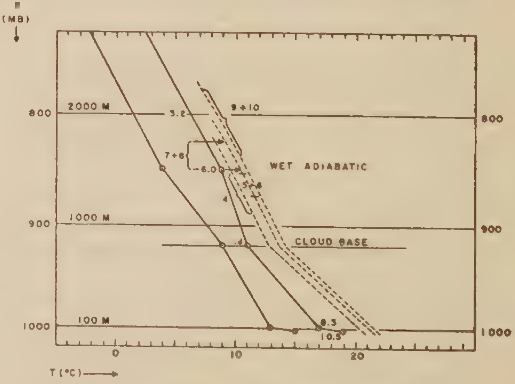

FIG. 10. Radiosonde observation made in clear air over Nantucket Island, 1500 *GCT* 8 August 1950. Right-hand solid curve is temperature. Left-hand curve is dew-point. Mixing ratios (g/kg) are entered next to temperature curve. Dotted curves are adiabats followed by individual bubbles. Height range in which each numbered bubble was studied is delimited on appropriate adiabat.

excesses of about 2.6C for the individual bubbles. Unfortunately, during the latter part of its history (from $-t = 120$ sec onward) the composite bubble was being followed closely and pushed upward by bubble 8 (see lower left part of fig. 8), and thus the vertical motions measured are too high, giving excessively low values of G in table 4. Nevertheless, it may be considered to obey the laws for a single bubble fairly well, as is supported by the calculation of R from (14). At $-t = 240$ sec with use of $E = 50$ sec, R comes out as 540 m, giving an angular half-aperture, θ_m, of about 28 deg. From (3), with use of the calculated R, w_L comes out as 325 cm/sec, which is within observational error of the measured w.

Certain other deductions concerning the composition and formation of this bubble may be drawn from fig. 9 and the tables. At $-t = 180$ sec on the composite bubble's time scale, its top was at 1300 m. It was then composed of bubbles 5 and 6. Extrapolating with the formula $R = -EgBt$ at this frame, we find that the composite bubble would have a radius of curvature equal to about 400 m, while bubble 5 would have dwindled to about 100 m and bubble 6 to about 300 m. If the volume is assumed proportional to the cube of this linear dimension, it may be hazarded that approximately 30 per cent of the large bubble volume came from undilute individuals and 70 per cent from wake material. No inferences are drawn about the degree of mixing or homogeneity within the large bubble, which must however be fairly high for it to retain coherent identity. If the individual bubbles possessed, at the time, a buoyancy gB of 10.0 cm/sec^2, and the composite bubble a gB of 4.5 cm/sec^2, this means the wake material had buoyancy of roughly $gB = 2.0$ cm/sec^2. This would imply a virtual-temperature excess in the wake of 0.58C. With use of the entrainment method of Stommel (1947), it is possible to determine what degree of mixing between cloudy air and environment would give rise to this latter buoyancy at this height. When the virtual-temperature excess possessed by bubble 5 at cloud base was assumed, to derive initial values of temperature and moisture, the entrainment rate between cloud base and 1200 m averaged about 1.5×10^{-5} cm^{-1}. This is in good agreement with the entrainment rate (2.0×10^{-5} cm^{-1}) calculated by Malkus (1952b) for the same clouds from their observed slopes.

5. Interaction of cloud bubbles with one another and with their environment

Most of the important recent work on cumulus clouds has emphasized the critical role of the ambient air in regulating the formation, growth and development of the clouds. In particular, it has been shown (Austin, 1948; Byers and Braham, 1949; Byers and Battan, 1949; Malkus, 1952a) that strong wind shear and environment dryness are inhibitory to the growth of large clouds and precipitation. The present study has so far dealt with individual bubbles whose life history in relative isolation has been shown to be rather unaffected by the latter parameters. Nevertheless, in the course of this work certain information has been derived which may provide a start on the vital problems of the protection of bubbles by one another and their interaction with the surroundings.

Although wind shear and environment dryness do not affect, in the first approximation, the life cycle of an individual isolated bubble, the rate at which bubbles succeed in each other's wakes, protect each other, and amalgamate to form a large cloud, will be affected by these parameters. Strong shear carries the first bubbles and their wakes far to one side and prevents their being joined by successors, while dryness in the surroundings destroys the protective pathway offered by a moist wake. Indeed, on reviewing the observational work in this article, it may be seen (table 3) that the "good" days for convection (such as 8 August 1950) were days on which bubbles amalgamated readily into larger towers and really isolated bubbles were hard to find. On these occasions, the environment was relatively moist and the wind shear weak. On the "poor" days for convection (such as 14 August 1950, and especially 2 April 1953) clouds built only marginally and isolated bubbles were readily found. On these latter days, the environment was either abnormally dry, the wind shear strong, or both, while the stability conditions differed rather little.

A preliminary attempt may now be made to formulate some of these ideas quantitatively. Each bubble's life may be divided into two sections: first, that spent within cloud from origin level to emergence at the top (protected range); and second, the section of its life studied here where it is eroding in clear air (unprotected). In the first place, it was found that, for all bubbles studied in table 3, the maximum radius R at emergence from cloud top is very nearly equal to the unprotected height range (see captions to tables 1 and 2). In the second place, the total range covered by each bubble (protected plus unprotected) is nearly the same as the measured width of the cloud body from which the bubble emerged, as predicted by Ludlam and Scorer (1953).

Finally, good days for convection were apparently characterized by high values of the ratio of the total height range to the maximum radius (at emergence). This ratio is essentially a measure of how large a fraction of its total height range a bubble is protected by neighbors and wakes, since we have shown that once they become isolated all bubbles obey the same erosion laws. It was thus desired to determine what relation, if any, this ratio of total range to maximum dimension bore to the significant environment parameters, wind shear and dryness. To make a rough estimate of such a relation, the environment dryness was represented by the average difference between bubble and clear-air mixing ratio; this quantity was multiplied by the wind shear; and the product was correlated with the ratio of total height range to maximum radius. For the twelve cases of table 3, the correlation coefficient is -0.7. With this many pairs, random numbers would produce a correlation this high once in a hundred times. Although so simple a correlation may or may not prove physically meaningful, these data do suggest a negative relation between protected height range and environment shear and dryness, and a positive relation between good cumulus building and a high value of protected height range. Thus, in building a cumulus from individual bubbles, the role of the environment indeed appears to be critical.

6. Concluding remarks: Comparison between present results and previous work on cumulus-cloud dynamics

The critically time-dependent nature of the size and velocity of an individual convective element has been emphasized in this work. In fact, referring again to (13), we can see that the vertical velocity w obeys a $(-t)^{\frac{1}{2}}$ power law throughout a large portion of the bubble's life cycle. Since G has been established constant, this law will be obeyed very accurately when the buoyancy gB is constant, up until the time near the end of the cycle when $\dot{w}$ becomes comparable to gB in magnitude. Furthermore, it has been shown that the life cycle of the isolated bubble, once formed, is to first order independent of all environment parameters except lapse rate.

These results might, at first glance, appear in distinct contradiction to the basic hypothesis of the entrainment model of a cumulus evolved by Stommel (1947; 1951), Malkus (1949; 1952a; 1952b; 1954) and others, which treats a cloud as consisting of steady or quasi-steady columnar updrafts and strongly emphasizes the effects of the environment upon the cloud. The apparent contradiction is only superficial, however. The present work may be considered as the next logical step forward from the entrainment model, since it attempts to describe the mechanism of the entrainment, the interaction of cloud elements with one another and with the environment, and begins to introduce some time-dependent features, at least with respect to individual cloud turrets. The necessity to progress to a time-dependent model has been long felt by workers in this field (Malkus, 1952a; 1954), and its commencement herein retrospectively sheds considerable light upon the results obtained by use of the steady-state hypothesis. Indeed, the present work raises the question of how it was possible that the model of entrainment in a steady-state updraft compared so very well with the features of observed clouds, most notably in the cases described by Malkus (1954). The answer to this question should provide some clues concerning how large clouds are built up.

It should be recalled that most of the testing of the steady-state model has been carried out in the trade-wind region, where clouds of 1 to 1.5-km vertical extent have been observed to remain in apparently steady conditions for well over an hour, sometimes longer. It must also be emphasized that during the latter study (Malkus, 1954) only those clouds were picked for measurement which appeared to be in this condition, and data were not used for those clouds in which this proved not to be the case. The fact that so much selection had to be applied in obtaining cases to test the theory clearly indicated that, at any given instant, the clouds chosen were not typical of the cloud population, although it was assumed that a large fraction of this population went through a quasi-steady phase in the life cycle. Furthermore, near the tops and tower portions of these clouds, the steady-state model began to give less consistent and satisfactory results, although it checked excellently in the lowest two-thirds of the cloud body.

It can now be seen that, for the main body of a cumulus to maintain itself in a nearly steady condition (*i.e.*, so that a set of airplane traverses made through it at one instant could be similar to another set 15 min or so later), bubbles must be forming within and rising through it in fairly rapid succession. Also, the individual bubbles which agglomerate to form the large turrets must be small compared with the size of the cloud; otherwise the character of the drafts as measured would be greatly altered by the passage of one bubble. Since the observed draft diameters in trade-wind clouds were about 1 km, and the turrets from 1 to 1.5 km in diameter, the clouds could indeed be considered large with respect to 200- to 300-m bubbles.

In conclusion, although one of the aims of the bubble model may eventually be the building up of such large, quasi-steady clouds, there are many intervening steps which, at least, are now suggested by comparison of the results of the two approaches. The first of the steps should probably concern the process of wake formation by a single bubble, and the effect upon a succeeding bubble of rising in this wake.

Acknowledgments.—The writers would like to thank the Woods Hole Oceanographic Institution for making possible Dr. Scorer's visit to the United States, during which time the major fraction of this work was done.

Gratitude is further due several individuals who made important contributions to the study. The writers are indebted to Sir Geoffrey Taylor and Dr. W. V. R. Malkus for critical comment and much important new insight shed upon this problem in the course of discussions with them. The writers would

also like to thank Mr. Claude Ronne, without whose skill, as both photographer and observer, the data used here on trade cumuli would not exist, and Mr. Andrew Bunker, who participated indispensably in all phases of the observational work and made many valuable suggestions concerning the theory.

REFERENCES

Austin, J. M., 1948: A note on cumulus growth in a non-saturated environment. *J. Meteor.*, **5**, 103–107.

Bunker, A. F., B. Haurwitz, J. S. Malkus, and H. Stommel, 1949: Vertical distribution of temperature and humidity over the Caribbean Sea. *Pap. phys. Ocean. Meteor., Mass. Inst. Tech. and Woods Hole ocean. Instn.*, **11**, No. 1, 82 pp.

Byers, H. R., and L. J. Battan, 1949: Some effects of vertical wind shear on thunderstorm structure. *Bull. Amer. meteor. Soc.*, **30**, 168–175.

Byers, H. R., and R. R. Braham, 1949: *The thunderstorm.* Washington, U. S. Govt. Print. Off. 282 pp.

Davies, R. M., and G. I. Taylor, 1950: The mechanics of large bubbles rising through extended liquids and through liquids in tubes. *Proc. roy. Soc.* (*London*), A, **200**, 375–390.

Ludlam, F. H., and R. S. Scorer, 1953: Reviews of modern meteorology, 10: Convection in the atmosphere. *Quart. J. r. meteor. Soc.*, **79**, 317–341.

Malkus, J. S., 1949: Effects of wind shear on some aspects of convection. *Trans. Amer. geophys. Union*, **30**, 19–25.

——, 1952a: Recent advances in the study of convective clouds and their interaction with the environment. *Tellus*, **2**, 71–87.

——, 1952b: The slopes of cumulus clouds in relation to external wind shear. *Quart. J. r. meteor. Soc.*, **78**, 530–542.

——, 1954: Some results of a trade-cumulus cloud investigation. *J. Meteor.*, **11**, 220–237.

——, and A. F. Bunker, 1952: Observational studies of the air flow over Nantucket Island during the summer of 1950. *Pap. phys. Ocean. Meteor., Mass. Inst. Tech. and Woods Hole Ocean. Instn.*, **12**, No. 2, 50 pp.

Malkus, J. S., and M. E. Stern, 1953: The flow of a stable atmosphere over a heated island, Part I. *J. Meteor.*, **10**, 30–41.

Scorer, R. S., and F. H. Ludlam, 1953: Bubble theory of penetrative convection. *Quart. J. r. meteor. Soc.*, **79**, 94–103.

Stommel, H., 1947: Entrainment of air into a cumulus cloud. *J. Meteor.*, **4**, 91–94.

——, 1951: Entrainment of air into a cumulus cloud II. *J. Meteor.*, **8**, 127–129.

Contribution No. 710

Reprinted from the AMERICAN JOURNAL OF BOTANY, Vol. 42, No. 1, 92-98, January, 1955
Printed in U.S.A.

GAS EXCHANGE IN THE ROOTS OF MANGROVES[1]

P. F. Scholander, L. van Dam, and Susan I. Scholander

ALONG THE southern and western coasts of the Florida peninsula occurs one of the greatest developments of mangrove swamp in the world. *Rhizophora mangle* L., the red mangrove, perching on its arched stilt roots, is the dominant species and the most marine. Another important component is *Avicennia nitida* Jacq., the black mangrove, which is restricted to the tidal zone and reaches its most luxuriant development on intertidal mud flats in more sheltered inland localities. Both species have a considerable tolerance for fresh water (Davis, 1943).

Familiar to anyone who has visited the mangrove region are the air roots which protrude in great numbers from the mud under and around *Avicennia* bushes or trees. A single tree may produce several thousand of these air roots, usually 20–30 cm. high and a centimeter thick, soft and spongy, and studded with little whitish lenticels. In the mud they connect to radially-running main roots, which are also soft and spongy and contain large amounts of air (fig. 1). The vertical air-roots are often referred to as pneumatophores because it is believed that they may have the function of aerating the root system which lies buried in the mud.

If one of the arching stilt roots of *Rhizophora* is dug out of the mud it is found to terminate in a bunch of long, spongy, finger-thick, and air-filled roots (fig. 2). The stilt root has a conspicuous development of lenticels, and one may wonder whether these might serve as ventilating ports for the mud roots. If they do, one might ask by what process the ventilation takes place, as it seems almost incredible that the voluminous roots down in the mud could be effectively ventilated by simple diffusion alone, through little lenticels high up on the stilt roots. One might also wonder how such a system, which gets its oxygen from the air, avoids getting jammed with nitrogen.

However, before worrying over how the ventilation comes about one must first establish that such ventilation does take place, and this is the object of the present investigation.

GAS EXCHANGE IN SUBMERGED ROOTS OF VARIOUS PLANTS.—Several investigators have analyzed the gases in roots of plants growing in water or mud which is poor in oxygen. In general these roots have been found to be aerated; how is usually not clear.

Conway (1937), in a series of experiments on the sedge *Cladium mariscus* R. Br., found that air spaces were continuous from the leaves down into the roots. The gas connections were particularly free through dead leaves and old leaves, whereas growing young leaves were less pervious. The roots contained usually 16–18 per cent oxygen even though the medium might have zero oxygen. If the air connection was blocked by cutting the leaves off below the water surface, the oxygen in the roots would drop to 1–2 per cent. This would happen even if the roots were kept in well aerated water. Concomitant with the oxygen decrease there would usually be a slight increase in the carbon dioxide.

Laing (1940) found that there was a drop in the oxygen tension from the leaves and down into the roots in several aquatic plants (*Nuphar*, *Peltandra*, *Pontederia*, *Typha*, *Sparganium*, *Scirpus*). The oxygen tension in the roots was generally highest in sunshine and decreased during night or artificial darkness. It was inferred that oxygen produced by photosynthesis in the leaves found its way down into the roots by simple diffusion.

Van Raalte (1940) found that the roots of rice plants contained some 10–15 per cent oxygen even though the medium was practically anaerobic. By ringing or tying off the roots the oxygen tension fell to that of the medium. If the plant stem was cut off above the water line the root oxygen increased, but decreased if the plant was covered with agar. It was hence concluded that oxygen enters the aerial parts of the plant and is transported downward into the roots. Illumination had no effect upon the oxygen concentration in the roots.

Brown (1947), working on seedlings of *Cucurbita pepo*, found that when the root was placed in aerated water it gave off nitrogen. This stopped when the shoot was cut off. The experiments were interpreted to mean that oxygen and nitrogen flow from the cotyledons down into the root, not by simple diffusion but by active transport of the gases in solution. If the root was placed in nitrogen-saturated water, oxygen would enter the water which at the same time would lose nitrogen. Although not simple to interpret, these experiments certainly raise the question of exactly how the gases are transported in this plant.

Vallance and Coult (1951) determined the gas composition at five different heights in the bog bean (*Menyanthes*). They found that when the plant was kept in darkness with the roots in an anaerobic medium, the roots contained some 13–18 per cent oxygen. There was no clearly defined increase in the oxygen tension at levels above the roots. It was therefore concluded that a means other than simple diffusion might be responsible for the aeration of *Menyanthes* roots.

Amongst the several species of mangroves which have a conspicuous development of pneumatophores only *Sonneratia* has been investigated as to the function of these air roots. This plant has aerial

---

[1] Received for publication May 5, 1954.

Contribution No. 710 from the Woods Hole Oceanographic Institution.

Contribution No. 134 from the Marine Laboratory, University of Miami.

roots which in several respects resemble those of *Avicennia.* An excellent and most thorough anatomical description of the root system of *Sonneratia* is given by Troll and Dragendorff (1931). In the physiological part of their investigation they showed that the mud in which the roots were imbedded was generally completely anaerobic. They carried out a series of experiments in order to establish whether or not the air roots served as ventilatory chimneys for the root system buried in the mud. By blowing into the horizontal root, keeping the air root under water, air would bubble out through the lenticels, demonstrating that the pneumatophores were in direct gas connection with the buried root system. The respiration of detached air roots was then compared with the respiration of air roots in situ, but no systematic difference between the two was found. Hence the question as to the function of the air roots was left open.

A similar approach was used to find out whether the well known cypress knees (*Taxodium*) have any function in supplying the root system with oxygen (Kramer et al., 1952). Here the respiration of a series of knees in situ was compared with the respiration of the same knees detached. As in *Sonneratia* it was found that the knees in situ did not use more oxygen than when detached, and it was therefore concluded that they do not play any essential role as aeration structures for the root system.

We shall see in the following account that the air roots in *Avicennia* and the stilt roots in *Rhizophora,* through their lenticels, are indeed aeration structures which are essential for the ventilation of the roots buried in an anaerobic mud.

MATERIAL.—The *Avicennia* bushes used in the present investigations grow on Tokas Key near the Lerner Marine Laboratory on Bimini in the Bahamas and on Virginia Key near the Marine Laboratory of the University of Miami in Florida. All the *Rhizophora* experiments were performed at the latter place.

INVESTIGATIONS ON AVICENNIA.—In suitable localities *Avicennia* may grow to a stout tree 20 m. tall or more, but it is usually much smaller. For our investigations only smaller plants were used, usually 1–3 m. tall. The number of air roots an *Avicennia* may have varies a great deal with the habitat. For one tree used at Bimini (fig. 6) the number of roots was estimated by counting all roots within a wire frame of 0.5 m.^{2} area. From counts in six different places it was estimated that this tree, 2–3 m. tall, had well over ten thousand air roots. Surely such a spectacular development must have an important function.

The length of the air roots is usually 20–30 cm., but it may sometimes be almost twice as much. The thickness is generally around 1 cm. If the tree is standing isolated one may often see that the air roots are lined up in rows radiating from the tree, indicating the radial root from which they rise. Neighboring air roots are often 10–20 cm. apart. From the radial root many roots also branch down into the mud, often one for each air root (fig. 1, 3, and 4).

The radial roots are often a centimeter thick or more. They are soft and spongy, containing much air. They are covered by a thin cortex and have a thin woody central core. The lower, subterranean part of the air root is of the same general structure. Above the mud the root gets tougher, developing a green layer under the bark, and it is covered with numerous whitish lenticels, especially towards the apex.

If a half-meter section of a horizontal root is dug up with the air roots attached one can easily show that blowing into the radial root, with the air roots under water, will force air bubbles out through the lenticels. Air will also bubble out through the other end of the main root. The resistance to these air movements is rather considerable, but, as in *Sonneratia,* it shows that there is direct gas communication between adjacent chimneys through the radial root. The lenticels are hydrophobic and will not pass water inward.

Habitat.—A profile of the habitat of an *Avicennia* bush used in the Bimini study is given in fig. 6. The roots sprang up from a sloping bottom and the height of several hundred root tips was measured in relation to the level of high and low tide. The longest air roots were located farthest out from the shore, but their tips were lower than those of air roots nearer the shore. Consequently the outer ones would be the first to be covered by the rising tide and would be completely submerged at high tide, while many of the landward roots would remain out of water.

Oxygen content in the mud.—It was established by Troll and Dragendorff (1931) that the *Sonneratia* roots were imbedded in mud which was for the most part completely anaerobic. A series of oxygen analyses of the mud in which the roots of *Avicennia* and *Rhizophora* were embedded was undertaken at Virginia Key. A capillary glass tube, provided with a fine-mesh metal sieve was stuck on a slant into a narrow hole in the mud amongst the roots. After a few minutes a sample of muddy water was drawn anaerobically into a syringe. It was analyzed on the spot by a gasometric method (Scholander, P. F., and L. van Dam, unpublished material). Eleven out of 14 samples were oxygen-free, or showed indeed negative values, inasmuch as the mud water quickly used up the slight oxygen blank introduced by the reagents. The roots of these plants were therefore imbedded in a muck or mud which was completely anaerobic.

Gas pressures in the roots of Avicennia in relation to the tide.—Westermaier (1900) postulated that rising tide would compress the rather soft radial roots which he had observed in *Sonneratia.* This would cause the air to be exhaled through the pneumatophores. Then on falling tide they would

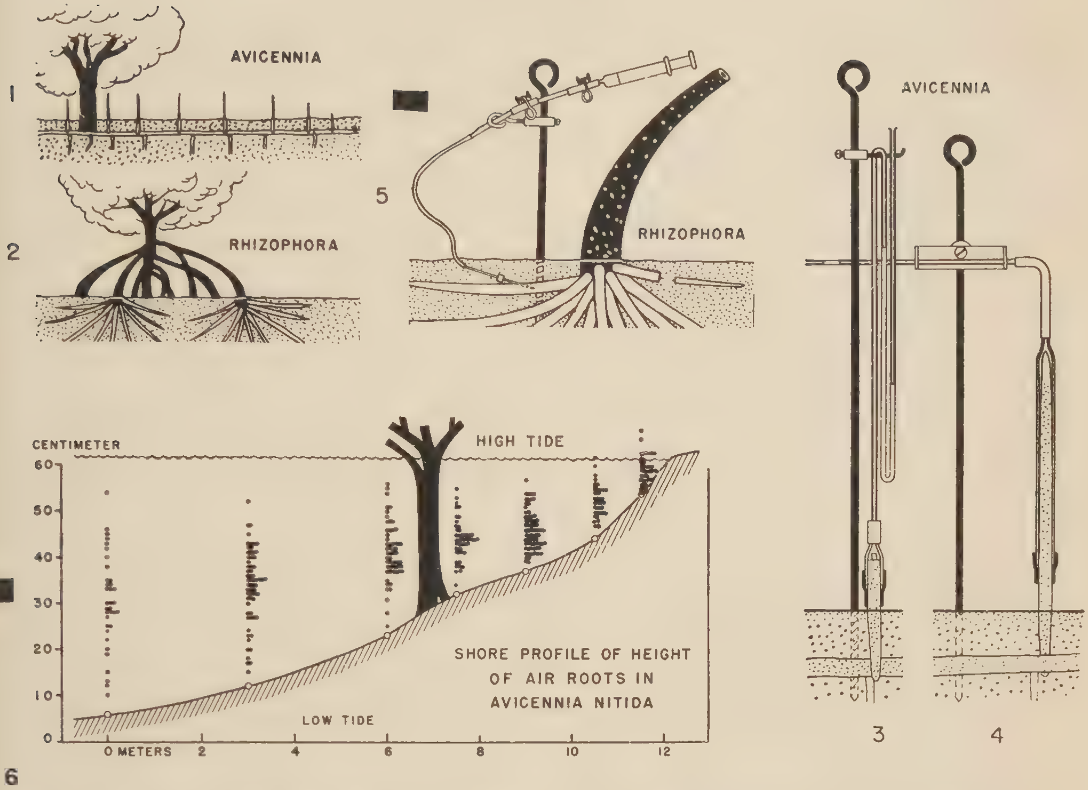

Fig. 1–6.—Fig. 1. *Avicennia* with radial roots and air-roots.—Fig. 2. *Rhizophora* with stilt roots terminating in a bunch of mud roots.—Fig. 3. Water manometer attached to stump of pneumatophore, the woody core of which is greased.—Fig. 4. Measurement of the volume of air drawn into (or given off by) an intact *Avicennia* pneumatophore. Horizontal calibrated tube contains a kerosene indicator drop.—Fig. 5. Gas sampling from mud root in *Rhizophora* by means of indwelling hypodermic needle. The lenticels on the stilt root are indicated as white spots.—Fig. 6. Habitat profile of *Avicennia* bush used for data in fig. 8 and 10. The level of the tip of each measured pneumatophore is indicated by one point.

inhale, resulting in long tidal breaths. This pictorial theory was never put to a test.

By applying manometers to *Avicennia* roots, as shown in fig. 3, pressure fluctuations were found which correlate with the tide but in a direction opposite to that expected from the tidal breathing theory. In the later stages of the rising tide suction starts to develop in the root system, and keeps on increasing during the first part of the falling tide whereupon rather suddenly the pressure rises to atmospheric (fig. 8).

The period of increasing suction corresponds in time to the period when the lenticels of the adjacent air roots are covered with water. It will be shown that artificial closure of the lenticels produces a progressive reduction in the gas pressure caused by the respiratory processes in the roots. This being the case one should be able to predict what would happen when the tide would act upon a root profile as the one given in fig. 6. This can best be done by considering a schematic situation such as presented in fig. 7. Here three air roots reach three different levels in relation to the high tide. We assume for the sake of simplicity that the lenticels are confined to the apex only. We also assume that the molar gas reduction (O_2–CO_2) due to respiration is a relatively slow process proceeding at a constant rate. As soon as the lenticels become covered with the water the pressure in the system begins to drop and keeps on dropping until at falling tide the lenticels are again freed. When this happens air enters through the lenticels and atmospheric pressure in the roots is rapidly restored. The tidal coverage and uncoverage of the three chimneys in fig. 7 will result in the pressure diagrams 1, 2, 3, which show that the peaks of the suction curves are delayed in relation to the time of high tide, and lead us to expect that the greatest suction would develop in those groups of air roots which are longest covered by water, i.e., which are deepest. By comparing the experimentally found curves of fig. 8 and 10 with the theoretical diagram of fig. 7 it would seem clearly indicated that the coverage sequence of the lenticels by the tide

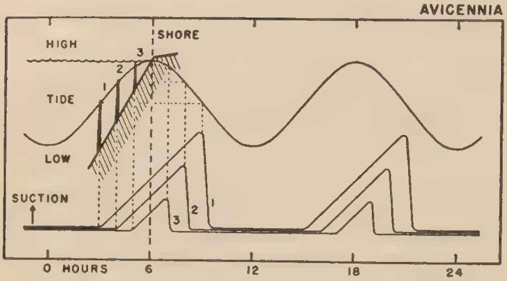

7

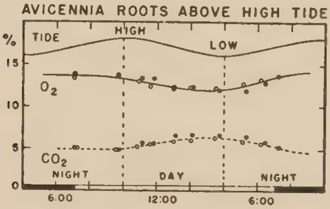

9

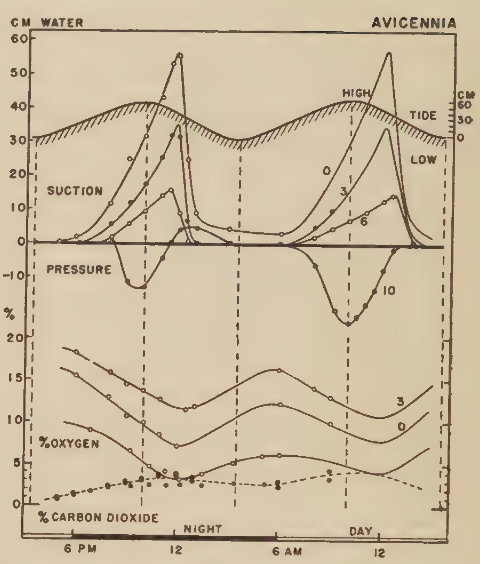

8

Fig. 7-9.—Fig. 7. Schematic diagram of tidal action upon 3 pneumatophores in *Avicennia* reaching to different heights. Lenticels are assumed to be located only at the apex of each root. Suction, caused by a steady and relatively slow respiratory gas shrinkage (O_2–CO_2) increases as long as the tip is covered by water. When uncovered by the falling tide atmospheric pressure is rapidly restored by aspiration of air. Curves 1, 2, and 3 are the suction curves constructed on these premises.—Fig. 8. Suction in four *Avicennia* roots in relation to tide action. They were located at 0, 3, 6, and 10 meters on the abscissa in fig. 6. The root at the 10-m. mark developed positive pressure almost synchronous with the rising tide. The oxygen concentrations in the roots at 3 and 0 m. show a marked tidal cycling. The lower oxygen curve belongs to another plant.—Fig. 9. Diurnal variations in the gas composition of two roots of *Avicennia* growing above tidal action.

essentially explains the magnitude, shape, and time relations of the suction curves in *Avicennia*.

In a few cases we have recorded that positive pressures developed in roots, which then rather closely synchronized with the tide (fig. 8). This could possibly be due to compression of the subterranean roots by the tide, as suggested by Westermaier's idea. However, pieces of the radial roots, when closed at the ends with paraffin and placed under water, are only very slightly compressible, especially when in the mud.

Gas composition in the roots of Avicennia in relation to tide.—The gas composition in the subterranean root system of *Avicennia* was followed during several tidal cycles. The gas samples were drawn from the base of a cut air root using the same attachment as for the suction measurements. The manometer was replaced with a glass capillary provided with a double clamp arrangement for anaerobic sampling (fig. 5). For the analyses 1.5 cc. gas were drawn into a syringe and analyzed in a 0.5 cc. analyzer (Scholander, 1947) for CO_2, O_2, and N_2.

It will be seen in fig. 8 that radial roots subjected to a moderate coverage of their chimneys by tidal action had an oxygen concentration often as high as 15–18 per cent, whereas roots in deeper water often had lower oxygen. In the zone of tidal coverage the oxygen concentration showed marked tidal fluctuations. During the time of lenticel coverage the oxygen decreased synchronously with the drop in pressure. It commenced to rise at the time when the lenticels were again uncovered and the pressure started to rise. The rise in oxygen concentration continued through the low and rising tide until the lenticels were again being covered. The fact that the restoration of the oxygen tension in the roots occupied all this time, while the pressure equalized much more quickly, shows that the restoration of the tension is essentially independent of the aspirated air, which in any event amounts to no more than a few per cent of the total gas volume in the root.

The carbon dioxide changed in the direction opposite to that of the oxygen, and very much less, as would be expected from its high solubility.

In plants growing more or less on dry land out of reach of the action of the average tides, no clear tidal rhythm could be traced in the gas composition of the roots. They did exhibit a faint diurnal rhythm, however, with lowest oxygen values in the daytime, higher at night (fig. 9). This diurnal variation may be seen to be superimposed upon the tidal rhythm, depressing the oxygen in the daytime (fig. 8, station 0 and 3).

The fact that the oxygen content in roots above the zone of average tidal action shows no tidal rhythm, but starts to drop immediately when the air connection is artificially blocked, shows that the ventilation through the lenticels is basically a continuous process, modified by the tide but not primarily caused by the tide.

From the very slight changes in the carbon dioxide concentrations as compared to the oxygen variations it follows that there will be appreciable changes in the nitrogen concentrations. From fig. 8 and 9 it may be inferred that the nitrogen tension in the roots is regularly higher than in the atmosphere. At times it may reach 90 per cent of one atmosphere or more.

In a closed, rigid gas space where respiration takes place a 1 per cent reduction in the molar amount of gas (O_2–CO_2, or RD) would develop a suction of 10 cm. water. Assuming that the amount of nitrogen remained constant one may calculate the pressure drop from the change in nitrogen concentration. In fig. 8 the pressure was found to decrease by 4–10 cm. per hr. Calculated from the nitrogen data it should have decreased by 8–12 cm. per hr. This is a close enough agreement to indicate that the suction is caused by the respiration, and it may also indicate that the root system is not quite rigid but shrinks very slightly as a result of the suction and increased hydrostatic pressure. It was found that pieces of horizontal roots closed at the ends with paraffin shrink by 0.2–0.3 per cent when subjected to a hydrostatic pressure increase of 10 cm. water. In the mud this shrinkage would probably be even less. Influx of sap into the spongy cells lining the gas space may also be a factor in the slight volume reduction.

Air drawn in through the lenticels of Avicennia.—The rapid return from suction to atmospheric pressure when the air roots are being uncovered at falling tide indicates that air is being sucked into the roots through the lenticels. That this actually happens was shown by enclosing air roots in situ in gas-tight glass or rubber tubes which fitted snugly around them without obstructing the lenticels (fig. 4). A volume-calibrated glass tube, open at both ends, was adjusted so it lay strictly horizontal and a kerosene indicator drop would remain stationary in it. It was then connected to the root. The amount of gas moving out of or into the air roots could be measured by the movement of the kerosene drop. A big beach umbrella shaded the setup. As soon as the tide began to cover the neighboring pneumatophores air began to be drawn in at accelerated rates (fig. 10). Here then is a direct demonstration that the lenticels serve as ventilatory ports for respiratory gas exchange. Although this has been assumed reasonably enough from the anatomical structure and from the gas connections with the interior of plants, yet such a ventilatory function does not seem to have been previously demonstrated. It has been shown, however, that closing of the lenticels with lacquer or wax may reduce the evaporation loss from a stem (Haberlandt, 1875; Klebahn, 1884).

In a few cases we have observed that a slight amount of gas was exhaled from roots in the upper tidal zone, confirming the observation that positive pressures may sometimes develop.

Effects of eliminating the air roots in Avicennia.—A young *Avicennia* bush was selected which had a well developed system of 5 major radial roots, as indicated by the 5 straight, orderly rows of air roots rising from them above the mud. On two of these radial systems the outermost air root was cut off and provided with a volume-indicating horizontal tube (fig. 4). For one hour, only a very minute amount of air was drawn into the roots (fig. 11). Now all the rest of the air roots coming off the two radial roots were cut off, the cut surfaces greased, and the stumps covered with wet mud. The result was that the measuring root immediately began to suck in air, confirming once more the idea that coverage of the air roots by the tide is the cause of the suction development.

In another *Avicennia* bush with a similar root system the outermost chimneys of two radial root systems were cut off and connected with a glass capillary for gas sampling. The oxygen concentration was respectively near 10 and 13 per cent, and slightly falling due to tidal action (fig. 12). As soon as the chimneys were eliminated, the oxygen started to drop and reached in two days one per cent or less. The CO_2 rose by about 2 per cent in both cases. This again clearly demonstrates that the suction is respiratory and that the radial root system is ventilated through the air roots.

EXPERIMENTS WITH RHIZOPHORA.—The root system of the red mangrove is quite different from that of *Avicennia.* Whereas *Avicennia* has long radial roots ventilated by more or less evenly spaced chimneys, *Rhizophora* perches on the mud on arched stilt roots, each of which (when mature) terminates in a cluster of swollen, spongy, air-filled roots (fig. 2, and 5). These all radiate from the club-shaped ending of the stilt root, which from the mud line to the trunk bears large (2–5 mm.) brownish lenticels. If one digs out a stilt root with its complement of mud roots and blows through a mud root, with the stilt root under water, air bubbles will emerge from the lenticels, showing that there is direct air communication through them from the outside air down into the roots. Here therefore is a system where all of the mud roots in one clump must be ventilated by the lenticels on their common stilt. The roots are arranged in parallel, so to speak, with respect to ventilation, whereas in *Avicennia* the ventilation system is arranged with the chimneys in series.

The *Rhizophora* plants used in these investigations grew together with the *Avicennia* on the Virginia Key, where the oxygen tension in the mud was zero.

In *Rhizophora* gas could easily be drawn from the

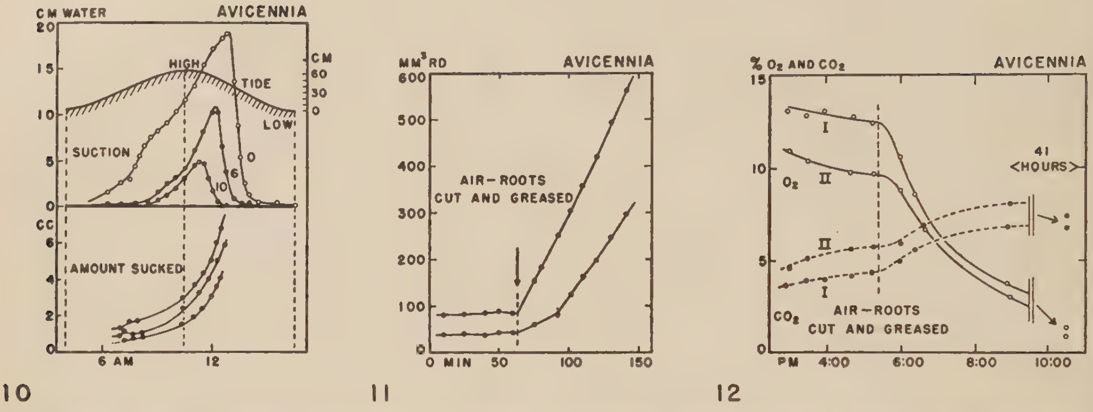

Fig. 10–12.—Fig. 10. Amount of air sucked in through three different air-roots enclosed in a tube (fig. 4) when the neighboring roots were being covered by the tide. Three suction curves are given for reference, obtained from locations 0, 6, and 10 m. in fig. 6.—Fig. 11. The amount of air (RD) drawn into two pneumatophores of *Avicennia* before and after the remaining air-roots on the same radial root were eliminated.—Fig. 12. Asphyxiation of root system in *Avicennia* when air-roots are eliminated.

mud roots by inserting a number 20 blood-taking needle in the root. The needle was attached with a polyethylene tubing to a double clamp arrangement for taking gas samples with a syringe (fig. 5). With the needle in place and the root covered over with mud, gas samples could be taken at any desired time.

Needles were put into 3 roots, each from a different bush and the gases were analyzed. In all of these roots the oxygen was initially 14–19 per cent and the CO_2 4–6 per cent. After three hours the gas exchange through the lenticels was eliminated in two of the plants, keeping the third as control. This was done by covering the stilt root with grease from the mud line up to the trunk. The oxygen concentration in these roots started to drop as compared to the control, and in 36 hr. it had fallen to near 2 per cent. Correspondingly the CO_2 in the greased plants rose from the normal 4–6 per cent to some 8–12 per cent (fig. 13).

The control plant showed a diurnal cycle in the oxygen concentration in the root like that in *Avicennia*, i.e., a decrease in the daytime and increase during night. This rhythm is also reflected in the greased plants by the accelerated drop in the oxygen during the day.

These experiments have demonstrated that in *Rhizophora* the roots submerged in the anaerobic mud maintain their high oxygen tension by means of a ventilation which takes place through the lenticels located on the stilt roots.

SUMMARY

The respiratory gas exchange in the roots of two common mangroves has been investigated. *Avicennia nitida* has a system of radial, spongy, gas-filled roots running horizontally in the mud. These send up numerous air roots, often called pneumatophores. There is direct gas connection between these and the radial roots. The latter are embedded in mud which was found to be completely oxygen free. When the tide covers the lenticels on the air roots the pressure in the root system starts to drop and continues to drop until the lenticels are again uncovered by the falling tide. At low tide the oxygen concentration in the radial roots is usually around 10–18 per cent. Synchronously with the tidal drop

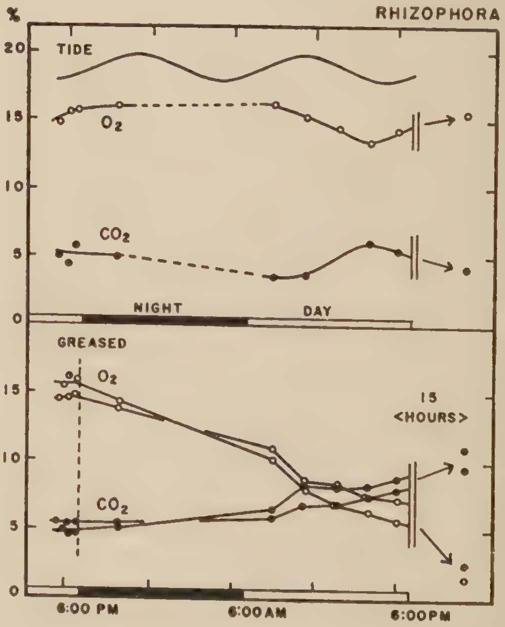

13

Fig. 13. Lower curve: Asphyxiation of root system in *Rhizophora* when the lenticels of the stilt root are plugged. Upper curve: Control showing diurnal variations in the oxygen and carbon dioxide content of the roots.

in gas pressure the oxygen concentration in the roots falls. In comparison the CO_2 rises very little. This respiratory gas shrinkage is the cause of the pressure drop. When the lenticels are freed by the falling tide the oxygen rises in the roots until they are covered by the next high tide. This tidal rhythm is not found in roots situated above the tidal action. In such roots a diurnal variation in the oxygen concentration may be apparent, with the oxygen lowest in daytime. Sometimes this diurnal rhythm may be seen to superimpose upon the tidal rhythm. On falling tide the gas pressure returns to atmospheric. This is caused by air being drawn in through the lenticels on the pneumatophores. When the pneumatophores are eliminated the oxygen in the roots drops, reaching in two days one per cent or less, proving that the pneumatophores in *Avicennia* are chimneys serving as ventilators for the root system in the anaerobic mud. The stilt roots of *Rhizophora* end in a bunch of spongy, gas-filled roots embedded in the mud which was found to be entirely oxygen free. The roots in the mud maintain a high oxygen concentration of 15–18 per cent, which showed diurnal variations with lowest oxygen during daytime, like *Avicennia*. There is direct gas connection between the mud roots and the lenticels on the stilt roots. When the lenticels were plugged by grease the oxygen in the buried roots fell and reached in two days 2 per cent or less. The high oxygen tension in the roots of *Rhizophora* is therefore maintained by means of a ventilation which takes place through the lenticels on the stilt roots.

Woods Hole Oceanographic Institution,
Woods Hole, Massachusetts;
Lerner Marine Laboratory,
Bimini, Bahamas
and
The Marine Laboratory,
University of Miami,
Coral Gables, Florida

LITERATURE CITED

Brown, R. 1947. The gaseous exchange between the root and the shoot of the seedling of *Cucurbita pepo*. Ann. Bot. N. S. 11: 417–437.

Conway, Veronica M. 1937. Studies in the autecology of *Cladium mariscus* R. Br. III. The aeration of the subterranean parts of the plant. New Phytol. 36: 64–96.

Davis, J. H., Jr. 1943. The natural features of southern Florida. Florida Dept. Conservation Geol. Bull. 25. Tallahassee.

Haberlandt, G. 1875. Beiträge zur Kenntniss der Lenticellen. Arbeit. pflanzenphysiol. Inst. K. K. Wiener Univ. V. Sitzungsber. K. Akad. Wiss. Wien, Math.-Naturwiss. Cl. 72 (1): 175–203.

Klebahn, H. 1884. Die Rindenporen. Zeitschr. Naturwiss. N. S. 10: 537–592. Jena.

Kramer, P. J., W. S. Riley, and T. T. Bannister. 1952. Gas exchange of cypress knees. Ecology 33: 117–121.

Laing, H. E. 1940. The composition of the internal atmosphere of *Nuphar advenum* and other water plants. Amer. Jour. Bot. 27: 861–868.

Scholander, P. F. 1947. Analyzer for accurate estimation of respiratory gases in one-half cubic centimeter samples. Jour. Biol. Chem. 167: 235–250.

Troll, W., and O. Dragendorff. 1931. Über die Luftwurzeln von *Sonneratia* Linn. f. und ihre biologische Bedeutung. Mit einem rechnerischen Anhang von Hans Fromherz. Planta 13: 311–473.

Vallance, K. B., and D. A. Coult. 1951. Observations on the gaseous exchanges which take place between *Menyanthes trifoliata* L. and its environment. 1. The composition of the internal gas of the plant. Jour. Exp. Bot. 2: 212–222.

Van Raalte, M. H. 1940. On the oxygen supply of rice-roots. Ann. Jard. Bot. Buitenzorg 50: 99–114.

Westermaier, M. 1900. Zur Kenntniss der Pneumatophoren. Botanische Untersuchungen im Anschluss en eine Tropenreise. Heft I. Freiburg (Quoted from Bot. Centralbl., 1901, 86: 392–393 and from Troll and Dragendorff, 1931.)

Contribution No. 712

Reprinted from *The Luminescence of Biological Systems*, Frank H Johnson, Editor, published by the American Association for the Advancement of Science, Washington, D.C., 1955.

Ecology of Autotrophic Marine Dinoflagellates with Reference to Red Water Conditions*

John H. Ryther
Woods Hole Oceanographic Institution, Woods Hole, Massachusetts

Although dinoflagellate luminescence was at one time believed to be restricted to a few highly specialized forms (i.e., *Noctiluca, Pyrocystis*), as early as 1830 Michaelis described 9 luminous species of the common genera *Ceratium*, *Peridinium*, and *Prorocentrum*. Kofoid and Swezy (1921) attribute this property to "many if not most of the Perindiniales and Gymnodiniales." The extent to which bioluminescence occurs in the group as a whole has not been systematically investigated, but the opinion now appears to be widespread among workers in the field that most dinoflagellates, at least under certain conditions, exhibit luminescence. Kofoid, in a personal communication to Harvey (1952), went so far as to suggest that perhaps all dinoflagellates have this property.

The dinoflagellates are found in all the oceans of the world and at least a few are usually present at every time of the year. Among all forms of marine life, they are probably second in abundance only to the diatoms and, in many cases, may greatly outnumber them. Together with the diatoms they constitute the bulk of the so-called phytoplankton, the community of unicellular, autotrophic organisms that are the basis for all life in the sea.

In view of the widespread occurrence of dinoflagellates in the ocean and the apparent preponderance of luminous forms, this group must be considered as one of the principal producers of biolumines-

---

[*] Contribution No. 712 from the Woods Hole Oceanographic Institution.

cence in the sea. Allen (1939) stated categorically that they are the most common cause of this phenomenon. It follows that any consideration of the factors contributing to the occurrence of marine bioluminescence must include a consideration of the ecological factors that influence and control the growth and distribution of its principal causitive agents, the dinoflagellates. The following discussion will be concerned with the general ecology of these organisms. In addition, special attention will be devoted to a possible explanation for the frequently reported occurrences of dense "blooms" or "swarms" of dinoflagellates in many parts of the world.

No attempt will be made in the following discussion to differentiate between luminous and nonluminous dinoflagellates, but it will be assumed that the presence or absence of this property will not appreciably affect the interrelationships between the organisms and their environment. A consideration of their ecology as a group is complicated, however, by the fact that individual species may employ almost any type of nutritional habit, including autotrophic, holozoic, saprophytic, and parasitic. Although the number of species which employ the second mode of nutrition, either obligatorily or facultatively, is apparently quite large (Kofoid and Swezy, 1921), in total abundance they are probably insignificant in comparison with the photosynthetic forms. For this reason we will consider here primarily the autotrophic dinoflagellates.

General Ecology of Dinoflagellates

Temperature

Dinoflagellates are found in all parts of the ocean and are usually present in some quantity at all times of the year. It is therefore impossible to make broad generalizations concerning the temperature relationships of so large and widespread a group. Some species are obviously arctic forms and may be observed living in subzero temperatures associated with the polar seas (Gran, 1924; Braarud, 1935). However, there does appear to be some justification for classifying the great majority of the dinoflagellates as warm-water organisms. This is particularly true if they are compared as a group with the diatoms, which, in contrast, are often considered cold-water forms.

In the temperate regions of the ocean, the relatively unproductive winter season is normally followed by a spring "flowering" or "bloom" of phytoplankton, which consists predominantly of diatoms. This spring maximum, which usually develops into the largest population of the year, becomes limited by the supply of available nutrients and may pass through its entire cycle of growth and decline in a few weeks. As the nutrient level falls and the temperature rises, the numbers of diatoms decrease and many species may disappear entirely from the plankton.

By late spring, the dinoflagellates appear in significant numbers, and while they seldom attain the abundance of the spring diatom bloom, they often persist as the dominant member of the plankton community throughout the summer months.

The sequence of events described above occurs in temperate regions in the open ocean (Herdman, 1922), in coastal and slope waters (Gran and Braarud, 1935), and in estuarine situations (Gaarder and Gran, 1927; Marshall, 1947; Braarud, 1945).

While northern waters support larger populations of dinoflagellates, the number of temperate species is extremely small compared with the number of tropical forms (Sverdrup, Johnson, and Fleming, 1942). This is particularly true of the highly specialized Dinophysiales, which are characteristic of tropical seas (Fritsch, 1935) but also applies to the ubiquitous genus *Ceratium* of which Peters (1932) found 33 of 55 South Atlantic species confined to warm water.

The dense populations of dinoflagellates which create "red water" conditions are known only in the tropics or in temperate water during the warmer (and usually the warmest) time of the year. This subject will be discussed in more detail in another section. Dinoflagellate luminescence shows a similar seasonal periodicity in the temperate parts of the ocean. Allen (1939) reported that luminous displays by these organisms are common in the La Jolla region during the summer months, but never occur between October and May.

Such fragmentary physiological evidence as is available concerning the temperature relations of dinoflagellates appears to support the view that they are predominantly a warm-water group. Barker (1935), who is one of the pioneers in developing successful culture methods for dinoflagellates, observed optimal temperatures for the growth of some 14 species between 18° and 25° C. Braarud and Pappas (1951) noted a temperature optimum for *Peridinium triquetrum* at 18° C, while Nordli (1953) found that *Ceratium fusus* and *C. furca* grew most rapidly at temperatures of 15° and 20° C respectively. Provasoli (personal communication) finds temperatures of 20–25° C most suitable for growing *Gyrodinium californicum.* Although the preceding experimental evidence is obviously insufficient to form a basis for generalization, it is perhaps significant that all the above species, despite their relatively high temperature optima for growth, were isolated from temperate regions of the ocean.

Salinity

Dinoflagellates occur in fresh, brackish, and full sea water, and it is again impossible to define optimal or limiting salinity conditions for the group as a whole. The unarmored dinoflagellates appear to be most abundant in the open ocean plankton, while the armored forms are more typical of coastal and estuarine regions (Fritsch, 1935). This suggests that the optimal growth conditions for the latter may occur at somewhat lower salinities than are observed in the open ocean.

Several plankton investigations have revealed that dinoflagellate maxima may often be correlated with the seasonal or geographical occurrence of relatively low salinity water (Gran, 1924; Marshall, 1947; Gaarder and Gran, 1927; Marshall and Orr, 1927; Gran and Braarud, 1935). It is noteworthy that the majority of such studies have been concerned principally with the armored species and have largely neglected the smaller, naked dinoflagellates owing to the difficulties involved in collecting and preserving them.

Nordli (1953) found optimum salinities for the growth of three species of *Ceratium* (*C. furca*, *C. fusus*, and *C. tripos*) at 20–25 $^0/_{00}$. He was able to correlate the relatively low salinity and high-temperature optima of these forms with similar conditions in the regions where they occur along the Norwegian coast. Nordli suggests that the so-called Tripos-plankton region of Gran (1902) off the northern coast of Norway may be a biogeographical area limited by high-temperature and low-salinity borders.

Table I gives a summary of the optimum and maximum range of

TABLE I

Optimum and Maximum Range of Salinity for Growth of Some Neritic Dinoflagellates

Reference	Species	Optimum, $^0/_{00}$	Range, $^0/_{00}$
Nordli (1953)	*Ceratium furca*	25	10–40
	Ceratium tripos	20	10–35
	Ceratium fusus	20	10–40
Braarud (1951)	*Amphidinium* sp.	15	5–45
	Exuviella balitca	18	5–35
	Peridinium trochoideum	20	5–60
Braarud and Rossavik (1951)	*Prorocentrum micans*	15–20	10–45
Braarud and Pappas (1951)	*Peridinium triquetrum*	15–20	10–40

salinity for the growth of several species of common neritic dinoflagellates as determined by Braarud and his co-workers.

While all the species have salinity optima well below that of full sea water, it is perhaps of even greater significance that they are also able to grow within an extremely wide range of salinities. This high degree of adaptability is a definite advantage to life in the variable environment of coastal and estuarine waters, and it is perhaps one of the means by which the neritic dinoflagellates are able to compete successfully with other organisms, such as diatoms, which in general have a more narrow range of salinity tolerance.

Nutrient Requirements

The autotrophic dinoflagellates, as other members of the phytoplankton, are dependent upon dissolved mineral salts for their nutrition. According to Vinogradov (1935) the peridinians contain approximately the same relative concentrations of nitrogen, phosphorus, calcium, and iron as does sea water.

The dinoflagellates have often been credited with the ability to utilize and flourish in extremely low concentrations of nitrogen and phosphorus (Gran, 1926–27; Gilson, 1937). This concept has stemmed largely from observations that dinoflagellate maxima, in temperate waters, follow the decline of the spring diatom flowerings and relatively large populations often persist throughout the summer months when the supplies of these nutrients are almost undetectable. Gran (1926–27) has proposed that the dinoflagellates require less nutrition for growth than the diatoms on account of their relatively low rate of metabolism.

There is some experimental evidence that dinoflagellates can utilize nitrogen and phosphorus at rather low concentrations. Thus Barker (1935) observed that increasing the nitrogen content of aged sea water by 1000 to 10,000 times did not increase the growth rates of *Prorocentrum micans, P. gracile,* or *Peridinium* sp. Similarly *P. micans* grew equally well in K_2HPO_4 concentrations ranging from 5×10^{-6} to $5 \times 10^{-3}\%$. King (1950) found that increasing nitrogen and phosphorus 1 to 200 times their concentrations in aged sea water did not increase the growth rate of *Gymnodinium simplex.*

There is no indication, however, that such low nutrient concentrations are necessary for the optimum growth of these organisms. Braarud (1945) found that maximum populations of several dinoflagellates occurred in the regions of heaviest pollution in the Oslofjord. Marshall (1947) observed a dense growth of *P. triquetrum* in Loch Craiglin immediately following fertilization of the loch. In the following section, a factor other than the nutritional physiology of the dinoflagellates will be discussed as a possible explanation for their occurrence and growth in nutrient-poor waters.

As mentioned earlier, dinoflagellates as a group show a continuous variation in their modes of nutrition from autotrophic to holozoic, while many species are facultative, obtaining their food by either or both methods (Kofoid and Swezy, 1921). We are concerned here principally with the former type of nutrition. However, it is perhaps questionable whether any of the dinoflagellates are completely autotrophic, in the literal sense of the term.

For many years they have remained among the most difficult of marine organisms to grow and maintain in culture. The author knows of no case in which dinoflagellates have been grown in a completely inorganic medium, either of the completely artificial or the enriched sea water type. The few media which have been developed and used successfully for growing these organisms include, almost without exception, soil extract as their common ingredient (Barker, 1935; Gross, 1937; Braarud, 1951; Sweeney, 1951).

Sweeney found that this substance best supported the growth of *Gymnodinium splendens* when aged for 4–6 weeks, and it was relatively ineffective when freshly prepared or aged for more than two months. Neither Barker nor Sweeney was able to replace soil extract with trace element mixtures. The latter author concluded that the active ingredient is probably organic in nature, and later (Sweeney, in press) succeeded in replacing soil extract with vitamin B_{12}.

King (1950) cultured *Gymnodinium simplex* in a medium consisting of McClendon's artificial sea water, Hoagland's trace element mixture, and yeast extract. Again, she was unable to obtain growth with the inorganic constituents alone, but was able to replace yeast extract with a mixture of amino acids added as pure chemicals in the same ratio as they occur in the yeast extract.

Provasoli and Pintner (1953) synthesized an artificial medium for the growth of *Gyrodinium californicum* which contained, in addition to the common inorganic nutrients and trace metals, a chelating agent (EDTA), NaH glutamate, *dl*-lycine, *dl*-leucine, and vitamin B_{12}.

Although the growth-promoting ingredients of soil extract have not been identified, it would appear likely, in view of the preceding evidence, that they include growth factors such as vitamin B_{12}. The organisms may also derive some benefit from humic acid and other ingredients which may act as chelating agents, reducing the concentrations of some one or more of the trace metals to a nontoxic or noninhibitory concentration.

In inshore waters dinoflagellates are often abundant, and in many parts of the world their populations may develop bloom proportions. Here the close association of the plankton with land masses and the contribution of runoff water to their environment provide what may be considered as a natural "soil extract," and, in the vicinity of heavily populated areas, frequently a source of organic pollutants. As mentioned earlier, Braarud (1945) observed a heavy growth of dinoflagellates in the highly polluted regions of the Oslofjord. Braarud and Pappas (1951) later found that the addition of small amounts of raw sewage to the medium stimulated the growth of *Peridinium triquetrum*.

In the open ocean, the presence of free organic compounds is more difficult to account for. In this case it is perhaps the metabolites or decomposition products of other plankton organisms which create the necessary growth conditions for the dinoflagellates.

It has been pointed out that many of the dinoflagellates found in temperate waters have relatively high-temperature optima, a fact which may explain their paucity in the winter plankton community and the spring blooms. However, there are certainly many species which are able to show some growth in temperatures of 0° C and below (Braarud, 1935). Yet even these are conspicuously absent from the usual spring flowering of diatoms. Thus temperature alone may not be sufficient to account for the seasonal periodicity of the dinoflagellates. It would appear that, in many cases, the growth of these organisms may be also dependent upon, or at least benefited by, the previous existence of a flowering of diatoms.

The underlying cause for this type of succession is probably nutritional, but its exact mechanism is obscure. The diatoms may reduce the concentrations of one or more of the nutrients or trace metals to a level favorable for the growth of the dinoflagellates. This type of relationship was proposed as an explanation of the succession of plankton elements in freshwater by Pearsall (1932) and Hutchinson (1944). A somewhat different type of relationship has been suggested by Lucas (1947, 1949), who has proposed the production of external metabolites or "ectocrines" by one group of plankton organisms which may have a beneficial effect upon the succeeding population and an inhibitory effect upon other competing organisms. This has been demonstrated in fresh water by Rice (1954).

Ecological Significance of Motility in Dinoflagellates

The presence of motility in the dinoflagellates, and its absence in the diatoms, may have an important bearing in the relationships of these organisms with such environmental conditions as temperature, salinity, and the nutrient concentration of the water. This is the hypothesis of Gran (1926–27) and is supported by Braarud (1935).

The diatoms are dependent upon vertical mixing and their natural buoyancy for remaining in the upper, photosynthetic zone of the ocean. They may derive some benefit from the synthesis of fats and its inclusion as oil droplets in their protoplasm and may possess structural adaptations of various types which increase their surface area and hence retard sinking (Gran, 1912; Russell, 1927; Sverdrup, Johnson, and Fleming, 1942). Gross and Zeuthen (1948), on the other hand, attribute the buoyancy of diatoms to their ability to maintain extremely low concentrations of divalent ions in their cell sap. According to these authors, under suitable physical conditions plankton diatoms have a specific gravity equal to that of sea water and do not sink, but at temperatures of 20° C or above, this equilibrium does not exist and the cells settle to the bottom. In general diatoms may be said to thrive in cold, fully saline ocean water at times of the year when there is considerable mixing of the surface water.

In temperate or northern summer conditions, the density of the water decreases as its temperature rises. For example, an increase in temperature from 0–25° C decreases the viscosity of sea water by one-half (Sverdrup, Johnson, and Fleming, 1942). In addition, vertical mixing is usually at a minimum in summer. Under these conditions, the diatoms find it increasingly difficult to remain in the upper water layers, and in Gran's opinion, their populations are unable to maintain themselves in the euphotic zone.

In the tropics, this situation usually prevails throughout the year and provides a definite disadvantage to the diatoms. For the same reason, they may encounter suboptimal conditions in the low-salinity (and hence low-density) waters of many coastal and estuarine situations.

The dinoflagellates, on the other hand, possessing the advantage of motility, are able to maintain themselves in water of low density with comparative ease and are relatively independent of vertical mixing. Furthermore, they, too, are often assisted by morphological adaptations which increase their surface area and thereby retard sinking. In the tropical forms, these structures far surpass similar features of the diatoms. Thus *Ceratium* is reputed to have the ability of prolonging or shedding its horns as it moves into warmer or colder water masses (Fig. 1). Others, like *Ornithocercus,* grow wide, wing-shaped membranes (Fig. 2). Some species, such as *Triposolenia*, have asymetrically arranged appendages so that, as soon as they stop swimming and start to sink, they are quickly oriented horizontally in the water,

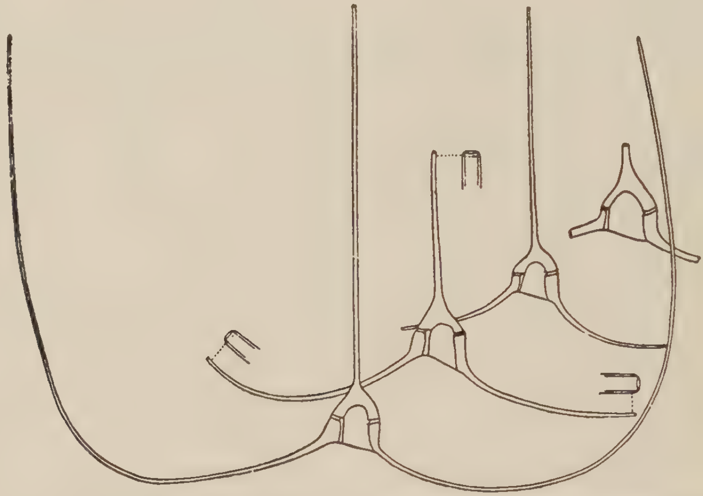

FIG. 1. *Ceratium trichoceros,* showing progressive and proportionate reduction of the horns in autotomy. (After Murray and Hjort.)

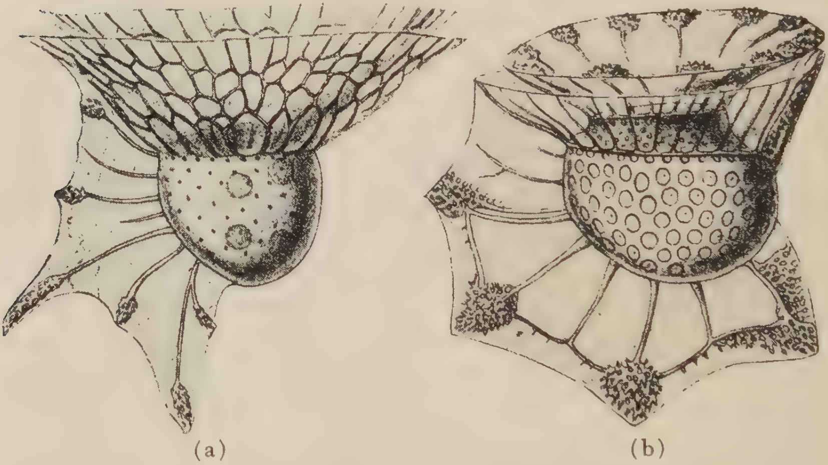

(a) (b)

FIG. 2. (a) *Ornithocercus splendidus;* (b) *Ornithocercus steinii.* (After Murray and Hjort.)

providing a maximum surface as resistance to sinking (Kofoid, 1906). Thus the dinoflagellates, in contrast to the diatoms, appear to be particularly well adapted for life in relatively calm, low-density water.

In addition, and of perhaps greater significance, the same factor of motility provides the dinoflagellates with an advantage in waters of low nutrient content. The nonmotile diatoms are dependent upon the dissolved nutrients contained in the water which immediately surrounds them and through which they sink (see Munk and Riley, 1952). In contrast, the dinoflagellates, though not strong swimmers, can move about for considerable distances and localize in the most advantageous depth for photosynthesis. If the nutrient level of the water is low, they may, by their vertical migrations, utilize all the nutrients available within the entire photic zone. According to Peters (1929) *Ceratium* can move through 5 to 10 meters in 12 hours or less.

Thus motility may be equally as important as the basic physiological characteristics of dinoflagellates in providing the means for their existence in waters of high temperature, low salinity, and reduced nutrient concentration.

"Red Water" Phenomena

Background

In certain parts of the world, usually in coastal or estuarine regions, dinoflagellates either grow or aggregate to such an extent that they impart a distinct coloration to the water. Such manifestations are known popularly as "red tide" or "red water," since the predominant color is of a reddish hue, although yellow or brown dinoflagellate blooms are not uncommon.

According to Allen (1946) a cell concentration of one-half to one million organisms per liter may give a chocolate-brown color to the water, while a doubling or trebling of this number is sufficient to produce red water. Concentrations of over 50 million cells per liter are not uncommon in patches of red water (Woodcock, 1948; Davis, 1948).

Frequently these aggregations of dinoflagellates are accompanied by a mass mortality of marine organisms (Whitelegge, 1891; Aiyar, 1936; Gunter *et al.*, 1948; Connell and Cross, 1950). However, many red water reports make no reference to such calamities. In many instances these outbursts are also accompanied by brilliant displays of luminescence.

The reported occurrences of red water are too numerous to review

TABLE II

Summary of Some Occurrences of "Red Water" Conditions in Various Parts of World
(M = mass mortality, L = luminescence)

Reference	Location	Time	Organism(s)	Ecological conditions
Whitelegge (1891)	Port Jackson, Australia	March, 1890	*Glenodinium rubrum*	Hot weather following heavy rainfall. Occurred in streaks or patches. (M)
Nishikawa (1901)	Bay of Aug, Japan	Sept., 1900	*Gonyaulax polygramma*	Occurred in patches, concentrated at surface. Floated on surface of container. (L)
Hirasaka (1922)	Gokasho Bay, Japan	Dec.–March, 1921	*Gymnodinium sanguineum*	Entire bay chocolate or red color. Restricted to layer approx. 1 meter thick. Diurnal vertical migrations. (L)
Ritchie (1952)	South coast of Honshu	May, 1950	*Noctiluca* sp.	Occurred in streaks offshore. Driven onshore by southerly winds. (L)
Hornell and Nayudu (1923)	Malabar coast, India	Annually, Aug.–Sept.	peridinians	Follow southwest monsoons, diatom blooms, and heavy rainfall. Occur during calm, hot weather. In bands along shore or patches which moved with tide.
Aiyar (1936)	Madras coast, India	June, 1935, and other years	*Noctiluca miliaris*	Follow diatom blooms in hottest time of the year. Salinities 34–35$^{0}/_{00}$. (M)
Menon (1945)	Trivandrum coast, India	Annually, June–Sept.	*Gymnodinium* sp.	Follow rains and diatom maxima.
Bhimacher and George (1950)	Malabar coast, India	Oct., 1948	*Noctiluca miliaris*	After southwest, before northeast monsoon; calm, hot weather; salinity ca. 35$^{0}/_{00}$.

Gilchrist (1914)	Walvis Bay, So. Africa	Annually in December	*Noctiluca* sp.	Follow periods of offshore wind. (M, L)
Brongersma-Sanders (1948)	Walvis Bay, So. Africa	Annually in Dec.	*Noctiluca* sp.	During periods of minimal upwelling. Water temperatures highest of year. (M, L)
Allen (1946 and ref.)	California coast	Frequently in midsummer	*Gonyaulax polyedra* *Prorocentrum micans*	Usually during periods of calm, hot weather, smooth seas. (L)
Bonnot and Phillips (1938)	Monterey Bay, Calif.	Aug.–Sept., 1937	*Gonyaulax catenella*	Developed inshore, spread seaward in bands. (L)
Torrey (1902)	San Pedro, Calif.	July, 1902	*Gonyaulax* sp. *Noctiluca* sp.	Occurred in patches of same temp. and salinity as surrounding seawater. (M, L)
Gunter *et al.* (1948)	West coast of Florida	Nov., 1946–Aug., 1947	*Gymnodinium brevis*	Calm, hot weather, preceded by hurricane and heavy rains. Temperature 24–27° C salinities 36–37$^0/_{00}$. (M)
Chew (1953)	West coast of Florida	Nov., 1952	*Gymnodinium brevis*	Occurred in patches. Temperature 23–25° C, salinity 33–34$^0/_{00}$.
Connell and Cross (1950)	Offats Bayou, Texas	Midsummer, 1949	*Gonyaulax* sp.	Calm, hot weather following heavy rainfall. (M, L)
Lund (1936)	Texas coast	June–Aug., 1935	?	Calm, hot weather following heavy rainfall.
Martin and Nelson (1929)	Delaware Bay, N.J.	July–Aug., 1928	*Amphidinium fusiforme* *Gymnodinium* sp.	Clear, fine weather. Occurred in bands. Temp. 25–28° C.
Mead (1898)	Narragansett Bay, R. I.	Aug.–Oct., 1898	*Peridinium* sp.	Calm, hot weather. (M)
Marshall and Orr (1927)	Loch Striven, Scotland	June, 1925	*Peridinium triquetrum*	Period of high temperature, and low salinity.
Braarud (1945)	Oslofjord, Norway	Aug., 1938	*Peridinium triquetrum*	In polluted part of fjord, concentrated at surface.

here completely. Table II gives a partial review of the red water literature, including the time and place of the occurrence, the causative organism, and a brief statement of the ecological conditions preceding or accompanying the outbreak, in so far as these have been observed.

Prerequisites for Red Water Conditions

The basic requirements for an outbreak of red water may be summarized under the following three headings: (1) a seed population of dinoflagellates, (2) the existence of favorable conditions for the growth of one or more of the species present, and (3) either the concentration of sufficient nutrients to permit the dense growth of the organisms, or the concentration of the organisms themselves, to the degree to which they are found in "red water."

The presence of a seed population of dinoflagellates is a condition which is probably always met, for there are at least a few of these organisms in almost every part of the ocean at all times. However, this is undoubtedly an important factor, together with the environmental conditions, in determining the particular species of dinoflagellate dominating a red water outbreak. Thus, it is somewhat more difficult to account for the origin of *Gymnodinium brevis*, the causative agent of the Florida "red tide," which appears to be present in the region only during its periods of blooming. Slobodkin (personal communication) is of the opinion that seed populations of this organism are maintained in the brackish to freshwater regions of the Florida Everglades.

In maximum developments of "red water," the optimal growth conditions for the species involved are perhaps met or closely approached. However, such ideal situations are probably less common than the existence of an environment in which the growth of some one species of dinoflagellates is favored over that of all other phytoplankton forms. In most parts of the ocean the diatoms are the principal competitors of the dinoflagellates, though other forms, such as Chrysophceae, Chlorophyceae, and Euglenineae may be important in estuarine conditions.

In the preceding sections of this report we have seen that the dinoflagellates can compete successfully with the diatoms under conditions of high temperature, low salinity, and reduced nutrient concentrations. They appear to require the presence of some one or more unknown organic substances, and there is some indication that they benefit from the previous existence of a large population of diatoms. It is doubtful if all these conditions are usually satisfied at any one time, and unlikely that they are all necessary for the dominance of dinoflagellates.

An examination of Table II reveals one factor which is almost universal in red water outbreaks, the occurrence of a high water temperature. In temperate or boreal regions of the ocean, red water appears to be restricted to the summer months, and the notation is frequently made that it is preceded by periods of unusually hot, calm weather. Along the Indian coast, red water occurs during the clear, hot periods between the southwest and the northeast monsoons (Hornell and Nayudu, 1923; Menon, 1945; Bhimachar and George, 1950). Off the Peruvian and Southwest African coasts it appears during the southern summer when the upwelling of cold water is at a minimum and water temperatures are the highest of the year (Brongersma-Sanders, 1948). Allen (1946) described a number of occurrences of red or yellow water along the California coast which have always occurred in mid-summer during periods of hot, calm weather and smooth seas.

There is less evidence that low salinity is an important factor in red water outbreaks. Slobodkin (1953) has shown a close correlation of red tides along the west coast of Florida with previous periods of exceptionally heavy rainfall. He has proposed that the organisms develop in small, discrete masses of relatively low-salinity water which result from the increased land drainage during heavy rains and are maintained in the ocean by density gradients. Table II gives several other instances in which red water has been preceded by heavy rainfall (Whitelegge, 1891; Hornell and Nayudu, 1923; Lund, 1936; Menon, 1945; Connell and Cross, 1950). However, this situation is by no means universal. On the South African, Peruvian, and California coasts, red water occurs during periods when precipitation is at a minimum. Furthermore, where such measurements have been made, the salinity in patches of red water does not appear to be significantly lower than that of the surrounding, clear ocean water (Ketchum and Keen, 1948; Chew, 1953; Torrey, 1902).

It is quite likely, however, that land drainage is important to the dinoflagellates from another aspect, that of providing their necessary organic matter. Whatever the function of these substances, it is possible that they are required in such minute concentrations as to satisfy the requirements of the organisms, although the entraining freshwater may not appreciably dilute the sea water.

The concentration of dissolved nutrient salts in a given water mass prior to the onset of red water has not, to the author's knowledge, been determined. There are, to be sure, small, local occurrences which appear to be related to the introduction of domestic pollutants (Braarud, 1945; Connell and Cross, 1950). In these instances there are perhaps sufficient nutrients, as well as the necessary organic growth factors, to support populations approaching red water proportions. However, in the majority of red water occurrences there is no indication of an unusually high enrichment of the water prior to the outbreak.

Brongersma-Sanders (1948) emphasized that red water is associated with those regions of the world where upwelling brings deep, cold, nutrient-rich water to the surface (i.e., Southwest Africa, Peru, California). She also pointed out, however, that such upwelled water normally supports a luxuriant growth of diatoms, and that red water occurs in these regions only during the summer months when upwelling, and presumably the nutrient level, is greatly reduced. On the Indian coast, the southwest monsoon is associated with high enrichment and maximum productivity of the waters. Under these conditions it is again the diatoms which flourish, and red water appears only when the monsoon has ended.

Ketchum and Keen (1948) measured the total phosphorus content of sea water collected in and outside of patches of red water which occurred off the west coast of Florida in 1946–47. They found concentrations of total phosphorus in the red water (including that contained in the organisms) up to ten times as high as that of the clear water outside of the local patches. These authors emphasize the necessity for a mechanism either for accumulating these concentrations of phosphorus in the water prior to the growth of the organisms, or for concentrating the organisms after they have grown. There was no indication that the first of these alternatives was true.

The maximum concentration of phosphorus in the deep offshore waters of the Caribbean (2 microgram atoms per liter), as determined by Rakestraw and Smith (1937), does not approach the maximum observed in the red water patches (20 microgram atoms per liter), so upwelling could not have provided sufficient enrichment to be an important factor. It is also unlikely that land drainage could account for this phosphorus. Since the red water region contained only about 10% freshwater, runoff would have to carry tremendous concentrations of this element to account for the amount present in the organisms (estimated at 17,000 lb of pure phosphorus per square mile of red water). Chew (1953), who investigated a minor outbreak of red water in the same region in 1952, found that the lower salinity, coastal water, which contained the river drainage, had lower concentrations of phosphorus than the open waters of the Gulf of Mexico.

Thus it would appear that there may be insufficient nutrients normally present in sea water, and no known mechanism for concentrating them to a sufficiently high level, to support the development of a typcial red tide. The remaining possibility, that the organisms themselves become concentrated after growth, will be discussed below.

In every case in which the vertical distribution of dinoflagellates in red water has been examined, it was found that the organisms were concentrated in relatively narrow bands usually at the surface of the water (Whitelegge, 1891; Nishikawa, 1901; Hirasaka, 1922; Martin and Nelson, 1929). In three instances of small, local outbreaks of red water, cell counts were made in a vertical column, revealing in each case that the maximum concentration of dinoflagellates occurred at the surface (Table III).

It is very doubtful that the organisms could have grown in such a pattern of distribution. As pointed out above, there would appear to be insufficient nutrients available to support such populations. Furthermore the high light intensities at the surface of the ocean are normally inhibitory to photosynthesis (Stanbury, 1931; Jenkin, 1937), particularly in the case of dinoflagellates, many of which appear to prefer reduced illumination (Barker, 1935; King, 1950). Hence, dense aggregations of dinoflagellates at the surface of the water must be

TABLE III

Vertical Distribution of Dinoflagellates in Red Water
(Figures indicate organisms per liter)

Depth (meters)	*Peridinium triquetrum*		*Gonyaulax monilata*
	Braarud (1945)	Marshall (1927)	Slobodkin (1953)
0	361,000	32–56,000	8,200,000
0.3			5,700,000
2.0	45,000	—	
2.6			450,000
4.0	11,000	—	
6.0	—	800	—

explained by concentrations of the organisms themselves, either by means of their active motility, or by passive floatation, should they become less dense than sea water.

Gran and Braarud (1935) observed that *Peridinium triquetrum* was often found in maximum concentrations at the surface, but that this organism could occur at any depth from 0 to 25 meters. They concluded that it could seek out the level at which the general conditions for growth were most favorable. Halse (1950) demonstrated marked vertical diurnal migrations in several dinoflagellates, the characteristics of which differed considerably from species to species. Thus *Ceratium fusus* and *C. tripos* rose to the surface at night and sank to the lower depths during the day, while *Gonyaulax polyedra* and *Prorocentrum micans* showed the opposite response to light, rising in the daytime and sinking at night.

Concentration of dinoflagellates by means of such migrations may, at times, create red water conditions. Hirasaka (1922) observed red water in Gokasho Bay, Japan, in which the entire bay was apparently affected, in contrast to the usual situation in which red water is restricted to patches or streaks. According to this author, the organisms were confined to a band no more than 3 to 4 ft thick which appeared to migrate diurnally, the red color being most conspicuous in the late afternoon.

In many cases, however, the red water organisms remain at the surface of the water at all times. Woodcock (personal communication) collected samples of *Gymnodinium brevis* during the 1946–47 red tide off Florida and observed that the organisms remained at the surface of the vessel at all times of the day and night. Ketchum (personal communication) observed the same behavior in *Noctiluca miliaris* collected during a bloom at Friday Harbor. Hornell and Nayudu (1923) and Nishikawa (1901) found that the red water organisms remained floating at the surface of a bottle apparently until they encysted; then they sank to the bottom.

Harvey (1917) and Ketchum (unpublished) studied the specific gravity of *Noctiluca* collected from patches of red water. In each case the organisms remained floating at the surface of the sea water if the latter was diluted with fresh water until the dilution approached 50%, beyond which they became suspended or sank. It must be emphasized, however, that these observations were made upon cells collected during typical red water conditions. It must not be assumed that such low densities are typical of *Noctiluca* at all times, and it cannot be so assumed if one subscribes to the theory that they accumulate at the surface after their growth. In this connection, the present author has observed a healthy culture of *Noctiluca* grown by Dr. L. Provasoli in which the organisms were evenly distributed throughout the medium.

Pratje (1921) has suggested that *Noctiluca* undergoes physiological changes in response to its environment, and that senescent, nondividing cells lose density and become buoyant in sea water. He subscribes to the theory suggested above that the concentration of these organisms at the surface does not result from active migration, but from floatation. Spoehr and Milner (1949) and others have demonstrated that *Chlorella* ceases to divide and stores fats when the nitrogen in its medium becomes limiting. Fat storage in the autotrophic dinoflagellates is common. Many species accumulate bright yellow or red oil droplets (Graham, 1951). *Noctiluca* apparently does not store fats, but its buoyancy is explained on the basis of the low specific gravity of its cell sap possibly through the accumulation of NH_4^+ ions (see Krogh, 1939). Such mechanisms as these are adequate to account for the floatation of dinoflagellates. It remains to be demonstrated that changes occur in their metabolism or osmo-regulation such as to make them buoyant only at certain stages of their development.

The accumulation of buoyant organisms at the water surface would, of course, be enhanced in the absence of vertical mixing of the water, which would tend to carry them down again into deeper layers. Harvey (1917) mentions that *Noctiluca* could not be observed at the surface during windy days. A re-examination of Table II will reveal that most of the occurrences of red water throughout the world were accompanied or preceded by periods of calm weather and smooth seas. Such conditions, together with the high temperatures which usually accompany them, may further stabilize the water through thermal stratification, providing additional resistance to the vertical mixing of the organisms.

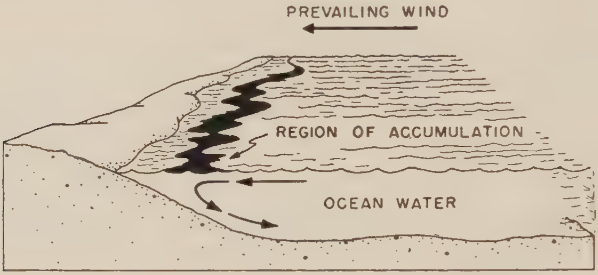

FIG. 3. Accumulation of floating material along shore by prevailing onshore wind.

Once the organisms have accumulated at the surface of the water, there are several means by which they may become further concentrated. Three such mechanisms will be discussed briefly below.

(1) Prevailing onshore winds: Surface water driven shoreward by prevailing onshore winds establishes a circular pattern, sinking at the waters edge and returning seaward at lower depths. Buoyant organisms will accumulate in windrows along shore or at the region of descent (Fig. 3).

(2) Where brackish coastal water, particularly in the vicinity of river mouths, meets open ocean water, there is a mixing and sinking of the two water masses along a line of convergence. Both types of water flow toward this line, and buoyant organisms will accumulate at or near the convergence line, producing streaks of floating material. (Fig. 4).

(3) Convection cells: Wind-driven vertical convection cells may be established which rotate alternately clockwise and counterclockwise

with their vertical axes perpendicular to the direction of the prevailing wind. Floating objects will accumulate in the region between the descending components of two such adjoining cells. Under these conditions parallel streaks of floating matter are produced (Fig. 5). (For a more detailed description of this process, see Langmuir, 1938; Stommel, 1949.)

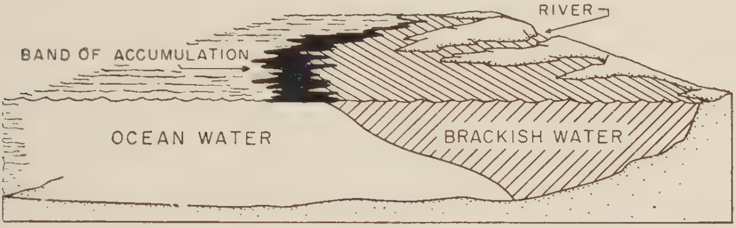

Fig. 4. Accumulation of floating material at convergence of water masses of different density.

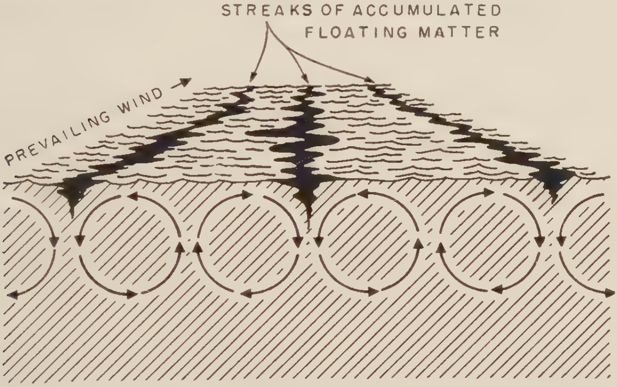

Fig. 5. Accumulation of floating material by wind-driven convection cells.

These and other similar mechanisms are undoubtedly important means of concentrating dinoflagellates to the extent to which they are observed in red water conditions. The existence of such processes is indicated by the repeated mention of patches or streaks of organisms in many descriptions of red water (see Table II). Bary (1953) has indicated that convection cells are responsible for the streaky distribution of floating masses of the ciliate *Cyclotrichium meunieri* in Wellington Harbor, New Zealand.

Thus through the combined processes of floatation and surface concentration, a method is possible by means of which red water conditions may be produced without the excessive enrichment of the water, and, indeed, without an unusually heavy growth of dinoflagellates. This may be illustrated by the following hypothetical situation.

According to Riley (1937, 1938) phosphate-phosphorus values for the surface waters of the Gulf of Mexico range from 0.02 to 0.5 microgram atom per liter. Since red water often occurs when nutrient levels are low, let us propose a situation in which the phosphate-phosphorus concentration is 0.05 microgram atom or 1.55×10^{-6} gram per liter. Let us further assume that other mineral nutrients, organic growth factors, etc., are present in the same or higher concentrations as phosphorus relative to the requirements of a given species of dinoflagellate.

No data are available concerning the dry weight and elementary analysis of red water organisms. However, these may be roughly estimated from known figures for other plankton organisms, and values may be obtained which are probably reliable within an order of magnitude.

Gymnodinium brevis, the dinoflagellate responsible for the Florida red tide of 1946–47, measures approximately 28 by 28 by 13 microns (Davis, 1948), and its volume may be roughly estimated at 7.5×10^{-9} cc. If it is assumed to have about the same density as sea water (at about $34^0/_{00}$ and 25° C in the coastal waters of the Gulf of Mexico), its wet weight will approximate 7.7×10^{-9} gram per cell.

Ketchum and Redfield (1949) found that the dry weight of a variety of planktonic algae was approximately 25% of their wet weight, and that their phosphorus content was rather constant at about 2.5% of the dry weight. Using these figures for *Gymnodinium* (which are probably somewhat high for dinoflagellates in general) a value of 0.48×10^{-10} gram of phosphorus per cell is obtained.

A dissolved phosphorus concentration of 1.55×10^{-6} gram per liter will then support a population of

$$\frac{1.55 \times 10^{-6}}{0.48 \times 10^{-10}} = 3.2 \times 10^{4} \text{ cells per liter}$$

if all of the phosphorus were utilized and no other nutrient was limiting.

If the dinoflagellates in this hypothetical situation are also able to utilize all the nutrients in a water column 10 meters deep, and then, due to changes in their specific gravity, accumulate in the upper meter, their concentration at the surface will be in the range of 3.2×10^5 cells per liter. The action of winds, convergence, or convection may then easily concentrate this surface layer by another factor of 10 or 20, producing concentrations of organisms typical of red water conditions, which range anywhere from 10^6 to 10^8 cells per liter.

Thus there is no necessity to postulate obscure factors which would account for a prodigious growth of dinoflagellates to explain red water. It is necessary only to have conditions favoring the growth and dominance of a moderately large population of a given species, and the proper hydrographic and meteorological conditions to permit the accumulation of organisms at the surface and to effect their further concentrations in localized areas.

References

Aiyar, R. G. 1936. Mortality of fish of the Madras Coast in June, 1935. *Current Sci.*, **4**, 488–89.

Allen, W. E. 1939. Phosphorescence in the sea. *Naut. Gaz.*, Aug. 26, 1939.

Allen, W. E. 1946. "Red water" in La Jolla Bay in 1945. *Trans. Amer. Microscop. Soc.*, **65**, 149–53.

Barker, H. A. 1935. The culture and physiology of marine dinoflagellates. *Arch. Mikrobiol.* **6**, 157–81.

Bary, B. M. 1953. Sea-water discoloration by living organisms. *New Zealand J. Sci. Technol.* **B34**, 393–407.

Bhimachar, B. S., and P. C. George. 1950. Abrupt set backs in the fisheries of the Malabar and Kanara Coasts and "red water" phenomenon as their probable cause. *Proc. Indian Acad. Sci.*, **B31**, 339–50.

Bonnot, P., and J. B. Phillips. 1938. Red water, its cause and occurrences. *Calif. Fish and Game,* **24**, 55–59.

Braarud, T. 1935. The Øst expedition to the Denmark Strait, 1929. II. The phytoplankton and its condition of growth. *Hvalradets Skrifter, Norske Videnskaps—Acad. Oslo,* **No. 10.**

Braarud, T. 1945. A phytoplankton survey of the polluted waters of inner Oslofjord. *Hvalradets Skrifter, Norske Videnskaps-Akad. Oslo,* **No. 28.**

Braarud, T. 1951. Salinity as an ecological factor in marine phytoplankton. *Physiol. Plant.,* **4,** 28–34.

Braarud, T., and I. Pappas. 1951. Experimental studies on the dinoflagellate *Peridinium triquetrum* (Ehrb.) Lebour. *Avhandl. Norske Videnskaps-Acad. Oslo Mat-Naturv. Klasse,* **1951,** No. 2.

Braarud, T., and E. Rossavik. 1951. Observations on the marine dinoflagellate *Prorocentrum micans* Ehrenb. in culture. *Avhandl. Norske Videnskaps-Akad. Oslo Mat. Naturv. Klasse,* **1951,** No. 1.

Brongersma-Sanders, M. 1948. The importance of upwelling water to vertebrate paleontology and oil geology. *Verhandl. Konin. Nederland. Akad. Wetenschap. Natuur.,* Tweede Sectie, **45,** No. 4, 112 pp.

Chew, F. 1953. Results of hydrographic and chemical investigations in the region of the "red tide" bloom on the West Coast of Florida in Nov., 1952. *Bull. Marine Sci., Gulf and Carib.,* **2,** 610–25.

Connell, C. H., and J. B. Cross. 1950. Mass mortality of fish associated with the protozoan *Gonyaulax* in the Gulf of Mexico. *Science,* **112,** 359–63.

Davis, C. C. 1948. *Gymnodinium brevis* sp. nov., a cause of discolored water and animal mortality in the Gulf of Mexico. *Botan. Gaz.,* **109,** 358–60.

Fritsch, F. E. 1935. The structure and reproduction of the algae. Vol. I. The University Press, Cambridge, Mass.

Gaarder, T., and H. H. Gran. 1927. Production of plankton in the Oslofjord. Cons. Perm. Int. Explor. Mer; *Rapport et Proc. Verb.* **42,** 1–48.

Gilchrist, J. D. F. 1914. An enquiry into fluctuations in fish supply on the South African Coast. *Marine Biol. Rept., Union South Africa,* **2** (2), 8–35.

Gilson, H. C. 1937. The Nitrogen Cycle. *John Murray Exped.,* **2,** 21–81.

Graham, H. W. 1951. *Pyrrophyta.* In *Manual of Phycology:* An Introduction to the Algae and Their Biology. The Chronica Botanica Co., Waltham, Mass.

Gran, H. H. 1902. Das plankton des norwegischen Nordmeers von biologischen und hydrographischen Gesichtspunkten behandelt. Bergen. *Rept. on Norwegian Marine—und Fishery—Investigations,* **2.** No. 5.

Gran, H. H. 1912. Pelagic Plant Life. In J. Murray and J. Hjort, *The Depths of the Ocean.* MacMillan and Co., London.

Gran, H. H. 1924. Quantitative plankton investigations carried out during the expedition with "Michael Sars" July–Sept., 1924. *Cons. Perm. Exp. Mer; Rapport et Proc. Verb.,* 56.

Gran, H. H. 1926–27. Investigation of the production of plankton outside the Romsdalfjord. *Cons. Int. Exp. Mer; Rapport et Proc. Verb.,* 56.

Gran, H. H., and T. Braarud. 1935. A quantitative study of the phytoplankton in the Bay of Fundy and the Gulf of Maine. *J. Biol. Board Canada,* **1,** 279–467.

Gross, F. 1937. Notes on the culture of some marine plankton organisms. *J. Marine Biol. Assoc.*, **21**, 753–68.

Gross, F., and E. Zeuthen. 1948. The buoyancy of plankton diatoms: a problem of cell physiology. *Proc. Roy. Soc. (London)*, **B135**, 382–89.

Gunter, G., R. H. Williams, C. C. Davis, and F. G. Walton Smith. 1948. Catastropic mass mortality of marine animals and coincident phytoplankton bloom on the west coast of Florida, November 1946 to August 1947. *Ecol. Monographs*, **18**, 309–24.

Halse, G. R. 1950. Phototactic vertical migration in marine dinoflagellates. *Oikos*, **2**, 162–75.

Harvey, E. B. 1917. A physiological study of specific gravity and of luminescence in *Noctiluca* with special reference to anaesthesis. *Carnegie Inst. Wash., Papers Dept. Marine Biol.*, **11**, 235–53.

Harvey, E. N. 1952. *Bioluminescence*. Academic Press, New York.

Herdman, W. A. 1922. Spolia Runiana V. Summary of results of continuous investigation of the plankton of the Irish Sea during 15 years. *J. Linnean Soc. London Botany*, **46**, 141–70.

Hirasaka, K. 1922. On a case of discolored sea-water. *Annot. Zool. Japan*, **10**, 161–64.

Hornell, J., and M. R. Nayudu. 1923. A contribution to the life history of the Indian Sardine. *Madras Fish. Bull.*, **17**, 129–97.

Hutchinson, G. E. 1944. Limnological studies in Connecticut. VII. A critical examination of the supposed relationship between phytoplankton periodicity and chemical changes in lake waters. *Ecology*, **25**, 3–26.

Jenkin, P. M. 1937. Oxygen production by the diatom, *Coscinodiscus excentricus* Ehr. in relation to submarine illumination in the English Channel. *J. Marine Biol. Assoc. U. K.*, **22**, 301–43.

Ketchum, B. H., and J. Keen. 1948. Unusual phosphorus concentrations in the Florida "red tide" sea water. *J. Marine Research*, **7**, 17–21.

Ketchum, B. H., and A. C. Redfield. 1949. Some physical and chemical characteristics of algae grown in mass culture. *J. Cellular and Comp. Physiol.*, **33**, 281–300.

King, G. S. 1950. Production of red tide in the laboratory. *Proc. Gulf and Carib. Fish. Inst. 2nd Ann. Sess.*, Nov., 1949, 107–109.

Kofoid, C. A. 1906. On the significance of the asymmetry in *Triposolenia*. *Univ. Calif. Publ. Zool.*, **3**, 127–33.

Kofoid, C. A., and O. Swezy. 1921. The free living unarmored Dinoflagellata. *Mem. Univ. Calif.*,**5**, 1–562.

Krogh, A. 1939. *Osmotic Regulation in Aquatic Animals*. The University Press, Cambridge.

Langmuir, I. 1938. Surface motion of water induced by wind. *Science*, **87**, 119–23.

Lucas, C. E. 1947. The ecological effects of external metabolites. *Biol. Revs.*, **22**, 270–95.

Lucas, C. E. 1949. External metabolites and ecological adaptation. *Symp. Soc. Exptl. Biol.* III. Selective toxicity and antibiotics. Academic Press, New York.

Lund, E. J. 1936. Some facts relating to the occurrence of dead and dying fish on the Texas Coast during June, July, and August, 1935. Cited from: G. Gunter *et al.* 1948. Catastrophic mass mortality of marine animals and coincident phytoplankton bloom on the west coast of Florida, November, 1946 to August, 1947. *Ecol. Monographs,* **18,** 309–24.

Marshall, S. M. 1947. An experiment in marine fish cultivation III. The plankton of a fertilized loch. *Proc. Roy. Soc. Edinburgh,* **B63,** 21–33.

Marshall, S. M., and A. P. Orr. 1927. The relation of the plankton to some chemical and physical factors in the Clyde Sea area. *J. Marine Biol. Assoc.*, **14,** 837–68.

Martin, G. W., and T. C. Nelson. 1929. Swarming of dinoflagellates in Delaware Bay, New Jersey. *Botan. Gaz.*, **88,** 218–24.

Mead, A. D. 1898. *Peridinium* and the "red water" in Narragansett Bay. *Science,* **8,** 707–709.

Menon, M. A. S. 1945. Observations on the seasonal distribution of the plankton of the Trivandrum Coast. *Proc. Ind. Acad. Sci.*, **B22,** 31–62.

Michaelis, G. A. 1830. Ueber das Leuchten der Ostsee nach eigenen Beobachtungen. Cited from: C. A. Kofoid and O. Swezy. 1921. The free-living unarmored Dinoflagellata. *Mem. Univ. Calif.*, **5,** 1–562.

Munk, W. H., and G. A. Riley. 1952. Absorption of nutrients by aquatic plants. *J. Marine Research,* **11,** 215–40.

Nishikawa, T. 1901. *Gonyaulax* and the discolored water in the Bay of Agu. *Annot. Zool. Japon,* **4,** 31–34.

Nordli, E. 1953. Salinity and temperature as controlling factors for distribution and mass occurrence of *Ceratia. Saertrykk av. Blyttia,* **11,** 16–18.

Pearsall, W. H. 1932. Phytoplankton in the English lakes. II. The composition of the phytoplankton in relation to dissolved substances. *J. Ecol.*, **20,** 241–62.

Peters, N. 1929. Über Orts- und Geisselbewegund bei marinen Dinoflagellaten. Archiv. f. Protistenk. 67: 291–321.

Peters, N. 1932. Wissenschaftliche Ergebnisse der deutschen atantischen Expedition auf dem Forschungs-und Vermessungsschiff "Meteor" 1925–1927. Bd 12, Lief 1: Die Bevölkerung des Südatlentischen Ozeans mit *Ceratien.* Cited from: *Bot. Centr.* [N. F.] **21,** 412–13.

Pratje, A. 1921. *Noctiluca miliaris* Suriray. Beitrage zur Morphologie, Physiologie, und Cytologie. I. Morphologie und Physiologie, *Arch. Protistenk.*, **42,** 1–98.

Provasoli, L., and I. J. Pintner. 1953. Ecological implications of *in vitro* nutritional requirements of algae flagellates. *Ann. N. Y. Acad. Sci.*, **56**, 839–51.

Rakestraw, N. W., and H. P. Smith. 1937. A contribution to the chemistry of the Caribbean and Cayman Seas. *Bull. Bingham Oceanog. Coll.*, **6** (1), 1–41.

Rice, T. R. 1954. Biotic influences affecting population growth of planktonic algae. *U. S. Fish Wildlife Service Fishery Bull.*, **54**, 227–45.

Riley, G. A. 1937. The significance of the Mississippi River drainage for biological conditions in the northern Gulf of Mexico. *J. Marine Research*, **1**, 60–74.

Riley, G. A. 1938. Plankton studies. I. A preliminary investigation of the plankton of the Tortugas region. *J. Marine Research*, **1**, 335–52.

Ritchie, G. S. 1952. H. M. S. *Challanger's* investigations in the Pacific Ocean. *J. Inst. Nav.*, **5**, 251–61.

Russell, F. S. 1927. The vertical distribution of plankton in the sea. *Biol. Revs.* **2**, 213–62.

Slobodkin, L. B. 1953. A possible initial condition for red tides on the coast of Florida. *J. Marine Research*, **12**, 148–55.

Spoehr, H. A., and H. W. Milner. 1949. The chemical composition of *Chlorella;* effect of environmental conditions. *Plant Physiol.*, **24**, 120–49.

Stommel, H. 1949. Trajectories of small bodies sinking slowly through convection cells. *J. Marine Research*, **8**, 24–29.

Stanbury, F. A. 1931. The effect of light of different intensities, reduced selectively and non-selectively, upon the rate of growth of *Nitzschia closterium*. *J. Marine Biol. Assoc.*, **17**, 633–53.

Sverdrup, H. U., M. W. Johnson, and R. H. Fleming. 1942. *The Oceans, Their Physics, Chemistry, and General Biology*. Prentice-Hall, New York.

Sweeney, B. M. 1951. Culture of the marine dinoflagellate, *Gymnodinium* with soil extract. *Am. J. Bot.*, **38**, 669–77.

Sweeney, B. M. *Gymnodinium splendens,* a marine dinoflagellate requiring vitamin B_{12}. In press.

Torrey, H. B. 1902. An unusual occurrence of dinoflagellates on the California Coast. *Am. Naturalist*, **36**, 187–92.

Vinogradov, A. P. 1935. Elementary chemical composition of marine organisms. Part I. Cited from: H. U. Sverdrup, M. W. Johnson, and R. H. Fleming. 1942. *The Oceans, Their Physics, Chemistry, and General Biology.* Prentice-Hall, New York.

Whitelegge, T. 1891. On the recent discoloration of the waters of Port Jackson. *Rec. Aust. Mus., Sydney*, **1**, 179–92.

Woodcock, A. H. 1948. Note concerning human respiratory irritation associated with high concentration of plankton and mass mortality of marine organisms. *J. Marine Research*, **7**, 56–62.

DISCUSSION

Dr. Sweeney: Dr. Ryther has made clear in his presentation, an understanding of the nutritional requirements of the dinoflagellates is prerequisite to any explanation of the occurrence of "red tides." These organisms have been found to require for growth, substances not present in aged autoclaved sea water and usually supplied by the addition to the culture medium of small amounts of soil extract. In our laboratory, an analysis of the activity of soil extract with respect to the growth of bacteria-free *Gymnodinium splendens* has shown that soil extract may be replaced by vitamin B_{12}, the optimum concentration being at 0.01 microgram vitamin B_{12} per liter. Provasoli has shown that the dinoflagellate *Gyrodinium* sp. also requires vitamin B_{12}. The organic requirements of *Prorocentrum micans* and *Gonyaulax polyedra* appear to be more complex and cannot be met by vitamin B_{12} alone.

Gonyaulax polyedra may be grown successfully in mineral-enriched aged sea water with soil extract. Maximum populations reached are of the order of 40,000 cells per milliliter and the generation time is 40 to 60 hours. This organism is bioluminescent in culture. (*Prorocentrum micans, Gymnodinium splendens,* and *Gyrodinium* in our cultures are not luminescent.) Because it is both luminescent and photosynthetic, *Gonyaulax* provides interesting material for the study of bioluminescence.

Contribution No. 724

Transactions, American Geophysical Union Volume 36, Number 3 June 1955

SOUTHWEST PACIFIC CRUSTAL STRUCTURE

Charles B. Officer

(Woods Hole Oceanographic Institution Contribution No. 724)

Abstract--This investigation has been concerned with the determination of the crustal thicknesses of the various features of the Southwest Pacific from Love- and Rayleigh-wave dispersion characteristics. The crustal thickness of the Tasman Basin between New Zealand and Australia is the same, five to ten km, as that for the South Pacific Basin to the east of New Zealand. The thickness of East Cape - Kermadec - Tonga Ridge bordering the South Pacific Basin on the west and that of the Lord Howe Rise bordering the Tasman on the northeast is 20-25 km. A crustal refraction profile over New Zealand gives a thickness of 20 km. The interior region of ridges and troughs, northeast of New Zealand, has an average thickness of 15-20 km. The results are indicative of an origin from successive orogenic belts built out over an oceanic crust. The area is not part of an extensive continent.

Introduction--Recently the author has had the opportunity to be in New Zealand on a Fulbright research fellowship and to be able to examine the crustal structure of the Southwest Pacific from the New Zealand network of stations and from the Australia stations at Brisbane and Sydney. The purpose of the research has been to determine the crustal thicknesses of the various features in this rather complex area for the conclusions that they might add to its geologic history and to a general knowledge of the geology of suboceanic areas.

The method used was to examine the dispersive characteristics of the surface wave trains from selected distant earthquakes. These waves travel in the wave guide bounded at the bottom by the familiar Mohorovicic discontinuity. This boundary represents a discontinuity in seismic velocity from a value of 6.5-7.0 km/sec to a value of 8.1 km/sec. It is a datum which has been observed from both earthquake and explosion seismology over the Earth. Under the continents, it is at a depth of 35 to 60 km being deepest under the high mountain ranges. Under all explored ocean-basin areas, it is at a depth of 10 to 13 km below sea level. This shallow depth is found uniformly under all ocean basin areas and is a distinguishing feature of these areas, indicative of their stability and their lack of direct association in the geosynclinal and resultant tectonic activities in the past. The seismic velocity of the material below this discontinuity is higher than measured on surface rocks; it is probably ultrabasic [HESS, 1954], the exact nature of the physical or chemical change across the discontinuity remaining a question to be answered. That such material has taken part in tectonic activity is evinced by its depression under the mountain ranges, but that it represents the depth of isostatic compensation, as has been considered by some, is doubtful. In this paper it is used in the seismic sense only to distinguish between areas of thin crust, 5-10 km, typical of the ocean basins and those of thick crust, 35-60 km, typical of the continents and to determine the thickness under the active geologic regions of the island arcs.

Previous investigations have been limited for the most part to the determination of the crust under New Zealand. HAYES [1935], BULLEN [1936; 1939], and EIBY [1949] have obtained results from travel time curves for local earthquakes. In addition, E. I. Robertson and the staff of the New Zealand Geophysics Division made a crustal refraction profile on a line northeast from Wellington. DE JERSEY [1946] studied Rayleigh waves recorded at Brisbane from the Solomons, Samoa, and the Kermadecs.

Figure 1 is a bathymetric map of the Southwest Pacific with the earthquake paths that were used. The nomenclature is that of BRODIE [1952]. To the east is the broad expanse of the South Pacific Basin extending over to the Easter Island Rise. Between New Zealand and Australia there is an extension of this deep water area in the Tasman Basin. Bordering the South Pacific Basin is the sequence of the Kermadec and Tonga Trenches and the East Cape - Kermadec - Tonga Ridge extending from New Zealand to Samoa. The major belt of shallow-focus earthquakes, not shown, follows along the eastern side of the Ridge with the intermediate and deep focus belts along the same trend further to the west. This sequence appears again in the New Hebrides and Solomons

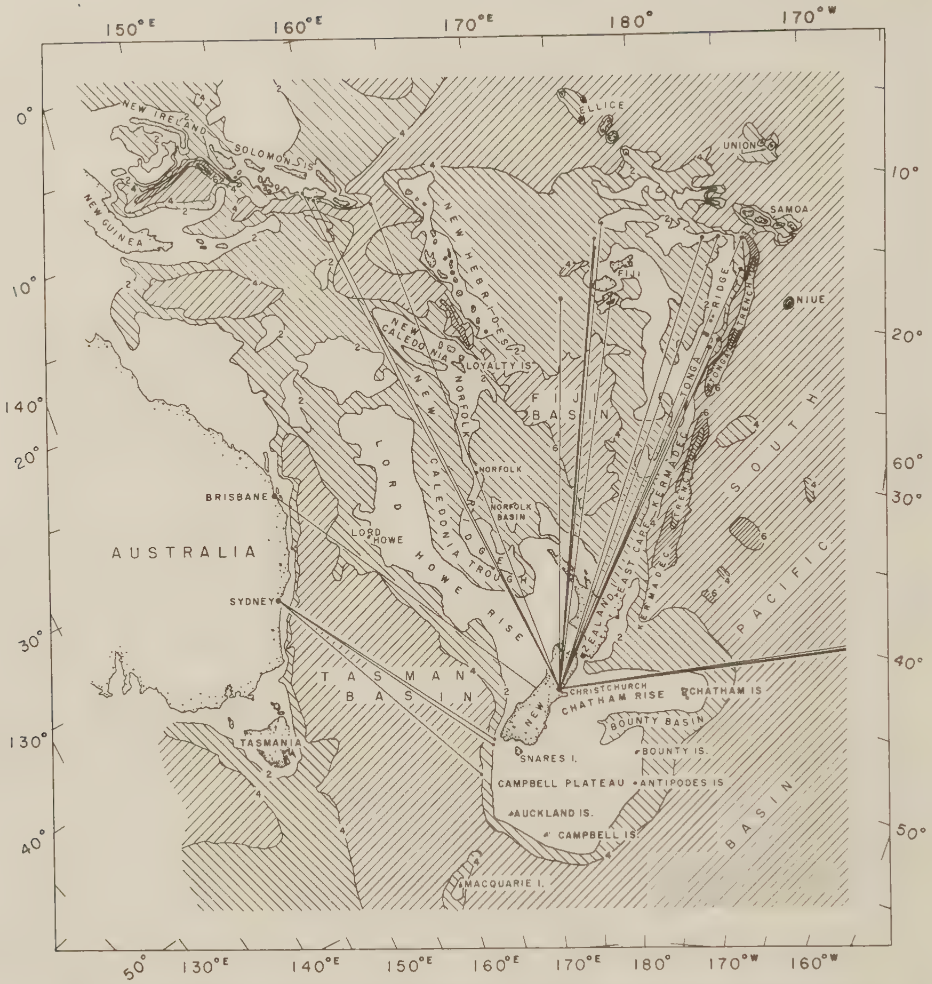
150°E
160°E
170°E
180°
170°W
0°
10°
20°
30°
40°
140°
130°
50°
10°
20°
60°
30°
40°
50°
130°E
140°E
150°E
160°E
170°E
180°
170°W
160°W
NEW IRELAND
SOLOMON IS
NEW GUINEA
ELLICE
UNION
SAMOA
NIUE
NEW HEBRIDES
FIJI
NEW CALEDONIA
LOYALTY IS
FIJI BASIN
TONGA RIDGE
TONGA TRENCH
NORFOLK
NEW CALEDONIA TROUGH
NORFOLK RIDGE
NORFOLK BASIN
LORD HOWE RISE
LORD HOWE
BRISBANE
AUSTRALIA
SYDNEY
EAST CAPE
KERMADEC RIDGE
KERMADEC TRENCH
SOUTH PACIFIC BASIN
TASMAN BASIN
NEW ZEALAND
CHRISTCHURCH
CHATHAM RISE
CHATHAM IS
BOUNTY BASIN
BOUNTY IS.
SNARES I.
CAMPBELL PLATEAU
ANTIPODES IS
AUCKLAND IS.
CAMPBELL IS
TASMANIA
MACQUARIE I.
2
4
6

Fig. 1--Bathymetric chart of the Southwest Pacific including earthquake paths

with the trenches now on the side away from the Pacific Basin. Between these two is the Fiji area and the Fiji Basin. Bordering the Tasman Basin on the northeast is the Lord Howe Rise. Further to the northeast are the New Caledonia Trough, Norfolk Ridge, and Norfolk Basin.

For the South Pacific Basin earthquakes from the Easter Island region recorded at Christchurch were used. For the Tasman Basin the travel path was fairly short, and it was advantageous to pick earthquakes and a station for which no correction would be needed for travel through a different structure. Earthquakes off the southwest of New Zealand to the Riverview station, Sydney, met this requirement. No earthquake paths were available to the station at Samoa for the investigation of the crust under the Kermadec and Tonga Trenches. For the East Cape - Kermadec - Tonga Ridge earthquakes from Samoa and Tonga recorded at Christchurch were used. Fortunately the composite thickness along the whole path was the same as that found from the local earthquake studies and the crustal refraction profile for New Zealand so that no correction was necessary. For the Lord Howe Rise two earthquakes from New Zealand to Brisbane along the edge of the Rise were available. For the interior region a composite thickness was obtained along paths from the Solomons to Christchurch. For the Fiji Basin earthquakes from the Fiji area to Christchurch were used. A correction was made for the portion of the path across New Zealand and Fiji in order to determine the thickness of the crust under the Fiji Basin.

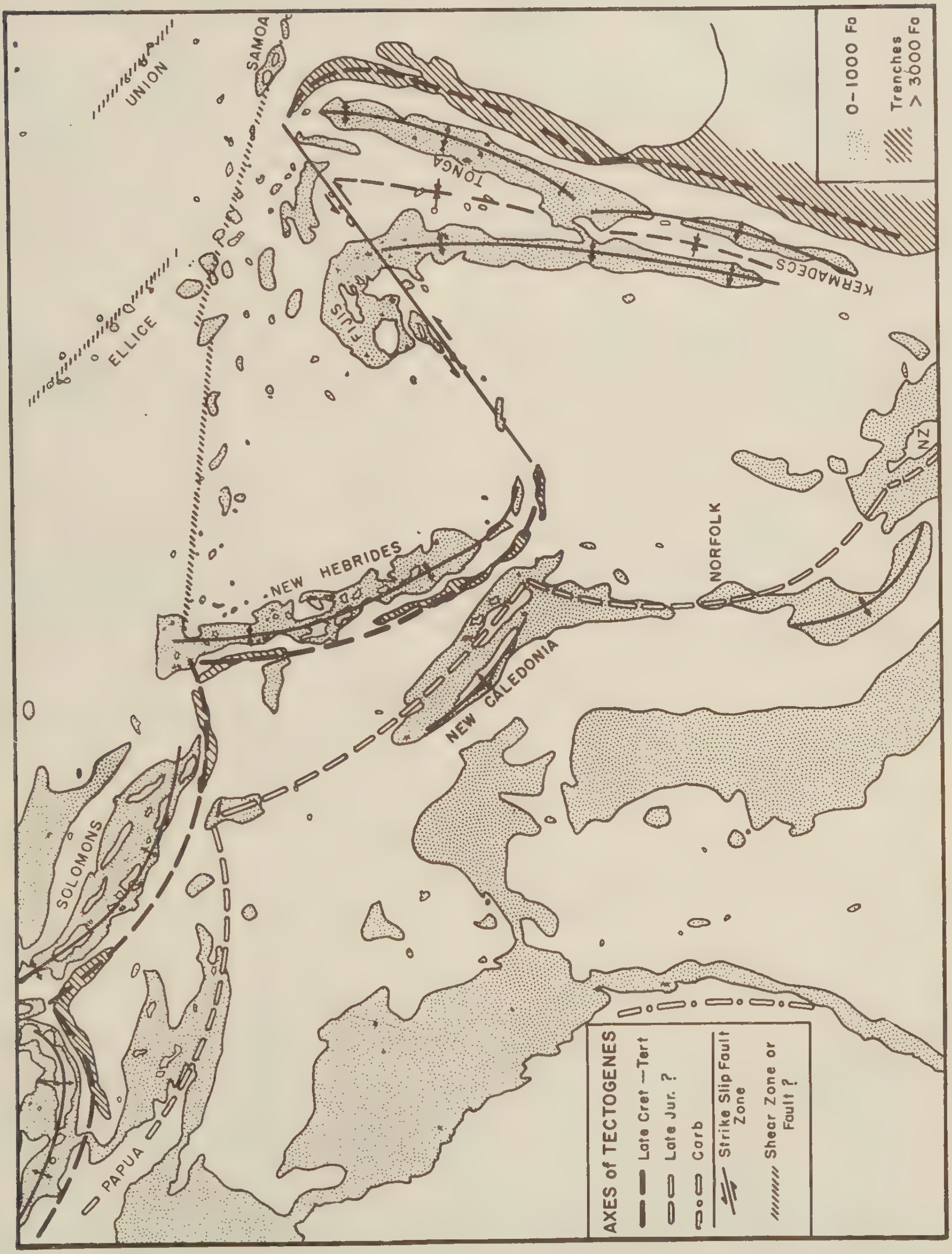
UNION
ELLICE
SAMOA
FIJIS
TONGA
KERMADECS
NEW HEBRIDES
NORFOLK
NEW CALEDONIA
NZ
SOLOMONS
PAPUA
0-1000 Fa
Trenches > 3000 Fa
AXES of TECTOGENES
Late Cret —Tert
Late Jur. ?
Carb
Strike Slip Fault Zone
Shear Zone or Fault ?

Fig. 2--Summary of the geology of the region according to HESS and MAXWELL [1949]

The regional geology is summarized in Figure 2, taken from a paper by HESS and MAXWELL [1949]. Five orogenic belts are recognizable. The first of Precambrian age extends north-south across Western Australia. The second of late Ordovician age extends from Melbourne toward Cape York. The third of late Paleozoic age, shown in Figure 2, is in the vicinity of Brisbane. A fourth of probable late Jurassic age is found along the inner island arcs from New Guinea and the Louisades, New Caledonia, and the western margin of New Zealand. The fifth and presently active belt follows the outer island arcs from New Britain, the Solomons, to the New Hebrides, then offset to Tonga and the Kermadecs. The geology of New Zealand is summarized in the geologic map of the North and South Islands and accompanying pamphlet by the NEW ZEALAND GEOLOGICAL SURVEY [1947; 1948] and in a memoir by MacPHERSON [1946]. The orogenic belt from Tonga and the Kermadecs is continued along the eastern margin of the North Island in the northeast trending Cretaceous and Tertiary geosynclinal deposits, the extension of the Kermadec Trench at shallower depth offshore from the North Island, and the zones of shallow, intermediate, and deep focus earthquakes. Cretaceous and thick Tertiary deposits are also present on the western side of the North Island along the northwest trend of the older orogenic belt of the inner island arcs. The region between these two converging belts is a volcanic plateau traversed by the Taupo - Rotorua graben. GLAESSNER [1952] and GILL [1952] have recently summarized two views on the geology of the Tasman Basin.

Theory--Surface waves from shallow focus earthquakes are the guided waves which have been propagated by multiple reflection in the Earth's crust. The net effect of adding up the mutual interferences of the multiple reflections is to produce a dispersive wave train, that is, a wave train in which the observed frequency changes in a regular manner with time of arrival. The dispersive characteristics depend upon the physical constants of the crust and subcrust and the thickness of the crust. Two types of surface waves are possible. In one, Love waves, the particle motion is transverse to the direction of propagation and polarized parallel to the reflecting boundary. In the other, Rayleigh waves, the particle motion is retrograde elliptical in the direction of propagation. These differences in the types of particle motion for Love and Rayleigh waves and the fact that Love waves travel faster than Rayleigh waves allow one to identify the two trains separately and read the dispersive characteristics of each. The theory of surface waves has been given by several authors and will not be repeated here. A recent contribution has been made by EWING and PRESS [1950; 1952] in the recognition that the observed Rayleigh waves across oceanic areas travel in the combined wave guide of ocean and crust whereas the Love waves, being a shear vibration, are confined to the crust.

Table 1--Crustal thicknesses

Area	Crustal thickness
	km
North Pacific Basin	5
South Pacific Basin	10, 5-10
Tasman Basin	5-10, 10
East Cape - Kermadec - Tonga Ridge	25
New Zealand (refraction profile)	20
New Zealand (earthquakes)	20-30
Lord Howe Rise	20
Solomons to New Zealand	15-20
Fiji Basin	15

The practice here will be to compare the experimental results with a single layered crust of constant velocity underlain by subcrust of different velocity to arrive at a value for the thickness of the crust. For both surface waves theoretical curves were calculated for two crustal velocities, one lower than the average velocity obtained from earthquake and crustal refraction profiles elsewhere and the other higher. The values given in Table 1 for the crustal thicknesses are a mean of these two curves. The velocity of P_n was taken as 8.1 km/sec for all cases. This graphical method has been chosen to compare the experimental results with theory so that the reader may judge for himself how well the thicknesses have been determined and what variations in thickness would be realized on the assumption of different crustal velocities. A change in the subcrustal structure, P_n, which is a definite possibility for the disturbed areas of the island arcs, will alter the thicknesses quoted in Table 1 but will not change the general conclusion for the structure of the area.

The theoretical curves for Love waves were calculated for two values of α_1, using α_2 as constant: $\alpha_1 = 6.50$ km/sec, $\beta_1 = 3.65$, $\alpha_2 = 8.10$, $\beta_2 = 4.55$, $\rho_2/\rho_1 = 3.00/2.67$; and $\alpha_1 = 6.05$ km/sec,

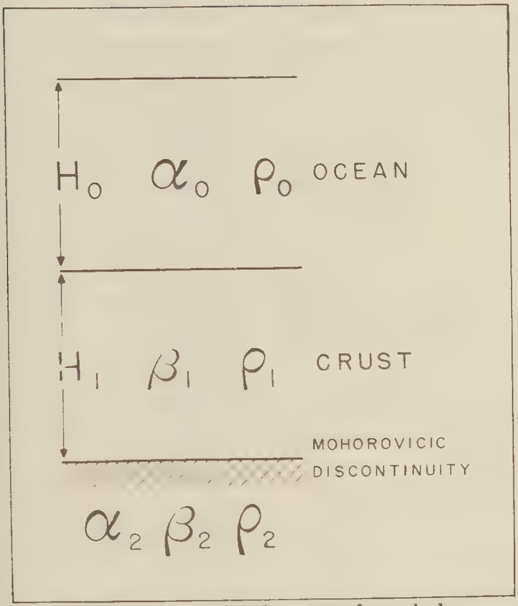
H_0 α_0 ρ_0 OCEAN
H_1 β_1 ρ_1 CRUST
MOHOROVICIC DISCONTINUITY
α_2 β_2 ρ_2

Fig. 3--Chart showing use of symbols

$\beta_1 = 3.40, \alpha_2 = 8.10, \beta_2 = 4.55, \rho_2/\rho_1 = 3.00/2.67$; where α and β are the P and S velocities, and ρ the density as shown in Figure 3. A value of $\sigma = 0.27$ was taken for Poisson's ratio for this range of velocities. Following **JARDETSKY** and **PRESS** [1953] Rayleigh waves were calculated for the two cases: $\alpha_0 = 1.52$ km/sec, $\alpha_1 = 6.90$, $\beta_1 = 3.98, \alpha_2 = 8.10, \beta_2 = 4.68, \rho_1/\rho_0 = 2.67$, $\rho_2/\rho_0 = 3.00$; and $\alpha_0 = 1.52$ km/sec, $\alpha_1 = 5.50$, $\beta_1 = 3.18, \alpha_2 = 8.10, \beta_2 = 4.68, \rho_1/\rho_0 = 2.67$, $\rho_2/\rho_0 = 3.00$. For ease in calculation Cauchy's value of $\sigma = 0.25$ was taken for Poisson's ratio. Jardetsky and Press calculated the Rayleigh wave dispersion curves for these two cases for $H = H_0$. For this investigation it was necessary to extend the calculations to ratios $H = 2H_0$, $5H_0$, and $10H_0$. These calculations are fairly laborious and are given in Table 2 in dimensionless form for the use they may be to other investigators. The period T is related to kH_0 by $T = 2\pi H_0/(kH_0)\,C$. C is the phase velocity and U the group velocity.

South Pacific Basin--In the investigations to be discussed in the following sections, an attempt at objectivity was made by including all the earthquakes which had appropriate paths in a given span of years long enough to give adequate coverage and which had good epicenters and origin times and readable records at the receiving station. The consistency of the results for each area testifies to the usefulness of surface waves for the investigation of crustal properties. The earthquake epicenters, origin times, magnitudes, and the source of their determination are summarized in Table 3. The constants of the instruments are shown in Table 4. The method of determining the period was to assign consecutive half numbers to the peaks and troughs of a given train of waves and to plot the arrival time of the peak or trough against its respective number, the periods being tangents to the resulting curve. The theoretical curves on each graph are labeled with the assumed thickness and crustal velocity.

Table 2--Calculated H values for two values of α_1 ($\alpha_0 = 1.52$ km/sec, $\alpha_2 = 8.10$ km/sec, $\rho_1 = 2.67, \rho_2 = 3.00, \sigma = 0.25$)

α_1	C/α_0	$H = H_0$[a]		$H = 2H_0$		$H = 5H_0$		$H = 10H_0$	
		kH_0	U/α_0	kH_0	U/α_0	kH_0	U/α_0	kH_0	U/α_0
km/sec									
5.5	2.80	0.070	2.76	0.043	2.76	0.019	2.76	0.010	2.77
5.5	2.77	0.135	2.71	0.083	2.71	0.039	2.71	0.020	2.72
5.5	2.75	0.175	2.68	0.109	2.68	0.051	2.69	0.027	2.68
5.5	2.73	0.231	2.63	0.148	2.64	0.070	2.65	0.037	2.64
5.5	2.70	0.290	2.55	0.194	2.58	0.094	2.60	0.050	2.59
5.5	2.60	0.449	2.23	0.352	2.35	0.187	2.39	0.101	2.40
5.5	2.50	0.540	1.76	0.464	1.97	0.265	2.12	0.144	2.12
5.5	2.40	0.603	1.30	0.544	1.59	0.329	1.87	0.180	1.90
5.5	2.30	0.656	0.99	0.607	1.34	0.388	1.61	0.217	1.72
6.9	2.80	0.101	2.77	0.071	2.78	0.039	2.78	0.022	2.78
6.9	2.77	0.214	2.71	0.167	2.72	0.104	2.72	0.065	2.72
6.9	2.75	0.263	2.67	0.217	2.68	0.144	2.68	0.092	2.68
6.9	2.73	0.334	2.60	0.292	2.63	0.200	2.63	0.121	2.63
6.9	2.70	0.398	2.48	0.366	2.54	0.256	2.56	0.152	2.55
6.9	2.60	0.521	1.97	0.504	1.95	0.381	2.20	0.236	2.27
6.9	2.50	0.583	1.34	0.566	1.43	0.463	1.87	0.307	2.14
6.9	2.40	0.631	1.11	0.617	1.17	0.538	1.68	0.414	2.07
6.9	2.30	0.682	0.97	0.670	1.02	0.614	1.62	0.562	1.99

[a] The figures for $H = H_0$ differ slightly from Jardetsky and Press.

Table 3--Data on earthquake epicenters, origins, and magnitudes

Location	Date	Original time GMT	Epicenter		Epicentral distance	Magnitude	Reference	Symbol	Figure
			Lat.	Long.					
		h m s	°	°	°				
South Pacific Basin (Easter Island to Christchurch)	Apr. 30, 1950	10 29 03	24 1/2 S	112 1/2 W	6.28	....	USC&GS 42-50	▼	4ab
	July 9, 1950	01 39 29	33 S	112 W	58.1	....	USC&GS 74.50	▲	4ab
	Sep. 22, 1950	07 52 07	25 S	114 W	61.4	6 1/2 - 6 3/4	USC&GS 111-50	■	4ab
	Feb. 19, 1951	22 11 54	25 S	117 W	59.2	6 1/2	USC&GS 18-51	●	4ab
Tasman Basin (SW New Zealand to Riverview)	Sep. 4, 1945	17 14 18	46 1/4 S	165 3/4 E	16.7	5 1/2 - 6	N. Z. and Riverview	◆	6ab
	Aug. 8, 1947	05 32 48	46 S	166 E	16.6	5 1/2 - 6	N. Z. and Riverview	▲	6ab
	Aug. 8, 1947	20 18 38	46 S	166 E	16.6	5 1/2 - 6	N. Z. and Riverview	▼	6ab
	Aug. 9, 1947	05 33 16	46 S	166 E	16.6	5 1/2 - 6	N. Z. and Riverview	■	6ab
	Feb. 6, 1950	22 53 30	48 S	164 E	17.2	6 - 6 1/4	N. Z. and Riverview	●	6ab
East Cape - Kermadec - Tonga Ridge (Samoa and Tonga to Christchurch)	Jan. 27, 1950	19 18 09	17 S	173 W	28.8	....	USC&GS 8-50	▼	7ab
	Nov. 24, 1950	13 03 43	15 S	173 W	31.1	6 1/4 - 6 1/2	USC&GS 140-50	◆	7ab
	Nov. 24, 1950	20 18 48	15 S	173 W	31.1	6 1/4 - 6 1/2	USC&GS 140-50	●	7ab
	Apr. 1, 1952	14 08 47	15 S	175 1/2 W	30.3	6 1/4	USC&GS 43-52	▲	7ab
	Sep. 16, 1953	01 48 42	15 S	174 1/2 W	30.6	6 1/4 - 6 1/2	USC&GS 124-53	■	7ab
	Mar. 3, 1952	07 12 39	21 1/2 S	174 1/2 W	24.5	6	USC&GS 28-52	△	7ab
	Aug. 12, 1953	16 53 42	22 S	175 W	23.9	6 - 6 1/2	USC&GS 104-53	▽	7ab
Lord Howe Rise (W New Zealand to Brisbane)	June 19, 1948	06 18 39	43 1/4 S	169 1/4 E	20.4	5 3/4	N.Z. Stations	▲	9
	June 19, 1948	07 05 36	43 1/4 S	169 1/4 E	20.4	5 3/4	N.Z. Stations	▼	9
Solomons to New Zealand (Solomons to Christchurch)	July 7, 1950	16 46 55	11 S	163 1/2 E	33.7	....	USC&GS 73-50	●	10
	Oct. 15, 1950	15 59 33	10 S	160 E	35.3	6 1/2	USC&GS 122-50	▲	10
	Nov. 8, 1950	02 18 09	9 1/2 S	159 1/2 E	35.9	7 1/4 - 7 1/2	USC&GS 136-50	▼	10
Fiji Basin (Fiji to Christchurch)	Dec. 22, 1940	12 31 44	14 S	178 E	29.9	6 1/2	Gutenberg and Richter	▼	11
	Oct. 21, 1943	23 08 13	15 S	177 1/2 E	28.8	7	Gutenberg and Richter	●	11
	Sep. 27, 1950	08 23 52	18 1/2 S	175 E	25.1	6 1/2	USC&GS 114-50	■	11
	Apr. 5, 1952	08 33 12	15 1/2 S	177 1/2 E	28.4	6 - 6 1/4	USC&GS 46-52	▲	11

The results for the South Pacific Basin are presented in Figure 4. For the Love waves the experimental points predict a crustal thickness slightly greater than 10 km for a mean crustal velocity between 6.0 and 6.5 km/sec. For the Rayleigh waves the experimental points predict a thickness of 5-10 km for a mean velocity. If the lower crustal velocity of 5.5 km/sec were chosen, the thickness would be 5 km; and if the higher velocity of 6.9 km/sec were chosen, the thickness would be somewhat greater than 10 km. These two graphs illustrate the kind of results that can be obtained. The crustal thicknesses are quoted to 5 km for an average crustal velocity of 6.2-6.3 km/sec, and to that order of magnitude the results are correct for any reasonable variation from this average velocity that might occur under particular structures.

It is interesting to compare these results with those obtained by OLIVER, EWING, and PRESS [in press] for the North Pacific. Figure 5 is a replot from their paper. The Love wave data are from earthquakes around the perimeter of the Pacific at various azimuths to Hawaii. The data from the southwest are from earthquakes in South America whose travel path is across the basin between

Table 4--Instrumental constant

Station	Instrument	Pendulum period	Galvanometer period	Magnification
		sec	sec	
Christchurch	Galitzin N-S	24	24	265
	Galitzin E-W	24	24	275
	Galitzin Z	13	13	465
Riverview	Galitzin N-S	12	12	540
	Galitzin E-W	12	12	530
	Galitzin Z	11	11	460
Brisbane	Milne-Shaw N-S	12	...	250
	Milne-Shaw E-W	12	...	250

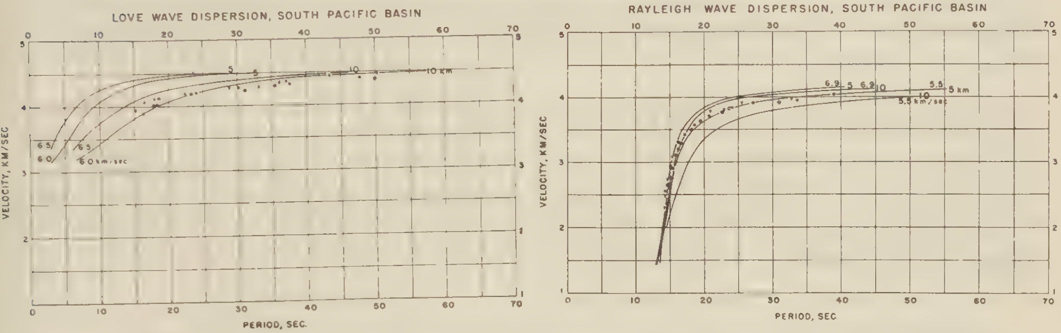

Fig. 4--Wave dispersion in the South Pacific Basin; (a) Love waves, (b) Rayleigh waves

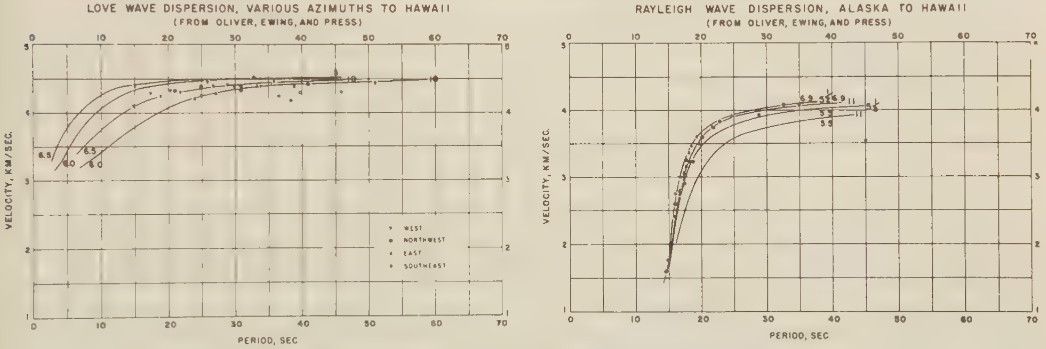

Fig. 5--Wave dispersion, various azimuths to Hawaii (after Oliver, Ewing, and Press); (a) Love waves, (b) Rayleigh waves

South America and the Easter Island Rise and is interpreted by them as indicating a thicker crust under this basin. The data from the other azimuths are consistently higher than that for the South Pacific indicating a thickness somewhat greater than 5 km. The Rayleigh wave data show the same pattern giving a crustal thickness of 5 km. The crust is slightly thicker under the South Pacific Basin than under the North Pacific Basin.

Tasman Basin--The results for the Tasman Basin are presented in Figure 6. The Love waves give a thickness of 5-10 km. The experimental points do not fit any of the four theoretical curves very well; a more satisfactory agreement could be obtained by taking an 8-km crust in which the velocity varied from 6.0 km/sec near the top to 6.5 km/sec near the bottom. The Rayleigh waves predict a thickness of slightly greater than 10 km for a mean crustal velocity.

An important conclusion from these results is that the crustal structure under the Tasman Basin is oceanic and not continental. The hypothesis that the area from Australia to New Zealand

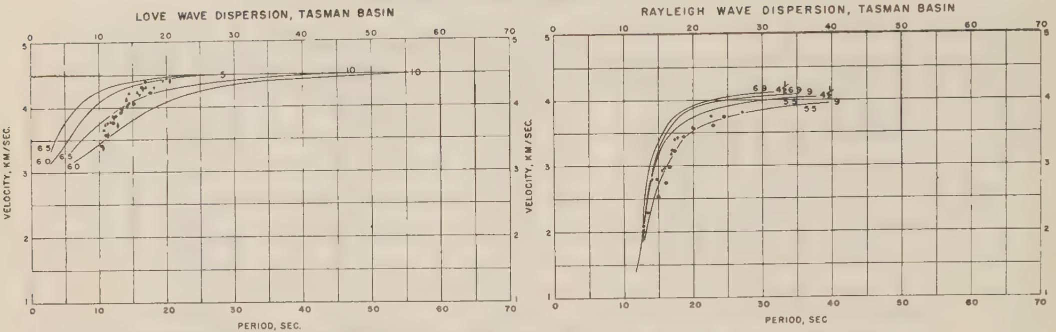

Fig. 6--Wave dispersion, Tasman Basin; (a) Love waves, (b) Rayleigh waves

is part of the Australian continent is definitely disproved. The thickness of the crust under the Tasman Basin to the west of New Zealand is the same as that under the South Pacific Basin to the east of New Zealand.

East Cape - Kermadec - Tonga Ridge--The results for the East Cape - Kermadec - Tonga Ridge bordering the South Pacific Basin are quite different than those for either the South Pacific, North Pacific, or Tasman Basins. They are presented in Figure 7. For the Love waves the thickness is 25 km for a mean crustal velocity between 6.0 and 6.5 km/sec. For the Rayleigh waves part of the path is across an ocean of average depth 1 1/2 km and part across land. No correction has been made for this difference, and the results are to be taken only as a check on the Love waves. From the lower velocity curves the thickness would be 20 km and from the higher velocity curves greater than 30 km.

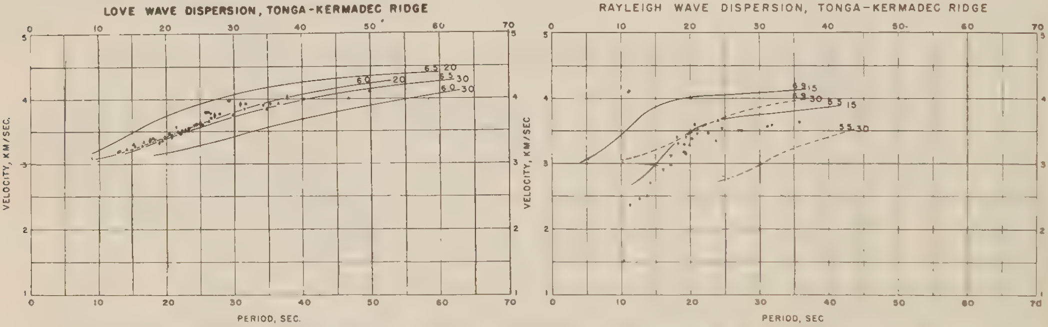

Fig. 7--Wave dispersion, Tonga - Kermadec Ridge; (a) Love waves, (b) Rayleigh waves

New Zealand--The structure of New Zealand has been investigated from local earthquake studies. HAYES [1935] recognized that crustal pulses could be read from the records of the New Zealand stations. He obtained lines with the velocities: P_n, 8.3; P_q, 7.3; P^*, 6.5; P_g, 5.4; S_n, 4.5; S^*, 3.8; and S_g, 3.4 km/sec. BULLEN [1936] determined a three-layered crust with P and S velocities respectively of 4.7 and 2.8 km/sec, 5.5 and 3.3 km/sec, 6.3 and 3.7 km/sec, and 8.10 and 4.37 km/sec for the successive layers and the subcrust; a formal solution for the thicknesses gave a total depth to the Mohorovicic discontinuity of 18 km. Later from additional data BULLEN [1939] revised this to a structure of an upper layer of 5-10 km with a P velocity of 5.0 km/sec, a second questionable layer of 4 km with a P velocity of 5.5 km/sec, and a third layer of 10-20 km with a P velocity of 6.3 km/sec. For the total depth to the Mohorovicic discontinuity he preferred an upper value of 30 km. EIBY [1949] has verified the identification of the phases traveling through the sedimentary basement, 'intermediate' layer, and subcrust and has pointed out from routine local seismogram interpretation that there is a strong probability of regional differences in the crustal properties under New Zealand.

In 1947, E. I. Robertson and the staff of the New Zealand Geophysics Division carried out a crustal refraction profile on a line northeast from Wellington. A series of strings of depth charges were fired in Wellington harbor and recorded at portable stations on the greywacke basement out to a distance of 175 km. All the records were taken with high speed recording equipment, from two to 12 inches per second, and with accurate shot instants. The experiment and the results will be given in detail in a memoir from the New Zealand Geophysics Division. Various people have examined the data; the following is the author's interpretation. The first arrivals from the records determine a straight line with a velocity of 5.54 km/sec out to a distance of 28 km (Fig. 8). This refraction can continue to be read as a strong second arrival for another 20 km. The layer above it in Wellington harbor was not determined; but it is thin, not greater than 0.3 km, with a velocity less than 2.0 km/sec. The second refractor with a velocity of 6.04 km/sec first appears as a second arrival at 15 km. At the longer ranges it has a velocity of 6.40 km/sec. The nature of the transition from a velocity of 6.04 km/sec to 6.40 km/sec can be seen from the second graph of Figure 8, which is a plot of the observed travel time minus the distance divided by a velocity of 6 km/sec, giving an expanded time scale. The change from 6.04 to 6.40 km/sec is fairly abrupt occurring at a distance of 90 km, more indicative of a discontinuity than a gradual change in velocity throughout the layer. The definition of P_n is not as satisfactory as one might desire. Two clear first arrivals out in front of the 6.04-6.40 km/sec lines from 85 to 95 km and three strong second arrivals from 70 to 80 km determine a line with a velocity of 8.10 km/sec. The three records from 95 to 120 km are not of sufficiently good quality to allow an early arrival to be read, and on the records at greater distance no early arrival can be detected. Support for the P_n line comes from a strong reflection, the most prominent on the records, which is observed at all stations from 15 to 40 km. The depth of this reflector agrees with that obtained for the Mohorovicic discontinuity from the P_n refraction line. The resulting thicknesses are 3 km of 5.54 km/sec, 7 km of 6.04 km/sec, and 8 km of 6.40 km/sec giving a total depth to the Mohorovicic discontinuity of 19 km.

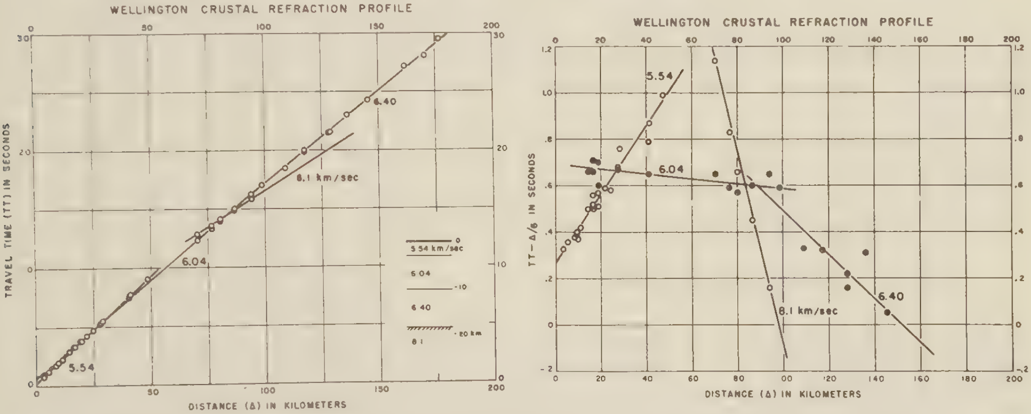

Fig. 8--Wellington crustal refraction profile; (a) using observed travel times, (b) using travel times minus Δ/6

The upper layer of 3 km of 5.54 km/sec is the greywacke basement on which the recording stations were located. It is of undifferentiated Jurassic - Triassic - Permian age. From its seismic velocity and its stratigraphic position the 7 km of 6.04 km/sec is interpreted as metamorphosed greywacke and probably older metamorphosed rock. The total of 10 km for the present thickness of the original geosynclinal sediments is of the order expected by BRODIE [1953] from a stratigraphic section near Wellington and by WELLMAN, GRINDLEY, and MUNDEN [1952] from the Alpine schists and Upper Triassic of the South Island. Indeed from a direct extrapolation of the surface geology to depth over parts of the South Island still greater thicknesses are expected by these authors. From its seismic velocity and its position above the Mohorovicic discontinuity the 8 km of 6.40 km/sec is interpreted as the 'intermediate' layer of seismology.

This crustal section argues for an origin of New Zealand from an original oceanic crust, not a reworked continental mass. The geosynclinal sediments deposited in earlier deep sea trenches have been uplifted and reach a thickness of 10 km under this profile. They are underlain by a crust of 'intermediate' layer velocity typical of that found under the undisturbed ocean basin areas. New Zealand has been part of the presently active orogenic belt of the outer island arcs, the previous belt of the inner island arcs, and possibly a still earlier belt along the Lord Howe Rise. Whereas the orogenic belts to the northwest have progressed outward with geologic time, the active region around New Zealand has remained central with the sediments from the older orogenic belts being eroded and deposited in the new.

Lord Howe Rise--The results for the Rayleigh wave dispersion along the Lord Howe Rise are presented in Figure 9. It was not possible to read a train of Love waves from the records for these two earthquakes. A curve for a 15 km crust with a mean velocity between 5.5 and 6.9 km/sec would be somewhat too thin to fit the experimental data. A thickness of 20 km is chosen. The paths for these two earthquakes to Brisbane are along the flank of the Lord Howe Rise; the crust may be thicker along the central portion of the Rise.

Solomons to New Zealand--The results for earthquake paths from the Solomons to Christchurch are presented in Figure 10. With the variable depth of water over the path only the Love waves were considered. The thickness for a mean crustal velocity between 6.0 and 6.5 km/sec would be 15-20 km. This value is a composite thickness over the entire path. The actual crustal thickness under the northern, basin area is probably thinner than this value and that under the southern, ridge and rise area thicker.

DE JERSEY [1946] examined Rayleigh waves from the Solomons, Samoa, and the Kermadecs to Brisbane. Neglecting the effect of the ocean on the Rayleigh wave dispersion curves, he obtained too great a thickness, which varied with the period of the surface waves. Including the ocean in the Rayleigh wave dispersion curves his results all lie on the same line and are in agreement with results given above. He also examined the ratio PP/P of the reflected to direct P phases and concluded that the Southwest Pacific was of continental structure. A. A. Thomson of the Seismological Observatory, Wellington, in a paper at the Geophysical Conference of 1951, has carried out a similar investigation and obtained results showing oceanic (4), intermediate (2), and continental (1) PP/P ratios for the Southwest Pacific. He concluded that the method was unsuitable for differentiating between crustal structures in this area.

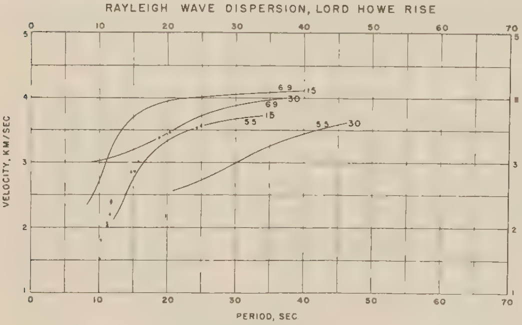

Fig. 9--Rayleigh wave dispersion, Lord Howe Rise

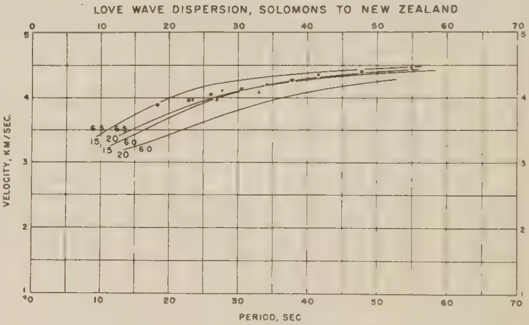

Fig. 10--Love wave dispersion, Solomons to New Zealand

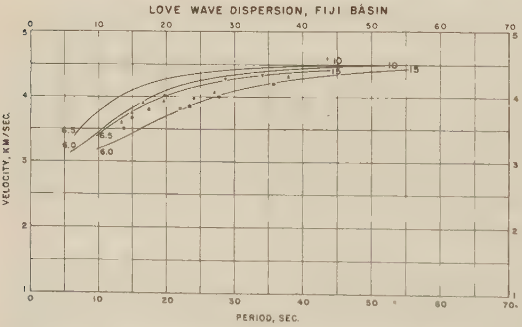

Fig. 11--Love wave dispersion, Fiji Basin

Fiji Basin--The results for the Fiji Basin are presented in Figure 11. Again only the Love waves were considered. The plotted data have been corrected for the portion of the path across New Zealand from the offshore slope and for the Fiji area on a 25-km crust to isolate the effect due to the Fiji Basin alone. From the graph a thickness of 15-20 km is predicted for a mean crustal velocity. This is greater than the thickness of the deep basins exterior to the orogenic belts.

Conclusions--The values for the crustal thicknesses are summarized in Table 1. From the surface waves the crustal thickness under the South Pacific Basin is slightly greater than that under the North Pacific Basin. The thickness of the crust under the Tasman Basin is the same as that under the South Pacific Basin. It is an oceanic and not a continental type crust. The interior region of the orogenic belts including New Zealand have been built up with succeeding geologic time on an oceanic crust. They are not part of an extensive continent. The thicknesses are not of continental proportions nor does the structure indicate a continental origin. The structure is that of successive orogenic belts built out over an oceanic crust.

Acknowledgments--The author is indebted to R. C. Hayes, Director, Seismological Observatory, Wellington, for making the Christchurch records available; to O. A. Jones, Director, Seismological Observatory, Brisbane, and N. Burke-Gaffney, Director, Seismological Observatory, Riverview, Sydney, for sending records from their respective stations; and to E. I. Robertson, Director, New Zealand Geophysics Division, for allowing him to examine the crustal refraction profile records. The author wishes to express his thanks to E. I. Robertson, J. W. Brodie, N. Modriniak, and F. F. Evison of the New Zealand Geophysics Division; R. C. Hayes, G. A. Eiby, and A. A. Thomson of the Seismological Observatory, Wellington; and H. W. Wellman of the New Zealand Geological Survey for valuable discussions during the course of the investigation; and to J. E. Oliver, F. Press, and R. R. Revelle for reviewing the paper.

References

BRODIE, J. W., Features of the sea floor west of New Zealand, N. Z. J. Sci. and Tech. B, v. 33, pp. 373-384, 1952.

BRODIE, J. W., Stratigraphy and structure of the greywackes and argillites on the south coast of Wellington peninsula, N. Z. J. Sci. and Tech. B, v. 34, pp. 205-226, 1953.

BULLEN, K. E., On near earthquakes in the vicinity of New Zealand, N. Z. J. Sci. and Tech., v. 18, pp. 493-507, 1936.

BULLEN, K. E., The crustal structure of the New Zealand region as inferred from studies of earthquake waves, Proc. Sixth Pacific Sci. Cong., pp. 103-110, 1939.

DE JERSEY, N. J., Seismological evidence bearing on crustal thickness in the Southwest Pacific, Univ. Queensland papers, Dept. Geology, v. 3, no. 2, pp. 1-18, 1946.

EIBY, G. A., The Waiau earthquakes of May, 1948, Proc. Seventh Pacific Sci. Cong., v. 2, pp. 493-507, 1949.

EWING, M., and F. PRESS, Crustal structure and surface wave disperson, Bull. Seis. Soc. Amer., v. 40, pp. 271-280, 1950.

EWING, M., and F. PRESS, Crustal structure and surface wave dispersion, pt. II, Solomon Islands earthquake of July 29, 1950, Bull. Seis. Soc. Amer., v. 42, pp. 315-325, 1952.

GILL, E. D., Paleogeography of Australia - New Zealand in Lower Devonian time, Trans. R. Sci. N. Z., v. 80, pp. 171-185, 1952.

GLAESSNER, M. F., The geology of the Tasman Sea, Aus. J. Sci., v. 14, pp. 111-114, 1952.

HAYES, R. C., Seismic waves and crustal structure in the New Zealand region, N. Z. J. Sci. and Tech., v. 17, pp. 519-528, 1935.

HESS, H. H., Geological hypotheses and the Earth's crust under the oceans, Proc. R. Soc. A, v. 222, pp. 341-348, 1954.

HESS, H. H., and J. C. MAXWELL, Major structural features of the Southwest Pacific: a preliminary interpretation of H. O. 5484, bathymetric chart, New Guinea to New Zealand, Proc. Seventh Sci. Cong., v. 2, pp. 1-18, 1949.

JARDETSKY, W. S., and F. PRESS, Crustal structure and surface wave dispersion, pt. III, Theoretical dispersion curves for suboceanic Rayleigh waves, Bull. Seis. Soc. Amer., v. 43, pp. 137-144, 1953.

MacPHERSON, E. O., An outline of Late Cretaceous and Tertiary diastrophism in New Zealand, N. Z. Geol. Surv., Mem. 6, 1946.

NEW ZEALAND GEOLOGICAL SURVEY, Geological map of New Zealand, North Island and South Island, scale 1/1,013,760, 1947.

NEW ZEALAND GEOLOGICAL SURVEY, Outline of the geology of New Zealand to accompany the Geological map, 47 pp., 1948.

OLIVER, J., M. EWING, and F. PRESS, Crustal structure and surface wave dispersion, pt. IV, Atlantic and Pacific Ocean Basins, Bull. Seis. Soc. Amer., in press.

WELLMAN, H. W., G. W. GRINDLEY, and F. W. MUNDEN, The Alpine schists and the Upper Triassic of Harpers Pass (Sheet S52), South Island, New Zealand, Trans. R. Soc. N. Z., v. 80, pp. 213-227, 1952.

Woods Hole Oceanographic Institution,
Woods Hole, Massachusetts

(Manuscript received May 3, 1954; presented at the Thirty-Fifth Annual Meeting, Washington, D. C., May 4, 1954; open for formal discussion until November 1, 1955.)

Contribution No. 725

OSMOTIC PRESSURES OF SEA WATER SOLUTIONS COMPUTED FROM EXPERIMENTAL VAPOR PRESSURE LOWERING[1]

By

K. G. WILSON AND A. B. ARONS

Woods Hole Oceanographic Institution
Woods Hole, Mass.

ABSTRACT

Osmotic pressures of sea water solutions for temperatures between 0 and 35°C and for chlorinities between 5 and 100 ‰ have been computed from experimental vapor pressure measurements.

The osmotic pressure, π, of sea water as a function of chlorinity and temperature is given in Table I. The osmotic pressure was calculated by using the equation

$$\pi = -\frac{RT\ln a_1}{\bar{V}_1\left(1 - \frac{\alpha\pi}{2}\right)}$$

TABLE I. SEA WATER OSMOTIC PRESSURE (ATMOSPHERES) FOR VARIOUS TEMPERATURES AND CHLORINITIES

Cl ‰ \ *Temp* °C	0	5	10	15	20	25	30	35
5	5.4	5.8	5.6	6.2	6.1	5.7	5.6	6.0
10	10.9	11.8	11.3	11.4	11.5	11.5	11.7	11.6
20	21.9	23.5	22.7	23.9	24.6	24.8	24.5	24.7
30	33.1	35.5	37.1	37.6	37.9	39.5	39.6	40.4
40	47.2	47.6	50.2	51.5	52.2	53.7	55.3	56.6
50	61.6	61.9	65.0	68.9	70.7	73.0	74.5	76.6
60	76.1	78.5	83.0	86.5	90.3	94.0	96.4	99.1
70	91.0	95.4	99.9	103.4	108.7	112.7	116.9	120.2
80	109.0	114.8	120.2	126.2	130.8	136.4	139.7	143.6
90	127.5	136.8	142.5	150.8	156.8	163.7	169.8	173.6
100	152.5	159.2	166.9	174.8	181.8	190.5	196.3	203.6

[1] Contribution No. 725 from the Woods Hole Oceanographic Institution.

Reprint from SEARS FOUND. JOURN. MAR. RES.

(Glasstone, 1949), where a_1 is the activity of the water, $\bar{V}_1$ its partial molal volume at atmospheric pressure, and α is defined by

$$\bar{V}_p = \bar{V}_1[1 - \alpha(p - p_0)].$$

Thus α is approximately the compressibility of sea water, which is about 4×10^{-5} atm^{-1}; since $\pi \leqslant 200$, $\alpha\pi/2$ is $< .004$ or 0.4%; we have therefore neglected the $(1 - \alpha\pi/2)$ term. The activity coefficient a_1 was calculated from measurements of vapor pressure lowering made by Arons and Kientzler (1954). $\bar{V}_1$ was calculated by the equation

$$\bar{V}_1 = \frac{18}{\rho}\left[1 + \left(\frac{\partial ln\rho}{\partial lnS}\right)_{T,P}\right],$$

where ρ, S are density and salinity respectively. ρ was assumed to vary linearly with S, using the densities of Higashi, et al. (1931) and Dorsey (1940); this probably introduces an error of about 0.4%.

It is estimated that the vapor pressure data have an error of 2% or 0.010 mm Hg, whichever is larger. The error in π corresponding to 0.010 mm Hg is shown in Table II.

TABLE II. ESTIMATED ERRORS IN OSMOTIC PRESSURE RESULTS

Temp. (°C)	*Estimated Error* (*atm*)	*Temp.* (°C)	*Estimated Error* (*atm*)
0	±2.8	20	±.7
5	2.0	25	.6
10	1.4	30	.5
15	1.0	35	.4

In summary, a reasonable estimate of the maximum error is 0.8% + 2%, or 0.8% + the value given in Table II, whichever is larger.

The numerical data of Table I do not lend themselves readily to empirical curve fitting. We suggest that an individual, wishing to interpolate for intermediate values, plot the data in any manner suited to his needs and draw smooth curves through the given points.

Precipitation was noticed in the samples (used for obtaining vapor pressures) when the chlorinity exceeded 40 ‰. Rough data by Thompson (1932) indicated that the amount of precipitation would not be sufficient to affect the results, compared with other errors, in the 40–100 ‰ chlorinity range.

Fig. 1 compares our results with values calculated from the equation:

$$\pi = \frac{2.317\ TS}{1000 - S},$$

with S in ‰ and π in atmospheres for 20°C. This equation is based on ideal solution theory and can be obtained from the consideration given by Sverdrup, et al. (1942:67). On the average, values calculated by this method are about 1–2 atm higher than those calculated from vapor pressure data in the 0–30 chlorinity range.

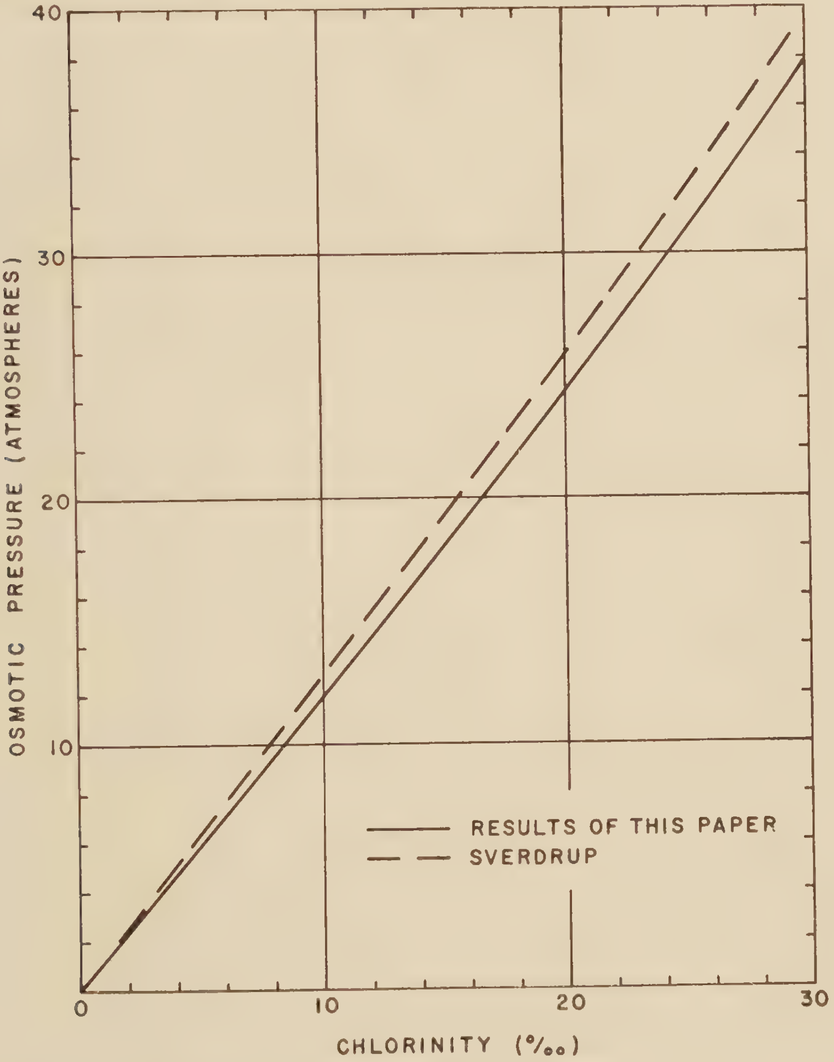

Figure 1. Comparison of the results of this work with equation based on ideal solution theory (Sverdrup, et al., 1942: 67), temperature 20°C.

The preparation of samples for the vapor pressure determinations consisted of obtaining sea salt solutions that varied in concentration from that of natural sea water to a saturated solution. Attempts were made to use a formula for artificial sea water (Lyman and Fleming, 1940) to obtain the concentrated solutions, but large amounts of precipitate were observed in the concentrated solutions, so the use of artificial sea water was abandoned.

The samples were prepared from natural sea water obtained at Woods Hole, Massachusetts. The concentration of the first six samples of sea water (which had been previously filtered to remove the organic matter) was carried out in 2000 ml Erlenmeyer flasks heated over a low flame. The other five samples were concentrated in boiling flasks by passing air through the solution while maintaining a temperature of 80°C. It was found that the saturation point was at about 10 times the normal concentration or at a chlorinity of about 155 ‰. For concentrations of 40 ‰ or greater, some precipitate appeared. Thompson and Robinson (1932) state that $CaCO_3$ is first deposited, this being followed by $CaSO_4 . 2H_2O$ at a concentration of about 70 ‰.

REFERENCES

Arons, A. B. and C. F. Kientzler
1954. Vapor pressure of sea salt solutions. Trans. Amer. geophys. Un., *35*: 722.

Dorsey, N. E.
1940. Properties of ordinary water-substances. Reinhold Publishing Corp., New York. 673 pp.

Glasstone, S.
1949. Thermodynamics for chemists. D. Van Nostrand Co., New York. 522 pp. (p. 373).

Higashi, K., K. Nakamura and R. Hara
1931. The specific gravities and the vapor pressure of the concentrated sea water at 0–175°C. J. Soc. chem. Ind. Japan, *34*: 166–172 (Abstr. 72B).

Lyman, John and R. H. Fleming
1940. Composition of sea water. J. Mar. Res., *3*: 134–146.

Sverdrup, H. U., M. W. Johnson and R. H. Fleming
1942. The Oceans. Prentice-Hall, Inc., New York. 1087 pp.

Thompson, T. G.
1932. The physical properties of sea water. Physics of the Earth, 5, Oceanography. Bull. Nat. Res. Council, No. 85: 63–94.

Thompson, T. G. and R. J. Robinson
1932. Chemistry of the sea. Physics of the Earth, 5, Oceanography. Bull. Nat. Res. Council, No. 85: 187–188.

Contribution No. 726

ON THE FORMATION AND STRUCTURE OF DOWNDRAFTS IN CUMULUS CLOUDS

By Joanne Starr Malkus
Woods Hole Oceanographic Institution[1,2]

(Original manuscript received 16 August 1954; revised manuscript received 15 January 1955)

ABSTRACT

With use of the model of the steady-state entraining cumulus draft, it is possible to describe the formation and structure of the downdraft observed at the down-shear edge of an oceanic trade-cumulus cloud. The observations are airplane traverses made at several levels giving the temperature, humidity, and vertical draft structure in cloud and environment, and a nearby pilot-balloon run.

It is found that this downdraft must be mixing primarily with the updraft; that it gains its negative buoyancy mainly from evaporation; and that it is permitted to go through a life cycle of formation, strengthening, and decay which is closely dependent upon that of the updraft.

Downdrafts, exhibiting speeds and mass transports comparable to those of the main updrafts, are a common feature of the cumulus clouds studied by the Woods Hole Oceanographic Institution's PBY aircraft in the trade-wind region. These downdrafts are observed to be most pronounced at the extreme down-shear edge of the visible cloud and are generally stronger the greater the age of the cloud tower, although they are normally present at the edge of even rapidly growing turrets.

The cloud data obtained by the PBY on the 1952 Caribbean trip [reported on by Malkus (1954) in a paper hereafter referred to as I] suggested that these downdrafts mixed primarily with the air of the adjacent updraft, rather than with the drier air of the clear environment. This is plausible in view of the hypothesis voiced by the writer (1949; 1952) that air is moving through an updraft in the direction pointed by the shear vector; that is, an updraft entrains air mainly on the up-shear side and sheds air mainly from its down-shear side. Regarding a cumulus draft in terms of the bubble-like elements which compose it (see Malkus and Scorer, 1955), we reach the same conclusion when we consider that, in a shearing wind field, the wake region is found down-shear of the ascending buoyant elements.

The data available from the March–April 1953 trade-wind cloud flights now make it possible to set up a tentative physical theory concerning the origin and structure of these downdrafts at the edge of the clouds. It is suggested, and made plausible by the calculations to follow, that the downdraft originates at the top of the cloud from air which has recently been part of the updraft. Air shed from the updraft at cloud top may, because of slight dilution by the surroundings and evaporation of roughly 10 per cent

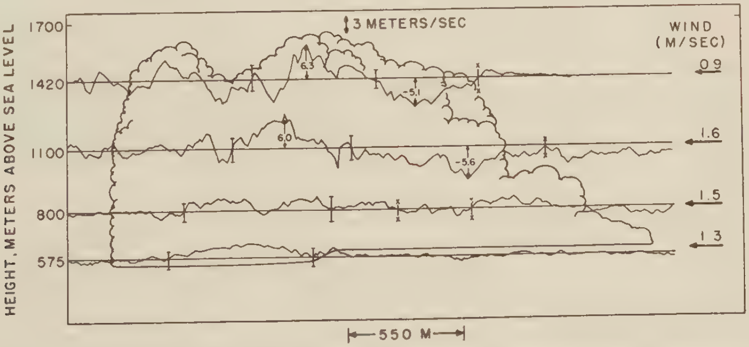

FIG. 1. Reconstructed cross-section of cloud studied by PBY on 7 April 1953, showing measured vertical draft profile. Cloud formed over open ocean, about 100 mi NE of San Juan, Puerto Rico. Airplane passes were made from top downward, in alternate directions. Wind component along section flown is given at right. Major up- and down-drafts used in calculations are denoted by vertical lines drawn at each level. Peak draft velocities (m/sec) are indicated. Averages across drafts are presented in text.

---

[1] Contribution No. 726 from the Woods Hole Oceanographic Institution.

[2] The work described in this article was carried out under Contract N6onr-27702 (NR-082-021) between the Office of Naval Research and the Woods Hole Oceanographic Institution.

of its liquid-water content, acquire sufficient negative buoyancy to begin a rapid downward acceleration, once given a small initial downward velocity of the order of magnitude observed in the turbulent fluctuations at cloud boundaries. In fact, the low stability of the common trade-cumulus environment would permit extreme downward velocities to develop were there not constant braking due to entrainment of air with upward momentum, as will be illustrated.

The set of cloud traverses discussed here (through a single cloud observed on 7 April 1953) were made in a manner identical to those described in I, except that the vertical draft records are considerably more accurate. This improvement is due primarily to the fact that, in integration of the accelerometer records, corrections to the aircraft's sinking speed caused by airspeed and attitude fluctuations are now incorporated rather than assumed to be negligible as in I. $\frac{1}{5}$-sec averages of w (draft values over horizontal distances of about 10 to 12 m) are presented in fig. 1. The reliability of these determinations has been discussed in detail by Bunker (1954), who has also shown the results of a comparison with a tower-mounted sonic anemometer. The latter comparison indicated root-mean-square values of w agreeing within 12 per cent and nearly identical frequency distributions.

The calculations from this set of traverses are based upon the steady-state model of an entraining cumulus draft described in I. In that article, the relations between parameters prescribed by the steady-state model were shown to hold fairly adequately even when the cloud visibly departed from steady conditions (see cloud II in I) and for two separate clouds in widely differing phases of their life cycles. It is therefore contended that the development and decay of a single cloud may be approximated by a series of quasi-steady states.

Under steady conditions, the equation for conservation of vertical momentum [(8) in I] states that

$$\frac{1}{w_{d0} - w_E}\frac{dw_d}{dz} = -\frac{1}{M}\frac{dM_i}{dz} + \frac{\bar{\alpha}}{w_{d0}(w_{d0} - w_E)}, \quad (1)$$

where the z-axis points upward, and a small height interval between z and $z + dz$ is considered. Vertical velocities are denoted by w, where w_d is the average velocity across the draft at $z + dz$, w_{d0} is the corresponding value at z, and w_E is the average vertical motion of the nearby environment (actually of the entrained air). M is the average mass flux across the draft, so that $(1/M)\, dM_i/dz$ is the gross entrainment between z and $z + dz$ calculated by Stommel's method, M_i being the total mass flux entrained in the height interval. The buoyancy acceleration, α, is defined as $g(T_v - T_v')/T_v'$, where g is the acceleration of gravity, T_v is the mean virtual temperature of the draft air, and T_v' is the virtual temperature of the environment. The value $\bar{\alpha}$ denotes an averaging of the mean draft buoyancy between z and $z + dz$. Equation (1) is exact (under the assumed conditions) except for the omission of an additional drag term due to form drag and weight of suspended hydrometeors, which omission was justified by the previous observations. A further approximation to (1) was introduced in I, since it was felt that the 1952 draft measurements were not sufficiently accurate to estimate w_E. This approximation has now been dropped, and the obser-

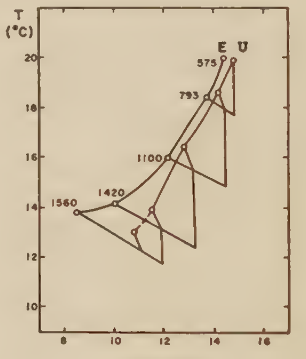

Fig. 2. Entrainment calculation for major updraft in cloud shown in fig. 1, with use of Stommel's method. Vertical coordinate is temperature (deg C); horizontal coordinate is mixing ratio (g/kg). Curve E gives properties of nearby environment of draft observed at each of levels (msl) indicated; curve U gives corresponding properties of draft observed at all levels except 1560 m, which value was obtained by calculation described in text. Vertical lines downward from each point represent dry adiabatic cooling. Line joining end of vertical line to corresponding environment point is mixing line, and final slanting line to draft point represents condensation of liquid water. Ratio of entrained air (mass flux) to mass flux already in draft between successive levels is, thus, ratio of right-hand to left-hand portion of mixing line intercepted by condensation line.

Table 1. Gross entrainment in the updraft.

Level (m)	$\bar{T}$ (draft) (deg C)	$\bar{q}$ (draft) (g/kg)	T (env.) (deg C)	q (env.) (g/kg)	$\frac{1}{M}\frac{dM_i}{dz}$ (10^{-5} cm^{-1})	Increment liquid water (g/kg)	Wind shear (m sec^{-1} km^{-1})
575	19.9	14.8	20.0	14.4			
793	18.6	14.2	18.4	13.7	2.6	0.3	+0.9
1100	16.4	12.8	16.0	12.2	3.7	0.4	+0.3
1420	13.9	11.5	14.15	10.0	2.4	0.4	−2.2
(1560)	13.0	10.8	13.85	8.5	2.4	0.35	
						Σ = 1.45	

vations are used directly in (1) as follows: the draft boundaries are defined at the point where the vertical velocity becomes zero. The major up- and downdrafts so defined are readily traceable from one level to the next on the reconstructed cloud cross-section (draft profile presented in fig. 1). The average values across draft boundaries of w, T (actual temperature), T_v, q (mixing ratio), *etc.* are then made graphically, at each level traversed, from plotted diagrams similar to figs. 4 to 9 of I. The main updraft in the cloud (marked on fig. 1) is first considered. The gross entrainment between each two successive observed levels of this draft is calculated, and the results are presented in table 1 and fig. 2.

Next the draft profile in the updraft is calculated with use of (1) and the horizontal traverses, similarly to the procedure in I. The first step is made by taking for w_{d0} in the equation the observed average updraft at 575 m, calculating dw_d/dz from there up to 793 m, *etc.* The results are presented in table 2, in which the last two columns give side-by-side the calculated w at each height compared to the value arrived at by a graphical averaging across the draft of the observed values shown in fig. 1.

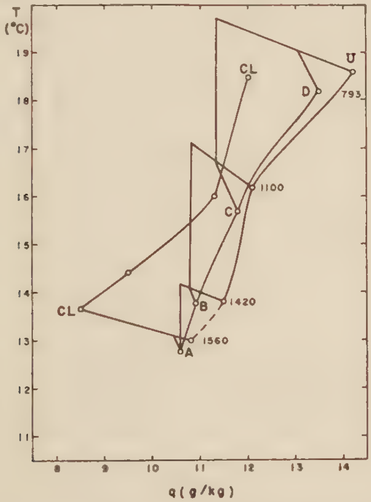

FIG. 3. Entrainment calculation for major downdraft in cloud shown in fig. 1. Same procedure was followed as illustrated in fig. 2, except that processes are in reverse, as described in text. Curve CL gives observed points for clear-air environment of downdraft; curve U gives observed or calculated nearby updraft properties; curve D gives observed downdraft properties, except for point A, which was calculated. Updraft curve, U, is not everywhere quite the same as U curve in fig. 2, since here that portion of updraft nearest downdraft was considered, while fig. 2 gives average properties across entire updraft.

The highest level at which measurements were made within the cloud was at 1420 m or 4500 ft. The highest traverse made by the airplane was at 5400 ft, which however passed above the cloud top by about 300 ft.

To discuss the formation of the downdraft, the updraft has been constructed upward from the 1420-m traverse to 1560 m (≈ 5000 ft). This was done by assuming that rate of entrainment (comparable to values measured in nearby levels) which will give cloud properties at 1560 m such that the updraft is reduced to approximately zero velocity there. This could be used as a criterion, since the tower top was observed to be rising no longer. These calculated values are the ones presented for the 1560-m level in tables 1 and 2. A hypothesis concerning the manner in which the downdraft formed near the down-shear edge of the visible cloud at this height will now be tested. It will be determined whether air with these calculated properties, after dilution with environment air of known properties, could show up at the successively lower levels with the observed properties of the downdraft actually studied and marked in fig. 1. If the cloud is not precipitating (this cloud never did), and if the major fraction of its liquid water lies in drops of low fall velocity (≤ 1 mm), the liquid-water content at the cloud top will be approximately the sum of the increments in column seven of table 1, namely 1.45 g/kg. Since we are considering that a quasi-steady situation obtains, we must inquire what proportions of the surrounding air must be admixed to the cloudy air starting at 1560 m in order that it reach the 1420-m level with the observed properties of the downdraft at that level. Trial computations show that the entrainment into the downdraft must be mostly from the updraft rather than from the clear-air environment, as was suggested by the downdraft calculations for the 1952 clouds (see table 6 of I).

Fig. 3 shows the entrainment calculation for the downdraft on the assumption that at the upper cloud edge, after the updraft has gone nearly to zero, a mixture is made consisting of 84 per cent updraft air (curve U) and 16 per cent clear air (curve CL) and that thereafter the downdraft entrains air only from the updraft. Point A is obtained by mixing the updraft and environment air in the stated proportions and then evaporating 0.15 g/kg of liquid water. To

TABLE 2. Draft calculation for the updraft.

Level (m)	T_v (deg C)	T_v' (deg C)	$\overline{a}$ (cm/sec²)	w_{d0} (cm/sec)	w_E (cm/sec)	Δw (cm/sec)	w_d (calc.) (cm/sec)	w_d (obs.) (cm/sec)
575	22.50	22.50	0.50	150	−20	− 24		
793	21.10	20.80	1.35	126	−60	+114	126	110
1100	18.60	18.10	0.85	240	−50	−110	240	220
1420	15.90	15.90	−0.78	130	0	−128	130	140
(1560)	14.85	15.30					2	≈0

TABLE 3. Results of mixing higher proportions of clear air with the downdraft.

Height range (m)	Magnitude entrainment rate: $\lvert(1/M)\, dM_i/dz\rvert$ (10^{-5} cm^{-1}) 80% updraft, 20% clear	 67% updraft, 33% clear	 50% updraft, 50% clear
1560–1420	5	∞	Impossible
1420–1100	3.5	6.3	>28
1100–793	13.0	~50.0	Impossible

arrive at point B, the observed downdraft properties at 1420 m, air with properties A ($T = 12.8$C, $q = 10.6$ g/kg, liquid water $= 1.45 - 0.15 = 1.3$ g/kg) must entrain from the updraft at a rate 2.0×10^{-5} cm^{-1} and evaporate 0.15 g/kg additional liquid water. From 1420 to 1100 m (the lowest level to which this downdraft penetrated vigorously on the cross section), for the air to arrive with the observed properties C, the entrainment rate from the updraft must have stayed nearly the same and an additional 0.47 g/kg liquid water must have been evaporated. The resulting entrainment rates, presented in table 4, are quite reasonable. On the other hand, table 3 shows the entrainment rates arrived at from similar computations by using various larger proportions of air from the environment relative to that from the updraft.

It is seen that even for 80 per cent updraft and 20 per cent clear air, the entrainment rates are very high; and for 67 per cent updraft and 33 per cent clear air, there could not be adequate entrainment to explain the observed properties of the downdraft. By "impossible" in the right column of table 3 is meant the situation in which, in a diagram similar to fig. 3, the sloping evaporation line through the final draft image-point has no intersection with the mixing line. The increase in the calculated entrainment rates as the proportion of environment air is increased may be visualized physically as follows: the more the air entrained by the downdraft contains air from the clear, the drier is the entrained air. As the properties of the entrained air approach those of the air observed in the downdraft, the higher is the calculated entrainment rate, up to that point where the average properties of the entrained air become drier than the draft, when the calculated proportion entrained decreases again. However, fig. 3 shows that reasonable entrainment rates of drier air than that in the downdraft would give draft air far drier than actually observed. Thus it must be concluded that, at this stage of this cloud, the observed downdraft is composed almost entirely of air originally in the updraft. This gives rise to a downdraft in which the temperature lapse rate is steeper than moist adiabatic, rather than more stable than moist adiabatic as in fig. 33 of *The thunderstorm* in which the downdraft is entraining clear air.

The chosen entrainment calculation for the downdraft is presented in table 4, in which, after 1560 m, the mixture is entirely with updraft air. The resulting entrainment rates are now comparable in magnitude to those of the updraft, similar to the 1952 clouds. It will be noted that, in the case of the downdraft, $(1/M)\, dM_i/dz$ must be written as negative for later use in (1), since the mass flux increases in the direction of the current, which is downward. The total evaporation of liquid water by the time the 1100-m level is reached is the sum of the figures in the last column of table 4 plus the original 0.15 g/kg hypothesized evaporated at 1560 m, namely a total of 0.77 g/kg. By 793 m, it is seen that this downdraft must have essentially disappeared. The entrainment rate becomes large, and 1.25 out of the maximum possible 1.45 g/kg liquid-water content has been evaporated. The disappearance of the downdraft by 793 m is even better illustrated in table 5, which gives the draft calculation for the downdraft. Table 5 may be regarded as a check upon the previous assumptions and calculations, since it is possible to compare the velocity profile arrived at by use of the temperatures, mixing ratios and entrainment rates obtained with the actually measured velocity profile of the downdraft. This comparison is made in the last two columns of the table.

The virtual temperature of the downdraft air at 1560 m was taken as that of air at 12.8C, 10.6 g/kg

TABLE 4. Gross entrainment in the downdraft.

Level (m)	$\bar{T}$ (downdraft) (deg C)	$\bar{q}$ (downdraft) (g/kg)	T (updraft) (deg C)	q (updraft) (g/kg)	T (clear) (deg C)	q (clear) (g/kg)	$-\dfrac{1}{M}\dfrac{dM_i}{dz}$ (10^{-5} cm^{-1})	Evap. (g/kg)
(1560)	12.8	10.6	13.0	10.8	13.65	8.5		
1420	13.75	10.9	13.8	11.5	14.4	9.5	2.0	0.15
1100	15.7	11.8	16.2	12.1	16.0	11.3	1.9	0.47
793	18.2	13.5	18.6	14.2	18.5	12.0	4.7	0.48

TABLE 5. Draft calculation for the downdraft.

Level (m)	T_v (deg C)	T_v' (deg C)	$\bar{a}$ (cm/sec^2)	w_{d0} (cm/sec)	w_E (cm/sec)	Δw (cm/sec)	w_d (calc.) (cm/sec)	w_d (obs.) (cm/sec)
(1560)	14.6	14.95		− 60				
1420	15.65	16.0	−1.20	−290	+100	−230	−290	−250
1100	17.70	18.3	−1.65	−240	+100	+ 50	−240	−230
793	20.55	21.1	−1.96		+100	+230	− 10	− 30

water vapor. The virtual temperature of its environment was found from the average figures for updraft and environment given in table 4. The initial downward velocity, w_{d0}, at 1560 m was taken simply from the magnitude of turbulent fluctuations in w near the cloud boundaries at that height. The remaining figures were obtained from the cloud traverses in the same manner as in I.

The disappearance of the downdraft at 793 m is also plausible in view of the fact that below this level the wind shear is reversed in sign, being positive, so that a downdraft should appear thenceforth on the opposite, *i.e.*, downwind side of the cloud. The observational evidence on this point is in the present case inconclusive. It is pertinent to note, however, that the normal situation in the trade-wind cloud layer is a reversal of wind shear, from positive up to about 1100 m to negative above that. If the present hypothesis concerning the origin and structure of cumulus downdrafts is correct, this reversal of shear should make it difficult for the main downdraft, which starts near the top of the cloud on the upwind side, to penetrate downward to cloud base or lower before exhausting its liquid water. Exceptions might be found in the cases of very large cumulonimbus clouds, such as those studied by Malkus and Ronne (1955) which reached great heights and possessed undilute cores with presumably high liquid-water contents.

It may be seen by reference to fig. 3 that, although the observations in this particular case preclude significant entrainment of clear air by the downdraft, such a situation [as described by the U. S. Weather Bureau (1949)] is by no means physically proscribed. If the downdraft entrained outside air, it could maintain the same or even greater negative buoyancy merely by evaporating liquid water at a faster rate. It would, of necessity, have to do this if mixing with clear air, because so long as any liquid water remains it will evaporate until the draft air is nearly saturated.

In fact, this situation may be quite pertinent to a still later stage in the life cycle of the cloud tower. As the tower ages, its updraft weakens and the air in the updraft becomes closer in its properties to the air of the clear environment with which it is mixing. The downdraft, thus, receiving the majority of its air from the updraft, will be entraining air of properties somewhat closer to curve CL in fig. 3 than curve U, *i.e.*, drier and colder. To remain saturated, the downdraft then must evaporate its liquid water faster. If such water is available in large enough quantities, it may be shown by a calculation similar to those foregoing that the downdraft then will exhibit negative buoyancy equal to or greater than that calculated in table 5. With the weakened braking effect of the updraft, w_E will be smaller; and it may be shown for the environment studied here, and reasonable values of the updraft parameters, that the downdraft may reach 1420 and 1100 m increased in intensity by 1 m/sec or more. As the updraft dies completely and the cloud top begins to evaporate, the downdraft, too, cannot last much longer, as its source of cooling, namely, evaporation of liquid water, will soon give out.

Conversely, it may be shown that in an earlier stage of the updraft, although the downdraft is enabled to be more economical with its liquid water, the larger braking effect of the adjacent updraft will, under reasonable assumptions, restrain the downdraft magnitudes below the values given in table 5.

It is thus possible to describe quantitatively the structure of the cumulus downdraft in one stage of its development in terms of a steady-state model. It is plausible, in view of these calculations, to believe that most of the air composing the downdraft was originally entrained from the updraft and that the primary source of the downward acceleration is due to the evaporation of liquid water. It does not appear to be necessary to call upon the weight of, nor the drag exerted by, the liquid drops to assure the needed downward force. It further seems possible, by regarding a series of quasi-steady states, to project the downdraft both backward and forward in its life cycle and to see how its time-dependent behavior is related to that of the updraft upshear of it. It seems evident from this work that the behavior of the downdraft is intimately dependent upon that of the updraft which, in this study, was measured or extrapolated from measurements. The time-dependent behavior of the updraft itself has not been analyzed herein, although it may be suggested in conclusion that a similar approach might be applied to that more fundamental problem.

Acknowledgments.—The writer is indebted to Prof. P. A. Sheppard of the Imperial College, London, who closely collaborated with her on the observational work described here, and whose group provided the wind records. The draft observations were reduced from the original data by the skill and diligence of Mrs. Mary C. Thayer and Miss Martha A. Walsh, who devised many of the reduction procedures.

REFERENCES

Bunker, A. F., 1954: *WHOI airplane turbulence and flux measurements, O'Neill, Nebraska, August 21–28, 1953.* (Unpubl. manuscript, Ref. No. 54-25), Woods Hole, Woods Hole Ocean. Instn., 14 pp.

Malkus, J. S., 1949: Effects of wind shear on some aspects of convection. *Trans. Amer. geophys. Union*, **30**, 19–25.

——, 1952: Recent advances in the study of convective clouds. *Tellus*, **4**, 71–87.

——, 1954: Some results of a trade-cumulus cloud investigation. *J. Meteor.*, **11**, 220–237.

——, and C. Ronne, 1954: On the structure of some cumulonimbus clouds which penetrated the high tropical troposphere. *Tellus*, **6**, 351–366.

——, and R. S. Scorer, 1955: The erosion of cumulus towers. *J. Meteor.*, **12**, 43–57.

U. S. Weather Bureau, 1949: *The Thunderstorm.* Washington, U. S. Govt. Print. Off., 282 pp.

Contribution No. 727

Contribution No. 727 from the Woods Hole Oceanographic Institution

The effects of a large island upon the trade-wind air stream

By JOANNE S. MALKUS
Woods Hole Oceanographic Institution, Massachusetts, U.S.A.

551.558.1 : 551.555.1

The effects of a large island upon the trade-wind air stream

By JOANNE S. MALKUS

*Woods Hole Oceanographic Institution, Massachusetts, U.S.A.**

(Manuscript received 5 April 1955, in revised form 28 June 1955)

SUMMARY

A series of four helical aircraft soundings across the island of Puerto Rico on a sea-breeze day are analyzed and interpreted. The existence of a fairly symmetrical orographic-convection cell with ascent over the island and compensating subsidence in a surrounding ring is established. The field of motion in the convection cell is deduced from the observations together with the theoretical work on flow over heated islands by Malkus and Stern (1953). The plausibility of the motion field is tested by construction of a moisture budget for part of the cross-section delineated by the soundings, and the effects of the subsidence, lifting, heating and other processes imposed upon the air stream by its passage over the island are discussed, with particular emphasis upon alterations in the upward transport of water vapour and cumulus cloud structure.

1. INTRODUCTION

Although diurnal variations in a trade-wind air mass over the ocean are extremely slight, the presence of an island or land-body introduces marked changes from night to day. The alteration in cloud patterns is particularly striking. Over Puerto Rico and even the smaller Virgin Islands, the build-up of land and orographic clouds during the morning is commonly accompanied by clearing at the coastlines and the formation of a clear ring surrounding the island. Except in the localities where the land-formed clouds may extend seaward in a ' street,' the cloud-free ring extends off-shore with a radius comparable to the island width. In the late afternoon as diurnal convection subsides, the clear ring shrinks and trade cumuli again drift in across the coast. This sequence suggests a simple orographic-convection cell, with ascending motion over the heated land and mountains, and compensating subsidence over the coastal waters. With such a picture in mind, Riehl (1947) undertook an interpretation of diurnal moisture and rainfall patterns at San Juan, Puerto Rico. His work was handicapped, however, by being confined to the use of sounding observations for the coastal region only. In Hawaii, more complicated patterns of interaction between island convection and trade winds have been studied by Leopold (1949).

Since the work of Leopold and Riehl, a theoretical study of the flow of a slightly stable air stream over a heated island has been carried out by Malkus and Stern (1953; see also Stern and Malkus 1953, Stern 1954). These theoretical results, coupled with the relatively simple shape and orography of Puerto Rico, suggested a more detailed study of the convection pattern produced by that island. Such a study, carried out on 25 June 1952, forms the subject of this paper. The basic data consist of a series of vertical soundings performed by a slow-flying aircraft on a line approximately parallel to the low-level wind. Their location relative to the island and cloud formations is mapped in Fig. 1. Figs. 2 to 5 (Plates VI to IX) depict the cloud configurations. The first sounding was made about 50 km ENE of the windward coast, in apparently undisturbed oceanic air. The second was made in the clear ring just off the windward shore; the third over the foothills where island convection was active; and the fourth near the seaward edge of the wider clear ring to the lee (WSW) of the island.

---

* At present at the Department of Meteorology, Imperial College, London.

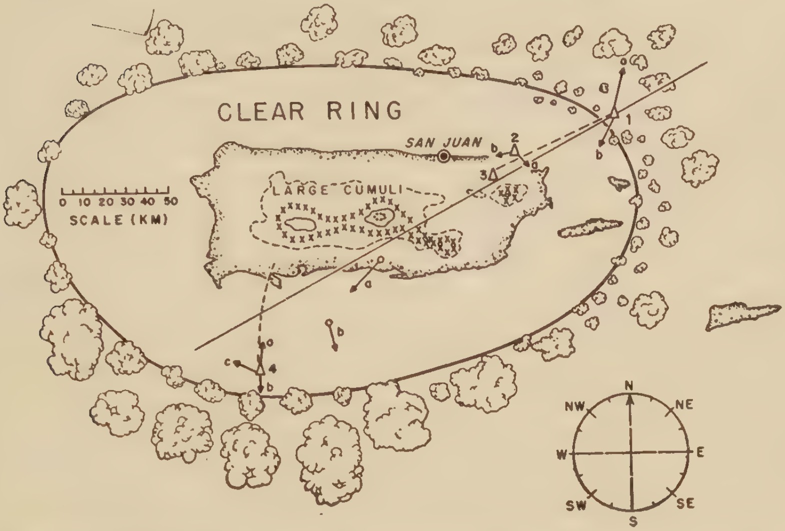

Figure 1. Map showing the topography of Puerto Rico, the locations of the four soundings, and the cloud distribution (schematically) near noon on 25 June 1952. The 1,000-ft contour is dashed; the 2,000-ft, ×-ed; the 3,000-ft solid, and the 4,000-ft, dotted. The light solid line through the sounding locations is the cross-section constructed (see Figs. 7 to 9); the arrows show the directions aimed by the camera in the photographs to follow (Figs. 2 to 5). The dashed lines running from soundings 1 and 4 to shore indicate where horizontal runs were made by the observing aircraft. The latter data are omitted from the discussion since little new information was added by them.

One of the primary reasons for performing these observations was to study the effects of divergence, subsidence, turbulence, and heating upon the various layers of the undisturbed trade-wind atmosphere, and upon the structure and height of the trade inversion. In an analysis of the Pacific trade (Riehl, Yeh, Malkus and La Seur 1951), budgets of moisture, momentum, and heat were calculated along a section of the flow about 2,500 km in length. This was a mean picture, averaged over a two months' series of observations. In it was illustrated the role of subsidence in strengthening the trade-wind inversion and the counter-working role of cumulus convection in raising and weakening it. Along the present cross-section, just over 200 km in length, the air is first subjected to subsidence (windward clear ring), then to violent turbulence, convection, and heating (over island and mountains) and then again to subsidence (leeward clear ring).

To discuss the resulting effects upon the air structure, it is first necessary to establish the motion field. This will be done after a brief presentation of the methods of measurement and several cross-sections.

2. The data

(a) *Method of sounding*

The basic instrumentation of the sounding aircraft was a modified form of the M.I.T. psychrograph, described previously by McCasland (1951). The plane (Catalina) was flown in helical ascents of about 2 mi diameter at air-speeds of 50-60 m/sec and at a sufficiently slow rate of climb (200 ft/min) for lag-free values of temperature and humidity to be obtained at about 30-m height intervals. The soundings are thus well suited to accurate determination of vertical gradients of these properties. A water-column accelerometer was operated to record small-scale turbulence which has been described by a parameter called ' turbulence index ' defined by Malkus and Bunker (1952). Values are obtained by planimetering the accelerometer trace over five-second intervals and are only suitable for comparisons, since the actual magnitudes depend upon the aircraft. Supplementary observations included photographs (Figs. 2 to 5, Plates VI to IX) and wind determinations. Surface-wind directions were ascertained by smoke drifts; over the water, smoke flares were dropped. Winds at 1,000 ft were determined by double drift, using two independent sights and observers.

The four soundings are plotted in Fig. 6. Unfortunately an hour's delay occurred between the end of sounding 3 and the commencement of sounding 4 owing to the failure of the aeroplane's interphone, and sounding 4 cannot be considered synoptic with the other three. Furthermore, just as that last sounding was being made, the wind was shifting to a few degrees south of east owing to the passage of a weak easterly wave. Thus the trajectory of the air at the location marked 4 on Fig. 1 was not along the cross-section. The fact that the shift was so recent, however, and the character of sounding 4 itself suggest that the air at that location had an over-island trajectory. Sounding 4 is thus included in the discussion, although the calculations are restricted to the remaining three which were performed in rapid succession between 1115 and 1415 LMT. The San Juan time-section (not reproduced) shows that the weak easterly wave-system produced no noticeable variations in the properties of the air in the region. Upon the aircraft's return to San Juan at 1730 LMT conditions there, including the height of the inversion which was checked just off shore, were the same (except for the slight wind shift) as they had been early in the morning.

(*b*) *Construction of the cross-sections*

The observations are more readily interpreted in conjunction with Figs. 7 and 8, which are sections across the island in the plane of the soundings (see map in Fig. 1). Fig. 7 shows the distribution of potential temperature and mixing ratio. Within the region delineated by the light rectangle (soundings 1-3) the picture may be considered synoptic for about noon. The remainder of the section was put together using sounding 4, theoretical calculations, other information and speculation. The potential-temperature gradient along the island surface was chosen consistent with the figures presented by Riehl (1954). He gives maximum temperatures for normal sea-breeze days at San Juan, Yayuya (elevation $\simeq$ 600 m), and Mayaguez (lee shore). Since the sea breeze on 25 June was weaker (9 mi hr^{-1}) than Riehl's median figure (15 mi hr^{-1}) his maximum gradients have been slightly reduced in Fig. 7. The mountain top in the section, for example, is 6°A potentially warmer than San Juan, while Yayuya (same elevation) often is 7-8°A potentially warmer on well-developed sea-breeze days. The potential-temperature configuration between lee shore and sounding 4 was drawn consistent with the patterns downwind of Nantucket, observed by Malkus and Bunker (1952). The potential-temperature field is everywhere consistent with the velocity field presented later. The heights to which superadiabatic and adiabatic lapse rates are shown to extend have been governed by the height of cloud base, which in general limits the top of the mixed ground layer.

Fig. 8 is a schematic reconstruction of the section. The stabilities, cloud configurations, winds at 1,000 ft, and the trade-inversion base are denoted. The latter was determined by the dual criteria of a decrease in temperature lapse-rate and a discontinuity in vertical moisture-gradient towards more rapid drying. On soundings 1, 2 and 4, these criteria were clearly met at the levels indicated. The inversion base possessed a mixing ratio of 8·7, 8·7, and 8·4 g/kg, respectively, at these locations. Between soundings 1 and 2 the additional criterion of constant potential temperature (303·4°A) could also be

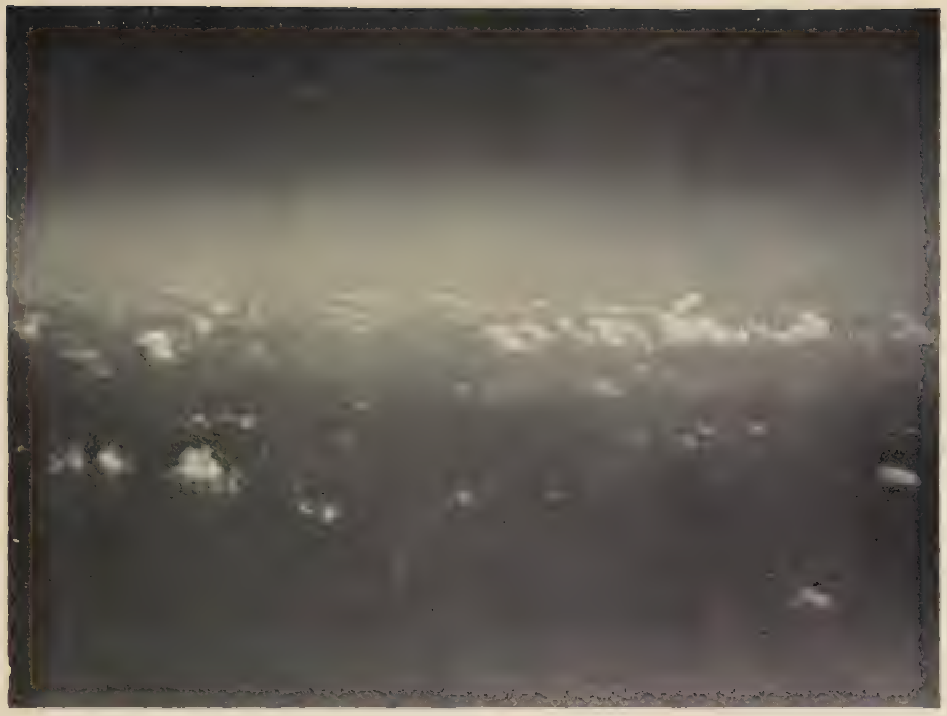

(a)

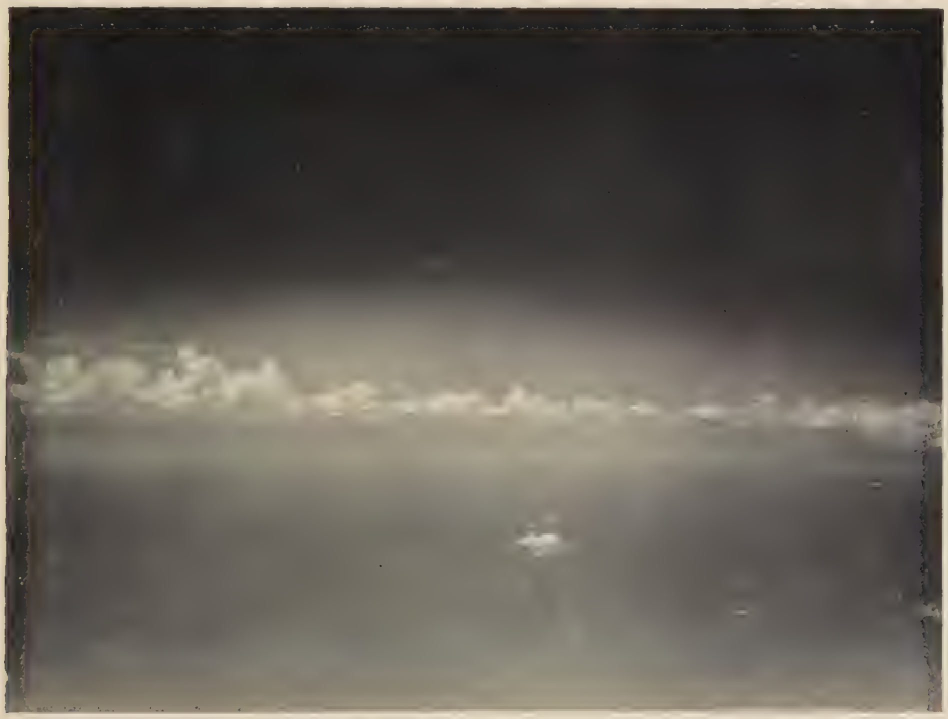

(b)

Figure 2. Photographs taken at location of sounding 1, 1200 LMT, 6,000-ft elevation. (a) Photograph of trade cumuli seaward of subsidence ring, along direction of arrow a on Fig. 1. (b) Photograph of clear ring and clouds along coastal plane (over island), along direction of arrow b on Fig. 1. Coastline is visible in right foreground.

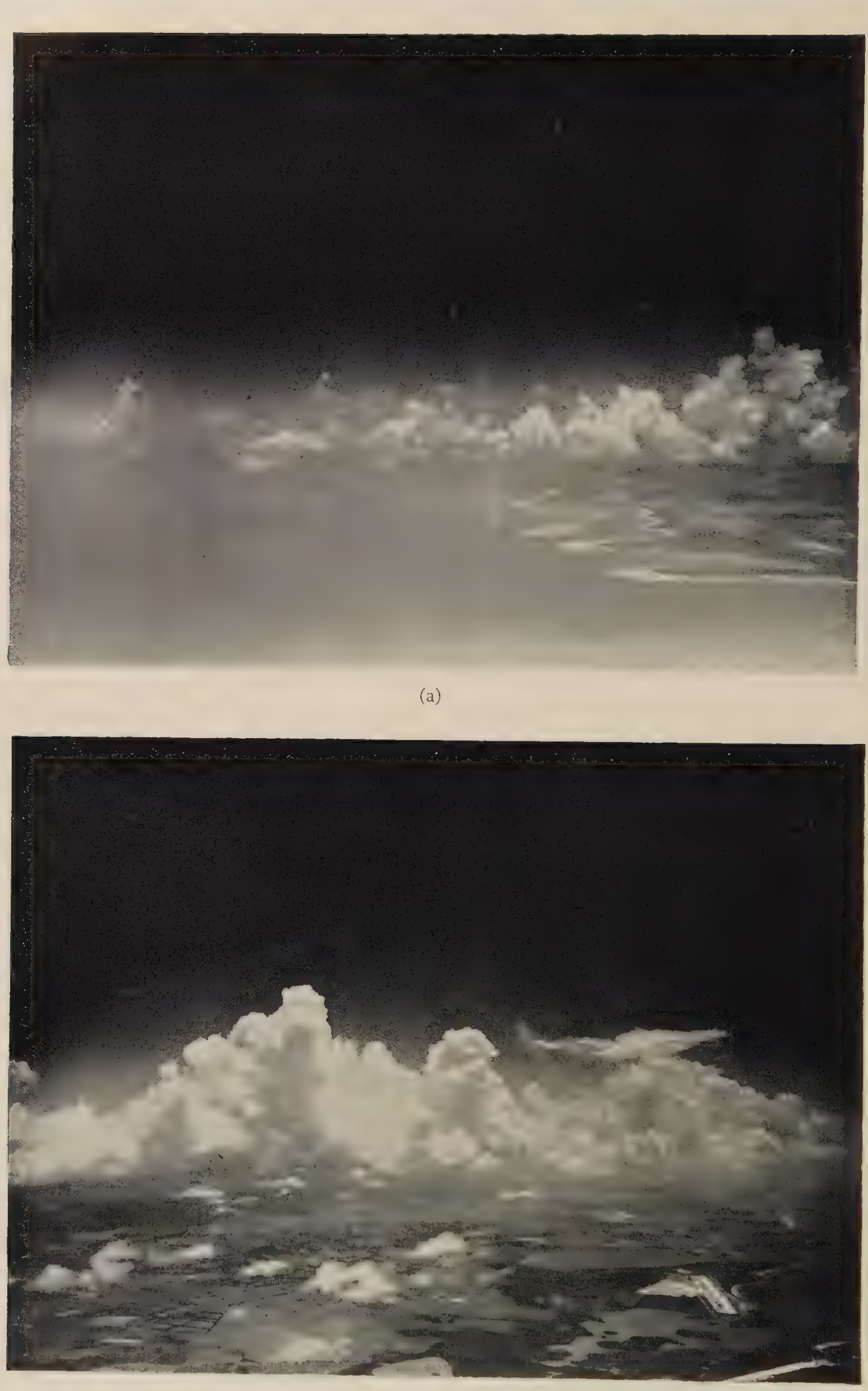

Figure 3. Photographs taken at location of sounding 2, 1333 LMT, 6,000-ft elevation. (a) Photograph along arrow a of coastal plane clouds. All clouds seen here are land-formed. (b) Photograph along arrow b of coastal plane clouds. Outskirts of San Juan are in right foreground.

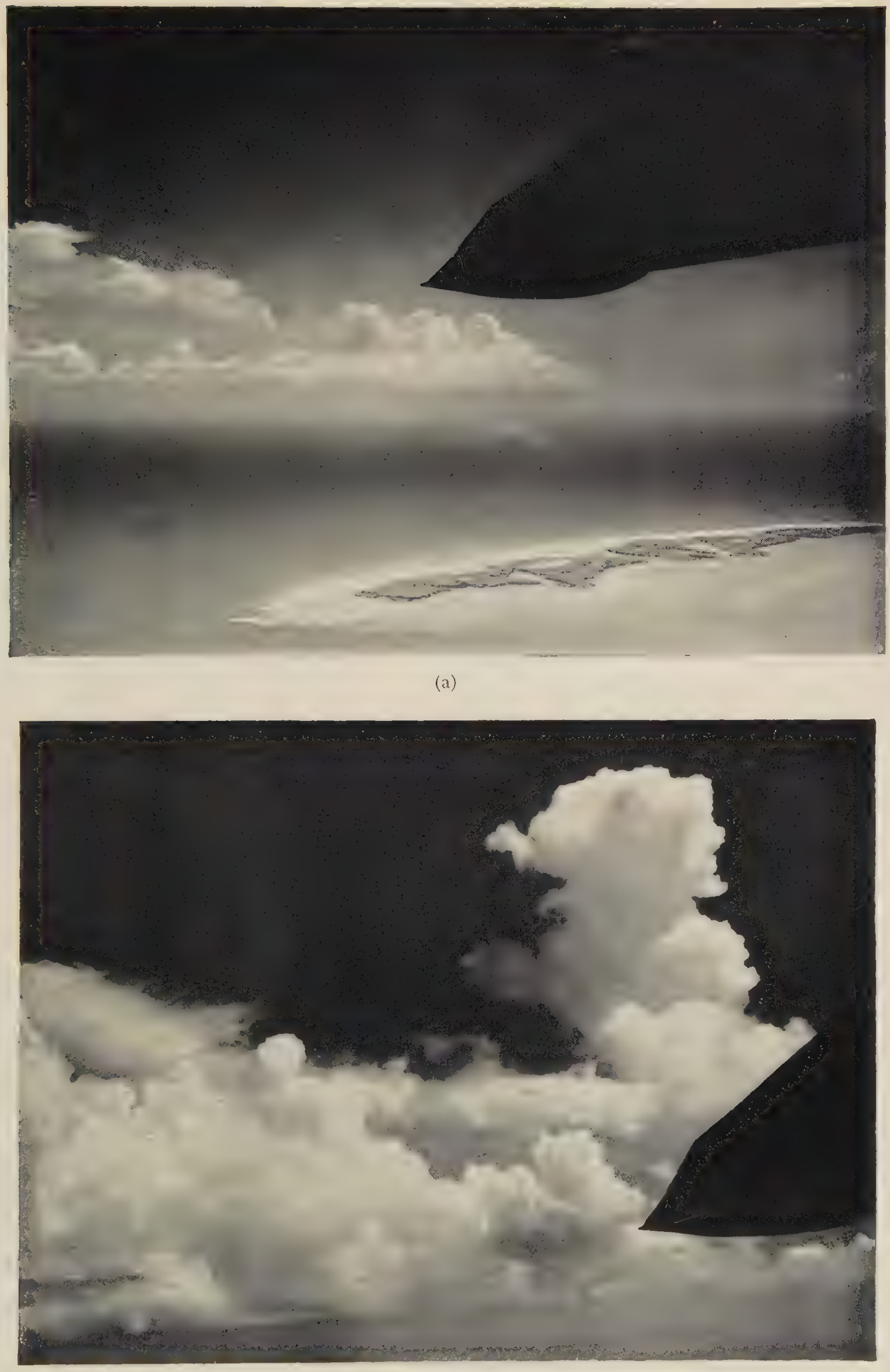

(a)

(b)

Figure 4. Photographs taken on way to location of sounding 4, 1436 LMT, about 2,000-ft elevation. (a) Photograph taken at location and in direction of arrow a showing lee coast of Puerto Rico, lee side subsidence ring, and oceanic cumulus farther to seaward. (b) Photograph taken at location and in direction of arrow b showing oceanic trade cumuli to seaward of subsidence ring off lee shore.

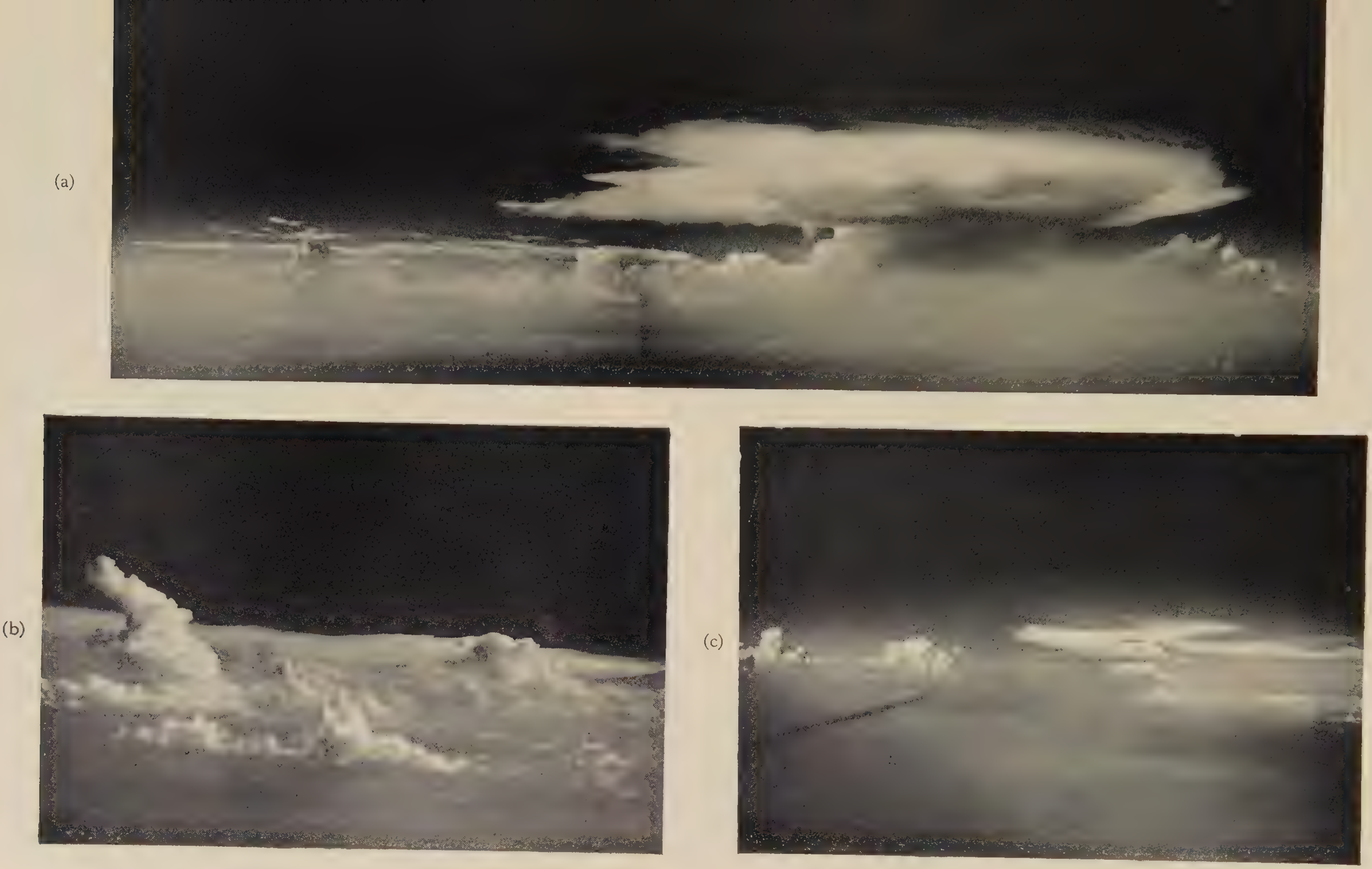

Figure 5. Photographs taken at location of sounding 4, 1600 LMT, 8,400-ft elevation. (a) Photograph along arrow a showing coastline and cumulonimbus cloud over mountain range. (b) Photograph along arrow b showing oceanic trade cumulus to south of leeward subsidence ring. (c) Photograph taken along arrow c showing land clouds to the right, clear ring, and oceanic clouds to the left.

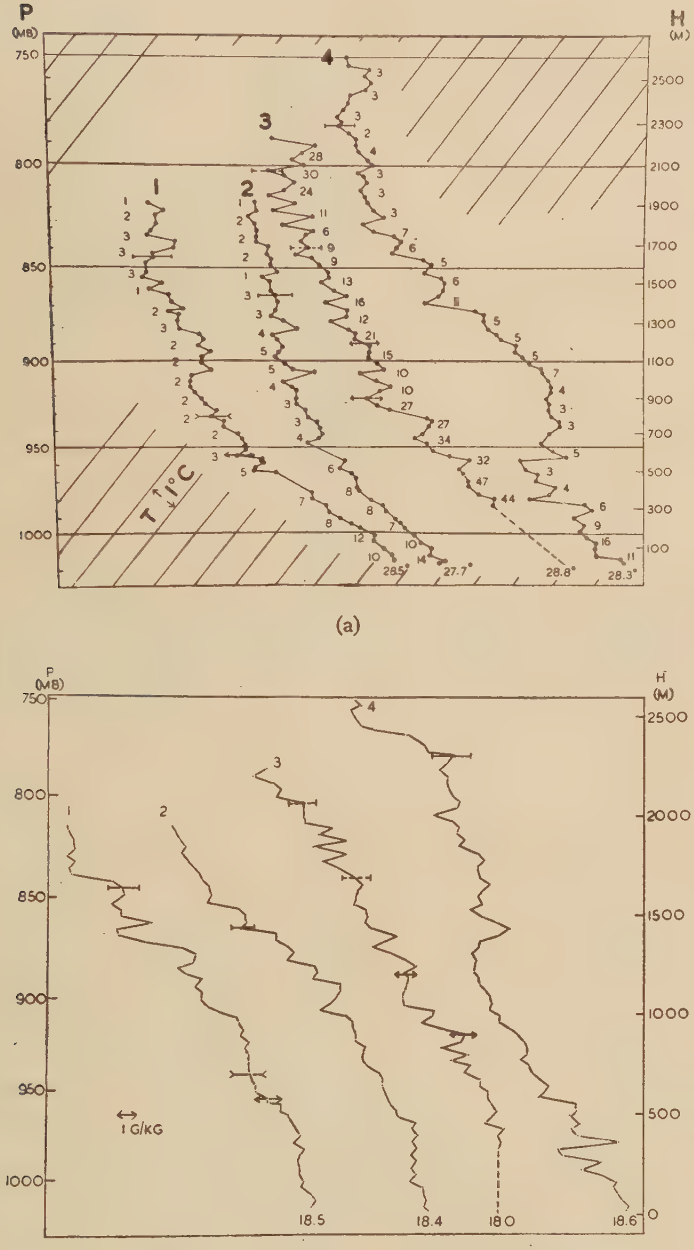

(a)

(b)

Figure 6. (a) Tephigram showing temperature (°C) as a function of pressure (left vertical axis) and height (right vertical axis) for each of the four aircraft soundings, the first sounding being on the left. The temperatures at the lowest observation point are given at the base of each sounding curve. Each curve thus has the same scale but a different origin. Dry adiabats are normal to the slanting isotherms. Sounding 3 (over land) began at 300-m elevation and was extrapolated dry-adiabatically to sea level. The figures beside each curve are values of the turbulence index averaged over 7 mb (or about 65 m) height intervals, and plotted at the centre of each interval. The trade-inversion base (not located entirely from information plotted directly on these graphs) is denoted by the lines with vertical ends; cloud base is denoted by arrows, and cloud-top level by an inverted arrow where it differed from inversion base. (b) Mixing ratio in g/kg as a function of pressure (left vertical axis) and height on a linear scale (right vertical axis) for the sounding curves of Fig. 6a. The mixing ratio at the lowest level is given below each sounding, sounding 3 being extrapolated downward at constant mixing ratio.

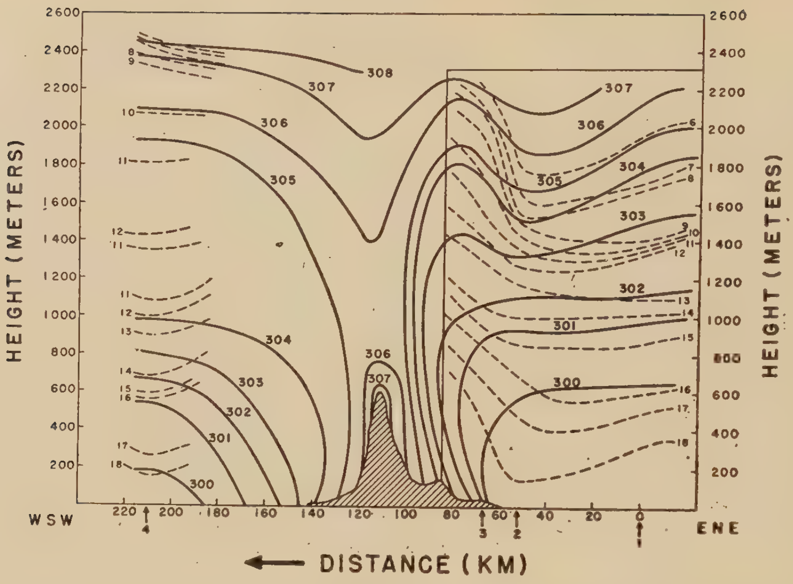

Figure 7. Cross-section of potential temperature and mixing ratio along the line indicated on Fig. 1, near noon, 25 June 1952. The contours of Puerto Rico are shown by the hatched profile. Isentropes are solid lines; lines of constant mixing ratio are dashed. The region outside the light rectangle (soundings 1 to 3) is partly speculative (see text) and not used in quantatitive calculations.

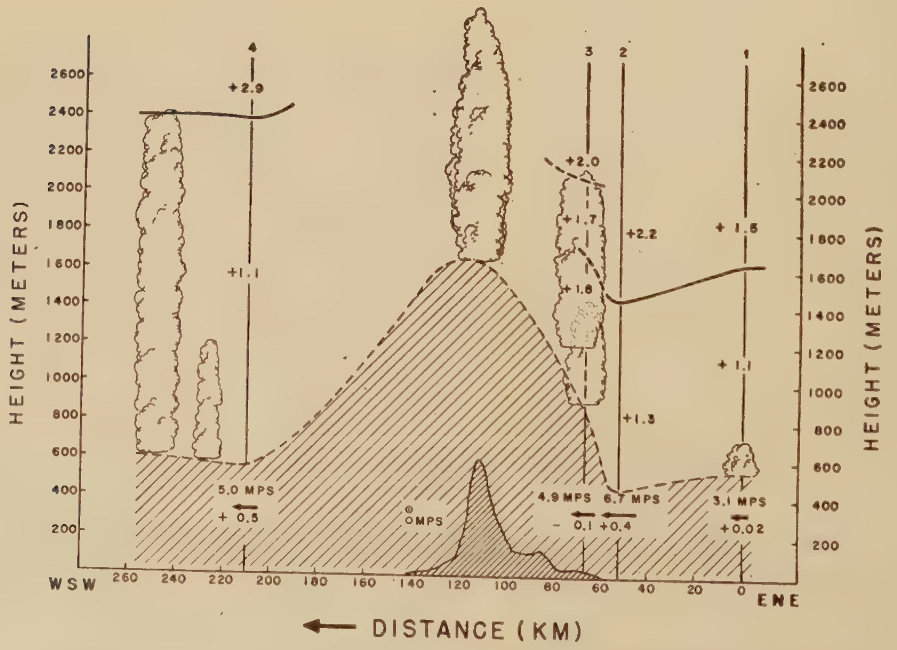
HEIGHT (METERS)
2600
2400
2200
2000
1800
1600
1400
1200
1000
800
600
400
200
4
3
2
1
+2.9
+1.1
+2.0
+1.7
+1.8
+2.2
+1.3
+1.5
+1.1
5.0 MPS
+ 0.5
0 MPS
4.9 MPS
6.7 MPS
- 0.1
+0.4
3.1 MPS
+0.02
WSW
260
240
220
200
180
160
140
120
100
80
60
40
20
0
ENE
← DISTANCE (KM)

Figure 8. Schematic reconstruction of the cross-section shown in Fig. 7, giving the thickness of the subcloud layer (hatched); the distribution of the inversion base (solid, dashed on sounding 3), average stabilities for the layers indicated ($\times 10^7$ cm^{-1}), cloud configurations and 1,000-ft winds. It should be noted that the stabilities were calculated by layers and are therefore not comparable for the same height interval from one sounding to the next.

used to follow the inversion base, since condensation and non-adiabatic heating were absent. On sounding 3 the inversion was indefinite and appeared to have a multiple structure, a weak transition being indicated at 1,690 m (mixing ratio 10·6 g/kg) and another more pronounced stabilization and drying at 2,070 m (mixing ratio 8·0 g/kg). The stability is defined as $\frac{1}{\theta}\frac{d\theta}{dz}$, where θ is potential temperature. The average stability for each layer was obtained from the soundings by graphical averaging over each 100-m height-interval and numerical averaging of these averages over the layer in question. It was checked graphically for each layer as a whole using Fig. 6a. The heights of cloud bases and tops were measured, except for the tops over the mountains, which at noon were estimated to be at about 10,000 ft. These built up to huge anvils surpassing 30,000 ft (see Fig. 5a) by mid-afternoon and died away near sundown.

4. THE FIELD OF MOTION

(a) *The observed wind structure*

Surface smoke showed directions fluctuating between 60°-88° on soundings 1-3. Double drift-readings at 1,000 ft in each of these locations indicated little or no shift in direction with height. The 1100 LMT radio-wind observation at San Juan showed small wind shear up to 3 km. Thus the average 1,000-ft wind at soundings 1 and 4, namely 4 m/sec, is taken as a constant basic current throughout the section, upon which the calculated mean convective motions are to be superposed.

(b) *Calculation of the mean convective motions*

It is assumed that the sea-breeze cell is in a nearly steady state during the hours around noon, as has been justified for smaller islands by the work of Malkus and Stern (1953).

The velocities in this cell are computed as follows : a circular island of radius 50 km is considered, with an elliptical subsidence ring around it; the ring is 40 km across on the upwind side and 80 km across on the downwind side. An inward-pointing sea breeze is taken, around the coast line, of 3·6 m/sec on the upwind coast (difference between observed winds at 1,000 ft at soundings 1 and 3), increasing to 4 m/sec on the lee coast (owing to calm at 1,000 ft observed there). Inland, the sea breeze is assumed to fall linearly to zero at the island centre and, out to sea, it goes linearly to zero at the periphery of the subsidence ring. If we assume strictly radial velocities, the low-level divergence pattern is thus specified, and to complete the determination of the velocity field it is only necessary to find the height at which the sea breeze reverses. Stern and Malkus (1953) have derived an expression for this height, namely

$$h = \tfrac{1}{2}\,\pi\,(U^2/gs)^{\frac{1}{2}}$$

where U is the basic current; g is the acceleration of gravity; and s is the stability of the undisturbed current. Taking $U = 4$ m/sec, and s as the mean stability of the moist layer on sounding 1, this height h becomes 850 m. Therefore, the horizontal-divergence field is taken as constant from the surface to 300 m, is decreased linearly from there to zero at 900 m over the water (1,000 m over the island) and increased linearly in the opposite sense up to surface magnitude at 1,500-1,800 m. The last is not critical for the budgets which follow and was done in agreement with the theoretical results of Malkus and Stern.

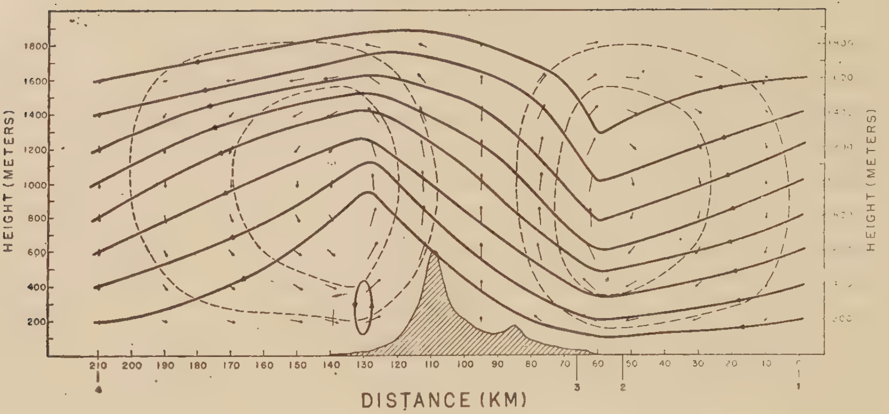

Figure 9. Streamlines (calculated) of the air flow along the cross-section of Figs. 7 and 8. The streamlines of the convection cell are dashed; the total streamlines are solid (obtained by adding constant basic wind of 4 m/sec from right to left).

Thus $\partial w/\partial z$ and w (the vertical velocity) are specified. When w is so calculated, the convective and total (4 m/sec basic current added) velocities along the section give the streamlines shown in Fig. 9. The maximum rate of descent in the subsidence ring is 3·3 cm/sec at 900 m, and the maximum average rate of ascent over the island is about 10 cm/sec at 1,000 m. The rate of descent in the subsidence ring at 1,500 m is found to be 1·2 cm/sec in fair agreement with the 0·8 cm/sec calculated from the sinking of the inversion between soundings 1 and 2. In constructing Fig. 9, the presence of the actual mountain ridge has been ignored, for although it undoubtedly disturbs the flow and adds to the circulation, the ‘ equivalent mountain ’ due to the heating may be shown (see Stern and Malkus, Eqs. 34 and 35, 1953) to be at least $1\frac{1}{3}$ times as high as the actual 600-m mountain, provided that the average island surface-temperature exceeds that of the sea by 1·5°C. Since the temperature at the lee shore (Fig. 7) is 4°C greater than that at the windward, this mean temperature-excess is not exaggerated, and the ‘ equivalent mountain ’ amplitude of 800 m is consistent with the vertical amplitude of the streamlines, as also was found in the previous studies.

An independent test of the velocity field is, however, possible. The calculated motions must transport water vapour through and within the section in such a way that mass continuity is satisfied, using the observed mixing ratios and gradients. The next section is thus concerned with the moisture balance.

5. The moisture budget of the section

Soundings 1, 2, and 3 are assumed synoptic to describe a steady-state air flow. We consider a volume of unit width normal to this section (see Riehl *et al.* 1951) and approximately 2 km high. Since no precipitation was occurring in this part of the section, the processes which must achieve a balance in the lowest layer are : evaporation into the section from the surface; influx at the upstream side and efflux at the downstream side; efflux or influx along the top depending on whether the mean motions are subsiding or ascending; and efflux from the top due to turbulence. Symbolically we may write

$$\rho \int_0^H U_i\, q_i\, dz + Ed - \bar{w}\, \rho\, q_H d - \rho \int_0^H U_E\, q_E\, dz - \int_0^d A \left(\frac{\partial q}{\partial z}\right)_H dx = 0$$

where the z-direction is vertically upward; the x-direction points along the basic flow;

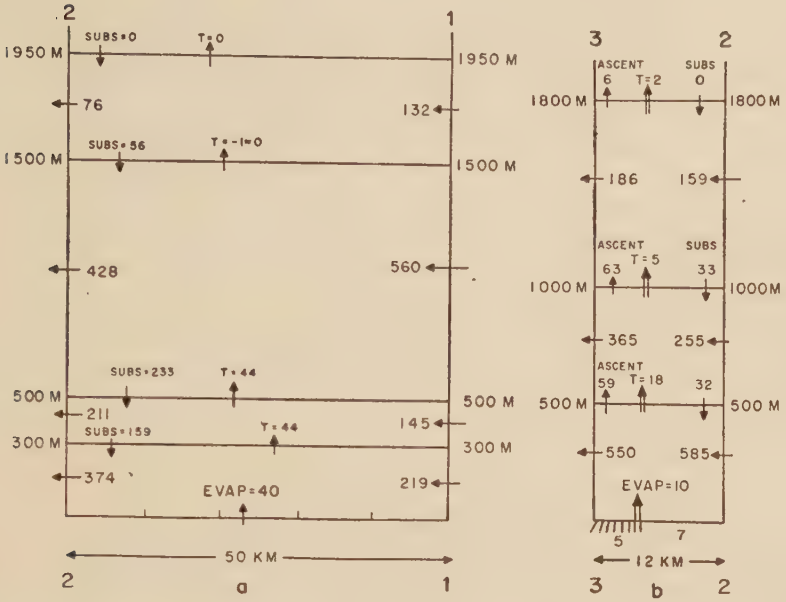

Figure 10. Moisture budget for the volume 1 cm normal to the section of Figs. 7 to 9. The numbers accompanying the arrows are moisture fluxes in g/sec into and out of the sub-volumes. (a) Budget for the volume 50 km in length between soundings 1 and 2, which was divided into four layers: lower subcloud (0-300 m); upper subcloud (300-500 m); cloud (500-1,500 m); inversion (1,500-1,950 m). The turbulent transport through the 1,500 and 1,950 m levels was zero despite a strong rate of decrease of mixing ratio upward, thus indicating a negligible Austausch at these levels. (b) Budget for the volume 12 km in length between soundings 2 and 3, which was divided into three layers: lower subcloud (0-500 m); upper subcloud (500-1,000 m); cloud (1,000-1,800 m). The much shorter length of this section makes its figures rather unreliable compared to the previous one, especially since some gradients and transports (those indicated by double arrows) were averaged across the top which includes a water-land transition. Nevertheless the results are consistent with one another and with the sounding data.

the section has a height H and a length d. The first term is the influx at the upstream end due to the horizontal motion along the section, U_i; q_i is the mixing ratio at the influx end; and ρ is the air density, assumed constant throughout the section. The second term is the moisture addition due to evaporation, E being the evaporation rate per unit area. The third term is the flow through the top of the section, where $\bar{w}$ is the mean vertical motion along the length of the top, and q_H is the mean mixing-ratio along the top. The fourth term is the horizontal efflux at the downstream end and the last term is the efflux through the top due to turbulence. The vertical gradient of moisture at the level H is $\partial q/\partial z$ and A is the Austausch or coefficient of turbulent moisture exchange. All these quantities except the evaporation rate and the Austausch are determined by the field of motion and the soundings. If the evaporation rate can be estimated, the Austausch at the upper boundary of the lowest layer may be calculated and a similar budget-equation evolved for the next higher layer of the section. Since two terms are unknown for the first sub-section, it might appear that quite a wide leeway is permitted in their choice and that the field of motion is not thereby rigorously tested. The calculations show, however, that small variations in the velocity field require rather implausible choices of evaporation and Austausch distribution to achieve a balance in all the subsections, since the fluxes in each one depend upon those in all the others, both vertically and in the horizontal (see Fig. 10). Large variations in velocity field prohibit balance in one or more sub-sections under any reasonable assumptions concerning the remaining two fluxes.

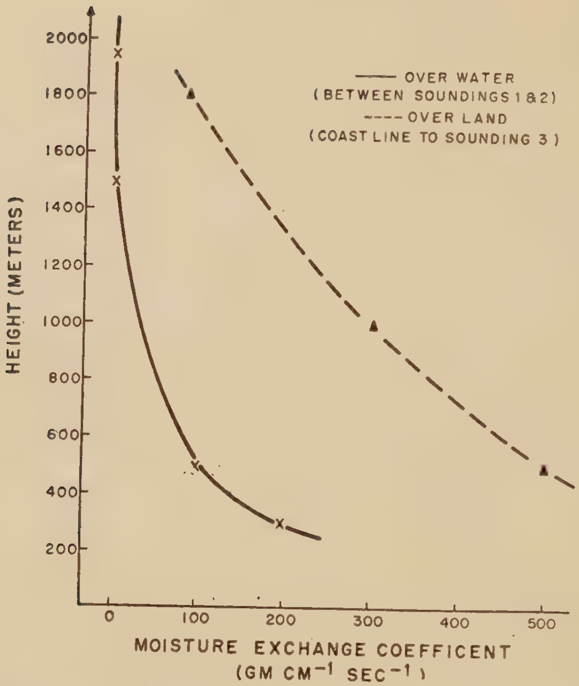

Figure 11. Austausch, or moisture-exchange coefficient, as a function of height, calculated from the results of Fig. 10 taking the turbulent transport, T, and the vertical moisture gradient at the level in question. The values over land (dashed curve) are computed by obtaining the average value between soundings 2 and 3 (Fig. 10b) and extrapolating the value over water (solid curve) up to the coastline.

An evaporation rate has therefore been taken which is plausible and gives a reasonable distribution of Austausch. The process is illustrated in detail for the lowest 300-m layer between soundings 1 and 2, and the remaining calculations are shown in Figs. 10 and 11. The Austausch distribution over land was found from the average between soundings 2 and 3 by extrapolating the overwater value up to the coastline.

The figures for the lowest 300-m section between soundings 1 and 2 are as follows :

Horizontal influx term $= \rho \bar{U}_i \bar{q}_i H = 10^{-3} \times 4 \times 10^2 \times 18{\cdot}2 \times 10^{-3} \times 3 \times 10^4 = 219$ g/sec

Horizontal efflux $= \rho \bar{U}_E \bar{q}_E H = 10^{-3} \times 7 \times 10^2 \times 17{\cdot}8 \times 10^{-3} \times 3 \times 10^4 = 347$ g/sec

Subsidence through top $= \rho \bar{w} q_{300}\, d = 10^{-3} \times 1{\cdot}8 \times 17{\cdot}6 \times 10^{-3} \times 50 \times 10^5 = 159$ g/sec

These figures are fixed by the soundings and calculated velocities. An evaporation rate of 8×10^{-6} g cm^{-2} sec^{-1} is now assumed, which is twice the mean annual evaporation rate for the region (Sverdrup 1942). This gives the remaining two fluxes as :

Evaporation $= Ed = 8 \times 10^{-6} \times 50 \times 10^5 = 40$ g/sec

Turbulent flux $= A_{300}\, (\partial q/\partial z)_{300}\, d = A_{300} \times 5 \times 10^{-9} \times 50 \times 10^5$

Applying the balance equation, A_{300} is found to be 176 g cm^{-1} sec^{-1}, or 200 g cm^{-1} sec^{-1}, within the errors of the calculations. Clearly the balance within this sub-section can be achieved with many alternative arrangements between the last two fluxes, including equating both of them to nearly zero. However, when the remaining three upper and three downstream sections are considered it will be seen that those two fluxes can be varied only little if plausible balances are required throughout, since the fluxes into each section depend on the effluxes from the neighbouring ones.

The height distribution of Austausch coefficient in Fig. 11 compares well with values obtained for the Caribbean (Bunker, Haurwitz, Malkus and Stommel 1949) and in the Pacific trade by Riehl *et al.* (1951). The higher values and greater vertical extent of the turbulence over land are also indicated by the much higher ' turbulence index ' on sounding 3 compared with the others (see Fig. 6a).

5. EFFECTS UPON THE TROPICAL AIR MASS ON PASSING THROUGH THE CONVECTION CELL

It is now possible to return to the cross-sections to examine the effects of the processes established above upon the meteorologically important features of the trade stream. For this purpose it is again convenient to divide the section into vertically superposed layers.

(*a*) *The properties of the subcloud or ground layer*

The subcloud layer is defined in Fig. 8 as the layer of air between the surface and the region of slight stabilization and drying which usually marks the level of cloud base. The subcloud layer exhibited by sounding 1 is typical of undisturbed oceanic trade-wind air (see Bunker *et al.* 1949). Its depth is 575 m; it is barely stable with respect to dry adiabatic processes; it is also well-mixed and homogeneous with a nearly constant mixing-ratio. At the location of sounding 2, the character of the layer is markedly changed. Subsidence and divergence have caused it to shrink to 450 m depth; *it has stabilized by a factor of about twenty*, and dried slightly (mean mixing ratio reduced by 5 per cent compared to sounding 1).

Over the plains, the lapse rate is superadiabatic up to 300 m (using the 1100 LMT San Juan sounding up to the height where the aeroplane sounding commenced) and adiabatic from there up to 900 m, the lowest height of a highly variable cloud base. The mean stability in the lowest 900-m layer is negative and the moisture uniformly distributed. Turbulence is intense and the turbulence index reached extreme values. On the last sounding, at the outer edge of the leeward subsidence ring, the subcloud layer has shrunk again to about 575-m thickness, but its structure is markedly different from the normal oceanic ' homogeneous ' layer. The mean stability is even greater than that at sounding 2 and the average moisture lapse-rate is three times greater than in the undisturbed trade-wind air at sounding 1. Most striking, however, are the intense fluctuations in mixing ratio with height, indicating that the layer was not well mixed at all, but suggesting that masses of drier air had been brought down from aloft and not yet incorporated.

(*b*) *The relation between the structure of the subcloud layer and the initiation of cumulus growth*

Small trade cumuli uniformly based at 575 m are present at sounding 1, while clouds are entirely absent at sounding 2. Since calculations using normal rates of mixing show that the lowest 300 m of the ' cloud ' layer at sounding 2 are less inhibitory (by drying) to cumulus growth than at sounding 1, the reason for the suppression of cumuli at sounding 2 must be sought in the subcloud layer. The work of Bunker *et al.* (1949) indicated that trade cumuli generally were found in localities where the lifting condensation level (LCL) of the lowest air fell below the top of the mixed layer, and clear spaces occurred where the LCL was more than about 30-50 m above its top. At sounding 1, the LCL of the lowest air is 585 m, the same within observational error as the top of the mixed layer and the observed cloud base. At sounding 2, the LCL of the lowest air is 560 m, which exceeds the top of the mixed layer by 110 m. Sounding 4, however, suggests that a lifting condensation level close to the top of the ground layer is not a sufficient condition for cumulus formation. No clouds appeared at sounding 4, although the LCL for the lowest air was at 600 m. Apparently the stability of the subcloud layer inhibited the upward mixing of water vapour from the sea surface and the turbulent eddying necessary for the initiation of clouds. A few kilometres seaward of sounding 4, small cumuli based at 600 m began to appear, increasing in size still farther off shore, suggesting that the mixed layer and its transport functions were re-established after leaving the region influenced by subsidence.

At sounding 3 over the plains of Puerto Rico, cloud-base height ranged from 900 to about 1,200 m. Here the heating condensation level is probably more pertinent than the LCL. For air with a mean mixing ratio of 1 g/kg (or 6 per cent) in excess of the sounding, the HCL was at 900 m and no further heating was required for cloud production since the lapse rate is adiabatic up to that level. For air with the mixing ratio of the sounding, the HCL was at 1,275 m, requiring a 1°C increase in surface temperature. Local fluctuations in temperature and moisture can therefore easily account for the height variations in cloud base. In contrast to the oceanic cumuli, it appears that the land clouds were associated with thermals extending well below their bases, since cloud-scale 'bumps' could be traced under clouds down to the lowest level flown (approximately 300 m).

(c) *The properties of the cloud layer*

The cloud layer is defined as lying between the top of the ground layer and the base of the trade inversion, regardless of whether clouds may actually be present. One obvious variation in that layer was the great rise in cloud base from 575 m over water, to 900-1,200 m over the plains, and to more than 1,600 m in the mountainous area. This common island effect is explained by more rapid warming than moistening of the lower air. A second is the very different appearance of the clouds themselves (see Figs. 2 to 5). The land and mountain clouds exhibit an appearance similar to middle-latitude cumulus, with hard, cauliflowerlike edges and boiling motions, in contrast to the softer, more slanting, more slowly overturning trade cumuli. The stability in the cloud layer is, however, far greater over the land than over the ocean, being nearly the same at soundings 1, 2, and 4, and larger by 50 per cent at sounding 3. This feature (namely stabilization over land in the middle and upper cloud layer) was noted by Riehl (1947) who attributed its cause to the intense turbulence below, which creates a stable region at its upper limit. Many of the clouds over the plains terminated at the first weak inversion at 1,690 m and the tallest ones stopped at the stronger one at 2,070 m.

Downstream variations in cloud layer humidity are also pertinent. Between soundings 1 and 2, the average mixing ratio of the cloud layer (roughly 500-1,500 m vertical extent) decreased by 13 per cent. On soundings 3 and 4 the cloud layer has thickened so much that mean mixing ratios are not comparable. The difference in mixing ratio between sounding air and saturated air at the same temperature was therefore taken as a measure of the probable difference in vapour content between clouds and environment. For the 1,500-m level, at sounding 1 this difference is 6·2 g/kg; at sounding 2, it is 6·0 g/kg, at sounding 3, 3·3 g/kg; and at sounding 4, 4·4 g/kg. Thus, over the island, the greater stability in the cloud layer was far more than offset by three factors, (a) strong thermals below cloud base, (b) general ascent in the mean motion, and (c) reduced resistance due to entrainment (a less dry environment).

(*d*) *Features of the moist layer as a whole and of the trade-wind inversion*

In the tropics, the moist layer is defined as extending from the surface up to inversion base. Sounding 4 shows clearly the effects of passage across the island; the moist layer extends up to 2,300 m, compared to 1,600 m on sounding 1. Relative to sounding 1, the air from 500-1,300 m has dried, decreasing its mean mixing ratio by 10 per cent, and the air from 1,300-2,000 m has been moistened increasing its mean mixing ratio by 38 per cent. Fig. 9 shows that the effects of the subsidence and divergence had become small by 1,300 m, while mean ascent and cumulus activity over the land reached far greater heights. The net effects of passage through the convection cell were thus such that the moist layer as a whole accumulated water vapour.

We saw that the trade inversion-layer sank 200 m between soundings 1 and 2, stabilized, and conserved its potential temperature. After the coastline is passed, the isentropes begin to cross the inversion contours very rapidly and at sounding 4 the potential temperature of the base of the layer has increased by 4·5°C. Level for level, sounding 4 shows (compared with sounding 1) a net warming up to 1,000 m, a net cooling above about 2,000 m, and a marked destabilization between, to be expected as a result of the convective overturning. The intensified inversion on sounding 4, both in respect of stability and vertical rate of drying, must be due to the fact that the inversion marks the upper boundary of the convection, rather than to the subsidence, which vanished well below that level. Thus although it may be useful throughout such a section to refer to the stable boundary between moist and dry air as ' the ' trade inversion, this inversion is physically continuous only between soundings 1 and 2. Thereafter it is controlled in strength and height by differing processes at different stages as the air passes through the cell.

6. Conclusions

In addition to establishing the existence and magnitude of the orographic-convection cell suggested visually, the present study illustrates the critically sensitive balance between the processes normally at work in the trade stream. An island serves to intensify some of these processes relative to others as the air passes across it and thus suddenly alters the balance, quickly bringing about results which may occur imperceptibly slowly on a long over-ocean trajectory.

Particular attention has been focused on the moisture budget and upward transport of water vapour. The trade cumuli are the main effectors of this transport through a deep layer, and their suppression over large areas or times may cause not only local drought but a disturbing influence on larger-scale circulations. It has been shown here that small alterations in the subcloud layer due to subsidence may prevent the appearance of cumuli, despite little or no change in the cloud layer itself. This is due to the marginal condition of the normal subcloud layer. Under ordinary conditions, a decrease in lapse rate of less than 0·1°C per 100 m may increase the stability by more than a factor of five; or a decrease of mixing ratio of 0·5 g/kg at the top of the layer may double the moisture gradient. Either of these changes alters the eddy transports through the layer. Subsidence is a particularly effective suppressor of cumuli since it both stabilizes and thus damps the eddies and may also lower the top of the mixed layer below the lifting condensation level of the air within it. At higher levels, subsidence serves to lower and strengthen the trade inversion, the contours of which we see from Fig. 8 would be far different without the normally observed counteraction of the cumuli.

A heated land mass produces the opposite effects. Over an island the size of Puerto Rico on even a slightly subnormal sea-breeze day, the height of cloud top is raised from an undisturbed 700 m over water to 3 km over land by noon and to more than 9 km by mid-afternoon. After leaving the island the air had experienced a net 800-m raising of the trade inversion and a 23 per cent accumulation of water vapour in the moist layer. Clearly an observer's picture of the trade-wind atmosphere will depend critically upon whether he observes over water or over land, and, if over land, upon the size of the land mass and his particular location with respect to it.

Finally the very delicate equilibrium governing the trade-wind air stream raises the possibility of artificial attempts to alter it in limited areas. In particular, the critical condition of the subcloud layer indicates that man-made efforts to increase tropical rainfall might more fruitfully be concentrated upon the air below cloud and upwind of the islands rather than upon the already existent clouds over the region where rain is desired, which this study suggests are in a far less marginal balance.

ACKNOWLEDGMENTS

The writer is indebted to Mr. Kenneth McCasland who both conceived this experiment and made possible its performance.

The observational work was carried out under the sponsorship of the United States Office of Naval Research.

REFERENCES

Bunker, A. F., Haurwitz, B., Malkus, J. S. and Stommel, H. 1949 'Vertical distribution of temperature and humidity over the Caribbean Sea,' *Pap. Phys. Ocean. Met. M.I.T. and Woods Hole Ocean. Inst.*, **11**, No. 1.

Leopold, L. B. 1949 'The interaction of trade wind and sea breeze, Hawaii, *J. Met.*, **6**, p. 312.

Malkus, J. S. and Bunker, A. F. 1952 'Observational studies of the airflow over Nantucket Island during the summer of 1950, *Pap. Phys. Ocean. Met. M.I.T. and Woods Hole Ocean. Inst.*, **12**, No. 2.

Malkus, J. S. and Stern, M. E. 1953 'The flow of a stable atmosphere over a heated island, I,' *J. Met.*, **10**, p. 30.

McCasland, K. 1951 'Modifications of the airplane psychrograph and adaptation of the humidity strip to airplane soundings, W.H.O.I. Ref. No. 51-59. Unpublished manuscript submitted to the Office of Naval Research under Contract No. N6onr-27702 (NR-082-021).

Riehl, H. 1947 'Diurnal variation of moisture and stability aloft in the vicinity of San Juan, Puerto Rico,' *Bull. Amer. Met. Soc.*, **28**, p. 137.

Riehl, H. 1954 *Tropical Meteorology*, New York (McGraw-Hill).

Riehl, H., Yeh, T. C., Malkus, J. S. and La Seur, N. E. 1951 'The north-east trade of the Pacific Ocean, *Quart. J. R. Met. Soc.*, **77**, p. 598.

Stern, M. E. 1954 'The theory of the mean atmospheric perturbations produced by differential surface heating,' *J. Met.*, **11**, p. 495.

Stern, M. E. and Malkus, J. S. 1953 'The flow of a stable atmosphere over a heated island, II,' *J. Met.*, **10**, p. 105.

Sverdrup, H. U. 1942 *Oceanography for Meteorologists*, New York (Prentice Hall).

Contribution No. 729

Deep-Sea Research, 1954, Vol. 2, pp. 145 to 151. Pergamon Press Ltd., London.

Underwater telemetering

A telemetering depth meter

WILLARD DOW

Summary—This report describes an inexpensive telemetering depth meter capable of determining depth of towed gear and other information, and of transmitting the data acoustically through the water to the surface. The device is somewhat unusual in that it uses the ocean rather than the air as the metering medium. Built into a torpedo-shaped fish for towing purposes, the instrument is self-contained and may be quickly attached to any trawl wire.

INTRODUCTION

A TELEMETERING depth meter which can be made to determine depth of gear, current flow, or other information and then transmit the data acoustically through the water has been developed at the Woods Hole Oceanographic Institution. The acoustic signal is detected at the surface by a hydrophone connected to a sonar or low frequency radio receiver in the ship. The depth meter unit is self-powered and may be clamped on to any trawl wire in a few moments.

The device is somewhat novel in that it uses the ocean itself as the telemetering medium. That sound travels great distances through water with little attenuation has been known for many years, and highly efficient echo ranging and echo sounding equipment has been developed which takes advantage of this phenomenon. A sound " carrier " signal can be modulated or coded at the transmitter in accordance with the information desired by employing the same principles and coding techniques already developed for sonobuoys and radiosonde. The carrier is " tuned in " at the ship much as a broadcast is tuned in on a radio, and then demodulated or decoded to recover the original information just as music or speed is detected and reproduced by a radio set. In fact, a long wave radio receiver can be used without alteration for detecting the acoustic signal by replacing the radio antenna with an underwater antenna – i.e., a receiving hydrophone.

REVIEW OF CURRENT METHODS

Equipment developed to date for oceanographic research may be roughly divided into classes. The first consists of instruments which, when lowered over the side of the ship, produce a reading or a record which can be inspected when the device is recovered. The Bathythermograph (SPILHAUS 1937), bucket thermometer, and Nansen Bottle are examples of this type of instrument and they have a number of special advantages. They are simple, rugged, and compact. Being self-contained, they require no electrical cable to the ship. They have the disadvantage of providing data which may be valid only for a very small area or during a short space of time, and of making such information available only upon recovery of the instrument. In those parts of the world where conditions in the sea are reasonably homogeneous these factors are of minor importance, but in regions where conditions may vary significantly within a relatively small area, or are subject to rapid changes, instruments which can supply continuous information without constant attendance are much to be preferred, and may be essential in some instances.

The second class of instruments, exemplified by various depth (VON ARX 1950) and current meters (UFFORD 1946) do provide continuous monitoring, but have the disadvantage of requiring electrical cables to transmit the information to the ship. Anyone who must operate such equipment at sea soon discovers that cables are a nuisance to handle on deck, that they readily become tangled with trawl wires, nets, or other gear being towed at the same time and even on occasion become fouled in the screws. Often they are subjected to sufficient strain and wear as to eventually leak or break. Replacement can be a time consuming and expensive process.

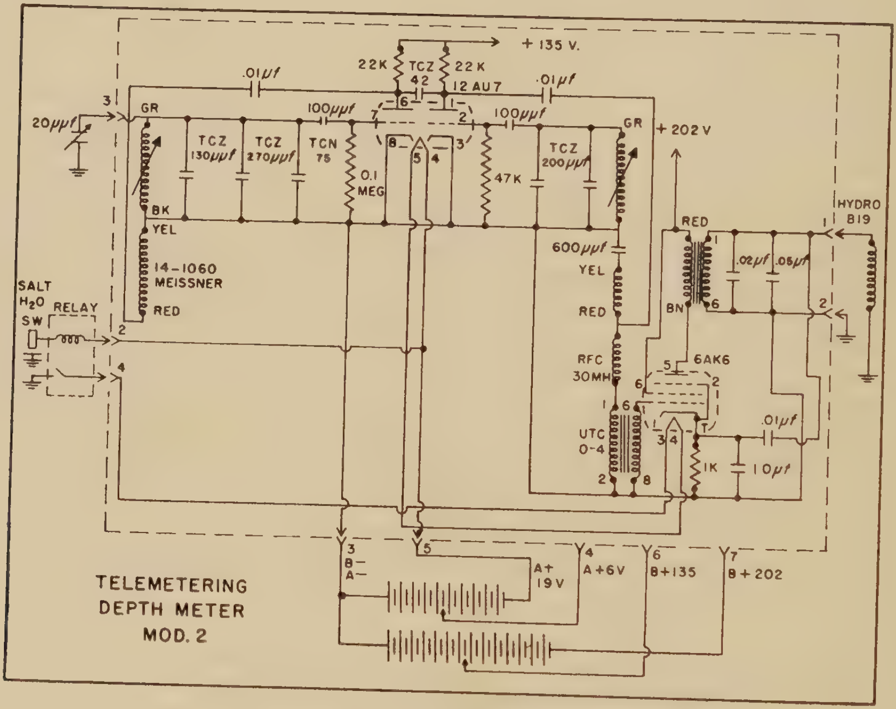
+ 135 V.
22K
TCZ 42
22 K
12 AU7
.01μf
.01μf
3
GR
20μμf
100μμf
100μμf
7
6
1
2
TCZ 130μμf
TCZ 270μμf
TCN 75
0.1 MEG
8
5
4
3'
47K
TCZ 200μμf
GR
+ 202 V
BK
YEL
14-1060 MEISSNER
RED
SALT H₂O RELAY SW
2
4
600μμf
YEL
RED
RFC 30MH
UTC 0-4
6AK6
.01μf
1K
10μf
RED
BN
.02μf
.05μf
HYDRO B19
1
2
3 B- A-
5
A+ 19V
4 A+6V
6 B+135
7 B+202
TELEMETERING DEPTH METER MOD. 2

Fig. 1. Schematic diagram of telemetering depth meter.

Telemetering equipment can be designed to incorporate the best features of both classes of instruments without incurring their disadvantages. It can be made rugged, compact, self-contained and yet capable of supplying continuous information to the ship. Once submerged, the gear operates without attention for long periods of time. In fact, if data is desired from a point somewhat remote from the ship, the telemetering unit can be attached to a floating buoy by an ordinary wire or rope and suspended at any desired depth below the surface. A remote hydrophone could be effected by equipping such a buoy with a receiving hydrophone and amplifier-modulator. The information received by the hydrophone would be amplified and transmitted through the water to the ship as modulation of the carrier signal in the manner described above. Alternatively the same instrument might be used as a deep hydrophone by suspending it from the ship's hydrographic wire, thereby eliminating the necessity for a special electrical cable capable of withstanding the severe strain.

These are only a few of the many possible applications. Telemetering units of this nature can do much to satisfy the long existent need for compact self-contained instruments capable of supplying continuous information about the ocean to a ship at sea.

GENERAL DESCRIPTION OF THE TELEMETERING SYSTEM

The telemetering depth meter makes use of the principles described above. The need for this equipment became particularly pressing when it was required to tow plankton nets and fish trawls in scattering layers. This operation requires that the depth of the plankton nets and fish trawls be known and monitored continuously.

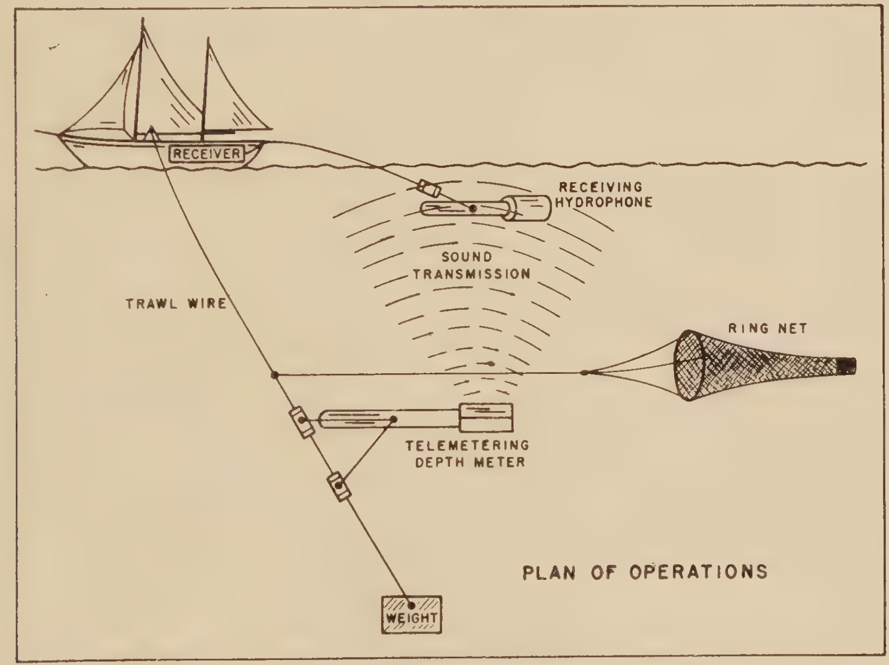

Fig. 2. Plan of operations.

The instrument determines this depth and continuously transmits the information acoustically through the water to the ship. The submerged fish contains a stable heterodyne oscillator (Fig. 1), the frequency of which is varied between 16 and 26 kc. by a variable capacitor which in turn is driven by a bourdon tube sensitive to pressure and having access to the sea. As the instrument descends, the increasing water pressure causes the bourdon tube to rotate the capacitor and the frequency of the oscillator increases. The oscillator output is amplified by a power vacuum tube and applied to a transducer in the tail of the fish. The sound radiated by the transducer is picked up by a receiving hydrophone, which is towed behind the ship at the surface (Fig. 2). The hydrophone is connected to a tuned receiver in the vessel. A the tuning dial of this receiver is calibrated in terms of frequency, reference to frequency vs. depth curve gives the depth of the instrument, or alternatively, the dia may be calibrated directly in terms of depth. Current or temperature informatio can be applied as a modulating signal on the depth " carrier signal " in accordanc with the principles outlined above.

STRUCTURE

The instrument is self-contained in a torpedo shaped housing, or fish, abou 53 inches long and 3½ inches diameter (Fig. 3). The housing is divided into three compartments separated by watertight bulkheads (Fig. 4). The forward compartment contains the bourdon tube and the variable capacitor fastened to it as well as the relay which acts as a power switch. The middle compartment contains the electronic chassis and battery stack. The aft compartment houses the forward end of the transducer and its cable and is removable from the rest of the housing as a unit. Connections between compartments are made by sealed feed-through connectors. The watertight bulkheads prevent damage to the electronics if either the bourdon tube or transducer should become damaged or leak.

MOUNTING

The depth meter fish is mounted on the trawl wire by a triangular bracket (Fig. 3). The fish is free to rotate in a vertical plane in the bracket so that it can always swim parallel to the surface. The bracket is free to swivel about the wire but cannot move vertically because of the stops. The swivels and stops are of a new quick-disconnect design which permits the instrument to be mounted or removed in a few seconds time (Fig. 5). The trawl wire slips into a slot on the side of the clamp. An L-shaped piece of brass is then inserted from the top into a slot at right angles to the first slot. The handle on the opposite side is then turned clockwise. This operates a screw which in turn forces a vertical grooved bar against the wire. The wire is thereby effectively clamped between this bar and the L-shaped insert. To disconnect, the procedure is simply reversed. The swivels are of similar construction except that the clamping feature is omitted. A weight or depressor is hung on the lower end of the wire to obtain a reasonable angle of tow.

OPERATING PROCEDURE

Hydrophone Placement. Experiments at sea indicate that the main obstacle to good reception of the depth meter signal is screw noise from the towing ship. For example, the non-directional hydrophone (Fig. 6), must be towed 1,000-1,500 feet behind the vessel before this background ceases to limit the sensitivity of the system. However the performance of the directional unit (Fig. 7) appears far superior in this regard, as might be expected, and tests are under way to determine if revised towing arrangements and orientation will permit it to be used close to the ship.

Depth Meter Placement. When the hydrophone is in the water the depth meter is lowered just below the surface. This automatically starts the electronic oscillators by completing a relay circuit through a salt water switch which is mounted on the nose of the fish. (The switch also insures that the device cannot accidentally be left operating when not in use and thus prolongs battery life.) The instrument

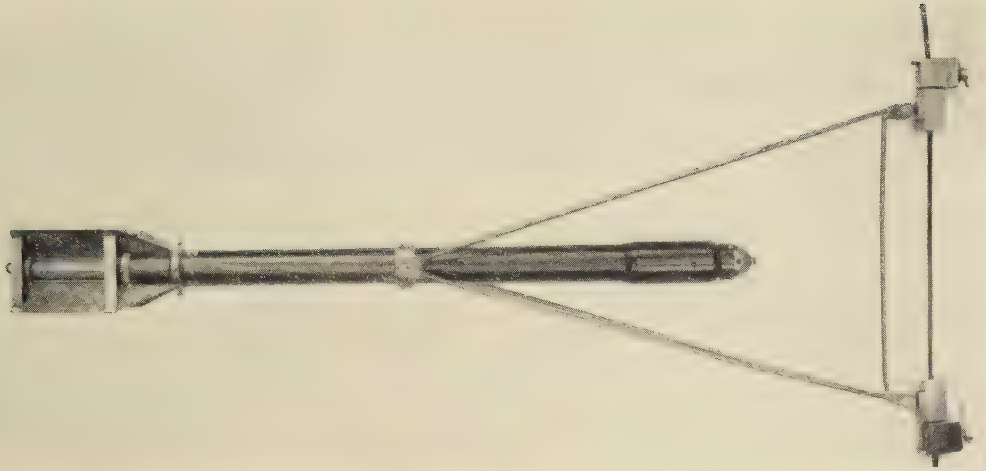

Fig. 3. Depth meter mounted on trawl wire in towing position.

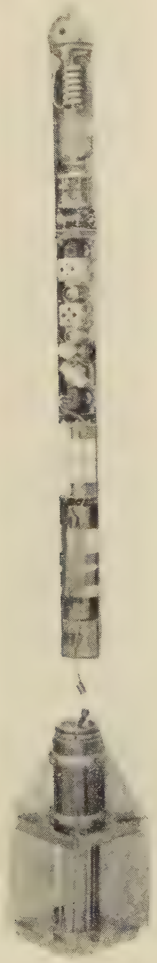

Fig. 4. Telemetering depth meter interior chassis and transducer.

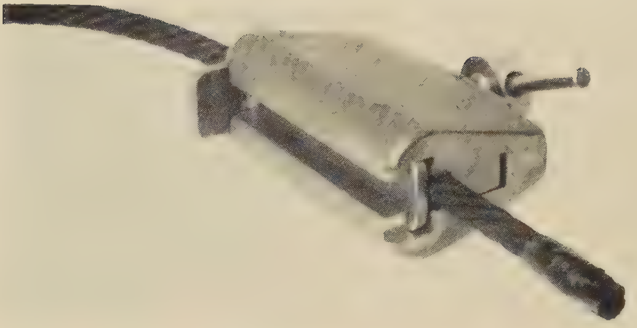

Fig. 5. Wire clamp.

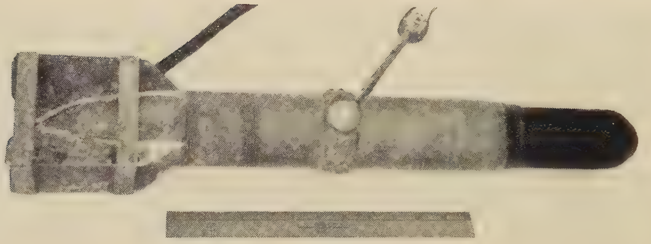

Fig. 6. Non-directional towed hydrophone.

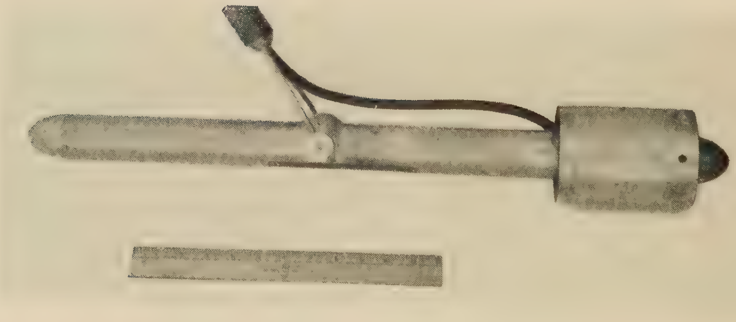

Fig. 7. Directional receiving hydrophone.

should remain in this position a few moments until a stable zero depth reading on the receiver indicates that the electronics have reached operating temperature, the unit may then be lowered to the desired depth.

Operating Time. Battery life, using mercury batteries, is approximately four hours. Since the average net tow does not usually exceed this time period, and since battery pack replacement is quick and easy, it was deemed inadvisable to increase the bulk and weight of the instrument to provide longer battery life.

Receiver Tuning. To receive the depth meter signal, the beat frequency oscillator is turned on and the main receiver tuning dial adjusted until an audible note indicates the carrier has been picked up. This note is then adjusted for zero beat and the frequency read from the receiver dial. A glance at the frequency versus depth calibration curve will then give the depth, or alternatively the dial may be calibrated directly in terms of depth. If the signal becomes weak some readjustment of hydrophone position may be to advantage.

SEA TRIALS

"*Blue Dolphin*" *Cruise.* A preliminary model of the device was given a sea trial during a 10-day fishing cruise aboard the schooner *Blue Dolphin* in August 1953, where it was used to determine the depth of fishing nets during trawling operations. It was found that the signal could be heard reliably at depths up to 1,500 feet by means of a non-directional hydrophone towed behind the ship (see below), but was intermittently lost in screw noise at greater depths. However, the meter could readily be heard to 3,200 feet when the ship was not under way. Calibration of the instrument was checked during the towing operations by echo sounding on the unit from a following vessel. Comparisons of the echo sounder and depth meter records for these runs yielded differences ranging from 4·8% to 8·3% of the depth (as determined by the echo sounder). However, it was found that the depth meter oscillators had been somewhat over compensated for temperature changes. A rough determination of the error from this source was made before the final run and applied as a correction to the telemetered signal. Comparison of records for this run indicated a deviation of only 6 feet in a 343-foot determination. This would correspond to an error of 1·8% for the depth meter reading, but since the echo sounder readings may also have been in error by this amount, this value is only an approximation. In the course of these runs a complete depth versus wire out curve was established for the net and depressor unit, and the curve was used in tests on a second expedition as described below.

"*Atlantis*" *Cruise.* Following the *Blue Dolphin* cruise, the depth meter was stabilized for temperature changes in the laboratory and then given additional tests on *Atlantis* cruise 196 to Puerto Rico. During this cruise the readings of the instrument were checked in two ways.

First a net-depressor-depth meter assembly practically identical to the one used on the *Blue Dolphin* cruise was towed at various depths and depth meter readings were taken to depths of 1,080 feet. The length of wire out and the wire angle were recorded, and the depth meter readings then compared with values taken from the depth vs. wire out curve described above (Fig. 8). While there was undoubtedly some error in applying this curve to the *Atlantis* operation, nevertheless the mean difference between values taken from the curve and the depth meter readings was only 13·0 feet which represents 0·9% of full scale for the depth meter (1,530 feet).

The second check consisted of a vertical lowering with the ship hove to. During this test the depth meter frequencies were plotted against length of wire out as read by the *Atlantis* meter wheel for 18 different depths. The resulting curve was then compared with the original laboratory calibration curve (Fig. 9).

There are thought to be two principal sources of error in these experiments. First, the laboratory calibration follows a smooth curve, but the meter wheel calibration curve is erratic particularly at shallow depths (Fig. 9). This may be due to slippage between the wheel and trawl wire when the tension is light. Secondly, the receiver dial was calibrated only to 0·1 kc. which with this depth range corresponds to 16 feet. Since the mean difference between the meter wheel and laboratory curves is approximately 13 feet, a considerable portion of this discrepancy could be due to reading error. A more finely divided receiver dial is desirable for future work.

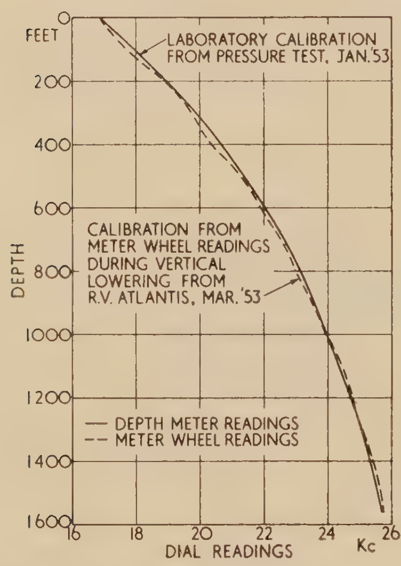

Fig. 8. Depth vs. frequency curve for depth meter. (Depth readings from depth vs. wire out curve described in text).

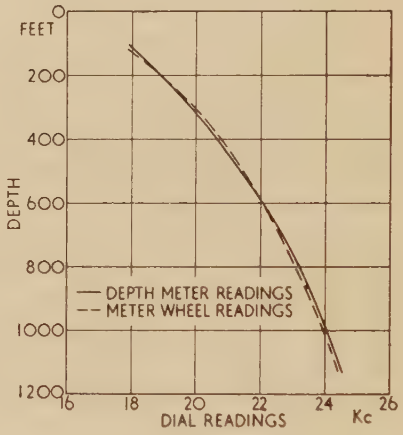

Fig. 9. Depth vs. frequency calibration curves for telemetering depth meter.

It should be pointed out that if greater accuracy is desired at shallow depths, an alternative "nose" for the fish containing a low pressure bourdon tube can be plugged in. One of these units containing a 500-foot bourdon was taken on the *Atlantis* cruise, but was not used because the scattering layer investigations were concentrated around greater depths.

NEW DEVELOPMENTS

A new and more efficient model of the instrument having higher output power and lower battery drain has recently been developed at the Woods Hole Oceanographic Institution. The new instrument has provision for applying temperature information as modulation of the carrier signal. The carrier frequency simultaneously provides depth information as in the older unit. If the instrument proves successful it will be made the subject of a future report.

ACKNOWLEDGMENTS

The author wishes to thank the following people for substantial contribution to this project:

Dr. J. B. Hersey made suggestions concerning types and placement of transducers involved in the acoustic link as well as recommendations concerning the towed fish. Mr. S. T. Knott designed and helped fabricate the structure of the depth meter, mounting bracket, towed hydrophones, etc. and helped test the equipment both in the laboratory and at sea. He also contributed substantially to other phases of the work. Mr. W. E. Witzell assisted Mr. Knott in the work outlined above. Dr. Benjamin B. Leavitt assisted in the overall design of the towing assembly and he and Dr. R. H. Backus helped test the equipment at sea. Mr. M. E. Edwards constructed the electronic chassis for Mod. 1 and 2 of the equipment. Mr. H. A. Cain constructed the special battery packs designed for the instrument.

Contribution No. 729 *of the Woods Hole Oceanographic Institution. This work was supported under Contract NObsr-*43270 *with the Bureau of Ships.*

REFERENCES

Spilhaus, A. F. (1938), A bathythermograph. *J. Mar. Res.*, **1** (2): 95-100.
Ufford, C. W. (1946), An electronic bathythermograph. Unpublished Manuscript.
Von Arx, W. S. (1950), Some current meters designed for suspension from an anchored ship. *J. Mar. Res.*, **9** (2), 93-99.

Printed in Great Britain by The Salisbury Press Ltd., Publicity House, Wilton Road, Salisbury, Wilts. (88014)

Contribution No. 731

A DEEP-SEA SEISMIC REFLECTION PROFILE

BY

CHARLES B. OFFICER

Reprinted for private circulation from
GEOPHYSICS
Vol. XX, No. 2, April, 1955

GEOPHYSICS, VOL. XX, NO. 2 (APRIL, 1955), PP. 270–282, 8 FIGS.

A DEEP-SEA SEISMIC REFLECTION PROFILE*

C. B. OFFICER†

ABSTRACT

This paper presents a detailed seismic reflection profile taken over the deep ocean. Clear sub-bottom reflections and refractions are obtained which are interpretable to show the variation of velocity with depth. From the travel-time difference between the bottom reflection and a prominent sub-bottom reflection as a function of range and frequency and from the variation of the amplitudes of the bottom and sub-bottom reflections with frequency and angle of incidence, the conclusion is reached that the sediment is dispersive, i.e, that the velocity of sound propagation through it is a function of frequency. Further it is concluded that at lower frequencies the velocity in the sediment near the bottom is less than that in the adjacent ocean. This rather unexpected geophysical phenomenon is explained theoretically in terms of propagation in a porous media.

The low velocity sediment forms a wave guide between the higher velocity ocean above and the higher velocity sediment beneath. This resulant wave guide explains previously observed single-frequency arrivals.

INTRODUCTION

A great deal of work has been done in recent years in the study of suboceanic geologic structure by the seismic refraction method. Reports, published and in preparation, from Lamont Geological Observatory, Columbia University; Scripps Institution of Oceanography; Dept. of Geodesy and Geophysics, Cambridge University; and Woods Hole Oceanographic Institution describe much of this work. The amount of effort put into seismic reflection measurements has not been so vast. This has been because information was at first primarily desired on the gross features of the oceanic areas. Among such features are the depth of the Mohorovičić discontinuity, the properties of the crustal material, and the total volume of sediment under the abyssal plains. Geophysicists were also concerned with the changes that occur across continental margins, oceanic islands and ridges, island arcs, and interior basins.

At present the emphasis is changing toward a closer examination of the sediment column itself. The seismic reflection method is finding important use in these studies. Weibull (1947) and Hersey and Ewing (1949) describe vertical reflection measurements, and the latter discuss various types of reflection records that are obtained over the Western Atlantic. Hill (1952) and Katz and Ewing (unpublished manuscript) describe wide angle reflections obtained during the course of their seismic refraction measurements. More will be said about their results and conclusions later. This report is the first on a *detailed* seismic reflection profile over deep oceanic areas; one of the main conclusions is that the characteristics of the sedimentary column, principally the seismic velocities and thicknesses, can be determined by this method.

---

* Manuscript received by the Editor October 19, 1954. Contribution No. 731 from the Woods Hole Oceanographic Institution.

† Woods Hole Oceanographic Institution, Woods Hole, Mass.

Independent investigations have been carried out on this problem by J. Nafe and J. Ewing at Columbia and C. B. Officer at Woods Hole. The investigation by Nafe and Ewing, to be published soon, involves a broad areal coverage by sub-bottom reflection techniques, whereas this report contains a more detailed discussion of the sediment characteristics on the basis of a single profile.

OPERATIONAL TECHNIQUES

A series of seismic reflection measurements were made during the summer of 1953 on a cruise of the research vessels *Atlantis* and *Caryn* from Woods Hole to Bermuda and return. The data were obtained over the continental slope, continental rise, abyssal plain, Bermuda rise, Bermuda slope, and Kelvin banks (Fig. 1). This paper presents the results from one of the abyssal plain profiles; the same conclusions can be reached from the other profiles over this feature.

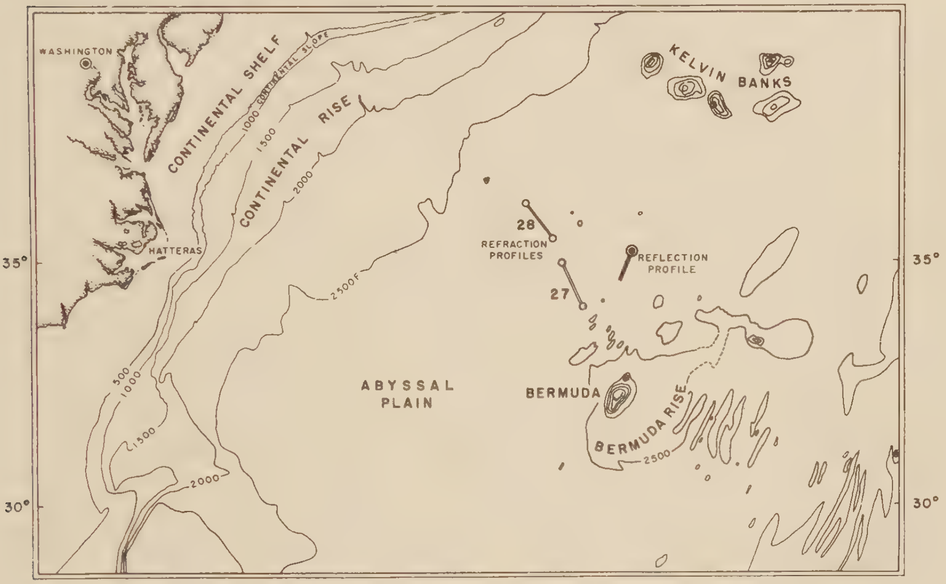
WASHINGTON
CONTINENTAL SHELF
CONTINENTAL SLOPE
1000
1500
CONTINENTAL RISE
2000
HATTERAS
2500F
KELVIN BANKS
28
REFRACTION PROFILES
27
REFLECTION PROFILE
ABYSSAL PLAIN
BERMUDA
BERMUDA RISE
2500
500
1000
1500
2000
35°
35°
30°
30°

FIG. 1. Location of deep-sea seismic reflection profile.

The method is similar to that for any two-ship seismic operation. The *Atlantis* recorded from a hydrophone at 50 ft and from another at 1,000 ft below the ocean surface. The ship was hove to, and all rotating machinery and other noise makers were silenced. The charges, fired from the *Caryn*, were one-half pound TNT-tetryl, and a balloon was tied to them by a piece of string so that they would fire at 2 feet below the surface. At this shallow depth the explosion gas bubble will not oscillate to complicate the sub-bottom reflection patterns and also will not break the surface and thus lose energy into the atmosphere. In this paper,

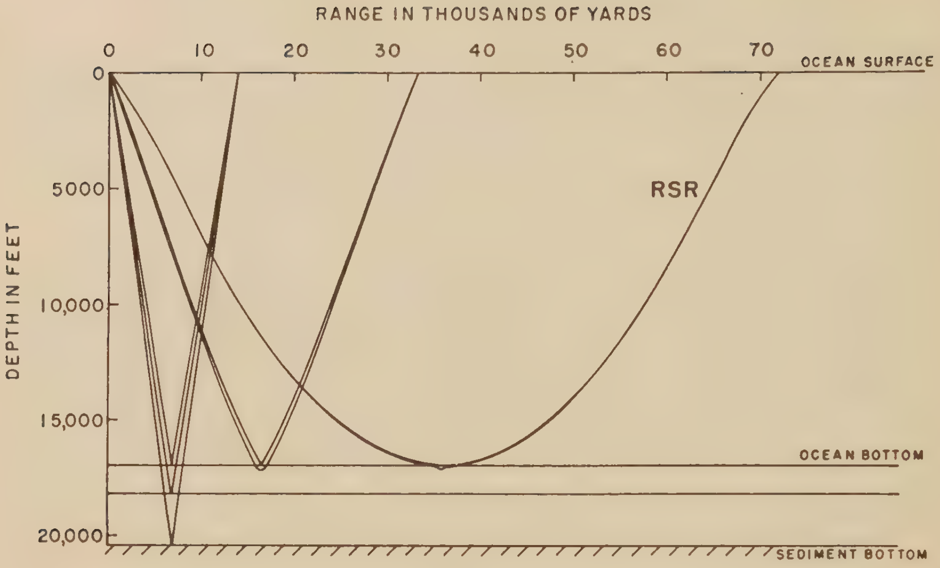

FIG. 2. Ray diagram of bottom and subbottom reflections and refractions.

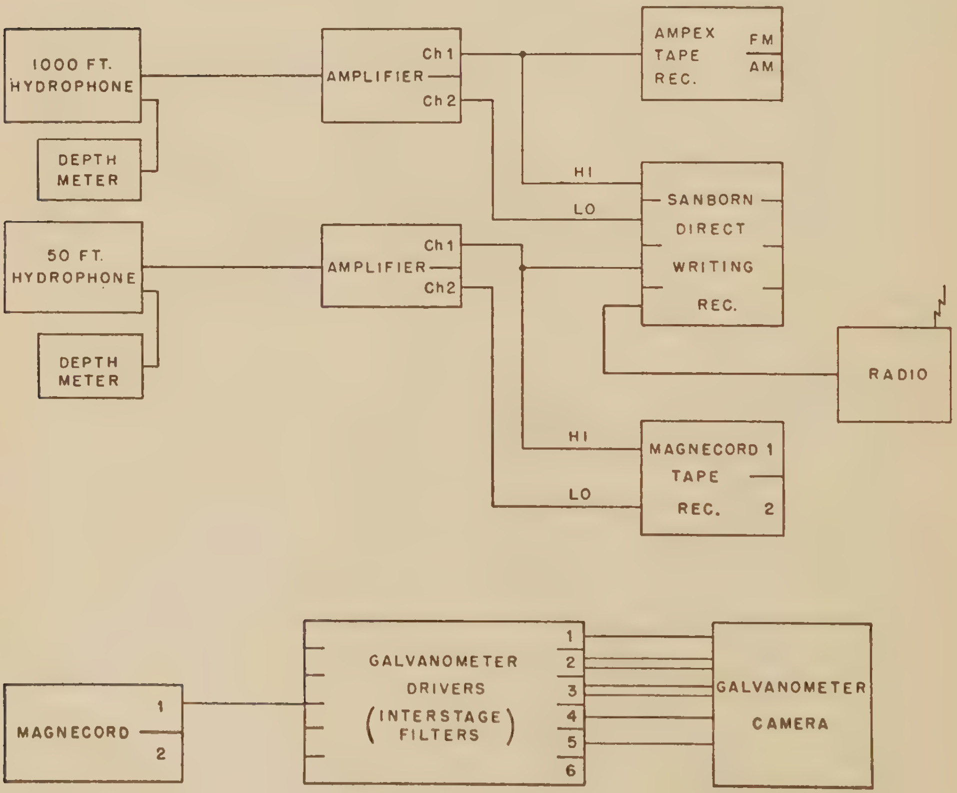
1000 FT. HYDROPHONE
DEPTH METER
50 FT. HYDROPHONE
DEPTH METER
AMPLIFIER
Ch 1
Ch 2
AMPLIFIER
Ch 1
Ch 2
AMPEX TAPE REC.
FM
AM
HI
LO
SANBORN DIRECT WRITING REC.
RADIO
HI
LO
MAGNECORD TAPE REC.
1
2
MAGNECORD
1
2
GALVANOMETER DRIVERS
(INTERSTAGE FILTERS)
1
2
3
4
5
6
GALVANOMETER CAMERA

FIG. 3. Block diagram of recording and analyzing equipment.

only the recordings from the 50-ft hydrophone are presented, for these do not have the additional complication of arrivals reflected from the ocean surface back to the hydrophone as do the recordings from the phone at 1,000 ft. All recordings were taken on magnetic tape without the use of filters. The range was determined from the travel time of the direct arrival from shot to receiver guided in the small, 100-ft sound channel at the ocean surface (Fig. 8). This time interval was observed with a direct-writing recorder. The depth of water on this profile was 16,750 ft and shots were fired about every 500 or 2,500 yards along the

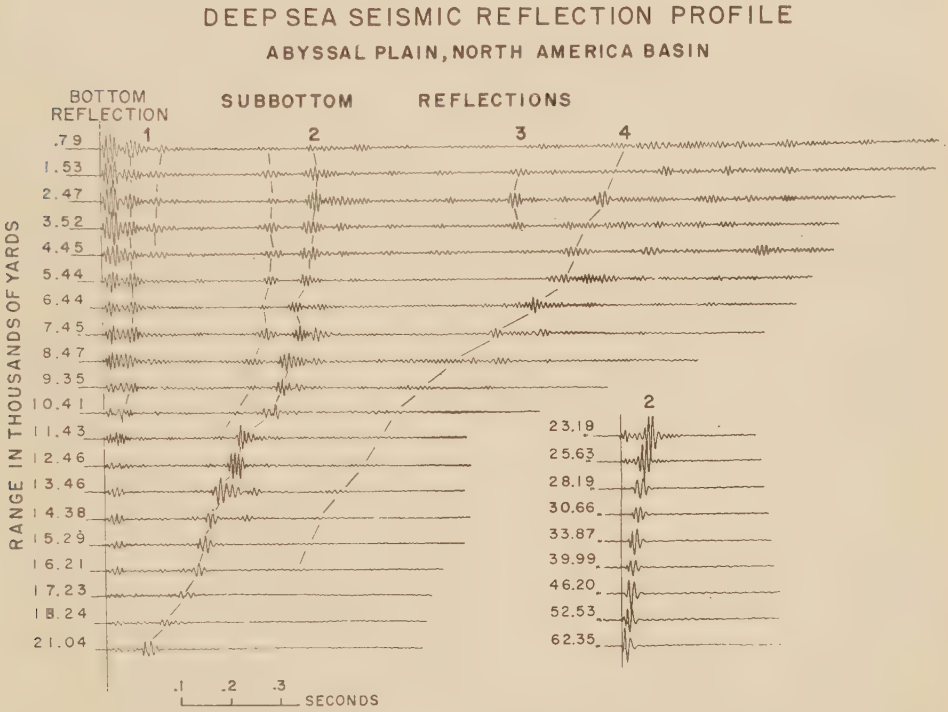

FIG. 4. Deep-sea seismic reflection profile, abyssal plain, 80–100 cps.

shooting ship's traverse until it was 100,000 yards from the recording ship. This distance was beyond the range at which energy is no longer received from a single bottom reflection, the limitation resulting from the sound velocity structure in the ocean (Fig. 2). The profile was not reversed.

In the laboratory the magnetic tapes were replayed through two-stage amplifiers and interstage variable-bandpass electronic filters into a galvanometer camera. Block diagrams of the original recording and analysis arrangements are shown in Figure 3 and sample records are shown in Figures 4 and 5. With the one-half pound near-surface shots, only frequencies down to 50 cps were excited.

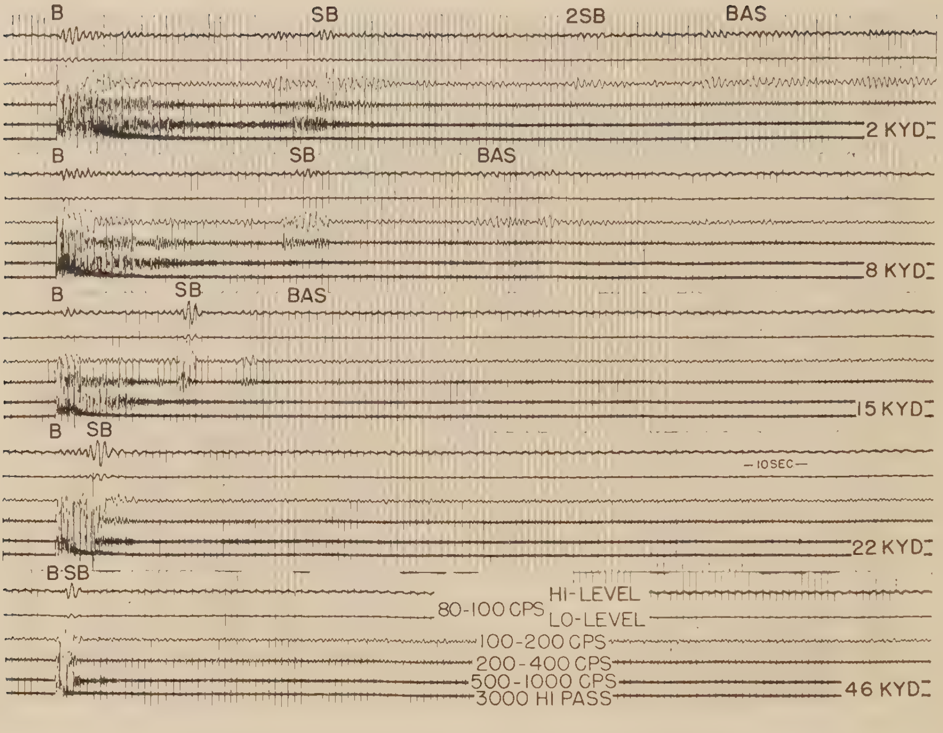

FIG 5. Deep-sea seismic reflections as a function of frequency.

REFLECTION DATA

There are many features of a deep-sea seismic reflection profile which can be seen directly on the records. The sub-bottom reflections are clearly observed at frequencies below 300 cps; there is little penetration by the higher frequencies. The sub-bottom reflections are quite clear and distinct and can be easily followed from record to record. They appear more distinctly at a long range than at near-vertical incidence. This is because the reflections approach their critical angles at the longer ranges. Further, the noise level between the groups of reflection events is low, indicating the presence of homogeneous material between the reflecting interfaces.

Four reflection groups are identified and can be followed from record to record. A group of reflections, marked (1) on Figure 4, at .04–.06 sec after the bottom reflection can be followed out to a range where it becomes difficult to resolve them from the bottom reflection. A second group of three reflections, marked (2), at .30–.50 sec are observed at the closer ranges. The middle one of these reflections can be followed for the entire length of the profile and is the most prominent and useful event. The multiple of this reflection, marked (3), is observed over a short range interval. A fourth reflection, marked (4), with a longer duration is observed at 1.00–1.10 sec at the near ranges and can be followed out to 16,000 yards. This reflection is believed to come from near the bottom of the sediment. The noise level for about a second after this reflection is higher than that between the earlier reflections; after event (4) some other arrivals can be followed for a few records.

Considering the length of the spread and the distance between shots for this deep-ocean reflection profile, the correlation here must be between reflection groups rather than between particular cycles, as is done in oil exploration. This kind of correlation is not, of course, as refined as that employed in exploration and it requires a higher signal-to-noise ratio than can be tolerated with a closely spaced, multi-element spread such as is used in commercial prospecting.

A first interpretation of the data was made using average velocities through each column. This was adequate and accurate for the near-vertical reflections out to 15,000 yards. The sound-velocity structure in the ocean was determined from hydrographic stations and from bathythermograph lowerings. The latter measure the temperature as a function of depth for the variable near-surface water down to 900 ft. The sound-velocity structure of the deeper water is more stable, and the information for depths below 900 ft can be assumed on the basis of previous hydrographic data taken in the vicinity. The sound velocity in the ocean varied from a maximum of 5,050 ft/sec near the surface to a minimum of 4,890 ft/sec at 4,000 ft and increased to a maximum of 5,070 ft/sec at the bottom. The average vertical velocity was 4,960 ft/sec. In great depths of water it was expedient to plot the time differences between the sub-bottom reflections and the bottom reflections against range rather than the total travel time of the sub-bottom reflections. Theoretical curves have been computed for average sediment velocities, and those that gave a reasonable fit to the data are shown in Figure 6.

The velocity in the sediment to the first horizon at 100–150 ft below the bottom cannot be determined. Curves are shown for ratios between sediment and water velocities of 0.9, 1.0, and 1.1, and no one curve fits the plotted data better than the others. This would be expected in measuring a layer of this thickness from an elevation of 17,000 ft. The next reflection from a depth of 1,170 ft below the sea bottom, indicates an average veolcity of 5,460 ft/sec for the overlying sediment. This prominent reflector is found on all the deep-sea profiles examined to date, and the geological and geophysical significance of this discontinuity in the sediment column is an interesting question. The observed data points diverge noticeably from the theoretical curves beyond 30,000 yards; this is indicative of the fact that the overlying sediment has a varying rather than a constant velocity. Further, the fact that this sub-bottom reflection has not crossed the bottom reflection at grazing incidence indicates that the sediment velocity just below the ocean bottom must be lower than that of the overlying ocean water. The curve fitting the third reflection group is the multiple of the second.

The fourth reflection, from 3,350 ft below the bottom, indicates an average

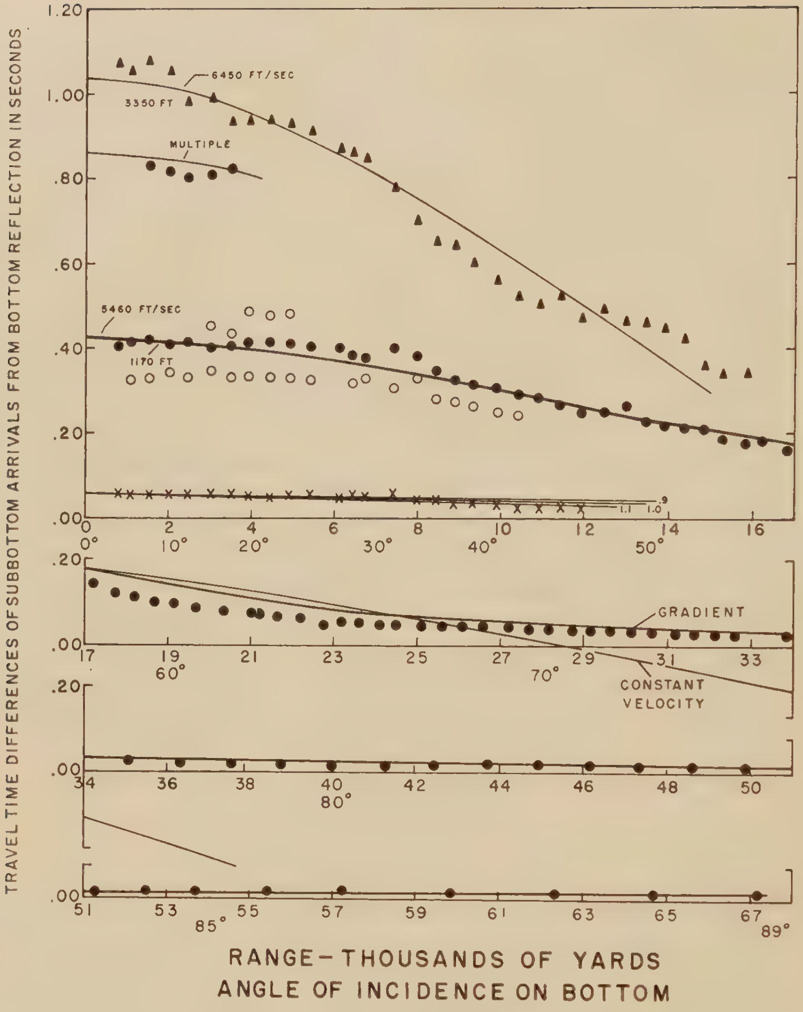

Fig. 6. Travel time graphs of subbottom reflections. Different symbols indicate times for various events correlated across parts or all of profile.

velocity from the ocean bottom to this depth of 6,450 ft/sec or an interval velocity from the depth of the second reflection to this depth of 7,150 ft/sec. This reflecting horizon is near the bottom of the sedimentary column, as determined from adjacent refraction profiles. Ewing, Sutton, and Officer (1954) report data from two refraction profiles in the same vicinity (Fig. 1): station 27 gave 3,950 ft of sediments and station 28 gave 4,300 ft.

The refraction measurements, such as those at stations 27 and 28, have all shown a high velocity basement underneath the sedimentary column in the deep ocean basins. The velocity of this basement material is characteristic of basaltic rocks. The reflection profile measurements demonstrate that almost the entire sedimentary column is of low-velocity material and must be for the most part unconsolidated. It would be interesting to have an age scale through this column.

DISPERSIVE SEDIMENT—LOW VELOCITY CONTRAST

One of the most interesting conclusions arrived at from this profile is the discovery that the deep-sea sediment is dispersive and, further, that at low frequencies the velocity in the sediment just below the bottom is lower than that in the ocean water just above the bottom. To begin, let us consider the theory of propagation in a gross mixture of sediment particles and water. For the static case, the velocity of propagation can be derived directly from fundamental principles (Heiland, 1940, pp. 474–475; Urick, 1947; and Chambré, 1954) and it can be written in the form

$$C_s = \sqrt{\frac{1}{(fm + f_1 m_1)(f\rho + f_1\rho_1)}}, \tag{1}$$

where f and f_1 are the respective volume fractions of water and sediment particles, m and m_1 are the compressibilities, and ρ and ρ_1 are the densities. The porosity of the sediment is f. m_1 is generally much smaller than m, whereas ρ_1 and ρ are of comparable size. Thus as the sediment mixture is built up, say from 100 percent water, the effect of adding sediment particles is first to load the mixture, therefore decreasing its sound velocity. As the porosity decreases, the effect of the compressibility term becomes important; and the velocity begins to increase. A hypothetical case is shown in Figure 7. The velocity contrast of sediment-mixture to water is plotted against porosity. At high porosity values of 0.7–0.8, the velocity of sound in the sediment can be as low as 0.97 that in water. Measurements of the porosity of deep-sea sediment by Kullenberg (private communication) give values ranging from 0.65 to 0.85. The porosity is generally high, and it is higher for the finer sediments, so that from theory alone one would expect that the velocity of sound propagation in deep-sea sediments should be lower than that in water.

For the dynamic case, one must introduce permeability, or viscosity, to account for the resisting effect of the water motion in the matrix of sediment particles. As the frequency is increased, the sediment begins to act more as a rigid body; and the velocity of sound propagation through it increases. Morse (1951) and Ament (1953) have derived an approximate theory for the dynamic case, and on the basis of Ament's treatment the velocity and absorption coefficient can be written in the following form for low frequencies:

$$C = C_s\left(1 + F^2 \frac{8\pi^2 f f_1 r^4 (\rho_1 - \rho)^2 (f\rho_1 + f_1\rho)}{81\eta^2\rho_s}\right) \tag{2}$$

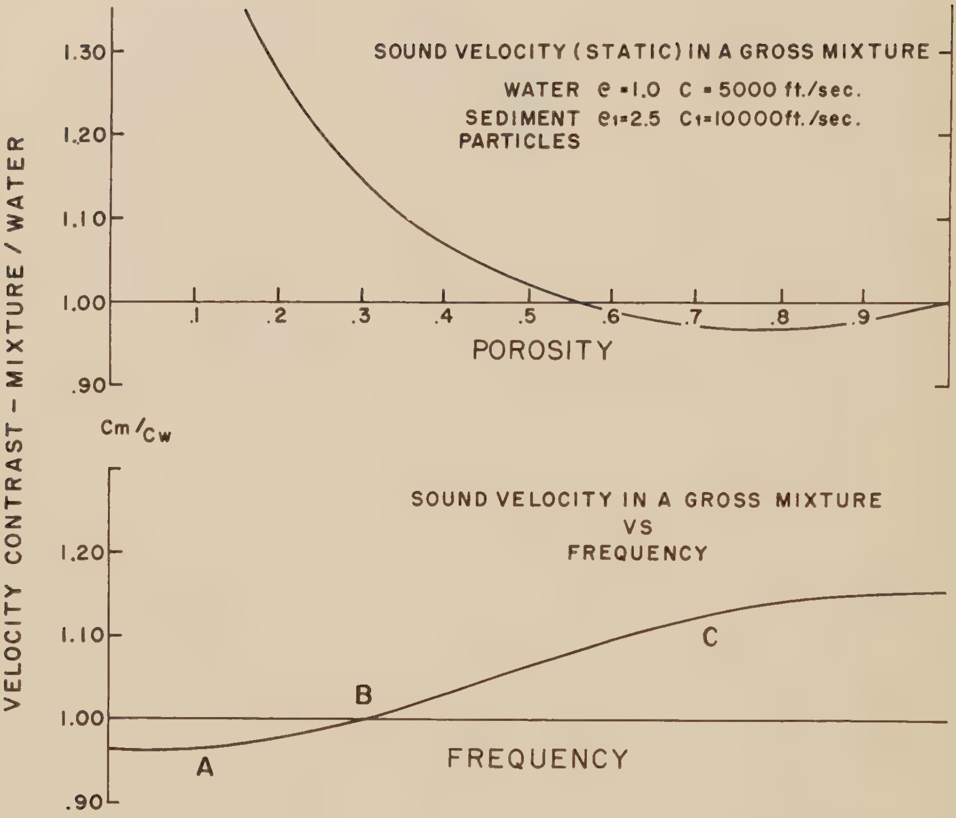

FIG. 7. Sound velocity as a function of porosity and frequency in sedimentary materials.

and

$$\beta = F^2 \frac{4\pi^2 f f_1 r^2 (\rho_1 - \rho)^2}{9\eta \rho_s C_s}, \tag{3}$$

where C and C_s are the dynamic and static velocities; ρ_s is the static density, $f\rho + f_1\rho_1$; F is the frequency in cps; β the absorption coefficient; η the viscosity; and γ the radius of the sediment particles. It is difficult to specify numbers for γ and η. The curve for equation (2) shown in the lower portion of Figure 7 has been drawn for an unspecified frequency scale. The radii of deep-sea sediment particles range from less than 1 micron to greater than 100 microns; Revelle (1944) has an excellent tabulation of these radii for Pacific deep-sea samples. To the author's knowledge, no values have been published for the viscosity or permeability of deep-sea sediments. For the case of a radius of 5 microns and a viscosity of 10^{-1} cgs units the velocity contrast would become greater than 1.0

at 2,700 cps; this is a higher frequency than is observed on our profile. The absorption would be 0.3 db per thousand yards at 100 cps and 30 db at 1,000 cps.

There are three ways in which a sediment with these properties should be observed from a deep-sea reflection profile. First, the energy reflected from the ocean bottom as a function of the angle of incidence should show a marked change from low frequencies, at which the bottom shows a low velocity contrast, to high frequencies, at which the bottom shows a high velocity contrast. The first-order theory for reflectivity can be taken from the Rayleigh reflection law. For sound reflected from a dicontinuity across which there is an increase in velocity, the reflectivity will increase from normal incidence to a value of unity at an intermediate angle, the critical angle. For angles of incidence greater than this the reflectivity remains unity. For sound reflected from a discontinuity across which there is a decrease in velocity, the reflectivity will decrease from normal incidence to zero at nearly grazing incidence. The reflectivity then rises rapidly to unity. Thus for frequencies in the range *A* of Figure 7, the reflectivity should decrease with angle of incidence and for frequencies in the range *C* it should increase to a critical angle. This is strikingly evident on the records of Figures 4 and 5. At the low frequencies, 75–150 cps, the bottom reflected energy decreases with range to a faintly observable level at the long ranges. At the high frequencies, 500–1,000 cps, the bottom reflectivity does indeed increase from normal to critical-angle incidence and remains uniform for increasing angles.

Second, for a dispersive sediment the travel times of the sub-bottom reflections should be a function of frequency. This can be seen on the records of Figure 4, particularly at the longer ranges; the higher frequencies of the prominent sub-bottom reflection arrive earlier.

Third, the travel times observed from the reflection profile should demonstrate that there is a low-velocity contrast. In fitting a constant velocity to the prominent second reflection group it was observed that there was poor agreement at the longer ranges, indicating that there must be a gradient in the sediment; moreover, since the sub-bottom reflection had not crossed the bottom reflection at grazing incidence, the velocity in the sediment near the ocean bottom must be lower than that in the adjacent ocean. Consideration of the sound-velocity structure in the ocean alone will not resolve this discrepancy.

Of the simple velocity gradients which might be used for calculation, a parabolic gradient was chosen *a priori*. The velocity at the top of the sedimentary column was chosen to be 0.97 times that of the water at the sea bottom, or 4,920 ft/sec. The gradient was calculated from the observation at close ranges that the average vertical velocity to the horizon at 1,170 ft below the bottom was 5,460 ft/ sec. The final equation is

$$v = 4{,}920(1 + 4.17 \times 10^{-4} z)^{1/2}, \tag{4}$$

where v is the velocity in ft/sec and z the depth in ft below the bottom. The velocity at the bottom of the column would be 6,000 ft/sec. This velocity gradient gave a good fit to the data over the entire range of reception. The reflection becomes a refraction at a range of about 10,000 yards and at ranges beyond 40,000 yards it is penetrating 250 ft or less of the sediment. The porosity can be computed as a function of depth from equations (4) and (1), and it is plotted along with the sound velocity section of Figure 8; this curve should give the correct order of magnitude of the decrease of porosity with depth but it cannot give the exact shape of the curve or reliable values of porosity at a particular depth. Hill (1952) recorded this sub-bottom refraction at intermediate ranges on a series of seismic refraction profiles in deep water off the coast of Ireland. He concluded as here, that the arrival was a refraction in the sediment. His measurements were taken at low frequencies, and he did not record the bottom reflection itself.

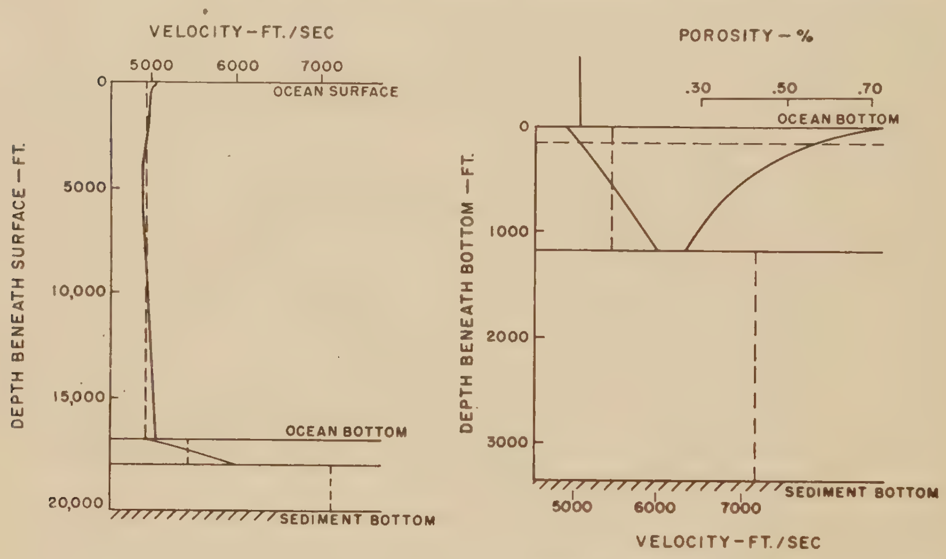

FIG. 8. Sound velocity and porosity sections.

All three of these observations form a clear geophysical demonstration that the deep-sea sediment is dispersive and that its upper portion has a velocity lower than that in water.

WAVE GUIDE—LOW VELOCITY LAYER

In one of the early deep sea seismic refraction measurements, Hersey, Officer, Johnson, and Bergstrom (1952) reported a single-frequency forerunner which appeared beyond the range at which the first bottom reflection arrival should be received. At this range, the first bottom reflection becomes a refraction at depth in the ocean, following the path of the RSR rays of Ewing and Worzel (1948); at greater ranges it is transmitted by leakage from the surface sound channel and RSR paths. From its travel time plot, the single-frequency forerunner was interpreted as a wave which travelled over a portion of its path near the ocean bottom, travelling to and from the bottom by the RSR path which was grazing at the bottom. It was not possible to state from the physical data then available whether the wave travelled in the bottom water or in the sediment, but it was felt that in order for such an arrival to exist and to have the single frequency characteristic, there must be trapping of energy near the bottom in a wave guide. Such trapping would take place by a coupling process such as that proposed by Lamb (1932, p. 413–415) and extended by Press and Ewing (1951) and Jardetsky and Press (1952) to particular geophysical cases. According to this mechanism, a disturbance travelling across a boundary in an extended medium, the ocean, will couple to a low-velocity layer, the sediment, at the frequency for which the phase velocity in the sediment is equal to the velocity of sound in the extended medium. This will give reinforcement at all points on the boundary.

Subsequently Katz and Ewing (unpublished manuscript) observed the same phenomenon and arrived at the same conclusion. They were able to show that the frequency is determined by local conditions and that it is not related to the depth of water. Assuming a low-velocity section in the sediment, for which they had indirect evidence from shallow water measurements by others, they showed that the thickness of this section varied from 50 ft to 150 ft over the range of observed forerunner frequencies, which was from 30 to 100 cps. The velocity contrast for the section was taken to be 0.98.

In the results reported in this paper, we have *direct* evidence that there is a low-velocity sedimentary layer, which should be excited as a coupled wave guide for ranges beyond which the RSR ray travels across its surface at grazing incidence. The thickness of the low-velocity section as computed from the frequencies of the coupled wave is in agreement with that indicated in Figure 8 on the basis of the seismic reflection profile.

ACKNOWLEDGMENTS

The author wishes to express his thanks to Dr. J. B. Hersey for cooperation and helpful discussions during this investigation, to Messrs. Johnson, Bergstrom, and Duys and Drs. Dietz and Wheeler for their cooperation in the scientific work at sea, and to Capts. Bray and Karlson and the crews of the research vessels *Atlantis* and *Caryn*. This work was done under contract Nobsr 43270 with the Bureau of Ships, U. S. Navy.

REFERENCES

Ament, W. S., 1953, Sound propagation in gross mixtures: J. Acoust. Soc. Am., v. 25, p. 638–641.

Chambré, P. L., 1954, Speed of a plane wave in a gross mixture, J. Acoust. Soc. Am., v. 26, p. 329–331.

Ewing, M., and Worzel, J. L., 1948, Long range sound transmission, *in* Propagation of sound in the ocean: Geol. Soc. Am. Memoir 27.

Ewing, M., Sutton, G. H., and Officer, C. B., 1954, Seismic refraction measurements in the Atlantic ocean, Part VI. Typical deep profiles: Bull Seis. Soc. Am., v. 44, p. 21–38.

Heiland, C. A., 1940, Geophysical exploration: New York, Prentice-Hall Publ. Co.

Hersey, J. B., and Ewing, M., 1949, Seismic reflections from beneath the ocean floor: Trans. A.G.U., v. 30, p. 5–14.

Hersey, J. B., Officer, C. B., Johnson, H. R., and Bergstrom, S., 1952, Seismic refraction measurements north of the Brownson Deep: Bull. Seis. Soc. Am., v. 42, p. 291–306.

Hill, M. N., 1952, Seismic refraction shooting in an area of the eastern Atlantic: Phil. Trans. Roy. Soc. London, A, v. 244, p. 561–569.

Katz, S., and Ewing, M., unpublished manuscript, Seismic refraction measurements in the Atlantic Ocean.

Jardetsky, W. S., and Press, F., 1952, Rayleigh wave coupling to atmospheric compression waves: Bull. Seis. Soc. Am., v. 42, p. 135–144.

Lamb, H., 1932, Hydrodynamics, sixth edition: New York, Dover Publ.

Morse, R. W., 1951, Acoustical propagation in granular media: J. Acoust. Soc. Am., v. 24, p. 696–700.

Press, F., and Ewing, M., 1951, Theory of air-coupled flexural waves: J. Appl. Phys., v. 22, p. 892–899.

Revelle, R. R., 1944, Marine bottom samples collected in the Pacific Ocean by the Carnegie on its seventh cruise, Scientific Results of Cruise 7 of the Carnegie: Oceanography, v. 2, Carnegie Inst. of Wash. Publication 556.

Urick, R. J., 1947, A sound velocity method for determining the compressibility of finely divided suspensions: J. Appl. Phys., v. 18, p. 983–987.

Weibull, W., 1947, The thickness of ocean sediments measured by a reflection method: Med. Oceanograf. Inst., Goteborg, Goteborg Kungl, Vetenskaps—Och Vitterhets—Samhalles Handlingas, Siatte Foljden, B, v. 5, p. 1–17.

Contribution No. 732

Bulletin of the Museum of Comparative Zoology
AT HARVARD COLLEGE
Vol. 113, No.2

OCCURRENCE OFF THE MIDDLE AND NORTH ATLANTIC UNITED STATES OF THE OFFSHORE HAKE *MERLUCCIUS ALBIDUS* (MITCHILL) 1818, AND OF THE BLUE WHITING *GADUS* (*MICROMESISTIUS*) *POUTASSOU* (RISSO) 1826

BY HENRY B. BIGELOW AND WILLIAM C. SCHROEDER

Museum of Comparative Zoology and
Woods Hole Oceanographic Institution

CAMBRIDGE, MASS., U.S.A.
PRINTED FOR THE MUSEUM
April, 1955

No. 2.—*Occurrence off the Middle and North Atlantic United States of the Offshore Hake Merluccius albidus (Mitchill) 1818, and of the Blue Whiting Gadus (Micromesistius) poutassou (Risso) 1826*[1]

By Henry B. Bigelow and William C. Schroeder

INTRODUCTION

Among the more interesting of the bony fishes trawled by the dragger "Cap'n Bill II," from the Woods Hole Oceanographic Institution, in deep water between the offings of Virginia and of middle Nova Scotia in 1952 and 1953 (Bigelow and Schroeder, 1954, p. 39), were many specimens of the western Atlantic representative of the European silver hake *Merluccius merluccius,* recently described by Ginsburg (1954, p. 192) under the specific name *albidus* Mitchill 1818, and four specimens of the blue whiting *Gadus* (*Micromesistius*) *poutassou* (Risso) 1826, which has not been reported before from the western side of the Atlantic.

OFFSHORE HAKE

Merluccius[2] albidus (Mitchill) 1818

It had been taken for granted, until very recently, that the hordes of silver hake or whiting inhabiting the continental waters of the western Atlantic from New Jersey to the outer coast of Nova Scotia all belonged to the one species *Merluccius bilinearis* (Mitchill) 1814. But it has developed, of late, that the *Merluccius* populations over the outer part of the continental shelf, and along the upper belt of the continental slope also include a second member of the genus that is more nearly related to the hake of northern European seas (*Merluccius merluccius* Linnaeus 1758), but differing sufficiently from the latter to deserve recognition as a separate species.

Our own first hint of this was the discovery that the sample that was retained from the "Cap'n Bill II" trawlings of 1952 fell into two categories, the one with the numbers of anal fin rays (39-41), of scales (103-110), and of gill rakers (16-20) that characterize *M. bilinearis*, the other group with fewer anal

[1] Contribution No. 732 from the Woods Hole Oceanographic Institution.

[2] The so-called silver hakes have been referred for many years to the genus *Merluccius* of Rafinesque 1810. According to Whitley (1948, p. 83) this name is equivalent to *Merlangius* Geoffroy 1767 (vol. 5, p. 401, pl. 661), hence should be replaced by the latter. But the heading to Geoffroy's description of his *Merlangius* included only this one name; i.e. it was not binomial. And in any case his illustration of it, showing three separate dorsal fins, seems to have been of the European whiting *Gadus merlangus* Linnaeus 1758. Indeed, the caption ("Merlangius, Merlan") indicates as much, for merlan is the common French name for that fish. We owe to the library of the Arnold Arboretum our opportunity to consult Geoffroy's work.

rays (36-39), and fewer (9-11) gill rakers (Fig. 1), but a larger number of scales (132-148) as is the case in *M. merluccius*. Armed with this knowledge, the 2962 silver hakes that were taken in 1953 were examined in these respects, with the result that while 535 of them proved to be typical *bilinearis*, 2427 of them yielded the counts that had been credited to *M. merluccius* in published accounts of the latter. And comparison between these "Cap'n Bill II" specimens and 20 *M. merluccius*, 360-595 mm. long (14 of them from Plymouth, England, 6 of them from Portugal, received through the kindness of Dr. F. S. Russell and Dr. A. M. Ramalho) has confirmed their unity in these respects.

This result is in line with Ginsburg's (1954) recent announcement that the U. S. National Museum's collection of silver hakes from the east coast of the United States — presumably all *M. bilinearis* — also includes representatives of a second form that resembles *M. merluccius* more closely than it resembles *bilinearis*, and which (from his excellent account) we judge to be identical with the "Cap'n Bill II" series of *M. merluccius* affinity.

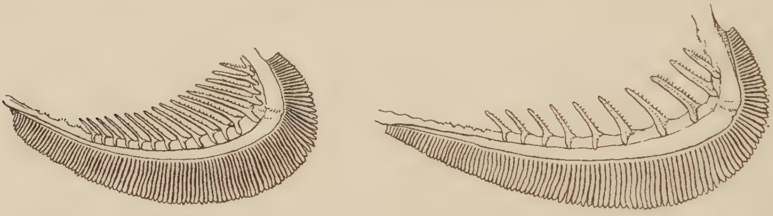

Fig. 1. Right, first gill arch from *Merluccius albidus* 368 mm. long, and left, from *Merluccius bilinearis* 331 mm. long, about 0.9x.

Ginsburg described this hake as a species distinct from *M. merluccius* under the name *albidus* Mitchill 1818, with pectoral fins consistently a little longer, number of 1st dorsal fin rays ranging larger by about one, and number of scales ranging lower in the western Atlantic population than in the eastern Atlantic (for details, see Tables I, II, also Ginsburg, 1954, p. 193). These differences justify his specific separation of the one from the other. We refer the reader to Ginsburg, 1954, page 194 [1] for the reasons for applying the old name *albidus* to the western Atlantic form, in preference to coining a new specific name for it.

---

[1] The early nomenclatural history of the genus *Merluccius* in northeastern American waters is a confused one.

TABLE I. *Merluccius merluccius* and *M. albidus*

Species Locality		*M. merluccius* Plymouth, England	*M. merluccius* Lisbon, Portugal	*M. albidus* off New England
Number of specimens		14[1]	6[2]	14
Total length	mm.	277-595	353-363	300-590
Standard length	mm.	249-540	318-327	272-539
Eye, horizontal	percent of head	13.8-19.9	18.4-20.7	17.7-21.0
Snout	percent of head	31.1-40.2	30.3-33.7	28.2-36.3
Head	percent of S.L.	26.5-30.3	27.6-29.8	27.5-30.3
1st dorsal, base	percent of S.L.	8.7-10.5	8.9-10.2	9.1-12.3
Pectoral, length	percent of S.L.	15.9-17.6	15.7-17.6	17.6-21.2
Pelvic, length	percent of S.L.	13.7-17.0	15.0-16.5	12.1-17.6
1st dorsal, rays	number	9-11	9-10	11-12
2nd dorsal, rays	number	37-40	37-39	36-40
Anal, rays	number	36-39	36-39	36-39
Pectoral rays	number	14-15	14-15	14-15
Pelvic rays	number	7	7	7
Scales	number	152-170	163-180	132-148
Gill rakers, 1st arch	number	9-11	9-11	9-11
Gill rakers, longest	percent of eye length	40.7-57.0	35.8-47.0	41.4-54.5

[1] Kindly contributed by Dr. F. S. Russell.
[2] Kindly contributed by Dr. A. M. Ramalho.

The "Cap'n Bill II" specimens of *albidus* were from 4 to 28 inches in total length, thus covering the range from yearlings to adults perhaps 9-10 years old, if their rate of growth is about the same as it is for *M. merluccius* off Ireland (Belloc, 1929). And the presence of ovaries nearing ripeness in large females of *albidus* taken off Virginia, off Long Island, New York, and off Martha's Vineyard, June 26 and 29, 1953 and July 7, 1954,

TABLE II

1st dorsal rays, Number	*M. merluccius* Specimens	*M. albidus* Specimens
9	6	
10	13	
11	1	8
12		6
Pectoral rays, Number	Specimens	Specimens
14	18	2
15	2	12
Scales Number	Specimens	Specimens
131-140		10
141-150		4
151-160	6	
161-170	11	
171-180	3	
Pectoral length in percent of S.L.	Specimens	Specimens
15.7-16.0	3	
16.1-17.0	13	
17.1-18.0	4	3
18.1-19.0		1
19.1-20.0		4
20.1-21.0		5
21.1-21.2		1

is evidence that the large adults, at least, are midsummer spawners. The stomach contents of the specimens opened consisted chiefly of black pelagic fishes, mostly myctophids, with snipe eels (*Nemichthys*) and squids. And many myctophids were disgorged by the larger of the hakes, enough in fact on one occasion to make the deck slippery. Thus their feeding habits correspond to those of the European *M. merluccius* (p. 212).

The 37 stations where ''Cap'n Bill II'' took *albidus* in the summer of 1953 were distributed from the southeastern slope of Georges Bank (Lat. 40°46′N; Long. 66°48′W) to the most southerly haul off Virginia (Lat. 37°38′N, Long. 74°15′W) without evident concentration within any particular sector. And in the summer of 1954 it was taken by ''Atlantis'' at 10 stations between Lat. 40°47′N, Long. 66°40′W and Lat. 39°54′N, Long. 70°47′W. This is in line with Ginsburg's (1954, p. 193) published report of *albidus* from various localities between the southwestern part of Georges Bank and the offing of Cape Henry, Virginia (Fig. 2). The list of localities whence it is represented in the collection of the U. S. National Museum (information contributed by letter from Dr. Ginsburg) also includes the offings of Savannah, Georgia, and Cape Canaveral, Florida. And a probable record from Tortugas, Florida, (Ginsburg 1954, p. 193) suggests that its geographic range is continuous around Florida with that of the new species *magnoculus* recently described by Ginsburg (1954, p. 194) from the Gulf of Mexico. We suspect, however, that the center of population for *albidus* lies off the middle Atlantic coast, for silver hakes of whichever species are not caught in commercial quantities south of Chesapeake Bay; very few in fact, southward beyond New Jersey (landings, 1951: New England 118,466,000 pounds; New York 684,000 pounds; New Jersey 897,000 pounds; Maryland 11,200 pounds; Virginia 17,200 pounds).

Failure to pick up even a single *albidus* in any of the successful hauls that were made by ''Cap'n Bill II'' at appropriate depths along the Nova Scotian shelf and slope in 1953, though 5 hauls did take a few *bilinearis*, suggests that *albidus* did not range eastward beyond Georges Bank at the time. And even if it should prove to occur as far as the Newfoundland Banks in that direction, as *bilinearis* does, the geographic range of *M. albidus* in the

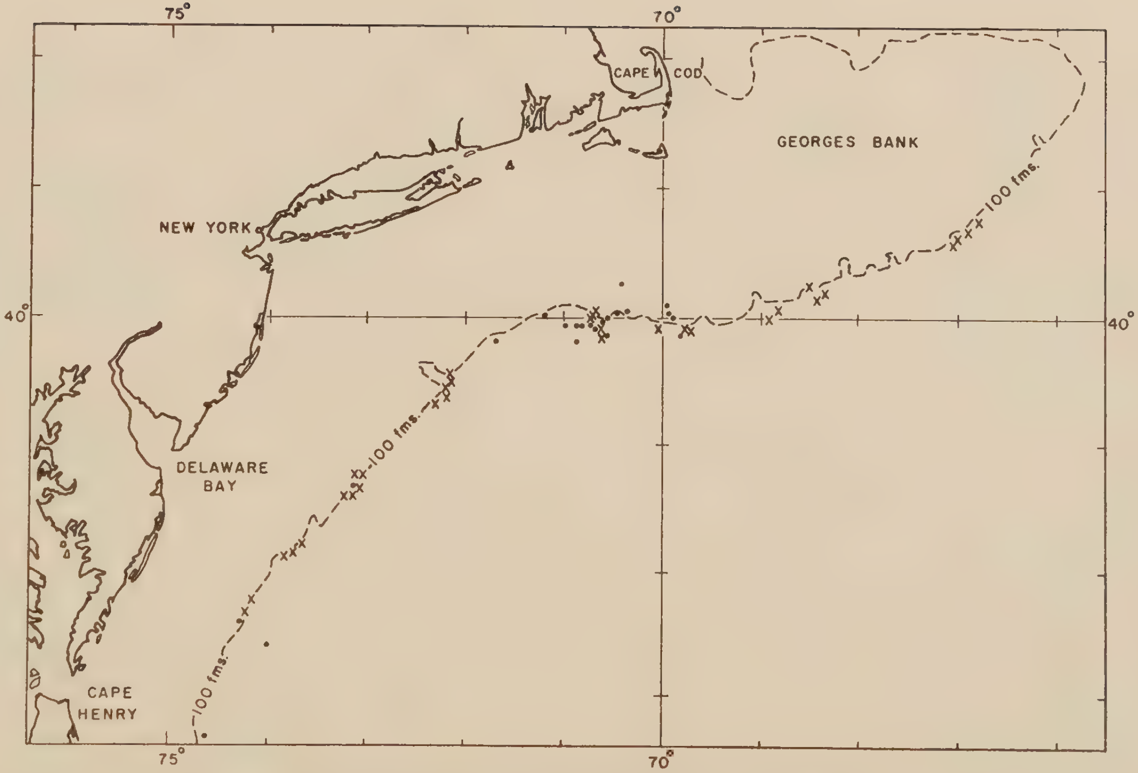
75°
70°
40°
40°
75°
70°
CAPE COD
GEORGES BANK
100 fms.
NEW YORK
DELAWARE BAY
100 fms.
100 fms.
CAPE HENRY

Fig. 2. Localities (●) whence *Merluccius albidus* is represented in the U. S. National Museum from north of Cape Hatteras (information contributed by Dr. Isaac Ginsburg), and (x) where it was taken by "Cap'n Bill II" in 1953.

one side of the Atlantic, and of *M. merluccius* in the other would still be separated by a gap somewhere near 1400 miles wide, for old reports of the genus off southwestern Greenland are not reliable (Täning, 1938, footnote).

The "Cap'n Bill II" captures, and the earlier locality records as well, were scattered along the outer part of the continental shelf and upper part of the continental slope. Along this zone *albidus* intermingles with the offshore fringe of the population of *M. bilinearis* — the two were taken side by side repeatedly by "Cap'n Bill II" — and it greatly outnumbered *bilinearis* there at the time of the "Cap'n Bill II" cruises as appears from the relative numbers of the two species that were taken (p. 206). It was also more generally distributed than *bilinearis*, to judge from the capture of *albidus* in 47 hauls in 1953 and 1954, but of *bilinearis* in 32 hauls only.

Ginsburg (1954, p. 193) has reported *M. albidus* off Long Island, New York from 58-67 fathoms, also from 317 fathoms (depth of capture of the specimen selected by him as neotype of the species), and the National Museum series includes a record on the southwestern slope of Georges Bank (Lat. 40°01′N, Long. 68°56′W) from as deep as 640 fathoms (information contributed by letter from Dr. Ginsburg). The shoalest "Cap'n Bill II" haul that yielded it was at 50-55 fathoms (shoalest haul made, off Delaware Bay), the deepest was at 545-600 fathoms, the relationship between numbers taken and depth being as follows:

TABLE III

Numbers of *M. albidus* taken at different depths in 1953

Depth in fathoms	No. hauls with *albidus*	Total specimens	Specimens per haul	Average number per haul
50-100	5	27	1–16	5.4
101-200	14	1165	2–220	83.3
201-300[1]	10	1034	48–270	103.4
301-400	6	178	1–84	29.7
401-500	1	1	1	1
501-600	1	22	22	22

[1] One haul working between 250 and 340 fathoms yielded 58 specimens.

TABLE IV

Generality of distribution of *M. albidus,* versus depth, west of Longitude 66°40′W

Depth in fathoms	No. hauls with *albidus*	Total no. hauls	% with *albidus*
50-100	5	14	35.7
101-200	14	14	100.
201-300	10	10	100.
301-400	6	8	75.
401-500	1	6	16.7
501-600	1	6	16.7

The hauls that took it were all made during the daytime. Hence, from analogy, it seems safe to assume that most of the specimens (if not all of them) were on the bottom when picked up, or very close to it, for European experience is that its close relative *M. merluccius* keeps to the bottom by day, to rise in the water by night in pursuit of the mid-water fishes and squids on which they feed (Hickling, 1927, pp. 78-79; Täning, 1938).

Evidently the center of population for *M. albidus* lies between the 100 fathom and the 300 fathom depth zone. And the "Cap'n Bill II" catches suggest some concentration at about 150-225 fathoms, for the 3 hauls that yielded more than 200 specimens each were at 150 fathoms, at 150-155 fathoms, and at 225 fathoms. This parallels the vertical distribution of *M. merluccius* in north European seas, where it is reported as most frequent between 55 and 275 fathoms (100-500 meters, Belloc, 1929, p. 178), most of the stock wintering deeper than 100 fathoms, but many of them making incursions into water as shoal as 40-60 fathoms in summer (Hickling, 1927), the adults in connection with spawning, the young in pursuit of the smaller fishes on which they prey. The "Cap'n Bill II" catch of 22 *albidus* in a haul working at 545-600 fathoms, and the earlier capture of the species from 640 fathoms (Fish Hawk Sta. 1124; see above), are a little deeper than the greatest depth to which *M. merluccius* has been reported definitely in the eastern side of the Atlantic — 440-550 fathoms (800-1000 meters) according to Belloc (1929, p. 178).

It is interesting, in passing, that while the closely allied *M. bilinearis* comes so close inshore that great numbers are taken in pound nets, the center of abundance for the offshore fringe of the population of *bilinearis* was at about the same depth as for *M. albidus,* i.e. at 100-300 fathoms, as illustrated by Table V.

TABLE V

Numbers of *M. bilinearis* taken at different depths in 1953

Depth in fathoms	No. hauls with *bilinearis*	Total specimens	Specimens per haul	Average no. per haul
50-100	10	47	1-15	4.7
101-200	7	250	1-88	35.7
201-300	6	235	1-100	39.2
301-400	0	0	0	0
401-500	1	3		3

The eight stations where *albidus* was taken shoaler than 100 fathoms in 1953 and 1954 were off Delaware Bay (1 specimen, 50-55 fathoms; 16 specimens, 95-100 fathoms) ; off Long Island, New York (5 specimens, 81-83 fathoms) ; off Martha's Vineyard (1, 1, 1 and 2 specimens at 80-93 fathoms, 75 fathoms, 70-72 fathoms and 70 fathoms respectively) and on the southwestern slope of Georges Bank (4 specimens, 85-92 fathoms) ; 2 specimens were also taken at 100-105 fathoms on the southeastern slope of Georges. Thus it seems as likely to come into shoal water off one part of the coast as another.

These records do not locate the upper limit to its vertical range for the shoalest haul that yielded it (50-55 fathoms, 1 specimen) was the shoalest of the series. But we think it unlikely that it comes nearer to the land than the 70-80 fathom line with any frequency, or in any numbers, partly for the reason that the numbers taken per haul at depths down to 100 fathoms were so small, but chiefly because its presence off the Atlantic coast of the United States could hardly have been overlooked until so recently, if it came close inshore there in numbers at all rivaling those of *M. bilinearis.*

Location of the usual inshore boundary for *albidus* as somewhere between the 55 and 75 fathom lines implies at the same time that strays only are to be expected closer to the coast than perhaps 50-60 miles anywhere, between the offings of Delaware Bay and of Martha's Vineyard, or between about 90 miles and 180 miles out from the nearest land along the seaward slope of Georges Bank, depending on locality.

An interesting question for the future is whether *M. albidus* ever enters the Gulf of Maine along the bottom of the channel between Georges and Browns Banks, to form a part of the plentiful population of silver hakes that we trawled at depths greater than 65 fathoms in the inner parts of the Gulf in the summer of 1936, i.e. before the possibility was foreseen that two species might be in question, not *bilinearis* alone (Bigelow and Schroeder, 1939, p. 308, Table I).

Our only indications as to the offshore boundary to the range of *M. albidus* are that 22 specimens were taken in the haul that was made the farthest out on the slope, at 545-600 fathoms in 1953 and that the "Fish Hawk" took it at 640 fathoms on the southwestern slope of Georges Bank in 1882 (see above). These depths agree so closely with the maximum recorded for *M. merluccius* in the other side of the Atlantic (p. 212), as to make it unlikely that *albidus* ranges much farther seaward, provided that a wholly pelagic mode of life is not more characteristic of *albidus* than of *M. merluccius,* which regularly seeks the bottom in daytime (p. 212). If this be the case, the breadth of the geographic range of *albidus* is only some 10 to 15 miles at most, anywhere between the offing of Virginia, and the southeastern slope of Georges Bank. And even if it does occur within the Gulf of Maine, the contrast is striking between the breadth of the belt populated by *albidus* in the western side of the Atlantic, and of *M. merluccius* in the eastern, where the range of this hake extends from the mouth of the Baltic to southwestern Iceland in the north, and from the eastern part of the Mediterranean to the continental slope off Gibraltar in the south.

If the range of *albidus* is no more extensive in reality than suggested above, it seems a safe assumption that its total population is much smaller than that of the eastern Atlantic *M. merluccius,* the total catch of which for 1947 (most recent year of record) was about 409,163,270 pounds (185,187 thousands of kilos, see Rosén, 1951, p. 16), shared among Norway, Sweden, Germany, Denmark, Holland, Belgium, Scotland, England, Ireland, France, Portugal and Spain. This was about 81 per cent as great as the north European catch of haddock, and about 5 times as great as the catch of *M. bilinearis* landed along the middle and north Atlantic coasts of the United States in that same year.

The temperatures at which *M. albidus* was taken in 1953 ranged from 53° down to 38-39°, with the great majority of the catch made at 40.5-52°, as follows:

TABLE VI

Bottom temperatures at stations where *M. albidus* was taken in 1953

Depth in fathoms	Temperature
70-110	53°-49.3°
110-200	52°-42.4°
205-300	42°-39.2°
300-400	40.5°-39°
420-600	39°-38°

A final point of interest is that the distributional status of *albidus* proved about the same for the summer of 1953 as it had been in the 1880's (Fig. 2).

BLUE WHITING

GADUS (subgen. MICROMESISTIUS) POUTASSOU (Risso) 1826

Goode and Bean, writing in 1895 (1895, p. 355), thought it probable that this wide ranging eastern Atlantic member of the cod tribe would "yet be found among the captures of the cod schooners of the offshore banks" off New England. And their forecast has been verified at last, for "Cap'n Bill II" trawled one specimen, about 355 mm. in standard length, on the seaward slope of Georges Bank, Lat. 40°18′N, Long. 68°01′W, at 230-250 fathoms, July 15, 1952, and three others, 349 mm. to 416 mm. long, at 240-280 fathoms on the slope of Browns Bank, between Lat. 42°09′ N, Long. 65°21′W, and Lat. 42°08′N, Long. 65°27′W, July 16,

TABLE VII. Blue Whiting of Western and Eastern Atlantic

Specimen no.		1	2	3	4	5	6	7	8
Total length	mm.	349	380	387	416	243	289	291	427
Standard length	mm.	322	347	357	388	224	271	270	401
Eye, horizontal	Percent of head	27.3	24.4	26.1	24.2	28.4	29.4	26.6	24.0
Body, depth	Percent S.L.	13.7	16.8	18.2	16.7	14.7	15.5	14.1	15.5
Head	Percent S.L.	**23.9**	**23.8**	**24.4**	**23.9**	**26.8**	**25.1**	**25.7**	**25.0**
Snout to 1st dorsal	Percent S.L.	33.5	36.3	35.9	35.3	37.1	36.5	35.9	37.3
1st, 2nd dorsals, interspace	Percent S.L.	6.8	7.6	7.1	6.4	5.4	6.3	6.5	8.2
2nd, 3rd dorsals, interspace	Percent S.L.	12.4	15.1	14.7	14.3	13.8	11.4	14.8	12.8
1st, 2nd anals, interspace	Percent S.L.	2.2	2.9	1.4	2.6	2.7	1.5	1.9	2.3
Pectoral, length	Percent S.L.	14.9	14.8	15.0	15.2	15.6	14.7	13.7	12.2
Pelvic, length	Percent S.L.	7.5	6.5	8.5	6.4	8.0	6.3	6.7	5.6
1st dorsal, rays	Number	11	11	12	13	12	13	12	12
2nd dorsal, rays	Number	11	12	11	13	11	13	14	12
3rd dorsal, rays	Number	**24**	**23**	**24**	**24**	**22**	**23**	**25**	**24**
1st anal, rays	Number	37	33	36	35	36	39	36	34
2nd anal, rays	Number	**26**	**25**	**25**	**25**	**22**	**23**	**23**	**26**
Scales	Number	166	181	180	174	170	166	163	167
Gill rakers	Number	5+25	5+24	5+23	5+24	5+23	5+22	5+23	5+23
Pectoral, rays	Number	20	21	21	22	19	21	20	18
Pelvic, rays	Number	6	6	6	6	6	6	6	6
Pyloric caeca	Number	11	9	9	8	a)	a)	a)	10

Specimens Nos. 1 and 4 are from Lat. 42°09′N, Long. 65°21′W, 240-280 fathoms, July 16, 1953; specimen 2 is from Lat. 40°18′N, Long. 68°01′W, 230-250 fathoms, July 15, 1952; specimen 3 is from Lat 42°08′N, Long. 65°27′W, 250-280 fathoms, July 16, 1953; specimen 5 is from off Nice, France; specimens 6 and 8 are from Bergen, Norway; specimen 7 is from Christiania, Norway, these latter four all taken many years ago.

a) The viscera were in such condition that the pyloric caeca either could not be recognized or counted with accuracy.

1953. These have been compared with a *poutassou* about 224 mm. in standard length in the Museum of Comparative Zoology from Nice, France, and 3 others 270 to 401 mm. long, from Bergen and Christiania, Norway, in the U. S. National Museum, loaned to us through the kindness of Dr. Leonard Schultz. The illustration (Fig. 3) and the preceding table (VII) are added so that the reader may judge, first-hand, as to the correctness of our identification:

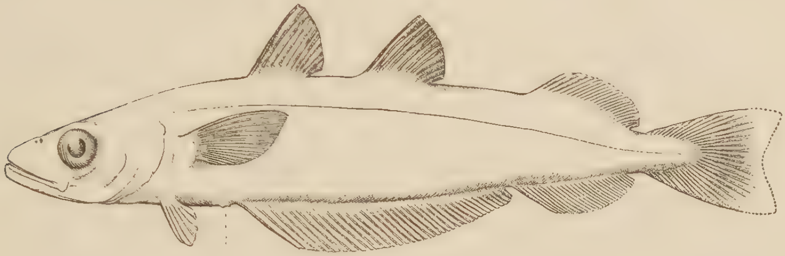

Fig. 3. ***Gadus (Micromesistius) poutassou*, 387 mm. long, from Lat. 42°08'N, Long. 65° 27'W, taken in 250-280 fathoms.**

It has been known for many years that the range of *poutassou* in the eastern Atlantic extends from the Mediterranean to Iceland and northern Norway, and from the coastline out across the continental slope. Schmidt (1909, pp. 83-84) has pointed out, also, that the localities where its early stages were taken during the cruises of the "Thor" locate its spawning grounds as near the 550 fathom line, or even deeper still. And since it has been reported recently from the Julianehaab district, West Greenland (Jensen, 1948, p. 182) the "Cap'n Bill II" captures of it off Georges and Browns Bank are not astonishing.

The number of specimens reported so far from the western side of the Atlantic has not been large enough to show whether we are dealing with stragglers, only, as seems true of the European ling (*Molva molva*) recently reported by Templeman and Fleming (1954, p. 11) from the southwestern part of the Grand Bank of Newfoundland, or whether a permanent population exists in the western side of the Atlantic. We are inclined to favor the second alternative, for it does not seem likely that the number of strays crossing the Atlantic would be large enough for "Cap'n Bill II" to have picked some of them up in two successive summers.

If so, Smitt's (1892, p. 465) account of *poutassou* as without pyloric caeca, would suggest an important anatomical difference between the two populations for there are 8 to 11 of these structures in the "Cap'n Bill II" specimens. But we have recently been informed by Denys W. Tucker of the British Museum (Natural History) that four specimens 241-274 mm. in standard length from Lousy Bank, Lat. 60°20′N, Long. 12°40′ W, 108-200 fathoms, which he examined, had 9, 10, 11 and 12 pyloric caeca, respectively, while one of the Norwegian specimens, mentioned above, has 10 caeca. Thus Smitt's account was incorrect in this respect.

If the blue whiting is in fact a permanent resident of the northwestern Atlantic, the inshore boundary to its regular range probably lies outside the 100 fathom line there, for a fish so easily recognizable could hardly have been overlooked in waters as hard fished as those fronting Nova Scotia and northern New England, if it came close inshore there in such numbers as in the Mediterranean (Risso 1826, p. 228, as *Merlangus vernalis*), in British seas (Day 1880-1884, p. 293), and along the coast of Norway (Smitt 1892, p. 514).

A summary of the nomenclatural history of this species seems appropriate here, to justify our use of the subgenus *Micromesistius* Gill 1863 for it, rather than of any of the other generic or subgeneric names under which it has appeared in scientific literature. The earliest account of it was by Risso (1810, p. 115), as *Gadus merlangus* Linnaeus, 1758. This specific name, however, actually was that of the common whiting of northern Europe, a very different fish, as Risso evidently realized, for he added to his excellent account of it that "ce poisson me paroît une nouvelle espèce" (Risso, 1810, p. 116). Accordingly, he not only proposed the new specific name *poutassou* for it in his next mention of it (Risso, 1826, p. 227), but transferred it from *Gadus* to *Merlangus,* Oken, 1817, a subdivision that had been proposed by Cuvier (1817, p. 213) for such of the gadids as agree with the cod and the haddock in the number of dorsal and anal fins but differ from them in lacking a barbel on the chin.

Merlangus was proposed by Oken (1817, p. not numbered, but following p. 1182; the latter misprinted "1782") as the latinized form of Cuvier's (1817, p. 213) "les merlans." See, on this, Jordan, 1917, pp. 97, 100.

This generic allocation for the species *poutassou* was accepted by several subsequent authors; by Moreau (1881, p. 245) for example, and by Jensen (1948) recently. But it has long been realized that *poutassou* differs from the members of the genus *Gadus* as typified by the cod, not only in lacking a chin barbel, but also in a lower jaw projecting beyond the upper, in a vent situated much farther forward with body cavity correspondingly shorter, in a much longer 1st anal fin, in a lateral line that is almost straight, and in having only 1-3 teeth on either side of the front of the vomer (Smitt, 1892, p. 512).

Views have differed as to which of these characters are the more significant, from the taxonomic standpoint. Thus Bonaparte (1846) referred *poutassou* to the genus *Pollachius* Nilsson 1846[1] because of its projecting lower jaw. But Günther (1862, p. 338), followed by Malm (1877, p. 486) and by several subsequent authors, placed it in *Boreogadus* Günther 1862, proposed by Günther (1862, p. 327) as a ''group'' of *Gadus,* distinct from *Pollachius* (which he treated also as a ''group'') because with ''teeth in the outer series of the upper jaw stronger than the others.'' The next landmark in the history of the species was Gill's 1863 (p. 231) proposal of a new genus *Micromesistius* for it, which Gill set off from *Pollachius* Nilsson 1846 by ''dentition, the very short abdomen, very long first anal and short second dorsal which is widely separated from the first and third.''[2] *Micromesistius* was accepted by Goode and Bean (1895, p. 355). Most, if not all, of the references that were made to the species *poutassou* for the next 40 years were either under *Gadus,* as by Smitt (1892, p. 511), Schmidt (1905, p. 58; 1906, p. 11), Damas (1909, p. 210), Williamson (1909), Hickling (1927, p. 79), D'Ancona (1931), Koefoed (1927, p. 118), Nobre (1935, p. 169) and Lübbert and Ehrenbaum (1936, p. 117), or under *Boreogadus* as a subgenus of *Gadus,* as by Day (1880-1884, Vol. 1, p. 275), by Holt and Calderwood (1895, p. 430) and by Cligny (1905). But Norman (1937, p. 51) revived *Micromesistius* for his new species *australis* from southern Argentina, and this revival of the genus has been accepted by Svetovidov (1948) also, to include both *australis* and *poutassou.*

---

[1] Nilsson gave no definition for his genus *Pollachius.* But Bonaparte (1846, p. 45) listed *Gadus pollachius* Linnaeus 1758 as its type. And subsequent authors have followed Bonaparte in this regard.

[2] Two pages farther along in the same publication Gill (1863, p. 233) proposed a second new genus *Brachymesistius* for *poutassou,* apparently having forgotten that he had already proposed *Micromesistius* for it.

This disagreement as to the generic status of the species *poutassou* expresses the divergence of opinion now current as to whether it is preferable to emphasize the points of difference among the various gadids that have three separate dorsal fins and two separate anals (Subfamily Gadinae), or the points of resemblance. At the one extreme, Svetovidov (1948) has distributed the 21 full species that he recognizes in the Gadinae among 12 genera, restricting the old genus *Gadus* to the cod (*G. morrhua* Linnaeus 1758) alone, but split into 7 subspecies. And Jensen (1948, p. 140) has recently proposed still another genus (*Phocaegadus*) and a new species (*megalops*) for a West Greenland gadid that had been erroneously reported earlier by Johansen (1912, p. 666) as *G. saida* Lepechin 1773. Similarly, North American ichthyologists as a group have distributed the four common Gadinae of the northeastern United States and of the maritime provinces of Canada, cod, tomcod, haddock, and American pollock among as many genera, *Gadus* Linnaeus 1758, *Microgadus* Gill 1865, *Melanogrammus* Gill 1862, and *Pollachius* Nilsson 1846. And Jordan and Evermann (1898) not only retained the genus *Eleginus* Fischer 1813 for *navaga,* with *Boreogadus* Günther 1862 for *saida,* but recognized a separate genus, *Therargra* Lucas 1898 for the so-called Alaska pollock or Alaska whiting, *chalcogramma* Pallas 1814, in their survey of the Gadidae of North America.

On the other hand, Day (1880-1884), Smitt (1892), Williamson (1909) and Damas (1909), as well as European fisheries biologists in general have interpreted the old genus *Gadus,* or one or other subgenus of the latter, widely enough to include all the Gadinae of northern European and Greenland waters, except for *argenteus* Guichenot 1850, with its close ally *thori* Schmidt 1914, which have commonly been referred to the genus *Gadiculus* Guichenot 1850.

One reason for this divergence of opinion is that students have disagreed as to how much weight should be accorded in taxonomy to skeletal characters in this particular group of bony fishes; a second reason is that all of the external characters that have been proposed as generic in this case are intergrading in nature. Thus an unbroken series of intermediates connects the projecting upper jaw of cod and haddock with the projecting lower jaw of European pollack (*pollachius*), American pollock (*virens*), and Alaskan pollock (*chalcogrammus*). Similarly, while the contrast in the relative lengths of the two anal fins is sharp between *poutassou*, in which the first is about 2⅓ times as long as the second, and *saida* in which it is only a little the longer of the two, the gap is bridged by *minutus* and by *merlangus* in which the first anal is about twice as long as the second, and by the cod, by the European whiting (*merlangus*), and by *esmarki* in which it is only 1.3-1.5 times as long as the second.

Corresponding to this variation in the relative lengths of the two anal fins, the position of the vent ranges from below the point of origin of the first dorsal fin or a little anterior to the latter, as in *poutassou* and in *luscus*, to about under the mid-length of the first dorsal as in *merlangus* and below the point of origin of the second dorsal fin, or a little farther rearward still, as in cod, haddock, and several others. Similarly, the rather deeply forked tail fin of *saida* is connected, in form, with the rounded caudal of the tomcod of eastern North America (*tomcod* Walbaum, 1792) by a series of intermediates among fishes as well known as the American pollock (*virens*), European pollack (*pollachius*), European whiting (*merlangus*), and European bib (*luscus*).

The lateral line, the dark color of which was the basis on which Gill (1862, p. 280) originally instituted the genus *Melanogrammus* for the haddock, ranges from black in the latter, through somewhat darker than the sides as in the European whiting (*merlangus*), about the same hue as the sides in *poutassou*, and slightly but definitely paler than the sides in American pollock (*virens*) to conspicuously paler than the sides as in the cod. Again, the gap between the various Gadinae with well developed chin barbel, such as cod and haddock, and those which have none, such as *merlangus*, *pollachius* and *poutassou*, is bridged by *virens*, where young specimens usually have a small barbel, but the adults do not. Finally, the number of vomerine teeth in *poutassou* (1-3 on each side of the anterior end of the vomer) links the state in the cod, with a cardiform group of about 30 on each side, to the state in *argenteus* with only about

2 flat and seemingly deciduous vomerines on either side on some specimens, but perhaps none at all on others.

Obviously, the various European students of late years who have been content to leave the haddock in the same genus as the cod, despite its heavier, denser clavicular bones, have not given this character as much weight as their American colleagues who place the haddock in the separate monotypic genus *Melanogrammus*. And while the hyomandibular bone of *poutassou*, and of its close ally *australis* of southern Argentina, is more simple in outline than in most of the other Gadinae as pictured by Svetovidov (1948, pls. 41-64), we think it unlikely that its nature would be accepted any more generally as a generic character for *poutassou* than the nature of the clavicular bones has been for the haddock. In short we face, in the *poutassou,* one of those situations where a species, or group of species, is set apart from the type of the genus nearest to which it falls by a combination of characters that give it a strikingly different aspect, though no one of these characters is strictly alternative. Under these circumstances we think the course the most likely to stand is to retain *Micromesistius* for it, but as a subgenus of *Gadus* rather than as a separate genus.

REFERENCES

BELLOC, GÉRARD

1929. Étude monographique du merlu *Merlucius merluccius.* Part I. Revue des Travaux, Off. Pêches Maritimes [France], vol. 2, fasc. 2, pp. 153-199.

BIGELOW, HENRY B., and W. C. SCHROEDER

1939. Notes on the fauna above mud bottoms in deep water in the Gulf of Maine. Biol. Bull., vol. 76, pp. 305-324.

1954. Deep water elasmobranchs and chimaeroids from the northwestern Atlantic slope. Bull. Mus. Comp. Zool., vol. 112, no. 2, pp. 37-87.

BONAPARTE, C. L.

1846. Catalogo metodico dei pesci Europei. Naples, 97 pp.

CLIGNY, A.

1905. Poissons des côtes d'Espagne et de Portugal. Ann. Sta. Aquicole Boulogne-sur-Mer (not seen).

CUVIER, (G.)

1817. Le Règne Animal. Paris, vol. 2, xviii, 531 pp.

DAMAS, D.

1909. Contribution à la biologie des Gadides. Rapp. Conseil Perm. Internat. Explor. Mer, vol. 10, spec. part, no. 3, 277 pp., 21 pls.

D'ANCONA, U.

1931. *Gadus poutassou.* Faune Ichthyologique. Teleostei. Conseil Perm. Internat. Explor. Mer, text to accompany plate not numbered.

DAY, FRANCIS

1880–1884. The fishes of Great Britain and Ireland. London and Edinburgh, vol. 1, cxii, 336 pp.; vol. 2, 388 pp., 179 pls.

FISCHER VON WALDHEIM, GOTTHELF

1813. Recherches zoologiques, no. 3. Mém. Soc. Imp. Nat. Moscow, vol. 4, pp. 252-275. Reprinted 1830 (not seen).

GEOFFROY, ÉTIENNE LOUIS

1767. Description . . . de 719 plantes et de 134 animaux . . . Paris, 5 vols., 472 pp., 730 pls.

GILL, THEODORE

1862. Notes of a collection of the fishes of California . . . Proc. Acad. Nat. Sci. Phila., 1862, pp. 274-282.

1863. Descriptions of the genera of gadoid and brotuloid fishes of western North America. Proc. Acad. Nat. Sci. Phila., 1863, pp. 242-254.

1865. On the cranial characteristics of *Gadus proximus* Grd. Proc. Acad. Nat. Sci. Phila., 1865, p. 69.

GINSBURG, ISAAC

1954. Whitings on the coasts of the American continents. Fisheries Bull. U. S. Fish and Wildlife Service, vol. 56, Fisher. Bull. 96, pp. 187-208.

GOODE, GEORGE BROWN, and TARLETON H. BEAN

1895. Oceanic ichthyology . . . Smithsonian Contrib. Knowl., vol. 30, xxv, 553 pp.; vol. 31, 123 pls. Also Special Bull. U. S. Nat. Mus., 2, 1896; and Mem. Mus. Comp. Zool., vol. 22, 1896.

GUICHENOT, A.

1850. Histoire naturelle des reptiles et des poissons. Explor. Sci. Algérie 1840-1842, Zool. 5, 6, iv, 144 (4) pp.; Atlas, 12 pls.

GÜNTHER, ALBERT

1862. Catalogue of the fishes of the British Museum. London, vol. 4, xxi, 534 pp.

HICKLING, C. F.

1927. The natural history of the hake, parts 1 and 2. Fisher. Invest. Gt. Britain, vol. 10, no. 2, 99 pp., 18 charts.

HOLT, E. W. L., and W. L. CALDERWOOD

1895. Survey of fishing grounds, west coast of Ireland, 1890-1891. Report on the rarer fishes. Sci. Trans. Roy. Dublin Soc., ser. 11, vol. 5, pp. 361-512 [513-524], pls. 39-44.

JENSEN, A. S.
1948. Contributions to the ichthyofauna of Greenland, 8-24. Skrifter Univer. Zool. Mus. Copenhagen, Spolia Zool. Mus. Hauniensis, vol. 9, 182 pp., 4 pls.

JOHANSEN, FRITS
1912. The fishes of the Danmark expedition. Meddel. om Grønland, vol. 45, pp. 631-675, pls. 44-46.

JORDAN, D. S. [assisted by B. W. Evermann]
1917. Genera of fishes, Leland Stanford Junior Univ. Publ., Univ. Ser., Part 1, 161 pp.

JORDAN, D. S., and B. W. EVERMANN
1898. The fishes of North and Middle America. Bull. U. S. Nat. Mus., No. 47, Part 3, pp. xxiv, 2183-3136.

KOEFOED, EINAR
1927. Fishes from the sea bottom. Rept. Sci. Results "Michael Sars" North Atlantic Deep-Sea Exped. 1910, vol. 4, part 1, 148 pp., 6 pls.

LEPECHIN, IVAN IVANNOVICH
1773. Descriptio piscis, e gadorum genere, russis Saida dicti (*Gadus saida*). Novi Comment. Acad. Petropol., vol. 18, pp. 512-521, 1 pl.

LINNAEUS, CAROLUS
1758. Systema Natura. Ed. 10, vol. 1, ii, 824 pp.

LUCAS, FREDERICK AUGUSTUS
1898. [Genus *Therargra* proposed]. In Jordan and Evermann, 1898, p. 2535.
1899. Also in Jordan and others. The fur seals and fur-seal islands of the North Pacific Ocean, part 3, p. 486. Washington.

LÜBBERT, H., and L. EHRENBAUM
1936. Handbuch der Seefischerei Nordeuropas. Stuttgart, vol. 2, 337 pp.

MALM, AUGUST WILHELM
1877. Göteborgs och Bohusläns fauna. Göteborg, 674 pp., 9 pls.

MITCHILL, SAMUEL L.
1814. Report in part on the fishes of New York. New York, 30 pp. Reprinted 1898, under editorship of Theodore Gill, with introduction. Washington.
1818. Description of three species of fish . . . Jour. Acad. Nat. Sci. Phila., vol. 1, pp. 407-412.

MOREAU, ÉMILE
1881. Histoire naturelle des poissons de la France. Paris, vol. 3, 697 pp.

NILSSON, SVEN
1846. *In* Bonaparte, C. L., Catalogo Metodico dei Pesci Europei. Naples, p. 45.

NOBRE, AUGUSTO

1935. Vertebrados. *In* Fauna Marinha de Portugal. Porto. vol. 1, lxxxiv, 574 pp., 77 pls.

NORMAN, J. R.

1937. Coast fishes. Part II. Patagonian region. ''Discovery'' Rept., vol. 16, pp. 1-150, 5 pls.

OKEN [LORENZ]

1817. Cuviers und Okens Zoologien neben einander gestellt. Isis von Oken, oder Encyclop. Zeitung, vol. 1, 1817, no. 8, pp. 1147-1185 (incl. 1780-1782 bis, misnumbered).

PALLAS, PETER SIMON

1814. Zoographia Rosso-Asiatica . . . Petropoli, vol. 3, vii, 428, cxxv pp. For date of publication, see Sherborn, Ibis, vol. 4, p. 167, 1934.

RAFINESQUE, CONSTANTINE SAMUEL

1810. Carratteri di alcuni nuovi generi e nuove specie di animali e piante della Sicilia . . . Palermo, 4, 105 pp., 2 pls.

RISSO, A(NTOINE)

1810. Ichthyologie de Nice. xxxvi, 388 pp., 11 pls., Paris.

1826. Histoire naturelle des principales productions de l'Europe méridionale, vol. 3, xvi, 480 pp., 16 pls., Paris.

ROSÉN, NILS

1951. Bulletin statistique des pêches maritimes des pays du nord et de l'ouest de l'Europe. Conseil Perm. Internat. Explor. Mer, vol. 33, 39 pp.

SCHMIDT, JOHANNES

1905. The pelagic post-larval stages of the Atlantic species of *Gadus*. Part 1. Meddel. Komm. Havunders, Copenhagen, Ser. Fiskeri, vol. 1, no. 4, 77 pp., 3 pls.

1906. The pelagic post-larval stages of the Atlantic species of *Gadus*. Part 2. Meddel. Komm. Havunders, Copenhagen, Ser. Fiskeri, vol. 2, no. 2, 20 pp., 1 pl.

1909. The distribution of the pelagic fry and the spawning regions of the gadoids in the North Atlantic from Iceland to Spain. Rapp. Conseil Perm. Internat. Explor. Mer, vol. 10, spec. part, no. 4, 227 pp., 10 charts.

1914. *Gadiculus argenteus* und *Gadiculus thori*. Mindeskrift . . . Jap. Steenstrup, vol. 1, no. 14, 10 pp.

SMITT, F. A.

1892. A history of Scandinavian fishes. Stockholm and London, 2nd ed., vol. 1, vii, 566 pp., Atlas, 27 pls.

SVETOVIDOV, A. N.

1948. The gadoid fishes of the U.S.S.R. and neighboring countries. Fauna of the U.S.S.R., Fishes, vol. 9, no. 4, 221 pp., 72 pls., Acad. Sci., Moscow [In Russian].

Templeman, Wilfred, and A. M. Fleming

1954. European ling — first record from North American waters. Jour. Fisher. Res. Board Canada, vol. 11, no. 1, pp. 11, 13.

Täning, A. V.

1938. Faune Ichthyologique. Conseil Perm. Internat. Explor. Mer; *Merluccius merluccius.* pl. not numbered.

Walbaum, J. J.

1792. Petri Artedi Sueci Genera Piscium . . . pars 3, 723 pp., 3 pls.

Whitley, Gilbert P.

1948. Studies in ichthyology, no. 13. Rec. Australian Mus., vol. 22, no. 1, pp. 70-94.

Williamson, Henry Charles

1909. On the specific characters . . . with a key to the species of *Gadus* found in northern waters. 26 Ann. Rept. Fishery Board Scotland, pt. 3, pp. 97-134, 6 pls., diagram.

Contribution No. 733

Deep-Sea Research, 1954, Vol. 2, pp. 134 to 139. Pergamon Press Ltd., London.

The ratio of photosynthesis to respiration in marine plankton algae and its effect upon the measurement of productivity

JOHN H. RYTHER

Summary—Simultaneous measurements of photosynthesis in tropical ocean waters using STEEMANN NIELSEN'S C^{14} method and RILEY'S "light-and-dark bottle" oxygen technique showed wide disagreement, with C^{14} values consistently lower by a factor of 10-100. Similar comparisons made in coastal waters, gave good agreement between the two methods.

Laboratory experiments suggest that plankton algae respire to a large extent the newly-formed products of their photosynthesis. Thus, in measuring photosynthesis by C^{14} uptake, a considerable loss of activity may be incurred through respiration.

The magnitude of the error introduced by the respiratory loss of C^{14} is proportional to the ratio of respiration to photosynthesis. During exponential growth of *Chlamydomonas*, respiration is 5-10% of photosynthesis, but in nutrient starved, non-growing, cultures respiration may equal photosynthesis.

Under condition of both exponential growth and nutrient starvation, photosynthesis measurements by the C^{14} method agree with net photosynthesis (the difference between photosynthesis and respiration) as measured by the increase in oxygen in light bottles.

C^{14} values compare with total photosynthesis, determined from light-and-dark bottle experiments, only when the ratio of respiration to photosynthesis is low (e.g., during active growth). In nutrient-starved cultures, where the ratio approaches unity, C^{14} experiments give values which are lower by an order of magnitude.

THE use of C^{14} as a tracer for measuring photosynthesis rates in natural populations of phytoplankton was first described by STEEMANN NIELSEN (1952). This paper, which also included some preliminary data for mid-ocean photosynthesis from the *Galthea* expedition, was at once both stimulating and disturbing. While it provided marine biologists with a new technique, much more sensitive than existing methods, it also appeared to give values which were generally lower by a factor of 10 or more than earlier measurements of photosynthesis in similar areas of the ocean as made by RILEY *et al.* (1949) by means of the familiar "light-and-dark bottle" oxygen experiments.

Experiments were carried out at Woods Hole by RYTHER and VACCARO (1954) in which the photosynthesis of healthy algal cultures and natural plankton populations from Vineyard Sound was measured by both methods simultaneously. In general, agreement between the two techniques was extremely good. While photosynthesis values obtained by the C^{14} method were consistently lower, they were always within 50-90% of those obtained by "light-and-dark bottle" oxygen experiments*.

It was the author's tentative conclusion, based on these experiments, that the differences between RILEY'S and STEEMANN NIELSEN'S data may have reflected the seasonal or geographical variability of photosynthesis in the sea. Subsequent investigations, however, have proved this position to be untenable.

---

* A systematic error in the determination of C^{14} activity resulted in an overestimation of C^{14} photosynthesis by approximately 10%. Correction for this error did not appreciably effect the data or alter the authors' conclusions.

During the spring of 1954 the research vessels *Atlantis* and *Caryn* visited respectively the Antilles current north of Puerto Rico and the Sargasso Sea south-east of Bermuda. During both cruises there was a limited opportunity to conduct photosynthesis experiments using both methods simultaneously. In every case, the C^{14} method gave values which were less by a factor of 10-100 than those obtained by " light-and-dark bottle " oxygen experiments. Furthermore, in a more recent paper by STEEMANN NIELSEN (1954) an experiment was described in which the two methods were employed to measure photosynthesis of paper-filtered Sargasso Sea surface water. In this case, a discrepancy of almost 200-fold was observed. (Table I).

Table I. Simultaneous measurements of photosynthesis in tropical ocean water by C^{14} and oxygen experiments. (Expressed as mgC/litre/day).

Atlantis. 196. Antilles Current : Feb.-March, 1954. Samples from 9 m measured at 1,200 foot candles.

Lat.	*Long.*	*Oxygen method*	C^{14} *method*	O_2/C^{14}
24°28′	74°29′	·0127	·0011	11·5
23°54′	73°46′	·0348	·0007	49·7
24°12′	73°42′	·0660	·0058	11·4
20°30′	79°32′	·0264	·0029	9·1
26°37′	79°14′	·0132	·0012	11·0

Caryn. 72. Sargasso Sea : June, 1954. Samples from 10 m measured under natural surface illumination.

Lat.	*Long.*	*Oxygen method*	C^{14} *method*	O_2/C^{14}
28°53′	61°38′	·070	·0007	100·0

Galthea. Sargasso Sea : June, 1952 (STEEMANN NIELSEN). *Coarse-filtered surface water.* C^{14} *experiments for 12 hours at 1,800 foot candles.* O_2 *experiments for 3 days under natural surface illumination.*

Oxygen method	C^{14} *method*	O_2/C^{14}
·03	·00017	176·0

It became apparent from these data that, while the two methods gave good agreement in coastal waters, they did not give comparable results in the open ocean. Further laboratory experiments, which will be discussed below, suggest a possible explanation for the inconsistency of the agreement between the two methods.

In STEEMANN NIELSEN'S original description of the C^{14} method, he estimated that in a three hour experiment one-third of respiration is based upon substances produced by photosynthesis during the course of the experiment. Further studies by STEEMANN NIELSEN (personal communication) and the present author indicate that this figure may have been low, and that the algae may utilize almost exclusively the newly-formed products of photosynthesis for their respiration.

Fig. 1 illustrates that from 10% to 40% of the C^{14} fixed during two hours of photosynthesis may be lost, presumably through respiration, in the ensuing four to six hours. Since additional respiration of C^{14} undoubtedly occurred during the two hours of photosynthesis, these figures are minimal.

These and other similar experiments indicate that, while the loss of activity through respiration may be relatively large and must be taken into consideration, this loss is also extremely variable and hence cannot be accounted for by application of a constant correction factor.

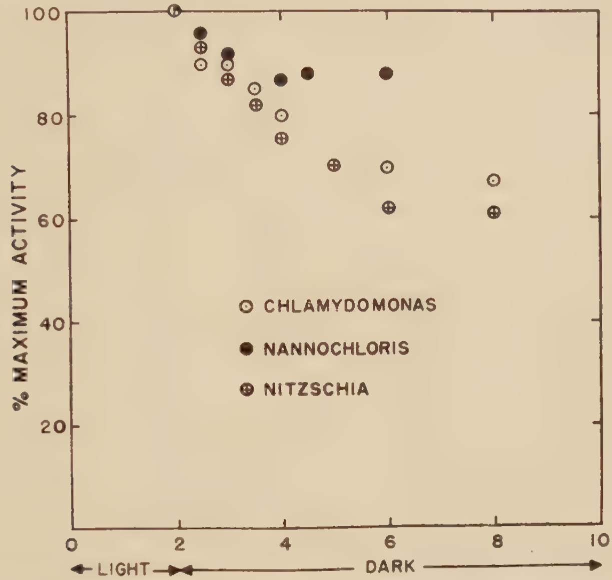

Fig. 1. Loss of activity of three species of marine algae when placed in dark after two hours exposure to light in $C^{14}O_3^=$.

The extent to which the respiration of C^{14} may effect the measurement of photosynthesis by the C^{14} method will depend, among other things, upon the ratio of respiration to photosynthesis. It is well known that this ratio increases with depth (and decreasing illumination) in the ocean. The term " compensation point " refers to the light intensity at which photosynthesis and respiration are equal (JENKIN, 1937) and " compensation depth " to the depth at which compensation intensity occurs. It may be assumed, however, that the respiration : photosynthesis ratio is dependant not only upon light, but equally as well upon any other factor or factors which have a differential effect upon the two processes.

KETCHUM (1939) reported a decrease in the growth rate of *Nitzschia closterium* at phosphate concentrations below ·55 mgA/m³. RILEY *et al.* (1949) considered that photosynthesis in the ocean is limited when phosphate falls below this level, but assumes that respiration is not affected. The effects of nutrient depletion upon these two processes were investigated in the following experiment.

Photosynthesis and respiration were determined at various stages in the population development of a pure culture of marine *Chlamydomonas* by means of " light-and-dark bottle " experiments (Table II). The *Chlamydomonas* was grown in a medium deficient in nitrogen and phosphorus and cell division occurred for only 4-5 days.

Photosynthesis per cell was relatively high during exponential growth, but decreased rapidly as nutrients became limiting and continued to decline throughout the experiment. Respiration per cell also decreased during the first four days, but then remained constant. While respiration decreased by a factor of two, photosynthesis decreased 20-fold in the course of the experiment.

Respiration was 5-10% of photosynthesis during the exponential growth phase of the culture, about 50% as the population asymptote was reached, and equal to photosynthesis after the culture had stopped dividing for 15 days. In the last instance the population was at a compensation point, but resulting here from nutrient deficiency rather than from limitation of light.

Table II. Photosynthesis (P) and respiration (R) in a nutrient-deficient pure culture of marine Chlamydomonas (Expressed in ml. O_2/24 hrs.)

Days	*Mean cell count* (10^6 *cells/litre*)	*P/litre*	*R/litre*	*P/cell* ($\times 10^3$)	*R/cell* ($\times 10^3$)	*R/P* × 100
0	26					
1-2	61	6·89	·82	113·0	13·4	11·8
2-3	135	16·40	1·35	121·0	10·0	8·3
3-4	290	5·30	2·48	18·3	8·6	47·2
4-5	390	4·10	2·30	10·5	5·9	56·3
5-6	470	4·10	2·32	10·1	5·7	56·3
6-7	427	4·08	2·70	9·5	6·3	63·0
14-15	410	3·18	2·40	7·5	5·9	78·9
28-29	415	2·47	2·52	6·0	6·1	101·8

If, as suggested, the phytoplankton respire largely the newly-formed products of photosynthesis, their up-take of C^{14} would appear to represent more nearly their net photosynthesis, or the difference between photosynthesis and respiration, rather than total or gross photosynthesis. The oxygen method, on the other hand, corrects for respiration by means of the dark bottle. By taking the difference between the oxygen produced in the light bottle (or consumed if respiration exceeds photosynthesis) and that consumed in the dark bottle, a measurement is made of total or gross photosynthesis. The preceding experiment has demonstrated that gross and net photosynthesis may be almost equal or may differ widely depending upon the state of nutrition of the organisms.

The effect which the relation between gross and net photosynthesis may have upon photosynthesis measurements is illustrated in the following experiment. Photosynthesis was measured simultaneously by C^{14} and oxygen experiments in a nutrient-deficient, pure culture of *Chlamydomonas*. Three such comparisons were made, (1) during the exponential growth phase, (2) when the population asymptote was reached, and (3) after the culture had stopped dividing for about two weeks (Fig. 2). Photosynthesis values obtained by both methods are expressed in mg. C fixed per liter per day. In the oxygen experiments (clear bar graphs) the values above the base line are equivalent to the oxygen increase in the light (the difference between photosynthesis and respiration, or net photosynthesis), the value below the base line is equivalent to the oxygen decrease in the dark bottle (respiration), and the entire graph represents gross photosynthesis. In every case photosynthesis measured by C^{14} uptake (cross-hatched bar graphs) was 70-80% of net photosynthesis. During exponential growth C^{14}-photosynthesis was 75% of gross photosynthesis. In the nutrient-deficient culture, C^{14}-photosynthesis was lower than gross photosynthesis by a factor of 20.

In the preceding experiments measurement of net photosynthesis could be made because bacteria-free cultures were used. In "light-and-dark bottle" experiments with natural populations it is not possible to separate respiration of the phytoplankton from that of bacteria and other organisms, and no estimate of net photosynthesis may be made. Consequently, the extent to which the relationships described above may occur in the ocean must remain a matter for speculation.

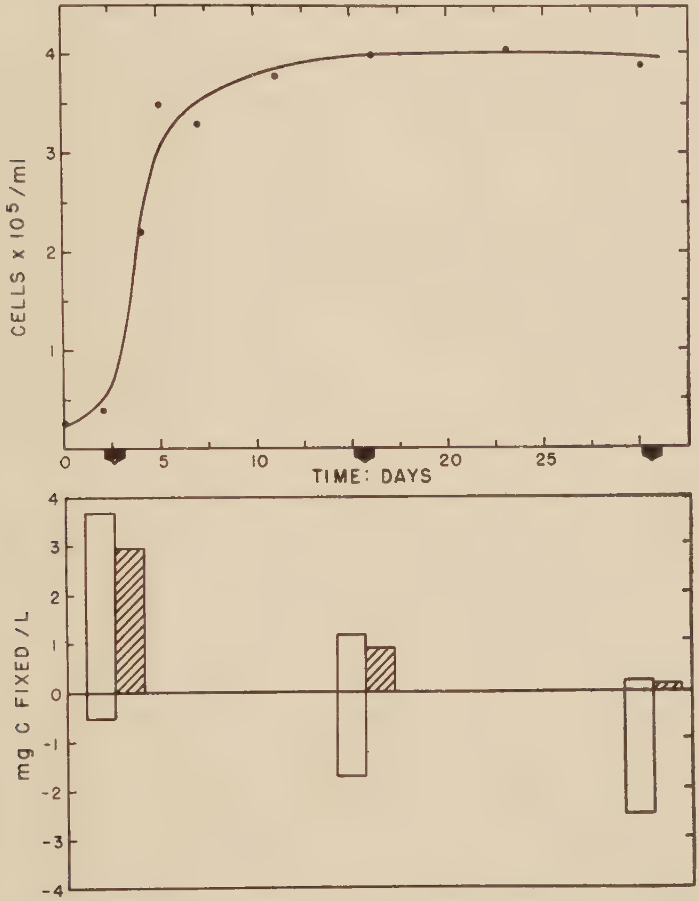

Fig. 2. Photosynthesis measured by oxygen production (clear bar graphs) and C^{14} uptake (hatched bar graphs) in a nutrient-deficient, pure culture of marine *Chlamydomonas*. Upper figure represents growth of culture determined by cell counts. (See text for full explanation of lower figure).

It may be postulated, however, that whenever nutrients (and presumably other factors) become limiting to the photosynthesis of an existing population of phytoplankton, a large difference between gross and net photosynthesis and a resulting large discrepancy between photosynthesis measurements by the C^{14} and oxygen method may be expected. In this connection, it is at least suggestive that the areas showing this disagreement occur in the tropical mid-ocean where surface concentrations of nitrogen and phosphorus are generally low and presumably are frequently limiting to photosynthesis (cf. Riley, 1949). On the other hand, good agreement between the two methods is normally observed in relatively eutrophic coastal waters.

Photosynthesis measurements at sea were made by R. F. VACCARO and D. B. FOSTER. The author wishes to acknowledge the participation of MR. VACCARO and Dr. R. R. L. GUILLARD in the laboratory phase of the investigation. This work was carried out with the assistance of a research grant from the National Science Foundation and under contract with the Office of Naval Research.

Woods Hole Oceanographic Institution Contribution No. 733 *from the Woods Hole Oceanographic Institution.*

REFERENCES

JENKIN, P. M. (1937), Oxygen production by the diatom *Coscinodiscus excentricus* in relation to submarine illumination in the English Channel. *J. Mar. Biol. Assoc., U.K.* **22** 301-342.

KETCHUM, B. H. (1939), The absorption of phosphate and nitrate by illuminated cultures of *Nitzschia closterium. Amer. J. Bot.* **26** 399-407.

RILEY, G. A., H. STOMMEL and D. F. BUMPUS (1949), Quantitative ecology of the plankton of the Western North Atlantic. *Bull. Bing. Oceanog. Coll.* **12**, Art. 3: 1-169.

RYTHER, J. H. and R. F. VACCARO (1954), A comparison of the oxygen and C^{14} methods of measuring marine photosynthesis. *Jour. Cons. Internat. Explor. Mer.* 20 25-37.

STEEMANN NIELSEN, E. (1952), The use of radio-active carbon (C^{14}) for measuring organic production in the sea. *Ibid.* **18** 117-140.

STEEMANN NIELSEN, E. (1954), On organic production in the oceans. *Ibid.* **19** 309-328.

Printed in Great Britain by The Salisbury Press Ltd., Publicity House, Wilton Road, Salisbury, Wilts. (88345)

Contribution No. 735

EXTRAIT DU JOURNAL DU CONSEIL INTERNATIONAL
POUR L'EXPLORATION DE LA MER
VOL. XXI. No. 1. 1955

Winds and Temperatures in Relation to the Brood-Strength of Georges Bank Haddock.[1]

By

Joseph Chase.

Introduction.

The wide year-to-year variation in the brood-strength of haddock has long been of much concern to fisheries investigators on both sides of the Atlantic. Recently, British investigators (Carruthers, 1951) have developed a function of average wind which correlates very well with the brood-strength of North Sea haddock. For Georges Bank, which is situated off the north-east coast of the United States (i.e., on the windward side of the Atlantic), the comparison of brood-strength with average wind has shown only a weak correlation.

The idea of dependence on wind arises from the fact that for some 4 months after spawning begins, the eggs and larvae are normally concentrated in the upper 10 metres of water where they are subject to movement by wind-blown currents. At the end of the pelagic period, the larvae sound, and their survival at the bottom as "zero age" fish depends on their finding bottom at a depth of 150 fathoms or less. The British formula takes cognizance of the mean wind for the pelagic season and therefore of the position of the larvae relative to shoal water at the end of the season. Brood-strength has been shown (Parrish, 1950) to be largely independent of events occurring outside the pelagic season.

The hydrography of Georges Bank and adjacent waters suggests the necessity of examining daily winds in order to reach a better correlation for that area. The easterly current, which lies just off the shelf (Bigelow, 1924, pp. 936—942) at a distance of some 50—75 miles south-south-east of the middle of the bank, provides the possibility of loss of eggs and larvae after a régime of north-westerly winds, regardless of a later régime of south-easterlies. There is an indication of this type of action in drift-bottle records. Another possible source of loss is found in the much higher temperatures which exist off the shelf.

---

[1] Contribution No. 735 from the Woods Hole Oceanographic Institution.

This situation is in contrast to that of the North Sea, where currents flow in a general counter-clockwise circulation, so that average wind more nearly indicates the net travel of eggs and larvae, and where the temperature gradients are smaller.

Brood-Strength.

The data on Georges Bank haddock brood-strength were furnished by the Fish and Wildlife Service of the U. S. Department of the Interior. They include final figures for the year-classes of 1928 to 1949 and estimates for 1950 and 1951 (Figure 1). The year-class strength is determined at Boston, Massachusetts, by a careful sampling count of 3-year-old fish from the catches of commercial fishermen and is believed to be accurate to within one unit. Ten units on the scale represents a normal brood-strength and the range is from 1 (1928) to 26·3 (1948) units.

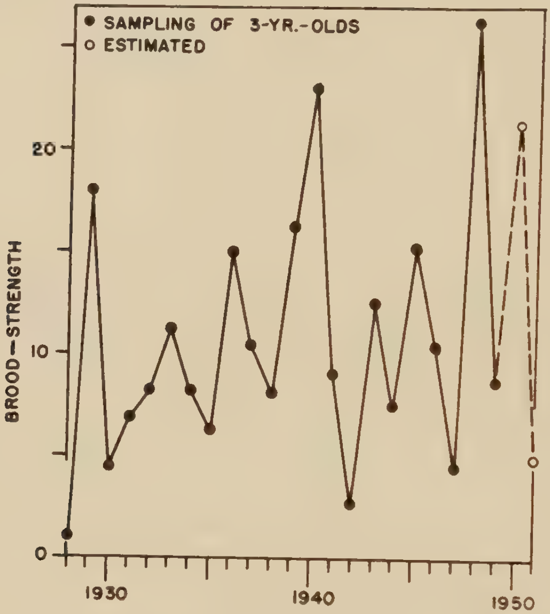

Figure 1. Brood-strength of Georges Bank haddock.

Wind.

The wind values are expressed in terms of daily (1230 GMT) pressure difference between Nantucket, Massachusetts, and Yarmouth, Nova Scotia. This pressure difference is proportional to the component of geostrophic wind normal to the Nantucket—Yarmouth line. It corresponds to the component of wind-driven current normal to the southern edge of Georges Bank if wind-driven currents in this region move at an angle of 25° to the right (clockwise) of the geostrophic wind. This angle is reasonable if it can be assumed that surface wind direction is about 20° to the left of the geostrophic wind and that surface water is driven in a direction 45° to the right of the surface wind.

The study is confined to the offshore components on the assumption that very little, if any, loss of eggs and larvae results from wind and current in other directions. According to their lengths and strengths, the principal régimes of offshore components are presumed to carry off eggs and larvae in varying amounts, i.e., to do varying amounts of "damage" to the potential brood-strength. The greater the total of damage during the pelagic season, the smaller the brood-strength should be.

Damage Assessment.

"Damage units" were assigned to the principal offshore régimes according to an empirical table. This table (Table 1) lists increasing numbers of damage units according to the number of days for which the Nantucket—Yarmouth pressure difference was continuously 5 mb. or more, and extra units for the number of days of continuous pressure difference of 10 mb. or more.

Table 1.

Days of continuous pressure difference	Damage units for régime
of 5 mb. or more	
1	1
2	2
3	4
4	7
5	10
6	13
7	16
of 10 mb. or more	
1	1
2	3
3	5

The form of the table and the non-linearity of the early part of the damage-units column was suggested by an inspection of daily winds for a few pelagic seasons. The empirical damage-unit scale is the result of trial-and-error fitting to the pressure-difference data and brood-strength data for the years 1928—1931.

A 5 mb. difference corresponds to a surface wind of about 20 m.p.h. At a ratio of current in knots to wind in m.p.h. of 0·035, this gives a water movement of about 17 nautical miles per day, which is enough to transport eggs and larvae from the normal edge of the pelagic field at the 50 fathom curve to the easterly current. This ratio is a little

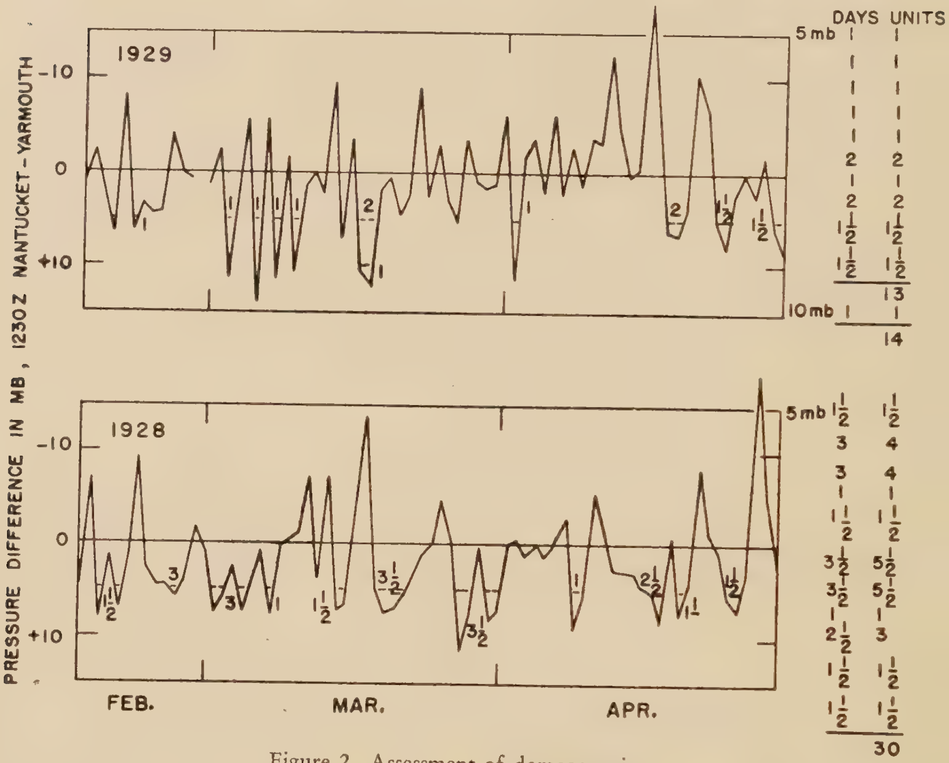

Figure 2. Assessment of damage units.

higher than most of those found by Haight (1942, p. 70) in a study of coastal lightship data but seems reasonable in view of the offshore position of Georges Bank. The proportionally greater damage-unit figures listed for the longer régimes are to account for the denser distribution near the centre of the pelagic field and for the greater water speeds probably attained after the first two or three days.

In assessing the length of the régimes, some allowance was made for the rate of change of pressure differences near and during each régime. Variations due to subjectivity in the counting of damage units probably do not exceed two units for any season.

The normal pelagic season is from 17. February to 15. June. The period from 2. May to 15. June has been left out of the damage-unit calculations because of its generally light winds and small year-to-year variation in damage count.

Examples of damage count are shown in Figure 2.

Fixed Date Correlogram.

When damage counts for the period 17. February—1. May for each of the 24 years were compared with the corresponding brood-strength figures on a correlogram, some correlation was apparent, seventeen of

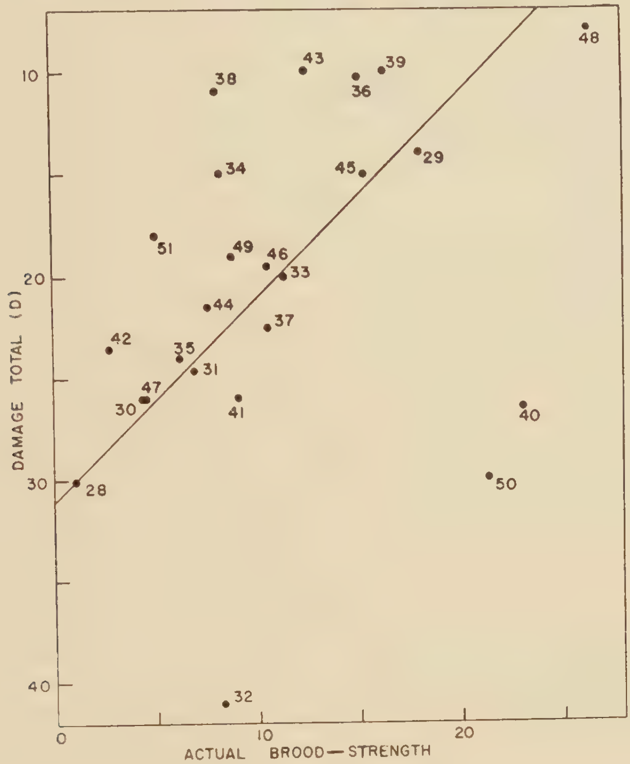

Figure 3. Fixed date correlogram.

the points lying within 6 units of a straight line (Figure 3). The other seven points probably reflect the influence of other variables such as are often present in biological problems. Some other danger to haddock than wind may have reduced the brood-strength for the years 1934, 1938, 1943, and 1951. More of a problem are the cases of 1932, 1940, and 1950, where the brood-strength was higher than the damage totals indicate.

A factor which might account for deviations on either side of the line is variation in the spawning time. Variations of this nature are often associated with temperature and it is interesting that in 6 of the 7 years showing large deviations, there were anomalous air temperatures at New England coastal stations. There are indications that spawning time does vary but the details of this variation are unknown at present. Though any attempt to introduce temperature into the formula at this time must be somewhat arbitrary, it nevertheless seems warranted in view of the anomalous temperatures.

Temperature Sequence.

Perhaps the best available data for indicating the water temperature

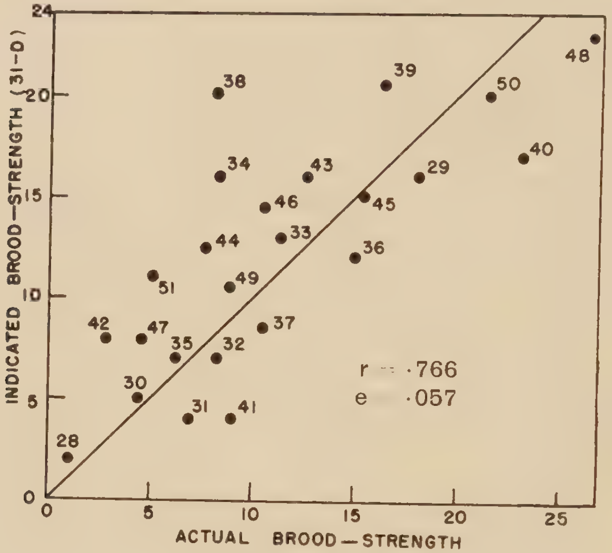

Figure 4. Variable date correlogram.

of Georges Bank are the 5-day means of surface water temperature at "Nantucket Shoals" lightship, the available file of which covers the 16 years 1928—1932, 1934—1941, 1948, 1949, and 1951. These temperatures may be more influenced by short-period weather than are those of the bank but it is believed that the difference in influence is small.

These data show that on the average a definite lessening of the rate of cooling occurs at about normal spawning time, i.e., 17. February, the drop in temperature for the period from 16. February to the minimum on 6. March being about $^1/_3$ that of a like period ending on 16. February. This time of the change of rate on the individual years was taken as the starting date for damage count. The date varied between 1. February and 21. March.

Due to oscillations resulting from short-period weather, this change was sometimes not well marked. However, in a majority of cases it was well marked and occurred at a temperature 1·5°F. above that of the minimum. To make the selection as objective as possible, the count was started when the temperature last fell to within 1·5°F. of the eventual minimum.

To handle the eight cases not covered by the "Nantucket Shoals" data, the monthly mean air temperatures (U. S. W. B.) for Nantucket, Massachusetts, and Eastport, Maine, were used. The normal time of the minimum of the mean temperature between the two stations is about 30. January, which is 18 days before the normal beginning of spawning. The starting date for damage count was therefore set, for each of the years, at a date 18 days after the date (interpolated) of the minimum air temperature.

Variable Date Correlogram.

The application of temperature to the formula resulted in the correlogram of Figure 4. For the ordinate of the figure, the seasonal damage (D) has been replaced by the indicated brood-strength (31-D). The correlation coefficient between indicated and actual brood-strengths is 0·766 ± 0·057, which is well above 0·515, the 1 % level of significance for 24 cases.

The principal improvement is in the reduction of the deviations for 1932, 1940, and 1950, which years had late temperature minima. Also improved are the points for 1943 and 1951. The points for 1934 and 1938 remain unchanged. February of 1934 had the lowest water and air temperatures of all of the period examined, while 1938 had a very normal winter. The hurricanes of 1938 and 1944 may have reduced the brood-strengths of those years.

The relative merits of air and water temperatures for use in the formula were tested by calculating indicated strengths with air temperatures for the 16 years already treated with water temperatures. The water temperatures led to better results in 7 cases, poorer results in 2 cases, and equal results in 7 cases.

Acknowledgements.

The writer wishes to thank Dr. C. O'D. Iselin and Mr. F. C. Fuglister, of the Woods Hole Oceanographic Institution, for their interest and guidance in this study, and Mr. G. G. Pasley, Jr., for the drafting of the figures.

Summary and Conclusions.

1. An empirical formula for predicting the brood-strength of Georges Bank haddock is presented. The formula makes use of the wind during the pelagic season and of the winter water or air temperatures. While the formula works well for the 24 years of available brood-strength data, the need for more research on haddock and their environment is apparent.

2. A correlation of 0·766 ± 0·057 has been found between the actual brood-strength of Georges Bank haddock and an indicated brood-strength. This indicated brood-strength is a function of offshore wind during a part of the pelagic season beginning with a date determined by temperature sequence and ending on 1. May.

3. At the present time there is insufficient knowledge of the variations in the spawning time of Georges Bank haddock and their possible connexion with environmental temperatures to establish a firm ecological basis for the formula for indicated brood-strength. Intensive study of spawning and the establishment of a programme of water temperature observations appear to be in order for purely scientific reasons as well as for the practical importance which the forecasting of brood-strengths has in the conservation of a commercially valuable fish.

References.

Bigelow, H. B., 1924. "Physical Oceanography of the Gulf of Maine". Bull. Bur. Fish., **40**, Part II, 1027 pp.

Carruthers, J. N., A. L. Lawford, V. F. C. Veley, & B. B. Parrish, 1951. "Variations in Brood-strength in the North Sea Haddock in the Light of Relevant Wind Conditions". Nature, London, **168**, 4269, pp. 317—9.

Haight, F. J., 1942. "Coastal Currents along the Atlantic Coast of the United States". U. S. Dept. of Commerce, Coast and Geodetic Survey, Spec. Publ., 230, 73 pp.

Parrish, B. B., 1950. "Brood Fluctuations in the North Sea Haddock Population". Abstract of paper read at Aberdeen Joint Meeting (October 1949) of the Challenger Society, 3, II, p. 18.

U. S. Weather Bureau. *Monthly Weather Review*, 1927—1949, and *Climatic Data National Summary*, 1950—1951.

Contribution No. 736

THE ESTIMATION AND CHARACTERIZATION OF PLANKTON POPULATIONS BY PIGMENT ANALYSIS. III. A NOTE ON THE USE OF "MILLIPORE" MEMBRANE FILTERS IN THE ESTIMATION OF PLANKTON PIGMENTS.[1, 2]

By

GRACE I. CREITZ AND FRANCIS A. RICHARDS
Woods Hole Oceanographic Institution

ABSTRACT

Collection of plankton samples on "AA" (aerosol assay) type "Millipore" membrane filters has been substituted for centrifugation in the method of Richards with Thompson for estimating plankton pigments. Although the filter dissolves in the 90% acetone that is subsequently used for extracting the pigments, its solution does not interfere with the spectrophotometric determination of the chlorophyll and carotenoid components. Comparison between retention by Millipore filters and the Foerst plankton centrifuge indicates that the filters are significantly more efficient. Plankton samples can be stored dry, in the dark, under vacuum, for at least three weeks without affecting the pigments for subsequent analysis.

During the work reported in the second paper of this series (5), various methods for removing plankton from water were investigated, and the Foerst plankton centrifuge was selected as the most satisfactory. Since that time, Millipore membrane filters[3] have become

---

[1] Contribution No. 736 from the Woods Hole Oceanographic Institution.

[2] Part of this work has been supported by a grant from the National Science Foundation. This financial aid is gratefully acknowledged.

[3] Manufactured under the name "Millipore" by the Lovell Chemical Company, Watertown, Massachusetts (4); available in two grades, designated "HA" (hydrosol assay) and "AA" (aerosol assay).

Reprint from SEARS FOUND. JOURN. MAR. RES.

readily available and the procedures previously described have been varied to incorporate their use.

The method, as revised, is as follows: filter an adequate quantity of water containing about 0.1 g of powdered magnesium carbonate through an AA Millipore filter, trim the filter to the size of its effective filtering area, fold and roll it into a cylinder and drop it into a 16 × 125 mm screw-cap test tube. Place the tube in a vacuum desiccator to be dried and stored if immediate extraction is impractical. Preliminary investigations indicate that dried plankton samples may be stored at least three weeks without apparent change in the absorption spectra of their extracts by refrigerating the samples in a vacuum desiccator. This procedure protects them from oxygen, moisture, light and high temperatures. Extraction and estimation are carried out according to the procedures of Richards with Thompson (5).

Membrane filters have been described by Goetz and Tsuneishi (2) and by Bush (1), and their use in plankton collection has been described by Goldberg, Baker and Fox (3).

Despite their designation as AA filters, they have proved applicable for use with aqueous suspensions. According to a personal communication from W. B. Krabek of the Lovell Chemical Company, a suspension of *Serratia marcescens* (coccoid, 0.5 μ, or short rods, $0.5 \times 0.5 - 1.0$ μ) containing 8×10^6 organisms was almost completely retained by AA filters, 25 or fewer colonies appearing in the filtrate. In this laboratory, aerosol filters have retained completely the cells of a *Nannochloris* species culture ($1.0 - 2.5$ μ). These observations as well as those on the retention of a large number of natural plankton populations lead to the conclusion that AA filters will retain all natural plankton organisms down to 1 μ in diameter. The HA filter, though it has a somewhat smaller pore size, filters less freely, is more brittle and bulky, and has a somewhat greater absorbancy when placed in 90% acetone solution (Table I); therefore, the AA filter is now used exclusively in this laboratory.

Table I. Absorbancies (log I_0/I) of solutions of Millipore filters in five ml of 90% acetone, in absorption cells of 5 cm light path.

Wavelength mμ	*AA Type (Entire, 4.7 cm. diam.)*	*AA Type (Trimmed to ca. 3.9 cm diam.)*	*HA Type (Entire, 4.7 cm diam.)*
480	.005	.002	.012
510	.004	.001	.010
630	.002	.000	.006
645	.001	.000	.006
665	.001	.000	.005
750	.001	.000	.004

The volume to be filtered varies with the type of water under investigation. The filters act as two-dimensional screens, permitting water to pass through them rapidly until all pores are covered; after that time, additional water can be filtered only very slowly. The amount of water which can be filtered in a reasonable time depends on the amount and kind of particulate matter present. Small volumes can be filtered when the plankton crop is large, large volumes when the crop is small. Nonpigmented detritus can also clog the filters, and in extreme cases sufficient amounts of plankton for a satisfactory analysis might not be collected. The volumes of natural waters which have been used in this laboratory have varied from a few hundred milliliters to more than six liters. Much smaller volumes of algal cultures have been used. To insure representative sampling, precautions must be taken against the settling onto the membrane of particulate matter from water which will not be filtered.

Absorbancy of Millipore Filters. Millipore filters are almost completely soluble in 90% acetone. Clear solutions are obtained on centrifuging for about 5 minutes in a clinical centrifuge in the presence of magnesium carbonate. Solutions of AA Millipore filters have negligible absorbancies at all wavelengths that are used to compute pigment concentrations (Table I). The absorbancy is decreased when the filters are trimmed to remove the unexposed edge; this removes about 30% of the total bulk of the filter.

Millipore filters were added to a large number of solutions containing plankton pigments, and the resultant spectra were compared with those of the original pigment solutions. Examples of two such experiments are shown in Table II. There is no evidence of chemical interaction between the filter and the pigments to create discrepancies in the absorption spectra. The small effects which the filters have on the pigment spectra are similar to Rayleigh scattering and probably result from incomplete solution of the filter and (or) gel-stabilized colloidal suspensions of particulate matter. In these studies, representing a variety of concentrations, average deviation of chlorophyll *a* estimates, either with or without added filters, was less than 5%.

Scattering can be detected from the absorbancy at 750 mμ, where pigment absorbancies are nearly negligible. If the absorbancy at this wavelength is appreciable, further centrifugation in the presence of magnesium carbonate is probably necessary. Even slight turbidities cause erroneously high estimates of components other than chlorophyll *a*. The chlorophyll *a* estimates are not as greatly affected but tend to be slightly low.

Table II. Absorbancies (log I_0/I) in 5 cm absorption cells, computed pigment concentrations of plankton extracts with and without added Millipore (AA) filter.

	Station 11		Station 12	
Wavelength, mμ.	*Without M.F. added*	*With M.F. added*	*Without M.F. added*	*With M.F. added*
	ABSORBANCY			
480	1.020	1.015	.455	.468
510	.390	.395	.185	.202
630	.197	.197	.076	.075
645	.220	.220	.089	.088
665	.790	.795	.239	.238
750	.009	.015	.009	.012
	COMPUTED CONCENTRATIONS			
Chlorophyll *a*,mg/1	11.72	11.80	3.49	3.48
Chlorophyll *b*,mg/1	0.05	0.02	0.43	0.42
Chlorophyll *c*,MSPU/L	5.28	5.23	2.75	2.70
Non-astacin carotenoids, MSPU/L	3.41	3.56	1.33	1.24
Astacin-type carotenoids, MSPU/L	1.16	1.21	0.75	0.78

Comparisons of Retention by the Foerst Plankton Centrifuge and Millipore Filters. It is well known that the recovery of plankton organisms by the continuous-feeding plankton centrifuge depends on several factors, including the speed of the instrument, the size and relative density of the plankton organisms, and the rate of flow through the centrifuge. The membrane filters provide a good means for investigating the retention by the centrifuge.

Aliquot samples of sea water were passed through AA Millipore filters and through the Foerst plankton centrifuge at a rate of about seven minutes per liter. The material passed by the centrifuge was subsequently filtered. The differences in retention by the two methods were large, the chlorophyll *a* retained by the centrifuge varying between 69 and 86% of that retained by the filters. The sum of the pigment contents of the material retained and passed by the centrifuge agreed well with the pigments retained by filtration.

In the examples in Table III, the material retained by the centrifuge was comparatively poor in chlorophyll *c* whereas the material recovered on filtration of the centrifugate was rich in this compound.

Table III. Comparison of retention by Foerst plankton centrifuge and AA type Millipore filters.

Sample			*Chlorophyll a* mg/M^3	*Chlorophyll b* mg/M^3	*Chlorophyll c* $MSPU/M^3$		$\frac{Chph\ b}{Chph\ a}$	$\frac{Chph\ c}{Chph\ a}$
21	Retained by Centrifuge		2.52	0.76	3.33		0.30	1.32
	Passed by Centrifuge		1.04	0.48	2.17		0.46	2.05
			—	—	—			
		Sum	3.56	1.24	5.50	$\Sigma/\Sigma Ca$	0.35	1.54
	Retained by M.F.		3.58	1.05	5.80		0.29	1.62
15	Retained by Centrifuge		4.68	0.76	4.83		0.16	1.03
	Passed by Centrifuge		0.97	0.48	2.65		0.50	2.74
			—	—	—			
		Sum	5.65	1.24	7.48	$\Sigma/\Sigma Ca$	0.22	1.32
	Retained by M.F.		5.94	1.40	8.00		0.24	1.35
8	Retained by Centrifuge		8.04	2.31	2.51		0.29	0.31
	Passed by Centrifuge		1.06	0.57	1.67		0.54	1.58
			—	—	—			
		Sum	9.10	2.88	4.18	$\Sigma/\Sigma Ca$	0.32	0.46
	Retained by M.F.		11.60	2.26	5.56		0.19	0.48

This suggests that the centrifuge is effecting a separation of plankton species.

Other work, now in progress, shows that dinoflagellates are particularly rich in this compound and that they are thrown down by centrifuging less readily than diatoms and other plankton organisms. The samples in Table III contained an abundance of dinoflagellates, and the enrichment of chlorophyll *c* in the material passed by the centrifuge could reflect the failure of the instrument to retain dinoflagellates or fragments of them. Similar though less marked changes in the ratios of chlorophyll *b* to *a* could be interpreted as a selective failure of the centrifuge to retain small green algae.

LITERATURE CITED

1. Bush, J. H.
1952. A basic new tool in bacteriology. Sci. Mon., *75* (5): 303–305.

2. Goetz, A. and N. Tsuneishi
1951. Application of molecular filter membranes to the bacterial analysis of water. J. Amer. Wat. Wks. Ass., *43* (12): 943–984.

3. Goldberg, E. D., M. Baker, and D. L. Fox
1952. Microfiltrations in oceanographic research. I. Marine sampling with the molecular filter. J. Mar. Res., *11* (2): 194–204.

4. Lovell Chemical Company
(undated) Characteristics and uses of the MF Millipore filters. Lovell Chemical Company, Watertown, Massachusetts. Brochure, 22 pp.

5. Richards, F. A. with T. G. Thompson
1952. The estimation and characterization of plankton populations by pigment analyses. II. A spectrophotometric method for the estimation of plankton pigments. J. Mar. Res., *11* (2): 156–172.

Contribution No. 739

Transactions, American Geophysical Union Volume 36, Number 4 August 1955

ON THE FORMATION OF BOTTOM WATER IN THE NORWEGIAN BASIN

William G. Metcalf

(Contribution No. 739 from the Woods Hole Oceanographic Institution)

Abstract--The formation of Norwegian Basin bottom water has generally been considered to result from surface cooling during March, April, and early May followed by overturning of the water column to produce homogeneity throughout. Recent data confirm much of the earlier theory but suggest that the cooled surface water may flow toward the bottom along a gently tilted path, and that a homogeneous water column may not play any role in bottom water formation.

The problem of bottom water formation in the Norwegian Basin was considered by NANSEN [1906] and HELLAND-HANSEN and NANSEN [1909]. They believed that bottom water is formed during March, April, and early May in a part of the region between Jan Mayen and Svalbard where there is very little current movement. To a lesser extent, part of the region between Iceland and Jan Mayen was also considered to be of importance in such formation.

According to these investigators, cooling increases the density of the water at the surface causing it to sink. This brings from below to the surface slightly warmer water with a higher salinity. As this process continues, the entire water column is gradually overturned until homogeneity is obtained throughout. Actually, owing to the lateness of the season, the subsurface data presented by these oceanographers do not show this process actively taking place. Surface observations showing the requisite temperature and salinity for bottom water formation were observed during the proper season, but they were not accompanied by subsurface observations. NANSEN [1902] mentions that the sinking of the heavier surface water may not take place at once upon its formation and may be very slow.

Since the time of the above-mentioned papers, the problem has received little attention until recent wintertime observations were made in the central areas of the Norwegian Sea. In the light of the ideas of Nansen and Helland-Hansen, some recent data have been examined for evidence of bottom water formation.

The water below 1500 m in the Norwegian Basin shows a high degree of homogeneity. The recent data show it to have a temperature varying between -0.90 and -1.02°C, the colder temperature being found in the northern parts of the basin. NANSEN [1906] described it as being between -1.0 and -1.1° in the early years of the century with somewhat colder temperatures present in the north The recent salinity values of between 34.89 and 34.95 °/oo agree with those reported by Nansen.

At Station B the surface temperature was -0.9° with a salinity of 34.93 °/oo (Table 1). Had the water been homogeneous throughout the column, the early theory would finally have been supported by field data. However, at Station B the shallowest subsurface observation (44 m) showed a temperature of -0.47° and a salinity of 34.88 °/oo. The σ_t at this level was 28.05 compared with a surface σ_t of 28.12. At 1420 m, bottom water conditions were present.

The surface density inversion at both Stations B and C (Table 1) is caused by high surface salin ty as well as low temperature. No ice was being formed at the surface at the time, there is no evidence of overturning within the water column, and the water just below the surface is less rather than more saline. It is thus apparent that the overturning mechanism as described by Nansen and Helland-Hansen for increasing the salinity of the water being cooled at the surface is not in operatio here. Instead, the surface water of high salinity must have come from the region to the east where surface values of over 35.00 °/oo are evidence of North Atlantic Water (see Station D, Table 1). The low surface temperature is due to local cooling.

In comparing the surface and bottom water characteristics in Station B, two things should be kept in mind. First, the surface temperature was observed only to the nearest tenth of a degree whereas the bottom water temperatures were observed to a hundredth, and second, surface water

Table 1--Data on the bottom water in the Norwegian Basin

Depth	Temperature	Salinity	σ_t	O_2 saturation	Depth	Temperature	Salinity	σ_t	O_2 saturation
m	°C	0/00		pct	m	°C	0/00		pct
	Station B, March, 1951					Station C, March, 1951			
0	-0.9	34.94	28.12	98	0	-0.9	34.93	28.11	92
44	-0.47	34.88	28.05	71	41	-0.30	34.86	28.03	96
88	-0.48	34.87	28.05	73	84	-0.31	34.86	28.03	88
177	-0.50	34.88	28.05	70	170	-0.34	34.88	28.05	87
268	-0.53	34.86	28.04	71	259	-0.20	34.88	28.04	85
361	-0.22	34.92	28.07	65	351	-0.21	34.92	28.07	86
457	-0.35	34.90	28.06	66	446	-0.36	34.91	28.07	79
555	-0.47	....	....	..	497	-0.43	34.92	28.08	81
745	-0.64	34.90	28.08	74	669	-0.57	34.94	28.11	83
935	-0.80	34.89	28.08	63	843	-0.77	34.91	28.09	83
1130	-0.77	34.92	28.10	66	1200	-0.83	34.91	28.09	83
1420	-0.89	34.93	28.11	70	1568	-0.93	34.92	28.10	80
1720	-0.92	34.92	28.10	74	1949	-0.91	34.92	28.10	80
	Station D, March, 1951					Station E, April, 1951			
0	+2.30	35.04	28.00	97	0	+2.9	35.07	27.97	..
46	+2.43	35.06	28.01	95	86	+3.04	35.04	27.93	..
93	....	35.05	....	..	259	....	35.05	....	..
188	+2.41	35.05	28.00	94	440	+0.82	34.95	28.04	..
284	+1.05	34.95	28.02	90	624	-0.03	34.90	28.05	..
380	-0.11	34.89	28.04	84	815	-0.42	34.90	28.07	..
478	-0.29	34.91	28.07	84	1010	-0.64	....	....	..
587	-0.31	34.96	28.11	66	1207	-0.82	34.95	28.12	..
785	-0.57	34.93	28.10	76	1381	....	34.92	....	..
983	-0.70	34.93	28.10	75	1738	-0.93	34.92	28.10	..
1283	-0.87	34.93	28.11	78	2100	-0.95	34.94	28.12	..
1584	-0.94	34.92	28.11	77	2460	-0.96	34.94	28.12	..
1889	-0.95	34.91	28.10	74	2820	-0.95	34.93	28.11	..
	Station M, February, 1952								
0	-1.4	34.91	28.11	..					
49	-0.76	34.80	28.00	..					
96	-0.77	34.81	28.01	..					
187	....	34.85	....	..					
352	-0.60	34.87	28.05	..					
428	-0.45	34.90	28.07	..					
498	-0.17	34.89	28.04	..					
560	-0.68	34.88	28.06	..					
650	-0.75	34.88	28.06	..					
830	....	34.90	....	..					
1312	....	34.90	....	..					
1840	-1.02	34.91	28.10	..					
2400	-1.09	34.88	28.07	..					

at -0.9° would be heated adiabatically by 0.06° upon sinking 1500 m. However, it is felt that it is pertinent to point out the close similarity between the surface and bottom water at this station and also at Station C.

The temperature-salinity relationship of each surface observation and also of each observation from below 1500 m from a recent March-April cruise has been plotted in Figure 1. The individual points in the figure represent surface observations and, as expected, show a wide scatter. The deep observations fall into two closely bunched groups shown by the shaded areas in the figure. The area marked North Atlantic includes 11 deep observations from south of the Scotland-Iceland-Greenland Ridge. The area marked Norwegian Sea includes 18 deep observations from the Norwegian Basin. As can be seen, two surface observations, Stations B and C, fall directly within the shaded area representing the Norwegian Basin Bottom Water.

It should be mentioned that the area around Station B and C is one of very little horizontal circulation according to computations based on the circulation theorem, the density structures of the

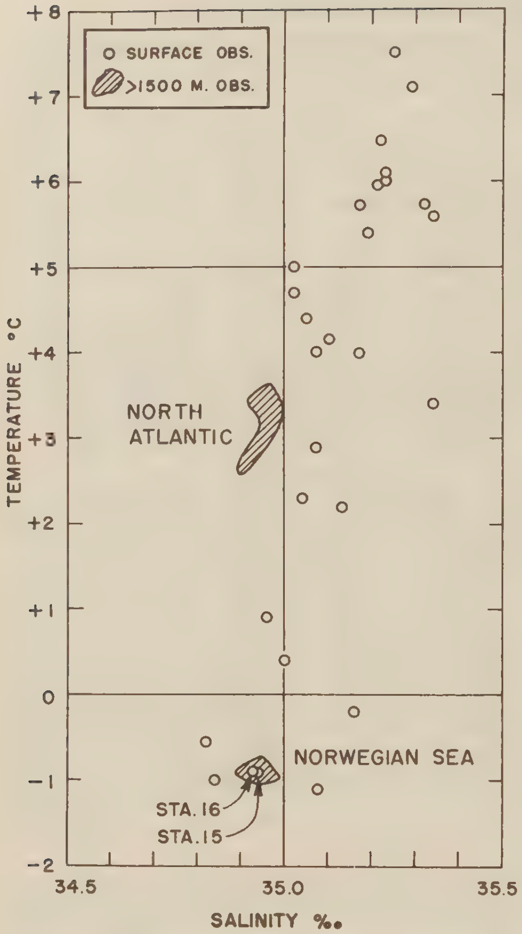

Fig. 1--Temperature-salinity correlation for 1951 cruise

water columns at the two stations and at station to the northwest and southeast being very simila

Although only at Stations B and C of the Marc April cruise might bottom water formation be suspected on the basis of surface conditions, these two were by no means the only stations showing unstably high surface densities. In a total of 30 stations for which the surface data ar available, 23 showed surface density inversions. Of these, 15 stations showed surface densities equal to or exceeding the density of the deepest water sampled at the station.

It is at stations exhibiting high surface densities that according to the early theory one woul expect to find a homogeneous water layer extendi well down the water column. Yet only rarely wa homogeneity found even between the surface and the shallowest subsurface observation, and in thes few cases there was no question of bottom water formation taking place, the surface water being either much too fresh or much too warm.

During a January-February cruise the following year, the occurence of surface density inversions was not nearly as wide-spread as it had been during the previous March-April cruise. In 49 stations for which surface data are availabl 21 showed such inversions and only one, Station had a surface temperature and salinity such that bottom water formation might be suspected (see Table 1). It will be noted that the bottom water a this station, which was in the area north of Jan Mayen, is about 0.1° colder than that observed south of that island.

If it is hypothesized that the frequent occurrence of the density inversions during the March-April cruise is associated with the production at the surface of water destined to sink to a deeper level, then it can be further hypothesized that onl the preliminary stages of this process would be i evidence during the January-February cruise if the theory of Helland-Hansen and Nansen is correct as to the season during which such formation takes place. Fitting in with this is the fact that it was at the far northwestern station (Station M), where winter conditions may be presumed to be the most advanced, that surface water was found in February which might conceivably be associated with bottom water formation.

Thus the recent data support Helland-Hansen's and Nansen's theory on bottom water formation except that evidence of the formation of an homogeneous water column is lacking. Even if the supposed overturning were very slow and came about only after a considerable lag as suggested by Nansen, it seems strange that none of the recent observations shows a homogeneous water layer which appears to be related with bottom water formation. This naturally gives rise to the question of whether there is some explanation possible to account for the sinking of this water other than by the gradual overturning within the column.

Figure 2 presents temperature, salinity and σ_t profiles in a northwest-southeast section across the Norwegian Basin between Iceland and Jan Mayen which includes Station B and C. The interpretation of the data given in this figure demonstrates a path along which the cold saline surface water noted at Stations B and C could flow into the bottom water along the isopleths. The exact thickness of such a flow is, of course, not known.

It could be speculated that somewhere in the 75 mi separating Stations B and C a homogeneous water column exists as a result either of vertical flow or overturning as described by Helland-Hanse

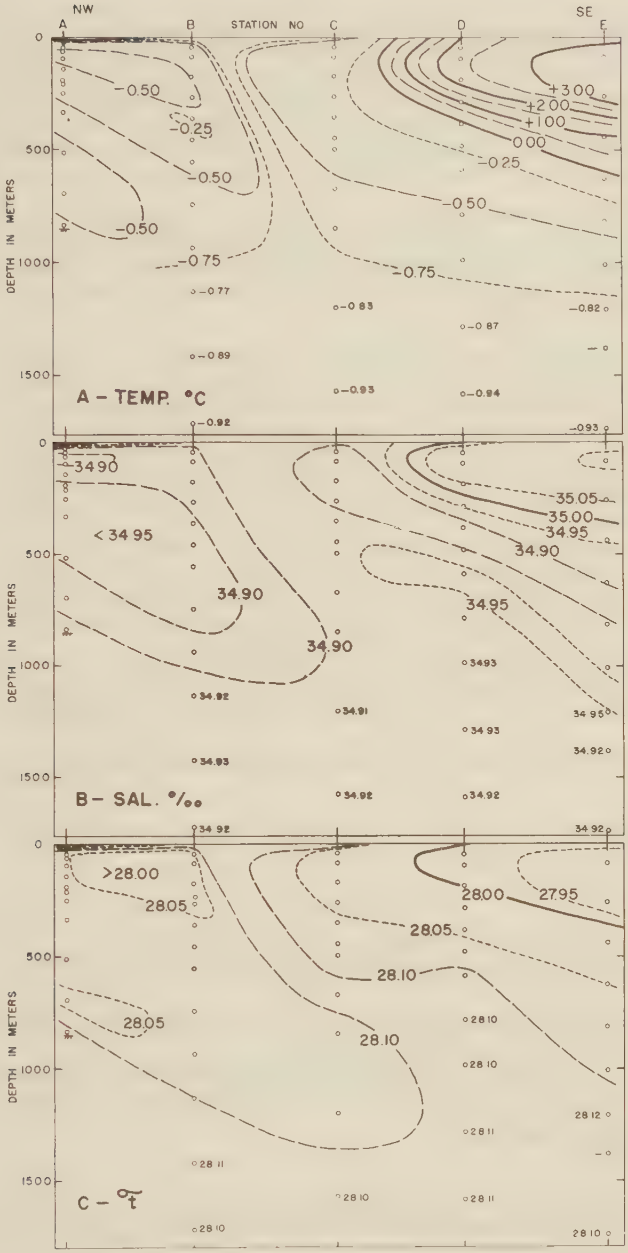

Fig. 2--Temperature, salinity, and σ_t profiles from March-April cruise

and Nansen. However, the particular interspersal of lighter and heavier water layers at those two stations appears to indicate a horizontal component to the flow. In fact, the horizontal component may be by far the dominant one, a point which is obscured by the exaggerated vertical scale used in the profile. It is interesting to note that a flow of water could take place reaching from the surface to a depth of 1500 m between Stations B and C along a path tilted only 0.6° from the horizontal.

Contribution No. 740

TURBULENCE AND SHEARING STRESSES MEASURED OVER THE NORTH ATLANTIC OCEAN BY AN AIRPLANE-ACCELERATION TECHNIQUE

By Andrew F. Bunker

Woods Hole Oceanographic Institution[1]

(Manuscript received 8 December 1954)

ABSTRACT

A method of measuring the horizontal and vertical turbulent components of the wind has been developed to meet the need for these measurements over the open ocean. An anemometer, a vertical accelerometer, and a gyroscope mounted in an airplane (U. S. Navy PBY-6A) yield simultaneous records of the total air-speed, vertical accelerations, and the attitude of the airplane. From these records, and from airplane-lift theory and the characteristics of the particular type of aircraft, the vertical and horizontal fluctuations of the wind, the root-mean-square deviation velocities, and the shearing stress can be computed. The method allows the phugoid oscillations of the airplane to contribute nearly periodic velocity terms to both components; these must be eliminated by a computational step. A different reduction method can give phugoid-free vertical velocities, but an additional instrument will be required for phugoid-free horizontal velocities. The airplane lift has a response of from 80 to 100 per cent to gusts of radius 20 meters or more, and the method fails to measure reliably gusts larger than 350 m. This limits the contributions to the quantities presented to those by gusts within the 20- to 350-m range. In the lower levels of polar-continental air masses, root-mean-square vertical velocities have been observed to attain 191 centimeters per second over land and 120 cm/sec over water, while stresses reached maxima of 16.6 dyne/cm^2 over land and 3.8 dy/cm^2 over water. Shearing stresses in the lowest 60 m in the trade winds averaged 0.2 dy/cm^2 over seven days, while vertical velocities averaged 26 cm/sec. The influence of atmospheric stability and convective activity upon the turbulent velocities is discussed.

1. Introduction

The present investigation was carried out to develop a satisfactory means of measuring atmospheric turbulence in regions not accessible to ground-based instruments. Emphasis has been placed on developing a rapid means of computing total stresses and turbulent components, so that a large number of samples may be obtained and reduced for use in a study of air-mass modification and turbulence structure in the atmosphere over the ocean. Spectral analysis of the turbulent components has not been attempted, although data have been made available to other workers interested in the basic nature of atmospheric turbulence. The next three sections of this article are devoted to an explanation of the physical principles on which the method is based, of the computational steps followed, and the estimated errors. In the last section, turbulence and stress measurements obtained over the western North Atlantic Ocean are presented.

Horizontal and vertical components of the wind are computed from the aircraft records. As a measure of the turbulence, the root-mean-square velocities have been formed from the turbulent components. The shearing stresses have been formed by averaging the cross products of the horizontal and vertical components of the wind fluctuations. Reynolds (1895) first showed the importance of these cross products, when he redeveloped the Navier-Stokes equations for a turbulent atmosphere. In his equations, the products appeared as apparent stresses which have been shown to be orders of magnitudes larger than laminar stresses. For many years after Reynolds' work, relatively few determinations of the turbulent stresses were made; but in recent years, superior instruments have been developed and many workers are engaged in the measurements and analysis of this quantity. If the stresses and wind shear are known, the eddy viscosity of the air mass can be determined from the Newtonian friction law. This law may be written as follows to describe a turbulent atmosphere:

$$\mu = \tau/(dU/dz) = -\overline{\rho u'w'}/(dU/dz). \qquad (1)$$

Here μ is the eddy viscosity, dU/dz the vertical shear of the mean horizontal wind, u' and w' are the horizontal and vertical components of the rapid fluctuations of the wind, τ is the shearing stress, and the bar denotes a time average. Similarly, the roughness coefficient c, defined by

$$\tau_0 = c\rho U_a^2, \qquad (2)$$

may be found if the shearing stress at the lowest determined level is assumed equal to τ_0, the surface stress, and U_a, the horizontal speed at anemometer height is known. More generally, the stress at any height may be referred to the gradient wind squared,

---

[1] Contribution No. 740 from the Woods Hole Oceanographic Institution. This research was conducted under a contract with the Office of Naval Research.

to obtain a value of c representative of the atmospheric condition at any height. The values of c obtained in this manner may be compared with laboratory experiments such as Laufer's (1950).

The hope of using the airplane for studies of the basic nature of atmospheric turbulence depends upon the development of means of obtaining more reliable measurements throughout the turbulence spectrum. Other workers (see Press and Mazelsky, 1953) have been attacking this problem with the aid of generalized harmonic analysis and airplane frequency-response functions. Their success with this approach may well lead to a more satisfactory theory in the free atmosphere.

The problem of finding τ and μ resolves itself into obtaining a suitable series of simultaneous values of w' and u' and a corresponding value of dU/dz. This problem has been solved satisfactorily by analyzing and accounting for the flight and lift characteristics of the airplane, and by installing a pressure anemometer, a vertical accelerometer, a gyroscope, and a drift sight on the airplane. Reduction of the observations in accordance with lift theory yields the desired velocity fluctuations. Numerous tests were conducted to prove that the values found were true shearing stresses and not meaningless values reflecting an instability in the flight of the aircraft. The complications introduced by the phugoid motion of the airplane are eliminated from the turbulence values, but only at the cost of losing the atmospheric contribution in the large-gust range.

The aircraft used for this study is a U. S. Navy, two-engined patrol bomber of the amphibian type, denoted PBY-6A. Several characteristics of this nearly obsolete airplane make it ideal for meteorological studies of this nature. As it is a very slow airplane, cruising at about 110 kn, temperature and humidity elements can respond to smaller-scale fluctuations than they would if mounted on a faster aircraft. The rigidity of the wing and fuselage is far greater than on other transports or bombers. This characteristic has been a great help in the reduction of data, since wing flutter and fuselage oscillations are negligibly small.

2. Application of simplified airplane-lift theory to computation of vertical-velocity fluctuations

Whenever an airplane flies through a turbulent air mass, the airplane experiences a rapid succession of changes in angle of attack and speed of the apparent air flow. The effect of these changes is to modify the lift of the airplane, producing irregular vertical motions of the airplane. Recorded vertical accelerations of the airplane and recorded changes in the indicated airspeed can be used to compute the variations in the angle of attack. From these quantities, determinations of gust velocity can be made. Their significance and trustworthiness depend to a great degree on the simplifying assumptions made concerning the flight of the airplane and its reaction to gusts. A vast amount of work, both theoretical and observational, has been done by aerodynamicists (see Durand, 1935) on the performance of aircraft.

The incremental lift equation applicable to the gust problem (see Duncan, 1952), derived from the definition of the lift coefficient,

$$L = \tfrac{1}{2}\rho V^2 S C_L, \tag{3}$$

is

$$\Delta L = \tfrac{1}{2}\rho S \left(V^2 \frac{dC_L}{d\alpha} \Delta\alpha + 2VC_L\,\Delta V \right), \tag{4}$$

where ΔL is the change in the lifting force of the airplane, ρ the density of the air, S the effective wing area, V the true air speed, C_L the coefficient of lift, and α the angle of attack.

Conditions required for the correct application of this equation to the determination of gust velocities are as follows:

1. The airplane is a rigid body.
2. The attitude of the airplane does not change.
3. A steady flow has been established over the airfoils.
4. The airplane flight is level, rectilinear and properly trimmed.
5. The gust is sharp-fronted and symmetrical across the span of the wing.

The PBY and its performance have been investigated to see if they fulfill these conditions. Whenever they failed to fulfill one and consequent large errors could be expected in gust determination, the situation was studied to determine whether an additional instrument would rectify the failure.

Comparisons by Brewer (1954) of accelerometer records with records of strain gauges attached to the PBY's struts showed that the PBY has an essentially rigid body. An additional check is the wing-period rule of Kordes and Houbolt (1953), which shows that the PBY may be considered rigid for all gusts larger than 18 m.

The problem of a changing attitude was solved by adding a recording gyroscope to the airplane's equipment. From the record of this instrument, the effect of attitude changes is eliminated from the vertical-velocity computation [see (8)].

The condition of a steady circulation around the airfoil can never be fulfilled in a turbulent air mass, but the observations may be treated in such a way as to minimize this failure. Donely (1949), in a study of gust loads on airplanes, discusses the results of many workers in the field of non-steady flow. He presents graphs of the ratio of the non-steady flow circulations and lift coefficients as functions of gust penetration in wing-chord lengths, *i.e.*, the fore and aft dimension. This ratio rises from zero outside the gust to about 0.85 at 5 chord-lengths penetration, and to nearly 1 at 10 to 15 chord-lengths penetration.

To arrive at an average value of the transient lift ratio that can be applied to the measured accelerations, the atmospheric turbulence may be considered to be composed of a complete spectrum of sharp-fronted gusts. As many of the different-sized gusts will be affecting the lift simultaneously, it is obvious that all degrees of gust penetration are also present simultaneously. A satisfactory ratio has been determined by averaging the ratios given by Donely over 0 to 200 chord-lengths penetration into a gust. Weights proportional to the value of the accelerations for each degree of gust penetration were found from the acceleration record of a flight through an atmosphere with a turbulence typical of that desired for study. The weighted average ratio determined was 0.88. If we correct the measured acceleration increment, Δn, for this diminution due to unsteady flow, we have

$$\Delta n_{\text{true}} = 1.1\ \Delta n_{\text{meas.}} \tag{5}$$

If the airplane is not flying level and rectilinear in accordance with the fourth assumption, a mean value of the acceleration that is other than zero will be recorded. Whenever the airplane describes a smooth arc either in the vertical or horizontal plane, the resulting mean acceleration can be eliminated in the computation and will have no effect upon the final computation.

A more difficult problem is the unstable oscillatory flight of the airplane called "phugoid motion" [see Durand (1935) or Duncan (1952)]. This pendulum-like motion of the airplane arises whenever a perturbation upsets the balance between the lift of the airplane and the force of gravity. At the beginning of the present study, ΔV_t was defined arbitrarily as a deviation from the average of the previous 10 sec. Later this definition was found to allow phugoid motion to affect the final computation of w' and u'. Definition of ΔV_t as the deviation from the proper equilibrium velocity can be demonstrated to give phugoid-free vertical velocities. The horizontal velocity requires an additional instrument, such as an accelerometer or camera, as well as the deviation from the equilibrium velocity. The original computing method has been adhered to throughout the present article, so that the horizontal and vertical turbulent components would be consistent.

The effect of phugoid motion has been eliminated from the computed quantities by subtracting values averaged over a quarter period of the phugoid oscillation from the instantaneous values of the turbulent components. This step has been used as an approximation to subtracting a properly phased and damped curve, representing the phugoid influence, from the instantaneous values. It does have the great disadvantage of reducing to zero any contribution of atmospheric gusts of larger sizes. Since the quarter period of the PBY's motion is about 7 sec, the contributions from gusts greater than 350 m in radius are lost. The effective range of gust contribution with the present equipment and method of reduction is from 20 to 350 m.

From the data obtained by the airplane method, two values may be found for each quantity. One represents the turbulence plus the fictitious quantity added by the phugoid motion. The other value represents the turbulence with both the phugoid contribution and the atmospheric contribution of gusts larger than 350 m subtracted. A comparison shows that in most cases there is a surprisingly small difference between the two values, although a few cases show decreases of about 45 per cent.

Adverse effects upon the vertical-velocity computation resulting from asymmetry of the gusts are of a rather minor nature. This is so because the smallest gusts cannot change the circulation about the wing enough to change the lift measurably. Therefore only gusts large enough to change the lift have any significant influence upon velocity computation, and the probability of the large gusts affecting the airplane symmetrically is correspondingly larger.

As the accelerometer records the accelerations normal to the flight of the airplane, (4) may be rewritten in terms of this normal acceleration, Δn, and the mass, M, of the airplane:

$$\Delta n = \tfrac{1}{2}\rho(S/M)\left(V^2\frac{dC_L}{d\alpha}\,\Delta\alpha + 2C_L V\,\Delta V\right). \tag{6}$$

The factor $\Delta\alpha$ may be broken down into its three components: $\Delta\alpha_{\text{turb}}$, the change in angle of attack due to the turbulent gusts; $\Delta\alpha_{\text{att}}$, the change in angle of attack due to the varying attitude of the airplane; and $\Delta\alpha_{\text{ap}}$ the change in angle of attack due to the vertical motions of the airplane. Since $\sin\Delta\alpha \approx \Delta\alpha$ for small angles, $\Delta\alpha_{\text{turb}}$ may be written as w'/V_t, where w' is the vertical velocity of a gust, and V_t is the instantaneous value of the true air speed. Likewise, $\Delta\alpha_{\text{ap}}$ may be written $-W_{\text{ap}}/V_t = -(\Sigma\,\Delta n\,t_i + w_0)/V_t$, where W_{ap} is the vertical velocity of the airplane, w_0 the initial vertical velocity of the airplane, and t_i is the time of the individual observation. Proof that a summation of individual $\Delta n\,t_i$'s gives a sufficiently accurate value of W_{ap} is given by Brewer (1954), who determined W_{ap} both by integrating accelerations and differentiating the altitude record. Differences between $\Sigma\,\Delta n\,t_i$ and W_{ap} may become significant if the attitude of the airplane changes rapidly, so that $V_t(d\theta/dt)$ is large in comparison with Δn.

Equation (6) may be solved for w' by making the above substitutions and cancelling V_t against V, which is now identified as the average true airspeed. Noting that the lift of the airplane equals Mg, we obtain

$$w' = \frac{\Delta n\, M}{\frac{1}{2}\rho V S (dC_L/d\alpha)} - \frac{4Mg\, \Delta V_t}{\rho V^2 S (dC_L/d\alpha)} - \Delta\alpha_{\text{att}}\, V_t + \Sigma\, \Delta n\, t_i + w_0. \quad (7)$$

This equation gives the vertical velocity of the gust in terms of the vertical accelerations of the airplane and changes in airspeed and attitude.

Applying the non-steady flow factor to the Δn of (7), and substituting the values of the constants for the PBY-6A, we obtain

$$w' = 4.98 \frac{\Delta n}{\rho V} - \frac{8.9 \times 10^3\, \Delta V_t}{\rho V^2} - \Delta\alpha_{\text{att}}\, V_t + \Sigma\, 1.1\, \Delta n\, t_i + w_0. \quad (8)$$

The values entered into (8) are as follows: $M = 1.34 \times 10^7$ g (varies with gas load, *etc.*, $\pm 0.05 \times 10^7$ g), $S = 1.30 \times 10^6$ cm², and $dC_L/d\alpha = 4.54$. The value of $dC_L/d\alpha$ was determined for the PBY-6A, loaded and equipped in a manner similar to the loading during observational runs, by flying at various attitudes and velocities and plotting the computed lift-coefficient against angle of attack.

3. Computation of velocity fluctuations, root-mean-square velocities, and shearing stresses

In development of the system of stress measurement, each (1/5)-sec average of the observed quantities was measured, reduced, and deviations from lines of regression and averages were formed in accordance with (8). The final squares and cross products were formed from these values. Later, once the system was established, short cuts were introduced that reduced the work by a factor of five without reducing the accuracy of the computation.

Values of ΔV_t and $\Delta\alpha_{\text{att}}$ to enter into (8) were found by computing deviations from the average of the preceding 10 sec. The V_t entered in (8) is formed from the deviations from the average velocity plus an average velocity indicated by the aircraft's pitot-tube airspeed indicator. The coefficient of the $(\Delta n)/\rho V$ term should be determined for each series of runs according to the weight of the airplane at the time. Therefore, a record of the gas load of the airplane is necessary.

The value of u', the horizontal turbulent component of the wind, is defined as deviation from the mean horizontal component of the measured airspeed. As a pitot tube measures total airspeed, the horizontal component should be found from the vector difference of w' and V_t. However, as even maximum values of w' are small (about 1/50) compared to V_t, u' is approximately equal to $V_t - \bar{V}$, or $\bar{V} - V_t$ in the case of downwind runs.

One source of difficulty in the stress determination is that the airplane accelerates and decelerates with the gusts. From the power requirements of the PBY listed in the *Navy Pilots Handbook*, the deceleration can be computed. A PBY flying 120 mi/hr (true airspeed) at 1000 ft, and weighing 29,000 lb, will decelerate 1 cm/sec² if it encounters a sudden increase of head wind speed of 2 m/sec. From this computation, it will be seen that shearing stresses determined from short-period (≈1 sec) fluctuations will be valid; but determinations of longer-period (≈30 sec) fluctuations are subject to uncertainties over and above those introduced by phugoid motion. A camera is being adapted to photograph the ground or sea surface through the ship's drift meter. If such a device is used in conjunction with the recording altimeter, the ground speed of the airplane may be computed each second. From these observations, the long-period fluctuations can be measured with assurance, as the inertia of the airplane is no longer depended upon for the horizontal velocity computation. This problem is of the utmost importance, as Panofsky and Singer (1951) have shown that the larger gusts contribute a large portion of the total shearing stress.

The reduction of the observations to individual values of w' and u' is very laborious, so a short-cut method was devised which allows faster calculations of $w'u'$, w'^2 and u'^2 without an appreciable sacrifice of accuracy. The short cut takes full advantage of the graphic nature of the traces and use of reading scales. A scale is made up in terms of $[(1.1\, M)/(\frac{1}{2}\rho V S\, dC_L/d\alpha)]\, \Delta n$, so that the first term of (8) can be read directly from the record. The $\Sigma\, 1.1\, \Delta n\, t_i$ term can be summed on a calculator and entered on the reduction sheet during the reading process. Similar scales are made for reading the velocity term of (8). In the case of the $\Delta\alpha_{\text{att}}$ term, a special plastic scale is used so that one can read directly the product of $\bar{V}_t$ times the deviation of the attitude from the 10-sec average, since $\Delta\alpha\, V_t \approx \Delta\alpha\, \bar{V}_t$.

From these readings, values of w_i and u_i, the instantaneous velocities, can be formed. They are not the desired turbulent deviations, w' and u', but the sums of deviations from a line of regression plus the value of the point on the line of regression plus an average value not necessarily zero. Thus,

$$w_i = \bar{w} - a t_i + w', \quad (9a)$$

and

$$u_i = \bar{u} - b t_i + u', \quad (9b)$$

where a and b are the slopes of the lines of regression of w and u upon time. From these equations, mean square velocities and mean cross products can be computed without the necessity of forming the deviations from the line of regression. The following three equations for the means are exact:

$$\overline{w'^2} = \overline{w_i^2} - \bar{w}^2 - a^2\overline{t^2}, \quad (10a)$$

$$\overline{u'^2} = \overline{u_i^2} - \bar{u}^2 - b^2\overline{t^2}, \quad (10b)$$

and

$$\overline{w'u'} = \overline{w_i u_i} - \bar{w}\,\bar{u} - ab\bar{t}^2. \qquad (10c)$$

It will be seen that the conditions $\overline{\Delta n} \neq 0$ and $\overline{\Delta V_t} \neq 0$ affect only the values of $\bar{w}$, $\bar{u}$ and a, but not $\overline{w'^2}$, $\overline{u'^2}$ and $\overline{w'u'}$. Similarly, any vertical velocity that the airplane may possess at the beginning of the run will be included in the value of $\bar{w}$. If attitude variations become too extreme (>2 deg) in certain parts of the run, those parts either may be discarded or, if used, accepted as unreliable. In the roughest air, $(\overline{w'^2})^{\frac{1}{2}} >$ 150 cm/sec, even larger variations do not make the computations invalid.

The effect of the phugoid motion plus the atmospheric contribution in the quarter-period range can be eliminated with a minimum of computation by the following equations:

$$\overline{w^2{}_{(s-m)i}} = \overline{w_i{}^2} - \overline{w^2{}_{mi}} \qquad (11a)$$

$$\overline{u^2{}_{(s-m)i}} = \overline{u_i{}^2} - \overline{u^2{}_{mi}}, \qquad (11b)$$

and

$$\overline{w_{(s-m)i}\, u_{(s-m)i}} = \overline{w_i u_i} - \overline{w_{mi} u_{mi}}. \qquad (11c)$$

In these equations, $w_{(s-m)i}$ and $u_{(s-m)i}$ are defined as the difference of the instantaneous velocities from the quarter-period mean, and w_{mi} and u_{mi} are the quarter-period means.

Before discussion of the observational results, it is desirable to check the order of accuracy of the computed quantities. Probable errors due to reading, calibration and instrumental inaccuracies are small. This probable error for a shearing stress determination from 150 observational points is estimated to be ±0.1 dy/cm². Probable errors for $(\overline{w'^2})^{\frac{1}{2}}$ and $(\overline{u'^2})^{\frac{1}{2}}$ are ±2 cm/sec and ±1 cm/sec. These values represent the accuracy of the measurements exclusive of the effects of phugoid motion, airplane deformation, and unsteady lift. The effects of airplane deformation are small, since the strain-gauge tests showed the assembly of the fuselage, struts and wing center-panel to be very rigid. It is possible that the higher-frequency gusts have a 5 per cent amplification factor for a fuselage-mounted accelerometer. For lower-frequency gusts, this error must be nearly zero. The unsteady lift of the wings in first penetrating a gust adds an uncertainty factor to the acceleration measurements. The 1.1 correction factor for unsteady lift described earlier was not rigorously determined or proven. The error arising from this source may be estimated to be half the correction itself or ±5 per cent. When (11) is used, little or no error due to the phugoid motion of the airplane is introduced. If (10) is used, errors of an individual run due to phugoid oscillations may remain small or become as high as 100 per cent. This wide range in error depends on whether the airplane happened to start oscillating or not and points up the necessity for eliminating the long-period variations by use of (11). The objectiveness of (11) is preferred at the present time to any subjective method of evaluating the contribution of phugoid motion and eliminating it from the result.

Table 1. Shearing-stress comparisons, O'Neill, Nebraska, August 1953.

	Johns Hopkins stresses		PBY stresses		
Date	Time (CST)	Stress (dy/cm²)	Time (CST)	Altitude (m)	Stress (dy/cm²)
22	1400–1500	2.5	1450	30	0.1
24	1900–2000	0.8	1547	30	0.2
25	1000–1100	2.6	1045	30	2.1
25	1600–1700	2.6	1650	18	1.8

An opportunity to compare the w' measurements of the airplane method with the tower-based sonic anemometer of the University of Wisconsin was arranged on 25 August 1953 over the flat plains of Nebraska. Dr. Verner Suomi had his anemometer mounted at 12 m, while the PBY flew past the tower twice at an altitude that turned out to be 6 m higher than the anemometer height. The sonic anemometer gave 19 per cent higher readings of $(\overline{w'^2})^{\frac{1}{2}}$ than did the airplane data when reduced in accordance with (10a). If no line of regression is used, the airplane values exceed the anemometer values by 10 per cent. The closeness of the agreement confirms the reliability of the system. With exclusion of phugoid motion and the effects of gusts larger than 350 m, by means of (11a), from the PBY measurements, the sonic anemometer gives values 30 per cent higher.

A confirmation of the ability of the airplane method to measure shearing stresses is given by a comparison of PBY values to stresses obtained by the Johns Hopkins University Laboratory of Climatology group at O'Neill, Nebraska, in August 1953. The project used the Sheppard type shear-meter mounted flush with the level grass-covered ground. All available comparisons are listed in table 1. The PBY stresses listed are corrected for phugoid motion. It is seen that the airplane values have a lower average than the shear-plate values and have a larger scatter. The lower values arise from the dropping off of shear with height and the loss of the contributions of the large-scale gusts. The poorest agreement occurred on 22 August, when the double-theodolite pilot-balloon observations of the U. S. Air Force showed the wind to be stratifying into layers of zero and negative gradients. The large scatter may arise from too small a sampling of the atmosphere by the airplane. All this considered, the table is accepted as additional confirmation of the reliability of the method.

4. Observing procedures and aircraft instrumentation

Observations for the shearing-stress computation were taken during short horizontal flights lasting 1 or 2 min. Many of these horizontal runs were made during vertical helical soundings to obtain temperatures and humidities. As the sounding progressed to a selected altitude, the airplane was leveled and flown upwind. During this upwind run, complete records of the airspeed, normal accelerations, and attitude were obtained. Also, if no pilot-balloon observations of the wind were available, drift-sight readings were made during the run and again after the airplane had turned 90 deg. After the run was completed, the vertical sounding was continued on up to the next level at which a turbulence measurement was desired.

At the beginning of each turbulence run, care was taken in trimming the airplane for rectilinear level flight and in damping oscillatory motions. After several runs with and without the auto-pilot in operation, it was found that the pilot could control the attitude of the airplane sufficiently well for the work at hand, and considerable time was saved by not resetting the control for each run. A standard pilot's attitude-indicator was modified and connected to a gyroscope potentiometer, so that a greatly magnified indication of the ship's attitude was available to the pilot.

One observer is stationed in the bunk compartment of the PBY, where he can operate the oscillograph, calibrate, and adjust the sensitivities and zero positions of the instruments. Another observer is required in the navigator's compartment, to operate a psychrograph, use the drift meter, record altitudes and airspeeds, and direct operations.

Only a brief description of the equipment installed in the PBY will be given here, as a complete report of the PBY and its instrumentation has been written.[2] The final instruments used in the study are an electric pressure-gauge anemometer, an electric accelerometer, a gyroscope and a dry-bulb thermopile. The thermopile was installed to allow the computation of heat transports from the cross products of w' and T'. The Statham electric accelerometer is mounted rigidly near the center of gravity and perpendicular to the plane of level flight. The pressure gauge is mounted on the bulkhead of the navigator's compartment, in a horizontal cross-ship position to minimize the effects of accelerations. The gyroscope, a unit from an auto-pilot system, has been connected to send a voltage signal of the ship's attitude to the oscillograph, the pilot's attitude indicator and to a meter on the observer's control panel. This oscillograph control-panel is mounted over the bench in the bunk compartment. Only one recorder, a nine-galvanometer oscillograph, is used for the turbulence measurements. The outputs of all the gauges record photographically on a chart 5-in wide. A self-balancing potentiometer is installed to record the dry- and wet-bulb temperatures of the air.

5. Presentation and discussion of data

During the development of the airplane technique of measuring turbulent components, many shearing-stress runs were made and their results will be given here together with other computed and supplementary quantities. A discussion of the significance of the observations is given. The earliest observations were made with rather crude equipment, and their reliability is lower than that defined in the previous section. The first observations taken with the oscillograph arrangement as described were obtained in March 1953 in the trade-wind region. Minor changes have been made from that time on, but the over-all accuracy has remained about the same.

29 June 1952 observations, Atlantic Ocean north of San Juan, Puerto Rico.—Twelve turbulence runs were made on this day at various altitudes in the trade-wind current. The accelerations were measured with a water-column accelerometer, while the wind fluctuations were determined with a hot-bead anemometer mounted about a meter ahead of the forward gunner's turret. The attitude recorder had not been constructed at this time, so the third term of (8) could not be evaluated. In spite of these shortcomings, the deviations of w' and u' from 7-sec averages are believed to be reliable.

The weather on this day was disturbed easterly flow resulting in extreme convective activity over the ocean and thunderstorms over Puerto Rico. The first seven runs were made in a large clear area about 40 mi north of San Juan. This area was about 10 mi in diameter

TABLE 2. Shearing stress and turbulence, 29 June 1952, North Atlantic north of San Juan, P. R.

Run	Height (m)	Sky condition	$(\overline{w'^2})^{\frac{1}{2}}$ (cm/sec)	$(\overline{u'^2})^{\frac{1}{2}}$ (cm/sec)	Stress (dy/cm²)	Wind (m/sec)	Eddy viscosity (g cm⁻¹ sec⁻¹)	Roughness coef. × 10⁴
1	1460	Clear	7	28	0.1	9.6	—	1
2	960	Clear	20	19	−0.2	8.6	—	3
3	640	Clear	24	29	0.3	9.0	—	4
4	320	Clear	11	14	0.1	6.4	17	1
5	160	Clear	53	31	0.7	6.6	78	9
6	60	Clear	24	34	0.4	6.6	27	5
7	15	Clear	37	44	1.0	5.3	50	12 (30)
8	580	Cloudy	33	32	0.0	9.9	—	0
9a	320	Lge Cu overhead	47	81	−0.9	7.2	neg.	9
9b	320	Clear overhead	29	23	0.4	7.2	67	5
10	160	Cloudy	44	60	−0.4	9.2	neg.	5
11	60	Cloudy	39	89	0.2	5.5	13	3
12	15	Cloudy	40	54	0.1	4.5	5	1 (5)

---

[2] Unpublished manuscript, Woods Hole Oceanographic Institute, Reference Number 54–82.

and had only a few small cumulus clouds with only slight vertical development. Runs eight to twelve were made in a region where the cumulus clouds covered a large fraction of the sky and frequently developed into cumulonimbus clouds.

During these runs, two observers were making independent drift-sight runs, so the average winds at the different altitudes in the area are known quite accurately. Knowledge of the wind gradient allows computation of the eddy viscosity and roughness coefficients from the shearing stress. The turbulence values observed have been studied in relation to the vertical distribution of the potential temperature and mixing ratio. A shallow ground layer extending to 300 m was topped by a thin wafer of warmer drier air. Above this wafer, the air was stable and progressively drier to the 1200-m level, where a stronger inversion existed. Above this level, the air continued to get warmer and drier. The average wind speed as observed by drift sight shows a rapid increase with height in the lowest 300 m and a more moderate shear above this level.

The computed values are entered in table 2. Columns 1, 2 and 3 give the run number, height in meters, and the sky conditions above the airplane. Columns 4 and 5 give the vertical and horizontal root-mean-square velocities. Column 6 gives the shearing stress of the atmosphere. Column 7 gives the average drift-sight winds. Column 8 gives eddy viscosities computed from (1). Column 9 gives the roughness coefficient computed from (2), but with use of the gradient wind in place of the anemometer-height wind. The values in parentheses at the 15-m level are computed from the wind at that level. The stability, defined as $[(dT/dz) + \Gamma]T^{-1}$ is given for the ground layer, here 0 to 300 m, and for the cloud layer, 300 to 1500 m.

Considering first the measurements made in the clear region, one sees that the shearing stress is high near the surface and decreases to low values at the higher levels, as predicted by turbulence theory and pilot-balloon measurements of the geostrophic departure. The $(\overline{w'^2})^{\frac{1}{2}}$ values show a slight increase with height in the lowest 150 m, and then decreases to the low value of 7 cm/sec at the highest level. On the other hand, the $(\overline{u'^2})^{\frac{1}{2}}$ values have the highest values at the lowest level and decrease with height to a minimum at 300 m. This phenomenon of increasing $(\overline{w'^2})^{\frac{1}{2}}$ and decreasing $(\overline{u'^2})^{\frac{1}{2}}$ in the lowest hundred meters of the atmosphere is a characteristic of the turbulence that reappears frequently in the measurements made to date. The characteristic sharp decrease of turbulence and stress above the ground layer is very pronounced in this set of values. The 320-m run was made just above the ground layer, and the $(\overline{w'^2})^{\frac{1}{2}}$ values dropped from 53 cm/sec in the ground layer to 11 cm/sec above the layer. The values of the eddy viscosity show considerable scatter, but the order of magnitude is well established.

Looking at the values measured in the area of cumulus and cumulonimbus, one sees that the turbulence and stress pattern has changed markedly from the clear-air pattern. The greatest change takes place in the stress values. Instead of an orderly decrease with height, the stress varies widely from 0.4 to −0.9 dy/cm^2, with a value of only 0.1 at the 15-m level. The sharp drops in $(\overline{w'^2})^{\frac{1}{2}}$ and $(\overline{u'^2})^{\frac{1}{2}}$ are noticeable at the top of the ground layer only in the case of run 9b, which was made in a small clear spot. Run 9a, which was made directly under a large cumulus cloud, shows an increase in both $(\overline{w'^2})^{\frac{1}{2}}$ and $(\overline{u'^2})^{\frac{1}{2}}$. One of the greatest differences between the clear area and the cloudy area lies in the great increase of $(\overline{u'^2})^{\frac{1}{2}}$ which is more than doubled.

The significance of the comparison is that the cumulus and cumulonimbus have a great effect upon the horizontal turbulence and the stress values in the ground layer below the clouds. These data clarify the findings of a previous expedition to the trade-wind region, described by Bunker *et al* (1949). In that report, it was shown that no significant increase in the vertical turbulence occurred under the trade-wind cumulus. From the present data, it is seen that a disturbance in the ground layer does exist, but most of the increase in turbulent energy lies in the horizontal component. The table shows that in the ground layer proper, that is, below the 300-m level, the vertical root-mean-square velocities increased only 8 per cent while the horizontal root-mean-squares increased 86 per cent. As the cumuli and cumulonimbi on this day were many times more vigorous than the normal trade cumuli, the disturbance of the trade cumuli to the ground layer must be proportionally smaller and close to the threshold of detection.

5 November 1952 observations, New Bedford, Weather Ship H, and Bermuda.—This flight to Bermuda was made just after a strong cold front passed the east coast of North America and Bermuda. The sky was clear over the land, but small cumuli appeared a few miles offshore and continued to increase until the sky was 8/10 covered at the location of the weather ship. Their tops were flattened by the stable layer which had risen from 1300 m over land to 2000 m in the region of the ship. Temperature and humidity measurements were made at New Bedford (Mass.), Weather Ship H, and Bermuda. Turbulence measurements were made at the weather ship and Bermuda.

The air that was measured at New Bedford arrived at Ship H some 7×10^4 sec later and was remeasured. From these measurements, the vertical flow of moisture was found to be 8.8×10^{-6} g cm^{-2} sec^{-1} and the coefficient of turbulent mass exchange to be 880 g cm^{-1} sec^{-1}.

TABLE 3. Stress and turbulence measurements, 5 November 1952, North Atlantic Ocean Weather Ship H.

Height (m)	$(\overline{w'^2})^{\frac{1}{2}}$ (cm/sec)	$(\overline{u'^2})^{\frac{1}{2}}$ (cm/sec)	Stress (dy/cm²)	Wind (m/sec)	Eddy viscosity (g cm⁻¹ sec⁻¹)	Roughness coefficient × 10⁴
1525	—	—	—	2.2	—	—
1220	33	42	0.1	2.2	neg.	2
915	84	61	−1.7	2.7	760	190
610	88	62	0.1	3.6	neg.	6
305	90	67	−2.6	4.5	1250	107
150	74	62	−0.8	4.9 (Sfc)	575	28
			20 km NW of Bermuda			
305	—	—	—	7.2	—	—
150	101	75	0.8	—	63	23
Sfc	—	—	—	3.6	—	—

Table 3 gives the turbulence and stress measurements. The winds were obtained from the weather ship and Bermuda rawin reports. A wave developed on the cold front to the east of the ship, causing NNE winds decreasing with height as shown in the table. The negative shearing stresses are consistent with the negative wind gradient. Values of the eddy viscosity were computed from the stresses and the wind gradients. They agree quite well with the mass exchange-coefficient computed from the moisture flow. The roughness coefficients were computed from the wind at the given height, since no definite gradient level was attained. The large scatter of stress and coefficient values probably arises from too small a sampling of the atmosphere and too rapid changes in the wind field.

It is of interest to note that the turbulence, as evidenced by the root-mean-square velocities, is much greater on this day than on 29 June 1952 off San Juan. The primary reason for this difference is found in the slight stability (2×10^{-8}) of the air at Weather Ship H as opposed to the greater stability (7×10^{-8}) in the San Juan region.

7 November 1952, 50 km SW of Bermuda.—By 7 November, the northwesterly flow of air had ceased and a strong southwest wind was blowing. A well defined ground layer had developed at 950 m, and a few tenths of the sky were covered by cumulus clouds with bases at about 700 m and tops around 1400 m. The stability of the air was slight (3×10^{-8}) in the ground layer, large (14×10^{-8}) in the cloud layer, and even greater (22×10^{-8}) above the clouds. The stress and turbulence values are given in table 4.

The measured stresses show the usual pattern of large stresses nearest the water surface, decreasing with height. The one negative stress at 305 m is inconsistent with the Bermuda wind profile but may be caused by local variations and a sample that is too small. The root-mean-square velocities follow the pattern of $(\overline{w'^2})^{\frac{1}{2}}$ being smaller than $(\overline{u'^2})^{\frac{1}{2}}$ at the 60-m level and larger at the higher levels. The vertical velocities increase in the cloud layer, rather than decrease as is usually the case. The reason for this is not apparent, although proximity to a cumulus tower may be the cause. It is of interest to note that the root-mean-square velocities are only about one-half the velocities observed on 5 November, when the wind speed was only about one third of this day's speed. The critical role of stability in suppressing turbulence is brought out by this comparison, for the stability on the 7th was only 1×10^{-8} greater than on the 5th.

16 March to 7 April 1953, Anegada Island, British West Indies.—The following series of observations of stress were made during cooperating expeditions to the West Indies by the meteorologists of Imperial College, London, under the direction of Prof. P. A. Sheppard, and the Woods Hole marine meteorology group. The purpose of the Imperial College group was to obtain pilot-balloon observations from which stress values were computed by the geostrophic-departure method. The pilot-balloon observations were made available to the Woods Hole group through the kindness of Prof. Sheppard. While the balloon runs were being made on Anegada, the airplane flew a few miles off the windward shore, making turbulence and stress runs or cumulus-cloud observations.

TABLE 4. Stress and turbulence measurements, 7 November 1952, 50 km SW of Bermuda.

Height (m)	$(\overline{w'^2})^{\frac{1}{2}}$ (cm/sec)	$(\overline{u'^2})^{\frac{1}{2}}$ (cm/sec)	Stress (dy/cm²)	Wind (m/sec)	Eddy viscosity (g cm⁻¹ sec⁻¹)	Roughness coefficient × 10¹
1850	—	—	—	16.6	—	—
1525	49	41	0.03	16.6	30	0.1
1220	52	39	0.13	16.2	430	0.4
915	31	58	0.44	16.1	1500	1.5
610	28	35	0.09	16.1	90	0.3
305	55	29	−0.32	15.6	—	1.0
150	38	33	0.47	—	31	1.4
60	48	61	1.08	—	54	7.7*
0	—	—	—	10.8	—	—

* Surface wind used.

Table 5. Stress and turbulence measurements, March and April 1953, north of Anegada Island, British West Indies.

Date	Time (GCT)	Height (m)	$(\overline{w'^2})^{\frac{1}{2}}$ (cm/sec)	$(\overline{u'^2})^{\frac{1}{2}}$ (cm/sec)	Stress (dy/cm²)	Wind (m/sec)	Eddy viscosity (g cm⁻¹ sec⁻¹)	Roughness coef. × 10⁴	Stability × 10⁸
16 March	1840	702	—	—	—	5.0	—	—	2
16 March	1913	610	9	10	0.02	4.9	15	0.7	2
16 March	1908	150	25	18	−0.12	5.4	indeter.	3	2
16 March	1837	78	—	—	—	5.4	—	—	2
18 March	1925	2160	18	10	−0.05	—	—	—	19
18 March	2000	1482	—	—	—	2.0	—	—	19
18 March	1915	1370	12	7	−0.02	1.6	neg.	0.8	
18 March	1910	610	30	19	0.20	7.5	22	3	0.0
18 March	1900	305	55	24	0.52	6.5	neg.	10	0.0
18 March	1850	150	40	30	0.71*	7.4	indeter.	11	0.0
18 March	1947	78	—	—	—	7.4	—	—	0.0
22 March	1750	1326	—	—	—	7.2	—	—	19
22 March	1640	1220	12	7	−0.01	7.7	2	0.1	19
22 March	1744	860	—	—	—	8.3	—	—	19
22 March	1630	760	17	12	0.00	7.8	0	0	19
22 March	1625	485	29	20	−0.07	7.5	neg.	1.0	2
22 March	1620	305	23	11	−0.01	6.5	3	0.2	2
22 March	1615	150	25	29	0.12	6.2	17	3	2
22 March	1737	78	—	—	—	5.6	—	—	2
22 March	1612	30	24	19	0.05	—	—	—	2
22 March	1610	15	25	26	0.39	—	—	—	2
1 April	1727	702	—	—	—	4.0	—	—	16
1 April	1510	610	23	19	0.03	4.4	neg.	1	3
1 April	1500	425	13	16	0.09	3.8	10	5	3
1 April	1455	305	20	16	−0.02	2.8	neg.	2	3
1 April	1722	78	—	—	—	1.9	—	—	3
1 April	1450	30	31	34	0.68	—	—	—	3
1 April	1445	15	27	30	0.01	—	—	—	3
4 April	1727	390	—	—	—	6.7	—	—	0.8
4 April	1605	305	25	11	0.02	5.6	1	0.5	0.8
4 April	1600	150	29	11	0.08	4.4	42	3	0.8
4 April	1725	78	—	—	—	4.2	—	—	0.8
4 April	1555	30	32	12	0.2*	—	—	—	0.8
4 April	1550	15	18	17	0.1	—	—	—	0.8
5 April	1645	78	—	—	—	4.8	—	—	10
5 April	1700	15	26	15	0.05	—	—	—	10
7 April	1650	1015	—	—	—	3.8	—	—	23
7 April	1425	950	24	17	0.2	4.5	neg.	9	23
7 April	1420	520	34	19	0.1	5.3	neg.	4	1
7 April	1415	335	21	19	−0.06	6.1	neg.	1	1
7 April	1410	150	43	16	−0.08*	5.6	neg.	2	1
7 April	1640	78	—	—	—	5.2	—	—	1
7 April	1405	60	24	18	0.09	—	—	—	1
7 April	1400	15	24	18	0.08	—	—	—	1

* Unreliable.

The turbulence existing in the ground layer of the trade-wind region is established by the numerous measurements of $(\overline{w'^2})^{\frac{1}{2}}$ and $(\overline{u'^2})^{\frac{1}{2}}$ presented in table 5. From the table, it is seen that root-mean-square velocities average nearly 30 cm/sec but vary from this value by more than ±20. In the upper region, away from clouds, the turbulent velocities drop to low values of less than 10 cm/sec. It should be pointed out that the trade winds were lighter than average during the measurement period, and the turbulence may be presumed to have been subnormal.

One of the more important aspects of the work,

Table 6. Average values of stress and turbulence measurements, March and April 1953, Anegada Island, British West Indies.

Number of observations	Height (m)	$(\overline{w'^2})^{\frac{1}{2}}$ (cm/sec)	$(\overline{u'^2})^{\frac{1}{2}}$ (cm/sec)	Stress (dy/cm²)	Wind (m/sec)	Eddy viscosity (g cm⁻¹ sec⁻¹)	Roughness coef. × 10⁴	Stability × 10⁸
1	2160	18	10	−0.05	4.4	—	—	17.7
2	1220	12	7	−0.02	4.1	2	0.5	17.7
1	930	24	17	0.23	4.7	0	4.5	17.7
6	610	24	18	0.05	5.6	19	2.0	2.7
5	305	29	16	0.09	5.5	5	3.2	2.7
5	150	34	21	0.14	5.0	30	4.3	2.7
1	60	24	18	0.09	—	—	—	2.7
3	30	29	22	0.31	—	—	—	2.7
5	15	24	21	0.13	—	—	—	2.7

particularly to oceanographers, is the establishment of the shearing stress of the atmosphere over the ocean in the trade-wind belt. Table 6 shows that the stress averaged 0.13 dy/cm^2 at 15 m and 0.31 dy/cm^2 at 30 m. Sheppard and Omar (1952) have reported values of 0.85 dy/cm^2, determined in this same region by the geostrophic-departure method under similar wind conditions.

The change from small positive stresses in the 1000-m region to small negative stresses above this level reflects the decrease in the intensity of the easterlies with height, which continues until a strong westerly flow is attained at the 5000-m level.

The measurement of eddy viscosities from the wind-shear equation was not very successful, primarily because of the existence of transient regions of positive and negative shears and stresses. Unfortunately, drift-sight winds were not obtained from the airplane as it was thought that the island pilot-balloon winds would be representative of the ocean areas. On 7 April, it appears that the winds measured over the island were, by chance, always out of phase with stresses measured over the water. This resulted in negative values of the viscosities. In spite of this sampling difficulty, the order of magnitude of the viscosity is established in both the sub-cloud and cloud layers. The roughness coefficient was computed from the wind at the given levels and is seen to be smaller than those found by Sheppard and Omar (1952). This should be expected, for the present stresses are smaller, while the winds at the given levels are greater than the anemometer-height winds used by Sheppard.

20 October 1953 to 29 January 1954, Gulf of Maine region.—A few root-mean-square velocity and shearing-stress values obtained over the Gulf of Maine and surrounding land are presented in table 7, for comparison with the values just described. Only the values representing extremes of stability and instability are tabulated and discussed briefly, as all will be discussed in detail at a later date. Viscosity and roughness co-

TABLE 7. Stress and turbulence measurements, Gulf of Maine, 20 October 1953, 7 December 1953, and 29 January 1954.

Date	Place	Height (m)	$(\overline{w'^2})^{\frac{1}{2}}$ (cm/sec)	$(\overline{u'^2})^{\frac{1}{2}}$ (cm/sec)	Stress (dy/cm^2)	Stability $\times 10^8$
20 October	Portland, Me.	1500	13	9	0.01	10
		1200	26	15	−0.27	0
		900	96	31	−0.89	0
		600	57	37	0.07	0
		300	97	47	−1.6	19
		150	88	65	2.7*	19
20 October	10 km offshore	900	17	8	0.10	5
		600	11	11	0.05	5
		300	11	13	0.06	5
		150	12	13	0.04	5
		60	12	11	−0.02	5
20 October	42°30′N, 68°30′W	900	12	17	0.01	9
		600	10	5	0.03	9
		300	12	5	0.03	36
		150	9	8	0.00	36
		60	11	26	−0.10	36
7 December	Beverly, Mass.	1800	27	20	0.13*	0
		1500	44	13	0.01*	71
		900	37	38	−0.50	2
		600	81	75	0.64	2
		300	191	130	16.6	−10
		150	103	96	6.1	−10
7 December	42°20′N, 70°15′W	1680	15	22	−0.02	60
		1200	30	30	−0.33	60
		900	20	29	0.04	4
		600	40	43	−0.12	4
		300	46	42	0.08*	−7
29 January	Portland, Me.	1320	18	12	0.15	55
		1000	10	7	0.00	55
		690	24	22	0.25	55
		390	45	43	0.94	11
		240	73	36	−0.08*	11
29 January	42°30′N, 68°30′W	1560	17	8	0.13	40
		1230	11	10	0.01	40
		930	18	13	−0.05	40
		660	43	33	0.20	3
		360	120	41	−1.51*	3
		190	117	51	−0.50*	3
		100	111	48	3.8*	3
		0 to 80				−180

* Unreliable.

efficients were not computed, as winds were not measured over the Gulf. Turbulence conditions on each of the three days were characterized by different controlling physical processes. On 20 October 1953, the Gulf water was 10C colder than the air, with the result that a root-mean-square vertical velocity of 97 cm/sec over land dropped to 12 cm/sec by 10 km offshore. On 7 December 1953, a condition of extreme turbulence and instability was encountered in the lowest 500 m over Beverly, Mass., three or four hours after a cold front passage. The root-mean-square vertical velocity was measured as 191 cm/sec at 300 m, while the shearing stress reached the record height of 16.6 dy/cm^2. The same air was remeasured after it had passed over 50 km of Gulf water. It was found that the turbulence had subsided, while the shearing stress had diminished to only 0.1 dy/cm^2. 29 January 1954 is characterized by moderate stability and turbulence over Portland, Me., changing to pronounced instability in the lowest 80 m and to increased turbulence over the warmer Gulf water. Intense convective activity increased the root-mean-square vertical velocity to 120 cm/sec, while the shearing stress reached 3.8 dy/cm^2. These few measurements are sufficient for the purpose of comparison with the more moderate values found in the trade-wind region.

6. Conclusion

The studies conducted to date have proven that the airplane offers a reliable method of determining the turbulent components of the atmosphere within a limited spectral range. Its greatest advantage lies in its ability to obtain measurements in regions completely inaccessible, or accessible only at great cost or time expenditure. With the technique in its present state of development, a vast amount of material can be collected and reduced concerning the turbulent components occurring under various meteorological conditions. It is planned to use the technique to study turbulence and diffusion over the western North Atlantic Ocean in continuation of work already done by Bunker (1952). The technique will also be applied to a study of the relation between diffusion and air-mass modification, thermal wind shears, and subsequent large-scale meteorological developments over the Atlantic.

Acknowledgments.—The investigation described in this article is the result of the work of many people besides that of the writer. All members of the Woods Hole meteorological group have contributed to the solution of the problem. Mr. Kenneth McCasland skillfully handled the job of building and installing the equipment in the PBY. Dr. Joanne Malkus has contributed to the understanding of the problem through applying the same techniques to the measurement of vertical velocities in cumulus clouds. Miss Martha Walsh did all of the computations of shearing stress and has aided in developing the techniques of reducing the observed quantities.

The help of the U. S. Navy is gratefully acknowledged for not only sponsoring the present work through the Office of Naval Research, but also for loaning the PBY aircraft to the Woods Hole Oceanographic Institution through the Bureau of Aeronautics.

Mr. Given A. Brewer, engineering consultant retained by the project, helped the writer in the analysis of aerodynamic problems and improved the instrumentation by applying a multichannel oscillograph and electric gauges to the problem.

Mr. Philip Donely of the National Advisory Committee for Aeronautics has contributed much to the writer's understanding of the problems involved in the measurement of gust velocities. Innumerable pitfalls were avoided due to his advice and help.

REFERENCES

Brewer, G. A., 1954: Calibrating the PBY-6A airplane for meteorological purposes. *Aero. Engr. Rev.*, **13**, No. 2, 24–28.

Bunker, A. F., B. Haurwitz, J. S. Malkus, and H. Stommel, 1949: Vertical distribution of temperature and humidity over the Caribbean Sea. *Pap. phys. Ocean. Meteor., Mass. Inst. Tech. and Woods Hole ocean. Instn.*, **11**, No. 1, 82 pp.

Bunker, A. F., 1952: Measurements of the vertical water vapor transport and distribution within unstable atmospheric ground layers and the turbulent mass exchange coefficient. *Pap. phys. Ocean. Meteor., Mass. Inst. Tech. and Woods Hole ocean. Instn.*, **12**, No. 3, 42 pp.

Donely, P., 1949: Summary of information relating to gust loads on airplanes. *Natl. adv. Com. Aero., Tech. Notes*, No. 1976, 145 pp.

Duncan, W. J., 1952: *The principles of the control and stability of aircraft.* London, Cambridge Univ. Press, 384 pp.

Durand, W. F., 1935: *Aerodynamic theory.* (Vol. II, Div. E; Vol. V, Div. N), Berlin, J. Springer, 367 pp. and 347 pp.

Kordes, E. E., and J. C. Houbolt, 1953: Evaluation of gust response characteristics of some existing aircraft with wing bending flexibility included. *Natl. adv. Com. Aero., Tech. Notes*, No. 2897, 31 pp.

Laufer, J., 1950: Some recent measurements in a two-dimensional turbulent channel. *J. aero. Sci.*, **17**, 277–287.

Panofsky, H. A., and I. A. Singer, 1951: *Annual progress report.* (A.E.C.—Air pollution project, Meteorological phase, NYO. 1559), Oak Ridge Tech. Inf. Ser., 66 pp.

Press, H., and B. Mazelsky, 1953: A study of the application of power-spectral methods of generalized harmonic analysis to gust loads on airplanes. *Natl. adv. Com. Aero., Tech. Notes*, No. 2853, 48 pp.

Reynolds, O., 1895: On the dynamical theory of incompressible viscous fluids and the determination of the criterion. *Phil. Trans. roy. Soc.*, **186**, 123–164.

Sheppard, P. A., and M. H. Omar, 1952: The wind stress over the ocean from observations in the trades. *Quart. J. r. meteor. Soc.*, **78**, 583–589.

Contribution No. 741

Reprinted from
PHOTOGRAMMETRIC ENGINEERING
March
1955

AERIAL STEREO-PHOTOGRAPHY AND OCEAN WAVES*

Wilbur Marks, Research Associate in Physical Oceanography, and F. Claude Ronne, Research Associate in Photography,
Woods Hole Oceanographic Institution, Woods Hole, Massachusetts

ABSTRACT

A need for experimental verification of new ocean wave theories is discussed. The use of aerial stereo-photography as a means to this end is outlined. A brief summary of the operational plan is given and special attention is focused on those aspects of the operation which make photography of a moving target, which changes shape with time, unique. The reduction of the stereo-pairs to data form and the application of this information to ocean wave research is discussed. Results of the operation are given.

INTRODUCTION

RECENT investigations have produced theories which explain the generation, propagation and decay of ocean waves (Pierson, 1952, Neumann, 1953); in general the behavior of the waves can be predicted, if certain parameters are known. To describe any motion it is necessary to know the initial state of the system and the laws which govern the motion. These laws are known for waves, to a fair degree of approximation; it is the initial state which must be determined. The complexity of the sea surface rules out a precise mathematical description, of every configuration, in time and space, but a way to describe the features of ocean surface has been found in a statistical approach to the problem.

The energy in the waves can be described by a spectrum which is a function of wave frequency and direction of travel of the spectral components. The energy spectrum can be found if the sea surface is "captured" in either time or space. Many methods have been tried, with only partial success. A wave pole, for example, may record a time history of the waves as they pass a fixed point. The energy spectrum as a function of wave frequency is determined (Pierson and Marks, 1952) but nothing is known about the distribution of energy with respect to direction of travel. This argument holds for all such single point observers. Perhaps a battery of wave poles is the answer, but the theory governing the analysis of such data has not yet been derived An attempt has been made to record the sea surface with a sensitive radio altimeter mounted in an airplane which makes a run over the sea surface. (Deacon, Darbyshire and Smith, 1949). In this case, wave frequencies (periods) are distorted because the plane cannot fly perpendicularly to all the wave crests all the time, and directional information is at best inferred. Some other attempts at wave measurement have been: pressure elements placed on the ocean bottom to record the pressure of the water column above; submarines moving and stationary, equipped with pressure elements and accelerometers (to compensate for the submarines' vertical motions), (Ewing and Press, 1949); ships equipped with pressure elements and accelerometers; and several other methods which are variations of the above.

A good deal of thought was given to the Sonne strip camera as a means of "laying a carpet down on the sea surface," that is, a narrow strip of the sea surface is recorded by a fast, low flying airplane (Sawyer, 1949). Here again, the field of view is too narrow to determine the direction spectrum. The next logical step is consideration of high altitude stereophotography. This satisfies all of the conditions imposed above with respect to determination of the energy distribution as a function of frequency and direction of travel of the wave components. From the stereo-pairs, elevations are read at discrete points, where the spacing of the points depends on the properties of the sea surface and the resolution (of the spectrum) desired. The information is fed into an electronic computer and the end result is the two-dimensional energy spectrum of the waves (Marks, 1954).

---

* Contribution No. 741 from the Woods Hole Oceanographic Institution. Publication authorized by the Institution on Nov. 22, 1954.

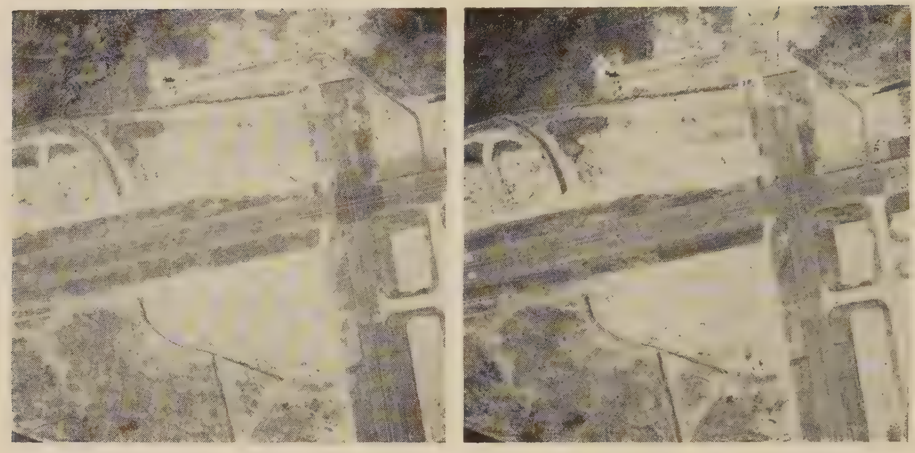

FIG. 1.—Stereo-pair showing the truck on the runway.

TEST FLIGHT

In order to capture enough of the sea surface for analysis purposes, it was necessary to use two planes. The cameras were triggered at the same instant by an FM signal sent out by the master plane.

It was desired to prove that the electronic link would actually fire the two cameras simultaneously. Oscillograph measurements made on the ground with the engines of the two airplanes turned up, indicated that the cameras could be fired within one millisecond of each other, or better. To substantiate further the ability of the F. M. link to trigger the cameras simultaneously, a test flight was made over the airfield, along the runway. A truck traveled in the opposite direction at 40 mph (the fastest wave speed anticipated); the plane moved at 160 mph. The photographs were made with various delays installed in the cameras. That is, one camera was purposely fired 5 milliseconds after the other one. Then the delay was reversed. The result was that in no pair of photographs could it be visually ascertained that there was any change in position of the truck. Furthermore, the photos were enlarged 25 times and no difference could be measured that was greater than the measuring error itself. Figure 1 shows a stereo-pair of the truck on the runway.

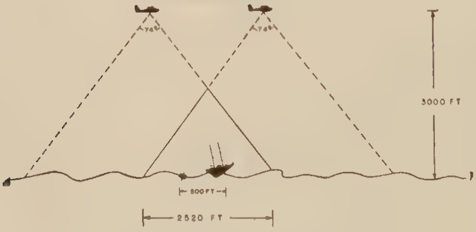

FIG. 2.—Schematic representation of operational procedure.

OPERATIONAL PROCEDURE

Stereo-photography of the sea surface involves certain problems not encountered over land. The sea presents a relief pattern which is always moving and changing its shape, and it offers no fixed marks which can be used for ground control.

However, in the case of a rough sea (waves 15 to 20 feet high) such as are required for this experiment, there is a great deal of contrast between the foam (due to breaking wave crests) and the water, and this can be utilized for the separation of tonal values in the photographs. The serious problem of reflection glare can be overcome if the pictures are taken at a time of day when the sun is at a relatively low altitude (40°) or, ideally, when there is a high overcast.

Attempts have been made to obtain oblique stereo-pairs from a ship (Schumacher, 1932) but this method is not altogether satisfactory. The camera base line is too short to be useful except over a small area, the backs of the waves are not recorded, and the nearer waves obstruct those more distant.

To satisfy the needs of the oceanographer for a statistical analysis of the sea surface, it is essential to have vertical photographs covering a large area.

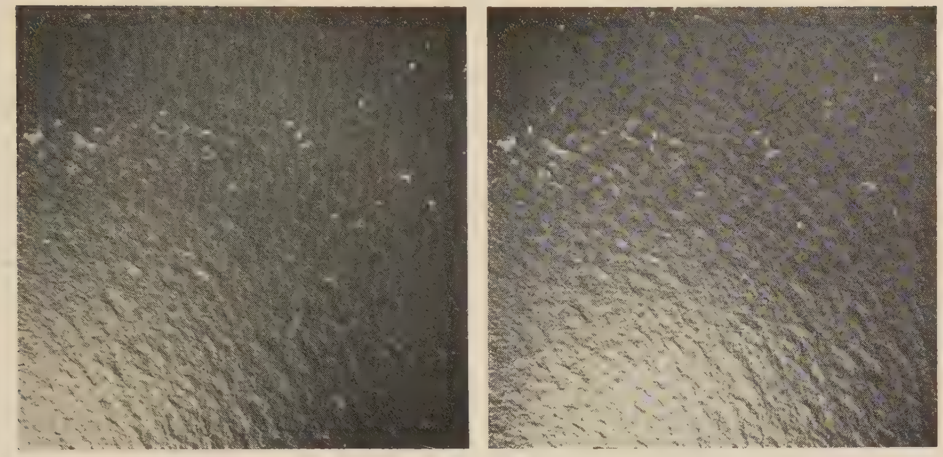

FIG. 3.—A stereo-pair showing ocean waves.

The operational procedure involved the use of two airplanes flying in tandem 2,000 feet apart and at an elevation of 3,000 feet. Each plane was equipped with a standard mapping camera (CA-8) and the cameras were triggered simultaneously from the forward (master) plane, by an FM radio link. The planes flew directly into the wind. This eliminated crabbing, reduced the air speed and allowed the major wave fronts to pass at right angles to the line of flight.

To help establish some sort of ground control, the WHOI research vessel *Atlantis* was stationed in the area of operation. The vessel towed a target raft 500 feet behind it. The distance between the raft and the ship was monitored during the entire exercise by a sonar buoy located on the raft which received a radio impulse through air from the vessel and retransmitted the signal to the vessel, through water. The travel time was recorded every 2 seconds by a Speed-O-Max installed in the research vessel. (See Figure 2.)

The planes adjusted their altimeters to the barometer on the ship at the time the pictures were taken. The distance between the two planes was maintained nearly constant at about 2,000 feet by means of a range finder located in the slave plane, and utilizing the wing span of the master plane as base line.

The research vessel was instructed by radio at the moment each run started and made a side-mark on the record paper of the Speed-O-Max. Since only 10 pairs of photographs are made during the run (a time interval of about 36 seconds), it was felt that if the ship and raft appeared in one of the pairs, this control may be inferred for each of the other pairs in the run. A stereo-pair of ocean waves appears in Figure 3.

ANALYSIS OF STEREO-PAIRS

It is necessary for the purposes of prediction that a select number of photo pairs be contoured. The exact number depends on the highest frequency waves present and on the short-crestedness of the sea surface. In order to determine the energy spectrum of the sea surface a grid of spot heights must be made; the spacing of the grid depends on the parameters mentioned above. The points on the grid might be read from the contours directly, but the interpolation between contours is difficult even when the shape of the sea surface between contours can be seen from the pictures. After the elevations are read from the photographs the values are tabulated for analysis by an electronic computer. The end results is the two-dimensional energy spectrum of the sea surface.

CONCLUSION

High altitude stereo-photography of the sea surface from two airplanes flying in tandem has produced a sequence of 100 stereo-pairs which show waves ranging in height from one to ten feet. The heights at discrete points on these photographs will yield the two dimensional energy spectrum of the sea surface. It is hoped that this information will establish confidence in new theories which describe the behavior of ocean waves.

ACKNOWLEDGMENT

Professor W. J. Pierson, Jr., N.Y.U., initiated the project and served as advisor to the group. The Naval Air Development Unit, South Weymouth, Mass. contributed the planes and flight personnel. The Aerial Photographic Experimental Laboratory, Naval Air Development Center, Johnsville, Pa. tested the cameras for mechanical efficiency, and installed them in the planes. The Hydrographic Office, Photogrammetry Division is analyzing the photographs. The Hydrographic Office, Forecasting Section prepared all meteorological intelligence and signaled the start of the exercise. The Woods Hole Oceanographic Institution provided a research vessel, ground baseline and the electronic link for synchronous photography.

Lastly, the Office of Naval Research has sponsored the project under contract Nonr 769(00), assembled all of the interested parties, procured equipment and personnel, arranged meetings, organized schedules, and in general administered and coordinated the entire project.

All of the groups above offered suggestions and criticisms which were extremely useful.

REFERENCES

Deacon, G. E. R., J. Darbyshire and N. D. Smith (1949). "Use of the airborne sea and swell recorder to measure changes in the wave spectrum from west to east across the Irish Sea." Admiralty Research Laboratory, Teddington, Middlesex.

Ewing, M. and F. Press (1949). "Notes on surface waves. Ocean surface waves." *Annals of the New York Academy of Sciences*, Vol. 51, pp. 453–462.

Marks, W. (1954). "The use of a filter to sort out directions in a short-crested sea surface." *Transactions of the American Geophysical Union*, Vol. 35, no. 5, Oct. 1954.

Neumann, G. (1953). "On ocean wave spectra and a new method of forecasting wind generated sea." *Technical memo. 43. Beach Erosion Board.*

Pierson, W. J. Jr. (1952). "A unified mathematical theory for the analysis, propagation and refraction of storm generated ocean surface waves." Parts I and II. Research Division, College of Engineering, New York University.

Pierson, W. J. Jr., and W. Marks (1952). "The power spectrum analysis of ocean wave records." *Transactions of the American Geophysical Union*, Vol. 33, no. 6, Dec. 1952.

Sawyer, D. W. (1949). "Preliminary report on the determination of water surface profiles." U. S. Naval Photographic Interpretation Center, U. S. Naval Receiving Station, Washington 25, D. C., Report No. 103–49.

Schumacher, A. (1932). "Stereophotogrammetric measurement of waves." *Zeitschrift der Gesellschaft für Erdkunde zu Berlin*, Erganzungsheft III: 105–120.

Contribution No. 742

SUMMER ECOLOGY OF OCEANIC BIRDS OFF SOUTHERN NEW ENGLAND

BY MALCOLM S. GORDON

Reprinted from The Auk, Vol. 72, April, 1955

SUMMER ECOLOGY OF OCEANIC BIRDS OFF SOUTHERN NEW ENGLAND

BY MALCOLM S. GORDON

Between June 13 and August 27, 1953, I spent a total of twenty-six days at sea off southern New England on the research vessel *Blue Dolphin*. Some notes on the distribution and ecology of the oceanic birds observed during this period are presented here. Indications of quantitative correlations between hydrographic conditions, food supply, as plankton populations, and bird abundance were found.

More than 95 per cent of the bird observations used in this paper were made by the author. The remainder were made by Dr. Richard H. Backus, of the Woods Hole Oceanographic Institution, and by various members of the ship's company, to whom sincere appreciation is here expressed.

Thanks are also due to David C. Nutt, master of the *Blue Dolphin*, Drs. John C. Ayers, LaMont C. Cole, J. Brackett Hersey, Robert C. Murphy, and Charles G. Sibley, and Messrs. John T. Nichols and Charles F. Powers, all of whom have aided in various ways.

This paper is Contribution Number 742 from the Woods Hole Oceanographic Institution and is part of a thesis submitted in partial fulfillment of the requirements for the degree of Bachelor of Arts with Honors in Zoology at Cornell University.

Observations.—The ship worked fairly intensively in two areas, an inshore area hereafter called Area I and an offshore area called Area III. The intervening sea is called Area II. These areas, shown in figure 1, are covered by U. S. Coast and Geodetic Survey Chart No. 1108.

The three areas were visited as follows, an observer being on deck at least 90 per cent of the daylight periods. The numbers in parentheses are the column numbers in table 1 which include observations made on the dates indicated.

Area I: traversed June 13 (1); all day July 11 and 12(2); traversed July 28(3); all day August 4(4); all day August 6(5); late afternoon August 11(6); morning August 12(6); and all day August 13(6).

Area II: parts B and C traversed July 16(1); B and C traversed July 18(2); A, B, and C traversed July 28(3); C traversed July 30(4); C traversed August 7(5); and A and B traversed August 27(6).

Area III: area less than ten miles to the eastward traversed June 29(1); all day July 16 and 17(2); morning and early afternoon July 18(2); all day July 29(3); morning and early afternoon July 30(3); morning and early afternoon August 7(4); and all day each day August 18 through 26(5).

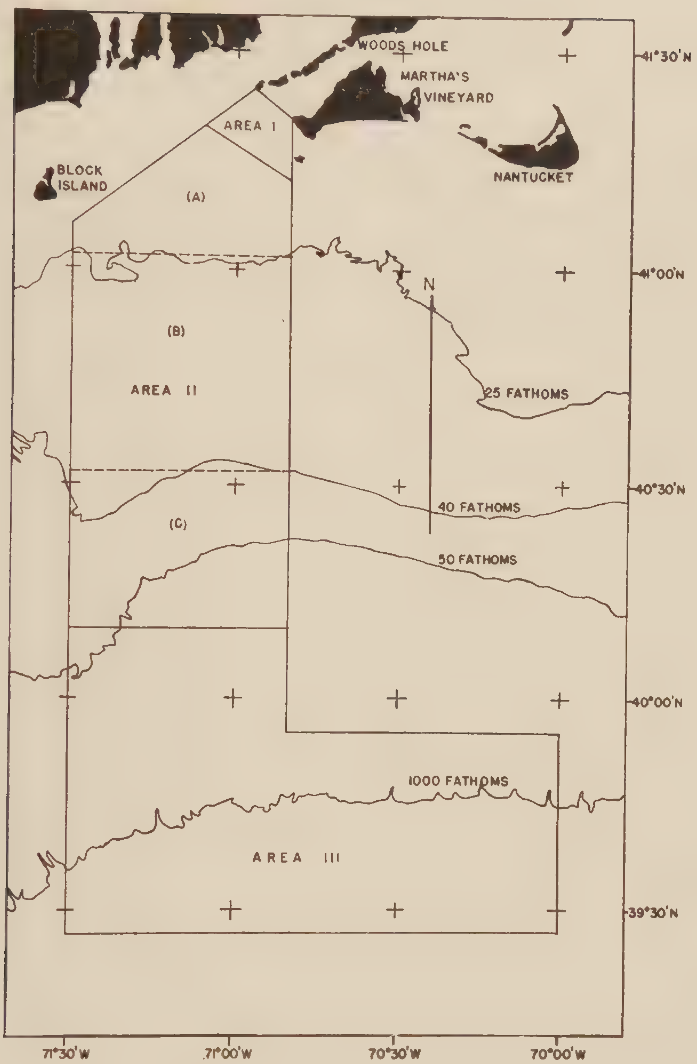
WOODS HOLE
MARTHA'S VINEYARD
NANTUCKET
BLOCK ISLAND
AREA I
(A)
(B)
AREA II
(C)
AREA III
N
25 FATHOMS
40 FATHOMS
50 FATHOMS
1000 FATHOMS
41°30'N
41°00'N
40°30'N
40°00'N
39°30'N
71°30'W
71°00'W
70°30'W
70°00'W

Figure 1. Bird Observation Areas.

The major weather disturbances during the period June 13 to August 27 were as follows: strong lows passed June 14–15 and 18–19; squall line July 3; lows passed July 12–13, 15, 21–22, 23–24, and August 3, 5, and 9; hurricane "Barbara" August 15; and a low on August 19.

Comparisons with Fuglister (1947) show that the sea-surface temperatures throughout the area were normal for the season. The temperature of the surface water in Area III rose from approximately 70° F. to 76° F. between June 29 and August 26.

The bird species observed were as follows: Sooty Shearwater (*Puffinus griseus*), Audubon's? Shearwater (*Puffinus ?lherminieri*), Greater Shearwater (*Puffinus gravis*), Cory's Shearwater (*Puffinus diomedea*), Leach's Petrel (*Oceanodroma leucorhoa*), Wilson's Petrel (*Oceanites oceanicus*), Frigate Petrel (*Pelagodroma marina hypoleuca*), Gannet (*Moris bassana*), and Pomarine Jaeger (*Stercorarius pomarinus*).

The identity of the small black and white shearwaters seen during the summer is uncertain. An examination of numbers of skins of Audubon's, Manx (*P. puffinus*), and Allied (*P. assimilis*) shearwaters (the subspecies which might be expected on the basis of distribution) in the American Museum of Natural History indicates that the color of the under tail coverts is not a reliable character for distinguishing these species from one another (see Peterson, 1947: 246). The color of the feet was not distinguishable on any bird seen during the present study. The color of the under tail coverts was observed on three birds; on two, the coverts were white, on the third, black. Thus, no definite statement may be made about the identity of all such shearwaters seen. It should be noted, though, that all these birds seen flew with very rapid wing beats and that, where such comparisons were possible, they appeared much smaller than Cory's Shearwaters. Dr. R. C. Murphy, in conversation, has likened the size relation between the Cory's and Audubon's shearwaters to that between a Rock Dove and a Robin, while that between the Cory's and Manx is similar to that between a Robin and a Catbird. Since the Allied Shearwater is only accidental in this area, I think the present birds were probably Audubon's Shearwaters.

The observations made are shown in Table 1.

For Area I: the shearwaters under column 6 were east of Area I proper—approximately over the twenty-fathom curve south of eastern Martha's Vineyard. The Audubon's Shearwater in column 5 was about four miles southwest of Gay Head.

For Area II: the letters following the numbers signify the subdivisions of the Area in which the birds were seen. (B, C) means that the birds were about equally numerous in B and C; (B-C) means that the birds were seen in northern C and southern B. The figures in column 2 are for one half the birds seen on July 18, either in III or IIC (but no distinction made in my notes).

For Area III: the column 2 figures include one half the birds seen on July 18 (see above).

The bird observations indicate the following pattern: oceanic birds were generally scarce in Area I; Wilson's Petrel, while not common,

TABLE 1

SUMMARY OF OBSERVATIONS ON BIRDS

Species	*Area*	*1*	*2*	*3*	*4*	*5*	*6*
Sooty Shearwater	I	0	0	0	0	1–2	0
	II	0	1(C)	0	0	0	0
	III	0	3–4	0	0	0	–
Audubon's Shearwater	I	0	0	0	0	1	0
	III	0	0	0	0	15	–
Greater Shearwater	I	0	0	0	0	2–3	1
	II	0	20–25(C)	3–4(B-C)	0	0	0
	III	20–25	60–70	2–3	0	5	–
Cory's Shearwater	I	0	0	0	0	1–2	2
	II	0	40–50(C)	4–5(B-C)	0	0	3(A)
	III	0	75–100	4–6	0	6	–
Leach's Petrel	III	0	2 prob.	0	0	4–5	–
Wilson's Petrel	I	0	5–7	0	0	2–3	3–4
	II	100–150 (B,C)	30–40(C)	3–4(B-C)	0	20–30(C)	10–15(B)
	III	abt. 100	300–380	40–50	0	1000–1400	–
Frigate Petrel	III	0	0	0	0	1[1]	–
Gannet	I	0	0	0	0	1	1
Pomarine Jaeger	I	3	0	0	0	0	2
	II	0	1	0	0	0	2
	III	1	1	0	0	2	–

[1] Collected August 18 at 39° 48′ N., 71° 02′ W. See Gordon (1955) for details.

being the most abundant. Areas IIA and B were rather barren, although occasionally Wilson's Petrels were moderately common in B. Area IIC occasionally had numbers of birds present in it but in general was quite barren, except for Wilson's Petrels. Area III usually had a fairly large population of birds. Wilson's Petrels were continuously common and became abundant in late August; Greater Shearwaters were the most abundant of the shearwaters in late June but lost this numerical dominance to Cory's Shearwater in the latter part of July. All of the larger shearwaters became quite scarce in late July and August, while Audubon's Shearwater became the most numerous form in late August. Jaegers were scarce, the only species seen in any of the areas being the Pomarine.

In Area III, the late July decrease in numbers of Greater Shearwaters and the mid-July increase of Cory's Shearwaters were probably due to a completion of the northward migration and to completion of nesting activities and start of post-breeding season wandering, respectively. Similar conclusions were reached by Wynne-Edwards (1935).

The late July and August scarcity of all species of the larger shearwaters is not explained. There was no significant change in the surface temperature of the water covering the area during the summer. It seems unlikely that the small change observed could have been the cause of the great change in population makeup. It is also unlikely that hurricane "Barbara" caused the change, for it apparently began at least three weeks before the hurricane.

The marked increase in Wilson's Petrels and the appearance of many Audubon's Shearwaters in late August seem at least partially explicable by observation. Sargassum weed had earlier been virtually absent from the area. In late August, however, as usual in this region, it became very abundant, carrying with it its usual large community of small animals (shrimp, crabs, fishes, isopods, etc.). The food habits of Audubon's Shearwater and of Wilson's Petrel (Murphy, 1936, and Bent, 1922) make it appear likely that this influx of sargassum was the direct cause of both phenomena. This increase, however, further obscures the cause of the scarcity of the larger shearwaters (especially Cory's), for the food habits of these birds, as described by Bent (1922), are such that one would expect an increase in sargassum to attract them.

A consideration of the variations in abundance and distribution of birds follows. This is made on the basis of two major assumptions:

1. No birds were seen twice. This assumption is considered reasonable due to the wide-ranging habits of the birds involved. Though watched carefully, no shearwaters were ever observed to follow the ship. Wilson's Petrels followed the vessel for varying lengths of time, but never for as long as an entire day. The numbers of petrels recorded daily contain an estimated correction for this duplication.

2. The total number of birds seen in each area is proportional to the total population of birds present in that area at the time. No other assumption in this regard seems justified.

Table 2 summarizes the total bird numbers observed in the various areas during the summer. Column 4 of this table was calculated as follows: Column 2 (observed number) is the sum of all the numbers of shearwaters and petrels observed in each area (see Table 1), using the mid-point of the range when a range of numbers was recorded. Column 4 gives estimates of the numbers of birds that would have been seen in Areas I and III if six days only had been spent in these areas. These numbers were calculated by multiplying the Area I number by 6/7, and taking a random sample of six days from the time spent in Area III (numbering the days from 1–16, the days used were

1, 4, 7, 10, 13, 16—substantially the same results were obtained using other random samples of six days). Differences between the records for the three areas resulting from differing lengths of observing time are thus at least partially compensated for; I believe the "observing effort per unit time" was the same in all areas. The time-corrected numbers bear to one another the relation 1:18:45; the ratio between Areas II and III is 2:2.6.

TABLE 2

NUMBERS OF OCEANIC BIRDS

Area	*Observed number*	*Observing time (day)*	*6-day time-corrected number*
I	19	7	16
II	280	6	280
III	1910	16	717

"Land shyness" of the oceanic birds may have been responsible for the paucity of birds in Area I (the other areas are completely out of sight of land). It is therefore omitted from further consideration.

The time equalization in Table 2 also roughly equalizes the sea-surface areas observed in each Area. As a first order approximation, the *Blue Dolphin* may be considered to have steamed at a constant speed throughout each of the twelve days involved in Areas II and III. Since, on the basis of the vessel's tracks, about the same amount of overlap of observed areas appears to have occurred in each area, approximately equal areas of sea-surface were observed. The 1: 2.6 ratio between Areas II and III thus appears to be the best estimate of the "true" ratio available.

It should be pointed out that approximately one-third of IIC is covered by water of greater than fifty fathoms depth, hence rightfully belongs in the Slope Water area (Area III—see Miller, 1950). The above treatment of the data and the roughness of the known time-distribution of the records do not allow any reasonably simple correction of the bird ratio for this effect. Suffice it to say that the ratio would be somewhat increased by any such correction.

Why such a distribution exists now becomes a question. The uniformity of the birds' immediate aerial environment makes it seem likely that something in the sea is responsible, probably food supply.

The dependence of sea-birds on planktonic food or plankton-dependent food has previously been pointed out by Jesperson (1924, and other papers). Wynne-Edwards (1935) considers Jesperson to have shown clearly that food supply is "the chief controlling factor in regulating local abundance of plankton-feeding birds." Off southern California, Miller (1936, 1940) has shown qualitatively a correlation between oceanic bird abundance and the edge of the Continental Shelf similar to that shown here. He considered it likely that plankton population sizes were significant in this. Redfield (1941) has also demonstrated an apparent direct qualitative correlation between plankton abundance and oceanic bird abundance (primarily for Wilson's Petrel) during the summer in the Gulf of Maine.

An analysis of plankton population figures for the areas studied here has been made. Two hypotheses, possibly alternatives, possibly supplementary to one another, have been developed. On the basis of present knowledge no indication of preference for one or the other seems justified.

First hypothesis: Hydrographic conditions in the water masses covering Areas II and III (the Continental Shelf and Continental Slope waters, respectively) are such that it would seem likely that Area III can maintain a larger total plankton population than Area II (Iselin, 1936; Miller, 1950; Riley *et al.*, 1949; Sverdrup *et al.*, 1942). Data showing that this actually is the case, in the summertime, are presented by Riley and Gorgy (1948).

Phytoplankton population figures (see table on p. 121 of Riley and Gorgy) are indicative of this but, unfortunately, are inconclusive. Figures for total zooplankton, based on observations made in the areas here being discussed, are as follows: From surface to near bottom on the Shelf, and for the upper 800 meters in the Slope area, "the averages for total zooplankton were of the order of 30 gm. wet weight per square meter of sea surface in the coastal zone . . . and upwards of 80 gm. in the slope water area" (Riley and Gorgy, p. 116). From these figures the zooplankton population ratio of coastal (Shelf) to Slope water is 1:2.7.

These figures become pertinent to the present hypothesis when the occurrence of "deep scattering layers" is noted in Area III (see Hersey, Johnson, and Davis, 1952, and various of the papers referred to in their bibliography). An at least partially similarly behaving phenomenon was observed fairly consistently in Area II in the course of the present work. In Area III during the months of July and August the fauna of the deep layers appears to be primarily copepods, amphipods, euphausian shrimps, and fishes (mostly small lanternfishes of the family Myctophidae).

Data on the food habits of the birds under consideration here (Murphy, 1936, and Bent, 1922) indicate that the shearwaters feed primarily on fish, squid, crustacea, and almost any reasonably edible oily substance. Both Wilson's and Leach's petrels feed primarily on crustacea—especially euphausians for Wilson's—small fish, and oily substances. Thus the birds eat exactly what occurs in the scattering layers.

However, the scattering layers are at the surface at night only. Do the birds feed at this time?

No reference to this problem has been found in any of the papers on oceanic birds consulted. However, from the fact that most of these birds are very active during the night while on their breeding grounds (Bent, 1922), also from my own observations of large amounts of nocturnal activity among Leach's Petrels at sea, it does seem reasonable to suppose that at least some feeding goes on in the dark.

There are usually casualties of the previous night's activities floating on the sea-surface (at least in Area III) in the morning, however. Many times during the course of the summer I observed dead squid (deep water forms possessing photophores) floating about. It may be that the birds do not feed at night but merely clean up the battleground after the war has retreated.

In addition, fairly extensive schools of small silvery fish were observed on several occasions during the daytime swimming near the surface in Area III. Schools of Round Herring (*Etrumeus teres*) were similarly observed in Area IIA. All these fishes are probably fed upon by the birds. The fishes in Area III were probably, the Round Herring almost definitely, feeding upon plankton.

Clarke (1940) supplies further evidence regarding this hypothesis, at first glance contradictory.

Clarke states that the Shelf water appears to support more plankton than the Slope water. This, however, is based upon a consideration of tows made throughout the year. When Clarke's summer data (between May 28 and September 3) alone are considered, essentially the same conclusion is reached as was reached by Riley and Gorgy (1948). Clarke's station 4 (apparently right over, or very near, the 100-fathom curve) is within the Slope area as defined in this paper; further, his Slope area tows went down to only 275 meters, hence only his night tows in this area sampled the entire significant population. Comparisons between summer night tows in the two areas give an average total plankton population ratio of 1:2.4.

Fairly strong evidence thus exists for a reasonably close quantitative correlation between bird population size and total plankton population size. A weakness exists in the above argument, however, which allows a somewhat different interpretation also to be made.

Second hypothesis: As was pointed out above, the large numbers of Wilson's Petrels observed in Area III in late August (which make up the greatest part of the birds observed in Area III) may well have been feeding upon the animals carried by the surface-drifting sargassum weed. These animals are certainly not considered in any of the plankton figures presented by either Clarke or Riley and Gorgy. One might, therefore, easily say that the correlation indicated above is merely fortuitous and, while interesting, has little significance. No way of correcting the present data for this effect is available. It might be pointed out, though, that Clarke (1940) gives figures for total plankton population in the upper twenty-five meters, for daytime hauls during the summer, that give an Area II: Area III ratio of 1:0.28.

It thus seems apparent to me that the critical observations regarding the relations of oceanic birds to their watery substratum are still to be made. Analyses of the stomach contents of petrels and shearwaters taken very shortly after sunrise and also at a variety of times of day in areas having abundant sargassum weed are needed before any reasonable approach to the difficulties mentioned may be made. That there is a correlation between food supply and bird abundance, however, seems quite clearly demonstrated.

Summary.—Observations of oceanic bird occurrence and distribution were made during the course of twenty-six days at sea off southern New England between June 13 and August 27, 1953. The areas covered and the observations made are described, and weather and sea-surface temperature data are presented.

Off southern New England in summer, oceanic birds appear to be more numerous, by a factor of 2.6, over Continental Slope water than they are over Continental Shelf water. The major mixing processes occurring in these water masses appear to supply more nutrients to the plankton of the Slope water than to that of the Shelf water. The ratio of total zooplankton populations of the Shelf water to those of the Slope water is 1:2.7. A consideration of "deep scattering layer" behavior and known feeding habits of the birds makes this appear to be something more than just an interesting parallel. However, deficiencies in our present knowledge, combined with complication of the food supply picture owing to the appearance of sargassum weed in the study area, do not allow definite conclusions to be reached. In any case, the general correlation between seabird abundance and food supply, first pointed out by Jesperson, seems strongly supported.

Temporal variations in species abundance of various of the birds

are also considered. Possible reasons for these variations are discussed. The field identification of the western North Atlantic species of small black and white shearwaters is considered, with the conclusion that sight indentifications are not trustworthy.

LITERATURE CITED

BENT, A. C. 1922. Life histories of North American petrels and pelicans and their allies. Bull. U. S. Nat. Mus. No. 121, 343 pp.

CLARKE, G. L. 1940. Comparative richness of zooplankton in coastal and offshore areas of the Atlantic. Biol. Bull. **78**: 226–55.

FUGLISTER, F. C. 1947. Average monthly sea surface temperatures of the western North Atlantic Ocean. Pap. Phys. Ocean. and Meteor. **10**(2): 1–25.

GORDON, M. S. 1955. A western North Atlantic record for the Frigate Petrel (*Pelagodroma marina hypoleuca*). Auk, **72**: 81–82.

HERSEY, J. B., H. R. JOHNSON, and L. C. DAVIS. 1952. Recent findings about the deep scattering layer. Jour. Mar. Res. **11**(1): 1–9.

ISELIN, C. O'D. 1936. A study of the circulation of the western North Atlantic. Pap. Phys. Ocean. and Meteor. **4**(4): 101 pp.

JESPERSON, P. 1924. The frequency of birds over the high Atlantic Ocean. Nature **114**: 281–3.

MILLER, A. R. 1950. A study of mixing processes over the edge of the continental shelf. Jour. Mar. Res. **9**(2): 145–60.

MILLER, L. 1936. Some maritime birds observed off San Diego, California. Condor **38**: 9–16.

MILLER, L. 1940. Observations on the Black-footed Albatross. Condor **42**: 229–38.

MURPHY, R. C. 1936. Oceanic birds of South America. Macmillan Co., N. Y. 2 vols., 1245 pp.

PETERSON, R. T. 1947. A field guide to the birds (2nd ed., revised). Houghton Mifflin Co., Boston, 290 pp. illus.

REDFIELD, A. C. 1941. The effect of the circulation of water on the distribution of the calanoid community in the Gulf of Maine. Biol. Bull. **80**: 86–110.

RILEY, G. A., and S. GORGY. 1948. Quantitative studies of summer plankton populations of the western North Atlantic. Jour. Mar. Res. **7**(2): 100–21.

RILEY, G. A., H. STOMMEL, and D. F. BUMPUS. 1949. Quantitative ecology of the plankton of the western North Atlantic. Bull. Bingham Ocean. Coll. **12**(3): 169 pp.

SVERDRUP, H. U., M. W. JOHNSON, and R. H. FLEMING. 1942. The Oceans. Prentice-Hall Inc., N. Y., 1087 pp.

WYNNE-EDWARDS, V. C. 1935. On the habits and distribution of birds on the North Atlantic. Proc. Boston Soc. Nat. Hist. **40**(4): 233–346, pls. 3–5.

Department of Zoology, Yale University, New Haven, Connecticut, *February 2, 1955.* (*First submitted March 26, 1954.*)

Contribution No. 743

Deep-Sea Research, 1955, Vol. 2, pp. 253 to 260. Pergamon Press Ltd., London.

Geologic interpretation of a series of seismic reflection profiles from Bermuda to the continental margins

C. B. OFFICER*

INTRODUCTION

THE GEOLOGIC exploration of oceanic areas has proceeded in several directions. Echo sounders are used to study the morphology of the ocean bottom, cores to study the near surface sediments, and seismic refraction profiles to study the properties of the sub-oceanic crust. A further method is that of seismic reflections. Previous investigations over deep water have dealt with vertical reflection measurements from a single ship, WEIBULL (1947) and HERSEY and EWING (1949). Both demonstrated that sub-bottom horizons do exist, and the latter discuss the various types of reflection records that are obtained over the western Atlantic and the differences in sediment structure that they represent. Here, the results from a series of seismic reflection profiles are discussed.

Such reflection profile investigations have been carried out by J. NAFE and J. EWING at Lamont Geological Observatory from profiles giving a broad aereal coverage and by OFFICER (1955) from profiles designed to give a more detailed examination of the physical properties of the sediment. Both show that the sub-bottom reflections can be followed from one record to the next on a profile and that the seismic velocity structure in the sediments can be determined from such profiles. In general, a velocity gradient of the order of 1 ft./sec. per ft. of depth is measured so that beyond a moderate range the angle of incidence on the bottom is such that the energy is returned from a refraction in the sediment column without a deep reflection. The existence of this velocity gradient in the sediment had been demonstrated previously by HILL (1952). The interest in this paper is with the arrivals from records at closer ranges where sub-bottom reflections are received.

On these seismic reflection profiles over deep water two ships were used. The first ship, R/V *Atlantis*, recorded from a hydrophone near the ocean surface. The second ship, R/V *Caryn*, fired small charges at closely spaced intervals on a prescribed track away from the *Atlantis*. A balloon was tied from a piece of string to each charge so that it would fire two feet below the surface. This procedure eliminated the explosion bubble pulse, and the near surface hydrophone eliminated the sometimes complicating effect of surface reflected energy, recorded on a deeper hydrophone. The information was preserved on magnetic tape to be replayed in the laboratory to a galvanometer camera.

STRUCTURE FROM SEISMIC REFRACTION PROFILES

The several published seismic refraction investigations over the North America Basin allow one to draw a rough geologic section along the line of the reflection profiles (Fig. 3). Under the abyssal plain portion the sediment is 3,000 to 4,000 ft.

---

* Woods Hole Oceanographic Institution, Contribution No. 743.

thick (EWING, SUTTON, and OFFICER, 1954). Under the Bermuda rise southeast of Bermuda the sediment is 1,000 ft. thick and is underlain by a layer of volcanics, and possibly consolidated sediment, varying in thickness from 5,000 to 10,000 ft. (OFFICER, EWING, and WUENSCHEL, 1952). It is inferred that a similar structure is present under the western portion of the Bermuda rise along the line of the reflection profiles. Investigations over the continental rise from Nova Scotia to Georges Bank show an extensive sediment of geosynclinal proportions with a maximum thickness of upward of 15,000 ft. (OFFICER and EWING, 1954). These sediment layers under the continental rise are continuous with those under the continental shelf and Atlantic coastal plain. Wells over the Atlantic coastal plain determine the age of the boundary between the two sediments, shown in Fig. 3, to be of Upper Cretaceous age such that the lower sediment is primarily Lower Cretaceous and possibly Jurassic and the upper layer Upper Cretaceous and Tertiary (EWING, WORZEL, STEENLAND, and PRESS, 1950) ; this age is again checked by samples dredged from the sides of the canyons which incise the continental slope (STETSON, 1949). The basement beneath these sediment layers, from Nova Scotia to New England, is metamorphosed rock of Palezoic and pre-Cambrian ages. The seismic velocities that are measured over the continental shelf for the basement are characteristic of metamorphics ; however, as one progress out over the continental rise there is a significant decrease in the basement velocity down to values which are more characteristic of lithified sediments. It is interpreted that this decrease in basement velocity represents decreasing metamorphism away from the main orogenic belt and that the basement under the continental rise is the now lithified sediment deposited seaward from sources on the continental shelf during the time when large thickness of sediment were being deposited landward to the Appalachian geosyncline. This basement thins and pinches out under the continental rise and is not present under the ocean basin areas. Here, the sediment is underlain by the simatic crust with seismic velocities characteristic of basic to ultrabasic rocks. The Mohorovicic discontinuity, which is at a depth of around 130,000 ft. (40 km.) below sea level under eastern North America, is at a depth of 30,000 ft. (10 km.) under the ocean basin areas.

SEISMIC REFLECTION PROFILES

The locations of the seismic reflection profiles are shown in Fig. 1. Profile 6 is over the Bermuda rise, 5 and 8 over the abyssal plain, 4 at the beginning of the continental rise, and 3 further up the continental rise. A sequence of records from profiles 3, 4, 5, and 6 illustrate the differences in the sediment structure between the areas, (Fig. 2). The subbottom reflections, where observed on each set, can be followed from one record to the next until they merge into the sub-bottom refraction arrival. On profile 6 a strong sub-bottom reflection is observed at a depth of 800 ft. below the bottom plus a strong multiple reflection from the same horizon. This depth correlates with the top of the volcanics from the seismic refraction profiles. On profile 5 a well defined although not quite as strong, reflection is observed at a depth of 1,000 ft. and a second reflection from a depth of 2,800 ft. The deeper reflection is near the bottom of the sediment column as measured from the refraction profiles. Profile 8, which has been discussed in a previous paper (OFFICER, 1955), illustrates the same type of records and measures a similar structure with the two reflectors at 1,200 and 3,400 ft. and in addition a weak multiple of the 1,200 ft. horizon.

is observed. On profile 4 the lower reflector at 2,600 ft. is observed. An upper reflector can be followed for a few records. On profile 3 a deep reflection or possibly deep refraction is observed at range, but the correlation back toward zero range cannot be followed.

These profiles present a consistent picture. The lower horizon of profiles 4, 5, and 8 is near the bottom of the sediment column, probably not the actual contact with the underlying simatic crust but a consolidated sediment zone above this contact. The upper reflector at a depth of around 1,000 ft. is the top of the volcanics under the Bermuda rise. Proceeding away from the Bermuda rise, this horizon is present on profiles 5 and 8, is questionable on 4, and is not present on 3. It is interpreted that the volcanics of the Bermuda rise extend out over the abyssal plain disappearing near the continental rise (Fig. 4). That the volcanic layer under the abyssal plain is thin, of the order of a few hundred feet, is known from the fact that it is not observed on the seismic refraction profiles. It is inferred that at the time of the volcanic activity associated with the building of the Bermuda islands and the Bermuda rise, some of the lava flows, perhaps from fissures on the outer portion of the rise, extended out over the abyssal plain.

The volcanic layer allows an age to be given to a portion of the sediment column under the abyssal plain. A boring on Bermuda (PIRSSON, 1914) reaches the volcanic platform: miocene and eocene foraminifera are found in the sediment immediately above the volcanics. PIRSSON gives the age of the volcanism as Triassic from the last period along the east coast of North America ; however, it may be later and contemporaneous with the volcanism of the Caribbean island arc. Either gives a compressed age scale for the sediment column under the abyssal plain and indicates that the upper third, at least, is Cretaceous or younger. This age agrees with that which might be given from an extrapolation of the known age for the intermediate horizon in the sediment under the continental shelf.

That there is not a uniform age scale through the deep ocean sediment column argues for the premise that, in a geological sense, the abyssal plain areas are not static, that there has not been a uniform increase in sediment with time. Rather there has been a more rapid increase in sedimentation associated with the Atlantic coastal plain. It might be reasoned further that the compressed age scale argues for a previous emergence of the ocean basins; however the author finds this incompatible with the evidence from the measured geologic structure under the oceanic and continental areas. It seems more reasonable to assume that such agencies as mid-ocean canyons (EWING *et al*, 1953) which today transport sediment from one abyssal plain to the next lowest and so on operated in the past in the same manner.

ACKNOWLEDGMENTS

The author wishes to express his thanks to Dr. J. B. HERSEY and Mr. H. R. JOHNSON for valuable discussions during this investigation and to those who took part in the work at sea and the analysis in the laboratory. This work was done under the sponsorship of contract NObsr-43270 with the Bureau of Ships, U.S. Navy.

Woods Hole Oceanographic Institution.

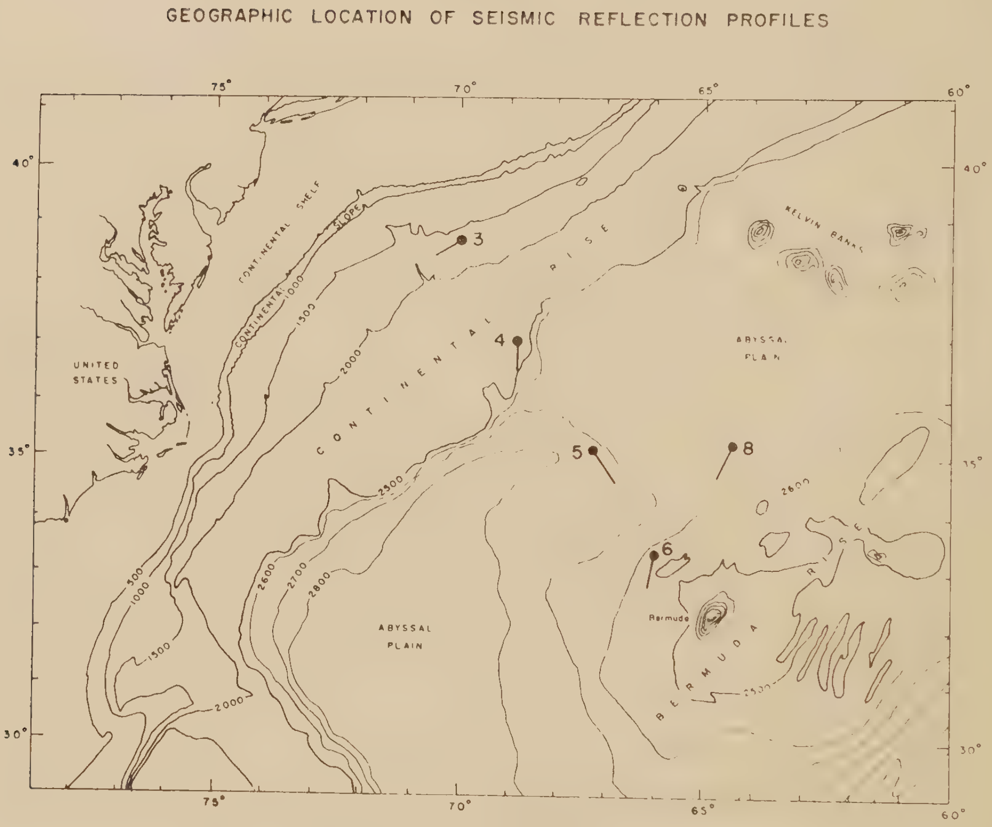
GEOGRAPHIC LOCATION OF SEISMIC REFLECTION PROFILES
75°
70°
65°
60°
40°
35°
30°
UNITED STATES
CONTINENTAL SHELF
CONTINENTAL SLOPE
CONTINENTAL RISE
ABYSSAL PLAIN
ABYSSAL PLAIN
KELVIN BANKS
BERMUDA RISE
Bermuda
3
4
5
6
8
500
1000
1500
2000
2500
2600
2700
2800

Fig. 1. Geographic location of seismic reflection profiles.

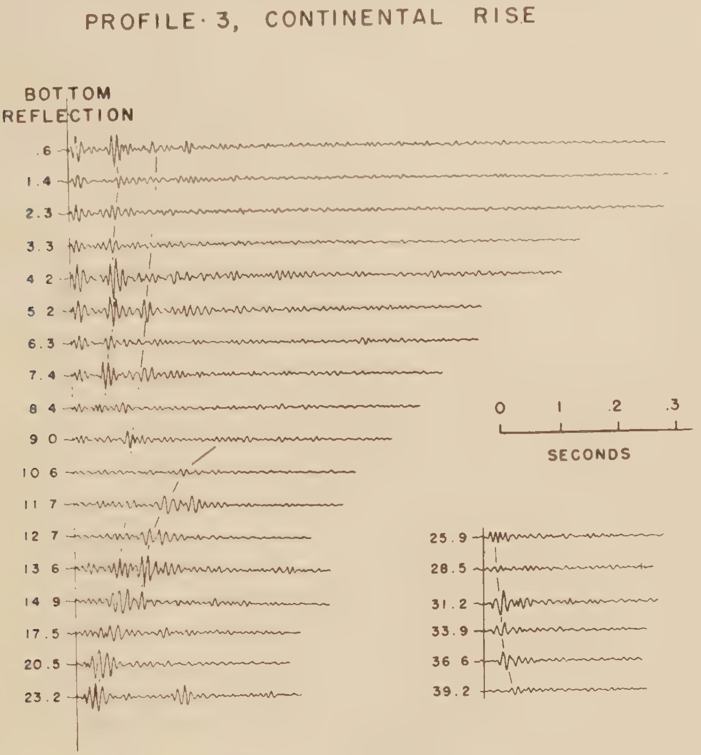

Profile 3, continental rise.

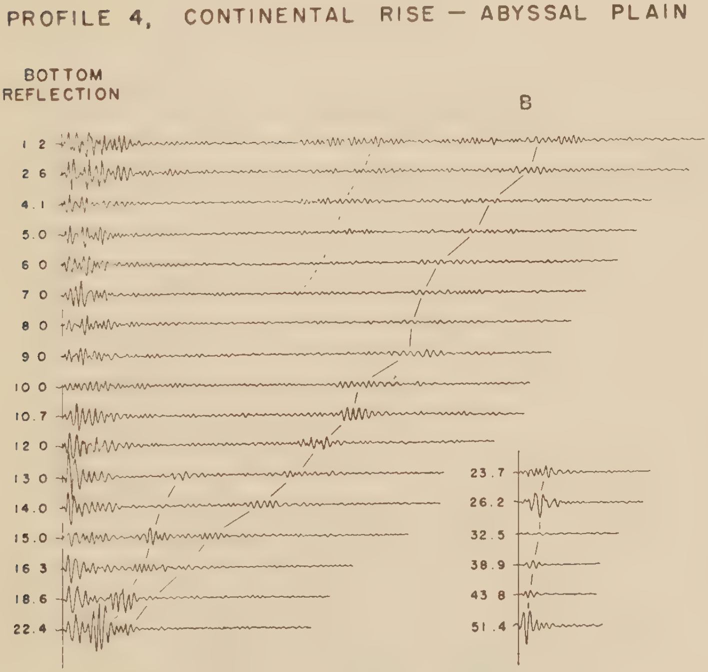

Profile 4, continental rise – abyssal.

Fig. 2.

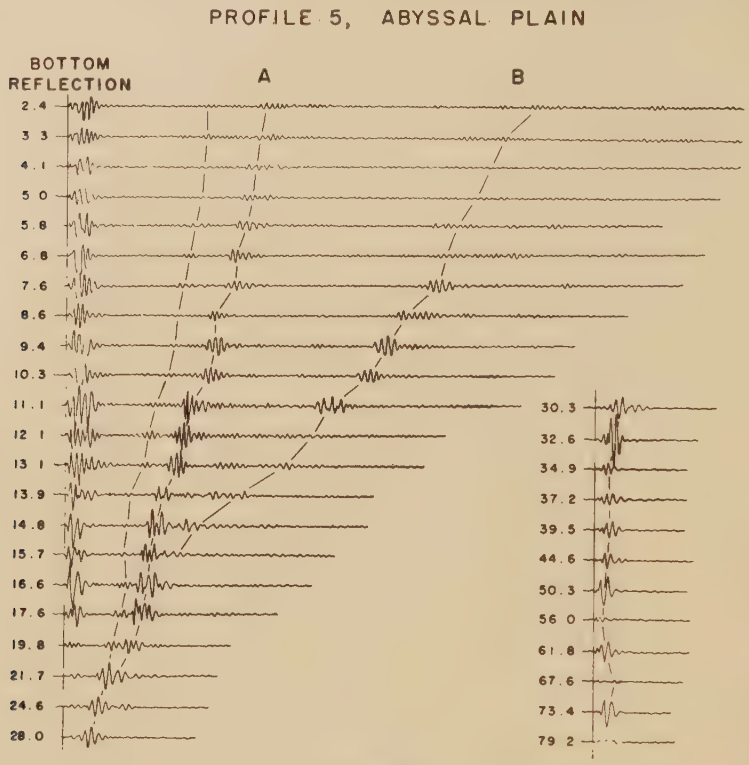

Profile 5, abyssal plain.

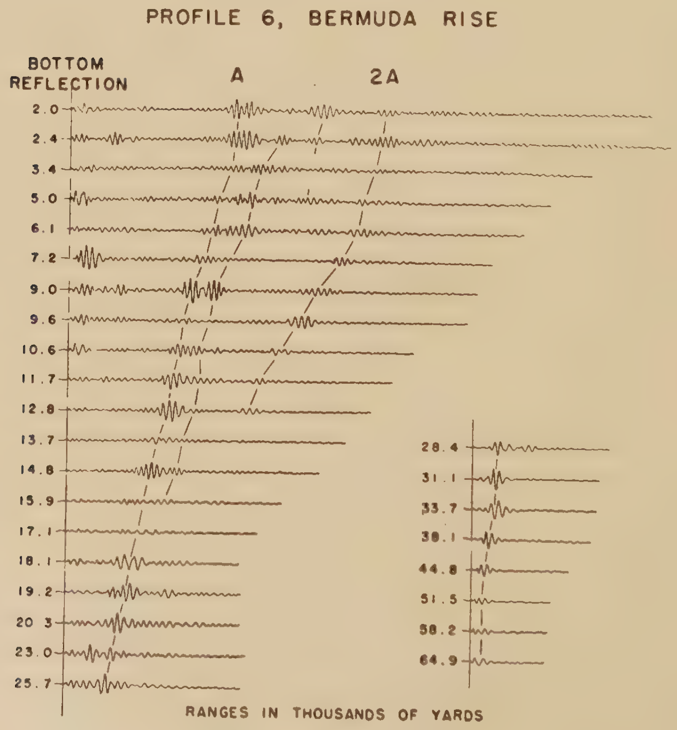

Profile 6, Bermuda rise.

Fig. 2.

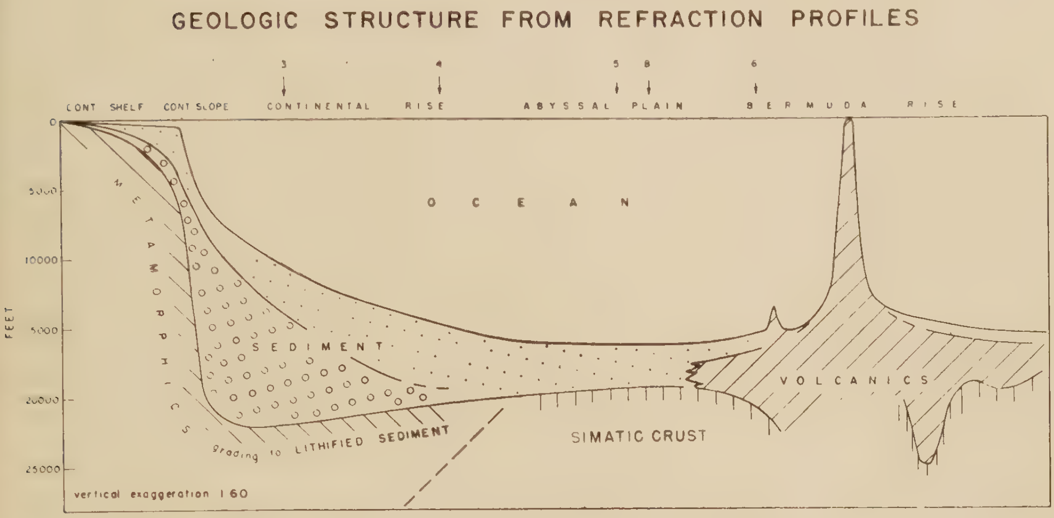
GEOLOGIC STRUCTURE FROM REFRACTION PROFILES
3
4
5
8
6
CONT SHELF
CONT SLOPE
CONTINENTAL RISE
ABYSSAL PLAIN
BERMUDA RISE
FEET
0
5000
10000
15000
20000
25000
OCEAN
METAMORPHICS
SEDIMENT
VOLCANICS
SIMATIC CRUST
grading to LITHIFIED SEDIMENT
vertical exaggeration 1 60

Fig. 3. Geologic structure from refraction profiles.

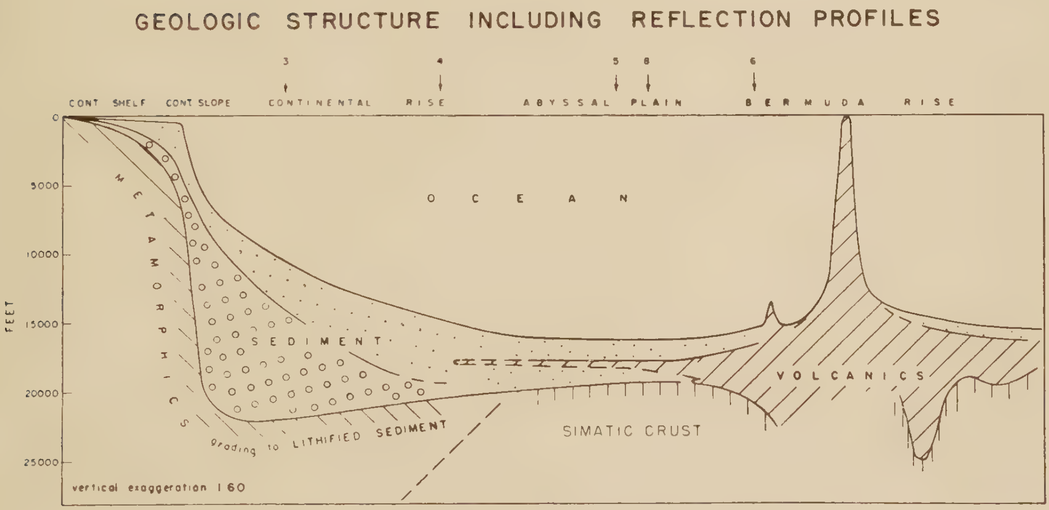
GEOLOGIC STRUCTURE INCLUDING REFLECTION PROFILES
3
4
5
8
6
CONT SHELF
CONT SLOPE
CONTINENTAL RISE
ABYSSAL PLAIN
BERMUDA RISE
FEET
0
5000
10000
15000
20000
25000
OCEAN
METAMORPHICS
SEDIMENT
VOLCANICS
SIMATIC CRUST
grading to LITHIFIED SEDIMENT
vertical exaggeration 1 60

Fig. 4. Geologic structure including reflection profiles.

REFERENCES

Ewing, M., Worzel, J. L., Steenland, N. C. and Press, F. (1950), Geophysical investigations in the emerged and submerged Atlantic coastal plain: Part V. Woods Hole, New York, and Cape May sections. *Bull. Geol. Soc. Amer.*, **61**, 877-892.

Ewing, M., Heezen, B. C., Ericson, D. B., Northrop, J., and Dorman, J. (1953), Exploration of the northwest Atlantic mid-ocean canyon. *Bull. Geol. Soc. Amer.*, **67**, 865-868.

Ewing, M., Sutton, G. H., and Officer, C. B. (1954), Seismic refraction measurements in the Atlantic ocean- Part VI. Typical deep stations, North America basin. *Bull. Seis. Soc. Amer.*, **44**, 21-38.

Hersey, J. B. and Ewing, M. (1949), Seismic reflections from beneath the ocean floor. *Trans. Amer. Geophys. Union*, **30**, 5-14.

Hill, M. N. (1952), Seismic refraction shooting in an area of the Eastern Atlantic. *Phil. Trans. Roy. Soc. London* A, **244**, 561-596.

Officer, C. B., Ewing, M. and Wuenschel, P. C. (1952), Seismic refraction measurements in the Atlantic ocean: Part IV. Bermuda, Bermuda rise, and Nares basin. *Bull. Geol. Soc. Amer.*, **63**, 777-808.

Officer, C. B. and Ewing, M. (1954), Geophysical investigations in the emerged and submerged Atlantic coastal plain: Part VII. Continental shelf, continental slope, and continental rise south of Nova Scotia. *Bull. Geol. Soc. Amer.*, **65**, 653-670.

Officer, C. B. (1955), A deep sea seismic reflection profile. *Geophysics* (in press).

Pirsson, L. V. (1914), Geology of the Bermuda island, the igneous platform. *Amer. J. Sci.*, **38**, 189-206.

Stetson, H. C. (1949), The sediments and stratigraphy of the east coast continental margin; Georges bank to Norfolk canyon. *Paper in Physical Oceanography and Meteorology*, **11**, (2), 1-60.

Weibull, W. (1947), The thickness of ocean sediments measured by a reflexion method. *Göteborg Vetenskaps och Vitterhets-Samhälles Handl.*, Sjatte Foljden, B. 5 (4), 1-17.

Printed in Great Britain by The Salisbury Press Ltd., Publicity House, Wilton Road, Salisbury, Wilts. (91430)

Contribution No. 744

Reprinted from SCIENCE, January 21, 1955, Vol. 121, No. 3134, pages 108–109.

Scattering Layer Observation

The deep-scattering layer has been shown to be esent over most of the oceans with the possible ex- ption of the polar areas. It is generally believed to nsist of marine organisms, and one of its remark- e features is the constancy with which it shows an echo sounding record as a ship moves along. is constancy is surprising in view of the relative tchiness of plankton indicated by the towing of ntinuous plankton samplers (*1*).

At the depth of the scattering layer an echo sounder licates only the presence or absence of a scatterer thin a large area. In an effort to obtain better reso- ion in recording the layer a transducer was lowered various depths. With the echo sounder set on its ortest range, only a small volume of sea was return- echoes at any one time. The drifting of the ship ved the transducer through the water and resulted scanning. Figure 1 shows the type of record ob- ned under these conditions. Two conclusions can mediately be drawn. First, the scattering is patchy though it was caused by individuals or small ools. Second, the size of the "individuals" is small ative to 25 ft. This is indicated by the concave derside of the patches on the record even at ranges short as 50 ft. As the scatterer passes through the am its distance from the transducer varies. It is tially further away, reaches a point of closest ap- oach directly beneath the transducer and then again edes as it passes out of the conic sound beam. If scatterer were longer than the beam width it would urn sound from a greater range when part of it s at a minimum range. Since this is not the case en at a range of 50 ft, where the sound beam is 25 wide, the second conclusion seems justified.

The velocity of the scatterers relative to the trans- cer can be computed from the curvature of the per sides of the patches. Nearly the same value is tained for all patches; therefore it would seem that scatterers are not affected by the sound and are moving about randomly. For this reason it is aightforward to count the number of patches in a own volume of water scanned and calculate their nsity.

So far it has been possible to do this only outside scattering layer. The scatterers occur on the aver- e of one for every 3×10^5 ft^3 of sea. This is in reement with the frequency of large individual noes found by Raitt (*2*) outside the scattering layer the Pacific Ocean. It is also in substantial agree- nt with the numbers of fish caught by a mid-water wl of efficient design described in some unpub- ned work of Backus. Backus' investigation was de in the same area of the Atlantic as ours.

The scattering layer in the North Atlantic is usually t developed during the day at a depth of about 250 homs. Consider that some transducers are sensitive over an angle of about 30 deg. Then from the surface the sound beam is sampling a circular section of the layer 750 ft in diameter. Echoes are returned from a thickness of half a pulse length, which for the records here is 20 ft. The volume of sea returning sound at any instant is then about 10^7 ft^3.

Unfortunately the only figures here are for outside the main region of scattering. Even in this sparsely populated area there are 30 individuals in the sound beam at one time. Backus (personal communication) reports a density of fish in the layer that would place at least 500 in the beam at one time. Marshall (*1*) has presented plausible evidence that bathypelagic fish are widespread and nonschooling in behavior. It is not surprising then that the scattering layer record appears continuous. Such a large average number would only rarely be expected to fluctuate to a low value and thus give no echo.

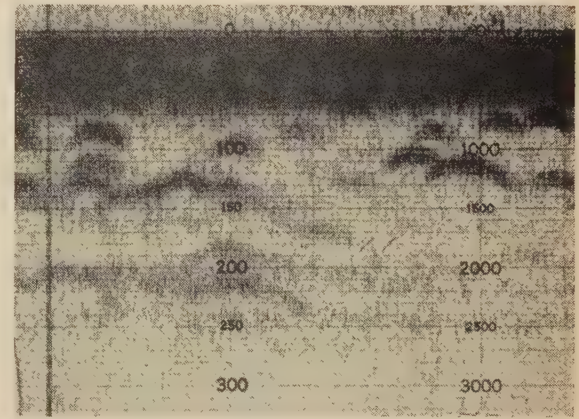

Fig. 1. Section of recording tape with the transducer at a depth of 200 m. The vertical scale is 0 to 500 ft. This represents depths below the transducer. The frequency of the sound was 12 kcy/sec.

Work will be done to narrow the cone angle and shorten the pulse length. This will permit the counting of scatterers in more densely populated regions. In addition, a measurement of the echo intensity will help to establish the size range of the scatterers. The possibility exists of using a surface-controlled camera in conjunction with the transducer. This should constitute marked improvement over the random picture-taking technique now in use.

JOHN KANWISHER
GORDON VOLKMANN

Contribution No. 744,
Woods Hole Oceanographic Institution,
Woods Hole, Massachusetts

References

1. N. B. Marshall, "Bathypelagic fishes as sound scatterers in the ocean," *J. Marine Research* **10**, 1 (1951).
2. R. W. Raitt, "Sound scatterers in the sea," *ibid.* **7**, 393 (1948).

1 November 1954.

Contribution No. 746

Reprinted from Proceedings of the First Conference
on "SHIPS AND WAVES", Chapter 2, Pages 11-32, 1955.
Council on Wave Research and Society of
Naval Architects and Marine Engineers.

CHAPTER 2

A TECHNIQUE FOR OCEAN WAVE MEASUREMENTS[1]

H. G. Farmer, W. Marks, R. G. Walden, G. G. Whitney, Jr.
Woods Hole Oceanographic Institution
Woods Hole, Massachusetts

ABSTRACT

A general description of the WHOI wave poles, a theoretical analyses of their approximate motions and results to date are presented. Detailed mechanical drawings and circuit diagrams are included in the appendix.

INTRODUCTION

In recent years intensive investigation of the generation and propagation of waves in deep water has created a demand for open ocean wave measurements. Great success in the measurement of ocean waves has been achieved in the near shore zone where an instrument is placed on the bottom or attached to some permanent structure and connected to the shore by cable. The major problem in moving into a region of deep water is to retain the stable platform from which the heights of the waves may be measured. The purpose of this paper is to describe the WHOI wave poles which from tests to date, appear to satisfy this requirement.

DESCRIPTION OF WHOI WAVE POLE

In the design of a wave measuring instrument it was felt that several basic requirements should be met. (a) To avoid the cumbersome equipment and inherent difficulties in anchoring a buoy to the bottom, it was considered that a freely floating buoy should be used. Further, this does away with the problem of strong currents tending to tow under an anchored surface buoy. (b) The buoy should have no physical connection to a ship standing by. From experience at sea it has been observed to be very difficult and most likely generally unsuccessful for a ship of any size in even a moderate sea to keep from imparting any motion to a floating buoy when the two are connected by a cable. (c) A freely floating buoy should respond to the forces acting on it with only small to negligable motions. Hence the buoy should be highly stable in pitch and roll, and in order that its amplitude in vertical oscillation be small, its vertical natural period of oscillation should be large compared to the period of waves encountered, Holmes (1954). Also the physical size of the buoy should be small in order to keep down the magnitude of the viscous forces.

---

[1] Contribution No.746 from the Woods Hole Oceanographic Institution. This work was supported from funds made available by the Bureau of Ships, Department of the Navy, through their contract with the Woods Hole Oceanographic Institution.

(d) Consideration should also be given to ease in launching and retrieving the buoy. (e) In connection with the sensing element it should respond not only to the gross features of the sea but also to as much of the fine structure as possible. Clearly the sensing element and necessary electronics should be rugged and dependable. (f) The final desired information is a displacement profile of the sea surface as a function of time. Presumably the vertical acceleration, velocity or displacement of the sea surface could be sensed. However, in the former two cases double or single integration would be required. Due to the inherent difficulties of this processing, particularly in the double integration, it was decided to sense the actual displacement of the sea surface about some reference datum.

To accomplish these aims two wave poles have been built, their general arrangement being shown in Fig. 1. By a proper distribution of weight the center of gravity of the main section can be kept well below its center of buoyancy, the distance between C.G. and C.B. being in the order of two to three feet. Hence the wave poles are very stable against a pitching or rolling motion. The natural period of vertical oscillation is made large by keeping the cross sectional area of that portion of the wave pole piercing the water surface as small as practicable and by keeping the overall mass of the system large. The latter is accomplished in the following manner. In reference to Fig. 1, additional lengths of pipe or hot water tanks are secured end to end and attached to the bottom of the main section. For the Capacitance Wave Pole, No. 1 tank is buoyant and Nos. 2, 3 and 4 are open so that they flood with water. The weight necessary for final ballasting is usually secured at the very bottom. If the wave pole is in vertical oscillation the total mass of the system now comprises not only the additional mass of the four tanks but also the water mass trapped within the bottom three tanks. A similar arrangement is used on the Inductance Wave Pole except that only two twenty foot lengths of tubing are used. A natural period of approximately forty seconds is obtained for each wave pole.

In launching either of the wave poles from a ship it is highly desirable that there be a minimum of rigging due to the long length of the top section alone. So far, in putting the wave poles overboard, it has been the practice to put the separate sections, starting from the bottom, singly over the side, securing them as each new section goes over and gradually lowering away. This procedure becomes increasingly more difficult as the sea state rises. An alternative procedure would be to fully assemble the wave pole along the rail of a ship and then, using loops of rope, lower the complete assembly horizontally into the water. When released the wave pole will gradually right itself. Retrieving the wave pole would follow the former procedure but in reverse. During a rough sea it would be a relatively dangerous operation not only to the safety of the wave pole but to the personnel involved. The life of the batteries in the wave poles on a transmitting schedule of twenty minutes every three hours is about four days. Hence it should be possible to place and retrieve the wave poles during the relative calm before and after the development and decay of a state of sea.

The two wave poles have been built in order to investigate two distinctly different types of sensing elements. In one case the top part of the wave

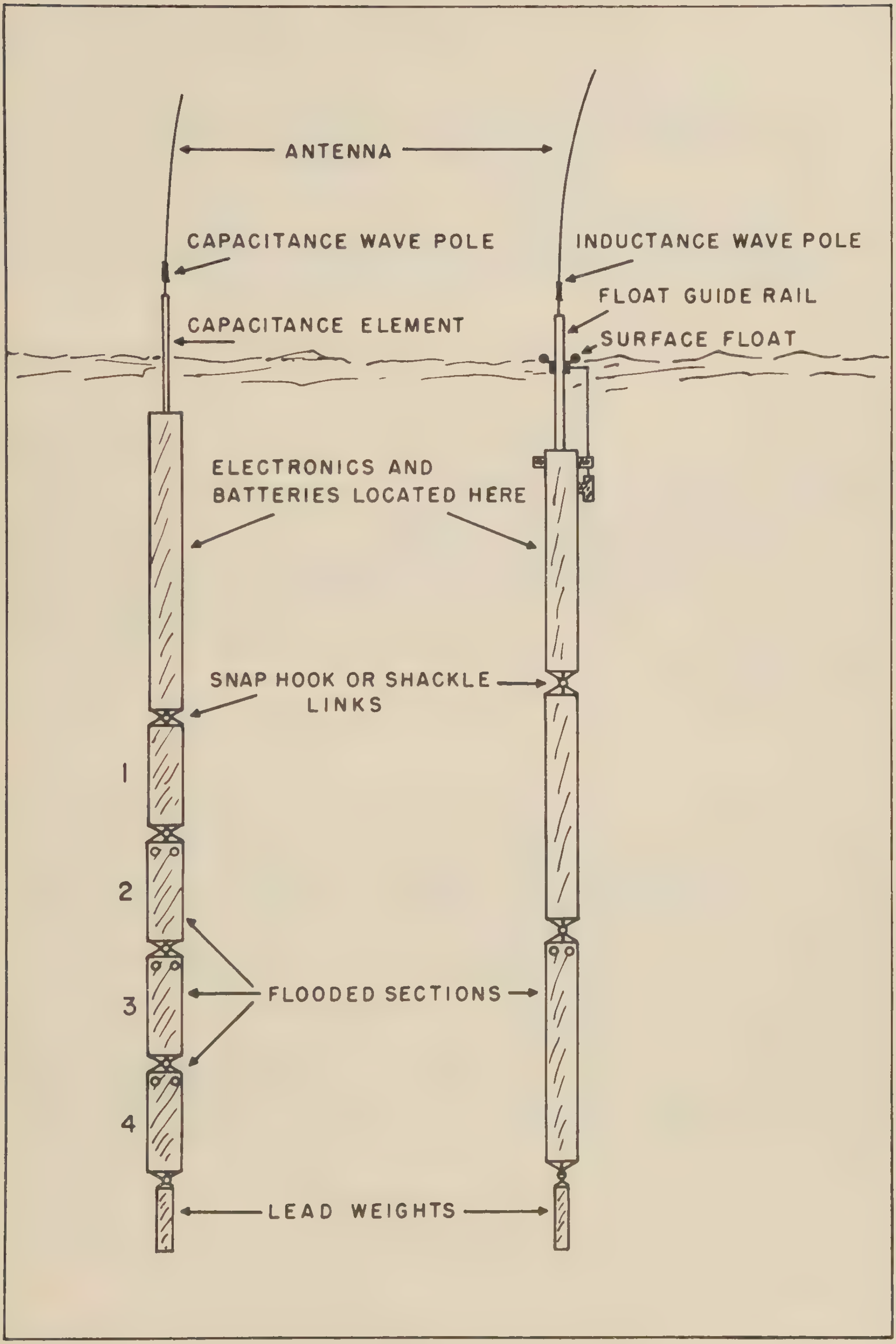
ANTENNA
CAPACITANCE WAVE POLE
INDUCTANCE WAVE POLE
FLOAT GUIDE RAIL
CAPACITANCE ELEMENT
SURFACE FLOAT
ELECTRONICS AND BATTERIES LOCATED HERE
SNAP HOOK OR SHACKLE LINKS
1
2
3
4
FLOODED SECTIONS
LEAD WEIGHTS

Fig. 1. Schematic diagram, W.H.O.I. wave poles.

pole is a 1 1/2" diameter steel tube 18' long which is insulated from the water. Mean water level is at the midpoint of this tube. The capacitance of the steel tube to the water is a direct measure of the immersion of the pole by a passing wave. In the other case a small float is constrained to move vertically along a small diameter tube, the vertical motion being transmitted by a fine wire to a variable inductance mounted inside the body of the wave pole. For brevity the two wave poles will subsequently be referred to as the Capacitance and/or Inductance wave pole. The purpose for investigating these two types of sensing elements was that foam and water clinging to the capacitance sensing element could introduce an unknown error whereas the mechanical float would not respond erroneously to these causes. The capacitance sensing element, however, is simple and without any mechanical workings which could fail.

Fig. 1 illustrates the general arrangement of both wave poles. The capacitance element is attached to a Formica plug which fits into the 6" dia. pipe and is sealed by "O" rings. The electronic unit is placed immediately below this plug and the batteries slide to the bottom, Fig. 2. When comletely assembled the antenna, capacitance element and top section are an integral unit nearly 50' long. The steel tube, forming the core of the sensing element, is wrapped with Scotch Electrical Tape #33 to provide insulation and act as dielectric. As discussed in more detail under Electronic Description, the thickness of the wrapping is varied to provide a linear variation of frequency with wave height. To facilitate the water running off the pole as the water level recedes, run-off rings are placed every six inches, Fig. 3. As the water runs over the rings it forms droplets and falls free of the pole. To further resist the water clinging to the pole, a thin coating of Dow-Corning DC-4 Silicone grease is applied.

For the Inductance Wave Pole, the main section is a four-inch dia. steel tube. The float guide rail is specially constructed. The float guide rail is attached to a Formica plug and fits into the main section in a similar manner as the capacitance pole. This guide rail consists of a three-quarter inch diameter aluminum tube with two aluminum strips attached in a manner to give the overall cross section a strut-like shape. The float may be a scooter-type tire tube or can be built up of balsa wood and suitably painted. This is connected through gimbals to the guide wheels which allow vertical motion without rotation about the vertical axis. A fine stainless steel braided wire, 16x1x.003 construction, connects the float to the inductance take-up wheel, Fig. 4. This in turn drives in and out the iron slug and consequently changing the inductance of a solenoid which is mounted inside the main section. To provide smooth and continuous transfer of motion from the float to the inductance take-up wheel the connecting wire must always be kept taut. This is accomplished by a spring-driven take-up wheel mounted and connected to the other take-up wheel as shown in Fig. 4.

ELECTRONIC DESIGN

The wave poles contain a radio transmitter, audio oscillator, timing motor and the necessary batteries. The circuitry is essentially similar for

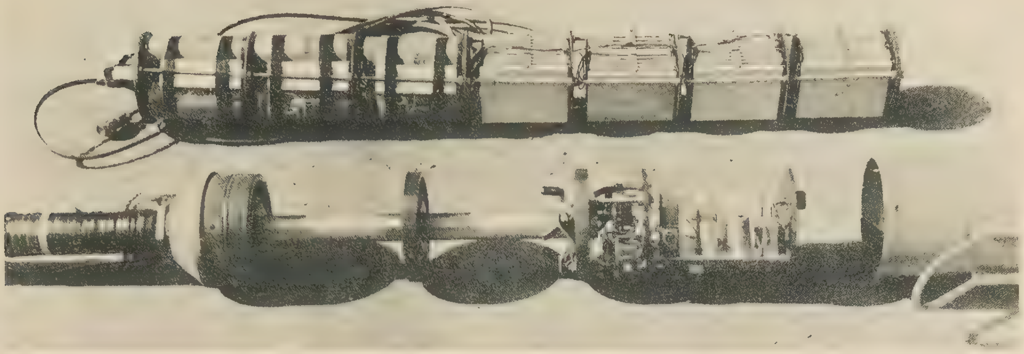

Fig. 2. Capacitance wave pole, coupling of sensing element to top section, electronics and battery supply.

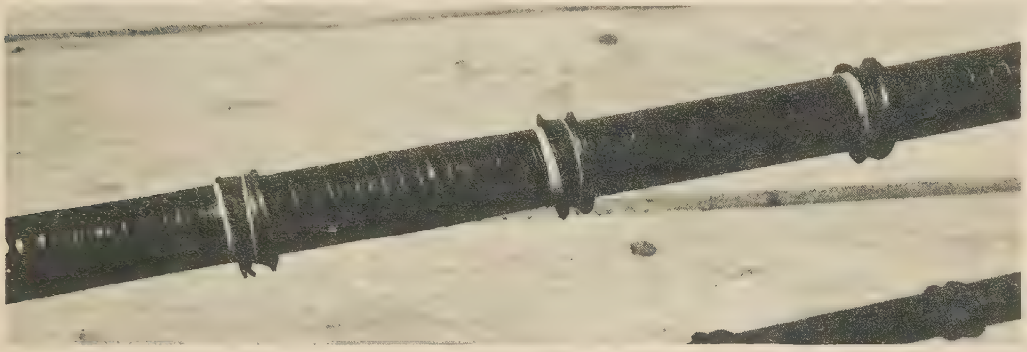

Fig. 3. Capacitance wave pole, sensing element and run-off rings.

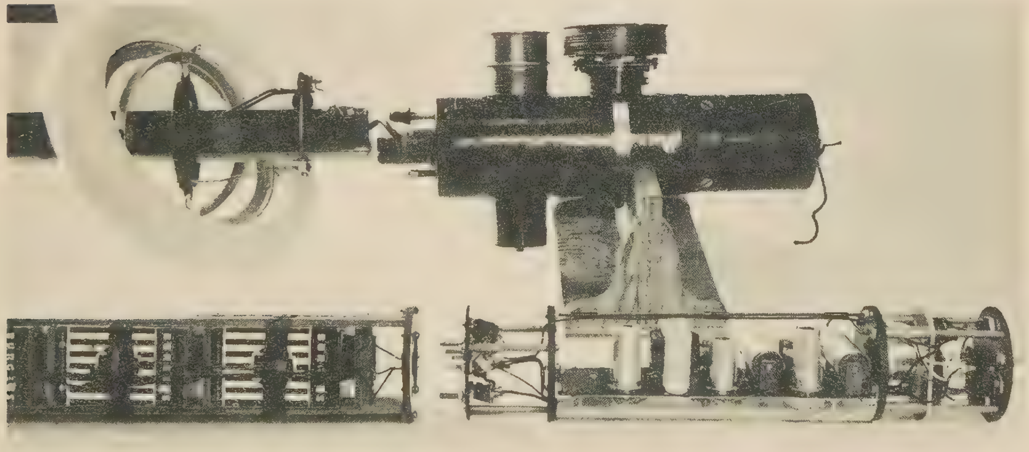

Fig. 4. Inductance wave pole, coupling of guide rail to top section, float assembly, take-up wheels, electronics and battery supply.

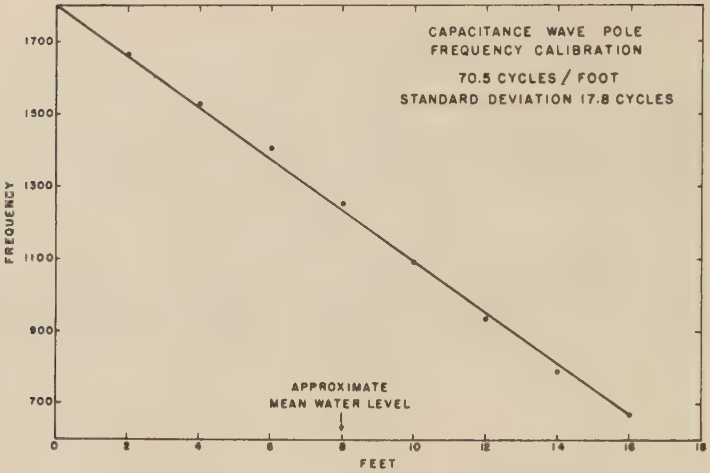

Fig. 5. Capacitance wave pole, typical calibration curve, audio frequency output vs depth of immersion of sensing element.

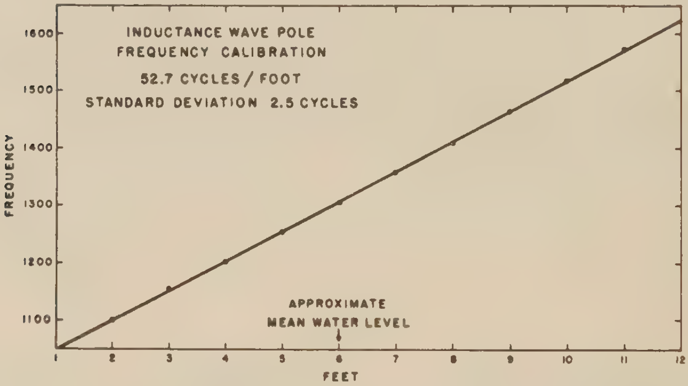

Fig. 6. Inductance wave pole, typical calibration curve, audio frequency output vs depth of immersion of guide rail.

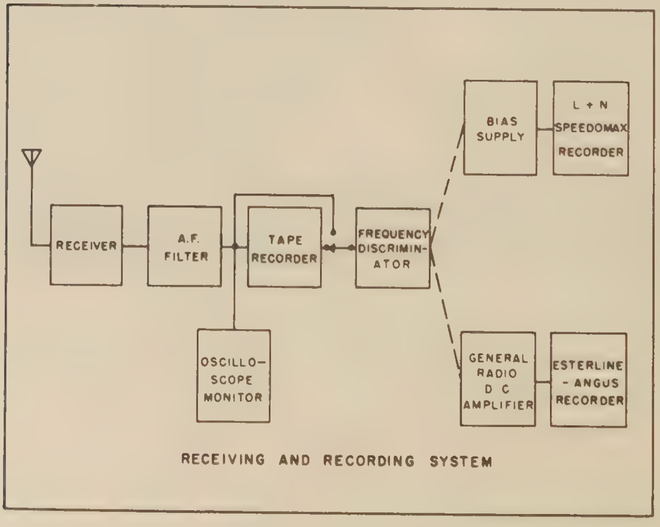
RECEIVER
A.F. FILTER
TAPE RECORDER
FREQUENCY DISCRIMIN- ATOR
OSCILLO- SCOPE MONITOR
BIAS SUPPLY
L + N SPEEDOMAX RECORDER
GENERAL RADIO D C AMPLIFIER
ESTERLINE - ANGUS RECORDER
RECEIVING AND RECORDING SYSTEM

Fig. 7. Block diagram of receiving and recording apparatus.

both the capacitance and the inductance wave pole. The change of capacitance of the sensing element in the former directly causes the frequency of the audio oscillator to vary, whereas the change in level of the float in the latter causes a change in the inductance and a consequent frequency change in the audio oscillator. This audio frequency oscillator amplitude modulates the R.F. amplifier of the transmitter. The transmitter is crystal controlled and operates on approximately 5.4 megacycles. The antennae, located at the very top of the wave poles, are electrically equivalent to a quarter wavelength. The range of the transmitter is approximately eight to ten miles.

To obtain linearity from the capacitance element, the necessary thickness of tape as a function of length was first computed. This served as a starting point and experimentation determined what additional tape was necessary to obtain the desired linearity. Fig. 5 illustrates a typical calibration of audio frequency versus immersion of the capacitance wave pole.

The winding on the solenoid used in the Inductance wave pole was rewound so as to provide sufficient inductance to keep the audio frequency in the desired range. A typical calibration of audio frequency versus float position is given in Fig. 6.

The calibration curves will shift slightly with battery use, however, this shift is essentially parallel to the given lines. It is, therefore, the frequency change per foot of immersion which is the information needed for final interpretation of the records.

The monitoring and receiving apparatus may be either shore based or located on a ship standing by the wave pole. The audio output from a receiver may be directly recorded on a magnetic tape for future use or the tone can be fed to a frequency discriminator whose output is then put on a pen and ink recorder such as the Leeds Northrup Speedomax. The latter procedure gives a direct graphic representation of the sea surface.

Fig. 7 illustrates the receiving station equipment.

ANCHORED WAVE BUOY

For use in bays, estuaries or other inshore work where swell and waves are not excessive an anchored telemetering wave buoy has been built. This unit utilizes the capacitance sensing element as previously described except that its length has been shortened to twelve feet. This wave buoy can be anchored in water as shallow as twelve feet and has been used successfully in water up to seventy feet in depth. A strong upward pull from positive buoyancy and a taut mooring line maintain vertical stability of the buoy. The electronic circuitry and the receiving and recording apparatus are essentially the same as that of the capacitance wave pole. Sufficient batteries are included to permit continuous operation for thirty to forty hours. The transmitter is turned on and off by means of a relay which may be energized, at will, by applying a D.C. pulse between the antenna and the sea water. The complete buoy, disassembled, is shown in Fig. 8.

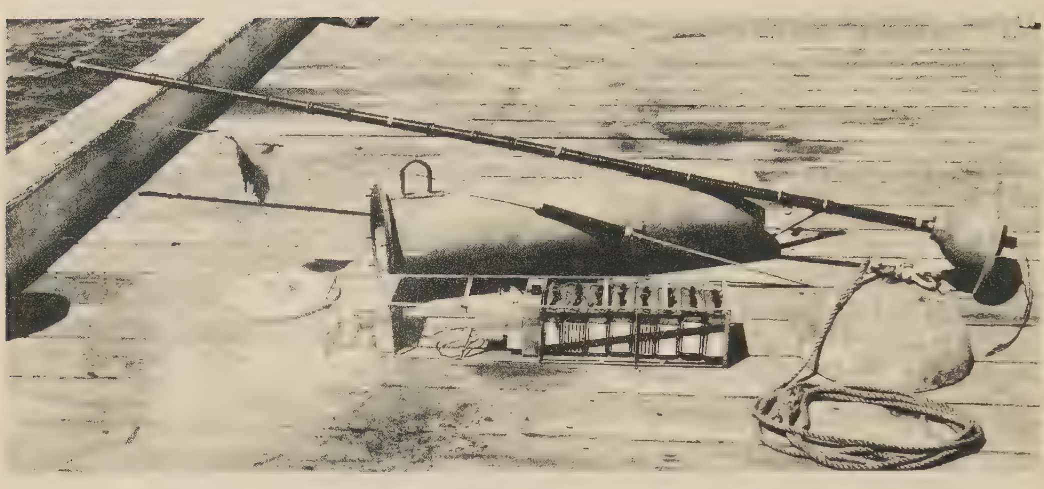

Fig. 8. Anchored wave pole, disassembled, sensing element, antenna, tank, electronics battery supply and anchor.

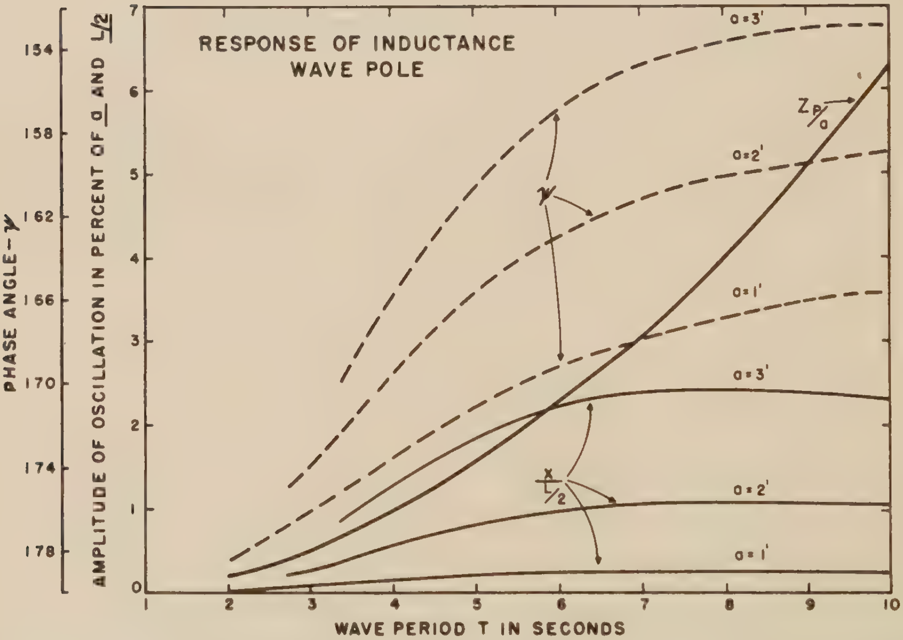

Fig. 9. Theoretical response of inductance wave pole to a sinusoidal sea surface. The abscissa is the wave period T. The ordinates are the phase angle and the amplitude of the vertical and horizontal motion expressed as the percent of the wave amplitude, a, and half the wave length, L/2, respectively.

A TECHNIQUE FOR OCEAN WAVE MEASUREMENTS

THEORETICAL ANALYSIS

The purpose of the following analysis is to present the approximate magnitude of the motions of the wave pole when subjected to a sinusoidally varying sea surface. It is not intended that the results of the analysis are applicable to any particular component of a sea surface which comprises an infinite number of waves of different frequencies. Whereas the theory is linear, if the actual response of the wave pole to a confused sea is also linear, then it would be possible to use the theory to indicate an approximate error in the recorded amplitude or energy of any particular constituent wave. However, before such use can be made the actual motion of the wave pole when under a sea condition must be observed and compared to the theory. The results of this section, therefore, should not be extrapolated beyond the assumed sea surface condition prior to further testing, at least not without considerable caution being shown.

Several basic assumptions will first be made. (a) The main section of the wave pole and the buoyant and flooded tanks are a single rigid member of constant cross section. (b) There is no wind effect. (c) The capacitance element and the float guide rail are sufficiently small that the viscous forces acting on them are negligible. Also their cross section is constant over their length. (d) The variation in height of the sea surface is sinusoidal.

The equation of vertical motion for the wave pole may be written as

$$M Z'' + f Z' + kZ = F_o(t) \tag{1}$$

where M is the mass of the system, f the damping coefficient, k the spring constant, $F_o(t)$ the forcing function, and Z the vertical displacement about the mean position. Symbols used subsequently are defined at the end of this section. To facilitate the solution it has been assumed that the viscous term follows a linear law with velocity.

The forcing function $F_o(t)$ is composed of two parts. The first part F_1, is the fluctuating buoyant force imparted on the system due to the rise and fall of the sea surface as waves pass by.

$$F_1 = ka \sin wt \tag{2}$$

The second part, F_2, is the viscous drag resulting from the vertical component of the particle velocities. The magnitude of this force at any depth will be assumed to be proportional to the square of the magnitude of the vertical velocity component, and will vary in time as the cosine, hence,

$$F_2 = F \cos wt \tag{3}$$

and

$$F = C_f \frac{\rho}{2} \pi d \int_{y_1}^{y_2} |v|^2 \, dy \tag{4}$$

From wave theory

$$v = \frac{2\pi a}{T} e^{-\frac{2\pi y}{L}} \cos wt \tag{5}$$

then

$$F = C_f \pi \frac{\rho g}{4} d a^2 b \tag{6}$$

with

$$b = e^{-\frac{4\pi y_1}{L}} - e^{-\frac{4\pi y_2}{L}} \tag{7}$$

$$L = \frac{gT^2}{2\pi} \tag{8}$$

The complete solution to equation 1 is

$$Z = Z_c + Z_p \tag{9}$$

where

$$Z_c = e^{-\frac{f}{2M} t} (C_1 \cos \beta t + C_2 \sin \beta t) \tag{10}$$

$$\beta = \sqrt{\frac{k}{M} - \left(\frac{f}{2M}\right)^2} \tag{11}$$

and

$$Z_p = \frac{\sqrt{\left(\frac{F}{k}\right)^2 + a^2}}{\sqrt{\left(1 - \left(\frac{w}{w_o}\right)^2\right)^2 + \left(2\frac{f\,w}{f_c w_o}\right)^2}} \sin (wt - \psi) \tag{12}$$

$$\tan\psi = \frac{\frac{F}{ka}\left(1 - \left(\frac{w}{w_o}\right)^2\right) - 2\frac{f\,w}{f_c w_o}}{\frac{F}{ka} 2 \frac{f\,w}{f_c w_o} + \left(1 - \left(\frac{w}{w_o}\right)^2\right)} \tag{13}$$

Eq. 10 depicts the transient resulting from specified initial conditions. This equation is useful in determining the damping coefficient, f, and the effective mass. The effective mass is greater than the true mass because of the entrapped water in the flooded tanks and also because of the thin film of water dragged along with the wave pole when in motion. After sufficient time the transient will become negligible and the vertical motion of the wave pole will be given by equation 12. From inspection of this equation it is apparent that as the frequency of the waves of encounter approaches the natural frequency of the pole the displacement, Z_p, will become very large. As resonance is approached the term F/k becomes small and there remains only the usual amplification factor.

To determine the horizontal motion of the wave pole it will be assumed that the only force acting is that due to the drag of the horizontal component of the particle velocity. Hence

$$M X'' = R \sin wt \tag{14}$$

The amplitude of the drag force, R, is constructed similarly to that of F_2.

$$R = C_D d \frac{\rho}{2} \int_{y_1}^{y_2} |u|^2 \, dy \tag{15}$$

With

$$u = -\frac{2\pi a}{T} e^{\frac{2\pi y}{L}} \sin wt \tag{16}$$

$$R = C_D \frac{\rho g}{4} d a^2 b \tag{17}$$

It should be noted that C_D is the coefficient of drag of a cylinder whose axis is perpendicular to the direction of flow. C_f is the mean drag coefficient of a flat plate parallel to the direction of flow.

The horizontal motion of the wave pole is then given by

$$X = -\frac{R}{Mw^2} \sin wt \tag{18}$$

Prior to using these equations to estimate the magnitude of the wave pole oscillations it is first necessary to determine the effective mass and damping coefficient. Approximate values may be obtained by putting the wave pole into vertical oscillation under still water conditions and recording the resultant motion. From the damped natural period and the slope of the exponential decay, M and f may be computed from equations 10 and 11.

Fig. 9 shows the results of equations 12, 13, and 18 for data pertinent to the Inductance wave pole. The abscissa is the period, in seconds, of the sinusoidal surface waves. The ordinates are the phase angle ψ, in degrees, and the amplitude of the vertical and horizontal motion expressed as the percent of the amplitude of the wave, a, and half the wave length, respectively. The three curves correspond to waves of amplitude one, two, and three feet. The following data was used in the computations:

$$T_o = \frac{2\pi}{w_o} = 40 \text{ seconds}$$

$f/f_c = 0.25$

$y_1 = 6'$, $y_2 = 68'$

$A = 0.00458 \text{ ft}^2$

$\gamma = 64 \ \#/\text{ft}^3$

$d = 0.33 \text{ ft}$

$M = 14 \ \# \text{ sec/ft}$

$C_D = 1.0$

$C_f = 0.003$

It is clear that these results depend on the selection of C_D and C_f. Also, it is interesting to note that, from the computations for the vertical motion, the effect of the viscous drag compared to rise and fall of the sea surface is less than 1% for a = 1 ft, 6% for a = 2 ft and 20% for a = 3 ft. Whereas Fig. 9 extends out to only 10 seconds, the displacement Z_p will become equal to the wave amplitude a at a wave period of about 32 seconds. Further, the phase angle in the desired range of wave periods is in the order of 180°. Hence in order that the wave pole respond with a minimum error to the recorded signal, the natural period of oscillation of the wave pole should be as large as practicable.

SYMBOLS

A	Cross sectional area of capacitance element or float guide rail
a	Amplitude of wave
C_D, C_f	Drag coefficients, defined in text
C_1 C_2	Constants
d	Diameter of wave pole
F	Force
f	Damping coefficient
f_c	$= 2\sqrt{kM}$, critical damping coefficient
g	Gravitational acceleration

k	$= \gamma A$ spring constant
L	Wave length
l	$y_2 - y_1$, total length of submerged part of wave pole
M	Mass of wave pole
T	Wave period
T_o	Undamped natural period
t	Time
u	Horizontal component of particle velocity
v	Vertical component of particle velocity
w	Angular wave frequency
X	Coordinate, horizontal displacement
y_1 y_2	Distance from sea surface to top and bottom of main part of wave pole, respectively
Z	Coordinate, vertical displacement
β	Damped natural frequency
γ	Unit weight of water
ρ	Unit mass of water
ψ	Phase angle

RESULTS

The wave poles were tested at four different locations. Two tests were made at George's Bank, July 18, 1954 and Nantucket Shoals, July 28, 1954. At George's Bank both the inductance and capacitance poles participated, and in addition, a second capacitance pole was rigidly attached to a piling sunk into the bottom. At Nantucket Shoals only the capacitance pole was used. On neither occasion, however, was the maximum wave height greater than 2 1/2 feet, not did the periods exceed 3 seconds. This made it difficult to evaluate the effectiveness of the stable platforms and the sensing elements, as the theoretical analysis indicated that significant motions of the wave pole would not appear until waves with periods of approximately 10 seconds or more were encountered.

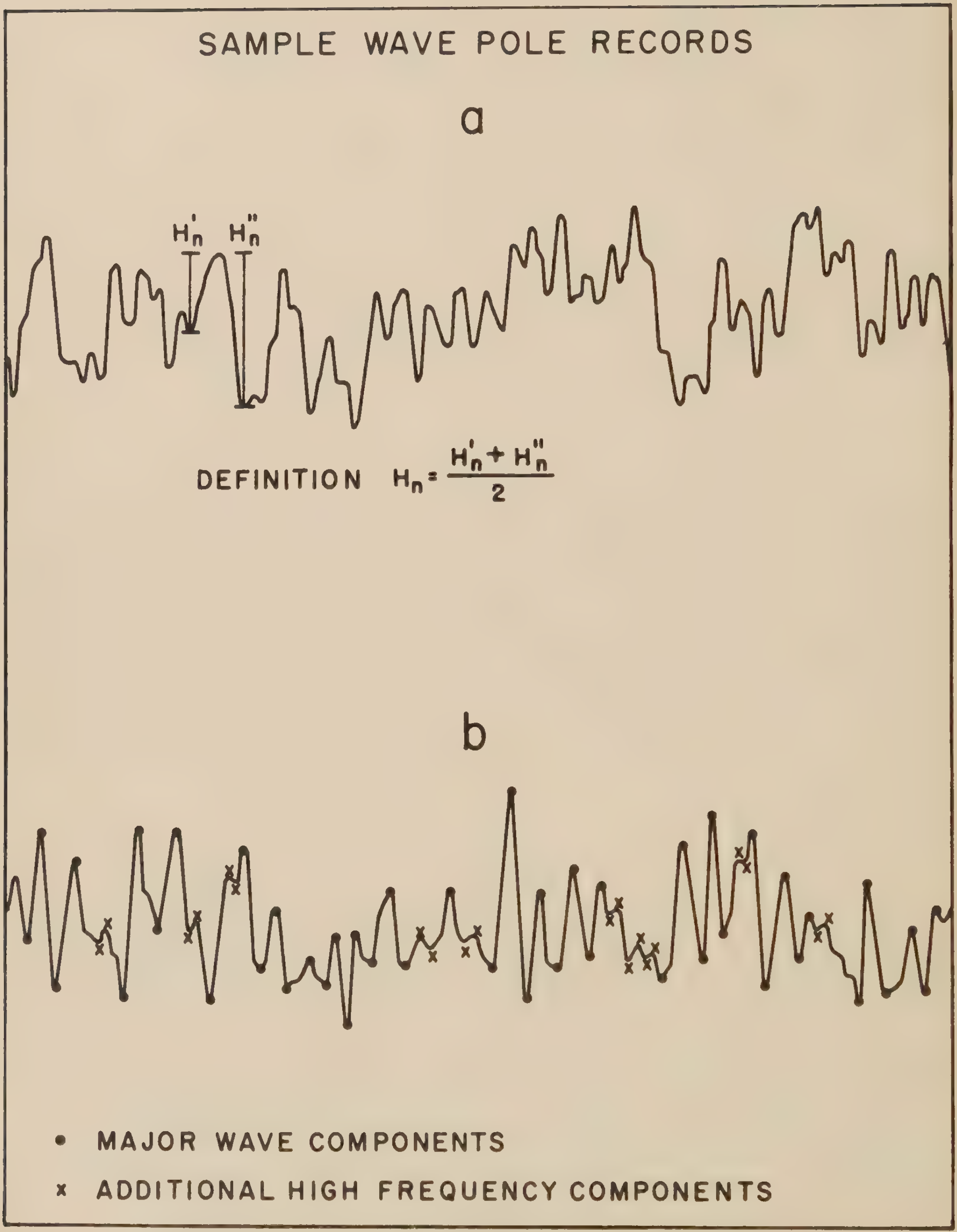

Fig. 10. Sample wave records obtained with the capacitance wave pole. The method of reading the records is indicated.

The other two locations were roughly 250 miles ESE of Nantucket Island. These tests took place on the 21st and 25th of October 1954. The highest waves were about 9.3 feet and the maximum period was about 8 seconds. Unfortunately, only the capacitance pole was used in these tests.

As the mechanics of the system appear to be theoretically sound, it was believed that if the wave records compare favorably with the distribution of wave heights predicted by Longuet-Higgins (1952) and observed by other investigators then a certain degree of confidence might be established in the wave measuring system.

To make this comparison, the wave heights were measured and the ratios $\overline{H}_{1/3}/\overline{H}$ and $\overline{H}_{1/10}/\overline{H}$ computed. $\overline{H}$ is the average wave height, $\overline{H}_{1/3}$ the average of the one-third highest waves or significant height, and $\overline{H}_{1/10}$ is the average of the one-tenth highest waves. The height, H_n of any wave was defined as

$$H_n = \frac{H_n' + H_n''}{2}$$

where H_n' is the height measured from the wave crest to the preceding trough and H_n'' is the height measured from the wave crest to the following trough. This is shown in Fig. 10a. In comparison to the records obtained from pressure recorders, the wave poles appear to sense a relatively wide band of frequencies. It was decided that the records would be analyzed in two fashions. In one case the major wave components alone were measured and in the other case all of the waves present were measured on the basis of the definition that a wave is a bump on the water surface whose slope changes sign somewhere.

Table I shows the results obtained from the Woods Hole wave poles, the theoretical prediction, and the results of investigations by others. In the case of the pressure records it should be remembered that only the major wave components were measured because the pressure recorder receives a pressure signal which has had the higher frequencies filtered out. Column IV, which indicates the depth of the wave recorder is only pertinent to the pressure records; the wave poles sense the free surface directly. In lines 12 - 16 various arrangements of the wave poles were used. The results, however, indicate nothing significant about any one particular arrangement. In lines 17 - 23 the complete wave pole as indicated in Fig. 1 was used. The average per cent difference for these last seven data are

$\overline{H}_{1/3}/\overline{H}$	$\overline{H}_{1/10}/\overline{H}$	
10.5	15.6	All comp.
3.9	5.4	Maj. comp.

Table I

Evaluation of wave records obtained by WHOI capacitance wave pole and inductance wave pole. % error is measured in terms of the theoretical results of Longuet-Higgins

	I	II	III	IV	V	VI	VII	VIII	IX	X
	Date	Place	Record. Elem.	Depth	No. of Waves	$\overline{H}_{1/3}/\overline{H}$	% diff.	$\overline{H}_{1/10}/\overline{H}$	% diff.	Remarks
1.	1950	---	Theor.	---	---	1.598		2.034		Reference 2
2.	1944	Scripps	Pr.Rec.	---	---	1.539	3.7	1.985	2.4	Reference 3
3.			Pr.Rec.	---	---	1.492	6.7	---	---	Reference 3
4.	1953	L.Br. N.J.	Pr.Rec.	32	---	1.595	0.2	2.034	0.0	Reference 4
5.	1949	Cuthk.	Pr.Rec.	---	---	1.562	2.3	---	---	Reference 6
6.		Bermud.	Pr.Rec.	---	---	1.562	2.3			Reference 6
7.	1949	Pt.Sur	Pr.Rec.							Reference 8
8.		Heceta Hd.	Pr.Rec.							Reference 8
9.		P.Arguello	Pr.Rec.							Reference 8
10.	1948	Pt.Sur	Pr.Rec.	60	116	1.495	6.5			Extreme values of 25 wave records, Reference 5
11.			Pr.Rec.	64	112	1.827	14.3			
12.	7/18/54	G. B.	Ind.Pole	0	218	1.500	6.3	1.916	5.8	Maj. comp. top section only
13.	7/18/54	G. B.	Cap.Pole	0	456	1.602	0.3	2.101	3.3	All comp. tank #2 only
14.	7/18/54	G. B.	Cap.Pole	0	120	1.423	11.0	1.754	13.8	All comp. complete
					96	1.599	0.1	1.955	3.8	Maj. comp. wave pole
15.	7/28/54	Nan. S.	Cap.Pole	0	282	1.820	13.9	2.520	23.9	All comp. fixed
					253	1.756	9.1	2.305	13.3	Maj. comp. wave pole
16.	7/28/54	Nan. S.	Cap.Pole	0	360	1.806	13.0	2.516	23.7	All comp. top section
					302	1.722	7.8	2.298	13.0	Maj. comp. only
17.	10/25/54	39N 65W	Cap.Pole	0	380	1.767	10.6	2.337	14.9	All comp. complete
					319	1.640	2.5	2.088	2.7	Maj. comp. wave pole
18.	10/25/54	39N 65W	Cap.Pole	0	416	1.748	9.4	2.308	13.5	All comp. complete
					367	1.633	2.2	2.129	4.7	Maj. comp. wave pole
19.	10/25/54	39N 65W	Cap.Pole	0	388	1.751	9.6	2.324	14.3	All comp. complete
					356	1.660	3.9	2.153	5.9	Maj. comp. wave pole
20.	10/25/54	39N 65W	Cap.Pole	0	422	1.780	10.0	2.376	16.8	All comp. complete
					376	1.729	8.2	2.198	8.1	Maj. comp. wave pole
21.	10/21/54	38N 67.5W	Cap.Pole	0	385	1.740	8.9	2.293	12.7	All comp. complete
					330	1.647	3.1	2.150	5.7	Maj. comp. wave pole
22.	10/21/54	38N 67.5W	Cap.Pole	0	358	1.782	11.5	2.402	18.1	All comp. complete
					292	1.620	1.4	2.084	2.4	Maj. comp. wave pole
23.	10/21/54	38N 67.5W	Cap.Pole	0	430	1.812	13.4	2.427	19.3	All comp. complete
					371	1.706	5.9	2.206	8.5	Maj. comp. wave pole

CONCLUSIONS

1. From the results indicated in Table I the wave height distribution determined from wave pole records agree favorably with the theoretically predicted values and the results of other investigators.

2. The wave pole sensing elements appear to be responsive to a relatively wide band of wave frequencies. To obtain agreement with the predicted height distribution it was necessary to use only the major wave components, thus forming a relatively narrow frequency band. This is consistent with the assumption made by Longuet-Higgins.

3. Further tests in seas with waves of longer period than those so far encountered are necessary to adequately evaluate the stable platform and the two types of sensing elements.

REFERENCES

1. Holmes, J. F.
1954 Deep water wave pole (unpublished manuscript). Ref. No. 54-13. Woods Hole Oceanographic Institution.

2. Longuet-Higgins, M. S.
1952 On the statistical distribution of the heights of sea waves. J. Mar. Res. 11(3).

3. Munk, W. and R. S. Arthur
1951 Forecasting Ocean Waves. Compendium of Meteorology.

4. Neumann, G.
1953 On ocean wave spectra and a new method of forecasting wind-generated sea. Tech. Memo. No. 43. Beach Erosion Board, U. S. Army Corps of Engineers.

5. Putz, R. R.
1952 Statistical distributions for ocean waves. Trans. Amer. Geophys. Union 33(5).

6. Seiwell, H. R.
1949 Sea surface roughness measurements in theory and practice. Ocean surface waves. N. Y. Acad. Sci. 51(3).

7. Walden, R. G. and G. G. Whitney, Jr.
1954 An anchored wave telemetering buoy (unpublished manuscript). Ref. No. 54-37. Woods Hole Oceanographic Institution.

8. Wiegel, R. L.
1949 An analysis of data from wave recorders on the Pacific Coast of the United States. Trans. Amer. Geophys. Union 30(5).

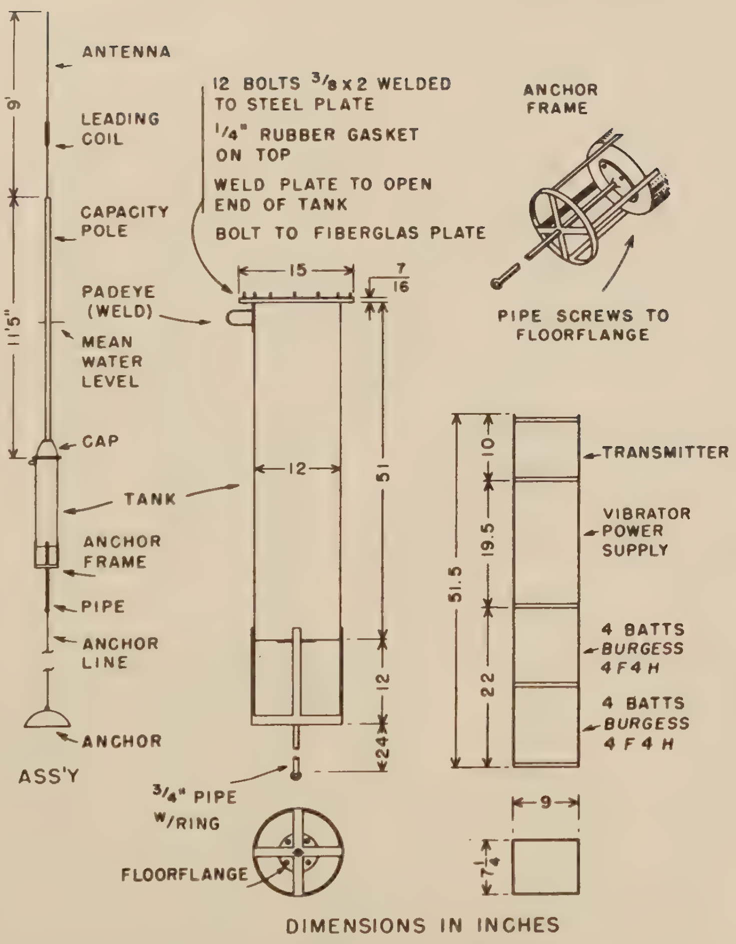
9'
11'5"
ANTENNA
LEADING COIL
CAPACITY POLE
PADEYE (WELD)
MEAN WATER LEVEL
CAP
TANK
ANCHOR FRAME
PIPE
ANCHOR LINE
ANCHOR
ASS'Y
12 BOLTS 3/8 x 2 WELDED TO STEEL PLATE
1/4" RUBBER GASKET ON TOP
WELD PLATE TO OPEN END OF TANK
BOLT TO FIBERGLAS PLATE
15
7/16
12
51
12
24
3/4" PIPE W/RING
FLOORFLANGE
ANCHOR FRAME
PIPE SCREWS TO FLOORFLANGE
10
19.5
22
51.5
TRANSMITTER
VIBRATOR POWER SUPPLY
4 BATTS BURGESS 4 F 4 H
4 BATTS BURGESS 4 F 4 H
9
7 1/4
DIMENSIONS IN INCHES

(a) Mark 1 anchored capacitance wave pole assembly.

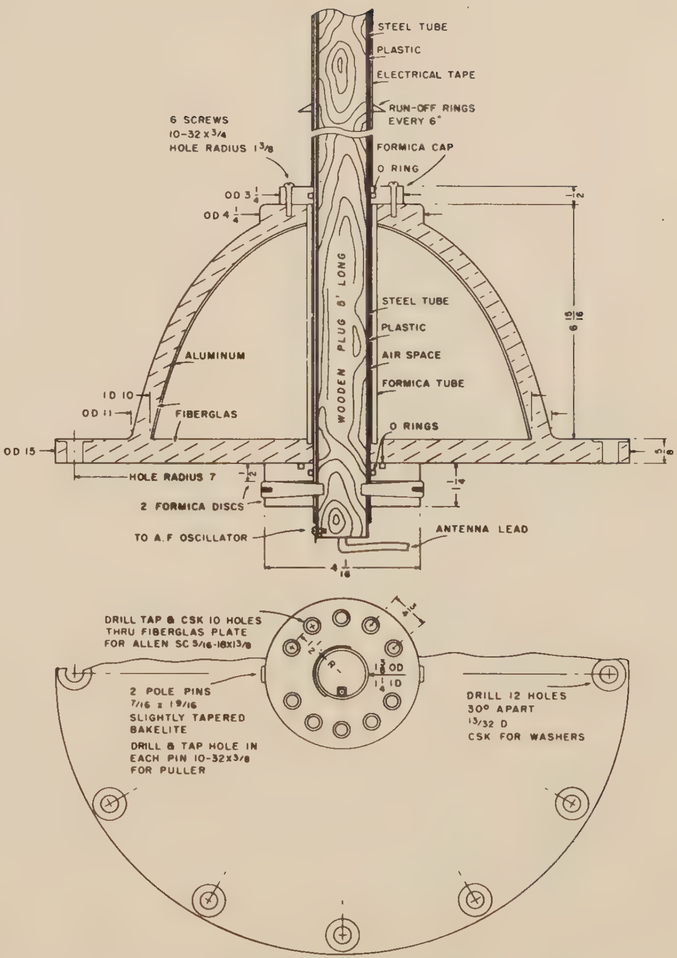
STEEL TUBE
PLASTIC
ELECTRICAL TAPE
RUN-OFF RINGS EVERY 6"
FORMICA CAP
O RING
6 SCREWS 10-32 x 3/4 HOLE RADIUS 1 3/8
OD 3 1/4
OD 4 1/4
WOODEN PLUG 8' LONG
STEEL TUBE
PLASTIC
AIR SPACE
FORMICA TUBE
O RINGS
ALUMINUM
FIBERGLAS
ID 10
OD 11
OD 15
6 15/16
5/8
1/2
1 1/4
HOLE RADIUS 7
2 FORMICA DISCS
TO A.F OSCILLATOR
ANTENNA LEAD
4 1/16
DRILL TAP & CSK 10 HOLES THRU FIBERGLAS PLATE FOR ALLEN SC 5/16-18X1 3/8
1 3/8 OD
1 1/4 ID
2 POLE PINS 7/16 x 1 9/16 SLIGHTLY TAPERED BAKELITE
DRILL & TAP HOLE IN EACH PIN 10-32x3/8 FOR PULLER
DRILL 12 HOLES 30° APART 13/32 D CSK FOR WASHERS

(b) Mark 1 anchored capacitance wave pole cap.

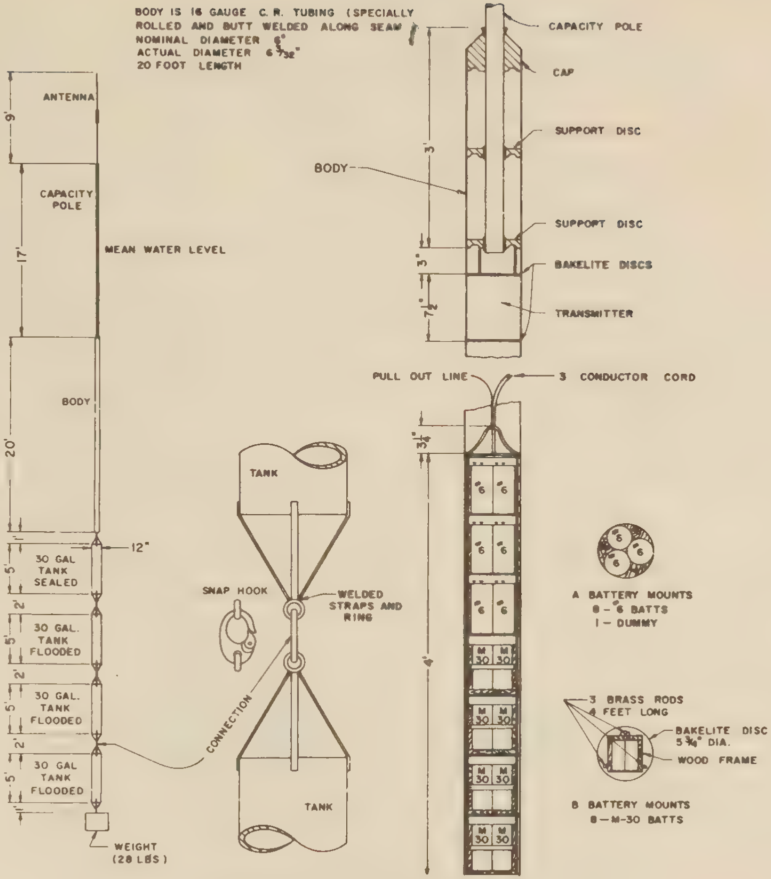
BODY IS 16 GAUGE C. R. TUBING (SPECIALLY ROLLED AND BUTT WELDED ALONG SEAM
NOMINAL DIAMETER 6"
ACTUAL DIAMETER 6 7/32"
20 FOOT LENGTH
ANTENNA
9'
CAPACITY POLE
17'
MEAN WATER LEVEL
BODY
20'
12"
1'
30 GAL TANK SEALED
5'
2'
30 GAL. TANK FLOODED
5'
2'
30 GAL. TANK FLOODED
5'
2'
30 GAL TANK FLOODED
5'
1'
WEIGHT (28 LBS)
CONNECTION
SNAP HOOK
WELDED STRAPS AND RING
TANK
TANK
CAPACITY POLE
CAP
SUPPORT DISC
BODY
3'
SUPPORT DISC
3"
BAKELITE DISCS
7 1/2"
TRANSMITTER
PULL OUT LINE
3 CONDUCTOR CORD
3 1/4"
4'
6
M 30
A BATTERY MOUNTS
8 - 6 BATTS
1 - DUMMY
3 BRASS RODS
4 FEET LONG
BAKELITE DISC
5 3/4" DIA.
WOOD FRAME
B BATTERY MOUNTS
8 — M-30 BATTS

(c) Mark 2 capacitance wave pole assembly.

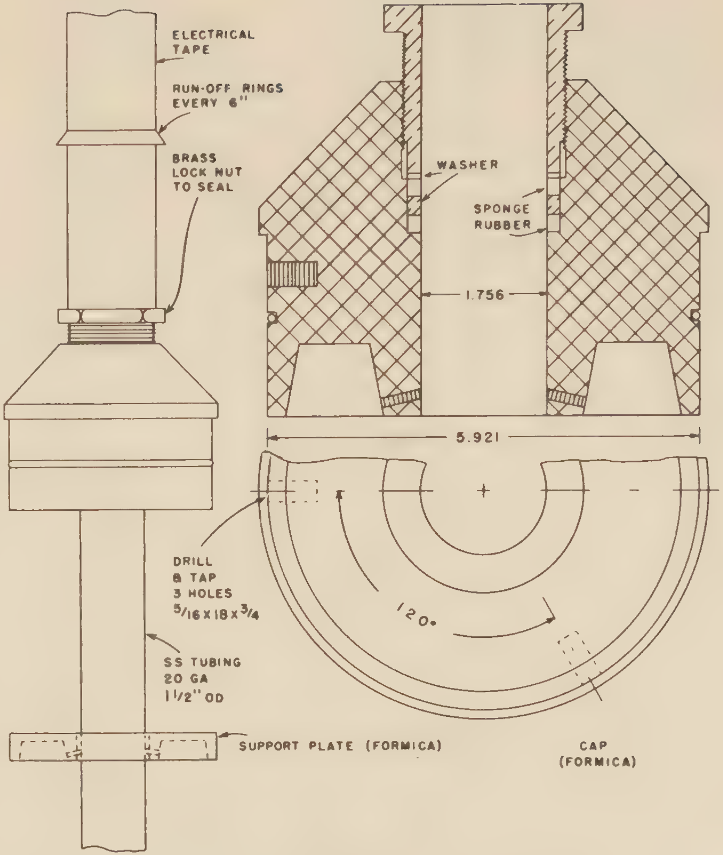
ELECTRICAL TAPE
RUN-OFF RINGS EVERY 6"
BRASS LOCK NUT TO SEAL
DRILL & TAP 3 HOLES 5/16 X 18 X 3/4
SS TUBING 20 GA 1 1/2" OD
SUPPORT PLATE (FORMICA)
WASHER
SPONGE RUBBER
1.756
5.921
120°
CAP (FORMICA)

(d) Mark 2 capacitance wave pole. Base of sensing element and cap.

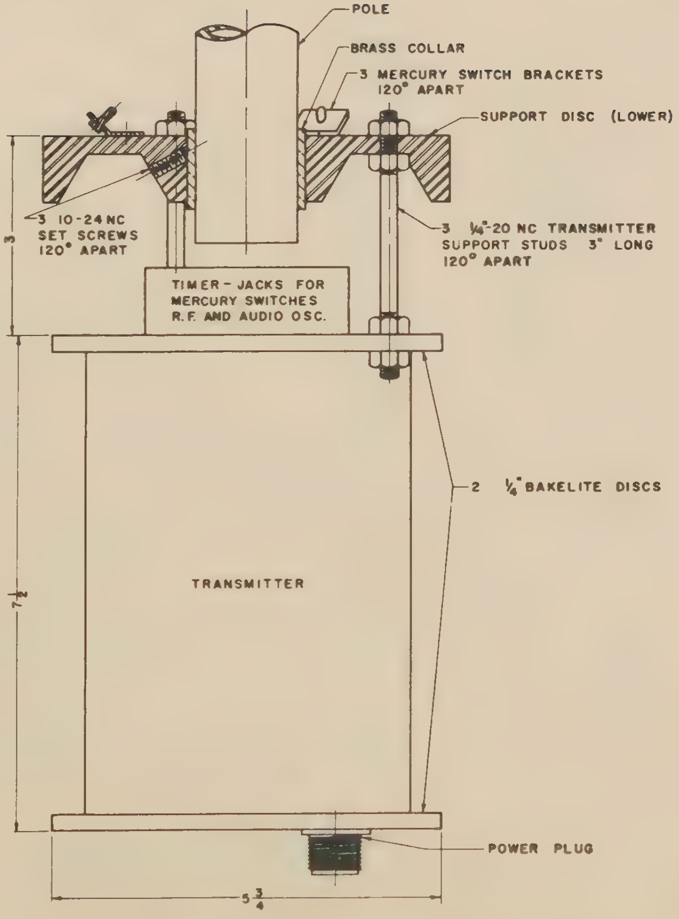
POLE
BRASS COLLAR
3 MERCURY SWITCH BRACKETS 120° APART
SUPPORT DISC (LOWER)
3 10-24 NC SET SCREWS 120° APART
3 ¼"-20 NC TRANSMITTER SUPPORT STUDS 3" LONG 120° APART
TIMER-JACKS FOR MERCURY SWITCHES R.F. AND AUDIO OSC.
2 ¼" BAKELITE DISCS
TRANSMITTER
POWER PLUG
3
7½
5¾

(e) Mark 2 capacitance wave pole. Transmitter section.

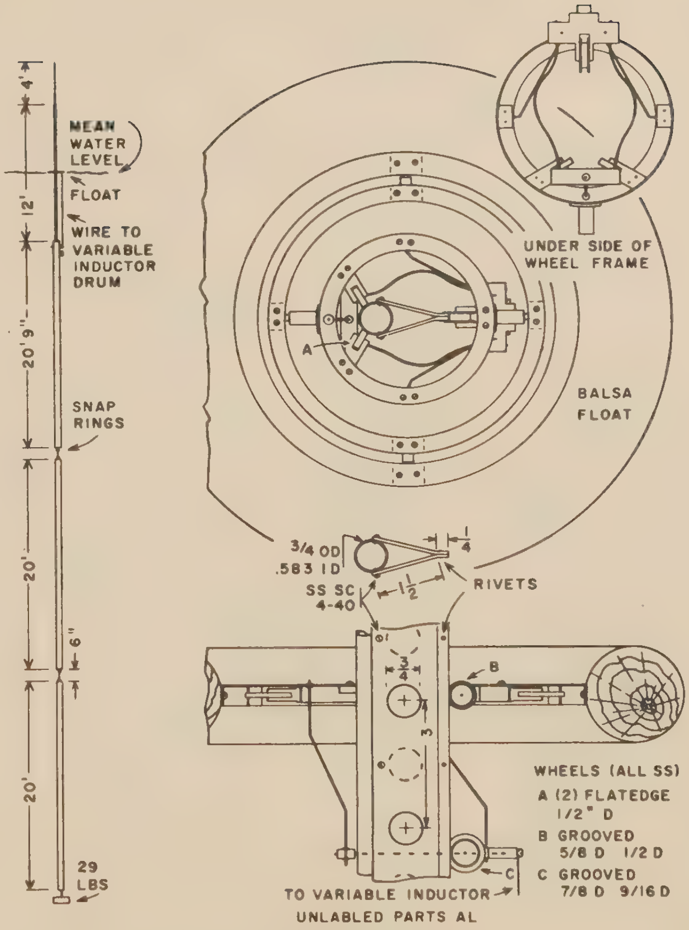
4'
MEAN WATER LEVEL
FLOAT
12'
WIRE TO VARIABLE INDUCTOR DRUM
20'9"
SNAP RINGS
20'
6"
20'
29 LBS
UNDER SIDE OF WHEEL FRAME
A
BALSA FLOAT
3/4 OD
.583 ID
SS SC 4-40
1½
¼
RIVETS
¾
B
3
C
TO VARIABLE INDUCTOR
UNLABLED PARTS AL
WHEELS (ALL SS)
A (2) FLATEDGE 1/2" D
B GROOVED 5/8 D 1/2 D
C GROOVED 7/8 D 9/16 D

(f) Mark 3 inductance wave pole. Assembly and float detail.

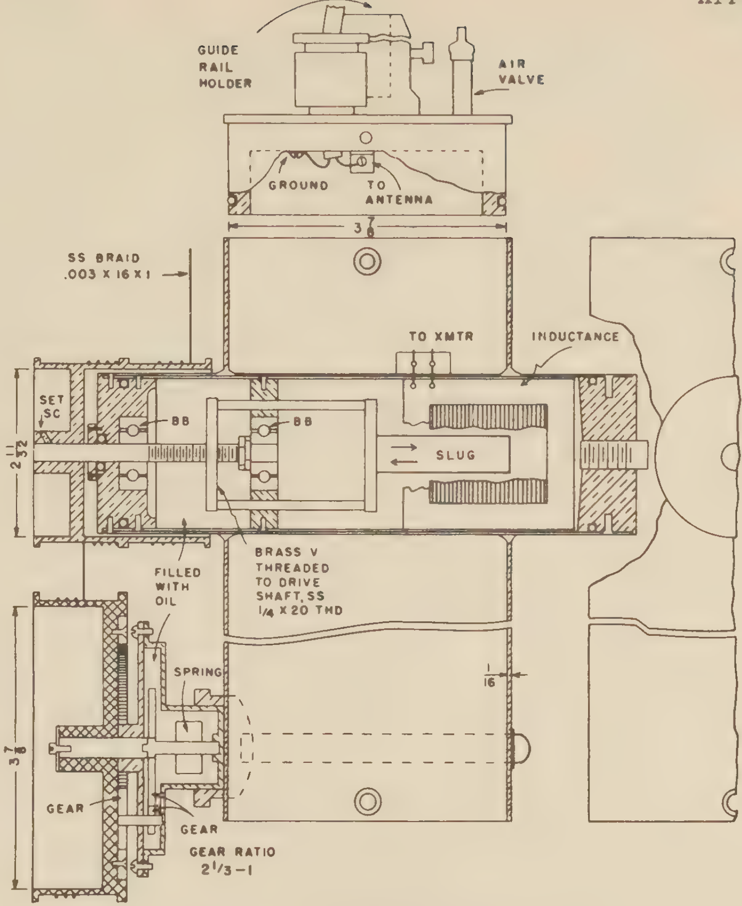
GUIDE RAIL HOLDER
AIR VALVE
GROUND
TO ANTENNA
3 7/8
SS BRAID .003 X 16 X 1
TO XMTR
INDUCTANCE
SET SC
BB
BB
SLUG
2 11/32
BRASS V THREADED TO DRIVE SHAFT, SS 1/4 X 20 THD
FILLED WITH OIL
SPRING
1/16
3 7/8
GEAR
GEAR
GEAR RATIO 2 1/3 – 1

(g) Mark 3 inductance wave pole. Sensing element assembly.

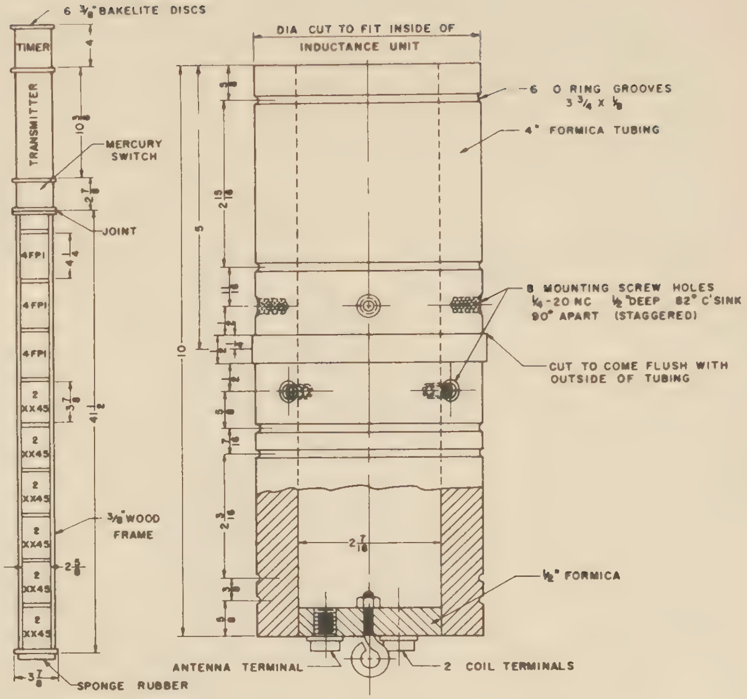
6 3/8" BAKELITE DISCS
TIMER
TRANSMITTER
MERCURY SWITCH
JOINT
4FPI
4FPI
4FPI
2 XX45
2 XX45
2 XX45
2 XX45
2 XX45
2 XX45
3/8" WOOD FRAME
SPONGE RUBBER
4
10 3/8
2 7/8
4 1/4
3 7/8
41 1/2
2 5/8
3 7/8
DIA CUT TO FIT INSIDE OF INDUCTANCE UNIT
6 O RING GROOVES 3 3/4 X 1/8
4" FORMICA TUBING
8 MOUNTING SCREW HOLES 1/4-20 NC 1/2" DEEP 82° C'SINK 90° APART (STAGGERED)
CUT TO COME FLUSH WITH OUTSIDE OF TUBING
1/2" FORMICA
ANTENNA TERMINAL
2 COIL TERMINALS
10
5
2 15/16
2 3/16
2 7/16

(h) Mark 3 inductance wave pole coupling.

APPENDIX

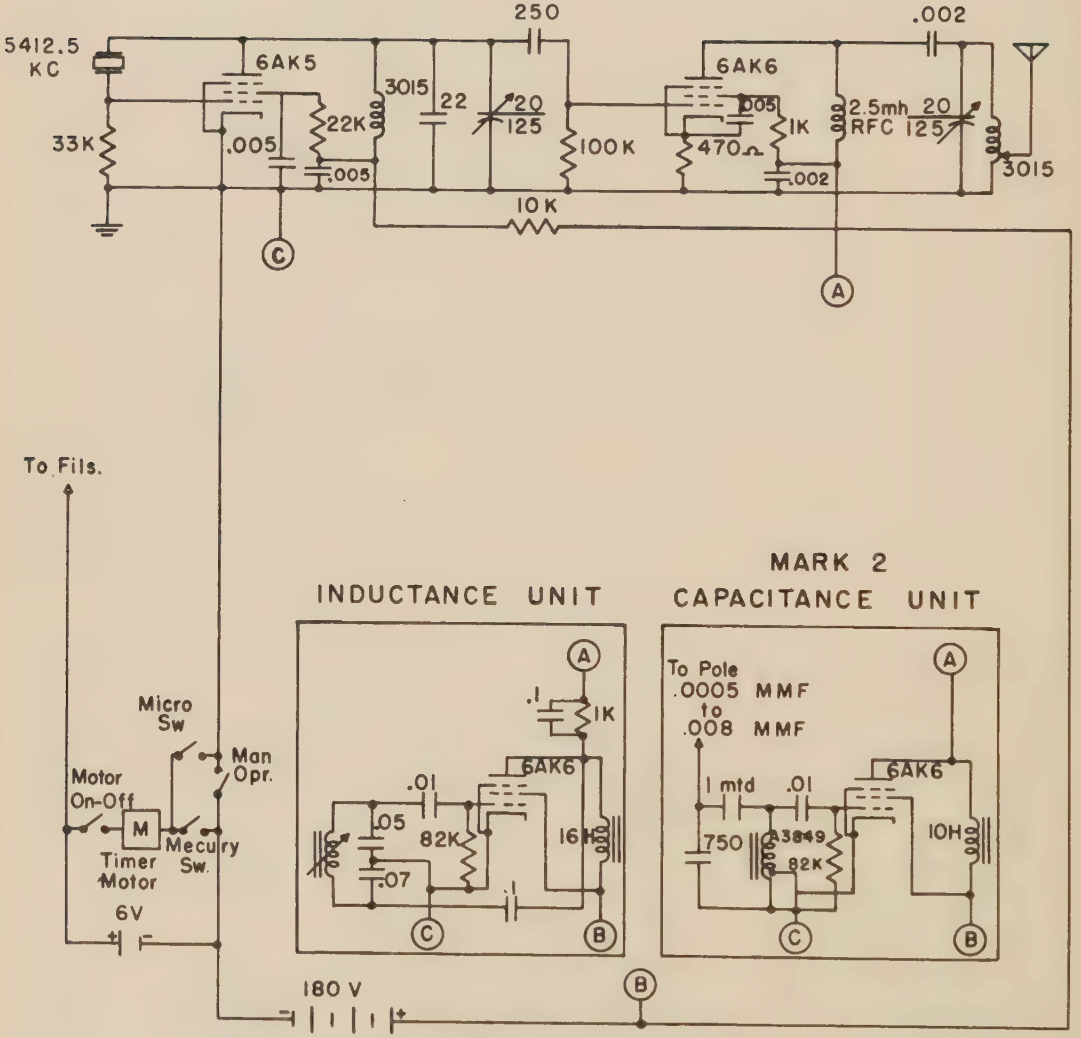
5412.5 KC
33K
6AK5
.005
22K
.005
3015
22
250
20
125
100K
6AK6
.005
1K
470Ω
.002
2.5mh RFC
.002
20
125
3015
10K
Ⓒ
Ⓐ
To Fils.
Micro Sw
Man Opr.
Motor On-Off
M
Timer Motor
Mecury Sw.
6V
INDUCTANCE UNIT
Ⓐ
.1
1K
6AK6
.01
.05
82K
.07
16H
Ⓒ
Ⓑ
MARK 2
CAPACITANCE UNIT
To Pole
.0005 MMF
to
.008 MMF
Ⓐ
1 mfd
.01
6AK6
750
A3849
82K
10H
Ⓒ
Ⓑ
180 V
Ⓑ

(i) Transmitter schematic diagram.

Contribution No. 747

(*Reprinted from Nature, Vol.* 175, *p.* 334, *February* 19, 1955)

ELECTRIFIED DROPLETS FROM THE BURSTING OF BUBBLES AT AN AIR–SEA WATER INTERFACE*

By DUNCAN C. BLANCHARD
Woods Hole Oceanographic Institution, Mass.

THE bursting of a bubble at an air–sea water interface is an effective mechanism for the production of airborne droplets[1,2]. For small bubbles the large majority of these droplets evolve from the vertical water jet which forms upon collapse of the bubble cavity. This jet, we have found, moves upward at a high velocity and is transformed into five or six droplets. The height of projection of these droplets, a function of bubble size, may reach a maximum of 18 cm. It seems certain that this process significantly contributes to the production of the airborne salt particles present over the oceans.

Early in our study of breaking bubbles[1], it was found that the droplets produced by the vertical jet were electrically charged. With the apparatus schematically shown in Fig. 1, measurements were carried out on the sign and magnitude of this charge as a function of the radius of the droplet. Bubbles were produced at a rate of 3–10 sec.$^{-1}$ by pumping air under 10–30 lb./sq. in. through a finely drawn-out section of glass capillary tubing E. These bubbles burst at the surface of the sea water in the inner container F and ejected electrically charged droplets into the observation region G. This region was sealed off from the outside air by an open-bottomed rectangular 'Plexiglass' housing B which made contact with the sea water in the outer container D. It was necessary to use the outer container as a water seal since the distortion of the water surface near the 'Plexiglass' made it impossible to make observations near the water surface. The d.c. power supply A was used for producing a uniform, vertical electric field between the brass plate C and the earthed surface of the sea water in the inner container F by increasing the plate potential to any desired plus or minus value up to a maximum of 12 kV.

The determination of the electrical charge and radius of a droplet ejected by the jet from a bursting bubble was made in the following way. Before the droplet returned to the water surface, the voltage on the plate was adjusted until the droplet was stationary in the electric field. The gravitational force could then be equated to the electric force, giving an equation with two unknowns, the droplet radius and charge. The field-strength was then decreased to allow the droplet to move slowly downward. An equation of motion could then be obtained which, when solved simultaneously with the first equation, gave the droplet radius and charge. A cathetometer was used for observing the droplet and to determine its motion in the electric field. To avoid evaporation of the droplet while under observation, it was necessary that the air and water temperature were essentially the same.

---

* Contribution No. 747 from the Woods Hole Oceanographic Institution.

All the results obtained to date, including those shown in Fig. 2, were from bubbles less than about 150 μ in radius, the ejected droplets of which rose less than 20 mm. The weight of salt contained in droplets produced from this range of bubbles is comparable to that found by Woodcock[3] over the oceans. Curve *A* of Fig. 2 is for droplets from bubbles which were allowed to break in the presence of an electric field. In this manner all the droplets originating via the jet mechanism obtained, by electrostatic induction, a charge of opposite sign from that of the plate potential. For a given droplet radius, this charge was substantially the same in the range of fields from 50 to 300 V. cm.$^{-1}$. Curves *B*, *C* and *D* are for the natural charge on the droplets. In these cases the bubbles were allowed to produce droplets before the balancing electric field was applied. It will be noted that the results, unlike those for the induced charges, tend to fall into three separate groupings. The first, for droplets less than 3μ radius, indicates an increase of charge nearly proportional to the fifth power of the radius. The second, for droplets between 3 and 6μ in radius, shows approximately a second-power relationship.

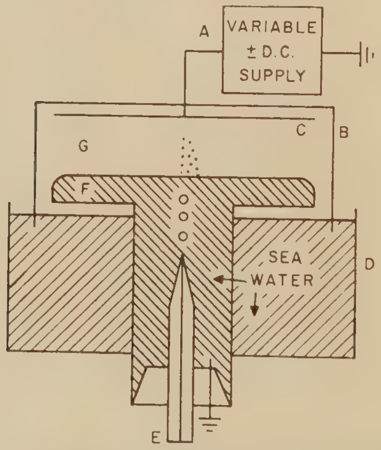

Fig. 1. A schematic view of the apparatus for suspending an electrically charged droplet in a vertical electric-field

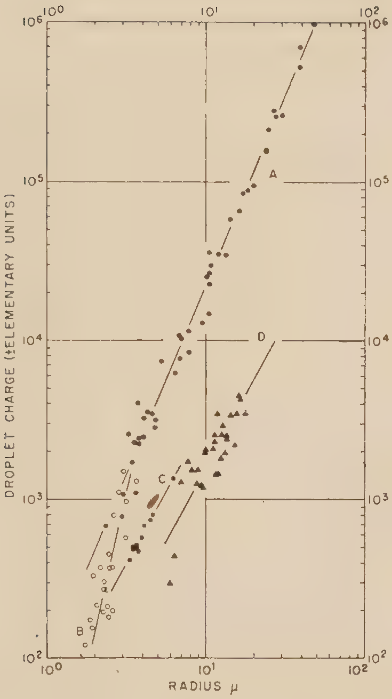

Fig. 2. Natural and induced charge on droplets from bursting bubbles

Other results suggest that this curve is not unique but that a family of curves exists in this region. The third grouping, for droplets greater than 6μ radius, is similar to the second. The maximum charge per unit volume is obtained by droplets of about 3μ radius. At this radius the quantity of charge is nearly identical with that obtained when the bubbles break in the presence of an electric field. To date no explanation has been given for these groupings.

If the maximum height of ejection of droplets is less than about 2 mm., the sign of the charge on all the drops is, almost without exception, positive. For ejection heights of 2–20 mm., which implies larger bubbles, the charge on the droplet ejected to the maximum height is still positive, while the lower droplets may show either sign.

These results lead to some very interesting speculations as to what might happen under various natural conditions. Consider, for example, a thunderstorm passing over the sea with a peak field-strength at the sea surface of 100 V. cm.$^{-1}$. From curve *A* of Fig. 2, one finds that all droplets less than 10 μ in radius originating from the jets of breaking bubbles will be carried upward towards the cloud. One might also wonder about the electric field at the surface of these droplets and its tendency to induce corona discharge. With the equation of curve *A* and Gauss's law, one finds that the field strength E (V. cm.$^{-1}$) at the surface of a droplet of radius R (microns) is $E = 1{\cdot}24 \times 10^{3} R^{0{\cdot}4}$. With E varying only as the 0·4 power of the radius, the field-strength at the surface of droplets 3–50μ radius varies only from about 1,900 to 5,900 V. cm.$^{-1}$. These calculations assume that the charge is uniformly distributed over the surface of the drop. It is well known that a charged conducting sphere in a vertical electric field will have an intensification of the field on the top and bottom of the sphere. This intensification was computed, with Laplace's equation, for the droplets of curve *A* when they are subjected to an electric force just sufficient to balance the gravitational force. The computed fields were in no case more than 15 per cent larger than those given above. These fields are not sufficient for breakdown; but evaporation of the droplets, which almost invariably occurs under natural conditions, might raise the surface field to breakdown values.

It is likely that the positively charged droplets from the smallest bubbles alone carry an appreciable electrical current between the atmosphere and the earth. If one assumes a positive charge totalling 3,000 elementary units carried by the several droplets from a small bubble and, on the average, about one bubble per second per square centimetre breaking over the entire ocean area of the world, then a current of 1,800 amp. will be obtained. It is assumed, of course, that winds and turbulent diffusion will transport these small droplets upward. This current is of the same magnitude but in the opposite direction to the observed current-flow in fair-weather areas over the earth[4]. It is probable that the above estimate of the current carried by these low-mobility droplets is high; but, nevertheless, this mechanism may contribute significantly to the earth's counter or supply current, which at present is attributed to thunderstorms.

Further laboratory- and field-studies should lead to other interesting aspects of this production of charge on droplets from bubbles breaking at the sea surface. This work is being continued, and more detailed publication is planned for the future.

This work was supported by the Office of Naval Research, under contract number *Nonr*-798(00) (*NR*-082–124). [Oct. 6.

[1] Woodcock, A. H., Kientzler, C. F., Arons, A. B., and Blanchard, D. C., *Nature*, **172**, 1144 (1953).

[2] Knelman, F., Dombrowski, N., and Newitt, D. M., *Nature*, **173**, 261 (1954).

[3] Woodcock, A. H., *J. Meteor.*, **10**, 362 (1953).

[4] Gish, O. H., "Compendium of Meteorology", 101 (Waverley Press, Inc., 1951).

Printed in Great Britain by Fisher, Knight & Co., Ltd., St. Albans.

Contribution No. 749

Deep-Sea Research, 1955, Vol. 2, pp. 213 to 229. Pergamon Press Ltd., London.

Alternative analyses of current surveys*

F. C. FUGLISTER

(*Received 22nd January* 1955)

Summary—Ocean current nomenclature, with respect to average and instantaneous currents, is discussed. Temperature data from the Gulf Stream System, obtained in 1948, 1951 and 1953, and from the Kuroshio System in 1933 are analysed with alternative points of view. A 1954 survey of a portion of the Gulf Stream System substantiates the analyses which show relatively small scale structure in these current systems.

INTRODUCTION

IN 1951 this writer advanced an hypothesis of multiple currents in the Gulf Stream System. This large scale breakdown of the current system differed from the generally accepted pattern in that it showed a series of overlapping currents and relatively weak countercurrents rather than one continuous, branching current. A breakdown in this current system on a smaller scale was suggested by VON ARX and RICHARDSON (1953). They showed that the " surface outcrop " of the currents could be followed by a plane for distances of not more than about 300 kilometres. Their interpretation of the observations showed a series of currents similar to those suggested by the author but on a considerably smaller scale and with no evidence of counter currents.

It is evident that as more detailed observations of ocean currents are obtained many heretofore unknown structural characteristics will come to light, and the simple concept of a major ocean current " flowing like a river through the sea " may become a thing of the past. It will become increasingly important that the time and space scales employed in any study or description of these currents be clearly understood. An associated problem, of real importance in this connection, is one of nomenclature. By attaching a name to an observed current, many factors are implied – or assumed on the part of the reader – that are not correct or justified on the bases of the actual observations. Since this paper deals with currents, and it is difficult to avoid using names, a brief discussion of the subject of ocean current nomenclature is in order.

NOMENCLATURE

Most of our knowledge of ocean currents is based on data collected and averaged over many years. These data are of many different kinds but primarily they consist of ships' drift reports. The subsurface data are meagre in comparison and consist almost entirely of temperature and salinity observations ; direct sub-surface current measurements are negligible in number. The ocean current names in the literature, therefore, refer to long period average water movements at the surface and, what in effect is, a mixture of average and quasi-instantaneous water movements at depth.

Ocean currents are named in order to locate, at least approximately, the geographical positions of the currents and to differentiate one from another. Names are

---

* Contribution No. 749 from the Woods Hole Oceanographic Institution. This research was sponsored by the Office of Naval Research under contract N6 onr-27701.

applied only to those currents that are considered to be relatively permanent features of the general circulation. Whether the name applies to an average or to an instantaneous current is not generally made clear. The same name, with the singular form of the word " current " or " stream," is used to denote either or both.

Confusion could be avoided if it was generally accepted that the major ocean currents named in the literature refer to large scale, long term average water movements and that the plural form of the word " current " should be used. A current observed at a particular place and time is best described not by a name but by an accurate statement as to its location, velocity, transport, water-mass characteristics, etc. It may be referred to as part of a larger scale average water movement but it should not be considered the same thing.

In particular, it is suggested that the term Gulf Stream should not be used in reference to a particular current observed at a particular time. The Gulf Stream is a large scale water movement in the central, western North Atlantic where, on the average, the flow is to the north and east. It is narrowest and swiftest in the area from the Straits of Florida to the offing of Cape Hatteras where it is close to the Continental Shelf. To the north and east of Cape Hatteras the average water movement is not close to the shelf and it is more wide spread, deeper and slower. To the east of about 45° west longitude it is even more diffuse and to the east of about 25° west longitude it is no longer recognizable as a particular average water movement. Individual surveys in these areas do not show any such current (ISELIN and FUGLISTER 1948). This definition of the Gulf Stream differs from those given by ISELIN (1936) and by FUGLISTER and WORTHINGTON (1951). ISELIN confined the term Gulf Stream to that portion of the system flowing between Cape Hatteras and longitude 50° west. FUGLISTER and WORTHINGTON went a step further and restricted its application to a single continuous current in this same region. One purpose of the following analyses is to show that the Gulf Stream is a single continuous current only in a large scale statistical sense, and any particular current observed in this area is not the Gulf Stream and should not be confused with it by being given the same name.

TEMPERATURE DATA

Following the system used for other studies (FUGLISTER 1951, 1954) the assumption will be made here that major currents exist wherever there is an abrupt horizontal temperature gradient at a depth of 200 metres. The relationship that has been repeatedly observed between the temperature gradients at 200 metres and the slope of the sigma-*t* surfaces at greater depths is the justification for assuming that these temperature gradients are associated with more than just superficial currents. The direction of flow is such that, facing down stream, warm water is to the right and cool water to the left. This does not apply where the 200 metre temperatures are below 5° centigrade. At these lower temperatures the salinity differences are the determining factor and the direction of flow is generally in the opposite direction.

All of the surveys to be discussed cover periods of less than one month and the thermal conditions are presented without regard to time changes. The spacing of the observations vary but are generally less than 10 miles apart along the ships' tracks. In the case of the Pacific data the spacing of the observations is irregular, being close together near the coast but quite widely spaced in other areas. In all cases except with the Japanese data, the temperature was obtained by means of the bathythermograph and the Fahrenheit scale is used**.

ALTERNATIVE ANALYSES

Alternative analyses of the temperature fields at a depth of 200 metres in various portions of the Gulf Stream System (Charts 1 to 3) and in the Kuroshio System (Chart 4) will be presented. In each case there is more than one interpretation of the data. Other interpretations are, of course, possible but not many that would be fundamentally different from these shown. Along the tracks of the vessels a linear interpolation between observations is adhered to, thus restricting the number of interpretations.

The method of surveying the temperature field differed in each of the surveys. In the first case (Chart 1) the Canadian Research Vessel H.M.C.S. *New Liskeard* crossed and recrossed the currents, changing course by 180° at the end of each run. In the second case (Chart 2) the *Albatross* III* made more widely spaced sections in a much longer survey. The third case (Chart 3) is quite different from the first two in that no attempt was being made to follow a current, and the temperature field is the result of combining data from two independent surveys. The Woods Hole Oceanographic Institution vessels *Atlantis* and *Caryn* were studying the western portion of the area while the H.M.C.S. *Sackville* was surveying the eastern sector. Finally, the Kuroshio investigation (Chart 4) was a Japanese, multi-ship survey of a very large area.

In each case presented here the temperature field obviously consists of a cool and warm water area separated by a zone in which abrupt thermal gradients occur. If the data had consisted of many hundreds of observations averaged over the years it is easy to visualize what the average thermal field would look like in each case. There would be one, relatively diffuse, gradient separating the cool and warm water areas. According to present terminology, this average gradient in the areas covered by Charts 1 and 3 would be termed the Gulf Stream ; in the area of Chart 2 it would be the northern branch of the North Atlantic Current. If this terminology is carried over and applied to these short period surveys there is a natural tendency to analyse the data in such a way as to produce a Gulf Stream or a branch of the North Atlantic Current. In other words, the isotherms are drawn so as to show one abrupt gradient crossing the charts.

Occasionally an analysis is forced in order to obtain a single gradient. An extreme example is shown here (Chart 3A) in order to point out the fact that it is always possible to twist and turn the isotherms in such a manner as to produce a single abrupt gradient. A less obvious example (Chart 2A) is the interpretation carried out aboard the *Albatross* III. The object of this survey was to locate and follow the northern branch of the North Atlantic Current and it is easy to see why the data were interpreted as shown here but it is entirely possible that, if the object of this cruise had been to survey a system of currents, the data might have been analysed as shown on Chart 2B. This latter analysis has, at least, the virtue of not suggesting that a current was following in the path of the ship.

** All the bathythermograph instruments were calibrated in the Fahrenheit system. The data were not converted to the metric system because the scale used is relatively unimportant in the analyses presented in this paper.

* Chartered by the Woods Hole Oceanographic Institution.

Another type of analysis shows a single current but manages to avoid violent and improbable meandering (Chart 1B, 1C and 3B). The " Gulf Stream " or single group of isotherms crosses the entire area ; the " extra " gradients are accounted for as eddies. The analysis carried out aboard the H.M.C.S. *New Liskeard* showed the " Gulf Stream " with an anticyclonic eddy to the north of it (Chart 1C) but these same data could be interpreted to show a current with a cyclonic eddy to the south of it (Chart 1B). A more complicated analysis of this type retains a " Gulf Stream " but several other currents and eddies are required to account for the " extra gradients (Chart 3B).

A third type of analysis, usually used only to cover very large areas, tends to show that, although numerous currents exist in an area, they all stem from a single current. The temperature field in the Kuroshio System for August, 1933, as drawn by UDA (1935), is an example of this point of view. UDA'S chart was drawn with 3°C intervals ; the 1° intervals are interpolated here (Chart 4A) in order to compare this analysis with one carried out by the author (Chart 4B). The branching currents in the Kuroshio System, according to UDA, are shown on Chart 4C. A quite different picture of this system of currents (Chart 4D) is based on an interpretation of the 200 meter temperature field discussed below. Where several currents are shown stemming from a single one, it is generally necessary to introduce some eddies or countercurrents because the sum of the gradients that make up the branches is greater than the gradient in the single current.

Finally, there is an analysis that essentially dismisses the idea, introduced originally by the long period average picture, that there is necessarily a continuous single current passing through the zone that separates the cool and warm water areas. Although this type of analysis results in a much more complicated picture of the temperature fields and probable currents (Charts 1A, 2B, 3C, 4B and D) it may partially explain some of the peculiar behaviour of the " Gulf Stream " as pictured by the other types of analysis. The extreme meandering, the tendency for the current to follow the lines of observations, the downstream fluctuations in width, transport, velocity etc., all these questions take on new and different meanings with the introduction of these new " turbulent " pictures of the currents. Whether these interpretations are correct or not, they are clearly possible and should be given due consideration when studying the Gulf Stream or any other major ocean current system.

Two studies, that may throw more light on the validity of this last type of analysis, are first, a detailed examination over a period of days of one of the abrupt thermal gradients and second, a survey of the right hand or warm water environment of the Gulf Stream. Studies of the first kind are being made and the results of one such study will be discussed below. A thorough survey of the vast warm water environment of the currents in this area will require a great deal of ship time and in all probability will eventually require a multiple ship survey.

A DETAILED SURVEY OF A PORTION OF THE GULF STREAM

In August, 1954 a survey of a small portion of the Gulf Stream in the area south and east of Georges Bank and south of Nova Scotia was undertaken aboard the *Caryn*. From a position at approximately 35° north, 68° west the *Caryn* followed a current over a distance of 240 miles to a point near 29° north, 64°west. The dead reckoning – Loran – calculations gave speeds in this current of from 4 to 5 knots.

Near 39° north, 64° west (Chart 5) a short section was run across the thermal gradient associated with the current and a drift station was occupied. The current velocity, averaged over a period of 4 hours, was 3·7 knots, 053° true. Immediately after this section was completed another run was made, this time toward the north (section C on the chart). There was a marked change in the thermal structure which, taken together with the calculated drift, indicated a slowing down of the current speed and a bending to the north and northwest. The next section in point of time, section B, was essentially in the same geographical position as section A but 30 hours later. This section gave the same results as section A but the current had shifted 8 miles to the south during the time interval. At the end of section B the ship was again hove to and a drift station occupied.

On the bases of the data obtained up to this point it was to be expected that the ship would drift first toward the northeast and then gradually toward the north and west with diminishing speed. Actually, the drift started off toward the northeast but as the speed of drift diminished the direction changed, not toward the north, but east and then as the speed increased again, toward the south of east. The very light winds, less than Beaufort force two, and smooth seas together with excellent Loran conditions made it possible to get quite accurate and relatively small scale measurements of the surface current velocities during this drift. For each 2 hour period of this 14 hour drift station the velocities of the current were as follows ;

direction	070°	070°	070°	093°	098°	103°	120°
knots	4·5	3·9	3·6	3·1	3·9	3·8	3·8

After this drift station and a short excursion into the warm water area to the south, section D was occupied. Again the abrupt thermal gradients of the first two sections were crossed with even colder water in evidence. The diminishing gradients and changing conditions of section C were not encountered.

These sections are approximately 25 miles apart, which is considerably closer together than most sections made across these currents, yet if either of the last two sections were left out any interpretation of the data from this survey would be in error. If the last section was omitted it would be concluded that the current turned north in this area accounting for the warm water found to the north and west. On the other hand if the middle section, section C, was not available there would be no doubt that the current continued to the eastward and the warm water to the north would be considered to be part of a separate eddy. Certainly, all the data show that the abrupt thermal gradients, associated with these currents, can become diffuse or concentrated over a remarkably short, downstream, distance.

CONCLUSION

The data presented in this paper represent only a small part of the data examined during the past year. A collection of data, covering a period of five years, from the California Currents was examined at the Scripps Institution of Oceanography. It was while studying these data and the Kuroshio data that it first became apparent to the writer that a major difficulty in the way of understanding these currents is the tendency to force the quasi-instantaneous picture to conform with the statistical mean.

Relatively narrow and swift currents occur in the Gulf Stream System but our present knowledge is not sufficient to tell us over what distances these currents remain narrow and swift. It is evident, however, that these characteristics of the currents can change over relatively short distances.

Theoretical conclusions concerning downstream changes in the physical characteristics of major ocean currents will frequently be erroneous as long as the present conglomoration of time and space scales is used to describe these currents.

REFERENCES

FUGLISTER, F. C. (1951), Multiple currents in the Gulf Stream system. *Tellus* 3 (4), 230-233.

FUGLISTER, F. C. (1954), Average temperature and salinity at a depth of 200 meters in the North Atlantic. *Tellus* **6** (1), 46-58.

FUGLISTER, F. C. and WORTHINGTON, L. V. (1951), Some results of a multiple ship survey of the Gulf Stream. *Tellus* **3** (11), 1-14.

ISELIN, C. O'D. (1936), A study of the circulation of the western North Atlantic. *Pap. Phys. Oceanogr. Meteorol.* **4** (4), 1-101.

ISELIN, C. O'D. and FUGLISTER, F. C. (1948), Some recent developments in the study of the Gulf Stream. *J. Mar. Res.* **7** (3), 317-329.

VON ARX, W. S. and RICHARDSON, W. S. (1953), The surface outcrop of the Gulf Stream front. *Woods Hole Oceanographic Institution. Ref.* No. 53-24. Unpublished manuscript.

UDA, MITITAKA (1935), The results of simultaneous oceanographical investigations in the North Pacific Ocean adjacent to Japan made in August, 1933. *J. Imp. Fish. Exp. Sta. Paper* No. 43, 126-130.

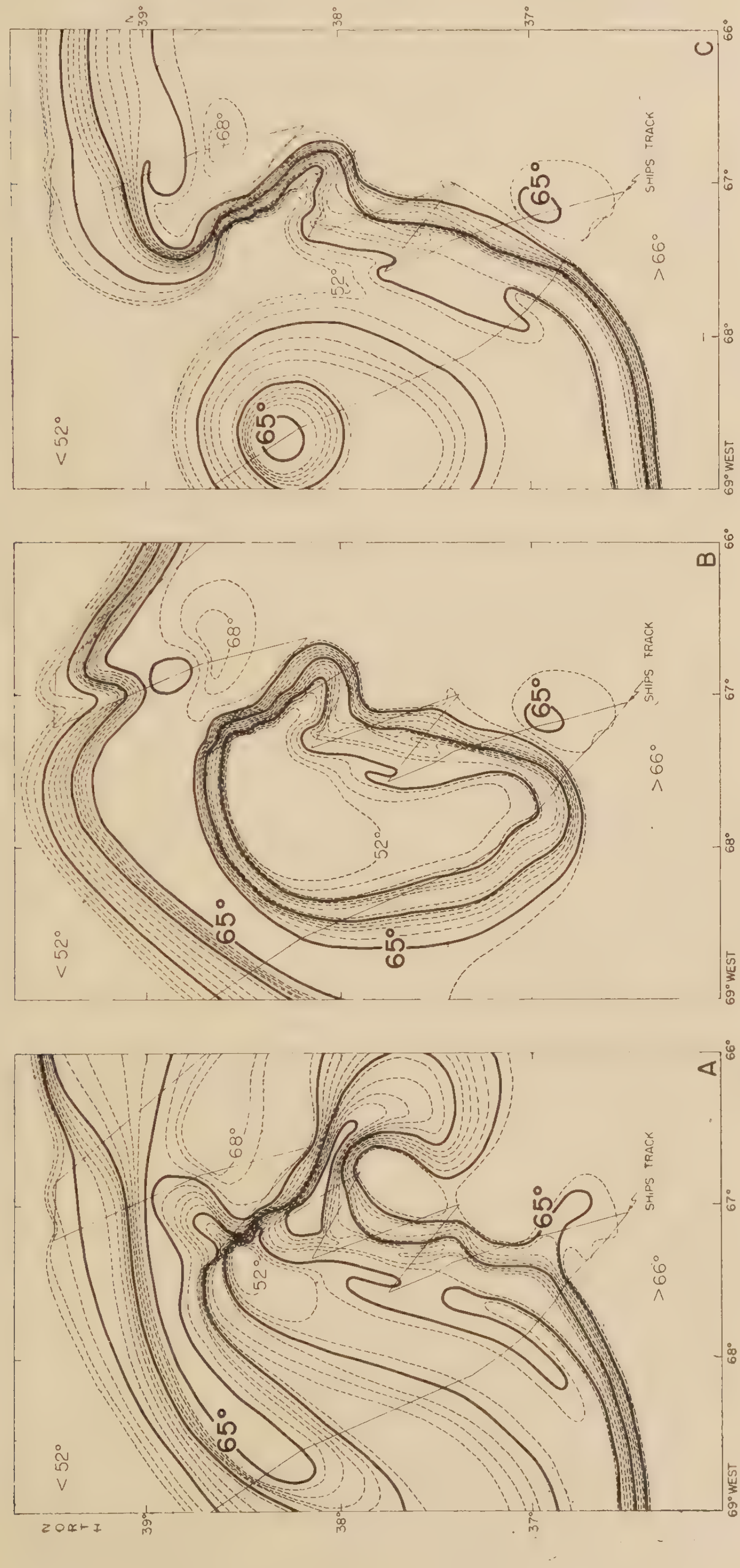
A
B
C
NORTH
< 52°
> 66°
65°
68°
52°
SHIPS TRACK
69° WEST
68°
67°
66°
39°
38°
37°

Chart 1. Three analyses of the temperature field (degrees F), at a depth of 200 metres in the Gulf Stream System south of Georges Bank. From data obtained by the Canadian Research Vessel H.M.C.S. *New Liskeard*, 15-18 November, 1948.

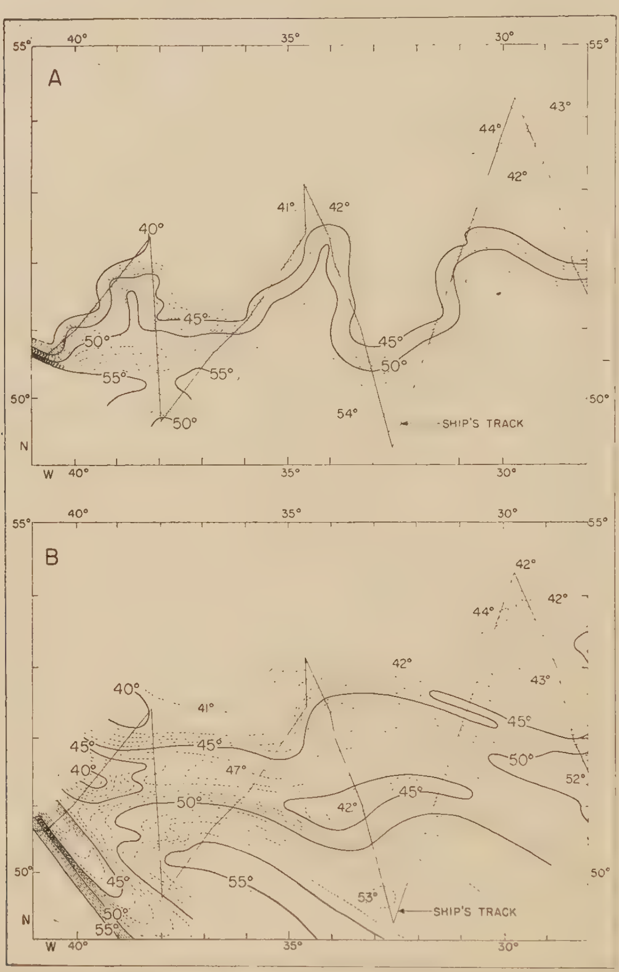
A
B
55°
50°
40°
35°
30°
N
W
SHIP'S TRACK
40°
41°
42°
43°
44°
45°
47°
50°
52°
53°
54°
55°

Chart 2. Two analyses of the temperature field (degrees F), at a depth of 200 metres in a portion of the Gulf Stream System in Mid-Atlantic. From data obtained by the Woods Hole Oceanographic Research Vessel *Albatross III*, 7-23 July, 1951.

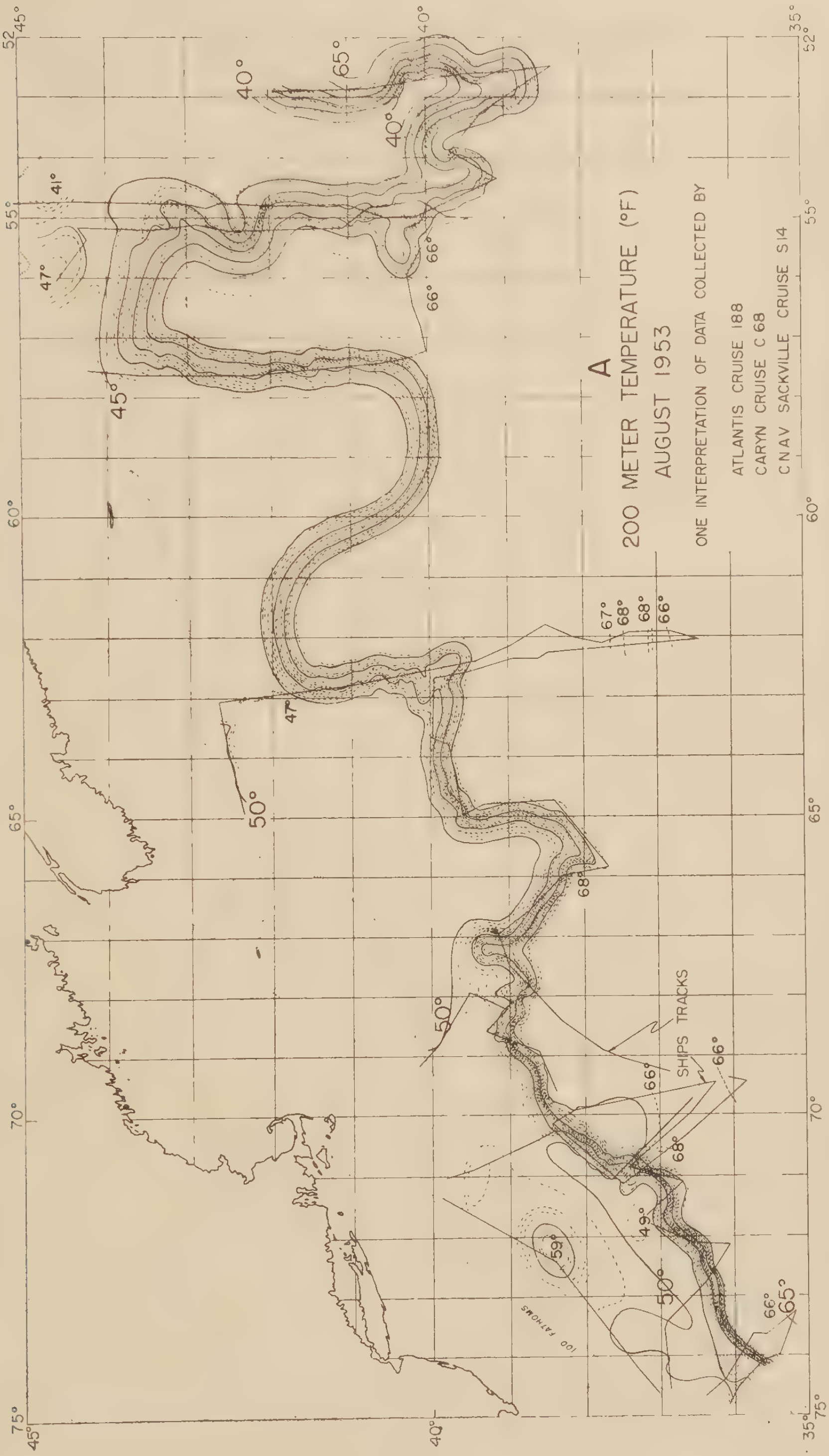
A
200 METER TEMPERATURE (°F)
AUGUST 1953
ONE INTERPRETATION OF DATA COLLECTED BY
ATLANTIS CRUISE 188
CARYN CRUISE C 68
CNAV SACKVILLE CRUISE S14
SHIPS TRACKS
100 FATHOMS
75°
70°
65°
60°
55°
52°
45°
40°
35°
41°
47°
45°
50°
65°
40°
66°
67°
68°
68°
66°
47°
50°
68°
50°
66°
66°
68°
49°
59°
50°
66°
65°

Chart 3a. An analysis of the temperature field (degrees F) at a depth of 200 metres in the Gulf Stream between 75° and 52° West longitude.

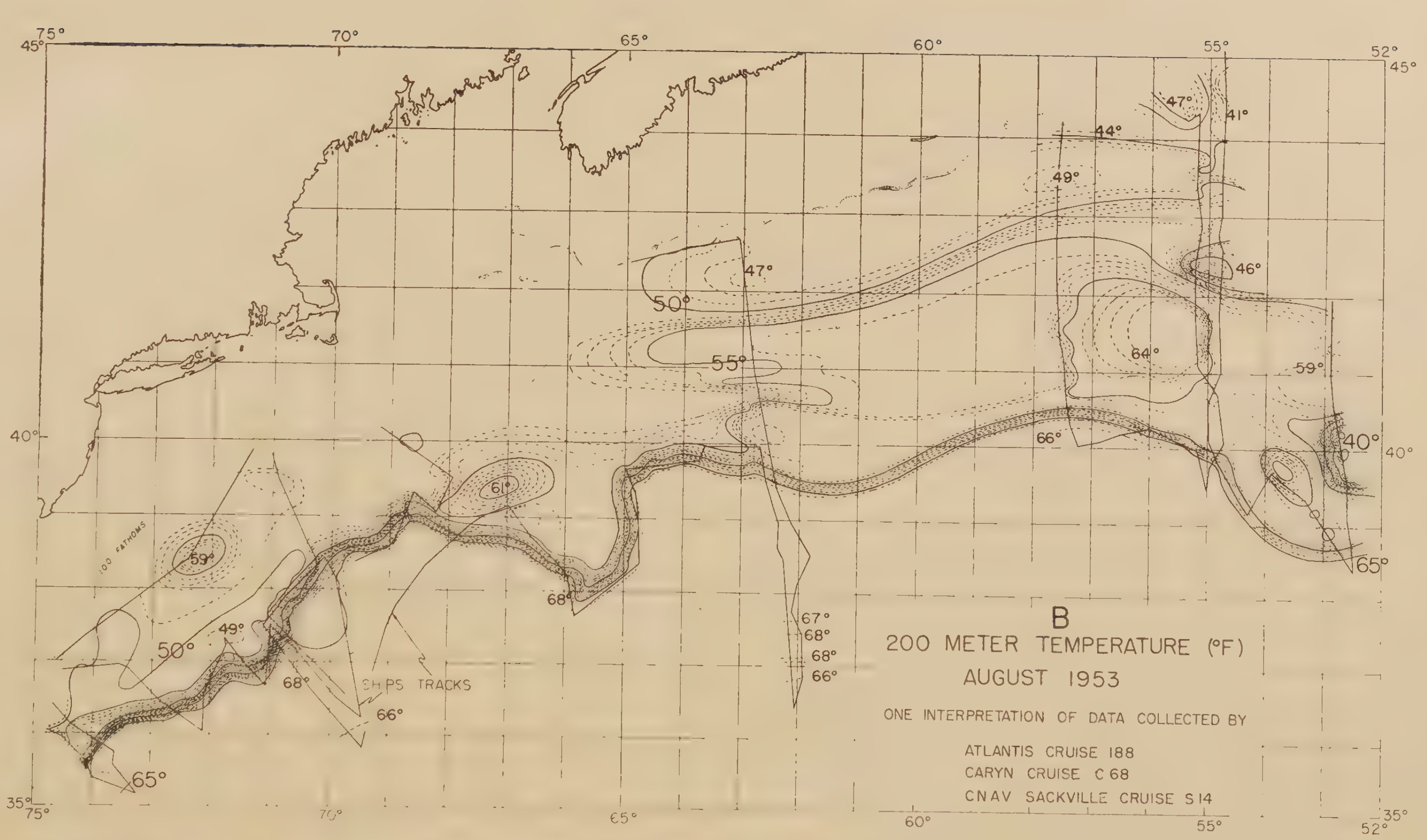
75°
70°
65°
60°
55°
52°
45°
40°
35°
100 FATHOMS
47°
41°
44°
49°
46°
47°
50°
55°
64°
59°
40°
66°
61°
59°
68°
49°
50°
68°
66°
SHIPS TRACKS
65°
67°
68°
68°
66°
65°
B
200 METER TEMPERATURE (°F)
AUGUST 1953
ONE INTERPRETATION OF DATA COLLECTED BY
ATLANTIS CRUISE 188
CARYN CRUISE C 68
CNAV SACKVILLE CRUISE S 14

Chart 3b. An analysis of the temperature field (degrees F), at a depth of 200 metres in the Gulf Stream between 75° and 52° West longitude.

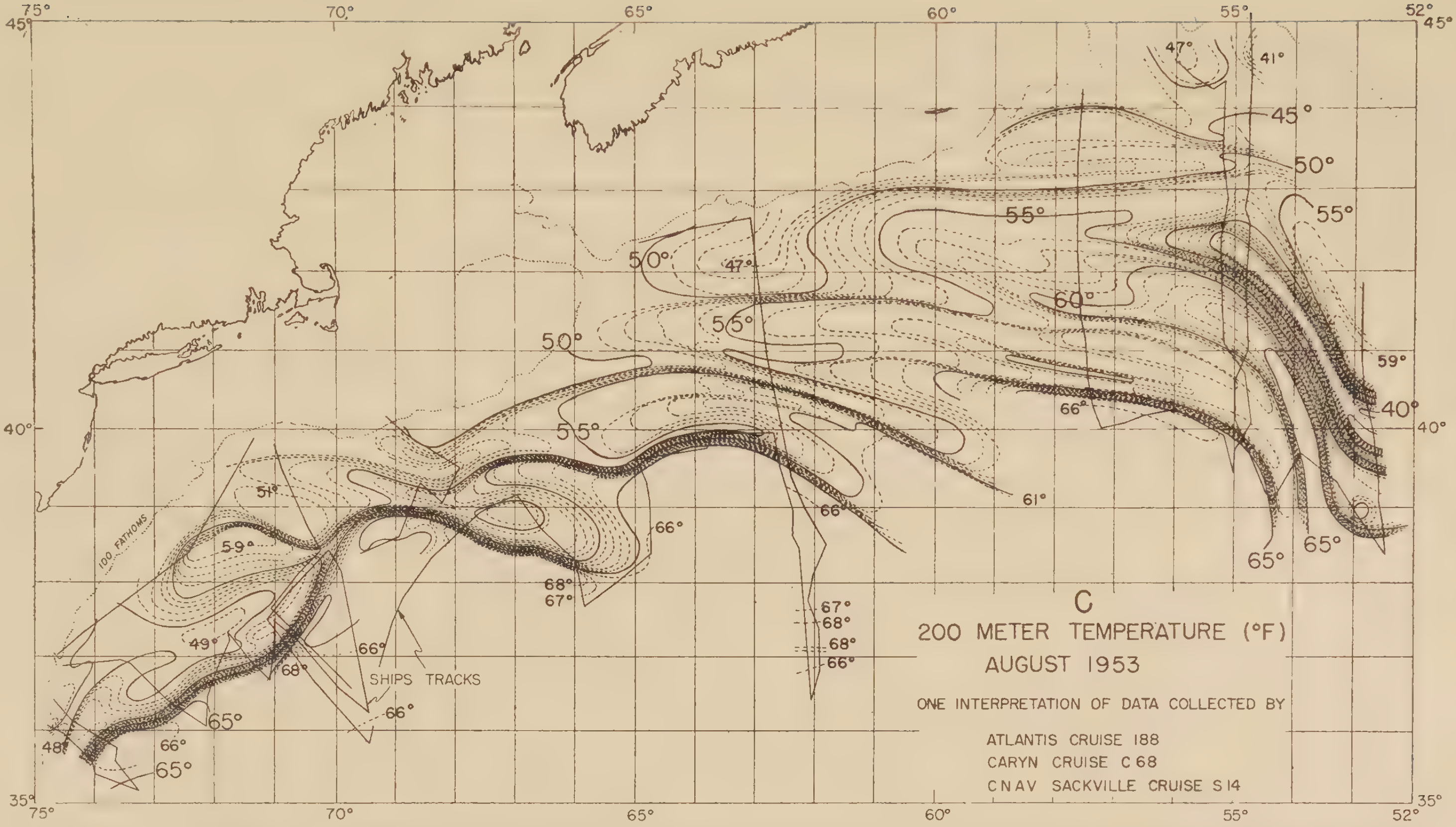
C
200 METER TEMPERATURE (°F)
AUGUST 1953
ONE INTERPRETATION OF DATA COLLECTED BY
ATLANTIS CRUISE 188
CARYN CRUISE C 68
CNAV SACKVILLE CRUISE S 14
SHIPS TRACKS
100 FATHOMS
75°
70°
65°
60°
55°
52°
45°
40°
35°
47°
41°
45°
50°
55°
55°
60°
50°
47°
55°
50°
55°
59°
40°
66°
61°
65°
65°
66°
66°
51°
59°
68°
67°
67°
68°
68°
66°
49°
66°
68°
65°
66°
66°
65°
48°

Chart 3c. An analysis of the temperature field (degrees F), at a depth of 200 metres in the Gulf Stream between 75° and 52° West longitude.

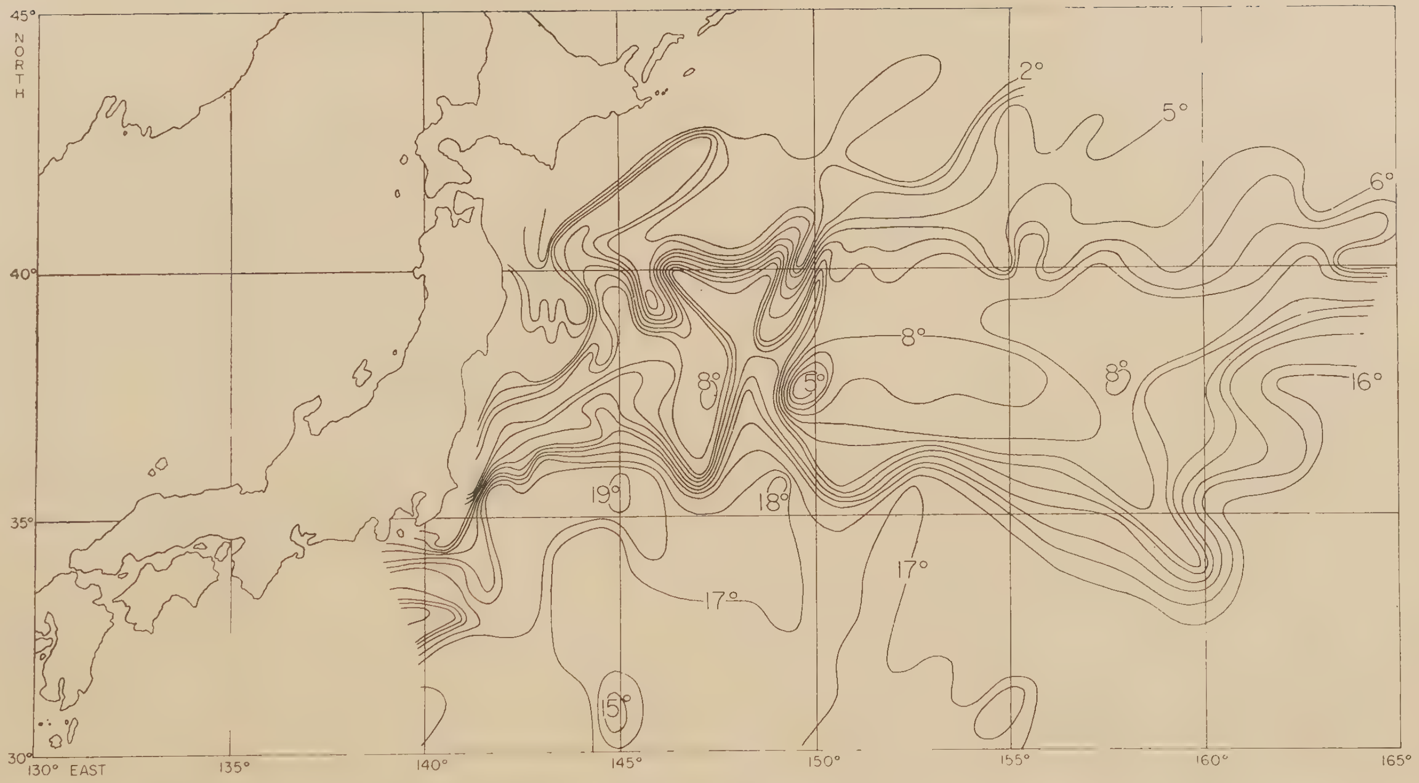
45°
NORTH
40°
35°
30°
130° EAST
135°
140°
145°
150°
155°
160°
165°
2°
5°
6°
8°
8°
8°
5°
16°
19°
18°
17°
17°
15°

Chart 4a. One analysis of the temperature field (degrees C), at a depth of 200 metres in the Kuroshio System, after UDA (1935). From data obtained by numerous Japanese vessels, 1-14 August, 1933.

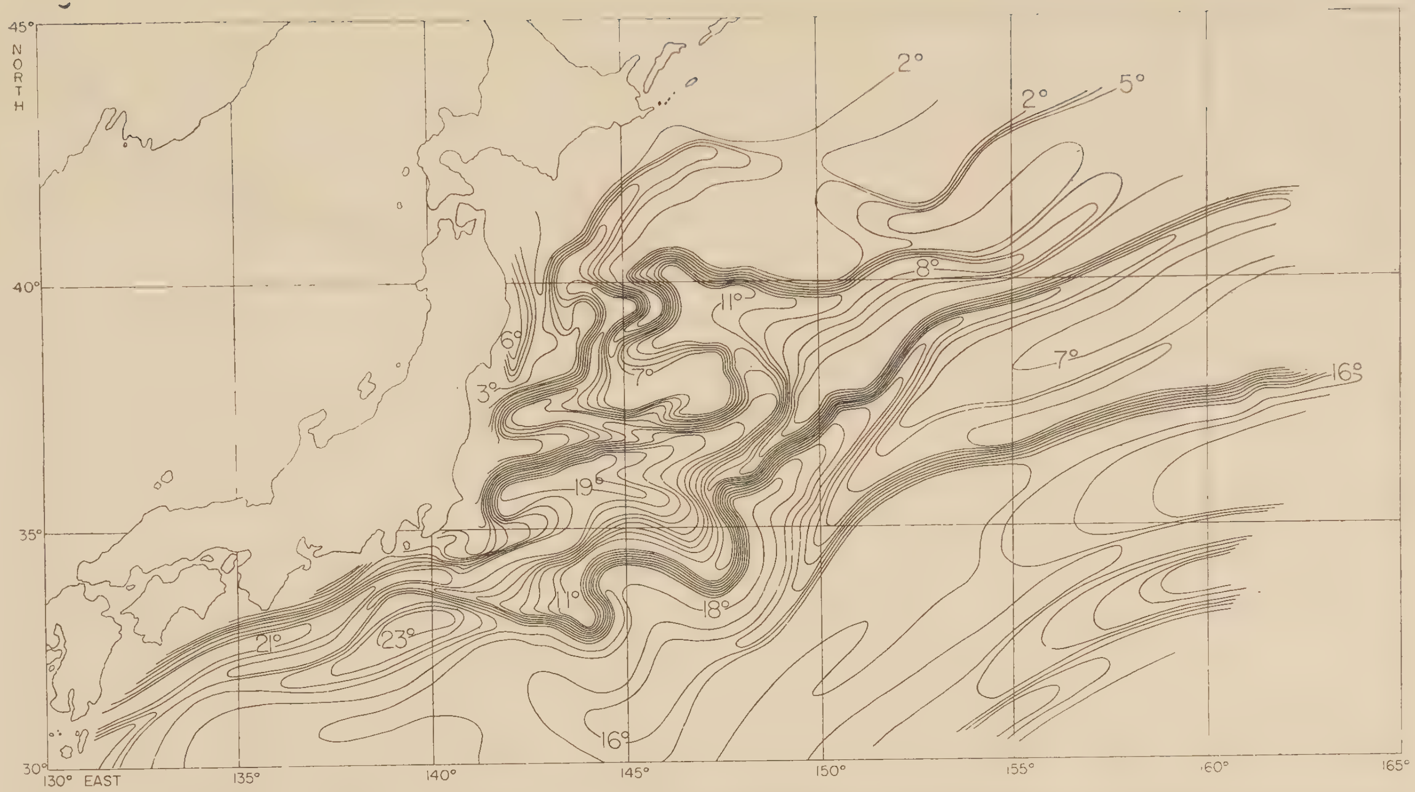
45°
NORTH
40°
35°
30°
130° EAST
135°
140°
145°
150°
155°
160°
165°
2°
2°
5°
8°
11°
6°
3°
7°
7°
16°
19°
11°
18°
21°
23°
16°

Chart 4b. One analysis of the temperature field (degrees C), at a depth of 200 metres in the Kuroshio System. From data obtained by numerous Japanese vessels, 1-14 August, 1933.

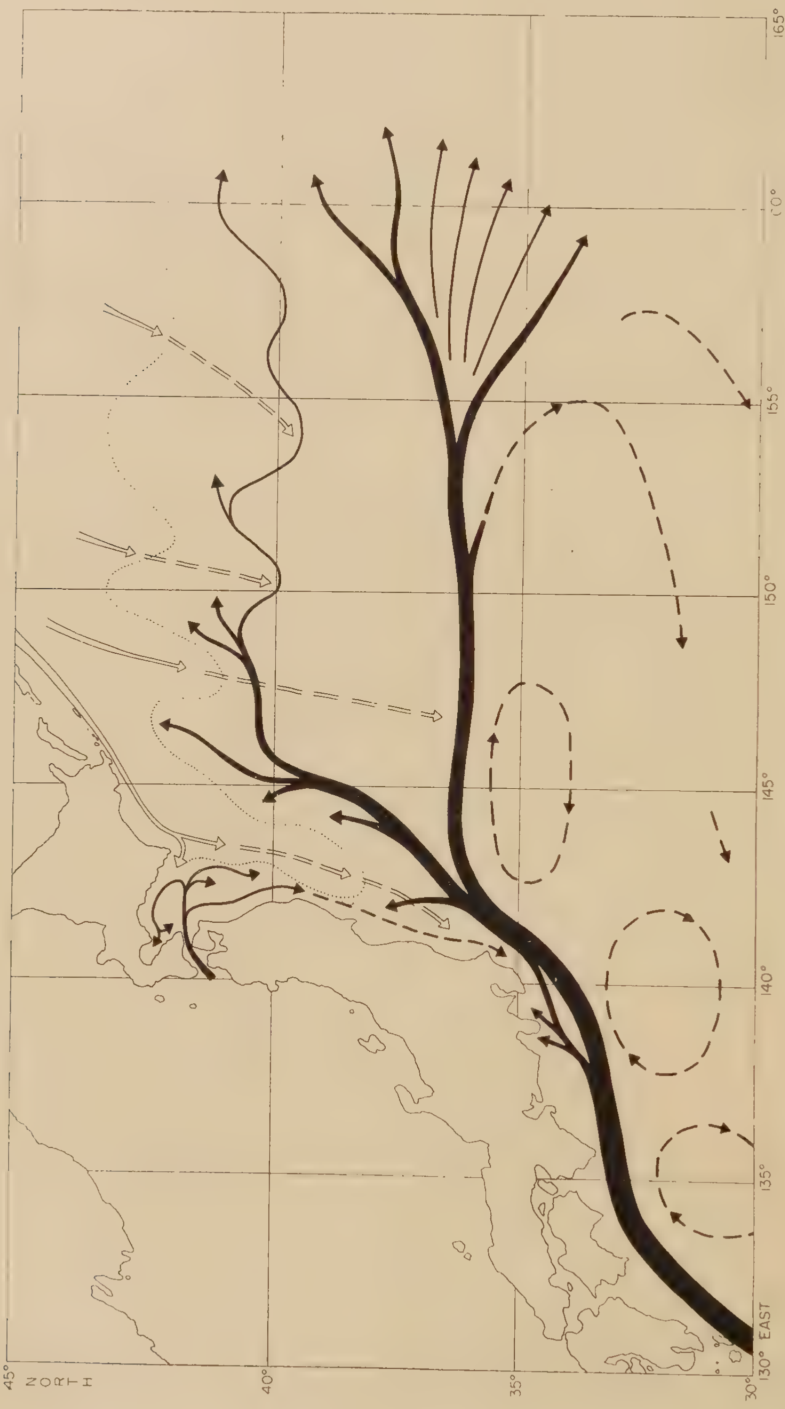
45°
NORTH
40°
35°
30°
130° EAST
135°
140°
145°
150°
155°
160°
165°

Chart 4c. The currents in the Kuroshio System during August, 1933, after Uda (1935).

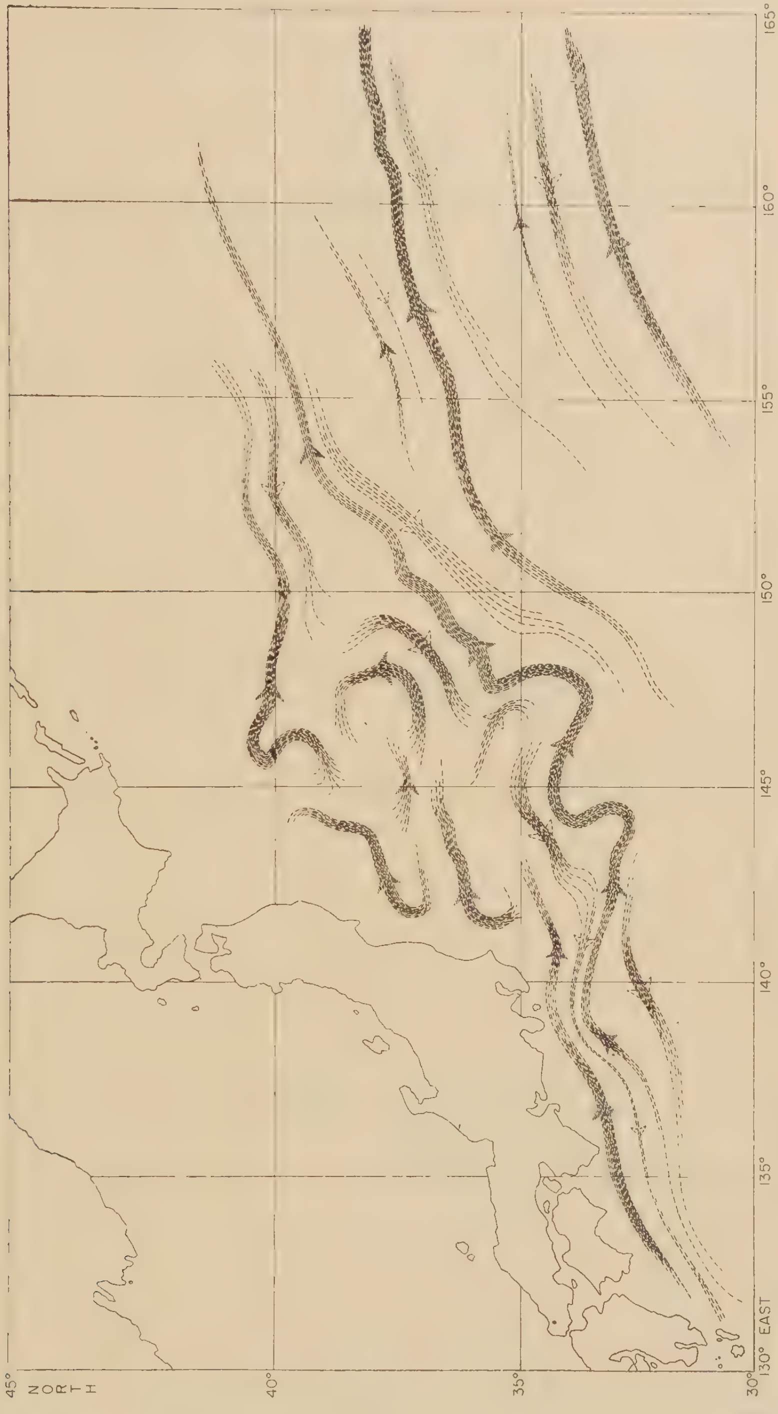
165°
160°
155°
150°
145°
140°
135°
130° EAST
45° NORTH
40°
35°
30°

Chart 4d. The currents in the Kuroshio System, based on the 200 metre temperature field shown on chart 4b.

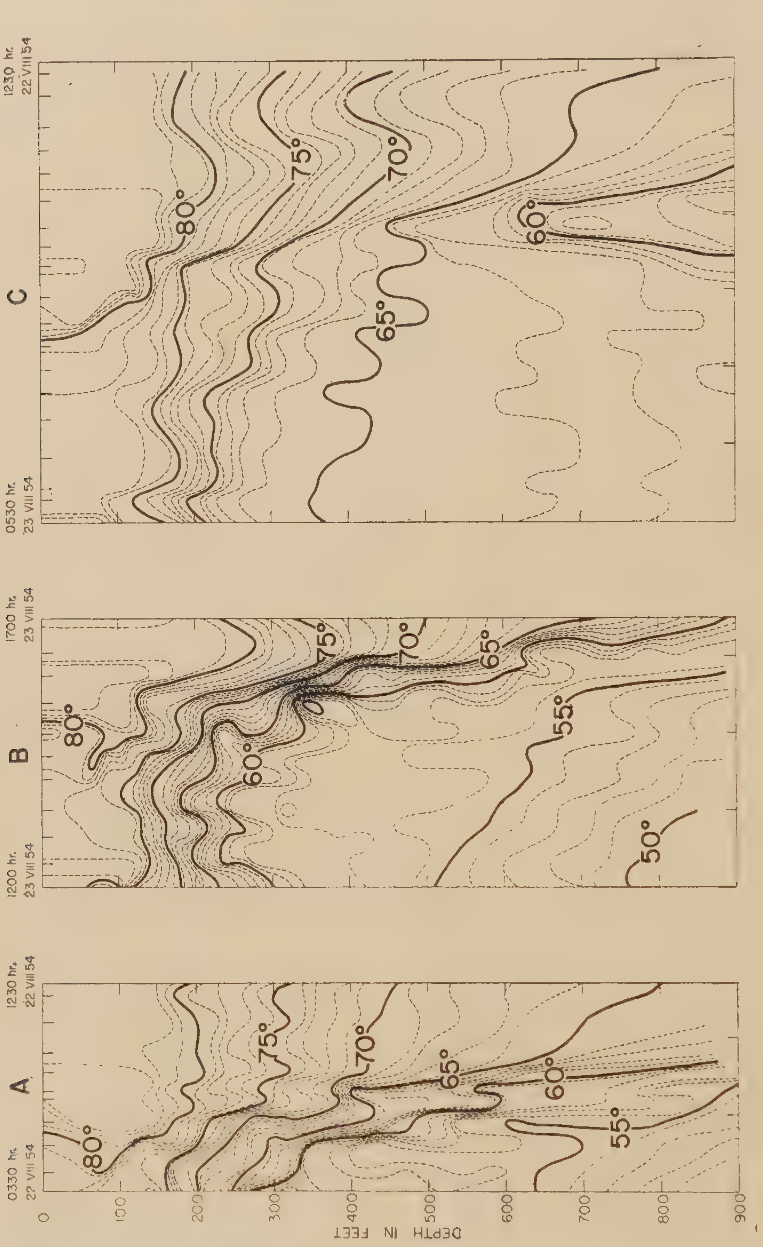
C
1230 hr.
22 VIII 54
0530 hr.
23 VIII 54
80°
75°
70°
65°
60°
B
1700 hr.
23 VIII 54
1200 hr.
23 VIII 54
80°
75°
70°
65°
60°
55°
50°
A
1230 hr.
22 VIII 54
0330 hr.
22 VIII 54
80°
75°
70°
65°
60°
55°
0
100
200
300
400
500
600
700
800
900
DEPTH IN FEET

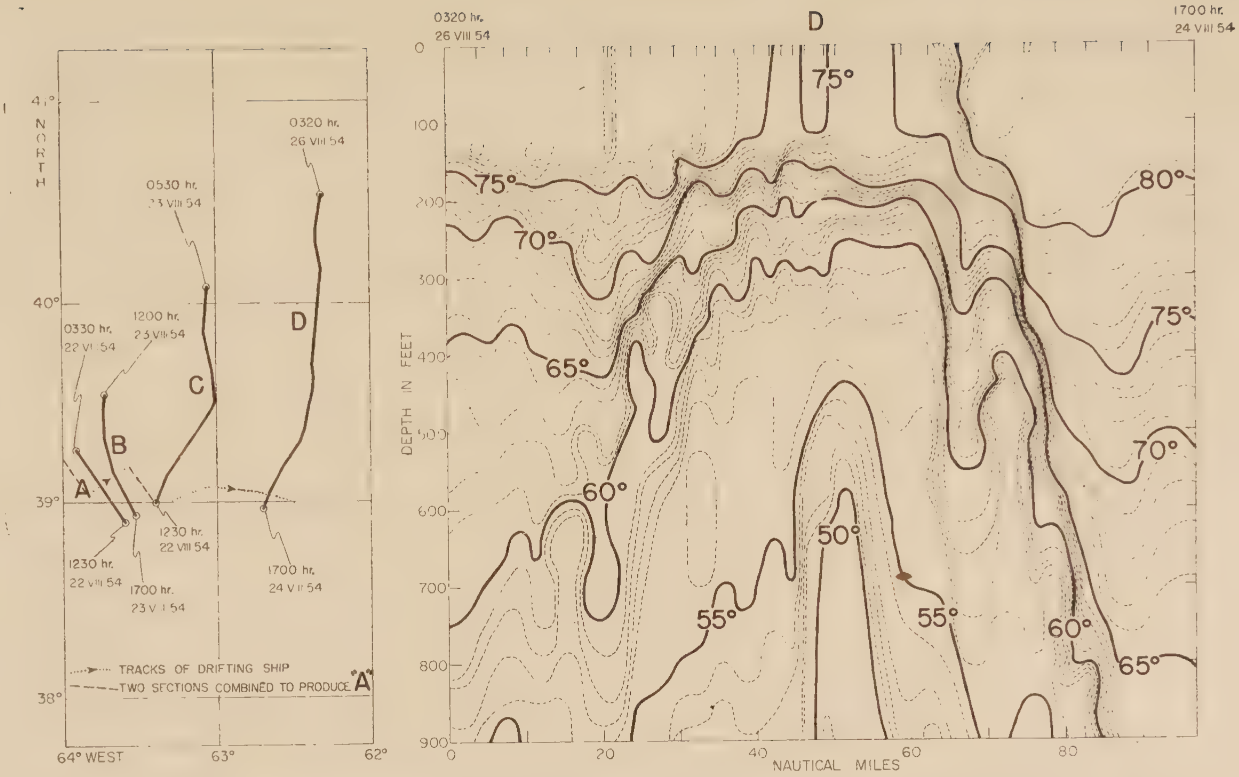

Chart 5. Four temperature-depth profiles in the Gulf Stream System south of Novia Scotia. From data obtained by the Woods Hole Oceanographic Institution Research Vessel *Caryn*, 22-25 August, 1954.

Printed in Great Britain by The Salisbury Press Ltd., Publicity House, Wilton Road Salisbury, Wilts. (89859)

Contribution No. 750

Reprinted from
BULLETIN OF MARINE SCIENCE
OF THE GULF AND CARIBBEAN
Vol. 5, No. 2, pp. 81-115
JUNE, 1955

THE CEPHALOPODA OBTAINED BY THE HARVARD-HAVANA EXPEDITION OFF THE COAST OF CUBA IN 1938-39[1]

GILBERT L. VOSS
The Marine Laboratory, University of Miami

ABSTRACT

The collections of cephalopods obtained by the ATLANTIS off the coasts of Cuba in 1938 and 1939 contained 253 specimens representing 21 genera and 25 species of which 1 genus and 4 species are new to science. All of the species are recorded together with their ranges and distribution. *Rossia antillensis* n. sp., *Heteroteuthis atlantis* n. sp., *Abralia redfieldi* n. sp., and *Tetracheledone spinicirrus* new genus and species, are described and figured. *Rossia brachyura* Verrill is figured for the first time. A key to all of the cephalopods definitely known to occur in Cuba is included.

INTRODUCTION

The collection of cephalopods obtained by the ATLANTIS off the coasts of Cuba in 1938 and 1939 contain 253 specimens representing 21 genera and 25 species of which 1 genus and 4 species are new to science.

It is interesting to note that over half of the species contained in this report are represented by only 1 specimen and 5 by only 2 specimens, while the remaining are well represented. Of these latter *Rossia* is by far the most common genus containing over half of the total number of cephalopods taken by the expedition. Of the remaining myopsid squid *Lolliguncula brevis, Doryteuthis plei,* and *Nectoteuthis pourtalesi* are the most numerous. The latter species, not reported since Verrill described it in 1883, is probably much more numerous than was formerly thought. The oegopsid squid are mainly represented by *Illex illecebrosus* and *Abralia veranyi.* The octopods, surprisingly, are best represented by two species, *Pteroctopus tetracirrhus* recently first recorded from the Western Atlantic by Voss (1954), and a new genus and species, *Tetracheledone spinicirrus,* of which 4 specimens were obtained.

---

[1] Contribution No. 750 from the Woods Hole Oceanographic Institution.
Contribution No. 142 from The Marine Laboratory, University of Miami.

The literature on Cuban cephalopods is very scarce. The first work appeared in 1841 by d'Orbigny as part of the larger work, "Histoire physique, politique et naturelle de l'Isle de Cuba," by Ramon de la Sagra, in which 16 species are recognized. Of these, 3 are synonyms of others in the list, and one is not native to the Western Atlantic.

In 1875 Arango published a list of cephalopods which apparently was copied from d'Orbigny's work. From that time until 1945 no cephalopod papers appeared with particular mention of Cuban species. In the latter year Pickford, in her revision of the littoral octopods of the Western Atlantic, listed *Octopus vulgaris* and *O. hummelincki* as found in Cuban waters. Lately, Dr. C. G. Aguayo has begun a publication listing all of the known species of mollusks from the island. The cephalopod section is as yet fragmentary since many of the genera and families have not been covered at the present time. The work is primarily a survey of previously published records.

Thanks to the kindness of C. G. Aguayo and Isabel Farfante the author has been privileged to examine several small collections of littoral cephalopods from Cuba in the course of several years, and this has confirmed the presence in Cuban waters of *Octopus briareus* and *Doryteuthis brasiliensis,* the latter collected this year (1954) from the vicinity of the Isle of Pines.

The author wishes to thank the Woods Hole Oceanographic Institution and the associate director, Dr. Alfred C. Redfield, for the financial aid in the form of a Research Fellowship to carry out this study. He also wishes to thank William J. Clench, Curator of Mollusks, Museum of Comparative Zoology, Harvard University for the loan of the collections for study and Harald A. Rehder, Curator of Mollusks, U. S. National Museum for permission to study certain comparative material in the collections of the latter institution and for facilities placed at his disposal during the summer of 1953.

Key to the Cephalopods of the Island of Cuba

The following artificial key is presented for the convenience of those interested in the cephalopods found in the waters of Cuba. In it are listed all of the species known to occur in the area, as well as those contained in the present report. Those not taken by the ATLANTIS, but recorded from other sources, are preceded by an asterisk. It is probable that many other species will be reported from Cuba with the increased activity in exploratory fisheries investigations. Thus the key alone should not be relied upon for final determinations.

I. Tentacles present; suckers stalked, usually provided with a horny ring or hooks (Decapoda).
1. Eyes covered by a continuous membrane or open by a minute pore (Myopsida).
2. An internal coiled, chambered shell.
**Spirula spirula* Linnaeus
2^{1}. Internal shell straight, feather-shaped, or absent.
3. Adult small; body short and rounded posteriorly with round or ovate lateral fins; internal shell reduced or absent.
4. Antero-ventral mantle margin strongly produced as a shelf nearly covering the funnel.
5. Arm suckers raised on prominent pedicels, suckers extending to tips of all arms.
Nectoteuthis pourtalesi Verrill
5^{1}. Arm suckers normally stalked; distal half of second pair of arms blade-like, devoid of suckers.
Heteroteuthis atlantis n. sp.
4^{1}. Antero-ventral margin of mantle not strongly produced.
5. Tentacular suckers in few rows (5-8), left dorsal arm of male hectocotylized.
Rossia (Semirossia) sp.
5^{1}. Tentacular suckers minute, in many rows; both dorsal arms of male hectocotylized.
6. Suckers of sessile arms in 4 rows.
Rossia brachyura Verrill
6^{1}. Suckers of sessile arms in 2 rows, rectal papillae present.
Rossia antillensis n. sp.
3^{1}. Adult medium to large; body elongate, pointed posteriorly; fins unite posteriorly, internal shell feather-like.
4. Fins marginal, extending nearly to anterior edge of mantle.
Sepioteuthis sepioidea (Blain.)
4^{1}. Fins terminal.
5. Body short; fins terminal, rounded; female with spermatophore pad within mantle cavity.
Lolliguncula brevis (Blain.)
5^{1}. Body elongate; fins rhombic; spermatophore pad of female on lower lip of buccal membrane.
6. Lateral edges of gladius straight, thickened, brownish.
7. Mantle long, slender, width about 1/8 the length, lightly pigmented; ventral mantle surface streaked with reddish brown in the male.
Doryteuthis plei (Blain.)
7^{1}. Mantle stout, pigmented with purplish brown; no ventral streaks in the male.
**Doryteuthis brasiliensis* (Blain.)
6^{1}. Lateral edges of gladius curved, not thickened.
**Loligo pealei* Lesueur
1^{1}. Eyes not covered by a continuous membrane (Oegopsida).

2. Some of the suckers of the arms and/or tentacles converted into slender curved hooks.

3. Arms with two rows of hooks.

4. Fins drawn out to a point posteriorly, united; ventral surface of mantle with numerous rows of light organs.

5. Arms with 2 rows of hooks; tentacular clubs with one row of hooks; 5 light organs on ventral surface of eyeball.

6. 3 nearly equal size hooks on tentacular club; 1st, 3rd and 5th light organs on eyeball twice as large as 2nd and 4th, round.

Abralia redfieldi n. sp.

6^{1}. 4 hooks on tentacular club, proximal minute, 2nd largest, decreasing in size distally; 1st and 5th light organs on eyeball much larger than middle three, oval, the 5th often with a slight sinus in dorsal edge.

Abralia veranyi (Rüppell)

5^{1}. Both arms and tentacular club with 2 rows of hooks.

**Thelidioteuthis alessandrini* Verany

4^{1}. Fins lateral, reaching beyond the pointed posterior end of the the body, not united; no light organs on mantle.

5. Arms with 2 rows of hooks; tentacular club with small number of hooks on ventral row.

Pyroteuthis margaritifera aurantiaca Joubin

5^{1}. Arms with two rows of hooks; no hooks on tentacular club.

**Pterygioteuthis giardi* H. Fischer

3^{1}. No hooks on arms.

4. Body fleshy, stout, strongly colored with purplish brown; mantle with short point posteriorly; 2 rows of hooks and 2 rows of suckers on tentacular club; fins less than half the mantle length; animal small.

**Onychia caribaea* (Lesueur)

4^{1}. Body slender, with long drawn out posterior point; adults with fins longer than half the mantle length; 2 rows of hooks on tentacular club; animal medium to large.

Onychoteuthis banksi (Leach)

2^{1}. No hooks on either arms or tentacles.

3. Mantle locking at sides of funnel by means of locking grooves and ridges.

4. Connective apparatus on tentacles indistinct; no folds or pockets in funnel groove.

Illex illecebrosus (Lesueur)

4^{1}. A distinct carpal cluster on tentacles; folds and side pockets in funnel groove.

5. 0-2 cups on the tentacular stalk proximal to last cup of carpal cluster.

**Sthenoteuthis pteropus* (Steenstrup)

5^{1}. 4-7 cups on the tentacular stalk proximal to last cup of carpal cluster.

**Sthenoteuthis bartrami* (Lesueur)

3^{1}. Mantle fused to head at dorsum and on each side of the funnel.

4. Body either covered with tubercles or with tubercles arranged in V-shaped lines at fusion of mantle and funnel.

5. Mantle smooth; V-shaped lines of tubercles at point of fusion of mantle and funnel.
Liocranchia reinhardti (Steenstrup)

5^1. Mantle completely covered with tubercles.
Cranchia scabra Leach

4^1. No tubercles on mantle.
Verrilliteuthis hyperborea (Steenstrup)

II. Tenetacles absent; 8 arms; suckers not stalked and without horny rings (Octopoda).

1. A single pair of fins present; cirri bordering suckers; deep water forms.

2. Body globular; fins large; arms long with simple velum.

3. Length of cirri bordering suckers about 2½ times the diameter of suckers.
Grimpoteuthis umbellata (Fischer)

3^1. Cirri bordering suckers no longer than the diameter of the suckers.
?*Grimpoteuthis meangensis* (Hoyle)

2^1. Body flattened; fins small and dorsal; arms nearly completely involved in the velum.
Opisthoteuthis agassizi Verrill

1^1. No fins.

2. Suckers in 2 rows.

3. Large and conspicuous aquiferous pores on head; dorsal arms of female connected by a broad velum.
**Tremoctopus violaceus* Delle Chiaje

3^1. No aquiferous pores on head; dorsal arms of female not connected by a broad velum.

4. Left third arm of male hectocotylized.

5. Male minute; female with dorsal arms with terminal expansions modified for secretion of an external shell or egg case; pelagic.

6. Shell of female small; keel broad, knobs few and large, broad auricular expansions.
Argonauta hians Solander

6^1. Shell large, keel narrow, knobs numerous and small, auricular expansions narrow.
Argonauta argo Linnaeus

5^1. No sexual dimorphism in size; female without an egg case; no terminal expansions of the dorsal arms; benthic.

6. A thickened fold or ridge surrounding the mantle; a single cirrus over each eye; surface covered with small papillae.
Scaeurgus unicirrhus d'Orbigny

6^1. No fold surrounding mantle; 2 cirri over each eye; skin smooth.
Pteroctopus tetracirrhus (Delle Chiaje)

4^1. Right third arm of male hectocotylized.

5. A persistent purple, blue or dark ring or ocellus at base of arms below eye on each side.
**Octopus hummelincki* Adam

5^1. No persistent ring or ocellus.

6. Arms large, long, and stout, especially the 3rd pair; gills 6-8; ligula index 3-4.

**Octopus briareus* Robson

6[1]. Arms subequal except 1st pair which is much shorter; gills 7-11; ligula index below 2.5.
**Octopus vulgaris* Lamarck

2[1]. Suckers in a single row.

3. Body gelatinous, soft, semi-transparent; planktonic, size small.
Eledonella pygmaea Verrill

3[1]. Body firm, covered with coarse sharp tubercles; 2 large cirri over each eye; hectocotylus spade-shaped; benthic, moderate size.
Tetracheledone spinicirrus n. sp.

Systematic Discussion

Suborder *DECAPODA*

Division MYOPSIDA

Family Sepiolidae Leach.

Rossia (Austrorossia) antillensis n. sp.

(Figures 1A-E)

Holotype. Male, Sta. 2987, 280-300 fms. off Sagua la Grande, March 13, 1938. MCZ Cat. No. 203976.

Paratype. Gravid female, Sta. 3485, 385 fms. off Cayo Romano, May 11, 1939. MCZ Cat. No. 203977.

This is a large species of *Rossia* with a rather flabby consistency (Figure 1A). The surface is smooth and densely covered dorsally, less so ventrally, with small purple and red chromatophores. The body is sacular, rounded posteriorly, with the dorsomedian border slightly projecting. The fins are large, 80 to 88.5 per cent of the mantle length, thick and fleshy, their anterior edges reaching to the anterior border of the mantle. The width across the fins is 163 to 200 per cent of the mantle length. The funnel is stout, tubular, free for half of its length. The locking apparatus is normal but strongly developed. The funnel organ is shown in Figure 1B.

The head is large. In the holotype the head width is 135 per cent of the mantle length; in the paratype the head was too distorted to obtain a useful measurement. The eyes are very large and conspicuous.

The arms are of medium length, in the order 2=3.4.1 or 3.4=2.1 with the suckers arranged distinctly in two rows. The suckers on the female are rather small, but the male holotype has suckers of medium size with those in the middle of the arms slightly enlarged. In the holotype the dorsal pair of arms is hectocotylized in the following manner. Proximally there are about six pairs of small suckers. These are followed by about six pairs of enlarged suckers which are about twice the diameter of the basal suckers. In the only male available, it is impossible to tell whether these are enlarged to the tip of the arm as

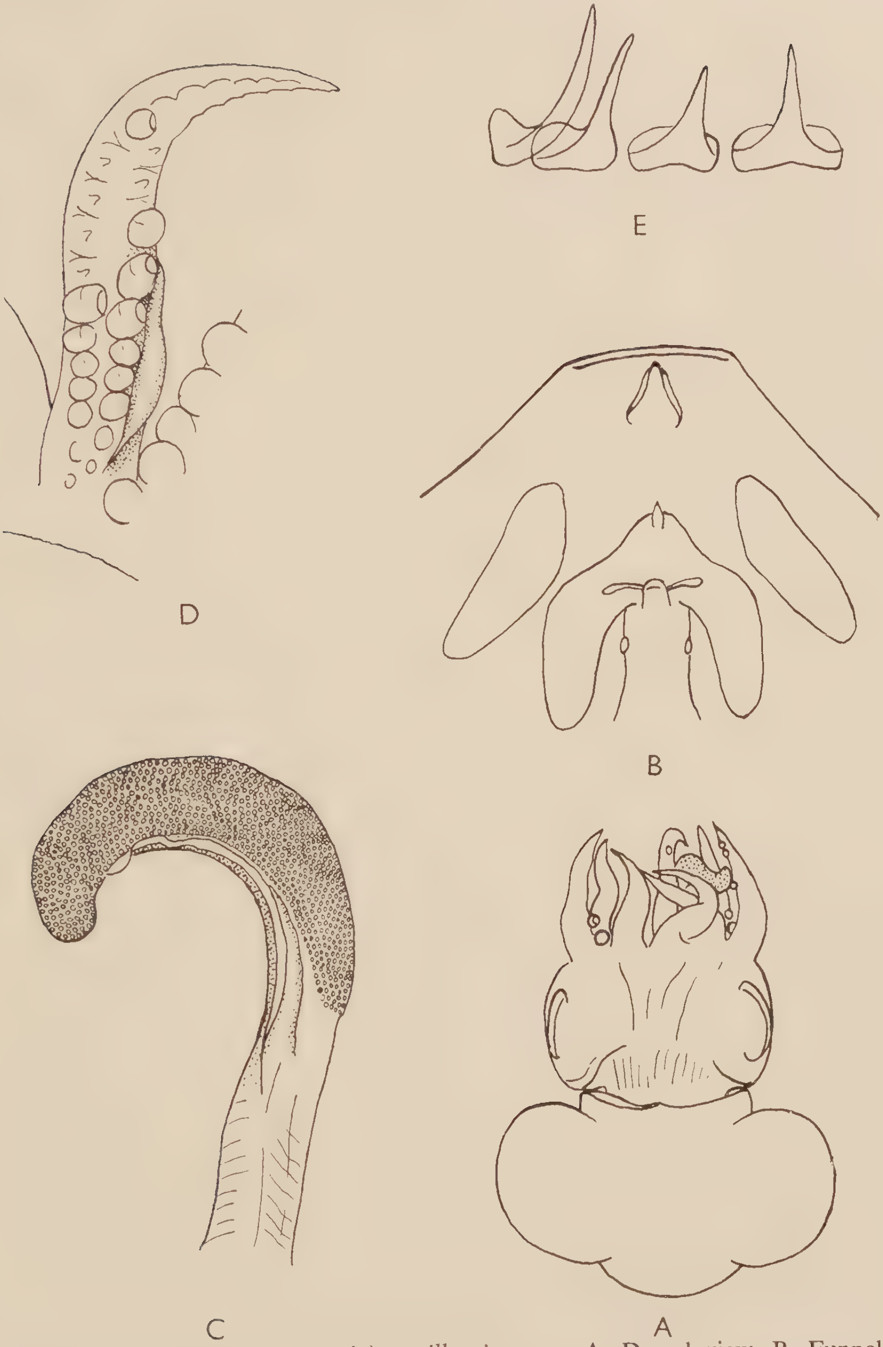

FIGURE 1. *Rossia* (*Austrorossia*) *antillensis* n. sp. A. Dorsal view, B. Funnel organ and rectal papillae, C. Left tentacle, D. Left dorsal arm showing hectocotylization, E. Radula.

the distal suckers are missing. Starting at the base of the third pair of suckers from the base of the arm is a thick, fleshy pad or fold on the outer or ventral side of the arm. This peculiar pad extends to the base of the eighth pair of suckers and is similar on both dorsal arms (Figure 1D).

Measurements (in mm) of two specimens of *Rossia antillensis* n. sp.

	Holotype	Paratype
Mantle length	43.0	72.0
Mantle width	40.0	——
Head width	47.5	47.0
Fin insertion	25.5	48.0
Fin length	31.0	57.5
Fin width	70.0	118.0
Arm length, 1st pair	33.0	71.5
2nd "	42.0	76.0
3rd "	42.0	87.5
4th "	37.0	77.0
Length tent. club	18.0	——

The tentacles (Figure 1C) are short, stout, the stalks generally oval in cross section, but squared on the ventral edge. The clubs are over half of the mantle from the proximal sucker to the tip, and are rounded instead of expanded, and no wider than the stalk. A well developed swimming membrane borders the dorsal edge from slightly below the suckers to within a millimeter of the distal end. The suckers are very minute, their total diameter about 0.25 mm, the diameter of the opening of the horny circle about 0.12 mm. The suckers are so small and crowded that it is not possible to distinguish the number of rows with certainty, but they appear to number about 30 to 40 rows.

The radula has seven rows of teeth, long and slender. The rhachidian teeth are long, slender with wide bases; first laterals slightly shorter and broader; second laterals long and slender, curving, longer than the rhachidian teeth; marginals long, strongly curving and arcuate, nearly twice as long as the rhachidian teeth (Figure 1E).

The spermatophores of the holotype had disintegrated within the outer capsule so that although they were measureable in total length, 12.0 mm and 34.2 per cent of the mantle length, none of the internal structures can be described. The eggs of the gravid female are oblong, somewhat reticulated and measured 7.0 x 4.5 mm.

A complete dissection of the internal anatomy was not considered advisable on the holotype and the paratype is in such a poor state of preservation that a dissection of it would have been useless. However, an examination of the surface of the visceral mass disclosed that this species has a pair of papillae on the sides of the rectum as has been described for *R. mastigophora* Chun and *R. bipapillata* Sasaki.

Remarks. This species appears to be most closely comparable to Berry's *R. australis* for which he constructed the subgenus *Austrorossia* to accommodate both this species and *R. mastigophora* Chun. Whether this subgenus is valid seems to be open to question on several points. The very numerous and minute suckers of the tentacular club are also found in *R. brachyura,* which however, has four rows of suckers on the sessile arms. Some of the suckers of all of the arms are slightly enlarged or greatly so in the males of *Semirossia.* Also the nature of the pad on the dorsal pair of arms in the male is apparently lacking in *R. mastigophora* and unknown in *R. bipapillata,* but present in *R. australis* and *R. antillensis.* In most of these species there is a papillary organ on either side of the rectum. This is undescribed in *R. australis,* but may be present.

With the possible exception of the subgenus *Semirossia* there does not appear to be any homogeneity of characters within the genus *Rossia* which permits well characterized subgeneric division. However, on the basis of the composite characters listed by Berry (1918) it seems at present that the subgenus *Austrorossia* is comprised of four species: *R. australis, R. mastigophora, R. bipapillata,* and *R. antillensis.*

The present species may be separated from *R. mastigophora* and *R. australis* by the nature of the fleshy pad on the dorsal arms. Until the nature of the males of *R. bipapillata* is known this species cannot be separated except by the somewhat larger and less numerous tentacular suckers.

Rossia brachyura Verrill, 1883
(Figures 2A - C)

Rossia brachyura Verrill, 1883, p. 110.

Material. 1 female in alcohol, Sta. 2982B off Punta Alegre, Camaguey Prov. in 205 fms., otter trawl, March 11, 1938. MCZ Cat. No. 203978.

Verrill described this species from a single female of 18mm dorsal mantle length, taken by the BLAKE in 208 fms. off the island of St. Kitts. The present specimen is in an excellent state of preservation; only the end of the right tentacular club is missing. No other specimens are known.

As Verrill's description of this species is rather brief, the following

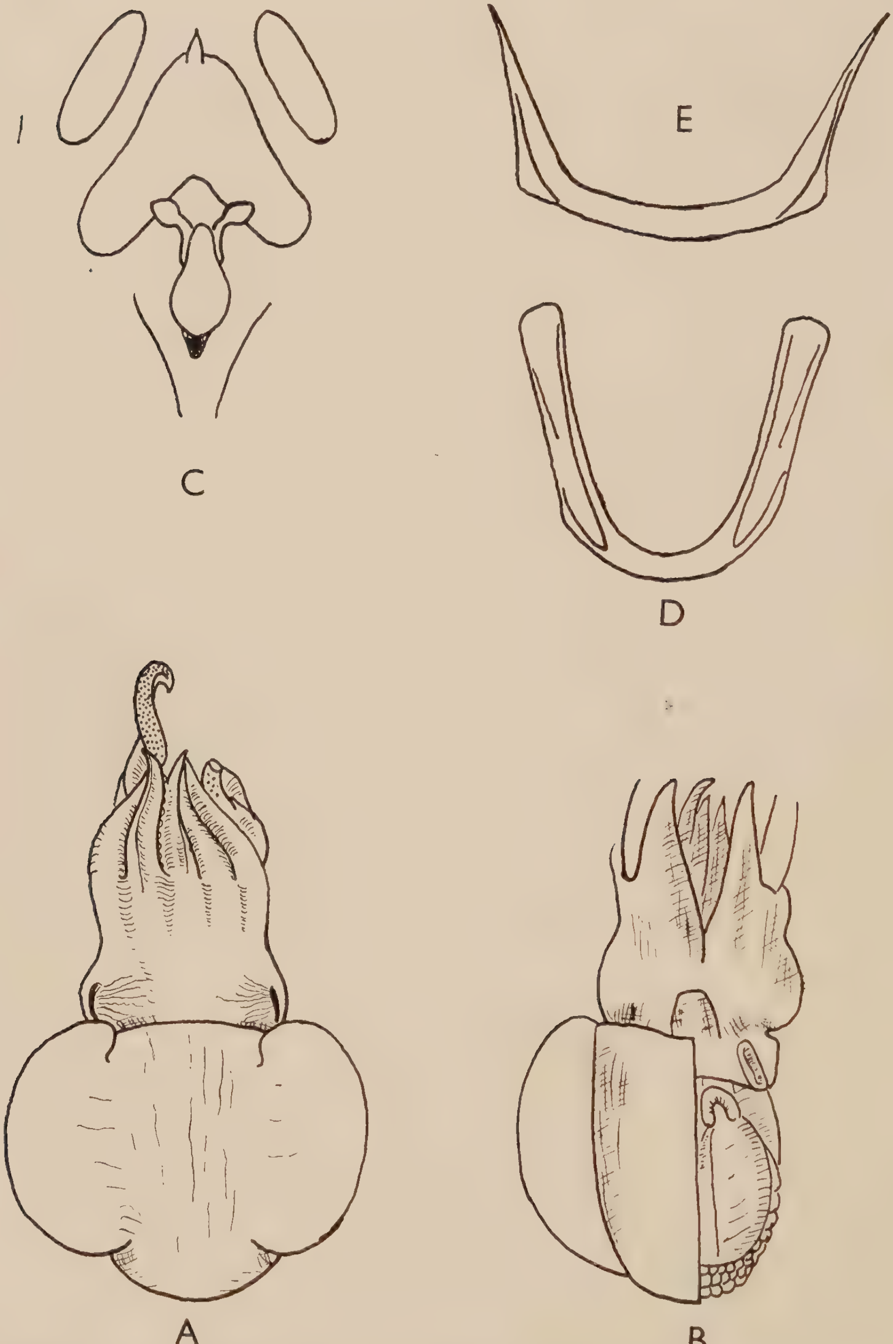

FIGURE 2. A-C *Rossia brachyura* Verrill. A. Dorsal view, B. Ventral view, mantle cavity open, C. Funnel organ. Figure 2D. Shell vestige of *Grimpoteuthis umbellata* (Fischer), Figure 2E. Shell vestige of *?Grimpoteuthis meangensis* (Hoyle).

somewhat more detailed description is given. To it are added Figure 2 A-C which supplement the figure given by Verrill of the left second arm of his specimen, which is of somewhat dubious value.

The body is short, thick and fleshy, rounded posteriorly, and with large, fleshy fins, somewhat resembling those of *R. megaptera* Verrill. The fin insertion is about 2/3 of the mantle length. The anterior lobe of the fin is free while the fin itself projects slightly anteriorly of the mantle edge. The head is large, with prominent eyes, and is about ¾ as wide as the mantle. The integument is smooth.

The sessile arms are about ¾ of the mantle length, stout, in the order 3.2=4.1, the dorsal pair prominently keeled. The fourth pair of arms are stout and bordered laterally by a stout membrane which connects the third arms to form a deep pocket for the reception of the tentacle stalks. The arms are united by a deep web which is about 40 per cent of the arm length, deepest in the sector between the third and fourth arms, and completely disappearing between the ventral arms which are deeply cleft. The arm suckers are as described by Verrill, small, with small apertures, arranged in two rows proximally but immediately being distinctly four rowed and crowded medially, less so distally.

The tentacular arms are rather stout, of moderate length, triangular, rounded on the aboral surface, but flat and slightly grooved orally. The club is only slightly expanded, round, and bordered dorsally by a broad swimming membrane or keel which has its origin slightly proximal to the club and extends to the tip. The suckers are small and are arranged in about 16 rows. They have very short, slender stalks.

The funnel is short, thick, with a rounded, subterminal flap. The funnel organ is an inverted V-shaped body, small, compact with a slender, broadly triangular papilla anteriorly. The ventral pads are narrowly oval (Figure 2C).

Measurements (in mm) of a gravid female of *Rossia brachyura.*

Mantle length	43.0	Arm length	
Mantle width	30.0	1st pair	29.0
Head width	30.0	2nd "	32.0
Fin insertion	26.0	3rd "	34.0
Fin length	36.0	4th "	32.0
Fin width	56.0		

In the gravid female the nidamental glands are large, conspicuous, and occupy the major part of the visceral cavity. A small U-shaped accessory nidamental gland is also present. The eggs are about 3.0 x 4.0 mm.

In alcohol the color is pale with small reddish chromatophores dorsally and larger ones which are crowded and somewhat fused ventrally.

Rossia (Semirossia) sp.

Among the cephalopods taken by the ATLANTIS are 148 specimens from 37 stations located on both coasts of Cuba of sepiolids here tentatively identified as members of the subgenus *Semirossia.* They represent over half of the total cephalopods taken during the cruises and are one of the commonest benthic forms of the West Indies. With few exceptions the specimens are females, and as none of the males can be definitely linked to the females, the specific identity must remain in doubt.

The males, although distinctly belonging to the *Semirossia,* cannot at this stage of our knowledge of the group be assigned to any of the known species. With the material at hand and the problematical status of the females it was felt that they should not be described as a new species until such time as the entire genus can be revised.

Detailed studies of the hectocotylized arm, the tentacular suckers, and the spermatophores were undertaken without success. Evidently there are two types of spermatophores involved in the group at hand, part of them approaching the structure of *Semirossia tenera,* the others deviating in certain respects. The external morphology is nearly identical.

If the females belong to the same species as the males then there is a strong difference in size between the sexes, a fact not hitherto recorded.

The whole problem of the genus *Rossia* is a perplexing one and cannot be solved until all of the species have been critically examined upon a sounder basis than has formerly been used. Some species have been thrown into synonymy without adequate comparison and others have been created upon minor details which, it is felt, will not stand up under critical observation.

It is possible, due to their size and locality, that the females might belong to *Rossia equalis* Voss (1950), but as no males referrable to this species were found in the collections this must also remain in doubt.

Genus *Heteroteuthis* Gray

Subgenus *Stephanoteuthis* Berry, 1909, emended

Body sepiolid-like, somewhat pointed posteriorly; mantle margin free, ventral mantle margin produced forward covering or nearly covering the funnel; fins large, semicircular, placed somewhat posteriorly; head large, broad; arms short, stout, the suckers arranged biserially; the distal portion of the second pair of arms and some of the others devoid of suckers; tentacles stout, club not expanded, covered with minute suckers.

Remarks. The genus *Stephanoteuthis,* formerly considered synonymous with *Heteroteuthis* Gray, 1849, is here emended for the reception of those species which have at least some of their arms devoid of suckers on their extremities. At the present state of our knowledge of this group it appears to be distinct from *Heteroteuthis* s. s. in having a somewhat more elongate body, part of the extremities of some of the arms devoid of suckers, and the smooth bladelike conformity of the second pair of arms. The subgenus *Stephanoteuthis* contains the species *hawaiiensis, hawaiiensis dagamensis,* and *atlantis* n. sp.

Heteroteuthis (*Stephanoteuthis*) *atlantis* n. sp.

(Figures 3A-F)

Holotype. Female, in alcohol, from Sta. 3367, off Puerto Tanamo in 640 fms., April 19, 1939. MCZ Cat. No. 155019.

Description. This beautiful little squid is very compactly built. The body is stout, roundly pointed posteriorly, slightly projecting on the dorsal margin, and about ½ as wide as long. Ventrally the mantle extends sharply forward of the dorsal margin, emarginated on the anterior edge, and nearly covers the tip of the funnel.

The fins are large, semicircular, about 60 per cent of the mantle length, and inserted obliquely with free anterior and posterior lobes. The posterior edges of the fins do not reach the end of the mantle. (Figures 3A, B).

The head is large with prominent eyes which project beyond the mantle width. The sessile arms are in the order 2.1.3.4. The second pair of arms is the longest (Figure 3E). The arms of this pair are broadened, somewhat flattened, and have the distal 60 per cent of the arms devoid of suckers. The suckerless portion is smooth, slightly recurving and blade-like. The remaining arms have the suckers in two rows; those of the ventral and dorsal pairs rather small, the suckers of the third pair rather large. The suckers of all of the arms become minute distally, the tips of the dorsal pair of arms devoid of suckers and ridged on the oral surface. There are no keels on the dorsal arms.

The tentacles (Figure 3D) are stout, flattened on their oral surface and slightly grooved. The clubs are conspicuously smaller than the

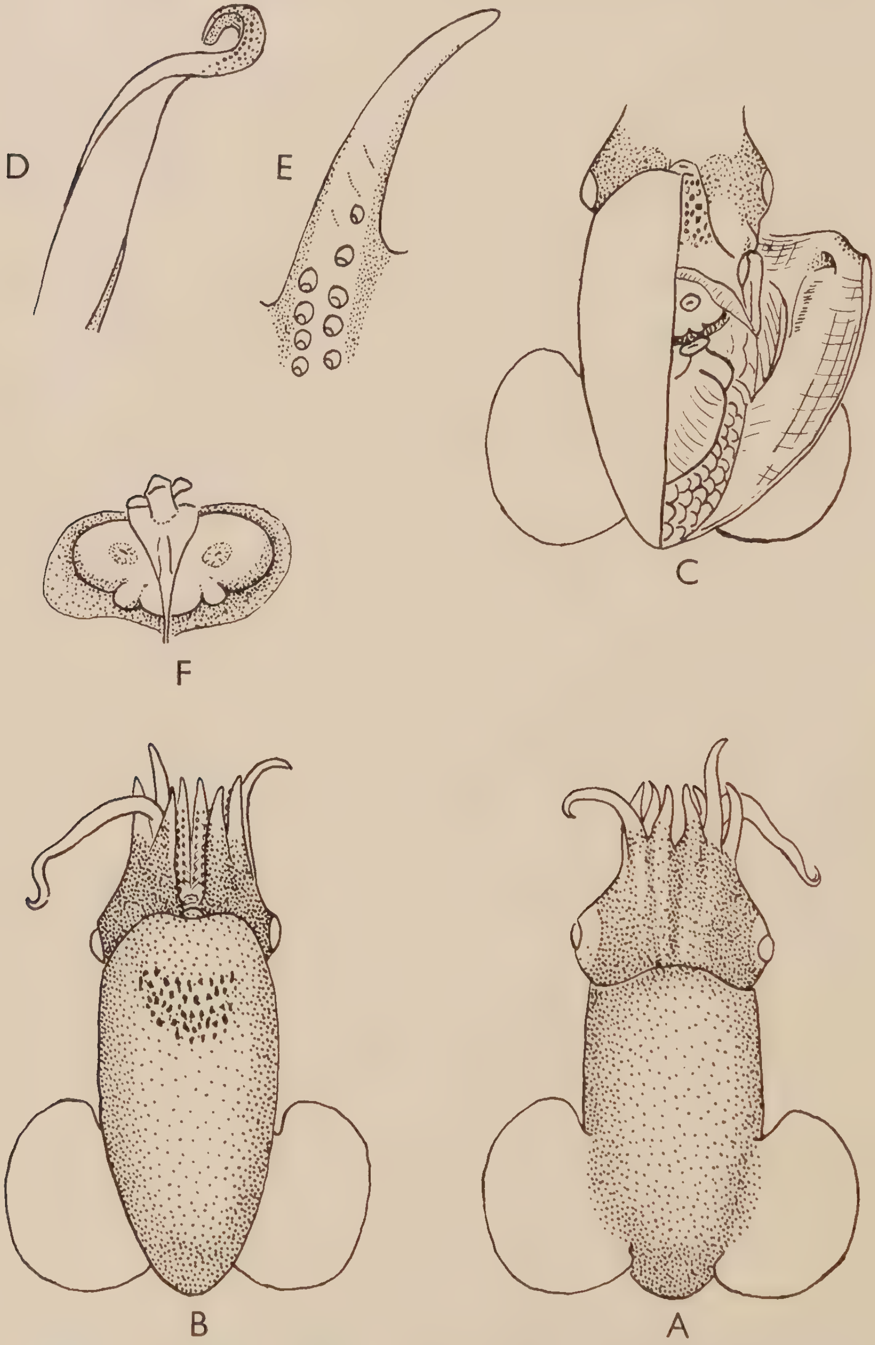

FIGURE 3. *Heteroteuthis atlantis* n. sp. A. Dorsal view, B. Ventral view, C. Ventral view, mantle cavity open, D. Left tentacle, E. Left dorso-lateral arm, F. Photogenic organ on ventral surface of ink sac.

stalks, round, and covered with minute pedunculate suckers crowded into numerous rows.

The funnel is short, stout, free for the distal 1/3 and covered with purple chromatophores over its entire length. The funnel organ is not distinguishable.

Internally a large, broad, five-lobed photogenic organ (Figure 3F) almost completely covers the ventral surface of the free ink sac. The lateral lobes each have a prominent pore situated in the middle of the lobe, appearing as a mammilar projection with a large central pit. A large nidamental gland (Figure 3C) occupies the majority of the mantle cavity and posteriorly covers the rather large eggs which have a diameter of 1.3 x 2.0 mm in diameter.

Measurements (in mm) of the holotype of *Heteroteuthis atlantis* n. sp.

		Arm length	
Mantle length, dorsal	27.0		
Mantle length, ventral	31.0	1st pair	9.1
Mantle width	15.0	2nd "	12.0
Head width	17.0	3rd "	9.0
Fin insertion	10.0	4th "	9.0
Fin length	16.0		
Fin width	31.0		

The color in alcohol was a deep purplish red dorsally, with smaller, more scattered chromatophores on the ventral surface. These become larger and more crowded in an oval area on the ventral surface near the anterior edge. The fins and the distal ¾ of all of the arms are devoid of color.

Remarks. The present species is distinct from all of the other known species; *H. dispar, H. sirventyi, H. weberi,* and *H. hawaiiensis,* by (1) the distal ends of the first and second pairs of arms alone being devoid of suckers, (2) the curious enlargement and flattening of the second pair of arms into blade-like structures, (3) the arm formula 2.1=3=4, and (4) the five-lobed photogenic organ of the ink sac. It has a close affinity with *H. hawaiiensis* Berry but as is seen from the description, it is quite distinct from this species. Unfortunately a detailed examination of the last named species is impossible at this date. The type, USNM Cat. No. 214311, is no longer extant, and no other specimens are available. Hence any comparison between the species is impossible for the purpose of more clearly defining the subgenus. It is entirely possible that such an examination may reveal the advisability of raising it to generic rank.

Robson's (1924) description of *H. hawaiiensis* var. *dagamensis* shows that his subspecies is not similar to the present species. In his specimen all but the second arms have a keel, a character lacking in the present species. Although I am not certain that Robson's species does not represent a distinct species, it cannot be shown at the present time as certain features, such as the photogenic organ, are undescribed.[1]

Nectoteuthis pourtalesi Verrill, 1883

Nectoteuthis pourtalesi Verrill, 1883, p. 108.

Material. 1 male, ML 9.8 mm, Sta. 3466, 200 fms. off Matanzas, 14 foot Blake trawl, May 9, 1939. MCZ Cat. No. 154503.

1 male, ML 9.8 mm, Sta. 3427, 240 fms. off Caibarien, 35 foot otter trawl, May 1, 1939. MCZ Cat. No. 155012.

1 gravid female, ML 9.2 mm, Sta. 3467, 215 fms. off Bahia de Matanzas, 14 foot Blake trawl, May 9, 1939. MCZ Cat. No. 155016.

1 juv., ML 5.5 mm, Sta. 3396, 180 fms. off Cayo Coco, 35 foot otter trawl, April 28, 1939. MCZ Cat. No. 155018.

1 female, ML 8.0 mm, Sta. 3401, 230 fms. off Cayo Coco, 35 foot otter trawl, April 28, 1939.

This small and beautiful species of myopsid squid has been well described and illustrated by Verrill (1883) from the BLAKE cruises and little can be added here. A minute examination of the males and females disclosed no apparent trace of hectocotylization. The spermatophores of the specimens from Sta. 3466 were examined, but the details of the structure were obscure. The spermatophores are very large; in the specimen of 9.8 mm the spermatophore was about 9.0 mm in length and rather stout.

Verrill's single specimen was captured from 180 fms. off Barbados The conjecture that the curious pedicels of the suckers and the union of the dorsal arms by a web are male characteristics is disproved and they are instead shared by both sexes.

Family LOLIGINIDAE d'Orbigny

Lolliguncula brevis (Blainville, 1823)

Loligo brevis Blainville, 1823. p. 133.

Loligo brevipinna Lesueur, 1824. p. 282.

Loligo hemiptera Howell, 1868. p. 239.

Material. 2 juv., Sta. 3421, 235 fms. off Cayo Frances, April 30, 1939.

2 juv., Sta. 3418, 195 fms. off Cayo Frances, April 30, 1939.

---

[1] Since this paper was written another specimen of *H. atlantis* has come to hand. This specimen was taken from the Mediterranean in the Straits of Messina. It corresponds exactly to the description of the holotype in all characters described for the species. Thus the distribution of this species well overlaps that of the well known *H. dispar*.

1 juv., Sta. 3428, 240 fms. off Cayo Fragoso, May 1, 1939.
8 juv., Sta. 3416, 200 fms. off Cayo Frances, April 30, 1939.
5 juv., Sta. 3417, 200 fms. off Cayo Frances, April 30, 1939.
8 juv., Sta. 3423, 245 fms. off Cayo Fragoso, April 30, 1939.
8 juv., Sta. 3422, 235 fms. off Cayo Fragoso, April 30, 1939.
1 juv., Sta. 3414 fms. off Cayo Frances, April 29, 1939.

It is interesting to note that of the 35 specimens contained in the collections, none of them were adult or even half grown. This species is more or less confined to coastal areas, bays and lagoons of average salinity and it is seldom recorded in the literature from offshore waters.

The presence of these young specimens from depths of from 195 to 235 fathoms is difficult to explain as the adults are surface or shallow water dwellers. It can only be conjectured that the adults retire to deep water to spawn and that the young continue to dwell in moderate depths until nearing maturity when they seek the shallow coastal waters. As can be seen by referring to the station lists, all of the specimens were collected within a rather small area and in a short interval of time. This is one of the commonest Western Atlantic species and ranges from Rio de Janeiro, Brazil to Chesapeake Bay and Bermuda.

Sepioteuthis sepioidea (Blainville, 1823)

Loligo sepioidea Blainville, 1823, p. 133.
Sepioteuthis biangulata Rang, 1837, p.73.
" *sepioidea,* d'Orbigny, 1839, p. 34.
" *sloani* Leach, 1849, p. 81.
" *ovata* Gabb, 1868, p. 193.
" *ehrhardti* Pfeffer, 1884, p. 63.
" *occidentalis* Robson, 1926, p. 352.

Material. 1 female,1 male, in alcohol, taken with a dip net and light at surface, Bahia Cochina, February 23, 1938.

These are both adults of large size and are the only specimens of this species taken by the expedition. It is a coastal species ranging from the West Indies northward to Cape Canaveral on the Florida coast and the Bermudas, but it is absent from the Gulf of Mexico. This species is found most abundantly in inshore waters, and is a rather agile and rapid swimmer.

Both of the specimens were dissected and the stomach contents examined. They were found to have been feeding on a polychaete worm, *Nereis glandulata* Hoagland, which apparently was swarming at the time.

Doryteuthis plei (Blainville, 1823)

Loligo plei Blainville, 1823, p. 132.
Doryteuthis plei, Naef, 1912, p. 742.

Material. 11 juveniles taken at night on the surface with a dipnet at Bahia Cochina, April 3, 1939.

These are rather small specimens, the largest with a mantle length of 35.0 mm, and no attempt was made to determine their sex. This species was first described from the West Indies by Blainville in 1823. It was later listed by d'Orbigny (1835), but was not reported again in the literature until Adam (1937) redescribed it. Apparently this is the species which has been listed from the Gulf of Mexico by Verrill (1882) and others as *Loligo gahi,* which is a Pacific coast species from Chile and Peru. It is commonly known as the arrow squid and is very common in the area around Key West and Dry Tortugas. It is known from as far north as Sea Island, Georgia but its southern range is unknown. It is an extremely active and swift swimmer, but is taken in fair quantities in shrimp hauls in Florida waters.

Division OEGOPSIDA

Family Enoploteuthidae Pfeffer

Abralia veranyi (Rüppell, 1844)

Enoploteuthis veranyi Rüppell, 1844, p. 3.
Abralia veranyi, Hoyle, 1886, p. 38.

Material. 1 male, Sta. 3432, 250 fms. off Cayo Fragoso, May 1, 1939.

1 male, Sta. 2980, 250 fms. off Cayo Frances, Blake trawl, March 16, 1938.

2 females, gravid, at night on the surface in Corrientes Bay Anchorage, March 26, 1939.

The only previous record of this species from the Western Atlantic is by Adam (1941) from Cockburn Town, San Salvador. Naef (1923) has given an excellent description of this species from the Mediterranean, including synonymy, anatomy, and development. Adam (1952) has beautifully illustrated this species from the west coast of Africa. Pfeffer (1912) and others have used the absence of light organs in a narrow strip down the median-ventral surface of the mantle as a specific character, but of the four specimens collected by the ATLANTIS two only show signs of this stripe, one very distinctly, while the others have no indication whatever. It would seem that such a character would be affected by contraction of the skin due to preservation, but Naef (1923) suggests that it may be an individual variation.

In the four specimens at hand all have 4 hooks on the hand part of the tentacular club; the proximal minute, the second the largest, and then gradually decreasing distally. The light organs on the eyeball are 5 in number, the two end ones much larger, the posterior sometimes with a slight sinus in the dorsal edge. The three intermediate light organs are small and nearly equal in size.

Abralia redfieldi n. sp.

(Figures 4A-H)

Holotype. Gravid female, University of Miami Marine Laboratory Sta. SL23 B, at surface off Gun Cay, Bahamas, December 10, 1953. MCZ Cat. No. 203979.

Paratype. Gravid female, Sta. 3436, 255 fathoms off Caibarien, May 2, 1939. MCZ Cat. No. 203980.

Description. Among the *Abralia* collected by the ATLANTIS was a single female with a mantle length of 28.0 mm. Upon examination this specimen, which is in rather poor condition, proved to represent a second and hitherto unknown species of *Abralia* from the Atlantic Ocean. The specimen is extremely flaccid, the tentacular hooks are missing and the specimen is in generally poor condition. Fortunately, while this paper was in the process of being written, another specimen, a female of 29.0 mm mantle length, was obtained by the Marine Laboratory of the University of Miami from a haul off Gun Cay in the Bahamas. This specimen was in perfect condition and was therefore chosen as the holotype of the new species. The following description is based primarily upon this specimen but supplemented by the original specimen when necessary.

This is a small species of squid, compact, and rather stout with a mantle width of 41.5-46.5 per cent of the mantle length (Figures 4A, B). The anterior mantle margin is slightly produced in the median-dorsal line. Ventrally the anterior margin is emarginated beneath the funnel with small sharp projections on either side. Posteriorly the body is bluntly pointed but the union of the two fins at the posterior end gives it the appearance of a long, somewhat pointed extremity. The fins are large occupying 47.2-55.2 per cent of the mantle length and very wide, 93.0-89.4 per cent of the mantle length, typically *Abralia*-like in contour.

The head is large, broad, 39.6-39.3 per cent of the mantle length, with prominent eyes. The arms are long, 51.8-60.5 per cent of the mantle length, stout, tapering to slender tips. The bases of the arms

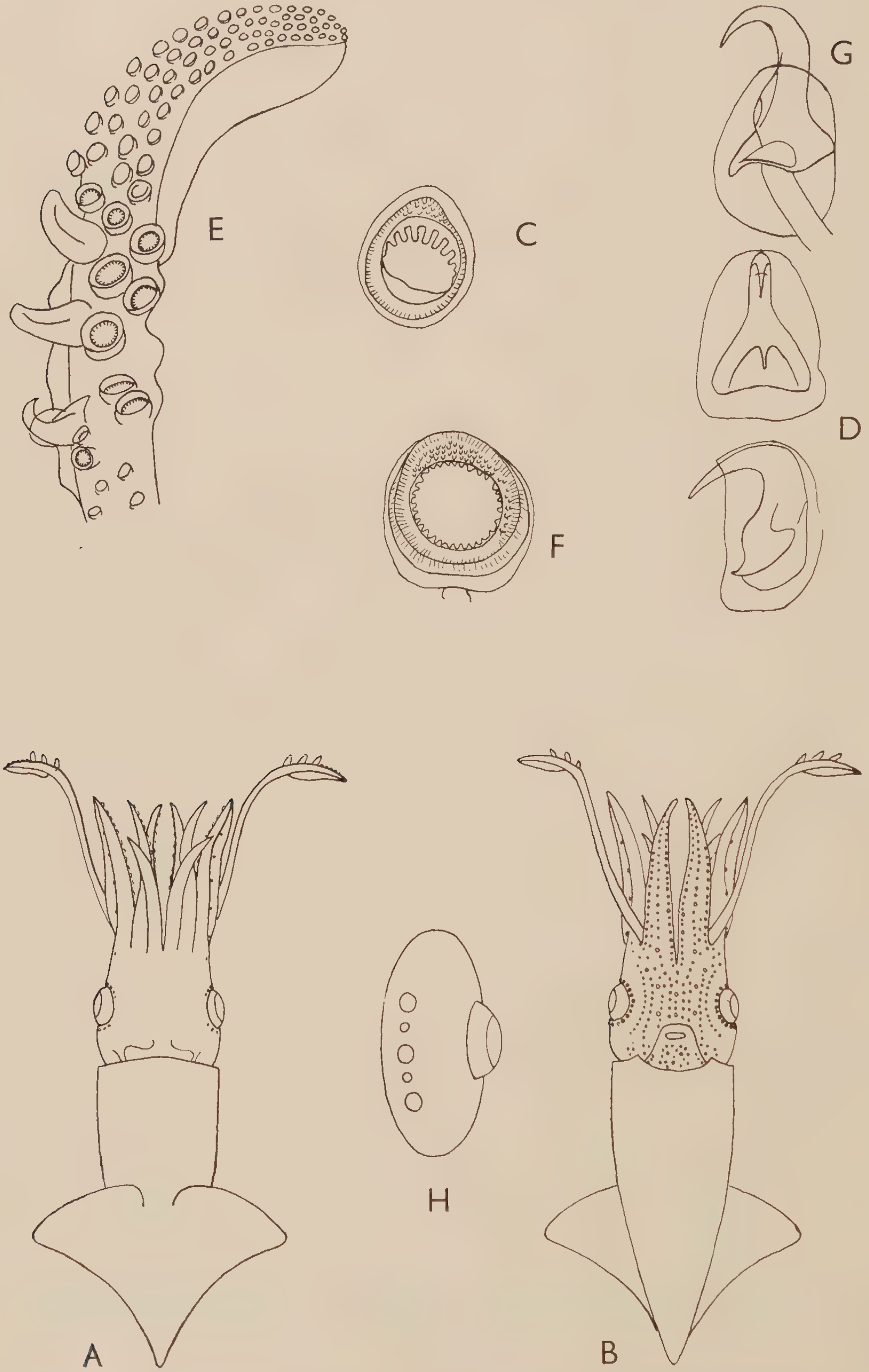

FIGURE 4. *Abralia redfieldi* n. sp. A. Dorsal view, B. Ventral view, C. Sucker of distal portion of left disto-lateral arm, D. Lateral and facing view of hook from left disto-lateral arm, E. Left tentacular club, F. Large marginal sucker from left tentacular club, G. Lateral view of tentacular hook, H. Eye, showing position of light organs.

are devoid of suckers or hooks, but soon become equipped with two rows of hooks which at the distal ends are replaced by suckers in two rows, whose horny rims bear about eight small square-tipped teeth in the distal margin (Figure 4C). The hooks (Figure 4D) are as follows on the arms: dorsal arms with 8 pairs of hooks, 2nd arms with 7 pairs of hooks, 3rd arms with 7 pairs of hooks, and ventral arms with 5 pairs of hooks. The third pair of arms are bordered by a broad swimming membrane.

Measurements (in mm) of two specimens of *Abralia redfieldi* n. sp.

	Holotype	Paratype
Mantle length	29.0	28.0
Mantle width	12.0	13.0
Head width	11.5	11.0
Fin width	27.0	25.0
Fin length	16.0	13.5
Arm length		
1st pair	13.5	15.0
2nd "	15.0	17.2
3rd "	15.0	17.1
4th "	14.0	17.2

The tentacles are of medium length, stout, with slightly expanded clubs equipped with both suckers and hooks (Figure 4E). The distal half of the club is bordered dorsally by a swimming membrane. The suckers and hooks are arranged in the following order: on the carpus is a cluster of 4 carpal cups and one or two pads; this is followed on the ventral margin by two small toothed suckers; there follows on the ventral margin three large hooks of nearly equal size, the middle one slightly larger than the other two (Figure 4G); the hooks are accompanied by three pairs of suckers (Figure 4F) on the dorsal side of the club; beyond these hooks and suckers are 4 rows of small toothed suckers which extend to the extremity of the club.

As in all the species of this genus the body, arms, head and eyes are liberally covered with light organs. As the distribution of these are of great taxonomic importance in this genus, the following account is given.

The mantle is sparsely supplied with light organs upon the sides and dorsal surface but ventrally they are crowded together so as to nearly cover the entire surface. In both the paratype and the holotype there is a clear strip down the median ventral line which is devoid of light organs. The light organs on the rest of the ventral surface are of two kinds: few but large somewhat clear organs with a darker periphery, and small and very numerous solid dark purple light organs. Both of these types extend over the ventral surface of the funnel.

Dorsally the head and arms are devoid of light organs. There is a ring of about 28 to 30 photophores around each eye, sparse dorsally and thickly crowded ventrally. The ventral surface of the head is covered with photophores of both types arranged in about 9-10 rows (Figure 4B). Of these, three rows extend onto the ventral surface of each of the ventral arms. The 3rd pair of arms has a single row of large, widely spaced light organs at the base of the swimming membrane, extending from the base of the arm to the tip.

On the eyeball, arranged in a line around the periphery of the bulbus, are five light organs (Figure 4H). These are of two sizes: the 1st, 3rd and 5th are about twice as large as the 2nd and 4th. All of them are round and of a similar appearance.

Remarks. The genus *Abralia* is primarily Indo-Pacific with 8 described species from that area. The sole representative, hitherto, in the Atlantic was *A. veranyi* which is known from the Mediterranean, Madeira, the West Coast of Africa, and the West Indies. The present species undoubtedly is closely related to this species but it differs from it in: (1) the shorter, heavier body, (2) somewhat shorter fins, (3) presence of only two rows of minute suckers on the tips of the sessile arms as contrasted with 4 in *A. veranyi,* (4) only 3 nearly equal hooks on the tentacular club, and (5) the size and arrangement of the light organs on the eyeball.

As the present specimens represent a new species of squid I have named it *Abralia redfieldi* for Dr. Alfred C. Redfield of the Woods Hole Oceanographic Institution through whose kindness I have been able to examine the present collections.

Pyroteuthis margaritifera aurantiaca Joubin, 1924.

Pyroteuthis margaritifera aurantiaca Joubin, 1924, p. 52.

Material. 1 gravid female, Sta. 2969, 1075-1145 fms. SE of Guantanamo Bay, Blake trawl, March 5, 1938, MCZ Cat. No. 203981.

A single specimen with a mantle length of 35 mm was taken at the above station. It is striking by the numerous and large reddish brown chromatophores crowded on the dorsal surface and the large scattered chromatophores on the bases of the fins. Ventrally the chromatophores are small, rather closely set, and not as noticeable as those on the dorsal surface.

The light organs are conspicuous within the mantle cavity and on the eyeball, but due to the fusion of the skin with the latter organ a definite count of the light organs was not obtainable. Joubin reported this species from the Azores, an area which shows a strong affinity with the Gulf of Mexico and the Caribbean in its fauna.

Family ONYCHOTEUTHIDAE Gray

Onychoteuthis banksi (Leach, 1817)

Loligo banksii Leach, 1817, p. 141.

Material. 1 male in alcohol, Sta. 3015, surface at night with light between Cat Cay and Miami, Florida, March 27, 1938. MCZ Cat. No. 203982.

A single specimen of this well known circumtropical squid was taken from the above station. This is an active and fast swimming species and is not generally taken in net hauls. Although commonly limited to warm waters it has been taken from as far north as Hammerfest, Norway and as far south as Cape Horn. The present specimen is a young male with a mantle length of 78.0 mm.

Family OMMASTREPHIDAE Gill

Illex illecebrosus (Lesueur, 1821)

Loligo illecebrosus Lesueur, 1821, p. 95
Ommastrephes illecebrosus, Verrill, 1872, p. 281
Illex illecebrosus, Steenstrup, 1880, p. 90?

Material. 1 female, Sta. 3432, 250 fms. off Caibarien, May 1, 1939.

2 females, Sta. 2984, 240-250 fms. off Caibarien, March 12, 1938.

1 female, Sta. 2981c, 195 fms. off Punta Alegre, March 10, 1938.

1 female, Sta. 3411, 260 fms. off Punta Alegre, April 29, 1939.

2 females, Sta. 3422, 235 fms. between Punta Alegre and Caibarien, April 30, 1939.

1 female, Sta. 2963, 190-180 fms. off Bahia de Cochinos, February 25, 1938.

1 female, Sta. 3421, 235 fms. between Punta Alegre and Caibarien, April 30, 1939.

1 female, Sta. 2999, 145-230 fms, off Matanzas, March 17, 1938.

2 females, Sta. 3423, 245 fms. off Caibarien, April 30, 1939.

1 female, Sta. 3387, 245 fms. off Cayo Romano, April 26, 1939.

1 male, Sta. 3414, 230 fms. between Punta Alegre and Caibarien, April 29, 1939.

This species is well represented in the collections by 14 specimens from 11 stations. This is a common squid of the Gulf of Mexico and Caribbean region. On the European side of the Atlantic it is represented by the subspecies *I. illecebrosus coindetti,* from which it differs in many respects (see Pfeffer, 1912, Adam, 1952). *I. illecebrosus illecebrosus* is found across the upper North Atlantic to the European coast. New England to Cape Hatteras, the Gulf of Mexico and Cuba.

Family CRANCHIIDAE Gray

Liocranchia reinhardti (Steenstrup, 1856)

Leachia reinhardti Steenstrup, 1856, p. 200.

Material. 1 specimen, in alcohol, Sta. 2999A, 145-230 fms. off Matanzas, March 17, 1938. MCZ Cat. No. 203983.

A single specimen with a mantle length of 66.0 mm is represented in the collections. This is probably an adult, although full grown specimens from Japanese and Philippine waters attain a much greater size. It is easily recognized by the dorsal row of tubercles in the midline and the inverted V-shaped row of tubercles on either side of the funnel at the point of fusion with the mantle.

This is apparently the first record of this species from the Western Atlantic. It is planktonic in habitat and cosmopolitan in distribution.

Cranchia scabra Leach, 1817.

Cranchia scabra Leach, 1817, p. 410.

Material. 1 specimen, in alcohol, Sta. 2972A, 1200 fms. Windward Passage off Oriente, May 6-7, 1938. MCZ Cat. No. 135081.

This specimen with a mantle length of 23.0 mm belongs to one of the common species of the Cranchiidae and is easily recognized by the subglobular form and heavily tuberculated skin. It attains a length of about two to three inches in mature individuals. This is the first record of this species from the Western Atlantic although the author has taken immature forms in the plankton hauls off Miami, Florida. In common with the other members of the family it is planktonic in habitat.

Verrilliteuthis hyperborea (Steenstrup, 1856)

Leachia hyperborea Steenstrup, 1856, p. 200
Desmoteuthis tenera Verrill, 1882, p. 412
Taonius hyperboreus, Hoyle, 1886, p. 191
Desmoteuthis hyperborea, Pfeffer, 1912, p. 708
Verrilliteuthis hyperborea, Berry, 1912, p. 643

Material. 1 specimen, in alcohol, Sta. 2959, 2050 fms. south of the Isle of Pines, 2 meter net, February 15-16, 1938. MCZ Cat. No. 203984.

1 specimen, in alcohol, Sta. 2999A, 145-230 fms. off Bahia de Matanzas, March 17, 1938. MCZ Cat. No. 203985.

Two specimens, which I have referred to this species, were obtained in very poor condition. This species is confused in the literature under several different names and has been recorded by Johnson (1934) under the name *Taonius tenera* Verrill and under its present name from Greenland to Massachussetts. It seems to be rather widely distributed in the North Atlantic, and is strictly planktonic.

Suborder *OCTOPODA*

Family Stauroteuthidae Robson

Grimpoteuthis umbellata (Fischer, 1883)

(Figure 2D)

Cirroteuthis umbellata Fischer, 1883, p. 404.

Material. 1 gravid female, Sta. 2967B, 1330-1650 fms. off Guantanamo, 14 foot Blake trawl, March 4, 1938. MCZ Cat. No. 203986.

This specimen is in fair condition, but the outer integument is missing and much of the web. It is tentatively placed in this species, but it presents some characters which cannot be settled without comparison with other specimens. The total length is about 250.0 mm with a dorsal mantle length of 46.0 mm. The mantle width is about 72.0 per cent of the mantle length, while the interocular width equals the mantle length. The eyes are large and prominent, about 38.0 per cent of the mantle length. The arms are 74.0 per cent of the total length and in the order 1.2.3.4. The suckers are 4.0 per cent of the mantle length, uniserial, and bordered on either side by cirri which are about 2½ times the diameter of the suckers, and extend to the distal extremity of the arms. The web is so damaged that no observations are possible.

The fins are long and slender, the length of the individual fin being 47.0 mm while the breadth across both fins is 129.0 mm. They are slender, rounded at the extremities, the width about 1/4 the length of the fin. The dorsal cartilage is horse shoe-shaped, the ends lying parallel, the posterior curve forming part of the arc of a circle (Figure 2D). The funnel is slender, compact, and projects through a narrow mantle opening.

The present specimen is a gravid female and contained 6 large eggs about 12.5 X 7.0 mm. The surface is sculptured by a series of rough irregular longitudinal ridges. Of the six large eggs one was lodged in the oviduct just below the large oviducal gland. A dozen small eggs about 1/4 the size of the others were situated on the dorsal surface of the ovary.

As can be seen this specimen shows a close affinity with *G. umbel-*

lata and also with *G. megaptera* (Verrill) due to the size of the fins. It differs from the latter, however, in the much larger eyes which seem to exclude it from that species. Joubin has described a specimen of *G. umbellata* from the Sigsbee Deep which, however, is not adequate for comparison with the present specimen. This species seems to be well distributed in the Eastern Atlantic although this is only the second record from the Western Atlantic.

?*Grimpoteuthis meangensis* (Hoyle, 1885)

(Figure 2C)

Cirroteuthis meangensis Hoyle, 1885, p. 234.

Material. 2 specimens, Sta. 3305, 330 fms. off Playa Baracoa, 14 foot Blake trawl, March 23, 1939. MCZ Cat. No. 203987.

The two specimens recorded above are doubtfully placed in this species on the basis of the record of this species from the Mediterranean by Lo Bianco and the illustrated shell vestige by Robson (1931). The arms and web are the sole remains and these are in such a bad state of preservation that little can be told from them. The suckers are small and bordered by small, conical short cirri which are continued to the arm extremities or nearly so. The shell vestige is shown in Figure 2C. It is unfortunate that both specimens are nearly completely destroyed and no detailed description can be given.

Family OPISTHOTEUTHIDAE Verrill

Opisthoteuthis agassizi Verrill, 1883.

Opisthoteuthis agassizi Verrill, 1883, p. 113.

Material. 1 specimen, Sta. 3370, 450 fms. off Puerto Tanamo, April 20, 1939. MCZ Cat. No. 203988.

The single specimen referred to this species was in a dried condition and returned to alcohol. Although most of the body characteristics have been destroyed the mantle length appears to be about 12.0 mm. The oral face of the web and arms is in fair condition and from the position and arrangement of the suckers it is placed without hesitation in the above species. It is known previously from the West Indies (Verrill) and off the southwestern coast of Ireland (Chun, from MICHAEL SARS material).

Family BOLITAENIDAE Chun

Eledonella pygmaea Verrill, 1884

Eledonella pygmaea Verrill, 1884, p. 145
Japetella prismatica Hoyle, 1885, p. 231
Eledonella massyae Robson, 1924, p. 202

Eledonella ijimai Sasaki, 1929, p. 13
Eledonella massyae purpurea Robson, 1930, p. 379
Material. 1 female, Sta. 2972A, 3510 m. off Baracoa, March 7, 1938. MCZ Cat. No. 203989.

This delicate, gelatinuous, bathypelagic species has recently been monographed by Sven Thore (1949) and little can be added here of value.

The present specimen is small and is in very poor condition so that a critical examination is not possible. Two other specimens, definitely assignable to this species, were captured in the central Bahamas on the voyage down. They agree in all ways with Thore's data. They have a nearly worldwide distribution, being found in all seas but the Arctic, in very deep water.

Family OCTOPODIDAE d'Orbigny

Genus *Tetracheledone* n. gen.

With the characters of the species.

Type species: *Tetracheledone spinicirrus* n. sp.

Tetracheledone spinicirrus n. sp.

(Figures 5A-H)

Holotype. Male, in alcohol, Sta. 2999A, 145-190 fms. off Matanzas, 10 foot Blake trawl, March 17, 1938. MCZ Cat. No. 203990.

Paratypes. Female, in alcohol, Sta. 3439, 295 fms. off Caibarien, 60 foot otter trawl, May 2, 1939. MCZ Cat. No. 203991.

Male, in alcohol, M/V Antillas, 105 fms. ESE of Jacksonville Beach, Florida, May 1, 1952. To be deposited in the U. S. National Museum.

Male, in alcohol, Sta. 2999A, 145-190 fms. off Matanzas, 10 foot Blake trawl, March 17, 1938. Museo Poey, Havana, Cuba.

Additional material. Fragmented female, Sta. 3432, 250 fms. off Bahia de Cochinos, 35 foot otter trawl, May 1, 1939.

Male, partly torn, M/V OREGON, Sta. 489, Gulf of Mexico.

This new and interesting tropical eledonid is a small species from moderate depths (Figure 5A). The body is globular and nearly as wide as the mantle length. The head is 63.0 to 75.0 per cent of the mantle length with rather small eyes. The arms are nearly subequal, in the order 3=2.1.4 in the holotype, and 59.0 to 66.0 per cent of the total length with a rather deep web which is 43.0 to 45.0 per cent of the arm length in the adult, the sectors C or B being the deepest but the others subequal. The suckers are uniserial, small and deeply set with an index of 5.3 to 9.0 per cent of the mantle length. The surface of the mantle, head, web and arms is closely set with large, stellate papillae which give this species a characteristically spinous appearance. In the small female a skinfold surrounds the mantle, similar in appearance to that of *Scaeurgus unicirrhus*. In the holotype this fold consists only of a raised line of stellate tubercles running around the mantle from the corner of the funnel opening. Additional specimens show this ridge distinctly. Over each eye there are two large cirri which are armed with spinous protuberances arranged in circles about the cirrus. In some specimens these cirri are retracted into pit-like depressions at their bases.

Measurements (in mm) of 3 specimens of *Tetracheledone spinicirrus* n. sp.

	Holotype		Paratype		Paratype	
Sex	Male		Female		Male	
Mantle length	37.0		15.0		42.0	
Mantle width	30.0		14.0		41.5	
Head width	25.5		10.5		26.5	
Sucker diameter	2.2		.8		3.8	
Arm width	4.8		1.8		4.5	
Length hect. arm	46.0		——		62.0	
Ligula length	2.0		——		4.5	
Calamus length	0.5		——		1.5	
Length penis and diverticulum	4.0		——		7.0	
Arm length	R	L	R	L	R	L
1st pair	53.0	51.0	20.5	23.0	77.0	72.0
2nd "	54.0	54.0	22.0	20.0	81.0	79.0
3rd "	46.0	54.0	20.0	25.0	62.0	71.0
4th "	51.5	52.0	——	21.5	64.0	71.0
Web depth						
Sector A	17.5		7.0		27.0	
" B	22.5		7.0		35.0	
" C	23.5		7.0		33.0	
" D	20.0		6.2		29.0	
" E	19.5		——		25.0	

The funnel is short and stout. The funnel organ is very distinctive (Figure 5B), consisting of four small stoutly oval, widely separated pads showing not the slightest trace of union with one another. They seem to correspond to the pads found in the genus *Teretoctopus*, but are not similar to those found in *Thaumeledone brevis* which are thin strips.

The internal anatomy was partially dissected out of the OREGON specimen. The radula consists of a simple, unicuspid rhachidian, small admedians, second laterals with a single stout tooth, saber like third

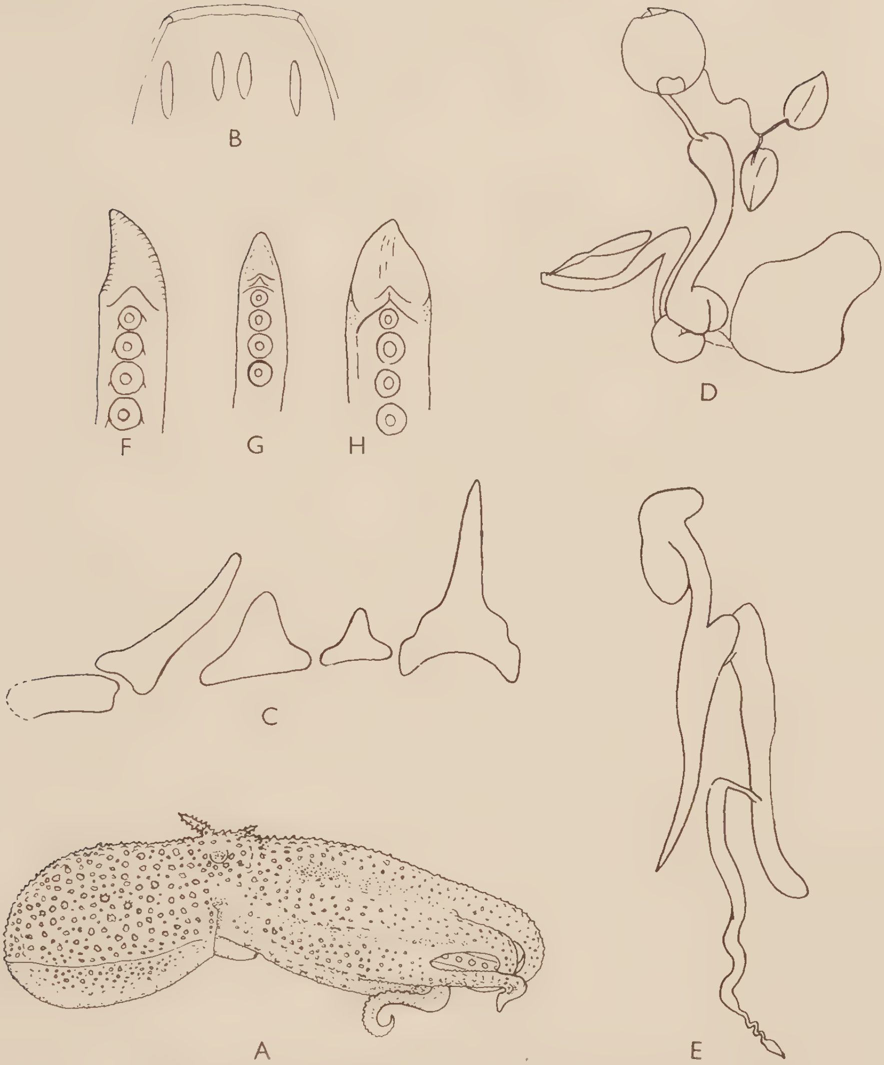

Figure 5. *Tetracheledone spinicirrus* n. sp. A. Lateral view, B. Funnel organ, C. Radula, D. Digestive tract, E. Male genitalia, F. Ligula of Gulf of Mexico specimen, G. Ligula of holotype, H. Ligula of paratype from Jacksonville, Florida.

laterals and flat, plate-like marginals (Figure 5C). The gills are rather large, with 7 to 9 filaments per demibranch and are 22.0 to 32.0 per cent of the mantle length. The inner and outer demibranchs seem similar.

The alimentary tract consists of closely adhering anterior salivary glands bright orange in color, rather large posterior glands attached to the buccal mass by long ducts, a stout esophagus and rather prominent crop. The stomach is externally divided into two parts, a heavy muscular proximal section and a thin walled distal section. There is a stout spiral caecum and large liver. There is a tendency towards a second stomach. An ink sac is present which is not involved in the liver except superficially.

The male genital organs were dissected out and are figured in Figure 5E. The penis is short and thick, and has a large diverticulum. There were no spermatophores present in any of the specimens. Externally the hectocotylized arm bears a small, spade-like ligula which is 4.3 to 7.2 per cent of the hectocotylized arm (Figures 5F-H). There are no transverse ridges apparent. The calamus is about 25.0 to 33.4 per cent of the ligula, consisting of a simple fold which is continuous with the spermatophoral groove.

Remarks. While I naturally hesitate to form a new genus to contain this single species there is none known in which it can properly be placed. The uniserial suckers, stellate warts, well developed ink sac, and peculiar four pads of the funnel organ preclude placing this species in any of the other eledonid genera. As known at present it is a tropical species occurring from north Florida on the Atlantic coast to both the north and south coasts of Cuba and the Gulf of Mexico.

In consideration of the above noted peculiarities I have given this species the generic name *Tetracheledone (tetracha,* in four parts, and *eledone,* a kind of octopus) in order to show its relationship to the eledonids and the peculiar four pads of the funnel organ, and the trivial name *spinicirrus* from the spiny appearance of the ocular cirri.

Octopus sp.

Material. 1 male, Sta. 2999A, 145-190 fms. off Matanzas, March 17, 1938.

A single male in rather poor condition was taken at the above station and for want of more material cannot be identified at this time. The body is saccular, somewhat soft and gelatinous, with a mantle length of 29.0 mm. The surface is mostly smooth, but bears a cluster of large papillae over each eye and about two cirri. The arms are long and there are indications of the presence of a deep web, especially between the dorsal arms. The third right arm is hectocotylized, and there is a very small ligula without a calamus. There are about 7 filament on the outer demibranch of the gill. The penis is long and slender with a small coiled diverticulum. The large ink sac is deeply involved in the liver.

Although this specimen is unlike any known species from this area it does not seem wise, considering the state of the specimen and no other material at hand, to describe it at this time.

Scaeurgus unicirrhus (d'Orbigny, 1840)

Octopus unicirrhus Orbigny, 1840, p. 70
Scaeurgus unicirrhus, Tiberi, 1880, p. 12
Scaeurgus patagiatus Berry, 1913, p. 564

Material. 1 female, Sta. 2999, 145-230 fms. off Matanzas, March 17, 1938. MCZ Cat. No. 203992.

This small specimen with a dorsal mantle length of 19.0 mm is the only specimen taken by the cruises. It has been reported by Voss (1951) from the Florida coast and a single specimen was taken by the Cuban hydrographic vessel YARA in the middle of the Florida Straits between Havana and Key West. It is a benthic species from moderate depths and is distributed from the Mediterranean Sea to the Azores, tropical Western Atlantic, the Pacific and Indian Oceans. The skin fold around the sides of the mantle, the rough surface, and the male hectocotylus on the third left arm serve to identify this species.

Pteroctopus tetracirrhus (Delle Chiaje, 1830)

Octopus tetracirrhus Delle Chiaje, 1830, p. 72.
Scaeurgus titanotus Troschel, 1857, p. 51.
Scaeurgus tetracirrhus, Tiberi, 1880, p. 12.
Pteroctopus tetracirrhus, Fischer, 1882, p. 334.

Material. 1 female, Sta. 3435, 255 fms. off Caibarien, 60 foot otter trawl, May 2, 1939. MCZ Cat. No. 203993.

2 females, Sta. 3439, 295 fms. off Caibarien, 60 foot otter trawl, May 2, 1939.

1 female, Sta. 3431, 245 fms. off Caibarien, 35 foot otter trawl, May 1, 1939.

2 females, Sta. 2982C, 195-225 fms. off Punta Alegre, 35 foot otter trawl, March 11, 1938.

1 female, Sta. 2995, 370-605 fms. off Bahia de Cardenas, 35 foot otter trawl, March 16, 1938.

1 female, Sta. 2982, 210 fms. off Punta Alegre, 35 foot otter trawl, March 11, 1938.

This species has previously been recorded by Voss (1954) from the Western Atlantic from specimens collected on the Florida coast. Previous to the Florida record it has been known from the Mediterranean, Cape Verde Islands, and recently from Africa by Adam (1952). It is easily recognized by the two large cirri over each eye and the hectocotylus of the male being on the third left arm as in *Scaeurgus*. The consistency is somewhat soft and gelatinous and the surface is covered with purplish red chromatophores.

Family Argonautidae Cantraine

Argonauta hians Solander, 1786.

Argonauta hians Solander, 1786, p. 44.

Material. 1 female, North Atlantic (information contained upon printed Harvard-Havana Exped. label) MCZ Cat. No. 203994.

The single specimen bearing the above label was taken by the ATLANTIS complete with shell. It is unfortunate that no other data are available as the label raises some doubts that the specimen came from Cuba. However, this species is widely distributed in the West Indies and there seems to be no valid reason for not including it in the present paper. The animal is badly distorted by the preservative so that measurements are unobtainable. The shell has a greatest diameter of 31.0 mm and a width of 25.0 mm across the ears.

Although this is a rather rare shell upon the beaches in the West Indies, the examination of a number of stomachs of the fish, *Coryphaena hippurus,* has revealed that they occur in considerable numbers in the open ocean. The species is world wide in distribution in tropical and subtropical waters.

LITERATURE CITED

ADAM, W.
1941. Cephalopoda. Res. Sci. Cros. Navire-ecole "Mercator" *3*. Mem. Mus. Hist. nat. Belg., serie 2, fasc. 21: 83-162.
1952. Cephalopodes. Exped. oceanogr. Belg. dans les Eaux Cotieres Africaines de l'Atlantique Sud (1948-1949) *3* (3): 1-142.
ALLAN, JOYCE
1945. Planktonic cephalopod larvae from the eastern Australian coast. Rec. Aust. Mus. *21* (6): 317-350.
ARANGO Y MOLINA, RAFAEL
1878. Contribucion a la fauna malacologica Cubana. Habana, 1878.
BERRY, S. S.
1909. Diagnoses of new cephalopods from the Hawaiian Islands. Proc. U. S. nat. Mus. *37* (1713): 407-419.
1912. Some necessary changes in cephalopod nomenclature. Science *36*: 643-646.
1913. Some new Hawaiian cephalopods. Proc. U. S. nat. Mus. *45* (1996): 563-566.
1918. Report on the cephalopods obtained by the F. I. S. "Endeavour" in

the Great Australian Bight and other southern Australian localities. Zool. Res. Fish. Exp. "Endeavour." *4*. Sidney.

1934. Cephalopoda. *In* List of marine mollusca of the Atlantic coast from Labrador to Texas, by C. W. Johnson, Proc. Boston Soc. nat. Hist. *40* (1): 160-165.

BLAINVILLE, H. D. DE

1823. Memoire sur les especes du genre Calmar (Loligo, Lamarck). J. Phys. *96*: 116-133.

CHUN, CARL

1913 Cephalopoda. Rep. Sars N. Atl. Deep Sea Exped. *3* (1). Bergen.

1914. Die Cephalopoden. II. Teil: Myopsida, Octopoda. Wiss. Ergebn. "Valdivia." *18* (2): 405-552.

DELLE CHIAJE, S.

1830. Memorie . . . animali senza vertebre del Regno di Napoli *4*. Naples.

FISCHER, H.

1882. Manuel de Conchyliologie. Paris.

FISCHER, P.

1883. Note preliminaire sur une nouvelle espece du genre *Cirroteuthis*. J. Conchyliol: *31*: 402.

GABB, W. M.

1868. J. Conch. *4*: 193-194.

GRAY, J. E.

1849. Catalogue of the mollusca in the collections of the British Museum. I. Cephalopoda antepedia, London.

HOYLE, W. E.

1885. Diagnoses of new species of cephalopoda. Ann. Mag. nat. Hist. (5) *15*: 222.

1885. On *Loligopsis* and some other genera. Proc. roy. Soc. Edinb. *8*: 313-333.

1886. Report on the cephalopoda collected by the HMS Challenger during the years 1873-76. 246 pp. 33 pls. Edinburgh.

1904. A diagnostic key to the genera of present dibranchiate cephalopoda. Mem. Manchr. lit. phil. Soc. *48* (23).

HOWELL, S. B.

1868. Description of two new species of cephalopods. Amer. J. Conch. *3*: 239.

JOUBIN, L.

1900. Cephalopodes provenant des campagnes de la Princesse- Alice (1891-1897). Result. Camp. sci. Monaco *17*: 135 pp.

1924. Contribution a l'Etude des Cephalopodes de l'Atlantique nord. Result. Camp. sci. Monaco *76*: 113 pp.

LEACH, W. E.

1817. Synopsis of the order, families and genera of the Class Cephalopoda. Zool. Miscell. *3*: 137-141.

1841. MS *in* Gray (see above).

LESUEUR, C. A.

1821. Descriptions of several new species of cuttlefish. J. Acad. nat. Sci. Philad. *2*: 86-101.

1824. Description of a new species of the genus Loligo (L. brevipinna). J. Acad. nat Sci. Philad. *3:* 282-284.

NAEF, A.

1912. Die Gattungen der Loliginidae. Zool. Anz. *39* (7): 741-745.

1923. Die Cephalopoden. Fauna u. Flora Neapel, Monogr. 35.

ORBIGNY, A. D' ET FERUSSAC
1839-40. Histoire naturelle generale et particulaire des cephalopodes acetabuliferes, vivantes et fossile. Paris.

ORBIGNY, A. D'
1841. Mollusques, *in* Histoire physique, politique et naturelle de l'Isle de Cuba, by Ramon de la Sagra. Paris. Spanish edition and atlas, 1845.

PFEFFER, GEORG
1884. Die Cephalopoden des Hamburger Naturhistorischen Museums. Abh. Naturw. Hamburg. *7* (1): 3.
1912. Die Cephalopoden der Planktonexpedition. Ergebn. Planktonexped. *2*.

PICKFORD, GRACE E.
1945. Le poulpe americain: a study of the littoral octopoda of the western Atlantic. Trans. Conn. Acad. Arts Sci. *36* (3): 701-811.

RANG, M. S.
1837. Documents pour servir a l'historie naturelle des cephalopodes cryptobranches. Mag. de Zool. *7*.

ROBSON, G. C.
1920. Cephalopoda: Octopoda. "Discovery" Rep. *2:* 371.
1924a. On new species, etc. of octopoda from South Africa. Ann. Mag. nat. Hist. (9), *13*: 202.
1924b. On the cephalopoda obtained in South African waters by Dr. J. D. F. Gilchrist in 1920-21. Proc. zool. Soc. Lond. 1924: 589-686.
1926. On a new species of *Sepioteuthis* from Tobago. Ann. Mag. nat. Hist. *18* (series 9): 352-356.
1929. A monograph of the recent cephalopoda. Part I. Octopodinae. British Museum, London.
1932. A monograph of the recent cephalopoda. Part II. The Octopoda (excluding the Octopodinae). British Museum, London.

RÜPPELL, E.
1844. Intorno ad alcuni Cefalopodi del Mare di Messina. Messina.

SASAKI, MADOKA
1929. A monograph of the dibranchiate cephalopods of the Japanese and adjacent waters. J. Coll. Agric. Sapporo. *20*. Suppl. Number. 357 pp.

SOLANDER, D.
1786. A catalogue of the Portland Museum.

STEENSTRUP, J.
1856. Hectocotyldannelsen hos Octopodslägterne Argonauta og Tremoctopus, oplyst ved Jagttagelse af ligmende Dannelsen hos Bläcksprutternes in Almindelighed. Dansk. Vid. Selsk. Afh. *4* (5).
1880. Orientering i de Ommatostrephagtige bläcksprutters inbyrdes forhold. overs. danske Vidensk. Selsk. Forh. pp. 73-110.
1881. Sepiadarium og Idiosepius, to nye Slagter af Sepiernes Familie. K. danske Vidensk. Selsk. *1* (6): 242.

THORE, S.
1949. Investigations on the "Dana" octopods. Part I. Bolitaenidae, Amphitretidae, Vitreledonellidae, and Alloposidae. Dana Rep. No. 33.

TIBERI, N.
1880. Cefalopodi . . . viventi nel Mediterraneo. Boll. Soc. ital. Malaco. *6*.

TROSCHEL, H.
1857. Bemerkungen über die Cephalopoden von Messina. Arch. Naturgesch. 32, Band I.

VERRILL, A. E.
1872. Amer. J. Sci. *3:* 281.

1882. Report on the cephalopods of the northeastern coast of America. U. S. Comm. Fish & Fisheries, pt. 7, Rep. Comm. for 1879, pp. 211-450, Washington, D. C.

1883. Reports on the results of dredging . . . . steamer "Blake" XXIV-Supplementary report on the "Blake" cephalopods. Bull. Mus. comp. Zool. *11* (5): 105-116.

1884. Second catalogue of mollusca . . . . . of the New England coast. Trans. Conn. Acad. Arts Sci. *6* (1): 139.

Voss, G. L.

1950. Two new species of cephalopods from the Florida Keys. Rev. Soc. Malaco. *7* (2): 73-79.

1951. A first record of the cephalopod, *Scaeurgus unicirrhus,* from the Western Atlantic. Bull. Mar. Sci. Gulf & Carib. *1* (1): 64-71.

1954. Cephalopods of the Gulf of Mexico. *In* Gulf of Mexico, its Origin, Waters, and Marine Life. Edit. by Paul S. Galtsoff. Fish. Bull. 89: 475-478.

Contribution No. 751

B R E V I O R A

Museum of Comparative Zoology

Cambridge, Mass. April 7, 1955 Number 43

SPEED-INDUCED SKIN FOLDS IN THE BOTTLE-NOSED PORPOISE, *TURSIOPS TRUNCATUS*[1]

By Frank S. Essapian

Marineland Research Laboratory

While engaged in a study of the behavior of bottle-nosed porpoises, *Tursiops truncatus* (Montagu), at Marine Studios, Marineland, Florida, over a period of three to four years, the author has observed on hundreds of occasions a remarkable modification of the skin contour of these animals whenever they resorted to rapid movement about the tank (Essapian 1953, p. 399). The circular tank, where the porpoises are on exhibit, is seventy-five feet in diameter and about fourteen feet deep at the center. It houses an average of ten animals.

Generally lost to view due to swiftness of action, this transformation of the skin contour takes place when an animal accelerates its speed in excess of its normal rate, or, when swimming rapidly, comes to a sudden stop. It is then that transverse skin folds may stand out in relief on part of an animal, or may extend over its entire length, from head to tail. The pattern of these formations depends on the speed and sex of the swimming animal, but is not restricted to any age group. The folds may be seen even in an animal only a day or two old.

The skin folds generated by a sudden burst of speed are by far the more common of the two categories, and are usually occasioned when the animals engage in pursuit of one another, are frightened and trying to escape, or when racing for a food fish tossed into the tank. The duration of folds is then conditioned by the factors which motivate the animals' movements. In the case of a brief dash, for example, when an animal exerts itself to snatch a fish, the skin folds may last only a second, or even a fraction of a second (Pls. 1 and 2). However, in the case of prolonged rapid movement around the tank, the animals may intermittently exhibit skin folds for a period of one or two or more seconds. Often an animal at play or during the mating season may suddenly leap out of water, exhibiting folds at the peak of acceleration, just prior to its emergence from water, and again after it has reentered the water (Pls. 3 and 4). At this point it may be of interest to note that the fat adult females tend to exhibit fewer folds, but greater in size and at less regular intervals, than are produced in the adult male or in the younger slimmer animals when swimming at comparable speeds. The same female in Plate 4 is also shown in Plate 5; here this animal's folds are shown in a transitory stage, just prior to full acceleration.

---

[1] Contribution No. 751 from the Woods Hole Oceanographic Institution.

The skin folds of the second category occur at less frequent intervals and are of very brief duration. These take place when an animal swimming rapidly without exhibiting any folds comes to an abrupt halt. Then the folds may suddenly be displayed (Pl. 6). The duration of folds of this sort is indicated by the fact that this entire sequence occupies only twelve frames of 16 mm. film at 16 frames per second. This would indicate a total elapsed time of three quarters of a second for the formation and disappearance of folds. Plate 6 is the fourth frame, showing that these folds were fully formed in one quarter of a second.

One feature in the production of skin folds is of particular interest. In an animal maintaining a high and sustained rate of speed the folds are stationary and do not progress wave-fashion. At times, when extremely high speeds are achieved by adult animals, the skin folds tend to slope posteriorly. Observations also indicate that the folds are more likely to occur on ventral and lower lateral surfaces.

While the superficial layer of the porpoise's skin is extremely thin, the blubber is of considerable thickness and is tough and fibrous. In a *Tursiops truncatus* fifteen days old and weighing thirty pounds, the skin, including blubber, is approximately half an inch thick. In an adult it is nearly one and a half inches thick on the ventral surface. Although normally not apparent to the view or touch, the porpoise's skin is, nevertheless, pliant and loose on the body. This slackness of the skin in a live animal held out of water in a sling is shown in Plate 7.

Discussion

It is tempting to speculate upon the causes of this phenomenon. The answer may lie in the possibility that these folds are caused by the unequal pressure of water upon the body of the animal, in which case the production of folds would appear to be beyond the muscular control of the animal. Clarke and Ruud (1954, p. 144), in discussing different types of marks used in whale marking, say: ". . . whenever a whale is moving naturally the envelope of blubber is always sliding, more or less, over the contracting and relaxing muscle beneath, so that a mark with stoppers which is set partly in blubber and partly in muscle would almost certainly be worked out." The Marineland porpoises while swimming normally do not display such looseness of skin as is here ascribed to the great baleen whales. However, this similarity in the flexibility of skin in such divergent species suggests that all animals of the order Cetacea may share this characteristic.

These speed-induced folds are to be distinguished from those caused simply by flexure, such as the ones shown in Plates 8 and 9.

Racovitza (1903, pp. 43-44, pl. 3, fig. 17) mentions a group of four *Hyperoodon* (bottle-nosed whales) of which one individual is sketched emerging from water and exhibiting an exaggerated likeness of skin folds on its trunk. Unfortunately the author has failed to explain whether this particular animal was swimming rapidly at the time or whether this deformity in the skin contour was apparent even when the animal had raised itself partly out of water. The author furnished no further explanation beyond expressing his astonishment and a conviction that the animal didn't appear to be sick or emaciated and that the projections on its trunk appeared to be composed of soft material. This animal didn't differ from the three other individuals in any other respect.

At sea, in conditions of greater freedom of movement, the porpoises may exhibit skin folds for more protracted periods than is feasible in the confines of a tank. In any case, these folds should be of interest to hydrodynamicists.

The author wishes to express his deep gratitude to Mr. William E. Schevill for his encouragement, as well as for his helpful suggestions and criticisms of the manuscript. The author is also thankful for the use of a motion picture camera and film which was made available by Mr. Schevill under a contract between the Office of Naval Research and the Woods Hole Oceanographic Institution.

REFERENCES

Clarke, Robert and Johan T. Ruud
1954. International cooperation in whale marking: The voyage of the "Enern" to the Antarctic 1953. Norsk Hvalfangst-Tidende, **43**(3): 128-146.

Essapian, Frank S.
1953. The birth and growth of a porpoise. Natural History (New York), **62**(9): 392-399, ills.

Racovitza, E. G.
1903. Cétacés. Résultats du voyage du S. Y. Belgica. 1897-1899. Rapports Scientifiques, Zoologie. 142 pp., 15 text figs., 4 pls.

All photographs by courtesy of Marine Studios; the porpoises shown are all *Tursiops truncatus* on exhibition at Marineland, Florida. Plate 7 is from a photograph by Bob Neelands; all the others are by the author.

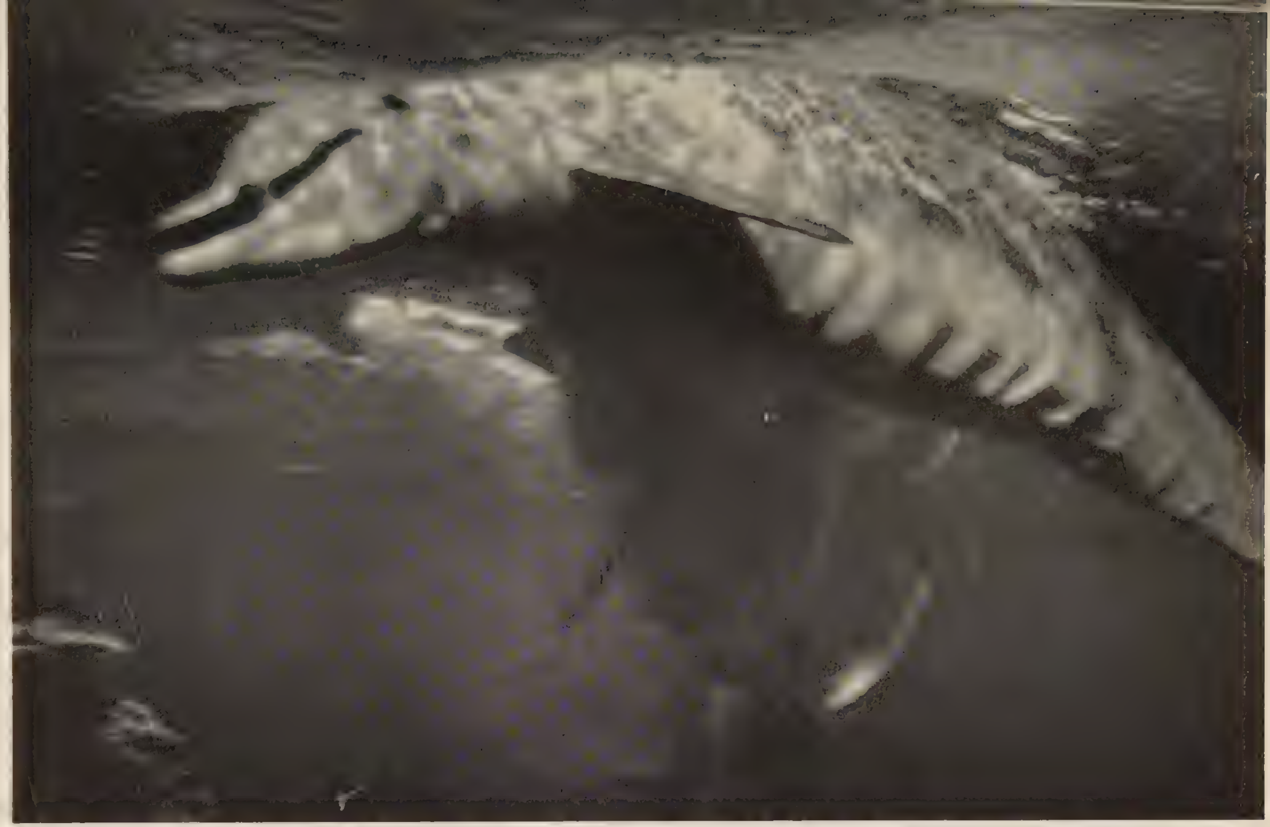

Pl. 1. A female, approximately eighteen months old, displays folds at the peak of acceleration. The fish she has just seized is seen in her mouth.
Photographed at F/3.5 at 1/500 of a second.

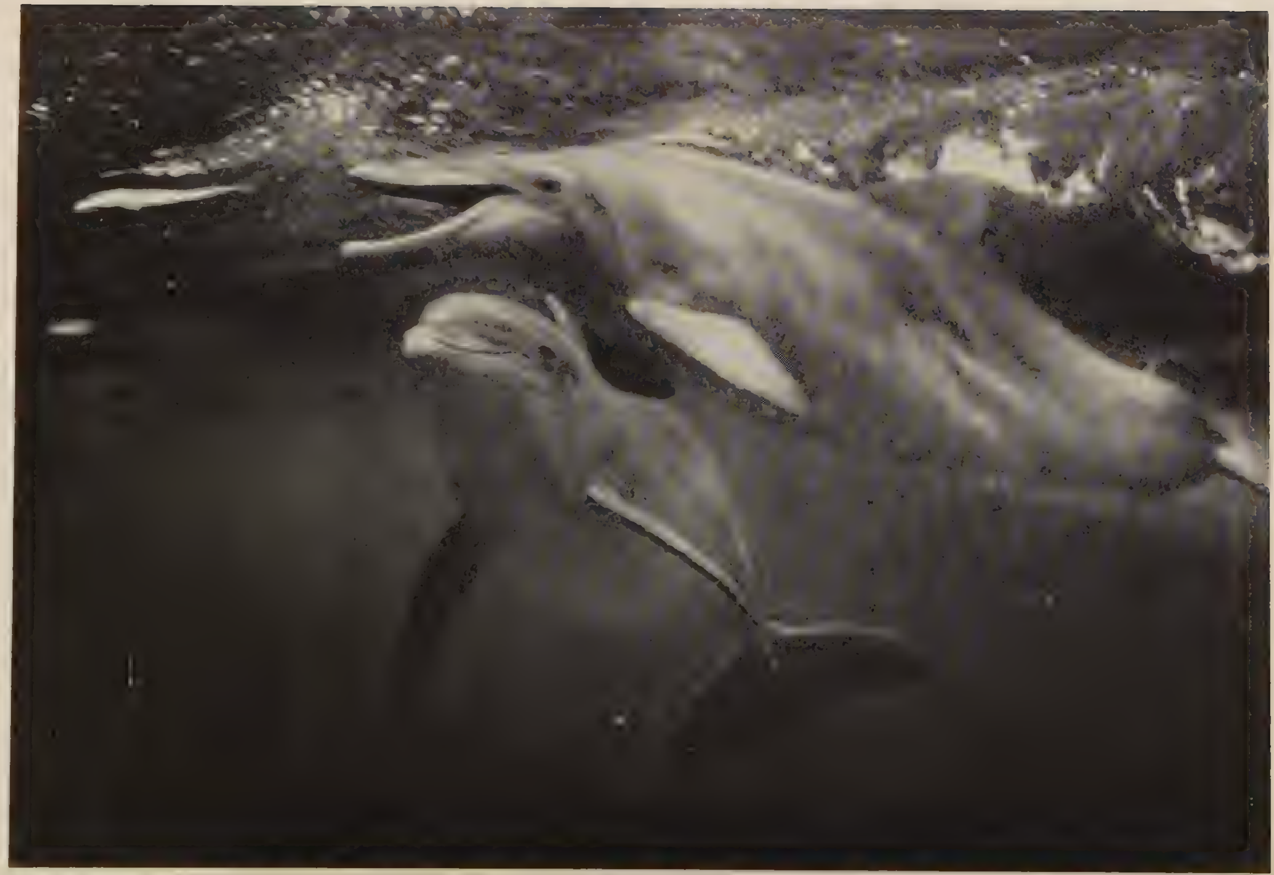

Pl. 2. An adult in a state of deceleration, about to seize a fish. Photographed at F/3.5 at 1/250 of a second.

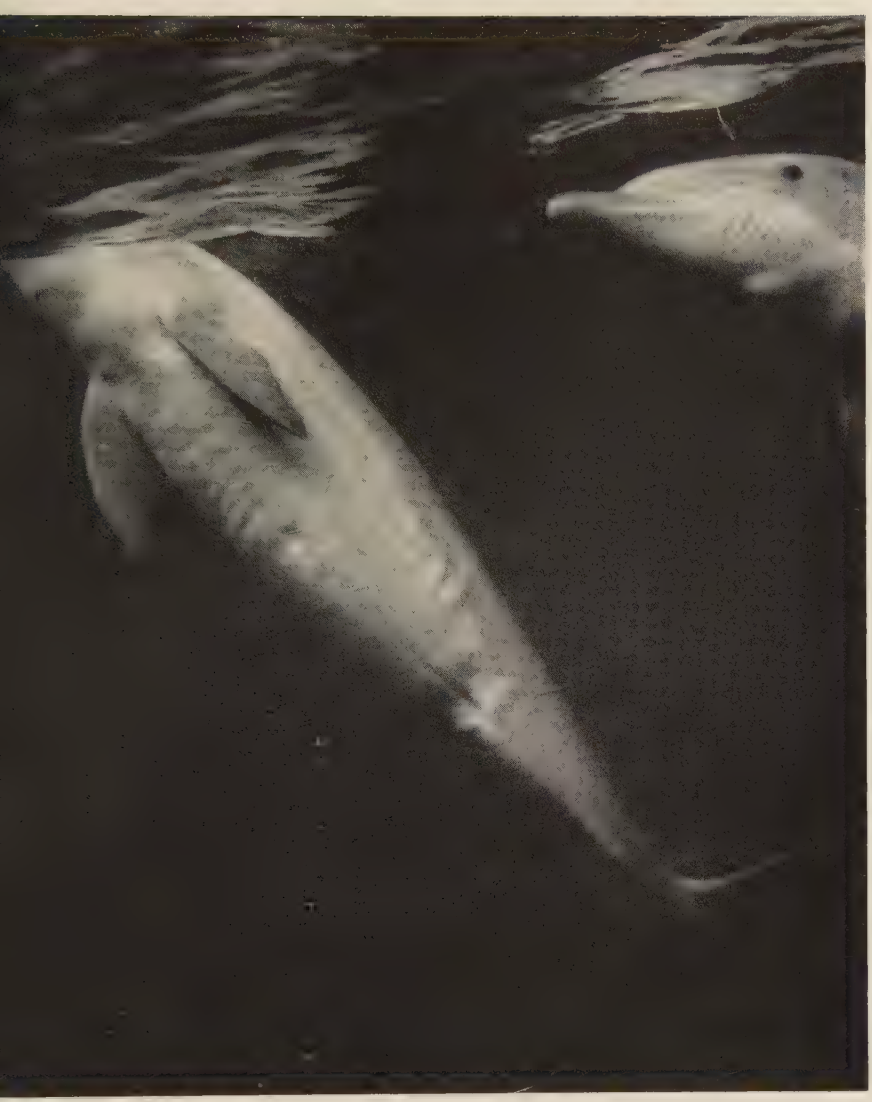

Pl. 3. A female, approximately eighteen months old, about to leap out of the water. Note also the folds on the head of the pursuing five-year-old male.

Photographed at F/3.5 at 1/500 of a second.

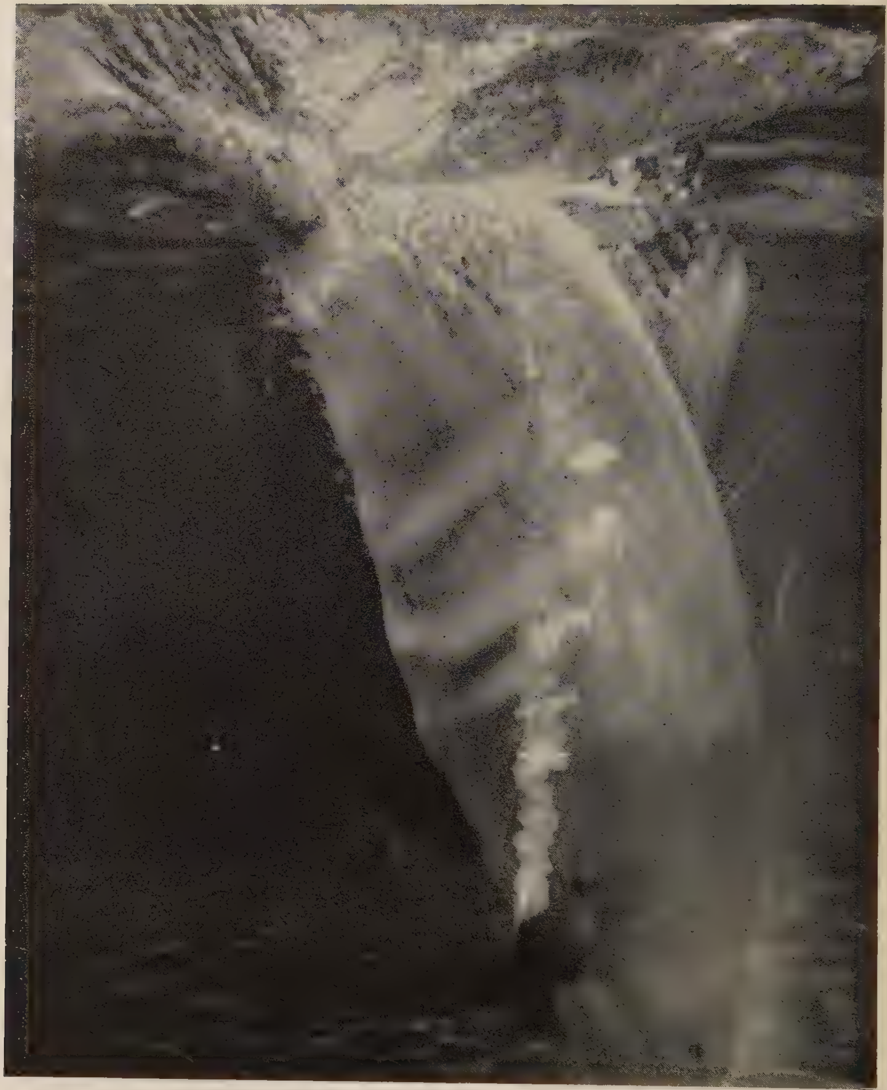

Pl. 4. An adult female displays folds as she reenters the water at completion of a leap.
Photographed at F/3.5 at 1/250 of a second.

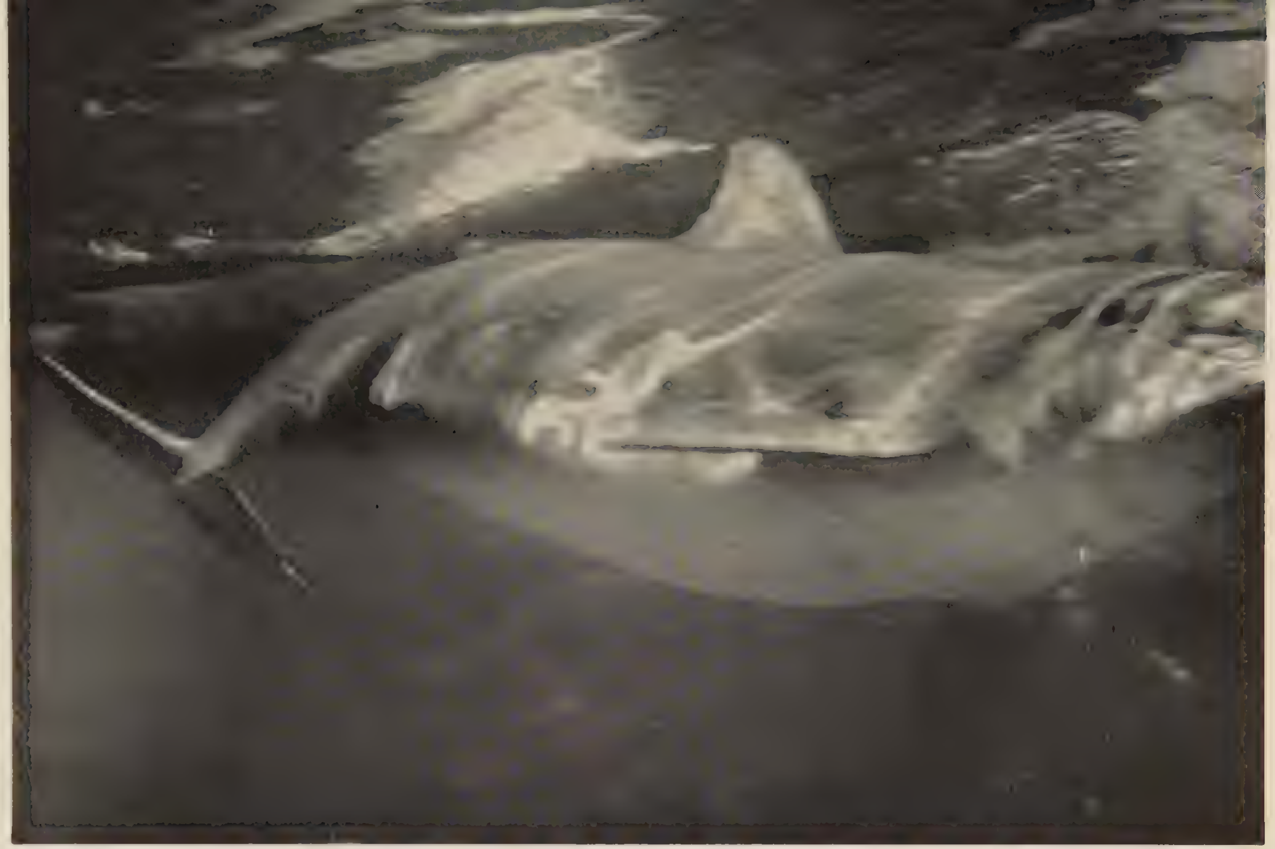

Pl. 5. The same animal as in Plate 4 exhibits widely spaced skin folds beginning at the angle of the jaw, prior to full acceleration. As in Plate 1, the irregular light and dark pattern is due to refraction of light through the surface water waves.

Photographed at F/3.5 at 1/250 of a second.

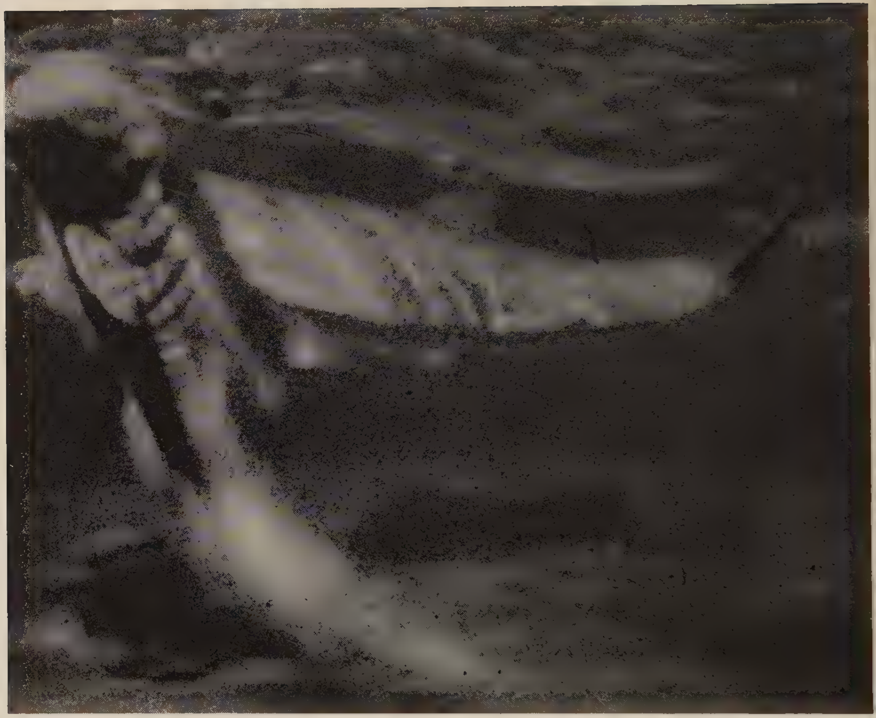

Pl. 6. An adult male displays folds as he comes to an abrupt stop in a vertical position (second porpoise in background shows no folds). Enlarged from 16 mm. film.
Photographed at 16 frames per second.

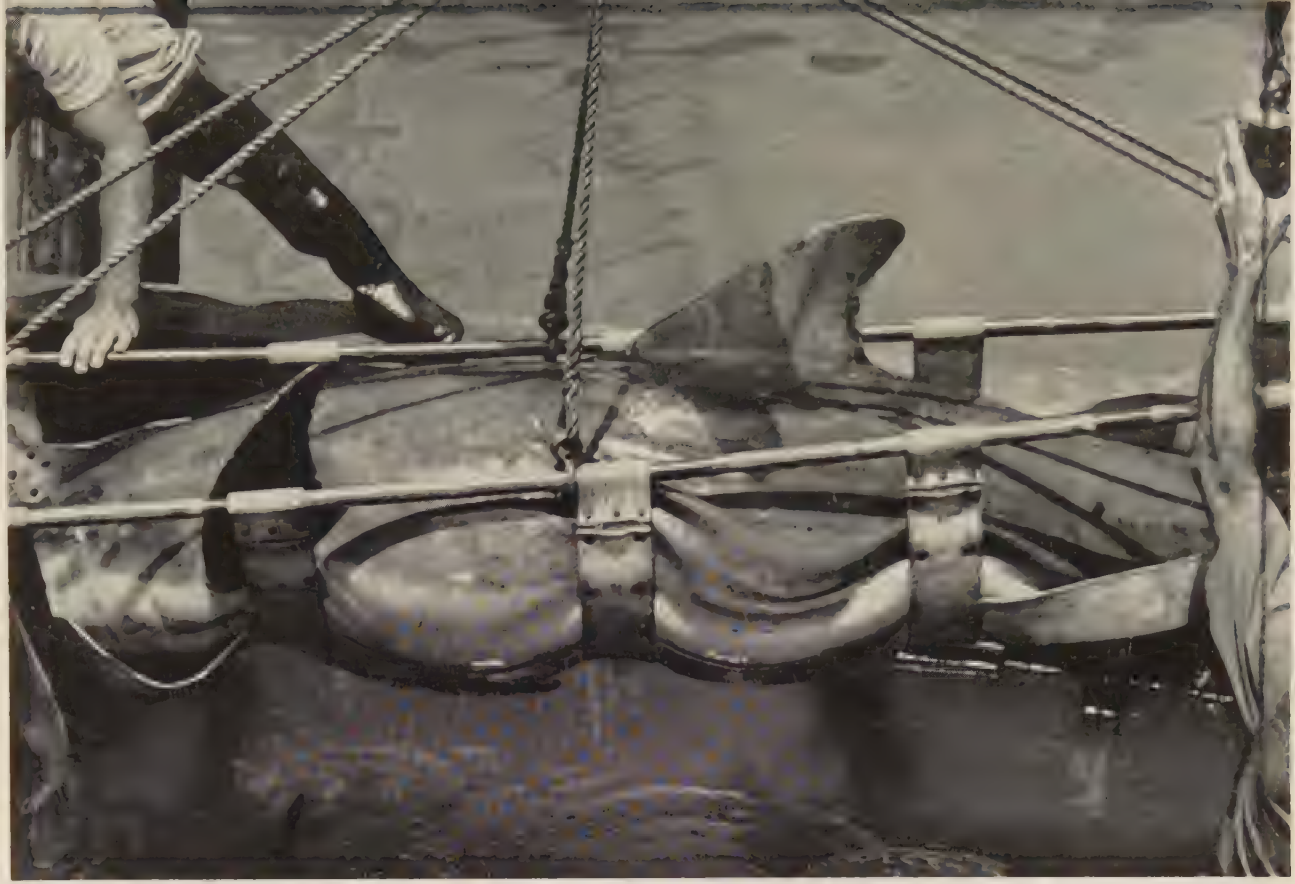

Pl. 7. A live adult female lifted in a sling displays the extreme looseness of the skin. Photograph by Bob Neelands.

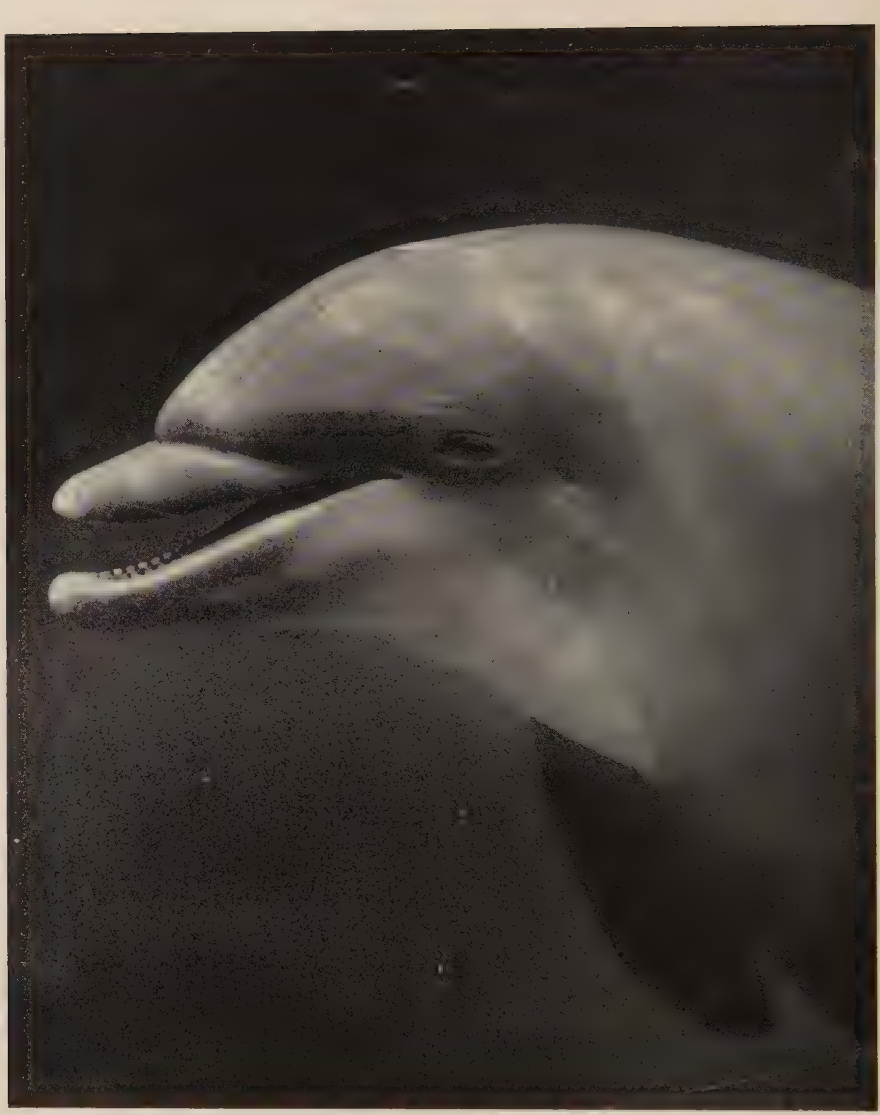

Pl. 8. Throat folds caused by downward flexion of head (esp. lower jaw). That these differ from the occasional speed folds is shown by the permanent creases between them (seen also on the unflexed throat of the porpoise in Plate 7). Note also the characteristic pigmentation. Photographed at F/3.5 at 1/250 of a second.

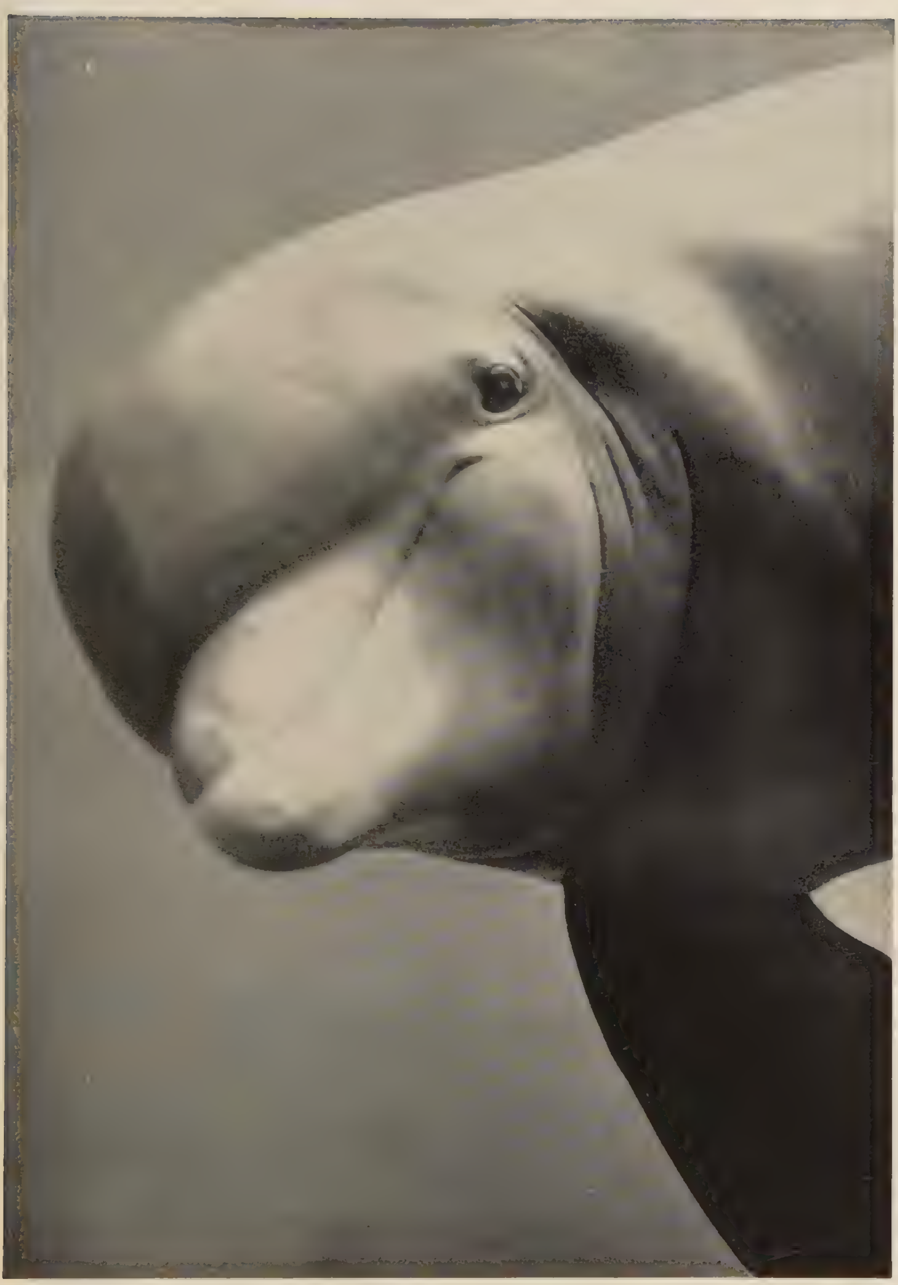

Pl. 9. Folds in the neck-shoulder region caused by turning the head sideways. This is the same animal as in Plates 4, 5, and [illegible].
Photographed at F/3.5 at 1/250 of a second.

Contribution No. 753

Reprinted from BIOLOGICAL BULLETIN, Vol. 109, No. 2, 211–225, October, 1955
Printed in U. S. A.

PHYSICAL AND BIOLOGICAL PROCESSES DETERMINING THE DISTRIBUTION OF ZOOPLANKTON IN A TIDAL ESTUARY[1]

JOHN P. BARLOW[2]

Woods Hole Oceanographic Institution, Woods Hole, Mass.

Plankton are at the mercy of the water movements that carry them about. These water movements also determine their physical and biological environments. As a result the study of the geographical distribution of plankton has an unique simplicity. The maintenance of an endemic plankton population and its distribution from its endemic center depends primarily on the dynamic balance between two processes: the translocation and dispersion of the population by the water movements, and the reaction of the population to the changes in environment caused by the water movements (Redfield, 1939, 1941; Redfield and Beale, 1940).

In spite of this simplicity, it is difficult in most environments to separate the effects of dispersal by the water movements on their distribution from the effects of reproduction and mortality of the organisms. The physical and analytical difficulties met in understanding and measuring the effects of these processes are, however, lessened by the characteristics of many tidal estuaries.

Estuaries are environments for which the land provides well defined boundaries. These boundaries permit a useful simplification in that the three dimensions in which events take place in the open sea can often be reduced to the two dimensions of a vertical plane in the land-sea axis of the estuary. Moreover, the rivers that drain into estuaries supply fresh water in a continuous and measurable fashion. This fresh water can become a useful tracer by which the rate of circulation of both fresh and salt water can be measured. The recent studies of the circulation in estuaries by Tully (1949), Ketchum (1951a, 1951b), Ketchum, Redfield and Ayers (1951), and Ketchum and Keen (1953) have given realistic descriptions of the circulation based on the behavior of this fresh water.

These studies show that there must be a net seaward movement of mixed salt and fresh water through an estuary adequate to remove the fresh water added by the river. This seaward movement must tend to transport the weakly swimming planktonic organisms. Ketchum (1954) has shown that the rate of this circulation determines the rate at which a plankton population must reproduce in order to maintain itself in an estuary. He has pointed out that the vigor of the circulation may thus limit the kind of plankton that is able to maintain an endemic population in an estuary. Bousfield (in press) has shown that in the Miramichee estuary the distribution of barnacles is influenced by seaward movements of mixed fresh and salt water and the landward counter current associated with it. Huntsman (1954) has used the estuarine circulation in the Bay of Fundy to explain the distribution of the herring populations there.

---

[1] Contribution No. 753 from the Woods Hole Oceanographic Institution.

[2] Present address: Department of Oceanography, A. and M. College of Texas, College Station, Texas.

This net seaward transport through an estuary implies that a population living in any part may be increased by additions from landward as well as decreased by losses to seaward. A knowledge of this circulation permits estimates to be made of the net rate at which a population in any part of the estuary is augmented or reduced by the physical processes. If the population is to be maintained, it must be increased or decreased by growth or mortality to offset the effects of the physical processes. Hence, if the rate of the circulation is taken into account, it is possible to determine the biological processes that underlie the distribution of plankton.

The distribution of zooplankton in a small estuary, Great Pond, near Woods Hole, Mass., has been studied. Rates have been computed at which some typical endemic zooplankton must have grown or died to maintain their distribution in face of the circulation. The rates of reproduction and mortality of these same zooplankton have also been estimated in various parts of the estuary from rates of increase or decrease of portions of the population isolated in bottles. There have thus been two independent estimates of the biological processes that maintain the distribution of these zooplankton. It is possible to give some understanding of both the physical and biological processes that determine the distribution of these zooplankton in Great Pond.

These investigations in Great Pond were suggested by Dr. Alfred C. Redfield. The author owes much to him for his continued encouragement, advice and critical analysis of this work. The author is also indebted to Dr. Bostwick H. Ketchum for his general interest in this problem, and his patient help in understanding the relations between plankton and the circulation in estuaries.

Mr. Edward M. Hulburt supplied much valuable information from his studies on the phytoplankton of the pond and helped greatly in the collection of the zooplankton samples.

METHODS

Zooplankton sampling

Great Pond (Fig. 1) is a small tidal estuary in the northern shore of Vineyard Sound. It is 3,300 meters long, with a maximum width of about 300 meters and a maximum depth of a little over two meters. The topography of its basin divides the pond into the several parts, the arm, narrows, main pond, shallows and entrance, as shown in Figure 1. The stations from which plankton samples were regularly taken are also shown. A full description of the pond has been previously given (Barlow, 1952).

Regular surveys of the plankton of Great Pond were made at 10- to 15-day intervals during the spring and summer of 1950 and at longer intervals during the following winter and spring. All zooplankton samples were taken with the quantitative plankton sampler (Clarke and Bumpus, 1950). Silk nets of No. 10 mesh (nominal aperture 0.158 mm.) were used except for samples taken in February, 1951, when the water was so turbid that it was necessary to use No. 2 mesh nets (nominal aperature 0.366 mm.).

On each survey samples were usually taken from the six stations in the pond and a station in the adjacent part of Vineyard Sound. At all stations a surface

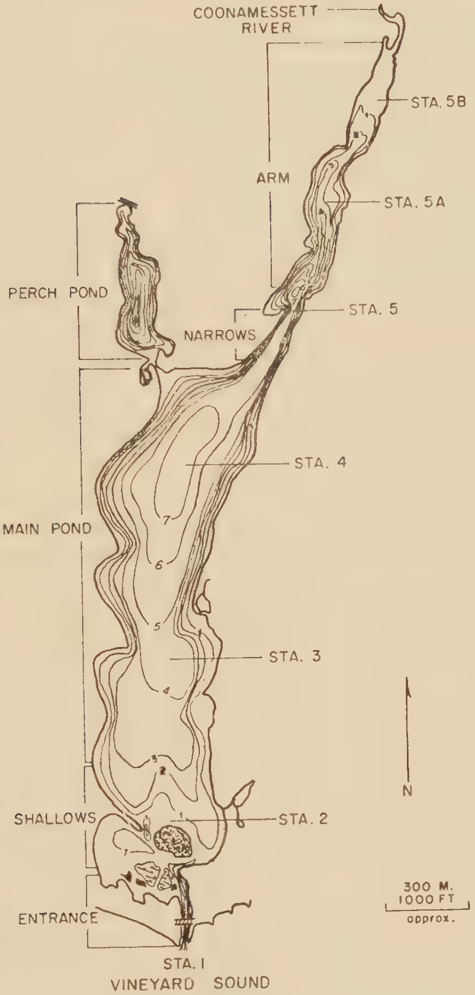
COONAMESSETT RIVER
STA. 5B
ARM
STA. 5A
PERCH POND
STA. 5
NARROWS
STA. 4
MAIN POND
7
6
5
STA. 3
4
N
SHALLOWS
STA. 2
300 M.
1000 FT
approx.
ENTRANCE
STA. I
VINEYARD SOUND

FIGURE 1. Bathymetric chart of Great Pond: depth in feet.

sample was collected by towing a sampler just below the surface. At stations 4, 5 and 5a, another sample was taken simultaneously as close as possible to the bottom. Tows were made, as far as possible, transverse to the long axis of the pond and at a velocity of two to three knots. The cyclometer readings indicated that usually two to three cubic meters of water were filtered for each sample.

Aliquots of each sample were counted under a dissecting microscope. The size of the aliquots was adjusted so that 50 to 100 of each of the important forms were counted. The concentrations in numbers per cubic meter have been computed from the numbers counted in these aliquots and the volume of water filtered for each sample.

The estimates of abundance of plankton are based on counts of single aliquots from single samples. The representativeness of such counts was tested by duplicate aliquots of a series of ten successive samples taken within two hours at station 3. Analysis for the variance between counts and the variance between hauls by the method of Silliman (1946) indicated that a sample could be considered to be significantly different from another only if it were less than half or more than twice the size of the other.

The samples have usually included so much detritus that the usual direct measurement of the weight or volume of the zooplankton could not be used. Instead, the average dimensions of each organism were determined in several representative samples. Each organism was considered to approximate in shape a simple geometric solid, and its average volume was calculated for each of these representative samples. These calculated average volumes were similar to those arrived at by more elaborate methods by Lohmann (1908) for the same or similar organisms. They have been used to compute the "calculated volume" of zooplankton in each sample.

Experiments with isolated water samples

A number of experiments were made with natural populations of phytoplankton and zooplankton imprisoned in bottles in order to study grazing rates, multiplication and growth. Water was pumped from the desired depth into a large wooden tub. After thorough mixing, one-liter aliquots of this water were poured alternately into a clean five-gallon carboy and through a No. 10 net. When the bottle contained 15 liters it was stoppered and moored where the sample had been taken. Thus filled, the bottle floated with its neck awash, and the water in it was stirred and aerated by wave motion. The sample collected in the net was preserved as a control. Usually bottles were filled and moored at five or six places in the pond. They were harvested after two or three days by pouring their contents through a plankton net. Occasionally some species not usually abundant in the pond would become very abundant in the bottle. Usually, however, the species composition changed very little during the course of an experiment.

As a measure of grazing rate this method was not entirely satisfactory, partly because large changes in the number and sizes of the animals during the course of the experiments made the results difficult to interpret. However, the multiplication and growth of the zooplankton in some of the jugs was so great that some conclusions could be drawn about the response of the animals to the differences in environment in different parts of the pond.

RESULTS

The zooplankton population of Great Pond

There have been a number of studies of the neritic plankton fauna of the Vineyard Sound region. Among these are Fish's (1925) seasonal study of the plankton of Woods Hole harbor and Wilson's (1932) description of the copepods of the Woods Hole region including several smaller estuaries. Deevey (1948) has described a population in Tisbury Great Pond, Martha's Vineyard, that was very similar in composition, seasonal distribution and abundance to that found in the central part of Great Pond.

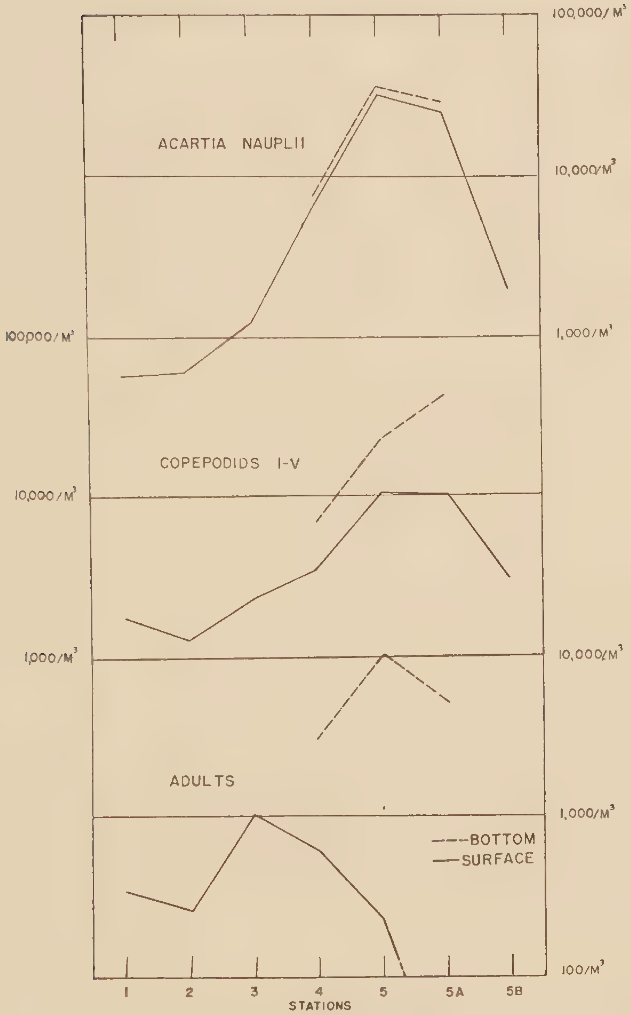

FIGURE 2. Distribution of *Acartia tonsa* copepodids and *Acartia* spp. nauplii in June 1950. Mean of surveys of June 5, 15 and 30.

The principal constituents of the catches from both the Sound and the pond have almost always been small neritic copepods, usually species of *Acartia*. During the late spring and summer these copepods were so much more abundant in parts of the pond than in the Sound that they must have been living endemically somewhere in the pond. The distribution of *Acartia tonsa* copepodid stages and *Acartia sp.* nauplii in the month of June is shown in Figure 2. The species of *Acartia* nauplii has not been determined, but since *A. tonsa* was by far the most abundant *Acartia* in June, it may be presumed that most of the *Acartia* nauplii were of *tonsa*. In addition to these copepods, several other endemic plankton organisms were abundant in this period. The cladoceran *Podon polyphemoides* and species of the rotifer *Synchaeta* were especially numerous in some parts of the pond but were scarce or not found in the Sound.

In contrast there were only a few forms, such as the copepod *Centropages hamatus,* that were more abundant in the Sound than in the pond.

The seasonal change in abundance of plankton has been summarized in Figure 3. This figure shows the seasonal distribution of the calculated volumes of all zooplankton except medusae, ctenophores, and gastropod veligers. The medusae and ctenophores were omitted because of their high water content. The gastropod veligers were omitted because their distribution must at least in part be determined by the distribution of the adult gastropods. Other temporary plankton made but small contributions to the calculated volumes shown in Figure 3.

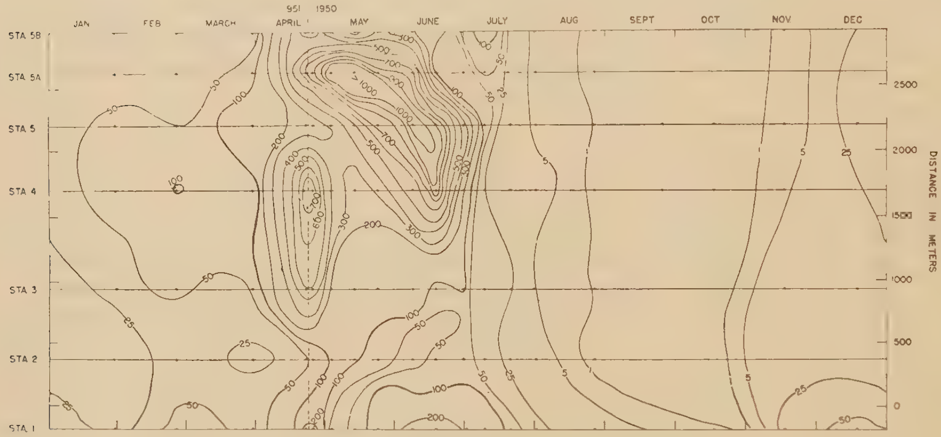

FIGURE 3. Seasonal distribution of zooplankton volume. Calculated volume in mm.^{3}/M^3. Gastropods, hydromedusae, and ctenophores not included. Mean of surface and deeper samples at Stations 4, 5 and 5a. Closed circles indicate observations. Distance in meters from entrance shown at right.

The fall and winter were periods of least abundance in both the pond and the Sound. The population increased from about the first of April through the spring to the period of greatest abundance in the early summer. In the latter part of July in both 1950 and 1951 there was a dramatic decrease in the abundance of all kinds of zooplankton in the pond. There were no obvious changes in physical, chemical or hydrographic conditions accompanying this decrease. In both years it coincided with the appearance of numbers of *Mnemiopsis leidyi.* These ctenophores were so poorly preserved that they could not be counted in the 1950 samples. Examination of some fresh samples in 1951 showed that at Station 5 they increased from less than one per cubic meter in early July to 35 per cubic meter near the end of July.

Since *Mnemiopsis* is known to be a zooplankton predator (Nelson, 1925), it seems possible that the late summer decrease in zooplankton in Great Pond was due to its depredations. Although Deevey (1948) found a similar late summer decrease in Tisbury Great Pond, she found no ctenophores in her samples. The number of zooplankton in Great Pond did not increase substantially again during the remainder of the year.

The greatest concentration of zooplankton in the pond was found on June 5, 1950, in the deeper water at Station 5a where there were 346,000 organisms per cubic meter having a calculated volume of 2,500 mm.^{3} per M^3. The smallest concentrations of plankton in the pond and Sound were found on September 18, 1950, when there were less than 100 organisms per cubic meter, having a calculated volume less than one mm.^{3} per M^3 at Station 5a. Thus there was a several thousand-fold seasonal decrease in both number and volume of zooplankton in the pond.

The concentrations in the Sound have usually been quite different from those in the pond. On June 5 the zooplankton in the Sound was nearly at its maximum, yet it was only 1/72 in numbers and 1/38 in volume of that in the pond. The zooplankton was never as low in the Sound as in the pond. At the time of the September minimum in the pond the zooplankton was about 20 times greater, in both numbers and volume, in the Sound. The winter minimum was about 1/15 the summer maximum in the Sound.

Vertical distribution of plankton in Great Pond

There were usually no significant differences in the concentrations of *Acartia* nauplii at the surface and near the bottom. The juveniles and adult copepodids were, however, found in significantly greater concentrations near the bottom than at the surface at some stations. The difference in surface and bottom concentrations did not appear to be related to the time of day when the samples were taken, as shown by samples taken near midday and midnight of the same day. The distribution of zooplankton does not, therefore, seem to be greatly affected by vertical diurnal migrations. Large differences in surface and bottom concentrations were found when and where there were large differences in surface and bottom salinities. It is probable that the passive sinking of the plankton from the less buoyant brackish surface layer and then active avoidance of this layer are more effective in influencing the concentration of the heavier and more active forms than is a migration influenced by light.

Horizontal distribution of plankton in Great Pond

Tidal exchanges of salt and fresh water play a large part in effecting the salinity distribution in many tidal estuaries. Ketchum (1951b) has given an empirical method for estimating the changes of salt and fresh water in tidal estuaries. This method has been used to estimate the tidal exchanges that account for the average summertime salinity distribution in Great Pond (Barlow, 1952). These tidal exchanges must affect the horizontal distribution of plankton as well.

Ketchum, Ayers and Vaccaro (1952) have pointed out that if organisms such as coliform bacteria were introduced at a constant rate with the river water, their eventual distribution within an estuary would be similar to that of the fresh water, providing there were no net reproduction or mortality of the organisms. It may also be pointed out that these tidal exchanges must tend to disperse organisms landward. Hence, if plankton were present in constant numbers in Vineyard Sound its eventual distribution in Great Pond would be similar to that of the salt water, providing there were no net reproduction or mortality of the organism as it was dispersed through the pond.

Estuaries are not uniform environments. The salinity of Great Pond, ranging as it does from about 32 °/₀₀ in Vineyard Sound to zero at the river mouth, provides in itself a significant environmental gradient. There must be similar gradients of other conservative environmental factors present in different quantities in the salt and fresh water.

It seems unlikely that there can be many organisms whose reproduction, growth and survival are not affected by such large environmental differences. We have found no zooplankton in Great Pond whose distribution landward or seaward from its center of abundance is consistently similar to that of the salt or fresh water. The distribution of the zooplankton is, therefore, determined not only by the exchanges of salt and fresh water but also by its own reproduction, mortality, and its specific behavior.

Ketchum, Ayers and Vaccaro (1952) have considered the effects of tidal exchanges and mortality on the distribution of coliform bacteria in the Raritan River. They have shown that after m tidal cycles the concentration C_n of coliform bacteria in a segment n of the river equal in length to one tidal excursion is

$$C_n = (C_0)_n \cdot r_n \cdot \frac{1 - (1 - r_n)^m e^{mk}}{1 - (1 - r_n)e^k}, \tag{1}$$

in which $(C_0)_n$ is the concentration of bacteria entering the segment n from the next landward segment and r_n is the exchange ratio of the segment n. The term e^k is the coefficient of net population change due to reproduction and mortality.

Since predation and the bactericidal action of sea water were always greater in their effects than reproduction, the sign of the coefficient k of the coliform bacteria was always negative. In some parts of the estuary reproduction will, however, tend to increase the size of the populations of many estuarine organisms. The sign of the coefficient k may thus often be positive.

Equation (1) can be simplified (see Ketchum, Ayers and Vaccaro, 1952) and solved for e^k to give

$$e^k = \frac{C_n - (C_0)_n(r_n)}{C_n(1 - r_n)}. \tag{2}$$

The simplification is valid only when $(1 - r_n)e^k$ is less than unity.

The term e^k in equation (2) defines the rate at which the population in a given segment must be increased to maintain it there at the concentration C_n in face of additions or withdrawals by tidal exchanges. This rate will be called the "replacement rate." If the sign of k in a specific segment of the estuary is positive, it implies that the population within the confines of that segment must be increasing by reproduction or by additions from deeper water below the limits of the segment to maintain the observed concentration in spite of the losses due to tidal exchanges. If the sign of k is negative, it implies that the population within the segment must be decreasing by mortality or by losses to the deeper water to maintain the observed concentration in spite of the gains due to tidal exchanges.

Estimates of the rates of the processes that maintain the observed distribution of Acartia

The replacement rates necessary to maintain a population at an observed steady state concentration C_n in any segment of Great Pond may be readily computed if the distribution of the population is well enough known that the contribution $(C_0)_n$ from the next landward segment can be estimated.

Both *Acartia* nauplii and *Acartia tonsa* copepodids were abundant and widespread throughout June and July, 1950. The *Acartia* copepodids were found in about the same abundance at the several stations in the pond on two successive surveys, June 30 and July 10, and the nauplii on three successive surveys, June 5, 15 and 30.

The nauplii were most abundant at the northern end of the main pond and in the arm, at stations 4, 5 and 5a, during June. An analysis of variance (Snedecor, 1946) of the June counts of nauplii at these three stations showed that none of the differences between surface and bottom concentrations, or between surveys, were significant. There were similar differences in abundance of *Acartia* copepodids in the June 30 and July 10 surveys. The distribution of these two forms appears to have been approximately in a steady state for the periods covered by these successive surveys.

The concentrations of *Acartia* nauplii and copepodids in the tidal excursion segments of the pond were estimated from the data of these surveys and are shown in Figures 4 and 5. At stations where samples were taken at both surface and bottom the average of surface and bottom concentrations has been considered to most nearly represent the average concentration in the mixed layer. The replacement rates necessary to maintain in each segment these observed steady state concentrations of *Acartia* nauplii and copepodids have been computed, using the relationship presented in equation (2). The replacement coefficients are shown in Figures 4 and 5. Each of these coefficients has been plotted against the mean salinity of its respective segment.

At salinities less than 15 $^0/_{00}$, representing values from the arm landward of station 5, the replacement coefficients were usually positive and relatively large. These large coefficients indicate that the concentrations of both nauplii and copepodids in the mixed layer of the arm were being maintained in face of seaward transport by very rapid replacement.

At the intermediate salinities of from 15 $^0/_{00}$ to 25 $^0/_{00}$, representing values from the narrows and the northern end of the main pond, the replacement coefficients were also usually positive but much smaller than in the arm. These coefficients indicate that, even though the populations were large in this part of the pond, they were being maintained by replacement at a moderate rate.

At salinities above 25 $^0/_{00}$, representing values from the southern half of the main pond and the shallows, the replacement coefficients were nearly all negative. These coefficients indicate that the *Acartia* must have been removed from this part faster than could be accounted for by exchanges with the Sound.

Production rate in isolated water samples

The replacement rates, e^k, calculated from equation (2) represent the rates of change in the population by reproduction and mortality which, under steady state conditions, balance the gains or losses by tidal exchanges. These rates would

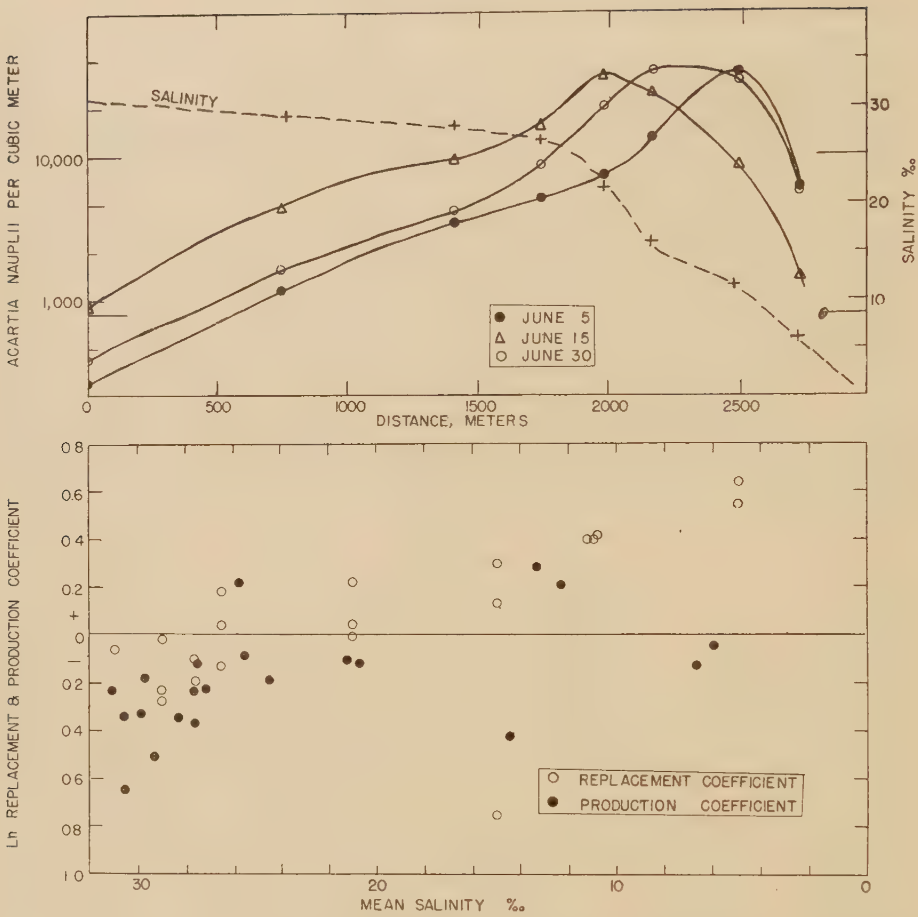

FIGURE 4. Distribution of *Acartia* nauplii (above) and replacement and production coefficients for *Acartia* nauplii (below). Replacement coefficients calculated from distributions of June 5, 15 and 30, 1950. Natural logarithms of replacement rates, e^k, plotted against mean salinity in tidal excursion segments. Production coefficients calculated from bottle experiments of June and July 1951. Natural logarithms of production rates, e^k, plotted against salinity in the bottles.

also reflect the effects of vertical exchanges between the mixed layer and the deeper layer, which may or may not be significant. The replacement rate thus gives an estimate of the rate at which the population would increase or decrease if purely horizontal tidal exchanges were eliminated.

An independent estimate of the value of e^k may be obtained by actually isolating a sample of water with its natural population from tidal exchanges and noting the rate at which its population actually changes when maintained under otherwise natural conditions. These two estimates should agree unless vertical exchanges are significant.

The change in numbers in an isolated parcel of water may be represented by

$$(C_0)e^{kt} = C_t, \tag{3}$$

in which C_0 is the initial concentration of the organism and C_t the concentration after t tidal cycles. The value of e^k determined from equation (3) will be called the "production rate," in distinction from the value obtained from equation (2) which is referred to as the replacement rate.

When applied to the numbers of some particular stage in the life history of an organism, as in the present case, these production rates are not, of course, true

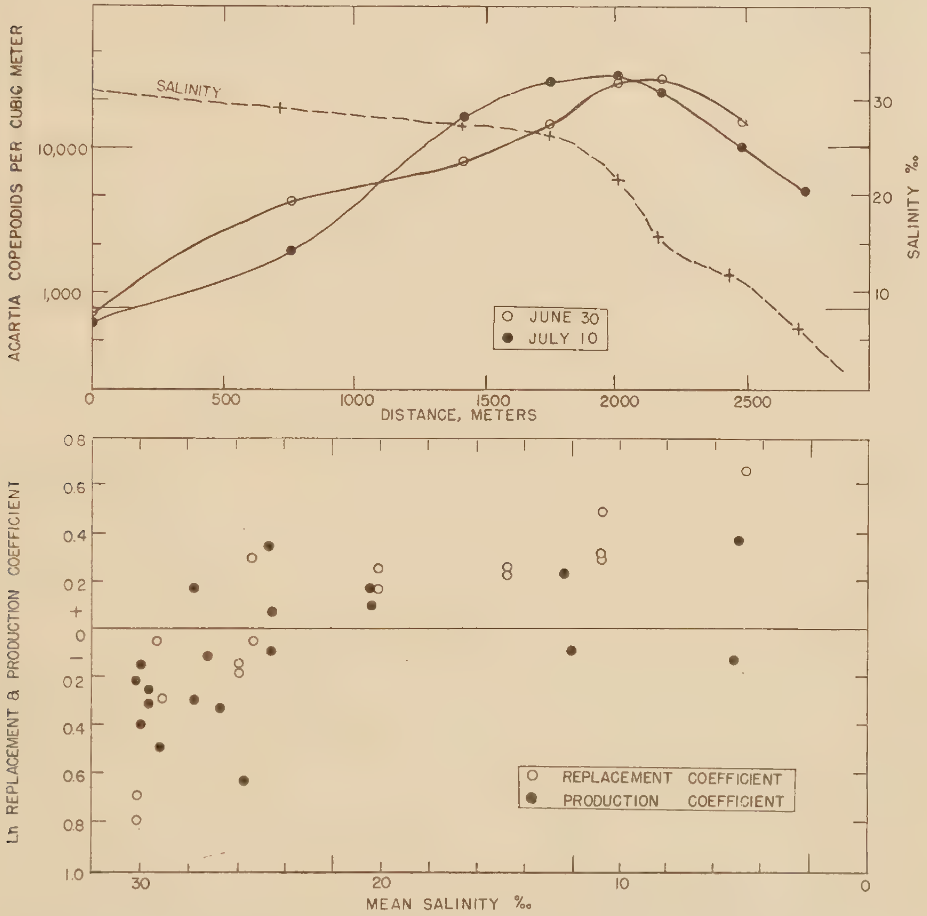

FIGURE 5. Distribution of *Acartia tonsa* copepodids (above) and replacement and production coefficients for *Acartia tonsa* copepodids (below). Replacement coefficients calculated from distributions of June 30 and July 10, 1950. Natural logarithms of replacement rates, e^k, plotted against mean salinity in tidal excursion segments. Production coefficients calculated from bottle experiments of June and July, 1951. Natural logarithms of production rates, e^k, plotted against salinity in the bottles.

measures of the rate of change of the entire population; they refer rather to the changes resulting from hatching, moulting, and the mortality of the particular stage in question.

In the bottle experiments portions of the *Acartia* population were effectively isolated from all exchanges with the surrounding water, but were maintained under natural conditions of temperature and illumination. Production coefficients have been computed from the change in numbers of *Acartia* nauplii and copepodids during these experiments using equation (3). Since it is reasonable to assume that the environmental conditions in the pond were essentially the same in 1950 and 1951, these production coefficients have also been shown in Figures 4 and 5 for comparison with the replacement coefficients. The production coefficients have been plotted against the salinity of the water enclosed in each bottle.

Comparison of the production rates with the replacement rates shows that in the main pond these two estimates of the rates of the biological processes are in general agreement. The greatest production rates were at the intermediate salinities of 10 to 15 $^0/_{00}$, typical of the narrows and northern end of the main pond. There the populations often reproduced fast enough to double themselves in less than two days. The agreement between the replacement and production rates indicates that there the *Acartia* population was replaced in the mixed layer by reproduction and by horizontal tidal exchanges with the population in the more landward part of the pond. The deeper layer could not have been a very potent source of recruits to the mixed layer since the *Acartia* population in the deeper layer in this part of the pond was little larger than that in the mixed layer.

At the higher salinities typical of the more seaward part of the pond the production coefficients were usually negative, showing that the *Acartia* brought in by exchanges with the landward parts of the pond were being reduced. Since the replacement rates were also negative these populations must have been reduced by some other means than by exchanges with the Sound. The hydrographic data show that most of this part of the pond was so thoroughly mixed that there could seldom be a distinct deeper layer which could receive the *Acartia* removed from the mixed layer. These populations must, therefore, have been reduced by an excess of mortality within this part of the pond over recruitment from the landward parts of the pond.

The cause of this mortality in the southern end of the pond is not known. Similar mortality rates have, however, been shown for lake zooplankton caught in outflowing rivers. Galtsoff (1924) has suggested that the mortality of this lake zooplankton may often be caused by the strong turbulence in the river. The strong turbulence in the shallows and entrance may have caused an excessive mortality of zooplankton in that part of the pond.

The replacement rates at the low salinities typical of the mixed layer of the arm were much higher than the production rates. These replacement rates indicate that the populations in this part of the pond must have been replaced very rapidly if they were to be maintained there. If they were to be replaced by reproduction alone, they would have had to double or triple themselves each day. As the rates of increase in the bottle experiments suggest, these are improbably high rates for an organism such as *Acartia*. A large part of the copepod population in the mixed layer may have been recruited by vertical mixing or migration from the deeper layer. This is possible because the deeper layer usually had a much richer population than the surface layer. The population in the deeper layer in turn must have been replaced rapidly if it were to provide a continuous supply to the mixed layer. This replacement may have been provided by landward transport in a deeper counter current from the regions of maximum abundance near Station 5.

The comparison of the replacement and production rates made above has shown that a high rate of reproduction served to maintain the populations in the narrows and northern end of the main pond. At higher salinities, in the more seaward parts of the pond, there was a decrease in the rate of the biological processes. The small populations in these parts of the pond were a result of mortality and exchanges with the Sound. At the lowest salinities, in the surface layer of the arm, the biological processes are insufficient to maintain the populations found there. The discrepancy between the rate at which these organisms reproduce and the rate at which they must be replaced in these parts of the pond appears to be made up by recruitment from the deeper layer.

Discussion

The distribution of plankton does not in itself give a reliable definition of the limits of the region in which the organism is able to maintain itself endemically by its own reproduction and growth. The analysis of the processes that maintain the distribution of *Acartia* has shown that nowhere in the surface mixed layer of Great Pond did this copepod maintain itself wholly by local reproduction. The population in the arm could not have maintained itself without continuous additions from the deeper layer. Even the population in the mixed layer of the northern end of the main pond was dependent to some extent on additions from the more landward parts of the pond. Mortality must have far exceeded reproduction to account for the observed concentrations of *Acartia* in the seaward part of the pond.

If any holoplankton organism is to attain an endemic relation to a specific region, it is necessary that the biological processes that maintain it balance the physical processes that disperse it. This necessity is lessened but not evaded by organisms seeking regions in which dispersion is less rapid such as the deeper layer in Great Pond. In the final analysis this necessity can be met only by a sufficient rate of population increase. The fitness of a plankton organism to establish an endemic relation to a specific region depends on its rate of reproduction and growth and on its survival in the environment of that region. Smaller organisms often have the higher reproductive rates and shorter periods of immaturity that contribute to high rates of population increase. It is perhaps significant that all the endemic plankton organisms of an estuary such as Great Pond are small.

The physical processes of advection and diffusion set the minimum rate at which a plankton organism must be able to increase to maintain itself endemically. In Great Pond this minimum rate was achieved by several zooplankton in the summer during the time when temperature is high and the phytoplankton abundant. In the late summer and early fall these zooplankton appear to be unable to reproduce fast enough to maintain their numbers, perhaps because of the depredations of ctenophores.

The higher salinities in the pond in the winter suggest that there may have been some change in the physical processes that dispersed the plankton. Whether the rate of these physical processes increased or not, the biological processes of reproduction and growth must have been decreased by the lower temperatures and sparser phytoplankton of the winter to the point where they may have been insufficient for any zooplankton to maintain themselves in the estuary by these processes. The zooplankton would, however, be able to tide themselves over such periods by the formation of resting stages on the bottom. It was not until the temperature and the phytoplankton began to increase in the spring that there was any clear evidence that any of the zooplankton in the pond was able to increase sufficiently to maintain itself endemically.

SUMMARY

1. The zooplankton of a small estuary, Great Pond, has been described. It has been shown that in the summer there were endemic populations of several zooplankton of which the copepod *Acartia* was the most numerous and widespread.

2. The rates at which *Acartia* must have been replaced to maintain its numbers in the surface mixed layer of Great Pond in face of dispersion by the tidal exchanges have been calculated. These rates are compared with the rates at which *Acartia* increased or decreased when isolated in bottles immersed in the pond.

3. This comparison shows that in the most landward parts of the pond the population in the mixed layer could not reproduce fast enough to maintain itself and was dependent on recruitment from the deeper layer. In the central part of the pond reproduction alone was sufficient to offset the seaward transport by the tidal exchanges. In the most seaward parts of the pond, mortality was so great that the small population was maintained only by transport from the landward parts of the pond.

4. Thus the comparison reveals the contribution of reproduction, growth and mortality and of tidal transport to the maintenance of the observed distribution of *Acartia*. Seasonal changes in these physical and biological processes account for the seasonal changes in the distribution of zooplankton in Great Pond.

LITERATURE CITED

BARLOW, J. P., 1952. Maintenance and dispersal of the endemic zooplankton population of a tidal estuary. Ph.D. Thesis, Harvard University.

BOUSFIELD, E. L., 1955. Ecological control of the occurrence of barnacles (Crustacea: Cirripedia) in the Miramichee Estuary. (In press). *Bull. National Mus. of Canada.*

CLARKE, G. L., AND D. F. BUMPUS, 1950. The plankton sampler—an instrument for quantitative plankton investigations. Spec. Publ. 5, *Amer Soc. Limn. and Ocean.* Revised 1950, 8 pages.

DEEVEY, G. B., 1948. The zooplankton of Tisbury Great Pond. *Bull. Bingham Ocean. Coll.,* **12**: 1–44.

FISH, C. J., 1925. Seasonal distribution of the plankton of the Woods Hole region. *Bull. U. S. Bur. Fish.,* **41**: 92–179.

GALTSOFF, P. S., 1924. Limnological observations in the upper Mississippi River, 1921. *Bull. U. S. Bur. Fish.,* **39**: 347–438.

HUNTSMAN, A. G., 1954. Movements and decline of large Quoddy Herring. *J. Fish. Res. Bd. Can.,* **10**: 1–50.

KETCHUM, B. H., 1951a. The flushing of tidal estuaries. *Sewage and Industrial Wastes,* **23**: 199–209.

KETCHUM, B. H., 1951b. The exchanges of fresh and salt water in tidal estuaries. *J. Mar. Res.,* **10**: 19–38.

KETCHUM, B. H., 1954. Relation between circulation and plantonic populations in estuaries. *Ecology,* **35**: 191–200.

KETCHUM, B. H., J. C. AYERS AND R. VACCARO, 1952. Processes contributing to the decrease of coliform bacteria in a tidal estuary. *Ecology,* **33**: 247–258.

KETCHUM, B. H., AND D. J. KEEN, 1953. Exchanges of fresh and salt water in the Bay of Fundy and Passamaquoddy Bay. *J. Fish. Res. Bd. Can.,* **10**: 97–124.

KETCHUM, B. H., A. C. REDFIELD AND J. C. AYERS, 1951. The oceanography of the New York Bight. *Pap. Phys. Ocean. and Met.,* **12**: 4–46.

LOHMANN, H., 1908. Untersuchungen zur Feststellung des vollstandigen Gehaltes des Meeres an Plankton. *Wiss. Meersunter. N. F.* **10**, Abt. Keil: 131–370.

NELSON, T. C., 1925. On the occurrence and food habits of ctenophores in New Jersey inland coastal waters. *Biol. Bull.,* **68**: 92–111.

REDFIELD, A. C., 1939. The history of a population of *Limacina retroversa* during its drift across the Gulf of Maine. *Biol. Bull.,* **76**: 26–47.

REDFIELD, A. C., 1941. The effect of the circulation of water on the distribution of the calanoid community in the Gulf of Maine. *Biol. Bull.,* **80**: 86–110.

REDFIELD, A. C., AND A. BEALE, 1940. Factors determining the distribution of populations of chaetognaths in the Gulf of Maine. *Biol. Bull.,* **79**: 459–487.

SILLIMAN, R. D., 1946. A study of variability in plankton townet catches of Pacific pilchard (*Sardinops caerulea*) eggs. *J. Mar. Res.,* **6**: 74–83.

SNEDECOR, G. W., 1946. Statistical methods. Iowa State College Press, Ames, Iowa.

TULLY, J. P., 1949. Oceanography and the prediction of pulp mill pollution in Alberni Inlet. *Fish. Res. Bd. Can. Bull.,* **83**: 1–169.

WILSON, C. B., 1932. The copepods of the Woods Hole region, Massachusetts. *Bull. U. S. Nat. Mus.,* **158**: 635 pages.

Contribution No. 755

Reprinted from EVOLUTION, Vol. IX, No. 1, March, 1955
Printed in U. S. A.

EVOLUTION OF CLIMATIC ADAPTATION IN HOMEOTHERMS[1]

P. F. SCHOLANDER

Woods Hole Oceanographic Institution, Woods Hole, Massachusetts

Received May 6, 1954

Climatic adaptation in warm-blooded animals has been a subject of much concern to ecologists and evolutionists. With the formulation of the climatic rules of Bergmann and Allen it has become almost dogma that a reduction in the surface area relative to weight is a morphogenic factor of prime importance in the evolution of cold-hardy species or races. This idea is based on the simple reasoning that, other factors being equal, the less surface area an animal has the less heat it would lose. Natural selection would therefore favor an arctic fauna tending towards large globular woolly balls with the least possible ears, tail, snout and legs. Tropical animals would tend in the opposite direction, towards smaller skinny forms, with long legs, snout, ears and tail. Clines of this sort have been looked for and have been found in many mammals and birds, and are given in textbooks on evolution as classical examples of the workings of adaptation by selection. Lately anthropologists have seen in the climatic rules a powerful tool by which to explain many racial features in man.

Adaptation, in the sense of "rendered fit for," implies an understanding of how and why the observed trend or response is useful, and is hence linked up with physiology. Sufficient information on the physiological adjustments of arctic and tropical animals is now available so that we may attempt an analysis of what phylogenetic pathways evolution has actually followed in the engineering of climatic adaptation of warm-blooded animals.

CLIMATIC ADAPTATIONS FOUND IN ARCTIC AND TROPICAL MAMMALS AND BIRDS

Most homeothermic animals require maintenance of a constant internal body temperature. This is generally higher than the environmental temperature. In arctic latitudes the temperature gradient to the outside is so great that the main problem becomes one of keeping warm. Thermally speaking there are three avenues open for adaptation to the arctic environment: (1) by lowering the gradient, (2) by increasing the heat production, and (3) by decreasing the heat dissipation. In a tropical environment overheating would be checked by changes in the opposite direction.

It is known that the body temperature is the same in species from all climates. (Compare Morrison and Ryser, 1952, and Irving and Krog, 1954.) Also the basal heat production has been found to be essentially the same in all climates, inasmuch as most arctic, temperate and tropical mammals fit the mouse-to-elephant curve of Benedict (1938). Birds show this regularity too. This leaves the heat dissipation as the only major avenue for phylogenetic adaptation to climate. (Compare the three papers by Scholander, Hock, Walters, Johnson and Irving, 1950.)

Major adaptations are traceable not only in the overall heat dissipation but also in the heat dissipation of localized peripheral structures. We shall consider the overall heat dissipation first.

ADAPTATION OF THE OVERALL HEAT DISSIPATION

At thermal equilibrium the heat dissipation balances the heat production.

---

[1] Contribution No. 755 from the Woods Hole Oceanographic Institution.

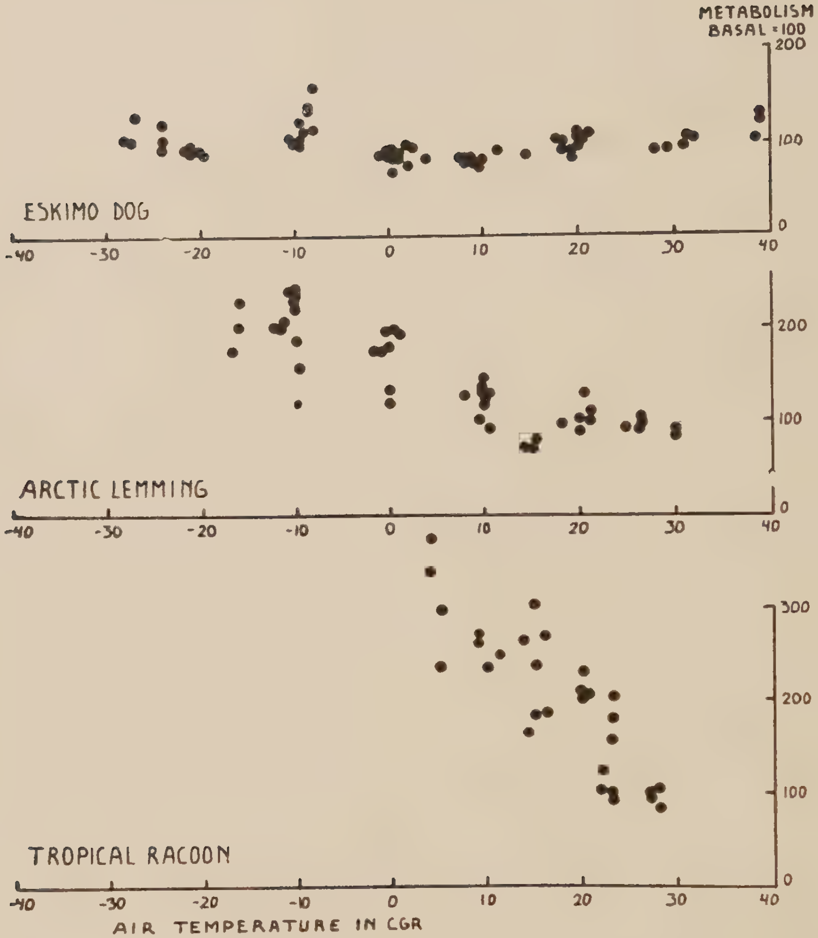

FIG. 1. Heat production versus environmental temperature in the husky, the lemming and the tropical racoon. Resting or basal rate is set at 100. Critical temperature is below −30° in the husky, 10–15° in the lemming and 25–27° in the tropical racoon. (From Scholander, Hock, Walters, Johnson and Irving 1950.)

The latter is usually determined indirectly from the oxygen consumption or the carbon dioxide output. It is reasonable to assume that a mammal or a bird when fully adapted to its normal environment can rest and sleep in it at essentially basal heat production. A fundamental measure of the overall adaptation to cold is therefore to determine the lowest air temperature at which the animal can maintain a resting or basal metabolic rate, without losing body temperature. This is its *critical temperature*.

If the temperature of the environment drops, our resting mammal or bird will compensate for it by decreasing the heat loss. This is done by raising hairs or feathers, decreasing peripheral circulation and by balling up. At the critical temperature the overall insulation has reached its maximal value. If the environmental temperature is lowered still further, shivering sets in as a gross sign of incipient metabolic heat regulation. From this point on there is an increase in the heat production which is approximately proportional to the difference between the body and air temperature, such as would be expected from Newton's law of cooling (cp. fig. 1).

In tropical mammals the critical temperature was found to be 25–27° C., the same as in naked man. In the arctic fox and husky the critical temperature was not yet reached at − 30° in laboratory experiments. In these and larger arctic mammals it is probably − 40° or lower since they can sleep unprotected on the snow at these temperatures. When curled up on the snow they may be likened to a man resting comfortably in an arctic sleeping bag at −40°.

Mammals and birds smaller than a rabbit have critical temperatures higher than the larger animals. Lemmings had a critical temperature of around +10° and a little shrew with much less body insulation must have one still higher. These and many other small mammals live in the cold northern forests or on the tundra through the winter, but they all seek shelter, often under the snow, where microclimates may be found which are only a few degrees below freezing (Johnson, 1951). Many of them build warm nests. If shelter is not available such small animals may have to pull through cold spells by sustained high metabolic rate. Snow buntings were kept outside in an open wire cage at Point Barrow, Alaska, during the whole winter. These birds had a critical temperature of 0° and nevertheless spent several months at − 20° or lower. They normally migrate south in the winter.

In humans the critical temperature is only known for the white man and is about 27°. In spite of much recent work on the Eskimo this, his most fundamental index of overall temperature adaptation, has not been determined. Neither has the microclimate inside his clothing or sleep-

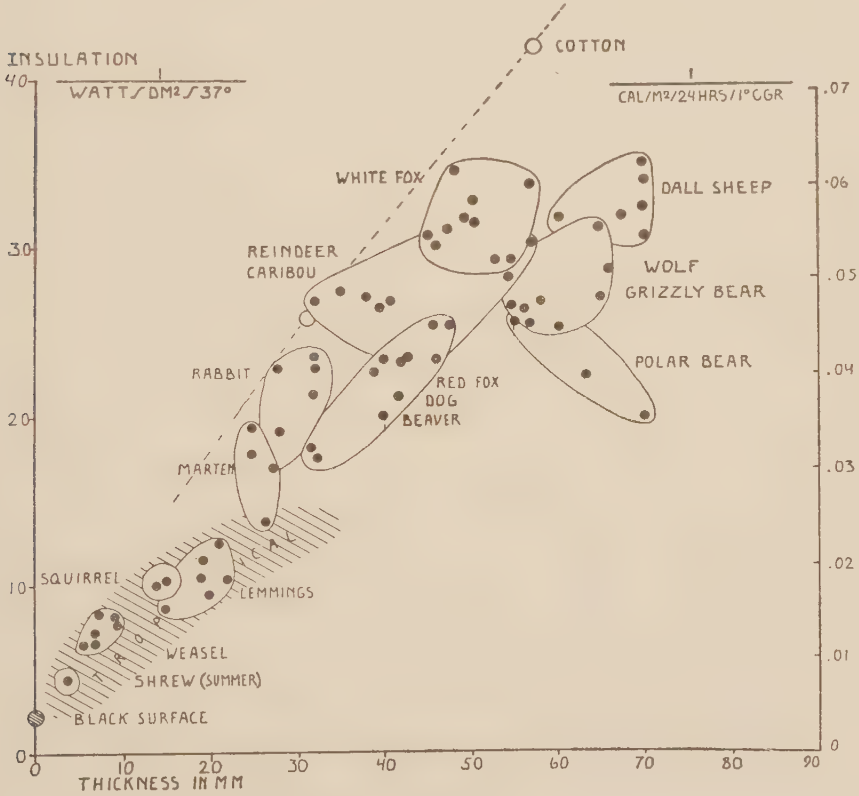

FIG. 2. Insulation of winter fur from arctic and tropical mammals. (Modified from Scholander, Walters, Hock, and Irving, 1950.)

ing bags been defined, but it is most likely as warm as ours. At least, his mittens, footwear and other clothing are excellent and sufficient to keep us warm. The really cold people, such as the Tierra del Fuegians of former days, or the Australian aborigines, have not been tested conclusively. Hicks, Moore, and Eldridge (1934) found that the Australians were able to rest at a basal heat production naked at 0° air temperature, but as they were surrounded by little fires their environmental temperature is unknown (Goldby, Hicks, O'Connor and Sinclair, 1938).

How have the observed great differences in the critical temperature come about? There are two major avenues available. One is the increase in body insulation as we go towards colder climates; another is an adaptation of extremities and other peripheral parts to tolerate, and remain functional at, low tissue temperatures, sometimes even approaching zero degrees.

Body Insulation

Measurement of the body insulation of mammals from the tropics to the arctic, on detached pieces of fur taken from the trunk, shows that it increases from warmer to colder climates (fig. 2). In arctic mammals the trunk insulation increases from the shrew to the rabbit, but from then on as the animals get bigger the insulation remains approximately constant (fig. 3). In the same environment a 5 kg hare or fox has about the same insulation as a 500 kg moose. For these animals the body-to-air gradient is the same, and hence the heat transfer per surface area should be about the same. This may be derived independently from the fact that the resting metabolic rate of a mammal is in general roughly proportional to the ¾ power of the weight (Brody and Procter, 1932; Brody, 1945; Kleiber, 1932, 1947). This makes it close enough to be proportional also to the ⅔ power of the weight, which is the relationship the surface area bears to weight. We should therefore not be surprised to find about the same insulation in all of the larger arctic species, including fur-clad man.

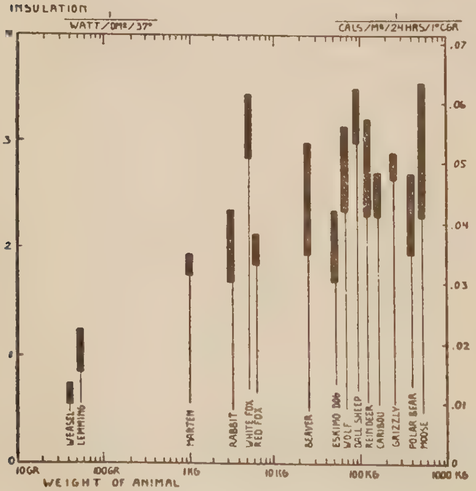

Fig. 3. Insulation of the winter fur versus size of arctic mammals. (From Scholander, Walters, Hock, and Irving, 1950.)

The non-adaptability of the resting rate shows that the heat production is not determined by the heat loss, as one might infer from the surface law of Rubner (1883), but vice versa. Whatever the surface area happens to be, the heat loss from it must be so regulated by various means that it balances the heat production. In a homeotherm one might say that body temperature plays the first violin, metabolic rate the second, and heat loss the third. The surface area is but one of the several factors which determine the heat loss.

In tropical animals the body insulation varies from almost complete nakedness to a sizeable amount of fur. A tropical sloth has a fur on its trunk as warm as that of an arctic lemming. This somewhat astounding fact is undoubtedly linked up with the very low metabolic rate of the sloth, which is no more than half of that of an ordinary mammal.

Adaptation in Peripheral Parts

It was shown that an arctic mammal like the husky or fox may sleep on the snow at − 40° at a resting metabolic rate (fig. 1). This is possible because of the very high overall body insulation. If this animal were to get up and run, let us say on a warm sunny winter day, it would have to increase suddenly its heat dissipation by some 10 to 20 times, in order not to heat up. Such a latitude in heat dissipation cannot be accomplished through the dense, thick body fur, but is achieved by other means. All arctic mammals and birds present a conspicuously uneven insulation. The extremities and face are generally very poorly insulated; in most mammals this is also true for the belly. A caribou, reindeer, or mountain sheep has three to five times less insulation on the legs than on the trunk (Scholander, Walters, Hock, and Irving, 1950).

It is a reasonable assumption that these poorly insulated parts, when warmed by increased circulation, would serve as essential avenues for an increased heat loss. Penguins and seals when out of water may keep their feet and flippers very hot, and seals are known to have an extremely efficient vasomotor control in the flippers (Scholander, 1940; Irving, Scholander, and Grinnell, 1942). Arctic sea gulls (*Larus glaucus*) avoid freezing their legs in subzero weather by increased circulation (Scholander, Walters, Hock, and Irving, 1950). Panting and exposure of the tongue are other well known avenues for increased heat dissipation.

When heat must be conserved the bare areas or parts may cool very considerably. This has been shown by measuring the leg temperature in many arctic mammals and birds (Irving, 1951). In cold weather reindeer and huskies and other arctic mammals and birds maintained their legs at 10° C. or even lower for prolonged periods. When resting, the animals usually coil up, shielding the bare parts from the cold.

Many species of more or less aquatic mammals and birds keep their naked feet, and sometimes the tail, in ice water for a long time. We may mention ducks, sea gulls, penguins, wading birds, whales, seals, beavers, muskrats, otters, moose and others. Some of these have greatly expanded flukes, fins, flippers or webbed feet. Temperature records from these structures are few. Irving found, however, that the feet of sea gulls (*Larus argentatus* and *L. glaucescens*) may be kept near zero degrees (Chatfield, Lyman, and Irving, 1953). When the feet of an arctic gull (*L. glaucus*) were kept in a thermous bottle of ice water their caloric output over two hours was only 1.5% of the basal rate of the bird. (Scholander, Walters, Hock, and Irving, 1950). From the handling of subarctic porpoises (*Phocaena*) in cold water and young arctic seals (*Cystophora*) in ice water it is known that their flukes or flippers may keep close to the water temperature (personal observations). It would be difficult to conceive how much animals could remain warm if they had to keep these expanded and thin organs at body temperature in the ice water.

As a corollary to the conspicuously low temperature which we may find in peripheral parts the nerves in the cold tolerant legs of a herring gull were found to conduct impulses at temperatures so low as to render the nerves of a hen's leg useless (Chatfield, Lyman, and Irving, 1953).

VASCULAR HEAT EXCHANGERS

Many mammals and birds show a vascular pattern in the extremities or other peripheral parts which may be interpreted as an adaptation to heat conservation. Claude Bernard (1876) considered that some of the heat from the arteries would be transmitted over to the cooler blood returning through the neighbor-

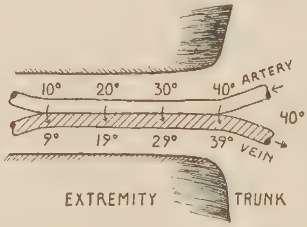

FIG. 4. Schematic presentation of arteriovenous counter current heat exchange in an extremity, resulting in a steep linear temperature gradient and consequent reduced peripheral heat loss.

ing veins. Bazett and his coworkers (1948) through numerous measurements in man showed that temperature gradients of as much as 3 degrees per decimeter could develop along a brachial or radial artery, mainly because of heat transfer from the artery across to the *venae commitantes.* The principle of operation of such a counter current exchange system will be seen from the diagram in figure 4.[2] The heat exchange system as we find it in man is a mere rudiment compared to those we find in many mammals and birds. The multichannel arteriovenous *rete* systems to be described below are by physical necessity heat exchangers and economizers of the body heat. Whether or not this is their primary or sole function is another matter.

In the manatee the flippers and tail are supplied with blood through a bundle of hundreds of arteries and veins intermingled in a *rete* (Murie, 1872; Fawcett, 1942). Fan-shaped arteriovenous bundles are prevalent in the peripheral structures of seals (Zuckerkandl, 1894; Müller, 1904; and personal observations). The tail and flippers of whales are supplied through arterio-venous *retes* (Stannius, 1841; Wilson, 1879; Braun, 1905; Slijper, 1936; Fawcett, 1942). The arteries in the tail fluke are surrounded by venous channels (personal observations). The capybara and to less extent the nutria, amphibious rodents of South America, have arteriovenous *retes* in the legs (Müller, 1904).

Penguins have an arterial *rete* in the axilla suggestive of heat exchange with the veins, which are fewer in number (Watson, 1883; Müller, 1908). Tall wading birds like cranes, herons, flamingos have tarsial arterio-venous *retes,* as have also several long-legged land birds (Hyrtl, 1863). Sea or lake waters are cooling even in the tropics, considering that the cooling power of water is some 20 to 50 times that of air of the same temperature.

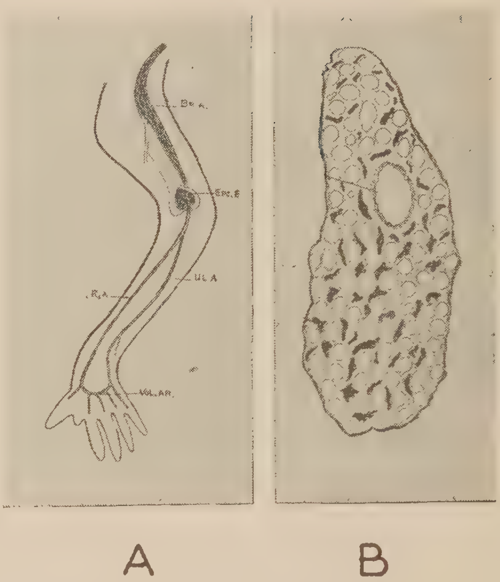

Fig. 5. A. Arm of loris (*Loris lyddekerianus*) with brachial vascular bundle. B. Section of the hind leg bundle; arteries white, veins black. (From Rau and Rao, 1930.)

Many terrestrial tropical mammals have arterio-venous bundles running out into the extremities and tail instead of, or in addition to, the conventional single arteries with their *venae* commitantes (fig. 5). The most striking development of such bundles or *retes* is found in sloths, anteaters, armadillos, pangolins, loris, tarsiers, and monotremes (Hyrtl, 1853, 1854; Zuckerkandl, 1894, 1895, 1907; Leche and Göppert, 1902–1906; Müller, 1904; Wislocki, 1928; Rau and Rao, 1930; Wislocki and Straus, 1932; Davies, 1947). Of these animals the sloth is known to be extremely temperature sensitive, and at times it may well need to keep its long arms and legs at a low reptilian temperature to be able to keep the trunk warm. Its resting metabolic rate is only half that of an ordinary mammal (Scholander, Hock, Walters, and Irving, 1950).

---

[2] The theory for a multi-channel counter current exchange system of this sort has been elaborated for the *rete mirabile* of the swimbladder of deep sea fishes. Here an oxygen gradient of some 100–200 atmospheres is maintained across the swimbladder wall, and the *rete* can be calculated to cut down the oxygen tension of the leaving blood to only a few millimeters of mercury (Scholander, 1954).

Monotremes are normally very temperature sensitive in their metabolic response to cold and have a low metabolic rate (Martin, 1902). The loris are very sluggish animals.

Other animals, such as ducks, geese, swans, sea gulls, have not been found to have macroscopic heat exchangers in their legs (Hyrtl, 1863), although one might well at first thought expect that they would need them. Irving found a steep temperature gradient below the feathered part of the leg in a sea gull (*L. glaucescens*) suggestive of a vascular heat exchange mechanism (Chatfield, Lyman, and Irving, 1953).

In any attempt to evaluate the thermal significance of the *retes,* one must remember that in well insulated animals, like the fox, which is capable of sleeping on the snow at −40°, there may arise a serious problem of heat dissipation, when the weather turns warm, or when the animal is running. Where heat conservation is the main problem one might find vascular heat exchangers; where heat dissipation is the more important point one might not find them. Final evaluation of the thermal significance of these striking structures must of course await experimental measurements. At all events the extremities and sometimes the tail and other bare parts of the body are essential for the heat regulation in northern species and show very significant adaptations to climate.

BERGMANN'S AND ALLEN'S RULES

In the above brief outline of known physiological pathways in the phylogenetic adaptation to hot and cold climates no mention is made of the possible importance of the overall size of the animal. Neither is there any reference to the absolute or relative size of the protruding parts such as legs, tail, and ears. Behind both Bergmann's and Allen's rules lies the idea that as we go to colder environments the surface of animals relative to weight should become reduced, bringing about a decrease in heat loss. These rules are conceived as applicable primarily on a sub-species level. (Compare Goldschmidt, 1940; Huxley, 1943.) There are two aspects here which are of interest to us: To what extent are clines of this sort of general occurrence, and what evidence is there that they are caused by a physiological response to cold?

To the first question one may point out that there is disagreement as to whether these clines constitute clear trends. Rensch (1936) is the chief proponent of the validity of the rules, whereas Reinig (1939) denies them, finding size clines radiating more or less in any direction from a common distribution center. Well-known cases where size increases southwards are among many others, the puma, the racoon and the otter (Allen, 1906). The rules evidently are not entirely above debate. For the physiological interpretation of established cases this does not matter a great deal, inasmuch as the basic measurements are often thermally irrelevant or reveal differences so small that they cannot be appraised.

The Biometrical Data. In the arguments for the validity of Bergmann's and Allen's rules Rensch has, for example, made use of data from Ridgeway's "The Birds of North and Middle America" (1904–1914). The measurements are based on dried museum skins. The size is taken as the wing length, which is the length from the wrist bend to the tip of the longest primary. There are a few short finger bones in this measurement, the rest is just wing feathers. These measurements may correlate with flight but bear no useful thermal significance. If we consider a five millimeter's difference in length of these feathers as thermally uninterpretable we find that 16 subspecies pairs out of a total of 43 have slightly longer feathers going north. If we consider it uninterpretable whether the tarsus is 30% or 32% of the length of the wing feathers then also Allen's rule disappears from physiology.

Rensch also compared subspecies pairs of southern and northern mammals based on skin measurements given in Anthony's "Field Book of North American Mammals" (1928). In a series of 30 pairs 80% of the subspecies were longer in the north; in a similar series of European forms 60% were longer in the north. The length difference was mostly less than 10%. The relative length of feet and tail versus body length was often a trifle smaller in the northern form of a pair. The correlation was considered positive at a difference of only 0.2% (i.e., 20.0% instead of 20.2%).

Physiological Significance. If, contrary to the view of Reinig, the slight biometrical trends found by Rensch are taken to reflect a general tendency, what is the evidence that they represent a physiological adaptation to temperature?

Exposure and resulting adaptation to cold do, of course, affect the whole population of northern mammals and birds. From a purely physiological standpoint, if relative surface reduction were a point of general adaptive importance, we should expect this to modify the animals not only on a subspecific level, but the whole northern warm-blooded fauna should by convergence tend towards large globular species. This quite obviously is not so. In some of the coldest areas on earth, the great northern Canadian and Siberian forests, there is a wide variety of sizes and shapes in both birds and mammals. There are little birds with naked legs thinner than match sticks, such as redpolls and chickadees, there are tiny shrews and mice, there are long-tailed foxes, long-legged, long-eared mammals, like the moose and deer. Some of the mammals of the cold forests or tundra have a considerable expanse of horns.

In the icy polar lakes and seas swim mammals and birds, such as whales, seals, and penguins, not with surface-saving, reduced extremities but with legs or tail naked and expanded into swimming surfaces. We also find numerous wading birds walking about with their tall, thin legs in ice water. Nowhere are extremities so regularly exposed to more severe chilling. Yet here we find no tangible evidence that the size of the surface area, absolute or relative, is in any way a critical factor in arctic or northern phylogenetic adaptation.[3] The prime point is *conservation of heat,* true enough, but in this the size of the surface area of the animal is of minor importance, at best. The factors that count are the *thermal properties of the surface*—its insulation, its exposure, its vascularization, and its ability to tolerate a cold tissue temperature. Poorly insulated and expanded areas do not disappear but are essential adjuncts in heavily insulated animals which ensure sufficient latitude in the heat regulation.

In the tropics the assortment of mammals and birds is similar to that in the arctic, but less well insulated. There are tiny birds and large ones, tiny mammals and large ones, some chubby and stocky like the rhinoceros, others long and lanky like the giraffe.

We are unable to see any evidence that the surface area as such has played a detectable role in the phylogenetic engineering of warm-blooded animals for hot and cold climates. The heat loss from the available surfaces, as a function of their insulation, their exposure and their surface temperature, drowns out in importance the numerical value of the areas.[4]

We may conclude that there is no physiological evidence to indicate that those cases of subspecific clines which accord with Bergmann's and Allen's rules are the result of a heat-conserving adaptation. One must be open for other interpretations. Cold climates do not produce a fauna tending towards large-sized globular forms with small protruding parts. The phylogenetic adaptation to heat conservation in the arctic took place through other means, which have been measured, which are understood, and which apply to every individual of every species.

---

[3] The hopeless inadequacy of cold adaptation via Bergmann's rule may be seen by the following consideration. Take a body-to-air gradient in the tropics of 7° and in the arctic of 70°, i.e., a tenfold increase. A tenfold greater cooling in the arctic animal is prevented by covering the surface with fur a few centimeters thick. A relative surface reduction of ten times would require a weight increase of the animal of one thousand times.

[4] For these same reasons it is conceptually an unfortunate custom to express basal or resting metabolic rate as per surface area.

Bergmann's and Allen's Rules Applied to Man

Hardly anywhere have these "rules" been taken more seriously than in modern anthropology. Coon, Garn and Birdsell (1950) in their stimulating book "Races. A Study of the Problems of Race Formation in Man" take the racial features of many people to be the result of an interaction between the climate and the surface area of man.

The stockiness and relatively short extremities found in many Eskimos are interpreted as the result of cold, working through generations on the hands and feet of these people, giving short-limbedness a selective advantage. Similarly the Mongolian face has been engineered by the cold wind and weather. This is evidently based on the concept that the Eskimo is a people perpetually shivering from cold. As already mentioned, there are no measurements to substantiate such an idea. They are clever in clothing. You are warm when you stay with them and when you use their mittens and leg wear. Furthermore, it would seem that tall Eskimos could easily cheat evolution out of shortening arms and legs simply by getting long enough sleeves on their parkas and long enough legs on their pants. Extra mittens and socks could also be had if needed. Where then would be the stimulus to drive the selection?

If subjected to a suitable cold stress, circulation will improve in our hands and feet so that they may remain warm and functional at an exposure which would render unadapted digits numb and useless (Balke, Cremer, Kramer, and Reichel, 1944; Carlson, Burns, Holmes, and Webb, 1953). In Eskimos adapted hands remain conspicuously well circulated and warm on cold exposure (Brown and Page, 1952, and personal observations in the field). This is a heat-wasting tropical type of emergency reaction. In sharp contrast to this we have the heat-preserving, cold, but functional extremities of arctic mammals and birds. This ultimate adaptation evolved in animals compelled to submit to the environment. In the Eskimo the main adaptation lies not in physiology, but in an age-long experience and technical skill in ducking the cold. They conquered the arctic not by submitting to it but by surrounding themselves successfully with a little piece of the same tropical microclimate upon which we also depend.

As the opposite of the allegedly cold-engineered Eskimos the tall Tuaregs of the hot and dry Sahara have been cited, and with them the Australian aborigines. Several tribes of the latter were studied by Hicks, Moore, and Eldridge (1934), who observed that these *naked* people expose themselves seasonally to very low, even freezing, temperatures, something neither we nor an Eskimo would ever venture to do naked. This certainly confuses the idea that the Eskimo features are a result of cold exposure and the Australian features a result of heat exposure. There is hardly any valid evidence from physiology that the surface area as such, in man or beast, is a factor of general morphogenic importance in the evolution of races inhabiting hot or cold climates.

Summary

Mammals and birds have the same body temperature in hot and cold climates, and within the same weight range they have roughly the same basal heat production per unit weight. This leaves them with *heat dissipation* as the only main avenue for climatic thermal adaptation. The lowest air temperature at which a mammal or bird can rest at a basal heat production, maintaining its body temperature, is the critical temperature. This is 25–27° in naked man and in many tropical species, and − 40° in the larger arctic species, and is a fundamental measure of the overall climatic thermal adaptation. The major reason for the low critical temperature in the arctic species is the heavy body insulation provided by fur or feather coats, combined with an outstanding tolerance of low tissue temperature (often near 0°) in poorly insulated peripheral parts such as legs, tail and face. There are good indications that arctic species depend upon vascular control of these poorly insulated parts for heat dissipation. Without them they would over-heat during exercise when the heat output may be increased 10–20 times over the resting rate. Aquatic species, especially, expose their naked feet, fins or tail to the most severe chilling in ice water. Yet these organs are usually thin and greatly expanded for swimming. In many arctic and tropical species cold extremities, and consequently low heat loss, are assured by arterio-venous counter current heat exchangers at the base of the limbs or tail. In spite of the low temperature which may prevail in the extremities when the animal needs heat conservation, these organs are fully functional.

There is no physiological evidence, in beast or man, that the minor and erratic subspecific trends expressed in Bergmann's and Allen's rules reflect phylogenetic pathways of heat-conserving adaptation. Arctic species do not tend towards large spheres with reduced extremities and tail. The phylogenetic adaptations which have taken place are fairly well known in their main physiological aspects, as outlined above. They are major and general, as is the stimulus of the climate, and they know no taxonomic barriers.

Literature Cited

Allen, J. A. 1906. The influence of physical conditions in the genesis of species. Ann. Rep. Smithsonian Inst. (1905), pp. 375–402.

Anthony, H. E. 1928. Field Book of North American Mammals. G. P. Putnam's Sons, New York.

Balke, B., H. D. Cremer, K. Kramer, and H. Reichel. 1944. Untersuchungen zur Kälteanpassung. Klin. Wochenschr., **23**: 204–210.

Bazett, H. C., L. Love, M. Newton, L. Eisenberg, R. Day, and R. Forster, II. 1948. Temperature changes in blood flowing in arteries and veins in man. Jour. Applied Physiol., **1**: 3–19.

Bazett, H. C., E. S. Mendelson, L. Love, and B. Libet. 1948. Precooling of blood in the arteries, effective heat capacity and evaporative cooling as factors modifying cooling of the extremities. Jour. Applied Physiol., **1**: 169–182.

Benedict, F. G. 1938. Vital energetics. Carnegie Inst. Washington Publ. no. 503.

Bergmann, C. 1847. Ueber die Verhältnisse der Wärmeökonomie der Thiere zu ihrer Grösse. Göttinger Studien, pt. 1, 595–708.

Bernard, C. 1876. Leçons sur la chaleur animale. Libr. J.-B. Baillière et Fils, Paris.

Braun, M. 1905. Einiges über *Phocaena communis* Less. Zool. Anz., **29**: 145–149.

Brody, S. 1945. Bioenergetics and Growth. Reinhold Publ. Corp., New York.

Brody, S., and R. C. Procter. 1932. Relation between basal metabolism and mature body weight in different species of mammals and birds. Univ. Missouri Agr. Exper. Sta. Res. Bull., **166**: 89–101.

Brown, G. M., and J. Page. 1952. The effect of chronic exposure to cold on temperature and blood flow of the hand. Jour. Applied Physiol., **5**: 221–227.

Carlson, L. D., H. L. Burns, T. H. Holmes, and P. P. Webb. 1953. Adaptive changes during exposure to cold. Jour. Applied Physiol., **5**: 672–676.

Chatfield, P. O., C. P. Lyman, and L. Irving. 1953. Physiological adaptation to cold of peripheral nerve in the leg of the herring gull (*Larus argentatus*). Amer. Jour. Physiol., **172**: 639–644.

Coon, C. S., S. M. Garn, and J. R. Birdsell. 1950. Races. A Study of the Problems of Race Formation in Man. Charles C. Thomas, Springfield, Ill.

Davies, D. V. 1947. The cardiovascular system of the slow loris (*Nycticebus tardigradus malaianus*). Proc. Zool. Soc. London, **117**: 377–410.

Fawcett, D. W. 1942. A comparative study of blood-vascular bundles in the Florida manatee (*Trichechus latirostris*) and in certain cetaceans and edentates. Jour. Morph., **71**: 105–133.

Goldschmidt, R. 1940. The Material Basis of Evolution. Yale Univ. Press, New Haven.

Hicks, C. S., H. O. Moore, and E. Eldridge. 1934. The respiratory exchange of the Australian aborigine. Australian Jour. Exper. Biol. Med. Sci., **12**: 79–89.

Huxley, J. 1943. Evolution. The Modern Synthesis. Harper and Bros., New York.

Hyrtl, J. 1853. Beiträge zur vergleichenden Angiologie. IV. Das arterielle Gefäss-System der Monotremen. Denkschr. K. Akad. Wissensch., Math.-Naturwiss. Classe, Wien, vol. 5, Abth. 1, 1–20.

Hyrtl, J., 1854. Beiträge zur vergleichenden Angiologie. V. Das arterielle Gefäss-System der Edentaten. Denkschr. K. Akad. Wissensch., Math.-Naturwiss. Classe, Wien, vol. 6, Abth. 1, 21–64.

Hyrtl, J. 1863. Neue Wundernetze und Geflechte bei Vögeln und Säugethieren. Denkschr. K. Akad. Wissensch., Math.-Naturwiss. Classe, Wien, **22**: 113–152.

Irving, L. 1951. Physiological adaptation to cold in arctic and tropic animals. Fed. Proc., Amer. Soc. Exper. Biol., **10**: 543–545.

Irving, L., and J. Krog. 1954. Body temperatures of arctic and subarctic birds and mammals. Jour. Applied Physiol., **6**: 667–680.

Irving, L., P. F. Scholander, and S. W. Grinnell. 1942. The regulation of arterial blood pressure in the seal during diving. Amer. Jour. Physiol., **135**: 557–566.

Johnson, H. M. 1951. Preliminary ecological studies of microclimates inhabited by the smaller arctic and subarctic mammals. Science in Alaska, 1951. Proc. Second Alaska Sci. Conf., Alaska Div. AAAS, pp. 125–131.

Kleiber, M. 1932. Body size and metabolism. Hilgardia, **6**: 315–353.

Kleiber, M. 1947. Body size and metabolic rate. Physiol. Rev., **27**: 511–541.

Leche, W., and E. Göppert. 1902–1906. Das Gefässsystem. *In* H. G. Bronn, Klassen und Ordnungen des Thier-Reichs, vol. 6, Abt. 5, Buch 5, Teil 1, 1171–1330.

Martin, C. J. 1902. Thermal adjustment and respiratory exchange in monotremes and marsupials.—A study in the development of homoeothermism. Phil. Trans. Roy. Soc. London, ser. B, **195**: 1–37.

Morrison, P. R., and F. A. Ryser. 1952. Weight and body temperature in mammals. Science, **116**: 231–232.

Müller, E. 1904. Beiträge zur Morphologie des Gefässsystems. II. Die Amarterien der Säugetiere. Anat. Hefte, **27**: 71–241.

Müller, E. 1908. Beiträge zur Morphologie des Gefässsystems. III. Zur Kenntnis der Flügelarterien der Pinguine. Anat. Hefte, **35**: 553–648.

Murie, J. 1872. On the form and structure of the manatee (*Manatus americanus*). Trans. Zool. Soc. London, **8**: 127–202.

Rau, A. Subba, and P. Krishna Rao. 1930. Contributions to our knowledge of the anatomy of the Lemuroidea. I. Arterial system of *Loris lyddekerianus*. Half-Yearly Jour. Mysore Univ., **4**: 90–121.

Reinig, W. F. 1939. Besteht die Bergmannsche Regel zu Recht? Arch. Naturgesch., N.F., **8**: 70–88.

Rensch, B. 1936. Studien über klimatische Parallelität der Merkmalsausprägung bei Vögeln und Säugern. Arch. Naturgesch., N.F., **5**: 317–363.

Ridgeway, R. 1904–1914. The birds of North and Middle America. Bull. U. S. Natl. Mus. no. 50, pts. 2–6.

Rubner, M. 1883. Ueber den Einfluss der Körpergrösse auf Stoff-und Kraftwechsel. Zeitschr. Biol., **19**: 535–562.

Scholander, P. F. 1940. Experimental investigations on the respiratory function in diving mammals and birds. Hvalraadets Skr. no. 22.

Scholander, P. F. 1954. Secretion of gases against high pressures in the swimbladder of deep sea fishes. II. The *rete mirabile*. Biol. Bull., **107**: 260–277.

Scholander, P. F., R. Hock, V. Walters, and L. Irving. 1950. Adaptation to cold in arctic and tropical mammals and birds in relation to body temperature, insulation, and basal metabolic rate. Biol. Bull., **99**: 259–271.

Scholander, P. F., R. Hock, V. Walters, F. Johnson, and L. Irving. 1950. Heat regulation in some arctic and tropical mammals and birds. Biol. Bull., **99**: 237–258.

Scholander, P. F., V. Walters, R. Hock, and L. Irving. 1950. Body insulation of some arctic and tropical mammals and birds. Biol. Bull., **99**: 225–236.

Slijper, E. J. 1936. Die Cetaceen vergleichend-anatomisch und systematisch. Capita Zool., vol. 7.

Stannius, H. 1841. Ueber den Verlauf der Arterien bei *Delphinus phocaena*. Arch. Anat., Physiol. Wissensch. Med., 379–402.

Watson, M. 1883. Report on the anatomy of the Spheniscidae collected during the voyage of H.M.S. Challenger. Rep. Sci. Results Voyage H.M.S. Challenger, Zool., vol. 7, pt. 18.

Wilson, H. S. 1879. The *rete mirabile* of the narwhal. Jour. Anat. Physiol., **14**: 377–398.

Wislocki, G. B. 1928. Observations on the gross and microscopic anatomy of the sloths (*Bradypus griseus griseus* Gray and *Choloepus hoffmani* Peters). Jour. Morph., **46**: 317–397.

Wislocki, G. B., and W. L. Straus, Jr. 1932. On the blood vascular bundles in the limbs of certain edentates and lemurs. Bull. Mus. Comp. Zool., **74**: 1–15.

Zuckerkandl, E. 1894. Zur Anatomie und Entwickelungsgeschichte der Arterien des Vorderarmes (1. Teil). Anat. Hefte, **4**: 1–98.

Zuckerkandl, E. 1895. Zur Anatomie und Entwickelungsgeschichte der Arterien des Unterschenkels und des Fusses. Anat. Hefte, **5**: 207–291.

Zuckerkandl, E. 1907. Zur Anatomie und Morphologie der Extremitatenarterien. Sitzungsber. K. Akad. Wissensch., Wien, Math.-Naturwiss. Klasse, vol. 116, Abt. 3, 459–730.

Contribution No. 756

Reprinted from BIOLOGICAL BULLETIN, Vol. 108, No. 2, 175–181, April, 1955
Printed in U. S. A.

VARIATIONS IN TEMPERATURE AND LIGHT RESPONSE WITHIN A PLANKTON POPULATION

HILARY B. MOORE

The Marine Laboratory, University of Miami,[1] *Coral Gables 34, Florida*

Zooplankton tends to concentrate about a particular depth, this depth being characteristic of certain external conditions, of the species concerned, and frequently also of the stage of maturity and brood of the organism. Diurnal and seasonal rhythms in external conditions are frequently reflected in vertical migrations of the animals, and geographical gradients in such factors as light and temperature have been shown to be associated with correlated changes in the vertical distribution of the species concerned. There is an extensive literature on the subject, that part pertaining to the Crustacea having been well reviewed by Cushing (1951). He describes also the experiments on tropisms, taxes, etc., which have been made in an attempt to understand the behavior observed in the field. Although widely differing and sometimes contradictory results have been obtained by different workers, it appears that such differences are characters of particular species rather than of whole groups. So far as it is possible to visualize a typical copepod, etc., it appears that the general pattern of behavior is much the same at least in copepods, chaetognaths, siphonophores and pteropods (Moore *et al.,* 1953). With the exception of larval fishes, which rarely exhibit diurnal migration, it is probable that the principles are generally applicable to such zooplankton as are capable of vertical movements.

Cushing shows how light and temperature are generally accepted as the major environmental factors controlling vertical distribution, with only a minor part played by salinity, CO_2 and other factors. There are many instances where, during most of the 24 hours, the plankton migrates vertically as if it were following a level of optimal illumination. On the other hand, there are instances of a thermocline proving a barrier to the vertical movement of a species, and the upper or lower limits of some species have been shown to follow closely the seasonal movements of particular isotherms (Nikitine, 1929). Vertical movements in response to light and temperature stimuli have been demonstrated experimentally, although the results sometimes appear to conflict with observations of natural behavior. It has also been shown that the nature of the response to light may be modified by the temperature.

Laboratory experiments, at least with marine zooplankton, suffer from the difficulty of reproducing natural conditions. Comparatively few marine zooplankton have been successfully kept for any long period in the laboratory. The ecologist has the uncomfortable feeling that the more successful laboratory species are the least typical, and can be reared only because of this. There are factors such as food, previous treatment, internal rhythms and others which may well modify behavior. On the other hand, any attempt to analyze behavior under natural conditions suffers from the large number of simultaneously varying factors, none of which can be controlled. It has the advantage, though, that the animals may be assumed to be behaving typically, and that, particularly in the tropics, a large number of species may be studied, so that the pecularities of atypical species will not seriously affect the observations. The present paper is a study of the relative responses to temperature and light of some zooplankton in the Florida Current, and how these vary in a vertical section through the plankton population.

---

[1] Contribution No. 756 from Woods Hole Oceanographic Institution; Contribution No. 137 from the Marine Laboratory, University of Miami.

Material and Methods

The material was collected in a region of the Florida Current lying from ten to forty miles east of Miami, Florida. This is ocean water with isotherms sloping very steeply across the current so that a wide range of temperatures is available at any depth. Seasonal variations in the current pattern and velocity result in a wide range in conditions at any one station throughout the year. An account of the hydrographic conditions at the ten mile station has already been published by Miller *et al.* (1953) and the methods used in collecting plankton were described in the same paper. The material was drawn from samples, collected for other purposes, in part under a joint program of the Marine Laboratory of the University of Miami and the National Geographic Society, and in part by the Marine Laboratory under contract number NObsr-57146 for the Office of Naval Research. The analyses were carried out under the latter contract and under Bureau of Ships contract number NObsr-43270 at Woods Hole Oceanographic Institution. The siphonophore examination was carried out in part by the author and in part by D. C. Roane (1954). The chaetognaths were examined by H. Owre and her results will be included in a doctorate thesis at the University of Michigan. To all of these the author wishes to express his indebtedness.

The present work is restricted to the period within about two hours either side of noon, when the illumination is not changing rapidly, and it is assumed that the plankton has had time to stabilize at the depth at which it is found. Vertical temperature sections were available for each station. The vertical distribution of illumination was calculated by methods previously used (Moore, 1950) and from these the depths of selected isotherms and isolumes were obtained. For each station, the percentage vertical distribution of each species was calculated as follows. First, the count from each of the oblique net hauls was scaled to the equivalent of a tow of one mile, the factor being obtained from the trace on the depth-distance recorder towed along with the nets. Each count was assumed to be applicable to a column of water reaching from half way between the mid-depth of that tow and the mid-depth of the tow above it to half way to mid-depth of the tow below it. The top tow was assumed to terminate at the surface, and the lowest at the deepest point shown on its trace. Integration of the whole column was performed by multiplying each count by the length of water column to which it applied, and adding the products. By the use of a calculating maching, the levels were found corresponding to 10%, 20%, etc., of this total. These, referred to as the 10% level, etc., are the depths above which this percentage of the species occurred on the particular occasion. Values from 10% to 90% were calculated, but the 0% and 100% levels were not sufficiently clearly defined to be usable.

The following species, used in previous work, were present in sufficient numbers to be significant. It should be noted that, with the inclusion of more stations, some of the regressions obtained differ from ones previously quoted.

SIPHONOPHORA

Chelophyes appendiculata (Esch.)
Diphyes bojani (Esch.)
D. dispar Chamisso & Eysenhardt
Eudoxoides mitra (Huxley)
E. spiralis (Bigelow)
Abylopsis eschscholtzii Huxley
A. tetragona Otto.
Bassia bassensis (Quoy & Gaimard)

CHAETOGNATHA

Sagitta enflata Grassi
S. hexaptera D'Orb.
S. lyra Krohn
S. bipunctata Quoy & Gaimard
S. serratodentata Krohn
S. minima Grassi
S. decipiens Fowler
Pterosagitta draco (Krohn)
Krohnitta subtilis (Grassi)

The various species characteristically occupy different levels. In order that the data for the various species could be combined, the mean 10%, 20%, etc., levels were calculated for each species, these being the means of all stations. For each station, the results were then expressed as deviations from the mean on that occasion, a positive value being deeper, and a negative shallower. The deviation of a typical siphonophore on that occasion was the mean deviation for the eight species available, and that of a typical chaetognath was the mean for nine species. For comparison, the levels of the 15° C. isotherm and of the 10^{-2} isolume were similarly expressed as deviation from their respective means.

After testing for correlations between the deviations of the plankton and the isolume and isotherm, and finding that these were significant, partial regressions were calculated with the results shown in Figures 1 and 2. The regression coefficients show the extent of vertical movement of the plankton in relation to a one-meter shift in the 15° C. isotherm or 10^{-2} isolume. In all cases the coefficients are positive, that is to say, the plankton movement is in the same direction as the movements of the isotherm and isolume.

For simplicity it may be assumed that the temperature and light graphs in the above figures are straight lines. If the regressions of plankton movements on isotherm and isolume movements are referred to as temperature and light responses, then the regressions of the responses on percentage level can be calculated. From these, the levels occupied by the typical siphonophore or chaetognath may be predicted for any given hydrographic conditions for this region. As a verification of the goodness of fit between such predicted levels and those actually observed, six stations were selected which offered a particularly wide range of hydrographic conditions. Figures 3 and 4 show the comparison of the values from the 10, 50 and 90% levels as predicted and as observed. These cover a more than five-fold range of depth under different conditions, and the agreement appears to be good.

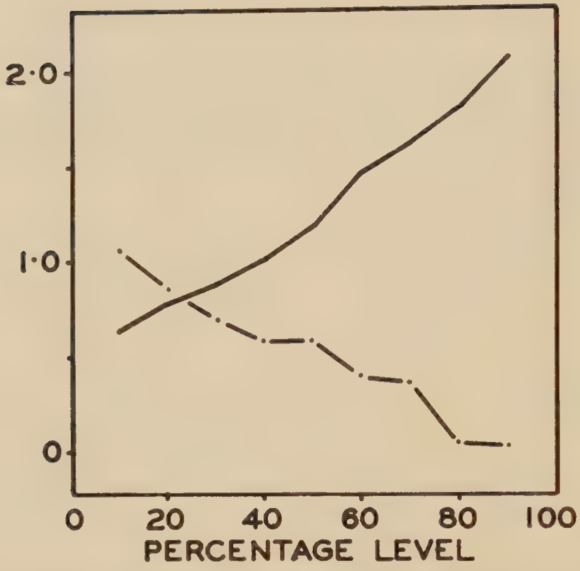

FIGURE 1. Typical siphonophores. Partial regression of plankton movement on movement of the 15° C. isotherm (whole line) and of the 10^{-3} isolume (broken line), and the variation of these regressions with percentage level; 0% represents the top, and 100% the bottom of the plankton column.

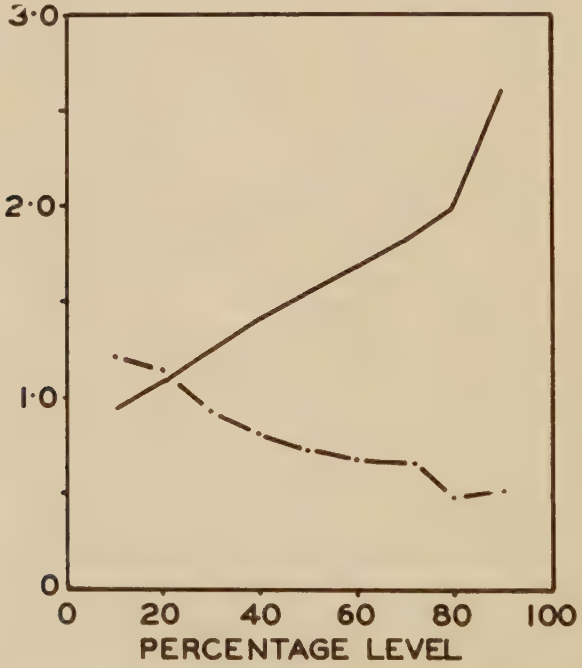

FIGURE 2. Typical chaetognath regressions indicated as in Figure 1.

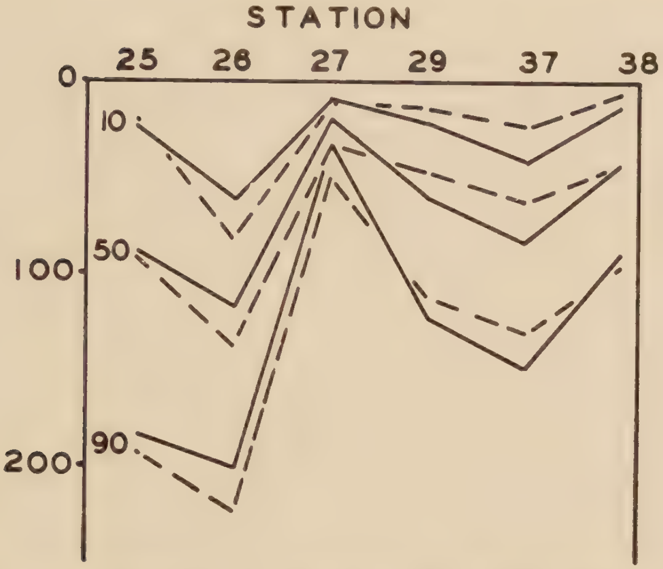

Figure 3. Typical siphonophore. Comparison of the observed depths, in meters, of the 10%, 50% and 90% levels at six stations (whole lines) with the depths predicted by the regressions referred to in the text (broken lines).

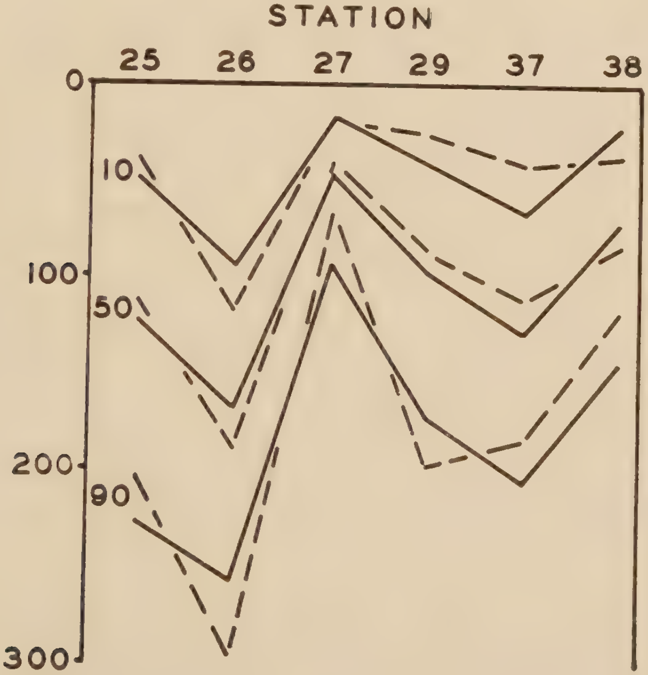

Figure 4. Typical chaetognath comparisons indicated as in Figure 3.

DISCUSSION

Cushing (1951) summarizes many examples of plankton whose day level varies on different occasions. Where these variations have been correlated with changes in an environmental factor, this has usually been illumination. The Florida Current provides an unusually wide range of temperature variation at depth, and so may be particularly advantageous for demonstrating the role of temperature. Further, most previous workers have been concerned with the level of maximum concentration of the plankton and have not differentiated between the behaviors of the shallower and deeper members of the population of a given species. In an earlier study (Moore, 1953; Moore *et al.*, 1953) in which considerably fewer data were available than in the present work it was shown that there was an increase in temperature response and a decrease in light response in the lower levels of the plankton as a whole. The same trend was indicated in the four separate groups studied, but many of the values could not be considered statistically significant. J. B. Lewis (in press) has studied the euphausids of this area, and shown that illumination plays the major part in controlling both day level and vertical diffuseness, with little or no demonstrable effect of temperature. Roane (1954) compared the average day level of a group of siphonophores at two stations in the Florida Current and found these to be 79 and 253 meters. The corresponding extinction coefficients were 0.062 and 0.051 while the depths of the 15° C. isotherms were 151 and 619 meters, respectively. It seemed probable that the great range in depth of the animals was associated with both illumination and temperature differences. The present work shows that the observed vertical distributions can be accounted for if both temperature and light play a part in regulation of level, and if it is assumed that their effects are additive.

Two characteristics of the graphs in Figures 1 and 2 call for explanation. The temperature and light responses change more or less linearly with percentage level, and the regressions of plankton movement on isotherm and isolume movement may have values well in excess of unity. The author has, so far, been able to find little information on how the nature or strength of a reaction varies among the individuals in an invertebrate population. The frequency distribution may perhaps be expected to follow either a symmetrical or a skewed normal curve. The latter is true in what is perhaps a parallel case, the variations in rate of hemolysis of red cells in a sample (Ponder, 1930, 1932). Too much reliance cannot be placed on the exact form of the present curves, and unfortunately the ends of the curves are lacking, even the 10% and 90% values probably being based on too small counts to have much significance. It seems clear, though, that they cannot represent a frequency distribution rising to a marked peak at any particular value. Subsequent work on single species suggests that they may, with more data available, prove to be flat-peaked curves. Another explanation of their shape lies in the probability that, as shown below, temperature and light are not sufficient alone to account for the observed behaviors, and a further environmental factor will have to be considered.

The extent to which the regression coefficients may exceed unity can hardly be attributed to error due to inadequate data. They indicate that the animals may respond to a change in depth of an isotherm or isolume by moving considerably further. In other words, although the movements of the animal are in such direction as could maintain them at a constant temperature or illumination, they do not, in fact congregate at the depth corresponding to such a constant value. Finally, very much poorer correlations are obtained if an attempt is made to relate the depth at which the animals are found to *in situ* temperatures and illuminations, than if the correlations are made between the depth changes of the animals, the isotherms and the isolumes. All this suggests that a third factor, related to depth, and which we tentatively suggest may be pressure, must be included in the complex. Although pressure has received much less consideration in this connection that the other two factors, there is some evidence that it may affect vertical movement of zooplankton (Hardy and Bainbridge, 1951).

The similarity of Figures 1 and 2 gives support to the statement already made that there may be a pattern of depth control mechanism typical of widely different animals. Within the species which we have grouped together, specific differences may be expected both in the strengths of the responses and in the relative response to light and temperature. Such would be in agreement with the very different behavior patterns observed in the many forms which have been worked with. We have found a marked difference in response in different parts of a population. There is no evidence as to whether this represents permanent differences among the individuals or whether it represents a sorting, resulting from varying responses, of individuals whose responses fluctuate continually. Differences between individuals may be expected, but so may changes in the reactions of a single individual. The latter might be more or less random, they might vary in relation to previous condition or to some control such as a feeding cycle, or they might vary with an inherent diurnal or other rhythm. Whatever may prove to be the case, a significant point seems to emerge in connection with the interpretation of experiments with plankton. Firstly, if the experimental animals are not always collected from the same part of the plankton column then differences may be expected in the nature of the experimental behavior. Secondly, experiments made with animals taken from the top or bottom of the population may yield results which are not applicable to the main concentration of the population.

LITERATURE CITED

Cushing, D. H., 1951. The vertical migration of planktonic crustacea. *Biol. Rev.*, **26**: 158–192.

Hardy, A. C., and R. Bainbridge, 1951. Effect of pressure on the behaviour of decapod larvae (Crustacea). *Nature*, **167**: 4244, 354–355.

Miller, S. M., H. B. Moore and K. R. Kvammen, 1953. Plankton of the Florida Current. I. General conditions. *Bull. Mar. Sci. Gulf and Caribbean*, **2**: 465–485.

Moore, H. B., 1950. The relation between the scattering layer and the Euphausiacea. *Biol. Bull.*, **99**: 181–212.

Moore, H. B., 1953. Plankton of the Florida Current II. Siphonophora. *Bull. Mar. Sci. Gulf and Caribbean*, **2**: 559–573.

Moore, H. B., H. Owre, E. C. Jones and T. Dow, 1953. Plankton of the Florida Current. III. The control of the vertical distribution of zooplankton in the daytime by light and temperature. *Bull. Mar. Sci. Gulf and Caribbean*, **3**: 83–95.

Nikitine, B., 1929. Les migrations verticales saisonnières des organismes planktoniques dans la Mer Noire. *Bull. Inst. Océanogr. Monaco*, **540**: 1–24.

Ponder, E., 1930. The form of frequency distribution of red cell resistances to saponin. *Proc. Roy. Soc. London, Ser. B*, **106**: 543–559.

Ponder, E., 1932. On certain correction terms required in the equations for the kinetics of simple haemolysis. *Proc. Roy. Soc. London, Ser. B*, **110**: 1–17.

Roane, D. C., 1954. A study of some siphonophores of the Florida Current. Thesis for Masterate at the University of Miami, 1–77.

Contribution No. 757

Särtryck ur Tellus nr 3, 1955

Salt Nuclei, Wind and Daily Rainfall in Hawaii

A. H. WOODCOCK[1] and W. A. MORDY[2]

(Manuscript received March 12, 1955)

Abstract

The discovery of large sea-salt particles at cloud levels led to the hypothesis that these particles act as nuclei on which raindrops initially form within clouds and to the suggestion that the amount of rainfall on an oceanic island might be a function of the number of the salt particles in the air. Exploratory observations of rain and airborne salt in Hawaii, which were intended to test this suggestion, are presented and discussed. These observations do not prove that greater numbers of salt nuclei are related to greater amounts of rain. They do, however, indicate that such a relationship may exist, and that additional field studies should be made which utilize the pertinent results of the present study.

Introduction

The presence of large sea-salt particles at cloud heights (Woodcock, 1952) and the recent theoretical indications of the possible role of large particles in the growth of raindrops by accretion (Bowen, 1950; Langmuir, 1948; Ludlam, 1951), caused us to suppose that the amount of rainfall from warm clouds might be related to the quantity of salt in the air. The physical basis for this supposition lies in the computations of the accretional growth of droplets made by Langmuir (1948). These computations show that large cloud drops should grow more rapidly than do smaller drops while falling through a cloud of much more numerous and smaller cloud droplets. The amount of water removed accretionally from clouds by drops falling through them might be expected, therefore, to be a function of the initial size of these drops and of the number, other relevant quantities being equal.

It seems most probable that the initially largest cloud drops form on the largest sea-salt nuclei, as indicated in the laboratory study of the condensational growth rates of sea-salt nuclei which was made by Keith and Arons (1954). Hence, it was thought that the amount of rain falling at a dominantly marine location might be related to the number of large salt nuclei in the air.

Ideas such as those sketched above led to the present study of the salt aerosols and the rainfall in Hawaii. It was felt that Hawaii would be a favorable marine location to test the rain-salt hypothesis, since the northeast trade-wind inversion tends to limit the vertical development of the clouds, producing more uniform cloud heights (Riehl, Yeh, Malkus, Laseur, 1951). A further factor in the selection of Hawaii for this study was the fact that U.S. Weather Bureau problems of forecasting shower rains had suggested that physical factors other than those routinely considered might be involved in the rain-forming processes (Anon, 1950).

---

[1] Contribution No. 757 of the Woods Hole Oceanographic Institution. This work was supported by the Office of Naval Research under contract Nonr-798 (00) (Nr-085-001).

[2] Meteorology Department, Pineapple Research Institute and Hawaiian Sugar Planters Association. Technical paper no. 232 of the Pineapple Research Institute.

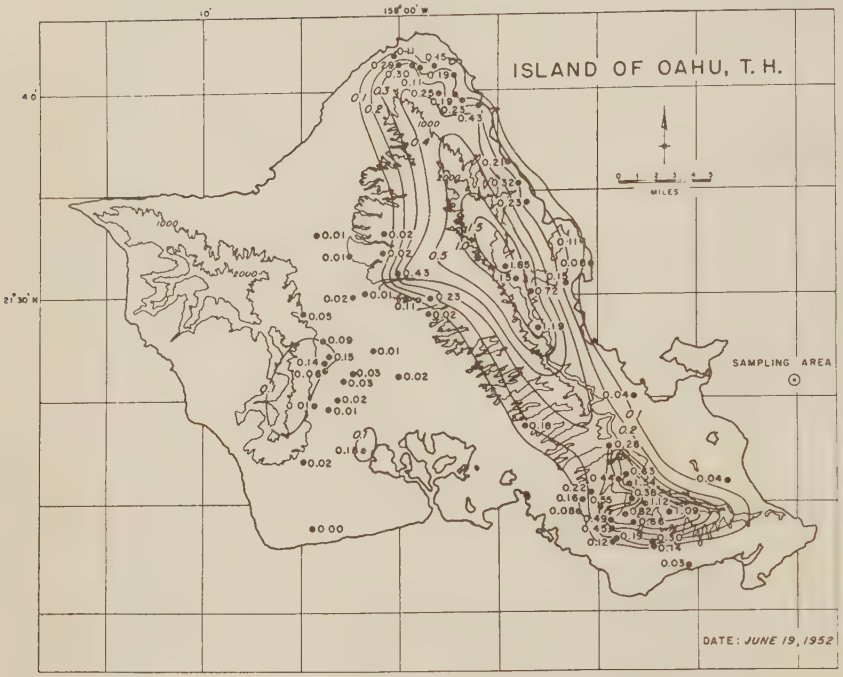

Fig. 1. Example of isohyetal maps used in deriving the total rain amounts shown on table 1, column 2. Rainfall amounts shown here are given in inches.

Numerous measurements of the quantity of salt nuclei in the air were made from aircraft over the sea on the windward side of the island of Oahu. An attempt is made here to relate this quantity of salt, which was usually sampled once a day, to the total amount of rain which fell on the island during each twenty-four hour period. These and other observations are presented in Table I and are discussed in sections 1, 2, 3, and 4 below.

Other properties of the air, such as mixing ratio, wind shear, instability, etc., which are potentially related to rainfall, are discussed briefly in sections 4 and 5, though they are not used directly in this exploratory study. These additional data are included in Table I so that other workers may examine their relevancy to the problem.

1. *Airbone salt particles*

The salt particles impinged upon and adhered to small glass sampling slides which were exposed to the atmosphere from aircraft. The slides were then taken to the laboratory, where particle diameters and numbers were determined with a microscope and at a controlled relative humidity of 90 %. At this relative humidity all salt nuclei were droplets, and the weights of salt in the individual droplets were computed from the droplet diameters. The detailed description of the techniques used to sample and measure the minute atmospheric salt particles has already been published and will not be discussed further in the present paper (Woodcock, Gifford, 1949; Woodcock, 1952).

On each flight an attempt was made to obtain the salt-nuclei samples at an altitude which was about one-hundred meters less than the altitude of the bases of the scattered local cumulus clouds but not necessarily under these clouds. The sampling position was over the sea and several miles up-wind (NE) of the island of Oahu (see Fig. 1). The air around and below the bases of the clouds had a higher water vapor and salt particle content than was found at greater altitudes in the cloud layer. I is supposed here that it is this lower air and its salt aerosols which flows into and forms the clouds. Thus the attempt here is to relate the quantities of the large salt aerosols present i the subcloud layer of air to the rain whic subsequently falls from the clouds as the trade winds pass over the island.

Columns 3 and 4 of Table I show the sal amounts sampled on fifty-two flights, whic

TABLE I

Observations arranged in chronological order

e	2 Total daily rainfall unit= 10^6 m³	3 Salt nuclei number l^{-1} of air >120 × 10^{-12} g	4 Salt nuclei weight m^{-3} of air unit= 10^{-6} g	5 Cloud-base to-inversion distance m	6 Wind shear 915—1,830 meters m sec⁻¹	7 Av. wind speed at cloud levels m sec⁻¹	8 Wind force	9 Av. wind direction at cloud levels ° true	10 Mixing ratio near cloud-base altitudes gm/kg	11 Mixing ratio in clear air at 1,525 m (from radio-sonde) gm/kg	12 Mixing ratio in clouds at 1,525 m gm/kg	13 Instability; cloud-base-to inversion cm²	14 Time of sampling flights LCT	15 Minimum cloud-base altitude m
51	0.4	3.2	1.1	1700	2.0	5.7	3	57	13.0	7.8	12.1	1.42	13	640
51	0.8	4.7	1.4	1550	4.3	6.7	3.5	74	13.9	8.2	12.5	1.67	14	610
51	1.4	13.5	6.3	1360*	5.3	9.3	5	79	13.0	7.3	12.3	0.58	14	655
51	2.6	5.3	1.8	1920	3.0	8.2	5.5	71	12.8	7.1	12.3	1.55	11	580
51	0.8	18.6	6.0	1550	6.0	7.2	4	62	13.0	8.8	13.0	1.42	14	550
51	1.9	8.7	3.4	1260	2.6	11.3	4.5	70	13.6	9.1	13.2	1.03	10	560
51	3.7	11.5	5.0	1370	—	8.2	4.5	71	14.1	9.7	12.8	1.22	15	460
51	1.1	8.4	3.6	1160	3.2	9.3	4.5	65	13.6	9.6	12.3	1.16	10	510
51	0.8	6.1	2.0	1130	4.3	5.7	4	63	13.5	10.4	12.5	0.84	11	610
51	0.1	1.9	0.4	1100	3.0	3.1	3	74	13.7	10.8	13.4	0.65	14	640
51	0.3	3.2	1.0	1400	2.7	2.1	4	78	14.9	9.0	13.5	0.90	12	510
51	0.5	1.5	0.4	> 3000*	3.4	2.1	3	variable	14.5	7.2	13.2	—	08	460
c 51	2.7	3.7	1.2	2710*	4.3	7.2	3.5	83	12.2	7.2	11.5	1.35	14	700
c 51	2.3	2.7	1.0	2850	2.1	4.6	4	61	12.2	6.5	11.7	1.22	11	560
c 51	1.5	1.0	0.3	2220	4.0	6.2	3	65	11.2	8.0	11.4	0.77	10	400
c 51	6.0	7.4	3.8	> 3000*	5.6	5.7	5	88	11.3	8.5	12.0	—	14	855
52	3.5	4.5	1.5	> 3000*	3.8	9.3	3.5	86	15.6	10.3	13.5	—	09	335
52	9.9	11.3	8.1	> 3000*	3.8	11.8	6	89	14.4	9.5	12.4	—	09	460
52	0.6	21.5	16.4	425*	3.5	8.2	7	89	13.2	8.3	11.3	0.13	11	580
52	trace	18.0	13.0	305	4.2	10.3	7	95	8.1	6.0	10.2	0.19	10	940
52	11.0	12.1	4.9	2130	4.3	9.8	5	99	12.0	8.7	11.5	0.90	14	610
52	8.7	25.9	16.2	2090	4.7	12.9	6	83	12.5	10.5	12.0	0.90	15	655
52	6.7	23.3	13.2	2330*	8.2	17.0	7	90	10.6	5.2	11.1	2.12	10	870
52	1.2	47.0	31.0	730*	9.7	15.9	7	77	10.9	3.3	10.5	0.06	10	790
52	4.2	19.3	13.7	1830	4.7	13.9	6	94	13.0	9.4	11.7	0.39	11	510
52	3.5	0.3	0.1	> 3000*	5.3	2.6	1	variable	13.8	8.1	11.0	—	14	510
52	0.6	2.9	0.7	975	4.6	7.7	4	64	8.7	6.4	10.5	0.32	15	580
52	2.6	11.7	7.0	1620	3.1	6.7	4.5	85	10.9	8.8	11.5	1.10	14	790
r 52	3.2	28.3	11.2	> 3000*	4.2	12.9	5	74	11.5	7.3	11.0	—	14	685
r 52	1.9	10.3	4.2	1700	8.5	12.9	5	49	10.4	8.2	10.6	1.22	11	790
y 52	1.1	1.5	0.5	2200*	4.6	6.7	3	86	13.7	9.0	11.8	1.68	15	460
y 52	0.4	9.5	3.0	1130	4.0	9.8	4.5	77	12.6	6.8	12.3	1.29	14	640
52	3.7	16.9	6.5	1830	6.8	5.7	5	55	12.8	8.7	11.9	0.84	11—16	610
52	3.2	7.5	2.3	1980	5.0	6.3	3.5	78	11.6	9.2	12.5	2.38	10—16	700
52	6.0	9.0	4.1	2440	3.3	9.8	4	80	14.0	9.7	13.0	2.38	10—16	245
52	0.1	9.9	3.7	1190	3.3	10.8	4	90	13.2	7.2	12.2	1.42	10—16	610
52	4.0	10.9	3.3	1630	4.6	11.3	3.5	80	13.9	7.7	12.5	1.35	10—16	530
52	4.3	15.8	6.1	1720	—	11.3	4	73	15.0	7.8	13.0	1.35	10—16	440
52	2.7	12.3	5.3	1620	3.5	11.3	4.5	75	13.5	8.1	12.7	0.97	10—16	520
52	4.3	8.9	3.2	1920	4.8	5.7	4	81	13.0	10.6	13.1	0.97	10—16	670
52	1.3	5.1	2.0	1740	3.5	8.2	3.5	46	12.8	9.9	13.4	0.97	10—16	610
52	2.7	4.3	1.3	2160	3.1	9.3	3.5	88	13.7	8.9	12.9	2.00	10—16	550

temperature inversion observed on these days.

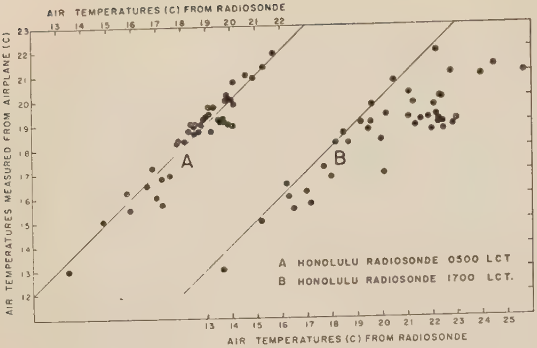

Fig. 2. Comparison of air temperatures observed from the salt-nuclei-sampling aircraft near cloud-base altitudes (see sampling area on fig. 1), with Honolulu radiosonde temperatures on the same day and at comparable altitudes.

were made on forty-two different days during 1951 and 1952. The quantities in these columns are limited to salt particles larger than $1.2 \times \times 10^{-10}$ grams. This limitation is due entirely to the fact that on many of the sampling days, and as a labor-saving step, only the larger nuclei on the slides were counted.

2. *Total rainfall measurements on Oahu*

Daily readings of many rain gages, scattered over the windward and central portions of the island, were used in drawing isoheytal maps for each of the forty-two days on which salt sampling flights were made. An example of these maps is shown in Figure 1. The rain data were assembled and the rain maps drawn by the second author, quite independently of the salt-nuclei-sampling activities of the first author.

Column 2 in Table I shows the values for total rainfall on Oahu, which were derived by planimeter-area measurements on the isoheytal maps. For instance the total rainfall obtained from the map shown in Figure 1 is 6×10^6 metric tons, a value derived by summing the products of the areas and the average rainfall amounts in each isohyetal contour. The rain amounts indicated in Table I were, in each case, collected in the time interval from 0800 LCT of one day to 0800 LCT of the following day. The date of the Hawaiian rain records is that of the day when the gages were read. In using these records here, however, it should be noted that the date of the preceding day is used; that is, the date when the salt-nuclei sample was taken. Thus the rainfall amount of 6×10^6 metric tons taken from the isoheytal map for 19 June 1952 (see Fig. 1), is listed in Table I as occurring on 18 June 1952.

3. *Inversion altitude and cloud-base-to-inversion distance*

In deriving the cloud-base-to-inversion distance, the minimum cloud-base altitude measurements (column 15) were used to mark the point where cloud temperatures would depart from the dry- lapse rate curves of the Honolulu soundings. This is illustrated in Figure 3. The point at which this cloud-lapse curve, or wet adiabat, intersects the dry bulb temperature line on the chart is taken as the altitude of the cloud tops. Cloud-base-to-inversion distance (column 5) is, therefore, simply the altitude of this intersection point minus cloud-base altitude, and is thought to represent roughly the maximum size of the clouds to be expected.

Inversion altitudes were taken from the Honolulu radiosonde records, using the soundings showing the maximum inversion altitudes observed at 0500 LCT. For example, the

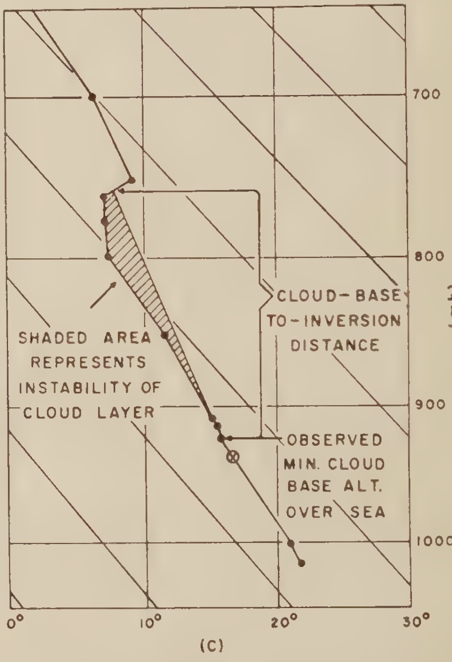
700
800
900
1000
(mb)
CLOUD-BASE TO-INVERSION DISTANCE
SHADED AREA REPRESENTS INSTABILITY OF CLOUD LAYER
OBSERVED MIN. CLOUD BASE ALT. OVER SEA
0°
10°
20°
30°
(C)

Fig. 3. Pseudo-adiabatic chart of Honolulu radiosonde record (1500Z, 26 February 1952) illustrating derivation of the cloud-base-to-inversion distances and the instability areas shown on table 1, columns 5 and 13. The circled X marks a temperature and pressure observed on the same day from aircraft over the windward sea.

20th value in column 5, Table I is based upon the radiosonde record of 0500 LCT on 6 January 1952, whereas the 20th rain record (column 2) is for the period 0800 LCT, 5 January 1952 to 0800 on the 6th. If the 0500 sounding of January 5 had revealed a higher inversion, then this sounding would have been used in deriving the value in column 5. The reason for this selection of the higher inversion altitude measured at the 0500 soundings is discussed below.

The 1700 LCT radiosonde temperature records were not used here because of the marked evidence on many days of local heating over the island which extended up to cloud heights, as shown in Figure 2, B. Thus it is thought that the 0500 soundings more nearly represent conditions over the sea and over the windward parts of the island where most of the rain falls.

On those days when no temperature inversion occurred, the cloud wet-lapse line usually intersected the radiosonde temperature line in a near-isothermal region. In Table I, column 5, the asterisks mark the days when the inversion was not present. On six of these days the altitude of the intersection of the lapse rate lines exceeded 3,000 m. In column 5 the cloud-base-to-inversion distances for these six days are given as > 3,000 m.

The reason for selecting minimum cloud base altitude and maximum inversion altitudes for deriving the daily cloud-base-to-inversion distances, was the thought that these conditions would favor cloud growth, and that rain occurring during each 24 hour period would be most likely to occur during the periods of greatest potential vertical extent of the clouds. These distances are, however, somewhat uncertain, due to the question of how many hours any observed inversion or cloud base ltitude may persist. This question is discussed n some detail later.

In deriving cloud-base-to-inversion distances, ossible effects of the diurnal variation of nversion height (LEOPOLD, 1948) are minimized by the consistent use of the 0500 LCT oundings[3].

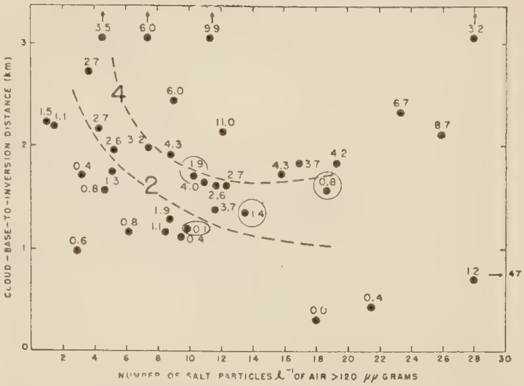

Fig. 4. Total daily amounts of rainfall on Oaho, expressed in units of 10^6 metric tons, related to the numbers of salt nuclei in the air and to the cloud-base-to-inversion distances. See text for further discussion.

4. *Winds and cloud-base altitudes*

The wind force at the sea surface was judged from the aircraft during sampling flights and is largely based upon the number, size and appearance of the white caps (breaking waves). The average winds at 915, 1,220, 1,525, and 1,830 meters altitude, were taken from the six-hourly records of the U.S. Weather Bureau at the Honolulu Airport. These wind velocities are given in columns 7 and 9, Table I.

The cloud-base altitudes shown in column 15, Table I, were measured from the airplane during a period of about one hour.

5. *Wind shear, stability and mixing ratios*

Among the various factors tending to reduce cloud growth and rain formation, the amount of shear present in the air through which the clouds must develop was thought to be important (MALKUS, SCORER, 1955). Other factors, such as the instability of the clear air in the cloud layer and the difference in mixing ratios are given in Table I, columns 6, 10, 11, 12, and 13. Though these quantities are not used in the present paper, they are included here so that the reader may examine their relevance to the problem.

6. *Relating rainfall to cloud-base-to-inversion distance and to salt particle number*

Assuming that cloud-base-to-inversion distance and the number of salt particles might be the major factors causing variations in total

---

[3] One exception to this rule was made on January 11, 952, when a 1900 LCT sounding was used. This sounding, made one hour after sunset, showed none of the diurnal heating indications evident in most of the 1700 CT soundings.

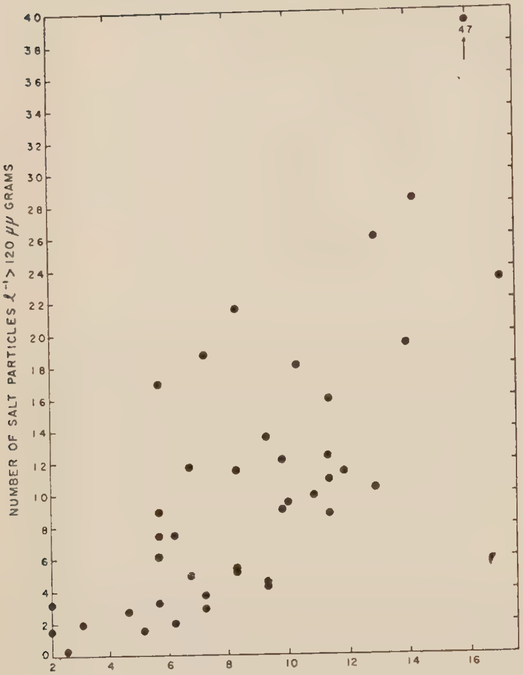

Fig. 5. Number of salt particles near cloud-base-altitudes, related to the average wind speed at altitudes between 900 and 1800 meters. (See Woodcock, 1953, for more detailed indication of dependence of salt nuclei upon wind).

rain amount, these three variables were plotted as shown in Figure 4[4].

The dashed lines on this figure are intended as an aid to the eye in roughly separating the values of rain amount into those less than two, those between two and four, and those greater than four. The units of rain amount equal 10^6 metric tons.

The most seriously divergent exceptions to the isoheytal pattern suggested by the dashed lines in Figure 4 are the rainfall amounts which are enclosed in circles. These observations will be discussed later. At the present time it is sufficient to point out that, with the above exceptions, the data in Figure 4 may be interpreted as indicating a crude quantitative relationship of the rainfall to the other variables on about two-thirds of the graph. For instance, note that increased values of cloud-base-to-inversion distance and of salt-nuclei numbe are generally attended by increased rainfal amounts, with a faint suggestion of an optimum rain amount in the middle range o nuclei number. On the right-hand portion o the figure the data are too sparse to justify a extension of the dashed isohyetal lines.

7. *Relating rainfall to cloud-base-to-inversion distance and to wind speed*

As shown in Figure 5 and in an earlie paper (Woodcock, 1953), the number of sal particles tends, however, to increase as th winds become stronger. Thus one migh reasonably ask to what extent wind speed ma contribute to rainfall. As a first test of th possible relationship of wind to rainfall, win speed at cloud levels (see Table I, column 7 was substituted for salt-particle number on diagram similar to Figure 4. The resultin distribution of values for rain amount is show in Figure 6, and is clearly considerably les systematic than the distribution shown i Figure 4. Does this mean that wind has les effect upon rain in Hawaii than do the sal nuclei?

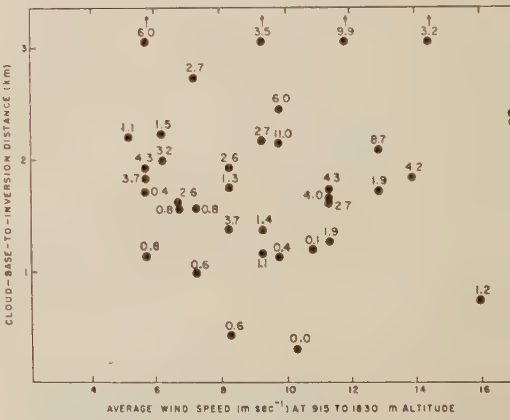

Fig. 6. Repetition of Figure 4, substituting wind speed cloud levels for numbers of salt particles.

---

[4] The only data excluded from Figure 4 are those obtained on the five days when winds at cloud levels averaged less than 5 m sec^{-1} (see column 7, Table I). The reason for this exclusion is that low wind conditions favor a marked development of convective activity over the island during the daylight hours, thus making it very unlikely that the cloud-base-to-inversion distances, derived from the 0500 radiosonde temperature record, will represent the maximum cloud heights developed during the day.

The rainfall amounts on four of the six days when the cloud-base-to-inversion distance exceeded 3,000 meters, are simply plotted slightly above the maximum ordinate value (3,000 m) given in Figure 4.

In many of the previous studies of Hawaiian rainfall it has been pointed out that it is reasonable to expect increased rainfall with stronger winds, since these winds transport more moist air over the mountains. The amount of water vapor moving over the island daily should be nearly a linear funcion of wind speed, other factors remaining constant. Assuming that rainfall also might be a linear function of wind speed, the rainfall values plotted in Figure 4 were divided by the ratios of the observed wind speeds to the minimum wind speed of 5 m sec^{-1}. By this device it was hoped to subtract wind effects on rainfall from possible salt-nuclei effects. The resulting modified rain amounts are shown in Figure 7. It is interesting that the general pattern of distribution of rain amount shown in Figure 4 is still evident in Figure 7. In other words, increased values of cloud-base-to-inversion distance and of salt-nuclei number are still generally attended by increased rainfall amounts. Does this mean that the remaining pattern of change in rain amount with different values for salt-nuclei number is due to the effects of salt nuclei on rainfall?

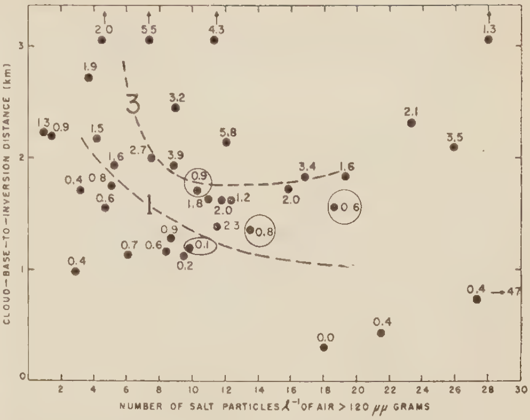

Fig. 7. The quotient of the total daily rain amounts and a function of wind speed, related to the number of salt nuclei in the air and to the cloud-base-to-inversion distances. See text for further discussion.

8. *Discussion*

The above questions cannot be answered at this time. The salt aërosols from the sea probably add still another variable to the already complex problem of Hawaiian rainfall. The contribution of wind to the daily rainfall in Hawaii remains unknown (Stidd, 1954 b) and there is at the present time little justification for assuming that rainfall might (or might not) be a simple linear function of wind speed, as was done in producing the "modified rain amounts" given in Figure 7. Further more detailed measurements are needed. The primary usefulness of the present study is that it further excites the curiosity about the role of salt nuclei in rain formation and it leads reasonably to pertinent suggestions about where, when and how future measurements should be made in an attempt to separate the wind and/or salt-aerosol contributions to rainfall.

In thinking about the possible significance of the distribution of values shown in Figure 4, it is well to remember that the twenty-four hour rainfall amounts represent an island-wide integration, whereas the values for number of salt particles and for cloud-base-to-inversion distances were usually taken from measurements obtained only once or twice a day and during relatively short periods of time. The proportion of each of the twenty-four hour periods during which these later values actually existed in the air over the island is of course unknown.

Changes in inversion height of as much as 1,000 m within a few hours have been indicated by Leopold (1948), and are occasionally evident in the Honolulu radiosonde records used in the present study. These changes will, of course, add uncertainty to the ordinate values in Figure 4, since these values are derived from the radiosonde records as described in section 3.

The usefulness of the cloud-base-to-inversion distances as a measure of cloud thickness and rainfall potential, probably depends upon the length of time these distances actually existed on the various sampling days. There is no adequate information about the hours of duration of any specific cloud-base-to-inversion distance, nor of the extent to which this duration is comparable from one sampling day to the next. In the absence of this information, further discussion of this point does not seem to be useful. It should be remarked, however, that Figures 4 and 7 suggest strongly that the cloud-base-to-inversion distances determined on the various days are related to the

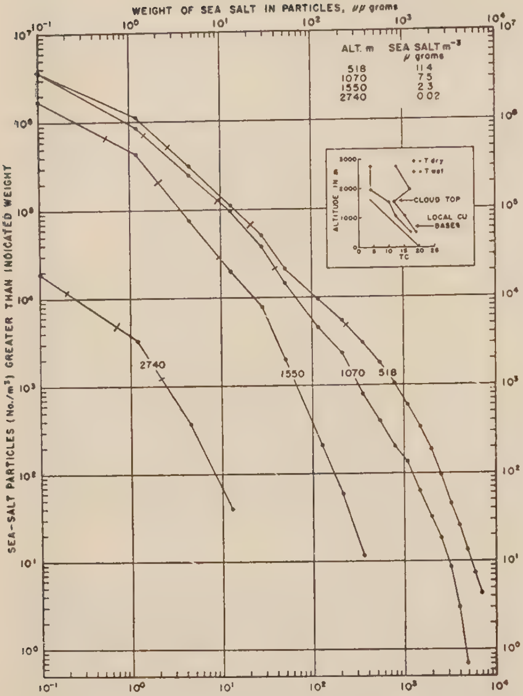

Fig. 8. An example of the decrease, with altitude, in the numbers of salt particles in Hawaii. Approximate position 21° 30′ N, 157° 40′ W; Time 1300 LCT, 30 May 1952. Surface wind 80 deg. force 4 to 5. Note that the region of cloud development is one of rapid decrease with height in the numbers of the larger nuclei. (The lines are drawn between the observed values as an aid to the eye in following the trends of the various observed distributions.)

rainfall. This result is thought to indicate that the durations of these distances are, on the average, sufficient to markedly influence the rainfall during each twenty-four hour period.

The amount of airborne salt also varies considerably during short periods of time. On ten of the days represented in Table I and Figures 4, 6, and 7, counts of salt nuclei were obtained at 1000 and 1600 hours, instead of the usual single observation per day. An average of these salt-particle counts is used in Figures 4 and 7. The ratios of the maximum to the minimum of these two values for salt-nuclei number averaged 1.56. On each of the remaining 27 days, when only one observation was made, the nuclei content of the air may have varied an equal or greater amount.

Thus it is evident that the two important quantities cloud-base-to-inversion distance and salt-nuclei number can be far from constant during a twenty-four hour period. It is thought that this lack of constancy may account for some of the observations which differ widely from the proposed pattern (see circled values of Figures 4 and 7). In view of the variability of the above quantities, it is rather surprising that there is any pattern in the distribution of the values in these figures. The suggestion of a pattern, despite the above variability, may be due to a real relationship between the quantities involved.

It is clear that numerous observations are needed throughout each twenty-four hour period in order to properly test the reality of the rainfall pattern suggested by Figures 4 and 7. At this early exploratory stage of this study, it does not seem fruitful to speculate about the meaning of this precipitation pattern and what it may imply about the rain-forming mechanism.

No consideration is given to the probable change in the slope of the cloud temperature-lapse line which would result from mixing of the cloud air with the environmental air during ascent. (Note on Fig. 3 that a wet lapse rate is assumed in the clouds.) This mixing would tend to decrease the cloud-top temperature and as is evident from the gradient of salt-nuclei number in the cloud layer (see Figure 8), would also cause a reduction of the number of salt nuclei in the cloud. The omission of consideration of these variables here is due to the impression that their effect upon the rainfall amounts is of secondary importance in this preliminary study.

Solot (1950) and others have pointed ou that wind speed determines the rate of moisture flow over the islands of Hawaii, and thus may directly affect rainfall intensity. Stidd (1954 a has recently found evidence of a correlation of rainfall with the pressure over certain areas of the North Pacific and he suggests that this correlation is due to the influence of stronger trade winds in increasing rainfall. The fact tha the number of salt nuclei in the air increases with increasing winds, poses a problem con cerning the detailed nature of the effects of wind on rainfall. To what extent is the rainfall due to the amount of moist air or cloud flowing over the mountains and to wha extent is it due to the quantities of potential raindrop-forming nuclei which are in this air?

The salt nuclei show a persistent pattern of relationship to rain amount which is not revealed by wind speed and rain amount (compare Figures 4 and 7 to Figure 6). This apparent relationship of nuclei to rainfall may not be due, however, to quantitative effects of the number and size of salt particles upon the number and size of raindrops. It is possible that the determination of the number of the large salt nuclei in the air is a better measure of the 24 hour average wind speed over the sea and the mountains than are the Honolulu winds-aloft measurements. If this is true then Figures 4 and 7 may be interpreted as reflecting the wind effects upon total rainfall. The authors consider, however, that at the present stage of the study, these figures are clear evidence that salt nuclei will have to be considered in future studies of the Hawaiian rainfall problem.

Detailed short period studies, made during or immediately after rapid changes in wind speed, may supply an answer to this problem. It is expected that the changes in the quantities of airborne salt at cloud levels will be found to lag behind the changes of wind speed, due to the time requirements for the upward diffusion of the salt particles in the case of increased wind, or for their sedimentation when the wind is reduced. The duration of this time lag is uncertain, however. If the lag proves to be long enough, perhaps of several hours duration, it may be possible to answer the question of the contribution of salt nuclei to rain amount through the use of hourly measurements.

Most of the shower rains which occur on Oahu are produced by cumulus clouds which are immersed in and drifting with the trade-wind stream. Many, if not most, of these clouds are formed before arriving over the island, and from some of them rain is falling as they approach the island from over the windward sea. This rain often continues to fall as the clouds pass over the windward beaches and move inland to the mountains. The time these clouds remain over the island is thus a function of wind speed at cloud altitudes.

One effect of greater cloud speed is of course to increase the number of clouds passing over the island in a given twenty-four hour period. If orographic lifting of clouds and of the ambient air accounts for the increased rainfall in the mountain areas, and this seems to be generally accepted (see LEOPOLD, 1948; SOLOT, 1950; STIDD, 1954 b), then the greater the number of clouds streaming over the island in a day the greater the chances of rain formation. That presupposes, of course, that other rainforming factors are equal.

However, since it is assumed that the Hawaiian shower rains are formed by accretional and/or condensational growth processes, which may be critically time-dependent, it is possible that high winds may move the clouds off the mountain areas before the rain-forming processes, which bring about the rain excess in these areas, have time to proceed to completion. In this case one might expect a tendency towards a reduction of rain amount as winds exceed some optimum speed. This speed may be regarded as one which will cause a maximum number of clouds to be lifted over a mountain area within a given time, the duration of the lifted state being sufficient for a completion of the accretional and/or condensational growth processes. The rainfall and other data given here are not sufficiently numerous throughout the range of values given to indicate an optimum wind speed.

The authors are inclined to think that the increased rain amount which falls from the clouds behind the crest of the Koolau Mountain Range (see Figure 1 and HALSTEAD, LEOPOLD, 1948) is due in large part to the modification, over the mountains, of shower clouds which form over the windward sea and drift down upon the island in the trade-wind stream.

The night maximum of rain on Oahu, which has been noted by LEOPOLD (1948) and others, may be due to the night maximum of cloudiness over the sea noted by RIEHL (1947). Thus a night maximum of rainfall does not necessarily suggest a night maximum of nuclei or wind speed, as might be supposed from the present study.

YEH and others (1951) have suggested that wind direction will affect the rainfall on Oahu, due to the fact that the flow is sometimes parallel to the mountain ridges and sometimes normal. As can be seen in column 9, Table I, and in Figure 1, most of the wind directions were nearly normal to the long axis of the Koolau Range. This relative constancy of the wind has caused us to ignore direction as one of the variables possibly affecting rainfall in this series of days.

Remarks about further study

In order to make a further test of the relationship of salt particles and/or wind to Hawaiian rainfall, it seems to be necessary to make additional measurements from aircraft. These measurements should be made over the sea, many kilometers upwind from the high-rainfall area on Oahu, and should include as many of the variables as possible. Four or more flights a day would be desirable, especially after a time of rapid change in wind speed.

An increase in the number of recording rain gages along the Koolau Range would add to the accuracy of the isoheytal maps. As shown in Figure 1, there are rather large areas in the high-rainfall regions of the mountain range where there are no gages. This relative sparsity of gages in this region adds a considerable uncertainty to the drawing of the isohyetal lines and hence to the total rainfall values derived from the maps. Errors due to this uncertainty add another factor to be considered in the evaluation of Figures 4, 5, and 7.

If further study confirms the general pattern of rainfall distribution suggested on Figures 4 and 7, the question of the forecast value of the measurements used in deriving this pattern will arise, and it will also become necessary to seek an explanation of the result in terms of the detailed mechanics of raindrop formation.

Acknowledgements

The authors want to thank Dr's Harry Wexler and Irving Langmuir, who originally suggested the study of salt nuclei and rain in Hawaii. The first author also wishes to express his appreciation of the skill, interest and effort of Mr. William Stearn and Mr. Wallace Waterhouse of Murray Air, Ltd., Honolulu, in the successful completion of the many airplane flights required in this study.

Mr. Larry Eber of the Pineapple Research Institute and Mr. Saul Price of the U.S. Weather Bureau, Honolulu, contributed much time and effort to this study by supplying numerous transcriptions of weather data.

REFERENCES

ANON, 1950: Physical basis for the production of rain in Hawaii (A statement by members of the forecast staff, U.S. Weather Bureau, Honolulu, Hawaii). Unpublished.

BOWEN, E. G., 1950: The formation of rain by coalescence. *Austr. J. Sci. Res.*, A, 3, 193—213.

HALSTEAD, M. H., and LEOPOLD, L. B., 1948: Monthly median rainfall maps. Meteorology Dept., Pineapple Research Institute and Experiment Station, Hawaiian Sugar Planters Association, Honolulu, Hawaii, Report No. 2.

KEITH, C. H., and ARONS, A. B., 1954: The growth of sea-salt particles by condensation of atmospheric water vapor. *Jour. Met.*, **11**, 173—184.

LANGMUIR, IRVING, 1948: The production of rain by chain reaction in cumulus clouds at temperatures above freezing. *J. Meteor.*, **5**, 175—192.

LEOPOLD, LUNA B., 1948: Diurnal weather patterns on Oahu and Lanai, Hawaii. *Pacific Science*, **2**, 81—95.

LUDLAM, F. H., 1951: The production of showers by the coalescence of cloud droplets. *Quart. J. r. meteor. Soc.*, **77**, 402—417.

MALKUS, JOANNE STARR, and SCORER, R. S., 1955: The erosion of cumulus towers. *J. meteor.*, **12**, 43—57.

RIEHL, H., YEH, T. C., MALKUS, J. S., and LASEUR, N. E., 1951: The northeast trade of the Pacific Ocean. *Quart. J. r. meteor. Soc.*, **77**, 598—626.

RIEHL, HERBERT, 1947: Diurnal variation of cloudiness over the subtropical Atlantic Ocean. *Bull. Amer. Met. Soc.*, **28**, 37—40.

SOLOT, SAMUEL B., 1950: Further studies in Hawaiian precipitation. Research paper No. 32, Weather Bureau, U.S. Department of Commerce, Washington, D.C.

STIDD, C. K., 1954 a: Objective Hawaiian rainfall estimates from mean 700 mb charts. To be published.

— 1954 b: Personal communication.

WOODCOCK, A. H., and GIFFORD, MARY M., 1949: Sampling atmospheric sea-salt nuclei over the ocean. *J. Marine Res.*, **8**, 177—197.

WOODCOCK, A. H., 1952: Atmospheric salt particles and raindrops. *J. Meteor.*, **9**, 200—212.

— 1953: Salt nuclei in marine air as a function of altitude and wind force. *J. Meteor.*, **10**, 362—371.

YEH, T. C., WALLÉN, C. C., and CARSON, J. E., 1951: A study of rainfall over Oahu. *Meteorological Monographs*, Vol. 1, No. 3, 34—46, Amer. Met. Soc., Boston 8, Massachusetts.

PRINTED IN SWEDEN
ESSELTE, STHLM 55

Contribution No. 758

PHYSICAL OCEANOGRAPHY OF THE GRAND BANKS REGION AND THE LABRADOR SEA IN 1954 [1]

By Floyd M. Soule and J. E. Murray, U. S. Coast Guard

The U. S. C. G. Cutter *Evergreen* again served as oceanographic vessel of the ice patrol in 1954. There were no major ship changes affecting the oceanographic work. Earlier bulletins of this series contain descriptions of deck and laboratory equipment for carrying out the mission of ice patrol oceanography.

The work of dynamic topographic surveying for the 1954 ice patrol season began with the departure of the *Evergreen* from Argentia on the afternoon of 30 March. Because of the large number of early season bergs which had been in the vicinity of Flemish Cap, it was desirable to have some information as to the current pattern off the northeastern shoulder of the Grand Banks and north of Flemish Cap. To include this area in the first survey it was necessary to omit the area south of the Tail of the Grand Banks. The southern limit of the surveyed area therefore was fixed at about 42° N. The work of collection of data began at the southern end of the survey on the morning of 1 April and progressed northward. The weather was more boisterous than usual and the succession of gales was more like what might be expected in March than April. The work of collection of data was interrupted by weather for 4 hours on the 2d, 20 hours on the 4th, and 18 hours on the 7th and 8th. At the next to the last station three of the Nansen water bottles had to be taken to the laboratory to thaw out before the samples could be withdrawn. Similar conditions existed at the final station, but additional personnel were assigned to speed up the work of withdrawing the water samples from the Nansen bottles as they arrived on deck before they had time to freeze. The work of collection of data was completed on the morning of 15 April, 93 stations having been occupied. A course was then laid for Argentia where the *Evergreen* arrived on the afternoon of 16 April.

On the afternoon of 25 April, the *Evergreen* departed St. John's, Newfoundland, for the purpose of making a second current survey, this time of the waters over and immediately seaward of the eastern and southern slopes of the Grand Banks from the latitude of Flemish Cap southward and extending just westward of the Tail of the Banks.

---

[1] To be reprinted as Contribution No. 758 in the Collected Reprints of the Woods Hole Oceanographic Institution.

EXTRACT FROM U. S. COAST GUARD BULLETIN No. 40. PAGES 79 to 168.

The work of collection of data began on the morning of 26 April and progressed from north toward south. The first section had not been completed when it was necessary to heave to on account of weather at midnight on the first day. After 15½ hours, oceanographic work was resumed. No other major interruptions occurred and the collection of data was completed on the afternoon of 8 May. This survey was made up of 83 stations. The *Evergreen* then proceeded to a poin about 100 miles southeasterly of the Tail of the Banks, where a carboy of surface water was collected for use as a substandard of salinity during subsequent surveys. A course was then laid for Argentia where the *Evergreen* arrived on the morning of 10 May.

The *Evergreen* departed Argentia on the morning of 28 May to begin a third survey. The planned survey had the same northern limit as the second survey but had a western boundary of 50°15′ W. and extended farther seaward than usual in the hope of developing information as to the extent of the colder mixed-water salients which were known to exist south-southeastward of the Tail of the Banks and southward of Flemish Cap. The work of collection of data began at noon on 29 May and work progressed from south towards north. On 6 June the survey work was interrupted to intercept the U. S. C. G Cutter *Matagorda* to effect the emergency transfer of two men fo transportation to Boston. Work on the survey was resumed on th early morning of 7 June. It was not necessary to heave to on accoun of gales during this survey. No further interruptions occurred, and the work of collection was completed on the afternoon of 11 June the survey including 90 stations. The *Evergreen* then proceeded t Argentia, arriving there on the afternoon of 12 June.

A fourth survey was begun with the departure of the *Evergree* from Argentia on the morning of 21 June. This survey was intended to include the waters over and immediately seaward of the northern and northeastern slopes of the Grand Banks and the Flemish Ca area northward of about 46°50′ N., and eastward to about 43°30′ W The work of collection of data began on the evening of 22 June at th offshore corner of the Bonavista triangle and progressed counter clockwise around the triangle, after which a network was occupie working southeastward to the final station which was completed o the afternoon of 2 July. It was not necessary to heave to on accoun of gales at any time, nor were there any other interruptions durin the survey. From the final station the *Evergreen* proceeded to a poin about 75 miles southeastward of Flemish Cap, where a carboy c surface water was collected for subsequent use as a substandard c salinity. The *Evergreen* then proceeded to Boston, arriving there o the afternoon of 7 July. During this survey 95 stations were occupied

The *Evergreen* departed Boston on 15 July to begin the postseaso cruise. En route to the first station, when off Trepassey Bay, Newfoundland, an electrical fire in the main propulsion motor disable the *Evergreen*, which was then towed to Boston for repair. Upon completion of the repairs the *Evergreen* again departed Boston on 17 August and the work of collection of data began at the offshore corner of the Bonavista triangle on the evening of 21 August. Work progressed in a counterclockwise direction around the triangle, and the last station of the triangle was completed on the afternoon of 24 August. From here the *Evergreen* proceeded to South Wolf Island, Labrador, and there, on the evening of 25 August, began a section across the Labrador Sea to Cape Farewell, Greenland. The final station of this section, and the initial station of a triangle southeastward of Cape Farewell, was completed on the late afternoon of 29 August. Work progressed in a clockwise direction around the Greenland triangle until the morning of 3 September, when increasing winds halted oceanographic work prior to the final approach to Cape Farewell. The following morning, work was resumed after a delay of 23 hours and the final station of the Greenland triangle and of the cruise was completed on the late evening of 4 September. The *Evergreen* then proceeded toward Argentia, stopping briefly en route to collect a carboy of surface water for subsequent use as a substandard of salinity. Argentia was reached on the afternoon of 8 September and, after loading freight and replenishing, the *Evergreen* departed on the evening of 8 September for Woods Hole with arrival there on the evening of 12 September. Oceanographic equipment and personnel were offloaded at the shore laboratory upon arrival to complete the field work for 1954. During the postseason cruise 28 stations were occupied in the Bonavista triangle, 24 stations made up the section across the Labrador Sea, and an additional 27 stations formed the Greenland triangle. Thus 79 stations were occupied during the post-season cruise.

The oceanographic work was under the supervision of Oceanographer Floyd M. Soule, who was assisted by LT John E. Murray. Other assistants in the observational work were Francis N. Brown, yeoman first class; Elwood C. Gray, aerographer's mate first class; Lewis M. Lawday, aerographer's mate second class; Hugh R. McCartney, Jr., aerographer's mate second class; Donald Zacher, aerographer's mate third class; and, during the fourth survey, Verne W. Schuenke, boatswain's mate third class.

Of the 440 stations occupied during season and post-season cruises, the 51 stations comprising the section across the Labrador Sea and the Greenland triangle were occupied from the surface to as near bottom as was practicable, and at the remaining 389 stations the observations extended to a depth of about 1,500 meters where the depth of water permitted. As in previous years the intended depths of observation, in meters, were 0, 25, 50, 75, 100, 150, 200, 300, 400, 600, 800, 1,000, and thence by 500-meter intervals. The dynamic heights have been referred to the 1,000-decibar surface, except for the section across the Labrador Sea and the Greenland triangle where the heights have been referred to the 1,500-decibar surface.

In addition to the usual measurements of temperature and salinity 617 samples were taken during the occupation of the South Wol Island-Cape Farewell section and the Greenland triangle for ultimate determination of total phosphorus concentration. At 293 stations observations were made with black and white Secchi disks varying in time from April to September and in location from the Gran Banks region to the Greenland triangle with a variety of sky conditions and with the sun's altitude varying from 71° to 2° below the horizon.

Temperatures were measured with deep-sea reversing thermometers. Most of the protected thermometers used were of Richter an Wiese manufacture, but a small percentage were made by Negrett and Zambra, G. M. Manufacturing Co., and Kahl Scientific Instrument Corp. The depths of observation were based on unprotecte thermometers made by Richter and Wiese and by Kahl. Th thermometers were used in pairs and a program of intercompariso of protected thermometers was carried out by periodically changin the individual thermometers comprising the pairs. This permitte the identification of thermometers which were not functioning satisfactorily and which needed some thermal and mechanical manipulation to restore them to normal performance. It also provided a measure of the uncertainty of the temperature measurements. Afte eliminating constant corrections, these comparisons (2,994 in all) gav a probable difference between the corrected readings of a pair thermometers of 0.011° C. Many of the thermometers had recen laboratory comparisons with thermometers tested by the Nationa Bureau of Standards, and as in most cases the temperatures are mean of the corrected readings of a pair of thermometers, it is considere that the observed temperatures listed in the table of oceanographi data have a probable error of about ±0.01° C.

The pressure coefficients of the unprotected thermometers used i 1954 are possibly in error by about one-half percent. The sign of th error is such that the tabulated depths are too great. Further wor on the problem of more accurately determining the pressure coefficient an unprotected thermometer will have under field conditio is in progress at the Woods Hole Oceanographic Institution.

As in previous years routine salinity measurements were made wit a Wenner salinity bridge. Prior to the beginning of the 1954 fiel work, the bridge was overhauled and cleaned and its calibration curv redetermined. The 1950 determination had given the expression:

$$S=\frac{9891.881}{200.2+m}-4.520,$$

where S is salinity in parts per thousand and m is the X-dial reading of the bridge at balance. The similar expression determined in 1954 is:

$$S=\frac{9892.513}{200.1+m}-4.531.$$

Over the range of salinities encountered in the area (30.2 to 36.6°/oo) the difference between these two curves may be compensated for with negligible error by adjustment of the X-dial reading selected as corresponding to the salinity of the Copenhagen standard water used (batch P17).

The Y-cell, which is filled with sea water simply to provide a bridge arm having thermal characteristics similar to those of the arm made up of the X-cell, undergoes a slow drift in its impedance as its contents is gradually concentrated through evaporation. It has been surmised that there also are erratic changes in its impedance as discrete drops of condensate return to the solution from the neck of the cell. The first change is evidenced by the slow change in the setting of the Y-dials necessary to bring the bridge onto the calibration curve during successive standardizations. As the range of adjustable impedance covered by the Y-dials has a finite limit, the evaporation from the Y-cell eventually reaches a point where the solution must be changed. In an attempt to remedy both the slow drift and the supposed erratic changes in the impedance of the Y-cell, a layer of oil about 1 mm. thick was placed on the surfaces of the solution in the cell and in the exhaust tube. No noticeable changes in the rate of drift resulted during the approximately 3-month period covered by the preliminary measurements ashore and the first two surveys. The oil layer was then increased in thickness to about 1 cm., with the result that the slow drift in impedance was very much reduced.

During the routine measurements standardizations were made with water from an oil-sealed carboy of sea water, and at least twice during each run a sample of Copenhagen standard water of batch P17 was measured as an unknown. At the end of each survey these measurements of Copenhagen water were used to compute such corrections as had to be made to the salinities measured during the survey. For each of the four surveys and the postseason cruise, the indicated corrections did not exceed 0.005°/oo so no corrections have been made. These measurements of Copenhagen water indicate the salinity determinations were precise to about ±0.005°/oo. The accuracy is, of course, limited to that of the silver nitrate titrations involved in determining the calibration curve of the salinity bridge.

The determinations of the total phosphorus concentration were carried out by personnel of the Woods Hole Oceanographic Institution, and the probable error is about ±10 percent. With only minor modifications the methods and procedures were those reported by Harvey.[2]

Figures 15, 16, 18, and 19 show, in chronological order, the current charts resulting from the four surveys made during the season. Figure 15 shows that at the time of the first survey, although the dynamic heights in the lowest part of the area were about normal, the highs of 971.72 in the Atlantic Current and 971.18 on the Grand Banks were exceptionally high and indicated a very active circulation both in the Labrador Current along the eastern slope of the Grand Banks and in the margins of the Atlantic Current shown in the southeastern part of the surveyed area. In the area south-southeastward of the Tail of the Banks, a pool of colder mixed water of undetermined extent was indicated beyond the southwestern limits of the survey. In the northeastern part of the survey there was a slow clockwise circulation around Flemish Cap, with a diversion of some of the Labrador Current water northward of it. This pattern persisted throughout the season and was probably responsible for the early season drift of bergs to the vicinity of Flemish Cap.

Comparison of figures 15 and 16 shows the extent to which the intrusion of Atlantic Current water spread northward between the first and second surveys. In the second survey, water of Atlantic Current characteristics was found as far north as 45°20′ N., and at single levels at stations 5411 and 5412 just north of 46° N. The Labrador Current along the eastern edge of the Grand Banks continued to feed the cold mixed-water pool which extended south of the southern limits of the survey. Labrador Current water did not extend westward of about 50°20′ W., and warm salty water had reached to the Grand Banks at 43° N., westward of 50°15′ W. This intrusion of water of the Gulf Stream was most in evidence at the section extending southwestward from station 5468. Figure 17 shows the temperature distribution along this section.

Figure 18, showing the results of the third survey, does not completely enclose all of the cold mixed-water pool even though the survey was extended unusually far to the south. The probable southern limit of berg drift was judged to be the 971.36-dynamic meter contour line, the course of which has been estimated in figure 18. Comparing figures 16 and 18 permits of following changes in pattern features common to both. The axis of the major valley in the southern part of the chart remained at about the 48th meridian. The branch valley which extended southwestward from the Tail of the Banks in the second survey moved southeastward, and in the third survey extended southwestward from about 42° N., 49° W. The topography along the southeastern edge of the surveyed area straightened out and the minor salients between it and the valley, only hinted at in

---

[2] Harvey, H. W., "The estimation of phosphate and of total phosphorus in sea waters." Journ. Mar. Biol. Assoc., vol. XXVII, pp. 337–359 (1948), Plymouth, Eng.

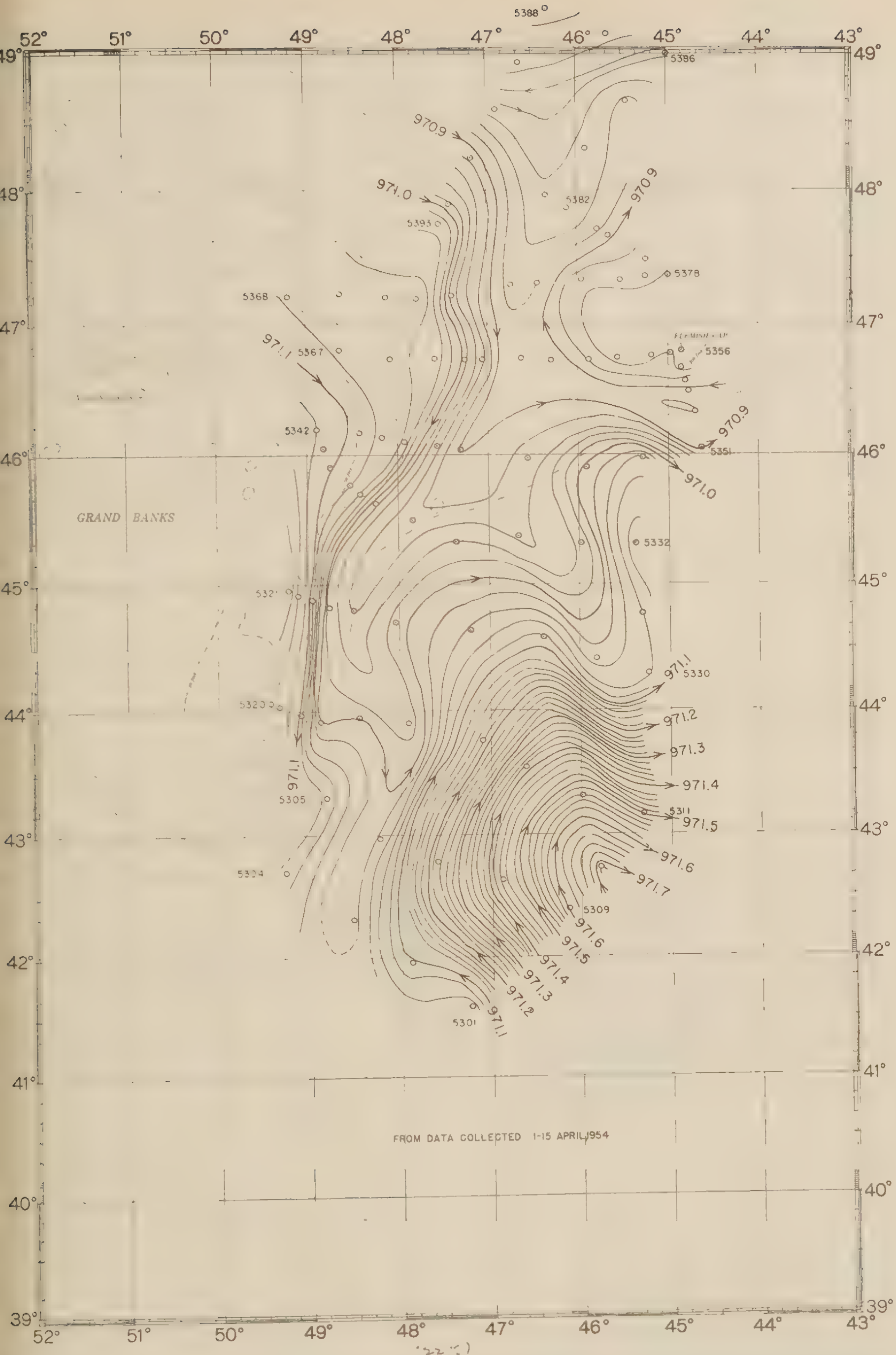
52°
51°
50°
49°
48°
47°
46°
45°
44°
43°
42°
41°
40°
39°
970.9
971.0
971.1
971.2
971.3
971.4
971.5
971.6
971.7
5388
5386
5382
5393
5378
5368
5367
5356
5342
5351
5332
5330
5320
5311
5309
5305
5304
5301
GRAND BANKS
FLEMISH CAP
FROM DATA COLLECTED 1-15 APRIL 1954

FIGURE 15.—Dynamic topography of the sea surface relative to the 1,000-decibar surface from data collected 1–15 April 1954. Oceanographic station positions are indicated and the station numbers given at turning points.

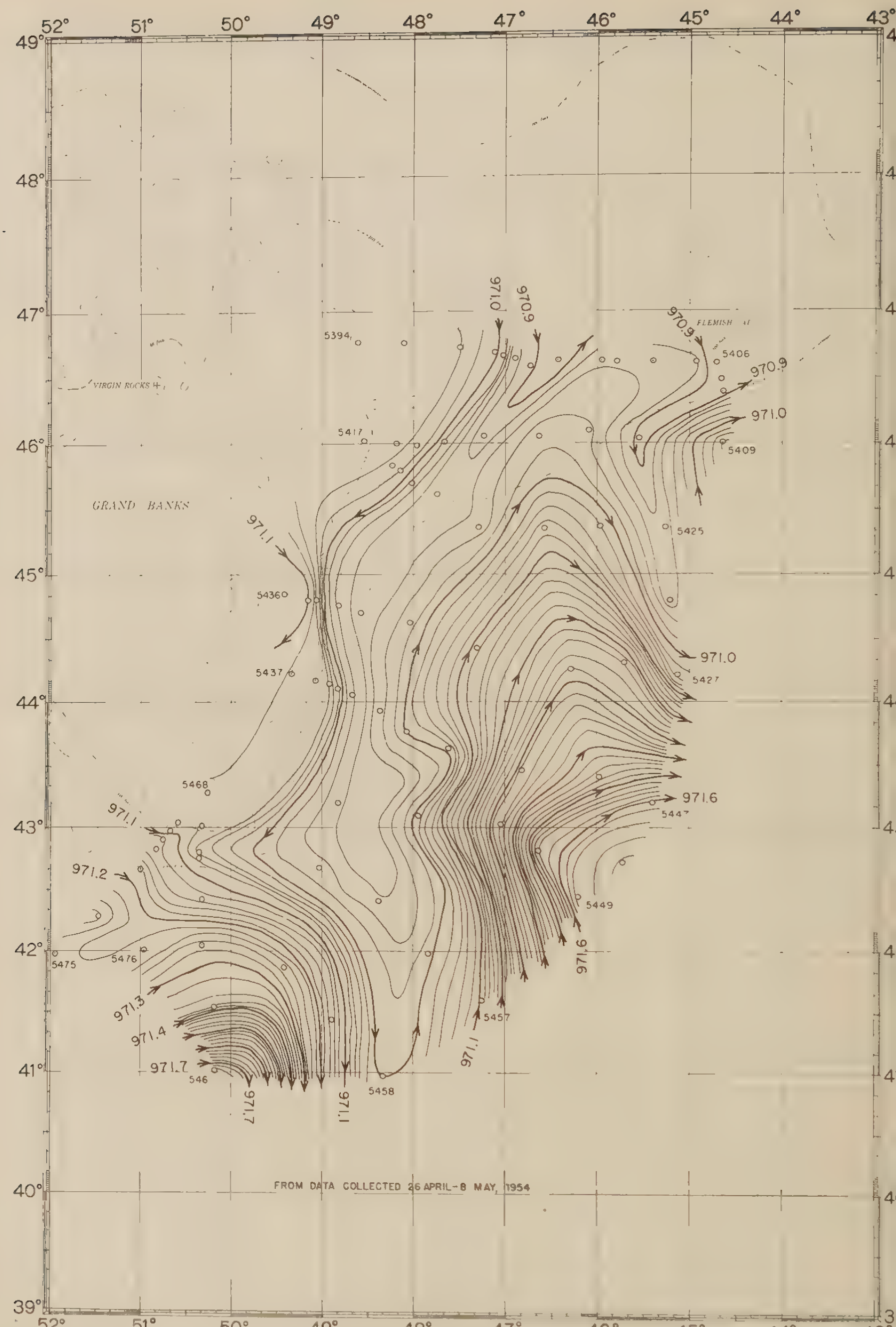
52°
51°
50°
49°
48°
47°
46°
45°
44°
43°
49°
48°
47°
46°
45°
44°
43°
42°
41°
40°
39°
VIRGIN ROCKS
GRAND BANKS
FLEMISH
5394
5417
5406
5409
5425
54360
5437
5427
5468
5447
5449
5457
5458
546
5475
5476
971.0
970.9
970.9
970.9
971.0
971.1
971.0
971.1
971.2
971.3
971.4
971.7
971.7
971.1
971.1
971.6
971.6
FROM DATA COLLECTED 26 APRIL–8 MAY, 1954

Figure 16.—Dynamic topography of the sea surface relative to the 1,000-deciba surface from data collected 26 April–8 May 1954. Oceanographic station positio are indicated and the station numbers given at turning points

figure 16, developed into interlocking high and low meanders in figure 18. One of these, developing westward along the 44th parallel, was accompanied by a greater eastward diversion of Labrador Current water in the lower dynamic heights northward of that latitude. The high meander, centered at 46° N., on the eastern edge of the second survey, developed westward and was centered at about 45°20′ N., in the third survey.

Figure 19, representing the dynamic topography found during the fourth survey, shows in greater detail the pattern of diversion of Labrador Current water eastward north of Flemish Cap and southward east of Flemish Cap. From the standpoint of berg mortality it is worthy of mention that in this survey the minimum temperatures in the cold core of the Labrador Current were uniformly about −1.5° C at all sections over the slopes of the Grand Banks, but the minimum temperatures in the cold core of the water in the eddy around Flemish Cap were about 2.0° at the periphery and about 3.5° at the center.

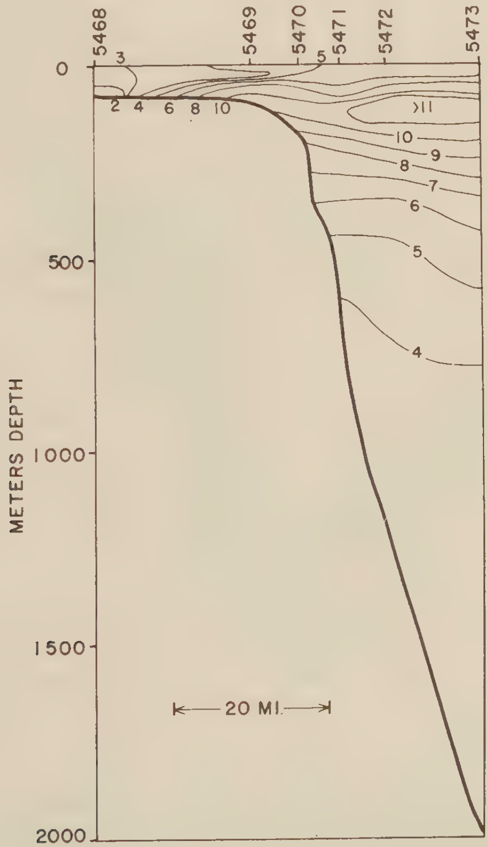

Figure 17.—Temperature distribution off southwestern slope of Grand Banks from data collected 7 May 1954.

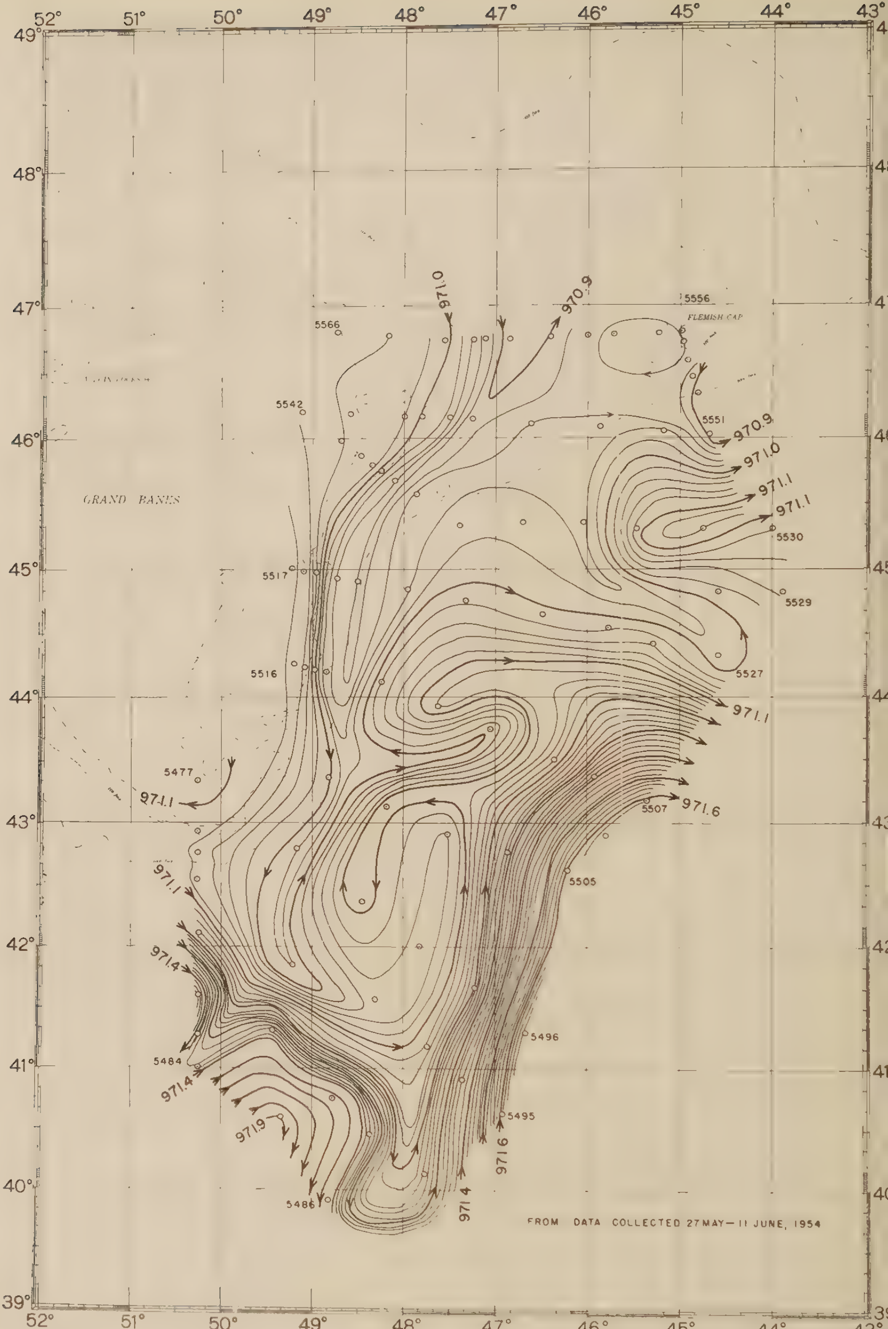
52°
51°
50°
49°
48°
47°
46°
45°
44°
43°
39°
40°
41°
42°
GRAND BANKS
FLEMISH CAP
971.0
970.9
5556
5566
5542
5551
970.9
971.0
971.1
971.1
5530
5517
5529
5527
5516
971.1
5477
971.1
5507
971.6
971.1
5505
971.4
5496
5484
971.4
5495
971.9
971.6
5486
971.4
FROM DATA COLLECTED 27 MAY — 11 JUNE, 1954

FIGURE 18.—Dynamic topography of the sea surface relative to the 1,000-decib surface from data collected 27 May–11 June 1954. Oceanographic station positio are indicated and the station numbers given at turning points.

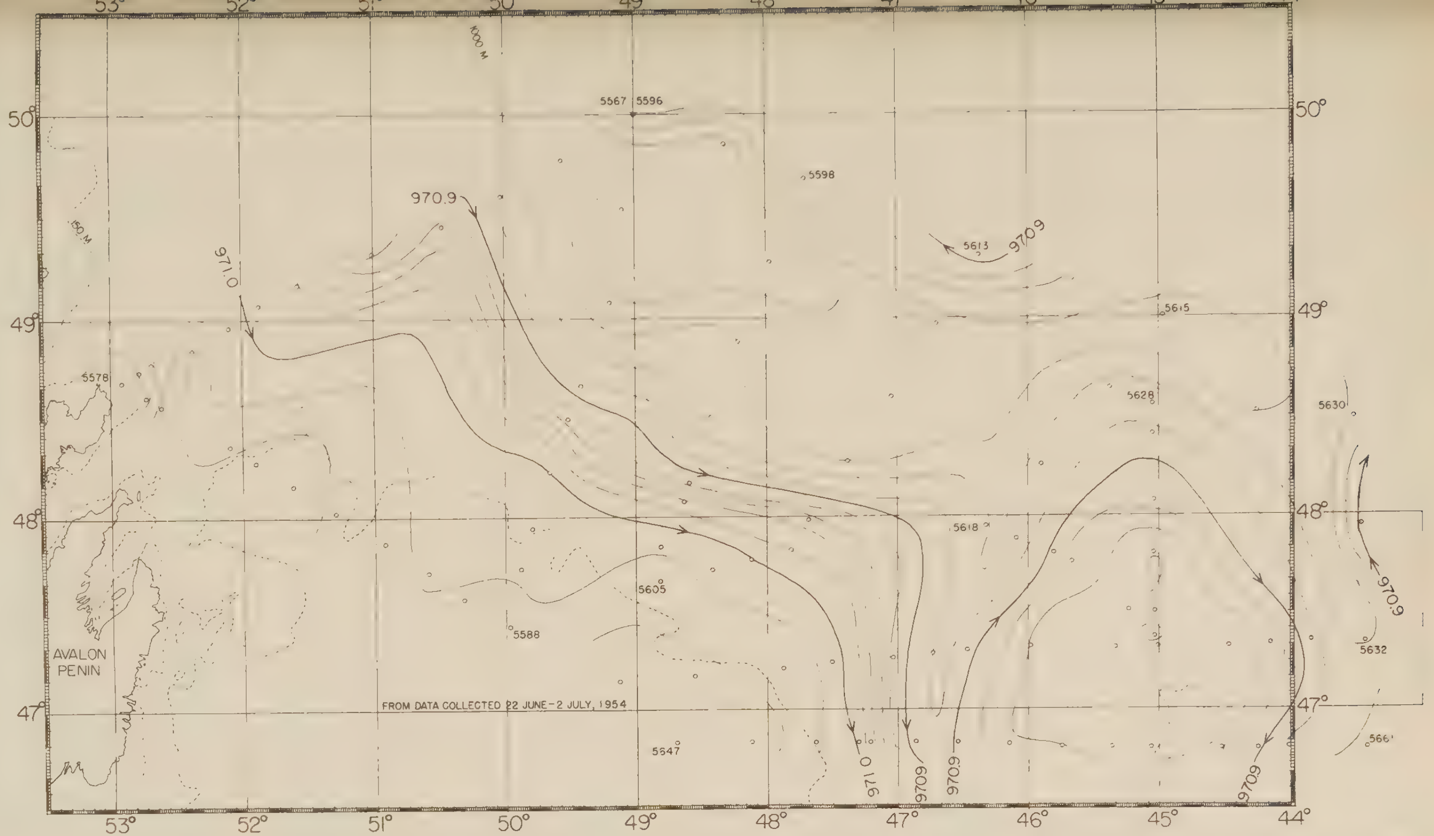
50°
49°
48°
47°
53°
52°
51°
50°
49°
48°
47°
46°
45°
44°
1000 M
150 M
5567
5596
5598
970.9
971.0
9709
5613
5615
5628
5630
5578
5618
5605
5588
5547
5632
5661
970.9
9709
9709
971.0
9709
AVALON PENIN
FROM DATA COLLECTED 22 JUNE–2 JULY, 1954

FIGURE 19.—Dynamic topography of the sea surface relative to the 1,000-decibar surface from data collected 22 June–2 July 1954. Oceanographic station positions are indicated and the station numbers given at turning points.

Table 1.—SUMMARY OF VELOCITY SECTIONS ACROSS LABRADOR CURRENT OCCUPIED IN 1954

Section	Volume transport			Mean temperature			Minimum observed temperature			Heat transport		
	1954	Normal	Anomaly	1954	Normal	Anomaly	1954	Normal	Anomaly	1954	Normal	Anomaly
1st survey:												
H	3.90	------	------	0.89	------	------	−1.56	------	------	3.46	------	------
F	3.16	------	------	0.61	------	------	−1.51	------	------	1.92	------	------
T	3.73	3.28	+0.45	1.09	1.97	−0.88	−1.42	−1.43	+0.01	4.05	6.46	−2.41
U	5.28	5.40	−0.12	0.80	1.42	−0.62	−1.16	−1.24	+0.08	4.25	7.67	−3.42
2d survey:												
F	3.64	------	------	1.33	------	------	−1.50	------	------	4.84	------	------
T	2.87	3.58	−0.71	1.68	1.85	−0.17	−1.44	−1.32	−0.12	4.83	6.62	−1.79
U	4.37	4.78	−0.41	0.82	2.02	−1.20	−1.09	−1.15	+0.06	3.58	9.66	−6.08
W	0.26	4.12	−3.86	5.35	2.90	+2.45	0.07	−0.55	+0.62	1.38	11.95	−10.57
3d survey:												
F	2.45	------	------	1.56	------	------	−1.59	------	------	3.81	------	------
T	2.19	2.67	−0.48	2.04	1.83	+0.21	−1.23	−1.55	+0.32	4.47	4.89	−0.42
U	4.52	3.63	+0.89	1.81	2.32	−0.51	−0.63	−1.24	+0.61	8.17	8.42	−0.25
W	0.65	4.12	−3.47	2.42	3.20	−0.78	−1.09	−0.35	−0.74	1.57	13.18	−11.61
4th survey:												
NW	2.80	3.81	−1.01	0.17	1.26	−1.09	−1.73	−1.66	−0.07	0.49	4.80	−4.31
SW	0.89	0.54	+0.35	−0.16	−0.19	+0.03	−1.61	−1.64	+0.03	−0.14	−0.10	−0.04
SE	1.72	3.20	−1.48	1.68	1.81	−0.13	−1.25	−1.55	+0.30	2.90	5.79	−2.89
H	3.44	------	------	1.97	------	------	−1.25	------	------	6.80	------	------
F	2.90	------	------	2.45	------	------	−1.49	------	------	7.10	------	------
Postseason:												
NW	3.36	4.55	−1.19	1.89	1.73	+0.16	−1.67	−1.52	−0.15	6.34	7.87	−1.53
SW	0.45	0.80	−0.35	1.26	0.62	+0.64	−1.65	−1.66	+0.01	0.56	0.50	+0.06
SE	2.84	3.58	−0.74	1.63	2.36	−0.73	−1.59	−1.65	+0.06	4.64	8.45	−3.81
South Wolf Island	7.84	4.73	+3.11	2.39	2.49	−0.10	−1.58	−1.48	−0.10	18.72	12.30	+6.42

More detailed study of the circulation in the upper 1,000 meters, with special reference to the Labrador Current, has been made in recent years through the examination of the volume of flow, mean temperature, and heat transport of that current across selected vertical sections. In 1954 this study included 21 occupations distributed among 9 different sections. Sections T, U, and W are located as follows: T extending southeasterly from about 46°20′ N., 49°00′ W.; U extending eastward from the Grand Banks at about 45° N.; W extending southward from the Grand Banks at about 50° W. Rough approximations to normal seasonal variation relationships have been developed for these three sections and were published in bulletin No. 36 of this series. Rough normal seasonal variation relationships for the sections NW, SW, and SE, comprising the sides of the Bonavista triangle, were published in bulletin No. 39 of this series. The results of the 1954 occupations of these sections have been compared with these seasonal normals. The South Wolf Island section has been occupied 17 times in as many different years from 1928 to 1954, most of the measurements having been made at about the same time of year. The results of the 1954 occupation of this section have been compared with average values. For the sections F (between Flemish Cap and the Grand Banks) and H (between sec. F and the Bonavista triangle) there are insufficient data on which to base average values for comparison. Table 1 summarizes the results of the velocity sections across the Labrador Current occupied in 1954 compared with normal or average values where available. In this table as well as in subsequent tables, figures and discussion, the units are as follows: volume of flow, 1 million cubic meters per second; mean temperature and minimum observed temperature, degrees C; heat transport, 1 million cubic meter degrees C per second.

From table 1 it will be noted that, in spite of the considerable diversion of Labrador Current water eastward north of Flemish Cap, the volume transport past section T was above normal during the first survey and that past section U was nearly normal and the mean temperature was decidedly colder than normal. During the second survey the normal seasonal increase in volume of flow did not occur and the transport past sections T and U dropped below normal. As the Labrador Current was not rounding the Tail of the Banks to the westward, the transport past section W was small. The mean temperature at section T was nearly normal, but that at section U held its early season value so that it was more than a degree colder than normal. By the time of the third survey the transport past section T was still below normal, but at section U a slight increase instead of the seasonal decrease brought the volume well above normal. The mean temperature rose at each of these sections to bring that at section T above normal and leaving that at section U about a half degree below normal. The minimum temperatures, which had been close to normal at both sections during the first two surveys, rose to 0.3° and 0.6° above normal during the third survey. The interpretation of the tabulated values in table 1 and the surface topography shown in figures 15, 16, and 18 is that the larger volume transport at section U compared with section T represented contributions of waters from the northward west of section T during the first and second surveys and that during the third survey some of this additional volume transport was contributed by a closed circulation over the Grand Banks.

Figure 20 shows the dynamic topography found during the post-season cruise at the Bonavista triangle. This is separated in point of time by about 2 months from the occupation of the triangle during the fourth survey. Also, its date in the latter part of August is later than the season of the year covered by the normal seasonal variation relationships given in bulletin No. 39. The normals with which it has been compared are therefore of doubtful applicability. Table 1 shows the volume transport as below normal past sections NW. and SE. and above normal past section SW. at the time of the fourth survey. The tabulated values are for the net transport past each of the sections. Usually the offshore corner of the triangle is close enough to the line of zero velocity between the Labrador Current and the northward flow offshore of it so that the net transport for the section is a good measure of the Labrador Current at the triangle. At the time of the fourth survey, however, the offshore corner was well into the northbound current, and in fact included about 1.0 million cubic meters per second of northward-moving water. The tabulated transport values should therefore be increased by about 1.0 for both sections NW. and SE. to obtain the transport of the Labrador Current for the fourth survey. Thus the transport was about normal at these sections and about 0.4 above normal at section SW. The proportion of the total Labrador Current following the eastern branch was 78 percent, which is below normal for this time of year. At the time of the postseason cruise the volume transport had dropped to values even smaller than the supposed normals for the time of year. Although the proportion of the total Labrador Current flowing in the eastern branch normally decreases seasonally, it increased in 1954

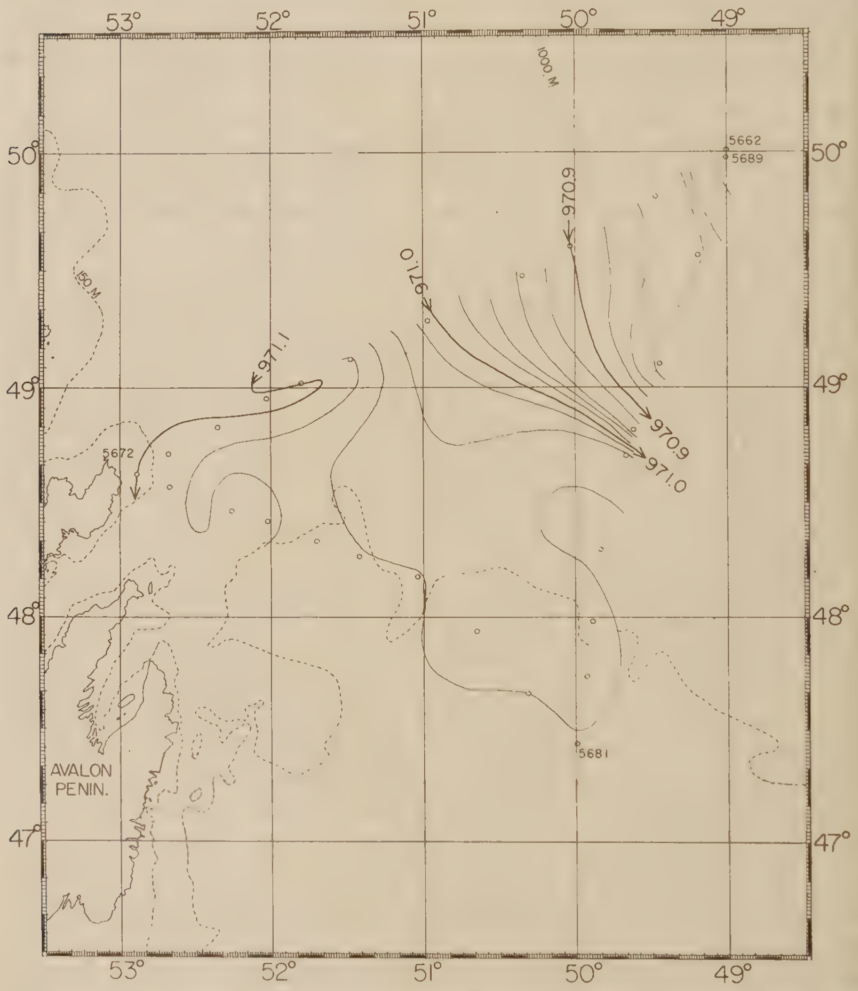

FIGURE 20.—Dynamic topography of the sea surface relative to the 1,000-decibar surface from data collected 21–24 August 1954. Oceanographic station positions are indicated and the station numbers given at turning points.

and was 86 percent at the time of the postseason cruise instead of the supposed normal of 81 percent. As figure 20 indicates, there also was some northward-flowing water inside the offshore corner of the Bonavista triangle during the postseason cruise. The volume transport of the Labrador Current past the triangle was therefore somewhat larger than tabulated for the postseason cruise, but the difference was much smaller than for the fourth survey. It has been neglected here and is not of the same order of magnitude as the difference between the volume transport at the triangle and that of the Labrador Current off South Wolf Island only 3 days later.

The circulation deduced from table 1 has been shown schematically in figure 21. In this figure the volume transports have been rounded off and adjusted in the Bonavista and Greenland triangles on the assumption that there was no appreciable vertical transport past the reference surfaces. Further reference will be made to this figure after consideration of the sections occupied in the Greenland area during the postseason cruise.

It was pointed out in bulletin No. 39 of this series that more often than not the minimum observed temperature was colder at the Bonavista triangle than at the South Wolf Island section. This was true again in 1954 when the minimum observed temperature at the triangle was −1.67° C with a corresponding salinity of 33.15°/₀₀, whereas the minimum observed temperature off South Wolf Island was −1.58° C with a corresponding salinity of 32.85°/₀₀. Comparable average values for the 7 years during which observations have been made are −1.65° C, 33.14°/₀₀, −1.53° C, and 32.81°/₀₀. Since 1949 the volume transport of the Labrador Current at the South Wolf Island section has been greater than average with the transport in 1954 exceeding any of the other 16 years. Since 1950 its mean temperature has been consistently above average until 1954, when it dropped to 0.1° below average. The heat transport in 1954 is consequently a high value, exceeded only by that in 1933, when a large volume transport was accompanied by a high mean temperature.

Labrador Current water and Atlantic Current water present in the Grand Banks region have been found to have characteristic temperature-salinity relationships identifying them as water masses. Usually also the mixed water formed from these parent water masses has a sufficiently uniform proportion of the parent water masses so that it can be regarded as a virtual water mass. The first three surveys of the 1954 season were examined for T–S relationships. The fourth survey was omitted as being located outside the area which has been the source of the T–S data considered in the past. Figure 22 shows the relationships found in 1954, as solid lines, in comparison with the averages for the 8-year period 1934-41, shown in broken lines. In general, all three water masses were lighter than the prewar average. The differences were least in the Labrador Current water and here

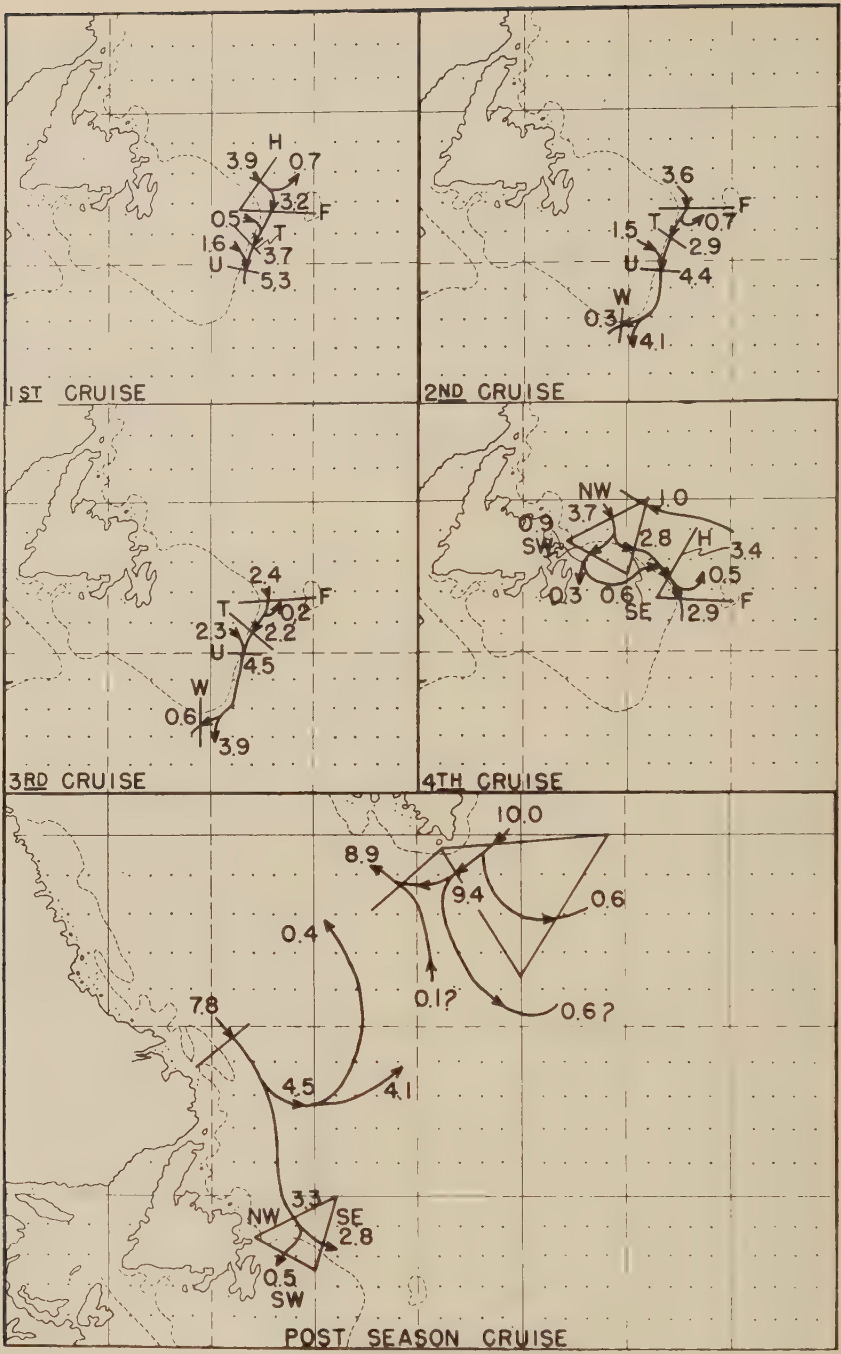
H
3.9
0.7
3.2
F
0.5
T
1.6
3.7
U
5.3
1ST CRUISE
3.6
F
1.5
T
0.7
2.9
U
4.4
W
0.3
4.1
2ND CRUISE
2.4
F
T
0.2
2.3
2.2
U
4.5
W
0.6
3.9
3RD CRUISE
NW
1.0
3.7
0.9
SW
2.8
H
3.4
0.5
0.3
0.6
SE
12.9
F
4TH CRUISE
10.0
8.9
9.4
0.6
0.4
0.1?
0.6?
7.8
4.5
4.1
3.3
NW
SE
2.8
0.5
SW
POST SEASON CRUISE

Figure 21.—Schematic representation of circulation deduced from sections occupied during 1954. Numerals indicate volume transport in units of cu. m/sec. x 10^6.

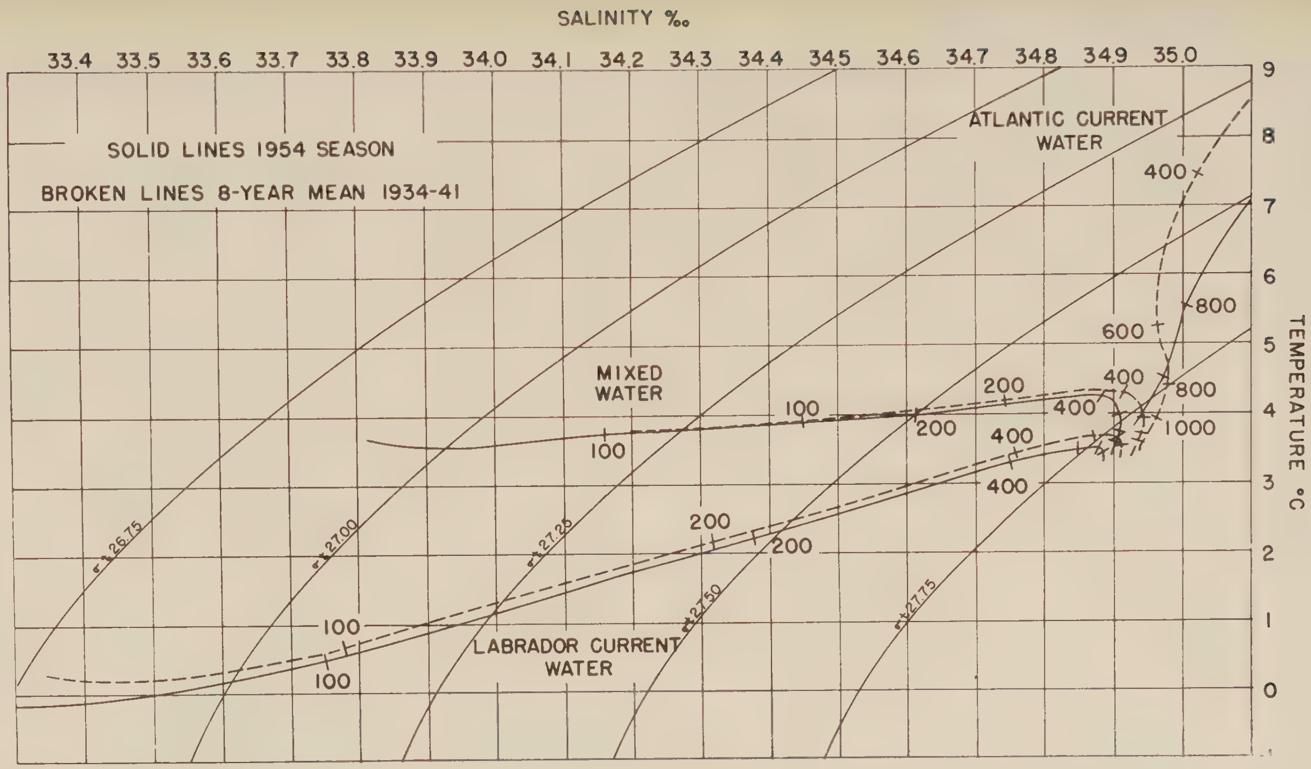

Figure. 22.—Temperature-salinity relationships for Labrador Current water, Atlantic Current water, and mixed water found in the Grand Banks region. Solid lines show conditions during the 1954 season and broken lines represent the 8-year mean for the period 1934–41. An approximate depth scale in meters is given.

(except for the 200-meter level) lower salinities were largely compensated for by lower temperatures. In the mixed water the principal difference is in the salinity which was less than the 8-year average in 1954. The shape of the characteristic curve for Atlantic Current water was materially different in 1954 from that of the 8-year average. The bulge toward lower salinity at a temperature of about 6° was markedly less. This is probably because more of the 1954 stations were farther into the Atlantic Current than is usual and the bulge is a feature of the outer margins of this current in the Grand Banks sector. The lower densities were the result of higher temperature, with the temperature effect outweighing the effect of higher than average salinities down to about 1,000 meters. Below 1,000 meters in the Atlantic Current the salinities found in 1954 were about average.

The second and third surveys each contained a number of stations where the water was atypical and irregularly intermediate between Atlantic Current water and mixed water. In the second survey the warm water thrust toward the southwestern edge of the Grand Banks was made up of these stations. The third survey had these stations

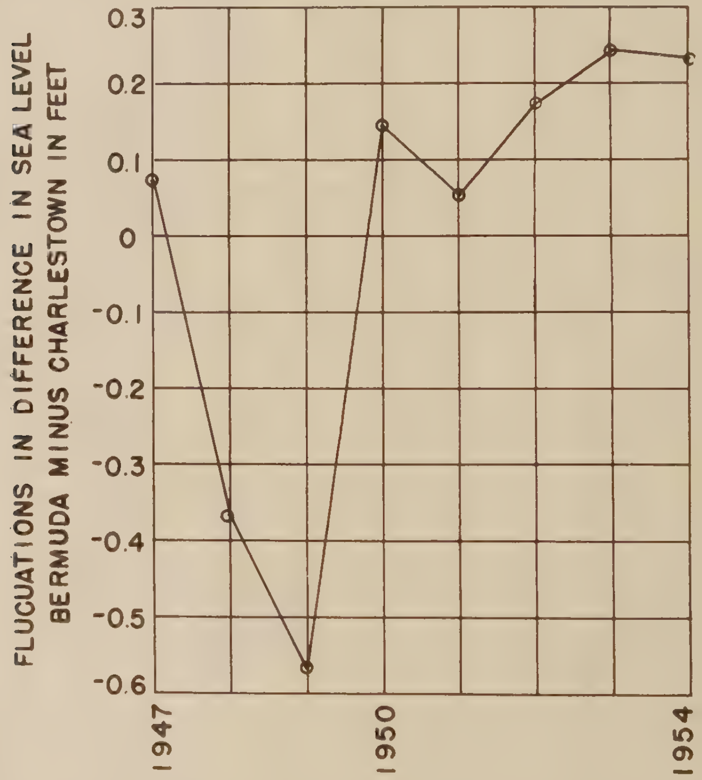

FIGURE 23.—Fluctuations in the activity of the North Atlantic eddy during the years 1947–54 as indicated by the changes in the difference in sea level Bermuda minus Charleston.

distributed downstream between the mixed water and the Atlantic Current water.

The position of the cold wall is an important factor in determining the southern limits of berg-infested waters in the vicinity of the Grand Banks. Its fluctuations have been studied and reported on in earlier bulletins of this series. As it is not necessarily a vertical boundary, the boundary selected for study is the horizontal projection of the line along which a temperature of 6° corresponds to a salinity of 34.95‰. The position of this boundary has been described numerically by the area between it and fixed rhumb lines northwestward of it (the 45th parallel, the 49th meridian from 45° N., to 43° N., and a line from 43° N., 49° W., through 42° N., 47° W.). Thus, as the boundary moves toward the Grand Banks, the area decreases. It was considered that the position taken up by the boundary was determined partly by forces associated with the North Atlantic eddy and partly by forces associated with the Labrador Current. An assumption was made that the area would be increased by 10,000 square kilometers for each million cubic meters per second volume transport of the Labrador Current entering the area past section U. After subtracting such an amount from the area to obtain an adjusted area, A, this adjusted area was considered as representing the effects of causes associated with the Gulf Stream system. A further assumption was made that these causes were related to the difference in sea level between Bermuda and Charleston, S. C., and hence that fluctuations in A would be related to fluctuations in this sea-level difference. With sea level at Charleston minus the departure from average sea level at Bermuda, in feet, designated as H, and A in units of 10,000 square kilometers with a time lag of 13½ months, 27 surveys made during the ice patrol seasons 1934–41 gave the expression

$$\mathrm{A}=6.8\ (H-5.07)+1.34.$$

Following the interruption of World War II, surveys were resumed in 1948. The postwar surveys have not agreed with the above relationship but followed a similar relationship if 11½ months was used as the time lag instead of 13½ months. Ten surveys made during the period 1948–52 were combined with the 27 prewar surveys, using 11½ months for the postwar time lag, to derive the expression

$$A=6.97\ (H-5.07)+1.67.$$

Two further surveys made in 1953 did not fit either of the above expressions, and examination of the fluctuations in sea level indicated that the time lag might have been either 11½ or 13½ months. Three surveys made in 1954 indicated the 11½ month time lag was still applicable and the actual values of A were −0.03, 1.31, and 3.35

compared with values computed with the 1952 expression of 0.83, 0.07, and 2.65.

The quantity H involves the sea level at Charleston and the departure from average sea level at Bermuda. Average sea level at Charleston enters the constant 5.07. Part of the difficulty in obtaining a good correlation in the postwar years is believed to be the changes in relative sea level which have taken place at both stations. The average sea level at Charleston for the 8-year period 1947–54 is 0.27 foot higher than during the prewar 8-year period 1933–40, and the postwar average sea level at Bermuda is 0.10 foot higher than that for the prewar period. Another possible difficulty is the exceptionally large variation in difference in sea level at these stations during the postwar period. Figure 23 shows the fluctuations in annual average values of the difference in sea level Bermuda minus Charleston. If this is taken as a measure of the activity of the North Atlantic eddy and if the total difference in sea level is inferred from density distribution, the range of 0.8 foot shown in figure 23 represents a fluctuation of about 30 percent. It is possible that the simple expressions given above may represent the relationship between the sea-level difference, the strength of the Labrador Current and the position of the cold wall in the Grand Banks region adequately for small changes, but become inadequate when major changes in the driving forces require the establishment of large compensating circulation patterns.

Figure 24 shows the dynamic topography of the sea surface relative to the 1,500-dicibar surface from the observations made during the 1954 postseason cruise along the section acrosss the Labrador Sea and the Greenland triangle. The temperature and salinity distribution along these four sections are shown in figures 25 to 32. In figure 25 it will be noted that the temperature minimum in the Labrador Current over the shelf has only a small cross section colder than −1.5°. The temperature maximum reaching bottom at intermediate depths along the continental shelf is defined by the 3.5° isotherms and contains observed temperatures up to 3.79°. The temperature minimum at intermediate depths in the central part of the section is indicated by the area enclosed in the 3.2° isotherm. Although the area thus enclosed is small, the temperature of the minimum is close to that of the colder years 1934–39 and 1950 when the minimum was about 3.17°. During the other 7 years for which data are available (1940–41, 1948–49, and 1951–53), the minimum was about 0.10° to 0.15° warmer. The temperature maximum below this minimum was for the most part less than 3.3°. At the Greenland end of the section the warm water of the West Greenland Current had about the same cross-sectional area with water warmer than 4° as was found in 1953, but the areas enclosed by the 5° and 6° isotherms was greater in 1954.

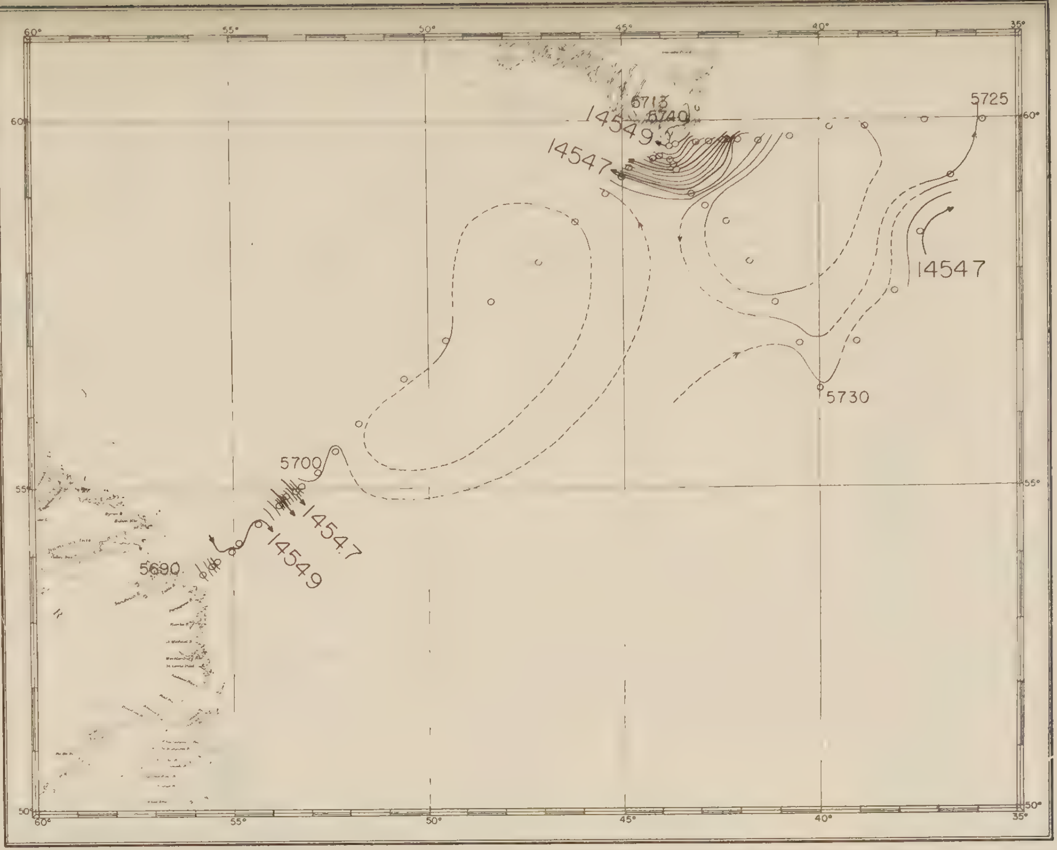
60°
55°
50°
45°
40°
35°
5725
6713
5740
14549
14547
14547
5730
5700
14547
14549
5690

FIGURE 24.—Dynamic topography of the sea surface relative to the 1,500-decibar surface from data collected 25 August–4 September 1954. Oceanographic station positions are indicated and the station numbers given at turning points.

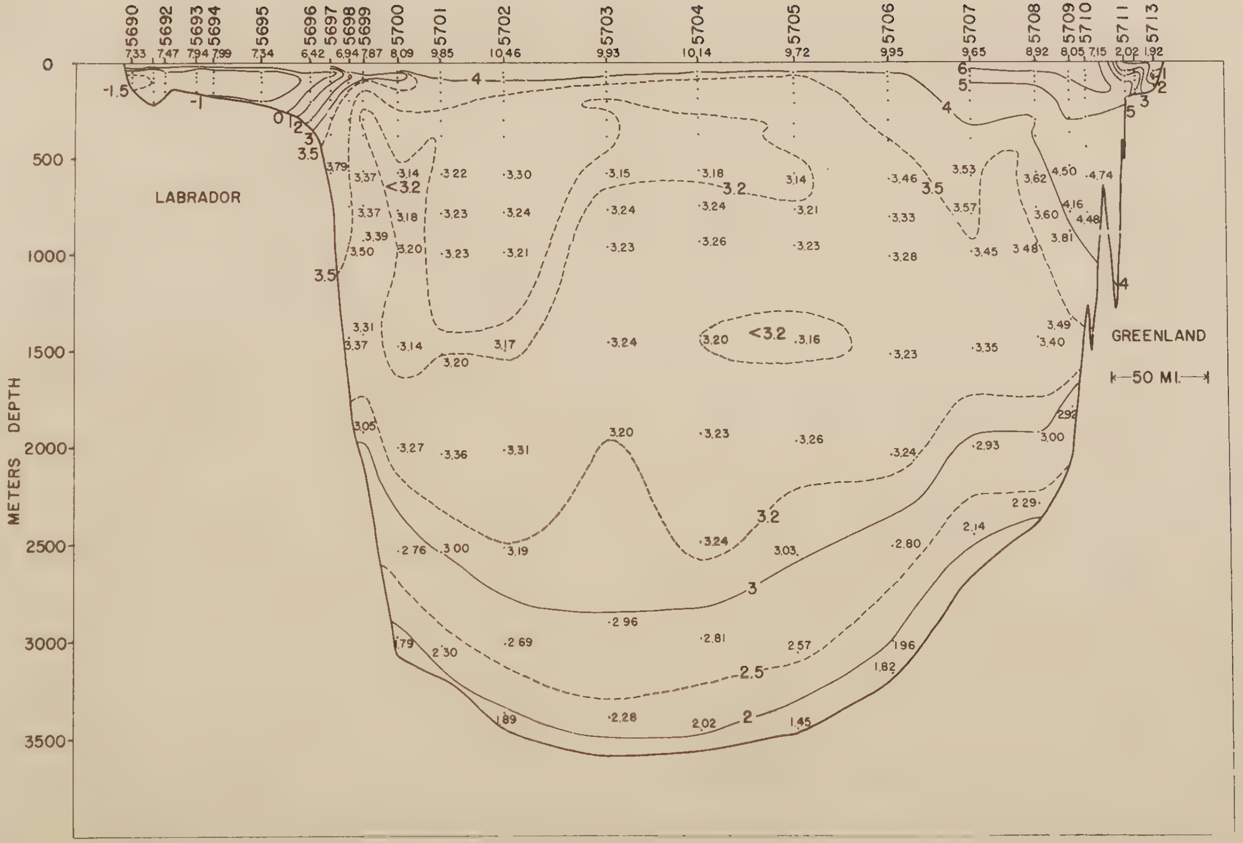

FIGURE 25.—Temperature distribution between South Wolf Island, Labrador and Cape Farewell, Greenland, 25–29 August 1954.

The surface topography shown in figure 24 indicates a simpler pattern in the Labrador Sea than that found in 1952 and 1953, when the extreme outer margins of the North Atlantic eddy reached northwestward as far as this section. The contribution of offshore water of the Labrador Current to the offshore part of the West Greenland Current between stations 5708 and 5709 may not be as direct as indicated in figure 24. The higher temperatures of this water in the

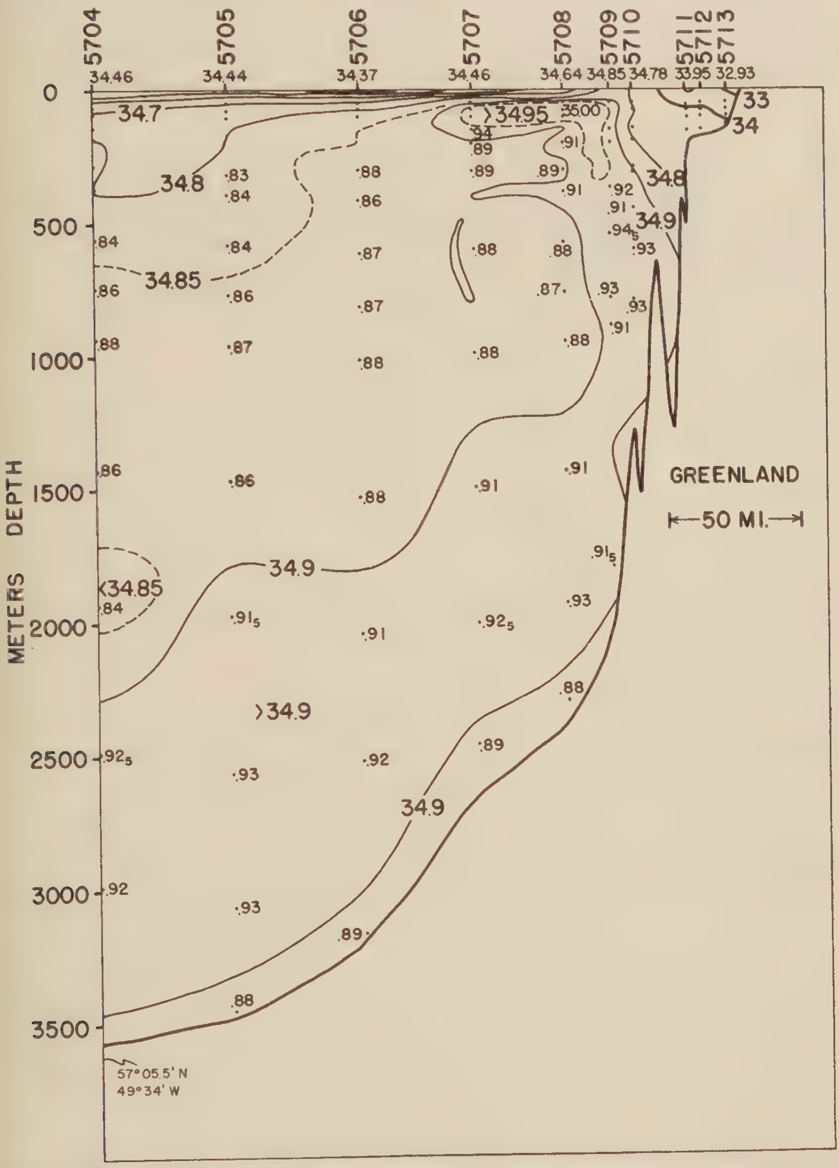

FIGURE 26.—Salinity distribution southwest of Cape Farewell, Greenland, 27–29 August 1954.

West Greenland Current suggests that the Labrador Current water has been mixed with some North Atlantic Current water in its journey northeastward although this may be the result of seasonal warming. Below the surface in the West Greenland Current the salinity reached a maximum of 35.00°/₀₀, with a small cross-sectional area of greater than 34.95°/₀₀ as shown in figure 26. While this is a decided increase over 1953 when the maximum found was 34.925°/₀₀, it is still short of the 35.04°/₀₀ found consistently during the prewar years.

The volume transport of the West Greenland Current past this section was found to be 8.95, with a mean temperature of 4.95° and a heat transport of 44.33. On the basis of constant mean temperatures

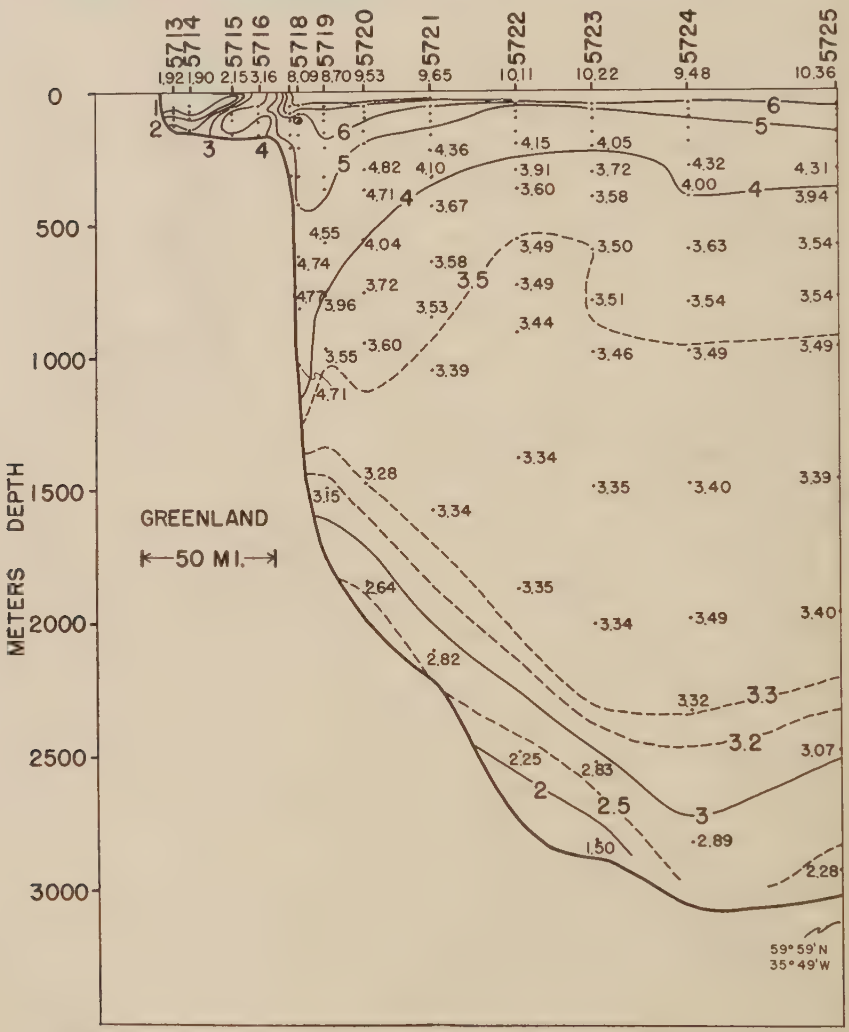

Figure 27.—Temperature distribution east of Cape Farewell, Greenland, 29–31 August 1954.

of 3.2° for the East Greenland Current component and 5.5° for the Irminger Current component, the observed volume transport breaks down into 2.13 and 6.82, respectively, for these components, compared with seasonal normal volume transports for these components of 0.09 and 4.42. On this basis then, each of the components were about 2 above normal in volume with a resulting heat transport 24.60 above normal. In view of the low salinity maximum it is quite possible that more of the West Greenland Current past this section approaches from the south than the 0.1 estimate shown in figure 21.

In examining the complete South Wolf Island-Cape Farewell section for volume of flow it was found that, if the velocities are referred to

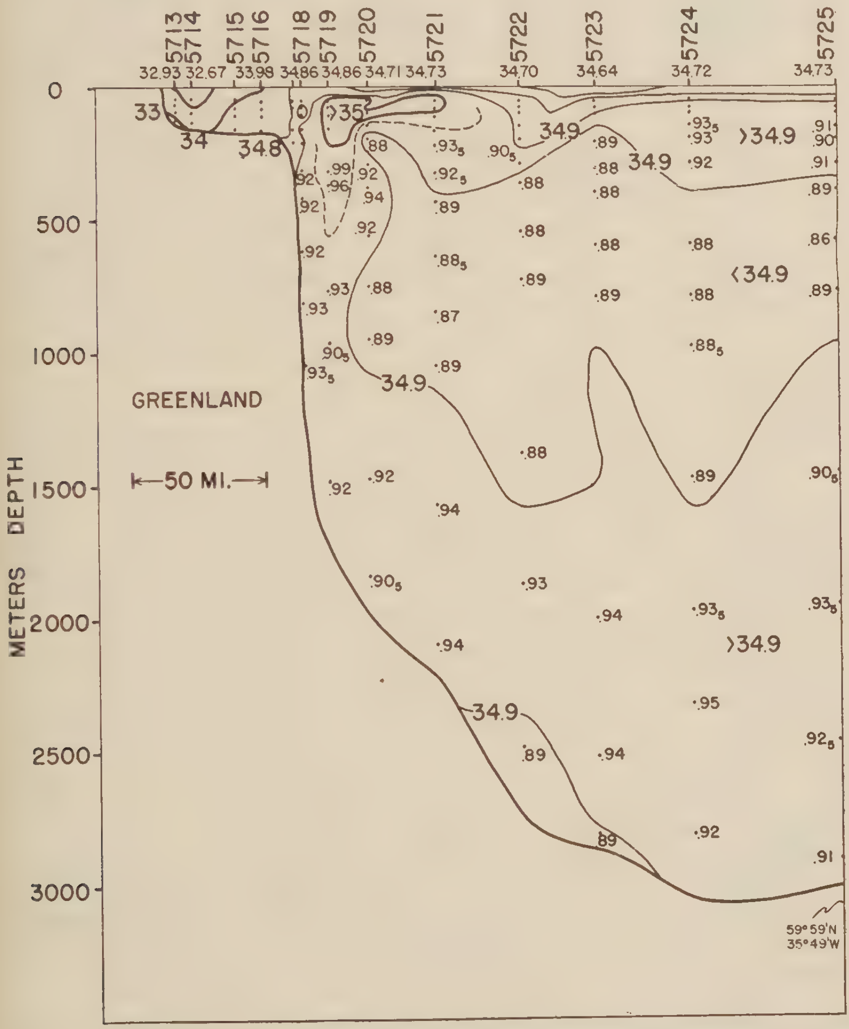

Figure 28.—Salinity distribution east of Cape Farewell, Greenland, 29–31 August 1954.

the 1,500-decibar surface, the net volume transport was 1.46 northwesterly. Although available observations are few, our conception of the circulation balance is that there is a small net contribution through the northern openings into the Baffin Bay-Labrador Sea system and a small sinking and outflow into the North Atlantic below the reference surface. These have been estimated to be of the order of a million cubic meters per second. If the reference surface of 1,500 decibars is acceptable, the sinking and outflow below it must have exceeded the

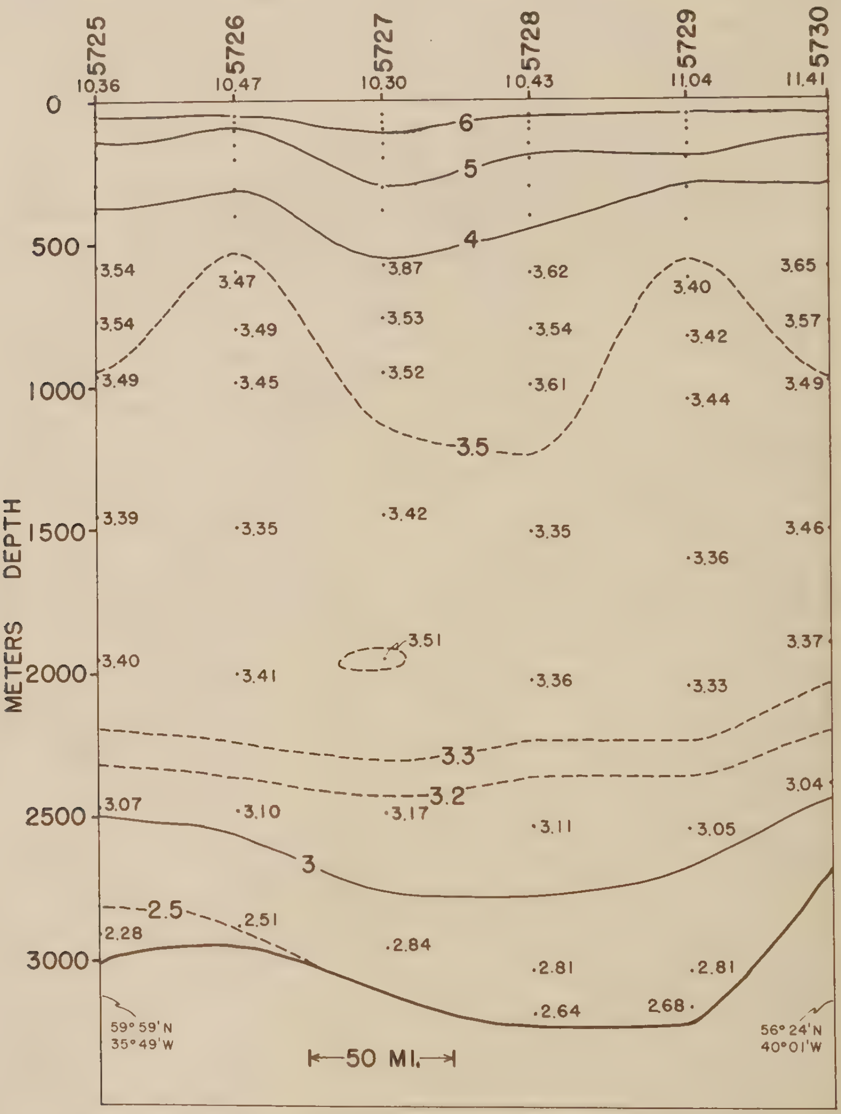

FIGURE 29.—Temperature distribution along offshore leg of Greenland triangle 31 August–2 September 1954.

contributions through the northern openings by the net northwesterly volume transport across this section. The value of 1.46 is larger than the errors of the methods used, and reference to the density distribution along the section indicates the 1,500-decibar surface was probably close to being the most nearly motionless at the time of the observations. The conclusion reached is that either the contributions through the northern openings were smaller or the sinking and outflow in the deep water was greater than usual or both.

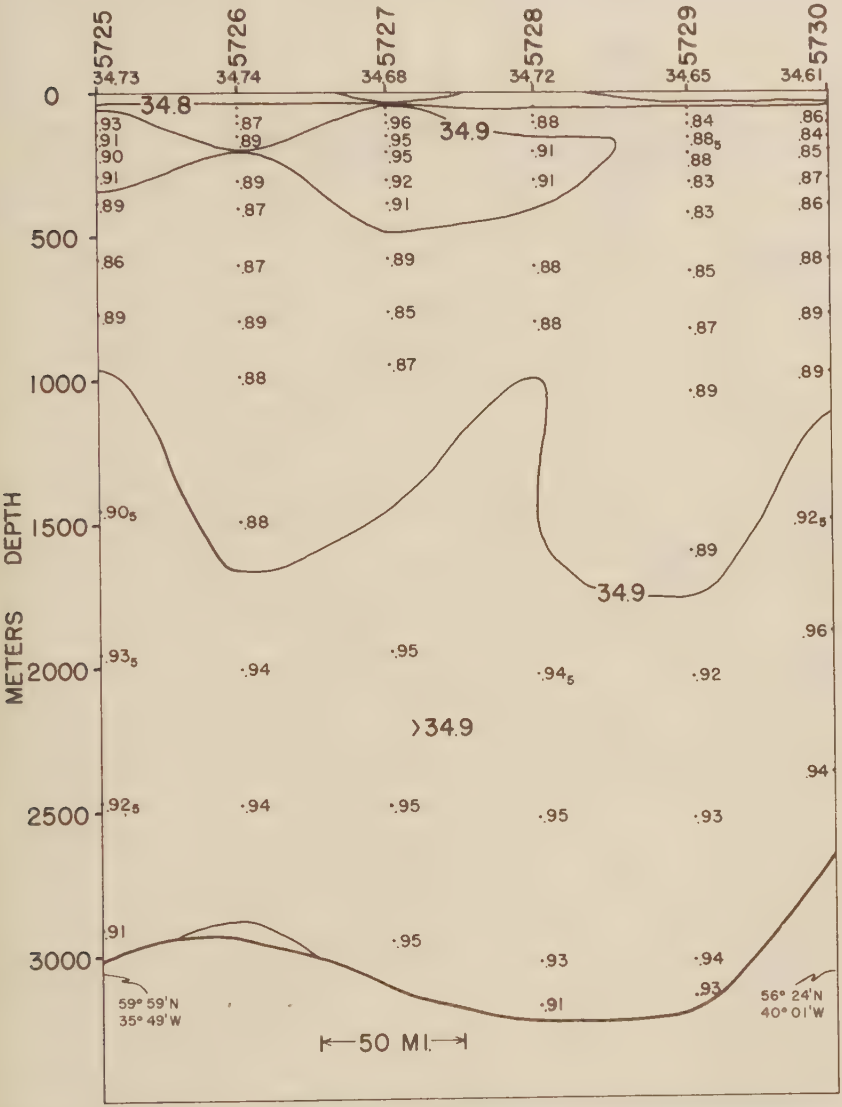

FIGURE 30.—Salinity distribution along offshore leg of Greenland triangle 31 August–2 September 1954.

Velocity profiles have been examined for each of the three sides of the Greenland triangle, and the resulting volume transports for the north, southeast, and southwest sides were 10.49, 0.47, and 8.99, respectively. As these figures indicate about 10 percent greater volume transport into the triangle than that leaving it, the computed volumes have been adjusted to equality for representation in figure 21. The mean temperatures for the sections, in the same order, were 5.37, 5.62, and 5.15, resulting in heat transports of 56.28, 2.65, and 46.25, respectively. As the point of beginning and ending was at the shallow corner of the triangle, it is difficult to make any straight-

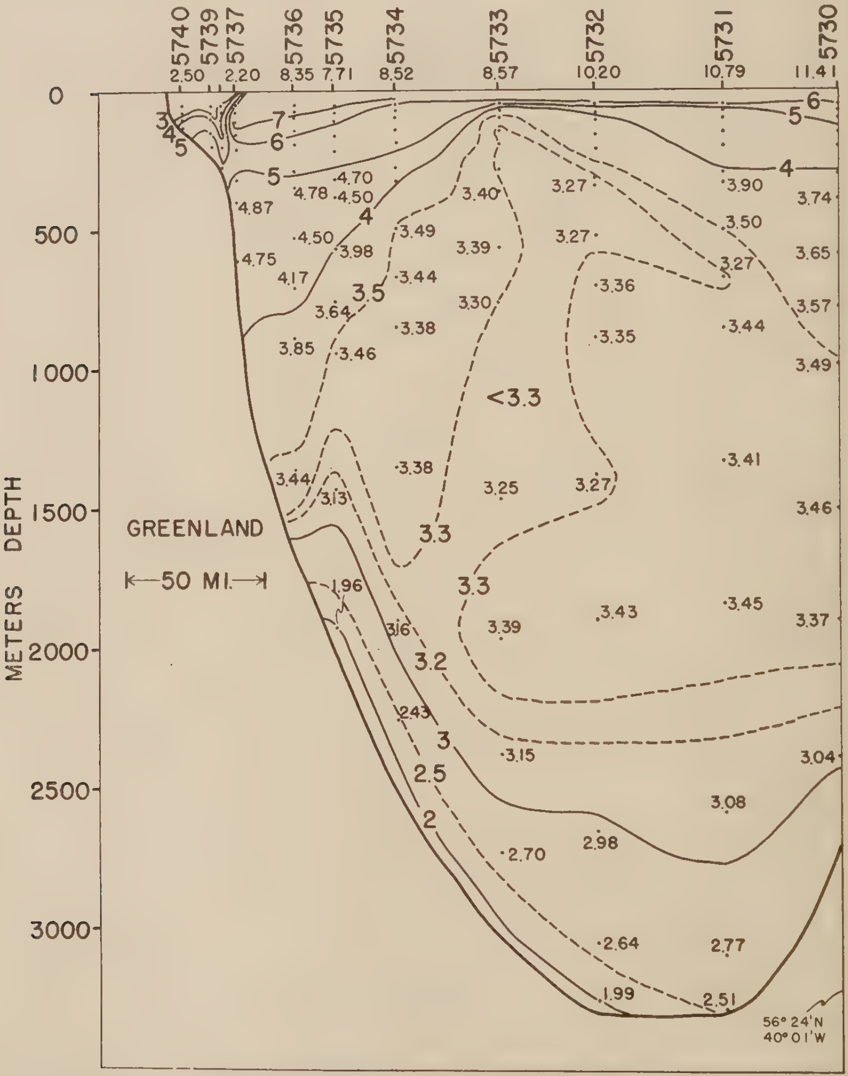

FIGURE 31.—Temperature distribution southeast of Cape Farewell, Greenland, 2–4 September 1954.

forward allowance for time changes which no doubt resulted from the gale which occurred between the occupation of stations 5734 and 5735. The loss of volume southward, both inside the triangle and between the triangle and the section across the Labrador Sea, is in accord with the reports of exceptional numbers of bergs south-southeastward of Cape Farewell. As suggested above, perhaps even more than the estimated 0.6 moved southward and eastward south of the triangle.

In considering the temperature sections forming the three sides of the triangle (figs. 27, 29, and 31), it will be noted that the temperature structure in the vicinity of Cape Farewell is markedly different in

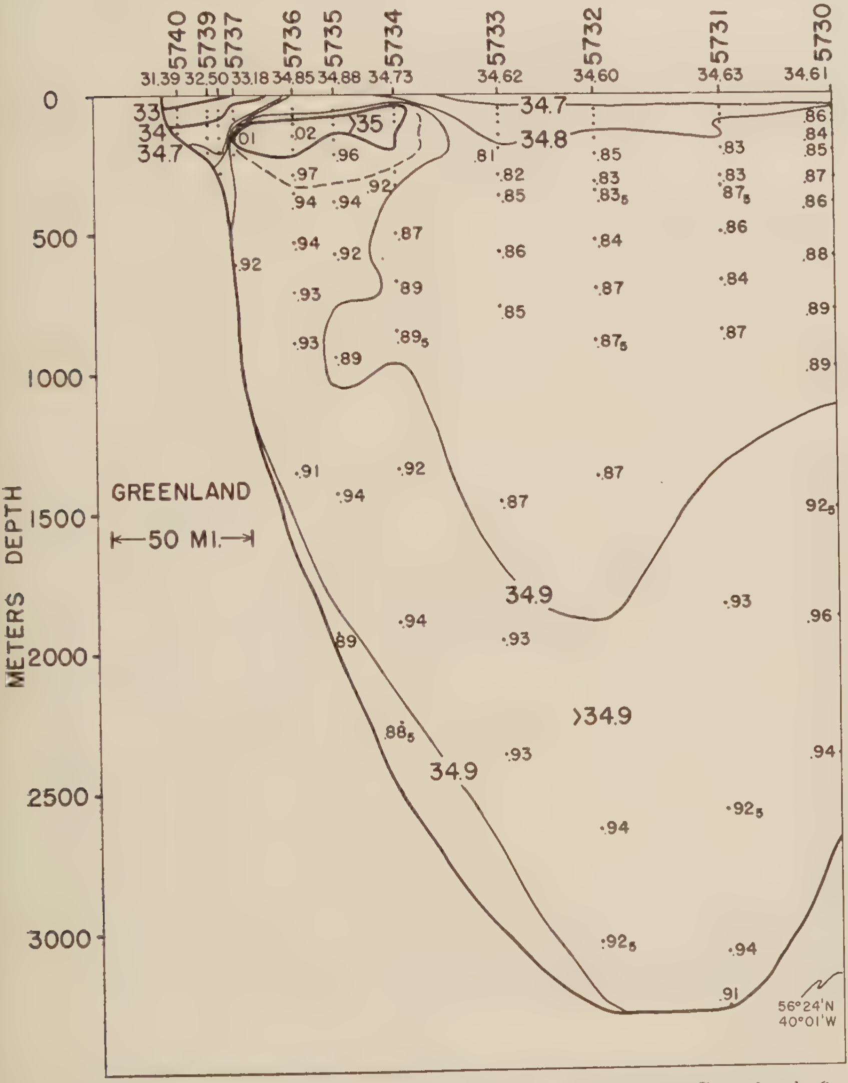

FIGURE 32.—Salinity distribution southeast of Cape Farewell, Greenland, 2–4 September 1954.

figures 27 and 31. In these two sections the deep water with temperatures of less than 3.2° is recognizably similar. Above this the intermediate water has but slight gradients between temperatures of 3.2° and 3.5°. In figure 31 there appears a poorly developed temperature minimum, with temperatures of between 3.25 and 3.3, which is similar to that found in the section across the Labrador Sea and it is probable that it is related to the Labrador Sea minimum in its formation. In the northern side of the triangle (fig. 27) such a minimum is hinted at, but the temperatures here are about 0.1° higher.

Figures 28, 30, and 32, showing the salinity distribution along the three sides of the triangle, all show a minimum with salinities of less than 34.90°/oo in the intermediate water with an underlying maximum greater than 34.90°/oo in the deep water. In figures 28 and 32 this maximum is connected along the continental slope with the maximum associated with the Irminger Current. Here the highest observed salinities were 35.055 and 35.04°/oo in the north and southwest sections, respectively. These are of the magnitude found in the section extending southwest from Cape Farewell in the prewar years and not found there since 1949.

In the hope that the concentration of total phosphorus might be useful as a water-mass tracer in the vicinity of southern Greenland, samples were taken from all levels at most of the stations during the May survey of the Grand Banks region in 1952 and characteristic phosphorus-density curves were derived from this survey for each of the three water masses (Labrador Current water, mixed water, and Atlantic Current water) present in that region. Samples were also taken from all levels at all stations comprising the South Wolf Island-Cape Farewell section in July 1952 and July 1953. The results of these observations have been reported in bulletin No. 39 of this series. In 1954 similar sampling was carried out during the occupation of the South Wolf Island-Cape Farewell section and the Greenland triangle. The results of the 1954 phosphorus determinations are tabulated at the end of the usual table of oceanographic data, and the phosphorus distribution has been shown graphically in figures 33 to 36. In each of these figures isentropic surfaces of equal potential density [3] have been shown as solid lines. In the South Wolf Island-Cape Farewell section (fig. 33), the phosphorus concentration shows very little variation at depths greater than 50 meters. There is a slight maximum at intermediate depths along the outer part of the Labrador Current and a somewhat greater maximum similarly located along the offshore part of the West Greenland Current. Elsewhere the range is for the most part between 1.1 and 1.3 microgram-atoms per liter. Some slight instabilities are present and the course of the 1.2

---

[3] $\sigma_{t\theta}$, where $t\theta$ is the temperature a water particle would have if its pressure were reduced adiabatically to atmospheric pressure, and where $\sigma_{t\theta}$ is 1,000 (density −1) at atmospheric pressure and temperature $t\theta$.

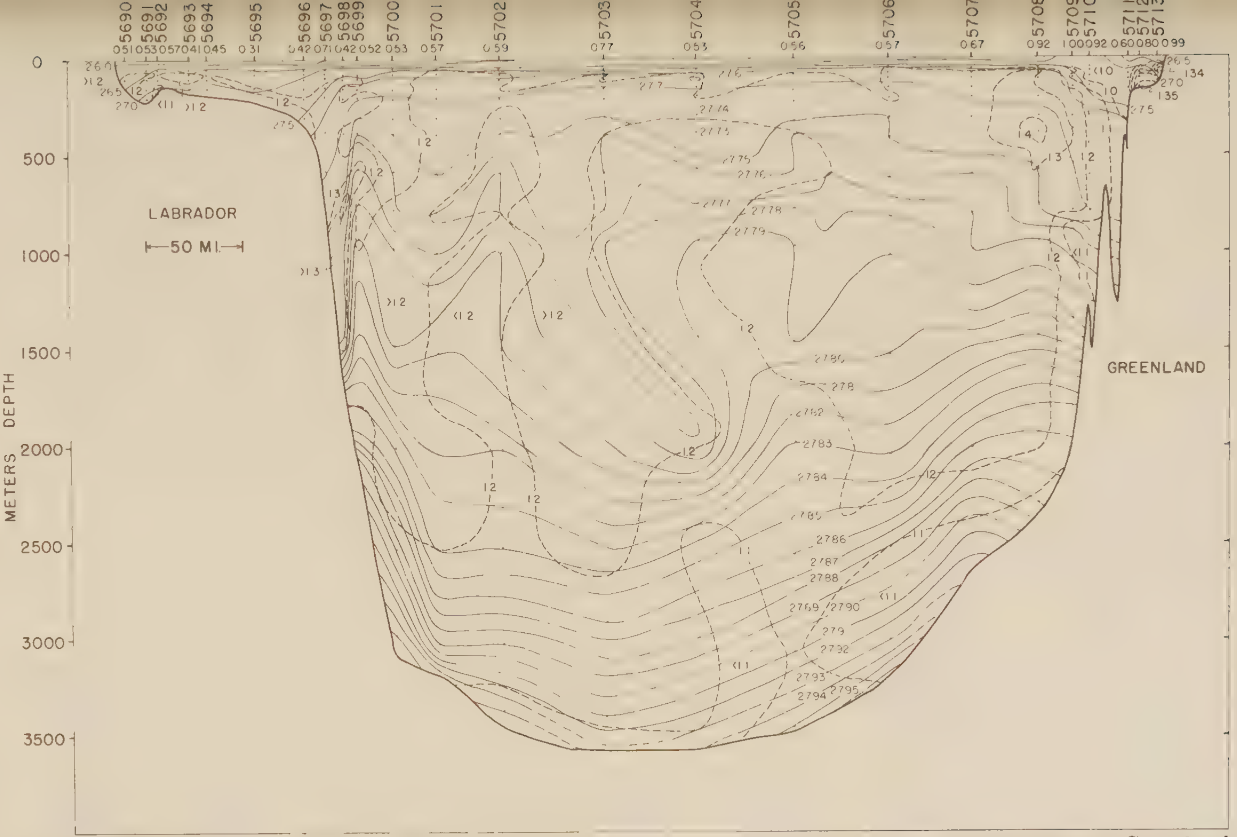

Figure 33.—Distribution of total phosphorus between South Wolf Island, Labrador, and Cape Farewell, Greenland, 25-29 August 1954. Concentration is given in microgram-atoms per liter. Solid lines show isentropic surfaces of equal σ_{t_θ}.

phosphorus line seems to show a correspondence with the distortions of the density pattern.

Figure 34 shows a more complicated pattern with higher phosphorus concentrations and in the intermediate water a split maximum with values in excess of 1.5μga/*L*. As in figure 33 the phosphorus concentration decreases toward the bottom. In figures 35 and 36 the southern corner of the triangle is seen to be in a phosphorus maximum, while figure 36 shows a slight maximum at intermediate depths at about station 5735 and another farther inshore at station 5738.

When individual station curves were drawn with total phosphorus concentration plotted against potential density, those in the Labrador

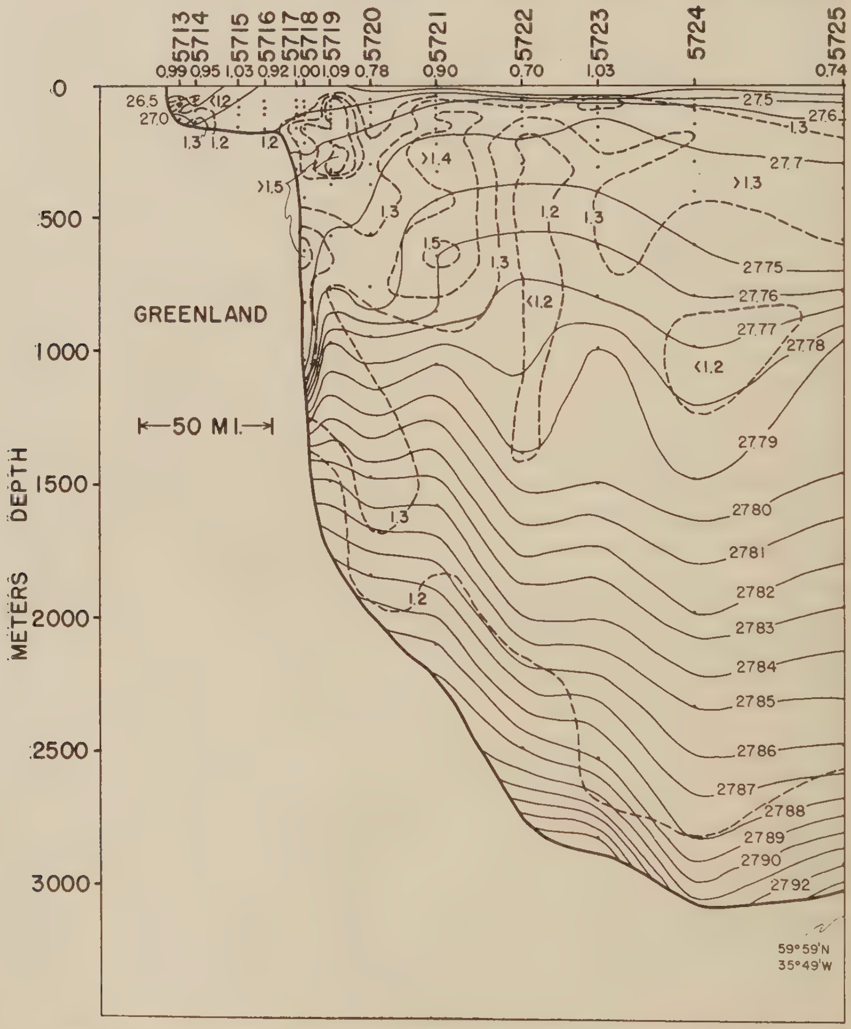

FIGURE 34.—Distribution of total phosphorus east of Cape Farewell, Greenland, 29–31 August 1954. Concentration is given in microgram-atoms per liter. Solid lines show isentropic surfaces of equal σ_{t_θ}.

Current off South Wolf Island fell into a group the mean curve for which is shown in figure 37 beginning at a phosphorus concentration of less than 0.6μga/L near the surface, increasing to about 1.15 at about 26.60 and continuing constant at that value in greater densities. This was about 0.15 higher in phosphorus than found for the Labrador Current in the Grand Banks region in 1952 and off South Wolf Island in July 1953, and about 0.15 lower than found off South Wolf in July 1952. The stations in the central Labrador Sea fell into

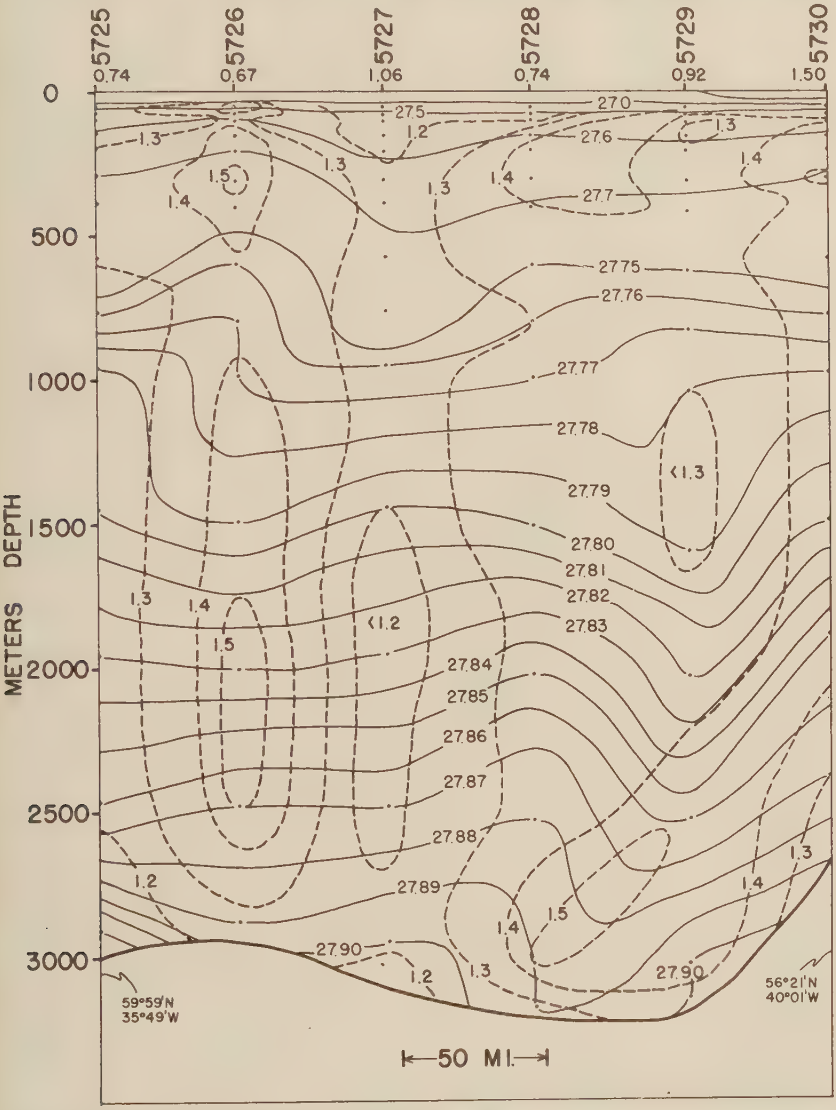

FIGURE 35.—Distribution of total phosphorus along offshore leg of Greenland triangle 31 August–2 September 1954. Concentration is given in micro-atoms per liter. Solid lines show isentropic surfaces of equal σ_{t_θ}.

another group the mean curve for which is shown in figure 37. This has a shape similar to that found for the mixed water in the Grand Banks region in 1952, but 0.1 to 0.2 poorer in phosphorus. It was also poorer in phosphorus than the central Labrador Sea in 1952 and similar to that found in 1953. In the stations southwest of Cape Farewell, only 5712 and 5713 departed from this central Labrador Sea group and they were richer in phosphorus. Except for the 25- and 50-meter values at station 5712, these two stations fell into the group from the Greenland triangle representative of the East Greenland

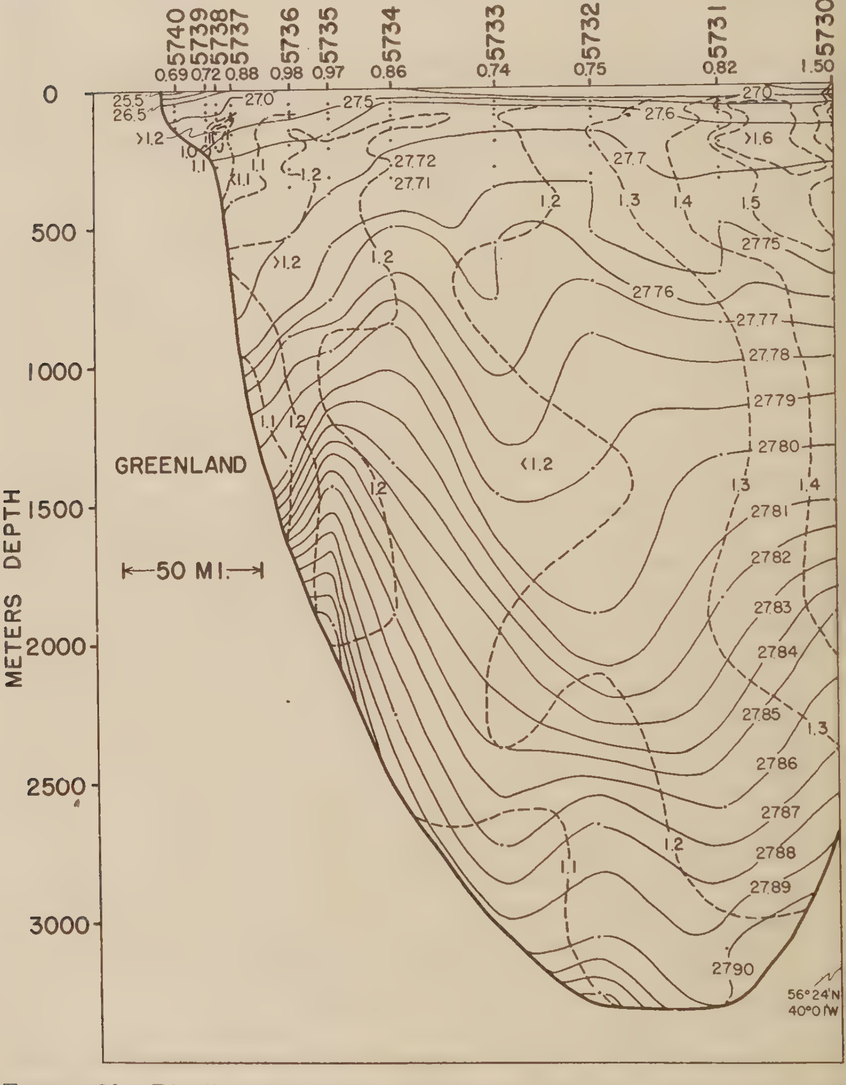

Figure 36.—Distribution of total phosphorus southeast of Cape Farewell Greenland, 2–4 September 1954. Concentration is given in microgram-atom per liter. Solid lines show isentropic surfaces of equal σ_{t_θ}.

Current water. This group was richer in phosphorus and similar to that for the Labrador Current in the density range common to both, and below which the high phosphorus Greenland triangle group increased to about 1.45 at 27.60 and then decreased slightly with increasing density. The other observations from the Greenland triangle fell into a low phosphorus group, shown in figure 37, similar in phosphorus-density relationship to the observations from the central Labrador Sea and only slightly higher in phosphorus.

The phosphorus values at all the locations in the Greenland triangle where the salinity was 35°/₀₀ or greater were examined and it was found that except for station 5719 these fell in the low phosphorus group. Water with salinities as great as this must have come from

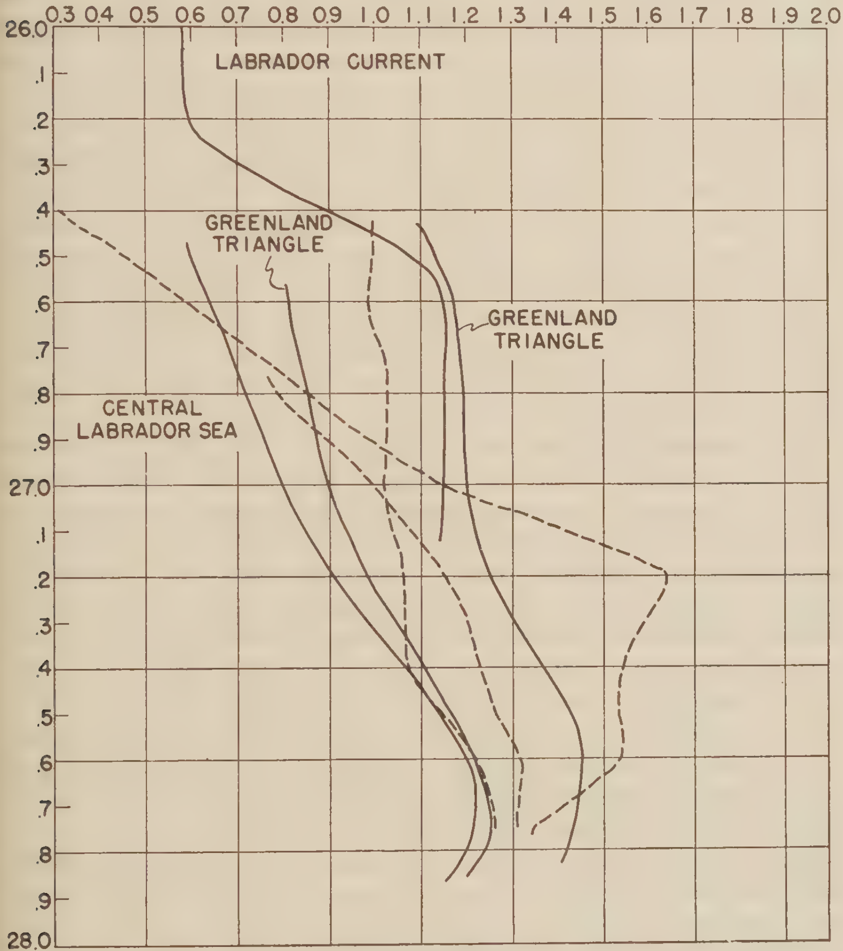

Figure 37.—Mean curves showing the relationship between total phosphorus concentration and potential density found in the South Wolf Island-Cape Farewell section and the Greenland triangle in 1954. Broken lines show the characteristic phosphorus-density curves for water masses found in the Grand Banks region in May 1952.

the North Atlantic eddy, either directly from its outer margins or indirectly such as by way of the Irminger Current. In the case of the salinity maximum water in the West Greenland Current, it is believed to have come from the outer margins of the North Atlantic eddy directly with some admixture of recirculating water of the Labrador Sea. In the case of the higher salinity maximum water in the Greenland triangle, its source is believed to have been the Irminger Current. If this is true then the high phosphorus values found at station 5719 were undergoing rapid depletion and had reached the level of the low phosphorus group by the time this water reached the southwestern side of the triangle. Total phosphorus, then, could be of little use as an indicator of the source of the salinity maximum water found in the West Greenland Current. When the location of the observations which form the high phosphorus group is considered, we find they are spottily present along the inshore half of the northern section to intermediate depths, present at one level only at station 5748 and present to all depths at the southern end of the triangle and weaving in and out of the southeastern section. Keeping in mind the similarity between the high phosphorus curve and the Grand Banks Atlantic Current curve at their deeper ends, the possibility is suggested that the high phosphorus water at the southern end of the triangle and along the southeastern side is supplied by the North Atlantic eddy in the deeper levels. This would mean that the high phosphorus curve for the Greenland triangle is a composite made up of the phosphorus characteristics of waters contributed by the Atlantic Current and by the East Greenland Current.

The alternative explanation is that all of the high phosphorus water is supplied by the East Greenland Current. This accords with the limitation to intermediate depths at the north side where it first reaches the triangle and extending to all depths at the southern end and southeastern side which is farther downstream. The almost complete absence of high phosphorus water from the southwest side of the triangle (except the southern corner) contradicts this explanation. The Atlantic Current source of the high phosphorus water at the southern corner and in the southeastern side is contradicted by the low salinities in the upper 1,000 meters. The choice therefore, is not clear cut and the authors have relied on the distribution of density, temperature, and salinity in deducing the circulation, and have considered that the total phosphorus concentration may be too much affected by transient additions from the erratic migrations of the sea's flora and fauna and their associated detritus to be a reliable tracer of water masses.

SUMMARY

1. The surface circulation in the Grand Banks region during the 1954 ice patrol season has been discussed on the basis of four dynamic topographic surveys made between 1 April and 2 July.

2. The circulation in the upper 1,000 meters has been presented in greater detail based on the consideration of the volume transport, mean temperature, minimum temperature, and heat transport of the Labrador Current found during 19 occupations of 8 selected sections across that current. The values found have been compared with seasonal normals where such normals are available.

3. The temperature-salinity relationship characteristic of Labrador Current water, mixed water, and Atlantic Current water found in the Grand Banks region in 1954 have been compared with the 8-year means for the period 1934–41.

4. Three more surveys were added to the material available for the study of the relationship between the position of the cold wall in the Grand Banks region, the strength of the Labrador Current and the strength of the North Atlantic eddy as indicated by the difference in sea level between Bermuda and Charleston. The large postwar fluctuations in the mean sea level of these stations have been noted as possible causes of the poor agreement of postwar observations with the relationship developed for the prewar observations.

5. The repetition of the section across the Labrador Sea from South Wolf Island to Cape Farewell, Greenland, has been reported upon and the exceptionally vigorous circulation noted. The absence of contributions to the West Greenland Current by the Irminger Current continued in 1954 although the heat transport of the West Greenland Current was abnormally high through more direct contributions from the North Atlantic eddy.

6. A group of three sections disposed in a triangular array southeast of Cape Farewell and occupied during the 1954 postseason cruise has been examined and the results presented. The southward and eastward recurvature of the Irminger Current and a part of the East Greenland Current verifies the circulation pattern deduced from the Labrador Sea section, and the separation of the Labrador Sea from the circulation east of Cape Farewell is in accord with the larger numbers of East Greenland bergs recently found in positions exceptionally far to the south-southeast of Cape Farewell.

7. The distribution of total phosphorus found in the section across the Labrador Sea and the Greenland triangle in 1954 has been presented and the phosphorus-density relationships found have been examined, leading to the conclusion that total phosphorus is not sufficiently conservative to be useful as a water mass tracer in this region.

The data collected during 1954 are tabulated below. The individual station headings give the station number, date, geographical position, depth of water, and the dynamic height of the sea surface used in the construction of the dynamic topographic charts shown in figures 15, 16, 18, 19, 20, and 24. The depths of water are rough approximations, being uncorrected sonic soundings based on a sounding velocity of 800 fathoms per second and containing an additional mechanical speed error of about 1/60. Where the depths of scaled values are enclosed in parentheses, the data are based on extrapolated vertical distribution curves of temperature or salinity or both. Asterisks appearing before observed temperatures indicate that these temperatures were determined from the depth of reversal and the corrected reading of an unprotected thermometer. The symbol σ_t signifies 1,000 (density—1) at atmospheric pressure and temperature t.

Table of Oceanographic Data

STATIONS OCCUPIED IN 1954

Station 5301, Apr. 1; latitude 41°36′ N., longitude 47°16′ W.; depth 4,189 m.; dynamic height 971.050

Observed values			Scaled values			
Depth, meters	Temperature, ° C.	Salinity °/oo	Depth, meters	Temperature, ° C.	Salinity, °/oo	σ_t
0	8.30	33.56	0	8.30	33.56	26.12
25	7.98	33.58	25	7.98	33.58	26.19
50	5.15	33.58	50	5.15	33.58	26.55
75	2.99	33.70	75	2.99	33.70	26.87
100	2.65	33.88	100	2.65	33.88	27.04
150	4.19	34.30	150	4.19	34.30	27.23
200	5.41	34.63	200	5.41	34.63	27.35
300	5.73	34.91	300	5.73	34.91	27.54
409	5.13	34.89	400	5.20	34.89	27.58
605	4.57	34.95	600	4.55	34.95	27.71
796	4.29	34.98	800	4.30	34.98	27.75
998	4.01	34.96	1,000	4.00	34.96	27.78
1,507	3.57	34.93				

Station 5302, Apr. 1; latitude 41°56.5′ N., longitude 47°55′ W.; depth 3,658 m.; dynamic height 971.097

Observed values			Scaled values			
Depth, meters	Temperature, ° C.	Salinity °/oo	Depth, meters	Temperature, ° C.	Salinity, °/oo	σ_t
0	12.74	35.08	0	12.74	35.08	26.53
24	13.00	35.08	25	13.00	35.08	26.48
48	13.09	35.14	50	13.10	35.14	26.50
73	13.08	35.14	75	13.10	35.14	26.50
97	14.03	35.76	100	14.00	35.75	26.78
144	10.21	35.14	150	10.10	35.13	27.05
193	9.37	35.10	200	7.95	35.08	27.36
290	6.87	34.90	300	6.60	34.87	27.39
352	5.24	34.75	400	5.15	34.81	27.53
532	4.88	34.97	600	4.70	34.96	27.70
713	4.30	34.95	800	4.15	34.93	27.73
904	3.97	34.92	1,000	3.90	34.92	27.76
1,403	3.55	34.92				

Station 5303; Apr. 1-2; latitude 42°19′ N., longitude 48°33′ W.; depth 3,182 m.; dynamic height 971.013

Observed values			Scaled values			
Depth, meters	Temperature, ° C.	Salinity °/oo	Depth, meters	Temperature, ° C.	Salinity, °/oo	σ_t
0	4.62	33.02	0	4.62	33.02	26.17
25	4.54	33.42	25	4.54	33.42	26.50
50	4.71	33.60	50	4.71	33.60	26.62
76	4.64	33.94	75	4.65	33.94	26.89
100	5.56	34.21	100	5.56	34.21	27.01
201	3.47	34.46	150	4.50	34.34	27.23
301	4.61	34.76	200	3.45	34.45	27.42
376	4.28	34.85	300	4.60	34.76	27.55
575	4.44	34.96	400	4.30	34.87	27.67
783	3.90	34.93	600	4.40	34.96	27.73
991	3.64	34.90	800	3.90	34.93	27.76
1,529	3.42	34.91	1,000	3.65	34.90	27.76

Station 5304; Apr. 2; latitude 42°42′ N., longitude 49°18′ W.; depth 2,195 m.; dynamic height 971.073

Observed values			Scaled values			
Depth, meters	Temperature, ° C.	Salinity, °/oo	Depth, meters	Temperature, ° C.	Salinity, °/oo	σ_t
17	−0.44	32.87	0	−0.10	32.87	26.41
18	−0.46	32.88	25	−0.50	32.87	26.43
39	−0.44	32.92	50	−0.70	33.05	26.59
62	−0.93	33.20	75	−0.75	33.28	26.77
83	−0.65	33.33	100	−0.40	33.39	26.85
128	0.00	33.51	150	0.40	33.65	27.02
337	4.91	34.70	200	1.50	34.02	27.25
498	4.09	34.82	300	4.05	34.60	27.48
657	4.29	34.935	400	4.60	34.75	27.54
839	3.97	34.92	600	4.25	34.90	27.70
1,327	3.58	34.91	800	4.00	34.92	27.75
			1,000	3.85	34.92	27.76

Station 5305; Apr. 2; latitude 43°18′ N., longitude 48°51′ W.; depth 2,012 m.; dynamic height 971.075

Observed values			Scaled values			
Depth, meters	Temperature, ° C.	Salinity, °/oo	Depth, meters	Temperature, ° C.	Salinity, °/oo	σ_t
0	−0.37	32.88	0	−0.37	32.88	26.43
26	−0.43	32.88	25	−0.40	32.88	26.44
51	−0.44	32.92	50	−0.45	32.92	26.47
78	3.09	33.71	75	2.90	33.63	26.82
103	4.01	33.95	100	3.90	33.90	26.94
155	6.83	34.58	150	6.60	34.53	27.12
206	7.61	34.79	200	7.55	34.77	27.18
309	2.65	34.41	300	3.10	34.43	27.44
381	2.40	34.44	400	2.55	34.47	27.53
581	3.66	34.80	600	3.70	34.82	27.70
790	3.63	34.88	800	3.65	34.88	27.74
993	3.46	34.88	1,000	3.45	34.88	27.76
1,509	3.41	34.87				

Station 5306; Apr. 2; latitude 42°58.5′ N., longitude 48°15′ W.; depth 3,017 m.; dynamic height 971.025

Observed values			Scaled values			
Depth, meters	Temperature, ° C.	Salinity, °/oo	Depth, meters	Temperature, ° C.	Salinity, °/oo	σ_t
0	4.99	33.03	0	4.99	33.03	26.14
26	4.99	33.04	25	5.00	33.04	26.15
51	3.87	33.52	50	3.90	33.51	26.64
77	3.58	33.64	75	3.60	33.63	26.76
102	3.14	33.86	100	3.15	33.85	26.97
153	3.54	34.24	150	3.50	34.22	27.24
204	3.74	34.50	200	3.75	34.48	27.41
306	3.71	34.68	300	3.70	34.67	27.58
399	4.67	34.92	400	4.70	34.92	27.67
596	4.56	34.98	600	4.55	34.98	27.73
791	3.99	34.93	800	4.00	34.93	27.75
994	3.87	34.94	1,000	3.85	34.94	27.77
1,508	3.55	34.93				

Table of Oceanographic Data—Continued

STATIONS OCCUPIED IN 1954—Continued

Station 5307; Apr. 3; latitude 42°46.5′ N., longitude 47°37′ W.; depth 3,585 m.; dynamic height 971.223

Observed values			Scaled values			
Depth, meters	Temperature, ° C.	Salinity °/oo	Depth, meters	Temperature, ° C.	Salinity, °/oo	σ_t
0	13.95	35.48	0	13.95	35.48	26.58
26	14.00	35.48	25	14.00	35.48	26.57
51	14.03	35.49	50	14.05	35.49	26.57
77	14.13	35.505	75	14.10	35.50	26.57
102	14.06	35.50	100	14.10	35.50	26.57
153	11.25	35.03	150	11.30	35.04	26.77
204	12.53	35.55	200	12.50	35.54	26.93
306	8.50	34.93	300	8.70	34.93	27.13
408	7.43	34.97	400	7.55	34.96	27.33
610	5.76	35.04	600	5.85	35.04	27.62
809	4.94	35.04	800	5.00	35.04	27.73
1,013	4.22	34.97	1,000	4.25	34.97	27.76
1,530	3.62	34.915				

Station 5308; Apr. 3; latitude 42°37.5′ N., longitude 46°54′ W.; depth 4,024 m.; dynamic height 971.444

Observed values			Scaled values			
Depth, meters	Temperature, ° C.	Salinity °/oo	Depth, meters	Temperature, ° C.	Salinity, °/oo	σ_t
0	15.99	36.00	0	15.99	36.00	26.55
25	15.99	36.00	25	15.99	36.00	26.54
50	15.98	36.00	50	15.98	36.00	26.54
75	15.99	36.00	75	15.99	36.00	26.54
100	15.99	36.00	100	15.99	36.00	26.54
150	16.00	36.00	150	16.00	36.00	26.54
200	16.01	36.00	200	16.01	36.00	26.53
300	*14.90	35.96	300	14.90	35.96	26.75
360	12.99	35.66	400	12.05	35.52	27.00
514	9.37	35.17	600	7.00	34.91	27.37
663	5.58	34.76	800	6.10	35.07	27.62
827	6.15	35.10	1,000	5.30	35.02	27.68
1,249	4.25	34.97				

Station 5309; Apr. 3; latitude 42°24′ N., longitude 46°10′ W.; depth 4,555 m.; dynamic height 971.596

Observed values			Scaled values			
Depth, meters	Temperature, ° C.	Salinity °/oo	Depth, meters	Temperature, ° C.	Salinity, °/oo	σ_t
0	16.82	36.28	0	16.82	36.28	26.56
25	16.78	36.26	25	16.78	36.26	26.55
49	16.61	36.24	50	16.60	36.24	26.57
73	16.53	36.20	75	16.50	36.20	26.58
97	16.43	36.19	100	16.40	36.19	26.59
146	16.34	36.165	150	16.35	36.16	26.57
195	16.33	36.16	200	16.30	36.16	26.58
292	16.05	36.08	300	16.05	36.09	26.60
342	*16.25	36.14	400	15.30	35.99	26.68
513	12.85	35.64	600	10.95	35.38	27.10
684	9.13	35.16	800	7.25	35.07	27.46
862	6.59	35.05	1,000	5.50	35.03	27.65
1,319	4.36	34.98				

Station 5310; Apr. 3; latitude 42°44′ N., longitude 45°48′ W.; depth 4,572 m.; dynamic height 971.717

Observed values			Scaled values			
Depth, meters	Temperature, ° C.	Salinity °/oo	Depth, meters	Temperature, ° C.	Salinity, °/oo	σ_t
0	16.97	36.32	0	16.97	36.32	26.55
24	16.99	36.32	25	17.00	36.32	26.54
47	16.99	36.32	50	17.00	36.32	26.54
70	17.00	36.31	75	17.00	36.31	26.53
93	17.01	36.31	100	17.00	36.31	26.53
141	17.01	36.31	150	17.00	36.31	26.53
188	16.96	36.30	200	17.00	36.29	26.52
281	16.99	36.24	300	16.90	36.22	26.49
355	16.44	36.17	400	16.00	36.13	26.63
533	-----	35.99	600	13.50	35.83	26.95
712	*11.56	35.52	800	9.80	35.30	27.24
892	7.98	35.11	1,000	6.40	35.07	27.58
1,345	4.62	35.01				

Station 5311; Apr. 3–4; latitude 43°10′ N., longitude 45°19′ W.; depth 3,566 m.; dynamic height 971.491

Observed values			Scaled values			
Depth, meters	Temperature, ° C.	Salinity, °/oo	Depth, meters	Temperature, ° C.	Salinity, °/oo	σ_t
0	16.54	36.25	0	16.54	36.25	26.60
28	16.56	36.24	25	16.55	36.24	26.58
54	16.54	36.23	50	16.55	36.23	26.58
82	16.50	36.22	75	16.50	36.22	26.59
109	16.49	36.22	100	16.50	36.22	26.59
164	16.23	36.15	150	16.30	36.17	26.59
218	16.11	36.13	200	16.15	36.14	26.60
327	15.65	36.09	300	16.10	36.10	26.59
308	16.06	36.10	400	13.80	35.80	26.86
448	12.55	35.59	600	7.95	35.00	27.30
577	*8.13	35.00	800	6.20	35.00	27.55
699	7.39	35.02	1,000	4.40	34.95	27.72
958	4.71	34.96				

Station 5312; Apr. 4–5; latitude 43°19.5′ N., longitude 46°00′ W.; depth 4,427 m.; dynamic height 971.546

Observed values			Scaled values			
Depth, meters	Temperature, ° C.	Salinity, °/oo	Depth, meters	Temperature, ° C.	Salinity, °/oo	σ_t
0	16.49	36.21	0	16.49	36.21	26.59
25	16.62	36.21	25	16.62	36.21	26.56
50	16.57	36.22	50	16.57	36.22	26.57
74	16.57	36.21	75	16.55	36.21	26.57
99	16.55	36.21	100	16.55	26.21	26.57
148	16.31	36.17	150	16.30	36.17	26.59
198	16.31	36.17	200	16.30	36.17	26.59
297	16.01	36.09	300	16.00	26.08	26.59
445	12.69	35.57	400	13.75	35.74	26.83
666	8.18	35.00	600	9.55	35.11	27.13
886	5.47	34.97	800	6.25	34.97	27.52
1,110	4.76	34.98	1,000	5.05	34.97	27.67
1,671	3.68	--------				

Station 5313; Apr. 5; latitude 43°33′ N., longitude 46°38′ W.; depth 4,445 m.; dynamic height 971.388

Observed values			Scaled values			
Depth, meters	Temperature, ° C.	Salinity, °/oo	Depth, meters	Temperature, ° C.	Salinity, °/oo	σ_t
0	14.90	35.74	0	14.90	35.74	26.59
25	14.93	35.74	25	14.93	35.74	26.58
50	14.92	35.74	50	14.92	35.74	26.58
76	14.93	35.74	75	14.92	35.74	26.58
100	14.93	35.74	100	14.93	35.74	26.57
151	14.94	35.74	150	14.95	35.74	26.57
201	14.97	35.75	200	14.98	35.75	26.57
301	14.34	35.82	300	14.35	35.82	26.76
321	13.88	35.79	400	11.35	35.40	27.04
478	8.79	35.06	600	6.90	35.02	27.47
634	6.56	35.02	800	5.35	35.02	27.67
811	5.33	35.02	1,000	4.55	34.99	27.74
1,285	3.79	34.92				

Station 5314; Apr. 5; latitude 43°45.5′ N., longitude 47°06′ W.; depth 4,061 m.; dynamic height 971.171

Observed values			Scaled values			
Depth, meters	Temperature, ° C.	Salinity, °/oo	Depth, meters	Temperature, ° C.	Salinity, °/oo	σ_t
0	13.53	35.43	0	13.53	35.43	26.64
27	13.55	35.43	25	13.55	35.43	26.64
54	13.54	35.43	50	13.55	35.43	26.64
82	13.55	35.43	75	13.55	35.43	26.64
108	13.55	35.43	100	13.55	35.43	26.64
163	12.47	35.47	150	12.80	35.46	26.81
217	10.99	35.33	200	11.50	35.39	27.00
325	7.65	34.89	300	8.40	34.98	27.21
426	5.98	34.86	400	6.35	34.86	27.42
635	4.60	34.92	600	4.70	34.91	27.66
845	4.49	34.99	800	4.55	34.99	27.74
1,057	4.12	34.96	1,000	4.20	34.98	27.77
1,587	3.53	34.91				

---

*See lines 4, 5, 6, and 7 on p. 116.

Table of Oceanographic Data—Continued

STATIONS OCCUPIED IN 1954—Continued

Station 5315; Apr. 5; latitude 43°54′ N., longitude 47°56′ W.; depth 3,658 m.; dynamic height 970.972

Observed values			Scaled values			
Depth, meters	Temperature, ° C.	Salinity °/oo	Depth, meters	Temperature, ° C.	Salinity, °/oo	σ_t
0	2.60	33.13	0	2.60	33.13	26.45
23	0.41	32.95	25	0.35	32.95	26.46
46	0.01	32.99	50	0.05	33.07	26.57
69	1.38	33.49	75	1.55	33.63	26.93
92	1.84	33.89	100	2.00	33.99	27.18
139	2.95	34.40	150	3.15	34.45	27.45
185	------	34.60	200	3.55	34.63	27.55
277	3.81	34.71	300	3.85	34.74	27.61
388	*3.89	34.85	400	3.90	34.85	27.70
585	3.81	34.91	600	3.80	34.89	27.74
786	3.79	34.89	800	3.80	34.89	27.74
991	3.56	34.90	1,000	3.55	34.90	27.77
1,514	3.43	34.91				

Station 5316; Apr. 5; latitude 43°57′ N., longitude 48°28′ W.; depth 4,200 m.; dynamic height 971.004

Observed values			Scaled values			
Depth, meters	Temperature, ° C.	Salinity °/oo	Depth, meters	Temperature, ° C.	Salinity, °/oo	σ_t
0	3.88	33.28	0	3.88	33.28	26.45
25	3.92	33.29	25	3.92	33.29	26.45
49	3.00	33.40	50	3.00	33.42	26.65
73	4.55	34.00	75	4.75	34.05	26.97
97	6.57	34.47	100	6.60	34.50	27.10
147	6.20	34.61	150	6.15	34.61	27.25
196	4.60	34.53	200	4.50	34.54	27.39
293	3.57	34.64	300	3.60	34.66	27.58
301	3.55	34.68	400	4.25	34.87	27.68
473	4.72	35.00	600	4.30	34.92	27.71
661	4.08	34.90	800	3.90	34.93	27.76
846	3.83	34.93	1,000	3.70	34.92	27.78
1,340	3.40	34.90				

Station 5317; Apr. 6; latitude 43°55′ N., longitude 48°54′ W.; depth 1,609 m.; dynamic height 971.003

Observed values			Scaled values			
Depth, meters	Temperature, ° C.	Salinity °/oo	Depth, meters	Temperature, ° C.	Salinity, °/oo	σ_t
0	−1.11	33.04	0	−1.11	33.04	26.59
24	−1.10	33.06	25	−1.10	33.06	26.60
47	−1.12	33.06	50	−1.10	33.06	26.60
71	−0.98	33.13	75	−0.95	33.15	26.68
94	−0.84	33.32	100	−0.60	33.40	26.86
142	1.37	33.99	150	1.55	34.08	27.28
189	1.99	34.31	200	2.05	34.32	27.45
283	2.23	34.39	300	2.70	34.51	27.54
338	3.68	34.72	400	3.75	34.79	27.66
519	3.73	34.86	600	3.65	34.88	27.74
707	------	34.89	800	3.50	34.88	27.76
901	3.44	34.875	1,000	3.40	34.87	27.77
1,429	3.35	34.85				

Station 5318; Apr. 6; latitude 43°58.5′ N., longitude 49°07′ W.; depth 622 m.; dynamic height 971.094

Observed values			Scaled values			
Depth, meters	Temperature, ° C.	Salinity °/oo	Depth, meters	Temperature, ° C.	Salinity, °/oo	σ_t
0	−0.80	32.86	0	−0.80	32.86	26.43
24	−0.82	32.865	25	−0.85	32.87	26.44
47	−0.84	32.88	50	−0.85	32.89	26.45
71	−1.17	32.98	75	−1.15	33.03	26.58
94	−0.85	33.24	100	−0.80	33.26	26.75
141	−0.26	33.38	150	−0.10	33.43	26.86
188	0.55	33.74	200	0.70	33.79	27.11
282	1.51	34.12	300	1.75	34.23	27.39
326	2.06	34.36	400	2.65	34.53	27.56
489	3.06	34.68	(600)	3.40	34.80	27.71

Station 5319; Apr. 6; latitude 44°02′ N., longitude 49°21′ W.; depth 201 m.; dynamic height 971.132

Observed values			Scaled values			
Depth, meters	Temperature, ° C.	Salinity, °/oo	Depth, meters	Temperature, ° C.	Salinity, °/oo	σ_t
0	0.22	32.72	0	0.22	32.72	26.28
29	0.03	32.78	25	0.05	32.77	26.33
56	−0.31	32.86	50	−0.25	32.84	26.40
84	−0.62	32.92	75	−0.55	32.90	26.45
112	−0.72	33.08	100	−0.70	33.01	26.56
169	−0.41	33.31	150	−0.60	33.24	26.73
			(200)	−0.05	33.43	26.86

Station 5320; Apr. 6; latitude 44°04′ N., longitude 49°27′ W.; depth 73 m.; dynamic height 971.143

Observed values			Scaled values			
Depth, meters	Temperature, ° C.	Salinity, °/oo	Depth, meters	Temperature, ° C.	Salinity, °/oo	σ_t
0	0.58	32.70	0	0.58	32.70	26.24
26	0.37	32.73	25	0.40	32.73	26.28
40	0.14	32.77	50	0.05	32.79	26.35
68	−0.09	32.83				

Station 5321; Apr. 6; latitude 44°57′ N., longitude 49°15′ W.; depth 96 m.; dynamic height 971.177

Observed values			Scaled values			
Depth, meters	Temperature, ° C.	Salinity, °/oo	Depth, meters	Temperature, ° C.	Salinity, °/oo	σ_t
0	−0.27	32.86	0	−0.27	32.86	26.41
26	−0.28	32.86	25	−0.27	32.86	26.41
52	−0.31	32.87	50	−0.30	32.87	26.42
79	−0.34	32.87	75	−0.30	32.87	26.42

Station 5322; Apr. 6; latitude 44°55′ N., longitude 49°07′ W.; depth 512 m.; dynamic height 971.147

Observed values			Scaled values			
Depth, meters	Temperature, ° C.	Salinity, °/oo	Depth, meters	Temperature, ° C.	Salinity, °/oo	σ_t
0	−0.30	32.87	0	−0.30	32.87	26.42
24	−0.33	32.87	25	−0.30	32.87	26.42
48	−0.42	32.87	50	−0.45	32.87	26.43
73	−0.49	32.87	75	−0.50	32.87	26.43
97	−0.48	32.88	100	−0.50	32.89	26.44
145	−0.87	33.12	150	−0.85	33.15	26.66
193	−0.24	33.36	200	−0.10	33.42	26.86
290	1.31	34.02	300	1.40	34.04	27.27
397	1.67	34.18	400	1.70	34.19	27.36

Station 5323; Apr. 6; latitude 44°53′ N., longitude 48°59′ W.; depth 914 m.; dynamic height 971.103

Observed values			Scaled values			
Depth, meters	Temperature, ° C.	Salinity, °/oo	Depth, meters	Temperature, ° C.	Salinity, °/oo	σ_t
0	−0.71	32.84	0	−0.71	32.84	26.42
27	−0.75	32.82	25	−0.75	32.82	26.40
54	−1.16	32.85	50	−1.15	32.84	26.43
81	−0.94	33.15	75	−0.95	33.09	26.62
108	−0.86	33.21	100	−0.90	33.19	26.71
163	0.63	33.70	150	0.25	33.57	26.97
217	1.40	34.04	200	1.25	33.96	27.21
325	1.59	34.12	300	1.60	34.10	27.30
364	1.58	34.16	400	1.90	34.27	27.42
555	3.45	34.78				

STATIONS OCCUPIED IN 1954—Continued

Station 5324; Apr. 6; latitude 44°49′ N., longitude 48°48′ W.; depth 1,829 m.; dynamic height 970.977

Observed values			Scaled values			
Depth, meters	Temperature, ° C.	Salinity, ‰	Depth, meters	Temperature, ° C.	Salinity, ‰	σ_t
0	−1.03	33.08	0	−1.03	33.08	26.61
28	−0.96	32.97	25	−0.95	32.98	26.53
55	−1.02	33.10	50	−1.00	33.05	26.59
83	2.79	33.89	75	2.00	33.69	26.94
110	2.03	33.96	100	2.25	33.93	27.11
166	1.72	34.23	150	1.75	34.15	27.33
221	2.75	34.50	200	2.40	34.40	27.48
331	3.45	34.68	300	3.30	34.63	27.58
410	3.76	34.81	400	3.75	34.80	27.67
605	3.53	34.88	600	3.55	34.88	27.75
796	3.47	34.89	800	3.50	34.89	27.77
998	3.35	34.88	1,000	3.35	34.88	27.77
1,507	*3.40	34.89				

Station 5325; Apr. 6; latitude 44°48′ N., longitude 48°32′ W.; depth 2,286 m.; dynamic height 970.940

Observed values			Scaled values			
Depth, meters	Temperature, ° C.	Salinity, ‰	Depth, meters	Temperature, ° C.	Salinity, ‰	σ_t
0	0.47	33.21	0	0.47	33.21	26.66
27	0.41	33.22	25	0.45	33.22	26.67
53	0.77	33.36	50	0.70	33.33	26.74
79	1.93	33.91	75	1.75	33.82	27.07
105	2.76	34.20	100	2.65	34.16	27.27
159	3.20	34.47	150	3.10	34.43	27.44
211	4.16	34.72	200	4.00	34.68	27.55
316	4.34	34.88	300	4.35	34.87	27.67
428	4.20	34.93	400	4.25	34.93	27.72
632	3.88	34.91	600	3.95	34.91	27.74
830	3.55	34.90	800	3.60	34.90	27.77
1,042	3.44	34.90	1,000	3.45	34.90	27.78
1,582	3.30	------				

Station 5326; Apr. 7; latitude 44°42.5′ N., longitude 48°04′ W.; depth 3,329 m.; dynamic height 970.988

Observed values			Scaled values			
Depth, meters	Temperature, ° C.	Salinity, ‰	Depth, meters	Temperature, ° C.	Salinity, ‰	σ_t
0	−0.17	32.98	0	−0.17	32.98	26.51
24	−0.13	33.02	25	−0.15	33.03	26.55
48	−0.54	33.34	50	−0.55	33.35	26.82
72	------	33.53	75	0.20	33.55	26.95
96	0.83	33.78	100	0.90	33.81	27.12
144	1.47	34.08	150	1.65	34.13	27.32
192	4.56	34.62	200	4.50	34.62	27.45
288	3.02	34.59	300	3.05	34.60	27.58
287	3.04	34.59	400	4.05	34.80	27.64
432	4.26	34.84	600	4.00	34.91	27.74
579	3.99	34.91	800	3.70	34.89	27.75
729	3.80	34.90	1,000	3.50	34.88	27.76
1,115	3.37	34.87				

Station 5327; Apr. 7; latutude 44°38′ N., longitude 47°14′ W.; depth 3,695 m.; dynamic height 971.042

Observed values			Scaled values			
Depth, meters	Temperature, ° C.	Salinity, ‰	Depth, meters	Temperature, ° C.	Salinity, ‰	σ_t
0	3.47	33.07	0	3.47	33.07	26.32
26	2.34	33.01	25	2.35	33.01	26.38
52	6.31	33.85	50	6.20	33.83	26.62
78	3.94	33.79	75	4.05	33.79	26.83
104	3.73	33.99	100	3.75	33.95	27.00
157	5.71	34.48	150	5.50	34.46	27.21
208	3.41	34.31	200	3.70	34.32	27.30
312	4.77	34.78	300	4.70	34.73	27.51
401	4.54	34.85	400	4.60	34.85	27.62
603	4.28	34.93	600	4.30	34.93	27.71
808	4.10	34.95	800	4.15	34.95	27.75
1,017	3.76	34.92	1,000	3.75	34.92	27.77
1,551	3.45	34.92				

Station 5328; Apr. 7; latitude 44°35.5′ N., longitude 46°26′ W.; depth 3,658 m.; dynamic height 971.087

Observed values			Scaled values			
Depth, meters	Temperature, ° C.	Salinity, ‰	Depth, meters	Temperature, ° C.	Salinity, ‰	σ_t
0	10.16	34.50	0	10.16	34.50	26.55
20	10.35	34.52	25	10.30	34.53	26.55
41	10.29	34.56	50	10.90	34.75	26.62
62	12.00	35.02	75	12.65	35.30	26.71
82	12.84	35.39	100	11.35	35.19	26.88
123	9.43	34.90	150	9.20	34.96	27.07
165	9.03	35.00	200	7.70	34.82	27.20
247	5.78	34.64	300	6.25	34.89	27.45
219	6.89	34.73	400	5.35	34.91	27.58
315	6.28	34.94	(600)	4.50	34.91	27.68
400	5.34	34.91	(800)	4.10	34.90	27.72
			(1,000)	3.80	34.90	27.75

Station 5329; Apr. 8; latitude 44°26′ N., longitude 45°49′ W.; depth 3,841 m.; dynamic height 971.032

Observed values			Scaled values			
Depth, meters	Temperature, ° C.	Salinity, ‰	Depth, meters	Temperature, ° C.	Salinity, ‰	σ_t
0	3.06	33.37	0	3.06	33.37	26.60
29	3.01	33.37	25	3.00	33.37	26.61
56	2.94	33.38	50	2.95	33.38	26.61
84	2.78	33.34	75	2.85	33.35	26.60
112	1.59	33.56	100	2.05	33.46	26.77
169	2.02	33.98	150	1.90	33.85	27.08
225	2.22	34.20	200	2.15	34.10	27.26
337	4.60	34.96	300	3.95	34.74	27.60
404	4.27	-------	400	4.30	34.92	27.71
602	4.26	-------	600	4.30	34.93	27.71
872	3.96	34.94	800	4.10	34.94	27.75
1,004	3.73	34.92	1,000	3.75	34.92	27.77
1,537	3.31	34.89				

Sta. 5330; Apr. 8; latitude 44°18′ N., longitude 45°16 W.; depth 3,658 m.; dynamic height 971.058

Observed values			Scaled values			
Depth, meters	Temperature, ° C.	Salinity, ‰	Depth, meters	Temperature, ° C.	Salinity, ‰	σ_t
0	6.82	34.02	0	6.82	34.02	26.69
27	6.64	34.04	25	6.65	34.04	26.73
53	6.63	34.04	50	6.65	34.04	26.73
80	6.70	34.04	75	6.70	34.04	26.72
106	8.32	34.68	100	8.00	34.58	26.96
160	6.82	34.62	150	6.95	34.62	27.15
212	6.69	-------	200	6.70	34.71	27.25
318	7.08	34.95	300	7.05	34.93	27.37
442	4.94	34.92	400	5.60	34.93	27.56
657	4.46	34.99	600	4.55	34.97	27.73
869	4.04	34.96	800	4.20	34.97	27.77
1,086	3.73	34.925	1,000	3.85	34.94	27.77

Station 5331; Apr. 8; latitude 44°47′ N., longitude 45°19′ W.; depth 4,115 m.; dynamic height 971.059

Observed values			Scaled values			
Depth, meters	Temperature, ° C.	Salinity, ‰	Depth, meters	Temperature, ° C.	Salinity, ‰	σ_t
0	9.71	34.68	0	9.71	34.68	26.77
28	9.53	34.64	25	9.55	34.64	26.76
55	9.36	34.63	50	9.40	34.63	26.78
83	8.57	34.55	75	8.85	34.56	26.82
110	7.80	34.56	100	8.05	34.55	26.93
166	10.03	35.17	150	9.40	35.03	27.09
222	7.15	34.78	200	8.20	34.93	27.20
332	6.66	34.98	300	6.80	34.94	27.42
431	5.23	34.94	400	5.60	34.95	27.58
644	4.45	34.98	600	4.55	34.97	27.73
857	4.03	34.93	800	4.15	34.94	27.74
1,075	3.77	34.94	1,000	3.85	34.94	27.77
1,624	3.41	34.91				

Table of Oceanographic Data—Continued

STATIONS OCCUPIED IN 1954—Continued

Station 5332; Apr. 8; latitude 45°20′ N., longitude 45°23′ W.; depth 4,079 m.; dynamic height 971.096

Observed values			Scaled values			
Depth, meters	Temperature, ° C.	Salinity ‰	Depth, meters	Temperature, ° C.	Salinity, ‰	σ_t
0	7.34	34.20	0	7.34	34.20	26.76
25	7.36	34.20	25	7.36	34.20	26.76
50	7.39	34.20	50	7.39	34.20	26.75
75	8.58	34.52	75	8.58	34.52	26.83
100	10.18	34.99	100	10.18	34.99	26.93
151	7.58	34.57	150	7.60	34.57	27.02
202	8.12	34.85	200	8.10	34.84	27.15
302	6.56	34.79	200	6.60	34.78	27.32
367	5.98	34.85	400	5.75	34.88	27.51
553	4.93	34.95	600	4.75	34.95	27.68
741	4.33	34.95	800	4.25	34.95	27.74
933	4.05	34.95	1,000	4.00	34.95	27.77
1,424	3.65	34.92				

Station 5333; Apr. 9; latitude 45°20′ N., longitude 46°00′ W.; depth 3,466 m.; dynamic height 970.963

Observed values			Scaled values			
Depth, meters	Temperature, ° C.	Salinity ‰	Depth, meters	Temperature, ° C.	Salinity, ‰	σ_t
0	3.58	33.71	0	3.58	33.71	26.82
22	3.58	33.71	25	3.60	33.71	26.82
45	3.56	33.72	50	3.55	33.73	26.84
68	3.56	33.73	75	3.55	33.73	26.84
91	3.57	33.72	100	3.60	33.76	26.86
135	3.60	34.00	150	3.70	34.12	27.14
180	3.86	34.39	200	3.95	34.52	27.43
271	4.13	34.81	300	4.05	34.84	27.67
332	3.95	34.85	400	3.80	34.87	27.73
503	3.65	34.90	600	3.60	34.90	27.77
679	3.50	34.90	800	3.45	34.90	27.78
872	3.37	34.90	1,000	3.55	34.90	27.79
1,396	3.32	34.90				

Station 5334; Apr. 9; latitude 45°23′ N., longitude 46°41′ W.; depth 3,072 m.; dynamic height 970.937

Observed values			Scaled values			
Depth, meters	Temperature, ° C.	Salinity ‰	Depth, meters	Temperature, ° C.	Salinity, ‰	σ_t
0	3.00	33.76	0	3.00	33.76	26.92
28	2.99	33.76	25	3.00	33.76	26.92
55	3.16	33.78	50	3.10	33.77	26.92
83	3.32	33.90	75	3.30	33.86	26.97
111	3.91	34.21	100	3.75	34.09	27.11
167	3.97	34.54	150	4.00	34.46	27.38
222	4.09	34.68	200	4.05	34.63	27.50
333	4.36	34.88	300	4.30	34.83	27.64
442	4.07	34.93	400	4.15	34.92	27.73
653	3.67	34.92	600	3.75	34.92	27.77
859	3.50	34.90	800	3.55	34.90	27.77
1,078	3.37	34.90	1,000	3.45	34.90	27.78
1,627	3.32	34.91				

Station 5335; Apr. 9; latitude 45°20.05′ N., longitude 47°23′ W.; depth 2,743 m.; dynamic height 970.962

Observed values			Scaled values			
Depth, meters	Temperature, ° C.	Salinity ‰	Depth, meters	Temperature, ° C.	Salinity, ‰	σ_t
0	2.03	33.47	0	2.03	33.47	26.78
27	2.01	33.47	25	2.00	33.47	26.78
52	1.99	33.47	50	2.00	33.47	26.78
79	1.97	33.47	75	2.00	33.47	26.78
105	1.59	33.61	100	1.60	33.56	26.87
158	3.87	34.40	150	3.65	34.29	27.28
210	4.12	34.70	200	4.10	34.67	27.54
315	4.29	34.86	300	4.30	34.85	27.66
436	4.15	34.91	400	4.20	34.90	27.71
645	3.60	34.88	600	3.70	34.89	27.75
849	3.48	34.90	800	3.50	34.90	27.78
1,070	3.43	34.90	1,000	3.45	34.90	27.78
1,600	3.31	34.90	--------	------	------	------

Station 5336; Apr. 9; latitude 45°31′ N., longitude 47°52′ W.; depth 1,554 m.; dynamic height 970.922

Observed values			Scaled values			
Depth, meters	Temperature, ° C.	Salinity, ‰	Depth, meters	Temperature, ° C.	Salinity, ‰	σ_t
0	0.32	33.32	0	0.32	33.32	26.76
25	0.57	33.39	25	0.57	33.39	26.79
49	1.80	33.58	50	1.85	33.59	26.88
74	2.36	33.78	75	2.40	33.79	26.99
98	3.79	34.31	100	3.80	34.32	27.29
148	2.91	34.44	150	2.95	34.44	27.46
196	3.83	34.66	200	3.85	34.67	27.56
294	4.29	34.88	300	4.30	34.88	27.68
376	3.91	34.90	400	3.85	34.90	27.74
566	3.66	34.905	600	3.65	34.90	27.76
758	3.53	34.895	800	3.55	34.90	27.77
959	3.38	-------	1,000	3.40	34.90	27.79
1,374	3.32	34.89				

Station 5337; Apr. 9; latitude 45°38.5′ N., longitude 48°16′ W.; depth 631 m.; dynamic height 970.987

Observed values			Scaled values			
Depth, meters	Temperature, ° C.	Salinity, ‰	Depth, meters	Temperature, ° C.	Salinity, ‰	σ_t
0	−1.32	33.02	0	−1.32	33.02	26.58
24	−1.31	33.02	25	−1.30	33.02	26.58
48	−1.35	33.06	50	−1.35	33.08	26.63
72	0.03	33.65	75	0.35	33.70	27.06
96	1.11	33.98	100	1.20	34.00	27.25
144	1.74	34.18	150	1.80	34.19	27.36
192	1.92	34.26	200	1.95	34.27	27.42
288	2.16	34.42	300	2.20	34.43	27.52
355	2.52	34.49	400	2.90	34.55	27.56
552	3.57	34.84	(600)	3.60	34.86	27.74

Station 5338; Apr. 9; latitude 45°20′ N., longitude 48°27′ W.; depth 179 m.; dynamic height 971.063

Observed values			Scaled values			
Depth, meters	Temperature, ° C.	Salinity, ‰	Depth, meters	Temperature, ° C.	Salinity, ‰	σ_t
0	−1.11	32.92	0	−1.11	32.92	26.49
26	−1.11	32.92	25	−1.10	32.92	26.49
51	−1.41	33.00	50	−1.40	32.99	26.56
78	−0.84	33.25	25	−0.90	33.22	26.73
103	−0.13	33.51	100	−0.20	33.48	26.91
155	0.43	33.61	150	0.40	33.60	26.98

Station 5339; Apr. 9; latitude 45°46.5′ N., longitude 48°34′ W.; depth 123 m.; dynamic height 971.082

Observed values			Scaled values			
Depth, meters	Temperature, ° C.	Salinity, ‰	Depth, meters	Temperature, ° C.	Salinity, ‰	σ_t
0	−0.96	32.85	0	−0.96	32.85	26.43
27	−0.98	32.86	25	−0.95	32.85	26.43
53	−1.30	32.94	50	−1.25	32.93	26.50
80	−1.42	33.03	75	−1.40	33.01	26.58
106	−1.01	33.12	100	−1.15	33.10	26.64

Station 5340; Apr. 9; latitude 45°53.5′ N., longitude 48°46′ W.; depth 98 m.; dynamic height 971.100

Observed values			Scaled values			
Depth, meters	Temperature, ° C.	Salinity, ‰	Depth, meters	Temperature, ° C.	Salinity, ‰	σ_t
0	0.65	32.70	0	0.65	32.70	26.24
26	0.62	32.71	25	0.65	32.71	26.25
53	−0.12	32.83	50	−0.05	32.82	26.37
79	−0.66	32.86	75	−0.60	32.86	26.42

STATIONS OCCUPIED IN 1954—Continued

Station 5341; Apr. 10; latitude 46°03.5′ N., longitude 48°50′ W.; depth 93 m.; dynamic height 971.107

Observed values			Scaled values			
Depth, meters	Temperature, ° C.	Salinity ‰	Depth, meters	Temperature, ° C.	Salinity, ‰	σ_t
0	1.10	32.59	0	1.10	32.59	26.13
26	1.08	32.58	25	1.10	32.58	26.12
51	0.65	32.69	50	0.70	32.68	26.22
77	−0.14	32.94	75	−0.05	32.93	26.46

Station 5342; Apr. 10; latitude 46°12.5′ N., longitude 48°56′ W.; depth 82 m.; dynamic height 971.123

Observed values			Scaled values			
Depth, meters	Temperature, ° C.	Salinity ‰	Depth, meters	Temperature, ° C.	Salinity, ‰	σ_t
0	1.28	32.50	0	1.28	32.50	26.04
25	1.28	32.50	25	1.28	32.50	26.04
45	1.27	32.47	50	1.25	32.48	26.03
65	1.26	32.48	(75)	1.25	32.49	26.03

Station 5343; Apr. 10; latitude 46°10.5 N., longitude 48°26′ W.; depth 100 m.; dynamic height 971.090

Observed values			Scaled values			
Depth, meters	Temperature, ° C.	Salinity ‰	Depth, meters	Temperature, ° C.	Salinity, ‰	σ_t
0	0.28	32.82	0	0.28	32.82	26.36
26	0.25	32.82	25	0.25	32.82	26.36
53	−0.03	32.85	50	0.00	32.84	26.39
79	−0.23	32.88	75	−0.20	32.87	26.42

Station 5344; Apr. 10; latitude 46°08′5′ N., longitude 48°11/ W.; depth 115 m.; dynamic height 971.078

Observed values			Scaled values			
Depth, meters	Temperature, ° C.	Salinity ‰	Depth, meters	Temperature, ° C.	Salinity, ‰	σ_t
0	−0.93	32.83	0	−0.93	32.83	26.41
25	−0.93	32.82	25	−0.93	32.82	26.41
52	−1.10	32.86	50	−1.10	32.85	26.44
77	−1.38	33.06	75	−1.40	33.05	26.60
104	−0.93	33.23	100	−1.00	33.21	26.73

Station 5345; Apr. 10; latitude 46°06.5′ N., longitude 47°56′ W.; depth 170 m.; dynamic height 971.054

Observed values			Scaled values			
Depth, meters	Temperature, ° C.	Salinity ‰	Depth, meters	Temperature, ° C.	Salinity, ‰	σ_t
0	−1.35	32.90	0	−1.35	32.90	26.48
24	−1.34	32.91	25	−1.35	32.91	26.49
48	−1.47	33.01	50	−1.45	33.02	26.58
73	−1.10	33.30	75	−1.05	33.31	26.80
97	−0.28	33.52	100	−0.15	33.54	26.96
145	1.04	33.80	(150)	1.20	33.82	27.11

Station 5346; Apr. 10; latitude 46°05′ N., longitude 47°34′ W.; depth 604 m.; dynamic height 970.948

Observed values			Scaled values			
Depth, meters	Temperature, ° C.	Salinity ‰	Depth, meters	Temperature, ° C.	Salinity, ‰	σ_t
0	−1.24	33.09	0	−1.24	33.09	26.63
25	−1.26	33.14	25	−1.26	33.14	26.67
49	0.07	33.63	50	0.10	33.65	27.03
74	1.10	33.92	75	1.10	33.93	27.20
99	1.28	33.98	100	1.30	33.99	27.23
148	1.79	34.19	150	1.80	34.20	27.37
197	1.95	34.34	200	1.95	34.35	27.48
296	2.82	34.64	300	2.85	34.65	27.64
397	3.43	34.82	400	3.45	34.82	27.72
580	3.54	34.84	600	3.55	34.84	27.72

Station 5347; Apr. 10; latitude 46°03′ N., longitude 47°20′ W.; depth 1,445 m.; dynamic height 970.900

Observed values			Scaled values			
Depth, meters	Temperature, ° C.	Salinity, ‰	Depth, meters	Temperature, ° C.	Salinity, ‰	σ_t
0	−0.49	33.33	0	−0.49	33.33	26.80
25	−0.51	33.32	25	−0.51	33.32	26.79
49	0.23	33.65	50	0.25	33.67	27.05
74	1.28	34.15	75	1.30	34.16	27.37
98	1.57	34.26	100	1.60	34.26	27.43
148	2.50	34.54	150	2.55	34.55	27.59
197	2.88	34.64	200	2.90	34.64	27.63
295	3.55	34.77	300	3.55	34.77	27.67
421	3.79	34.86	400	3.75	34.85	27.71
619	3.56	34.89	600	3.60	34.89	27.76
812	3.42	34.885	800	3.45	34.88	27.76
1,025	3.38	34.885	1,000	3.40	34.88	27.77
1,350	3.36	34.88				

Station 5348; Apr. 10; latitude 45°59′ N., longitude 46°36′ W.; depth 531 m.; dynamic height 970.928

Observed values			Scaled values			
Depth, meters	Temperature, ° C.	Salinity, ‰	Depth, meters	Temperature, ° C.	Salinity, ‰	σ_t
0	3.43	33.82	0	3.43	33.82	26.92
24	3.47	33.81	25	3.45	33.81	26.91
48	3.45	33.82	50	3.45	33.82	26.92
72	3.62	33.91	75	3.65	33.91	26.97
96	3.56	33.98	100	3.60	34.02	27.07
145	3.87	34.51	150	3.95	34.56	27.46
193	4.41	34.76	200	4.45	34.77	27.58
289	4.13	34.89	300	4.15	34.90	27.71
365	4.36	34.96	400	4.30	34.95	27.73
504	3.70	34.90				

Station 5349; Apr. 10; latitude 45°55′ N., longitude 45°56′ W.; depth 2,816 m.; dynamic height 971.004

Observed values			Scaled values			
Depth, meters	Temperature, ° C.	Salinity, ‰	Depth, meters	Temperature, ° C.	Salinity, ‰	σ_t
0	7.76	34.26	0	7.76	34.26	26.75
26	7.82	34.28	25	7.80	34.28	26.75
52	7.72	34.27	50	7.75	34.27	26.76
78	8.58	34.56	75	8.50	34.52	26.84
104	8.34	34.77	100	8.40	34.76	27.04
156	7.23	34.80	150	7.35	34.80	27.23
208	6.52	34.86	200	6.65	34.85	27.37
312	4.25	34.75	300	4.50	34.76	27.56
400	4.67	34.93	400	4.70	34.93	27.67
597	4.27	34.91	600	4.30	34.91	27.70
794	3.89	34.94	800	3.90	34.94	27.77
1,000	3.69	34.92	1,000	3.70	34.92	27.78
1,529	3.36	34.89				

Station 5350; Apr. 10; latitude 45°59′ N., longitude 45°18′ W.; depth 3,292 m.; dynamic height 971.047

Observed values			Scaled values			
Depth, meters	Temperature, ° C.	Salinity, ‰	Depth, meters	Temperature, ° C.	Salinity, ‰	σ_t
0	9.12	34.56	0	9.12	34.56	26.78
26	9.16	34.57	25	9.15	34.57	26.78
53	9.13	34.58	50	9.15	34.58	26.78
79	9.14	34.61	75	9.15	34.60	26.80
105	7.69	34.69	100	7.90	34.67	27.05
157	7.50	34.82	150	7.55	34.82	27.22
209	7.09	34.81	200	7.20	34.81	27.26
314	5.23	34.80	300	5.40	34.80	27.49
414	4.69	34.90	400	4.75	34.90	27.64
612	4.52	34.90	600	4.60	34.90	27.66
806	3.69	34.82	800	3.75	34.82	27.69
1,009	3.55	34.89	1,000	3.60	34.89	27.76
1,522	3.30	34.85				

STATIONS OCCUPIED IN 1954—Continued

Station 5351; Apr. 11; latitude 46°03′ N., longitude 44°38′ W.; depth 3,603 m.; dynamic height 970.901

Observed values			Scaled values			
Depth, meters	Temperature, ° C.	Salinity, °/oo	Depth, meters	Temperature, ° C.	Salinity, °/oo	σ_t
0	3.33	33.95	0	3.33	33.95	27.04
24	3.36	33.94	25	3.35	33.94	27.03
50	3.30	33.95	50	3.30	33.95	27.04
74	3.10	34.02	75	3.10	34.02	27.12
100	2.99	34.21	100	3.00	34.22	27.29
149	3.06	34.51	150	3.10	34.50	27.50
198	3.23	34.64	200	3.25	34.64	27.59
298	3.74	34.84	300	3.75	34.84	27.70
386	3.76	34.86	400	3.75	34.86	27.72
573	3.55	34.89	600	3.55	34.89	27.76
756	3.41	34.89	800	3.40	34.89	27.78
952	3.33	34.89	1,000	3.35	34.89	27.78
1,454	3.29	34.91				

Station 5352; Apr. 11; latitude 46°21′ N., longitude 44°43′ W.; depth 2,195 m.; dynamic height 970.878

Observed values			Scaled values			
Depth, meters	Temperature, ° C.	Salinity, °/oo	Depth, meters	Temperature, ° C.	Salinity, °/oo	σ_t
0	4.07	34.15	0	4.07	34.15	27.12
26	4.08	34.18	25	4.10	34.18	27.14
52	3.90	34.20	50	3.95	34.20	27.18
78	3.81	34.22	75	3.85	34.22	27.21
104	3.57	34.45	100	3.60	34.40	27.37
154	3.59	34.64	150	3.60	34.63	27.55
206	3.77	34.80	200	3.75	34.79	27.66
310	3.73	34.86	300	3.75	34.86	27.72
399	3.69	34.885	400	3.70	34.88	27.74
594	3.56	34.905	600	3.60	34.90	27.77
786	3.46	34.90	800	3.55	34.90	27.77
985	3.38	34.89	1,000	3.40	34.89	27.78
1,489	3.30	34.885				

Station 5353; Apr. 11; latitude 46°30′ N., longitude 44°48′ W.; depth 732 m.; dynamic height 970.896

Observed values			Scaled values			
Depth, meters	Temperature, ° C.	Salinity, °/oo	Depth, meters	Temperature, ° C.	Salinity, °/oo	σ_t
0	3.28	33.96	0	3.28	33.96	27.05
26	3.22	33.95	25	3.25	33.95	27.04
51	3.32	34.06	50	3.30	34.05	27.12
77	3.47	34.24	75	3.45	34.23	27.24
103	2.87	34.26	100	2.90	34.25	27.32
153	2.94	34.49	150	2.95	34.47	27.49
205	3.11	34.60	200	3.10	34.59	27.57
308	3.85	34.79	300	3.80	34.78	27.65
379	3.83	34.88	400	3.80	34.88	27.73
572	3.55	34.89	(600)	3.50	34.89	27.77

Station 5354; Apr. 11; latitude 46°35′ N., longitude 44°49′ W.; depth 227 m.; dynamic height 970.919

Observed values			Scaled values			
Depth, meters	Temperature, ° C.	Salinity, °/oo	Depth, meters	Temperature, ° C.	Salinity, °/oo	σ_t
0	3.60	33.93	0	3.60	33.93	26.99
25	3.49	33.93	25	3.49	33.93	27.00
50	3.13	31.00	50	3.13	34.00	27.09
74	2.86	34.05	75	2.85	34.05	27.16
99	2.74	34.20	100	2.75	34.20	27.29
149	3.02	34.35	150	3.05	34.35	27.38
198	3.24	34.52	200	3.25	34.53	27.50

Station 5355; Apr. 11; latitude 46°41′ N., longitude 44°51′ W.; depth 172 m.; dynamic height 970.943

Observed values			Scaled values			
Depth, meters	Temperature, ° C.	Salinity, °/oo	Depth, meters	Temperature, ° C.	Salinity, °/oo	σ_t
0	3.57	33.88	0	3.57	33.88	26.95
25	3.28	33.88	25	3.28	33.88	26.98
50	3.11	33.92	50	3.11	33.92	27.04
74	2.89	33.95	75	2.90	33.95	27.08
99	2.80	33.99	100	2.80	33.99	27.12
149	2.87	34.09	150	2.90	34.09	27.19

Station 5356; Apr. 11; latitude 46°48′ N., longitude 44°51′ W.; depth 153 m.; dynamic height 970.942

Observed values			Scaled values			
Depth, meters	Temperature, ° C.	Salinity, °/oo	Depth, meters	Temperature, ° C.	Salinity, °/oo	σ_t
0	3.77	33.88	0	3.77	33.88	26.93
26	3.50	33.91	25	3.50	33.91	26.99
51	3.48	33.91	50	3.50	33.91	26.99
77	3.22	33.93	75	3.25	33.93	27.02
102	3.18	33.98	100	3.20	33.97	27.07
148	3.79	34.35	(150)	3.80	34.36	27.32

Station 5357; Apr. 11; latitude 46°47′ N., longitude 44°58′ W.; depth 174 m.; dynamic height 970.940

Observed values			Scaled values			
Depth, meters	Temperature, ° C.	Salinity, °/oo	Depth, meters	Temperature, ° C.	Salinity, °/oo	σ_t
0	4.13	33.90	0	4.13	33.90	26.91
26	3.65	33.91	25	3.65	33.91	26.97
52	3.64	33.91	50	3.65	33.91	26.97
77	3.51	33.98	75	3.55	33.97	27.03
103	3.59	34.14	100	3.60	34.12	27.15
155	3.46	34.34	150	3.45	34.32	27.32

Station 5358; Apr. 11; latitude 46°46.5′ N., longitude 45°12′ W.; depth 200 m.; dynamic height 970.950

Observed values			Scaled values			
Depth, meters	Temperature, ° C.	Salinity, °/oo	Depth, meters	Temperature, ° C.	Salinity, °/oo	σ_t
0	4.58	33.96	0	4.58	33.96	26.92
25	3.88	33.96	25	3.88	33.96	26.99
51	3.88	33.96	50	3.90	33.96	26.99
76	3.90	-------	75	3.90	33.96	26.99
101	3.64	33.98	100	3.65	33.97	27.03
152	3.05	34.15	150	3.10	34.14	27.21
203	3.52	34.42	200	3.50	34.41	27.39

Station 5359; Apr. 11; latitude 46°45′ N., longitude 45°34′ W.; depth 260 m.; dynamic height 970.950

Observed values			Scaled values			
Depth, meters	Temperature, ° C.	Salinity, °/oo	Depth, meters	Temperature, ° C.	Salinity, °/oo	σ_t
0	4.20	33.96	0	4.20	33.96	26.96
25	3.84	33.96	25	3.84	33.96	26.99
50	3.84	33.98	50	3.84	33.98	27.01
75	3.83	33.98	75	3.83	33.98	27.01
100	3.82	33.97	100	3.82	33.97	27.00
150	3.54	34.08	150	3.54	34.08	27.12
200	3.30	34.46	200	3.30	34.46	27.45
250	3.46	34.58				

Station 5360; Apr. 11; latitude 46°44′ N., longitude 45°54′ W., depth 327 m.; dynamic height 970.925

Observed values			Scaled values			
Depth, meters	Temperature, ° C.	Salinity, °/oo	Depth, meters	Temperature, ° C.	Salinity, °/oo	σ_t
0	2.50	33.62	0	2.50	33.62	26.85
25	2.31	-------	25	2.31	33.60	26.85
51	1.56	33.59	50	1.60	33.59	26.89
76	2.78	33.79	75	2.70	33.80	26.97
101	6.40	34.70	100	6.35	34.70	27.29
152	5.41	34.73	150	5.45	34.73	27.42
203	4.36	34.69	200	4.40	34.69	27.51
304	3.81	34.82	300	3.85	34.82	27.68

Station 5361; Apr. 11; latitude 46°44′ N., longitude 46°19′ W.; depth 640 m.; dynamic height 970.884

Observed values			Scaled values			
Depth, meters	Temperature, ° C.	Salinity ‰	Depth, meters	Temperature, ° C.	Salinity, ‰	σ_t
0	1.30	33.61	0	1.30	33.61	26.93
25	1.40	33.63	25	1.40	33.63	26.94
49	1.55	33.66	50	1.60	33.66	26.95
74	3.06	34.26	75	3.10	34.27	27.32
98	3.31	34.50	100	3.35	34.51	27.48
148	3.51	34.65	150	3.55	34.65	27.57
197	3.82	34.77	200	3.85	34.78	27.64
295	3.83	34.88	300	3.85	34.88	27.72
390	3.75	34.89	400	3.75	34.89	27.74
580	3.59	34.90	600	3.60	34.90	27.77

Station 5362; Apr. 12; latitude 46°44′ W., longitude 46°40′ W.; depth 1,188 m.; dynamic height 970.886

Depth, meters	Temperature, ° C.	Salinity ‰	Depth, meters	Temperature, ° C.	Salinity, ‰	σ_t
0	−0.18	33.39	0	−0.18	33.39	26.84
26	0.00	33.53	25	0.00	33.52	26.94
51	0.54	33.81	50	0.55	33.79	27.12
77	1.66	34.17	75	1.55	34.15	27.34
102	2.14	34.37	100	2.10	34.35	27.46
153	2.47	34.55	150	2.45	34.53	27.57
204	3.92	34.65	200	2.90	34.64	27.63
306	3.72	34.81	300	3.70	34.80	27.68
398	3.70	34.88	400	3.70	34.88	27.74
585	3.54	34.90	600	3.55	34.90	27.77
764	3.47	34.89	800	3.45	34.89	27.77
1,080	3.31	34.88	1,000	3.35	34.88	27.77

Station 5363; Apr. 12; latitude 46°44′ N., longitude 47°05′ W.; depth 631 m.; dynamic height 970.950

Depth, meters	Temperature, ° C.	Salinity ‰	Depth, meters	Temperature, ° C.	Salinity, ‰	σ_t
0	−1.23	33.15	0	−1.23	33.15	26.68
27	−1.12	33.24	25	−1.10	33.24	26.75
53	−0.98	33.32	50	−1.00	33.31	26.80
80	0.45	33.79	75	0.15	33.68	27.05
107	0.97	34.02	100	0.85	33.97	27.25
161	1.62	34.28	150	1.50	34.24	27.42
214	2.25	34.46	200	2.10	34.42	27.52
321	2.69	34.62	300	2.60	34.60	27.62
402	2.77	34.66	400	2.80	34.66	27.65
581	3.46	34.84	600	3.45	34.85	27.74

Station 5364; Apr. 12; latitude 46°44′ N., longitude 47°16′ W.; depth 308 m.; dynamic height 970.992

Depth, meters	Temperature, ° C.	Salinity ‰	Depth, meters	Temperature, ° C.	Salinity, ‰	σ_t
0	−1.39	32.98	0	−1.39	32.98	26.55
25	−1.45	33.06	25	−1.45	33.06	26.61
50	−1.48	33.12	50	−1.48	33.12	26.66
75	−1.42	33.24	75	−1.42	33.24	26.76
100	0.31	33.76	100	0.31	33.76	27.11
150	1.40	34.08	150	1.40	34.08	27.30
199	1.97	34.33	200	1.95	34.33	27.46
299	2.25	34.46	300	2.25	34.46	27.54

Station 5365; Apr. 12; latitude 46°45.5′ N., longitude 47°37′ W.; depth 183 m.; dynamic height 971.055

Depth, meters	Temperature, ° C.	Salinity ‰	Depth, meters	Temperature, ° C.	Salinity, ‰	σ_t
0	−1.35	32.81	0	−1.35	32.81	26.41
25	−1.39	32.81	25	−1.39	32.81	26.42
51	−1.42	32.83	50	−1.40	32.83	26.43
76	−1.46	32.93	75	−1.45	32.92	26.50
103	−1.51	33.09	100	−1.50	33.07	26.62
153	−0.01	33.44	150	−0.15	33.42	26.87

Station 5366; Apr. 12; latitude 46°45.5′ N., longitude 48°05′ W.; depth 119 m.; dynamic height 971.068

Depth, meters	Temperature, ° C.	Salinity, ‰	Depth, meters	Temperature, ° C.	Salinity, ‰	σ_t
0	−0.56	32.82	0	−0.56	32.82	26.39
27	−0.61	32.81	25	−0.60	32.82	26.39
53	−0.62	32.82	50	−0.60	32.82	26.39
81	−0.60	32.83	75	−0.60	32.83	26.40
107	−0.22	33.25	100	−0.35	33.11	26.61

Station 5367; Apr. 12; latitude 46°48.5′ N., longitude 48°40′ W.; depth 91 m.; dynamic height 971.077

Depth, meters	Temperature, ° C.	Salinity, ‰	Depth, meters	Temperature, ° C.	Salinity, ‰	σ_t
0	0.34	32.80	0	0.34	32.80	26.34
28	0.22	32.80	25	0.25	32.80	26.35
55	0.16	32.80	50	0.20	32.80	26.35
83	0.16	32.80	75	0.15	32.80	26.35

Sta. 5368; Apr. 12; latitude 47°13.5′ N., longitude 49°13′ W.; depth 89 m.; dynamic height 971.079

Depth, meters	Temperature, ° C.	Salinity, ‰	Depth, meters	Temperature, ° C.	Salinity, ‰	σ_t
0	−0.07	32.84	0	−0.07	32.84	26.39
29	−0.07	32.86	25	−0.05	32.86	26.40
56	−0.10	32.86	50	−0.10	32.86	26.40
85	−0.20	32.85	75	−0.15	32.85	26.40

Station 5369; Apr. 12; latitude 47°14′ N., longitude 48°39′ W.; depth 128 m; dynamic height 971.073

Depth, meters	Temperature, ° C.	Salinity, ‰	Depth, meters	Temperature, ° C.	Salinity, ‰	σ_t
0	−0.90	32.85	0	−0.90	32.85	26.43
19	−0.90	32.85	25	−0.95	32.85	26.43
46	−1.20	32.83	50	−1.20	32.83	26.42
73	−1.18	32.86	75	−1.15	32.87	26.45
100	−0.80	33.04	100	−0.80	33.04	26.58
112	−0.39	33.26				

Station 5370; Apr. 12; latitude 47°13′ N., longitude 48°08′ W.; depth 169 m.; dynamic height 971.066

Depth, meters	Temperature, ° C.	Salinity, ‰	Depth, meters	Temperature, ° C.	Salinity, ‰	σ_t
0	−0.90	32.85	0	−0.90	32.85	26.43
28	−0.90	32.87	25	−0.90	32.87	26.45
54	−1.31	32.88	50	−1.25	32.88	26.46
82	−1.36	32.92	75	−1.35	32.91	26.49
109	−0.98	33.14	100	−1.10	33.06	26.60
164	0.18	33.53	150	−0.10	33.46	26.89

Station 5371; Apr. 12; latitude 47°12.5′ N., longitude 47°48′ W. depth 229 m.; dynamic height 971.077

Depth, meters	Temperature, ° C.	Salinity, ‰	Depth, meters	Temperature, ° C.	Salinity, ‰	σ_t
0	−1.23	32.66	0	−1.23	32.66	26.29
26	−1.26	32.69	25	−1.25	32.69	26.31
52	−1.28	32.84	50	−1.25	32.83	26.42
78	−1.40	32.88	75	−1.40	32.87	26.46
104	−1.04	33.09	100	−1.10	33.05	26.60
157	−0.47	33.30	150	−0.55	33.27	26.75
209	0.85	33.71	200	0.65	33.64	26.99

Station 5372; Apr. 12; latitude 47°13.5′ N., longitude 47°24′ W.; depth 570 m.; dynamic height 970.970

Observed values			Scaled values			
Depth, meters	Temperature, ° C.	Salinity °/oo	Depth, meters	Temperature, ° C.	Salinity, °/oo	σ_t
0	−1.31	33.06	0	−1.31	33.06	26.61
24	−1.50	33.07	25	−1.50	33.07	26.62
48	−1.60	33.10	50	−1.60	33.10	26.65
72	−1.59	33.13	75	−1.55	33.14	26.68
96	−0.91	33.35	100	−0.75	33.48	26.93
144	1.37	34.13	150	1.45	34.22	27.41
192	1.80	34.32	200	1.85	34.34	27.47
288	2.44	34.58	(300)	2.50	34.61	27.64
			(400)	3.20	34.80	27.73

Station 5373; Apr. 13; latitude 47°18′ N., longitude 46°46′ W.; depth 1,046 m.; dynamic height 970.889

Observed values			Scaled values			
Depth, meters	Temperature, ° C.	Salinity °/oo	Depth, meters	Temperature, ° C.	Salinity, °/oo	σ_t
0	−0.40	33.23	0	−0.40	33.23	26.72
27	0.97	33.96	25	0.95	33.90	27.18
52	1.24	34.04	50	1.20	34.03	27.27
79	------	33.25	75	2.10	34.21	27.35
104	3.23	34.45	100	3.15	34.43	27.43
158	2.89	34.56	150	2.95	34.54	27.54
210	2.32	------	200	2.40	34.64	27.67
314	3.70	34.86	300	3.55	34.83	27.71
344	3.80	34.88	400	3.80	34.87	27.73
522	3.58	34.86	600	3.50	34.87	27.76
702	3.43	34.88	800	3.45	34.88	27.76
894	3.35	34.87	(1,000)	3.35	34.87	27.77

Station 5374; Apr. 13; latitude 47°19′ N., longitude 46°27′ W.; depth 531 m.; dynamic height 970.880

Observed values			Scaled values			
Depth, meters	Temperature, ° C.	Salinity °/oo	Depth, meters	Temperature, ° C.	Salinity, °/oo	σ_t
0	0.51	33.56	0	0.51	33.56	26.94
24	0.47	33.56	25	0.50	33.56	26.94
47	0.59	33.66	50	0.70	33.74	27.07
71	3.21	34.36	75	3.25	34.37	27.38
94	3.11	34.43	100	3.00	34.44	27.46
141	2.42	34.52	150	2.45	34.54	27.58
188	2.96	34.64	200	3.15	34.67	27.63
282	3.98	34.86	300	3.90	34.87	27.72
362	3.72	34.90	400	3.70	34.90	27.76
506	3.58	34.90				

Station 5375; Apr. 13; latitude 47°20′ N., longitude 45°57′ W.; depth 324 m.; dynamic height 970.933

Observed values			Scaled values			
Depth, meters	Temperature, ° C.	Salinity °/oo	Depth, meters	Temperature, ° C.	Salinity, °/oo	σ_t
0	4.30	34.04	0	4.30	34.04	27.01
24	4.28	34.04	25	4.30	34.04	27.01
47	4.27	34.04	50	4.25	34.04	27.02
70	4.28	34.05	75	4.25	34.05	27.03
93	4.20	34.045	100	4.20	34.06	27.04
141	4.07	34.35	150	3.95	34.37	27.32
188	3.49	34.45	200	3.55	34.49	27.44
281	4.17	34.79	(300)	4.20	34.86	27.68

Station 5376; Apr. 13; latitude 47°21′ N., longitude 45°32′ W.; depth 263 m.; dynamic height 970.930

Observed values			Scaled values			
Depth, meters	Temperature, ° C.	Salinity °/oo	Depth, meters	Temperature, ° C.	Salinity, °/oo	σ_t
0	3.99	33.97	0	3.99	33.97	26.99
27	4.09	34.02	25	4.10	34.02	27.02
53	4.38	34.075	50	4.35	34.07	27.03
80	4.38	34.07	75	4.35	34.07	27.03
106	4.42	34.085	100	4.40	34.08	27.03
159	3.77	34.38	150	3.85	34.32	27.29
212	4.91	34.74	200	4.70	34.68	27.47
249	4.52	34.77				

Station 5377; Apr. 13; latitude 47°22′ N., longitude 45°15′ W., depth 224 m.; dynamic height 970.932

Observed values			Scaled values			
Depth, meters	Temperature, ° C.	Salinity, °/oo	Depth, meters	Temperature, ° C.	Salinity, °/oo	σ_t
0	4.08	34.01	0	4.08	34.01	27.01
26	4.06	34.00	25	4.05	34.01	27.02
52	4.05	34.01	50	4.05	34.01	27.02
78	4.05	34.01	75	4.05	34.01	27.02
104	4.06	34.03	100	4.05	34.02	27.03
157	3.93	34.33	150	3.90	34.29	27.25
209	4.12	34.64	200	4.10	34.59	27.47

Station 5378; Apr. 13; latitude 47°22′ N., longitude 45°00′ W.; depth 216 m.; dynamic height 970.942

Observed values			Scaled values			
Depth, meters	Temperature, ° C.	Salinity, °/oo	Depth, meters	Temperature, ° C.	Salinity, °/oo	σ_t
0	3.88	33.94	0	3.88	33.94	26.97
24	3.85	33.94	25	3.85	33.94	26.98
47	3.75	33.94	50	3.75	33.94	26.99
71	3.73	33.94	75	3.75	33.94	26.99
95	3.72	33.94	100	3.75	33.95	27.00
142	3.82	34.20	150	3.80	34.25	27.23
189	3.82	34.46	(200)	3.85	34.51	27.43

Station 5379; Apr. 13; latitude 47°29′ N., longitude 45°15′ W.; depth 243 m.; dynamic height 970.927

Observed values			Scaled values			
Depth, meters	Temperature, ° C.	Salinity, °/oo	Depth, meters	Temperature, ° C.	Salinity, °/oo	σ_t
0	4.09	34.01	0	4.09	34.01	27.01
27	4.09	34.00	25	4.10	34.00	27.00
53	3.77	33.98	50	3.80	33.98	27.01
80	3.81	33.99	75	3.80	33.99	27.02
105	3.85	33.99	100	3.85	33.99	27.02
159	4.85	34.54	150	4.75	34.44	27.28
212	4.11	34.64	200	4.25	34.62	27.48

Station 5380; Apr. 13; latitude 47°40′ N., longitude 45°40′ W.; depth 326 m.; dynamic height 970.895

Observed values			Scaled values			
Depth, meters	Temperature, ° C.	Salinity, °/oo	Depth, meters	Temperature, ° C.	Salinity, °/oo	σ_t
0	2.37	33.79	0	2.37	33.79	26.99
19	2.25	33.79	25	2.25	33.79	27.00
38	2.34	33.82	50	1.90	33.82	27.06
58	1.58	33.82	75	2.55	34.00	27.15
77	2.73	34.04	100	3.30	34.31	27.33
115	3.61	34.50	150	4.15	34.63	27.49
153	4.15	34.64	200	4.15	34.76	27.60
230	4.08	34.83	(300)	3.95	34.90	27.73

Station 5381; Apr. 13; latitude 47°43′ N., longitude 45°47′ W.; depth 439 m.; dynamic height 970.876

Observed values			Scaled values			
Depth, meters	Temperature, ° C.	Salinity, °/oo	Depth, meters	Temperature, ° C.	Salinity, °/oo	σ_t
0	1.73	33.80	0	1.73	33.80	27.05
27	1.68	33.80	25	1.70	33.80	27.05
52	1.63	34.05	50	1.65	34.02	27.24
79	2.32	34.28	75	2.20	34.25	27.38
104	3.23	34.49	100	3.10	34.44	27.45
157	4.13	34.71	150	4.10	34.69	27.55
210	4.12	34.78	200	4.15	34.77	27.61
314	3.77	34.87	300	3.80	34.86	27.72
420	3.70	34.89	400	3.70	34.89	27.75

Table of Oceanographic Data—Continued

STATIONS OCCUPIED IN 1954—Continued

Station 5382; Apr. 13; latitude 47°52.5′ N., longitude 46°07′ W.; depth 1,067 m.; dynamic height 970.842

Observed values			Scaled values			
Depth, meters	Temperature, ° C.	Salinity °/oo	Depth, meters	Temperature, ° C.	Salinity, °/oo	σt
0	1.94	34.18	0	1.94	34.18	27.34
27	1.97	34.16	25	2.00	34.16	27.32
52	2.21	34.39	50	2.20	34.36	27.47
79	2.57	34.53	75	2.55	34.51	27.56
105	2.75	34.58	100	2.75	34.57	27.59
158	2.87	34.64	150	2.85	34.63	27.62
211	2.97	34.72	200	2.95	34.70	27.67
316	3.56	34.86	300	3.45	34.83	27.72
348	3.69	34.86	400	3.60	34.87	27.75
523	3.48	34.88	600	3.45	34.88	27.76
700	3.39	34.88	800	3.35	34.87	27.77
848	3.27	34.87	(1,000)	3.30	34.88	27.78

Station 5383; Apr. 13; latitude 47°58.5′ N., longitude 46°20′ W.; depth 1,165 m.; dynamic height 970.843

Observed values			Scaled values			
Depth, meters	Temperature, ° C.	Salinity °/oo	Depth, meters	Temperature, ° C.	Salinity, °/oo	σt
0	0.83	33.71	0	0.83	33.71	27.04
24	0.82	33.74	25	0.80	33.76	27.08
47	2.22	34.43	50	2.30	34.45	27.53
71	2.56	34.56	75	2.55	34.56	27.60
94	2.60	34.56	100	2.65	34.56	27.59
142	3.42	34.76	150	3.50	34.68	27.60
190	3.70	34.83	200	3.70	34.84	27.71
284	3.74	34.88	300	3.70	34.88	27.74
292	3.70	34.87	400	3.65	34.89	27.75
447	3.59	34.90	600	3.45	34.88	27.76
622	3.43	34.88	800	3.35	34.89	27.78
810	*3.32	34.89	(1,000)	3.30	34.89	27.79

Station 5384; Apr. 14; latitude 48°19′ N., longitude 45°54′ W.; depth 1,174 m.; dynamic height 970.844

Observed values			Scaled values			
Depth, meters	Temperature, ° C.	Salinity °/oo	Depth, meters	Temperature, ° C.	Salinity, °/oo	σt
0	2.47	34.40	0	2.47	34.40	27.47
25	2.47	34.41	25	2.47	34.41	27.48
48	2.50	34.40	50	2.50	34.40	27.47
73	2.64	34.42	75	2.65	34.42	27.48
96	3.04	34.58	100	3.05	34.58	27.56
145	2.76	34.60	150	2.80	34.61	27.61
194	3.80	34.79	200	3.80	34.79	27.66
290	3.72	34.86	300	3.40	34.82	27.73
317	3.10	34.765	400	3.45	34.84	27.73
498	3.46	34.87	600	3.45	34.88	27.76
682	3.42	34.88	800	3.40	34.88	27.77
873	3.36	34.88	(1,000)	3.35	34.88	27.77

Station 5385; Apr. 14; latitude 48°39.5′ N., longitude 45°27′ W.; depth 1,097 m.; dynamic height 970.864

Observed values			Scaled values			
Depth, meters	Temperature, ° C.	Salinity °/oo	Depth, meters	Temperature, ° C.	Salinity, °/oo	σt
0	2.46	34.33	0	2.46	34.33	27.41
25	2.47	34.35	25	2.47	34.35	27.43
50	2.46	34.36	50	2.46	34.36	27.44
75	2.48	34.38	75	2.48	34.38	27.45
99	2.53	34.39	100	2.55	34.39	27.46
149	2.38	34.40	150	2.40	34.40	27.48
199	3.24	34.63	200	3.25	34.63	27.58
298	3.76	34.84	300	3.75	34.84	27.70
333	3.71	34.86	400	3.60	34.87	27.75
513	3.52	34.88	600	3.55	34.89	27.76
704	3.54	34.89	800	3.50	34.89	27.77
930	3.34	34.88	(1,000)	3.35	34.88	27.77

Station 5386; Apr. 14; latitude 49°00′ N., longitude 45°00′ W.; depth 1,335 m.; dynamic height 970.817

Observed values			Scaled values			
Depth, meters	Temperature, ° C.	Salinity, °/oo	Depth, meters	Temperature, ° C.	Salinity, °/oo	σt
0	2.86	34.58	0	2.86	34.58	27.58
20	2.86	34.58	25	2.85	34.58	27.58
40	2.85	34.59	50	2.85	34.59	27.59
60	2.83	34.60	75	2.80	34.62	27.62
80	2.82	34.62	100	2.80	34.68	27.66
120	3.23	34.77	150	2.95	34.73	27.69
160	2.93	34.725	200	3.10	34.76	27.71
240	3.24	34.80	300	3.35	34.84	27.74
101	2.82	34.57	400	3.60	34.87	27.75
255	3.23	34.75	600	3.55	34.90	27.77
433	3.61	34.88	800	3.45	34.89	27.77
619	3.52	34.90	1,000	3.35	34.89	27.78
1,117	3.27	34.88				

Station 5387; Apr. 14; latitude 49°10′ N., longitude 45°40′ W.; depth 2,213 m.; dynamic height 970.850

Observed values			Scaled values			
Depth, meters	Temperature, ° C.	Salinity, °/oo	Depth, meters	Temperature, ° C.	Salinity, °/oo	σt
0	4.26	34.44	0	4.26	34.44	27.33
26	4.25	34.45	25	4.25	34.45	27.34
52	3.55	34.48	50	3.65	34.48	27.42
78	2.89	34.53	75	2.90	34.52	27.54
103	3.26	34.68	100	3.20	34.66	27.62
156	3.49	34.78	150	3.45	34.77	27.68
207	3.65	34.84	200	3.65	34.83	27.70
310	3.49	34.85	300	3.50	34.85	27.74
381	3.43	34.855	400	3.45	34.85	27.74
570	3.44	34.85	600	3.45	34.85	27.74
762	3.41	------	800	3.45	34.85	27.74
960	3.36	34.85	1,000	3.35	34.85	27.75
1,470	3.32	34.91				

Station 5388; Apr. 14; latitude 49°19′ N., longitude 46°21′ W.; depth 2,963 m.; dynamic height 970.897

Observed values			Scaled values			
Depth, meters	Temperature, ° C.	Salinity, °/oo	Depth, meters	Temperature, ° C.	Salinity, °/oo	σt
0	5.39	34.55	0	5.39	34.55	27.29
26	5.38	34.54	25	5.40	34.54	27.28
52	5.40	34.55	50	5.40	34.55	27.29
78	5.40	34.56	75	5.40	34.56	27.30
103	5.41	34.56	100	5.40	34.56	27.30
156	5.11	34.71	150	5.15	34.69	27.43
208	5.11	34.87	200	5.10	34.86	27.57
311	4.43	34.88	300	4.45	34.88	27.66
389	4.07	34.88	400	4.00	34.88	27.71
581	3.64	34.90	600	3.65	34.90	27.76
771	3.51	34.895	800	3.50	34.89	27.77
970	3.41	34.88	1,000	3.40	34.88	27.77
1,482	3.36	34.90				

Station 5389; Apr. 14; latitude 48°56′ N., longitude 46°39′ W.; depth 2,743 m.; dynamic height 970.854

Observed values			Scaled values			
Depth, meters	Temperature, ° C.	Salinity, °/oo	Depth, meters	Temperature, ° C.	Salinity, °/oo	σt
0	3.87	34.44	0	3.87	34.44	27.37
25	3.84	34.44	25	3.84	34.44	27.38
48	2.68	34.50	50	2.70	34.50	27.53
73	2.65	34.50	75	2.65	34.50	27.54
96	2.66	34.51	100	2.65	34.51	27.55
145	2.67	34.52	150	2.70	34.53	27.55
194	2.81	34.69	200	2.85	34.70	27.68
290	2.96	34.76	300	3.10	34.78	27.72
287	3.11	34.78	400	3.25	34.80	27.72
436	3.29	34.81	600	3.40	34.83	27.73
589	3.34	34.83	800	3.45	34.88	27.77
758	3.48	34.88	1,000	3.40	34.88	27.77
1,224	3.31	34.88				

STATIONS OCCUPIED IN 1954—Continued

Station 5390; Apr. 15; latitude 48°36′ N., longitude 46°54′ W.; depth 2,433 m.; dynamic height 970.829

Observed values			Scaled values			
Depth, meters	Temperature, ° C.	Salinity, ‰	Depth, meters	Temperature, ° C.	Salinity, ‰	σ_t
0	2.06	34.31	0	2.06	34.31	27.44
27	2.08	34.30	25	2.10	34.30	27.42
52	2.39	34.42	50	2.35	34.41	27.49
79	2.62	34.52	75	2.60	34.50	27.54
104	2.84	34.59	100	2.80	34.58	27.58
157	3.35	34.76	150	3.30	34.74	27.67
210	3.41	34.82	200	3.40	34.81	27.72
314	3.39	34.85	300	3.40	34.85	27.75
415	3.49	34.88	400	3.45	34.87	27.76
621	3.53	34.90	600	3.55	34.90	27.77
827	3.44	34.90	800	3.50	34.89	27.77
1,044	3.36	34.87	1,000	3.40	34.88	27.77
1,606	3.33	34.92				

Station 5391; Apr. 15; latitude 48°15′ N., longitude 47°11′ W.; depth 1,390 m.; dynamic height 970.918

Observed values			Scaled values			
Depth, meters	Temperature, ° C.	Salinity, ‰	Depth, meters	Temperature, ° C.	Salinity, ‰	σ_t
0	−1.41	33.21	0	−1.41	33.21	26.74
24	−1.40	33.21	25	−1.40	33.21	26.74
48	−1.46	--------	50	−1.45	33.21	26.74
73	−0.02	33.85	75	−0.95	33.86	27.25
97	1.10	34.12	100	1.15	34.15	27.37
144	2.00	34.42	150	2.05	34.45	27.55
193	2.54	34.59	200	2.60	34.61	27.63
290	3.09	34.71	300	3.10	34.72	27.68
380	3.21	34.74	400	3.20	34.75	27.69
566	3.39	34.84	600	3.45	34.86	27.75
750	3.58	34.89	800	3.60	34.89	27.76
944	3.48	34.89	(1,000)	3.45	34.89	27.77
1,394	-------	34.89				

Station 5392; Apr. 15; latitude 47°55′ N., longitude 47°26′ W.; depth 368 m.; dynamic height 970.962

Observed values			Scaled values			
Depth, meters	Temperature, ° C.	Salinity, ‰	Depth, meters	Temperature, ° C.	Salinity, ‰	σ_t
0	−1.42	33.14	0	−1.42	33.14	26.68
26	−1.44	33.16	25	−1.45	33.16	16.69
51	−1.45	33.19	50	−1.45	33.19	26.72
78	−1.12	33.44	75	−1.20	33.42	26.91
103	0.93	33.96	100	0.70	33.91	27.21
155	1.78	34.27	150	1.75	34.26	27.42
199	1.92	34.36	200	1.90	34.36	27.49
309	2.48	34.55	300	2.45	34.53	27.57

Station 5393; Apr. 15; latitude 47°46′ N., longitude 47°32′ W.; depth 320 m.; dynamic height 971.015

Observed values			Scaled values			
Depth, meters	Temperature, ° C.	Salinity, ‰	Depth, meters	Temperature, ° C.	Salinity, ‰	σ_t
0	−1.47	33.09	0	−1.47	33.09	26.63
26	−1.50	33.09	25	−1.50	33.09	26.63
51	−1.52	33.08	50	−1.50	33.09	26.63
78	−1.56	33.11	75	−1.55	33.10	26.65
103	−1 28	33.40	100	−1.35	33.36	26.85
155	1.37	34.04	150	1.15	33.98	27.23
206	1.57	-------	200	1.55	34.13	27.32
309	1.97	34.34	300	1.95	34.32	27.46

Station 5394; Apr. 26; latitude 46°46.5′ N., longitude 48°38′ W.; depth 84 m.; dynamic height 971.056

Observed values			Scaled values			
Depth, meters	Temperature, ° C.	Salinity, ‰	Depth, meters	Temperature, ° C.	Salinity, ‰	σ_t
0	0.31	32.84	0	0.31	32.84	26.37
28	0.29	32.83	25	0.30	32.83	26.36
55	0.28	32.84	50	0.30	32.84	26.37
80	−0.23	32.95	75	−0.10	32.91	26.44

Station 5395; Apr. 26; latitude 46°46′ N., longitude 48°06′ W.; depth 114 m.; dynamic height 971.055

Observed values			Scaled values			
Depth, meters	Temperature, ° C.	Salinity, ‰	Depth, meters	Temperature, ° C.	Salinity, ‰	σ_t
0	−0.11	32.82	0	−0.11	32.82	26.37
26	−0.18	32.82	25	−0.20	32.82	26.38
52	−0.21	32.82	50	−0.20	32.82	26.38
78	−0.80	32.87	75	−0.75	32.85	26.42
104	−0.33	33.26	100	−0.40	33.17	26.67

Station 5396; Apr. 26; latitude 46°44.5′ N., longitude 47°30′ W.; depth 172 m.; dynamic height 971.041

Observed values			Scaled values			
Depth, meters	Temperature, ° C.	Salinity, ‰	Depth, meters	Temperature, ° C.	Salinity, ‰	σ_t
0	−1.02	32.90	0	−1.02	32.90	26.47
26	−1.22	32.91	25	−1.20	32.91	26.49
51	−1.20	32.93	50	−1.20	32.93	26.50
77	−1.50	33.02	75	−1.50	33.01	26.58
103	−1.20	33.25	100	−1.25	33.21	26.73
154	0.27	33.59	150	0.15	33.56	26.96

Station 5397; Apr. 26; latitude 46°41.5′ N., longitude 47°08′ W.; depth 334 m.; dynamic height 971.002

Observed values			Scaled values			
Depth, meters	Temperature, ° C.	Salinity, ‰	Depth, meters	Temperature, ° C.	Salinity, ‰	σ_t
0	−1.17	32.97	0	−1.17	32.97	26.53
25	−1.15	33.09	25	−1.15	33.09	26.63
49	−1.40	33.22	50	−1.40	33.23	26.75
74	−0.56	33.42	75	−0.55	33.43	26.88
99	0.39	33.64	100	0.40	33.65	27.02
148	0.31	33.88	150	0.35	33.89	27.21
197	1.65	34.20	200	1.20	34.21	27.42
296	2.25	34.47	300	2.25	34.48	27.55

Station 5398; Apr. 26; latitude 46°44′ N., longitude 47°01′ W.; depth 644 m.; dynamic height 970.994

Observed values			Scaled values			
Depth, meters	Temperature, ° C.	Salinity, ‰	Depth, meters	Temperature, ° C.	Salinity, ‰	σ_t
0	−1.01	33.12	0	−1.01	33.12	26.65
24	−1.00	33.16	25	−1.00	33.16	26.68
48	−1.00	33.14	50	−1.00	33.15	26.68
72	−1.25	33.32	75	−1.20	33.36	26.85
96	−0.50	33.59	100	−0.35	33.64	27.04
144	1.23	34.08	150	1.35	34.10	27.32
193	1.60	34.20	200	1.65	34.22	27.40
289	2.70	34.58	300	2.75	34.59	27.60
393	2.83	34.63	400	2.85	34.63	27.62
576	3.30	34.78	600	3.35	34.80	27.71

Station 5399; Apr. 26; latitude 46°35.5′ N., longitude 46°44′ W.; depth 1,192 m.; dynamic height 970.929

Observed values			Scaled values			
Depth, meters	Temperature, ° C.	Salinity, ‰	Depth, meters	Temperature, ° C.	Salinity, ‰	σ_t
0	−0.69	33.25	0	−0.69	33.25	26.74
26	−0.69	33.26	25	−0.70	33.26	26.75
51	−0.16	33.32	50	−0.20	33.31	26.77
77	0.08	33.87	75	0.05	33.83	27.18
102	0.95	34.10	100	0.90	34.09	27.34
153	1.69	34.31	150	1.65	34.30	27.46
204	2.12	34.44	200	2.10	34.43	27.52
306	3.31	34.73	300	3.25	34.71	27.65
336	3.70	34.84	400	3.60	34.85	27.73
508	3.51	34.87	600	3.55	34.88	27.75
684	3.51	34.89	800	3.45	34.88	27.76
905	3.36	34.88	(1,000)	3.35	34.88	27.77

Table of Oceanographic Data—Continued

STATIONS OCCUPIED IN 1954—Continued

Station 5400; Apr. 27; latitude 46°39.5′ N., longitude 46°54′ W., depth 1,152 m.; dynamic height 970.913

Observed values			Scaled values			
Depth, meters	Temperature, ° C.	Salinity ‰	Depth, meters	Temperature, ° C.	Salinity, ‰	σ_t
0	−0. 86	33. 30	0	−0. 86	33. 30	26. 78
27	−0. 86	33. 32	25	−0. 85	33. 32	26. 80
53	−0. 78	33. 34	50	−0. 80	33. 34	26. 82
80	1. 12	33. 94	75	0. 75	33. 82	27. 14
106	1. 23	34. 18	100	1. 20	34. 14	27. 36
160	2. 11	34. 43	150	1. 95	34. 39	27. 51
214	2. 59	34. 60	200	2. 45	34. 56	27. 60
320	3. 23	34. 76	300	3. 10	34. 73	27. 68
356	3. 50	34. 81	400	3. 55	34. 84	27. 72
535	3. 56	34. 88	600	3. 55	34. 89	27. 76
715	3. 47	34. 89	800	3. 50	34. 89	27. 77
927	3. 38	34. 89	(1, 000)	3. 40	34. 89	27. 78

Station 5401; Apr. 27; latitude 46°38.5′ N., longitude 46°26′ W., depth 593 m.; dynamic height 970.879

Observed values			Scaled values			
Depth, meters	Temperature, ° C.	Salinity ‰	Depth, meters	Temperature, ° C.	Salinity, ‰	σ_t
0	0. 90	33. 51	0	0. 90	33. 51	26. 88
26	1. 13	33. 54	25	1. 15	33. 54	26. 88
53	1. 22	33. 56	50	1. 20	33. 56	26. 90
79	1. 52	34. 16	75	1. 45	34. 07	27. 29
106	2. 38	34. 46	100	2. 20	34. 43	27. 52
157	2. 68	34. 58	150	2. 65	34. 56	27. 59
210	3. 48	34. 74	200	3. 40	34. 72	27. 65
316	3. 80	34. 88	300	3. 80	34. 87	27. 73
407	3. 82	34. 90	400	3. 80	34. 90	27. 75
546	3. 57	34. 90				

Station 5402; Apr. 28; latitude 46°38′ N., longitude 45°58′ W., depth 366 m.; dynamic height 970.931

Observed values			Scaled values			
Depth, meters	Temperature, ° C.	Salinity ‰	Depth, meters	Temperature, ° C.	Salinity, ‰	σ_t
0	4. 52	34. 00	0	4. 52	34. 00	26. 96
27	4. 53	34. 00	25	4. 55	34. 00	26. 95
52	4. 53	34. 00	50	4. 55	34. 00	26. 95
79	4. 53	34. 00	75	4. 55	34. 00	26. 95
105	4. 10	34. 20	100	4. 20	34. 18	27. 13
158	3. 00	34. 31	150	3. 10	34. 29	27. 33
315	3. 78	34. 81	200	3. 20	34. 44	27. 44
			300	3. 75	34. 77	27. 65

Station 5403; Apr. 28; latitude 46°38′ N., longitude 45°48′ W.; depth 256 m.; dynamic height 970.936

Observed values			Scaled values			
Depth, meters	Temperature, ° C.	Salinity ‰	Depth, meters	Temperature, ° C.	Salinity, ‰	σ_t
0	4. 29	34. 00	0	4. 29	34. 00	26. 98
25	4. 29	34. 01	25	4. 29	34. 01	26. 99
48	4. 29	34. 01	50	4. 30	34. 01	26. 99
73	4. 26	34. 02	75	4. 25	34. 02	27. 01
97	4. 25	-------	100	4. 25	34. 03	27. 01
146	3. 94	34. 25	150	3. 90	34. 27	27. 24
194	3. 47	34. 54	200	3. 50	34. 56	27. 51
237	3. 62	34. 63				

Station 5404; Apr. 28; latitude 46°37.5′ N., longitude 45°24′ W.; depth 227 m.; dynamic height 970.924

Observed values			Scaled values			
Depth, meters	Temperature, ° C.	Salinity ‰	Depth, meters	Temperature, ° C.	Salinity, ‰	σ_t
0	3. 66	33. 92	0	3. 66	33. 92	26. 98
27	3. 69	-------	25	3. 70	33. 92	26. 98
53	3. 67	33. 92	50	3. 70	33. 92	26. 98
80	3. 63	33. 96	75	3. 65	33. 95	27. 00
106	3. 22	34. 15	100	3. 35	34. 12	27. 17
160	3. 28	34. 41	150	3. 25	34. 37	27. 38
213	3. 77	34. 62	200	3. 65	34. 37	27. 50

Station 5405; Apr. 28; latitude 46°37.5′ N., longitude 44°56′ W.; depth 201 m.; dynamic height 970.922

Observed values			Scaled values			
Depth, meters	Temperature, ° C.	Salinity, ‰	Depth, meters	Temperature, ° C.	Salinity, ‰	σ_t
0	3. 65	33. 92	0	3. 65	33. 92	26. 98
27	3. 66	33. 95	25	3. 65	33. 95	27. 00
53	3. 67	33. 95	50	3. 70	33. 95	27. 00
80	3. 64	33. 96	75	3. 65	33. 96	27. 01
105	2. 89	34. 12	100	3. 05	34. 08	27. 16
159	3. 75	34. 48	150	3. 55	34. 42	27. 39

Station 5406; Apr. 28; latitude 46°37′ N., longitude 44°42′ W.; depth 226 m.; dynamic height 970.888

Observed values			Scaled values			
Depth, meters	Temperature, ° C.	Salinity, ‰	Depth, meters	Temperature, ° C.	Salinity, ‰	σ_t
0	3. 67	33. 97	0	3. 67	33. 97	27. 02
24	3. 68	33. 97	25	3. 70	33. 97	27. 02
47	3. 51	33. 99	50	3. 45	34. 00	27. 07
71	3. 03	34. 29	75	2. 95	34. 31	27. 36
94	2. 89	34. 39	100	2. 90	34. 40	27. 44
141	3. 04	34. 45	150	3. 20	34. 49	27. 48
188	3. 99	34. 80	(200)	4. 00	34. 86	27. 70

Station 5407; Apr. 28; latitude 46°30′ N., longitude 44°40′ W.; depth 686 m.; dynamic height 970.888

Observed values			Scaled values			
Depth, meters	Temperature, ° C.	Salinity, ‰	Depth, meters	Temperature, ° C.	Salinity, ‰	σ_t
0	3. 08	34. 08	0	3. 08	34. 08	27. 16
28	3. 06	34. 10	25	3. 05	34. 10	27. 18
55	3. 11	34. 13	50	3. 10	34. 12	27. 20
82	3. 10	34. 20	75	3. 10	34. 17	27. 24
109	3. 22	34. 46	100	3. 20	34. 37	27. 39
165	3. 43	34. 60	150	3. 40	34. 56	27. 52
219	3. 50	34. 72	200	3. 50	34. 68	27. 60
328	3. 91	34. 86	300	3. 85	34. 84	27. 69
409	3. 78	34. 89	400	3. 80	34. 89	27. 74
584	3. 58	34. 87	600	3. 60	34. 87	27. 75

Station 5408; Apr. 28; latitude 46°24.5′ N., longitude 44°39′ W.; depth 1,371 m.; dynamic height 970.888

Observed values			Scaled values			
Depth, meters	Temperature, ° C.	Salinity, ‰	Depth, meters	Temperature, ° C.	Salinity, ‰	σ_t
0	3. 22	34. 15	0	3. 22	34. 15	27. 21
27	3. 17	34. 18	25	3. 15	34. 18	27. 23
53	3. 08	34. 20	50	3. 10	34. 20	27. 26
81	3. 01	34. 21	75	3. 05	34. 21	27. 27
107	3. 02	34. 25	100	3. 00	34. 24	27. 30
161	3. 30	34. 54	150	3. 25	34. 49	27. 47
215	3. 62	34. 68	200	3. 55	34. 64	27. 56
322	4. 31	34. 91	300	4. 20	34. 88	27. 69
422	3. 91	34. 91	400	3. 95	34. 91	27. 74
627	3. 44	34. 88	600	3. 45	34. 88	27. 76
827	3. 37	34. 89	800	3. 40	34. 89	27. 78
1, 036	3. 29	34. 88	1, 000	3. 30	34. 88	27. 78
1, 248	3. 31	34. 89				

Station 5409; Apr. 28; latitude 46°00′ N., longitude 44°38′ W.; depth 3,841 m.; dynamic height 917.061

Observed values			Scaled values			
Depth, meters	Temperature, ° C.	Salinity, ‰	Depth, meters	Temperature, ° C.	Salinity, ‰	σ_t
0	8. 68	34. 56	0	8. 68	34. 56	26. 84
26	8. 84	34. 60	25	8. 85	34. 60	26. 85
53	8. 89	34. 62	50	8. 85	34. 62	26. 87
79	9. 08	34. 68	75	9. 05	34. 67	26. 87
106	9. 10	34. 70	100	9. 10	34. 69	26. 88
158	7. 77	34. 78	150	7. 95	34. 76	27. 11
211	8. 03	35. 01	200	8. 00	34. 97	27. 27
317	6. 17	34. 92	300	6. 50	34. 93	27. 45
402	5. 38	34. 88	400	5. 40	34. 88	27. 55
602	4. 94	34. 98	600	4. 95	34. 98	27. 68
			(800)	4. 30	34. 97	27. 75
			(1, 000)	4. 00	34. 92	27. 75

STATIONS OCCUPIED IN 1954—Continued

Station 5410; Apr. 28; latitude 46°02′ N., longitude 45°34′ W.; depth 2,743 m.; dynamic height 970.892

Observed values			Scaled values			
Depth, meters	Temperature, ° C.	Salinity ‰	Depth, meters	Temperature, ° C.	Salinity, ‰	σ_t
0	4.07	34.18	0	4.07	34.18	27.15
24	4.08	34.18	25	4.10	34.18	27.14
48	4.03	34.20	50	4.05	34.20	27.17
72	4.03		75	4.05	34.22	27.19
97	3.91	34.25	100	3.90	34.25	27.21
145	3.55	34.57	150	3.55	34.58	27.51
193	3.37	34.66	200	3.40	34.67	27.61
290	3.71	34.83	300	3.75	34.84	27.70
399	3.96	34.91	400	3.95	34.91	27.74
591	3.55	34.89	600	3.55	34.89	27.76
778	3.45	34.90	800	3.45	34.90	27.78
972	3.41	34.90	1,000	3.45	34.90	27.78
1,458	3.32	34.89				

Station 5411; Apr. 28-29; latitude 46°06′ N., longitude 46°06′ W.; depth 1,723 m.; dynamic height 970.966

Observed values			Scaled values			
Depth, meters	Temperature, ° C.	Salinity ‰	Depth, meters	Temperature, ° C.	Salinity, ‰	σ_t
0	4.39	33.84	0	4.39	33.84	26.84
26	4.41	33.84	25	4.40	33.84	26.84
51	4.39	33.84	50	4.40	33.84	26.84
76	4.35		75	4.35	33.84	26.84
101	3.83	33.96	100	3.85	33.95	26.99
152	4.28	34.48	150	4.25	34.45	27.34
203	4.23	34.67	200	4.25	34.66	27.51
304	5.09	34.94	300	5.10	34.93	27.62
367	4.50	34.88	400	4.45	34.89	27.67
549	4.25	34.95	600	4.10	34.94	27.75
729	3.68	34.91	800	3.55	34.90	27.77
919	3.39	34.89	1,000	3.40	34.89	27.78
1,410	3.33	34.89				

Station 5412; Apr. 29; latitude 46°04′ N., longitude 46°39′ W.; depth 539 m.; dynamic height 970.966

Observed values			Scaled values			
Depth, meters	Temperature, ° C.	Salinity ‰	Depth, meters	Temperature, ° C.	Salinity, ‰	σ_t
0	3.47	33.47	0	3.47	33.47	26.64
25	3.48	33.44	25	3.48	33.44	26.62
50	3.49	33.46	50	3.49	33.46	26.63
75	2.69	33.86	75	2.69	33.86	27.02
99	4.70	34.40	100	4.75	34.41	27.26
149	6.54	34.77	150	6.55	34.77	27.32
199	4.64	34.63	200	4.65	34.63	27.44
298	4.87	34.87	300	4.90	34.87	27.61
383	4.24	34.90	400	4.20	34.90	27.71
470	4.04	34.92				

Station 5413; Apr. 29; latitude 46°03′ N., longitude 47°15′W.; depth 1,513 m.; dynamic height 970.910

Observed values			Scaled values			
Depth, meters	Temperature, ° C.	Salinity ‰	Depth, meters	Temperature, ° C.	Salinity, ‰	σ_t
0	1.46	33.52	0	1.46	33.52	26.85
26	1.75	33.57	25	1.75	33.57	26.87
51	1.93	33.64	50	1.95	33.63	26.90
77	1.74	34.04	75	1.75	33.99	27.20
102	1.81	34.26	100	1.80	34.24	27.40
154	3.37	34.56	150	3.35	34.54	27.50
205	3.37	34.66	200	3.40	34.65	27.59
307	4.22	34.90	300	4.20	34.89	27.70
388	4.10	34.90	400	4.05	34.90	27.72
577	3.67	34.89	600	3.65	34.89	27.75
763	3.52	34.89	800	3.50	34.89	27.77
962	3.47	34.89	1,000	3.50	34.89	27.77
1,342	3.34	34.885				

Station 5414; Apr. 29; latitude 46°01′ N., longitude 47°40′ W.; depth 745 m.; dynamic height 970.985

Observed values			Scaled values			
Depth, meters	Temperature, ° C.	Salinity, ‰	Depth, meters	Temperature, ° C.	Salinity, ‰	σ_t
0	−0.93	33.23	0	−0.93	33.23	26.74
26	−0.96	33.22	25	−0.95	33.22	26.73
52	−0.98	33.23	50	−1.00	33.23	26.74
77	−1.01	33.23	75	−1.00	33.23	26.74
103	0.67	33.77	100	0.55	33.70	27.05
154	0.62	34.04	150	0.65	34.02	27.30
206	1.71	34.30	200	1.65	34.27	27.44
309	2.52	34.58	300	2.50	34.56	27.60
421	2.94	34.70	400	2.90	34.68	27.66
620	3.50	34.84	600	3.45	34.83	27.72

Station 5415; Apr. 29; latitude 45°59.5′ N., longitude 47°58′ W.; depth 172 m.; dynamic height 971.038

Observed values			Scaled values			
Depth, meters	Temperature, ° C.	Salinity, ‰	Depth, meters	Temperature, ° C.	Salinity, ‰	σ_t
0	−1.21	32.93	0	−1.21	32.93	26.50
26	−1.34	32.96	25	−1.35	32.96	26.53
52	−1.42	33.00	50	−1.40	32.99	26.56
77	−1.53	33.13	75	−1.50	33.11	26.65
103	−0.74	33.38	100	−0.85	33.34	26.82
155	−0.08	33.52	150	−0.10	33.51	26.93

Station 5416; Apr. 29; latitude 46°00.5′ N., longitude 48°11′ W.; depth 121 m.; dynamic height 971.042

Observed values			Scaled values			
Depth, meters	Temperature, ° C.	Salinity, ‰	Depth, meters	Temperature, ° C.	Salinity, ‰	σ_t
0	−0.87	32.91	0	−0.87	32.91	26.47
25	−1.10	32.94	25	−1.10	32.94	26.51
50	−1.17	32.95	50	−1.17	32.95	26.52
75	−1.43	33.10	75	−1.43	33.10	26.64
100	−0.78	33.28	100	−0.78	33.28	26.77

Station 5417; Apr. 29; latitude 46°02′ N., longitude 48°33′ W.; depth 95 m.; dynamic height 971.048

Observed values			Scaled values			
Depth, meters	Temperature, ° C.	Salinity, ‰	Depth, meters	Temperature, ° C.	Salinity, ‰	σ_t
0	−0.28	32.82	0	−0.28	32.82	26.38
26	−0.54	32.84	25	−0.55	32.84	26.41
52	−0.68	32.84	50	−0.65	32.84	26.42
78	−1.15	33.15	75	−1.10	33.11	26.64

Station 5418; Apr. 29; latitude 45°50.5′ N., longitude 48°15′ W.; depth 121 m.; dynamic height 971.038

Observed values			Scaled values			
Depth, meters	Temperature, ° C.	Salinity, ‰	Depth, meters	Temperature, ° C.	Salinity, ‰	σ_t
0	−0.75	32.90	0	−0.75	32.90	26.46
25	−1.24	32.93	25	−1.24	32.93	26.50
50	−1.33	32.96	50	−1.33	32.96	26.53
76	−1.34	33.15	75	−1.35	33.14	26.68
101	−0.79	33.30	100	−0.80	33.30	26.78

Station 5419; Apr. 29; latitude 45°48′ N., longitude 48°08′ W.; depth 181 m.; dynamic height 971.024

Observed values			Scaled values			
Depth, meters	Temperature, ° C.	Salinity, ‰	Depth, meters	Temperature, ° C.	Salinity, ‰	σ_t
0	−1.13	33.03	0	−1.13	33.03	26.58
26	−1.44	32.97	25	−1.45	32.97	26.54
52	−1.39	32.99	50	−1.40	32.98	26.55
77	−0.47	33.44	75	−0.55	33.41	26.87
103	0.02	33.55	100	0.00	33.54	26.95
155	0.00	33.56	150	0.00	33.56	26.97

Table of Oceanographic Data—Continued

STATIONS OCCUPIED IN 1954—Continued

Station 5420; Apr. 29; latitude 45°42′ N., longitude 48°02′ W.; depth 690 m.; dynamic height 970.974

Observed values			Scaled values			
Depth, meters	Temperature, ° C.	Salinity °/oo	Depth, meters	Temperature, ° C.	Salinity, °/oo	σt
0	−0.66	33.10	0	−0.66	33.10	26.62
26	−1.08	33.25	25	−1.10	33.30	26.79
52	−1.10	33.25	50	−1.10	33.30	26.79
78	−1.09	33.50	75	−1.10	33.47	26.94
104	0.34	33.86	100	0.05	33.80	27.16
155	1.30	34.16	150	1.25	34.14	27.36
208	1.75	34.32	200	1.65	34.29	27.45
312	2.50	34.56	300	2.40	34.53	27.58
413	2.95	34.68	400	2.90	34.67	27.66
611	3.38	34.81	600	3.35	34.81	27.72

Station 5421; Apr. 29; latitude 45°37′ N., longitude 47°44′ W.; depth 1,420 m.; dynamic height 970.929

Observed values			Scaled values			
Depth, meters	Temperature, ° C.	Salinity °/oo	Depth, meters	Temperature, ° C.	Salinity, °/oo	σt
0	3.24	33.55	0	3.24	33.55	26.73
24	3.19	33.60	25	3.20	33.60	26.77
48	2.81	33.60	50	2.80	33.61	26.82
71	3.49	33.89	75	3.60	33.95	27.01
95	3.95	34.21	100	3.95	34.26	27.23
143	3.93	34.57	150	4.00	34.60	27.49
191	4.29	34.77	200	4.20	34.77	27.61
286	3.48	34.76	300	3.55	34.77	27.67
354	3.78	34.82	400	3.80	34.84	27.70
532	3.69	34.88	600	3.60	34.89	27.76
710	3.52	34.89	800	3.50	34.89	27.77
897	3.42	34.885	1,000	3.40	34.88	27.77
1,233	3.35					

Station 5422; Apr. 29–30; latitude 45°22.5′ N. longitude 47°17′ W.; depth 2,561 m.; dynamic height 970.949

Observed values			Scaled values			
Depth, meters	Temperature, ° C.	Salinity °/oo	Depth, meters	Temperature, ° C.	Salinity, °/oo	σt
0	3.79	33.64	0	3.79	33.64	26.75
25	3.63	33.66	25	3.63	33.66	26.78
50	3.08	33.63	50	3.08	33.63	26.80
75	3.21	33.73	75	3.21	33.73	26.87
101	3.49	34.07	100	3.50	34.07	27.12
150	3.83	34.44	150	3.85	34.44	27.38
201	4.02	34.62	200	4.00	34.62	27.51
302	4.00	34.79	300	4.00	34.78	27.63
389	3.92	34.85	400	3.90	34.86	27.71
581	3.75	34.91	600	3.75	34.91	27.76
772	3.52	34.90	800	3.50	34.90	27.78
968	3.48	34.90	1,000	3.50	34.90	27.78
1,474	3.35	34.91				

Station 5423; Apr. 30; latitude 45°22.5′ N., longitude 46°33′ W.; depth 3,017 m.; dynamic height 971.076

Observed values			Scaled values			
Depth, meters	Temperature, ° C.	Salinity °/oo	Depth, meters	Temperature, ° C.	Salinity, °/oo	σt
0	11.14	35.16	0	11.14	35.16	26.89
25	11.15	35.16	25	11.15	35.16	26.89
50	------	35.17	50	11.15	35.17	26.90
75	11.18	35.17	75	11.18	35.17	26.89
100	11.28	35.18	100	11.28	35.18	26.89
150	11.27	35.17	150	11.27	35.17	26.88
200	10.10	35.16	200	10.10	35.16	27.08
300	7.19	34.93	300	7.19	34.93	27.35
385	5.78	34.92	400	5.65	34.92	27.56
579	4.61	34.98	600	4.50	34.97	27.73
773	3.80	34.90	800	3.75	34.90	27.75
970	3.57	34.90	1,000	3.55	34.90	27.77
1,475	3.29	34.89				

Station 5424; Apr. 30; latitude 45°22.5′ N., longitude 45°57′ W.; depth 3,475 m.; dynamic height 971.022

Observed values			Scaled values			
Depth, meters	Temperature, ° C.	Salinity, °/oo	Depth, meters	Temperature, ° C.	Salinity, °/oo	σt
0	5.73	33.92	0	5.73	33.92	26.75
24	6.29	34.01	25	6.35	34.02	26.76
47	8.04	34 36	50	8.15	34.38	26.78
71	8.68	34.52	75	8.80	34.55	26.82
95	9.22	34.66	100	9.15	34.65	26.84
141	7.06	34.58	150	6.55	34.56	27.15
188	5.15	34.48	200	5.05	34.50	27.29
283	4.97	34.75	300	5.10	34.81	27.54
345	5.49	34.97	400	5.25	34.98	27.65
522	4.74	34.98	600	4.50	34.97	27.73
704	4.17	34.96	800	3.95	34.95	27.77
900	3.81	34.93	1,000	3.75	34.93	27.77
1,422	3.46	34.93				

Station 5425; Apr. 30; latitude 45°22′ N., longitude 45°15′ W.; depth 4,207 m.; dynamic height 970.935

Observed values			Scaled values			
Depth, meters	Temperature, ° C.	Salinity, °/oo	Depth, meters	Temperature, ° C.	Salinity, °/oo	σt
0	3.87	33.92	0	3.87	33.92	26.96
25	3.89	33.99	25	3.89	33.99	27.01
50	3.99	34.04	50	3.99	34.04	27.04
74	4.07	34.08	75	4.10	34.08	27.06
99	4.04	34.10	100	4.05	34.10	27.09
148	3.06	34.30	150	3.05	34.31	27.35
197	3.46	34.52	200	3.50	34.53	27.48
296	3.96	34.79	300	3.95	34.80	27.65
393	3.84	34.86	400	3.85	34.86	27.71
587	3.59	34.88	600	3.60	34.88	27.75
779	3.43	34.89	800	3.40	34.89	27.78
977	3.35	34.89	1,000	3.35	34.89	27.78
1,477	3.29	34.89				

Station 5426; Apr. 30; latitude 44°47.5′ N., longitude 45°12′ W.; depth 4,207 m.; dynamic height 970.928

Observed values			Scaled values			
Depth, meters	Temperature, ° C.	Salinity, °/oo	Depth, meters	Temperature, ° C.	Salinity, °/oo	σt
0	4.45	34.02	0	4.45	34.02	26.98
26	4.34	34.04	25	4.35	34.04	27.00
53	4.29	34.06	50	4.30	34.06	27.03
79	4.06	34.14	75	4.10	34.13	27.10
106	3.66	34.23	100	3.70	34.21	27.21
158	3.41	34.47	150	3.45	34.44	27.41
211	3.40	34.57	200	3.40	34.55	27.51
317	3.84	34.80	300	3.75	34.77	27.65
402	4.04	34.89	400	4.05	34.89	27.71
599	3.83	34.90	600	3.85	34.90	27.74
792	3 48	34.90	800	3.50	34.90	27.78
993	3.45	34.90	1,000	3.45	34.90	27.78
1,498	3.28	34.885				

Station 5427; Apr. 30; latitude 44°13′ N., longitude 45°08′ W.; depth 4,207 m.; dynamic height 971.030

Observed values			Scaled values			
Depth, meters	Temperature, ° C.	Salinity, °/oo	Depth, meters	Temperature, ° C.	Salinity, °/oo	σt
0	3.06	33.33	0	3.06	33.33	26.57
22	3.07	33.32	25	3.10	33.33	26.56
43	3.10	33.36	50	3.05	33.36	26.59
65	2.80	33.37	75	2.50	33.38	26.65
87	2.13	33.40	100	2.45	33.54	26.79
131	------	34.04	150	4.35	34.24	27.16
174	5.04	34.46	200	4.50	34.47	27.34
261	3.29	34.50	300	3.65	34.58	27.50
279	3.46	34.53	400	4.50	34.86	27.64
442	4.80	34.96	600	3.80	34.89	27.74
622	3.76	34.885	800	3.65	34.91	27.77
791	3.66	34.91	1,000	3.50	34.90	27.78
1,234	3.29	34.885				

Table of Oceanographic Data—Continued

STATIONS OCCUPIED IN 1954—Continued

Station 5428; May 1; latitude 44°19′ N., longitude 45°42′ W.; depth 4,024 m.; dynamic height 971.237

Observed values			Scaled values			
Depth, meters	Temperature, ° C.	Salinity °/oo	Depth, meters	Temperature, ° C.	Salinity, °/oo	σt
0	15.41	36.05	0	15.41	36.05	26.70
28	15.42	36.04	25	15.40	36.04	26.70
55	15.41	36.04	50	15.40	36.04	26.70
83	15.39	36.04	75	15.40	36.04	26.70
111	15.31	36.02	100	15.35	36.03	26.70
167	14.62	35.87	150	14.90	35.94	26.74
222	12.02	35.43	200	13.20	35.62	26.85
333	8.60	34.90	300	9.30	34.99	27.08
423	8.26	35.10	400	8.35	35.05	27.28
630	5.14	34.92	600	5.55	34.94	27.58
837	4.10	34.89	800	4.15	34.89	27.70
1,049	3.86	34.93	1,000	3.90	34.93	27.76
1,580	3.47	34.90				

Station 5429; May 1; latitude 44°16′ N., longitude 46°18′W.; depth 3,896 m.; dynamic height 971.280

Observed values			Scaled values			
Depth, meters	Temperature, ° C.	Salinity °/oo	Depth, meters	Temperature, ° C.	Salinity, °/oo	σt
0	14.72	35.87	0	14.72	35.87	26.72
28	14.73	35.87	25	14.72	35.87	26.72
55	14.75	35.89	50	14.75	35.88	26.72
83	14.74	35.885	75	14.75	35.89	26.72
111	14.72	35.87	100	14.70	35.88	26.73
167	14.47	35.82	150	14.60	35.85	26.73
222	12.27	35.41	200	13.15	35.58	26.83
333	10.96	35.29	300	11.35	35.32	26.98
426	*8.80	35.03	400	9.40	35.09	27.14
640	5.62	34.96	600	6.05	34.97	27.55
855	4.50	34.95	800	4.65	34.95	27.70
1,074	4.20	34.96	1,000	4.30	34.96	27.74
1,630	3.59	34.92				

Station 5430; May 1; latitude 44°26′ N., longitude 47°19′ W.; depth 3,695 m.; dynamic height 971.115

Observed values			Scaled values			
Depth, meters	Temperature, ° C.	Salinity °/oo	Depth, meters	Temperature, ° C.	Salinity, °/oo	σt
0	13.04	35.52	0	13.04	35.52	26.80
28	13.10	35.54	25	13.10	35.54	26.81
54	12.96	35.48	50	12.95	35.49	26.80
82	12.71	35.45	75	12.80	35.46	26.81
109	10.22	34.88	100	11.40	35.17	26.86
164	7.96	34.62	150	8.40	34.66	26.97
219	9.05	34.95	200	8.65	34.86	27.08
328	8.15	35.10	300	8.55	35.09	27.28
430	6.26	35.00	400	6.75	35.02	27.49
638	4.87	34.99	600	5.10	34.99	27.67
843	3.73	34.88	800	3.90	34.90	27.74
1,051	3.86	34.94	1,000	3.85	34.93	27.76
1,567	3.43	34.90				

Station 5431; May 1; latitude 44°37.5′ N., longitude 48°02′ W., depth 3,457 m.; dynamic height 970.974

Observed values			Scaled values			
Depth, meters	Temperature, ° C.	Salinity °/oo	Depth, meters	Temperature, ° C.	Salinity, °/oo	σt
0	2.80	33.18	0	2.80	33.18	26.48
25	2.64	33.20	25	2.64	33.20	26.51
49	1.58	33.24	50	1.55	33.24	26.62
74	1.20	33.60	75	1.25	33.61	26.93
99	2.70	34.14	100	2.75	34.15	27.25
148	5.77	34.73	150	5.80	34.73	27.38
197	3.75	34.52	200	3.75	34.52	27.45
296	3.98	34.77	300	4.00	24.78	27.63
400	4.68	34.96	400	4.70	34.96	27.70
594	4.18	34.94	600	4.20	34.94	27.74
783	3.86	34.93	800	3.90	34.93	27.76
978	3.61	34.91	1,000	3.60	34.91	27.78
1,466	3.44	34.90				

Station 5432; May 1; latitude 44°42.5′ N., longitude 48°34′ W.; depth 2,065 m.; dynamic height 970.928

Observed values			Scaled values			
Depth, meters	Temperature, ° C.	Salinity, °/oo	Depth, meters	Temperature, ° C.	Salinity, °/oo	σt
0	−0.24	33.17	0	−0.24	33.17	26.66
26	−0.29	33.18	25	−0.30	33.18	26.67
52	0.03	33.42	50	0.00	33.40	26.84
78	0.69	33.84	75	0.60	33.79	27.11
104	1.17	34.10	100	1.10	34.06	27.31
155	3.11	34.50	150	2.95	34.46	27.48
207	4.18	34.73	200	4.10	34.71	25.57
311	4.22	34.87	300	4.20	34.86	27.68
403	4.10	34.90	400	4.10	34.90	27.72
602	3.69	34.89	600	3.70	34.89	27.75
798	3.59	34.90	800	3.60	34.90	27.77
999	3.42	34.89	1,000	3.40	34.89	27.78
1,500	3.34	34.89				

Station 5433; May 2; latitude 44°45.5′ N., longitude 48°50′ W.; depth 1476 m.; dynamic height 970.957

Observed values			Scaled values			
Depth, meters	Temperature, ° C.	Salinity, °/oo	Depth, meters	Temperature, ° C.	Salinity, °/oo	σt
0	−0.72	33.20	0	−0.72	33.20	26.71
25	−0.78	33.21	25	−0.78	33.21	26.72
50	−0.92	33.22	50	−0.92	33.22	26.73
75	−0.38	33.64	75	−0.38	33.64	27.04
100	0.48	33.92	100	0.48	33.92	27.23
150	1.60	34.21	150	1.60	34.21	27.39
201	2.52	34.40	200	2.50	34.40	27.47
301	4.23	34.76	300	4.20	34.76	27.60
374	3.62	34.77	400	3.60	34.78	27.67
564	3.67	34.88	600	3.65	34.89	27.75
756	3.60	34.90	800	3.55	34.90	27.77
969	3.34	34.89	1,000	3.40	34.89	27.78

Station 5434; May 2; latitude 44°48′ N., longitude 49°04′ W.; depth 622 m.; dynamic height 971.064

Observed values			Scaled values			
Depth, meters	Temperature, ° C.	Salinity, °/oo	Depth, meters	Temperature, ° C.	Salinity, °/oo	σt
0	−0.97	32.96	0	−0.97	32.96	26.52
25	−0.96	32.96	25	−0.96	32.96	26.52
51	−0.91	32.97	50	−0.90	32.97	26.53
76	−1.09	33.19	75	−1.10	33.19	26.71
102	−0.86	33.28	100	−0.90	33.27	26.77
152	0.23	33.66	150	0.15	33.66	27.04
203	0.46	33.72	200	0.45	33.72	27.07
305	1.94	34.37	300	1.85	34.35	27.48
402	2.97	34.69	400	2.95	34.68	27.65
591	3.24	34.74	600	3.30	34.74	27.67

Station 5435; May 2; latitude 44°48.5′ N., longitude 49°10′ W.; depth 70 m.; dynamic height 971.108

Observed values			Scaled values			
Depth, meters	Temperature, ° C.	Salinity, °/oo	Depth, meters	Temperature, ° C.	Salinity, °/oo	σt
0	−0.73	32.96	0	−0.73	32.96	26.51
23	−0.74	32.97	25	−0.75	32.97	26.52
46	−0.94	33.06	50	−1.00	33.07	26.61
69	−1.03	33.12				

Station 5436; May 2; latitude 44°46.5′ N., longitude 49°24′ W.; depth 66 m.; dynamic height 971.115

Observed values			Scaled values			
Depth, meters	Temperature, ° C.	Salinity, °/oo	Depth, meters	Temperature, ° C.	Salinity, °/oo	σt
0	−0.02	32.85	0	−0.02	32.85	26.40
29	0.07	32.88	25	0.05	32.88	26.42
58	−0.56	32.98	50	−0.35	32.95	26.48

STATIONS OCCUPIED IN 1954—Continued

Station 5437; May 2; latitude 44°14′ N., longitude 49°21′ W.; depth 57 m.; dynamic height 971.078

Observed values			Scaled values			
Depth, meters	Temperature, ° C.	Salinity ‰	Depth, meters	Temperature, ° C.	Salinity, ‰	σ_t
0	−0.37	32.95	0	−0.37	32.95	26.48
27	−0.38	32.96	25	−0.35	32.96	26.49
46	−0.40	32.96	(50)	−0.40	32.96	26.50

Station 5438; May 2; latitude 44°10.5′ N., longitude 49°04′ W.; depth 93 m.; dynamic height 971.077

Observed values			Scaled values			
Depth, meters	Temperature, ° C.	Salinity ‰	Depth, meters	Temperature, ° C.	Salinity, ‰	σ_t
0	−0.65	32.95	0	−0.65	32.95	26.50
25	−0.71	32.96	25	−0.71	32.96	26.51
50	−0.71	32.96	50	−0.71	32.96	26.51
75	−0.75	32.95	75	−0.75	32.95	26.50

Station 5439; May 2; latitude 44°09′ N., longitude 48°56′ W.; depth 201 m.; dynamic height 971.066

Observed values			Scaled values			
Depth, meters	Temperature, ° C.	Salinity ‰	Depth, meters	Temperature, ° C.	Salinity, ‰	σ_t
0	−0.85	32.93	0	−0.85	32.93	26.49
24	−0.94	32.95	25	−0.90	32.95	26.51
48	−0.67	33.14	50	−0.70	33.14	26.66
73	−0.97	33.18	75	−0.95	33.18	26.70
97	−0.95	33.20	100	−0.90	33.21	26.73
146	0.74	33.78	150	0.80	33.81	27.12
194	1.10	33.95	(200)	1.15	33.97	27.23

Station 5440; May 2; latitude 44°06.5′ N., longitude 48°49′ W.; depth 615 m.; dynamic height 971.037

Observed values			Scaled values			
Depth, meters	Temperature, ° C.	Salinity ‰	Depth, meters	Temperature, ° C.	Salinity, ‰	σ_t
0	−0.86	33.04	0	−0.86	33.04	26.58
26	−0.89	33.04	25	−0.85	33.04	26.58
53	−1.14	33.19	50	−1.10	33.18	26.70
79	−0.65	33.40	75	−0.70	33.37	26.84
106	−0.26	33.49	100	−0.35	33.47	26.91
157	0.81	33.82	150	0.70	33.77	27.10
210	1.36	34.06	200	1.30	34.02	27.26
316	2.39	34.48	300	2.25	34.42	27.51
418	2.96	34.67	400	2.90	34.64	27.63
616	3.43	34.80	600	3.40	34.79	27.70

Station 5441; May 2; latitude 44°03.5′ N., longitude 48°40′ W.; depth 1,792 m.; dynamic height 970.965

Observed values			Scaled values			
Depth, meters	Temperature, ° C.	Salinity ‰	Depth, meters	Temperature, ° C.	Salinity, ‰	σ_t
0	−0.63	33.16	0	−0.63	33.16	26.66
26	−0.89	33.20	25	−0.85	33.20	26.71
51	−0.73	33.29	50	−0.70	33.29	26.77
76	−0.48	33.57	75	−0.50	33.57	27.00
101	0.31	33.82	100	0.30	33.81	27.15
153	1.71	34.19	150	1.70	34.17	27.35
204	2.32	34.46	200	2.30	34.44	27.52
305	3.06	34.66	300	3.05	34.65	27.62
413	3.29	34.75	400	3.25	34.74	27.67
616	3.66	34.87	600	3.65	34.86	27.73
819	3.58	34.88	800	3.60	34.88	27.75
1,025	3.46	34.87	1,000	3.45	34.87	27.76
1,543	3.39	34.88				

Station 5442; May 2; latitude 43°56′ N., longitude 48°23′ W.; depth 3,237 m.; dynamic height 970.950

Observed values			Scaled values			
Depth, meters	Temperature, ° C.	Salinity, ‰	Depth, meters	Temperature, ° C.	Salinity, ‰	σ_t
0	1.79	33.09	0	1.79	33.09	26.47
27	1.79	33.12	25	1.80	33.12	26.50
52	1.11	33.18	50	1.15	33.17	26.59
79	1.35	33.75	75	1.30	33.67	26.98
105	2.42	34.19	100	2.20	34.11	27.27
158	3.66	34.58	150	3.55	34.54	27.48
210	3.83	34.68	200	3.80	34.66	27.56
315	4.32	34.86	300	4.30	34.84	27.65
382	4.08	34.89	400	4.05	34.89	27.71
578	3.69	34.89	600	3.65	34.89	27.75
779	3.50	34.89	800	3.50	34.89	27.77
984	3.38	34.88	1,000	3.40	34.88	27.77
1,515	3.32	34.88				

Station 5443; May 2; latitude 43°46′ N., longitude 48°04′ W.; depth 3,475 m.; dynamic height 971.001

Observed values			Scaled values			
Depth, meters	Temperature, ° C.	Salinity, ‰	Depth, meters	Temperature, ° C.	Salinity, ‰	σ_t
0	5.71	33.67	0	5.71	33.67	26.56
24	6.17	33.82	25	6.20	33.83	26.62
47	6.79	34.26	50	6.80	34.26	26.89
71	4.99	34.17	75	5.00	34.19	27.05
95	5.98	34.41	100	6.25	34.46	27.12
141	8.09	34.94	150	7.85	34.93	27.26
188	6.56	34.83	200	6.25	34.82	27.40
283	4.75	34.78	300	4.65	34.80	27.58
285	4.86	34.82	400	4.15	34.81	27.64
420	4.13	34.82	600	4.30	34.90	27.69
551	4.33	34.94	800	4.00	34.94	27.76
708	4.13	34.94	1,000	3.75	34.93	27.77
1,130	3.53	34.90				

Station 5444; May 3; latitude 43°37.5′ N., longitude 47°37′ W.; depth 3,749 m.; dynamic height 971.008

Observed values			Scaled values			
Depth, meters	Temperature, ° C.	Salinity, ‰	Depth, meters	Temperature, ° C.	Salinity, ‰	σ_t
0	2.68	33.26	0	2.68	33.26	26.54
25	2.43	33.24	25	2.43	33.24	26.55
48	1.20	33.23	50	1.25	33.25	26.64
73	6.12	34.14	75	6.35	34.19	26.89
96	8.10	34.74	100	8.00	34.74	27.09
145	6.35		150	6.30	34.69	27.29
194	6.01	34.76	200	6.00	34.76	27.39
290	5.26	34.84	300	5.15	34.85	27.56
332	4.72	34.87	400	4.40	34.84	27.63
448	4.32	34.825	600	4.20	34.95	27.75
530	4.34	34.97	800	3.85	34.91	27.75
682	4.02	34.92	1,000	3.65	34.89	27.75
1,098	3.52	34.88				

Station 5445; May 3; latitude 43°27′ N., longitude 46°50′ W.; depth 4,024 m.; dynamic height 971.323

Observed values			Scaled values			
Depth, meters	Temperature, ° C.	Salinity, ‰	Depth, meters	Temperature, ° C.	Salinity, ‰	σ_t
0	16.44	36.21	0	16.44	36.21	26.60
27	16.39	36.20	25	16.40	36.20	26.60
53	16.35	36.19	50	16.35	36.19	26.60
80	16.30	36.175	75	16.30	36.18	26.60
106	15.16	35.86	100	15.40	35.94	26.62
160	13.85	35.56	150	13.90	35.60	26.69
213	13.74	35.57	200	13.80	35.58	26.69
319	12.66	35.61	300	13.00	35.64	26.90
311	12.85	35.65	400	10.60	35.31	27.11
448	9.24	35.20	600	6.20	35.00	27.55
572	6.59	35.01	800	4.85	34.97	27.69
718	5.22	34.98	1,000	4.25	34.95	27.74
1,086	3.99	34.94				

Station 5446; May 3; latitude 43°24.5′ N., longitude 46°01′ W.; depth 4,481 m.; dynamic height 971.452

Observed values			Scaled values			
Depth, meters	Temperature, ° C.	Salinity °/oo	Depth, meters	Temperature, ° C.	Salinity, °/oo	σ_t
0	17.06	36.34	0	17.06	36.34	26.54
28	17.00	36.33	25	17.00	36.33	26.55
55	16.99	36.33	50	17.00	36.33	26.55
83	16.99	36.33	75	17.00	36.33	26.55
110	16.97	36.33	100	17.00	36.33	26.55
166	16.94	36.305	150	16.95	36.32	26.55
221	16.05	36.10	200	16.40	36.18	26.58
331	*14.50	35.78	300	14.90	35.94	26.74
291	*15.02	36.07	400	13.25	35.91	27.06
429	------	35.90	600	9.65	35.33	27.28
563	10.36	35.44	800	6.30	35.09	27.60
692	7.92	35.15	1,000	4.70	35.04	27.76
995	4.65	35.04				

Station 5447; May 3; latitude 43°11.5′ N., longitude 45°24′ W.; depth 4,663 m.; dynamic height 971.611

Observed values			Scaled values			
Depth, meters	Temperature, ° C.	Salinity °/oo	Depth, meters	Temperature, ° C.	Salinity, °/oo	σ_t
0	17.09	36.35	0	17.09	36.35	26.54
28	16.92	36.31	25	16.95	36.32	26.55
55	16.91	36.32	50	16.90	36.32	26.57
83	16.91	36.31	75	16.90	36.31	26.56
111	16.84	36.30	100	16.85	36.30	26.56
167	16.58	36.25	150	16.65	36.27	26.59
222	16.46	36.23	200	16.50	36.24	26.60
333	16.35	36.22	300	16.40	36.22	26.61
417	*14.79	35.82	400	15.15	35.91	26.66
628	10.57	35.35	600	11.15	35.39	27.07
839	7.51	35.12	800	7.95	35.15	27.42
1,051	5.23	35.06	1,000	5.70	35.07	27.67
1,589	3.98	34.97				

Station 5448; May 3; latitude 42°43′ N., longitude 45°43′ W.; depth 3,572 m.; dynamic height 971.688

Observed values			Scaled values			
Depth, meters	Temperature, ° C.	Salinity °/oo	Depth, meters	Temperature, ° C.	Salinity, °/oo	σ_t
0	16.79	36.28	0	16.79	36.28	26.56
24	16.79	36.28	25	16.80	36.28	26.56
49	16.80	36.27	50	16.80	36.28	26.56
73	16.82	36.275	75	16.80	36.28	26.56
97	16.80	36.27	100	16.80	36.28	26.56
145	16.83	36.285	150	16.80	36.27	26.55
194	16.82	36.27	200	16.80	36.27	26.55
291	16.89	36.30	300	16.90	36.30	26.55
341	16.63	36.24	400	16.10	36.15	26.62
524	14.60	35.90	600	13.10	35.69	26.93
715	10.76	35.37	800	9.15	35.24	27.30
914	7.39	35.14	1,000	6.40	35.09	27.59
1,449	4.40	34.98				

Station 5449; May 4; latitude 42°26.5′ N., longitude 46°12′ W.; depth 4,390 m.; dynamic height 971.651

Observed values			Scaled values			
Depth, meters	Temperature, ° C.	Salinity °/oo	Depth, meters	Temperature, ° C.	Salinity, °/oo	σ_t
0	16.85	36.28	0	16.85	36.28	26.55
25	16.85	36.28	25	16.85	36.28	26.55
49	16.85	36.28	50	16.85	36.28	26.55
74	16.87	36.28	75	16.85	36.28	26.55
99	16.86	36.28	100	16.85	36.28	26.55
147	16.89	36.28	150	16.90	36.28	26.54
196	16.87	36.28	200	16.90	36.28	26.54
295	16.58	36.215	300	16.55	36.20	26.56
340	16.26	36.13	400	15.50	36.00	26.65
552	13.01	35.66	600	12.10	35.55	27.02
790	8.55	35.13	800	8.35	35.12	27.33
993	5.99	35.08	1,000	5.90	35.08	27.65
1,512	4.17	34.96				

Station 5450; May 4; latitude 42°49′ N., longitude 46°38′ W.; depth 4,390 m.; dynamic height 971.560

Observed values			Scaled values			
Depth, meters	Temperature, ° C.	Salinity, °/oo	Depth, meters	Temperature, ° C.	Salinity, °/oo	σ_t
0	17.02	36.32	0	17.02	36.32	26.54
25	17.02	36.31	25	17.02	36.31	26.53
51	17.00	36.305	50	17.00	36.31	26.53
76	16.98	36.29	75	17.00	36.30	26.53
102	16.94	36.295	100	16.95	36.29	26.54
151	16.90	36.29	150	16.90	36.29	26.55
202	16.87	36.28	200	16.85	36.28	26.55
304	16.23	36.16	300	16.30	36.17	26.59
457	13.91	35.80	400	15.05	35.96	26.72
677	8.42	35.08	600	10.35	35.32	27.16
892	5.86	35.05	800	6.70	35.06	27.53
1,113	4.65	35.00	1,000	5.15	35.03	27.70
1,668	3.77	34.93				

Station 5451; May 4; latitude 43°01.5′ N., longitude 47°02′ W.; depth 3,841 m.; dynamic height 971.336

Observed values			Scaled values			
Depth, meters	Temperature, ° C.	Salinity, °/oo	Depth, meters	Temperature, ° C.	Salinity, °/oo	σ_t
0	15.86	36.08	0	15.86	36.08	26.62
26	15.86	36.08	25	15.85	36.08	26.62
51	15.86	36.08	50	15.85	36.08	26.62
77	15.83	36.065	75	15.85	36.07	26.62
103	15.81	36.06	100	15.80	36.06	26.62
153	15.54	35.955	150	15.55	35.97	26.61
205	13.91	35.59	200	14.05	35.63	26.68
308	13.62	35.70	300	13.70	35.69	26.80
485	7.89	34.975	400	10.70	35.32	27.10
730	5.04	34.94	600	5.70	34.95	27.57
975	4.59	35.00	800	4.90	34.95	27.67
1,214	4.09	34.99	1,000	4.55	35.00	27.75
1,800	3.54	34.925				

Station 5452; May 4; latitude 43°06′ N., longitude 47°57′ W.; depth 3,365 m.; dynamic height 971.009

Observed values			Scaled values			
Depth, meters	Temperature, ° C.	Salinity, °/oo	Depth, meters	Temperature, ° C.	Salinity, °/oo	σ_t
0	1.34	33.17	0	1.34	33.17	26.58
25	0.46	33.12	25	0.46	33.12	26.59
50	2.73	33.45	50	2.73	33.45	26.70
76	1.37	33.58	75	1.35	33.58	26.90
101	8.32	34.74	100	8.30	34.74	27.04
150	1.19	33.96	150	1.20	33.96	27.22
200	2.11	34.28	200	2.10	34.28	27.40
301	5.10	34.86	300	5.10	34.86	27.57
378	4.24	34.78	400	4.25	34.79	27.61
565	4.46	34.975	600	4.40	34.97	27.74
752	3.97	34.93	800	3.85	34.92	27.76
943	3.68	34.89	1,000	3.65	34.90	27.76
1,428	3.46	34.89				

Station 5453; May 4; latitude 43°12′ N., longitude 48°50′ W.; depth 2,360 m.; dynamic height 970.947

Observed values			Scaled values			
Depth, meters	Temperature, ° C.	Salinity, °/oo	Depth, meters	Temperature, ° C.	Salinity, °/oo	σ_t
0	1.88	33.10	0	1.88	33.10	26.48
26	1.61	33.11	25	1.65	33.11	26.50
51	0.82	33.38	50	0.85	33.37	26.77
77	1.55	33.96	75	1.55	33.91	27.15
103	1.69	34.16	100	1.65	34.14	27.33
153	2.49	34.45	150	2.50	34.43	27.49
205	2.71	34.57	200	2.65	34.56	27.59
308	4.22	34.80	300	4.20	34.78	27.61
413	4.26	34.92	400	4.25	34.91	27.71
613	3.96	34.91	600	4.00	34.91	27.74
808	3.58	34.87	800	3.60	34.87	27.75
1,011	3.48	34.895	1,000	3.50	34.89	27.77
1,520	3.39	34.90				

Table of Oceanographic Data—Continued

STATIONS OCCUPIED IN 1954—Continued

Station 5454; May 5; latitude 42°50.5′ N., longitude 49°02′ W.; depth 2,260 m.; dynamic height 970.968

Observed values			Scaled values			
Depth, meters	Temperature, ° C.	Salinity, °/oo	Depth, meters	Temperature, ° C.	Salinity, °/oo	σ_t
0	3.40	33.07	0	3.40	33.07	26.33
25	3.54	33.39	25	3.54	33.39	26.57
50	------	34.81	50	9.65	34.81	26.88
75	2.93	33.98	75	2.93	33.98	27.09
100	1.00	33.87	100	1.00	33.87	27.16
149	6.57	34.80	150	6.55	34.80	27.34
199	6.13	34.93	200	6.10	34.93	27.50
299	4.20	34.81	300	4.15	34.81	27.64
362	3.75	34.81	400	3.75	34.82	27.69
538	3.72	34.88	600	3.70	34.88	27.74
712	3.58	34.88	(800)	3.55	34.88	27.75
903	3.49	-------	(1,000)	3.50	34.88	27.76
1,400	3.39	-------				

Station 5455; May 5; latitude 42°25′ N., longitude 48°24′ W.; depth 3,365 m.; dynamic height 971.094

Observed values			Scaled values			
Depth, meters	Temperature, ° C.	Salinity, °/oo	Depth, meters	Temperature, ° C.	Salinity, °/oo	σ_t
0	5.46	33.34	0	5.46	33.34	26.33
25	5.46	33.44	25	5.46	33.44	26.41
51	8.09	34.19	50	7.90	34.17	26.66
76	11.40	35.11	75	11.40	35.11	26.81
103	7.74	34.58	100	8.25	34.64	26.97
153	4.13	34.17	150	4.25	34.19	27.13
204	5.98	34.56	200	5.90	34.55	27.23
307	1.78	34.16	300	1.90	34.18	27.34
403	5.14	34.73	400	5.10	34.72	27.47
605	3.44	34.76	600	3.45	34.76	27.67
808	4.35	34.97	800	4.35	34.97	27.75
1,011	4.00	34.95	1,000	4.00	34.95	27.77
1,519	3.58	34.93				

Station 5456; May 5; latitude 41°59′ N., longitude 47°51′ W.; depth 3,749 m.; dynamic height 970.990

Observed values			Scaled values			
Depth, meters	Temperature, ° C.	Salinity, °/oo	Depth, meters	Temperature, ° C.	Salinity, °/oo	σ_t
0	5.47	33.24	0	5.47	33.24	26.24
25	4.78	33.26	25	4.78	33.26	26.34
50	3.65	33.48	50	3.65	33.48	26.63
75	2.73	33.88	75	2.73	33.88	27.03
99	2.84	34.16	100	2.85	34.16	27.25
149	4.09	34.54	150	4.05	34.54	27.43
199	3.83	34.58	200	3.85	34.58	27.48
298	4.58	34.82	300	4.60	34.82	27.60
400	4.80	34.94	400	4.80	34.94	27.67
595	3.83	34.88	600	3.85	34.88	27.72
788	3.73	34.90	800	3.75	34.90	27.75
985	3.83	34.93	1,000	3.80	34.93	27.77
1,479	3.59	34.93				

Station 5457; May 5; latitude 41°35′ N., longitude 47°16′ W.; depth 4,024 m.; dynamic height 971.103

Observed values			Scaled values			
Depth, meters	Temperature, ° C.	Salinity, °/oo	Depth, meters	Temperature, ° C.	Salinity, °/oo	σ_t
0	6.32	33.30	0	6.32	33.30	26.19
27	4.21	33.30	25	4.35	33.30	26.41
53	9.03	34.23	50	8.35	34.13	26.55
80	11.49	35.00	75	11.15	34.85	26.65
106	12.31	35.33	100	12.20	35.27	26.78
160	7.09	34.43	150	7.90	34.58	26.98
213	9.80	35.21	200	9.20	35.02	27.12
319	5.56	34.75	300	6.30	34.82	27.39
435	3.23	34.62	400	3.70	34.64	27.55
621	4.51	34.96	600	4.45	34.93	27.70
804	4.23	34.97	800	4.20	34.97	27.77
994	4.02	34.96	1,000	4.00	34.96	27.78
1,466	3.64	34.94				

Station 5458; May 6; latitude 40°58′ N., longitude 48°21′ W.; depth 3,475 m.; dynamic height 971.001

Observed values			Scaled values			
Depth, meters	Temperature, ° C.	Salinity, °/oo	Depth, meters	Temperature, ° C.	Salinity, °/oo	σ_t
0	3.11	33.07	0	3.11	33.07	26.36
23	2.10	33.14	25	2.05	33.16	26.52
47	1.89	33.54	50	1.90	33.58	26.87
70	3.21	33.85	75	3.60	33.91	26.98
93	4.91	34.14	100	4.75	34.15	27.05
140	3.38	34.26	150	3.25	34.30	27.32
187	3.17	34.52	200	3.25	34.55	27.52
280	4.21	34.70	300	4.50	34.75	27.55
405	5.69	35.04	400	5.65	35.03	27.64
609	4.65	34.99	600	4.70	34.99	27.72
814	3.96	34.91	800	4.00	34.91	27.74
1,012	3.70	34.91	1,000	3.70	34.91	27.77
1,542	3.43	34.90				

Station 5459; May 6; latitude 41°25.5′ N., longitude 48°55′ W., depth 3,146 m.; dynamic height 971.151

Observed values			Scaled values			
Depth, meters	Temperature, ° C.	Salinity, °/oo	Depth, meters	Temperature, ° C.	Salinity, °/oo	σ_t
0	5.52	33.32	0	5.52	33.32	26.30
24	5.36	33.36	25	5.35	33.37	26.36
48	7.11	33.94	50	7.40	34.03	26.62
72	11.92	35.12	75	11.90	35.12	26.72
96	11.64	35.12	100	11.20	35.10	26.84
144	6.54	34.37	150	6.60	34.40	27.02
193	8.60	34.82	200	8.50	34.81	27.07
289	6.37	34.66	300	6.05	34.62	27.27
338	4.80	34.50	400	5.05	34.66	27.42
502	5.47	34.91	600	5.40	35.02	27.67
662	5.23	35.04	800	4.30	34.94	27.72
835	4.16	34.93	1,000	3.95	34.93	27.75
1,283	3.73	34.93				

Station 5460; May 6; latitude 41°52′ N., longitude 49°25′ W.; depth 3,109 m.; dynamic height 971.251

Observed values			Scaled values			
Depth, meters	Temperature, ° C.	Salinity, °/oo	Depth, meters	Temperature, ° C.	Salinity, °/oo	σ_t
0	14.21	35.69	0	14.21	35.69	26.69
26	14.20	35.72	25	14.20	35.72	26.72
50	14.21	35.72	50	14.20	35.72	26.72
76	14.21	35.73	75	14.20	35.72	26.72
100	14.20	35.72	100	14.20	35.72	26.72
152	14.25	35.73	150	14.25	35.73	26.71
202	14.25	35.73	200	14.25	35.73	26.71
302	11.67	35.51	300	11.80	35.52	27.05
381	9.81	35.26	400	9.35	35.21	27.24
564	6.24	35.03	600	5.85	35.02	27.61
743	4.83	35.00	800	4.60	34.99	27.73
941	4.24	34.96	1,000	4.20	34.95	27.75
1,452	3.61	34.91				

Station 5461; May 6; latitude 41°00.5′ N., longitude 50°12′ W.; depth 3,530 m.; dynamic height 971.741

Observed values			Scaled values			
Depth, meters	Temperature, ° C.	Salinity, °/oo	Depth, meters	Temperature, ° C.	Salinity, °/oo	σ_t
0	19.21	36.48	0	19.21	36.48	26.12
25	19.23	36.53	25	19.23	36.53	26.15
49	18.53	36.46	50	18.50	36.46	26.28
74	18.21	36.45	75	18.20	36.45	26.35
99	18.17	36.46	100	18.15	36.46	26.37
149	18.04	36.45	150	18.05	36.45	26.39
198	17.98	36.45	200	17.95	36.45	26.42
297	17.62	36.42	300	17.55	36.41	26.48
389	16.12	36.13	400	15.95	36.11	26.63
592	13.23	35.70	600	13.05	35.68	26.92
801	8.52	35.14	800	8.50	35.14	27.32
1,001	5.16	34.94	1,000	5.15	34.94	27.63
1,504	3.91	34.94				

STATIONS OCCUPIED IN 1954—Continued

Station 5462; May 6; latitude 41°31.5′ N., longitude 50°13′ W.; depth 3,841 m.; dynamic height 971.355

Observed values			Scaled values			
Depth, meters	Temperature, ° C.	Salinity °/oo	Depth, meters	Temperature, ° C.	Salinity, °/oo	σ_t
0	16.61	35.94	0	16.61	35.94	26.34
24	16.39	35.89	25	16.40	35.88	26.34
48	15.06	35.62	50	15.00	35.61	26.47
72	14.18	35.40	75	14.20	35.40	26.47
95	14.25	35.46	100	14.20	35.47	26.53
144	13.94	35.51	150	13.90	35.51	26.62
191	13.58	35.51	200	13.45	35.51	26.72
286	12.26	35.53	300	12.05	35.51	27.00
440	9.62	35.24	400	10.30	35.31	27.16
653	6.50	35.02	600	7.10	35.04	27.45
862	5.04	35.01	800	5.35	35.01	27.66
1,078	4.43	34.98	1,000	4.60	34.99	27.73
1,615	3.81	34.96				

Station 5463; May 7; latitude 42°02′ N., longitude 50°19′ W.; depth 3,566 m.; dynamic height 971.272

Observed values			Scaled values			
Depth, meters	Temperature, ° C.	Salinity °/oo	Depth, meters	Temperature, ° C.	Salinity, °/oo	σ_t
0	13.99	35.54	0	13.99	35.54	26.62
27	14.06	35.55	25	14.05	35.55	26.62
53	14.09	35.56	50	14.10	35.56	26.62
81	14.14	35.61	75	14.10	35.60	26.65
107	14.28	35.66	100	14.20	35.64	26.66
161	14.72	35.84	150	14.65	35.81	26.69
215	14.03	35.70	200	14.25	35.75	26.73
322	11.06	35.40	300	11.65	35.46	27.03
416	8.92	35.14	400	9.20	35.18	27.24
620	5.60	34.96	600	5.80	34.97	27.58
822	4.39	34.92	800	4.45	34.92	27.70
1,027	4.23	34.96	1,000	4.25	34.96	27.75
1,535	3.64	34.92				

Station 5464; May 7; latitude 42°25′ N., longitude 50°20′ W.; depth 2,469 m.; dynamic height 971.128

Observed values			Scaled values			
Depth, meters	Temperature, ° C.	Salinity °/oo	Depth, meters	Temperature, ° C.	Salinity, °/oo	σ_t
0	3.13	32.96	0	3.13	32.96	26.27
24	3.36	33.05	25	3.40	33.10	26.35
50	9.17	34.31	50	9.20	34.31	26.57
74	11.37	34.95	75	11.40	34.96	26.69
100	12.36	35.36	100	12.35	35.36	26.82
149	11.44	35.40	150	11.40	35.40	27.03
198	10.02	35.20	200	9.95	35.19	27.13
298	8.44	35.10	300	8.40	35.10	27.31
397	6.55	34.97	400	6.50	34.96	27.48
594	3.55	34.77	600	3.55	34.77	27.67
791	3.60	34.85	800	3.60	34.86	27.74
989	3.79	34.92	1,000	3.80	34.92	27.77
1,485	3.43	34.89				

Station 5465; May 7; latitude 42°45′ N., longitude 50°22′ W.; depth 1,024 m.; dynamic height 971.073

Observed values			Scaled values			
Depth, meters	Temperature, ° C.	Salinity °/oo	Depth, meters	Temperature, ° C.	Salinity, °/oo	σ_t
0	1.95	32.97	0	1.95	32.97	26.37
25	−0.21	32.97	25	−0.21	32.97	26.50
50	−0.75	33.03	50	−0.75	33.03	26.57
76	0.38	33.41	75	0.35	33.40	26.82
101	3.39	33.98	100	3.30	33.98	27.06
151	4.41	34.17	150	4.40	34.16	27.10
202	6.58	34.64	200	6.55	34.62	27.20
303	6.90	------	300	6.90	34.95	27.41
404	3.25	34.64	400	3.35	34.65	27.59
601	3.64	34.81	600	3.65	34.81	27.69
795	3.66	34.84	800	3.65	34.84	27.71
993	3.57	34.88	1,000	3.55	34.88	27.75

Station 5466; May 7; latitude 42°48.5′ N., longitude 50°22′ W.; depth 338 m.; dynamic height 971.052

Observed values			Scaled values			
Depth, meters	Temperature, ° C.	Salinity, °/oo	Depth, meters	Temperature, ° C.	Salinity, °/oo	σ_t
0	5.02	33.02	0	5.02	33.02	26.12
23	3.52	33.00	25	3.55	33.05	26.30
46	------	34.93	50	12.45	35.04	26.55
70	------	35.28	75	11.40	35.10	26.80
93	7.65	34.50	100	7.35	34.50	27.00
139	6.48	34.50	150	6.60	34.54	27.13
185	7.08	34.69	200	6.80	34.73	27.25
278	5.17	34.87	(300)	4.80	34.89	27.63

Station 5467; May 7; latitude 43°01′N., longitude 50°20′ W.; depth 93 m.; dynamic height 971.075

Observed values			Scaled values			
Depth, meters	Temperature, ° C.	Salinity, °/oo	Depth, meters	Temperature, ° C.	Salinity, °/oo	σ_t
0	4.43	32.84	0	4.43	32.84	26.05
25	4.20	32.86	25	4.20	32.86	26.09
51	3.63	33.12	50	3.65	33.12	26.34
76	0.07	33.22	75	0.25	33.22	26.68

Station 5468; May 7; latitude 43°17′ N., longitude 50°16′ W.; depth 68 m.; dynamic height 971.079

Observed values			Scaled values			
Depth, meters	Temperature, ° C.	Salinity, °/oo	Depth, meters	Temperature, ° C.	Salinity, °/oo	σ_t
0	2.67	32.78	0	2.67	32.78	26.16
26	2.41	32.81	25	2.45	32.81	26.21
53	1.82	32.80	50	1.90	32.80	26.25

Station 5469; May 7; latitude 43°02.5′ N., longitude 50°35′ W.; depth 93 m.; dynamic height 971.067

Observed values			Scaled values			
Depth, meters	Temperature, ° C.	Salinity, °/oo	Depth, meters	Temperature, ° C.	Salinity, °/oo	σ_t
0	4.71	32.91	0	4.71	32.91	26.07
25	3.46	32.92	25	3.46	32.92	26.21
51	7.78	34.06	50	7.70	34.02	26.57
76	*10.24	34.83	75	10.20	34.82	26.80

Station 5470; May 7; latitude 42°58′ N., longitude 50°40′ W.; depth 176 m.; dynamic height 971.086

Observed values			Scaled values			
Depth, meters	Temperature, ° C.	Salinity, °/oo	Depth, meters	Temperature, ° C.	Salinity, °/oo	σ_t
0	4.67	32.70	0	4.67	32.70	25.91
26	5.16	33.03	25	5.15	33.15	26.11
51	7.77	33.87	50	7.65	33.85	26.44
77	8.95	34.28	75	8.90	34.23	26.55
103	10.91	35.05	100	10.70	34.95	26.81
154	9.15	34.96	150	9.30	34.96	27.06

Station 5471; May 7; latitude 42°54.5′ N., longitude 50°46′ W.; depth 640 m.; dynamic height 971.127

Observed values			Scaled values			
Depth, meters	Temperature, ° C.	Salinity, °/oo	Depth, meters	Temperature, ° C.	Salinity, °/oo	σ_t
0	5.37	32.92	0	5.37	32.92	26.00
25	5.29	32.98	25	5.29	32.98	26.06
50	5.98	33.24	50	5.98	33.24	26.19
75	7.70	33.87	75	7.70	33.87	26.45
101	10.89	34.85	100	10.85	34.84	26.70
151	10.20	35.14	150	10.25	35.03	26.95
201	8.39	34.93	200	8.45	34.93	27.17
302	6.84	35.00	300	6.80	35.00	27.47
403	5.29	34.88	400	5.30	34.88	27.56
593	4.04	34.88	600	4.00	34.88	27.71

STATIONS OCCUPIED IN 1954—Continued

Station 5472; May 7; latitude 42°50′ N., longitude 50°50′ W.; depth 1,192 m.; dynamic height 971.121

Observed values			Scaled values			
Depth, meters	Temperature, ° C.	Salinity, ‰	Depth, meters	Temperature, ° C.	Salinity, ‰	σ_t
0	5.36	32.89	0	5.36	32.89	25.98
25	5.47	33.03	25	5.47	33.03	26.08
51	7.94	33.92	50	7.90	33.90	26.44
76	10.29	34.60	75	10.25	34.59	26.61
101	11.70	35.19	100	11.65	35.18	26.81
152	10.91	35.28	150	11.00	35.28	27.01
203	9.19	35.04	200	9.20	35.05	27.14
304	6.71	35.02	300	6.80	35.02	27.48
403	5.42	34.85	400	5.45	34.85	27.52
601	4.15	34.89	600	4.15	34.89	27.70
795	3.89	34.89	800	3.90	34.89	27.73
995	3.64	34.88	1,000	3.65	34.88	27.74

Station 5473; May 7–8; latitude 42°40′ N., longitude 51°01′W.; depth 1,994 m.; dynamic height 971.185

0	5.21	32.80	0	5.21	32.80	25.94
24	5.25	32.94	25	5.30	32.98	26.06
49	8.22	34.00	50	8.30	34.04	26.49
73	9.72	34.48	75	9.85	34.50	26.61
98	11.39	35.00	100	11.40	35.02	26.74
147	11.14	35.13	150	11.05	35.13	26.88
195	10.03	35.08	200	9.90	35.07	27.05
293	7.92	-------	300	7.80	34.94	27.27
375	6.46	34.85	400	6.25	34.86	27.43
565	5.09	34.92	600	4.85	34.91	27.64
757	4.06	34.87	800	3.95	34.87	27.71
952	3.76	34.91	1,000	3.75	34.91	27.76
1,450	3.46	34.885				

Station 5474; May 8; latitude 42°17′ N., longitude 51°29′ W.; depth 3,017 m.; dynamic height 971.261

0	8.97	34.14	0	8.97	34.14	26.47
24	10.13	34.54	25	10.20	34.57	26.60
47	12.23	35.15	50	12.40	35.19	26.68
71	13.12	35.46	75	13.20	35.50	26.76
94	13.55	35.58	100	13.55	35.59	26.75
142	13.59	35.61	150	13.60	35.61	26.76
189	13.42	35.56	200	12.95	35.50	26.81
283	9.12	-------	300	8.35	34.87	27.14
387	5.31	34.36	400	5.30	34.38	27.17
583	5.23	34.78	600	5.20	34.81	27.52
779	4.85	34.98	800	4.80	34.98	27.71
977	4.28	34.94	1,000	4.25	34.94	27.73
1,476	3.78	34.94				

Station 5475; May 8; latitude 41°58.5′ N., longitude 51°58′ W.; depth 4,115m.; dynamic height 971.227

0	10.18	34.52	0	10.18	34.52	26.56
26	12.03	35.14	25	12.00	35.13	26.71
52	12.55	35.31	50	12.50	35.30	26.74
78	13.16	-------	75	13.10	35.44	26.73
103	13.25	35.50	100	13.20	35.49	26.75
154	13.23	35.52	150	13.25	35.52	26.76
206	13.49	35.59	200	13.45	35.59	26.77
309	11.69	35.49	300	11.90	35.50	27.02
411	9.20	35.47	400	9.45	35.47	27.43
614	5.98	35.00	600	6.10	35.02	27.58
813	4.94	35.01	800	5.00	35.01	27.71
1,021	4.27	34.97	1,000	4.30	34.97	27.75
1,548	3.79	34.94				

Station 5476; May 8; latitude 42°00′N., longitude 50°58′W.; depth 3,292 m.; dynamic height 971.226

Observed values			Scaled values			
Depth, meters	Temperature, ° C.	Salinity, ‰	Depth, meters	Temperature, ° C.	Salinity, ‰	σ_t
0	14.26	35.53	0	14.26	35.53	26.56
25	14.00	35.53	25	14.00	35.53	26.61
50	13.97	35.56	50	13.97	35.56	26.64
75	13.93	35.58	75	13.93	35.58	26.67
100	13.95	35.59	100	13.95	35.59	26.67
149	13.95	35.62	150	13.95	35.62	26.69
199	13.89	35.66	200	13.85	35.66	26.75
299	10.22	-------	300	10.20	35.33	27.19
380	8.48	35.07	400	8.15	35.06	27.32
569	5.92	35.00	600	5.65	35.00	27.62
759	4.60	34.98	800	4.40	34.96	27.73
958	3.83	34.90	1,000	3.80	34.90	27.75
1,474	3.57	34.90				

Station 5477; May 29; latitude 43°20′N., longitude 50°15′W.; depth 59 m.; dynamic height 971.104

0	6.14	32.72	0	6.14	32.72	25.76
25	4.36	32.75	25	4.36	32.75	26.08
51	2.07	32.81	50	2.15	32.81	26.24

Station 5478; May 29; latitude 42°55′N., longitude 50°15′W.; depth 91 m.; dynamic height 971.089

0	5.65	32.77	0	5.65	32.77	25.86
25	3.04	32.91	25	3.04	32.91	26.24
51	0.44	33.10	50	0.55	33.09	26.55
76	−0.74	33.27	75	−0.75	33.26	26.75

Station 5479; May 29; latitude 42°45′N., longitude 50°15′W.; depth 348 m.; dynamic height 971.077

0	3.96	32.90	0	3.96	32.90	26.14
24	1.41	32.93	25	1.30	32.93	26.34
47	−0.57	33.06	50	−0.60	33.07	26.59
71	−0.72	33.16	75	−0.80	33.18	26.69
94	−1.09	33.26	100	−1.05	33.28	26.78
140	−0.54	33.47	150	0.55	33.60	26.97
187	5.00	34.28	200	4.70	34.30	27.17
281	2.42	34.38	(300)	2.70	34.50	27.53

Station 5480; May 29; latitude 42°33′N., longitude 50°15′W.; depth 1,188 m.; dynamic height 971.078

0	3.78	32.84	0	3.78	32.84	26.12
25	3.67	32.84	25	3.67	32.84	26.13
49	3.02	33.05	50	3.05	33.06	26.35
74	3.70	33.44	75	3.70	33.44	26.60
98	0.64	33.52	100	0.65	33.53	26.90
148	1.29	33.77	150	1.30	33.78	27.06
196	0.91	33.86	200	0.95	33.88	27.16
294	2.15	34.39	300	2.25	34.42	27.51
297	2.21	34.41	400	2.95	34.64	27.62
447	3.20	34.71	600	3.70	34.85	27.72
598	3.71	34.85	800	3.75	34.88	27.73
811	3.76	34.88	(1,000)	3.75	34.89	27.74

STATIONS OCCUPIED IN 1954—Continued

Station 5481; May 29; latitude 42°06.5′ N., longitude 50°15′W.; depth 3,200 m.; dynamic height 971.167

Observed values			Scaled values			
Depth, meters	Temperature, ° C.	Salinity °/oo	Depth, meters	Temperature, ° C.	Salinity, °/oo	σ_t
0	7.26	32.67	0	7.26	32.67	25.58
23	7.04	32.67	25	6.90	32.68	25.63
45	5.84	33.00	50	5.95	33.18	26.15
68	7.06	33.78	75	7.70	33.96	26.52
90	9.22	-------	100	9.70	34.65	26.75
136	10.53	35.03	150	10.20	35.03	26.96
181	9.46	35.01	200	9.10	34.99	27.11
271	7.91	34.92	300	7.35	34.89	27.30
331	6.78	34.87	400	5.10	34.78	27.51
499	2.82	34.64	600	3.70	34.83	27.70
670	4.30	34.94	800	4.15	34.94	27.74
853	4.09	34.94	1,000	3.90	34.93	27.76
1,338	3.56	34.90				

Station 5482; May 30; latitude 41°37′N., longitude 50°15′W.; depth 3,658 m.; dynamic height 971.480

Observed values			Scaled values			
Depth, meters	Temperature, ° C.	Salinity °/oo	Depth, meters	Temperature, ° C.	Salinity, °/oo	σ_t
0	18.63	36.00	0	18.63	36.00	25.90
18	18.71	36.00	25	18.70	36.00	25.88
35	18.69	36.00	50	18.70	36.00	25.88
53	18.66	36.01	75	18.60	36.24	26.08
71	18.66	36.20	100	18.25	36.40	26.30
107	18.16	36.43	150	17.50	36.30	26.41
142	17.59	36.30	200	17.20	36.31	26.48
213	17.10	36.31	300	15.00	35.90	26.68
338	13.91	35.71	400	12.05	35.44	26.94
512	8.66	35.12	600	6.60	35.01	27.50
691	5.52	34.97	800	5.00	34.98	27.68
890	4.75	34.99	1,000	4.55	34.99	27.74
1,432	3.91	34.96				

Station 5483; May 30; latitude 41°16′N., longitude 50°16′W.; depth 3567 m.; dynamic height 971.391

Observed values			Scaled values			
Depth, meters	Temperature, ° C.	Salinity °/oo	Depth, meters	Temperature, ° C.	Salinity, °/oo	σ_t
0	18.29	35.60	0	18.29	35.60	25.68
24	18.10	35.58	25	18.05	35.58	25.72
47	16.90	35.50	50	16.80	35.51	25.97
70	15.94	35.87	75	15.75	35.86	26.48
93	15.14	35.77	100	14.90	35.73	26.57
140	13.76	35.46	150	13.75	35.49	26.63
187	13.97	35.62	200	13.95	35.63	26.70
280	13.46	35.65	300	12.90	35.58	26.88
275	13.55	35.66	400	10.10	35.21	27.12
404	9.96	35.20	600	6.70	35.01	27.49
529	7.67	35.05	800	5.05	34.99	27.68
677	5.79	35.00	1,000	4.45	34.98	27.74
1,075	4.30	34.98				

Station 5484; May 30; latitude 41°00′N., longitude 50°15′W., depth 3,749 m.; dynamic height 971.369

Observed values			Scaled values			
Depth, meters	Temperature, ° C.	Salinity °/oo	Depth, meters	Temperature, ° C.	Salinity, °/oo	σ_t
0	17.37	35.40	0	17.37	35.40	25.75
28	17.37	35.42	25	17.37	35.42	25.76
56	14.44	35.21	50	15.00	35.24	26.18
84	13.79	35.37	75	13.90	35.31	26.47
112	13.98	35.54	100	13.90	35.46	26.58
168	13.80	35.56	150	13.85	35.56	26.67
224	13.51	35.56	200	13.65	35.56	26.71
336	12.21	35.53	300	12.80	35.55	26.88
413	10.02	35.26	400	10.35	35.31	27.15
606	6.42	35.01	600	6.50	35.01	27.52
794	4.75	34.96	800	4.75	34.96	27.69
995	4.42	34.98	1,000	4.40	34.98	27.74
1,502	3.66	34.90				

Station 5485; May 30; latitude 40°35.5′ N., longitude 49°21′ W.; depth 3,713 m.; dynamic height 971.895

Observed values			Scaled values			
Depth, meters	Temperature, ° C.	Salinity, °/oo	Depth, meters	Temperature, ° C.	Salinity, °/oo	σ_t
0	22.34	36.23	0	22.34	36.23	25.07
29	22.19	36.22	25	22.25	36.22	25.09
56	21.67	36.28	50	21.80	36.26	25.25
84	20.17	36.44	75	20.70	36.39	25.65
112	19.02	36.46	100	19.45	36.45	26.03
169	18.56	36.48	150	18.70	36.48	26.25
225	18.24	36.46	200	18.35	36.47	26.33
337	17.80	36.46	300	17.90	36.46	26.44
443	17.38	36.36	400	17.55	36.43	26.49
654	12.58	35.60	600	14.50	35.80	26.71
861	7.01	35.05	800	8.05	35.16	27.41
1,075	4.88	35.00	1,000	5.45	35.00	27.64
1,611	3.95	34.96				

Station 5486; May 30; latitude 39°55′ N., longitude 48°48′ W.; depth 4,207 m.; dynamic height 971.464

Observed values			Scaled values			
Depth, meters	Temperature, ° C.	Salinity, °/oo	Depth, meters	Temperature, ° C.	Salinity, °/oo	σ_t
0	18.67	36.00	0	18.67	36.00	25.89
25	18.67	36.005	25	18.67	36.00	25.89
48	18.44	36.16	50	18.40	36.17	26.09
73	17.90	36.32	75	17.90	36.33	26.33
97	17.84	36.40	100	17.80	36.40	26.42
146	17.18	36.26	150	16.90	36.23	26.50
194	12.93	35.30	200	12.90	35.30	26.67
291	12.84	35.44	300	12.45	35.40	26.83
270	12.96	35.43	400	8.70	34.82	27.05
392	8.77	34.80	600	4.80	34.48	27.30
507	8.28	35.12	(800)	4.90	34.86	27.60
596	4.82	34.47	(1,000)	4.50	34.90	27.67
751	4.98	34.84				

Station 5487; May 31; latitude 40°07.5′ N., longitude 47°46′ W.; depth 4,024 m.; dynamic height 971.248

Observed values			Scaled values			
Depth, meters	Temperature, ° C.	Salinity, °/oo	Depth, meters	Temperature, ° C.	Salinity, °/oo	σ_t
0	14.45	34.71	0	14.45	34.71	25.89
28	13.25	35.34	25	13.30	35.27	26.56
54	13.54	35.52	50	13.50	35.51	26.71
82	13.56	35.56	75	13.55	35.55	26.72
108	13.57	35.56	100	13.55	35.56	26.73
163	13.69	35.64	150	13.65	35.63	26.76
217	13.56	35.63	200	13.60	35.64	26.78
325	10.63	35.34	300	11.45	35.42	27.04
415	7.90	35.01	400	8.25	35.05	27.30
622	5.10	34.93	600	5.25	34.93	27.61
832	4.32	34.94	800	4.40	34.94	27.71
1,045	4.19	34.97	1,000	4.25	34.97	27.76
1,587	3.68	34.94				

Station 5488; May 31; latitude 40°27′ N., longitude 48°22′ W.; depth 3,530 m.; dynamic height 971.373

Observed values			Scaled values			
Depth, meters	Temperature, ° C.	Salinity, °/oo	Depth, meters	Temperature, ° C.	Salinity, °/oo	σ_t
0	20.87	36.24	0	20.87	36.24	25.49
26	14.13	34.55	25	14.15	34.55	25.82
51	17.18	35.66	50	17.15	35.60	25.96
77	17.87	36.37	75	17.85	36.32	26.34
103	17.79	36.38	100	17.80	36.38	26.40
153	17.34	36.36	150	17.40	36.36	26.48
204	14.06	35.66	200	14.30	35.70	26.68
307	10.91	35.30	300	11.15	35.32	27.02
235	13.45	35.56	400	8.15	34.96	27.24
338	10.48	35.23	600	6.70	35.02	27.50
432	7.01	34.82	800	4.95	34.99	27.69
554	7.22	35.03	(1,000)	4.40	34.96	27.73
882	4.60	34.98				

Table of Oceanographic Data—Continued

STATIONS OCCUPIED IN 1954—Continued

Station 5489; May 31; latitude 40°45.5′ N., longitude 48°46′ W.; depth 3,658 m.; dynamic height 971.552

Observed values			Scaled values			
Depth, meters	Temperature, ° C.	Salinity °/oo	Depth, meters	Temperature, ° C.	Salinity, °/oo	σ_t
0	20.01	35.70	0	20.01	35.70	25.31
23	19.78	35.70	25	19.75	35.70	25.38
46	19.04	35.72	50	18.95	35.74	25.62
69	18.29	35.87	75	18.30	35.89	25.89
92	18.48	35.94	100	18.35	35.95	25.93
137	17.59	36.01	150	17.45	36.08	26.24
182	17.17	36.29	200	16.50	36.15	26.53
274	13.72	35.52	300	13.20	35.51	26.77
277	13.55	35.48	400	12.20	35.55	27.00
399	12.21	35.55	600	7.95	35.09	27.37
513	9.33	35.20	800	5.55	34.99	27.62
651	7.33	35.05	1,000	4.40	34.96	27.73
1,010	4.39	34.96				

Station 5490; May 31; latitude 41°18′ N., longitude 49°25′ W.; depth 3,475 m.; dynamic height 971.361

Observed values			Scaled values			
Depth, meters	Temperature, ° C.	Salinity °/oo	Depth, meters	Temperature, ° C.	Salinity, °/oo	σ_t
0	18.37	35.98	0	18.37	35.98	25.95
27	18.48	36.06	25	18.50	36.05	25.97
53	18.36	36.36	50	18.40	36.33	26.21
80	17.59	36.30	75	17.70	36.31	26.36
106	17.77	36.38	100	17.75	36.36	26.40
160	16.38	36.20	150	16.65	36.24	26.56
212	14.83	35.90	200	15.15	35.96	26.69
318	12.45	35.58	300	12.85	35.64	26.94
400	9.83	35.22	400	9.85	35.22	27.17
589	6.54	35.04	600	6.40	35.03	27.54
772	4.82	34.97	800	4.70	34.97	27.71
973	4.32	34.95	1,000	4.30	34.95	27.73
1,490	3.80	34.93				

Station 5491; May 31–June 1; latitude 41°50.5′ N., longitude 49°13′ W.; depth 3,200 m.; dynamic height 970.981

Observed values			Scaled values			
Depth, meters	Temperature, ° C.	Salinity °/oo	Depth, meters	Temperature, ° C.	Salinity, °/oo	σ_t
0	5.18	33.14	0	5.18	33.14	26.21
25	1.67	33.11	25	1.67	33.11	26.50
50	−0.67	33.42	50	−0.67	33.42	26.89
75	0.47	33.76	75	0.47	33.76	27.10
100	5.50	34.54	100	5.50	34.54	27.27
150	2.50	34.23	150	2.50	34.23	27.33
200	5.00	34.75	200	5.00	34.75	27.50
300	4.53	34.80	300	4.53	34.80	27.59
390	4.50	34.85	400	4.50	34.85	27.63
581	4.11	34.90	600	4.10	34.91	27.73
771	4.17	34.96	800	4.10	34.96	27.77
972	3.83	34.925	1,000	3.80	34.92	27.77
1,490	3.48	34.90				

Station 5492; June 1; latitude 41°34′ N., longitude 48°18′ W.; depth 3,566 m.; dynamic height 971.053

Observed values			Scaled values			
Depth, meters	Temperature, ° C.	Salinity °/oo	Depth, meters	Temperature, ° C.	Salinity, °/oo	σ_t
0	5.58	32.94	0	5.58	32.94	26.00
25	0.12	33.02	25	0.12	33.02	26.52
51	0.55	33.38	50	0.55	33.37	26.78
76	0.83	33.59	75	0.85	33.59	26.94
102	0.44	33.67	100	0.50	33.66	27.02
152	5.34	34.45	150	5.25	34.43	27.21
203	3.29	34.24	200	3.35	34.25	27.27
305	5.76	34.85	300	5.70	34.83	27.47
419	4.98	34.89	400	5.05	34.88	27.59
622	4.74	34.99	600	4.75	34.98	27.70
822	4.30	34.965	800	4.35	34.96	27.74
1,031	4.03	34.955	1,000	4.05	34.96	27.77
1,557	3.63	34.94				

Station 5493; June 1; latitude 41°10′ N., longitude 47°44′ W.; depth 3,475 m.; dynamic height 971.124

Observed values			Scaled values			
Depth, meters	Temperature, ° C.	Salinity, °/oo	Depth, meters	Temperature, ° C.	Salinity, °/oo	σ_t
0	7.94	32.76	0	7.94	32.76	25.55
26	3.07	33.16	25	3.10	33.15	26.42
51	8.70	34.31	50	8.35	34.28	26.67
77	12.82	35.42	75	12.75	35.38	26.76
102	11.35	35.19	100	11.55	35.21	26.86
152	6.56	34.41	150	6.70	34.44	27.04
203	5.75	34.38	200	5.75	34.38	27.11
305	7.55	34.95	300	7.55	34.92	27.30
409	6.46	35.01	400	6.55	35.01	27.51
607	4.02	34.86	600	4.05	34.86	27.69
801	3.74	34.89	800	3.75	34.89	27.74
1,010	3.58	34.89	1,000	3.60	34.89	27.76
1,550	3.43	34.89				

Station 5494; June1; latitude 40°54.5′ N., longitude 47°21′ W.; depty 3,566m.; dynamic height 971.345

Observed values			Scaled values			
Depth, meters	Temperature, ° C.	Salinity, °/oo	Depth, meters	Temperature, ° C.	Salinity, °/oo	σ_t
0	16.80	35.27	0	16.80	35.27	25.79
28	17.02	36.18	25	17.00	36.13	26.40
55	15.30	35.80	50	15.70	35.89	26.51
84	14.50	35.64	75	14.70	35.68	26.58
111	14.02	35.58	100	14.15	35.59	26.63
167	14.33	35.78	150	14.25	35.72	26.71
223	13.69	35.64	200	13.95	35.69	26.74
334	12.66	35.60	300	13.05	35.61	26.87
401	10.24	35.28	400	10.25	35.29	27.15
585	7.11	35.06	600	6.90	35.05	27.49
760	5.33	35.02	800	5.15	35.02	27.70
957	4.67	35.01	1,000	4.60	35.00	27.74
1,463	3.79	34.96				

Station 5495; June 1; latitude 40°38′ N., longitude 46°55′ W.; depth 3,713 m.; dynamic height 971.608

Observed values			Scaled values			
Depth, meters	Temperature, ° C.	Salinity, °/oo	Depth, meters	Temperature, ° C.	Salinity, °/oo	σ_t
0	18.46	36.35	0	18.46	36.35	26.20
26	18.38	36.36	25	18.40	36.36	26.24
52	18.31	36.40	50	18.30	36.39	26.28
78	18.23	36.45	75	18.25	36.45	26.34
103	18.17	36.45	100	18.15	36.45	26.37
156	17.84	36.41	150	17.85	36.42	26.41
208	17.45	36.36	200	17.50	36.37	26.46
311	16.40	36.18	300	16.50	36.20	26.58
413	15.12	35.96	400	15.30	35.99	26.68
626	10.53	35.38	600	11.10	35.44	27.12
844	5.93	34.96	800	5.85	35.01	27.60
1,065	4.62	34.96	1,000	4.85	34.96	27.68
1,634	3.87	34.95				

Station 5496; June 2; latitude 41°17.5′ N., longitude 46°40′ W.; depth 4,298 m.; dynamic height 971.668

Observed values			Scaled values			
Depth, meters	Temperature, ° C.	Salinity, °/oo	Depth, meters	Temperature, ° C.	Salinity, °/oo	σ_t
0	19.48	36.42	0	19.48	36.42	26.00
23	19.19	36.42	25	19.10	36.42	26.10
46	18.64	36.38	50	18.55	36.37	26.20
69	18.13	36.35	75	18.05	36.34	26.30
92	17.97	36.34	100	17.95	36.34	26.33
137	17.78	36.37	150	17.70	36.37	26.46
183	17.51	36.35	200	17.40	36.34	26.46
275	16.93	36.27	300	16.70	36.24	26.55
360	16.16	36.14	400	15.55	36.03	26.66
553	12.41	35.58	600	11.45	35.46	27.07
755	8.17	35.14	800	7.35	35.08	27.45
955	5.22	34.93	1,000	4.95	34.93	26.64
1,474	3.94	34.94				

Station 5497; June 2; latitude 41°39′ N., longitude 47°13′ W.; depth 4,142 m.; dynamic height 971.200

Observed values			Scaled values			
Depth, meters	Temperature, ° C.	Salinity °/oo	Depth, meters	Temperature, ° C.	Salinity, °/oo	σ_t
0	10.68	33.00	0	10.68	33.00	25.30
25	7.93	33.74	25	7.93	33.74	26.32
52	12.23	35.08	50	11.90	35.03	26.65
77	13.41	35.48	75	13.30	35.45	26.70
103	13.51	35.54	100	13.50	35.54	26.73
154	10.85	35.06	150	11.00	35.10	26.87
206	11.39	35.42	200	11.35	35.39	27.03
309	8.76	35.12	300	9.05	35.15	27.24
384	5.69	34.72	400	5.60	34.73	27.41
578	5.18	34.93	600	5.10	34.94	27.63
965	4.45	34.99	800	4.75	34.98	27.70
1,450	3.78	34.935	1,000	4.40	34.99	27.75

Station 5498; June 2; latitude 42°00′ N., longitude 47°49′ W.; depth 3,749 m.; dynamic height 971.050

Observed values			Scaled values			
Depth, meters	Temperature, ° C.	Salinity °/oo	Depth, meters	Temperature, ° C.	Salinity, °/oo	σ_t
0	8.89	33.34	0	8.89	33.34	25.85
25	7.28	33.51	25	7.28	33.51	26.23
51	4.91	33.91	50	4.95	33.89	26.82
76	7.22	34.47	75	7.10	34.45	26.99
101	8.00	34.76	100	8.00	34.76	27.11
152	7.28	34.75	150	7.30	34.75	27.20
203	6.80	34.78	200	6.80	34.77	27.29
304	6.55	34.98	300	6.55	34.97	27.48
389	6.14	35.05	400	6.05	35.05	27.60
577	4.69	34.98	600	4.60	34.97	27.72
760	4.23	34.95	800	4.15	34.95	27.75
957	3.83	34.93	1,000	3.80	34.93	27.77
1,460	3.64	34.90				

Station 5499; June 2; latitude 42°22′ N., longitude 48°27′ W.; depth 3,200 m.; dynamic height 971.114

Observed values			Scaled values			
Depth, meters	Temperature, ° C.	Salinity °/oo	Depth, meters	Temperature, ° C.	Salinity, °/oo	σ_t
0	11.98	34.58	0	11.98	34.58	26.28
25	11.85	34.59	25	11.85	34.59	26.31
50	11.50	34.57	50	11.50	34.57	26.37
74	13.33	35.39	75	13.35	35.39	26.64
99	13.16	35.37	100	13.15	35.36	26.66
149	9.80	35.03	150	9.75	35.03	27.03
198	9.28	35.15	200	9.25	35.15	27.22
297	7.49	35.02	300	7.04	35.01	27.39
360	6.09	34.93	400	5.90	34.95	27.55
535	5.35	35.04	600	5.00	35.01	27.71
708	4.50	34.97	800	4.20	34.95	27.75
892	4.03	34.94	1,000	3.95	34.93	27.75
1,365	3.64	34.92				

Station 5500; June 2; latitude 42°48′ N., longitude 49°10′ W.; depth 2,250 m.; dynamic height 970.988

Observed values			Scaled values			
Depth, meters	Temperature, ° C.	Salinity °/oo	Depth, meters	Temperature, ° C.	Salinity, °/oo	σ_t
0	7.64	33.08	0	7.64	33.08	25.84
25	1.58	33.10	25	1.58	33.10	26.50
51	3.10	33.82	50	3.10	33.80	26.94
76	3.23	33.99	75	3.20	33.98	27.07
102	4.81	34.38	100	4.65	34.34	27.21
153	6.74	34.82	150	6.65	34.81	27.34
204	2.89	34.41	200	2.95	34.43	27.45
306	4.95	34.85	300	4.85	34.83	27.57
397	5.16	34.99	400	5.15	34.99	27.67
591	4.57	34.99	600	4.55	34.99	27.74
782	4.20	34.98	800	4.15	34.98	27.77
981	3.87	34.93	1,000	3.85	34.94	27.77
1,483	3.46	34.89				

Station 5501; June 2–3; latitude 43°22′ N., longitude 48°50′ W.; depth 1,646 m.; dynamic height 971.003

Observed values			Scaled values			
Depth, meters	Temperature, ° C.	Salinity, °/oo	Depth, meters	Temperature, ° C.	Salinity, °/oo	σ_t
0	3.83	32.86	0	3.83	32.86	26.12
25	1.59	32.86	25	1.59	32.86	26.31
50	−0.85	33.02	50	−0.85	33.02	26.56
75	−1.01	33.17	75	−1.01	33.17	26.69
101	−0.68	33.40	100	−0.70	33.40	26.87
151	0.86	34.01	150	0.85	34.01	27.28
201	1.44	34.26	200	1.45	34.25	27.43
302	3.87	34.76	300	3.75	34.76	27.64
398	4.15	34.89	400	4.15	34.89	27.70
592	3.83	34.90	600	3.80	34.90	27.75
781	3.53	34.88	800	3.50	34.88	27.76
981	3.45	34.88	1,000	3.45	34.88	27.76
1,490	3.38	34.88				

Station 5502; June 3; latitude 43°08′ N., longitude 48°10′ W.; depth 3,054 m.; dynamic height 971.113

Observed values			Scaled values			
Depth, meters	Temperature, ° C.	Salinity, °/oo	Depth, meters	Temperature, ° C.	Salinity, °/oo	σ_t
0	12.64	34.70	0	12.64	34.70	26.25
25	13.98	35.20	25	13.98	35.20	26.36
50	13.45	35.18	50	13.45	35.18	26.46
75	9.20	34.38	75	9.20	34.38	26.62
100	5.70	34.05	100	5.70	34.05	26.86
150	9.08	34.92	150	9.08	34.92	27.07
201	7.96	34.84	200	7.95	34.84	27.17
301	6.89	34.87	300	6.90	34.87	27.35
334	7.30	35.04	400	6.35	35.00	27.53
490	5.28	34.95	600	4.85	34.97	27.69
638	4.70	34.98	800	4.20	34.96	27.76
803	4.18	34.95	1,000	3.90	34.93	27.76
1,223	3.57	34.90				

Station 5503; June 3; latitude 42°54′ N., longitude 47°30′ W.; depth 3,640 m.; dynamic height 971.062

Observed values			Scaled values			
Depth, meters	Temperature, ° C.	Salinity, °/oo	Depth, meters	Temperature, ° C.	Salinity, °/oo	σ_t
0	8.88	33.32	0	8.88	33.32	25.84
25	8.45	33.49	25	8.45	33.49	26.04
50	6.12	33.70	50	6.12	33.70	26.53
75	7.24	34.36	75	7.24	34.36	26.90
100	7.15	34.52	100	7.15	34.52	27.04
150	5.91	34.44	150	5.91	34.44	27.14
201	4.37	34.42	200	4.35	34.42	27.31
301	4.85	34.72	300	4.85	34.72	27.49
410	4.83	34.88	400	4.85	34.87	27.61
607	4.58	34.97	600	4.60	34.97	27.72
801	4.28	34.97	800	4.30	34.97	27.75
1,007	4.01	34.96	1,000	4.00	34.96	27.78
1,535	3.55	34.92				

Station 5504; June 3; latitude 42°45.5′ N., longitude 46°52′ W.; depth 4,042 m.; dynamic height 971.268

Observed values			Scaled values			
Depth, meters	Temperature, ° C.	Salinity, °/oo	Depth, meters	Temperature, ° C.	Salinity, °/oo	σ_t
0	12.33	33.58	0	12.33	33.58	25.45
27	13.64	34.81	25	13.60	34.70	26.06
53	13.57	35.44	50	13.60	35.40	26.60
80	13.77	35.56	75	13.70	35.54	26.69
106	13.86	35.61	100	13.85	35.60	26.70
160	13.59	35.58	150	13.60	35.58	26.74
212	13.28	35.64	200	13.35	35.62	26.82
318	10.71	35.35	300	11.20	35.41	27.08
316	10.65	35.34	400	7.65	34.97	27.32
464	5.52	34.72	600	5.45	34.94	27.59
608	5.44	34.95	800	4.40	34.92	27.70
777	4.46	34.92	1,000	4.15	34.93	27.73
1,228	3.98	34.95				

STATIONS OCCUPIED IN 1954—Continued

Station 5505; June 3; latitude 42°37.5′ N., longitude 46°12′ W.; depth 4,572 m.; dynamic height 971.608

Observed values			Scaled values			
Depth, meters	Temperature, ° C.	Salinity °/oo	Depth, meters	Temperature, ° C.	Salinity, °/oo	σt
0	19.33	36.37	0	19.33	36.37	26.01
26	19.27	36.37	25	19.30	36.37	26.01
51	18.25	36.29	50	18.30	36.29	26.21
78	17.88	36.36	75	17.90	36.35	26.34
103	17.70	36.38	100	17.75	36.38	26.41
155	17.10	36.27	150	17.15	36.28	26.48
206	16.66	36.19	200	16.70	36.20	26.53
309	15.71	36.07	300	15.75	36.08	26.64
393	14.89	35.96	400	14.80	35.95	26.76
577	11.05	35.40	600	10.55	35.33	27.13
754	7.27	35.04	800	6.60	35.02	27.51
949	5.54	35.00	1,000	5.25	35.00	27.67
1,450	4.07	34.96				

Station 5506; June 3; latitude 42°54′ N., longitude 45°46′ W.; depth 4,755 m.; dynamic height 971.632

Observed values			Scaled values			
Depth, meters	Temperature, ° C.	Salinity °/oo	Depth, meters	Temperature, ° C.	Salinity, °/oo	σt
0	17.65	36.34	0	17.65	36.34	26.40
26	17.45	36.32	25	17.45	36.32	26.43
51	17.44	36.32	50	17.45	36.32	26.43
77	17.44	36.32	75	17.45	36.32	26.43
102	16.98	36.24	100	17.00	36.25	26.48
155	16.88	36.26	150	16.85	36.26	26.53
206	16.69	36.26	200	16.70	36.26	26.57
308	16.44	36.22	300	16.45	36.23	26.60
367	15.98	36.13	400	15.45	36.04	26.68
543	12.71	35.62	600	11.45	35.46	27.07
714	8.99	35.16	800	7.40	35.05	27.42
899	6.30	35.00	1,000	5.50	34.99	27.62
1,370	4.13	34.94				

Station 5507; June 3; latitude 43°10.5′ N., longitude 45°21′ W.; depth 4,663 m.; dynamic height 971.621

Observed values			Scaled values			
Depth, meters	Temperature, ° C.	Salinity °/oo	Depth, meters	Temperature, ° C.	Salinity, °/oo	σt
0	18.58	36.33	0	18.52	36.33	26.16
24	18.58	36.34	25	18.55	36.34	26.18
48	18.04	36.34	50	18.00	36.34	26.32
72	17.76	36.32	75	17.70	36.32	26.37
97	17.57	36.32	100	17.55	36.32	26.41
144	16.97	36.23	150	16.90	36.23	26.50
192	16.74	36.22	200	16.70	36.22	26.54
289	16.34	36.19	300	16.25	36.18	26.61
337	15.97	36.12	400	15.05	35.96	26.72
498	13.23	35.67	600	10.70	35.36	27.13
655	9.45	35.20	800	7.25	35.06	27.45
824	6.99	35.05	1,000	5.55	35.04	27.66
1,250	4.57	35.02				

Station 5508; June 4; latitude 43°22′ N., longitude 45°55′ W.; depth 4,390 m.; dynamic height 971.389

Observed values			Scaled values			
Depth, meters	Temperature, ° C.	Salinity °/oo	Depth, meters	Temperature, ° C.	Salinity, °/oo	σt
0	19.28	36.26	0	19.28	36.26	25.93
19	19.26	36.24	25	19.00	36.23	25.98
36	18.12	36.21	50	16.80	36.07	26.40
55	16.44	36.03	75	16.75	36.06	26.40
73	16.52	36.06	100	16.10	36.03	26.53
110	15.95	36.01	150	15.30	35.93	26.64
146	15.42	35.94	200	14.10	35.68	26.71
219	13.67	35.59	300	13.25	35.60	26.82
286	13.64	35.65	400	10.40	35.21	27.07
413	10.09	35.16	600	5.35	34.79	27.49
530	6.44	34.785	800	4.55	34.87	27.65
673	4.87	34.81	1,000	4.40	34.96	27.73
1,053	4.34	34.97				

Station 5509; June 4; latitude 43°30.5′ N., longitude 46°22′ W.; depth 2,561 m.; dynamic height 971.176

Observed values			Scaled values			
Depth, meters	Temperature, ° C.	Salinity, °/oo	Depth, meters	Temperature, ° C.	Salinity, °/oo	σt
0	12.21	33.91	0	12.21	33.91	25.73
24	9.89	33.83	25	9.90	33.83	26.08
48	11.30	34.82	50	11.45	34.91	26.65
72	13.22	35.43	75	13.25	35.46	26.72
96	13.48	35.54	100	13.45	35.53	26.73
145	12.11	35.36	150	11.80	35.32	26.90
193	9.23	34.92	200	8.90	34.88	27.06
289	6.08	34.60	300	6.10	34.61	27.25
396	7.09	34.99	400	7.05	34.99	27.42
577	4.09	34.80	600	4.05	34.81	27.65
748	4.01	34.90	800	3.95	34.90	27.73
945	3.67	34.89	1,000	3.65	34.89	27.75
1,458	3.42	34.89				

Station 5510; June 4; latitude 43°44.5′ N., longitude 47°04′ W.; depth 4,042 m.; dynamic height 971.007

Observed values			Scaled values			
Depth, meters	Temperature, ° C.	Salinity, °/oo	Depth, meters	Temperature, ° C.	Salinity, °/oo	σt
0	6.18	33.12	0	6.18	33.12	26.07
23	5.40	33.21	25	5.25	33.22	26.26
45	2.96	33.25	50	2.85	33.30	26.56
68	2.47	33.61	75	2.10	33.64	26.90
90	1.26	33.70	100	1.60	33.80	27.06
135	3.49	34.35	150	4.15	34.50	27.39
180	5.30	34.73	200	5.10	34.73	27.47
270	4.13	34.73	300	3.75	34.71	27.60
312	3.69	34.71	400	4.35	34.86	27.66
481	4.70	34.98	600	4.25	34.94	27.73
658	4.09	34.93	800	4.05	34.94	27.75
849	4.04	34.94	1,000	3.95	34.94	27.76
1,371	3.55	34.92				

Station 5511; June 4; latitude 43°56′ N., longitude 47°38′ W.; depth 3,841 m.; dynamic height 971.120

Observed values			Scaled values			
Depth, meters	Temperature, ° C.	Salinity, °/oo	Depth, meters	Temperature, ° C.	Salinity, °/oo	σt
0	10.46	34.30	0	10.46	34.30	26.35
25	10.40	34.60	25	10.40	34.60	26.59
49	10.16	34.60	50	10.20	34.60	26.62
74	10.18	34.74	75	10.20	34.75	26.74
98	10.67	35.02	100	10.65	35.02	26.87
148	10.11	35.00	150	10.05	35.00	26.96
197	9.13	35.00	200	9.05	35.00	27.13
295	6.37	34.78	300	6.35	34.78	27.35
435	5.92	34.92	400	6.00	34.89	27.48
651	4.47	34.94	600	4.75	34.94	27.67
868	4.10	34.95	800	4.20	34.95	27.75
1,090	3.83	34.94	1,000	3.95	34.94	27.76
1,651	3.53	34.92				

Station 5512; June 4; latitude 44°03.5′ N., longitude 48°14′ W.; depth 3,457 m.; dynamic height 971.027

Observed values			Scaled values			
Depth, meters	Temperature, ° C.	Salinity, °/oo	Depth, meters	Temperature, ° C.	Salinity, °/oo	σt
0	5.58	33.10	0	5.58	33.10	26.12
27	6.17	33.66	25	6.15	33.62	26.47
53	6.89	34.04	50	6.80	34.00	26.68
80	7.76	34.60	75	7.55	34.50	26.97
106	8.93	34.89	100	8.75	34.85	27.06
160	5.67	34.48	150	6.15	34.55	27.20
212	6.26	34.76	200	6.10	34.69	27.31
318	4.01	34.68	300	4.15	34.69	27.54
407	4.20	34.82	400	4.15	34.81	27.64
605	4.57	34.99	600	4.55	34.99	27.74
802	4.13	34.95	800	4.15	34.95	27.75
1,009	3.82	34.93	1,000	3.85	34.93	27.76
1,539	3.49	34.91				

Station 5513; June 4–5; latitude 44°11′ N., longitude 48°50′ W.; depth 2,103 m.; dynamic height 970.948

Observed values			Scaled values			
Depth, meters	Temperature, ° C.	Salinity ‰	Depth, meters	Temperature, ° C.	Salinity, ‰	σ_t
0	2.39	33.12	0	2.39	33.12	26.46
25	2.36	33.11	25	2.36	33.11	26.45
50	1.93	33.22	50	1.93	33.22	26.58
75	0.47	33.80	75	0.47	33.80	27.13
101	0.88	34.04	100	0.90	34.04	27.30
150	2.79	34.44	150	2.80	34.44	27.47
200	3.79	34.69	200	3.80	34.69	27.58
301	4.00	34.79	300	4.00	34.79	27.64
404	3.99	34.83	400	4.00	34.83	27.67
602	3.70	34.92	600	3.70	34.91	27.77
799	3.43	34.89	800	3.45	34.89	27.77
1,006	3.36	34.89	1,000	3.35	34.89	27.78
1,536	3.32	34.90				

Station 5514; June 5; latitude 44°13′ N., longitude 48°58′ W.; depth 531 m.; dynamic height 971.016

Observed values			Scaled values			
Depth, meters	Temperature, ° C.	Salinity ‰	Depth, meters	Temperature, ° C.	Salinity, ‰	σ_t
0	2.39	32.90	0	2.39	32.90	26.28
25	0.17	33.05	25	0.17	33.05	26.54
51	0.21	33.29	50	0.20	33.29	26.73
76	−0.25	33.49	75	−0.25	33.48	26.91
103	0.22	33.72	100	0.15	33.70	27.07
153	0.58	33.91	150	0.55	33.90	27.21
204	0.89	34.05	200	0.90	34.03	27.29
307	2.18	34.50	300	2.10	34.46	27.55
322	2.47	34.59	400	2.80	34.64	27.63
518	3.04	34.70				

Station 5515; June 5; latitude 44°14′ N., longitude 49°05′ W.; depth 187 m.; dynamic height 971.067

Observed values			Scaled values			
Depth, meters	Temperature, ° C.	Salinity ‰	Depth, meters	Temperature, ° C.	Salinity, ‰	σ_t
0	1.77	32.84	0	1.77	32.84	26.29
26	0.28	32.99	25	0.35	32.99	26.49
53	−0.82	33.16	50	−0.80	33.14	26.66
79	−0.71	33.32	75	−0.70	33.30	26.78
105	−0.81	33.34	100	−0.80	33.33	26.81
157	−0.57	33.46	150	−0.60	33.44	26.89

Station 5516; June 5; latitude 44°16′ N., longitude 49°12′ W.; depth 59 m.; dynamic height 971.072

Observed values			Scaled values			
Depth, meters	Temperature, ° C.	Salinity ‰	Depth, meters	Temperature, ° C.	Salinity, ‰	σ_t
0	1.75	32.84	0	1.75	32.84	26.29
27	0.27	32.99	25	0.35	32.98	26.48
49	−0.07	33.08	50	−0.10	33.08	26.58

Station 5517; June 5; latitude 45°00.5′ N., longitude 49°13′ W.; depth 64 m.; dynamic height 971.083

Observed values			Scaled values			
Depth, meters	Temperature, ° C.	Salinity ‰	Depth, meters	Temperature, ° C.	Salinity, ‰	σ_t
0	2.62	32.84	0	2.62	32.84	26.22
27	−0.12	32.96	25	−0.05	32.95	26 48
55	−0.26	32.99	50	−0.25	32.98	26.51

Station 5518; June 5; latitude 44°59.5′ N., longitude 49°05′ W.; depth 98 m.; dynamic height 971.076

Observed values			Scaled values			
Depth, meters	Temperature, ° C.	Salinity ‰	Depth, meters	Temperature, ° C.	Salinity, ‰	σ_t
0	2.15	32.86	0	2.15	32.86	26.27
27	−0.28	33.10	25	−0.25	33.09	26.59
53	−0.63	33.21	50	−0.60	33.20	26.70
80	−0.57	33.22	75	−0.60	33.22	26.71

Station 5519; June 5; latitude 44°58.5′ N., longitude 48°57′ W., depth 659 m.; dynamic height 971.041

Observed values			Scaled values			
Depth, meters	Temperature, ° C.	Salinity, ‰	Depth, meters	Temperature, ° C.	Salinity, ‰	σ_t
0	2.09	32.88	0	2.09	32.88	26.29
25	0.89	32.98	25	0.89	32.98	26.45
49	0.70	33.16	50	0.70	33.17	26.61
74	−0.49	33.49	75	−0.50	33.49	26.93
98	0.14	33.69	100	0.15	33.71	27.08
147	0.64	33.94	150	0.65	33.95	27.24
196	0.75	34.02	200	0.75	34.03	27.30
294	1.27	34.26	300	1.30	34.28	27.46
366	1.85	34.42	400	2.10	34.48	27.56
545	2.98	34.70	600	3.10	34.75	27.70

Station 5520; June 5· latitude 44°56.5′ N., longitude 48°44′ W.; depth 1,646 m.; dynamic height 970.934

Observed values			Scaled values			
Depth, meters	Temperature, ° C.	Salinity, ‰	Depth, meters	Temperature, ° C.	Salinity, ‰	σ_t
0	3.10	33.12	0	3.10	33.12	26.40
27	1.86	33.24	25	1.95	33.23	26.58
53	1.15	33.50	50	1.15	33.46	26.82
80	1.48	33.94	75	1.40	33.86	27.12
106	2.09	34.24	100	2.00	34.18	27.33
160	2.83	34.52	150	2.70	34.46	27.50
213	4.18	34.76	200	3.90	34.71	27.59
319	3.88	34.83	300	3.90	34.82	27.68
404	3.85	34.86	400	3.85	34.86	27.71
606	3.85	34.90	600	3.85	34.90	27.74
809	3.51	34.89	800	3.50	34.89	27.77
1,017	3.45	34.89	1,000	3.45	34.89	27.77
1,543	3.35	34.89				

Station 5521; June 5; latitude 44°54.5′ N., longitude 48°30′ W., depth 2,689 m.; dynamic height 970.919

Observed values			Scaled values			
Depth, meters	Temperature, ° C.	Salinity, ‰	Depth, meters	Temperature, ° C.	Salinity, ‰	σ_t
0	4.08	33.21	0	4.08	33.21	26.38
27	1.04	33.27	25	1.10	33.26	26.66
53	0.88	33.92	50	0.90	33.84	27.14
80	1.72	34.17	75	1.55	34.13	27.32
107	2.33	34.34	100	2.15	34.30	27.42
161	5.34	34.86	150	4.90	34.79	27.54
214	4.87	34.84	200	5.00	34.85	27.58
321	4.46	34.88	300	4.50	34.87	27.65
390	4.40	34.91	400	4.35	34.91	27.70
605	3.85	34.92	600	3.85	34.92	27.76
834	3.67	34.91	800	3.70	34.91	27.77
1,048	3.51	34.88	1,000	3.55	34.90	27.77
1,594	3.39	34.88				

Station 5522; June 5; latitude 44°50′ N., longitude 47°57′ W., depth 3,292 m.; dynamic height 970.959

Observed values			Scaled values			
Depth, meters	Temperature, ° C.	Salinity, ‰	Depth, meters	Temperature, ° C.	Salinity, ‰	σ_t
0	6.29	33.50	0	6.29	33.50	26.35
24	5.49	33.56	25	5.50	33.56	26.50
49	5.35	33.66	50	5.35	33.68	26.61
73	3.76	34.00	75	3.80	34.03	27.05
97	4.00	34.24	100	4.10	34.27	27.22
146	4.61	34.54	150	4.60	34.55	27.38
195	3.93	34.61	200	3.95	34.62	27.51
292	4.51	34.87	300	4.50	34.87	27.65
381	4.28	34.91	400	4.25	34.91	27.71
568	3.98	34.93	600	3.90	34.92	27.76
753	3.56	34.90	800	3.50	34.89	27.77
946	3.45	34.89	1,000	3.45	34.89	27.77
1,436	3.38	34.90				

Table of Oceanographic Data—Continued

STATIONS OCCUPIED IN 1954—Continued

Station 5523; June 5–6; latitude 44°45′ N., longitude 47°19′ W.; depth 3,795 m.; dynamic height 971.018

Observed values			Scaled values			
Depth, meters	Temperature, ° C.	Salinity °/oo	Depth, meters	Temperature, ° C.	Salinity, °/oo	σ_t
0	6.25	33.30	0	6.25	33.30	26.20
23	3.63	33.22	25	3.65	33.23	26.43
46	4.83	33.47	50	5.25	33.71	26.65
69	7.64	34.57	75	7.85	34.64	27.03
92	8.08	34.73	100	8.00	34.75	27.10
137	7.09	34.80	150	6.80	34.79	27.30
184	5.98	34.74	200	5.65	34.74	27.41
276	4.63	34.75	300	4.70	34.78	27.55
334	4.76	34.82	400	4.65	34.87	27.64
500	4.34	34.90	600	4.05	34.89	27.71
666	3.92	34.88	800	3.80	34.89	27.74
850	3.73	34.89	1,000	3.65	34.89	27.75
1,341	3.40	34.89				

Station 5524; June 6; latitude 44°38′ N., longitude 46°28′ W.; depth 3,573 m.; dynamic height 971.007

Observed values			Scaled values			
Depth, meters	Temperature, ° C.	Salinity °/oo	Depth, meters	Temperature, ° C.	Salinity, °/oo	σ_t
0	7.07	33.46	0	7.07	33.46	26.22
24	7.53	33.90	25	7.55	33.91	26.50
50	8.67	34.69	50	8.70	34.69	26.94
74	8.82	34.79	75	8.85	34.79	27.00
100	9.12	34.89	100	9.10	34.89	27.03
149	7.49	34.80	150	7.45	34.80	27.22
198	5.95	34.77	200	5.90	34.77	27.41
298	4.95	34.79	300	4.90	34.79	27.54
415	3.62	34.73	400	3.75	34.73	27.61
610	4.08	34.92	600	4.10	34.92	27.74
797	3.82	34.92	800	3.80	34.92	27.77
1,001	3.54	34.90	1,000	3.55	34.90	27.77
1,517	3.32	34.88				

Station 5525; June 6; latitude 44°32.5′ N., longitude 45°46′ W.; depth 3,804 m.; dynamic height 971.017

Observed values			Scaled values			
Depth, meters	Temperature, ° C.	Salinity °/oo	Depth, meters	Temperature, ° C.	Salinity, °/oo	σ_t
0	6.92	33.47	0	6.92	33.47	26.25
25	5.23	33.45	25	5.23	33.45	26.44
50	5.61	33.58	50	5.61	33.58	26.50
75	2.70	33.57	75	2.70	33.57	26.80
101	0.96	33.68	100	0.95	33.67	27.00
151	2.04	34.14	150	2.05	34.13	27.29
201	2.30	34.35	200	2.25	34.34	27.44
302	4.55	34.80	300	4.55	34.79	27.58
387	4.35	34.86	400	4.35	34.87	27.67
578	4.47	34.96	600	4.45	34.95	27.72
767	3.89	34.89	800	3.85	34.89	27.73
966	3.74	34.92	1,000	3.70	34.92	27.78
1,473	3.45	34.91				

Station 5526; June 7; latitude 44°25.5′ N., longitude 45°16′ W.; depth 3,573 n.; dynamic height 971.040

Observed values			Scaled values			
Depth, meters	Temperature, ° C.	Salinity °/oo	Depth, meters	Temperature, ° C.	Salinity, °/oo	σ_t
0	10.39	34.36	0	10.39	34.36	26.40
25	11.50	34.80	25	11.50	34.80	26.55
51	10.13	34.74	50	10.20	34.74	26.73
76	6.56	34.28	75	6.60	34.28	26.92
102	7.10	34.58	100	7.10	34.56	27.08
152	6.45	34.58	150	6.45	34.58	27.18
202	6.57	34.80	200	6.55	34.79	27.33
304	5.13	34.77	300	5.15	34.77	27.50
415	4.79	34.86	400	4.80	34.84	27.59
615	4.42	34.94	600	4.45	34.94	27.71
810	4.02	34.92	800	4.05	34.92	27.74
1,017	3.73	34.91	1,000	3.75	34.91	27.76
1,544	3.38	34.88				

Station 5527; June 7; latitude 44°19.5′ N., longitude 44°34′ W., depth 4,572 m.; dynamic height 970.988

Observed values			Scaled values			
Depth, meters	Temperature, ° C.	Salinity, °/oo	Depth, meters	Temperature, ° C.	Salinity, °/oo	σ_t
0	7.46	33.45	0	7.46	33.45	26.16
25	6.36	33.46	25	6.36	33.46	26.32
49	4.70	33.72	50	4.70	33.74	26.73
74	4.55	34.08	75	4.55	34.09	27.02
99	4.75	34.30	100	4.75	34.30	27.17
148	4.17	34.44	150	4.15	34.45	27.35
197	4.17	34.60	200	4.15	34.60	27.47
296	4.22	34.77	300	4.20	34.78	27.61
400	4.44	34.92	400	4.45	34.92	27.70
593	4.12	34.93	600	4.10	34.93	27.74
780	4.09	34.93	800	4.05	34.93	27.74
965	3.69	34.91	1,000	3.65	34.91	27.77
1,411	3.41	34.89				

Station 5528; June 7; latitude 44°49′N., longitude 44°34′ W.; depth 4,481 m.; dynamic height 971.016

Observed values			Scaled values			
Depth, meters	Temperature, ° C.	Salinity, °/oo	Depth, meters	Temperature, ° C.	Salinity, °/oo	σ_t
0	7.84	33.45	0	7.84	33.45	26.10
25	6.23	33.51	25	6.23	33.51	26.37
50	6.42	33.76	50	6.42	33.76	26.54
75	4.41	33.83	75	4.41	33.83	26.83
100	4.31	34.12	100	4.31	34.12	27.08
150	4.96	34.48	150	4.96	34.48	27.29
199	4.44	34.50	200	4.40	34.50	27.37
299	3.85	34.65	300	3.85	34.65	27.54
388	4.11	34.83	400	4.10	34.85	27.68
576	4.16	34.93	600	4.15	34.93	27.73
760	3.83	34.92	800	3.85	34.92	27.76
955	3.82	34.93	1,000	3.80	34.93	27.77
1,450	3.55	34.90				

Station 5529; June 7; latitude 44°49′ N., longitude 43°53′ W.; depth 4,036 m.; dynamic height 971.048

Observed values			Scaled values			
Depth, meters	Temperature, ° C.	Salinity, °/oo	Depth, meters	Temperature, ° C.	Salinity, °/oo	σ_t
0	10.01	34.13	0	10.01	34.13	26.29
25	9.96	34.47	25	9.96	34.47	26.57
50	8.56	34.29	50	8.56	34.29	26.65
76	6.84	34.28	75	6.85	34.28	26.89
101	6.51	34.40	100	6.50	34.39	27.02
151	6.63	34.63	150	6.65	34.62	27.19
202	6.41	34.74	200	6.40	34.74	27.31
303	5.12	34.77	300	5.15	34.77	27.50
401	4.80	34.83	400	4.80	34.83	27.58
595	4.45	34.92	600	4.45	34.92	27.70
784	4.13	34.94	800	4.10	34.94	27.75
984	3.84	34.92	1,000	3.85	34.92	27.76
1,490	3.46	34.90				

Station 5530; June 7; latitude 45°19′ N., longitude 44°00′ W.; depth 4,390 m.; dynamic height 971.082

Observed values			Scaled values			
Depth, meters	Temperature, ° C.	Salinity, °/oo	Depth, meters	Temperature, ° C.	Salinity, °/oo	σ_t
0	10.05	33.87	0	10.05	33.87	26.08
25	11.25	34.60	25	11.25	34.60	26.43
50	12.68	35.12	50	12.68	35.12	26.57
75	12.22	35.25	75	12.22	35.25	26.76
100	10.19	34.94	100	10.19	34.94	26.89
150	9.07	34.95	150	9.07	34.95	27.08
201	8.54	35.02	200	8.55	35.02	27.23
301	4.43	34.59	300	4.45	34.59	27.43
407	5.42	34.94	400	5.40	34.93	27.59
599	4.30	34.93	600	4.30	34.93	27.71
784	3.97	34.90	800	3.95	34.90	27.73
981	3.65	34.90	1,000	3.65	34.90	27.76
1,473	3.32	34.88				

STATIONS OCCUPIED IN 1954—Continued

Station 5531; June 8; latitude 45°19′ N., longitude 44°44′ W.; depth 4,481 m.; dynamic height 971.120

Observed values			Scaled values			
Depth, meters	Temperature, ° C.	Salinity °/oo	Depth, meters	Temperature, ° C.	Salinity, °/oo	σt
0	8.09	33.43	0	8.09	33.43	26.04
25	10.81	34.55	25	10.81	34.55	26.48
50	12.25	35.02	50	12.25	35.02	26.58
75	12.86	35.37	75	12.86	35.37	26.73
100	11.93	35.25	100	11.93	35.25	26.82
150	9.21	34.86	150	9.21	34.86	27.00
201	8.40	34.84	200	8.40	34.84	27.10
301	4.66	34.51	300	4.70	34.51	27.34
399	5.02	34.74	400	5.05	34.74	27.48
			(600)	4.25	34.89	27.69
			(800)	3.95	34.92	27.75
			(1,000)	3.80	34.93	27.77

Station 5532; June 8; latitude 45°19′ N., longitude 45°28′ W.; depth 3,768 m.; dynamic height 971.088

Observed values			Scaled values			
Depth, meters	Temperature, ° C.	Salinity °/oo	Depth, meters	Temperature, ° C.	Salinity, °/oo	σt
0	11.43	34.68	0	11.43	34.68	26.47
25	11.37	34.94	25	11.37	34.94	26.69
50	11.32	35.00	50	11.32	35.00	26.73
75	11.12	34.99	75	11.12	34.99	26.77
101	10.88	35.03	100	10.90	35.03	26.83
150	9.34	34.93	150	9.35	34.93	27.02
200	8.27	34.88	200	8.25	34.88	27.16
301	5.59	34.70	300	5.60	34.70	27.39
354	4.16	34.64	400	4.25	34.70	27.54
530	4.52	34.90	600	4.30	34.90	27.69
708	4.00	34.90	800	3.85	34.90	27.74
898	3.78	34.90	1,000	3.70	34.90	27.76
1,398	3.38	34.89				

Station 5533; June 8; latitude 45°21.5′ N., longitude 46°02′ W.; depth 3,429 m.; dynamic height 970.958

Observed values			Scaled values			
Depth, meters	Temperature, ° C.	Salinity °/oo	Depth, meters	Temperature, ° C.	Salinity, °/oo	σt
0	8.02	33.81	0	8.02	33.81	26.36
26	6.37	33.80	25	6.40	33.80	26.58
51	5.88	33.86	50	5.90	33.86	26.69
77	3.42	34.01	75	3.45	34.00	27.07
102	3.74	34.22	100	3.70	34.20	27.20
155	4.17	34.54	150	4.10	34.51	27.41
206	5.15	34.85	200	5.10	34.83	27.55
308	4.64	34.87	300	4.70	34.87	27.63
384	4.55	34.95	400	4.50	34.95	27.71
572	4.00	34.94	600	3.95	34.93	27.75
759	3.65	34.90	800	3.60	34.89	27.76
958	3.38	34.88	1,000	3.40	34.88	27.77
1,474	3.29	34.87				

Station 5534; June 8; latitude 45°21.5′ N., longitude 46°42′ W.; depth 3,109 m.; dynamic height 970.973

Observed values			Scaled values			
Depth, meters	Temperature, ° C.	Salinity °/oo	Depth, meters	Temperature, ° C.	Salinity, °/oo	σt
0	8.03	33.77	0	8.03	33.77	26.32
26	6.56	33.87	25	6.60	33.87	26.61
51	5.93	34.00	50	5.95	33.99	26.78
77	4.45	34.12	75	4.45	34.11	27.05
102	4.44	34.22	100	4.45	34.21	27.13
153	4.28	34.47	150	4.30	34.45	27.34
204	4.26	34.63	200	4.30	34.62	27.48
306	4.35	34.81	300	4.35	34.80	27.61
390	4.48	34.92	400	4.45	34.92	27.70
581	3.96	34.90	600	3.90	34.90	27.74
771	3.71	34.90	800	3.70	34.90	27.76
974	3.55	34.90	1,000	3.55	34.90	27.77
1,495	3.38	34.90				

Station 5535; June 8; latitude 45° 20′ N., longitude 47°23′ W.; depth 2,834 m.; dynamic height 970.979

Observed values			Scaled values			
Depth, meters	Temperature, ° C.	Salinity, °/oo	Depth, meters	Temperature, ° C.	Salinity, °/oo	σt
0	6.99	33.46	0	6.99	33.46	26.23
27	5.45	33.47	25	5.50	33.47	26.43
53	5.14	33.74	50	5.15	33.70	26.65
80	3.97	34.06	75	4.10	34.00	27.00
106	4.16	---- --	100	4.10	34.24	27.19
160	3.86	34.53	150	3.90	34.50	27.42
214	4.29	34.69	200	4.25	34.65	27.50
320	4.08	34.80	300	4.10	34.78	27.62
417	4.23	34.88	400	4.20	34.86	27.68
621	3.75	34.89	600	3.80	34.89	27.74
823	3.59	34.88	800	3.60	34.88	27.75
1,034	3.45	34.86	1,000	3.45	34.86	27.75
1,574	3.33	34.88				

Station 5536; June 8; latitude 45°34′ N., longitude 47°51′ W.; depth 1,500 m.; dynamic height 970.945

Observed values			Scaled values			
Depth, meters	Temperature, ° C.	Salinity, °/oo	Depth, meters	Temperature, ° C.	Salinity, °/oo	σt
0	4.72	33.34	0	4.72	33.34	26.41
25	2.18	33.33	25	2.18	33.33	26.64
52	1.13	33.48	50	1.15	33.46	26.82
77	2.30	33.98	75	2.15	33.94	27.13
104	3.27	34.32	100	3.15	34.27	27.31
154	3.63	34.51	150	3.60	34.49	27.44
206	3.76	34.65	200	3.75	34.63	27.53
310	4.35	34.85	300	4.35	34.84	27.64
424	3.47	34.82	400	3.60	34.82	27.71
628	3.53	34.85	600	3.50	34.85	27.74
827	3.49	34.88	800	3.50	34.88	27.76
1,038	3.39	34.88	1,000	3.40	34.88	27.77
1,427	3.32	34.87				

Station 5537; June 8–9; latitude 45°40.5′ N., longitude 48°05′ W.; depth 649 m.; dynamic height 970.949

Observed values			Scaled values			
Depth, meters	Temperature, ° C.	Salinity, °/oo	Depth, meters	Temperature, ° C.	Salinity, °/oo	σt
0	3.66	33.01	0	3.66	33.01	26.26
24	1.59	33.54	25	1.60	33.55	26.86
48	1.85	33.84	50	1.85	33.85	27.08
71	0.93	33.97	75	0.95	34.00	27.26
95	1.03	34.11	100	1.10	34.13	27.36
143	1.47	34.26	140	1.55	34.28	27.44
190	1.72	34.39	200	1.75	34.40	27.53
285	2.06	34.50	300	2.15	34.52	27.60
361	2.57	34.62	400	2.80	34.67	27.66
549	3.18	34.76	(600)	3.25	34.77	27.70

Station 5938; June 9; latitude 45°45.5′ N., longitude 48°14′ W.; depth 167 m.; dynamic height 970.998

Observed values			Scaled values			
Depth, meters	Temperature, ° C.	Salinity, °/oo	Depth, meters	Temperature, ° C.	Salinity, °/oo	σt
0	2.60	32.70	0	2.60	32.70	26.10
26	1.15	33.06	25	1.20	33.05	26.49
52	−1.20	33.32	50	−1.15	33.03	26.80
78	−0.44	33.64	75	−0.55	33.60	27.02
104	0.41	33.89	100	0.35	33.87	27.20
155	0.65	33.96	150	0.65	83.95	27.24

Station 5539; June 9; latitude 45°48′ N., longitude 48°20′W.; depth 110 m.; dynamic height 971.024

Observed values			Scaled values			
Depth, meters	Temperature, ° C.	Salinity, °/oo	Depth, meters	Temperature, ° C.	Salinity, °/oo	σt
0	2.48	32.81	0	2.48	32.81	26.21
25	−0.63	32.88	25	−0.63	32.88	26.44
51	−1.23	33.09	50	−1.20	33.07	26.62
76	−1.14	33.19	75	−1.15	33.18	26.70
102	−0.90	33.37	100	−0.90	33.35	26.84

Table of Oceanographic Data—Continued

STATIONS OCCUPIED IN 1954—Continued

Station 5540; June 9; latitude 45°52′ N., longitude 48°28′ W.; depth 95 m.; dynamic height 971.026

Observed values			Scaled values			
Depth, meters	Temperature, ° C.	Salinity, ‰	Depth, meters	Temperature, ° C.	Salinity, ‰	σ_t
0	3.69	32.72	0	3.69	32.72	26.03
26	0.14	32.95	25	0.30	32.93	26.45
52	−1.04	33.11	50	−1.00	33.10	26.63
78	−0.93	33.24	75	−0.95	33.22	26.73

Station 5541; June 9; latitude 45°59′ N., longitude 48°42′W.; depth 80 m.; dynamic height 971.042

Observed values			Scaled values			
Depth, meters	Temperature, ° C.	Salinity, ‰	Depth, meters	Temperature, ° C.	Salinity, ‰	σ_t
0	4.27	32.64	0	4.27	32.64	25.91
26	2.11	32.78	25	2.20	32.78	26.20
52	1.11	32.87	50	1.20	32.86	26.34
67	−0.93	33.05	(75)	−1.10	33.13	26.66

Station 5542; June 9; latitude 46°13′ N., longitude 49°06′ W.; depth 67 m.; dynamic height 971.053

Observed values			Scaled values			
Depth, meters	Temperature, ° C.	Salinity, ‰	Depth, meters	Temperature, ° C.	Salinity, ‰	σ_t
0	5.15	32.50	0	5.15	32.50	25.70
26	3.62	32.56	25	3.70	32.56	25.90
53	0.65	32.85	50	1.00	32.82	26.32

Station 5543; June 9; latitude 46°11′ N., longitude 48°35′ W.; depth 88m.; dynamic height 971.037

Observed values			Scaled values			
Depth, meters	Temperature, ° C.	Salinity, ‰	Depth, meters	Temperature, ° C.	Salinity, ‰	σ_t
0	4.41	32.70	0	4.41	32.70	25.94
26	1.66	32.78	25	1.75	32.78	26.24
51	0.46	32.85	50	0.55	32.85	26.36
77	−0.97	33.12	75	−0.80	33.10	26.62

Station 5544; June 9; latitude 46°10′ N., longitude 47°59′W.; depth 117 m.; dynamic height 971.025

Observed values			Scaled values			
Depth, meters	Temperature, ° C.	Salinity, ‰	Depth, meters	Temperature, ° C.	Salinity, ‰	σ_t
0	3.53	32.71	0	3.53	32.71	26.03
26	0.93	32.75	25	1.00	32.75	26.26
51	−1.15	33.03	50	−1.10	33.03	26.58
77	−1.03	33.25	75	−1.05	33.24	26.75
103	−0.73	33.45	100	−0.80	33.43	26.89

Station 5545; June 9; latitude 46°09.5′ N., longitude 47°48′ W.; depth 176 m.; dynamic height 970.996

Observed values			Scaled values			
Depth, meters	Temperature, ° C.	Salinity, ‰	Depth, meters	Temperature, ° C.	Salinity, ‰	σ_t
0	3.15	32.74	0	3.15	32.74	26.10
24	0.28	33.07	25	0.25	33.08	26.57
49	−1.53	33.26	50	−1.50	33.26	26.78
73	−0.68	33.51	75	−0.65	33.53	26.97
97	0.23	33.81	100	0.30	33.83	27.16
146	0.72	33.99	150	0.75	34.00	27.28

Station 5546; June 9; latitude 46°09′ N., longitude 47°30′ W.; depth 652 m.; dynamic height 970.971

Observed values			Scaled values			
Depth, meters	Temperature, ° C.	Salinity, ‰	Depth, meters	Temperature, ° C.	Salinity, ‰	σ_t
0	3.76	32.78	0	3.76	32.78	26.07
25	−0.16	33.06	25	−0.16	33.06	26.57
50	−0.32	33.30	50	−0.32	33.30	26.76
75	−0.93	33.52	75	−0.93	33.52	26.98
99	0.01	33.75	100	0.05	33.76	27.13
149	1.11	34.15	150	1.15	34.16	27.38
199	2.13	34.42	200	2.15	34.42	27.52
298	2.64	34.63	300	2.65	34.63	27.64
377	3.17	34.76	400	3.25	34.77	27.70
565	3.35	34.81	(600)	3.35	34.81	27.72

Station 5547; June 9; latitude 46°08.5′ N., longitude 47°14′ W.; depth 1,463 m.; dynamic height 970.910

Observed values			Scaled values			
Depth, meters	Temperature, ° C.	Salinity, ‰	Depth, meters	Temperature, ° C.	Salinity, ‰	σ_t
0	3.35	33.32	0	3.35	33.32	26.53
27	1.72	33.57	25	1.85	33.55	26.85
53	1.18	33.82	50	1.20	33.80	27.09
79	1.26	34.00	75	1.25	33.97	27.22
105	1.53	34.26	100	1.45	34.21	27.40
159	2.27	34.51	150	2.20	34.48	27.56
211	2.56	34.60	200	2.50	34.58	27.61
316	3.10	34.73	300	3.05	34.71	27.67
425	3.33	34.82	400	3.30	34.80	27.72
629	3.48	34.87	600	3.50	34.85	27.74
830	3.45	34.88	800	3.45	34.88	27.76
1,044	3.43	34.88	1,000	3.45	34.88	27.76
1,482	3.36	34.88				

Station 5548; June 9; latitude 46°07′ N., longitude 46°37′ W.; depth 503 m.; dynamic height 970.940

Observed values			Scaled values			
Depth, meters	Temperature, ° C.	Salinity, ‰	Depth, meters	Temperature, ° C.	Salinity, ‰	σ_t
0	5.36	33.37	0	5.36	33.37	26.36
26	4.44	33.51	25	4.45	33.50	26.57
52	3.60	34.07	50	3.65	34.03	27.07
79	4.28	34.33	75	4.15	34.29	27.22
105	5.25	34.61	100	5.15	34.57	27.34
156	4.55	34.62	150	4.65	34.62	27.44
209	4.66	34.80	200	4.65	34.77	27.56
314	4.77	34.91	300	4.80	34.91	27.65
390	4.22	34.91	400	4.15	34.91	27.72
476	3.95	34.90				

Station 5549; June 10; latitude 46°05′ N., longitude 45°52′ W.; depth 1,737 m.; dynamic height 970.949

Observed values			Scaled values			
Depth, meters	Temperature, ° C.	Salinity, ‰	Depth, meters	Temperature, ° C.	Salinity, ‰	σ_t
0	4.48	33.33	0	4.48	33.33	26.42
25	2.91	33.36	25	2.91	33.36	26.61
50	3.32	33.63	50	3.32	33.63	26.78
74	3.81	34.16	75	3.85	34.16	27.16
99	3.98	34.36	100	4.00	34.36	27.30
149	4.02	34.58	150	4.05	34.58	27.46
198	4.33	34.74	200	4.35	34.74	27.56
297	4.11	34.83	300	4.10	34.83	27.66
406	3.61	34.81	400	3.65	34.81	27.69
606	3.63	34.86	600	3.65	34.86	27.73
804	3.53	34.87	800	3.55	34.87	27.75
1,008	3.40	34.88	1,000	3.40	34.88	27.77
1,525	3.30	34.89				

Station 5550; June 10; latitude 46°03′ N., longitude 45°10′ W.; depth 3,146 m.; dynamic height 970.971

Observed values			Scaled values			
Depth, meters	Temperature, ° C.	Salinity, ‰	Depth, meters	Temperature, ° C.	Salinity, ‰	σ_t
0	5.99	33.57	0	5.99	33.57	26.45
25	5.43	33.67	25	5.43	33.67	26.60
50	3.27	33.57	50	3.27	33.57	26.74
76	3.32	33.67	75	3.35	33.67	26.82
101	3.93	34.15	100	3.90	34.14	27.13
151	4.29	-------	150	4.30	34.51	27.39
202	4.01	34.64	200	4.00	34.63	27.51
303	4.69	34.89	300	4.70	34.88	27.63
408	4.58	34.95	400	4.65	34.95	27.70
610	4.03	34.93	600	4.05	34.93	27.74
810	3.80	34.93	800	3.80	34.93	27.77
1,016	3.62	34.90	1,000	3.65	34.91	27.77
1,542	3.45	34.91				

Table of Oceanographic Data—Continued

STATIONS OCCUPIED IN 1954—Continued

Station 5551; June 10; latitude 46°02′ N., longitude 44°40′ W., depth 3,585 m.; dynamic height 970.894

Observed values			Scaled values			
Depth, meters	Temperature, ° C.	Salinity ‰	Depth, meters	Temperature, ° C.	Salinity, ‰	σ_t
0	5.05	33.86	0	5.05	33.86	26.79
27	4.60	33.96	25	4.65	33.95	26.90
53	3.78	34.12	50	3.90	34.10	27.10
80	3.31	34.24	75	3.35	34.21	27.24
106	3.24	34.47	100	3.25	34.40	27.40
160	3.01	34.60	150	3.05	34.57	27.56
213	3.90	34.81	200	3.70	34.77	27.66
319	3.16	34.78	300	3.30	34.78	27.70
419	3.34	34.83	400	3.30	34.81	27.73
618	3.72	34.91	600	3.70	34.90	27.76
812	3.43	34.88	800	3.45	34.88	27.76
1,014	3.33	34.87	1,000	3.35	34.87	27.77
1,520	3.31	34.89				

Station 5552; June 10; latitude 46°20.5′ N., longitude 44°48′ W.; depth 2,195 m.; dynamic height 970.884

Observed values			Scaled values			
Depth, meters	Temperature, ° C.	Salinity ‰	Depth, meters	Temperature, ° C.	Salinity, ‰	σ_t
0	5.52	33.86	0	5.52	33.86	26.74
25	3.66	33.88	25	3.66	33.88	26.94
49	3.30	34.04	50	3.30	34.04	27.11
74	2.91	34.34	75	2.90	34.34	27.39
99	2.83	34.44	100	2.85	34.44	27.47
148	3.67	34.71	150	3.70	34.72	27.62
197	3.94	34.81	200	3.95	34.81	27.66
296	3.56	34.83	300	3.55	34.83	27.71
376	3.30	34.81	400	3.35	34.81	27.72
563	3.37	34.85	600	3.40	34.85	27.75
749	3.42	34.86	800	3.40	34.87	27.77
944	3.39	34.88	1,000	3.40	34.88	27.77
1,447	3.30	34.88				

Station 5553; June 10; latitude 46°28′ N., longitude 44°52′ W.; depth 805 m.; dynamic height 970.909

Observed values			Scaled values			
Depth, meters	Temperature, ° C.	Salinity ‰	Depth, meters	Temperature, ° C.	Salinity, ‰	σ_t
0	5.91	33.79	0	5.91	33.79	26.63
24	3.73	33.76	25	3.75	33.76	26.84
49	4.02	33.94	50	4.00	33.95	26.97
73	3.20	34.08	75	3.25	34.10	27.16
97	4.54	34.51	100	4.50	34.52	27.37
146	3.95	34.64	150	3.95	34.65	27.53
195	4.11	34.76	200	4.10	34.77	27.62
292	3.97	34.83	300	3.95	34.83	27.67
366	3.76	34.87	400	3.75	34.87	27.73
559	3.52	34.87	(600)	3.45	34.87	27.76

Station 5554; June 10; latitude 46°35′ N., longitude 44°54′ W.; depth 235 m.; dynamic height 970.935

Observed values			Scaled values			
Depth, meters	Temperature, ° C.	Salinity ‰	Depth, meters	Temperature, ° C.	Salinity, ‰	σ_t
0	6.05	33.73	0	6.05	33.73	26.56
27	4.69	33.79	25	4.80	33.78	26.75
53	3.72	33.86	50	3.80	33.85	26.91
80	4.07	34.07	75	3.90	34.02	27.04
106	5.19	34.49	100	5.00	34.38	27.20
160	4.23	34.57	150	4.35	34.55	27.41
213	4.11	34.70	200	4.15	34.67	27.53

Station 5555; June 10; latitude 46°43′ N., longitude 44°57′ W.; depth 180 m.; dynamic height 970.942

Observed values			Scaled values			
Depth, meters	Temperature, ° C.	Salinity ‰	Depth, meters	Temperature, ° C.	Salinity, ‰	σ_t
0	6.36	33.77	0	6.36	33.77	26.56
25	5.70	33.79	25	5.70	33.79	26.66
50	4.78	33.84	50	4.78	33.84	26.80
75	3.98	34.00	75	3.98	34.00	27.01
100	3.83	34.25	100	3.83	34.25	27.23
150	3.89	34.45	150	3.89	34.45	27.38

Station 5556; June 10; latitude 46°48′ N., longitude 44°58′ W.; depth 176 m.; dynamic height 970.939

Observed values			Scaled values			
Depth, meters	Temperature, ° C.	Salinity, ‰	Depth, meters	Temperature, ° C.	Salinity, ‰	σ_t
0	6.43	33.83	0	6.43	33.83	26.59
25	5.05	33.86	25	5.05	33.86	26.79
50	4.62	33.86	50	4.62	33.86	26.83
75	4.12	34.01	75	4.12	34.01	27.01
99	3.64	34.15	100	3.65	34.16	27.18
149	3.83	34.41	150	3.85	34.42	27.36

Station 5557; June 10; latitude 46°47.5′ N., longitude 45°14′ W.; depth 222 m.; dynamic height 970.953

Observed values			Scaled values			
Depth, meters	Temperature, ° C.	Salinity, ‰	Depth, meters	Temperature, ° C.	Salinity, ‰	σ_t
0	6.88	33.83	0	6.88	33.83	26.53
25	6.09	33.82	25	6.09	33.82	26.64
50	5.15	33.89	50	5.15	33.89	26.80
76	4.35	33.89	75	4.40	33.89	26.88
101	3.41	34.00	100	3.45	34.00	27.07
152	3.42	34.32	150	3.45	34.30	27.30
202	3.68	34.53	200	3.70	34.52	27.46

Station 5558; June 10; latitude 46°46.5′ N., longitude 45°43′ W.; depth 278 m.; dynamic height 970.949

Observed values			Scaled values			
Depth, meters	Temperature, ° C.	Salinity, ‰	Depth, meters	Temperature, ° C.	Salinity, ‰	σ_t
0	6.54	33.81	0	6.54	33.81	26.57
25	5.35	33.84	25	5.35	33.84	26.74
50	4.86	33.87	50	4.86	33.87	26.82
75	4.28	33.90	75	4.28	33.90	26.90
100	3.71	33.96	100	3.71	33.96	27.01
150	3.48	34.30	150	3.48	34.30	27.30
200	3.82	34.60	200	3.82	34.60	27.50
250	3.81	34.73				

Station 5559; June 10–11; latitude 46°46′ N., longitude 46°00′ W.; depth 326 m.; dynamic height 970.932

Observed values			Scaled values			
Depth, meters	Temperature, ° C.	Salinity, ‰	Depth, meters	Temperature, ° C.	Salinity, ‰	σ_t
0	6.34	33.79	0	6.34	33.79	26.57
25	5.09	33.87	25	5.09	33.87	26.80
50	4.82	33.87	50	4.82	33.87	26.83
74	4.47	33.91	75	4.45	33.91	26.89
99	3.67	34.11	100	3.65	34.12	27.15
149	3.48	34.46	150	3.50	34.46	27.43
173	3.80	34.59	200	3.95	34.69	27.56
198	3.92	34.69	300	3.70	34.83	27.70
297	3.72	34.83				

Station 5560; June 11; latitude 46°45.5′ N., longitude 46°24′ W.; depth 629 m.; dynamic height 970.901

Observed values			Scaled values			
Depth, meters	Temperature, ° C.	Salinity, ‰	Depth, meters	Temperature, ° C.	Salinity, ‰	σ_t
0	4.71	33.46	0	4.71	33.46	26.51
23	2.60	33.58	25	2.50	33.58	26.81
46	1.92	33.59	50	1.85	33.63	26.91
70	1.79	33.99	75	2.00	34.09	27.26
93	2.64	34.37	100	2.65	34.40	27.46
139	2.27	34.46	150	2.40	34.49	27.55
185	3.07	34.63	200	3.30	34.67	27.62
278	3.76	34.82	300	3.75	34.83	27.69
345	3.64	34.85	400	3.60	34.86	27.74
540	3.52	34.88	(600)	3.50	34.89	27.77

STATIONS OCCUPIED IN 1954—Continued

Station 5561; June 11; latitude 46°44.5′ N., longitude 46°51′ W.; depth 1,188 m.; dynamic height 970.887

Observed values			Scaled values			
Depth, meters	Temperature, ° C.	Salinity ‰	Depth, meters	Temperature, ° C.	Salinity, ‰	σ_t
0	4.74	33.55	0	4.74	33.55	26.58
27	3.14	33.89	25	3.20	33.87	26.99
53	2.19	33.94	50	2.25	33.94	27.12
80	1.23	34.22	75	1.35	34.16	27.37
106	1.71	34.34	100	1.60	34.32	27.48
160	2.24	34.55	150	2.15	34.51	27.59
214	2.66	34.65	200	2.60	34.63	27.64
320	3.18	34.78	300	3.10	34.76	27.71
379	3.45	34.81	400	3.50	34.82	27.72
581	3.53	34.87	600	3.50	34.87	27.76
793	3.47	34.88	800	3.45	34.88	27.76
1,012	3.37	34.87	1,000	3.40	34.87	27.77

Station 5562; June 11; latitude 46°44.5′ N., longitude 47°07′ W.; depth 622 m.; dynamic height 970.934

Observed values			Scaled values			
Depth, meters	Temperature, ° C.	Salinity ‰	Depth, meters	Temperature, ° C.	Salinity, ‰	σ_t
0	2.87	32.97	0	2.87	32.97	26.30
25	−0.16	33.35	25	−0.16	33.35	26.80
51	−0.43	33.69	50	−0.45	33.68	27.08
76	0.61	33.95	75	0.60	33.94	27.23
103	0.91	34.06	100	0.90	34.04	27.30
153	1.93	34.38	150	1.90	34.36	27.49
204	1.97	34.48	200	2.00	34.47	27.57
307	2.42	34.61	300	2.40	34.60	27.64
410	2.76	34.70	400	2.75	34.69	27.68
615	3.08	34.77	600	3.05	34.77	27.72

Station 5563; June 11; latitude 46°44.5′ N., longitude 47°14′ W.; depth 324 m.; dynamic height 970.957

Observed values			Scaled values			
Depth, meters	Temperature, ° C.	Salinity ‰	Depth, meters	Temperature, ° C.	Salinity, ‰	σ_t
0	2.72	32.95	0	2.72	32.95	26.30
24	−0.51	33.14	25	−0.60	33.14	26.65
47	−1.49	33.27	50	−1.45	33.29	26.79
71	−0.78	33.46	75	−0.70	33.51	26.96
94	−0.92	33.69	100	−0.15	33.74	27.12
141	0.94	34.06	150	1.10	34.14	27.37
189	1.60	34.38	200	1.70	34.41	27.54
283	2.33	34.58	300	2.45	34.60	27.63

Station 5564; June 11; latitude 46°44.5′ N., longitude 47°34′ W.; depth 172 m.; dynamic height 971.009

Observed values			Scaled values			
Depth, meters	Temperature, ° C.	Salinity ‰	Depth, meters	Temperature, ° C.	Salinity, ‰	σ_t
0	2.80	32.72	0	2.80	32.72	26.11
24	−0.04	32.96	25	−0.10	32.97	26.49
49	−1.55	33.16	50	−1.55	33.17	26.71
73	−1.59	33.23	75	−1.60	33.24	26.76
97	−1.46	33.32	100	−1.40	33.35	26.84
146	−0.14	33.75	150	0.00	33.79	27.15

Station 5565; June 11; latitude 46°46′ N., longitude 48°10′ W.; depth 112 m.; dynamic height 971.040

Observed values			Scaled values			
Depth, meters	Temperature, ° C.	Salinity ‰	Depth, meters	Temperature, ° C.	Salinity, ‰	σ_t
0	3.57	32.61	0	3.57	32.61	25.96
25	2.09	32.75	25	2.09	32.75	26.18
49	0.23	32.82	50	0.20	32.82	26.36
74	−0.89	33.02	75	−0.85	33.03	26.57
98	−0.71	33.26	100	−0.65	33.29	26.77

Station 5566; June 11; latitude 46°48′ N., longitude 48°43′ W.; depth 82 m.; dynamic height 971.043

Observed values			Scaled values			
Depth, meters	Temperature, ° C.	Salinity, ‰	Depth, meters	Temperature, ° C.	Salinity, ‰	σ_t
0	4.84	32.54	0	4.84	32.54	25.77
24	2.37	32.74	25	2.35	32.74	26.16
48	1.20	32.78	50	1.05	32.80	26.31
69	−0.98	33.05	75	−1.00	33.12	26.65

Station 5567; June 22; latitude 50°00′ N., longitude 49°00′ W.; depth 1,833 m.; dynamic height 970.846

Observed values			Scaled values			
Depth, meters	Temperature, ° C.	Salinity, ‰	Depth, meters	Temperature, ° C.	Salinity, ‰	σ_t
0	7.62	34.48	0	7.62	34.48	26.94
27	5.81	34.55	25	5.90	34.54	27.22
53	4.57	34.63	50	4.70	34.62	27.43
80	4.06	34.65	75	4.10	34.65	27.52
106	3.99	34.70	100	4.00	34.69	27.56
160	3.50	34.73	150	3.60	34.72	27.63
214	3.51	34.80	200	3.55	34.78	27.67
320	3.45	34.85	200	3.50	34.85	27.74
425	3.20	34.84	400	3.30	34.84	27.75
634	3.21	34.86	600	3.20	34.85	27.77
842	3.12	34.85	800	3.15	34.85	27.77
1,057	3.09	34.85	1,000	3.10	34.85	27.78
1,601	3.26	34.88				

Station 5568; June 22; latitude 49°46.5′ N., longitude 49°33′ W.; depth 1,412 m.; dynamic height 970.834

Observed values			Scaled values			
Depth, meters	Temperature, ° C.	Salinity, ‰	Depth, meters	Temperature, ° C.	Salinity, ‰	σ_t
0	6.30	33.89	0	6.30	33.89	26.66
27	6.14	34.51	25	6.15	34.46	27.13
53	3.99	34.59	50	4.35	34.58	27.43
80	3.17	34.67	75	3.30	34.66	27.61
106	3.06	34.72	100	3.10	34.71	27.67
160	2.85	34.76	150	2.90	34.76	27.73
213	2.84	34.78	200	2.85	34.78	27.74
319	2.86	34.78	300	2.85	34.78	27.74
386	2.88	34.80	400	2.95	34.80	27.75
582	3.13	34.84	600	3.15	34.84	27.76
780	3.12	34.85	800	3.10	34.85	27.78
991	3.13	34.86	1,000	3.15	34.86	27.78
1,334	3.23	34.87				

Station 5569; June 23; latitude 49°36′ N., longitude 50°01′ W.; depth 642 m.; dynamic height 970.869

Observed values			Scaled values			
Depth, meters	Temperature, ° C.	Salinity, ‰	Depth, meters	Temperature, ° C.	Salinity, ‰	σ_t
0	4.83	33.25	0	4.83	33.25	26.32
25	−0.20	33.87	25	−0.20	33.87	27.23
50	1.13	34.15	50	1.13	34.15	27.37
75	1.63	34.31	75	1.63	34.31	27.47
101	1.85	34.41	100	1.85	34.41	27.53
151	2.84	34.61	150	2.85	34.61	27.61
201	3.14	34.69	200	3.15	34.69	27.64
302	3.17	34.73	300	3.20	34.73	27.67
394	3.00	34.77	400	3.05	34.77	27.72
595	3.05	34.82	600	3.05	34.82	27.76

Station 5570; June 23; latitude 49°27′N., longitude 50°28′ W.; depth 326 m.; dynamic height 970.946

Observed values			Scaled values			
Depth, meters	Temperature, ° C.	Salinity, ‰	Depth, meters	Temperature, ° C.	Salinity, ‰	σ_t
0	5.18	32.86	0	5.18	32.86	25.98
24	−0,48	33.04	25	−0.50	33.05	26.58
48	−1.22	33.35	50	−1.25	33.36	26.85
72	−1.26	33.50	75	−1.25	33.52	26.99
96	0.29	33.78	100	0.45	33.82	27.15
144	1.12	34.09	150	1.20	34.12	27.35
193	1.62	34.33	200	1.70	34.36	27.50
289	2.48	34.63	(300)	2.60	34.66	27.67

Station 5571; June 23; latitude 49°19.5′ N., longitude 51°00′ W.; depth 333 m.; dynamic height 970.918

Observed values			Scaled values			
Depth, meters	Temperature, ° C.	Salinity ‰	Depth, meters	Temperature, ° C.	Salinity, ‰	σ_t
0	5.37	32.93	0	5.37	32.93	26.02
20	3.57	32.99	25	2.85	33.13	26.43
41	0.52	33.59	50	0.35	33.79	27.13
61	0.32	33.92	75	0.60	33.99	27.27
81	0.67	34.02	100	0.85	34.08	27.33
122	1.09	34.15	150	1.45	34.27	27.45
162	1.59	34.32	200	1.95	34.45	27.56
243	2.35	34.58	(300)	2.85	34.72	27.70

Station 5572; June 23; latitude 49°10.5′ N., longitude 51°34′ W.; depth 313 m.; dynamic height 970.983

Observed values			Scaled values			
Depth, meters	Temperature, ° C.	Salinity ‰	Depth, meters	Temperature, ° C.	Salinity, ‰	σ_t
0	5.63	32.31	0	5.63	32.31	25.50
25	1.66	32.99	25	1.66	32.99	26.41
49	−0.96	33.14	50	−1.00	33.15	26.68
74	−1.54	33.32	75	−1.55	33.33	26.84
98	−0.89	33.53	100	−0.85	33.55	26.99
147	0.08	33.90	150	0.15	33.92	27.25
196	1.24	34.17	200	1.30	34.19	27.39
294	2.34	34.58	300	2.40	34.60	27.64

Station 5573; June 23; latitude 49°04′ N., longitude 51°52′ W.; depth 297 m.; dynamic height 970.996

Observed values			Scaled values			
Depth, meters	Temperature, ° C.	Salinity ‰	Depth, meters	Temperature, ° C.	Salinity, ‰	σ_t
0	4.94	32.12	0	4.94	32.12	25.43
23	0.79	32.95	25	0.65	32.96	26.45
47	−0.93	33.10	50	−1.00	33.11	26.64
70	−1.44	33.24	75	−1.50	33.26	26.78
94	−1.59	33.35	100	−1.55	33.38	26.88
141	−0.08	33.76	150	0.20	33.83	27.17
188	1.11	34.06	200	1.30	34.12	27.34
277	2.16	34.50				

Station 5574; June 23; latitude 48°58′ N., longitude 52°06′ W.; depth 297 m.; dynamic height 971.007

Observed values			Scaled values			
Depth, meters	Temperature, ° C.	Salinity ‰	Depth, meters	Temperature, ° C.	Salinity, ‰	σ_t
0	4.99	31.99	0	4.99	31.99	25.32
25	−0.31	32.95	25	−0.31	32.95	26.48
50	−1.35	33.12	50	−1.35	33.12	26.66
74	−1.72	33.21	75	−1.70	33.21	26.75
99	−1.63	33.31	100	−1.60	33.31	26.82
149	−0.57	33.67	150	−0.55	33.68	27.08
199	0.92	34.07	200	0.95	34.08	27.32
283	2.11	34.46				

Station 5575; June 23; latitude 48°51′ N., longitude 52°22′ W.; depth 353 m.; dynamic height 971.048

Observed values			Scaled values			
Depth, meters	Temperature, ° C.	Salinity ‰	Depth, meters	Temperature, ° C.	Salinity, ‰	σ_t
0	5.66	31.81	0	5.66	31.81	25.10
25	−1.44	33.01	25	−1.44	33.01	26.58
50	−1.62	33.10	50	−1.62	33.10	26.65
75	−1.73	33.18	75	−1.73	33.18	26.72
100	−1.71	33.23	100	−1.71	33.23	26.76
150	−1.62	33.31	150	−1.62	33.31	26.82
201	−0.74	33.66	200	−0.75	33.65	27.07
301	1.66	34.31	300	1.65	34.30	27.46

Station 5576; June 23; latitude 48°47′ N., longitude 52°41′ W.; depth 220 m.; dynamic height 971.081

Observed values			Scaled values			
Depth, meters	Temperature, ° C.	Salinity, ‰	Depth, meters	Temperature, ° C.	Salinity, ‰	σ_t
0	5.85	31.45	0	5.85	31.45	24.79
25	−0.10	32.46	25	−0.10	32.46	26.08
50	−1.36	32.94	50	−1.36	32.94	26.52
75	−1.54	33.09	75	−1.54	33.09	26.64
100	−1.57	33.18	100	−1.57	33.18	26.71
151	−1.49	33.29	150	−1.50	33.28	26.79
201	−0.62	33.65	200	−0.60	33.64	27.05

Station 5577; June 23; latitude 48°45′ N., longitude 52°46′ W.; depth 165 m.; dynamic height 971.090

Observed values			Scaled values			
Depth, meters	Temperature, ° C.	Salinity, ‰	Depth, meters	Temperature, ° C.	Salinity, ‰	σ_t
0	4.94	31.39	0	4.94	31.39	24.85
24	−0.69	32.50	25	−0.75	32.51	26.15
49	−1.25	32.81	50	−1.30	32.82	26.42
73	−1.51	32.99	75	−1.50	32.99	26.56
97	−1.50	33.04	100	−1.50	33.04	26.60
136	−1.57	33.10	(150)	−1.55	33.16	26.70

Station 5578; June 23; latitude 48°42′ N., longitude 52°54′ W.; depth 104 m.; dynamic height 971.092

Observed values			Scaled values			
Depth, meters	Temperature, ° C.	Salinity, ‰	Depth, meters	Temperature, ° C.	Salinity, ‰	σ_t
0	4.82	31.43	0	4.82	31.43	24.89
25	0.50	32.17	25	0.50	32.17	25.82
49	−1.27	32.82	50	−1.30	32.83	26.42
74	−1.39	33.00	75	−1.35	33.01	26.58
			(100)	−1.50	33.08	26.63

Station 5579; June 23; latitude 48°37′ N., longitude 52°43′ W.; depth 247 m.; dynamic height 971.085

Observed values			Scaled values			
Depth, meters	Temperature, ° C.	Salinity, ‰	Depth, meters	Temperature, ° C.	Salinity, ‰	σ_t
0	5.77	31.34	0	5.77	31.34	24.71
24	0.20	32.40	25	0.15	32.45	26.06
47	−1.35	32.83	50	−1.35	32.84	26.43
71	−1.39	32.89	75	−1.40	32.91	26.49
94	−1.50	33.04	100	−1.50	33.05	26.60
141	−1.57	33.12	(150)	−1.55	33.15	26.69

Station 5580; June 24; latitude 48°34.5′ N., longitude 52°37′ W.; depth 261 m.; dynamic height 971.052

Observed values			Scaled values			
Depth, meters	Temperature, ° C.	Salinity, ‰	Depth, meters	Temperature, ° C.	Salinity, ‰	σ_t
0	5.59	31.32	0	5.59	31.32	24.72
26	1.44	32.55	25	1.50	32.51	26.04
51	−0.81	32.92	50	−0.75	32.91	26.47
77	−1.55	33.10	75	−1.55	33.08	26.63
103	−1.61	33.23	100	−1.60	33.21	26.74
153	−1.28	33.41	150	−1.30	33.40	26.89
205	−0.98	33.50	200	−1.00	33.49	26.95
247	−0.10	33.84				

Station 5581; June 24; latitude 48°22.5′ N., longitude 52°06′ W.; depth 190 m.; dynamic height 971.039

Observed values			Scaled values			
Depth, meters	Temperature, ° C.	Salinity, ‰	Depth, meters	Temperature, ° C.	Salinity, ‰	σ_t
0	4.38	32.14	0	4.38	32.14	25.50
25	0.88	32.51	25	0.88	32.51	26.07
49	−1.16	32.99	50	−1.20	33.00	26.56
74	−1.33	33.09	75	−1.30	33.10	26.64
98	−1.07	33.21	100	−1.05	33.22	26.73
147	−1.11	33.36	150	−1.10	33.37	26.85

Station 5582; June 24; latitude 48°17.5′ N., longitude 51°54′ W.; depth 185 m.; dynamic height 971.042

Observed values			Scaled values			
Depth, meters	Temperature, °C.	Salinity ‰	Depth, meters	Temperature, °C.	Salinity, ‰	σ_t
0	4.54	32.18	0	4.54	32.18	25.51
25	0.59	32.53	25	0.59	32.53	26.11
51	−0.93	32.88	50	−0.85	32.88	26.45
76	−1.44	33.06	75	−1.40	33.05	26.60
103	−1.61	33.23	100	−1.60	33.22	26.75
153	−1.51	33.32	150	−1.50	33.31	26.82
178	−1.02	33.49				

Station 5583; June 24· latitude 48°10′ N., longitude 51°37′ W.; depth 236 m.; dynamic height 971.053

Observed values			Scaled values			
Depth, meters	Temperature, °C.	Salinity ‰	Depth, meters	Temperature, °C.	Salinity, ‰	σ_t
0	4.71	32.08	0	4.71	32.08	25.42
25	−0.50	32.69	25	−0.50	32.69	26.28
50	−1.06	32.90	50	−1.06	32.90	26.47
75	−1.23	33.02	75	−1.23	33.02	26.58
100	−1.30	33.05	100	−1.30	33.05	26.60
149	−1.33	33.17	150	−1.30	33.17	26.70
199	−0.66	33.36	200	−0.60	33.36	26.82

Station 5584; June 24; latitude 48°02′ N., longitude 51°18′ W.; depth 155 m.; dynamic height 971.030

Observed values			Scaled values			
Depth, meters	Temperature, °C.	Salinity ‰	Depth, meters	Temperature, °C.	Salinity, ‰	σ_t
0	5.35	32.29	0	5.35	32.29	25.51
25	1.93	32.69	25	1.93	32.69	26.14
50	−0.89	32.87	50	−0.89	32.87	26.45
75	−1.17	33.00	75	−1.17	33.00	26.56
100	−1.30	33.14	100	−1.30	33.14	26.67
148	−0.71	33.48	150	−0.65	33.49	26.94

Station 5585; June 24; latitude 47°52.5′ N., longitude 50°56′ W.; depth 117 m.; dynamic height 971.026

Observed values			Scaled values			
Depth, meters	Temperature, °C.	Salinity ‰	Depth, meters	Temperature, °C.	Salinity, ‰	σ_t
0	5.49	32.55	0	5.49	32.55	25.70
25	2.40	32.67	25	2.40	32.67	26.10
50	−0.60	32.91	50	−0.60	32.91	26.46
76	−1.14	33.08	75	−1.10	33.07	26.61
101	−0.84	33.26	100	−0.85	33.25	26.74

Station 5586; June 24; latitude 47°43′ N., longitude 50°36′ W.; depth 128 m.; dynamic height 971.018

Observed values			Scaled values			
Depth, meters	Temperature, °C.	Salinity ‰	Depth, meters	Temperature, °C.	Salinity, ‰	σ_t
0	5.25	32.66	0	5.25	32.66	25.81
25	2.58	32.68	25	2.58	32.68	26.09
50	−0.89	33.01	50	−0.89	33.01	26.56
76	−1.13	33.20	75	−1.15	33.20	26.72
101	−1.16	33.31	100	−1.15	33.31	26.81

Station 5587; June 24; latitude 47°35.5′ N., longitude 50°19′ W.; depth 210 m.; dynamic height 971.022

Observed values			Scaled values			
Depth, meters	Temperature, °C.	Salinity ‰	Depth, meters	Temperature, °C.	Salinity, ‰	σ_t
0	5.49	32.65	0	5.49	32.65	25.78
24	3.09	32.66	25	2.70	32.66	26.06
48	−0.72	32.94	50	−0.70	32.95	26.50
72	−0.70	33.18	75	−0.70	33.20	26.71
97	−0.81	33.31	100	−0.80	33.32	26.80
145	−0.54	33.46	150	−0.50	33.48	26.92

Station 5588; June 24; latitude 47°27′ N., longitude 49°58′ W.; depth 77 m.; dynamic height 971.020

Observed values			Scaled values			
Depth, meters	Temperature, °C.	Salinity, ‰	Depth, meters	Temperature, °C.	Salinity, ‰	σ_t
0	5.95	32.64	0	5.95	32.64	25.73
25	3.56	32.67	25	3.56	32.67	26.00
50	0.19	32.86	50	0.19	32.86	26.39
64	−0.65	33.17	(75)	−0.75	33.40	26.87

Station 5589; June 24; latitude 47°44.5′ N., longitude 49°53′ W.; depth 119 m.; dynamic height 971.017

Observed values			Scaled values			
Depth, meters	Temperature, °C.	Salinity, ‰	Depth, meters	Temperature, °C.	Salinity, ‰	σ_t
0	5.16	32.47	0	5.16	32.47	25.68
25	2.39	32.56	25	2.39	32.56	26.01
50	−1.25	33.10	50	−1.25	33.10	26.64
76	−1.04	33.28	75	−1.05	33.27	26.77
101	−1.12	33.46	100	−1.10	33.45	26.92

Station 5590; June 24; latitude 47°57′ N., longitude 49°47′ W.; depth 172 m.; dynamic height 971.010

Observed values			Scaled values			
Depth, meters	Temperature, °C.	Salinity, ‰	Depth, meters	Temperature, °C.	Salinity, ‰	σ_t
0	5.90	32.26	0	5.90	32.26	25.42
25	1.95	32.87	25	1.95	32.87	26.29
49	−0.79	33.14	50	−0.80	33.15	26.66
74	−1.21	33.30	75	−1.20	33.31	26.81
98	−1.15	33.42	100	−1.10	33.43	26.90
147	−0.41	33.73	150	−0.35	33.76	27.14

Station 5591; June 24; latitude 48°14′ N., longitude 49°39′ W.; depth 224 m.; dynamic height 970.999

Observed values			Scaled values			
Depth, meters	Temperature, °C.	Salinity, ‰	Depth, meters	Temperature, °C.	Salinity, ‰	σ_t
0	5.67	32.31	0	5.67	32.31	25.49
25	2.29	32.77	25	2.29	32.77	26.19
50	−0.45	33.11	50	−0.45	33.11	26.62
75	−1.12	33.37	75	−1.12	33.37	26.85
100	−1.00	33.58	100	−1.00	33.58	27.02
149	0.53	33.96	150	0.55	33.97	27.27
199	1.06	34.12	200	1.10	34.12	27.36

Station 5592; June 25; latitude 48°30′ N., longitude 49°40′ W.; depth 659 m.; dynamic height 970.932

Observed values			Scaled values			
Depth, meters	Temperature, °C.	Salinity, ‰	Depth, meters	Temperature, °C.	Salinity, ‰	σ_t
0	5.13	32.66	0	5.13	32.66	25.82
22	1.64	33.04	25	1.20	33.07	26.51
43	−0.75	33.27	50	−0.70	33.34	26.82
65	−0.40	33.57	75	0.10	33.80	27.15
87	1.65	34.11	100	1.60	34.19	27.37
130	1.50	34.30	150	1.70	34.36	27.50
173	1.92	34.41	200	2.10	34.46	27.55
260	2.41	34.56	300	2.55	34.61	27.64
297	2.57	34.61	400	2.85	34.72	27.70
491	2.98	34.80	(600)	3.10	34.84	27.77

Station 5593; June 25; latitude 48°40.5′ N., longitude 49°25′ W.; depth 1,060 m.; dynamic height 970.884

Observed values			Scaled values			
Depth, meters	Temperature, °C.	Salinity, ‰	Depth, meters	Temperature, °C.	Salinity, ‰	σ_t
0	5.35	32.90	0	5.35	32.90	25.99
26	0.18	33.74	25	0.20	33.73	27.09
52	0.19	34.00	50	0.20	33.96	27.28
78	0.96	34.16	75	0.85	34.14	27.38
105	2.12	34.40	100	1.95	34.36	27.49
156	2.35	34.58	150	2.35	34.57	27.62
208	2.51	34.64	200	2.50	34.63	27.65
313	2.82	34.72	300	2.80	34.71	27.69
417	3.13	34.78	400	3.10	34.77	27.72
627	3.39	34.86	600	3.40	34.85	27.75
837	......	34.87	800	3.35	34.87	27.77
1,048	3.26	34.88	1,000	3.25	34.88	27.78

Station 5594; June 25; latitude 49°05′ N., longitude 49°12′ W.; depth 1,719 m.; dynamic height 970.823

Observed values			Scaled values			
Depth, meters	Temperature, ° C.	Salinity ‰	Depth, meters	Temperature, ° C.	Salinity, ‰	σ_t
0	6.71	33.98	0	6.71	33.98	26.67
25	5.34	34.34	25	5.34	34.34	27.13
50	3.65	34.58	50	3.65	34.58	27.50
74	2.97	34.66	75	2.95	34.66	27.64
99	2.73	34.69	100	2.70	34.69	27.68
149	2.62	34.72	150	2.65	34.72	27.72
198	2.70	34.76	200	2.70	34.77	27.75
297	2.94	34.81	300	2.95	34.81	27.76
379	3.08	34.84	400	3.10	34.84	27.77
569	3.15	34.86	600	3.15	34.86	27.78
760	3.15	34.85	800	3.15	34.86	27.78
957	3.14	34.86	1,000	3.15	34.86	27.78
1,461	3.24	34.88				

Station 5595; June 25; latitude 49°32.5′ N., longitude 49°06′ W.; depth 1,737 m.; dynamic height 970.813

Observed values			Scaled values			
Depth, meters	Temperature, ° C.	Salinity ‰	Depth, meters	Temperature, ° C.	Salinity, ‰	σ_t
0	7.36	34.16	0	7.36	34.16	26.73
25	4.73	34.40	25	4.73	34.40	27.25
49	3 44	34.67	50	3.40	34.68	27.61
74	3.04	34.73	75	3.00	34.73	27.69
98	2.94	34.75	100	2.95	34.75	27.71
147	2.87	34.77	150	2.85	34.77	27.74
197	2.78	34.78	200	2.80	34.78	27.74
295	3.19	34.84	300	3.20	34.84	27.76
326	3.10	34.84	400	3.10	34.84	27.77
528	3.08	34.85	600	3.05	34.85	27.78
756	3.09	34.85	800	3.10	34.85	27.78
952	3.10	34.855	1,000	3.10	34.86	27.79
1,455	3.24	34.89				

Station 5596; June 25; latitude 50°00′ N., longitude 48°59′ W.; depth 1,829 m.; dynamic height 970.872

Observed values			Scaled values			
Depth, meters	Temperature, ° C.	Salinity ‰	Depth, meters	Temperature, ° C.	Salinity, ‰	σ_t
0	8.04	34.50	0	8.04	34.50	26.89
23	7.86	34.50	25	7.55	34.50	26.97
46	5.40	34.58	50	5.20	34.59	27.35
69	4.58	34.64	75	4.50	34.64	27.46
92	4.26	34.65	100	4.20	34.66	27.52
138	4.07	34.69	150	4.05	34.70	27.56
183	3.90	34.74	200	3.85	34.76	27.63
275	3.67	34.82	300	3.70	34.84	27.71
330	3.65	34.85	400	3.45	34.85	27.74
501	3.18	34.84	600	3.05	34.82	27.76
676	3.02	34.82	800	3.10	34.83	27.76
859	3.10	34.84	1,000	3.10	34.85	27.78
1,343	3.13	34.86				

Station 5597; June 25; latitude 49°51.5′ N., longitude 48°19′ W.; depth 2,378 m.; dynamic height 970.872

Observed values			Scaled values			
Depth, meters	Temperature, ° C.	Salinity ‰	Depth, meters	Temperature, ° C.	Salinity, ‰	σ_t
0	8.29	34.50	0	8.29	34.50	26.85
26	6.09	34.63	25	6.15	34.62	27.26
52	4.02	34.69	50	4.10	34.68	27.54
78	3.57	34.72	75	3.60	34.72	27.63
103	3.38	34.74	100	3.40	34.74	27.66
156	3.05	34.76	150	3.10	34.76	27.71
207	2.92	34.79	200	2.95	34.78	27.73
310	2.91	34.81	300	2.90	34.81	27.77
406	2.99	34.84	400	3.00	34.84	27.78
607	3.04	34.845	600	3.05	34.84	27.78
810	3.08	34.85	800	3.10	34.85	27.78
1,018	3.12	34.875	1,000	3.10	34.87	27.80
1,549	3.10	34.92				

Station 5598; June 25; latitude 49°41.5′ N., longitude 47°42′ W.; depth 2,679 m.; dynamic height 970.868

Observed values			Scaled values			
Depth, meters	Temperature, ° C.	Salinity, ‰	Depth, meters	Temperature, ° C.	Salinity, ‰	σ_t
0	9.03	34.26	0	9.03	34.26	26.55
26	7.05	34.38	25	7.15	34.38	26.93
52	5.16	34.52	50	5.35	34.51	27.27
78	3.69	34.56	75	3.85	34.55	27.46
105	3.06	34.59	100	3.15	34.58	27.55
156	3.36	34.72	150	3.35	34.71	27.64
208	3.40	34.76	200	3.40	34.75	27.67
313	3.48	34.84	300	3.50	34.83	27.72
403	3.52	34.87	400	3.55	34.87	27.75
601	3.42	34.87	600	3.45	34.87	27.76
798	3.35	34.87	800	3.35	34.87	27.77
1,002	3.29	34.875	1,000	3.30	34.88	27.78
1,521	3.28	34.885				

Station 5599; June 26; latitude 49°16.5′ N., longitude 47°58′ W.; depth 2,332 m.; dynamic height 970.808

Observed values			Scaled values			
Depth, meters	Temperature, ° C.	Salinity, ‰	Depth, meters	Temperature, ° C.	Salinity, ‰	σ_t
0	8.76	34.48	0	8.76	34.48	26.77
24	6.63	34.58	25	6.55	34.58	27.17
48	3.74	34.69	50	3.65	34.70	27.60
72	3.36	34.74	75	3.30	34.74	27.67
96	3.16	34.77	100	3.15	34.77	27.71
144	3.01	34.81	150	3.00	34.81	27.76
191	3.00	34.83	200	3.00	34.83	27.77
287	3.02	34.84	300	3.05	34.84	27.77
369	3.03	34.85	400	3.05	34.85	27.78
554	3.12	34.86	600	3.15	34.86	27.78
739	3.09	34.86	800	3.05	34.86	27.79
933	3.06	34.86	1,000	3.05	34.86	27.79
1,431	3.16	34.91				

Station 5600; June 26; latitude 48°53.5′ N., longitude 48°13′ W.; depth 2,195 m.; dynamic height 970.840

Observed values			Scaled values			
Depth, meters	Temperature, ° C.	Salinity, ‰	Depth, meters	Temperature, ° C.	Salinity, ‰	σ_t
0	8.64	34.43	0	8.64	34.43	26.74
26	5.47	34.48	25	5.55	34.48	27.21
52	3.91	34.58	50	3.95	34.57	27.47
79	3.86	34.66	75	3.85	34.65	27.54
105	3.72	34.72	100	3.75	34.71	27.60
156	3.66	34.79	150	3.70	34.78	27.66
209	3.44	34.82	200	3.50	34.82	27.72
314	3.23	34.82	300	3.25	34.82	27.74
420	3.22	34.84	400	3.25	34.83	27.74
624	3.25	34.87	600	3.30	34.87	27.78
825	3.29	34.88	800	3.30	34.87	27.78
1,034	3.20	34.86	1,000	3.20	34.86	27.78
1,563	3.31	34.91				

Station 5601; June 26; latitude 48°31′ N., longitude 48°26′ W.; depth 1,792 m.; dynamic height 970.844

Observed values			Scaled values			
Depth, meters	Temperature, ° C.	Salinity, ‰	Depth, meters	Temperature, ° C.	Salinity, ‰	σ_t
0	7.26	33.74	0	7.26	33.74	26.42
22	4.84	34.11	25	4.50	34.15	27.08
45	2.43	34.49	50	2.40	34.51	27.57
67	2.37	34.56	75	2.40	34.57	27.62
90	2.40	34.59	100	2.45	34.61	27.64
135	2.75	34.68	150	2.75	34.69	27.68
179	2.69	34.71	200	2.75	34.72	27.71
269	2.92	34.77	300	3.05	34.79	27.73
363	3.32	34.84	400	3.30	34.84	27.75
553	3.18	34.84	600	3.20	34.84	27.76
749	3.25	34.86	800	3.25	34.86	27.77
950	3.18	34.86	1,000	3.20	34.86	27.78
1,476	3.24	34.89				

Station 5602; June 26; latitude 48°11′ N., longitude 48°36′ W.; depth 677 m.; dynamic height 970.915

Observed values			Scaled values			
Depth, meters	Temperature, ° C.	Salinity ‰	Depth, meters	Temperature, ° C.	Salinity, ‰	σ_t
0	5.48	32.70	0	5.48	32.70	25.82
25	1.88	33.18	25	1.88	33.18	26.55
50	0.46	33.74	50	0.46	33.74	27.08
74	0.25	33.96	75	0.25	33.96	27.28
99	1.76	34.31	100	1.80	34.32	27.47
148	2.58	34.58	150	2.60	34.59	27.61
198	3.07	34.71	200	3.10	34.71	27.67
297	2.88	34.74	300	2.90	34.74	27.71
341	2.87	34.74	400	2.85	34.74	27.71
528	2.85	34.75	(600)	2.85	34.75	27.72

Station 5603; June 26; latitude 48°05.5′ N., longitude 48°38′ W.; depth 324 m.; dynamic height 970.968

Observed values			Scaled values			
Depth, meters	Temperature, ° C.	Salinity ‰	Depth, meters	Temperature, ° C.	Salinity, ‰	σ_t
0	6.20	32.64	0	6.20	32.64	25.69
26	0.48	33.14	25	0.90	33.13	26.57
52	−1.02	33.46	50	−1.00	33.42	26.90
78	−0.59	33.72	75	−0.65	33.68	27.09
104	0.31	33.93	100	0.15	33.90	27.23
157	1.27	34.23	150	1.15	34.19	27.40
209	2.11	34.47	200	2.05	34.44	27.54
313	2.24	34.52	300	2.25	34.51	27.58

Station 5604; June 26; latitude 47°51′ N., longitude 48°44′ W.; depth 224 m.; dynamic height 971.018

Observed values			Scaled values			
Depth, meters	Temperature, ° C.	Salinity ‰	Depth, meters	Temperature, ° C.	Salinity, ‰	σ_t
0	6.74	32.22	0	6.74	32.22	25.29
26	−0.16	32.98	25	0.10	32.97	26.49
53	−1.00	33.15	50	−0.95	33.13	26.66
79	−1.54	33.33	75	−1.50	33.30	26.81
105	−0.75	33.59	100	−0.95	33.54	26.99
157	0.15	33.90	150	0.05	33.87	27.22
210	1.10	34.15	200	0.90	34.10	27.35

Station 5605; June 26; latitude 47°40.5′ N., longitude 48°49′ W.; depth 172 m.; dynamic height 971.033

Observed values			Scaled values			
Depth, meters	Temperature, ° C.	Salinity ‰	Depth, meters	Temperature, ° C.	Salinity, ‰	σ_t
0	5.87	32.62	0	5.87	32.62	25.72
25	−0.08	32.88	25	−0.08	32.88	26.42
51	−1.52	33.12	50	−1.50	33.11	26.65
76	−1.59	33.21	75	−1.60	33.21	26.75
101	−1.47	33.28	100	−1.45	33.28	26.79
152	−0.66	33.63	150	−0.70	33.61	27.04

Station 5606; June 26; latitude 47°44′ N., longitude 48°26′ W.; depth 226 m.; dynamic height 971.014

Observed values			Scaled values			
Depth, meters	Temperature, ° C.	Salinity ‰	Depth, meters	Temperature, ° C.	Salinity, ‰	σ_t
0	6.48	32.39	0	6.48	32.39	25.46
24	0.29	32.98	25	0.25	32.99	26.50
49	−0.50	33.17	50	−0.55	33.17	26.67
73	−1.50	33.29	75	−1.45	33.30	26.80
98	−0.83	33.51	100	−0.80	33.54	26.98
146	0.05	33.86	150	0.15	33.88	27.21
195	1.10	34.09	200	1.20	34.11	27.34

Station 5607; June 26; latitude 47°47′ N., longitude 48°08′ W.; depth 276 m.; dynamic height 971.001

Observed values			Scaled values			
Depth, meters	Temperature, ° C.	Salinity, ‰	Depth, meters	Temperature, ° C.	Salinity, ‰	σ_t
0	6.92	32.18	0	6.92	32.18	25.23
24	1.37	32.97	25	1.40	32.98	26.42
48	−1.02	33.22	50	−1.05	33.24	26.75
72	−1.07	33.38	75	−1.05	33.40	26.88
96	−0.60	33.62	100	−0.50	33.67	27.08
143	0.60	33.98	150	0.75	34.02	27.30
191	1.33	34.21	200	1.45	34.24	27.42
240	1.80	34.37				

Station 5608; June 27; latitude 47°50′ N., longitude 47°49′ W.; depth 309 m.; dynamic height 970.980

Observed values			Scaled values			
Depth, meters	Temperature, ° C.	Salinity, ‰	Depth, meters	Temperature, ° C.	Salinity, ‰	σ_t
0	6.54	32.46	0	6.54	32.46	25.50
27	1.89	33.16	25	2.30	33.12	26.47
52	−1.13	33.31	50	−1.05	33.30	26.79
78	−0.89	33.57	75	−0.95	33.53	26.98
103	−0.08	33.84	100	−0.15	33.81	27.18
156	1.24	34.17	150	1.15	34.14	27.36
208	1.77	34.40	200	1.70	34.37	27.51
278	2.10	34.46	(300)	2.20	34.48	27.56

Station 5609; June 27; latitude 47°59′ N., longitude 47°40′ W.; depth 368 m.; dynamic height 970.945

Observed values			Scaled values			
Depth, meters	Temperature, ° C.	Salinity, ‰	Depth, meters	Temperature, ° C.	Salinity, ‰	σ_t
0	6.20	32.68	0	6.20	32.68	25.72
25	0.71	33.20	25	0.71	33.20	26.64
51	−0.91	33.56	50	−0.90	33.54	26.99
76	−0.24	33.82	75	−0.25	33.81	27.18
102	0.34	33.99	100	0.30	33.98	27.28
151	1.32	34.27	150	1.30	34.26	27.45
202	2.22	34.51	200	2.20	34.50	27.58
304	2.72	34.66	300	2.70	34.65	27.65

Station 5610; June 27; latitude 48°17′ N., longitude 47°22′ W.; depth 1,654 m.; dynamic height 970.840

Observed values			Scaled values			
Depth, meters	Temperature, ° C.	Salinity, ‰	Depth, meters	Temperature, ° C.	Salinity, ‰	σ_t
0	6.29	33.47	0	6.29	33.47	26.33
26	1.79	34.32	25	1.80	34.28	27.43
52	1.90	34.42	50	1.90	34.41	27.33
78	2.07	34.49	75	2.05	34.48	27.57
104	2.28	34.56	100	2.25	34.55	27.61
155	2.55	34.65	150	2.55	34.64	27.66
208	2.81	34.71	200	2.75	34.70	27.69
312	3.24	34.79	300	3.20	34.78	27.71
399	3.19	34.82	400	3.20	34.82	27.75
596	3.30	34.86	600	3.30	34.86	27.77
789	3.28	34.87	800	3.30	34.87	27.78
992	3.20	34.87	1,000	3.20	34.87	27.79
1,509	3.29	34.89				

Table of Oceanographic Data—Continued

STATIONS OCCUPIED IN 1954—Continued

Station 5611; June 27; latitude 48°36.5′ N., longitude 47°02′ W.: depth 2,834 m.; dynamic height 970.839

Observed values			Scaled values			
Depth, meters	Temperature, ° C.	Salinity, ‰	Depth, meters	Temperature, ° C.	Salinity, ‰	σt
0	7.79	33.91	0	7.79	33.91	26.47
25	2.02	34.19	25	2.02	34.19	27.34
49	1.93	34.40	50	1.95	34.40	27.52
74	2.09	34.48	75	2.10	34.48	27.56
98	2.33	34.58	100	2.40	34.59	27.63
147	2.68	34.68	150	2.80	34.68	27.66
197	2.91	34.74	200	2.95	34.74	27.70
295	3.20	34.81	300	3.20	34.81	27.74
359	3.30	34.83	400	3.30	34.84	27.75
540	3.28	34.86	600	3.30	34.86	27.77
721	3.26	34.86	800	3.25	34.86	27.77
910	3.22	34.87	1,000	3.20	34.87	27.79
1,401	3.23	34.89				

Station 5612; June 27; latitude 48°58.5′ N., longitude 46°41′ W.; depth 2,726 m.; dynamic height 970.838

Observed values			Scaled values			
Depth, meters	Temperature, ° C.	Salinity, ‰	Depth, meters	Temperature, ° C.	Salinity, ‰	σt
0	9.61	34.29	0	9.61	34.29	26.48
25	5.55	34.42	25	5.55	34.42	27.17
50	4.06	34.52	50	4.06	34.52	27.42
75	3.15	34.58	75	3.15	34.58	27.55
99	2.73	34.65	100	2.75	34.65	27.65
149	2.79	34.72	150	2.80	34.72	27.70
199	3.05	34.78	200	3.05	34.78	27.72
298	3.09	34.82	300	3.10	34.82	27.76
391	3.22	34.85	400	3.25	34.85	27.76
584	3.35	34.88	600	3.35	34.88	27.77
774	3.25	34.865	800	3.25	34.87	27.78
973	3.27	34.87	1,000	3.25	34.87	27.78
1,479	3.30	34.90				

Station 5613; June 27; latitude 49°18.5′ N., longitude 46°22′ W.; depth 2,963 m.; dynamic height 970.914

Observed values			Scaled values			
Depth, meters	Temperature, ° C.	Salinity, ‰	Depth, meters	Temperature, ° C.	Salinity, ‰	σt
0	9.89	34.16	0	9.89	34.16	26.33
24	8.01	34.23	25	7.90	34.23	26.70
49	5.16	34.38	50	5.15	34.39	27.19
73	4.84	34.46	75	4.80	34.47	27.30
98	4.63	34.53	100	4.60	34.53	27.36
147	4.12	34.64	150	4.15	34.64	27.50
195	4.95	34.85	200	4.90	34.85	27.59
293	3.64	34.80	300	3.65	34.80	27.68
360	3.92	34.87	400	3.80	34.86	27.72
542	3.29	34.83	600	3.30	34.84	27.75
726	3.42	34.87	800	3.40	34.87	27.77
916	3.36	34.87	1,000	3.35	34.87	27.77
1,405	3.30	34.87				

Station 5614; June 27; latitude 49°11.5′ N., longitude 45°39′ W.; depth 2,743 m.; dynamic height 970.857

Observed values			Scaled values			
Depth, meters	Temperature, ° C.	Salinity, ‰	Depth, meters	Temperature, ° C.	Salinity, ‰	σt
0	9.12	34.24	0	9.12	34.24	26.53
24	5.68	34.37	25	5.60	34.37	27.13
49	4.55	34.47	50	4.50	34.47	27.34
73	3.22	34.44	75	3.20	34.44	27.44
97	3.03	34.56	100	3.00	34.57	27.57
145	2.77	34.64	150	2.80	34.65	27.64
194	2.77	34.71	200	2.80	34.72	27.70
291	3.34	34.83	300	3.35	34.83	27.73
330	3.41	34.84	400	3.40	34.85	27.75
503	3.38	34.86	600	3.40	34.87	27.77
681	3.38	34.87	800	3.35	34.87	27.77
860	3.32	34.87	1,000	3.30	34.87	27.78
1,320	3.20	34.86				

Station 5615; June 28; latitude 49°00.5′ N., longitude 44°58′ W.; depth 1,646 m.; dynamic height 970.836

Observed values			Scaled values			
Depth, meters	Temperature, ° C.	Salinity, ‰	Depth, meters	Temperature, ° C.	Salinity, ‰	σt
0	8.61	34.18	0	8.61	34.18	26.56
28	4.51	34.42	25	4.75	34.41	27.26
54	3.33	34.55	50	3.45	34.53	27.48
82	2.77	34.63	75	2.90	34.61	27.61
109	2.68	34.69	100	2.70	34.67	27.67
164	2.89	34.74	150	2.80	34.72	27.70
218	3.15	34.80	200	3.10	34.78	27.72
327	3.31	34.85	300	3.30	34.84	27.75
390	3.28	34.85	400	3.30	34.85	27.76
584	3.23	34.85	600	3.25	34.85	27.76
776	3.21	34.85	800	3.25	34.85	27.76
979	3.19	34.87	1,000	3.20	34.87	27.79
1,506	3.28	34.90				

Station 5616; June 28; latitude 48°39′ N., longitude 45°22′ W.; depth 1,042 m.; dynamic height 970.869

Observed values			Scaled values			
Depth, meters	Temperature, ° C.	Salinity, ‰	Depth, meters	Temperature, ° C.	Salinity, ‰	σt
0	8.15	33.95	0	8.15	33.95	26.45
26	5.55	34.06	25	5.60	34.06	26.88
52	3.54	34.30	50	3.70	34.29	27.27
78	2.96	34.39	75	3.00	34.37	27.41
105	2.93	34.53	100	2.95	34.51	27.52
156	2.63	34.65	150	2.65	34.64	27.65
208	3.07	34.76	200	3.00	34.75	27.71
313	3.30	34.82	300	3.30	34.81	27.73
409	3.40	34.85	400	3.40	34.85	27.75
610	3.47	34.88	600	3.50	34.88	27.76
808	3.38	34.88	800	3.40	34.88	27.77
994	3.29	34.875	1,000	3.30	34.88	27.78

Station 5617; June 28; latitude 48°16′ N., longitude 45°53′ W.; depth 1,097 m.; dynamic height 970.867

Observed values			Scaled values			
Depth, meters	Temperature, ° C.	Salinity, ‰	Depth, meters	Temperature, ° C.	Salinity, ‰	σt
0	8.17	33.84	0	8.17	33.84	26.36
25	2.43	33.82	25	2.43	33.82	27.01
50	2.85	34.29	50	2.85	34.29	27.35
75	2.39	34.39	75	2.39	34.39	27.47
100	2.76	34.53	100	2.76	34.53	27.55
150	3.26	34.69	150	3.26	34.69	27.63
200	3.32	34.75	200	3.32	34.75	27.68
300	3.43	34.82	300	3.43	34.82	27.72
409	3.60	34.87	400	3.60	34.87	27.75
610	3.51	34.89	600	3.55	34.89	27.76
809	3.34	34.88	800	3.40	34.88	27.77
1,028	3.26	34.88	1,000	3.25	34.88	27.78

Station 5618; June 28; latitude 47°57′ N., longitude 46°18′ W.; depth 1,143 m.; dynamic height 970.864

Observed values			Scaled values			
Depth, meters	Temperature, ° C.	Salinity, ‰	Depth, meters	Temperature, ° C.	Salinity, ‰	σt
0	7.97	33.55	0	7.97	33.55	26.17
25	2.62	34.05	25	2.62	34.05	27.18
50	2.82	34.36	50	2.82	34.36	27.41
76	2.69	34.48	75	2.70	34.48	27.51
101	3.06	34.62	100	3.05	34.62	27.60
151	2.90	34.69	150	2.90	34.69	27.67
202	3.22	34.77	200	3.20	34.77	27.71
303	3.35	34.83	300	3.35	34.83	27.73
394	3.44	34.85	400	3.45	34.85	27.74
589	3.48	34.85	600	3.50	34.85	27.74
781	3.41	34.88	800	3.45	34.88	27.76
998	3.33	34.88	1,000	3.30	34.88	27.78

STATIONS OCCUPIED IN 1954—Continued

Station 5619; June 28; latitude 47°53.5′ N., longitude 46°04′ W.; depth 860 m.; dynamic height 970.862

Observed values			Scaled values			
Depth, meters	Temperature, ° C.	Salinity, ‰	Depth, meters	Temperature, ° C.	Salinity, ‰	σ_t
0	8.11	33.48	0	8.11	33.48	26.08
25	3.85	34.07	25	3.85	34.07	27.09
50	2.53	34.32	50	2.53	34.32	27.41
76	2.15	34.41	75	2.15	34.41	27.51
101	2.80	34.57	100	2.80	34.57	27.58
151	2.72	34.63	150	2.70	34.63	27.63
202	3.25	34.76	200	3.25	34.75	27.68
303	3.35	34.80	300	3.35	34.80	27.71
427	3.50	34.86	400	3.50	34.85	27.74
634	3.46	34.89	600	3.45	34.89	27.77
839	3.34	34.89	800	3.30	34.89	27.79

Station 5620; June 28; latitude 47°48.5′ N., longitude 45°47′ W.; depth 425 m.; dynamic height 970.906

Observed values			Scaled values			
Depth, meters	Temperature, ° C.	Salinity, ‰	Depth, meters	Temperature, ° C.	Salinity, ‰	σ_t
0	8.69	33.36	0	8.69	33.36	25.89
25	4.43	33.63	25	4.43	33.63	26.67
50	3.38	33.93	50	3.38	33.93	27.01
75	3.41	34.23	75	3.41	34.23	27.25
100	.18	34.38	100	3.18	34.38	27.39
150	3.82	34.65	150	3.82	34.65	27.54
201	3.88	34.74	200	3.90	34.74	27.61
301	3.82	34.86	300	3.80	34.86	27.72
404	3.60	34.87	400	3.60	34.86	27.74

Station 5621; June 28; latitude 47°46′ N., longitude 45°40′ W.; depth 320 m.; dynamic height 970.932

Observed values			Scaled values			
Depth, meters	Temperature, ° C.	Salinity, ‰	Depth, meters	Temperature, ° C.	Salinity, ‰	σ_t
0	9.19	33.43	0	9.19	33.43	25.89
25	5.79	33.78	25	5.79	33.78	26.63
50	4.01	33.86	50	4.01	33.86	26.90
75	3.44	33.97	75	3.44	33.97	27.04
101	3.43	34.24	100	3.45	34.23	27.24
151	3.45	34.48	150	3.45	34.47	27.44
201	3.54	34.63	200	3.55	34.63	27.55
302	3.74	34.83	300	3.75	34.82	27.69

Station 5622; June 28; latitude 47°31′ N., longitude 45°13′ W.; depth 236 m.; dynamic height 970.950

Observed values			Scaled values			
Depth, meters	Temperature, ° C.	Salinity, ‰	Depth, meters	Temperature, ° C.	Salinity, ‰	σ_t
0	10.37	33.66	0	10.37	33.66	25.86
25	6.19	33.80	25	6.19	33.80	26.60
50	5.02	33.84	50	5.02	33.84	26.79
76	4.00	33.93	75	4.05	33.93	26.95
101	3.89	34.18	100	3.90	34.17	27.16
151	4.11	34.51	150	4.10	34.51	27.41
202	4.16	34.66	200	4.15	34.65	27.51

Station 5623; June 28; latitude 47°23′ N., longitude 45°02′ W.; depth 194 m.; dynamic height 970.961

Observed values			Scaled values			
Depth, meters	Temperature, ° C.	Salinity, ‰	Depth, meters	Temperature, ° C.	Salinity, ‰	σ_t
0	11.01	33.69	0	11.01	33.69	25.78
25	6.06	33.73	25	6.06	33.73	26.56
51	4.96	33.83	50	5.00	33.82	26.77
76	4.46	33.93	75	4.50	33.92	26.90
102	3.64	34.03	100	3.65	34.02	27.07
153	3.50	34.35	150	3.50	34.33	27.32

Station 5624; June 28; latitude 47°30.5′ N., longitude 45°01′ W.; depth 222 m.; dynamic height 970.951

Observed values			Scaled values			
Depth, meters	Temperature, ° C.	Salinity, ‰	Depth, meters	Temperature, ° C.	Salinity, ‰	σ_t
0	10.70	33.66	0	10.70	33.66	25.81
25	6.18	33.82	25	6.18	33.82	26.62
50	5.08	33.87	50	5.08	33.87	26.80
75	4.28	33.96	75	4.28	33.96	26.95
100	3.96	34.13	100	3.96	34.13	27.12
151	4.06	34.46	150	4.05	34.46	27.37
201	4.06	34.64	200	4.05	34.63	27.50

Station 5625; June 29; latitude 47°48.5′ N., longitude 45°02′ W.; depth 254 m.; dynamic height 970.959

Observed values			Scaled values			
Depth, meters	Temperature, ° C.	Salinity, ‰	Depth, meters	Temperature, ° C.	Salinity, ‰	σ_t
0	10.61	33.70	0	10.61	33.70	25.86
25	6.34	33.81	25	6.34	33.81	26.59
49	5.35	33.86	50	5.30	33.86	26.76
74	4.64	33.93	75	4.60	33.93	26.89
98	3.97	34.00	100	3.95	34.01	27.03
147	3.95	34.34	150	3.95	34.37	27.31
196	4.46	34.66	200	4.45	34.69	27.51

Station 5626; June 29; latitude 48°05′ N., longitude 45°02′ W.; depth 351 m.; dynamic height 970.918

Observed values			Scaled values			
Depth, meters	Temperature, ° C.	Salinity, ‰	Depth, meters	Temperature, ° C.	Salinity, ‰	σ_t
0	9.09	33.51	0	9.09	33.51	25.97
25	5.45	33.74	25	5.45	33.74	26.65
50	4.31	33.93	50	4.31	33.93	26.92
75	3.60	34.12	75	3.60	34.12	27.15
100	3.33	34.31	100	3.33	34.31	27.32
150	4.00	34.62	150	4.00	34.62	27.51
201	3.32	34.64	200	3.35	34.64	27.58
301	3.77	34.85	300	3.75	34.85	27.71

Station 5627; June 29; latitude 48°25′ N., longitude 45°02′ W.; depth 642 m.; dynamic height 970.886

Observed values			Scaled values			
Depth, meters	Temperature, ° C.	Salinity, ‰	Depth, meters	Temperature, ° C.	Salinity, ‰	σ_t
0	9.16	33.59	0	9.16	33.59	26.01
25	5.53	34.01	25	5.53	34.01	26.85
50	3.17	34.12	50	3.17	34.12	27.19
76	2.69	34.30	75	2.70	34.30	27.37
101	2.73	34.42	100	2.70	34.42	27.47
151	3.15	34.60	150	3.15	34.60	27.57
202	3.34	34.69	200	3.35	34.68	27.61
303	3.73	34.86	300	3.75	34.85	27.71
402	3.60	34.87	400	3.60	34.87	27.75
603	3.44	34.89	600	3.45	34.89	27.77

Station 5628; June 29; latitude 48°34′ N., longitude 45°02′ W.; depth 823 m.; dynamic height 970.867

Observed values			Scaled values			
Depth, meters	Temperature, ° C.	Salinity, ‰	Depth, meters	Temperature, ° C.	Salinity, ‰	σ_t
0	8.45	33.70	0	8.45	33.70	26.21
25	5.58	34.05	25	5.58	34.05	26.87
51	3.81	34.30	50	3.90	34.30	27.26
76	2.75	34.40	75	2.75	34.40	27.45
102	2.80	34.51	100	2.80	34.50	27.52
152	3.09	34.67	150	3.10	34.66	27.63
203	3.63	34.78	200	3.60	34.77	27.67
305	3.70	34.87	300	3.70	34.87	27.74
404	3.58	34.88	400	3.60	34.88	27.75
597	3.34	34.88	600	3.35	34.88	27.77
758	3.25	34.875	(800)	3.20	34.87	27.79

STATIONS OCCUPIED IN 1954—Continued

Station 5629; June 29; latitude 48°32′ N., longitude 44°15′ W.; depth 1,646 m.; dynamic height 970.840

Observed values			Scaled values			
Depth, meters	Temperature, ° C.	Salinity °/oo	Depth, meters	Temperature, ° C.	Salinity, °/oo	σ_t
0	9.24	33.91	0	9.24	33.91	26.25
25	4.47	34.31	25	4.47	34.31	27.21
51	3.13	34.52	50	3.15	34.51	27.50
76	2.71	34.63	75	2.75	34.62	27.63
101	2.69	34.67	100	2.70	34.67	27.67
152	2.83	34.72	150	2.85	34.72	27.70
203	3.05	34.78	200	3.05	34.78	27.72
304	3.27	34.82	300	3.25	34.82	27.74
413	3.26	34.84	400	3.25	34.84	27.75
610	3.29	34.86	600	3.30	34.86	27.77
800	3.25	34.86	800	3.30	34.86	27.77
1,003	3.26	34.87	1,000	3.25	34.87	27.78
1,517	3.30	34.88				

Station 5630; June 29; latitude 48°30′ N., longitude 43°30′ W.; depth 3,109 m.; dynamic height 970.862

Observed values			Scaled values			
Depth, meters	Temperature, ° C.	Salinity °/oo	Depth, meters	Temperature, ° C.	Salinity, °/oo	σ_t
0	10.17	33.95	0	10.17	33.95	26.12
25	7.62	34.26	25	7.62	34.26	26.77
50	4.08	34.47	50	4.08	34.47	27.38
75	3.51	34.56	75	3.51	34.56	27.51
100	2.76	34.65	100	2.76	34.65	27.65
150	2.82	34.70	150	2.82	34.70	27.68
199	3.25	34.79	200	3.25	34.79	27.71
299	3.32	34.83	300	3.35	34.83	27.73
389	3.26	34.84	400	3.30	34.84	27.75
580	3.35	34.88	600	3.35	34.87	27.77
768	3.31	34.87	800	3.35	34.87	27.77
965	3.31	34.87	1,000	3.30	34.87	27.78
1.469	3.30	34.885				

Station 5631; June 29; latitude 47°57.5′ N., longitude 43°28′ W.; depth 2,944 m.; dynamic height 970.909

Observed values			Scaled values			
Depth, meters	Temperature, ° C.	Salinity °/oo	Depth, meters	Temperature, ° C.	Salinity, °/oo	σ_t
0	12.36	34.16	0	12.36	34.16	25.89
25	5.63	34.13	25	5.63	34.13	26.93
50	6.50	34.66	50	6.50	34.66	27.24
76	5.28	34.58	75	5.30	34.58	27.32
101	5.78	34.87	100	5.75	34.87	27.51
151	5.44	34.86	150	5.45	34.86	27.53
202	4.75	34.86	200	4.80	34.86	27.61
303	3.63	34.79	300	3.65	34.79	27.67
406	4.07	34.91	400	4.05	34.91	27.73
601	3.74	34.90	600	3.75	34.90	37.75
792	3.56	34.895	800	3.60	34.89	27.76
994	3.43	34.88	1,000	3.45	34.88	27.76
1,507	3.35	34.89				

Station 5632; June 30; latitude 47°22′ N., longitude 43°26′ W.; depth 1,463 m.; dynamic height 970.858

Observed values			Scaled values			
Depth, meters	Temperature, ° C.	Salinity °/oo	Depth, meters	Temperature, ° C.	Salinity, °/oo	σ_t
0	10.58	33.61	0	10.58	33.61	25.79
25	6.28	34.23	25	6.28	34.23	26.92
50	3.88	34.50	50	3.88	34.50	27.42
75	3.26	34.53	75	3.26	34.53	27.50
101	2.87	34.59	100	2.90	34.58	27.58
151	2.77	34.69	150	2.80	34.69	27.67
201	3.07	34.78	200	3.10	34.78	27.72
302	3.30	34.83	300	3.30	34.83	27.74
387	3.29	34.85	400	3.30	34.85	27.76
577	3.30	34.87	600	3.30	34.87	27.78
765	3.26	34.87	800	3.30	34.87	27.78
963	3.26	34.87	1,000	3.25	34.87	27.78
1,472	3.29	34.90				

Station 5633; June 30; latitude 47°21′ N., longitude 43°51′ W.; depth 624 m.; dynamic height 970.887

Observed values			Scaled values			
Depth, meters	Temperature, ° C.	Salinity, °/oo	Depth, meters	Temperature, ° C.	Salinity, °/oo	σ_t
0	9.04	33.40	0	9.04	33.40	25.89
25	4.07	33.76	25	4.07	33.76	26.81
49	3.41	34.19	50	3.40	34.20	27.23
74	2.84	34.39	75	2.85	34.39	27.43
99	2.93	34.46	100	2.95	34.46	27.48
148	3.41	34.68	150	3.40	34.68	27.61
197	3.33	34.74	200	3.35	34.74	27.66
296	3.74	34.87	300	3.75	34.87	27.73
390	3.61	34.87	400	3.60	34.87	27.75
597	3.34	34.87	600	3.30	34.87	27.78

Station 5634; June 30; latitude 47°20.5′ N., longitude 44°09′ W.; depth 325 m.; dynamic height 970.934

Observed values			Scaled values			
Depth, meters	Temperature, ° C.	Salinity, °/oo	Depth, meters	Temperature, ° C.	Salinity, °/oo	σ_t
0	9.82	33.47	0	9.82	33.47	25.81
24	6.33	33.61	25	6.25	33.61	26.45
49	4.01	33.78	50	3.95	33.79	26.84
73	3.32	33.99	75	3.35	34.02	27.10
98	3.43	34.27	100	3.45	34.29	27.29
145	3.65	34.53	150	3.70	34.55	27.48
194	3.94	34.71	200	3.95	34.73	27.59
292	4.06	34.84	300	4.05	34.84	27.67

Station 5635; June 30; latitude 47°20′ N., longitude 44°28′ W.; depth 225 m.; dynamic height 970.955

Observed values			Scaled values			
Depth, meters	Temperature, ° C.	Salinity, °/oo	Depth, meters	Temperature, ° C.	Salinity, °/oo	σ_t
0	10.42	33.57	0	10.42	33.57	25.79
26	5.92	33.72	25	6.20	33.71	26.53
51	4.75	33.89	50	4.80	33.89	26.84
77	4.15	33.97	75	4.15	33.96	26.96
103	3.86	34.06	100	3.90	34.05	27.06
153	4.21	34.48	150	4.20	34.46	27.36
204	4.14	34.69	200	4.15	34.68	27.53

Station 5636; June 30; latitude 47°20′ N., longitude 45°00′ W.; depth 169 m.; dynamic height 970.959

Observed values			Scaled values			
Depth, meters	Temperature, ° C.	Salinity, °/oo	Depth, meters	Temperature, ° C.	Salinity, °/oo	σ_t
0	10.34	33.60	0	10.34	33.60	25.82
26	6.16	33.79	25	6.25	33.79	26.59
53	5.33	33.90	50	5.45	33.89	26.77
79	4.49	33.95	75	4.65	33.94	26.89
105	3.77	34.08	100	3.85	34.06	27.07
157	3.59	34.38	150	3.60	34.35	27.33

Station 5637; June 30; latitude 47°19.5′ N., longitude 45°20′ W.; depth 224 m.; dynamic height 970.957

Observed values			Scaled values			
Depth, meters	Temperature, ° C.	Salinity, °/oo	Depth, meters	Temperature, ° C.	Salinity, °/oo	σ_t
0	10.69	33.67	0	10.60	33.67	25.84
26	6.20	33.86	25	6.40	33.86	26.62
52	5.37	33.88	50	5.50	33.88	26.75
78	3.94	33.92	75	4.10	33.91	26.93
104	3.63	34.08	100	3.65	34.05	27.09
156	3.53	34.40	150	3.55	34.38	27.35
208	3.97	34.63	200	3.85	34.59	27.49

Station 5638; June 30; latitude 47°20′ N., longitude 45°40′ W.; depth 272 m.; dynamic height 970.955

Observed values			Scaled values			
Depth, meters	Temperature, ° C.	Salinity, °/oo	Depth, meters	Temperature, ° C.	Salinity, °/oo	σ_t
0	10.43	33.58	0	10.43	33.58	25.78
25	6.49	33.76	25	6.49	33.76	26.53
50	4.54	33.74	50	4.54	33.74	26.75
75	4.13	33.92	75	4.13	33.92	26.93
100	3.65	34.09	100	3.65	34.09	27.12
150	3.98	34.48	150	3.98	34.48	27.39
200	4.36	34.69	200	4.36	34.69	27.52

Table of Oceanographic Data—Continued

STATIONS OCCUPIED IN 1954—Continued

Observed values			Scaled values			
Depth, meters	Temperature, ° C.	Salinity °/oo	Depth, meters	Temperature, ° C.	Salinity, °/oo	σ_t
Station 5639; June 30; latitude 47°19.5′ N., longitude 45°58′ W.; depth 327 m.; dynamic height 970.940						
0	9.49	33.49	0	9.49	33.49	25.87
25	5.82	33.73	25	5.82	33.73	26.59
51	4.23	33.85	50	4.25	33.84	26.85
76	3.97	34.04	75	4.00	34.04	27.04
102	2.79	34.12	100	2.80	34.11	27.22
152	3.39	34.47	150	3.35	34.45	27.43
203	3.88	34.67	200	3.85	34.66	27.55
305	3.69	34.84	300	3.70	34.83	27.70
Station 5640; June 30; latitude 47°19′ N., longitude 46°28′ W.; depth 663 m.; dynamic height 970.895						
0	9.27	33.23	0	9.27	33.23	25.71
25	2.78	33.56	25	2.78	33.56	26.78
50	1.65	33.88	50	1.65	33.88	27.11
75	2.12	34.28	75	2.12	34.28	27.40
101	2.40	34.42	100	2.40	34.41	27.49
151	3.05	34.62	150	3.05	34.61	27.59
201	3.18	34.71	200	3.15	34.71	27.66
302	3.58	34.83	300	3.60	34.83	27.71
405	3.66	34.87	400	3.65	34.87	27.74
595	3.49	34.87	600	3.50	34.87	27.76
Station 5641; June 30; latitude 47°18′ N., longitude 46°43′ W.; depth 1,143 m.; dynamic height 970.880						
0	9.31	33.19	0	9.31	33.19	25.67
25	3.01	33.78	25	3.01	33.78	26.93
51	2.62	34.24	50	2.65	34.24	27.33
76	2.49	34.34	75	2.50	34.34	27.42
101	2.30	34.47	100	2.30	34.47	27.55
152	2.50	34.62	150	2.50	34.61	27.64
203	2.82	34.70	200	2.80	34.69	27.67
304	3.32	34.82	300	3.30	34.82	27.74
432	3.41	34.84	400	3.40	34.84	27.74
640	3.51	34.88	600	3.50	34.87	27.76
844	3.39	34.87	800	3.45	34.87	27.76
1,069	3.29	34.87	1,000	3.30	34.87	27.78
Station 5642; June 30; latitude 47°16.5′ N., longitude 47°02′ W.; depth 1005 m.; dynamic height 970.910						
0	7.15	32.63	0	7.15	32.63	25.56
25	4.76	33.69	25	4.76	33.69	26.69
51	1.01	34.10	50	1.00	34.09	27.33
76	1.07	34.19	75	1.05	34.19	27.41
101	1.91	34.41	100	1.90	34.40	27.52
152	2.44	34.56	150	2.40	34.56	27.61
203	2.52	34.61	200	2.50	34.61	27.64
304	2.60	34.63	300	2.60	34.63	27.64
404	2.75	34.70	400	2.75	34.70	27.69
600	3.20	34.81	600	3.20	34.81	27.74
793	3.34	34.85	800	3.35	34.85	27.75
1,006	3.31	34.88	1,000	3.30	34.88	27.78
Station 5643; July 1; latitude 47°15′ N., longitude 47°30′ W.; depth 220 m.; dynamic height 971.009						
0	8.21	32.24	0	8.21	32.24	25.10
26	1.07	33.06	25	1.40	33.04	26.47
51	−0.73	33.24	50	−0.70	33.24	26.74
77	−1.15	33.40	75	−1.15	33.39	26.88
102	−0.83	33.58	100	−0.85	33.56	27.00
154	0.36	33.97	150	0.25	33.95	27.27
205	1.48	34.29	200	1.40	34.26	27.45

Observed values			Scaled values			
Depth, meters	Temperature, ° C.	Salinity, °/oo	Depth, meters	Temperature, ° C.	Salinity, °/oo	σ_t
Station 5644; July 1; latitude 47°13′ N., longitude 47°53′ W.; depth 170m.; dynamic height 971.035						
0	8.77	32.62	0	8.77	32.62	25.31
25	3.05	32.73	25	3.05	32.73	26.10
51	−0.69	33.13	50	−0.65	33.11	26.63
76	−1.41	33.25	75	−1.40	33.25	26.76
101	−1.15	33.39	100	−1.15	33.38	26.87
152	−0.03	33.80	150	−0.10	33.78	27.14
Station 5645; July 1; latitude 47°11′ N., longitude 48°34′ W.; depth 121 m.; dynamic height 971.044						
0	8.46	32.55	0	8.46	32.55	25.30
25	2.88	32.69	25	2.88	32.69	26.07
51	−0.40	32.97	50	−0.30	32.95	26.48
76	−1.25	33.21	75	−1.25	33.20	26.72
102	−1.22	33.35	100	−1.20	33.34	26.84
Station 5646; July 1; latitude 47°09.5′ N., longitude 49°08′ W.; depth 89 m.; dynamic height 971.054						
0	8.85	32.58	0	8.85	32.58	25.27
26	3.54	32.66	25	3.90	32.66	25.96
53	0.79	32.79	50	0.95	32.78	26.29
79	−0.59	33.22	75	−0.45	33.14	26.65
Station 5647; July 1; latitude 46°50.5′ N., longitude 48°42′ W.; depth 87 m.; dynamic height 971.057						
0	10.65	32.50	0	10.65	32.50	24.91
26	3.96	32.69	25	4.20	32.68	25.95
51	0.64	32.84	50	0.75	32.83	26.34
77	−0.85	33.11	75	−0.75	33.08	26.61
Station 5648; July 1; latitude 46°50.5′ N., longitude 48°08′ W.; depth 117 m.; dynamic height 971.052						
0	10.21	32.56	0	10.21	32.56	25.04
25	3.29	32.64	25	3.29	32.64	26.00
50	0.31	32.82	50	0.31	32.82	26.36
76	−1.12	33.11	75	−1.10	33.10	26.63
101	−0.41	33.42	100	−0.40	33.41	26.87
Station 5649; July 1; latitude 46°50.5′ N., longitude 47°38′ W., depth 170 m.; dynamic height 971.023						
0	8.28	32.55	0	8.28	32.55	25.32
25	0.67	32.89	25	0.67	32.89	26.38
51	−1.44	33.15	50	−1.45	33.14	26.68
76	−1.49	33.31	75	−1.50	33.30	26.81
101	−1.08	33.43	100	−1.10	33.42	26.90
152	0.26	33.86	150	0.20	33.84	27.18
Station 5650; July 1; latitude 46°50.5′ N., longitude 47°18′ W.; depth 335 m.; dynamic height 970.998						
0	11.05	32.20	0	11.05	32.20	24.61
25	0.92	33.06	25	0.92	33.06	26.51
50	−1.11	33.33	50	−1.11	33.33	26.82
75	−0.66	33.61	75	−0.66	33.61	27.04
100	−0.29	33.78	100	−0.29	33.78	27.15
150	1.11	34.16	150	1.11	34.16	27.39
200	1.78	34.37	200	1.78	34.37	27.51
300	2.11	34.49	300	2.11	34.49	27.57

STATIONS OCCUPIED IN 1954—Continued

Station 5651; July 1; latitude 46°50.5′ N., longitude 47°12′ W.; depth 718 m.; dynamic height 970.971

Observed values			Scaled values			
Depth, meters	Temperature, ° C.	Salinity ‰	Depth, meters	Temperature, ° C.	Salinity, ‰	σ_t
0	11.02	32.61	0	11.02	32.61	24.93
25	2.25	33.28	25	2.25	33.28	26.60
51	−0.98	33.49	50	−0.95	33.47	26.94
76	−0.42	33.75	75	−0.45	33.73	27.12
101	0.11	33.94	100	0.10	33.93	27.25
152	1.16	34.23	150	1.10	34.22	27.44
203	1.88	34.42	200	1.85	34.41	27.53
304	2.51	34.60	300	2.50	34.59	27.62
412	2.65	34.68	400	2.65	34.67	27.68
608	2.87	34.74	600	2.90	34.74	27.71

Station 5652; July 1; latitude 46°50.5′ N., longitude 46°51′ W.; depth 1,188 m.; dynamic height 970.894

Observed values			Scaled values			
Depth, meters	Temperature, ° C.	Salinity ‰	Depth, meters	Temperature, ° C.	Salinity, ‰	σ_t
0	10.15	33.10	0	10.15	33.10	25.46
25	3.43	33.75	25	3.43	33.75	26.86
50	3.72	34.13	50	3.72	34.13	27.14
96	1.90	34.31	75	1.90	34.31	27.45
101	2.23	34.43	100	2.25	34.43	27.51
151	3.05	34.63	150	3.05	34.62	27.60
202	3.48	34.74	200	3.45	34.73	27.64
303	3.51	34.82	300	3.50	34.82	27.72
426	3.56	34.87	400	3.55	34.86	27.74
632	3.49	34.87	600	3.50	34.87	27.76
836	3.42	34.90	800	3.45	34.89	27.77
1,063	3.30	34.88	1,000	3.35	34.89	27.78

Station 5653; July 1; latitude 46°50′ N., longitude 46°32′ W.; depth 574 m.; dynamic height 970.903

Observed values			Scaled values			
Depth, meters	Temperature, ° C.	Salinity ‰	Depth, meters	Temperature, ° C.	Salinity, ‰	σ_t
0	11.01	33.24	0	11.01	33.24	25.43
25	3.02	33.54	25	3.02	33.54	26.74
51	1.23	33.88	50	1.25	33.87	27.14
76	1.73	34.16	75	1.70	34.14	27.32
101	2.35	34.39	100	2.35	34.37	27.46
152	3.40	34.66	150	3.35	34.65	27.59
304	3.97	34.81	200	3.95	34.80	27.65
203	3.89	34.85	300	3.90	34.85	27.70
405	3.65	34.86	400	3.70	34.86	27.73
551	3.45	34.86				

Station 5654; July 2; latitude 46°5′ N., longitude 46°08′ W.; depth 320 m.; dynamic height 970.941

Observed values			Scaled values			
Depth, meters	Temperature, ° C.	Salinity ‰	Depth, meters	Temperature, ° C.	Salinity, ‰	σ_t
0	11.87	33.64	0	11.87	33.64	25.58
25	5.84	33.80	25	5.84	33.80	26.65
50	5.56	33.88	50	5.56	33.88	26.74
75	4.00	33.98	75	4.00	33.98	26.99
100	3.45	34.10	100	3.45	34.10	27.14
150	2.57	34.36	150	2.57	34.36	27.44
200	3.76	34.68	200	3.76	34.68	27.57
300	3.60	34.85	300	3.60	34.85	27.73

Station 5655; July 2; latitude 46°49.5′ N., longitude 45°44′ W.; depth 260 m.; dynamic height 970.940

Observed values			Scaled values			
Depth, meters	Temperature, ° C.	Salinity ‰	Depth, meters	Temperature, ° C.	Salinity, ‰	σ_t
0	11.35	33.61	0	11.35	33.61	25.65
25	5.85	33.80	25	5.85	33.80	26.65
50	4.86	33.88	50	4.86	33.88	26.82
76	3.91	33.99	75	3.95	33.99	27.01
101	3.52	34.19	100	3.55	34.19	27.21
151	3.54	34.46	150	3.55	34.46	27.42
202	3.71	34.61	200	3.70	34.60	27.52

Station 5656; July 2; latitude 46°49′ N., longitude 45°21′ W.; depth 224 m.; dynamic height 970.946

Observed values			Scaled values			
Depth, meters	Temperature, ° C.	Salinity, ‰	Depth, meters	Temperature, ° C.	Salinity, ‰	σ_t
0	11.38	33.62	0	11.38	33.62	25.66
25	6.18	33.74	25	6.18	33.74	26.55
49	4.70	33.86	50	4.70	33.87	26.84
74	4.04	33.98	75	4.00	33.99	27.00
99	3.77	34.07	100	3.80	34.08	27.09
148	3.92	34.45	150	3.95	34.46	27.38
197	4.17	34.72	200	4.20	34.73	27.57

Station 5657; July 2; latitude 46°49′ N., longitud 45°04′ W.; depth 169 m.; dynamic height 970.95

Observed values			Scaled values			
Depth, meters	Temperature, ° C.	Salinity, ‰	Depth, meters	Temperature, ° C.	Salinity, ‰	σ_t
0	11.04	33.69	0	11.04	33.69	25.7
26	7.07	33.79	25	7.25	33.79	26.4
52	5.80	33.80	50	5.85	33.80	26.6
77	4.36	33.90	75	4.45	33.89	26.8
103	3.55	34.06	100	3.60	34.04	27.0
155	3.77	34.47	150	3.75	34.43	27.3

Station 5658; July 2; latitude 46°49′ N., longitud 44°32′ W.; depth 212 m.; dynamic height 970.94

Observed values			Scaled values			
Depth, meters	Temperature, ° C.	Salinity, ‰	Depth, meters	Temperature, ° C.	Salinity, ‰	σ_t
0	10.94	33.49	0	10.94	33.49	25.6
25	6.59	33.83	25	6.59	33.83	26.5
50	5.35	33.83	50	5.35	33.83	26.7
76	3.32	33.94	75	3.35	33.94	27.0
101	3.57	34.07	100	3.55	34.06	27.1
151	4.02	34.45	150	4.00	34.44	27.3
202	4.01	34.66	200	4.00	34.65	27.5

Station 5659; July 2; latitude 46°49′ N., longitu 44°15′ W.; depth 322 m.; dynamic height 970.9

Observed values			Scaled values			
Depth, meters	Temperature, ° C.	Salinity, ‰	Depth, meters	Temperature, ° C.	Salinity, ‰	σ_t
0	10.37	33.38	0	10.37	33.38	25.
25	4.87	33.57	25	4.87	33.57	26.
50	2.87	33.74	50	2.87	33.74	26.
75	3.53	34.27	75	3.53	34.27	27.
100	2.16	34.28	100	2.16	34.28	27.
150	2.98	34.56	150	2.98	34.56	27.
201	3.53	34.74	200	3.55	34.74	27.
301	3.78	34.86	300	3.75	34.86	27.

Station 5660; July 2; latitude 46°49′ N., longitu 44°01′W.; depth 622 m.; dynamic height 970.8

Observed values			Scaled values			
Depth, meters	Temperature, ° C.	Salinity, ‰	Depth, meters	Temperature, ° C.	Salinity, ‰	σ_t
0	10.36	33.45	0	10.36	33.45	25.
25	3.40	33.84	25	3.40	33.84	26.
50	3.73	34.25	50	3.73	34.25	27.
75	3.01	34.44	75	3.01	34.44	27.
101	3.15	34.55	100	3.15	34.54	27.
151	3.43	34.70	150	3.40	34.70	27.
201	3.44	34.77	200	3.45	34.77	27.
302	3.48	34.82	300	3.45	34.82	27.
411	3.46	34.87	400	3.45	34.87	27
611	3.28	34.87	600	3.30	34.87	27

Table of Oceanographic Data—Continued

STATIONS OCCUPIED IN 1954—Continued

Station 5661; July 2; latitude 46°49′ N., longitude 43°26′ W.; depth 2240 m; dynamic height 970.890

Observed values			Scaled values			
Depth, meters	Temperature, ° C.	Salinity, ‰	Depth, meters	Temperature, ° C.	Salinity, ‰	σ_t
0	12.61	33.66	0	12.61	33.66	25.45
25	4.64	33.96	25	4.64	33.96	26.91
49	3.93	34.16	50	3.95	34.16	27.15
74	3.96	34.39	75	3.95	34.39	27.33
98	3.16	34.47	100	3.20	34.48	27.47
148	3.44	34.68	150	3.45	34.68	27.60
197	3.18	34.73	200	3.20	34.73	27.67
295	3.21	34.79	300	3.20	34.79	27.72
402	3.28	34.84	400	3.30	34.84	27.75
600	3.29	34.86	600	3.30	34.86	27.77
795	3.28	34.865	800	3.30	34.86	27.77
1,001	3.26	34.86	1,000	3.25	34.86	27.77
1,526	3.29	34.90				

Station 5662; Aug 21; latitude 50°01′ N., longitude 48°59′ W.; depth 1,870 m; dynamic height 970.872

Observed values			Scaled values			
Depth, meters	Temperature, ° C.	Salinity, ‰	Depth, meters	Temperature, ° C.	Salinity, ‰	σ_t
0	11.48	33.11	0	11.48	33.11	25.24
25	5.71	34.39	25	5.71	34.39	27.13
49	4.55	34.85	50	4.55	34.58	27.41
74	3.92	34.62	75	3.95	34.62	27.51
99	3.93	34.68	100	3.90	34.68	27.56
148	3.41	34.71	150	3.45	34.71	27.63
197	3.81	34.83	200	3.70	34.83	27.70
268	3.34	34.85	300	3.50	34.85	27.74
553	3.14	34.84	400	3.30	34.85	27.76
740	3.21	34.84	600	3.15	34.84	27.76
934	3.18	34.83	800	3.20	34.84	27.76
1,432	3.22	34.89	1,000	3.20	34.84	27.76

Station 5663; Aug. 21; lat. 49°49′ N. longitude 49°29′ W.; depth 1,293 m.; dynamic height 970.851

Observed values			Scaled values			
Depth, meters	Temperature, ° C.	Salinity, ‰	Depth, meters	Temperature, ° C.	Salinity, ‰	σ_t
0	11.23	32.72	0	11.23	32.72	24.98
25	4.05	34.41	25	4.05	34.41	27.34
51	3.54	34.65	50	3.55	34.65	27.57
76	3.45	34.73	75	3.45	34.73	27.64
101	3.34	34.78	100	3.35	34.78	27.69
152	3.16	34.78	150	3.20	34.78	27.71
203	3.33	34.82	200	3.30	34.82	27.74
304	3.26	-------	300	3.30	34.81	27.73
398	3.09	34.79	400	3.10	34.79	27.73
593	3.03	34.84	600	3.05	34.84	27.77
784	3.10	34.84	800	3.10	34.84	27.77
960	3.12	34.84	1,000	3.15	34.84	27.76
1,287	3.17	34.86				

Station 5664; Aug. 22; latitude 49°36′ N., longitude 50°02′ W.; depth 626 m.; dynamic height 970.903

Observed values			Scaled values			
Depth, meters	Temperature, ° C.	Salinity, ‰	Depth, meters	Temperature, ° C.	Salinity, ‰	σ_t
0	9.74	31.63	0	9.74	31.63	24.38
25	3.02	34.12	25	3.02	34.12	27.20
49	1.62	34.21	50	1.65	34.32	27.48
74	2.44	-------	75	2.50	34.49	27.54
98	3.03	34.59	100	3.05	34.60	27.58
147	3.42	34.72	150	3.45	34.72	27.64
196	3.47	34.75	200	3.50	34.75	27.66
294	3.54	-------	300	3.55	34.78	27.67
395	3.55	34.79	400	3.55	34.79	27.68
597	3.23	34.81	600	3.20	34.81	27.74

Station 5665; Aug. 22; latitude 49°29′ N., longitude 50°21′ W.; depth 319 m.; dynamic height 970.936

Observed values			Scaled values			
Depth, meters	Temperature, ° C.	Salinity, ‰	Depth, meters	Temperature, ° C.	Salinity, ‰	σ_t
0	11.19	31.92	0	11.19	31.92	24.37
25	−0.86	33.54	25	−0.86	33.54	26.98
50	−0.46	33.81	50	−0.46	33.81	27.19
75	−0.02	33.94	75	−0.02	33.94	27.27
99	0.47	34.11	100	0.50	34.12	27.39
149	1.59	34.36	150	1.60	34.37	27.52
199	2.77	34.56	200	2.80	34.56	27.57
298	3.15	-------	(300)	3.15	34.72	27.67

Station 5666; Aug. 22; latitude 49°17′ N., longitude 50°59′ W.; depth 325 m.; dynamic height 971.010

Observed values			Scaled values			
Depth, meters	Temperature, ° C.	Salinity, ‰	Depth, meters	Temperature, ° C.	Salinity, ‰	σ_t
0	12.03	31.70	0	12.03	31.70	24.04
25	0.65	32.78	25	0.65	32.78	26.31
49	−1.41	33.17	50	−1.40	33.17	26.70
74	−1.19	33.41	75	−1.20	33.42	26.91
99	−1.06	33.62	100	−1.05	33.63	27.06
148	−0.01	33.96	150	0.00	33.98	27.30
197	1.39	34.25	200	1.45	34.26	27.44
296	2.86	-------	(300)	2.90	34.61	27.61

Station 5667; Aug. 22; latitude 49°07.5′ N., longitude 51°29′ W.; depth 317 m.; dynamic height 971.083

Observed values			Scaled values			
Depth, meters	Temperature, ° C.	Salinity, ‰	Depth, meters	Temperature, ° C.	Salinity, ‰	σ_t
0	11.48	31.40	0	11.48	31.40	23.92
25	0.66	32.76	25	0.66	32.76	26.29
50	−1.38	33.00	50	−1.38	33.00	26.57
74	−1.58	33.14	75	−1.55	33.14	26.68
99	−1.58	33.24	100	−1.55	33.24	26.75
149	−1.18	33.52	150	−1.15	33.53	26.99
198	−0.34	-------	200	−0.30	33.78	27.15
292	2.19	34.20	(300)	2.35	34.24	27.35

Station 5668; Aug. 22; latitude 49°01′ N., longitude 51°48′ W.; depth 324 m.; dynamic height 971.096

Observed values			Scaled values			
Depth, meters	Temperature, ° C.	Salinity, ‰	Depth, meters	Temperature, ° C.	Salinity, ‰	σ_t
0	11.72	31.29	0	11.72	31.29	23.78
23	0.38	32.63	25	0.10	32.70	26.27
46	−1.18	32.99	50	−1.30	33.01	26.57
69	−1.56	33.10	75	−1.60	33.11	26.66
93	−1.62	33.14	100	−1.60	33.17	26.71
139	−1.45	33.38	150	−1.35	33.43	26.91
185	−0.90	-------	200	−0.60	33.68	27.08
278	1.44	34.05	(300	1.95	34.17	27.34

Station 5669; Aug. 22; latitude 48°57′ N., longitude 52°02′ W.; depth 324 m.; dynamic height 971.110

Observed values			Scaled values			
Depth, meters	Temperature, ° C.	Salinity, ‰	Depth, meters	Temperature, ° C.	Salinity, ‰	σ_t
0	11.44	31.32	0	11.44	31.32	23.86
25	0.26	32.62	25	0.26	32.62	26.20
50	−1.44	32.99	50	−1.44	32.99	26.56
75	−1.62	33.12	75	−1.62	33.12	26.67
100	−1.63	33.16	100	−1.63	33.16	26.70
150	−1.51	33.34	150	−1.51	33.34	26.85
199	−0.94	-------	200	−0.95	33.56	27.01
299	1.51	34.00	300	1.50	34.00	27.23

Table of Oceanographic Data—Continued

STATIONS OCCUPIED IN 1954—Continued

Station 5670; Aug. 22; latitude 48°49.5′ N., longitude 52°21′ W.; depth 351 m.; dynamic height 971.090

Observed values			Scaled values			
Depth, meters	Temperature, ° C.	Salinity ‰	Depth, meters	Temperature, ° C.	Salinity, ‰	σt
0	11.20	31.32	0	11.20	31.32	23.90
24	−0.27	32.64	25	−0.30	32.67	26.26
49	−1.39	33.01	50	−1.40	33.02	26.58
73	−1.62	33.09	75	−1.65	33.09	26.64
98	−1.67	33.15	100	−1.65	33.16	26.70
147	−1.54	33.30	150	−1.50	33.31	26.82
195	−1.02	33.58	200	−0.95	33.62	27.06
293	1.01	34.19	(300)	1.20	34.24	27.44

Station 5671; Aug. 22; latitude 48°42.5′ N., longitude 52°41′ W.; depth 216 m.; dynamic height 971.087

Observed values			Scaled values			
Depth, meters	Temperature, ° C.	Salinity ‰	Depth, meters	Temperature, ° C.	Salinity, ‰	σt
0	10.93	-------	0	10.93	31.24	23.89
25	0.91	32.42	25	0.91	32.42	26.00
49	−1.12	32.90	50	−1.15	32.91	26.48
74	−1.51	33.05	75	−1.50	33.05	26.60
98	−1.59	33.12	100	−1.60	33.13	26.67
147	−1.39	33.40	150	−1.35	33.42	26.91
196	−1.19	-------	(200)	−1.15	33.75	27.17

Station 5672; Aug. 22; latitude 48°37′ N., longitude 52°53′ W.; depth 172 m.; dynamic height 971.099

Observed values			Scaled values			
Depth, meters	Temperature, ° C.	Salinity ‰	Depth, meters	Temperature, ° C.	Salinity, ‰	σt
0	11.49	31.18	0	11.49	31.18	23.74
25	0.82	32.24	25	0.82	32.24	25.86
51	−1.06	32.89	50	−1.00	32.88	26.45
76	−1.49	33.04	75	−1.45	33.04	26.60
101	−1.57	-------	100	−1.55	33.09	26.64
142	−1.56	33.21	(150)	−1.55	33.24	26.76

Station 5673; Aug. 22; latitude 48°34′ N., longitude 52°40′ W.; depth 260 m.; dynamic height 971.087

Observed values			Scaled values			
Depth, meters	Temperature, ° C.	Salinity ‰	Depth, meters	Temperature, ° C.	Salinity, ‰	σt
0	10.93	31.24	0	10.93	31.24	23.89
25	0.88	32.47	25	0.88	32.47	26.04
50	−0.68	32.82	50	−0.68	32.82	26.40
75	−1.39	33.05	75	−1.39	33.05	26.60
100	−1.58	33.14	100	−1.58	33.14	26.68
151	−1.44	33.36	150	−1.40	33.36	26.85
201	−1.06	-------	200	−1.05	33.58	27.02
241	−0.46	33.74				

Station 5674; Aug. 23; latitude 48°28′ N., longitude 52°16′ W.; depth 233 m.; dynamic height 971.083

Observed values			Scaled values			
Depth, meters	Temperature, ° C.	Salinity ‰	Depth, meters	Temperature, ° C.	Salinity, ‰	σt
0	11.08	31.35	0	11.08	31.35	23.94
23	0.09	32.67	25	−0.20	32.70	26.28
47	−1.20	32.92	50	−1.25	32.93	26.50
70	−1.49	33.07	75	−1.55	33.08	26.63
93	−1.60	33.11	100	−1.60	33.13	26.67
140	−1.60	33.25	150	−1.55	33.29	26.80
186	−1.30	33.46	(200)	−1.15	33.53	26.99

Station 5675; Aug. 23; latitude 48°25′ N., longitude 52°02′ W.; depth 210 m.; dynamic height 971.085

Observed values			Scaled values			
Depth, meters	Temperature, ° C.	Salinity ‰	Depth, meters	Temperature, ° C.	Salinity, ‰	σt
0	12.19	31.30	0	12.19	31.30	23.71
25	0.59	32.35	25	0.59	32.35	25.96
50	−1.07	32.96	50	−1.07	32.96	26.52
75	−1.61	33.11	75	−1.61	33.11	26.66
100	−1.62	33.14	100	−1.62	33.14	26.68
149	−1.40	33.36	150	−1.40	33.37	26.86
			(200)	−1.05	33.64	27.07

Station 5676; Aug. 23; latitude 48°20′ N., longitud 51°42′ W.; depth 178 m.; dynamic height 971.06

Observed values			Scaled values			
Depth, meters	Temperature, ° C.	Salinity, ‰	Depth, meters	Temperature, ° C.	Salinity, ‰	σt
0	12.26	31.30	0	12.26	31.30	23.6
26	0.17	32.78	25	0.25	32.68	26.2
52	−1.55	33.04	50	−1.50	33.03	26.5
78	−1.65	33.14	75	−1.65	33.14	26.6
104	−1.60	33.24	100	−1.60	33.23	26.7
155	−0.70	33.62	150	−0.80	33.57	27.0

Station 5677; Aug. 23; latitude 48°16′ N., longitud 51°25′ W.; depth 179 m.; dynamic height 971.06

Observed values			Scaled values			
Depth, meters	Temperature, ° C.	Salinity, ‰	Depth, meters	Temperature, ° C.	Salinity, ‰	σt
0	12.38	31.36	0	12.38	31.36	23.
25	1.19	32.88	25	1.19	32.88	26.
51	−1.11	33.05	50	−1.05	33.05	26.
76	−1.51	33.15	75	−1.50	33.15	26.
101	−1.45	33.25	100	−1.45	33.24	26.
153	−1.01	33.55	150	−1.05	33.53	26.

Station 5678; Aug. 23; latitude 48°10.5′ N., longitu 51°03′ W.; depth 172 m.; dynamic height 971.0

Observed values			Scaled values			
Depth, meters	Temperature, ° C.	Salinity, ‰	Depth, meters	Temperature, ° C.	Salinity, ‰	σt
0	12.69	31.27	0	12.69	31.27	23.
25	2.83	32.61	25	2.83	32.61	26.
50	−0.91	33.07	50	−0.91	33.07	26.
75	−1.49	33.22	75	−1.49	33.22	26.
100	−1.45	33.35	100	−1.45	33.35	26.
150	−0.44	33.72	150	−0.44	33.72	27.

Station 5679; Aug. 23; latitude 47°56′ N., longitu 50°39′ W.; depth 115 m.; dynamic height 971.0

Observed values			Scaled values			
Depth, meters	Temperature, ° C.	Salinity, ‰	Depth, meters	Temperature, ° C.	Salinity, ‰	σt
0	13.11	31.64	0	13.11	31.64	23.
25	0.04	32.92	25	0.04	32.92	26.
51	−1.20	33.06	50	−1.15	33.06	26.
76	−1.47	33.18	75	−1.45	33.18	26.
102	−1.18	33.37	100	−1.20	33.35	26.

Station 5680; Aug. 23; latitude 47°39.5′ N., longitu 50°19′ W.; depth 115 m.; dynamic height 971.0

Observed values			Scaled values			
Depth, meters	Temperature, ° C.	Salinity, ‰	Depth, meters	Temperature, ° C.	Salinity, ‰	σt
0	13.54	31.78	0	13.54	31.78	23.
26	3.97	32.64	25	4.20	32.62	25.
51	−1.01	33.10	50	−0.90	33.09	26.
77	−1.54	33.23	75	−1.50	33.22	26.
103	−1.32	33.40	100	−1.35	33.38	26.

Station 5681; Aug. 23; latitude 47°26′ N., longitu 50°00′ W.; depth 77 m.; dynamic height 971.

Observed values			Scaled values			
Depth, meters	Temperature, ° C.	Salinity, ‰	Depth, meters	Temperature, ° C.	Salinity, ‰	σt
0	13.96	31.66	0	13.96	31.66	23
27	1.88	32.76	25	2.10	32.69	26
53	−1.27	33.10	50	−1.25	33.08	26
69	−1.10	33.30	(75)	−1.00	33.37	26

Station 5682; Aug. 23; latitude 47°44′ N., longitu 49°56′ W.; depth 115 m.; dynamic height 971.

Observed values			Scaled values			
Depth, meters	Temperature, ° C.	Salinity, ‰	Depth, meters	Temperature, ° C.	Salinity, ‰	σt
0	13.38	31.76	0	13.38	31.76	23
24	1.68	32.76	25	1.40	32.79	26
48	−0.84	33.06	50	−0.90	33.07	26
72	−1.14	33.19	75	−1.10	33.22	26
96	−0.95	33.40	100	−0.90	33.45	26

STATIONS OCCUPIED IN 1954—Continued

Station 5683; Aug. 23; latitude 47°59′ N., longitude 49°54′ W.; depth 169 m.; dynamic height 971.073

Observed values			Scaled values			
Depth, meters	Temperature, ° C.	Salinity ‰	Depth, meters	Temperature, ° C.	Salinity, ‰	σ_t
0	13.05	31.64	0	13.05	31.64	23.80
23	6.55	32.44	25	5.60	32.51	25.66
45	−1.11	33.02	50	−1.25	33.04	26.59
68	−1.51	33.12	75	−1.55	33.16	26.70
91	−1.58	33.24	100	−1.50	33.29	26.80
136	−1.08	33.56	(150)	−0.90	33.69	27.11

Station 5684; Aug. 23; latitude 48°17.5′ N., longitude 49°51′ W.; depth 224 m.; dynamic height 971.043

Observed values			Scaled values			
Depth, meters	Temperature, ° C.	Salinity ‰	Depth, meters	Temperature, ° C.	Salinity, ‰	σ_t
0	11.68	31.48	0	11.68	31.48	23.56
23	−0.86	32.82	25	−1.00	32.86	26.44
46	−1.53	33.10	50	−1.55	33.13	26.67
69	−1.59	33.22	75	−1.55	33.25	26.77
93	−1.45	33.36	100	−1.35	33.40	26.89
139	−0.71	33.72	150	−0.50	33.80	27.18
185	0.17	33.99	(200)	0.45	34.06	27.34

Station 5685; Aug. 23; latitude 48°42′ N., longitude 49°41′ W.; depth 626 m.; dynamic height 970.935

Observed values			Scaled values			
Depth, meters	Temperature, ° C.	Salinity ‰	Depth, meters	Temperature, ° C.	Salinity, ‰	σ_t
0	10.98	32.08	0	10.98	32.08	24.53
27	4.24	33.28	25	4.65	33.23	26.33
53	0.93	33.93	50	1.10	33.84	27.12
80	1.53	34.25	75	1.45	34.21	27.40
106	2.38	34.47	100	2.20	34.43	27.52
160	2.97	34.64	150	2.90	34.62	27.62
213	3.31	34.72	200	3.30	34.71	27.65
319	3.34	34.73	300	3.30	34.73	27.66
402	3.51	34.79	400	3.50	34.79	27.69
606	3.20	--------	(600)	3.20	34.80	27.73

Station 5686; Aug. 24; latitude 48°48.5′ N., longitude 49°38′ W.; depth 1,064 m.; dynamic height 970.858

Observed values			Scaled values			
Depth, meters	Temperature, ° C.	Salinity ‰	Depth, meters	Temperature, ° C.	Salinity, ‰	σ_t
0	10.01	32.27	0	10.01	32.27	24.85
22	4.54	34.00	25	4.00	34.03	27.03
45	2.07	34.21	50	2.20	34.27	27.40
67	3.36	34.60	75	3.30	34.64	27.59
89	3.18	34.64	100	3.20	34.70	27.65
133	3.19	34.72	150	3.20	34.74	27.68
178	3.13	34.77	200	3.10	34.78	27.72
267	3.04	34.81	300	3.05	34.81	27.75
407	3.05	34.82	400	3.05	34.82	27.76
604	3.07	34.84	600	3.10	34.84	27.77
797	3.12	34.85	800	3.10	34.85	27.78
1,010	3.12	34.87	1,000	3.10	34.87	27.80

Station 5687; Aug. 24; latitude 49°06′ N., longitude 49°28′ W.; depth 1,485 m.; dynamic height 970.839

Observed values			Scaled values			
Depth, meters	Temperature, ° C.	Salinity ‰	Depth, meters	Temperature, ° C.	Salinity, ‰	σ_t
0	12.49	32.93	0	12.49	32.93	24.90
25	4.46	34.29	25	4.46	34.29	27.19
49	3.39	34.62	50	3.40	34.63	27.57
74	3.43	34.74	75	3.45	34.74	27.65
98	3.09	34.74	100	3.10	34.74	27.69
147	3.12	34.80	150	3.15	34.80	27.73
196	3.16	34.82	200	3.15	34.82	27.75
294	3.06	34.82	300	3.05	34.82	27.76
398	3.12	34.85	400	3.10	34.85	27.78
592	3.09	34.85	600	3.10	34.85	27.78
783	3.14	34.86	800	3.15	34.86	27.78
983	3.13	34.86	1,000	3.15	34.86	27.78
1,386	3.23	34.88				

Station 5688; Aug. 24; latitude 49°34′ N., longitude 49°13′ W.; depth 1,622 m.; dynamic height 970.841

Observed values			Scaled values			
Depth, meters	Temperature, ° C.	Salinity, ‰	Depth, meters	Temperature, ° C.	Salinity, ‰	σ_t
0	12.71	33.85	0	12.71	33.85	25.57
24	6.41	34.50	25	6.30	34.51	27.15
49	3.88	34.68	50	3.85	34.68	27.56
74	3.32	34.71	75	3.30	34.71	27.65
98	3.23	34.77	100	3.20	34.77	27.71
147	3.13	34.79	150	3.15	34.79	27.72
196	3.17	34.82	200	3.15	34.82	27.75
294	3.25	34.84	300	3.25	34.84	27.75
391	3.24	34.85	400	3.25	34.85	27.76
583	3.16	34.84	600	3.20	34.84	27.76
773	3.21	34.86	800	3.20	34.86	27.78
972	3.11	34.85	1,000	3.15	34.85	27.77
1,482	3.18	34.88				

Station 5689; Aug. 24; latitude 49°59′ N., longitude 49°00′ W.; depth 1,788 m.; dynamic height 970.863

Observed values			Scaled values			
Depth, meters	Temperature, ° C.	Salinity, ‰	Depth, meters	Temperature, ° C.	Salinity, ‰	σ_t
0	11.84	33.13	0	11.84	33.13	25.19
26	7.46	33.91	25	7.55	33.88	26.48
52	3.72	34.66	50	3.75	34.60	27.51
78	3.52	34.71	75	3.55	34.70	27.61
104	3.24	34.75	100	3.25	34.74	27.67
154	3.22	34.78	150	3.20	34.77	27.71
206	3.30	34.82	200	3.30	34.82	27.74
310	3.20	34.84	300	3.20	34.84	27.76
408	3.26	34.86	400	3.25	34.86	27.77
607	3.23	34.86	600	3.25	34.86	27.77
804	3.23	34.86	800	3.25	34.86	27.77
1,010	3.17	34.86	1,000	3.20	34.86	27.78
1,534	3.27	34.91				

Station 5690; Aug. 25; latitude 53°43′ N., longitude 55°49′ W.; depth 130 m.; dynamic height 1,454.985

Observed values			Scaled values			
Depth, meters	Temperature, ° C.	Salinity, ‰	Depth, meters	Temperature, ° C.	Salinity, ‰	σ_t
0	7.33	28.61	0	7.33	28.61	22.38
25	−0.79	32.55	25	−0.79	32.55	26.18
51	−1.45	32.76	50	−1.45	32.76	26.37
76	−1.54	32.81	75	−1.50	32.81	26.42
102	−1.58	32.85	100	−1.60	32.84	26.44

Station 5691; Aug. 25; latitude 53°50.5′ N., longitude 55°35′ W.; depth 218 m.; dynamic height 1,454.953

Observed values			Scaled values			
Depth, meters	Temperature, ° C.	Salinity, ‰	Depth, meters	Temperature, ° C.	Salinity, ‰	σ_t
0	7.37	28.90	0	7.37	28.90	22.60
25	−0.53	32.47	25	−0.53	32.47	26.11
50	−1.43	32.77	50	−1.43	32.77	26.38
75	−1.48	32.90	75	−1.48	32.90	26.48
100	−1.40	33.08	100	−1.40	33.08	26.63
151	−1.36	33.33	150	−1.35	33.33	26.83
201	−1.02	33.74	200	−1.05	33.73	27.14

Station 5692; Aug. 26; latitude 53°53.5′ N., longitude 55°26′ W.; depth 178 m.; dynamic height 1,454.912

Observed values			Scaled values			
Depth, meters	Temperature, ° C.	Salinity, ‰	Depth, meters	Temperature, ° C.	Salinity, ‰	σ_t
0	7.47	29.78	0	7.47	29.78	23.27
25	−0.13	32.60	25	−0.13	32.60	26.20
50	−1.30	33.02	50	−1.30	33.02	26.58
75	−1.38	33.17	75	−1.38	33.17	26.70
101	−1.36	33.31	100	−1.35	33.31	26.81
151	−1.18	33.64	150	−1.20	33.64	27.08

Station 5693; Aug. 26; latitude 54°04′ N.; longitude 55°04′ W.; depth 165 m.; dynamic height 1,454.910

Observed values			Scaled values			
Depth, meters	Temperature, ° C.	Salinity °/oo	Depth, meters	Temperature, ° C.	Salinity, °/oo	σt
0	7.94	30.75	0	7.94	30.75	23.98
25	−1.34	32.84	25	−1.34	32.84	26.43
50	−1.49	32.89	50	−1.49	32.89	26.47
75	−1.47	33.05	75	−1.47	33.05	26.60
99	−1.42	33.14	100	−1.40	33.14	26.68
149	−1.33	33.50	150	−1.35	33.51	26.98

Station 5694; Aug. 26; latitude 54°10.5′ N., longitude 54°54′ W.; depth 178 m.; dynamic height 1,454.891

Observed values			Scaled values			
Depth, meters	Temperature, ° C.	Salinity °/oo	Depth, meters	Temperature, ° C.	Salinity, °/oo	σt
0	7.99	30.87	0	7.99	30.87	24.06
25	−0.29	32.66	25	−0.29	32.66	26.25
50	−1.42	33.07	50	−1.42	33.07	26.62
76	−1.40	33.27	75	−1.40	33.27	26.78
101	−1.39	33.43	100	−1.35	33.43	26.91
151	−1.09	33.68	150	−1.10	33.68	27.11

Station 5695; Aug. 26; latitude 54°28′ N., longitude 54°24′ W.; depth 220 m.; dynamic height 1,454.911

Observed values			Scaled values			
Depth, meters	Temperature, ° C.	Salinity °/oo	Depth, meters	Temperature, ° C.	Salinity, °/oo	σt
0	7.34	30.95	0	7.34	30.95	24.22
25	−0.22	32.57	25	−0.22	32.57	26.18
50	−1.25	32.90	50	−1.25	32.90	26.48
75	−1.37	33.07	75	−1.37	33.07	26.62
100	−1.36	33.24	100	−1.36	33.24	26.76
151	−1.29	33.51	150	−1 30	33.51	26.98
201	−1.06	33.67	200	−1.05	33.67	27.10

Station 5696; Aug. 26; latitude 54°46′ N., longitude 53°51′ W.; depth 329 m.; dynamic height 1,454.843

Observed values			Scaled values			
Depth, meters	Temperature, ° C.	Salinity °/oo	Depth, meters	Temperature, ° C.	Salinity, °/oo	σt
0	6.42	31.50	0	6.42	31.50	24.77
25	3.46	32.87	25	3.46	32.87	26.17
50	−0.30	33.19	50	−0.30	33.19	26.68
75	−0.59	33.46	75	−0.59	33.46	26.91
100	−0.41	33.62	100	−0.41	33.62	27.04
150	0.27	34.00	150	0.27	34.00	27.30
201	0.87	34.19	200	0.90	34.19	27.42
301	2.15	34.41	300	2.15	34.41	27.51

Station 5697; Aug. 26; latitude 54°52′ N., longitude 53°38′ W.; depth 657 m.; dynamic height 1,454.754

Observed values			Scaled values			
Depth, meters	Temperature, ° C.	Salinity °/oo	Depth, meters	Temperature, ° C.	Salinity, °/oo	σt
0	4.80	32.80	0	4.80	32.80	25.98
24	1.30	33.39	25	1.15	33.40	26.77
48	−0.33	33.66	50	−0.30	33.67	27.07
71	0.11	33.86	75	0.20	33.89	27.22
95	0.68	34.06	100	0.80	34.10	27.35
143	1.82	34.35	150	1.95	34.38	27.50
190	2.53	34.49	200	2.65	34.51	27.55
285	3.34	34.66	300	3.45	34.67	27.60
372	3.70	34.72	400	3.75	34.74	27.62
574	3.79	34.83	(600)	3.80	34.84	27.70

Station 5698; Aug. 26; latitude 54°59′ N.; longitude 53°24′ W.; depth 1,719 m.; dynamic height 1,454.689

Observed values			Scaled values			
Depth, meters	Temperature, ° C.	Salinity, °/oo	Depth, meters	Temperature, ° C.	Salinity, °/oo	σt
0	6.94	33.27	0	6.94	33.27	26.09
25	7.63	33.73	25	7.63	33.73	26.35
50	2.09	34.05	50	2.09	34.05	27.22
75	1.87	34.29	75	1.87	34.29	27.43
100	2.42	34.48	100	2.42	34.48	27.53
150	3.58	34.75	150	3.58	34.75	27.65
200	3.63	34.78	200	3.63	34.78	27.66
300	3.59	34.79	300	3.59	34.79	27.68
377	3.50	34.84	400	3.50	34.84	27.73
565	3.50	34.83	600	3.50	34.84	27.73
754	3.53	34.88	800	3.55	34.88	27.75
946	3.50	34.88	1,000	3.50	34.88	27.76
1,432	3.37	34.86	(1,500)	3.35	34.86	27.76

Station 5699; Aug. 26; latitude 55°02′ N., longitude 53°14′ W.; depth 2,103 m.; dynamic height 1,454.646

Observed values			Scaled values			
Depth, meters	Temperature, ° C.	Salinity, °/oo	Depth, meters	Temperature, ° C.	Salinity, °/oo	σt
0	7.87	33.70	0	7.87	33.70	26.30
25	7.48	33.80	25	7.48	33.80	26.42
50	3.46	34.12	50	3.46	34.12	27.16
74	2.68	34.24	75	2.70	34.24	27.32
99	3.83	34.63	100	3.80	34.64	27.54
149	3.40	34.73	150	3.40	34.73	27.65
198	3.21	34.75	200	3.20	34.75	27.69
297	3.18	34.82	300	3.20	34.82	27.75
378	3.23	34.84	400	3.25	34.84	27.75
563	3.37	34.87	600	3.35	34.87	27.77
745	3.37	34.89	800	3.35	34.89	27.78
924	3.39	34.89	1,000	3.40	34.89	27.78
1,413	3.31	34.90	1,500	3.30	34.90	27.80
1,920	3.05	34.92	(2,000)	2.95	34.92	27.85

Station 5700; Aug. 26; latitude 55°14′ N., longitude 5251′ W.; depth 3,113 m.; dynamic height 1,454.639

Observed values			Scaled values			
Depth, meters	Temperature, ° C.	Salinity, °/oo	Depth, meters	Temperature, ° C.	Salinity, °/oo	σt
0	8.09	33.70	0	8.09	33.70	26.26
25	7.74	33.69	25	7.74	33.69	26.30
50	2.35	34.22	50	2.35	34.22	27.34
75	2.90	34.56	75	2.90	34.56	27.57
101	3.25	34.68	100	3.25	34.68	27.62
151	3.56	34.78	150	3.55	34.78	27.67
201	3.55	34.82	200	3.55	34.82	27.71
302	3.42	34.83	300	3.45	34.83	27.72
381	3.40	34.85	400	3.40	34.85	27.75
575	3.14	34.84	600	3.15	34.84	27.76
771	3.16	34.84	800	3.20	34.86	27.78
971	3.20	34.86	1,000	3.20	34.86	27.78
1,480	3.14	34.86	1,500	3.15	34.86	27.78
2,006	3.27	34.925	2,000	3.30	34.92	27.82
2,536	2.76	34.93	2,500	2.80	34.93	27.80
2,981	1.79	34.89	3,000	1.75	34.88	27.91

Station 5701; Aug. 26–27; latitude 55°31.5′ N., longitude 52°25′ W.; depth 3,182 m.; dynamic height 1,454.644

Observed values			Scaled values			
Depth, meters	Temperature, ° C.	Salinity °/oo	Depth, meters	Temperature, ° C.	Salinity, °/oo	σt
0	9.85	33.97	0	9.85	33.97	26.20
25	9.26	34.40	25	9.26	34.40	26.63
50	4.64	34.67	50	4.64	34.67	27.48
75	4.07	34.66	75	4.07	34.66	27.53
101	3.90	34.72	100	3.90	34.72	27.60
151	3.68	34.74	150	3.70	34.74	27.63
201	3.58	34.80	200	3.60	34.80	27.69
302	3.24	34.80	300	3.25	34.80	27.72
385	3.21	34.82	400	3.20	34.82	27.75
585	3.22	34.835	600	3.20	34.83	27.75
789	3.23	34.84	800	3.25	34.84	27.75
999	3.23	34.85	1,000	3.25	34.85	27.76
1,520	3.20	34.87	1,500	3.20	34.87	27.79
2,037	3.36	34.91	2,000	3.35	34.91	27.80
2,535	2.99	34.915	2,500	3.05	34.91	27.83
3,022	2.30	34.87	3,000	2.35	34.87	27.86

Station 5702; Aug. 27; latitude 55°56′ N., longitude 51°48′ W.; depth 3,457 m.; dynamic height 1,454.623

Observed values			Scaled values			
Depth, meters	Temperature, ° C.	Salinity °/oo	Depth, meters	Temperature, ° C.	Salinity, °/oo	σt
0	10.46	34.40	0	10.46	34.40	26.42
25	9.42	34.44	25	9.42	34.44	26.63
50	4.63	34.68	50	4.63	34.68	27.48
75	4.23	34.69	75	4.23	34.69	27.53
100	3.89	34.74	100	3.89	34.74	27.61
150	3.59	34.78	150	3.59	34.78	27.67
201	3.36	34.80	200	3.35	34.80	27.71
301	3.28	34.82	300	3.30	34.82	27.74
385	3.32	34.84	400	3.30	34.84	27.75
583	3.30	34.86	600	3.30	34.86	27.77
786	3.24	34.86	800	3.25	34.86	27.77
993	3.24	34.87	1,000	3.25	34.87	27.78
1,502	3.17	34.865	1,500	3.20	34.87	27.79
2,018	3.31	34.91	2,000	3.30	34.91	27.81
2,521	3.19	34.915	2,500	3.20	34.91	27.82
3,018	2.69	34.92	3,000	2.75	34.92	27.87
3,367	1.89	34.90				

Station 5703; Aug. 27; latitude 56°33.5′ N., longitude 50°38′ W.; depth 3,585 m.; dynamic height 1,454.623

Observed values			Scaled values			
Depth, meters	Temperature, ° C.	Salinity °/oo	Depth, meters	Temperature, ° C.	Salinity, °/oo	σt
0	9.93	34.44	0	9.93	34.44	26.54
25	8.78	34.56	25	8.78	34.56	26.83
50	4.65	34.66	50	4.65	34.66	27.47
75	3.87	34.75	75	3.87	34.75	27.62
99	3.57	34.76	100	3.60	34.76	27.66
149	3.27	34.79	150	3.25	34.79	27.71
199	3.18	34.80	200	3.20	34.80	27.73
298	3.21	34.82	300	3.25	34.82	27.74
387	3.23	34.84	400	3.25	34.84	27.75
580	3.15	34.84	600	3.15	34.84	27.76
771	3.24	34.85	800	3.25	34.85	27.76
962	3.23	34.86	1,000	3.25	34.86	27.77
1,460	3.24	34.85	1,500	3.25	34.86	27.77
1,967	3.20	34.865	2,000	3.20	34.87	27.79
2,426	------	34.91	2,500	3.15	34.91	27.82
2,908	2.96	34.91	3,000	2.90	34.91	27.85
3,392	2.28	34.90	(3,500)	2.00	34.90	27.91

Station 5704; Aug. 27; latitude 57°05.5′ N., longitude 49°34′ W.; depth 3,566 m.; dynamic height 1,454.623

Observed values			Scaled values			
Depth, meters	Temperature, ° C.	Salinity, °/oo	Depth, meters	Temperature, ° C.	Salinity, °/oo	σt
0	10.14	34.46	0	10.14	34.46	26.52
24	10.01	34.48	25	9.85	34.49	26.60
47	4.06	34.64	50	3.95	34.65	27.53
71	3.59	34.68	75	3.55	34.69	27.60
95	3.47	34.74	100	3.45	34.75	27.66
142	3.36	34.78	150	3.35	34.78	27.69
189	3.23	34.80	200	3.25	34.80	27.72
284	3.18	34.81	300	3.20	34.81	27.74
376	3.19	34.80	400	3.20	34.81	27.74
563	3.15	34.84	600	3.20	34.84	27.76
749	3.24	34.86	800	3.25	34.86	27.77
936	3.26	34.88	1,000	3.25	34.88	27.78
1,429	3.20	34.86	1,500	3.20	34.86	27.78
1,936	3.23	34.84	2,000	3.25	34.87	27.78
2,488	3.24	34.925	2,500	3.25	34.92	27.82
2,989	2.81	34.92	3,000	2.80	34.92	27.86
3,462	2.02	34.90	(3,500)	1.95	34.90	27.92

Station 5705; Aug. 28; latitude 57°38′ N., longitude 48°28′ W.; depth 3,475 m.; dynamic height 1,454.601

Observed values			Scaled values			
Depth, meters	Temperature, ° C.	Salinity, °/oo	Depth, meters	Temperature, ° C.	Salinity, °/oo	σt
0	9.72	34.44	0	9.72	34.44	26.58
27	6.38	34.59	25	6.70	34.59	27.15
53	3.63	34.69	50	3.70	34.68	27.58
80	3.45	34.75	75	3.45	34.74	27.65
106	3.44	34.77	100	3.45	34.77	27.68
160	3.30	34.80	150	3.30	34.80	27.72
214	3.30	34.80	200	3.30	24.80	27.72
320	3.21	34.83	300	3.25	34.82	27.74
389	3.23	34.84	400	3.25	34.84	27.75
581	3.14	34.84	600	3.15	34.84	27.76
771	3.21	34.86	800	3.20	34.86	27.78
960	3.23	34.87	1,000	3.25	34.87	27.78
1,461	3.16	34.86	1,500	3.20	34.86	27.78
1,975	3.26	34.915	2,000	3.25	34.92	27.82
2,560	3.03	34.93	2,500	3.10	34.93	27.84
3,062	2.57	34.93	3,000	2.65	34.93	27.88
3,450	1.45	34.88				

Station 5706; Aug. 28; latitude 58°09.5′ N., longitude 47°13′ W.; depth 3,200 m.; dynamic height 1,454.604

Observed values			Scaled values			
Depth, meters	Temperature, ° C.	Salinity, °/oo	Depth, meters	Temperature, ° C.	Salinity, °/oo	σt
0	9.95	34.37	0	9.95	34.37	26.49
25	5.44	34.58	25	5.44	34.58	27.31
50	3.94	34.74	50	3.94	34.74	27.60
75	3.80	34.79	75	3.80	34.79	27.66
100	3.79	34.81	100	3.79	34.81	27.68
150	3.76	34.85	150	3.76	34.85	27.71
201	3.69	34.85	200	3.70	34.85	27.72
301	3.64	34.88	300	3.65	34.88	27.74
411	3.47	34.86	400	3.50	34.86	27.75
613	3.46	34.87	600	3.45	34.87	27.76
814	3.33	34.87	800	3.35	34.87	27.77
1,012	3.29	34.88	1,000	3.30	34.88	27.78
1,525	3.22	34.88	1,500	3.25	34.88	27.78
2,041	3.24	34.91	2,000	3.25	34.91	27.81
2,515	2.80	34.92	2,500	2.85	34.92	27.86
3,000	1.96	34.90	3,000	1.95	34.90	27.92
3,168	1.52	34.89				

Table of Oceanographic Data—Continued

STATIONS OCCUPIED IN 1954—Continued

Station 5707; Aug. 28; latitude 58°40.5′ N., longitude 46°16′ W.; depth 2,562 m.; dynamic height 1,454.620

Observed values			Scaled values			
Depth, meters	Temperature, ° C.	Salinity °/oo	Depth, meters	Temperature, ° C.	Salinity, °/oo	σ_t
0	9.65	34.46	0	9.65	34.46	26.61
25	7.23	34.78	25	7.23	34.78	27.23
50	5.20	34.85	50	5.20	34.85	27.55
75	5.31	34.96	75	5.31	34.96	27.63
101	5.11	34.96	100	5.15	34.96	27.65
151	4.77	34.94	150	4.80	34.94	27.67
201	4.26	34.89	200	4.30	34.89	27.68
302	4.05	34.89	300	4.05	34.89	27.71
400	3.85	34.90	400	3.85	34.90	27.74
598	3.53	34.88	600	3.55	34.88	27.75
794	3.57	34.90	800	3.60	34.90	27.77
988	3.45	34.88	1,000	3.40	34.88	27.77
1,491	3.35	34.91	1,500	3.35	34.91	27.80
2,002	2.93	34.925	2,000	2.95	34.92	27.85
2,453	2.14	34.89	(2,500)	2.00	34.89	27.90

Station 5708; Aug. 29; latitude 59°03.5′ N., longitude 45°29′ W.; depth 2,378 m.; dynamic height 1,454.633

Observed values			Scaled values			
Depth, meters	Temperature, ° C.	Salinity °/oo	Depth, meters	Temperature, ° C.	Salinity, °/oo	σ_t
0	8.92	34.64	0	8.92	34.64	26.86
25	8.54	34.74	25	8.54	34.74	27.00
50	6.03	34.99	50	6.03	34.99	27.56
75	5.70	35.00	75	5.70	35.00	27.61
100	5.40	34.99	100	5.40	34.99	27.64
150	4.61	34.90	150	4.61	34.90	27.66
200	4.48	34.91	200	4.48	34.91	27.68
300	4.00	34.89	300	4.00	34.89	27.72
383	4.08	34.91	400	4.05	34.91	27.73
572	3.62	34.88	600	3.60	34.88	27.75
758	3.60	34.87	800	3.60	34.88	27.75
944	3.48	34.88	1,000	3.50	34.88	27.76
1,432	3.40	34.91	1,500	3.40	34.91	27.80
1,930	3.00	34.93	2,000	2.95	34.92	27.85
2,298	2.29	34.88				

Station 5709; Aug. 29; latitude 59°16′ N., longitude 45°05′ W.; depth 2,030 m.; dynamic height 1,454.687

Observed values			Scaled values			
Depth, meters	Temperature, ° C.	Salinity °/oo	Depth, meters	Temperature, ° C.	Salinity, °/oo	σ_t
0	8.05	34.85	0	8.05	34.85	27.17
25	8.11	34.86	25	8.11	34.86	27.17
50	7.80	34.91	50	7.80	34.91	27.25
75	6.46	34.965	75	6.46	34.965	27.48
99	5.74	34.95	100	5.75	34.95	27.57
149	5.48	34.94	150	5.50	34.94	27.59
199	5.34	34.94	200	5.35	34.94	27.60
298	5.03	34.95	300	5.00	34.95	27.66
364	4.73	34.92	400	4.70	34.92	27.67
541	4.59	34.945	600	4.55	34.94	27.70
781	4.16	34.93	800	4.10	34.93	47.75
883	3.81	34.91	1,000	3.70	34.91	27.77
1,343	3.49	34.90	1,500	3.40	34.90	27.79
1,792	2.92	34.915	(2,000)	2.25	34.91	27.90

Station 5710; Aug. 29; latitude 59°23′ N., longitude 44°54′ W.; depth 1,271 m.; dynamic height 1,454.749

Observed values			Scaled values			
Depth, meters	Temperature, ° C.	Salinity, °/oo	Depth, meters	Temperature, ° C.	Salinity, °/oo	σ_t
0	7.15	34.78	0	7.15	34.78	27.24
24	7.14	34.77	25	7.15	34.77	27.24
47	7.15	34.77	50	7.15	34.78	27.24
71	7.27	34.82	75	7.25	34.82	27.27
95	7.04	34.80	100	6.90	34.79	27.29
142	5.65	34.72	150	5.60	34.73	27.41
189	5.41	34.83	200	5.35	34.85	27.54
284	4.95	34.89	300	4.95	34.90	27.62
288	5.01	34.91	400	4.85	34.90	27.63
441	4.82	34.91	600	4.75	34.93	27.66
600	4.74	34.93	800	4.50	34.93	27.69
787	4.48	34.93	(1,000)	4.00	34.93	27.75

Station 5711; Aug. 29; latitude 59°30′ N., longitude 44°16′ W.; depth 196 m.; dynamic height 1,454.868

Observed values			Scaled values			
Depth, meters	Temperature, ° C.	Salinity, °/oo	Depth, meters	Temperature, ° C.	Salinity, °/oo	σ_t
0	2.02	32.95	0	2.02	32.95	26.36
26	2.34	33.09	25	2.35	33.09	26.43
52	2.53	33.61	50	2.50	33.56	26.80
78	4.76	34.15	75	4.60	34.11	27.04
105	5.00	34.28	100	4.95	34.26	27.12
156	5.30	34.52	150	5.25	34.50	27.27

Station 5712; Aug. 29; latitude 59°32′ N., longitude 44°07′ W.; depth 170 m.; dynamic height 1,454.843

Observed values			Scaled values			
Depth, meters	Temperature, ° C.	Salinity, °/oo	Depth, meters	Temperature, ° C.	Salinity, °/oo	σ_t
0	1.64	33.48	0	1.64	33.48	26.80
25	2.75	33.76	25	2.75	33.86	26.94
50	3.21	33.91	50	3.21	33.91	27.02
76	4.74	34.18	75	4.70	34.17	27.08
101	4.74	34.21	100	4.75	34.21	27.10
150	3.98	34.40	150	4.00	34.40	27.33

Station 5713; Aug. 29; latitude 59°40′ N., longitude 43°54′ W.; depth 151 m.; dynamic height 1,454.885

Observed values			Scaled values			
Depth, meters	Temperature, ° C.	Salinity, °/oo	Depth, meters	Temperature, ° C.	Salinity, °/oo	σ_t
0	1.92	32.93	0	1.92	32.93	26.35
24	1.56	33.08	25	1.55	33.09	26.49
47	1.18	33.14	50	1.10	33.14	26.57
71	0.87	33.15	75	0.90	33.18	26.61
94	1.24	33.59	100	1.40	33.68	26.98
124	2.24	34.02	(150)	3.15	34.31	27.34

Station 5714; Aug. 29; latitude 59°42′ N., longitude 43°44′ W.; depth 153 m.; dynamic height 1,454.926

Observed values			Scaled values			
Depth, meters	Temperature, ° C.	Salinity, °/oo	Depth, meters	Temperature, ° C.	Salinity, °/oo	σ_t
0	1.90	32.67	0	1.90	32.67	26.14
23	1.81	32.70	25	1.80	32.70	26.16
46	1.71	32.72	50	1.65	32.75	26.22
69	1.28	32.91	75	1.15	32.98	26.44
93	0.78	33.20	100	0.90	33.28	26.69
138	2.12	33.75	(150)	2.50	33.86	27.04

STATIONS OCCUPIED IN 1954—Continued

Station 5715; Aug. 29; latitude 59°44′ N., longitude 43°12′ W.; depth 174 m.; dynamic height 1,454.849

Observed values			Scaled values			
Depth, meters	Temperature, ° C.	Salinity, °/oo	Depth, meters	Temperature, ° C.	Salinity, °/oo	σ_t
0	2.15	33.32	0	2.15	33.32	26.64
26	0.07	33.34	25	0.15	33.34	26.78
52	2.22	33.72	50	2.10	33.70	26.94
79	4.33	34.18	75	4.20	34.12	27.09
104	4.54	34.29	100	4.55	34.28	27.17
157	3.89	34.32	150	4.00	34.32	27.27

Station 5716; Aug. 29; latitude 59°44.5′ N., longitude 42°53′ W.; depth 172 m.; dynamic height 1,454.822

Observed values			Scaled values			
Depth, meters	Temperature, ° C.	Salinity, °/oo	Depth, meters	Temperature, ° C.	Salinity, °/oo	σ_t
0	3.16	33.98	0	3.16	33.98	27.07
28	3.40	34.04	25	3.35	34.02	27.09
54	4.01	34.19	50	3.90	34.18	27.16
82	4.18	34.23	75	4.15	34.23	27.18
109	3.10	34.21	100	3.50	34.21	27.23
164	3.57	34.43	150	3.45	34.37	27.36

Station 5717; Aug. 29; latitude 59°45.5′ N., longitude 42°30′ W.; depth 340 m.; dynamic height 1,454.799

Observed values			Scaled values			
Depth, meters	Temperature, ° C.	Salinity, °/oo	Depth, meters	Temperature, ° C.	Salinity, °/oo	σ_t
0	8.00	34.83	0	8.00	34.83	27.16
26	7.96	34.83	25	7.95	34.83	27.16
53	7.96	34.83	50	7.95	34.83	27.16
79	7.83	34.82	75	7.90	34.82	27.17
105	5.44	34.80	100	5.70	34.80	27.45
157	5.32	34.90	150	5.35	34.89	27.56
209	4.88	34.85	200	4.95	34.85	27.58
314	4.92	34.89	300	4.95	34.88	27.60

Station 5718; Aug. 30; latitude 59°45′ N., longitude 42°24′ W.; depth 1,124 m.; dynamic height 1,454.783

Observed values			Scaled values			
Depth, meters	Temperature, ° C.	Salinity, °/oo	Depth, meters	Temperature, ° C.	Salinity, °/oo	σ_t
0	8.09	34.86	0	8.09	34.86	27.17
26	8.09	34.87	25	8.10	34.87	27.18
53	8.01	34.86	50	8.05	34.86	27.18
79	5.73	34.76	75	6.10	34.77	27.38
106	4.77	34.76	100	4.85	34.76	27.52
158	5.62	34.93	150	5.55	34.92	27.57
211	5.26	34.89	200	5.30	34.89	27.57
317	5.14	34.92	300	5.15	34.92	27.62
418	4.99	34.92	400	5.00	34.92	27.64
617	4.74	34.92	600	4.75	34.92	27.66
810	4.77	34.93	800	4.80	34.93	27.66
1,026	4.71	34.935	1,000	4.75	34.93	27.66

Station 5719; Aug. 30; latitude 59°45′ N., longitude 42°05′ W.; depth 1,737 m.; dynamic height 1,454.665

Observed values			Scaled values			
Depth, meters	Temperature, ° C.	Salinity, °/oo	Depth, meters	Temperature, ° C.	Salinity, °/oo	σ_t
0	8.70	34.84	0	8.70	34.84	27.06
26	8.59	34.84	25	8.60	34.84	27.07
53	7.19	35.03	50	7.25	35.03	27.42
79	6.88	35.03	75	6.95	35.03	27.47
106	6.62	35.055	100	6.70	35.05	27.52
157	6.19	35.03	150	6.25	35.04	27.57
210	5.67	35.00	200	5.75	35.00	27.60
316	5.34	34.99	300	5.40	34.99	27.64
368	5.11	34.96	400	5.00	34.96	27.67
561	4.55	34.95	600	4.45	34.95	27.72
762	3.96	34.93	800	3.85	34.92	27.76
963	3.55	34.905	1,000	3.55	34.90	27.77
1,482	3.15	34.92	1,500	3.20	34.92	27.83

Station 5720; Aug. 30; latitude 59°44′ N., longitude 41°36′ W.; depth 1,975 m.; dynamic height 1,454.664

Observed values			Scaled values			
Depth, meters	Temperature, ° C.	Salinity, °/oo	Depth, meters	Temperature, ° C.	Salinity, °/oo	σ_t
0	9.53	34.71	0	9.53	34.71	26.82
24	8.68	34.84	25	8.65	34.84	27.07
48	7.12	35.04	50	7.05	35.04	27.46
73	6.41	34.99	75	6.40	34.99	27.51
97	6.42	35.03	100	6.40	35.02	27.54
144	5.52	34.94	150	5.45	34.93	27.58
193	4.87	34.88	200	4.85	34.88	27.61
290	4.82	34.92	300	4.80	34.92	27.66
370	4.71	34.94	400	4.65	34.94	27.69
558	4.04	34.92	600	3.95	34.91	27.74
751	3.72	34.88	800	3.70	34.88	27.74
945	3.60	34.89	1,000	3.60	34.89	27.76
1,470	3.28	34.92	1,500	3.25	34.92	27.82
1,839	2.64	34.905				

Station 5721; Aug. 30; latitude 59°47′ N., longitude 40°48′ W.; depth 2,213 m.; dynamic height 1,454.606

Observed values			Scaled values			
Depth, meters	Temperature, ° C.	Salinity, °/oo	Depth, meters	Temperature, ° C.	Salinity, °/oo	σ_t
0	9.65	34.73	0	9.65	34.73	26.82
27	6.50	34.99	25	6.65	34.97	27.47
53	6.13	35.03	50	6.15	35.03	27.57
81	5.75	35.01	75	5.85	35.02	27.61
107	5.45	34.99	100	5.50	35.00	27.63
161	4.73	34.945	150	4.85	34.95	27.67
215	4.36	34.935	200	4.45	34.94	27.71
322	4.10	34.925	300	4.15	34.93	27.73
428	3.67	34.89	400	3.75	34.90	27.75
637	3.58	34.885	600	3.60	34.88	27.75
843	3.53	34.87	800	3.55	34.87	27.75
1,047	3.39	34.89	1,000	3.45	34.89	27.77
1,572	3.34	34.94	1,500	3.35	34.94	27.82
2,097	2.82	34.94	2,000	3.05	34.94	27.85

STATIONS OCCUPIED IN 1954—Continued

Station 5722; Aug. 30; latitude 59°53.5′ N., longitude 39°46′ W.; depth 2,743 m.; dynamic height 1,454.618

Observed values			Scaled values			
Depth, meters	Temperature, ° C.	Salinity °/oo	Depth, meters	Temperature, ° C.	Salinity, °/oo	σ_t
0	10.11	34.70	0	10.11	34.70	26.72
24	9.22	34.76	25	9.10	34.76	26.93
48	5.00	34.85	50	4.95	34.85	27.58
72	4.65	34.865	75	4.60	34.87	27.64
96	4.49	34.89	100	4.45	34.89	27.67
144	4.27	34.89	150	4.25	34.89	27.69
193	4.15	34.89	200	4.15	34.89	27.70
289	3.91	34.905	300	3.85	34.91	27.75
363	3.60	34.88	400	3.55	34.88	27.75
544	3.49	34.88	600	3.50	34.88	27.76
722	3.49	34.89	800	3.50	34.89	27.77
901	3.44	-------	1,000	3.45	34.88	27.77
1,377	3.34	34.88	1,500	3.35	34.89	27.78
1,870	3.35	34.93	2,000	3.35	34.93	27.81
2,481	2.25	34.89	(2,500)	2,15	34.89	27.89

Station 5723; Aug. 30; latitude 59°53′ N., longitude 38°49′ W.; depth 2,871 m.; dynamic height 1,454.620

Observed values			Scaled values			
Depth, meters	Temperature, ° C.	Salinity °/oo	Depth, meters	Temperature, ° C.	Salinity, °/oo	σ_t
0	10.22	34.64	0	10.22	34.64	26.65
25	9.91	34.66	25	9.91	34.66	26.72
51	5.33	34.87	50	5.60	34.87	27.52
76	4.79	34.88	75	4.80	34.88	27.62
101	4.50	34.90	100	4.50	34.90	27.67
152	4.10	34.90	150	4.10	34.90	27.72
203	4.05	34.89	200	4.05	34.89	27.71
304	3.72	34.88	300	3.75	34.88	27.73
396	3.58	34.88	400	3.55	34.88	27.75
592	3.50	34.88	600	3.50	34.88	27.76
787	3.51	34.89	800	3.50	34.89	27.77
981	3.46	34.90	1,000	3.45	34.90	27.78
1,485	3.35	34.90	1,500	3.35	34.90	27.79
1,999	3.34	34.94	2,000	3.35	34.94	27.82
2,518	2.83	34.94	2,500	2.85	34.94	27.87
2,810	1.50	34.89				

Station 5724; Aug. 31; latitude 59°58.5′ N., longitude 37°19′ W.; depth 3,054 m.; dynamic height 1,454.629

Observed values			Scaled values			
Depth, meters	Temperature, ° C.	Salinity °/oo	Depth, meters	Temperature, ° C.	Salinity, °/oo	σ_t
0	9.48	34.72	0	9.48	34.72	26.85
23	8.29	34.78	25	7.85	34.78	27.14
47	5.34	34.89	50	5.35	34.90	27.57
70	5.28	34.92	75	5.25	34.92	27.61
94	5.05	34.92	100	5.00	34.92	27.64
141	4.71	34.935	150	4.65	34.93	27.68
187	4.57	34.93	200	4.55	34.93	27.69
281	4.32	34.92	300	4.25	34.92	27.72
396	4.00	34.90	400	4.00	34.90	27.73
591	3.63	34.88	600	3.60	34.88	27.75
785	3.54	34.88	800	3.55	34.88	27.75
976	3.49	34.885	1,000	3.50	34.89	27.77
1,472	3.40	34.89	1,500	3.40	34.89	27.78
1,972	3.49	34.935	2,000	3.50	34.94	27.81
2,323	3.32	34.95	2,500	3.15	34.94	27.84
2,813	2.89	34.92	(3,000)	2.75	34.91	27.86

Station 5725; Aug. 31; latitude 59°59′ N., longitude 35°49′ W.; depth 3,033 m.; dynamic height 1,454.644

Observed values			Scaled values			
Depth, meters	Temperature, ° C.	Salinity, °/oo	Depth, meters	Temperature, ° C.	Salinity, °/oo	σ_t
0	10.36	34.73	0	10.36	34.73	26.70
24	10.22	34.74	25	10.10	34.74	26.75
48	6.33	34.88	50	6.15	34.89	27.46
73	5.57	34.92	75	5.55	34.92	27.57
97	5.55	34.93	100	5.55	34.93	27.57
145	5.12	34.91	150	5.05	34.91	27.62
193	4.69	34.90	200	4.65	34.90	27.66
290	4.31	34.91	300	4.25	34.91	27.71
386	3.94	34.89	400	3.90	34.89	27.73
578	3.54	34.86	600	3.55	34.86	27.74
768	3.54	34.89	800	3.55	34.89	27.76
958	3.49	34.90	1,000	3.50	34.90	27.78
1,450	3.39	34.905	1,500	3.40	34.91	27.80
1,952	3.40	34.935	2,000	3.40	34.93	27.81
2,466	3.07	34.925	2,500	3.00	34.92	27.85
2,907	2.28	34.91	(3,000)	2.05	34.91	27.92

Station 5726; Aug. 31; latitude 59°17′ N., longitude 36°40′ W.; depth 2,944 m.; dynamic height 1,454.640

Observed values			Scaled values			
Depth, meters	Temperature, ° C.	Salinity, °/oo	Depth, meters	Temperature, ° C.	Salinity, °/oo	σ_t
0	10.47	34.74	0	10.47	34.74	26.68
25	10.12	34.78	35	10.12	34.78	26.78
51	5.96	34.84	50	6.05	34.83	27.43
76	5.26	34.87	75	5.25	34.87	27.57
102	4.81	34.87	100	4.85	34.87	27.61
152	4.51	34.89	150	4.55	34.89	27.66
203	4.27	34.90	200	4.30	34.90	27.69
305	4.02	34.89	300	4.05	34.89	27.71
400	3.64	34.87	400	3.65	34.87	27.74
597	3.47	34.87	600	3.50	34.87	27.76
792	3.49	34.89	800	3.50	34.89	27.77
985	3.45	34.88	1,000	3.45	34.89	27.77
1,490	3.35	34.88	1,500	3.35	34.88	27.77
2,001	3.41	34.94	2,000	3.40	34.94	27.82
2,476	3.10	34.94	2,500	3.10	34.94	27.85
2,877	2.51	34.90	(3,000)	2.30	34.89	27.88

Station 5727; Sept. 1; latitude 58°31.5′ N., longitude 37°25′ W.; depth 3,109 m.; dynamic height 1,454.697

Observed values			Scaled values			
Depth, meters	Temperature, ° C.	Salinity, °/oo	Depth, meters	Temperature, ° C.	Salinity, °/oo	σ_t
0	10.30	34.68	0	10.30	34.68	26.67
25	10.16	34.68	25	10.16	34.68	26.69
50	6.39	34.91	50	6.39	34.91	27.45
76	5.99	34.92	75	6.00	34.92	27.51
101	6.02	34.96	100	6.05	34.96	27.54
151	5.83	34.95	150	5.85	34.95	27.55
202	5.64	34.95	200	5.65	34.95	27.58
303	4.94	34.92	300	4.95	34.92	27.64
381	4.70	34.91	400	4.60	34.91	27.67
571	3.87	34.89	600	3.80	34.88	27.73
759	3.53	34.85	800	3.55	34.85	27.73
948	3.52	34.87	1,000	3.50	34.88	27.76
1,442	3.42	34.90	1,500	3.45	34.91	27.79
1,947	3.51	34.95	2,000	3.50	34.95	27.82
2,480	3.17	34.95	2,500	3.15	34.95	27.85
2,950	2.84	34.95	(3,000)	2.80	34.95	27.88

STATIONS OCCUPIED IN 1954—Continued

Station 5728; Sept. 1; latitude 57°45′ N., longitude 38°04′ W.; depth 3,219 m.; dynamic height 1,454.668

Observed values			Scaled values			
Depth, meters	Temperature, ° C.	Salinity ‰	Depth, meters	Temperature, ° C.	Salinity, ‰	σ_t
0	10.43	34.72	0	10.43	34.72	26.68
25	10.36	34.72	25	10.36	34.72	26.69
50	6.34	34.79	50	6.34	34.79	27.36
76	5.54	34.86	75	5.55	34.86	27.52
101	5.44	34.88	100	5.45	34.88	27.54
151	5.12	34.90	150	5.15	34.90	27.60
202	4.91	34.91	200	4.95	34.91	27.63
303	4.58	34.91	300	4.60	34.91	27.67
403	4.19	34.90	400	4.20	34.90	27.71
602	3.62	34.88	600	3.65	34.88	27.74
797	3.54	34.88	800	3.55	34.88	27.75
992	3.61	34.90	1,000	3.60	34.90	27.77
1,502	3.35	34.90	1,500	3.35	34.90	27.79
2,021	3.36	34.945	2,000	3.35	34.94	27.82
2.526	3.11	34.95	2,500	3.10	34.95	27.86
3,027	2.81	34.93	3,000	2.85	34.93	27.86
3,178	2.64	34.91				

Station 5729; Sept. 1; latitude 57°02.5′ N., longitude 39°04′ W.; depth 3,200 m.; dynamic height 1,454.670

Observed values			Scaled values			
Depth, meters	Temperature, ° C.	Salinity ‰	Depth, meters	Temperature, ° C.	Salinity, ‰	σ_t
0	11.04	34.65	0	11.04	34.65	26.51
26	10.90	34.66	25	10.90	34.60	26.50
52	5.97	34.81	50	6.15	34.81	27.41
78	5.39	34.83	75	5.40	34.83	27.51
103	5.35	34.84	100	5.35	34.84	27.53
154	5.13	34.885	150	5.15	34.85	27.56
206	4.93	34.88	200	5.00	34.88	27.60
309	3.89	34.83	300	3.90	34.83	27.68
414	3.79	34.86	400	3.80	34.86	27.72
620	3.40	34.85	600	3.40	34.85	27.75
826	3.42	34.87	800	3.40	34.87	27.77
1,041	3.44	34.89	1,000	3.45	34.89	27.77
1,595	3.36	34.89	1,500	3.40	34.89	27.78
2,033	3.38	34.92	2,000	3.40	34.92	27.81
2,529	3.05	34.93	2,500	3.10	34.93	27.84
3,027	2.81	34.94	3,000	2.85	34.94	27.87
3,149	2.68	34.93				

Station 5730; Sept. 2; latitude 56°24′ N., longitude 40°01′ W.; depth 2,671 m.; dynamic height 1,454.662

Observed values			Scaled values			
Depth, meters	Temperature, ° C.	Salinity ‰	Depth, meters	Temperature, ° C.	Salinity, ‰	σ_t
0	11.41	34.61	0	11.41	34.61	26.42
25	11.04	34.62	25	11.04	34.62	26.49
50	5.85	34.82	50	5.85	34.82	27.45
75	5.44	34.86	75	5.44	34.86	27.53
100	5.34	34.86	100	5.34	34.86	27.54
150	4.64	34.84	150	4.64	34.84	27.61
200	4.36	34.85	200	4.36	34.85	27.65
300	3.98	34.87	300	3.98	34.87	27.71
388	3.74	34.86	400	3.75	34.86	27.72
580	3.65	34.88	600	3.65	34.88	27.74
772	3.57	34.89	800	3.60	34.89	27.76
976	3.49	34.89	1,000	3.50	34.89	27.77
1,490	3.46	34.925	1,500	3.50	34.93	27.80
1,882	3.37	34.96	2,000	3.30	34.96	27.85
2,374	3.04	34.94	(2,500)	2.90	34.93	27.86

Station 5731; Sept. 2; latitude 57°04′ N., longitude 40°34′ W.; depth 3,290 m.; dynamic height 1,454.659

Observed values			Scaled values			
Depth, meters	Temperature, ° C.	Salinity, ‰	Depth, meters	Temperature, ° C.	Salinity, ‰	σ_t
0	10.79	34.63	0	10.79	34.63	26.54
25	10.79	34.63	25	10.79	34.63	26.54
49	5.87	34.77	50	5.85	34.77	27.41
74	4.94	34.77	75	4.95	34.77	27.52
98	4.83	34.82	100	4.70	34.82	27.59
148	4.31	34.80	150	4.30	34.80	27.62
197	4.28	34.83	200	4.30	34.83	27.64
295	3.82	34.83	300	3.90	34.85	27.70
324	3.90	34.875	400	3.65	34.86	27.73
494	3.50	34.86	600	3.35	34.85	27.75
668	3.27	34.84	800	3.40	34.86	27.76
849	3.44	34.87	1,000	3.45	34.88	27.76
1,325	3.41	34.90	1,500	3.45	34.91	27.79
1,835	3.45	34.93	2,000	3.35	34.93	27.81
2,580	3.08	34.925	2,500	3.10	34.93	27.84
3,085	2.77	34.94	3,000	2.85	34.94	27.86
3,290	2.51	34.91				

Station 5732; Sept. 2; latitude 57°36.5′ N., longitude 41°08′ W.; depth 3,292 m.; dynamic height 1,454.626

Observed values			Scaled values			
Depth, meters	Temperature, ° C.	Salinity, ‰	Depth, meters	Temperature, ° C.	Salinity, ‰	σ_t
0	10.20	34.60	0	10.20	34.60	26.62
26	10.10	34.60	25	10.15	34.60	26.63
52	4.85	34.76	50	5.15	34.76	27.49
78	4.04	34.78	75	4.10	34.78	27.62
105	3.78	34.79	100	3.80	34.79	27.66
156	3.74	34.84	150	3.75	34.83	27.69
208	3.66	34.85	200	3.70	34.85	27.72
313	3.27	34.83	300	3.30	34.83	27.74
343	3.27	34.835	400	3.25	34.84	27.75
519	3.27	34.84	600	3.30	34.85	27.76
698	3.36	34.87	800	3.35	34.88	27.77
881	3.35	34.875	1,000	3.35	34.88	27.77
1,371	3.27	34.87	1,500	3.30	34.88	27.78
1,891	3.43	34.90	2,000	3.40	34.91	27.80
2,644	2.98	34.94	2,500	3.05	34.93	27.84
3,045	2.64	34.925	3,000	2.70	34.93	27.87
3,245	1.99	34.90				

Station 5733; Sept. 2–3; latitude 58°10′ N., longitude 41°49′ W.; depth 3,017 m.; dynamic height 1,454.609

Observed values			Scaled values			
Depth, meters	Temperature, ° C.	Salinity, ‰	Depth, meters	Temperature, ° C.	Salinity, ‰	σ_t
0	8.57	34.62	0	8.57	34.62	26.91
24	8.58	34.64	25	8.55	34.64	26.92
47	4.48	34.74	50	4.30	34.74	27.57
71	3.80	34.75	75	3.70	34.75	27.64
94	3.48	34.775	100	3.45	34.77	27.68
141	3.29	34.76	150	3.30	34.77	27.70
188	3.30	34.81	200	3.30	34.81	27.73
282	3.29	34.82	300	3.30	34.82	27.74
358	3.40	34.85	400	3.40	34.86	27.76
558	3.39	34.86	600	3.40	34.86	27.76
758	3.30	34.855	800	3.30	34.86	27.77
1,458	3.25	34.87	1,000	3.30	34.86	27.77
1,957	3.39	34.93	1,500	3.25	34.87	27.78
2,370	3.15	34.93	2,000	3.40	34.93	27.81
2,720	2.70	34.90	2,500	3.05	34.92	27.84
			(3,000)	1.95	34.87	27.90

STATIONS OCCUPIED IN 1954—Continued

Station 5734; Sept. 3; latitude 58°42′ N., longitude 42°23′ W.; depth 2,506 m.; dynamic height 1,454.600

Observed values			Scaled values			
Depth, meters	Temperature, ° C.	Salinity °/oo	Depth, meters	Temperature, ° C.	Salinity, °/oo	σ_t
0	8.52	34.73	0	8.52	34.73	27.00
23	7.58	34.88	25	7.30	34.90	27.32
46	6.06	35.04	50	6.00	35.04	27.60
69	5.84	35.02	75	5.80	35.02	27.62
92	5.61	35.01	100	5.55	35.01	27.64
138	5.32	35.00	150	5.25	35.00	27.67
184	5.13	35.00	200	5.05	34.99	27.68
276	4.18	34.915	300	4.25	34.92	27.72
325	4.29	34.92	400	3.75	34.88	27.73
494	3.49	34.87	600	3.45	34.88	27.76
667	3.44	34.89	800	3.40	34.89	27.78
845	3.38	34.895	1,000	3.40	34.90	27.79
1,343	3.38	34.92	1,500	3.35	34.93	27.81
1,892	3.16	34.94	2,000	3.05	34.93	27.84
2,252	2.43	34.885	(2,500)	1.75	34.86	27.90

Station 5735; Sept. 4; latitude 58°54.5′ N., longitude 42°58′ W.; depth 2,012 m.; dynamic height 1,454.629

Observed values			Scaled values			
Depth, meters	Temperature, ° C.	Salinity °/oo	Depth, meters	Temperature, ° C.	Salinity, °/oo	σ_t
0	7.71	34.88	0	7.71	34.88	27.24
27	7.72	34.88	25	7.70	34.88	27.24
53	7.69	34.90	50	7.70	34.89	27.25
79	6.17	35.04	75	6.30	35.03	27.55
105	6.05	35.02	100	6.10	35.03	27.58
159	5.60	34.98	150	5.70	34.98	27.59
211	5.27	34.96	200	5.35	34.96	27.62
316	4.70	34.95	300	4.80	34.95	27.68
378	4.50	34.94	400	4.45	34.94	27.71
566	3.98	34.92	600	3.90	34.92	27.76
754	3.64	34.90	800	3.60	34.90	27.77
940	3.46	34.89	1,000	3.45	34.89	27.77
1,428	3.13	34.94	1,500	3.10	34.93	27.84
1,926	1.96	34.89	2,000)	1.60	34.88	27.92

Station 5736; Sept. 4; latitude 59°04.5′ N., longitude 43°19′ W.; depth 1,646 m.; dynamic height 1,454.680

Observed values			Scaled values			
Depth, meters	Temperature, ° C.	Salinity °/oo	Depth, meters	Temperature, ° C.	Salinity, °/oo	σ_t
0	8.35	34.85	0	8.35	34.85	27.12
24	8.18	34.87	25	8.20	34.87	27.16
48	8.12	34.88	50	8.10	34.88	27.18
72	7.88	34.92	75	7.80	34.93	27.26
96	6.87	35.03	100	6.80	35.03	27.49
144	6.17	35.02	150	6.10	35.02	27.58
191	5.78	35.01	200	5.70	35.01	27.62
287	5.11	34.97	300	5.00	34.96	27.67
349	4.78	34.94	400	4.70	34.94	27.68
526	4.50	34.94	600	4.40	34.94	27.71
703	4.17	34.93	800	4.00	34.93	27.75
886	3.85	34.93	1,000	3.75	34.92	27.77
1,357	3.44	34.91	(1,500)	3.30	34.90	27.80

Station 5737; Sept. 4; latitude 59°22′ N., longitude 43°40′ W.; depth 666 m.; dynamic height 1,454.804

Observed values			Scaled values			
Depth, meters	Temperature, ° C.	Salinity, °/oo	Depth, meters	Temperature, ° C.	Salinity, °/oo	σ_t
0	2.20	33.18	0	2.20	33.18	26.52
26	4.37	34.01	25	4.30	34.00	26.98
52	7.35	34.69	50	7.35	34.68	27.13
79	6.12	34.51	75	6.25	34.52	27.16
105	7.21	34.80	100	7.10	34.74	27.22
156	6.53	35.01	150	6.65	35.00	27.49
209	5.37	34.91	200	5.55	34.92	27.57
314	4.90	-------	300	4.90	34.90	27.63
399	4.87	34.90	400	4.90	34.90	27.63
607	4.75	34.92	600	4.75	34.92	27.66

Station 5738; Sept. 4; latitude 59°26′ N., longitude 43°46′ W., depth 279 m.; dynamic height 1,454.841

Observed values			Scaled values			
Depth, meters	Temperature, ° C.	Salinity, °/oo	Depth, meters	Temperature, ° C.	Salinity, °/oo	σ_t
0	2.48	32.82	0	2.48	32.82	26.21
25	2.43	33.45	25	2.43	33.45	26.72
50	3.12	33.67	50	3.12	33.67	26.84
75	3.54	33.84	75	3.54	33.84	26.92
100	4.69	34.21	100	4.69	34.21	27.11
149	3.86	34.54	150	3.90	34.54	27.45
199	4.34	34.69	200	4.40	34.69	27.51
274	5.13	34.89				

Station 5739; Sept. 4; latitude 59°29′ N., longitude 43°51′ W.; depth 224 m.; dynamic height 1,454.862

Observed values			Scaled values			
Depth, meters	Temperature, ° C.	Salinity, °/oo	Depth, meters	Temperature, ° C.	Salinity, °/oo	σ_t
0	2.32	32.50	0	2.32	32.50	25.97
25	2.01	33.17	25	2.01	33.17	26.53
50	2.45	33.69	50	2.45	33.69	26.90
75	3.34	33.84	75	3.34	33.84	26.94
100	4.11	34.09	100	4.11	34.09	27.07
149	5.39	34.50	150	5.40	34.51	27.26
199	5.39	34.74	200	5.40	34.74	27.44

Station 5740; Sept. 4; latitude 59°40′ N., longitude 43°54′ W.; depth 144 m.; dynamic height 1,454.896

Observed values			Scaled values			
Depth, meters	Temperature, ° C.	Salinity, °/oo	Depth, meters	Temperature, ° C.	Salinity, °/oo	σ_t
0	2.50	31.39	0	2.50	31.39	25.07
25	2.15	32.73	25	2.15	32.73	26.17
50	2.29	33.34	50	2.29	33.34	26.64
76	2.60	33.48	75	2.60	33.48	26.73
101	3.58	33.91	100	3.55	33.90	26.97
131	4.48	34.36				

In the following table the potential density is represented by $\sigma_{t\theta}$ which signifies 1,000 (density−1) at atmospheric pressure and potential temperature t_θ. The concentration of total phosphorus is given in microgram-atoms per liter.

TOTAL PHOSPHORUS DATA COLLECTED IN 1954

Depth, meters	$\sigma_{t\theta}$	Total P µga L	Depth, meters	$\sigma_{t\theta}$	Total P µga/L
Station 5690; Aug. 25; latitude 53°43′ N., longitude 55°49′ W.; depth 130 m.					
0	22.38	0.51	76	26.42	1.20
25	26.18	0.52	102	26.45	1.21
51	26.37	1.12			
Station 5691; Aug. 25; latitude 53°50.5′ N., longitude 55°35′ W.; depth 218 m.					
0	22.60	0.53	100	26.63	1.15
25	26.11	0.77	151	26.83	1.15
50	26.38	1.08	201	27.15	1.88
75	26.48	1.30			
Station 5692; Aug. 26; latitude 53°53.5′ N., longitude 55°26′ W.; depth 178 m.					
0	23.27	0.57	75	26.70	1.16
25	26.20	0.60	101	26.81	1.13
50	26.58	1.04	151	27.08	1.05
Station 5693; Aug. 26; latitude 54°04′ N., longitude 55°04′ W., depth 165 m.					
0	23.98	0.41	75	26.60	1.31
25	26.43	1.07	99	26.68	1.24
50	26.47	1.09	149	26.97	1.15
Station 5694; Aug. 26; latitude 54°10.5′ N., longitude 54°54′ W.; depth 178 m.					
0	24.06	0.45	76	26.78	1.18
25	26.25	0.55	101	26.91	1.05
50	26.62	1.17	151	27.11	1.16
Station 5695; Aug. 26; latitude 54°28′ N., longitude 54°24′ W.; depth 220 m.					
0	24.22	0.31	100	26.76	1.12
25	26.18	0.53	151	26.98	1.23
50	26.48	0.57	201	27.10	1.13
75	26.62	1.09			
Station 5696; Aug. 26; latitude 54°46′ W., longitude 53°51′ W.; depth 329 m.					
0	24.77	0.42	100	27.04	1.09
25	26.17	0.55	150	27.30	1.11
50	26.68	1.08	201	27.42	1.21
75	26.91	1.15	301	27.51	1.19
Station 5697; Aug. 26; latitude 54°52′ N., longitude 53°38′ W.; depth 657 m.					
0	25.98	0.71	143	27.49	1.25
24	26.75	0.74	190	27.54	1.29
48	27.06	1.08	285	27.60	1.29
71	27.20	1.10	372	27.62	1.27
95	27.33	1.14	574	27.69	1.22
Station 5698; Aug. 26; latitude 54°58′ N., longitude 53°24′ W.; depth 1,719 m.					
0	26.09	0.42	300	27.68	1.35
25	26.35	0.38	377	27.73	1.12
50	27.22	0.83	565	27.72	1.22
75	27.43	1.08	754	27.76	1.42
100	27.53	1.27	946	27.77	1.38
150	27.65	1.18	1,432	27.77	1.31
200	27.66	1.19			
Station 5699; Aug. 26; latitude 55°02′ N., longitude 53°14′ W.; depth 2,103 m.					
0	26.30	0.52	297	27.75	1.20
25	26.42	0.56	378	27.76	1.18
50	27.16	0.76	563	27.77	1.32
74	27.33	0.95	745	27.78	1.16
99	27.53	1.21	924	27.79	1.19
149	27.65	1.19	1,413	27.81	1.25
198	27.69	1.30	1,920	27.85	1.17
Station 5700; Aug. 26; latitude 55°14′ N., longitude 52°51′ W.; depth 3,113 m.					
0	26.26	0.53	381	27.75	1.11
25	26.30	0.46	575	27.76	1.11
50	27.34	0.79	771	27.76	1.24
75	25.57	1.02	971	27.78	1.28
101	27.62	1.16	1,480	27.79	1.30
151	27.67	1.11	2,006	27.84	1.27
201	27.71	1.18	2,536	27.89	1.17
302	27.73	1.15	2,981	27.94	1.12
Station 5701; Aug. 26–27; latitude 55°31.5′ N., longitude 52°25′ W.; depth 3,182 m.					
0	26.20	0.57	385	27.74	1.27
25	26.63	0.68	585	27.75	1.19
50	27.48	1.25	789	27.76	1.24
75	27.53	1.29	999	27.77	1.16
101	27.60	1.28	1,520	27.80	1.16
151	27.63	1.29	2,037	27.82	1.24
201	27.69	1.30	2,535	27.84	1.20
302	27.72	1.23	3,022	27.89	1.15
Station 5702; Aug. 27; latitude 55°56′ N., longitude 51°48′ W.; depth 3,457 m.					
0	26.42	0.59	583	27.77	1.16
25	26.63	0.63	786	27.77	1.20
50	27.48	1.16	993	27.79	1.14
75	27.53	1.21	1,502	27.79	1.20
100	27.61	1.26	2,018	27.82	1.19
150	27.67	1.20	2,521	27.84	1.19
201	27.71	1.24	3,018	27.89	1.15
301	27.74	1.16	3,367	27.94	1.07
385	27.75	1.14			

TOTAL PHOSPHORUS DATA COLLECTED IN 1954—Continued

Station 5703; Aug. 27; latitude 56°33.5′ N., longitude 50°38′ W.; depth 3,585 m.

Depth, meters	$\sigma_{t\theta}$	Total *P* µga/*L*	Depth, meters	$\sigma_{t\theta}$	Total *P* µga/*L*
0	26.54	0.77	580	27.76	1.18
25	26.83	0.64	771	27.76	1.19
50	27.47	1.25	962	27.78	1.18
75	27.62	1.21	1,460	27.77	1.23
99	27.66	1.15	1,967	27.79	1.28
149	27.71	1.29	2,426	27.82	1.26
199	27.73	1.29	2,908	27.86	1.14
298	27.75	1.26	3,392	27.91	1.12
387	27.76	1.20			

Station 5704; Aug. 27; latitude 57°05.5′ N., longitude 49°34′ W.; depth 3,566 m.

Depth, meters	$\sigma_{t\theta}$	Total *P* µga/*L*	Depth, meters	$\sigma_{t\theta}$	Total *P* µga/*L*
0	26.52	0.53	563	27.76	1.14
24	26.56	0.57	749	27.77	1.16
47	27.51	1.06	936	27.79	1.19
71	27.59	1.26	1,429	27.79	1.15
95	27.65	1.31	1,936	27.77	1.21
142	27.69	1.28	2,488	27.84	1.05
189	27.72	1.19	2,989	27.88	1.11
284	27.74	1.22	3,462	27.93	1.10
376	27.73	1.14			

Station 5705; Aug. 28; latitude 57°38′ N., longitude 48°28′ W.; depth 3,475 m.

Depth, meters	$\sigma_{t\theta}$	Total *P* µga/*L*	Depth, meters	$\sigma_{t\theta}$	Total *P* µga/*L*
0	26.58	0.56	581	27.76	1.17
27	27.20	0.83	771	27.78	1.25
53	27.60	1.15	960	27.79	1.24
80	27.66	1.22	1,461	27.79	1.23
106	27.68	1.21	1,975	27.83	1.14
160	27.72	1.22	2,560	27.86	1.17
214	27.72	1.28	3,062	27.91	1.11
320	27.75	1.22	3,450	27.95	1.16
389	27.76	1.19			

Station 5706; Aug. 28; latitude 58°09.5′ N., longitude 47°13′ W.; depth 3,200 m.

Depth, meters	$\sigma_{t\theta}$	Total *P* µga/*L*	Depth, meters	$\sigma_{t\theta}$	Total *P* µga/*L*
0	26.49	0.57	411	27.75	1.23
25	27.31	1.13	613	27.76	1.24
50	27.60	1.30	814	27.78	1.25
75	27.66	1.26	1,012	27.79	1.21
100	27.68	1.22	1,525	27.80	1.30
150	27.71	1.25	2,041	27.83	1.24
201	27.72	1.16	2,515	27.88	1.10
301	27.75	1.23	3,000	27.93	1.06

Station 5707; Aug. 28; latitude 58°40.5′ N., longitude 46°16′ W.; depth 2,562 m.

Depth, meters	$\sigma_{t\theta}$	Total *P* µga/*L*	Depth, meters	$\sigma_{t\theta}$	Total *P* µga/*L*
0	26.61	0.67	400	27.74	1.25
25	27.23	0.85	598	27.76	1.20
50	27.55	1.16	794	27.77	1.22
75	27.63	1.21	988	27.77	1.28
151	27.67	1.21	1,491	27.81	1.20
201	27.69	1.22	2,002	27.86	1.25
302	27.71	1.22	2,453	27.91	1.07

Station 5708; Aug. 29; latitude 59°03.5′ N., longitude 45°29′ W.; depth 2,378 m.

Depth, meters	$\sigma_{t\theta}$	Total *P* µga/*L*	Depth, meters	$\sigma_{t\theta}$	Total *P* µga/*L*
0	26.86	0.92	383	27.73	1.47
25	27.00	0.89	572	27.75	1.30
50	27.56	1.18	758	27.75	1.22
75	27.61	1.38	944	27.77	1.25
100	27.64	1.23	1,432	27.81	1.25
150	27.66	1.30	1,930	27.86	1.25
200	27.68	1.31	2,298	27.88	1.07
300	27.72	1.30			

Station 5709; Aug. 29; latitude 59°16′ N., longitude 45°05′ W., depth 2,030 m.

Depth, meters	$\sigma_{t\theta}$	Total *P* µga/*L*	Depth, meters	$\sigma_{t\theta}$	Total *P* µga/*L*
0	27.17	1.00	298	27.65	1.24
25	27.17	0.90	364	27.66	1.30
50	27.25	0.97	541	27.70	1.24
75	27.48	1.15	781	27.73	1.22
99	27.57	1.07	883	27.76	1.02
149	27.59	1.17	1,343	27.79	1.15
199	27.60	1.25	1,792	27.85	1.13

Station 5710; Aug. 29; latitude 59°23′ N., longitude 44°54′ W.; depth 1,271 m.

Depth, meters	$\sigma_{t\theta}$	Total *P* µga/*L*	Depth, meters	$\sigma_{t\theta}$	Total *P* µga/*L*
0	27.24	0.92	189	27.51	1.11
24	27.24	0.87	284	27.61	1.18
47	27.24	0.95	288	27.63	1.09
71	27.26	0.93	441	27.64	1.19
95	27.27	0.96	600	27.67	1.19
142	27.40	1.02	787	27.70	1.17

Station 5711; Aug. 29; latitude 59°30′ N., longitude 44°16′ W.; depth 196 m.

Depth, meters	$\sigma_{t\theta}$	Total *P* µga/*L*	Depth, meters	$\sigma_{t\theta}$	Total *P* µga/*L*
0	26.36	0.60	78	27.05	0.88
26	26.44	0.66	105	27.12	0.90
52	26.84	0.91	156	27.28	0.94

Station 5712; Aug. 29; latitude 59°32′ N., longitude 44°07′ W.; depth 170 m.

Depth, meters	$\sigma_{t\theta}$	Total *P* µga/*L*	Depth, meters	$\sigma_{t\theta}$	Total *P* µga/*L*
0	26.00	0.80	76	27.08	1.12
25	26.94	0.90	101	27.10	1.22
50	27.02	0.93	150	27.33	1.35

Station 5713; Aug. 29; latitude 59°40′ N., longitude 43°54′ W.; depth 151 m.

Depth, meters	$\sigma_{t\theta}$	Total *P* µga/*L*	Depth, meters	$\sigma_{t\theta}$	Total *P* µga/*L*
0	26.35	0.99	71	26.59	1.34
24	26.48	0.99	94	26.91	1.20
47	26.57	1.11	124	27.19	1.28

Station 5714; Aug. 29; latitude 59°42′ N., longitude 43°44′ W.; depth 153 m.

Depth, meters	$\sigma_{t\theta}$	Total *P* µga/*L*	Depth, meters	$\sigma_{t\theta}$	Total *P* µga/*L*
0	26.14	0.95	69	26.37	0.94
23	26.16	1.15	93	26.64	1.22
46	26.19	1.22	138	26.98	1.31

Station 5715; Aug. 29; latitude 59°44′ N., longitude 43°12′ W.; depth 174 m.

Depth, meters	$\sigma_{t\theta}$	Total *P* µga/*L*	Depth, meters	$\sigma_{t\theta}$	Total *P* µga/*L*
0	26.64	1.03	79	27.12	0.91
26	26.79	1.02	104	27.18	0.99
52	26.95	1.00	157	27.28	1.02

Station 5716; Aug. 29; latitude 59°44.5′ N., longitude 42°53′ W.; depth 172 m.

Depth, meters	$\sigma_{t\theta}$	Total *P* µga/*L*	Depth, meters	$\sigma_{t\theta}$	Total *P* µga/*L*
0	27.07	0.92	82	27.18	1.04
28	27.10	1.02	109	27.27	0.99
54	27.16	0.97	164	27.39	1.09

TOTAL PHOSPHORUS DATA COLLECTED IN 1954—Continued

Station 5717; Aug. 29; latitude 59°45.5′ N., longitude 42°30′ W.; depth 340 m.

Depth, meters	$\sigma_{t\theta}$	Total *P* µga/*L*	Depth, meters	$\sigma_{t\theta}$	Total *P* µga/*L*
0	27.16	1.00	105	27.48	1.13
26	27.16	1.08	157	27.57	1.37
53	27.16	1.01	209	27.59	1.30
79	27.18	0.94	314	27.62	1.24

Station 5718; Aug. 30; latitude 59°45′ N., longitude 42°24′ W.; depth 1,124 m.

Depth, meters	$\sigma_{t\theta}$	Total *P* µga/*L*	Depth, meters	$\sigma_{t\theta}$	Total *P* µga/*L*
0	27.17	0.94	211	27.58	1.35
26	27.18	1.03	317	27.62	1.33
53	27.19	0.95	418	27.64	1.26
79	27.42	1.18	617	27.66	1.56
106	27.53	1.27	810	27.67	1.42
158	27.56	1.42	1,026	27.69	1.45

Station 5719; Aug. 30; latitude 59°45′ N., longitude 42°05′ W ; depth 1,737 m.

Depth, meters	$\sigma_{t\theta}$	Total *P* µga/*L*	Depth, meters	$\sigma_{t\theta}$	Total *P* µga/*L*
0	27.06	1.09	316	27.64	1.58
26	27.07	1.20	368	27.65	1.27
53	27.44	1.45	561	27.71	1.34
79	27.48	1.42	762	27.75	1.29
106	27.53	1.46	963	27.78	1.32
157	27.57	1.40	1,482	27.84	1.14
210	27.62	1.49			

Station 5720; Aug. 30; latitude 59°44′ N., longitude 41°36′ W.; depth 1,975 m.

Depth, meters	$\sigma_{t\theta}$	Total *P* µga/*L*	Depth, meters	$\sigma_{t\theta}$	Total *P* µga/*L*
0	26.82	0.78	290	27.65	1.29
24	27.07	0.93	370	27.68	1.27
48	27.45	1.08	558	27.74	1.30
73	27.51	1.13	751	27.74	1.38
97	27.54	1.15	945	27.77	1.26
144	27.59	1.17	1,470	27.83	1.38
193	27.62	1.20	1,839	27.87	1.24

Station 5721; Aug. 30; latitude 59°47′ N., longitude 40°48′ W.; depth 2,213 m.

Depth, meters	$\sigma_{t\theta}$	Total *P* µga/*L*	Depth, meters	$\sigma_{t\theta}$	Total *P* µga/*L*
0	26.82	0.90	322	27.74	1.45
27	27.50	1.13	428	27.75	1.36
53	27.58	1.30	637	27.76	1.59
81	27.61	1.37	843	27.76	1.35
107	27.63	1.40	1,047	27.79	1.22
161	27.68	1.38	1,572	27.84	1.24
215	27.72	1.44	2,097	27.89	1.16

Station 5722; Aug. 30; latitude 59°53.5′ N., longitude 39°46′ W.; depth 2,743 m.

Depth, meters	$\sigma_{t\theta}$	Total *P* µga/*L*	Depth, meters	$\sigma_{t\theta}$	Total *P* µga/*L*
0	26.72	0.70	289	27.74	1.21
24	26.91	0.82	363	27.75	1.17
48	27.58	1.26	544	27.76	1.19
72	27.63	1.28	722	27.77	1.20
96	27.66	1.31	1,377	27.79	1.19
144	27.69	1.29	1,870	27.83	1.25
193	27.70	1.18	2,481	27.90	1.13

Station 5723; Aug. 30; latitude 59°53′ N., longitude 38°49′ W.; depth 2,871 m.

Depth, meters	$\sigma_{t\theta}$	Total *P* µga/*L*	Depth, meters	$\sigma_{t\theta}$	Total *P* µga/*L*
0	26.65	1.03	396	27.75	1.30
25	26.72	0.75	592	27.76	1.30
51	27.55	1.44	787	27.77	1.26
76	27.62	1.46	981	27.79	1.28
101	27.67	1.36	1,485	27.80	1.26
152	27.72	1.35	1,999	27.84	1.24
203	27.71	1.35	2,518	27.89	1.23
304	27.74	1.26	2,810	27.95	1.18

Station 5724; Aug. 31; latitude 59°58.5′ N., longitude 37°19′ W.; depth 3,054 m.

Depth, meters	$\sigma_{t\theta}$	Total *P* µga/*L*	Depth, meters	$\sigma_{t\theta}$	Total *P* µga/*L*
23	27.08	0.98	591	27.75	1.25
47	27.56	1.25	785	27.76	1.23
70	27.60	0.84	976	27.77	1.15
94	27.63	1.35	1,472	27.79	1.24
141	27.68	1.31	1,972	27.82	1.23
187	27.69	1.30	2,323	27.85	1.25
281	27.71	1.32	2,813	27.88	1.20
396	27.73	1.31			

Station 5725; Aug. 31; latitude 59°59′ N., longitude 35°49′ W.; depth 3,033 m.

Depth, meters	$\sigma_{t\theta}$	Total *P* µga/*L*	Depth, meters	$\sigma_{t\theta}$	Total *P* µga/*L*
0	26.70	0.74	386	27.72	1.30
24	26.73	0.83	578	27.74	1.31
48	27.43	1.19	768	27.76	1.22
73	27.56	1.27	958	27.79	1.24
97	27.57	1.25	1,450	27.80	1.22
145	27.61	1.20	1,952	27.83	1.24
193	27.65	1.30	2,466	27.86	1.22
290	27.70	1.32	2,907	27.92	1.13

Station 5726; Aug. 31; latitude 59°17′ N., longitude 36°40′ W.; depth 2,944 m.

Depth, meters	$\sigma_{t\theta}$	Total *P* µga/*L*	Depth, meters	$\sigma_{t\theta}$	Total *P* µga/*L*
0	26.68	0.67	400	27.74	1.43
25	26.78	0.85	597	27.76	1.39
51	27.45	1.50	792	27.77	1.38
76	27.56	1.40	985	27.77	1.41
102	27.61	1.30	1,490	27.79	1.48
152	27.66	1.43	2,001	27.83	1.52
203	27.70	1.42	2,476	27.87	1.50
305	27.72	1.57	2,877	27.89	1.28

Station 5727; Sept. 1; latitude 58°31.5′ N., longitude 37°25′ W.; depth 3,109 m.

Depth, meters	$\sigma_{t\theta}$	Total *P* µga/*L*	Depth, meters	$\sigma_{t\theta}$	Total *P* µga/*L*
0	26.67	1.06	381	27.66	1.27
25	26.69	0.69	571	27.73	1.26
50	27.45	1.13	759	27.73	1.26
76	27.51	1.15	948	27.76	1.24
101	27.54	1.15	1,442	27.80	1.20
151	27.55	1.16	1,947	27.83	1.14
202	27.58	1.18	2,480	27.87	1.19
303	27.64	1.23	2,950	27.90	1.21

Station 5728; Sept. 1; latitude 57°45′ N., longitude 38°04′ W.; depth 3,219 m.

Depth, meters	$\sigma_{t\theta}$	Total *P* µga/*L*	Depth, meters	$\sigma_{t\theta}$	Total *P* µga/*L*
0	26.68	0.74	602	27.75	1.37
25	26.69	0.74	797	27.76	1.30
50	27.36	1.14	992	27.77	1.38
76	27.52	1.18	1,502	27.80	1.40
101	27.55	1.19	2,021	27.85	1.35
151	27.60	1.34	2,526	27.88	1.33
202	27.64	1.45	3,027	27.89	1.50
303	27.67	1.45	3,178	27.89	1.27
403	27.71	1.39			

Station 5729; Sept. 1; latitude 57°02.5′ N., longitude 39°04′ W., depth 3,200 m.

Depth, meters	$\sigma_{t\theta}$	Total *P* µga/*L*	Depth, meters	$\sigma_{t\theta}$	Total *P* µga/*L*
0	26.51	0.92	620	27.75	1.36
26	26.55	1.02	826	27.77	1.31
52	27.43	1.35	1,041	27.78	1.30
78	27.52	1.41	1,595	27.79	1.29
103	27.53	1.39	2,033	27.82	1.34
154	27.59	1.27	2,529	27.86	1.49
206	27.61	1.33	3,027	27.90	1.45
309	27.68	1.31	3,149	27.90	1.39
414	27.72	1.38			

TOTAL PHOSPHORUS DATA COLLECTED IN 1954—Continued

Station 5730; Sept. 2; latitude 56°24′ N., longitude 40°01′ W.; depth 2,671 m.

Depth, meters	$\sigma_{t\theta}$	Total *P* µga/*L*	Depth, meters	$\sigma_{t\theta}$	Total *P* µga/*L*
0	26.42	1.50	388	27.72	1.41
25	26.49	1.19	580	27.74	1.50
50	27.45	1.45	772	27.76	1.45
75	27.53	1.48	976	27.78	1.44
100	27.54	1.38	1,490	27.81	1.45
150	27.61	1.47	1,882	27.85	1.45
200	27.65	1.45	2,374	27.87	1.30
300	27.71	1.58			

Station 5731; Sept. 2; latitude 57°04′ N., longitude 40°34′ W.; depth 3,290 m.

Depth, meters	$\sigma_{t\theta}$	Total *P* µga/*L*	Depth, meters	$\sigma_{t\theta}$	Total *P* µga/*L*
0	26.54	0.82	494	27.75	1.48
25	26.54	1.08	668	27.75	1.33
49	27.41	1.40	849	27.77	1.29
74	27.52	1.59	1,325	27.80	1.27
98	27.57	1.44	1,835	27.82	1.31
148	27.62	1.42	2,580	27.86	1.27
197	27.64	1.65	3,085	27.90	1.18
295	27.69	1.39	3,290	27.90	1.15
324	27.72	1.47			

Station 5732; Sept. 2; latitude 57°36.5′ N., longitude 41°08′ W.; depth 3,292 m.

Depth, meters	$\sigma_{t\theta}$	Total *P* µga/*L*	Depth, meters	$\sigma_{t\theta}$	Total *P* µga/*L*
0	26.62	0.75	519	27.75	1.21
26	26.64	0.78	698	27.77	1.29
52	27.52	1.17	881	27.78	1.25
78	27.63	1.22	1,371	27.79	1.19
105	27.66	1.26	1,891	27.80	1.22
156	27.70	1.32	2,644	27.88	1.14
208	27.72	1.28	3,045	27.90	1.15
313	27.74	1.23	3,245	27.93	1.10
343	27.75	1.24			

Station 5733; Sept. 2–3; latitude 58°10′ N., longitude 41°49′ W.; depth 3,017 m.

Depth, meters	$\sigma_{t\theta}$	Total *P* µga/*L*	Depth, meters	$\sigma_{t\theta}$	Total *P* µga/*L*
0	26.91	0.74	358	27.75	1.15
24	26.92	0.77	558	27.76	1.20
47	27.55	1.16	758	27.76	1.23
71	27.63	1.16	1,458	27.79	1.11
94	27.68	1.19	1,957	27.83	1.20
141	27.69	1.18	2,370	27.85	1.20
188	27.73	1.18	2,720	27.87	1.05
282	27.74	1.14			

Station 5734; Sept. 3; latitude 58°42′ N., longitude 42°23′ W.; depth 2,506 m.

Depth, meters	$\sigma_{t\theta}$	Total *P* µga/*L*	Depth, meters	$\sigma_{t\theta}$	Total *P* µga/*L*
0	27.00	0.86	325	27.71	1.16
23	27.26	0.88	494	27.76	1.15
46	27.60	1.10	667	27.77	1.20
69	27.61	1.16	845	27.79	1.20
92	27.63	1.15	1,343	27.82	1.17
138	27.66	1.23	1,892	27.86	1.20
184	27.68	1.16	2,252	27.88	1.14
276	27.72	1.20			

Station 5735; Sept. 4; latitude 58°54.5′ N., longitude 42°58′ W.; depth 2,012 m.

Depth, meters	$\sigma_{t\theta}$	Total *P* µga/*L*	Depth, meters	$\sigma_{t\theta}$	Total *P* µga/*L*
0	27.24	0.97	316	27.69	1.22
27	27.24	0.95	378	27.70	1.24
53	27.26	0.94	566	27.75	1.24
79	27.58	1.13	754	27.76	1.30
105	27.58	1.17	940	27.78	1.13
159	27.60	1.16	1,428	27.86	1.25
211	27.63	1.24	1,926	27.92	1.21

Station 5736; Sept. 4; latitude 59°04.5′ N., longitude 43°19′ W.; depth 1,646 m.

Depth, meters	$\sigma_{t\theta}$	Total *P* µga/*L*	Depth, meters	$\sigma_{t\theta}$	Total *P* µga/*L*
0	27.12	0.98	287	27.66	1.21
24	27.16	0.96	349	27.67	1.13
48	27.18	0.98	526	27.70	1.20
72	27.25	1.05	703	27.73	1.24
96	27.48	1.18	886	27.77	1.21
144	27.55	1.20	1,357	27.80	1.10
191	27.61	1.17			

Station 5737; Sept. 4; latitude 59°22′ N., longitude 43°40′ W.; depth 666 m.

Depth, meters	$\sigma_{t\theta}$	Total *P* µga/*L*	Depth, meters	$\sigma_{t\theta}$	Total *P* µga/*L*
0	26.52	0.88	156	27.51	1.06
26	26.98	0.88	209	27.58	1.10
52	27.14	0.95	399	27.63	1.10
79	27.17	0.96	607	27.66	1.21
105	27.25	1.11			

Station 5738; Sept. 4; latitude 59°26′ N., longitude 43°46′ W.; depth 279 m.

Depth, meters	$\sigma_{t\theta}$	Total *P* µga/*L*	Depth, meters	$\sigma_{t\theta}$	Total *P* µga/*L*
0	26.21	0.77	100	27.11	0.90
25	26.72	0.86	149	27.45	1.48
50	26.84	0.85	199	27.52	1.20
75	26.92	0.79	274	27.67	1.17

Station 5739; Sept. 4; latitude 59°29′ N., longitude 43°51′ W.; depth 224 m.

Depth, meters	$\sigma_{t\theta}$	Total *P* µga/*L*	Depth, meters	$\sigma_{t\theta}$	Total *P* µga/*L*
0	25.97	0.72	100	27.07	0.95
25	26.53	0.90	149	27.25	0.94
50	26.90	0.80	199	27.44	1.00
75	26.94	0.83			

Station 5740; Sept. 4; latitude 59°40′ N., longitude 43°54′ W.; depth 144 m.

Depth, meters	$\sigma_{t\theta}$	Total *P* µga/*L*	Depth, meters	$\sigma_{t\theta}$	Total *P* µga/*L*
0	25.07	0.69	76	26.73	0.85
25	26.17	0.69	101	26.98	0.93
50	26.64	0.74			

U. S. GOVERNMENT PRINTING OFFICE: 1956

Contribution No. 759

Deep-Sea Research, 1955, Vol. 2, pp. 172 to 181. Pergamon Press Ltd., London.

The significance of organic phosphorus determinations in ocean waters*

BOSTWICK H. KETCHUM, NATHANIEL CORWIN and D. JEAN KEEN[†]

(*Received* 20*th January* 1955)

Summary—1. Total phosphorus can be measured by the Harvey method with an accuracy of about ± 5% (Standard deviation). The blank obtained using reagent grade chemicals without special purification is about 0·2 μgA/L.

2. Organic phosphorus is determined by the difference between the inorganic and the total phosphorus concentrations. Unless this difference exceeds 10% of the concentration it cannot be considered significant.

3. Analysis of almost a thousand samples from the equatorial Atlantic Ocean on which both inorganic and total dissolved phosphorus were determined indicates :

(a) that 95% of the surface water samples contain significant amounts of dissolved organic phosphorus.

(b) that the frequency of samples showing significant amounts of dissolved organic phosphorus decreases with depth and with the content of inorganic phosphorus.

(c) that at depths greater than 1,000 metres no measurable amounts of dissolved organic phosphorus are detectable by the present methods.

INTRODUCTION

ORGANIC phosphorus in sea water may be measured by the difference between the total phosphorus and the inorganic phosphorus content. The inorganic phosphorus must be measured as soon as possible after the removal of the samples from the sea but the total phosphorus samples can be stored and measured in the laboratory. Very few determinations of total phosphorus have been made, although it has been demonstrated that the concentration of organic phosphorus may exceed the concentration of inorganic phosphorus in the surface waters (KALLE, 1935 ; REDFIELD, SMITH and KETCHUM, 1937 ; HARVEY, 1948 ; HANSEN and ROBINSON, 1950 ; ARMSTRONG and HARVEY, 1953). HARVEY'S (1948) total phosphorus method is less laborious and time consuming than earlier methods, and it has been used on a routine basis in this laboratory for about three years. Samples can be obtained on any oceanographic cruise without the necessity of personnel trained in intricate chemical methods and they can be stored for periods of up to two years without measurable change in total phosphorus. This method should greatly facilitate studies of the distribution of phosphorus in the oceans.

During a joint cruise by the *Atlantis* and *Albatross* III in the equatorial Atlantic Ocean in 1952 nearly a thousand samples were collected on which both inorganic and total phosphorus determinations have been made. Since the organic phosphorus was frequently represented by a small difference between two relatively large values, it was found necessary to evaluate the methods statistically in order to determine whether or not the differences were significant.

---

*Contribution No. 759 from the Woods Hole Oceanographic Institution. This investigation was supported in part under contracts with the Office of Naval Research.

[†] Present Address, U.S. Navy Hydrographic Office, Wash., D.C.

This paper presents the results of the evaluation of the accuracy of the Harvey method for total phosphorus determinations, and of the method used on shipboard for the determination of inorganic phosphorus. The results indicate that about 95% of the surface water samples obtained from the equatorial Atlantic Ocean contained significant amounts of dissolved organic phosphorus. In water deeper than 1,000 metres the concentration of dissolved organic phosphorus was too small to be distinguished by the present methods.

TOTAL PHOSPHORUS

1. *Method :*

The method as described by HARVEY (1948) has been altered only slightly. It is briefly outlined below, but reference to the original is recommended.

1. Samples of sea water of about 200 ml. are placed in 8 oz. bottles with plastic screw caps and rubber liners. These bottles are carefully cleaned beforehand by scrubbing the walls and bottom with a rubber policeman and 10% HCl and are then rinsed thoroughly with tap water and 5 or 6 times with distilled water. They need not be rinsed with the sea water sample. Samples have been stored in the dark for periods up to two years without measurable change in total phosphorus.

2. When analyzed in the laboratory, 1 ml. of concentrated HCl is added to the bottle, the walls and bottom are vigorously scrubbed to remove any adhering bacterial film, and a 50 ml. sample is transferred by volumetric pipette to a 125 ml. " Vycor " flask.

3. Two ml. of 38% H_2SO_4 and 4 drops of saturated aqueous solution of Na_2SO_3 are added to each flask, which is covered with a 50 ml. " Pyrex " beaker.

4. The samples are digested in a steam autoclave for five hours at about 38 lb./sq. inch. pressure (140°C).

5. After cooling, each sample is diluted to 100 ml. with distilled water, transferred to a 250 ml. " Pyrex " flask and 2 ml. of 2·5% amonium molybdate is added. A measurement of light absorption is made with the photoelectric colorimeter described by FORD (1950) using a tube length of 29 cm and red light filters (Corning 2408). This gives a measure of the turbidity and is the zero reading for each determination.

6. Four drops of a stannous chloride solution containing 0·2 g of $SnCl_2 . 2H_20$ in 25 ml. of 10% HCl are added. This solution is made fresh each day.

7. The colour developed is read with the photoelectric colorimeter within 5-10 minutes after addition of the $SnCl_2$, using the same light filter and tube as were used in determining turbidity (paragraph 5).

8. One or more blanks are digested with each set of analyses. Distilled water is treated in exactly the same way as the samples (2 to 7 above).

9. The photoelectric colorimeter is calibrated by analyzing samples to which inorganic phosphate has been added to sea water in concentrations ranging from 0-3 μg atoms P/litre. The sea water used is surface Sargasso Sea water which is low in total phosphorus and usually ranges from 0·25 to 0·75 μg atoms P/litre. A linear relationship is found between concentration due to added phosphorus and reading within these limits.

The colour developed is temperature dependent, increasing about 1% per degree centigrade (see WOOSTER and RAKESTRAW, 1948). Our analyses have been conducted at ambient room temperatures and the calibrations have been made under the same conditions. The effect of temperature variations is included in the standard deviation of the method which will be discussed below.

ARMSTRONG and HARVEY (personal communication) have detected dissolution of phosphate from their glass bottles during storage. They report solution of less than 0·02 μg atoms/litre in one week from " good " glass and between 0·2 and 0·4 μg atoms/litre in one week from " poor " glass. We have been unable to detect measureable increases of phosphate during storage in the dark for periods up to two years, though a considerable increase in turbidity of the sample sometimes occurs when stored after the addition of the HCl. Analyses indicate that an increase in silicate is not responsible for this increased turbidity. We have not tested various types of glass for storage of samples, but our results indicate that the Duraglass bottles we have used are satisfactory.

The substitution of " Pyrex " for " Vycor " flasks during the digestion is unsatisfactory, owing to large blanks and erratic results. This confirms HARVEY'S (1948) conclusion that silica glass containers are essential for the digestion.

Two types of steam digesters have been used. The first was a high pressure vertical model (ten inches in diameter by eleven inches deep) (Eimer and Amend 1-811) in which only 16 samples could be digested daily. We now use an American Sterilizer Co. horizontal steam autoclave (20 in. in diameter by 36 in.) which has been modified with a bypass so that condensed steam in the chamber is returned directly to the gas fired steam boiler. In this apparatus over a hundred samples can be digested at once. We have found it convenient to digest about sixty at a time. The analysis of these can be completed on the following day while additional samples are digesting. The calibrations and results in these two digesters have been identical.

The recovery of organic phosphorus from a standard solution of 5 adenylic acid (adenosine 5 phosphoric acid) containing 1·01 μg atoms/L was tested. After digestion by the Harvey method three replicate samples gave recoveries ranging from 1·0 to 1·02 μg atoms/L.

The recovery of total phosphorus from a culture of *Nitzschia Closterium* was also tested. These samples were diluted ten-fold with distilled water before digestion. The original cultures contained 3,000 cells per millilitre and 13·8 μg atoms P/L. When the count had increased to 390,000 cells per millilitre the inorganic phosphorus in solution was 5·5 μg atoms/L, and the total phosphorus recovered was 13·6 μg atoms/L or 98·5%. With a cell count of 1,150,000 per millilitre, the inorganic phosphorus had decreased to 0·07 and the total phosphorus was 13·4 μg atoms/L or 97%. As will be shown below both of these recoveries are within the expected error of the method of the analysis.

2. *Comparison of Methods* :

Comparison between HARVEY'S (1948) method, and that described by REDFIELD *et al.* (1937) has shown that both yield similar results. Individual analyses, however, did not always agree as well as could be wished, HARVEY'S method giving results ranging from 0·75 to 1·40 times the result obtained by the earlier method. This ratio was calculated for analyses done by both methods on 43 separate samples of sea water. The mean ratio was 1·04 with a standard deviation of 0·143 (± 14%). The replicate results obtained with HARVEY'S method were superior to the replicates by the method of REDFIELD *et al.*, and it appeared that much of this variation was inherent in the older method. The reproducibility of the Harvey method will be discussed below.

These results indicated that identical amounts of total phosphorus were determined by the two methods. Because of the greater simplicity of the Harvey method it has been used exclusively by this laboratory since 1952.

3. *Reagent Blanks :*

The average of all reagent blanks determined between July, 1952 and December, 1954 are given in Table I. The results for each year are presented separately, since there has been a gradual improvement in the value. It should be pointed out that reagent grade chemicals are used throughout, and that no special purification of reagents has been attempted, since it was desirable to place the entire method on as routine a basis as possible. We have used " Baker Analyzed " Reagent grade Sulphuric and Hydrochloric acids, and Merck Reagent grade Sodium sulphite, Ammonium molybdate and Stannous chloride.

Table I

Total phosphorus reagent blanks obtained using the HARVEY *method.*

	1952	1953	1954
No. of analyses	60	125	216
Mode, μg atom P/L	0·33	0·23	0·18
Mean, μg atom P/L	0·36	0·27	0·22
Standard deviation μg atom P/L	0·10	0·07	0·11

The blank obtained during 1954 was 0·22 μg atoms P/litre with a standard deviation of 0·11. The distribution curves for the blank determinations are skewed toward the high values, as is indicated by comparison between the mode and the mean values. Small chance contaminations are difficult to avoid when working with such low concentrations. All determined values have been included in the data in Table I, although some of them were obviously contaminated and were not used in the actual calculation of total phosphorus. For example, the following blanks were obtained during one series of analyses : 0·63, 0·31, 0·32, 0·31, 0·31. The high value in this group was not used for the calculation, but it is included in the data in Table I. If these obviously high values are eliminated, the mean value for 1953 would be 0·25 and for 1954, 0·206. The elimination of these unusually high values does not eliminate the skew towards the high values, but it appears that they occur infrequently enough so that they have not substantially altered the mean blank value presented.

4. *Reproducibility of the Harvey Method :*

During the period January, 1953 – April, 1954, twenty-one calibrations of the photoelectric colorimeter were made. These permit an evaluation of the reproducibility of the method. An example of a single calibration is shown in Fig. 1. The factor to convert the photometer readings (in arbitrary units) to phosphorus is calculated as follows :

$$\frac{\text{Added } P}{R - R_s} = \text{factor}$$

in which R is the reading obtained for the standard solution and R_s is the reading obtained for the sea water used, which includes the reagent blank and any phosphorus present in the sea water. For this calibration the average of the factors for all samples was $8{\cdot}48 \times 10^{-3}$ or one photometer unit was equal to 0·00848 μgAP/L. The standard deviation was $\pm 0{\cdot}50 \times 10^{-3}$ (5·9%).

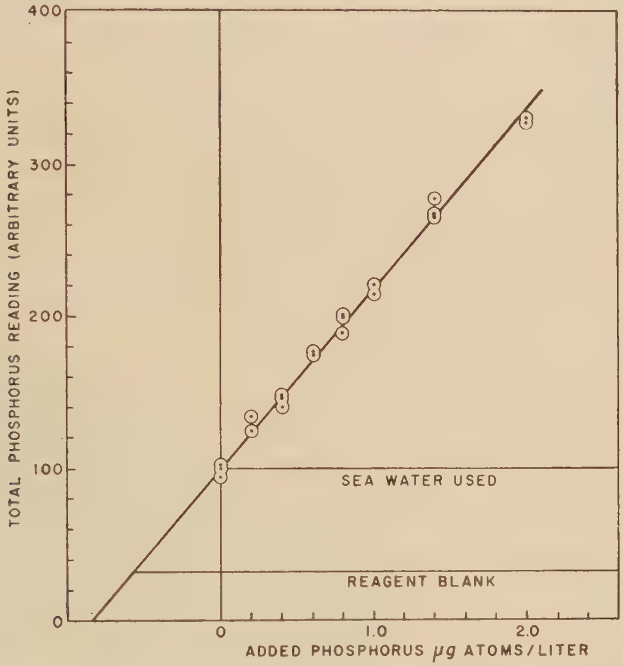

Fig. 1. Example of the calibration of the photometer for the determination of total phosphorus by the Harvey method.

In all, 297 standard solutions are included in the 21 calibrations, and for each of these solutions the factor relating the photometer reading to concentration has been calculated. The standard deviations within each calibration, and the group standard deviation for all of the calibrations performed during this period have been determined. The standard deviation most frequently found for the individual calibrations was 4-5%, though the range was from 2·4 to 11·6%. The average factor for all of the determinations (in arbitrary units) was $8{\cdot}49 \times 10^{-3}$, with a standard deviation of 5·14%. This standard deviation includes changes in reagents and in the photometer over a period of almost two years, as well as the random variations which would be expected within each calibration experiment.

It was mentioned above that the standard deviation of the comparison between the HARVEY and the REDFIELD, SMITH and KETCHUM method was 14%. Since the HARVEY method can be reproduced with an accuracy of about 5%, it would appear that much of the variation found in the comparison can be attributed to the older method. However, these were among the first samples analyzed by the HARVEY method, and it is not certain that the reproducibility of this method was as good at that time as it is now after three years of experience.

INORGANIC PHOSPHORUS

The inorganic phosphorus must be measured at sea at the time of collection to avoid biological changes. The method has been described by WATTENBERG (1937), WOOSTER and RAKESTRAW (1951) and ROBINSON and THOMPSON (1948). The colour developed was measured in the photoelectric colorimeter using a red light filter (Corning 2408) and a cell with a 29 cm light path for concentrations less than 1·0 μg AP/L and a cell with an 8 cm light path for higher concentrations.

The calibration of the photometer was made by adding known amounts of inorganic phosphorus to surface sea water containing little inorganic phosphorus. This procedure automatically compensates for the effect that sea salts have upon the intensity of colour developed. The accuracy of the determination of inorganic phosphorus was evaluated in the way described above for total phosphorus, with the results shown in Table II. The photoelectric colorimeter used on *Atlantis* was the same as that used in the laboratory for both inorganic and total phosphorus determinations. The differences in the factors obtained on *Atlantis* and *Albatross III* results from a different scale on the two instruments which were otherwise identical.

Table II

Variation in the determination of inorganic and of dissolved organic phosphorus.

Source of data	*Concentration range*	*Cell length (cm.)*	*No. of standards*	*Factor* $\times 10^3$	*Standard deviation*	
					inorganic %	*organic** %
Atlantis	0–1·0	29	10	3·68	6·7	8·4
	>1·0	8	20	12·4	9·3	10·3
Albatross III	0–1·0	29	27	8·0	8·4	10·0
	>1·0	8	20	29·3	8·9	10·6
Laboratory	0–1·0	29	92	3·54	7·6	—

* Obtained by $\sqrt{\sigma_1^2 + \sigma_2^2}$ where σ_1 is the standard deviation of the total phosphorus determination (5·14%) and σ_2 is the standard deviation of the inorganic phosphorus determination.

DISSOLVED ORGANIC PHOSPHORUS

The dissolved organic phosphorus is the difference between the total dissolved and the inorganic phosphorus. The accuracy with which it can be measured depends upon the accuracy of both methods. The combined standard deviation of the two methods is included in Table II. Unless the differences between the total and inorganic phosphorus determinations exceeds 10% of the measurement it cannot be considered significant. Actually almost a third of the random differences may be expected to lie outside the ± 10% limits, and about 5% may be expected to exceed ± 20% even though no organic phosphorus is present in any sample. Within these limits, negative differences should be found as frequently as positive differences.

Arsenic present in sea water as arsenate is included in the inorganic phosphorus determination, but is reduced and not included as total phosphorus. Consequently the amount of organic phosphorus may be underestimated by this method. However, the magnitude of this error is small and would produce an insignificant difference in most samples. GORGY, RAKESTRAW and FOX (1948) report arsenate contents of 0·03 to 0·07 μg atom/litre, and ROBINSON and THOMPSON (1948) conclude that the effect of arsenate on the determination of inorganic phosphorus is negligible for sea water containing more than 1 μg atom P/litre.

Both inorganic and total dissolved phosphorus were determined on 991 water samples collected at 94 stations by the *Atlantis* and *Albatross III* during a cruise to the equatorial Atlantic Ocean in 1952. The particulate matter in the water was removed by filtration on shipboard by the method described by REDFIELD, SMITH and KETCHUM (1937). The location of the stations is given in Fig. 2.

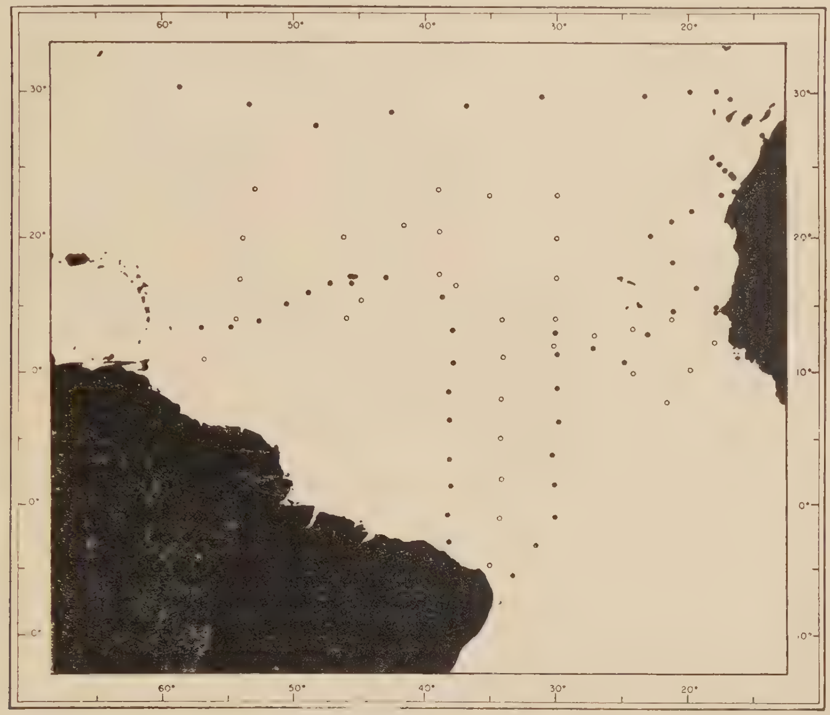

Fig. 2. Location of the stations occupied by *Atlantis* (●) and *Albatross III* (○) at which inorganic phosphorus and total dissolved phosphorus were determined.

When the total phosphorus analysis was completed the results were compared with the inorganic phosphorus concentrations. This was done by plotting the total phosphorus reading (corrected for reagent blank) against the inorganic phosphorus as measured on shipboard. The line determined by the most recent calibration data, and the ± 10% accuracy limits were drawn. One set of data treated in this way is shown in Fig. 3. Practically all of the samples which contained less than 1·0 μg atoms P/litre showed positive and significant differences between the total and inorganic phosphorus contents. This difference is attributed to dissolved organic phosphorus. Several of the samples containing more inorganic phosphorus also showed positive differences, but these were all within the expected errors of the methods and cannot be considered significant. One of these samples gave much less total phosphorus than had been found originally as inorganic. A recheck of this sample gave the analysis indicated by the special symbol. Presumably the bottle storing this sample was not adequately scrubbed before the aliquot was withdrawn for analysis.

The samples to be rechecked were selected as those containing more than 1·0 μg atoms P/litre in which the indicated total phosphorus differed from the inorganic by more than ± 10%. Some samples were selected for rechecking at random, and these included some of the samples containing the smaller amounts of phosphorus. Sixty-three of the *Atlantis* samples were rechecked with the following results: of 31 in which the total phosphorus was less than the inorganic, nine remained in this group, and 19 increased so that the difference did not exceed ± 10%; of 22 samples selected with positive significant differences, fifteen remained in this group and seven decreased so that the difference did not exceed ± 10%; of ten samples which were originally within the ± 10% limits, seven rechecks remained in this group, two decreased and one increased. Although some of these samples were stored for more than a year between the two determinations of total phosphorus, and as much as two years after the measurement of inorganic phosphorus, there is no evidence for a consistent increase which could be attributed to solution of phosphorus from the glass.

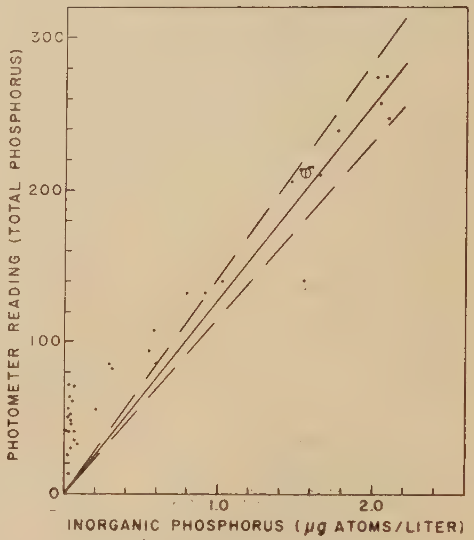

Fig. 3. Relation between the photometer readings for total dissolved phosphorus and the inorganic phosphorus for samples obtained on *Atlantis* stations 4983, 4985, 4986 and 4987. These stations were occupied March 30th to April 2nd, 1952, and the total phosphorus was analyzed on March 27th to April 1st, 1953.

The frequency of significant positive differences between total and inorganic phosphorus (organic phosphorus) and of insignificant and of negative differences is

Table III

Percentage of water samples from the equatorial Atlantic Ocean showing negative, insignificant and positive differences between total and inorganic phosphorus concentrations.

Inorganic Phosphorus (*μg* atoms *P/L*)	*No. of samples*	*Total minus % of inorganic phosphorus samples*		
		(−)	± 10%	(+)
0·00–0·5	370	0·8	4·3	94·9
0·51–1·0	55	0	32·8	61·8
1·01–1·5	125	1·6	76·8	21·6
1·51–2·0	259	1·5	88·0	10·5
> 2·01	182	1·1	92·3	6·6

shown in Table III for the comparison samples obtained on the *Atlantis* and *Albatross III* cruises in 1952. The observations have been separated into groups depending upon the concentration of inorganic phosphorus in the water. The depths at which these concentrations occur is quite variable, since the low nutrient water extends to several hundred metres in the northern part of the area, while it is limited to less than

100 metres near the equator. The concentration grouping, however, helps to identify the location of the water in relation to the ecological system.

About 95% of the water samples containing low inorganic phosphorus concentrations also contained significant amounts of dissolved organic phosphorus. This proportion decreased with increasing phosphorus concentrations, so that at the highest concentrations less than 10% of the samples showed significant amounts of organic phosphorus. Most of the differences observed among the samples containing more inorganic phosphorus than 1·0 μg atom per litre were within the ± 10% limits of error. At all concentrations, very few negative differences exceeding the 10% limit were found.

One of the difficulties in deciding whether the deep water, which contains the greater amount of inorganic phosphorus, also contains organic phosphorus, is that the inherent errors of the method eliminate positive values up to 10% of the concentration. As the concentration increases, the ability to identify larger and larger quantities of organic phosphorus by difference is lost. The question arises : are the low frequencies of organic phosphorus in the deeper waters an artifact produced by the errors of the method, or does this water really contain little or no organic phosphorus? No final answer can be given until our methods of analysis improve substantially.

The following further breakdown of the data in Table III is pertinent to this question. Nearly 50% of the surface (0–·5 μgAP/L) samples, contained dissolved organic phosphorus in concentrations greater than 0·25 μgAP/L. Such concentrations would be outside the limits of error of the method for practically all of the deep water samples, and would be identifiable if present. It is certain, therefore, that organic phosphorus occurs at a greatly decreased frequency in the waters containing the higher concentrations of phosphorus.

Of the thirty-nine samples containing more than 1·5 μg atom P/litre and significant amounts of dissolved organic phosphorus, twenty-six were obtained at depths of less than 1,000 metres and are not pertinent to the question. Two hundred and fifty-nine comparison samples were obtained from corrected depths greater than 1,000 metres. Only thirteen of these (5%) gave positive differences exceeding one standard deviation. Statistically this proportion of the samples could be expected to give differences greater than plus or minus two standard deviations, (± 20%), but only five of these thirteen samples (2%) gave differences this large.

It can be concluded, therefore, that the waters deeper than 1,000 metres in the equatorial Atlantic Ocean contain little if any organic phosphorus. Only thirteen of our samples gave positive results, and these can be attributed to chance errors in the methods of determination.

DISCUSSION

The advantages of the HARVEY method of determining total phosphorus in sea water include the facts that large numbers of samples can be handled by a routine procedure and that the samples can be collected on oceanographic expeditions by people who are not trained in intricate chemical methods. Our present procedure permits analysis of about 250 samples each week, and the capacity of the digester is enough so that the number of analyses could be doubled by providing an additional analyst to complete the photometry. The analysis can be performed with an acceptable accuracy for a colorimetric determination, and it is our experience that the accuracy of total phosphorus analyses conducted in the laboratory exceeds the accuracy of inorganic phosphorus analyses conducted on shipboard.

The HARVEY method gives results identical with the method of REDFIELD, SMITH and KETCHUM (1937). It has not been compared to the perchloric acid method described by HANSEN and ROBINSON (1953). Neither of these two methods, however, provide the simplicity and possibility of conducting large numbers of analyses on a routine basis comparable to the HARVEY method.

It would be desirable to have inorganic phosphorus determinations as well as total phosphorus determinations on the samples. It has been obvious in recent years, however, that there are not enough oceanographic chemists to go to sea on every expedition and the total phosphorus samples can be collected even when no chemist is aboard. Total phosphorus is a more conservative property of the water than is the inorganic phosphorus since it is not subject to as great seasonal changes. It differs from other conservative properties only in the gravitational effects on the particulate matter. ARMSTRONG and HARVEY (1950) have used total phosphorus as an index of the potential fertility of a water mass, and as a characteristic of different water masses in the English Channel. SOULE *et al.* (1954) have used total phosphorus to identify different water masses in the north Atlantic Ocean.

From our results in the equatorial Atlantic Ocean it is apparent that the total phosphorus will be found in greater concentrations than inorganic phosphorus in the surface waters. This makes comparison of total phosphorus with older determinations of inorganic phosphorus somewhat difficult. In water deeper than 1,000 metres, however, the total phosphorus results should not differ significantly from results of earlier measurements of inorganic phosphorus. The study of the phosphorus content of the deep waters of the oceans will, therefore, be greatly facilitated by the use of this method for determining total phosphorus

Woods Hole Oceanographic Institution.

REFERENCES

ARMSTRONG, F. A. J. and H. W. HARVEY (1950), The cycle of phosphorus in the waters of the English Channel. *J. Mar. Biol. Assoc. U.K.*, **29**, 145-162.

FORD, WILLIAM L. (1950), Seagoing photoelectric colorimeter. *Anal. Chem.*, **22**, 1431-1435.

GORGY, SAMY, N. W. RAKESTRAW and D. L. FOX (1948), Arsenic in the Sea. *J. Mar. Res.*, 7 (1), 22-32.

HARVEY, H. W. (1948), The estimation of phosphate and of total phosphorus in sea waters. *J. Mar. Biol. Assoc. U.K.* **27** (2), 337-359.

HANSEN, A. L. and R. J. ROBINSON (1953), The determination of organic phosphorus in sea water with perchloric acid oxidation. *J. Mar. Res.*, **12** (1), 31-42.

KALLE, K. (1935), Meereskundliche chemische Untersuchungen mit Hilfe des Zeisschen Pulfrich-photometers. V. Die Bestimmung des Gesamt Phosphorgehaltes, des Planktonphosphorgehaltes und Trubungsmessungen. *Ann. Hydrogr. Berl.*, **63**, 195-204.

REDFIELD, A. C., H. P. SMITH and B. H. KETCHUM (1937), The cycle of organic phosphorus in the Gulf of Maine. *Biol. Bull.*, **73**, 421-443.

ROBINSON, R. J. and T. G. THOMPSON, (1948), The determination of phosphates in sea water. *J. Mar. Res.*, 7 (1), 33-41.

SOULE, F. M., A. L. BUSH, and J. E. MURRAY, (1954), International observation and ice patrol service in the north Atlantic Ocean – season of 1953. *U.S. Coast Guard Bull.*, **39**.

WATTENBERG, H. (1937), Critical review of the methods used for determining nutrient salts and related constituents in salt water. 1. Methoden zur Bestimmung von Phosphat, Silikat, Nitrat, und Ammoniak im See-wasser. *Cons. p. l'Explor. de la Mer, Rapp. et Proc. Verb.*, **103**, 1-26.

WOOSTER, W. S. and N. W. RAKESTRAW, (1951), The estimation of dissolved phosphate in sea water. *J. Mar. Res.*, 10 (1), 91-100.

Contribution No. 761

Reprinted from SEWAGE AND INDUSTRIAL WASTES, Vol. 27, No. 10, October, 1955
Printed in U. S. A.

BURSTING BUBBLES AND AIR POLLUTION *

BY A. H. WOODCOCK
Woods Hole Oceanographic Institution, Woods Hole, Mass.

Photographic studies of small bubbles bursting at the surface of fresh and sea water have shown that aerosols are produced through the breakup of minute water jets formed by the collapse of the bubble cavities (1). It is the purpose of this paper to show a few of these photographs as evidence of the nature of the bubble-jet-droplet mechanism, and to suggest that this mechanism may cause bacteria to be ejected into the atmosphere from natural water surfaces. The interest of the author has centered around a study of the meteorological role of bubble-produced aerosols. However, studies of bursting bubbles as sources of natural aerosols have left a strong impression that these bubbles and the weather conditions which produce them may be of considerable significance in bacteriology.

Numerous studies have demonstrated the role of aerosols in the distribution of infectious and noninfectious bacteria (2) (3), and in the transport of bacteria by aerosols resulting from bubbling or splashing procedures in the laboratory (4). However, none of these studies of bubbles and air-borne droplets has indicated the nature of the mechanism of aerosol production by bursting bubbles, nor the fact that bubbling and aerosol production in natural waters is a common occurrence associated with a variety of weather conditions. Accordingly, the author's observations concerning bubbles and droplets may be useful to those working on the problems of the origin of air-borne infection and pollution.

Bubble-Jet-Droplet Mechanism

Figure 1 shows photographs of small bubbles forming jets and droplets. Similar photographs have been made of bursting bubbles 200 μ in diameter. Upon bursting at the surface of sea water, bubbles of a size range of about 20 to 2,000 μ in diameter are observed to produce droplets of about 2 to 200 μ in diameter, the larger bubbles forming the larger droplets. Each bubble produces about five droplets which are projected into the air 0.1 to 15 cm. above the surface (Figure 2), the larger bubbles projecting droplets higher. The smaller "microscopic" bubbles produce, upon bursting, much smaller droplets than those pictured. The average diameters of the droplets produced when a bubble bursts are usually about one-tenth of the diameter of the bubble.

At relative humidities commonly found over the sea, droplets of sea water of this size will evaporate quickly to form nuclei of about 1 to 45 μ in diameter. Such nuclei fall slowly (0.01 to 13 cm. per sec.), and atmospheric turbulence and winds cause them to be carried many miles and hundreds of feet into the air (5). Nuclei from droplets produced at the surface of less saline waters (lakes, rivers, etc.) would of course be smaller and hence have a lower settling rate.

Nature of Droplets From Jets

Measurements in the laboratory have shown that the bubble-jet-droplet mechanism is effective in removing films from water surfaces. This is readily demonstrated by placing an oleic acid

---

* Contribution No. 761 of the Woods Hole Oceanographic Institution.

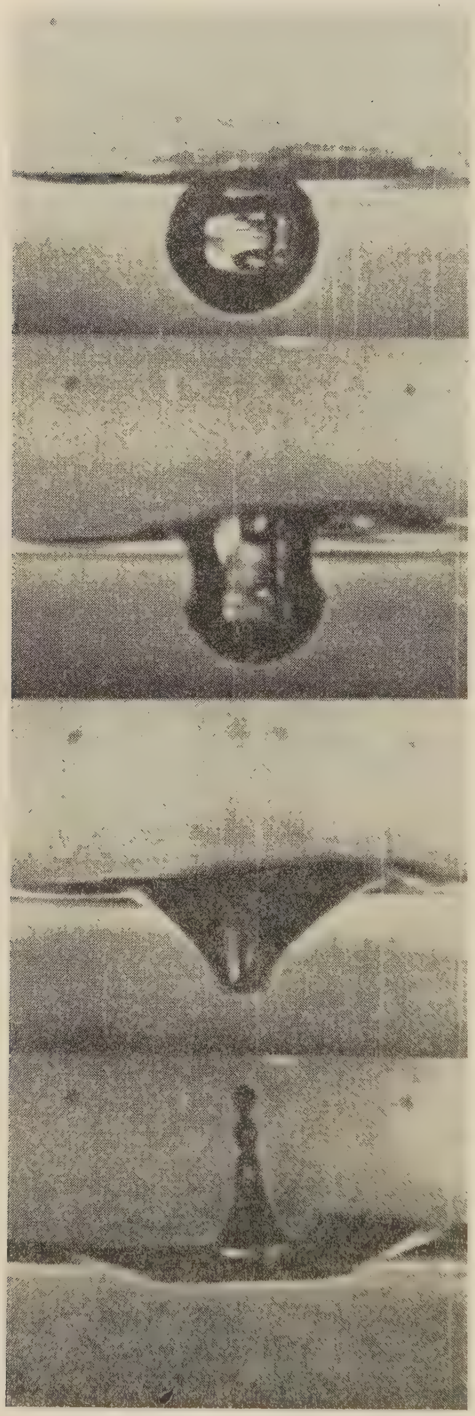

FIGURE 1.—Stages in bubble collapse and jet formation. Bubble diameter 1.7 mm.; time interval between top and bottom pictures 0.002 second.

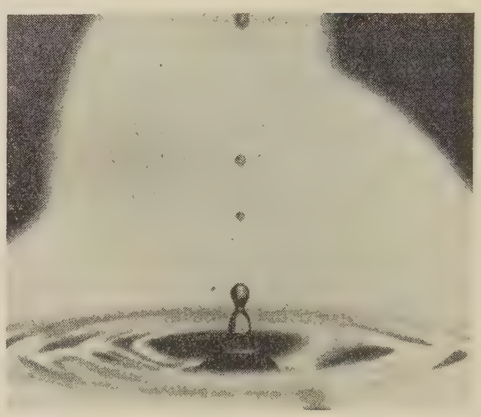

FIGURE 2.—Oblique view of jet and droplets from 1 mm. diameter bubble. Diameter smallest droplet 90 μ.

film on a water surface under which small bubbles are introduced through a fine capillary tube. Droplets produced by these bubbles, when allowed to fall upon a clean water surface which has been dusted with lycopodium, cause a characteristic oleic acid film to displace the powder in circular patches. Similar droplets, when produced at an uncontaminated water surface, show no displacement of the lycopodium dusted surface. This simple experiment shows that the mechanism can remove liquid from exceptionally thin surface layers. In fact, the mechanism is useful in completely removing contaminating films from water surfaces. Thus, aerosols produced by small bubbles may contain materials which are not present in the bulk of the water mass from which the aerosol is produced. A natural occurrence of this film-removing mechanism is indicated later in discussing the "red water" phenomenon of the Gulf of Mexico.

Since the bubble-jet-droplet mechanism removes materials from the superficial film of the water in the laboratory, it probably removes organic films present on natural water surfaces (6) as well. When bubbles are present in these waters, the nature of this film and the number of organisms in it becomes important to those concerned with air pollution.

Observations of Natural Aerosols

There is increasing evidence that droplets, arising naturally from sea water surfaces, sometimes contain materials other than water and sea salts. Zobell (3) found viable marine bacteria deposited on culture media exposed near the sea, and suggested that these marine bacteria were carried by sea-water droplets arising from the breaking of waves. He showed that some of these air-borne bacteria survive despite drying and exposure to sunlight.

During the "red water"* plankton bloom in the Gulf of Mexico, the air over the discolored sea water became quite irritating to the human respiratory tract. Woodcock (8) showed this irritation occurred only when bubbles were present on the sea surface, and he was able to reproduce the effect in the laboratory by inhaling aerosols produced by small bubbles bursting at the surface of stored "red water."

Microscopic examination of the aerosols from "red water" revealed that their surface tension was much reduced, compared to the surface tension of droplets of relatively clear sea water, and that some of the droplets contained parts of plankton organisms (9). It was clear that the droplets from the bursting bubbles were acting as a mechanism for the removal of an irritating agent from the water and for the dispersion of this agent in the air.† The bulk "red water" was, however, entirely non-irritating.

Evidence that the bubble-jet mechanism may produce droplets containing organic materials from the surface film of natural waters is reason to consider whether or not these droplets might contain pathogens. Zobell (3) and Proctor (12) found no pathogens among cultures of a great many aerosol samples taken at various altitudes and locations. However, there is no indication that any of the samples were taken at a place and time at which such organisms might have been most concentrated. For instance, no one seems to have made a study of the bacterial population of aerosols taken, with a modern impact sampler (13), directly downwind from a water area contaminated by sewage, though these areas are known to contain pathogens (14). Would aerosol samples taken in this manner contain pathogens?

A study which attempts to answer this question should be extended over a sufficient period of time to obtain results representing a variety of weather conditions which may effect the number of air-borne bacteria. Some of these important factors are the amount of sunlight, the relative humidity, and the amount of mixing within the air itself (15) (16) (17). The presence or absence of conditions which favor the concentration of bacteria in the surface film and cause the production of great numbers of small bubbles in the surface waters are significant.

Bubbles in Natural Waters

It is the presence of bubbles which is emphasized here, for it is this condition that causes a rapid transport of surface film waters into the atmosphere as droplets. Great numbers of small bubbles are produced in natural waters by the impact of rain drops, by the trapped air among the ice crystals of sleet, hail and snow and by the "white caps" caused by winds. For example, large snow flakes falling into and melting in sea water are observed to introduce microscopic bubbles (10 to 100 μ in diameter) at a rate of about 25 per sq. cm. of water per second. If these bubbles produce, upon bursting at the surface of natural waters, numbers of droplets comparable to similar bubbles in the laboratory, droplets will be ejected into the overlying air at a rate of about 100 per sq. cm. per second. Many of the droplets so produced are too small to fall out of the air quickly, or to be readily washed out through impingement upon precipitation particles.

---

* Sea water which was toxic to fish and which contained great numbers of the dinoflagellate of the genus *Gymnodinium*, see reference (7).

† It was suggested that the substance causing the respiratory irritation and, presumably, also killing the fish might be present in the sea and in the droplets as a surface-active organic material. It was also suggested that samples of this material might be obtained for analysis by filtering the aerosols arising from (experimentally introduced) bubbles bursting at the surface of "red waters." This mode of attack upon the problem of isolating the "red water" poison was not pointed out in the summarizing studies by Galtsoff (10) and by Brongersma-Sanders (11), though both authors concluded from a study of the literature that a toxic substance, produced in living plankton, is probably the cause of the mortality.

The author hopes that these remarks will aid bacteriologists in the investigation of the role of bursting bubbles in natural waters as sources of air-borne pathogens.

Acknowledgment

These observations resulted from a study of atmospheric sea salt nuclei supported by the Office of Naval Research.

References

1. Kientzler, C. F., "Photographic Investigation of the Projection of Droplets by Bubbles Bursting at a Water Surface." *Tellus*, **6**, 1 (1954).
2. Wells, W. F., and Stone, W. R., "On Air-Borne Infection. Study III. Viability of Droplet Nuclei Infection." *Amer. Jour. Hygiene*, **20**, 619 (1931).
3. Zobell, C. E., "Microorganisms in Marine Air." Contribution No. 157. Scripps Inst. Oceanography (1942).
4. Anderson, R. E., Stein, L., Moss, M. L., and Gross, N. H., "Potential Health Hazards of Common Bacteriological Techniques." *Jour. Bact.*, **64**, 473 (1952).
5. Woodcock, A. H., "Salt Nuclei in Marine Air as a Function of Altitude and Wind Force." *Jour. Meterology*, **10**, 362 (1953).
6. Ewing, Gifford, "Slicks, Surface Films and Internal Waves." *Jour. Marine Research*, **IX**, 161 (1950).
7. Gunter, G., Smith, F. G. W., and Williams, R. H., "Mass Mortality of Marine Animals." *Science*, **105**, 257 (1947).
8. Woodcock, A. H., "Note Concerning Human Respiratory Irritation Associated with High Concentration of Plankton and Mass Mortality of Marine Organisms." *Jour. Marine Research*, **VII**, 56 (1948).
9. Woodcock, A. H., Unpublished report to U. S. Fish and Wildlife Service (1947).
10. Galtsoff, P. S., Special Scientific Report No. 46. U. S. Fish and Wildlife Service, Washington, D. C. (1948).
11. Brongersma-Sanders, M., "The Importance of Upwelling Water to Vertebrate Paleontology and Oil Geology." *Kon. Ned. Ak. Wet., Verk. Afd.* (*Tweede Sectie*), **Dl. XLV**, 4, 1 (1948).
12. Proctor, B. C., "The Microbiology of the Upper Air. I." *Proc. Amer. Acad.*, **69**, 315 (1935).
13. Crumb, C., and Wells, W. F., "Air Sampling Performance." *Jour. Bact.*, **54**, 277 (1947).
14. Zobell, C. E., "Marine Microbiology." Chronica Botanica Co., Waltham, Mass. (1946).
15. Fair, G. M., and Wells, W. F., "Viability of *B. coli* Exposed to Ultraviolet Radiation in Air." *Science*, **82**, 28 (1935).
16. Wells, W. F. and Zappasodi, P., "The Effect of Humidity in *Beta Streptococci* (Group C) Atomized into Air." *Science*, **96**, 277 (1942).
17. Jacobs, W. C., "A Discussion of the Physical Factors Governing the Distribution of Microorganisms in the Atmosphere." *Jour. Marine Research*. **2**, 218 (1939).

Contribution No. 767

Transactions, American Geophysical Union Volume 36, Number 3 June 1955

HYDROSCOPES

Edward M. Thorndike

(Contribution No. 767 of the Woods Hole Oceanographic Institution)

Abstract--The construction and operation are described of a device for direct observation of submerged objects in fairly clear water to depths of 30 ft.

Introduction--During World War II, a need was felt for an instrument with which one could observe submerged objects in the neighborhood of docks and other installations down to depths of approximately 30 ft. The Woods Hole Oceanographic Institution undertook the development of such a hydroscope under Contract OEMsr-31 with OSRD during the period from June, 1942, to August, 1943. The need for speed, the lack of specialized staff, and the shortages of materials precluded a thorough, refined solution of the problem, but usable instruments were designed, constructed, and tested. They were easy to handle from a rigid platform such as a dock or dam and quite manageable from a small boat in sheltered water. Calculations indicated that the length could be increased to 100 ft or more. Thus, the hydroscope appeared to be a useful instrument for those concerned with work in fairly clear water of moderate depth.

During the past ten years, there has been considerable activity in shallow-water diving with the Aqualung and in underwater photography and television, but the hydroscope does not seem to have been used appreciably. It is probable that the hydroscope has been neglected in part because its possibilities have not been well known. This brief report is being made in order to bring the instrument to the attention of those interested in underwater research.

Description of the Woods Hole hydroscope--The complete hydroscope consists of three objectiv sections each one meter long, one two-meter and one four-meter intermediate section, and one 3.4-meter eyepiece section, as shown in Figure 1. The three objective sections differ only in that the center of the field of view of one lies on the axis of the hydroscope tube, while in the second it is at 45° and in the third at 90° from the axis. All sections are made of 1/16-inch steel tubing 2-7/8 inches OD. One of the three objective sections and the eyepiece section are always used. The length can be increased by adding either or both of the intermediate units. The sections are joined by bolting together flanges provided with rubber gaskets to make the joints watertight.

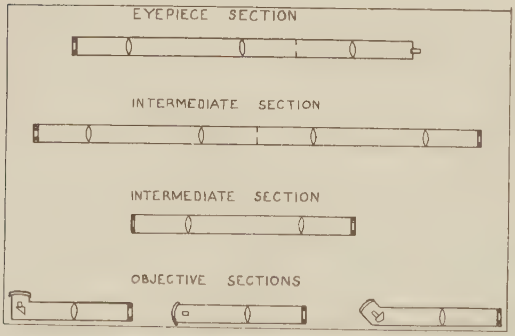

Fig. 1--Complete hydroscope

The optical system consists of an objective lens with several components which forms an image of the object being viewed, a series of achromatic lenses which pass this image up the tube, and a focusing eyepiece for viewing the fina image. A good objective must (1) have a wide field of view and (2) provide rays at the image making small angles with the axis of the tube. Condition (1) is important in order that objects can be found and kept in the field of view for a reasonable time. It is particularly necessary in water containing a considerable quantity of suspended matter or when the observer is in motion Condition (2) is, of course, essential if the light is to be confined to a long tube of small diameter An objective meeting these requirements is show in Figure 2. It has a total angular field in water of approximately 90°. The quality of the outer part of the image is not high, but experience has shown that the outer part of the field is used largely in finding an object which can then be brought to the center for study, and so the objective is satisfactory though far from perfect. A series of achromatic lenses with 50-cm focal lengths spaced 100 cm apart is used to pass the image up the tube. The first lens is located with its focal pla

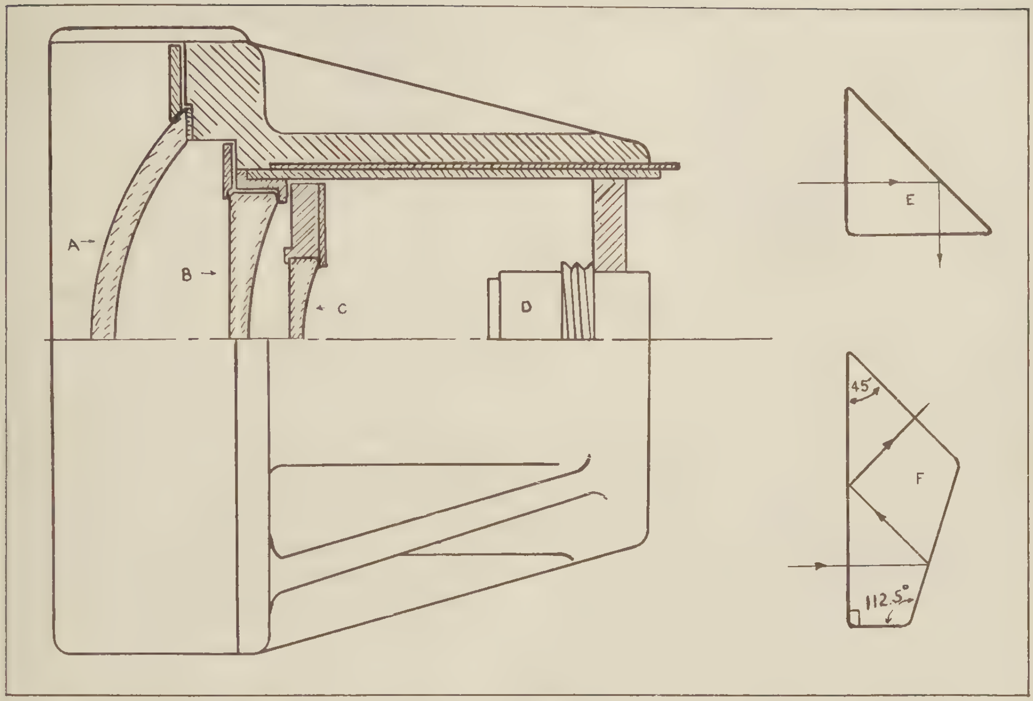

Fig. 2--Objective lens; A, window: outer radius 67 mm, inner radius 62 mm, axial thickness 5 mm, diameter 95 mm, crown glass of refractive index 1.52; B, plano-concave lens: radius 70 mm, axial thickness 3.5 mm, diameter 60 mm, crown glass of refractive index 1.52; C, plano-concave lens: radius 35 mm, axial thickness 3 mm, diameter 40 mm, crown glass of refractive index 1.52; D, Kellner eyepiece: focal length 27.4 mm, made for 7×50 binoculars; E, right-angle prism: square faces 1-1/4 inches on a side; F, prism: large face 1-1/4 by 2-1/4 inches, smaller face making an angle of 45° with the above 1-1/4 by 1-1/4 inches; the axial distances between the plane against which A is seated, the plane side of B, the plane side of C, and the plane against which the threaded part of D is pressed are 8, 12, and 62 mm; the three objective sections are obtained by using either prism E, prism F, or no prism at all.

coincident with the image formed by the objective lens. The plane waves formed by this lens are brought to focus by the second lens. This process is repeated by successive pairs of lenses. Stops with clear diameters of 1-11/16 inches are placed midway between the lenses of a pair in order to block off light which has been scattered or reflected from the walls of the tube. The arrangement of lenses, stops, and windows is shown in Figure 1. The mounting for the lenses is shown in Figure 3. It should be noted that the light passes from one section to the next as plane waves, so that the presence or absence of intermediate sections does not affect the final image in any important respect, and, in addition, the exact length of a section is not critical. A 27-mm Kellner eyepiece in a focusing mount, made for 7×50 binoculars, is used as the eyepiece. The focal lengths of the objective and eyepiece are such that the object appears slightly smaller than it would if the eye were at the window of the hydroscope. Each section is sealed with airtight glass windows in order that the tubes can be kept filled with dry air to prevent condensation and corrosion. The details of the mounting for the windows are shown in Figure 4.

Use of the hydroscope--In making observations with the hydroscope from a dock or dam, it has been found convenient to have a line attached near the lower end of the instrument. The observer holds the upper end by means of a handle clamped at right angles to the tube, while an assistant holds the line. It is sometimes suggested that strong lights can be used to 'pierce' turbid water. Actually, the suspended matter in water acts like fog and scatters the light back. Thus, strong lights usually give a loss in clarity rather than a gain. If artificial light must be used, the lamp should be kept at a distance from the window in order to illuminate as little of the water between

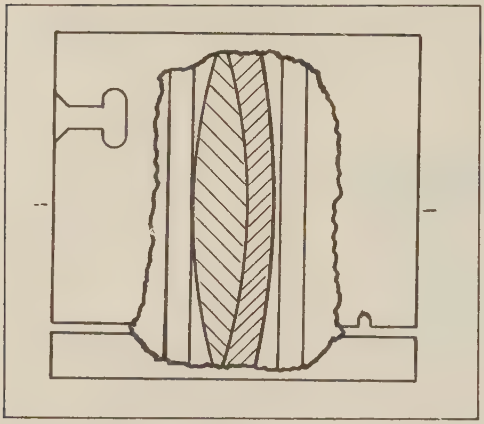

Fig. 3--Achromatic lens mounting; outside diameter is 2-3/4 inches, inside diameter 2-5/8 inches, and length 3 inches; the lens is held firmly between two split rings with three small pieces of cork; the mounting is pushed into the hydroscope tube with a tool having a crossbar that fits the T-slot shown at the upper left and its counterpart 180° away; the small notch in the slot shown at the lower right is used to hold the mounting in place; it is caught around a small screw which has been threaded through the hydroscope tube in the appropriate location and soldered in place.

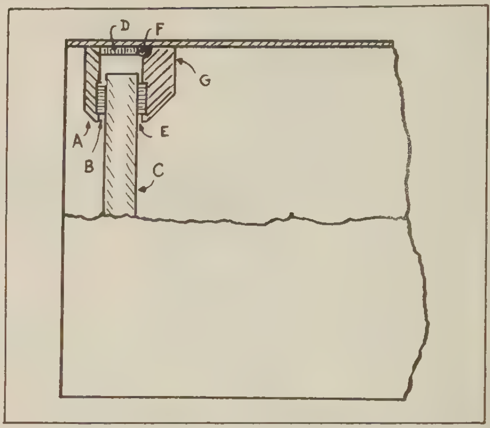

Fig. 4--Window mounting; the 1/4 inch crown glass window C is held between the rubber gaskets B and E by the brass ring A which is attac to the brass ring G by eight screws; at the sam time the rubber ring F is pressed into a groove in G by the brass ring D, thus securing G to the hydroscope tube and completing the seal; a sma hole through G which can be sealed with a steel ball pressed against it with a screw is used for filling the hydroscope section with dry air.

the object and the window as possible. As light at the blue end of the spectrum tends to be scatter more than that at the red end, a yellow filter is sometimes helpful.

In studying objects on the ocean bottom from a boat, the 45° objective has been valuable. A weighted line secured near the lower end of the tube can be used to control the distance between window and bottom. If a very limited region is to be studied, the boat can be anchored and its position controlled by lines. If a larger area is to be surveyed, the boat can be run against the current to give a very low speed over the ground. In either case, a camera can be mounted near the window and photographs taken when objects of interest come into view.

Various more complicated methods of operation involving adjustable vanes, motor-driven pro pellers, and the like have been considered. These hardly seem necessary for the 30-ft hydroscop but might be justifiable on a longer instrument.

Queens College
Flushing 67, N. Y.

(Communicated manuscript received August 19, 1954;
open for formal discussion until November 1, 1955.)

Contribution No. 768

Särtryck ur Tellus nr 4, 1955

Tests of the Salt-Nuclei Hypothesis of Rain Formation

By A. H. WOODCOCK and D. C. BLANCHARD, Woods Hole Oceanographic Institution,[1]
Woods Hole, Massachusetts

(Manuscript received May 18, 1955)

Abstract

Atmospheric chlorides in sea-salt nuclei and the chlorides dissolved in shower rainwaters were recently measured in Hawaii. A comparison of these measurements reveals the remarkable fact that the weight of chloride present in a certain number of nuclei in a cubic meter of clear air tends to be equal to the weight of chloride dissolved in an equal number of raindrops in a cubic meter of rainy air. This result is explained as an indication that the raindrops grow on the salt nuclei in some manner which prevents a marked change in the distribution of these nuclei during the drop-growth process.

The data presented add new evidence in further support of the salt-nuclei raindrop hypothesis previously proposed by the first author (Woodcock, 1952).

1. Introduction

The earlier study of atmospheric salt particles at cloud levels over Florida (Woodcock, 1952) showed that the number of the larger of these particles per cubic meter of air was similar to the average number of raindrops found during rain storms in other locations. This study also showed that the chloride in these nuclei, assuming that each raindrop forms around a single salt nucleus, was sufficient to account for the range of chloride concentrations usually observed in rains. This similarity of the number and chloride content of salt nuclei and the number of raindrops and the chloride content of rain waters led to the suggestion that raindrops form on the large salt nuclei. It was suggested that further studies should reveal a close relation between the salt in the clear air and salt in the rain falling from clouds subsequently formed in this air.

The purpose of this paper is to present the results of the first field tests of the salt-particle raindrop hypothesis. These tests were carried out during 1952 in Hawaii, where the salt nuclei content of the trade winds is well known and where shower rains occur with great regularity from orographic clouds over the mountains. These clouds form in the wind stream as it flows over the islands, and are usually restricted in vertical development to the lower atmosphere up to the trade-wind inversion at about 2,000 meters.

Rain samples were taken within the clouds at positions 1, 3, 4, and 5 (see fig. 1) on the island of Hawaii. Sampling of rain within the clouds made it possible to avoid the difficult problems of evaporation of raindrops and of the coalescence of drops with salt particles, which exists in rains which are sampled far below cloud base (Miyake, Suguira, 1950). The sampling positions were selected because positions 1 and 4 are within the bases of the clouds near the area where many of the first shower rains reach the ground, and because

---

[1] Contribution no. 768 of the Woods Hole Oceanographic Institution. Work supported by the Office of Naval Research, under contract number Nonr-798(00) (NR-082-124).

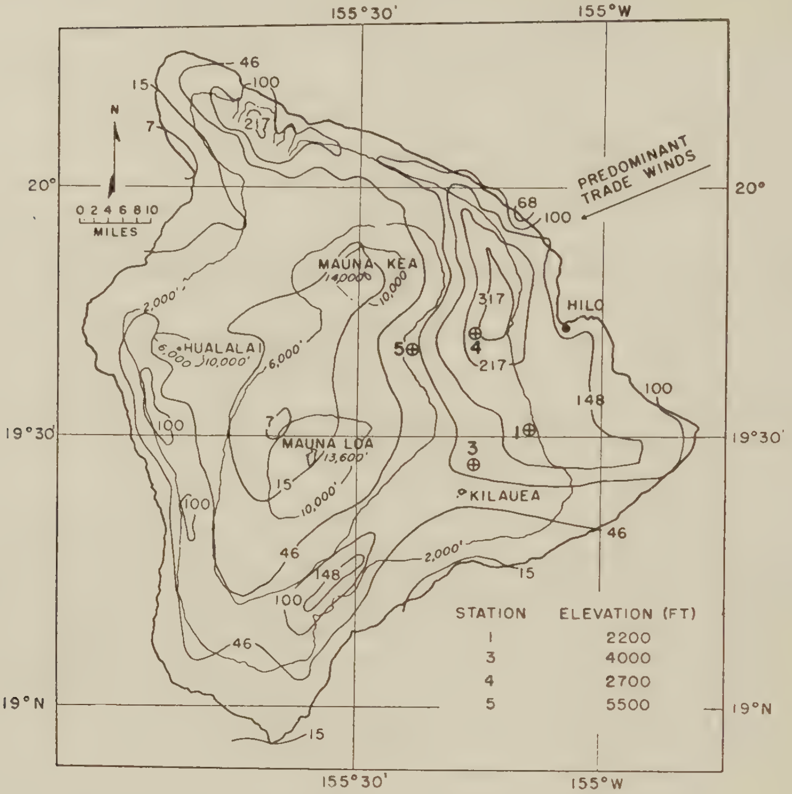
155°30'
155°W
20°
19°30'
19°N
N
0 2 4 6 8 10
MILES
PREDOMINANT TRADE WINDS
MAUNA KEA
14,000'
HUALALAI
10,000'
6,000'
2,000'
MAUNA LOA
13,600'
10,000'
KILAUEA
HILO
46
100
15
7
217
68
317
148
1
3
4
5
STATION ELEVATION (FT)
1 2200
3 4000
4 2700
5 5500

Fig. 1. Isohyetal map of the island of Hawaii, with the locations of the rain-sampling stations used in the present study. The rain-fall contours represent inches annually.

positions 3 and 5 are approximately downwind from 1 and 4 respectively and also within the clouds.

If the salt nuclei were growing to raindrop sizes in these shower clouds, we supposed that the larger less numerous nuclei, which are initially the larger of the cloud droplets (Keith, Arons, 1954), might become larger raindrops and fall out of the clouds at the windward stations 1 and 4 The remaining small and numerous drops, formed upon the smaller and more numerous nuclei, would be expected to fall more slowly and to reach the ground further downwind near positions 3 and 5. Thus it was anticipated that the raindrop number and the rain water chlorinity at stations 1 and 4 might be found to be related to the number of the larger salt nuclei in the air and that the rain at stations 3 and 5 might be similarly related to the smaller nuclei in the air.

The observations presented below give reasonably consistent support to this anticipated pattern of interrelationship of salt nuclei and rain.

2. Sampling rains and atmospheric salt in Hawaii

In this phase of our work in Hawaii the field problems were first, to measure from aircraft the number and the weight of the salt particles in the air stream before it arrived over the islands and second, to measure on the mountainside the drop size distribution, the salt content and intensities of the rains within the orographic clouds.

The filter-paper technique was used for measuring the sizes of the raindrops. Exposure of these filter papers was made at about the same time that bulk rain-water samples were

Table 1. Intensities, chlorinities, and drop size distributions in rains at stations 1 and 4. Sampling by filter-paper and bulk-water techniques

Position	Date (1952)	Time (LCT)	Bulk water samples		Rain drops sampled by filter paper technique										
			Rate mm hr⁻¹	Chloride mg l⁻¹	Rate mm hr⁻¹	Number of rain drops m⁻³ within various diameter ranges (mm)									
						.2—.4	.4—.6	.6—.8	.8—1.	1.—1.2	1.2—1.4	1.4—1.6	1.6—1.8	1.8—2.	2.—2.2
Part 1—Rain intensity range 0.4 to 2.0 mm/hour															
1	May 4	1810	1.9	6.3	0.71	4320	855	21							
1	» 4	1815	1.9	6.2	0.90	3200	1300	43							
1	» 4	1827	0.5	5.7	0.21	2620	19								
1	» 4	1832	1.8	2.8	1.00	6900	971	21	8						
4	» 6	1655	1.9	13.7	1.30	3210	890	287	20						
4	» 6	1706	0.4	24.8	0.71	4050	790	41							
4	» 6	1716	0.4	22.9	0.38	1600	580								
			1.26	11.8	0.74	3700	770	59	4						
Part 2—Intensity range 2.0 to 5.0 mm/hour															
1	May 1	1339	2.9	6.8	3.4	1500	385	390	265	52	26				
1	» 4	1835	2.3	2.9	3.2	1700	850	620	225	40					
1	» 4	1842	2.4	3.2	2.0	1800	1770	390	41	6					
4	» 6	1722	3.2	8.9	2.3	2170	524	590	168						
4	» 6	1734	3.9	8.0	3.8	1080	137	355	550	31					
			2.6	6.0	2.9	1650	733	468	250	26	5				
Part 3—Intensity range 5 to 10 mm/hour															
1	May 4	1848	7.0	1.3	8.0	111	520	690	670	194	54				
4	» 6	1735	7.9	7.7	8.4	790	280	82	87	121	65	125	14		
			7.45	4.5	8.2	450	400	386	379	158	60	63	7		
Part 4—Intensity range > 10 mm/hour															
1	May 1	1344			20.6	1282	369	76	206	164	198	202	23	55	7
1	» 4	1846	12.9	1.5	25.0	290	196	251	710	850	410	85	11		
			12.9	1.5	22.8	786	282	163	458	507	304	144	17	28	4

taken for chloride analysis. One-half square meter stainless steel funnels were used to obtain these bulk-water samples. Adequate volumes of water for chloride analysis could be taken with these funnels in from 10 to 300 seconds, the time depending upon the rain intensity. The filter-paper and funnel samples were taken only at times when the rain rate appeared to be constant. During the sampling periods rain showers were not observed to be drifting in over the land from the windward sea. Thus the samples were taken in orographic showers, with little rain falling to windward of stations 1 and 4.

The results of the rain sampling at stations 1 and 4 are shown on Table 1, and those at stations 3 and 5 on Table 2. In these tables averages are made from data which are separately tabulated into "parts" having similar rain intensities. The average raindrop distribution from the different rain intensities shown on Table 1 were plotted cumulatively as shown on the lower left part of figure 2.

In the present study it is also necessary to know the liquid water content and the rate of fall of the rain sampled with the filter papers. These quantities were derived as illustrated on Table 4, where rate of fall and liquid water content (columns 6 and 7) are determined from the raindrop distributions found in the highest intensity rains at stations 1 and 4 (see Table 1, part 4).

The chlorinities of the rains, which are given on Tables 1 and 2, were determined by the standard Mohr method, using a microburette and a one-hundredth normal silver nitrate solution.

Atmospheric salt particles were sampled in

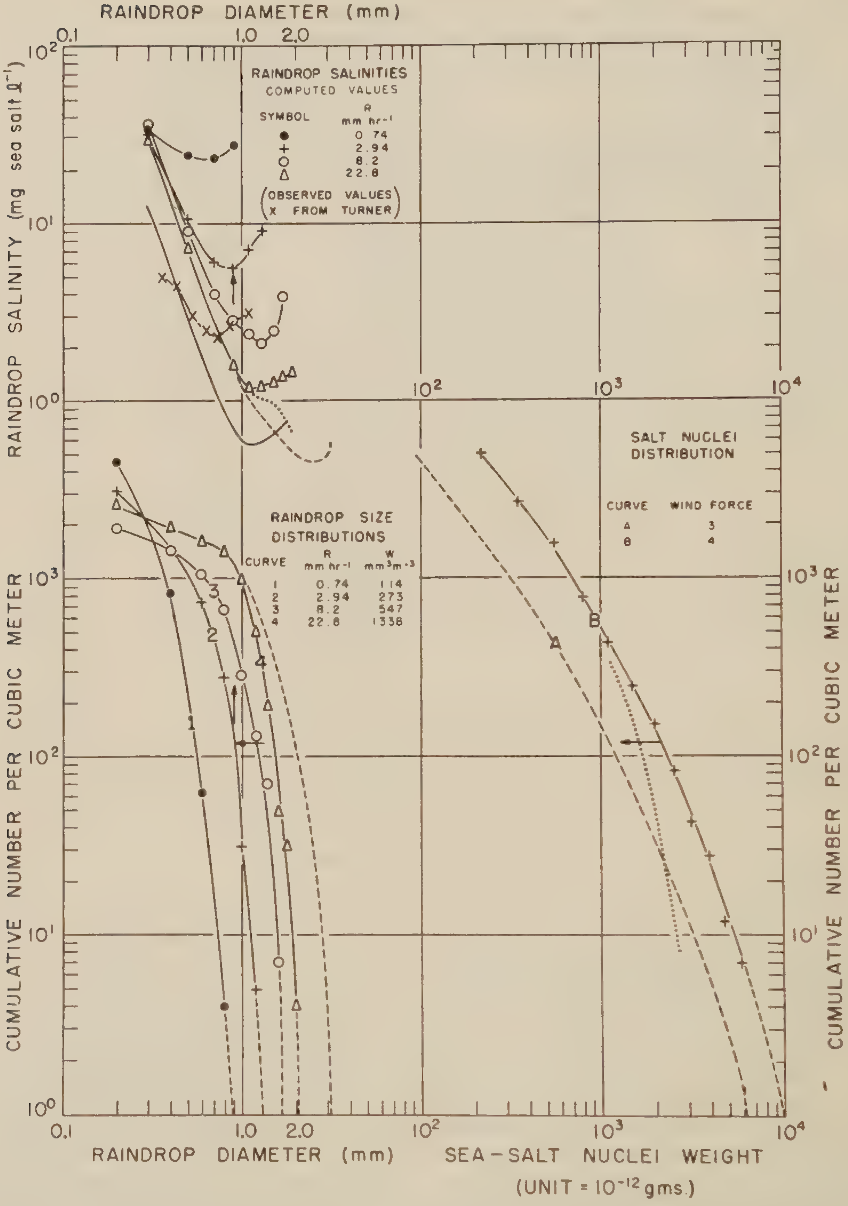

Fig. 2. The lower part of this figure shows cumulative average number distribution curves for salt nuclei and for drops in rains of various intensities (R). These curves are used, as described in the text, to compute the average chlorinity of the rain waters (fig. 5) and to compute the raindrop salinity values which are given above.

clear air at cloud levels over the sea by exposing small glass slides from aircraft. The methods used to sample atmospheric salt and those used to sample the rains have been described previously (Blanchard, 1953; Woodcock, Gifford, 1949; Woodcock, 1952), and w not be discussed further in this paper.

It proved impracticable, during the 19 field trip, to obtain simultaneous observatic of airborne salt and of rain. This difficulty w

Table 2. Intensities, chlorinities and drop size distributions in rains at stations 3 and 5. Sampling by filter-paper and bulk-water techniques

Position	Date (1952)	Time (LCT)	Bulk water samples		Rain drops sampled by filter paper technique						
			Rate mm hr⁻¹	Chloride mg l⁻¹	Rate mm hr⁻¹	Number drops m⁻³ in various diameter ranges (mm)					
						< 0.2	0.2—0.4	0.4—0.6	0.6—0.8	0.8—1.0	1.0—1.2
			Part 1—Intensity range 0.1 to 1.0 mm/hr								
5	Apr. 28	1702	0.13	2.10	0.09	48,700	85				
5	» 28	1740	0.22	2.3	0.19	41,500	2,040				
5	» 28	1812	0.23	6.8	0.06	25,400	243				
5	» 28	1819	0.23	6.8	0.19	78,500	930				
5	» 28	1834	0.33	2.9	0.18	110,000					
3	May 1	1513	1.00	0.8	0.58	800	5,800	485			
3	» 4	1710	0.74	0.8	0.87	20,000	8,600	56			
3	» 4	1737	0.29	0.4	0.37	28,500	5,400				
5	» 5	2043	0.80	0.6	0.65	101,000	7,030	144			
5	» 5	2116	1.00	0.3	0.53	80,800	6,400	33			
5	» 5	2138	0.22	0.4	0.19	66,200	1,360				
5	» 5	2149	0.11	1.4	0.25	149,000					
5	» 5	2222	1.00	0.2	0.26	29,500	3,600				
5	» 5	2235	0.92	0.2	0.45	51,000	6,100				
			0.52	1.9	0.35	59,400	3,400	51			
			Part 2—Intensity range 1.0 to 3.0 mm/hour								
5	Apr. 28	1727	1.09	2.00	1.43	116,000	11,500	1,150			
5	» 29	1759	2.28	1.2	1.95	2,450	5,400	2,060	270	24	
3	May 1	1455	2.70	0.7	2.40		8,300	3,860	31		
5	» 5	2053	1.10	0.4	1.34	65,000	11,200	1,120	27		
			1.79	1.1	1.78	45,800	9,100	2,050	82	6	

eliminated because it had been found, during many previous salt-sampling airplane flights, that a clear relationship existed between the wind force and the quantity of salt nuclei in the air at cloud levels. Figure 3 shows the averaged results from the salt nuclei samples taken in Hawaii on twenty-three different days between June 1951 and July 1952. Differences in the distribution of mass of salt among the nuclei on these days are shown cumulatively on figure 4. This figure also shows that the smoothed curves on figure 3 are based upon from nine to twenty-seven measured size-range categories.

Thus by using these salt-nuclei data and the average wind force observations from U.S. Weather Bureau surface maps (see Table 3), we were able to make a quantitative estimate of the average weight of salt as nuclei in the air during the interval of days when we sampled rain. This average salt amount was compared to the average weight of salt in the rain on these days.

3. Relating the salt in the nuclei to the salt in the rain at the windward stations 1 and 4

As previously stated, the purpose of the present study is to test the idea that a close relationship exists between the weight of the larger salt nuclei per cubic meter of clear air and the weight of salt dissolved in the rain in a cubic meter of rainy air. Expressed differently the above idea would mean that the largest salt nuclei form the raindrops, and that the individual drops which make up the first rains coming from a shower cloud should contain the salt found in an equal number of the largest salt nuclei.

The average numbers and sizes of raindrops for various rain intensities at stations 1 and 4 are plotted cumulatively on figure 2 (see curves, lower left), starting with the largest drops observed. On the same figure the average distribution of number and weight of salt nuclei is similarly presented at the lower right. This salt nuclei curve, taken from the data shown on figure 3 is used because the

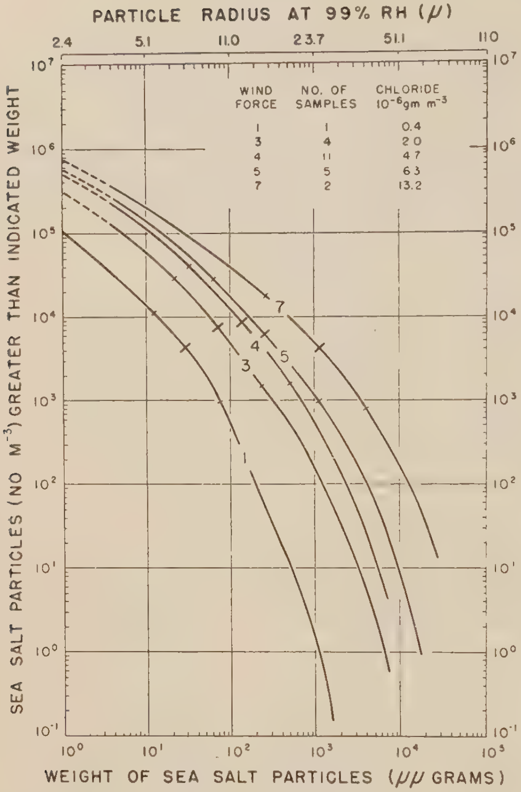

Fig. 3. Cumulative distribution curves for averaged salt nuclei number during winds of various forces in Hawaii. (Taken from Woodcock, 1954.)

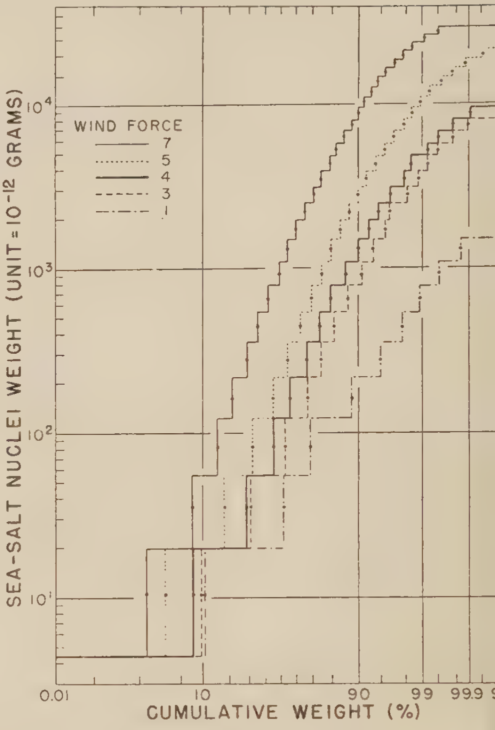

Fig. 4. Averaged cumulative per cent weight distributic curves for salt nuclei present in the atmosphere in Hawa under varying wind conditions (forces 1 through

Table 3. Surface winds over the sea, during t days when rain was sampled, as reported b ships and planes within 400 nautical miles Hilo, Hawaii. Taken from the four daily surfa maps of the North Pacific, which were obtaine from the US Weather Bureau, Honolulu, Hawa

Date 1952	Number of servations reported	Average win force
April 28	14	4.9
April 29	5	3.6
May 1	11	3.3
May 4	8	3.8
May 5	14	3.8
May 6	9	3.8
		av. = 3.9

observed average wind force during the days when the rains samples were taken was very nearly force 4 (see Table 3).

Figure 2 and Table 4 contain the information required to compute the chloride concentration which should be observed in rains if each of the larger salt particles has become a raindrop and if, in the process, little change has occurred in their distribution in the air. For example: rains averaging 6,328 mm^3 m^{-2} sec^{-1} intensity were made up of a definite number of drops of each size range falling per square meter per second (see Table 4, columns 4 and 5). The approximate weight of sea salt in the nucleus of each of these raindrops is taken from the force 4 cumulative salt nuclei curve on figure 2, using the appropriate cumulative raindrop curve to establish, in each case, this nucleus weight. These weights are shown on Table 4, column 8. As an indication of the derivation of these weights, note on salt curve B (fig. 2) that salt particles weighing 420 $\mu\mu$g, occur the cumulative number 2150, which corr sponds to the same number of 0.3 mm dro on raindrop curve number 4. Thus 420 μ is entered on Table 4, column 8, as the weig

Table 4. Averaged rain data derived from filter paper samples, table 1, part 4

1	2	3	4	5	6	7	8	9
Drop dia.	Drop no.	Drop vol.	Drop fall rate	Drop no. falling	Rain rate mm³	Rain water in air	Wt. sea salt in each drop. Unit=	Total sea salt falling in drops
mm	m^{-3}	mm^3	$m\ sec^{-1}$	$m^{-2}\ sec^{-1}$	$m^{-2}\ sec^{-1}$	$mm^3\ m^{-3}$	10^{-12} g	10^{-6} gm $m^{-2}\ sec^{-1}$
0.3	786	.0141	1.17	920	13	11.1	420	0.386
0.5	282	.065	2.06	581	38	18.3	485	0.282
0.7	163	.180	2.90	473	85	29.4	530	0.251
0.9	458	.375	3.65	1,670	628	172	600	1.000
1.1	507	.700	4.30	2,180	1,523	354	830	1.810
1.3	304	1.14	4.90	1,490	1,700	347	1,350	2.010
1.5	143	1.73	5.45	780	1,348	248	2,270	1.770
1.7	17	2.56	5.95	100	256	43	3,500	0.350
1.9	28	3.59	6.35	175	628	99	5,100	0.892
2.1	3	4.85	6.75	22	108	16	10,000	0.220
					6,328	1,338		8.971

of sea salt to be found in a 0.3 mm raindrop and in rains of the indicated average intensity. Column 9 gives the product of these nucleus weights and the numbers of raindrops (column 5). The computed salinity of the rain (S_c) is now simply the ratio of the total weight of sea salt falling, to the total amount of water falling.

$$S_c = \frac{Ms}{W} \qquad (1)$$

where S_c = computed sea-salt concentration of rain (mg l^{-1})

Ms = sea salt falling $m^{-2}\ sec^{-1}$ (mg)

W = liquid water falling $m^{-2}\ sec^{-1}$ (liters)

For the high-intensity rains averaged on Table 4, the amounts of sea salt and water falling are 8.97 μg $m^{-2}\ sec^{-1}$ and 6,328 $mm^3\ m^{-2}\ sec^{-1}$ respectively. The ratio of these quantities, with the units adjusted, yields a computed sea-salt concentration of 1.42 mg l^{-1}, or a chloride concentration 0.8 mg l^{-1}.

The above computed value for the average chloride concentration, plus other concentrations similarly computed from the averaged data concerning rains of lower intensity (see Table 1) are plotted on figure 5[1]. This also shows the observed average chlorinities of the rains at stations 1 and 4. These observed chloride concentrations are remarkably similar to the computed concentrations, and this similarity is regarded as suggesting that each large salt particle has formed a raindrop.

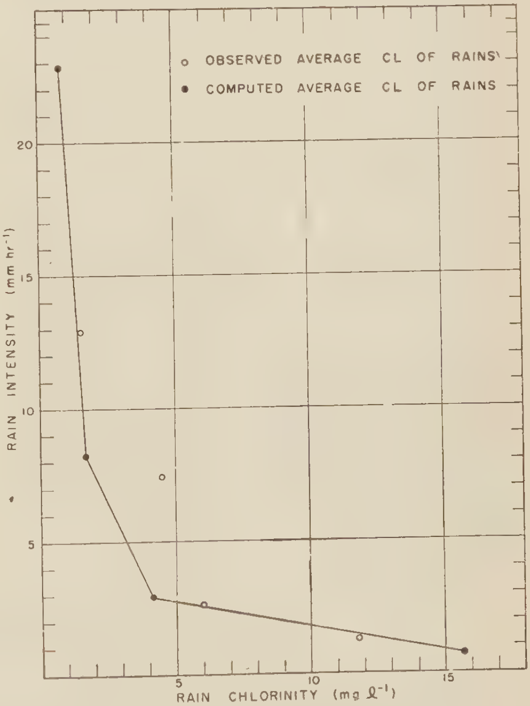

Fig. 5. Observed and computed chlorinities of rains related to rain intensity.

---

[1] These computed chloride concentrations for the rains of other intensities were derived in the manner shown on Table 4, but are not tabulated here in order to save space.

Table 5. Summary of averaged rain data from windward stations 1 and 4, Hawaii. May 1, 4, and 6, 1952

A	B	C	D	E	F	G	H	J	K	L
Rain from funnel sampler		Rain from filter paper samples			Rain Cl comput-ed from nuclei	Rain Cl m^{-3} of air (ExF)	Wt. of Cl falling in rain	Ratio of Cl in rain to Cl in air	Rain-drop size range	Total numbe of rain-drops
Rate mm hr^{-1}	Cl conc. mg l^{-1}	Rate mm hr^{-1}	Rate mm m^{-2} sec^{-1}	Water content mm^3 m^{-3}	mg l^{-1}	10^{-6} g	10^{-6} g m^{-2} sec^{-1}	G/4.7	mm dia.	m^{-3}
1.26	11.8	0.74	206	114	15.7	1.79	5.68	0.38	0.3—0.9	4,533
2.60	6.0	2.94	821	273	4.1	1.12	6.09	0.24	0.3—1.3	3,132
7.45	4.5	8.20	2,279	547	1.7	0.93	6.80	0.19	0.3—1.7	1,903
12.90	1.5	22.80	6,329	1,338	0.8	1.07	9.0	0.23	0.3—2.1	2,693

4. Relating the salt nuclei to the salinity of the rains at the leeward stations 3 and 5.

As previously suggested on pages 437 and 438 the rains falling at the leeward stations 3 and 5 were found to be made up of great numbers of small drops containing relatively little chloride (see Table 2). This character of these leeward rains tends to support the idea that they are composed of drops which have formed on the very numerous salt nuclei found among those particles weighing from about 5 to 20 $\mu\mu$g. The average chloride in these rains (see Table 6, column G) equals 6.2 per cent of the total chlorides found during force 4 winds (total $= 4.7 \times 10^{-6}$ g m^{-3}). On figure 4 it can be seen that during force 4 winds about 7.5 per cent of the chlorides in the air are between 4.5 and 20 $\mu\mu$g in weight, and in figure 3 the salt nuclei curve for force 4 winds shows that there are about 1.4×10^5 particles present in this weight range. Thus the chloride content and the numbers of the small salt nuclei are quite adequate to account for the chloride content and the numbers of the raindrops in the leeward rains.

Due to the nature of the techniques used to measure these small raindrops and small nucle it is not possible, with the present data, t relate the raindrops to the nuclei more precisel Such precision could be obtained in futur measurements by dividing the smaller raindro and salt nuclei number distributions during th measuring process into greater numbers c size-range categories. Note on Table 2 that th greatest numbers of the raindrops at statior 3 and 5 are in the first size category, whil figure 4 shows that all of the appropriate sa nuclei fall within a single measured size-rang category.

Most of the raindrops sampled at stations and 5 are so small that due to evaporation it very unlikely that they would survive a fa through many hundreds of meters of clear ai This probably explains why these small drop have not been reported in such great numbe by other observers.

5. Computed raindrop salinity compared t observed salinity

During the spring of 1954, TURNER (1955 measured the salinity of individual raindro size ranges in Hawaii. For obtaining rain wate

Table 6. Summary of averaged rain data from leeward stations 3 and 5, Hawaii. April 28 and 29, and May 1, 4, and 5, 1952

A	B	C	D	E	F	G	H	J
Rain-water samples					Rain Cl m^{-3} of air (BxE)	Ratio of Cl in rain to Cl in air	Raindrop size range	Raindrop number m^{-3} of air
funnel collector		filter-paper samples						
Rate mm hr^{-1}	Chloride mg l^{-1}	Rate mm hr^{-1}	Rate mm^3 m^{-2} sec^{-1}	Rain in air mm^3 m^{-3}	10^{-6} g	F/4.7	mm dia.	
0.52	1.9	0.35	97	119	0.22	.047	0.1—0.3	62,850
1.79	1.1	1.78	494	331	0.36	.077	0.1—0.9	57,038
					av. = 0.29			

from different drop size-range categories, he used a simple modification of the raindrop spectrograph which has been described by Bowen and Davidson (1951). Turner determined the sodium content of drops in many rain samples at cloud base near station 4, and it is useful here to compare his interesting observations to the raindrop salinities computed from our raindrop size distributions obtained at the same location. For this purpose his sodium chloride concentration values[1] were converted to total sea-salt concentration by multiplying by 1.3, the approximate ratio of total salts in the sea to the sodium chloride present.

On figure 2 (top) his average raindrop salinity values for 39 samples are compared to similar values computed from the average rain and salt nuclei data (lower curves on figure 2) used in the present paper. The method used to derive these latter raindrop salinities is given in equation (1) and is applied, for example, as follows. A nucleus, having a mass of approximately 2,100 $\mu\mu$g, corresponds in cumulative number per cubic meter of air, to the number of 0.9 mm diameter raindrops shown on one of the raindrop distribution curves (see arrow marks near lower curves on fig. 2). The ratio of this nucleus mass (2.1×10^{-6} mg) to the volume of a 0.9 mm raindrop ($.375 \times 10^{-6}$l), equals a concentration of 5.6 mg l^{-1}. This drop salinity is indicated by the arrow mark beside the second raindrop salinity curve at the top of figure 2. The other computed values for raindrop salinity were similarly derived.

It is interesting that the form of Turner's average observed raindrop salinity curve and those computed from our raindrop and salt nuclei data is similar, despite the differences in the sampling times, sampling durations, and in the methods used to derive the salinity values.

The occurrence of the pronounced salinity minimum in Turner's results and in our computed values is apparently a reflection of the average slopes and relative values of the cumulative raindrop and salt nuclei curves. For instance, if the observed cumulative average raindrop distribution curve represented by curve 4 (see figure 2, lower left) had actually followed the adjacent dashed line, then the computed raindrop salinity minimum would not have occurred at a drop diameter of 1.1 mm (see triangular symbols, upper diagram, fig. 2). Instead a different salinity curve would have occurred (see extended dashed line), with the salinity minimum falling at a drop diameter of about 2.5 mm. As an indication of the effects of changing nuclei distribution, the assumption of a force 3 salt-nuclei curve instead of the average force 4 curve (see curve A, fig. 2), simply shifts the computed drop salinity curves down. The unbroken drop salinity curve on figure 2 shows the dilution effects of the reduced nucleus sizes upon drop salt concentrations for the highest intensity rains. As a final example of the effects of the shape of the salt nuclei curve, note that the use of the dotted line modification of curve B in computing raindrop salinity, removes the salinity minimum from the drop salinity curve (see dotted line at top of fig. 2). This removal of the salinity minimum is mentioned here because Turner has remarked that about one-third of his results showed no salinity minimum. Thus the form and, of course, the slope of the computed raindrop salinity curves is clearly dependent upon the relative slopes and magnitudes of the cumulative raindrop and salt-nuclei curves.

Turner's raindrop salinity curve is based upon many hours of sampling, during which time the rain intensity probably varied greatly. Had he been able to collect his rain water during short periods of time (i.e., in about 100 seconds) and, in each case during rains of nearly constant intensity, it is supposed that he would have obtained different salinity curves for different rain rates similar to those which we compute from our observed raindrop and salt nuclei curves.

Turner's average values for the salinity of raindrops of each size range, probably represent an integrated quantity. Note for instance on figure 2 that the salinity of the 0.9 mm diameter raindrops computed from our curves may vary from 1.6 to 28 mg l^{-1}, depending upon the rain intensity in which they are sampled. The raindrop salinity values which will be obtained during a prolonged sampling period in orographic rains at station 4 would seem to depend, in part at least, upon the relative frequency of occurrence of rains of different intensities. They will also presumably depend upon the extent to which the samples are taken in the first rains from the showers, or in rains which are the winnowed remnants of showers occurring to windward of the raindrop spectrograph sampling position.

---

[1] Sodium concentrations, measured by flame photometry, were converted by Turner to equivalent NaCl values.

In future physical-chemical studies of rain, it would be very useful to combine raindrop spectrograph measurements of drop salinity, with simultaneous determinations of raindrop size distribution and of salt nucleus size distributions.

6. Discussion and conclusions

Clearly many more observations, such as those given on Tables 1 and 2, are needed in order to thoroughly test the consistancy of the pattern of interrelationship of nuclei to raindrops which has evolved from the present study. Data deficiencies are especially great among the higher intensity rains (see Table 1), and the lack of simultaneity of the rain and salt-nuclei observations introduces a further element of uncertainty. However, the authors feel that the data and ideas presented here, when considered as a whole, are sufficiently useful to justify publication at this time

Some of the above observational deficiencies were eliminated in further measurements recently made (1954) in Hawaii in connection with the co-operative cloud physics work of "Project Shower". These numerous measurements, which will require much time to completely analyse, will be presented in a later study of this problem.

A rather obvious result of the present study is the emphasis which is given to the importance, in the understanding of Hawaiian shower rain formation, of detailed knowledge of the salt particle size distribution in the clear air and the distribution of raindrop size and raindrop salinity within the clouds. It is also important to know where the rain samples are taken in relation to the stage of development of the showers. In the present study an effort was made to sample the first and the last rains falling from showers moving up the mountain slope. The authors feel that this detailed knowledge of the nuclei, the raindrops and the rain-sampling position, is essential to a further understanding of the evolution of raindrops in the shower rains of marine air masses. The techniques used here should a prove useful in exploring the role of sea-s nuclei in the formation of raindrops in con nental rains.

It should be pointed out that in the analy presented here, the quantities of salt falling the rains at stations 1 and 4 amount to or about 20 to 40 per cent of the total salt in t air (see summary Table 5, column J). Since, the remaining 60 to 80 per cent of the atmo pheric salt, only about 6 per cent falls at static 3 and 5 (see summary Table 6, column G), is supposed that the remaining salt rained-c in the drops falling between these stations, the rain showers were carried by the winds the mountain from the lower to the upp stations. In a later publication (of "Proj Shower" observations) the authors plan include an analysis of the effect of wind a wind shear upon the distribution of raindro at various locations on the mountainside.

In the Hawaiian shower rains, rapid chang in intensity with time are very common, shown on Tables 1 and 2, and by BLANCHA (1953; see fig. 2). Most of this change is thoug to be due to winds transporting the showe over the sampling stations. For instance t average clouds which were producing t showers in the present study were probab moving at about 7 meters per second up t mountain slope. During a sixty second interv between rain samples a shower-produci cloud could thus move almost one-h kilometer. The showers are seldom large diameter, and in aircraft a flight of one-h kilometer is often sufficient to carry the o server from the misty peripheral regions the relatively intense rains of the center.

The interpretation of the measuremen presented here, in terms of the details of t raindrop-forming processes operating in the Hawaiian rains, is uncertain. They see however, to be clearly useful in narrowi the areas of search for these "details". O can say from the present measurements th a drop-forming process seems to be requir which will, (a), involve most of the larger s nuclei in a simultaneous growth, (b) cau this growth to occur, presumably very rapidl in a manner which prevents marked chang in the distribution of the nuclei (or drop and (c) add water to the nuclei without at t same time greatly adding to their salt conte

Table 7. Weights of sea salt added to a 0.9 mm diameter raindrop due to coalescence with 10 and 20 μ radius cloud droplets containing sea-salt nuclei of various sub-micron sizes

Cloud droplet radius μ	Cloud droplet no. required to form 0.9 mm diameter raindrop	Weight sea salt (10^{-12} g) in 0.9 dia. raindrops (cloud droplet no × nucleus wt.)				
		(0.5 μ) 10^{-12} g	(0.2 μ) 10^{-13} g	(0.1 μ) 10^{-14} g	(0.05 μ) 10^{-15} g	(0.02 μ) 10^{-16} g
10	91,000	91,000	9,100	910	91	9.1
20	11,400	11,400	1,140	114	11.4	1.1

In the present study the quantities of salt in the individual large salt nuclei are adequate to account for all of the salt found in the rains. This suggests that the drops have grown entirely by condensation processes, or through coalescence with relatively chloride-free cloud droplets[1]. If one assumes, for instance, that the 0.9 mm diameter raindrops (which, on rain curve 2, fig. 2, are supposed to have formed on 2,100 $\mu\mu$g salt nuclei) have grown through coalescence with 10 μ radius cloud droplets, about 91,000 of these droplets would be required. Table 7 shows amounts of salt which would be added to the initial giant (2,100 $\mu\mu$g) nucleus due to coalescence with cloud droplets which have formed on sea-salt nuclei of various sub-micron sizes. On this table it is evident that the quantities of salt added through accretional growth might in some instances equal or greatly exceed the weight of the giant nucleus upon which the raindrop initially formed. The very small nuclei would, of course, require rather large water vapor supersaturations in the clouds to become activated.

Junge's work at Round Hill (Junge, 1954) indicates that most of the numerous nuclei which are less than about 0.8 μ in radius (or $< 5 \times 10^{-12}$ g, as shown on fig. 2) are composed largely of ammonium sulfate. However, in Hawaii Junge recently sampled aerosols which were less than 0.8 μ radius, and he found relatively very little ammonium sulfate present.

From the results of this paper, we cannot say that the raindrops in Hawaii do or do not grow by accretion. If the nuclei smaller than about 10^{-12} g are sea salt, then accretion would seem to be ruled out unless the nuclei are very small (see Table 7). Thus we feel that one of the important steps in future physical-chemical studies of raindrop formation in shower clouds is to determine the chemical nature and the number of the majority of the individual cloud-droplet nuclei which are smaller than about 0.8 microns and to relate these particles to the solutes found in the cloud and rain waters.

A conservation of the number of the larger nuclei per unit volume of air, during their growth to raindrops, is indicated by the results given here. This number conservation is not consistent with the model proposed by Bowen (1950), in which accretional growth involves marked alterations in drop distributions. If these Hawaiian raindrops grow largely by accretion, or by condensation, the authors feel that it is necessary to suppose that this growth occurs very rapidly in turbulent volumes of air which are ascending within clouds in a way similar to the "bubble parcels" proposed by Scorer and Ludlam (1953).

Acknowledgments

The writers are indebted to Mr W. A. Mordy, of the Pineapple Research Institute, the Hawaiian Sugar Planters Association and the Territorial Cattleman's Council, for the opportunity to work in Hawaii, and to the Honolulu office of the U.S. Weather Bureau for supplying north Pacific weather charts.

REFERENCES

Blanchard, D. C., 1953: Raindrop size distribution in Hawaiian rains. *Jour. Meteor.*, **10**, 457—473.

Bowen, E. G., 1950: The formation of rain by coalescence. *Aust. Jour. Sci. Res.*, A, **3**, 193—213.

---

[1] Hawaiian clouds, which are not producing rain, have been found to contain from 30 to 140 cloud droplets per cubic centimeter, though the air at sea level usually contains several hundred Aitken nuclei in an equal volume.

Bowen, E. G. and Davidson, K. A., 1951: A raindrop spectrograph. Quart. *J. R. Met. Soc.* **77**, 445—449.

Junge, C. E., 1954: The chemical composition of atmospheric aerosols, I: Measurements at Round Hill field station, June—July 1953. *J. Meteor.*, **11**, 323—333.

Keith, C. H. and Arons, A. B., 1954: The growth of sea-salt particles by condensation of atmospheric water vapor. *J. Meteor.* **11**, 173—184.

Miyake, Y. and Suguira, Y., 1950: The mechanism of the dissolution of the atmospheric chloride into rain water. *Pap. Meteor. Geophys.*, **1**, 222—226.

Scorer, R. S. and Ludlam, F. H., 1953: Bubble theory of penetrative convection. *Quart. J. R. Meteor. Soc.*, **79**, 94—103.

Sugawara, K., Oana, S., and Koyama, T., 194
Separation of the components of atmospheric s
and their distribution. *Bull. Chem. Soc. Japan*, 2
47—52.

Turner, J. S., 1955: The salinity of rainfall as a functi
of drop size. *Quart. J. R. Meteor. Soc.*, **81**, 418—42

Woodcock, A. H. and Gifford, M. M., 1949: Sampli
atmospheric sea-salt nuclei over the ocean. *Jo*
Marine Research, VIII, 177—197.

Woodcock, A. H., 1952: Atmospheric salt particles ar
raindrops. *J. Meteor.*, **9**, 200—212.

— 1954: Salt nuclei in marine air as a function of altitu
and wind force. *J. Meteor.*, **10**, 362—371.

PRINTED IN SWEDEN
ESSELTE, STHLM 55

Contribution No. 770

Särtryck ur Tellus nr 1, 1955

On the Chemical Climate and its Variation with the Atmospheric Circulation Pattern

By

C.-G. ROSSBY, University of Stockholm and the Woods Hole Oceanographic Institution, and
H. EGNÉR, Royal Agricultural College, Uppsala.*

(Manuscript received January 15, 1955)

A study of the chemical composition of monthly precipitation samples from a number of stations in Sweden brings out the existence of significant variations in the relative proportions of chlorides and sodium depending upon the general character of the prevailing circulation. In maritime westerly flows the weight ratio of chloride to sodium decreases eastward to values which lie far below the value characteristic of sea water. In precipitation falling from arctic or polar continental air masses the chloride component is almost completely absent. The highest amounts of chlorides relative to sodium are observed in precipitation from warm and most air masses reaching Sweden from the south or southeast.

Significant variations are observed also in the yearly means of the sodium and sulphur deposits depending upon the dominance of maritime or continental air currents.

A sketch map of the "average" chloride concentration in European precipitation prepared from miscellaneous older data lends support to the results of the analysis of the monthly data. The separation of the chemical components indicated by this study would seem to be of considerable geochemical interest since it would permit different maritime salts to be deposited in widely separated parts of the continents. It is not inconceivable that a detailed study of the association between different circulation patterns and the corresponding chemical climates might permit us to draw inferences concerning variations in the atmospheric circulation during post-glacial times, e.g. from the data on the chemical stratification in raised bogs now becoming available through the investigations by *Mattson* and *Koutler-Andersson*.

It is the specific purpose of this paper to show that the weight ratio of chloride to sodium ions determined through the analysis of monthly accumulated precipitation samples varies in a systematic manner from month to month, and that the value of this ratio closely reflects the trajectory and life history of the principal air mass from which or through which the month's precipitation is falling. The range over which this ratio varies extends from 0.0 to about 3.5, the average value for sea water being about 1.8 and for pure sodium chloride 1.5. The fluctuations here established clearly indicate that Cl^- and Na^+ are not inseparable but rather that they, through various processes about which our knowledge is as yet mainly conjectural, may be detached fron each other in leaving the surface of the se or shortly thereafter. Nuclei containing sodiun chloride and then certain other sodium salt appear to be precipitated at the most rapic rate while other chlorides seem to be capabl of travelling long distances from their oceani source regions without precipitation.

The more general purpose of our paper however, is to call attention to the wealth o fascinating problems created by the availability, since November 1, 1954, of synopti data (monthly means) on the chemical composition of precipitation and of the surface ai at a large number of stations in Denmark Finland, Norway and Sweden. The data fo November and December 1954 are publishe as an appendix to this issue of Tellus. It is ou intention to publish the data for subsequen months in quarterly installments.

The data available for the present stud consist of the following:

a) The amounts of the principal chemica constituents contained in monthly precipitatio

---

* The authors are indebted to the Knut and Alice Wallenberg Foundation for a generous grant which has enabled them to initiate the organization of an international network of chemical sampling points, and to the U. S. Office of Naval Research and the U. S. Weather Bureau which through their unfailing support have made it possible for the Institute of Meteorology to take up chemical meteorology as a major field of research. Contribution 770 from the Woods Hole Oceanographic Inst.

samples collected at a network of about 28 Swedish stations, operating from October 1, 1948, until September 30, 1950. A map showing the names and locations of these stations is given in a recent paper in Tellus (EMANUELSSON, ERIKSSON and EGNÉR 1954). Unfortunately, data on sulphur and magnesium are not available for this period.

b) Data on the amounts of various chemical components, including sulphur and magnesium, contained in monthly precipitation samples collected at seven stations in southern Sweden during the period July 1, 1951, until June 30, 1953. These stations were Alnarp, Bräkne-Hoby, Plönninge (Halmstad), Flahult, Bjärka-Säby, Skara (Lanna) and Ultuna. At these stations also air samples were collected monthly by means of continuously operating low capacity pumps (about 30 m^3 per month) and analyzed for the mean monthly concentration of the same elements (exclusive of NO_3—N) as those determined in the precipitation samples.

c) Data from an expanded net of Swedish stations at which both air and precipitation samples have been collected monthly since July 1, 1953. On November 1, 1954, this network was enlarged to include additional stations in Sweden, Norway, Finland and Denmark. The locations of these stations are given in the station map accompanying the chemical data appendix included in the present issue of Tellus. Since July 1, 1953, the hydrogen ion concentration (pH) and the electric conductivity of the monthly precipitation samples have been determined at all stations.

The chemical analyses were carried out at the Royal Agricultural College of Uppsala (Ultuna) under the supervision of one of us (Egnér). The meteorological analyses and the interpretation of the results were carried out at the University of Stockholm. The chemical technique now in use is described in the chemical data appendix.

In the report by Emanuelsson, Eriksson and Egnér, it was shown that during the two-year period October 1, 1948, to September 30, 1950, the weight ratio of the total amount of chloride to the total amount of sodium deposited per hectar and year decreased from a value of about 1.2 on the Skagerrack coast to about 0.6 in the vicinity of Stockholm—Ultuna. The separation of these two constituents was first brought out by CAUER (1949) in his studies of atmospheric condensation nuclei. Cauer states that the sodium and chloride ions added to the atmosphere from the sea through spray or bubble formation go through entirely different cycles. He believes that the chloride ions contained in the sea spray droplets, under the influence of the small amounts of ozone present in the lowest strata of the atmosphere (0—100 μg per m^3), may be oxidized to free chlorine gas which again, in the presence of sunlight and water vapour, is changed into hydrochloric acid. The escaping chlorine would be replaced in the initial droplets by bi-carbonate ions. Since the hydrochloric acid may be transported by the winds as a gas or may form droplets too small to serve as effective condensation nuclei, it is clear that the Cauer process would explain why rains falling within relatively short distances of the coast are characterized by relatively low and landward decreasing values of the weight ratio of chloride to sodium ions. Cauer's hypothesis is now being studied experimentally and theoretically by our collaborators and these studies will be reported in due time. It appears, however, that the effect observed by Cauer and verified by our precipitation data, might be accounted for by one or several alternative processes. KÖHLER and BÅTH (1952) have carried out an interesting experimental study of the separation of sea salt components, by blowing an air stream over a sample of sea water. Droplets of different size were analyzed separately for the main components. However, the maximum separation indicated by these experiments is insufficient to account for the observed geographical variation in Cl/Na.

The Cauer hypothesis, or any equivalent mechanism, carries with it one extremely important implication, apparently overlooked by Cauer but of considerable geochemical interest:

Presumably the proportions of chloride and sodium ions which leave the sea surface are the same as in the water but apparently some sodium is precipitated in combination with other negative ions than chloride in the coastal areas of western Europe. There must then develop an excess of chloride ions or of molecular chlorine in the free atmosphere. Unless one assumes that molecular chlorine is taken up directly by the ground or that

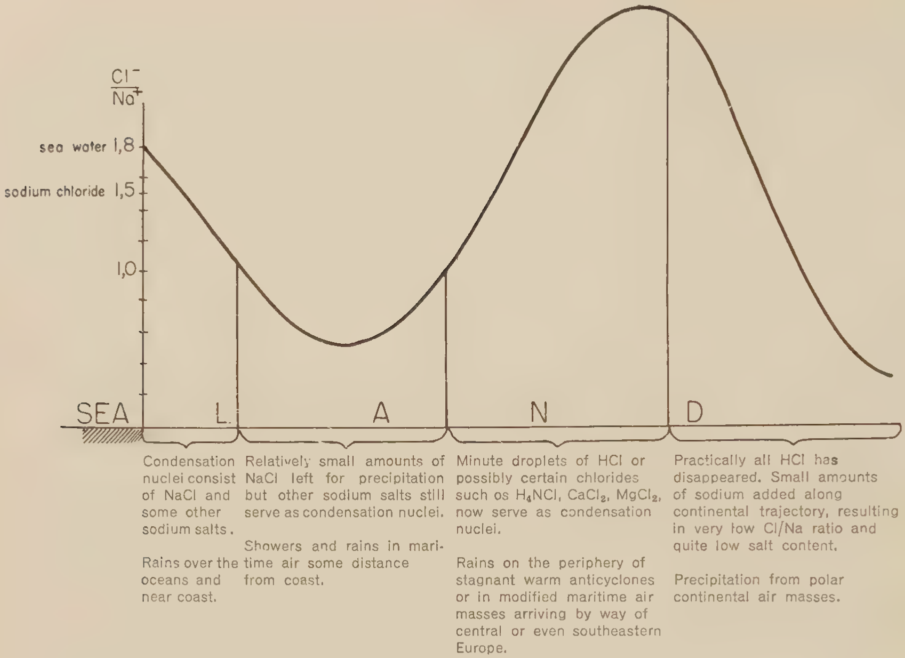

Fig. 1. Schematic representation of the variations in the weight ratio of chloride to sodium in precipitation from an air mass moving in over the continent.

chlorates or hypochlorites not now identified in our precipitation samples maintain the chlorine mass balance in the atmosphere, one is forced to conclude that there must exist continental regions far removed from the oceanic source regions, in which the weight ratio of chloride to sodium in precipitation must be very much in excess of the value characteristic of sea water or of coastal precipitation. If the chlorides (exclusive of sodium chloride) only slowly come into play as condensation nuclei it would in fact be possible for rains in such interior regions to reach a higher absolute chloride concentration than rains falling closer to the coast. It was this paradox that provided the starting point for the present study.

We have attempted to sketch the variation of the chloride to sodium ratio in precipitation as a function of distance from the oceanic source region in Fig. 1. Leaving out the many important nuclei not containing either sodium or chlorides one would have to assume that the precipitation falling from air masses near the coast contain a mixture of sodium chloride and some other sodium salt. As the air travels further away from the coast most of the sodium chloride would be used up and ultimately the rain drops would contain mainly sodium salts other than sodium chloride. Finally, when also these sodium salts have been consumed, the minute hydrochloric acid droplets or corresponding chlorides would come into play as condensation nuclei. When this happens the chloride to sodium ratio would, of course, rise far in excess of the 1.8 value characteristic of sea water. If the air continues along a continental trajectory without access to chloride sources but is able to pick up small amounts of sodium, it is probable that the chloride to sodium ratio of the precipitation would again decrease.

Figures 2, 3, 4 and 5 represent an attempt to verify the corollary formulated above through a study of the geographic distribution of the chloride to sodium ratio during four selected months of dissimilar circulation patterns. Each figure contains the mean sea level pressure pattern over northern and central Europe for the month in question. The monthly precipitation values in mm at the chemical stations have been entered on each map. In each figure the

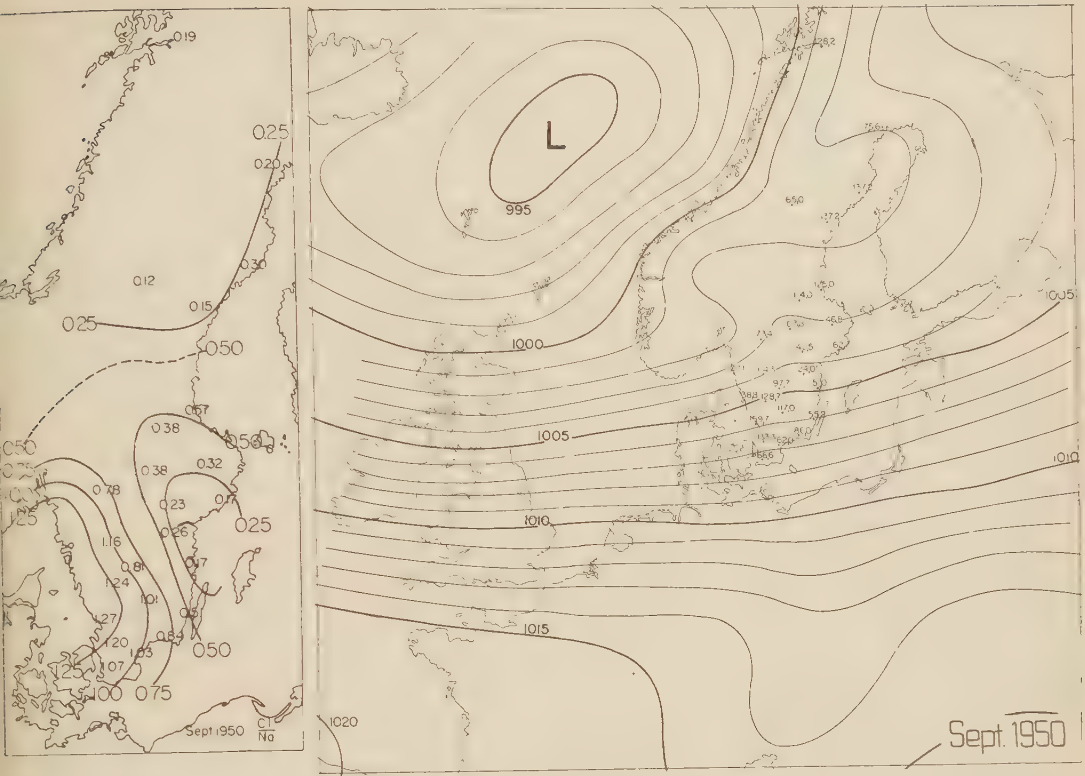

Fig. 2. Mean circulation pattern at sea level over Northwestern Europe during September 1950. The precipitation in mm at the chemical sampling points is entered on the pressure chart. The inset map gives the geographic distribution over Sweden of the weight ratio of chloride to sodium in the accumulated precipitation samples.

inset map gives the geographic distribution over Sweden of the weight ratio of chloride to sodium, expressed through isolines. It should not be necessary to stress that a monthly mean pressure pattern must be used with a great deal of caution in drawing conclusions concerning the paths of the rain-bearing winds; it has been suggested that mean charts should be constructed only for those days on which precipitation fell. However, the number of days with precipitation at any one station in Sweden is quite large and when twenty or thirty stations are considered such a map would become practically identical with the monthly mean chart. Figure 2 shows that in September 1950 straight westerly winds dominated the flow pattern in southern Sweden up to about the latitude of Stockholm. During this month the chloride to sodium ratio fell from about 1.3 on the Kattegatt coast to a minimum of 0.17, less than one tenth of the sea water value, on the Baltic coast. The precipitation decreased markedly from west to east.

December 1949 (fig. 3) was less uniform in its circulation characteristics but by and large it was dominated by strong west winds over southern Sweden. Also in this case the precipitation values decreased from Kattegatt to the Baltic coast and the chloride to sodium ratio decreased eastward, though less rapidly than in September 1950. In both cases this ratio reached very low values in northern Sweden, probably because the air reached that part of the country after a fairly long over-land journey and after considerable lifting over the mountains in Norway. Most of the sodium chloride must have been precipitated by the time the rain-bearing winds reached northern Sweden, other sodium salts than NaCl having taken over the role as condensation nuclei.

May 1950 (fig. 4) represents a month with a rather unusual circulation pattern, northerly

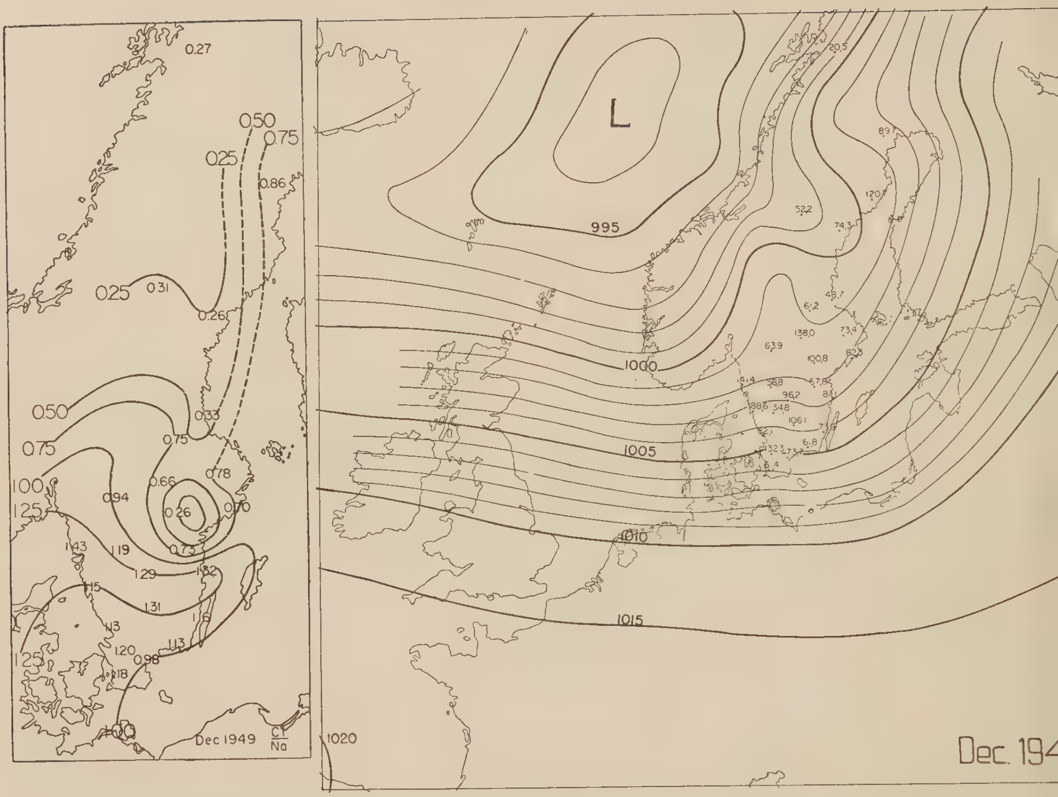

Fig. 3. Circulation pattern and weight ratio of chloride to sodium during December 1949. See legend to Fig for details.

or even northeasterly winds over the entire country. The precipitation amounts were low but sufficient for analysis. Amazingly low values of the chloride to sodium ratio are observed, less than 0.3 at all stations but one. In view of the hypothesis proposed by Cauer it should be pointed out that northerly winds during the spring presumably are characterized by relatively high ozone concentrations in the lower air strata.

November 1949 (fig. 5) was characterized by persistent advection of warm and moist air from the Mediterranean and Balkan region, air masses of Atlantic origin having made a long sweep eastward over southern Europe. The rainfall in southeastern Sweden during this month was profuse, up to two or three times the normal value. In these rains the chloride to sodium ratio reached values of up to 3.5 along the southern and southeastern coast of Sweden. The absolute amounts of chloride deposited in those districts were re tively large, in excess of 1 kg per hec (10^4 m^2) at several stations and reaching 2 kg per hectar at Tovehult.

The four cases presented above stron support the proposition that air masses leav the sea first lose sodium chloride throu precipitation, then certain other sodium sa but that the remaining chlorides, which not associated with sodium may stay with moist air masses until long after the ma portion of the sodium has been precipitat

The extremely low chloride ratios obser in May 1950 remain to be explained. I conceivable that the slight total precipitat observed during that month fell from masses with a very long continental histo air masses which had moved around blocked low pressure system located in White Sea region. In the course of this l continental history, the air would ultima

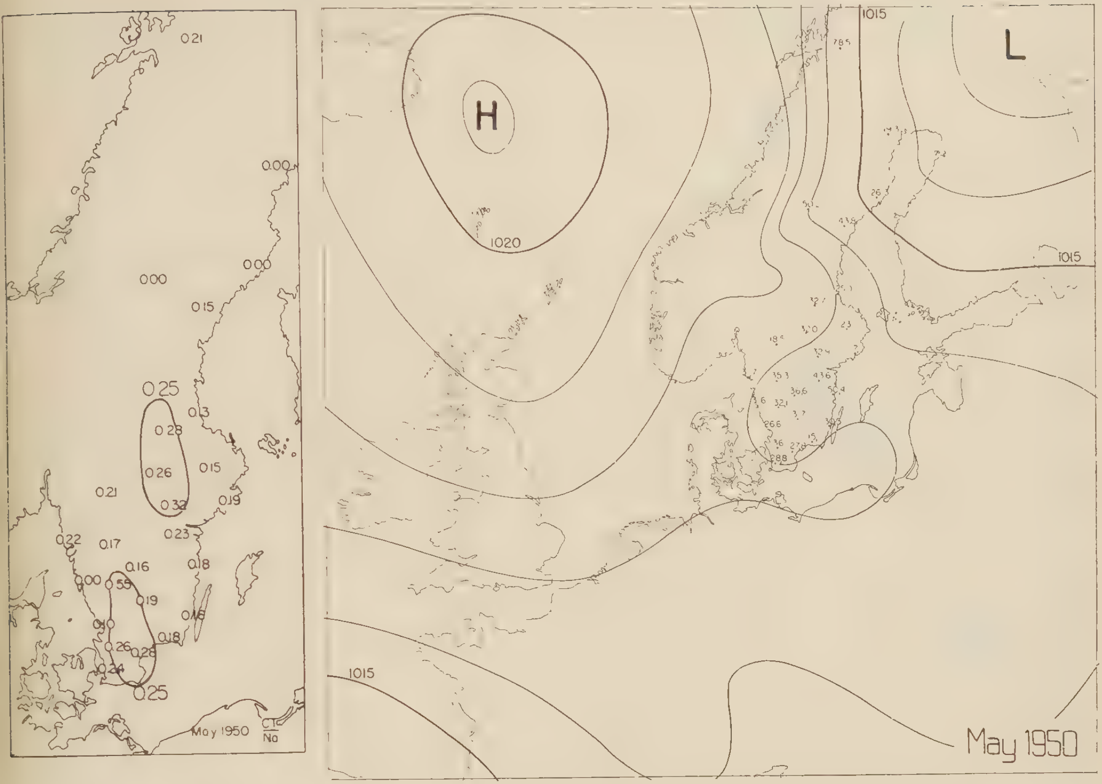

Fig. 4. Circulation pattern and weight ratio of chloride to sodium during May 1950. See legend to Fig. 2 for details.

lose the hydrochloric acid particles or chlorides through precipitation. Since there are no continental sources of chlorides, with the exception of industrial pollution and salt deserts, sources which hardly would have to be considered in these high latitudes, while there always would exist some opportunity for the air to pick up small amounts of sodium together with other typical continental cations, it is conceivable that the low chloride ratio in the precipitation of the northeasterly winds might be explained as associated with a second minimum in the chloride ratio curve, a minimum reached only after most of the chlorides have been precipitated without replacement. This second minimum would evidently be associated with very low salt concentration in the precipitation. To study this problem further we have looked into the precipitation chloride ratio for the month of April 1954. During this month, northerly to northeasterly winds prevailed over northern and central Sweden, northwesterly winds on the west coast of Sweden and in the southernmost parts of the country (fig. 6). It is probable that this last current to a large extent was fed by air from Central Europe brought towards southern Scandinavia in a broad sweep out of a stagnant anticyclone over the British Isles. The inset map shows the distribution of chlorides in mg per liter. On the same chart the lower number at each station gives the chloride to sodium ratio. The contrast between the low chloride concentration in the precipitation from the continental northeasterly current and the extremely high concentration in the precipitation over southern Sweden is striking. The high chloride ratio values in southern Sweden suggest that much of the pure sodium chloride particles already have been removed from the air and that other chlorides to a large extent have taken their place.

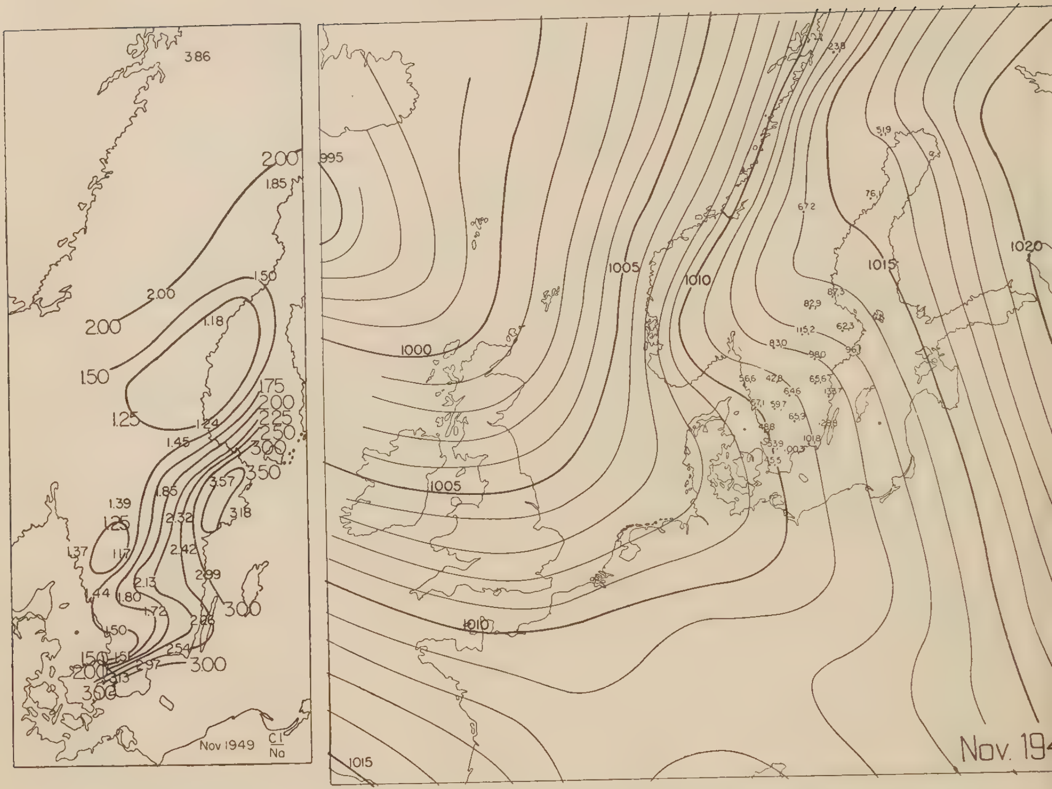

Fig. 5. Circulation pattern and weight ratio of chloride to sodium during November 1949. See legend to Fi for details.

We have attempted to make use of the combined precipitation and air analyses conducted since July 1, 1953, to study the chloride content in the surface air of currents reaching Sweden from the south. As a first step, we selected eleven stations (fig. 7) in the eastern half of Sweden and plotted for each one of these stations the monthly mean chloride content expressed in micrograms per m³ of air as a function of time (fig. 8). It is striking that all these curves are characterized by a well-defined maximum in December 1953. We then constructed (fig. 9) curves representing the mean concentration at these eleven stations of chloride, sulphur, sodium and magnesium as functions of time. The sodium and magnesium values for December 1953 exhibit no peculiarities, but the sulphur shows a minimum. (March 1954, on the other hand, is characterized by an extremely high sulphur value.) In December 1953 the ratio of the average chloride concentration to the corresponding sodium concentration as given the curves in figure 9 reached a value 4.0. The corresponding ratio computed fr the total precipitation deposits at the sa eleven stations was 1.74. This suggests presence in the lowest air layers of HCl gaseous form or in the form of minute drop too small to be collected effectively by falling rain.

The dominant circulation pattern of Dece ber 1953 is illustrated by figure 10. It repres the mean sea level pressure pattern for two-week period December 9—December inclusive, during which southern and cen Sweden were dominated by southerly or e southeasterly winds bringing in warm from southern and central Europe. In the and the last week of the month moist was brought into southern Sweden from southwest and west. The northernmost of the country was under the intermittent fluence of maritime air masses throughout

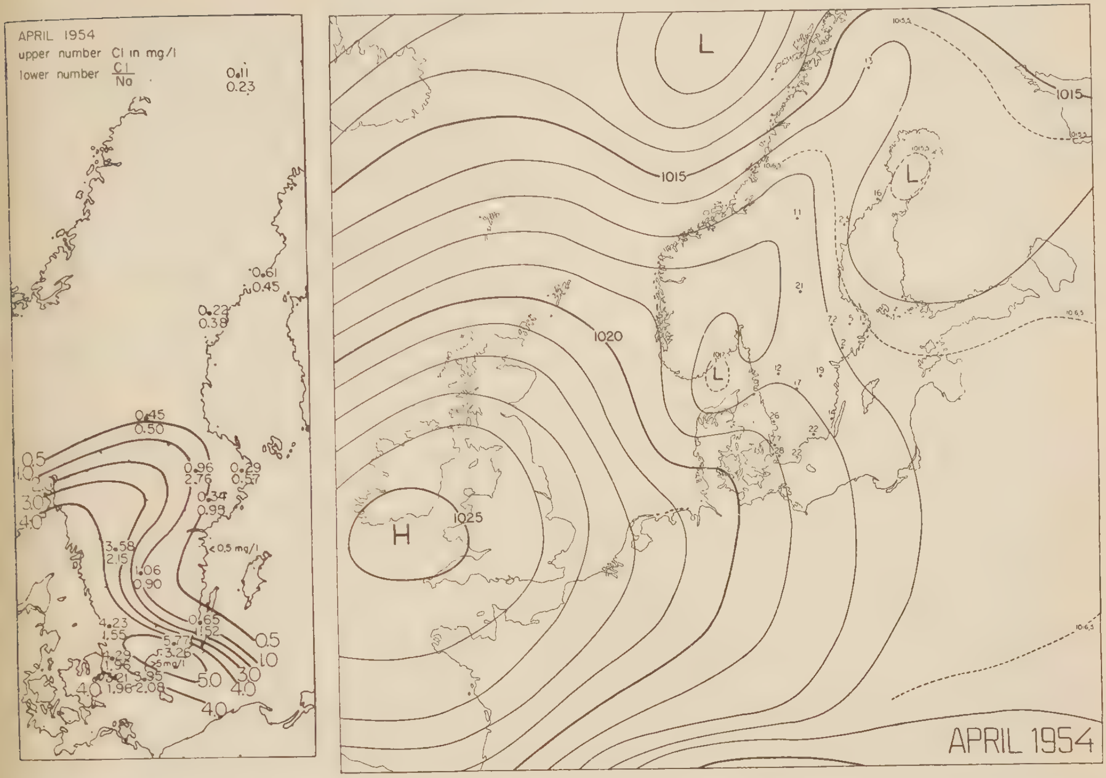

Fig. 6. Mean circulation pattern at sea level during April 1954, with precipitation amounts in mm at the chemical sampling points. The inset map gives the distribution of chlorides in the precipitation (mg pr liter) expressed through "isochlors". The lower figure at each sampling point gives the weight ratio of chloride to sodium.

major part of the month but received very small amounts of precipitation. The mean sea level pressure distribution for the entire month is not reproduced but it shows mean monthly pressures well above normal (10—11 mb in southern Sweden, 1—2 mb in northernmost Lappland). The flow was in the main anticyclonic and hence the precipitation was below normal practically everywhere except in the mountainous western part of northern Sweden.

The dominant southerly to southeasterly flow in southern Sweden during December 1953 was associated with a tongue of quite low pH-values in the precipitation samples (fig. 11). This observation supports the assumption that the prevailing air current contained droplets of hydrochloric acid. It is of some interest to compare this month with March 1954 (fig. 12), the month during which the concentration of sulphur (sulphate and sulphite ions) in the air samples from the eleven eastern stations reached a pronounced maximum. Also during this month southerly winds prevailed in southern and central Sweden, southerly to southwesterly winds in northern Sweden. In December 1953, temperatures were well above normal in southern Sweden, while March 1954 was characterized by about normal temperatures except in the north where they were in excess of normal. The March precipitation fell in the form of snow, except far south, the December precipitation mainly in the form of rain. One may perhaps infer that the December circulation pattern was dominated by air masses originally of maritime origin but having made a broad sweep over southern Europe. During March 1954 the country must at least at times have been under the influence of truly continental air masses from the interior of the Eurasian continent. The maximum of sulphur observed during this month may then have been the result, at least in part, of

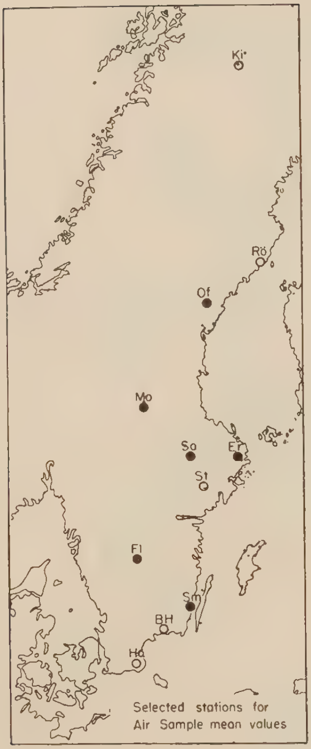

Fig. 7. Location of eleven sampling stations utilized in the analysis of the month-to-month fluctuations in the chemical content of the air.

increased winter time combustion in central and eastern Europe.[1]

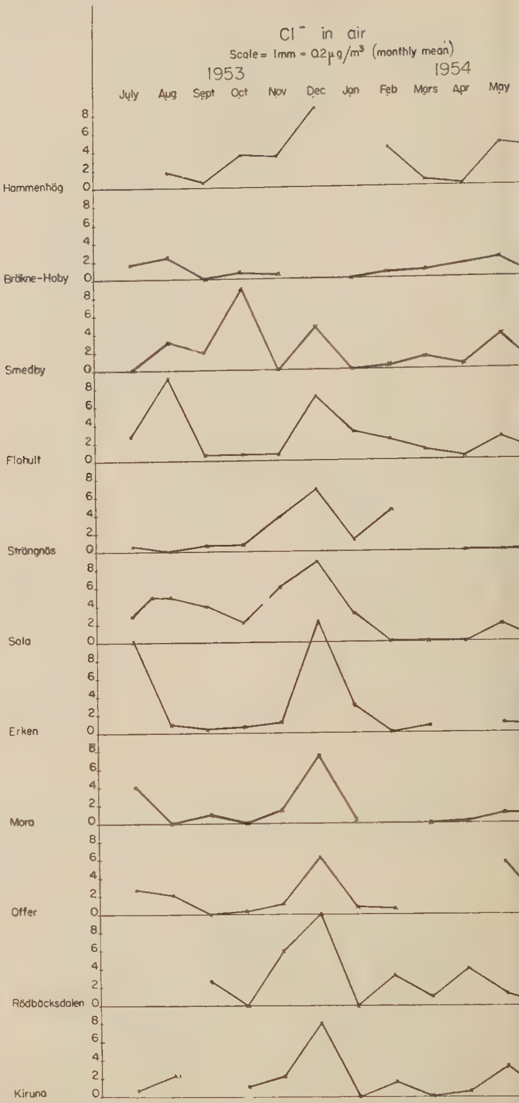

Fig. 8. Variation with time of the chloride conten the air (in μg per m^3) at eleven sampling point

The study of these two months sugg that blocking of the "normal" west-w circulation over northern Europe may associated with marked changes in the chemi composition both of the precipitation of the air. We have attempted to explore possibility further by a study of changes

---

[1] Mr. Claes Rooth of the Institute of Meteorology has looked into the air circulation over Europe in March 1954. His comments follow:

"The mean pressure chart for the month shows a well developed continental anticyclone together with a fairly deep cyclone over the north Atlantic. This indicates predominantly southerly flow over Scandinavia during the period. An inspection of the daily charts prepared by the Swedish weather service shows, as might be expected, a sequence of cyclonic and anticyclonic weather patterns over northern Europe. In central Europe, however, a weak anticyclonic circulation with wide areas of fog and low stratus dominated the month, preventing the vertical spreading of the pollution from the large industrial and urban areas. Extreme cases of such concentrations of highly polluted air under an inversion are known from Belgium, England and the United States where they have had even fatal consequences.

From the reservoir thus formed, contaminated air has apparently been brought up towards Scandinavia during the periods of SW—to SE flow. It has been stated by several workers that minute droplets of sulphuric acid are among the most persistent of the air pollutants that have been studied, which might explain partly why only the sulphur concentrations are abnormal in the air samples and partly why these high values are not reflected in the precipitation samples, which in fact show sulphur minima at several stations. In connection with the latter question it must be noted, however, that r of the precipitation fell during the first week of month before the characteristic pattern described al had developed."

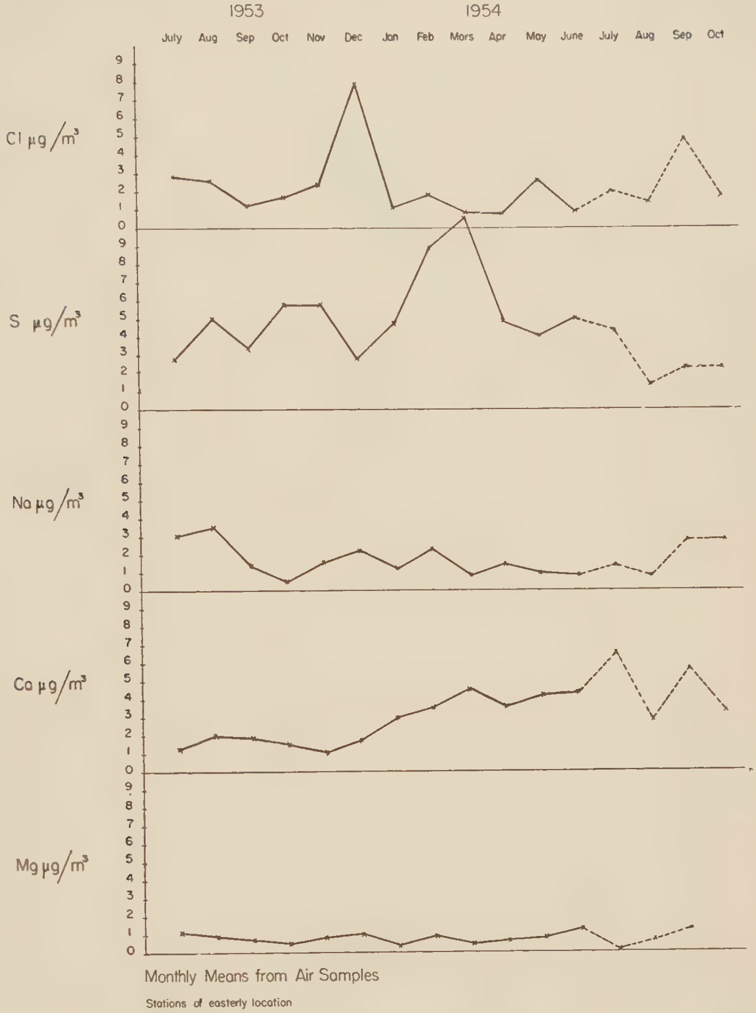

Fig. 9. Variation with time of the average concentration of chlorides, sulphur, sodium, calcium and magnesium (in µg per m³ of air). Curves represented in this figure obtained by averaging the concentrations measured in he monthly samples from the eleven stations in Fig. 7.

the annual mean values of the various chemical components brought to the ground by precipitation and by a comparison of these changes with the changes in the corresponding mean annual circulation patterns. The data at our disposal are inadequate but they suggest nevertheless that the "ventilation" of southern Sweden by fresh maritime air masses decreased successively from 1949 until 1953 and that southern and southeastern Sweden during these years gradually became more exposed to air masses which had spent some time over central Europe and thus lost much of their original sodium content. To demonstrate this, it is perhaps sufficient to point out the trends of the annual deposits of various chemical components at a few representative stations situated away from the coast where data are available for several years and where local sources of pollution appear relatively unimportant:

Sodium deposit in kg per har and year

	1949	1952	1953	July 1, 1953—June 30, 1954
Skara	9.46	4.46	4.48	3.92
Flahult	9.20	3.74	3.65	4.32
Bräkne-Hoby	5.80	5.23	3.90	4.88

Chloride deposit in kg per har and year

	1949	1952	1953	July 1, 1953—June 30, 1954
Skara	9.37	7.28	7.00	6.61
Flahult	10.34	5.72	5.14	5.71
Bräkne-Hoby	8.03	7.59	6.30	8.54

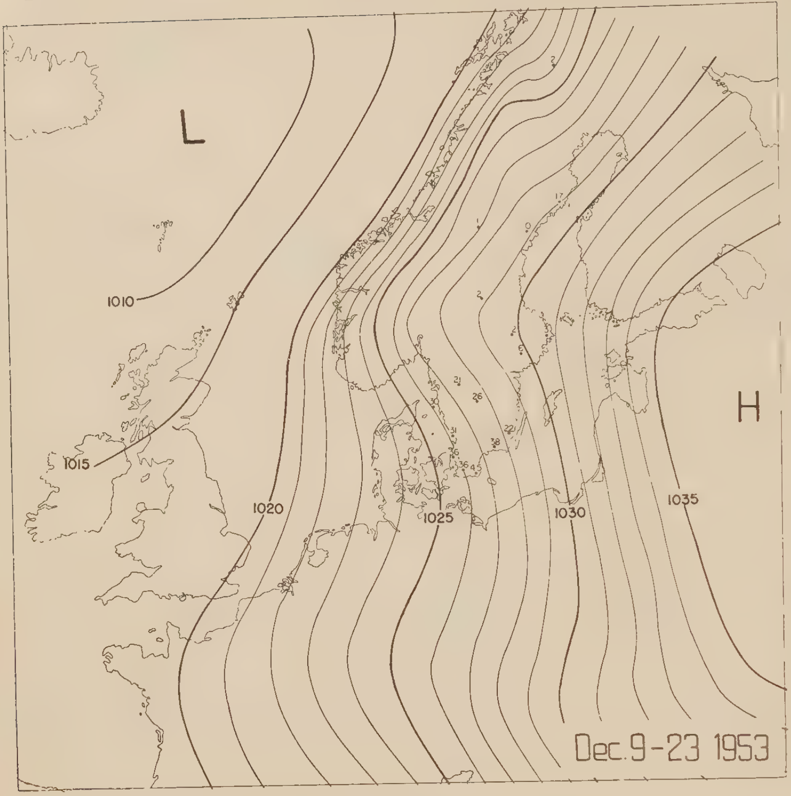

Fig. 10. Mean circulation pattern at sea level during the period December 9—23, inclusive, 1953.

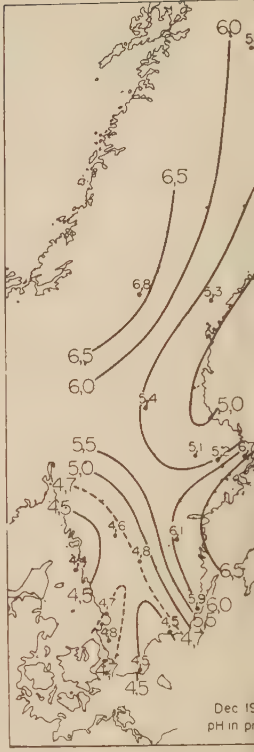

Fig. 11. Geographic distribu of the hydrogen-ion concer tion in the accumulated pre tation for December 195

Ratio of chloride to sodium	1949	1952	1953	1953—1954
Skara	0.99	1.63	1.56	1.69
Flahult	1.12	1.53	1.41	1.32
Bräkne-Hoby	1.05	1.45	1.62	1.75

Annual precipitation in mm	1949	1952	1953	1953—1954
Skara	547	398	624	516
Flahult	773	611	705	739
Bräkne-Hoby	515	645	346	470

Data on the sulphur content are not available for the entire period and thus we have been forced to group the observations differently to bring out such trends as may exist. Hence, one finds:

Annual deposit of sulphur in kg per hectar and year

12 month period	July 1951—June 1952	July 1952—June 1953	July 1953—June 1954
Skara	6.10	6.12	5.94
Flahult	5.24	5.28	7.05
Bräkne-Hoby	6.37	7.47	8.81

Between 1949 and 1953 the sodium depo fell off to one half or one third of their orig value. The chloride deposits decreased but much less markedly. On the other ha the two southeastern and eastern stat (Bräkne-Hoby and Flahult) showed ri deposits of sulphur. Taken together, the point to an increasing frequency of air invasions from central Europe. To test conclusion we have computed sea level m pressure charts for the two years 1949 1952. (Figures 13 and 14.) The chart for shows a marked west wind circulation the entire Scandinavian peninsula. In 1952 the other hand, the most striking featur the mean chart is a narrow high-pressure r which extends northward through the m part of Scandinavia. It follows that in the geostrophic winds across central Sw must have blown almost as often from

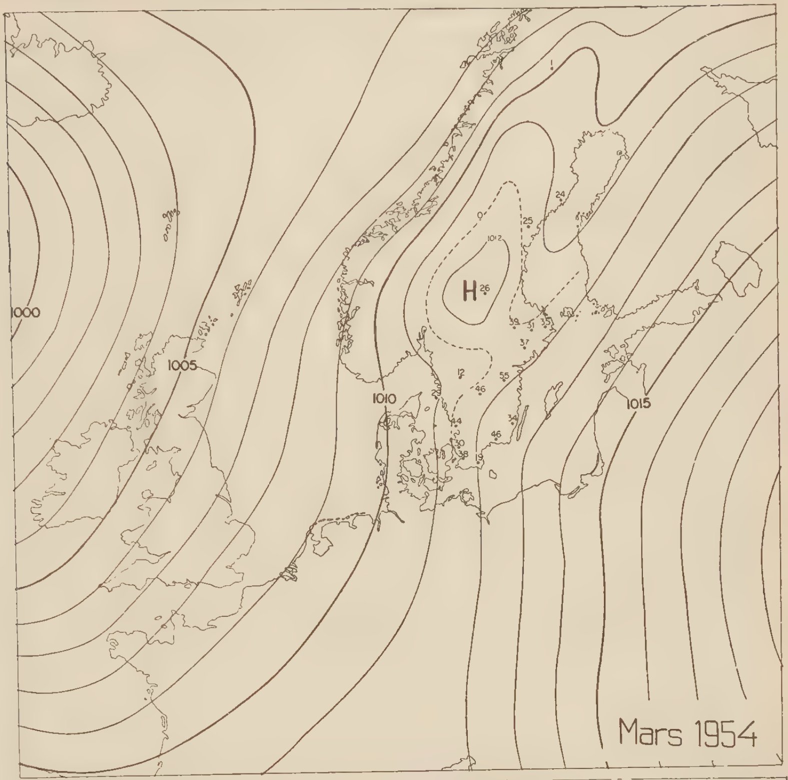
1000
1005
1010
1015
1012
H
25
24
Mars 1954

Fig. 12. Mean circulation pattern at sea level during March 1954.

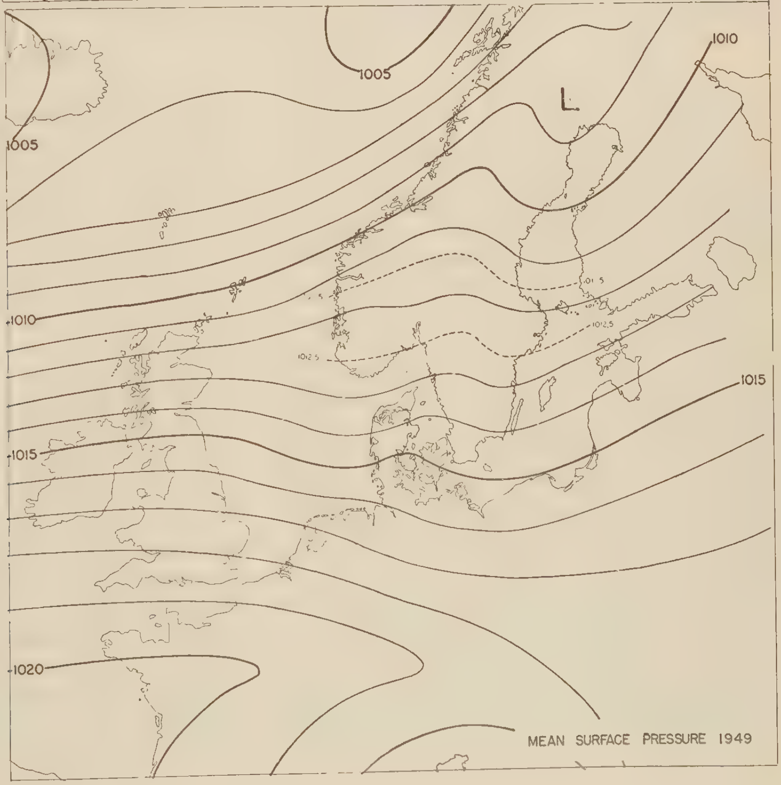
1005
1005
L
1010
1010
1012.5
1015
1015
1020
MEAN SURFACE PRESSURE 1949

Fig. 13. Mean circulation pattern at sea level during the calendar year 1949.

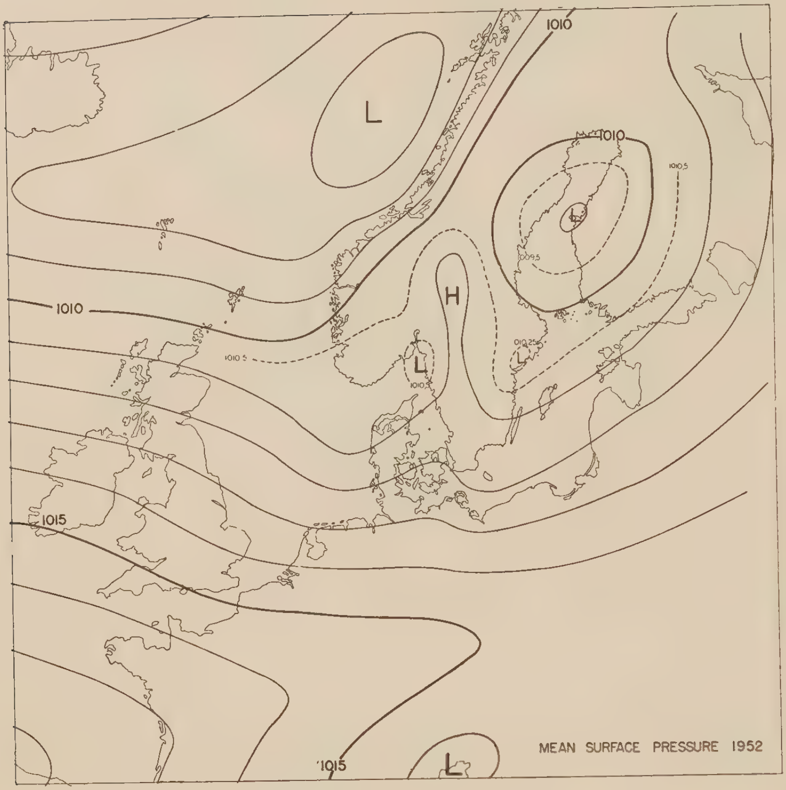

Fig. 14. Mean circulat
pattern at sea level dur
the calendar year 195

east as from the west, *i.e.* the normal westwind "ventilation" of the peninsula had to a large cxtent been replaced by air currents from the interior of the continent. This point is brought out quite clearly by the graphical representation in fig. 15 of the frequency distribution of easterly and westerly geostrophic sea level winds across a north-south section in south-central Sweden.

The great variations from year to year demonstrated above show that the mean charts presented by Emanuelsson, Eriksson and Egnér (loc. cit.) in no sense may be regarded as "normals" but merely as cartographic representations of the chemical composition of the precipitation in Sweden during one particular two-year period.

We shall finally attempt to check the various indications obtained from the study of our own data through an inspection of measurements in other parts of Europe. For this purpose we have attempted to sketch, in Fig. 16, the probable "average" distribution of chlorides in precipitation over northern central Europa generally. The data for sketch map have been obtained from rather complete references contained in survey by E. Eriksson (1952). A similar v useful tabulation of chloride data has b made by Drischel (1940).

All chloride values entered on the ske map in Fig. 16 have been expressed in mg liter and it has been necessary to piece toget data from periods widely separated in ti Observation series extending through than one full year have not been used s the variations in the chloride content f month to month are extremely large. Like we have omitted many observation series f sampling points near the exposed wes coasts of Europe, since the exact value the high concentrations in the immed vicinity of a coast clearly depend upon acci tal details of orography and exposure. V able general information concerning the st coastal gradients of the chloride concer tion may be obtained from the investigations by Farcy (1931) and by Leeflang (1938).

The data from the British Isles (for instance Russel and Richards 1919) show a well-defined minimum in the interior of England (Cirencester 3.2 mg per liter, 26 years, Rothamsted 2.4 mg per liter, 27 years). Apart from the excellent coastal gradient data collected by Farcy (l. c.) the observations from France are inadequate but there are old series from Paris (one year, 1851) which gives a concentration of 2.3 mg per liter, in good agreement with the data from Cirencester and Rothamsted. A similar series from Nantes (about 90 km from the coast) for 1863 gives 8.4 mg per liter (this value is placed in the wrong column in table 10, p. 286 of Erikssons survey (l. c.)).

In Germany data are available from several large industrial cities including Berlin, Dortmund and Essen. All these places show much higher values than the interior of England and represent undoubtedly the effects of strong local industrial pollution. There remains a one-year series from an apparently undisturbed sampling point at Müncheberg, approximately 50 km E of Berlin, with a concentration of 3.6 mg per liter (one year 1933—1934, Liesegang, 1934).

We have entered on the map the danish data (a one-year series for 1925—1926) obtained by Hansen (1931). Likewise we have included a selection of the Swedish sampling points analyzed by Emanuelsson, Egnér and Eriksson (1954). These data pertain to the calendar year 1949.

The data from the European part of the USSR are based on measurements made in 1909—1910 by Wituynj (1911). A statement by G. A. Maksimovitj (1953) in a lecture before the USSR Academy of Sciences seems to imply that these values still are accepted by USSR scientists as representative. Wituynj's measurements show notably high concentrations of chlorides in the Black Sea region decreasing northwards and towards Asia.

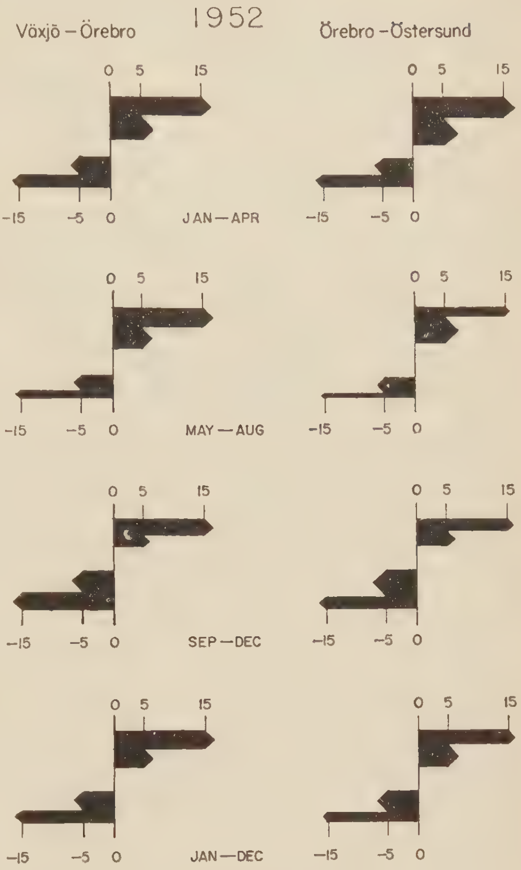

Fig. 15. Sea level frequency distributions for the year 1952 of geostrophic wind components from the west and from the east across two north—south sections in southern Sweden (Växjö—Örebro) and central Sweden (Örebro—Östersund). Thickness of arrows measures relative frequency of occurrence. Wind velocities expressed in mps.

The most striking features in our sketch map are the existence of a chloride minimum extending from the interior of France towards eastern Sweden and the existence of a marked second chloride maximum in the eastern and southeastern part of Europe. This second maximum fits in well with the high chloride concentrations observed in SE Sweden during November 1949 and in the air samples for December 1953. The explanation of this secondary maximum may lie in some process of ion separation operating on the sea salt nuclei but one can not a priori exclude as insignificant such other effects as volcanic and other continental sources of chlorides.

The separation of the individual chemical components of the nuclei brought out by some of the monthly patterns analyzed above would seem to fit in well with the results by Junge (1952, 1954) and Woodcock (1952) concerning the rôle of the giant nuclei in the precipitation mechanism. According to these authors the

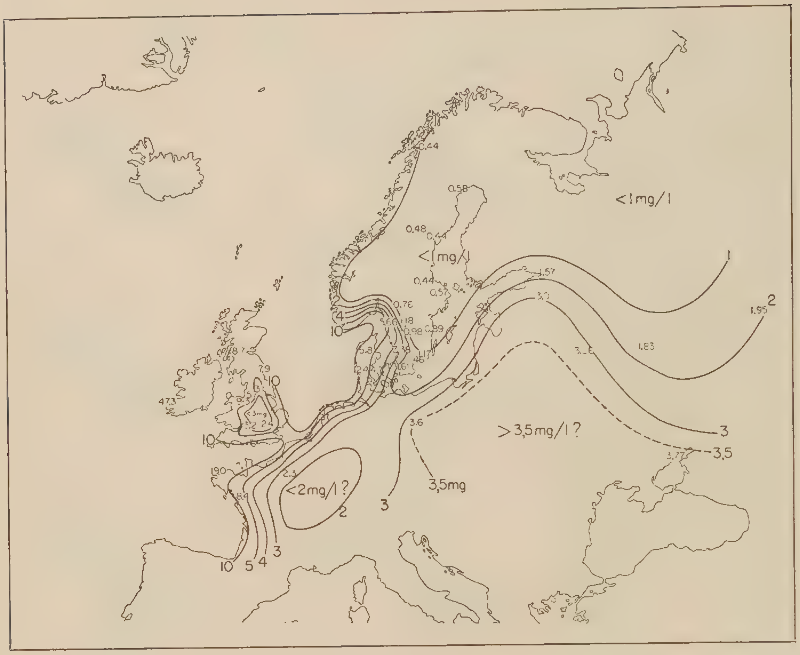

Fig. 16. A preliminary
of average concentratic
chlorides (in mg per l
in precipitation over
rope. Analysis based or
cords from different ep
and of very different len
Note proposed existen
minimum extending f
central France towa
eastern Sweden and
secondary maximum
southern Russia.

largest nuclei consist mainly of sodium chloride and it is these nuclei which most readily lead to the formation of cloud droplets of precipitable size. One should therefore expect precipitation at stations not too far removed from the coast to possess a characteristic chloride over sodium ratio of about 1.5. After the precipitation of the sodium chloride particles there would remain in the air, or in the clouds, an excess of chlorides, perhaps in the form of H_4NCl or $MgCl_2$. The fact that the Cl/Na ratio even in straight westerly flows may drop to values considerably below 1.5 suggests however, that other sodium-containing nuclei become active before the chloride nuclei take over the precipitation-forming mechanim. With Dr Junge's permission we include a statement in a recent letter (February 20, 1955) to one of us (C.-G.R.):

"... Es waren mir zwar schon, auch von eigenen Untersuchungen, starke Abweichungen des Cl/Na-Wertes von dem des Seewassers bekannt, dass sie aber so stark sind und so augenscheinlich mit der Grosszirkulation verbunden sind, war doch eine Überraschung. Wenn ich Ihre Ergebnisse mit den meinen vergleiche, kommt mir der Verdacht, dass wir möglicherweise drei Komponenten unterscheiden müssen, die zum Gehalt des Regenwassers beitragen: Die Seesalzkomponente,
im wesentlichen 1.8 liefert, eine Gaskom
nente, die eine Erhöhung dieses Wertes lie
würde und die ich jedenfalls in südlic
Breiten einwandfrei nachweisen konnte
drittens eine mineralische Staubkompone
die zusätzliches Na liefert und das Verhä
unter 1.8 sinken lässt.

"Das gefundene Verhältnis würde dann
Mischung dieser drei Komponenten darste
und natürlich von der Grosszirkulation
hängen. Nun ist die Lage Schwedens offe
so, dass selbst bei überwiegenden Westwir
keineswegs mit einer reinen Seesalzkon
nente zu rechnen ist. Den starken Anstieg
Werte bei südlicher Luftzufuhr würde
als das Auftauchen der Gaskomponente de
möglicherweise unterstützt von industri
Verunreinigungen. Das starke Absinken
östlichen und nördlichen Winden wäre
Überwiegen der mineralischen Staubkon
nent die ebenfalls noch bei westlichen Wi
von Einfluss ist."

Regardless of the nature of the mecha
or mechanisms responsible for the separ
of the individual chemical components
served in precipitation or in the air, it is
evident from the data presented above
the chemical climate varies in a str

manner with changes in the circulation patterns. In certain respects the association of a specific chemical climate with a specific circulation type may to some extent depend on man-made sources of pollution. By and large, however, one should expect the association to be stable and applicable also to past climates. The relative fluctuations in the temperature and precipitation climates with changes in circulation pattern are, at least in Northwestern Europe, small compared with the fluctuations in the chemical climate. There might therefore exist a possibility to trace post-glacial climatic fluctuations through their chemical consequences. In a recent major investigation Mattson and Coutler-Andersson (1954) have made a detailed study of the chemical composition of different strata in a raised bog in SW Sweden. They find striking variations in the relative proportions of various elements and in the pH. It is tempting to try to associate these variations with variations in the circulation pattern, to check conclusions concerning post-glacial climatic fluctuations which have been drawn previously mainly from pollen-analytical studies. Such an attempt would, however, require a detailed investigation of the association between the circulation pattern and the deposition through precipitation of the bivalent ions, for instance Ca^{++} and Mg^{++}, which are most closely bound by the humic acids, and which therefore are capable of exhibiting a measurable stratification.

Acknowledgement

In the preparation of this paper numerous members of the Institute of Meteorology have been of great assistance. The various sea level mean maps have been plotted and analyzed by Mr P. Bergthorsson of the Icelandic Weather Service, and by mr E. Edström of the Institute staff. The frequency analysis of west and east wind components and certain other calculations referred to in the text was carried out by Mr Cl. Rooth of the Institute staff. The pH-chart for December 1953 was prepared by mr Earl Barrett, of the Woods Hole Oceanographic Institution. The authors have benefitted from many fruitful consultations with these persons, and with Mr. E. Eriksson of the Institute staff. We are particularly indebted to Mr F. Ludlam of Imperial College, London, who throughout the autumn of 1954 in a most invigorating manner participated in and contributed to the discussion of our problem and to Dr. Ch. Junge, with whom we have maintained a steady correspondence.

REFERENCES

Cauer, H., 1949: Ergebnisse chemisch-meteorologischer Forschung, Archiv für Meteorologie, Geophysik und Bioklimatologie, Serie B, Band I, pp. 221—256.

Drischel, H., 1940: Chlorid-, Sulfat- und Nitratgehalt der atmosphärischen Niederschläge in Bad Reinerz und Oberschreiberhau im Vergleich zu bisher bekannten Werten anderer Orte, Der Balneologe, 7. Jahrgang, Heft 11, pp. 321—334.

Eriksson, E., 1952: Composition of Atmospheric Precipitation, II, Tellus, Vol. IV, No. 4, pp. 280—303.

Egnér, H., and Eriksson, E., 1955: Current Data on the Chemical Composition of Air and Precipitation, Tellus, Vol. VII, No. 1, pp. 134—139.

Emanuelsson, A., Eriksson, E., and Egnér, H., 1954: Composition of Atmospheric Precipitation in Sweden. Tellus, Vol. VI, No. 3, pp. 261—267.

Farcy, L., 1931: La composition des eaux de pluie de la région de Brest et du Nord finistère. Ann. Hyg., **9**, p. 504.

Hansen, F., 1931: Undersøgelser af regnvand. Tidskr. f. Planteavl., **37**, pp. 123—150.

Junge, Chr., 1953: Die Rolle der Aerosole und der gasförmigen Beimengungen der Luft um Spurenstoffhaushalt der Troposphäre. Tellus, Vol. V, No. 1, pp. 1—26.

— 1954: The chemical composition of atmospheric aerosols I: Measurements at Round Hill Field Station, June—July 1953. Journal of Meteorology, Vol. XI, No. 4, pp. 323—333.

Köhler, H., and Båth, M., 1952: Quantitative Chemical Analysis of Condensation Nuclei from Sea Water. Nova Acta Regiae Societatis Scientiarium Upsaliensis, Ser. IV, No. 7, pp. 1—24.

Leeflang, K. W. H., 1938: De chemische Samenstelling van den Neerslag in Nederland. Chem. Weekbl. **35**, pp. 658—664.

Liesegang, W., 1934: Untersuchungen über die Mengen der in Niederschlagswässern enthaltenen Verunreinigungen. Kleine Mitt. Mitgl. Ver. Wasser-, Boden- und Lufthygiene, **9**, pp. 350—355.

Maksimovitj, G. A., 1953: Atmospheric Precipitation and its rôle as carrier of dissolved substances (in Russian). Akademija Nauk SSSR, Doklady N S 92, p. 401.

Mattson, S., Koutler-Andersson, E., 1954: Geochemistry of a raised bog. Ann. Royal Agr. College, Sweden, 21, pp. 321—366.

Russel, E. J., and Richards, E. H., 1919: The amounts and composition of rain and snow falling at Rothamsted. J. Ag. Sci., **9**, pp. 309—337.

Wituynj, J., 1911: Die Mengen von Cl und SO_2, die in den Boden mit den atmosphärischen Niederschlägen gelangen. J. Exp. Landw. (Russian) 12, pp. 20—30.

Woodcock, A. H., 1952: Atmospheric Salt Particles and Raindrops. J. of Meteorology, **9**, pp. 200—212.

PRINTED IN SWEDEN
ESSELTE, STHLM 55

Contribution No. 771

Deep-Sea Research, 1955, Vol. 3, pp. 1 to 22. Pergamon Press Ltd., London.

Analysis of sound-scattering observations from non-uniform distributions of scatterers in the ocean

STEFAN MACHLUP and J. B. HERSEY

Abstract—A method is described for computing the vertical distribution of volume-scattering coefficient from a scattering experiment in which an explosion is used as the sound source, and a hydrophone having specified directional properties feeds a recorder through a band-pass filter.

Formulae for the echoes from several model distributions of scatterers are derived as functions of time and frequency. The information about marine scatterers obtainable from the scattering spectrum is discussed.

I. INTRODUCTION

SOUND scattering by both nekton and plankton has been one of the very intriguing problems in marine science for the past decade. Sound has proved to be an effective tool for revealing the presence and something of the behaviour of marine life, some of which could be identified, but most of which could not. Commercial fisheries have been able to do most of the identifying because they have followed up their acoustical observations with large-scale fishing operations, usually in rather shallow water. By contrast, no positive identification has been made of sound-scattering life in the deep scattering layers, partly because of inadequate fishing gear for the problem, and partly because the layers are found only in deep water and probably seldom represent dense concentrations. Most, if not all of the identifications have been made from a comparison of fish caught by net hauls or explosives with the characteristics of the echo sounder record. This sort of identification may eventually be useful in studying the deep water scattering layers, but not until we have made the first positive identifications and, in addition, learned how to interpret the characteristics of the acoustic records. As a step in this learning process we and others at Woods Hole have been studying the scattering layers in the deep ocean, using a small explosive charge as the sound source instead of the usual echo sounder. The explosion is an intense source of sound over a wide range of frequencies, and was anticipated to provide a means of discovering the frequency variation of scattering from the scattering layers in some detail. HERSEY, JOHNSON and DAVIS (1952) showed that there are scattering layers at different depths and different frequencies, and HERSEY and BACKUS (1954) have found evidence for a direct dependence of the peak frequency of certain scattering layers on their depth, suggesting that many of the sound scatterers in the layers are fish with swim bladders. Other work is in progress to use this general approach to the identification problem. The present paper discusses the kind of information to be found in the usual type of recording obtained by firing a shot at shallow depth, and receiving the scattered sound with a directional transducer pointing vertically downward near the shot. The first part is equally applicable to the analysis of volume scattering in general, and the rest considers the various questions having to do with analyzing the complex scattered sound from the shot with band-pass filters.

Typical observations at sea are made by detonating an explosive charge ($\frac{1}{2}$lb. TNT) at a shallow enough depth to blow out, thus eliminating the multiple sound pulses caused by oscillations of the gas globe. The scattered sound as well as the direct shock wave from the shot is received by a nearby hydrophone, either a circular piston type transducer pointed vertically downward or an omnidirectional hydrophone a few feet below the surface. In the early work the transducer fed a five channel amplifier, each channel of which was filtered by a rather narrow band-pass filter, so chosen as to cover a wide frequency range (cir. 1 to 20 kc). The channel outputs were rectified and recorded by an oscillograph camera. These recordings are described in more detail in HERSEY, JOHNSON and DAVIS (1952), and a sample record is shown in Fig. 1. Since 1951 single or dual channel amplifiers having a flat response over a wide frequency range have been used (cir. 100 to 15,000 or 30,000 cps.) to feed magnetic tape recorders of appropriate frequency range. These records are then played back through suitable filter systems for analysis. In the discussion below a sample analysis is presented from the earlier oscillograph records.

II. THE ANALYSIS

The problem discussed below may briefly be stated : Given an echo, what is the distribution of targets that caused it ? It is evident that we shall have to be satisfied with fragmentary information about the distribution ; there is the fundamental limitation of having only one signal (one receiver, hence one scalar function of one variable, time) to investigate a three-dimensional distribution. There is also the technical limitation on time resolution imposed by the finite length of any useful signal, and the finite response time of receiving and recording gear. The first limitation implies that one must make simplifying assumptions about the distribution to remove the indeterminacy. The second implies that the optimal description of the distribution will be in terms of averages over volumes whose dimensions have lower limits set by the time resolution.

We are interested in the frequency dependence of the scattering ; hence we must know how to separate out other frequency-dependent factors. The frequency spectrum of the outgoing energy – the explosion – can be arrived at theoretically (Section VI). So can the response of a filter to an impulsive signal (Section VII). The frequency dependence of the apparatus is taken care of by calibration at various frequencies. But one factor influences the " geometry " of the situation ; the resolution in *angle* is governed by the (frequency-dependent) directivity pattern of the receiver.

We shall discuss the echoes obtained from characteristic types of distributions, first for a non-directional receiver (low frequencies or small transducer) and then, briefly, for a directional receiver (higher frequencies or large transducer). Then we shall treat the general method of translating echo intensity (function of time) into volume scattering coefficient (function of depth).

Equation for the Echo.

If the energy flow per unit solid angle from the source of sound (assumed isotropic) is given by $F(\tau)$ (where τ is time measured from " the beginning of the signal "), then the intensity in a region of scatterers distant r from the source is $F(\tau)/r^2$. (For the moment, the acoustic approximation is assumed to hold, and dissipation is neglected). Let the differential cross-section for backward scattering of a unit volume

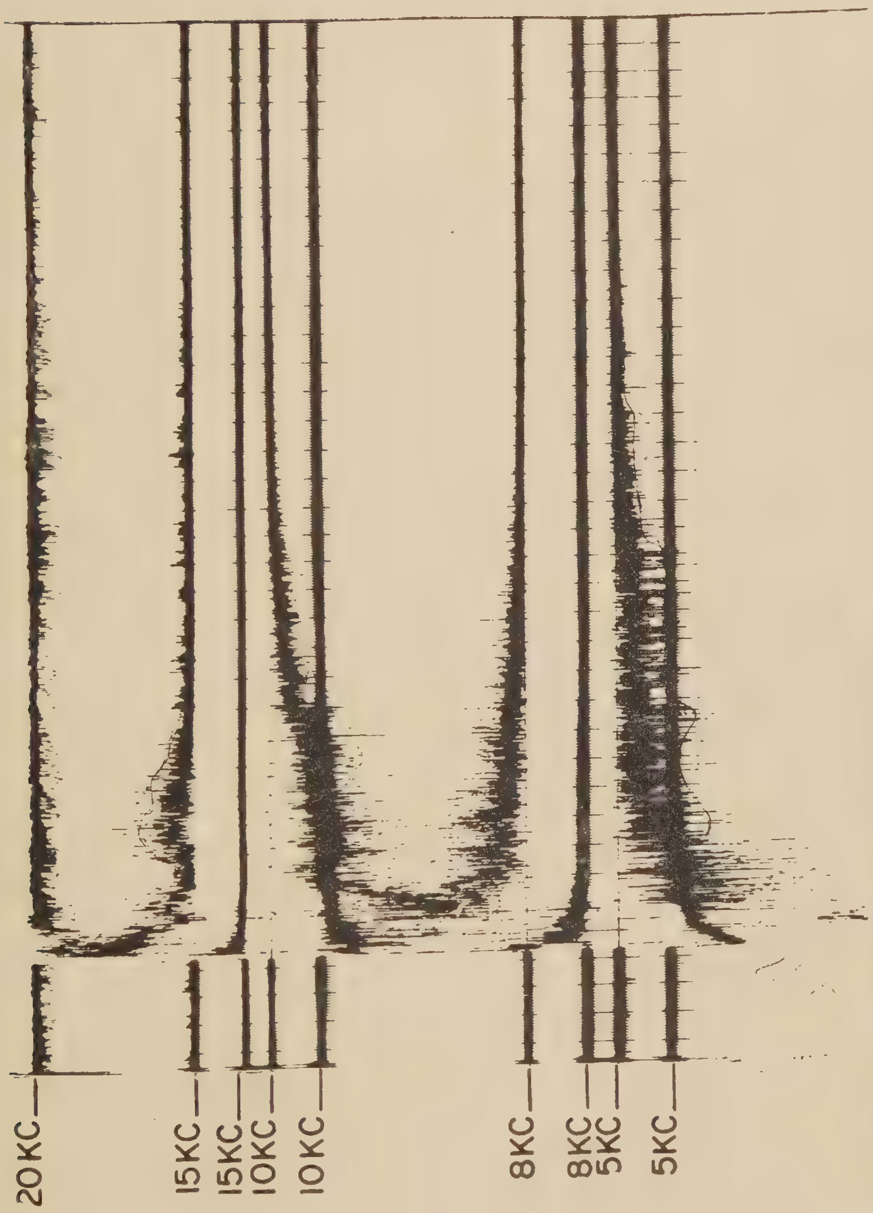

Fig. 1. 5 Channel amplifier record # 141, *Atlantis* cruise 160 made at 1113Q, 3rd April, 1950, Lat. 28° 03′N, Long. 54° 10′W

of ocean be m. (This " backward-scattering coefficient " is smaller than the usual " total scattering coefficient " (UCDWR, 1946) by a factor $1/(4\pi)$). Then the intensity of scattered sound at the receiver (considered coincident with the source) at time t is

2-1 $$I(t) = \int_{\text{VOLUME}} \frac{F(\tau)}{r^2} \frac{m(r, \theta, \psi)\, b(\theta, \psi)\, dV}{r^2}$$
$$= \int_{\tau=0}^{t} \int_{\theta=0}^{\pi/2} \int_{\psi=0}^{2\pi} \frac{F(\tau)}{r^2} \frac{m(r, \theta, \psi)\, b(\theta, \psi)}{r^2} r^2 \sin\theta\, dr\, d\theta\, d\psi$$

where

2-2 $$r = \frac{c}{2}(t - \tau).$$

c is the velocity of sound in the ocean, taken as constant. $(t - \tau)$ is the travel time out and back. $b(\theta, \psi)$, the " directivity function " of the receiver, is the ratio of the sensitivity of the receiver to plane waves coming from the direction (θ, ψ) to its sensitivity to plane waves coming in parallel to its axis.

The assumptions on which eq. (1) is based are those made in the standard treatments of volume reverberation (UCDWR, 1946) :

(1) Reverberation intensity from a given volume element is proportional to its volume. The proportionality constant is our coefficient m. The effect of this assumption is to " smear out " the individual scatterers into a continuum ; this is the averaging process mentioned above.

(2) A volume element begins to scatter sound at the instant it is insonified, and stops as soon as it is again " in the dark " ; i.e., there are no time lags – no storage of energy in the scatterers.

(3) Scattering cross-sections are small enough for us to neglect multiple scattering as well as attenuation of the outgoing beam due to scattering.

(4) The average reverberation intensity at the receiver is equal to the sum of the average intensities due to individual scatterers. This is a " randomizing " assumption, to average out interference effects.

(5) The backward-scattering coefficient m is independent of the direction of incidence of the beam.

To these we shall add two more assumptions :

(6) The receiver has axial symmetry $[b(\theta, \psi) = b(\theta)]$ and is pointed vertically down.

(7) The scattering coefficient m is a function only of depth $z = r\cos\theta$. Any horizontal plane is a surface of equal density of scatterers. It is this most unrealistic assumption which removes the indeterminacy in solving eq. (2-1) for m given $I(t)$.

Now we can perform the ψ-integration in (2-1), which becomes

2-3 $$I(t) = 2\pi \int_{\tau=0}^{t} \int_{\theta=0}^{\pi/2} \frac{F(\tau)}{r^2} m(r\cos\theta)\, b(\theta) \sin\theta d\theta dr$$
$$= \frac{4\pi}{c} \int_{\tau=0}^{t} \int_{\theta=0}^{\pi/2} \frac{F(\tau)}{(t-\tau)^2} m\left[\frac{c}{2}(t-\tau)\cos\theta\right] b(\theta) \sin\theta\, d\theta\, d\tau$$

using 2-2 to eliminate r.

For short signals, $F(\tau)$ is considerable only for $\tau \ll t$, and the τ-integration can be performed by setting $r = \frac{c}{2} t$. The total energy leaving the source is

$$E = 4\pi \int_0^\infty F(\tau)\, d\tau\,; \tag{2-4}$$

thus we can simply rewrite the echo intensity as

$$I(t) = \frac{Ec}{4r^2} \int_0^{\pi/2} m(r\cos\theta)\, b(\theta) \sin\theta\, d\theta. \tag{2-5}$$

This approximation limits the time resolution to times longer than the effective " signal length."

III. ECHOES WITH NON-DIRECTIONAL RECEIVER

We consider a receiver whose sensitivity is essentially the same at all angles of incidence less than $\pi/2$,

$$b(\theta) = 1,$$

and look at the time-dependence of the echo from some simple distributions of scatterers.

(i) *Uniform Distribution of Scatterers.*

For the case $m =$ constant, the echo simply falls off as t^{-2}. (In theory it is infinite at $t = 0$).

(ii) *Very Thin Layer at Depth D.*

Converting to an integral over depth $z = r\cos\theta$, we have

$$I(t) = \frac{Ec}{4r^2} \int_0^r m(z) \frac{dz}{r}$$

$$= \begin{cases} 0 & \text{for } t < 2D/c \\ \dfrac{Ec}{4r^3} \displaystyle\int_D^{D+\Delta} m(z)\, dz & \text{for } t > 2D/c. \end{cases}$$

Qualitatively : The wave-front " dips into " the layer, is " through it " in a very short time (rise-time of the echo), whereafter the echo falls off as t^{-3}.

(iii) *Uniform m Below Depth D.*

$$m(z) = \begin{cases} 0 \text{ for } z < D \\ m \text{ for } z > D \end{cases}$$

$$I(t) = \begin{cases} 0 & \text{for } t < 2D/c \\ \dfrac{Ec}{4r^2} \displaystyle\int_D^r m \frac{dz}{r} = \frac{Ecm}{4} \frac{r - D}{r^3} & \text{for } t > 2D/c. \end{cases}$$

As the wave-front " dips into " the layer, the echo builds up, reaching a maximum at $t = \frac{2}{c}(1{\cdot}5D)$, then falling off, becoming, as $r \gg D$, asymptotic to t^{-2}. (See

" uniform distribution of scatterers "). The curve $I(t)$ is plotted on a dimensionless time scale in Fig. 2 (solid curve), for a layer beginning at depth $D = 1$. $Ecm/4$ has been arbitrarily taken as unity.

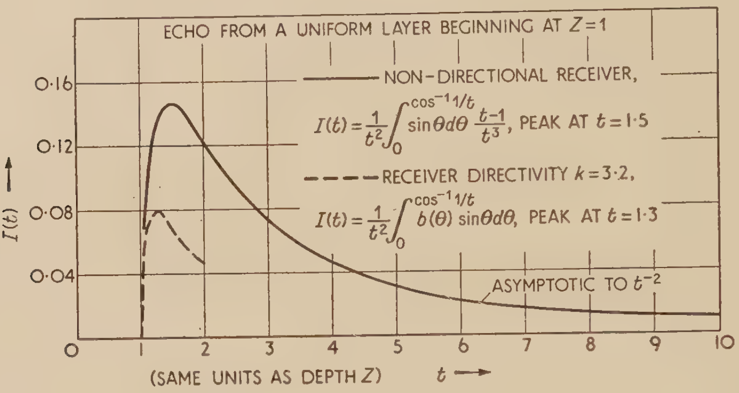

Fig. 2.

(iv) *Layer of Uniform m between Depths D_1 and D_2.*

Here three regions must be distinguished :

$$z < D_1, \qquad m(z) = 0, \qquad I(t) = 0$$

$$\left[t < \frac{c}{2} D\right]$$

$$D_1 < z < D_2, \qquad m(z) = m, \qquad I(t) = \frac{Ecm}{4} \frac{r - D}{r^3}$$

$$\left[\frac{c}{2} D_1 < t < \frac{c}{2} D_2\right]$$

This is as in (iii) : The echo does not yet " know " that the layer is going to end.

$$z > D_2, \qquad m(z) = 0, \qquad I(t) = \frac{Ec}{4r^2} \int_{D_1}^{D_2} m \frac{dz}{r}$$

$$\left[t > \frac{c}{2} D_2\right] \qquad\qquad = \frac{Ec}{4r^3} m (D_2 - D_1)$$

(Compare ii). A plot of $I(t)$ in decibels appears in Fig. 3 (solid curve), on a logarithmic time scale, for $D_1 = 1$, $D_2 = 2$; same normalization as above.

(v) *Gaussian Distribution of Scatterers.*

Such a distribution is given by

$$m(z) = m \frac{2}{\sqrt{\pi}} e^{-\frac{(z-D)^2}{2\sigma^2}}$$

for $z > 0$. The distribution centres at depth D, has $e^{-\frac{1}{2}}$ (= ·606) of its peak density at σ units above and below D. Then

$$I(t) = \frac{Ec}{4r^2} m \frac{2}{\sqrt{\pi}} \int_0^{\pi/2} e^{-\frac{(z-D)^2}{2\sigma^2}} \sin\theta \, d\theta.$$

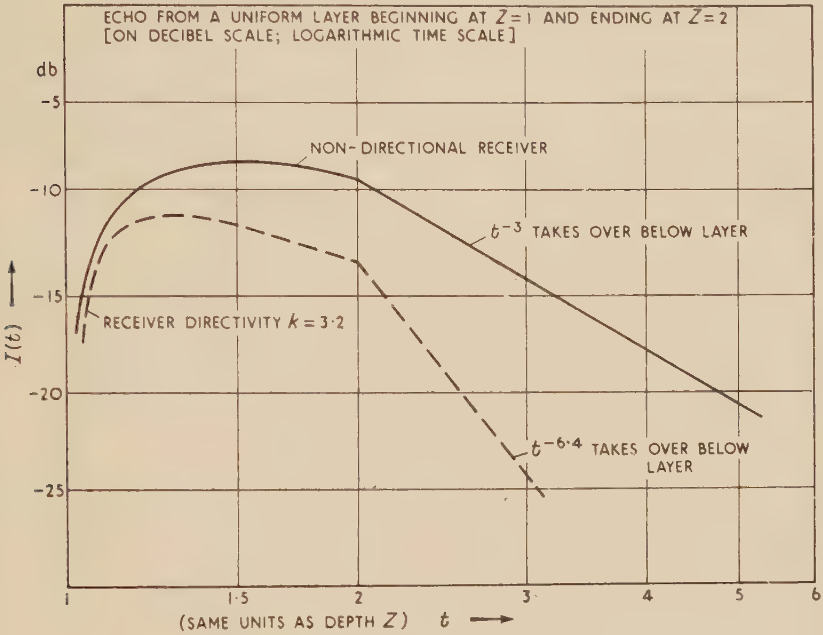

Fig. 3.

For simplicity we measure depth in units of $\sigma\sqrt{2}$ and echo intensity in units of $Ecm/4$. We must distinguish two regions :

$$r < D \qquad I(t) = \frac{1}{r^3}\{\Phi(D) - \Phi(D - r)\}$$

$$\left[t < \frac{c}{2} D\right]$$

$$r > D \qquad I(t) = \frac{1}{r^3}\{\Phi(D) + \Phi(r - D)\},$$

$$\left[t > \frac{c}{2} D\right]$$

where

$$\Phi(x) = \frac{2}{\sqrt{\pi}} \int_0^x e^{-y^2} dy$$

is the "error integral," tabulated in JAHNKE and EMDE (1945). The distribution and the echo are plotted for various values of D in Figs. 4-7. Since there are scatterers at $z = 0$, the echo is theoretically infinite at $t = 0$. For a deep enough (or thin enough) layer (Figs. 5-7), it falls to a minimum, peaks as the wave-front "dips" well into the dense part of the layer, and then falls off asymptotic to t^{-3}. Its peak is somewhat later than it would be with a very directional receiver. For a shallow

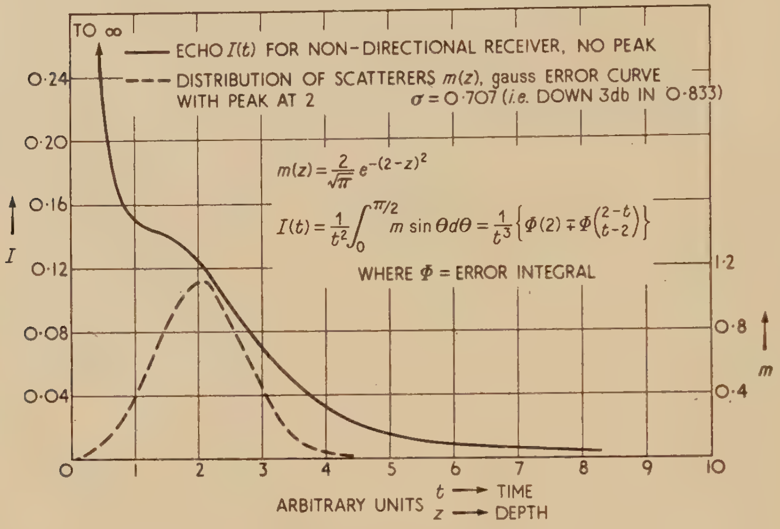

Fig. 4. Echo from a Gaussian distribution of scatterers centered at $z = 2$.

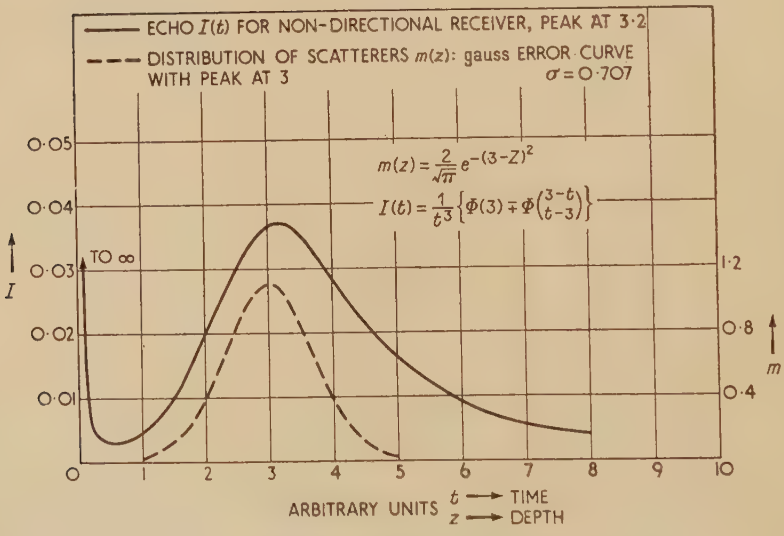

Fig. 5. Echo from a Gaussian distribution of scatterers centered at $z = 3$.

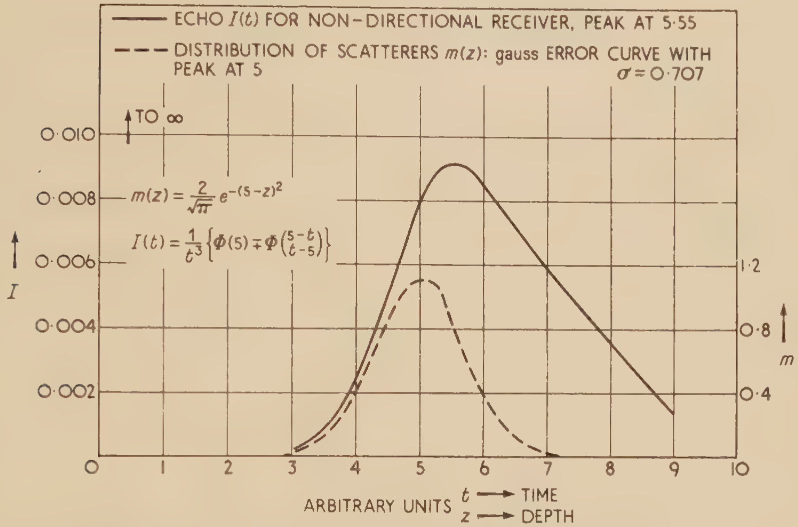

Fig. 6. Echo from a Gaussian distribution of scatterers centered at $z = 5$.

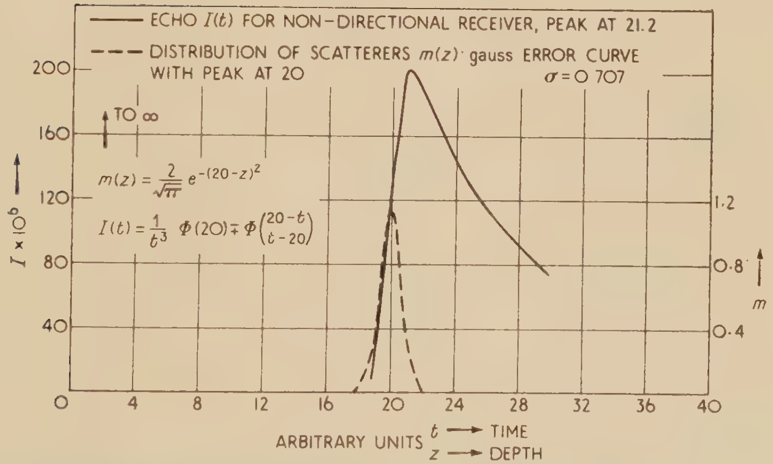

Fig. 7. Echo from a Gaussian distribution of scatterers centered at $z = 20$.

(or thick) layer (Fig. 4), it never goes to a minimum, and has a " ripple " instead of a peak.

IV. ECHOES WITH A DIRECTIONAL RECEIVER

When the receiver sensitivity is isotropic (non-directional), the time dependence and frequency dependence of the echo are separable. This is not true, however, for a directional receiver, since the directivity function depends on frequency and appears in the integrand of the expression giving the time dependence. Thus, whether we consider the echo as a function of time in a given frequency band, or as a function of frequency at a given instant of time, our curve will depend on the whole distribution of scatterers.

Directivity Function.

If the receiver is treated as a freely vibrating circular piston in an infinite, rigid baffle, theory predicts a directivity function (MORSE, 1948)

4-1 $$b(\theta) = \left|\frac{2J_1(k\sin\theta)}{k\sin\theta}\right|^2$$

where

J_1 = Bessel function of order one
$k = \pi d/\lambda$ = dimensionless number proportional to frequency and receiver size
d = diameter of the piston
$\lambda = c/f$ = wave-length, in the transmitting medium, of sound of frequency f.

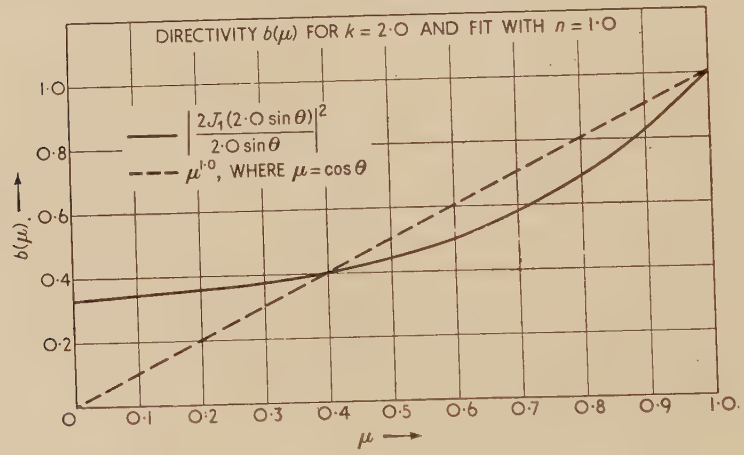

Fig. 8.

This function is tabulated in Table I as far as its first zero, i.e., out to the end of the " main lobe." The argument $\phi = k \sin\theta$ permits rapid use of the table for any frequency and receiver diameter. $b(\theta)$ is plotted against the argument $\mu = \cos\theta$ in Figs. 8-10 (solid curves) for $k = 2{\cdot}0$, $k = 3{\cdot}2$, and $k = 5{\cdot}3$. (Side lobes on $k = 5{\cdot}3$ not shown.)

The conventional *directivity index*,

$$N_{DI} = -10 \log \tfrac{1}{2} \int_0^{\pi} b(\theta) \sin\theta \, d\theta$$

becomes, for this theoretical directivity function,

4·2 $$N_{DI} = -10 \log \tfrac{1}{2} \int_0^{\pi} \left| \frac{2J_1(k \sin\theta)}{k \sin\theta} \right|^2 \sin\theta \, d\theta \simeq +20 \log k \qquad \text{for } k \gg 1$$

(Morse, 1948).

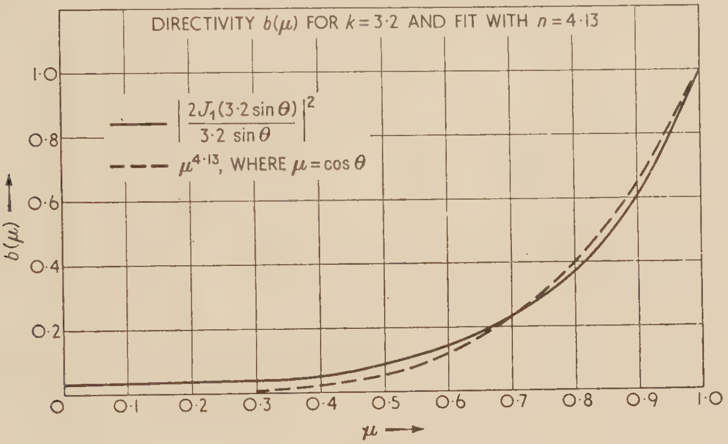

Fig. 9.

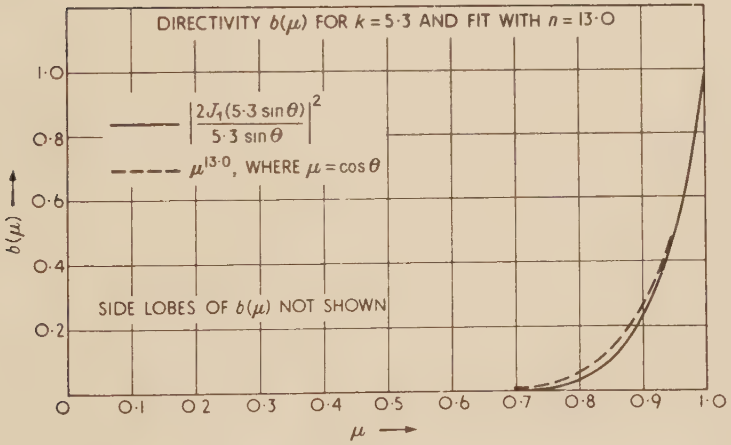

Fig. 10.

Directivity Calibration.

The hydrophone is calibrated off the ship in an experimental set-up. The results of this calibration are used in the final calculation of scattering coefficient. The frequency dependence of the directivity does not agree well with theory, but by choosing an " effective diameter " for each frequency, a good fit to the theoretical curves can be obtained at frequencies where the side lobes are not important. By integrating for N_{DI} numerically (see section VIII), k effective is chosen to satisfy $N_{DI} = +20 \log k$.

Approximate Directivity Function.

In section (V) it will be seen that it is desirable to find a simpler analytic function for $b(\theta)$ than the one given above, even if this new function has no theoretical significance. The function $\cos^n \theta$ has been tried. The condition on n shall be that the total energy received shall be the same for the " fit " function as for the theoretical one ; hence that

$$\int_0^{\pi} \left| \frac{2J_1(k \sin \theta)}{k \sin \theta} \right|^2 \sin \theta \, d\theta = \int_0^{\pi/2} \cos^n \theta \sin \theta \, d\theta.$$

Using eq. 4-2 and performing the integrations, one obtains

4-3 $$n = \frac{k^2}{2} - 1.$$

The dotted curves on Figs. 8-10 show the fit obtained. At high frequencies (large k) the fit is good close to the axis (small angles), where it matters most. It does not, of course, follow the side-lobes, nor does it ever cut off completely, as the Bessel function J_1 does. At low frequencies the fit is poor, but here the approximation of non-directionality becomes good.

Echoes from simple distributions.

Using the approximate directivity function $b(\mu) = \mu^n$ we now look at the echoes from some of the model distributions : (No confusion should be caused by use of the function symbol $b(z/r)$ when the argument is $\mu = \cos \theta$ instead of θ).

(i) *Thin Layer at Depth D . (Sec. III, case ii).*

The echo begins at $t = 2D/c$. It rises quickly, and then falls off according to

$$I(t) = \frac{Ec}{4} \frac{1}{r^2} \int_0^r m(z) \, b\left(\frac{z}{r}\right) \frac{dz}{r}$$

$$= \frac{Ec}{4} \frac{1}{r^3} b(D/r) \int_D^{D+\Delta} m(z) \, dz$$

$$= \frac{Ec}{4} \frac{1}{r^{3+n}} D^n \int_D^{D+\Delta} m(z) \, dz \quad \text{[this form displays the time dependence: } t = 2r/c\text{]}.$$

$$= \frac{Ec}{4} \frac{1}{r^3} (D/r)^{\frac{k^2}{2}-1} \int_D^{D+\Delta} m(z) \, dz \quad \text{[this form displays the frequency dependence : } f = kc/\pi d\text{]}.$$

This frequency dependence is shown graphically in Fig. 11 for time instants just after the beginning of the echo.

For very high frequencies (strongly directional receiver : narrow directivity pattern) the fall-off with time is so fast that the echo is just a sharp " spike." Then, in the integrand, $z \simeq r$, ($\cos \theta \simeq 1$) where $b(\theta)$ is appreciable, and we have

$$I(t) = \frac{Ec}{4r^2} m(r) \int_0^1 b(\mu) \, d\mu.$$

This is a case in which the frequency dependence can be separated out, since the integral no longer contains the time, and is, in fact, equal to $1/k^2$ (see eq. 4-2, and the definition of the directivity index).

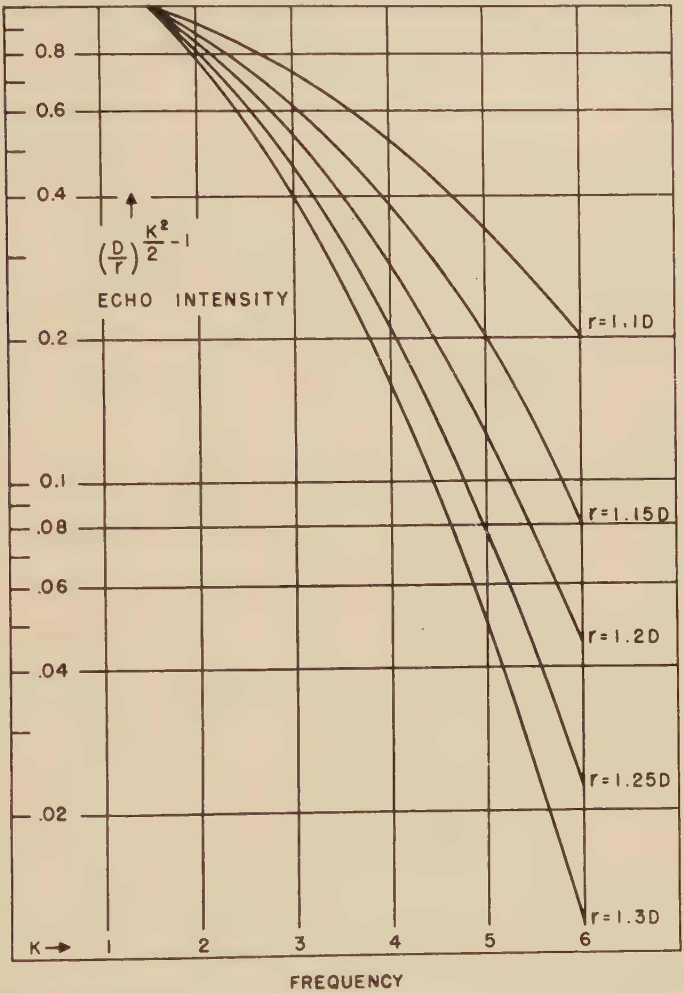

Fig. 11. Frequency dependence of the echo from a thin layer at depth D (directional receiver).

Of course, any distribution can be considered a superposition of thin layers, and we see that, for a very directional receiver, the echo is just proportional to the scattering coefficient corrected for $1/r^2$ " spreading loss ". More simply stated : $t^2 I(t)$ gives a true picture of the depth distribution of scatterers.

(*ii*) *Uniform m Below Depth D.* (*Sec. III, case iii*).

Again, the echo begins at $t = 2D/c$. Thereafter

$$I(t) = \frac{Ec}{4}\frac{m}{r^2}\int_D^r b(z/r)\,\frac{dz}{r}$$

$$= \frac{Ec}{4}\frac{m}{r^2}\int_D^r \left(\frac{z}{r}\right)^n \frac{dz}{r}$$

$$= \frac{Ec}{4}\frac{m}{r^2}\frac{1}{n+1}\left[1 - (D/r)^{n+1}\right]$$

$$= \frac{Ec}{4}\frac{m}{r^2}\frac{2}{k^2}\left[1 - (D/r).^{k^2/2}\right].$$

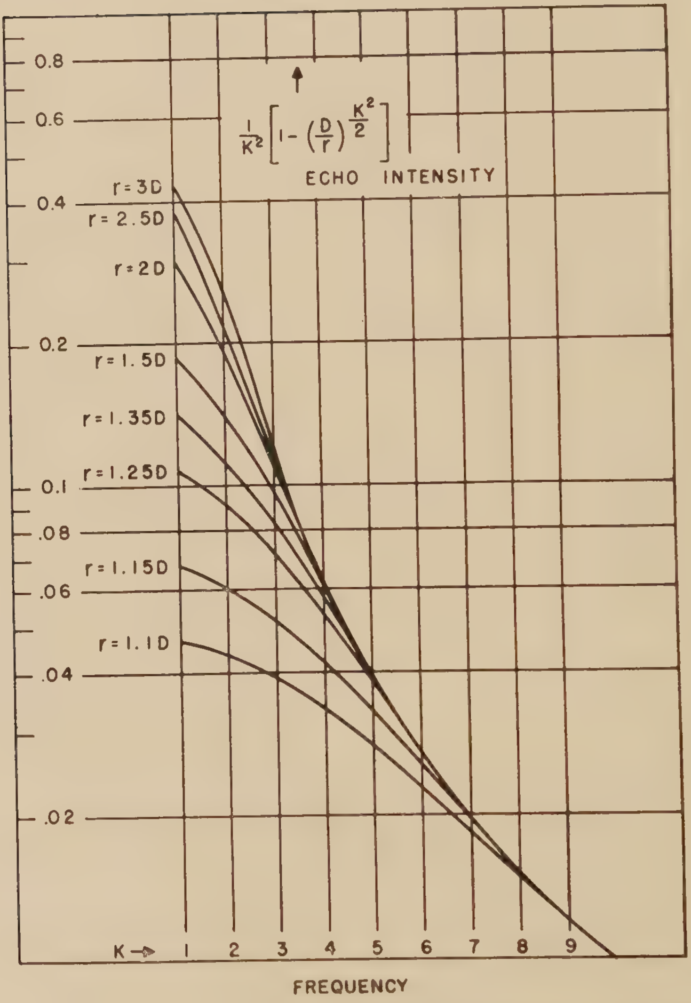

Fig. 12. Frequency dependence of the echo from a uniform distribution of scatterers below depth D (directional receiver).

The time dependence is shown in Fig. 2 for $k = 3{\cdot}2$. The frequency dependence is shown in Fig. 12 for time instants just after the beginning of the echo.

(iii) *Layer of Uniform m Between Depths D_1 and D_2.* (*Sec. III, case iv*).

For $t < 2D_2/c$ this is identical with (ii). Thereafter (the wave front being " through" the layer)

$$I(t) = \frac{Ec}{4}\frac{m}{r^2}\int_{D_1}^{D_2} b\left(\frac{z}{r}\right)\frac{dz}{r}$$

$$= \frac{Ec}{4}\frac{m}{r^2}\int_{D_1}^{D_2}\left(\frac{z}{r}\right)^n\frac{dz}{r}$$

$$= \frac{Ec}{4}\frac{m}{r^{3+n}}\frac{1}{n+1}\left[D_2^{\,n+1} - D_1^{\,n+1}\right] \text{ (this form displays the time dependence)}$$

$$= \frac{Ec}{4}\frac{m}{r^2}\frac{2}{k^2}\left[\left(\frac{D_2}{r}\right)^{k^2/2} - \left(\frac{D_1}{r}\right)^{k^2/2}\right] \text{ (this form displays the frequency dependence).}$$

The time dependence is shown in Fig. 2 for $k = 3{\cdot}2$. It may be instructive to note how this formula goes over into that of case (i) for a thin layer.

V. SOLUTION OF THE INTEGRAL EQUATION

Thus far $m(z)$ was considered given and $I(t)$ calculated. In practice, $I(t)$ appears on the records and $m(z)$ is to be found : The solution of an integral equation is required (Fredholm equation of the first kind) :

$$I(t) = \frac{Ec}{4}\frac{1}{r^2}\int_0^1 m(r\mu)\, b(\mu)\, d\mu.$$

This is equation (2-5) with $\mu = \cos\theta$ (Recall that $r = ct/2$).

The solution can be obtained in closed form when $b(\mu)$ is of the form μ^n, and this was our motivation for choosing this form for the " approximate directivity function " in the preceding section. Writing $\mathcal{J}(r) = I(t)$, we have

5-1 $$m(z) = \frac{1}{z^n}\frac{d}{dz}\left[\frac{4}{Ec}z^{n+3}\mathcal{J}(z)\right].$$

In logarithmic form, $\left(\text{using the relation } \frac{dy}{dx} = \frac{y}{x}\frac{d\log y}{d\log x}\right)$ this is written

5-2 $$10\log m(z) = -10\log\frac{Ec}{4} + 20\log z + 10\log\mathcal{J}(z) + 10\log\frac{d\log\left[z^{n+3}\mathcal{J}(z)\right]}{d\log z}.$$

In words : The shape of the depth distribution of scatterers is given by the curve $t^2 I(t)$ multiplied by the slope of the curve $t^{n+3} I(t)$ plotted on a logarithmic scale.

The term $t^2 I(t)$ is not unexpected in view of the remarks under (*i*) of the preceding section. The term in the slope of $t^{n+3} I(t)$ contains the effect of receiver directivity. It is also the " strong term " at the top and bottom of the layer : When the wavefront is just dipping into the layer – the echo is still small, but building up rapidly – the slope is large, showing there are many scatterers. When the wave-front is "through" the layer – the echo falls off as $t^{-(n+3)}$ – the slope is zero, showing there are no scatterers left. Incidentally, we may note that for a non-directional receiver, $n = 0$, the echo falls off as t^{-3} below the layers, as discussed in Section III.

VI. THE ENERGY OF THE SHOCK WAVE

The total energy of the outgoing signal can be calculated from empirical formulas given by ARONS (1954). The pressure pulse is considered to be of the form $Pe^{-\tau/\Theta}$ ($\tau > 0$), an exponential pulse with peak pressure P and decay time Θ (rise time essentially zero). For TNT,

6-1 $$P = 2{\cdot}16\,(10^4)\left(\frac{W^{\frac{1}{3}}}{R}\right)^{1{\cdot}13} \quad \text{p.s.i.}$$

6-2 $$\Theta = 58\,(10^{-6})\,W^{\frac{1}{3}}\left(\frac{W^{\frac{1}{3}}}{R}\right)^{-0{\cdot}22} \quad \text{sec.,}$$

where W = weight of TNT in pounds, R = range in feet.

The empirical formulas 6-1 and 6-2 are based on considerable data from measurements on larger charges at shorter ranges than we have used in the scattering layer studies. The change of shape of the pulse with range, and the associated deviation from a $1/R$ -dependence of the peak pressure, are effects due to the finite amplitude of the shock wave, i.e., the failure of the acoustic approximation. However, for 0·5 lb. TNT charges at distances greater than about 240′ (0·1 sec. echo travel time), we are well within the region where the acoustic approximation may be taken to hold. Any error resulting from our use of the formulae in the range 240′ to 3,000′, within which the present scattering data lie, is small compared to the uncertainty inherent in the analysis of the scattering records. According to ARONS (private communication), the error is more reasonably assigned to slightly variable performance of the TNT charges. In ARONS (1954) the maximum variation from 6-1 reported for peak pressure of 0·5 lb. TNT charges amounts to about 3 db.

At some mean distance R, the energy flow per unit solid angle is

6-3 $$F(\tau) = R^2\frac{p^2}{\rho c}$$

where p = pressure of the pulse and ρ = density of the water. The total energy E getting out through the sphere of radius R is

6-4 $$E = 4\pi\int F(\tau)\,d\tau = 4\pi R^2\frac{p^2}{\rho c}\int_0^\infty e^{-2\tau/\Theta}\,d\tau$$
$$= 4\pi R^2\frac{p^2}{\rho c}\frac{\Theta}{2}.$$

VII. RESPONSE OF THE FILTERS

The receiving gear is calibrated using sinusoidal signals, at the centre frequency of the separate filters. An investigation of the response of the filters to an exponential signal is therefore required.

The quantity of interest for each filter is the fraction A of the input energy that it puts out :

$$A = \frac{\text{Energy out}}{\text{Energy in}}$$

If the filter were perfectly flat and non-dissipative over its pass-band, and had vertical cut-off to zero at the edges, then the energy out would be the energy of the Fourier components of the input signal contained in the pass-band.

For a filter admittance approximating the actual filters, take a transfer characteristic

$$Y(\omega) = \frac{b}{b + i(\omega - \omega_0)}.$$

This is normalized to unity at the centre of the band ω_0 and is down 3 db at $\omega_0 \pm b$; $2b$ may be called the " band-width."

Consider an input $p(t)$ $(t > 0)$, expressed as an integral over angular frequency :

7-1 $$p(t) = \int_{-\infty}^{+\infty} \psi(\omega)\, e^{i\omega t}\, d\omega,$$

i.e., $\psi(\omega)$ is the Fourier transform of $p(t)$.

The output from a network with characteristic $Y(\omega)$ is then

7-2 $$v(t) = \int_{-\infty}^{+\infty} \psi(\omega)\, Y(\omega)\, e^{i\omega t}\, d\omega.$$

A purely dissipative (resistive) load will see the real part of $v(t)$. For an exponential input signal

7-3 $$p(t) = Pe^{-\lambda t} \qquad (\lambda = 1/\Theta)$$

we have

7-4 $$Re\left[v(t)\right] = Pa\left\{e^{-bt} \sin(\omega_0 t - \delta) + e^{-\lambda t} \sin \delta\right\},$$

where

$$a = \frac{b}{\sqrt{(\lambda - b)^2 + \omega_0^2}}$$

and $\tan \delta = \dfrac{\lambda - b}{\omega_0}$. The energy in a signal is proportional to the time integral of the square of the signal voltage.

Thus the energy in the input signal (7-3) is proportional to $P^2/2\lambda$; the energy in the output signal (7-4) is proportional to

$$P^2 a^2 \int_0^{\infty} [e^{-bt} \sin(\omega_0 t - \delta) + e^{-\lambda t} \sin \delta]^2\, dt.$$

Neglecting the cross-term in the squared parenthesis, the fraction of the energy " getting through " is approximately

7-5 $$A = a^2 \left\{\tfrac{1}{2} \frac{\lambda}{b} + \sin^2 \delta\right\}.$$

VIII. PRELIMINARY RESULTS

Some echoes have been analyzed using the method of section V. The equation 5-2,

$$10 \log m(z) = -10 \log \frac{Ec}{4} + 20 \log z + 10 \log \mathcal{J}(z) + 10 \log \frac{d \log [z^{n+3} \mathcal{J}(z)]}{d \log z}$$

may be written, recalling $z = \frac{c}{2} t$,

8-1
$$10 \log m(z) = - 10 \log E + 10 \log c + 20 \log t + 10 \log I(t) + 10 \log \frac{d \log [t^{n+3} I(t)]}{d \log t}.$$

In practice, the receiving gear has been calibrated so that the linear deflection on the galvanometer record can be read in db re 1 volt open circuit output of the hydrophone. The hydrophone has been calibrated so that this can be interpreted as db re 1 dyne/cm^2 sound pressure at the hydrophone incident on its axis. The effective attenuation A in the filters due to the shape of the input signal (see section VII, particularly eq. 7-5) may loosely be considered as applied to E. Then EA is the energy getting out through the " mean sphere " (see section VI) *and* through the filter.

With the incident intensity given in units of sound pressure p, one must recall

8-2
$$I(t) = \frac{p^2(t)}{\rho c}$$

and write

8-3
$$10 \log m(z) = Q_{f_0} + 20 \log t + 20 \log e(t) + 10 \log [\text{slope of } t^{n+3} e^2(t)],$$

where : 8-3-i $m(z)$ = back-scattering cross-section per unit volume,

8-3-ii $Q_{f_0} = - 10 \log E - 10 \log A_{f_0} - 10 \log \left|\frac{\text{gm}}{\text{cm}^3}\right| -$ db re 1 volt open circuit hydrophone response for 1 $\frac{\text{dyne}}{\text{cm}^2}$ sound field

8-3-iii E = energy, in ergs

8-3-iv A_{f_0} = fraction of the energy getting through a filter with centre frequency f_0

8-3-v t = time, in seconds

8-3-vi $e(t)$ = echo, in open circuit hydrophone output. Slope is taken on the db scale, with a logarithmic time scale.

Some Quantitative Results.

$10 \log E = 122{\cdot}8$ db re 1 erg for a $\frac{1}{2}$ lb. block of TNT, at 1,500 feet. There $\Theta = 250$ μ seconds, $\lambda = 4\,(10^3)$ sec^{-1}. We use the 5 kc trace from Fig. 1 for sample analysis.

The filter is fitted by the function $Y = \beta/[\beta + i(f - f_0)]$, using 5 kc as the centre frequency and a band-width, 2β, of 0·3 kc ($\beta = \frac{1}{2\pi} b, f_0 = \frac{1}{2\pi} \omega_0$) we have $10 \log A = - 22{\cdot}9$ db. From the hydrophone calibration $N_{DI} = - 5{\cdot}9$ db, and the open circuit response per dyne/cm^2 is $- 74{\cdot}5$ db re 1 volt. Using 8-3-ii, $Q_{5kc} = - 25{\cdot}4$ db.

A sample analysis is shown in Fig. 13. For 5 kc, $k = 2{\cdot}0$ gives the experimental directivity index. Hence $n = \frac{k^2}{2} - 1 = 1{\cdot}0$. The following curves are shown :

- the echo $I(t)$, in db re 1 millivolt (This curve is, of course, much smoother than the actual record. Fluctuations have been averaged out visually. Also the part of the record for $t < 0{\cdot}4$ sec. has been omitted since the first part is distorted, and the later part is of too high amplitude to be read).
- the curve $t^2 I(t)$, in db re 1 millivolt.
- the curve $t^4 I(t)$, arbitrary level.
- its slope in decibels.
- $m(z)$ in db re m^{-1}, obtained by solving equation 8-3.

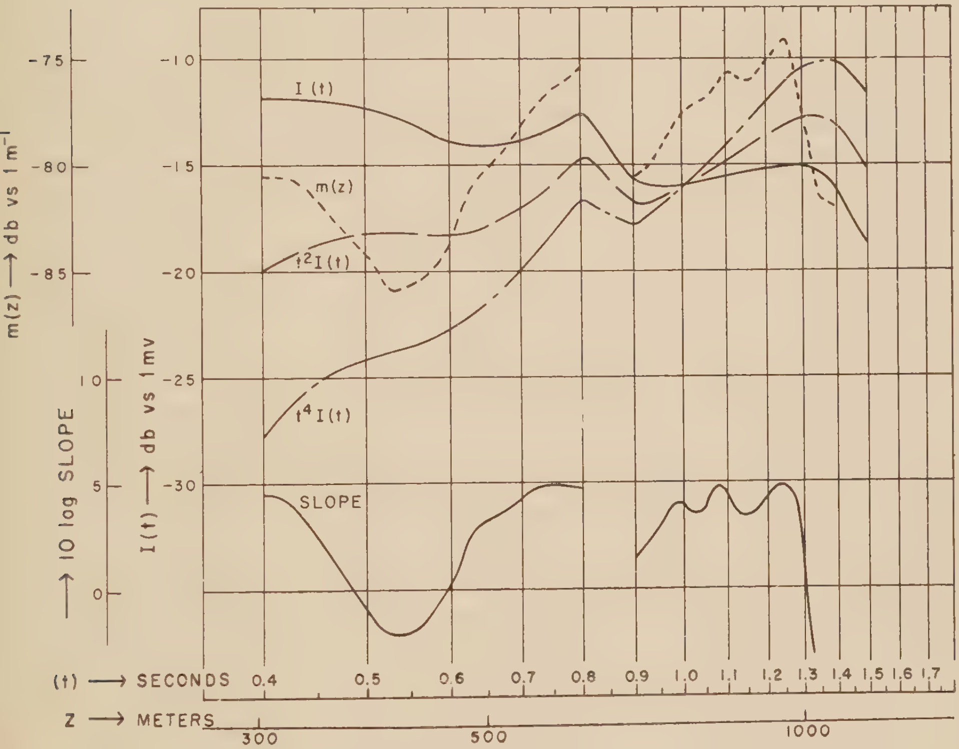

Fig. 13. Analysis of a sample record
Sargasso sea, 1113Q, 3rd April, 1950.
Echo from ½lb. TNT
5 kc filter, $n = 1{\cdot}0$.

Note that the slope goes negative in two intervals in this example. In such instances the solution of the integral equation fails and $m(z)$ cannot be computed. The negative slope is due to the patchiness of the layers ; i.e., they are not really uniform in a horizontal plane. In many recordings a reasonable smoothing of the typically spiky trace gives continuously positive slopes over most of the record.

Forty-five such traces have been thus analyzed, some for the filter centered at 5 kc as above, and some for a similar filter centred at 8 kc. There is considerable variety both in the shape and magnitude of $m(z)$. All the records were taken in the western North Atlantic, but scarcely provide enough data to make any generalizations. The peak values of $m(z)$ range from about -60 db re M^{-1} to -77 db re M^{-1}. This compares with a range of $\cdot 5 \times 10^{-6}$ yd^{-1} to 3×10^{-7} yd^{-1} or about -63 db re M^{-1} to -65 db re M^{-1} reported by UCDWR (1946) for various higher frequencies in the Pacific. Since our sampling is completely random and small we have no way of telling whether our range is representative. Where the 5 kc and 8 kc traces from the same record could be analyzed, there are about as many instances of striking dissimilarity between them as there are of qualitative similarity. This was to have been anticipated from preliminary inspection of the data reported by HERSEY, JOHNSON and DAVIS (1952).

Table I.

Directivity Pattern : Circular Piston in an Infinite Baffle

$b(\theta) = \left|\frac{2J_1(\phi)}{\phi}\right|^2$, $\phi = k \sin \theta$, $k = \pi d/\lambda$

ϕ	$b(\theta)$	$-10 \log b(\theta)$
0·0	1·0	0·0
0·5	·935	0·3
1·0	·773	1·1
1·5	·552	2·6
1·6	·508	2·9
1·7	·462	3·3
1·8	·418	3·8
1·9	·375	4·3
2·0	·333	4·8
2·1	·292	5·3
2·2	·255	5·9
2·3	·220	6·6
2·4	·188	7·3
2·5	·158	8·0
2·6	·131	8·8
2·7	·107	9·7
2·8	·0861	10·6
2·9	·0668	11·7
3·0	·0514	12·9
3·1	·0378	14·2
3·2	·0266	15·8
3·3	·0178	17·5
3·4	·0111	19·5
3·5	·00612	22·1
3·6	·00285	25·5
3·7	·000850	30·7
3·8	·0000468	43·3
3·83		∞

IX. REMARKS CONCERNING FREQUENCY DEPENDENCE

The preceding pages have been concerned exclusively with the volume scattering coefficient, not with individual scatterers. Our aim, however, is to use our " sound spectroscopy " to find out something about the size and number of the scatterers, and ultimately to tie in with other techniques (net hauls, photography . . . . .) to find out what the scatterers really are.

The acoustic scattering cross-section of a sphere as a function of frequency is discussed by ANDERSON (1950). At low frequencies, sufficiently low that the wave length is much greater than the size of the scatterer, the cross-section varies as the fourth power of the frequency (Rayleigh scattering; only the first and second spherical harmonics contribute). This holds regardless of the shape of the scatterer. At higher frequencies, when the wave length becomes of the order of the size of the scatterer, the cross- section goes through some maxima and minima, and higher order spherical harmonics become important. Then the differential cross-section becomes a rapidly varying (oscillating) function of angle. But any finite-sized receiver sees an average over a finite range of angle. As the frequency is further increased, these averages finally become independent of frequency, and we get into the region of geometrical reflection. The exact shape of the curve depends, of course, on the acoustic properties of the propagating and scattering media.

Knowledge of the frequency f_c at which the f^4 — law takes over, combined with ideas about the scattering medium (soft animal tissue, skeleton, swim bladder) can then tell us the approximate size of the individual scatterers.

If the receiver is approximately non-directional near f_c, we have no trouble recognizing this frequency : The echo – corrected for the frequency response of the apparatus – simply falls off as f^4 below f_c. With a directional receiver this fall-off point may be obscured by the frequency-dependence of the directivity function, but the discussion of section IV and the method of analysis of section V take account of this.

What complicates the problem is that – contrary to assumption (7) of section II – distributions in nature *do* have horizontal structure. Sharp peaks appear on the records which are due either to individual scatterers or to localized patches of them. The higher the frequency of observation (the greater the directivity of the receiver, the narrower the field of " view "), the " spikier " the echo traces look, and the worse our averaging over volume elements becomes as a method of analysis. The apparent advantage of better resolution is offset by the indeterminacy restored by the failure of assumption (7) : We do not know where the resolved individuals are ; specifically, at what angle to the receiver axis they lie. The frequency-dependence of a single echo-peak tells us nothing about the frequency-dependence of the scattering, since we do not know what angle θ to put into the directivity function $b(\theta)$.

On the records are many instances where peaks appearing at a low frequency are not present at higher frequencies. Unfortunately, these permit two interpretations: (a) Low frequency resonances. These would be strong if due to air bubbles (swim bladders). (b) The scatterer is located off the receiver axis and only comes into " view " at low frequencies, where the receiver is less directional.

Present techniques cannot remove this ambiguity. At least two observations on a single scatterer are needed to determine its θ. One might make simultaneous observations with two receivers of different size, or with two receivers differently oriented, or at different locations.

Another ambiguity in the interpretation of single echo-peaks might be pointed out here. This is due to the failure of assumption (4) of section II: There are interference effects, giving rise to fluctuations in echo intensity. If we consider a narrow frequency band, each echo signal is a sinusoid. Echoes from different scatterers come in with random phases and superpose. The fluctuations due to this randomness may have the same appearance as resolved echo-peaks from individual scatterers. If the number N of such (coherent) interfering signals is large, the Law of Large Numbers applies : The relative deviation is equal to $N^{-\frac{1}{2}}$ and therefore negligible.

But interference of two or three echoes can cause sizeable fluctuations : The relative deviation for the sum of two sinusoids of equal amplitude and random phase is equal to ·48.

Acknowledgements—We are indebted to G. W. WHEELER for his close collaboration in the early part of this work, Miss AUDREY BERRY for assistance in making several of the numerical computations, and to L. C. DAVIS, who carried out the analysis of the recordings. This work was done under Contract NObsr-43270 with the Bureau of Ships, U.S. Navy Department.

Contribution No. 771 of the Woods Hole Oceanographic Institution.

REFERENCES

ANDERSON, V. C. (1950), Sound scattering from a fluid sphere, *J. Acous. Soc. Amer.*, **22**, 426-431.
ARONS, A. B. (1954), Underwater explosion shock wave parameters at large distances from the charge, *J. Acous. Soc. Amer.*, **26**, 343-346.
HERSEY, J. B. and BACKUS, R. H. (1954), New evidence that migrating gas bubbles, probably the swim bladders of fish, are largely responsible for scattering layers on the continental rise south of New England, *Deep-Sea Research*, **1**, (3), 190-191.
HERSEY, J. B., JOHNSON, H. R. and DAVIS, L. C. (1952), Recent findings about the deep scattering layer, *J. Mar. Res.*, **11**, (1), 1-9.
JAHNKE, E. and EMDE, F. (1945), Tables of Functions, (Dover Publications), **24**.
MORSE, P. M. (1948), Vibration and Sound, McGraw-Hill, (Second Edition).
UNIV. CAL., DIV. WAR RES. (1946), Stratification of sound scatterers in the ocean, UCDWR File Report No. M397. Unpublished manuscript.

Printed in Great Britain by The Salisbury Press Ltd., Publicity House, Wilton Road, Salisbury, Wilts. (93305)

Contribution No. 772

Reprinted from SEWAGE AND INDUSTRIAL WASTES, Vol. 27, No. 11, November, 1955
Printed in U. S. A.

DISTRIBUTION OF COLIFORM BACTERIA AND OTHER POLLUTANTS IN TIDAL ESTUARIES *

BY BOSTWICK H. KETCHUM
Woods Hole Oceanographic Institution, Woods Hole, Mass.

In an estuary, any pollutant which is dissolved or freely suspended in the water is distributed by the circulation both upstream and downstream from the outfall location. A *conservative* pollutant, one which does not change with time, is distributed in a way that can be predicted from the salinity of the estuary. Many pollutants, including coliform bacteria and the biological and chemical oxygen demand, decrease with time in the water of the estuary, and this change is superimposed on the effects of the circulation. The distribution of these "time variable" or non-conservative pollutants can be derived if both the rate of the circulation and the independent rate of decay can be evaluated.

This paper attempts to explain the prediction of the distribution of pollution in estuaries. The prediction of the distribution of a non-conservative pollutant offers many difficulties which are as yet incompletely solved. The state of knowledge and ability to predict the distribution of coliform bacteria will be presented as an example of techniques available at present.

Distribution of Conservative Pollutants

When a conservative pollutant is introduced into an estuary at a constant rate, it will eventually achieve a steady-state distribution up and down the estuary which depends upon the rate of introduction and the rate of the circulation. Although the rate of circulation in estuaries may differ widely, the distribution of salt and fresh water is a direct indication of circulatory processes. The steady-state distribution of a conservative pollutant is directly related to the distribution of fresh and salt water, and can be derived from the results of a salinity survey of the estuary.

It should be pointed out that the conditions which will be discussed are average conditions and local concentrations will certainly differ. By the time the steady-state distribution is achieved, however, these local variations will be at a minimum. It is obvious the average concentrations of a pollutant in a total cross section will be much less than the local concentration immediately over the outfall. For the distribution immediately adjacent to the outfall the investigations of Rawn and Palmer (1) will be found a useful adjunct to the method described in this paper. The local distribution of pollutants will also be modified by different wind conditions. Local eddies and areas of slower than average circulation may be expected near headlands and in restricted basins. No effective general procedure for these local conditions has been developed, and a knowledge of the individual conditions and characteristics of the estuary is essential for the wise application of the methods described.

---

* Contribution No. 772 from the Woods Hole Oceanographic Institution, Woods Hole, Mass. Presented at 1955 Meeting, Texas Water and Sewage Works Assn.; College Station, Texas; Mar. 6–11, 1955.

Average Concentration of Pollutant

At the location of the outfall the pollutant will become mixed and its average concentration (C_o), achieved when steady-state conditions are reached, is given by:

$$C_o = \frac{P}{R} f_o \tag{1}$$

in which P is the rate of supply of the pollutant, R is the rate of river flow and f_o is the average fraction of fresh water in the complete cross section of the estuary which passes through the outfall location. This is calculated from the average salinity (S_o) at that location by:

$$f_o = \frac{S_b - S_o}{S_b} \tag{2}$$

in which S_b is the salinity of the source sea water in the mixture (2).

Downstream Distribution

In the steady-state, a conservative pollutant must pass seaward through every complete cross section at the same rate it is being introduced at the outfall. This same criterion of the steady-state condition applies to the fresh water, and the distribution of the pollutant downstream from the outfall is directly proportional to the distribution of river water. At any downstream location, the average concentration in the cross section, C_y, will be given by the relationship:

$$C_y = C_o \frac{f_y}{f_o} = \frac{P}{R} f_y \tag{3}$$

in which C_y and f_y are the average concentration of pollutant and river water in the complete cross section (y).

Upstream Concentration

The pollutant will also be carried upstream from the outfall by the mixing process and the flood and ebb of the tidal currents. Above the outfall there will be no net exchange across any boundary when the steady-state distribution is reached. The quantity carried upstream will be exactly balanced by the quantity carried downstream. This is the criterion of the steady-state condition that applies to the salt content of the water. The upstream distribution of a conservative pollutant will be directly proportional to the distribution of salinity, as given by:

$$C_y = C_o \frac{S_y}{S_o} \tag{4}$$

It is clear from these relationships that a knowledge of the distribution of salinity is essential in order to predict the expected distribution of pollutants. The salinity distribution in an estuary will be different at different times, depending largely upon fluctuations in river flow. However, an increase in river flow will produce an increase in the fraction of fresh water throughout the estuary. If there is a direct proportional relationship between river flow and the fraction of fresh water, the pollutant concentration will be independent of river flow, and will depend only upon the rate of supply. Its concentration may, therefore, be more nearly constant than the concentration of river water in the estuary.

Illustration

The foregoing relationships make it possible to predict the expected distribution of a conservative pollutant in an estuary. As an illustration, the expected distribution of a pollutant has been derived from the distribution of salt and fresh water in the Raritan River and Bay. An observed distribution of fresh water (3) is shown in Figure 1. Four locations have been selected arbitrarily for the position of an outfall, and the expected pollutant concentration from each is expressed as the percentage of the concentration obtained if the pollutant were uniformly mixed in the river water $\left(\frac{P}{R} = 1\right)$. Downstream from the out-

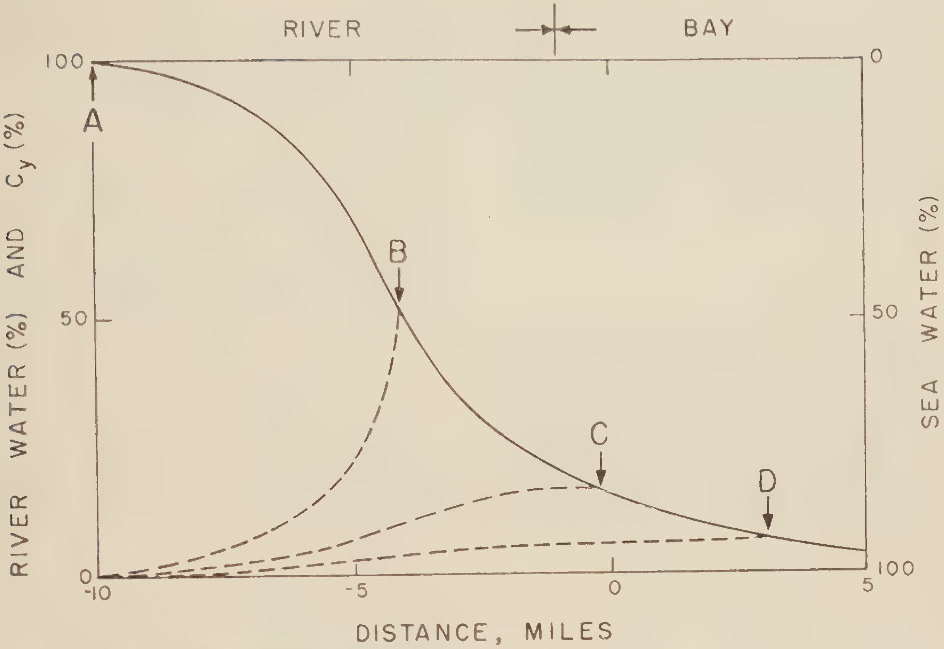

FIGURE 1.—The observed average distribution of river water, and the calculated distribution of a conservative pollutant (C_y) in Raritan River and Bay for four outfall locations.

fall the pollutant concentration is the same as that shown by the solid line, which describes the distribution of fresh water. Upstream from the outfall the dashed lines show the expected concentrations. Two important results of moving the outfall downstream are:

1. The concentration of pollutants upstream from the outfall is decreased.
2. The concentration of pollutants downstream from the outfall is unchanged.

Distribution of "Time Variable" Pollutants

Pollutants which decay or decrease with time will be less concentrated everywhere in the estuary than the predictions for the conservative pollutants. The change with time is superimposed on the circulation processes, and the joint and simultaneous effects of both determine the ultimate distribution. If the rate of supply is constant, a steady-state distribution will be attained also.

The mortality of coliform bacteria has been studied under laboratory conditions (4) (5) and a description given of the bactericidal effect of sea water which is found at all times of the year. The population change due to mortality alone is:

$$C_t = C_o e^{kt} \qquad (5)$$

in which C_o and C_t are the size of the population originally and at time t; e is the base of the natural logarithms, and k is the coefficient of mortality which is negative so that e^{kt} is less than unity. The laboratory experiments indicate the population of coliform bacteria decreases to a one-tenth its original size in a period of time ranging from one-half day to two or three days. Since the flushing time of most estuaries is longer than this, the bacterial mortality can be a most important factor in the distribution.

Practically all the decrease of coliform bacteria in the Raritan River can be accounted for by the circulation, the bactericidal action of sea water and the rate of consumption of the bacteria by zooplankton organisms in the water (6). The following relationship was used for this computation:

$$C_n = (C_o)_n \frac{r_n}{1 - (1 - r_n)e^k} \qquad (6)$$

in which n is a tidal excursion segment as defined by Ketchum (7) and r_n is the exchange ratio of that segment. The increment to the population in the segment considered $[(C_o)_n]$ from the adjacent segment $(n - 1)$ in the direction of the source of pollution, is given by:

$$(C_o)_n = C_{n-1} \frac{f_n}{f_{n-1}} \qquad (7)$$

Since the populations in the segments closer to the outfall ($n - 1$, $n - 2$, etc.) can also be defined by Eq. 6, successive substitutions relate the population in any segment to the average population at the outfall. At this location the rate of supply is given by Eq. 1 depleted by mortality while within the segment, *i.e.*, multiplied by the fraction $\left[\left(\frac{r_n}{1 - (1 - r_n)\, e^k}\right)\right]$. If the mortality coefficients and the exchange ratios are equal for all segments the relationship can be reduced to:

$$C_n = C_o \frac{f_n}{f_o}\left(\frac{r}{1 - (1 - r)e^k}\right)^n \qquad (8)$$

Similar reasoning indicates that the population upstream from the outfall can be given by:

$$C_n = C_o \frac{S_n}{S_o}\left(\frac{r}{1 - (1 - r)e^k}\right)^n \qquad (9)$$

In both Eqs. (8) and (9) the exponent (n) is the number of segments from the outfall to the locality considered, including the segment containing the outfall.

The effect of mortality can be di-

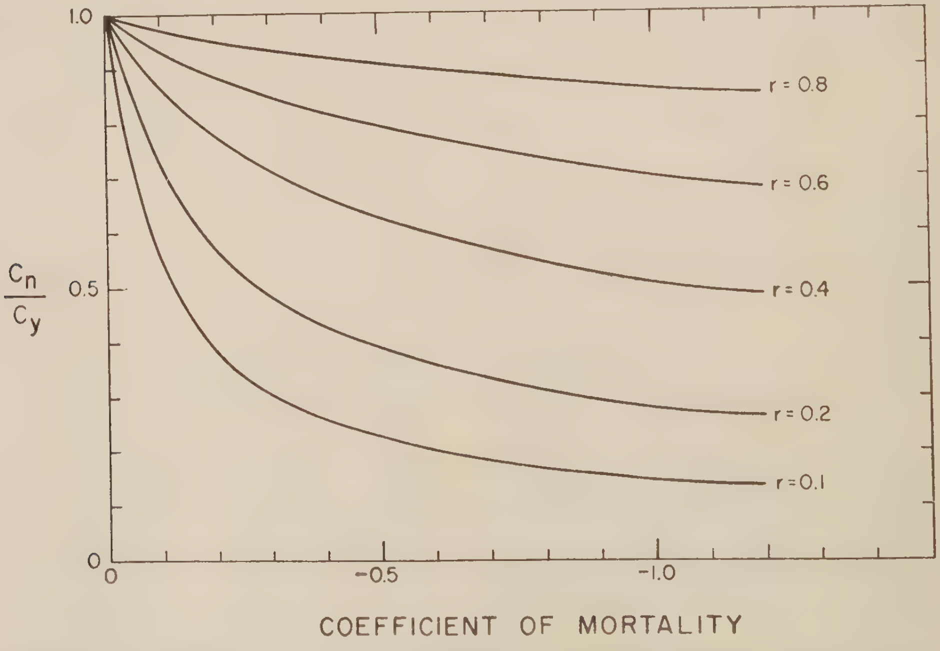

FIGURE 2.—Relative size (C_n/C_y) of a population of coliform bacteria, at the location of the outfall, produced by various circulation rates (r) and mortality coefficients.

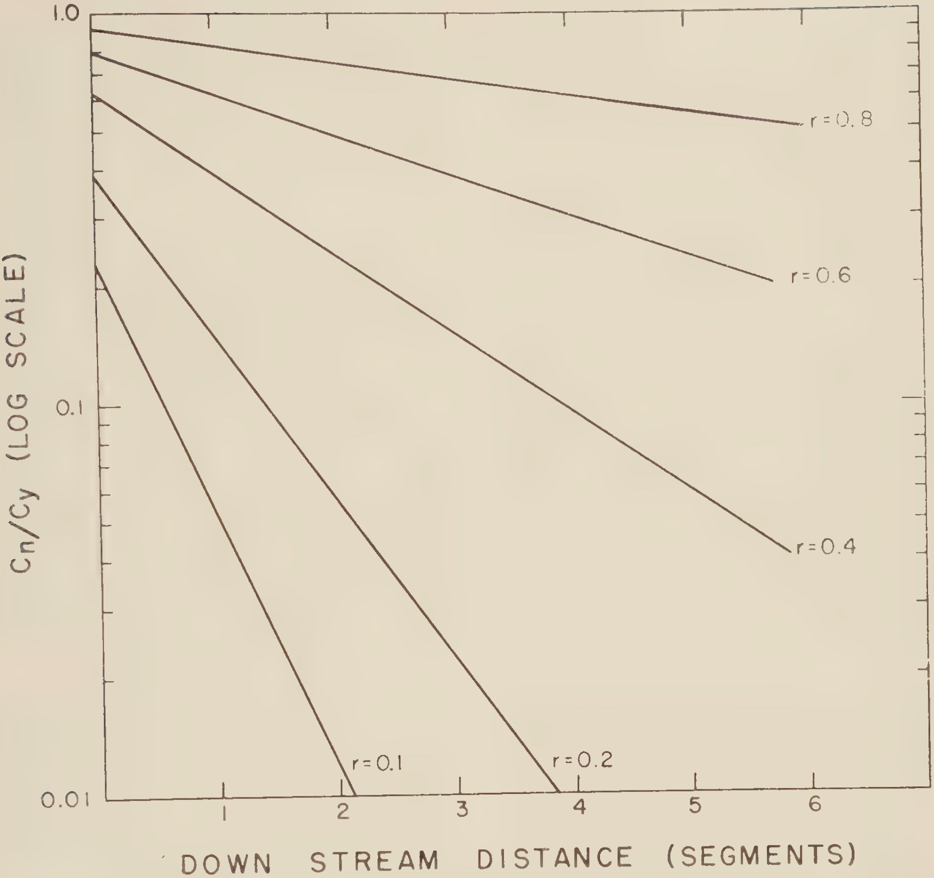

FIGURE 3.—Downstream decrease of a population of coliform bacteria as a result of various rates of circulation (r) for a coefficient of mortality of --0.51 tides^{-1}.

rectly assessed by dividing Eq. 8 by Eq. 3, or Eq. 9 by Eq. 4 so that both reduce to:

$$\frac{C_n}{C_y} = \left(\frac{r}{1-(1-r)e^k}\right)^n \qquad (10)$$

If the coefficient of mortality is zero ($e^k = 1$) Eqs. 8 and 9 reduce to Eqs. 3 and 4, and Eq. 10 gives C_n equal to C_y. It is also apparent that for any given exchange ratio, any increase in the rate of mortality will decrease the population. The larger exchange ratios, however, produce larger populations for a given mortality rate, since the water remains within the segment of the estuary for a shorter time. For example the average age of the river water in a segment with an exchange ratio of 0.8 is only 1.25 tidal cycles, whereas an exchange ratio of 0.1 indicates an average age of 10 tidal cycles (3). The expected populations for a variety of exchange ratios and coefficients of mortality are shown in Figure 2. The location of the outfall has been used ($n = 1$) so that successive effects of downstream circulation are eliminated and the value of the fraction $\left[\frac{r}{1-(1-r)e^k}\right]$, may be found directly from Figure 2.

The effects of the circulation are given in Figure 3 for a variety of exchange ratios (r) and a single coefficient of mortality ($k = -0.51$, $e^k = 0.6$). The more rapid the circulation the larger the relative population size at a distance from the outfall. This again, reflects the brief period of time required for the water to move through the successive segments. The slower circulations, however, permit a considerable population decrease as a result of mortality, and the resultant populations are much smaller than they would be if decreased by circulation alone.

The joint effects of the circulation of the estuary and the mortality of a coliform bacteria population have been computed for three possible outfall locations in Raritan River and Bay. The coefficient of mortality used was the same as previously observed (6). The exchange ratio for this estuary is nearly constant from segment III to segment X, a distance of nearly 10 mi. where it ranges from 0.285 to 0.397 (7), with an average value of 0.339. The upper curve of Figure 4 repeats the solid curve of Figure 1 and gives the population expected from dilution alone (C_y) with no mortality of the bacteria for an outfall at location *A*. The lower curves show the effects of mortality by indicating the fraction of the population (C_n/C_y) expected when the coefficient of mortality is -0.578 tides^{-1}. Multiplication of the value in the upper curve by the fraction at the corresponding location in the lower curve gives the population to be expected. These are relative to a population size of unity for the pollution bacteria mixed in the river water with no mortality. For example the maximum relative populations at the outfall locations would be 0.538 for *A*, 0.278 for

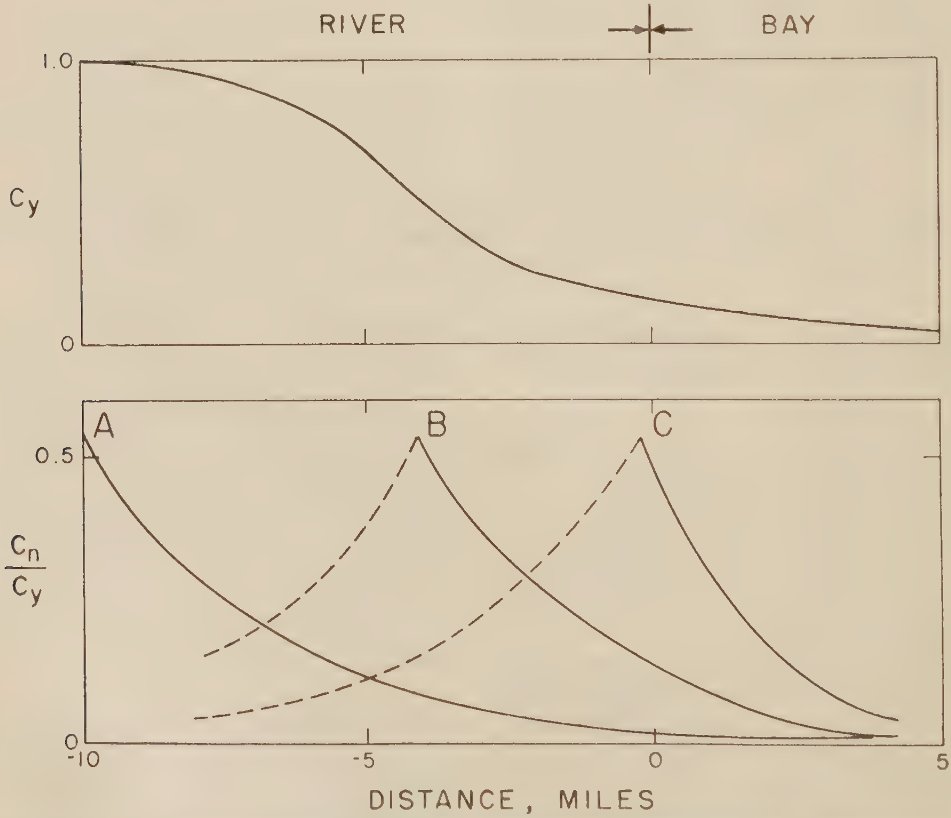

FIGURE 4.—The relative size (C_n/C_y) of a population of coliform bacteria calculated for three possible outfall locations in Raritan River and Bay.

B and 0.092 for *C*. The peak concentration, therefore, is decreased by downstream placement of the outfall, but to a greater extent than can be expected for a conservative pollutant.

Illustration

A discussion of the distribution of bacteria from an outfall at location *B* will clarify the effects of different locations on the distribution of time variable pollutants in general. At outfall location *B*, the population is greater than it would be if the outfall were located either upstream or downstream from *B*. The intersection with the curves for other locations (Figure 4) shows the extent of this greater population size. For an outfall at *B*, a stretch of the river nearly five miles in length would have a higher population of coliform bacteria then could be expected if the outfall were to be located at either *A* or at *C*. Also, the population would be greater than that from outfall *A* at all locations downstream from the intersection with curve A, but would be less than the population of outfall *C* at all locations downstream from the intersection with curve *C*.

Conclusion

For a time variable pollutant, therefore, it is clear that no location for an outfall can be selected which will improve conditions at all other locations in the estuary. The following conclusions concerning the effect of the location of the outfall on the distribution of time variable pollutants may be drawn:

1. The time variable pollutant will be less concentrated everywhere in the estuary than the conservative pollutant.
2. At and near the outfall, the pollutant concentration will be greater than would be obtained from an outfall located either upstream or downstream.
3. Like the conservative pollutant, the upstream concentration can be reduced by a downstream displacement of the outfall.
4. In contrast to the conservative pollutant, the downstream concentration can be reduced by an upstream displacement of the outfall.

Discussion

The methods described in this paper predict the distribution of both conservative and time variable pollutants in an estuary from the results of a salinity survey. The relative merits of different locations for an outfall within an estuary, therefore, can be evaluated. No assumptions concerning the mixing process are involved for the conservative pollutant, though the results are expressed in terms of average conditions, and local variations from the average may be expected. The prediction of the distribution of the time variable pollutant involves the determination of an exchange ratio, which may be based upon assumed mixing conditions.

Outfall Location

Some general rules concerning the location of an outfall in an estuary can be proposed. A displacement of the outfall location downstream decreases the upstream concentration of both conservative and time variable pollutants. If the objective is to improve conditions in the river end of the estuary, the outfall should be placed as far downstream as is economically practicable to obtain the maximum improvement. Downstream from the outfall, the concentration of a conservative pollutant is independent of the location of the outfall. For a time variable pollutant, however, the downstream concentration is increased as the outfall location is moved seaward. If bathing beaches or fishing grounds near the mouth of the estuary are important considerations, an upstream location of the outfall would be indicated. A precise evaluation of the conditions which it is desired to improve is necessary before the selection of an outfall location in an estuary is possible.

Stommel (8) has described a method for predicting the distribution of pollutants in a vertically mixed estuary. This depends upon the calculation of the average mixing conditions from the distribution of fresh water, and the determination of the expected pollutant distribution by relaxation methods. Relationships, similar to those described above, between the distribution of pollutants and the fresh and salt water downstream and upstream from the outfall were independently derived by Stommel.

Exchange Ratio

The prediction of the distribution of a pollutant which decreases with time requires the determination of an exchange ratio for each tidal excursion segment. This ratio is defined as the fraction of the water in a segment which is lost downstream with each tidal cycle. A method for computing an exchange ratio from the intertidal volume and the high tide volume of the various segments has been described by Ketchum (3, 7). This depends upon the assumption that the water is uniformly mixed at high tide within a segment defined in length by the excursion of water on the flooding tide.

This method was adequate for estuaries as widely different as the Raritan River, and the Bay of Fundy (7) (9). With modifications it was satisfactory for a small estuary, Great Pond, and for a fjord, Alberni Inlet. Austin (10) has found reasonable agreement in the Mobile River and the inner end of Mobile Bay, but found errors of about 25 per cent in the outer end of Mobile Bay. Stommel (8), however, found that this method could not be used to describe the salinity distribution in the Severn Estuary.

The calculation of exchange ratios from intertidal and high tide volumes within the estuary should not be used without adequate salinity data to verify that the assumption concerning mixing is a reasonable approximation. However, if adequate salinity data are available the exchange ratios can be determined directly from the accumulation of fresh water, since:

$$r_n = \frac{R}{Q_n} \tag{11}$$

in which Q_n is the total volume of river water accumulated in the tidal excursion segment (2) (9) (11). This calculation assumes steady-state conditions, but makes no assumptions concerning the mixing process. A valid exchange ratio is obtained provided river flow has been constant, so that the steady-state distribution has been attained. It is recommended that enough salinity data be collected in order to confirm the exchange ratio derived from tidal volumes, or to derive the exchange ratio directly from the accumulation of river water, before the results are used to predict the distribution of pollution.

References

1. Rawn, A. M., and Palmer, H. K., "Predetermining the Extent of a Sewage Field in Sea Water." *Trans. Amer. Soc. Civil Eng.*, **94**, 1036 (1930).
2. Ketchum, B. H., "Hydrographic Factors Involved in the Dispersion of Pollutants Introduced into Tidal Waters." *Jour. Boston Soc. Civ. Eng.*, **37**, 296 (1950).
3. Ketchum, B. H., "The Flushing of Tidal Estuaries." THIS JOURNAL, **23**, 2, 198 (Feb., 1951).
4. Ketchum, B. H., Carey, C. L., and Briggs, M., "Preliminary Studies on the Viability and Dispersal of Coliform Bacteria in the Sea." *in: Limnological Aspects of Water Supply and Waste Disposal*, p. 64, Amer. Assoc. Adv. Sci. (1949).
5. Vaccaro, R. F., Briggs, M. P., Carey, C. L., and Ketchum, B. H., "Viability of

Escherichia coli in Sea Water.'' *Amer. Jour. Publ. Health,* **40**, 1257 (1950).

6. Ketchum, B. H., Ayers, J. C., and Vaccaro, R. F., ''Processes Contributing to the Decrease of Coliform Bacteria in a Tidal Estuary.'' *Ecology,* **33**, 247 (1952).
7. Ketchum, B. H., ''The Exchanges of Fresh and Salt Water in Tidal Estuaries.'' *Jour. Marine Res.,* **10**, 18 (1951).
8. Stommel, H., ''Computation of Pollution in a Vertically Mixed Estuary.'' THIS JOURNAL, **25**, 9, 1065 (Sept., 1953).
9. Ketchum, B. H., and Keen, D. J., ''The Exchanges of Fresh and Salt Water in the Bay of Fundy and in Passamaquoddy Bay.'' *Jour. Fish. Res. Bd. Canada,* **10**, 97 (1952).
10. Austin, G. B., ''On the Circulation and Tidal Flushing of Mobile Bay, Alabama, Part I.'' Tech. Report No. 12, A. & M. College of Texas. Unpublished manuscript report (1954).
11. Tully, J. P., ''Oceanography and Prediction of Pulp Mill Pollution in Alberni Inlet.'' *Bull. Fish. Res. Bd. Canada,* **83**, 169 pp. (1949).

Contribution No. 773

Reprinted from THE AUK, Vol. 72, July, 1955

LAND BIRDS OVER THE WESTERN NORTH ATLANTIC[1]

BY SUSAN IRVING SCHOLANDER

LAND birds are regularly reported migrating over such great stretches of water as the Gulf of Mexico, the Mediterranean, and the North Sea. The Golden Plover may cross a thousand miles and more of ocean without sight of land. The Greenland Wheatear travels from Arctic America to the European coast every year, and Snow Buntings are found not infrequently flying far out at sea. Particularly during the fall months, any ship in the North Atlantic, even hundreds of miles offshore, may be visited by land birds of many different species. Most of the published references to such encounters are scattered in short notes on single occurrences or lie buried among extensive data on sea birds. In a few cases they have been given special attention, however, as by Helms (1897), Trumbull (1904, 1905), Jesperson (1930), Nicholson and Nicholson (1931), and Allison, Barras-Smith, Darlington, and Romer (1951).

For a number of years a record of biological observations has been kept on expeditions in the North Atlantic from the Woods Hole Oceanographic Institution, and notes on the birds sighted at sea form the major part of this record. Dr. A. C. Redfield began the series of observations in 1933 and 1934, and used them to determine the distribution of petrels in the Gulf of Maine in relation to the abundance of plankton (1941). The observations which Dr. Redfield started were continued by Mr. Harold Backus and Mr. Dean F. Bumpus, with contributions by Mr. Alfred H. Woodcock and Mr. Frank J. Mather III. In 1951 Dr. Hilary Moore undertook an extensive analysis of the records, and from this data as well as his own presented a detailed picture of the seasonal distribution of oceanic birds in the North Atlantic, which has contributed greatly to knowledge of the migration patterns of petrels, shearwaters, phalaropes, and jaegers. The work of assembling the material on land birds observed during the Oceanographic expeditions has been undertaken at Dr. Redfield's suggestion, to see whether these occurrences at sea could be related to season, migratory routes, or weather conditions. In this analysis birds which habitually light on the water, such as ducks and geese, have not been included in the category of land birds.

---

[1] Contribution Number 773 from the Woods Hole Oceanographic Institution.

Material.—The data were gathered during cruises in the years 1933 and 1934, 1936 through 1941, and 1949, most of them on the research vessel "Atlantis," with a few on the "Caryn." The area covered in this investigation extended from about 44° north latitude south through the West Indies, and from the coast of North America eastward to about 51° west longitude. The locations of all land birds recorded are given in figure 1, and all observations have been plotted on the maps in figures 2 and 3, according to month or season of the year.

Although every month is represented by notes from some section of this area, the extent of sea traversed and the number of observations made in each month vary considerably. Nevertheless for limited sections and periods, the data are sufficient to indicate prevailing seasonal conditions.

In plotting the data on the seasonal maps each time of entry in the biological notes was considered as one observation, regardless of whether land or sea birds or no birds at all were reported. In many cases one entry gives the total list of birds for one day. In other cases fairly regular watches were kept, and for one day there may be three or four entries made at different times. If only one entry was made per day the position of the point on the map is generally the ship's noon position; if there were several entries per day the positions may be somewhat closer to the actual location of observations.

Many of the birds seen were unidentifiable from the ship, but if they were clearly recognized as land birds they have been entered as such on the maps. Birds reported while the ship was in harbor or very close to shore have been omitted. A list of the species seen during these cruises, with their approximate distances from shore, is given in table 1, along with a number of records made by others in the same general area.

SEASONAL DISTRIBUTION

Winter, December–March (figure 2).—Through December and January practically no land birds were seen, and in February and

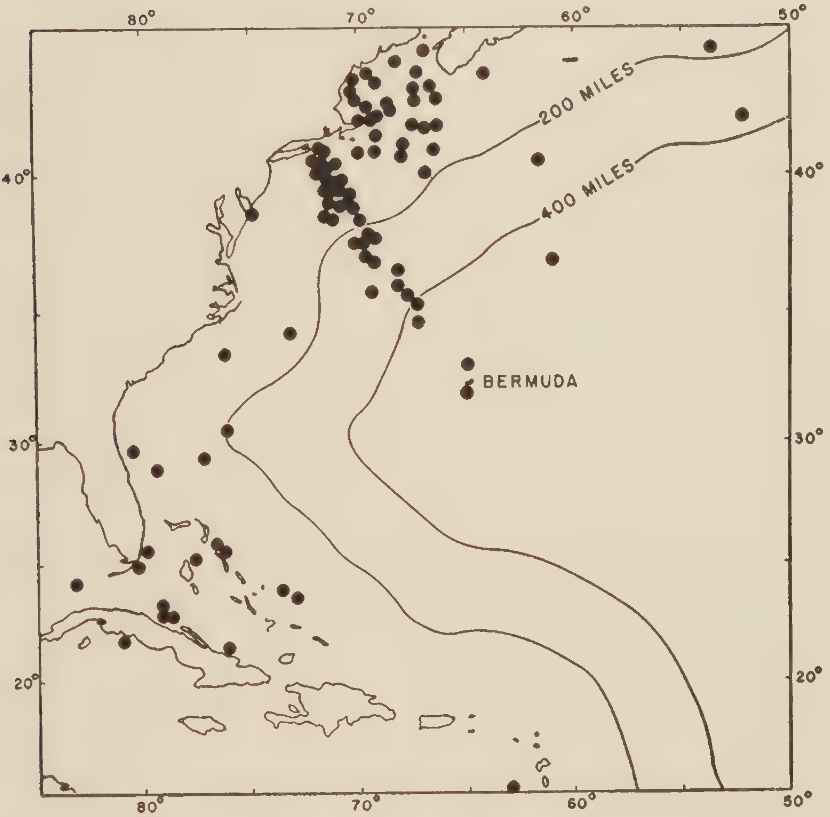

FIGURE 1. Positions of land birds seen from the Atlantis. Lines are drawn approximately 200 miles and 400 miles offshore; from these the distances from land were estimated for Table 1.

March there were only a few reported from southern waters. In fact, during this period entries in the notes frequently mention a complete absence of bird life of any kind for several days, even as long as a week at a time, in waters both to the north and south of Bermuda, to the east of the West Indies, and right among the West Indies themselves.

Spring Migration, April–May (figure 2).—Migratory activity during April and May is clearly reflected on the maps.

Off the coast of Florida and through the West Indies the movement appeared to be strongest around the middle of April, diminishing during the last week. Late in the month (April 27, 1952), however, at Bimini in the Bahamas, Mr. Marshall B. Bishop of the Lerner

TABLE 1

SPECIES OF LAND BIRDS OBSERVED AT SEA, WITH APPROXIMATE DISTANCES FROM SHORE.[1]

	Within 200 miles	*200 to 400 miles*	*Beyond 400 miles*	*Occurrence on Bermuda*[2]
Great Blue Heron (*Ardea herodias*)	5	8	1	F
Black-crowned Night Heron (*Nycticorax nycticorax*)	1	–	–	F
Sharp-shinned Hawk (*Accipiter striatus*)	5	–	–	A
Gray Sea Eagle (*Haliaeetus albicilla*)[3]	1	–	–	–
Osprey (*Pandion haliaëtus*)	6	–	–	A
Duck Hawk (*Falco peregrinus*)	1	–	–	A
Virginia Rail (*Rallus limicola*)	1	–	–	A
Semipalmated Plover (*Charadrius hiaticula*)[4]	2	–	–	F
Wilson's Plover (*Charadrius wilsonia*)	1	–	–	–
Ruddy Turnstone (*Arenaria interpres*)	2	–	–	F
Wilson's Snipe (*Capella gallinago*)	1	–	–	F
Whimbrel (*Numenius phaeopus*)[5]	1	–	–	–
Hudsonian Curlew (*Numenius hudsonicus*)	1	–	–	A
Baird's Sandpiper (*Erolia bairdii*)	sev.	–	–	–
Least Sandpiper (*Erolia minutilla*)	1	–	–	F
Semipalmated Sandpiper (*Ereunetes pusillus*)[6,7]	–	1	1	F
Sanderling (*Crocethia alba*)[4]	3	–	–	F
Domestic Pigeon (*Columba livia*)	–	2	1[8]	F
Barn Owl (*Tyto alba*)	1	–	–	A
Burrowing Owl (*Speotyto cunicularia*)[9]	1	–	–	–
Long-eared Owl (*Asio wilsonianus*)	1	–	–	F
Chimney Swift (*Chaetura pelagica*)	1	–	–	A
Belted Kingfisher (*Megaceryle alcyon*)	1	–	1	F
Flicker (*Colaptes auratus*)	4	–	1	A
Gray Kingbird (*Tyrannus dominicensis*)	2	–	–	A
Phoebe (*Sayornis phoebe*)	1	–	–	A
Yellow-bellied Flycatcher (*Empidonax flaviventris*)	1	–	–	–
Least Flycatcher (*Empidonax minimus*)	–	1	–	–
Olive-sided Flycatcher (*Nuttallornis mesoleucus*)	1	–	–	A
Horned Lark (*Otocoris alpestris*)[10]	sev.	–	–	F
Bank Swallow (*Riparia riparia*)[8]	–	–	1	A
Barn Swallow (*Hirundo rustica*)	6	1[8]	sev.[7, 8, 11]	F
Red-breasted Nuthatch (*Sitta canadensis*)	5	–	–	A
Robin (*Turdus migratorius*)	2	–	1[8]	F
Golden-crowned Kinglet (*Regulus satrapa*)	1	–	–	A
Cedar Waxwing (*Bombycilla cedrorum*)	5	1	–	F
Starling (*Sturnus vulgaris*)	3	2	–	A
Black and White Warbler (*Mniotilta varia*)	1[12]	1	–	F
Nashville Warbler (*Vermivora ruficapilla*)[13]	–	–	1	A
Parula Warbler (*Parula americana*)	2	–	–	A
Yellow Warbler (*Dendroica petechia*)	2	–	–	A
Cape May Warbler (*Dendroica tigrina*)	1	–	–	A
Black-throated Blue Warbler (*Dendroica caerulescens*)	–	1	–	A
Myrtle Warbler (*Dendroica coronata*)[14]	sev.	–	–	F
Yellow-throated Warbler (*Dendroica dominica*)	1	–	–	–
Black-poll Warbler (*Dendroica striata*)	1	1	–	A
Pine Warbler (*Dendroica pinus*)	6	–	–	F
Prairie Warbler (*Dendroica discolor*)[14]	–	1	–	A
Palm Warbler (*Dendroica palmarum*)	5	–	–	F
Oven-bird (*Seiurus aurocapillus*)[13]	–	–	1	A
Water-thrush (*Seiurus noveboracensis*)[15]	1	–	–	F
Yellow-throat (*Geothlypis trichas*)	1	1[11]	–	F
Yellow-breasted Chat (*Icteria virens*)	–	1	1	–
Wilson's Warbler (*Wilsonia pusilla*)	1	–	–	–
American Redstart (*Setophaga ruticilla*)	4	–	1[13]	A
Meadowlark (*Sturnella magna*)	1	1	–	–

TABLE 1—*Continued*

	Within 200 miles	*200 to 400 miles*	*Beyond 400 miles*	*Occurrence on Bermuda*[2]
Red-wing (*Agelaius phoeniceus*)	2	–		–
Baltimore Oriole (*Icterus galbula*)	1	1[17]	–	F
Cowbird (*Molothrus ater*)	2	–	–	A
Dickcissel (*Spiza americana*)	1[4]	1	–	–
Purple Finch (*Carpodacus purpureus*)	1	–	–	–
Pine Siskin (*Spinus pinus*)[10]	sev.	–	–	A
Goldfinch (*Spinus tristis*)	1	–	–	A
Crossbill (*Loxia curvirostra*)[18]	–	1	–	F
Savannah Sparrow (*Passerculus sandwichensis*)	2[19]	4	2	A
Slate-colored Junco (*Junco hyemalis*)	3	1	–	A
White-crowned Sparrow (*Zonotrichia leucophrys*)	–	1	–	–
Golden-crowned Sparrow (*Zonotrichia coronata*)[20]	–	1	–	–
Fox Sparrow (*Passerella iliaca*)[19]	1	–	–	A
Swamp Sparrow (*Melospiza georgiana*)[12]	sev.	–	–	A
Song Sparrow (*Melospiza melodia*)	1	–	–	A
Snow Bunting (*Plectrophenax nivalis*)	1[21]	6	–	F

[1] Species listed according to The A.O.U. Check-List of North American Birds, Fourth Ed., 1931, and supplements.

[2] According to Bradlee, Mowbray, and Eaton, 1931. F = Frequent or regular; A = Accidental or rare.

[3] Crandall 1915.

[4] Rand 1929.

[5] Brewster 1909.

[6] Nicholson and Nicholson 1931.

[7] Murphy 1915.

[8] Jesperson 1930.

[9] Bent 1938.

[10] Helmuth 1920.

[11] Dahl 1892.

[12] Furlong 1933.

[13] Moore 1941.

[14] Bent 1953.

[15] Penard 1926.

[16] Robbins 1901.

[17] Butler 1926.

[18] Brown 1896.

[19] Trumbull 1905.

[20] Riney 1946.

[21] Smith 1901.

Marine Laboratory listed 21 species of migratory birds which arrived, both in flocks and singly, after a period of high winds. The birds stayed a few days and then disappeared. According to residents of Bimini this influx after storms is a regular occurrence at about the same time every year, and Wetmore (1927) also mentions observations of flocks of migratory birds in the Bahamas in April and early May. Our list in May of birds observed in the vicinity of the Bahamas and West Indies is considerably smaller than in April.

To the north there were no land birds in the Gulf of Maine after the first week of May.

Summer, June–July (figure 2).—One Barn Swallow (*Hirundo rustica*) on June 1 constitutes the only land bird record, and it might perhaps better be added to the spring observations. The ocean in midsummer appears to be as barren of land birds as in midwinter. Nicholson and Nicholson (1931) and Allison, Barras-Smith, Darlington, and Romer (1951) have also reported that July was a poor month for non-oceanic birds at sea.

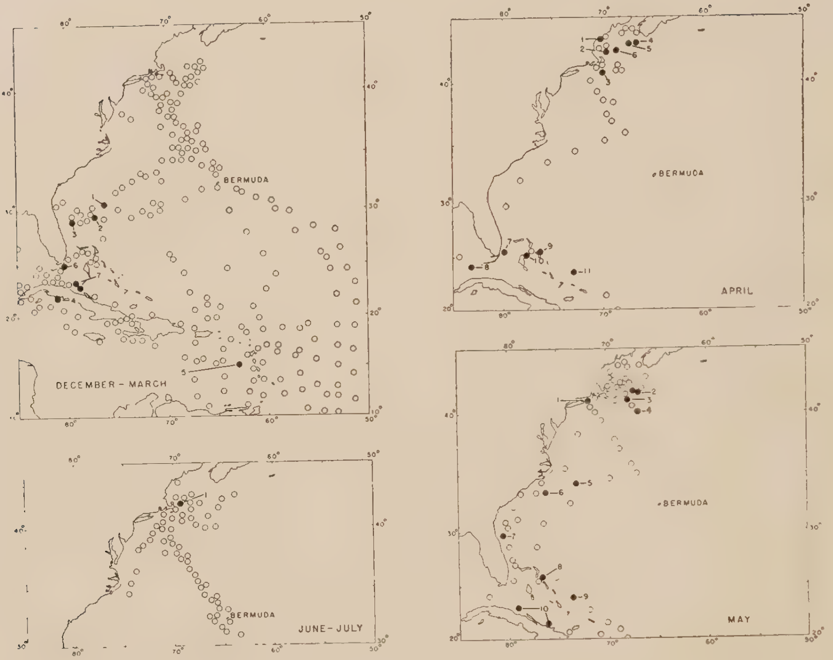

FIGURE 2. Observations during the winter, spring and summer. Dark circles indicate the positions of land birds; open circles show observations where no land birds were seen. Each circle usually represents from 1 to 3 observations, or as many as 10 in congested areas. The total number of observations, as well as the number of different years in which they were taken, is given below for each month. The land birds are listed under numbers corresponding to those on the map. An asterisk indicates that the bird landed on board or was caught.

December, 24 observations, between Cape Cod and Bermuda only, three years.

January, 179 observations, five years. 1. Domestic Pigeons.*

February, 132 observations, six years. 2. Wilson's Snipe ("lost"). 3. Landbird. 4. Yellow Warbler.* 5. Swallow.

March, 145 observations, six years. 6. Virginia Rail*; nuthatch. 7. Gray Kingbirds.* There were also, in March, 14 observations in the Gulf of Mexico not shown on the map. Five herons were recorded.

April, 140 observations, five years. 1. Landbirds. 2. Song Sparrow.* 3. Barn Swallow.* 4. Flicker; Palm Warbler. 5. Hawk; landbird. 6. Sharp-shinned Hawk. 7. Yellow-bellied Flycatcher*; Palm Warbler; Sharp-shinned Hawk*; Red-breasted Nuthatch*; landbirds. 8. Hawks; landbirds. 9. Pine Warbler. 10. Redstarts; Kingfisher; Palm Warbler; Cape May Warbler; finches; warbler. 11. Warbler. There were also 8 observations in the Gulf of Mexico in April, with 2 herons and 2 flocks of unidentified birds reported, all on southerly winds.

May, 132 observations, seven years. 1. Turnstones*; Red-wing; nuthatch; warbler; landbirds; all on one day after a storm in the vicinity of New York the day before. 2. Red-wing; Barn Swallow.* 3. Pine Warbler. 4. Barn Swallows. 5.

Fall Migration, August–November (figure 3).—In the last week of August the picture is different, and the first two weeks of September reflect a high point of activity in the Gulf of Maine. In October particularly, the presence of land birds is striking, especially if we make the reasonable assumption that the records obtained between Cape Cod and Bermuda constitute a representative cross section of large parts of the ocean. In November, land birds were reported during the first three weeks and not thereafter.

According to this reflection at sea of the migratory periods of land birds, the movement is under way in the spring from early April to early May. The much more striking southward movement is already well discernible in the last week of August, it increases markedly in early September, and may continue at this rate through October. In November the drop in numbers is pronounced, and the season is evidently over in this area by the end of November.

Warblers make up a considerable number of the birds reported from southern waters in the spring, and hawks were present there in the middle of April, with two records in April in the Gulf of Maine at a slightly later date. Five of the records in April and May were Barn Swallows, mainly from the waters off Cape Cod, or a little to the south. Swallows were seen again in August, but no later. The Cedar Waxwings (*Bombycilla cedrorum*), hawks, Red-breasted Nuthatches (*Sitta canadensis*), and Flickers (*Colaptes auratus*) seem to travel in August and September, and September is the only month in which sandpipers are mentioned. Warblers and flycatchers were also evident throughout September and October, and ducks (not recorded on the maps) were increasing in October, even considerably offshore. Starlings (*Sturnus vulgaris*), sparrows, Juncos (*Junco hyemalis*), Snow Buntings (*Plectrophenax nivalis*), and Great Blue Herons (*Ardea herodias*) are most conspicuous in October and November.

Weather conditions associated with the occurrence of land birds at sea.—In many cases, weather data were set down in the Atlantis records at the same time as the birds' appearance, and this information could be easily checked and supplemented by the ship's log. In table 2 the observation area has been divided into four regions from north to south, and the numbers of land birds are given for each region under the wind direction with which they were associated.

If the land birds seen at sea have been blown from their normal

---

Barn Swallow. 6. Chimney Swift. 7. Landbird. 8. Redstarts. 9. Black-poll Warbler; hawk. 10. Parula Warblers

June, 142 observations, five years. 1. Barn Swallow.

July, 70 observations, five years.

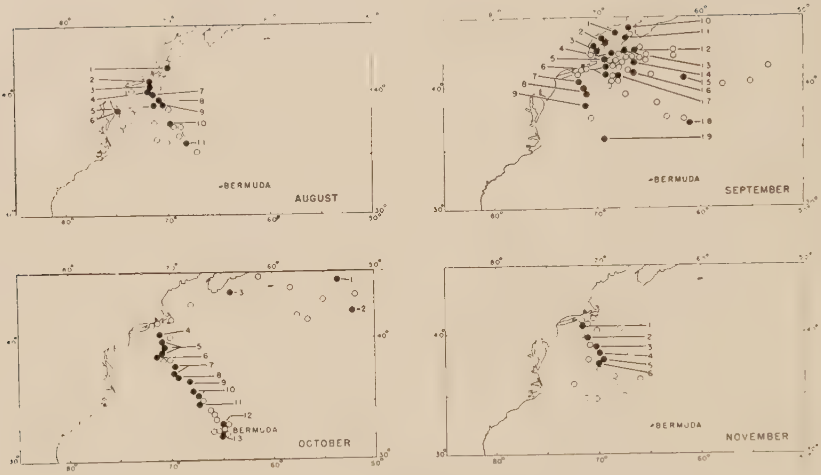

FIGURE 3. Observations during the fall.

August, 135 observations, six years. 1. Landbird. 2. Pine Warbler.* 3. Cedar Waxwing; landbirds. 4. Black-crowned Night Heron*; swallows. 5. Olive-sided Flycatcher*; landbirds. 6. Ospreys. 7. Warbler. 8. Landbird. 9. Cedar Waxwings.* 10. Swallow. 11. Cedar Waxwing.*

September, 120 observations, six years. 1. Least Sandpiper*; Cedar Waxwing*; Palm Warbler.* 2. Sandpipers; Long-eared Owl*; landbird. 3. Hudsonian Curlew; Yellow Warbler*; sandpipers; landbird. 4. Wilson's Warbler.* 5. Sandpipers. 6. Flycatcher; landbirds. 7. Red-breasted Nuthatch*; Flickers*; Ospreys; landbirds. 8. Cedar Waxwing*; Baird's Sandpipers, in a flock, one caught in the rigging; sandpipers. 9. Goldfinch; Pine Warbler*; Phoebe.* 10. Sharp-shinned Hawk. 11. Hawk. 12. Red-breasted Nuthatch. 13. Yellow-throat.* 14. Red-breasted Nuthatch; Palm Warbler*; landbirds. 15. Yellow-breasted Chat. 16. Baltimore Oriole. 17. Red-breasted Nuthatch. 18. Flicker.* 10. Least Flycatcher.*

October, 137 observations, five years. 1. Pine Warbler. 2. Snow Buntings.* 3. Duck Hawk; Flicker; landbirds. 4. Landbirds. 5. Cowbirds; Robin; Starlings; Golden-crowned Kinglet*; Yellow-throated Warbler*; warblers*; landbirds; a storm at sea may have accounted for the occurrence of 10 of these birds. 6. Wilson's Plover.* 7. Landbirds. 8. Great Blue Herons; Meadowlark; Starling; landbirds. 9. Landbird. 10. Starling; Black-poll Warbler*; White-crowned Sparrow*; Dickcissel*; Black and White Warbler*; Black-throated Blue Warbler*; Savannah Sparrows*; Slate-colored Junco*; flycatchers; Great Blue Herons; landbird. 11. Kingfisher; landbird. 12. Yellow-breasted Chat*; Savannah Sparrows. 13. Great Blue Heron.

November, 42 observations, three years. 1. Pine Warbler. 2. Slate-colored Juncos; landbird. 3. Purple Finch*; Meadowlark; Great Blue Heron; landbirds; all seen on one day after a storm recorded at Nantucket the day before. 4. Barn Owl; Robin; Great Blue Herons; landbirds; all these came on one day with wind NW 6. 5 Snow Buntings. 6. Great Blue Heron; landbird.

course, one would expect to find them associated chiefly with winds blowing offshore. This was generally true for the land birds seen from the Atlantis. It was also true that these winds were generally the prevailing winds of the region where the birds were seen, which may cloud the issue somewhat. In the three northern sections listed on table 2, the prevailing winds are the Westerlies, with a northeast component in the fall. In general the nearest land would lie to the west or north. Most of the land birds came on winds from these directions.

TABLE 2

NUMBER OF BIRDS IN RELATION TO DIRECTION OF WIND AT TIME OF BIRDS' APPEARANCE.

	Calm	SW	W	NW	N	NE	E	SE	S
1. *Latitudes from southern Nova Scotia to southern Cape Cod*									
Spring (Apr. and May)	1	1	1	1	4	2	0	0	0
Fall (Aug. thru Oct.)	4	8	9+	11+	1	0	0	2	0
Total (Jan. and Mar. thru Oct.)	5	9	15+	12+	5	3	0	2	0
2. *Latitudes from southern Cape Cod to Bermuda*									
Spring (Apr. and May)	0	2	0	9+	0	0	0	1	0
Fall (Aug. thru Nov.)	4	9	10	48+	17	37+	5	1	5+
Total (Jan. thru Dec.)	4	11	10	57+	17	37+	5	2	5+
3. *Latitudes from Bermuda to West Indies*									
Total (Jan. thru June, Oct. and Dec.)	0	7	0	1	0	0	0	3	1
4. *Latitudes from West Indies to coast of South America*									
Total (Jan. thru May)	1	0	0	1	0	7	19+	5+	0

Among the West Indies in the spring, the Northeast Trades are the prevailing winds, and it will be seen that in the southernmost section on table 2, all the land birds but one appeared on easterly winds. Since land occurred in almost every direction, its position in relation to the wind could not be considered.

A check of coastal weather conditions in the Daily Weather Maps for the two northern sections in table 2 indicated that offshore winds generally prevailed for the areas and times in which land birds were seen at sea. At least 140 out of about 195 birds during the spring and fall came in periods of offshore winds.

If it is assumed that the land birds observed from the Atlantis came almost directly from the nearest shore, the journey over the sea for most of them would have been well within 200 miles (table 1). This is a minimum estimation, and moreover it may not apply at all to the situation in the fall between Cape Cod and Bermuda, where almost as many birds were accompanied by winds from the north or northeast as by the west or northwest winds from the nearest land. If these birds actually came from land to the northeast, they might have been traveling for 400 miles or more, although in table 1 they might still appear in the category of 200 miles from shore. In the month of October only 26 birds appeared to be from the nearest land, whereas 34 apparently came from farther eastward. Of the latter group an unusually large proportion, 15, landed on the ship. In summary, it can be said that out of the total number of birds, some 240, reported from the Atlantis, about 128 were definitely associated with winds directly from the nearest land, and about 54 came in the fall when winds were blowing which might have carried them a considerably greater distance from the north or east.

When the wind was directly from the east, however, it is clear from table 2 that land birds were very rarely seen at sea north of the West Indies, and a number of the days and periods of easterly winds during the winter, even among the West Indies, were marked by a complete absence of both land and sea birds. Out of a total of 36 such days, which occurred in stretches of from two days to over a week, 25 had easterly winds.

Bad weather and the force of the wind, as well as its direction, might be expected to have some effect on the numbers of land birds over the sea, but in the Atlantis records this was not generally striking. Throughout the year most of the birds were recorded on days of fair weather in all areas, and the winds with which they came were in the majority of cases light to gentle, ranging between 1 and 3 on the Beaufort scale, or approximately 2 to 13 miles an hour. Between Cape Cod and Bermuda during the fall months, however, where birds were most frequently seen at some distance from shore, there seems to be some correlation between numbers and the force of the wind (table 3A); and in the month of October, it appears that the presence of a fair proportion of the birds could be attributed to ocean gales or storms in the vicinity (table 3B). This result is hardly surprising in a month which reflects not only the increasing storminess of the season but the height of the migration period as well. That the storms encountered in November were so few in table 3B is undoubtedly due to the comparatively small number of observations taken during the month. Except in the month of October there seems to be no marked relation between storms and numbers of land birds at sea. Out of the whole period only three of the many days which could be called outstanding for land bird occurrences (with more than five birds reported) could possibly be associated with storms either on land or sea. (These days are noted under the maps for May, October, and November, figures 2 and 3.) Williams

(1950) stated that night migration along the Gulf of Mexico ceased when strong winds were blowing, and Allison, Barras-Smith, Darlington, and Romer (1951) reported that a gale in September produced a marked cessation in the movements of birds at sea. In general birds must be able to cope with stormy weather, or avoid it; the fate of those that fail, on the other hand, is nowhere more evident than over the sea.

TABLE 3

A. NUMBER OF BIRDS IN RELATION TO THE FORCE OF THE WIND (BEAUFORT SCALE) BETWEEN CAPE COD AND BERMUDA DURING THE FALL.

Force	*Calm-1*	*2–3*	*4–5*	*6–7*
September	7	10+	5	1
October	3	23+	44+	1
November	2	6	10	7+

B. NUMBER OF BIRDS IN RELATION TO STORMS AT SEA OR ALONG COAST DURING SPRING AND FALL.[1]

Month	*Number of years*	*Total number of birds observed*	*Number of storms in vicinity of observation area*	*Number of birds observed in storm vicinity*
April	3	27+	7	1
May	3	13+	5	6+
August	4	18+	3	6
September	4	39+	8	3
October	5	79+	8	30
November	2	13+	3	3

[1] Storm data from Monthly Weather Review, 1933–1940.

Discussion.—The seasonal pattern of land birds over the North Atlantic is similar to that of the oceanic birds described by Moore (1951), allowing for differences in numbers and range. Periods of greatest activity and in many cases areas of concentration correspond rather closely. There are however at least two outstanding differences. For the oceanic birds, the migratory movement in the spring seems to be generally just as pronounced as in the fall. This is not true of the land birds. In addition it is evident in the numbers and behavior of the birds which Moore discussed that they are following a definite course over the sea. In the case of the land birds reported from the Atlantis there is nothing to suggest that they are flying over a normal route. The majority of records are of individual birds, seldom more than two of a kind during a month. There are only one or two references, in the fall, to migrating flocks. A comparatively large number of the birds landed on the ship, or were caught, and many of the smaller birds, particularly warblers, were either found dead or died shortly after landing, which would point to a rather common state of exhaustion, and probable disorientation.

In the case of Snow Buntings, occurrences over the Atlantic may be more than accidental, however. Three in October constitute the most easterly of the Atlantis land bird records, and they have been found by many others at much greater distances from shore. Helms (1897) mentions them with the Wheatears as the only birds seen regularly in the North Atlantic. A Snow Bunting banded in New York was recaptured a few months later in a flock west of Iceland (Cooke 1945), and Allison, Barras-Smith, Darlington, and Romer (1951) recorded 20 in September at a weather ship station west of the British Isles.

Swallows also appear rather often in lists of land birds at sea. Our records were not very far offshore, but Dahl (1892) and Murphy (1915) reported a number of Barn Swallows east of Bermuda, which were assumed to be on migration to South America. Murphy's record was made 360 miles from land, and Jesperson (1930) found them as much as 600 miles off shore. Both Snow Buntings and Barn Swallows are frequent visitors on Bermuda.

In view of the number of land birds southeast of Cape Cod in the fall, it was of interest to see how many of the species recorded there are known also from Bermuda (table 1), which lies near the eastern limit of most of the Atlantis observations, some 600 miles from the North American coast. According to the checklist of Bradlee, Mowbray, and Eaton (1931) 11 species of land birds are resident in Bermuda, four species are given as present during the winter, and 84 species appear fairly frequently or regularly during the migration seasons. By far the greatest number (138) are only occasional or accidental visitors. These include most (25) of the species seen in the region from the Atlantis. Of the four species recognized as winter residents on Bermuda, the Great Blue Heron, the Belted Kingfisher (*Megaceryle alcyon*), and the Black and White Warbler (*Mniotilta varia*) were seen from the Atlantis, as well as 13 of the species described as not uncommon in Bermuda in the fall. Only the Great Blue Herons and possibly the sandpipers appeared in any numbers which might suggest a regular migratory route. Several of the species seen at sea, in view of their location on the Atlantis maps, could well be expected in Bermuda, although they do not appear on the checklist of 1931. In comparison with the total list of species from Bermuda, the Atlantis list is meager. For a bird traveling over the ocean the chance of making a landfall on an island group some 200 square miles in area is considerably greater than the possibility of finding a ship at sea, and the list of Bermuda species is a compilation of the observations of nearly 100 years.

In October, fall migration in Bermuda is at its height; the spring migration is less noticeable, and the number of birds there is lowest in June and July (Bradlee, Mowbray, and Eaton 1931). The same general pattern appears also in the Atlantis records. There are many references to the effect of storms on the migratory bird population of Bermuda, and the presence of most of the species recorded on the island has been attributed to unfavorable winds which blow the birds off their regular courses (Reid 1884, Bradlee, Mowbray, and Eaton 1931). On Bermuda, as on the Atlantis, the appearance of land birds would seem to depend largely on wind conditions along the American coast.

There are many conflicting reports as to whether migratory flight is associated with certain wind directions, or proceeds regardless. These are mainly based on local observations of the arrival of migrant birds. In the two northern sections included on table 2, no clear seasonal difference in wind directions can be seen which might be associated with a seasonal difference in migration direction, but these birds at sea cannot be taken as representing the normal pattern. If a broader point of view is taken of the course of migration in relation to the pattern of prevailing winds, it appears that correlations may exist, as has been suggested by McMillan (1940), Landsberg (1948), and Lowery (1951). An easterly wind is a determining factor in the appearance of southbound migrants in the British Isles (Williamson 1952), and Bradlee, Mowbray, and Eaton (1931) found that the prevailing winds, from the south and southwest, were related to the preponderance of southern North American species among the "accidentals" on Bermuda.

All but 15 of the 248 land birds reported from the Atlantis came while the prevailing winds were blowing in the region where they were seen. In the spring the prevailing westerly or northerly winds along the Atlantic coast would be of little help to a northbound migrant, and the comparative scarcity of records at sea in the spring may indicate that at this season the main stream of migration does not pass along the coast, but farther inland. In the fall however, the prevailing north or west winds along the coast would correspond somewhat better to the direction of migration, and the numbers of land birds over the sea seem to indicate that the coastal route is much more popular at this season than it is in the spring. It is also evident that, although a fall migrant might derive some advantage from tail winds which would help it eastward to the coast and southward, it would have to pay the price of running special risks, such as overshooting the land in darkness, or blowing out to sea with the strong winds characteristic of the season. Whether or not the prevailing wind may be a factor in determining the course of migration along the coast in the fall, the vulnerability of such a route at that season is clearly illustrated in the Atlantis records of land birds at sea.

Summary.—A record of the birds observed in the western North Atlantic was kept for eight years by members of expeditions from the Woods Hole Oceanographic Institution. The data on land birds have been assembled from these notes and entered on a series of seasonal maps. Fifty-four species of land birds were identified from the ship. Most of them were within 200 miles from shore, but some were more than 400 miles from the nearest land. Only during the migration seasons were land birds found on the sea in any numbers, some in the spring and many more in the fall. Their appearance could generally be associated with winds blowing from the direction of land, and since a relatively large number lighted on the ship, exhausted, there seems to be little doubt that these birds at sea were blown off course and victims of the same conditions which determine the long list of "accidentals" on Bermuda. In the fall their numbers seemed also to have some correlation with the force of the wind, as well as with storms in October. From a comparison of spring and fall records it seems that the main course of migration may pass farther inland in the spring and nearer to the coast in the fall, where it would be particularly vulnerable to the stress of weather conditions.

LITERATURE CITED

ALLISON, F. R., M. A. BARRAS-SMITH, A. DARLINGTON, and M. L. R. ROMER, 1951. Migrants observed from ocean weather ships, July–October, 1950. Brit. Birds, **44**: 219–222.

AMERICAN ORNITHOLOGISTS' UNION. 1931. Check-List of North American birds, 4th edition. (Amer. Ornith. Union, Lancaster, Pa.), xx + 526 pp.

BENT, A. C. 1938. Life histories of North American birds of prey (Part 2). Orders Falconiformes and Strigiformes. Bull. U. S. Natl. Mus. 170: viii + 482 pp.

BENT, A. C. 1953. Life histories of North American wood warblers. Bull. U. S. Natl. Mus. 203: xii + 734 pp.

BRADLEE, T. S., L. L. MOWBRAY and W. F. EATON. 1931. A list of birds recorded from the Bermudas. Proc. Boston Soc. Nat. Hist., **39**: 279–382.

BREWSTER, W. 1909. Occurrence of the whimbrel (*Numenius phaeopus*) off the coast of Nova Scotia. Auk, **26**: 190–191.

BROWN, J. C. 1896. The American crossbill at sea. Auk, **13**: 176.

BUTLER, A. W. 1926. Land birds at sea. Auk, **43**: 103.

COOKE, M. T. 1945. Transoceanic recoveries of banded birds. Bird Banding, **16**: 123–129.

CRANDALL, L. S. 1915. Gray sea eagle off Nantucket. Auk, **32**: 368.

DAHL, F. 1892. Die auf der Plankton-Expedition beobachteten Säugethiere, Vögel und Schildkröten des Meeres. Ergebn. Plankton-Exp. Humboldt-Stiftung, vol. 1, Abth. A, 70–79.

FURLONG, W. R. 1933. Landbirds in a gale at sea. Bird Lore, **35:** 263–265.

HELMS, O. 1897. Ornithologiske Iagttagelser fra det nordlige Atlanterhav. Vidensk. Medd. Naturhist. Foren. Kjøbenhavn, ser. 5, **9:** 216–236.

HELMUTH, W. T. 1920. Extracts from notes made while in naval service. Auk, **37:** 255–261.

JESPERSON, P. 1930. Ornithological observations in the North Atlantic Ocean. Danish "Dana"-Exp. 1920–22, Oceanogr. Rep. no. 7.

LANDSBERG, H. 1948. Bird migration and pressure patterns. Science, **108:** 708–709.

LOWERY, G. H., JR. 1951. A quantitative study of the nocturnal migration of birds. Univ. Kansas Publ., Mus. Nat. Hist., **3:** 361–472.

MCMILLAN, N. T. 1940. Birds and the wind. Ann. Rep. Smithsonian Inst., for 1939, 355–363.

MONTHLY WEATHER REVIEW. 1933–1940. Weather on the Atlantic and Pacific oceans. Climatological tables. Vols. 61–68.

MOORE, H. B. 1941. Notes on Bermuda birds. Proc. Linnaean Soc. New York, **52–53:** 70–75.

MOORE, H. B. 1951. The seasonal distribution of oceanic birds in the western North Atlantic. Bull. Mar. Sci. Gulf Caribbean, **1:** 1–14.

MURPHY, R. C. 1915. A note on the migration at sea of shore birds and swallows. Auk, **32:** 236.

NICHOLSON, E. M., and B. D. NICHOLSON. 1931. An ornithological transect of the North Atlantic. Brit. Birds, **24:** 266–274.

PENARD, T. E. 1926. Warblers at sea. Auk, **43:** 376–377.

RAND, A. L. 1929. Birds on board ship between Nova Scotia and New York City. Auk, **46:** 246–247.

REDFIELD, A. C. 1941. The effect of the circulation of water on the distribution of the calanoid community in the Gulf of Maine. Biol. Bull., **80:** 86–110.

REID, S. G. 1884. The birds of Bermuda. Bull. U. S. Natl. Mus. 25, 163–279.

RINEY, T. A. 1946. Birds aboard ship. Auk, **63:** 250.

ROBBINS, R. C. 1901. Maryland yellow-throat at sea. Auk, **18:** 110–111.

SMITH, H. M. 1901. Snow bunting at sea. Auk, **18:** 195.

TRUMBULL, J. 1904. Notes on land-birds observed on the North Atlantic and Gulf of St. Lawrence. Zoologist, ser. 4, **8:** 134–141.

TRUMBULL, J. 1905. Notes on land-birds observed on the North Atlantic and Gulf of St. Lawrence, 1904. Zoologist, ser. 4, **9:** 293–300.

U. S. WEATHER BUREAU. 1933–1949. Daily Synoptic Series, Historical Weather Maps, Northern Hemisphere, Sea Level.

WETMORE, A. 1927. The migrations of birds. Cambridge.

WILLIAMS, G. G. 1950. Weather and spring migration. Auk, **67:** 52–65.

WILLIAMSON, K. 1952. Migrational drift in Britain in autumn 1951. Scottish Nat., **64:** 1–18.

Woods Hole Oceanographic Institution, Woods Hole, Massachusetts, June 21, 1954.

Contribution No. 777

Reprinted from THE NAUTILUS, Vol. 69, No. 1, July, 1955
Printed in U. S. A.

HOW CLAM DRILLS CAPTURE RAZOR CLAMS

By HARRY J. TURNER, JR. *

During the past few years, the author has observed a number of instances of predation by the carnivorous marine snail, *Polinices duplicatus,* on the razor clam, *Ensis directus.* In every case, the snail and the razor clam were found on the surface of the substratum with the clam enveloped in a coating of slime and the snail attached along the mid-ventral region with its proboscis inserted between the valves. No drilled razor clam shells have ever been found.

---

* Contribution No. 777 from the Woods Hole Oceanographic Institution.

It is difficult to imagine how *P. duplicatus* can capture a razor clam and hold it long enough to render it inactive, because razor clams normally retreat to considerable depths when disturbed. Burrowing is accomplished by extending the foot downward, expanding the distal portion as an anchor, and pulling the body down by strong contractions of the proximal portion of the foot. The process is then repeated so rapidly that a depth of ten inches can be reached in a matter of seconds and the force of the contractions is so great that the foot and part of the viscera may be torn out if the shells of a burrowing razor clam are held to prevent them from following the foot.

Recently, the author had the good fortune to make some observations on an attack by *P. duplicatus* on a razor clam which gave some indications as to how the snail may immobilize its prey. A 97 mm razor clam was found on the surface of the sand with a 15 mm snail attached to the posterior end. The clam was extending and retracting its foot in writhing motions as if making an attempt to escape. The clam finally managed to work its foot down into the sand, pull itself into an erect position, and begin to burrow. As soon as the clam had erected itself, the snail quickly crawled down the body and burrowed into the sand along side of its prey. The razor clam continued to dig in until ⅔ of its length was buried and then stopped.

After a two-minute period the razor clam suddenly forced its way out of the sand with violent thrusts of its foot. The snail was attached to the lower third of the body but the final thrust detached it. The razor clam immediately extended its foot and began to burrow, touching the snail as it did so. The snail then dug in along side of the clam which again stopped as soon as ⅔ of its length was buried. The clam made one or two feeble attempts at digging in deeper. The posterior end was just level with the surface when it suddenly forced its way out again with the snail attached to the lower portion. The last motions detached the snail and thrust it a few centimeters away from the clam. The clam and the snail then dug in independently although the activity of the clam was much slower than during the early part of the encounter.

No further activity was observed for the next ten minutes. The razor clam and the snail were then dug up and found to be separated from each other by five centimeters. The snail was expanded with its head oriented away from the clam. When placed on the sand, the clam showed no activity during the next 30 minutes after which observations were discontinued. All but the lower (anterior) end of the body of the clam was covered by an envelope of slime secreted by the foot of the snail.

It seems clear that *P. duplicatus* captures *Ensis directus* by approaching it below the surface of the substratum and by irritating the lower portion so that it retreats upward. The snail then coats the razor clam with an envelope of slime which appears to have anesthetic properties. Successful capture probably depends on the ability of the snail to maintain contact with its prey until anesthesia takes place.

Contribution No. 778

Reprinted from BIOLOGICAL BULLETIN, Vol. 109, No. 1, 56-63, August, 1955
Printed in U. S. A.

FREEZING IN INTERTIDAL ANIMALS

J. W. KANWISHER

Woods Hole Oceanographic Institution, Woods Hole, Massachusetts

FREEZING IN INTERTIDAL ANIMALS[1]

J. W. KANWISHER

Woods Hole Oceanographic Institution, Woods Hole, Massachusetts

Low temperature is frequently the chief environmental stress which eliminates a species in a given location. Marine life is generally exposed to a minimum of − 1.7° C., the freezing point of sea water. In the intertidal zone a much lower extreme must be met. On a high latitude shore in winter one finds an abundance of invertebrates exposed twice daily to a period of − 20° C. or lower. At these temperatures ice formation in the animals might be expected. This has been found to be the case and is the subject of this paper.

The observations on freezing in surviving macroscopic animals are scattered and frequently indefinite. The literature is reviewed by Luyet and Gehenio (1940) and more recently by Scholander *et al.* (1953). In spite of the large number of references only a few experiments are found in which quantitative ice measurements were made on surviving animals. Sacharov (1930) showed that as much as a third of the body water could be changed to ice in some insect larvae. More remarkable is the better than 90% frozen body water that Scholander measured in chironomid larvae. It seems likely that this large fraction of ice is present in the qualitative experiments reviewed by Luyet and Gehenio. These include the survival at liquid air temperatures of nematodes, rotifers, and tardigrades. Such forms would be expected to have a high water content.

In the Woods Hole region in winter the shore supports large numbers of mussels, snails, oysters, and barnacles. Many of these are high up on the shore where they are exposed to the air for six hours or more at low tide. They are frequently in completely exposed locations, where it seems they could not escape any adverse effects of the cold. The sea spray freezes on them and they may be imbedded in ice for days or even weeks at a time.

The rate of cooling of an animal can be estimated from the known values of heat conductivity in tissue and shell. This was done assuming that the animal is subjected to a sudden drop of 20°. Such is the case when it emerges from the water on the receding tide on a cold day. With even the larger mussels the temperature at the center will be within a degree of the air temperature after an hour's exposure.

To check these estimates the temperature of the interior of several molluscs was measured without moving the animals. For this purpose a small hole was drilled through the shell with the animal still in its natural location. A thermistor probe one mm. in diameter was inserted through this hole and could easily be pushed deep into the tissues.

Several such measurements were made on a day when the air temperature was − 15° C. The animals had been exposed for at least two hours by the receding

---

[1] Contribution No. 778 from the Woods Hole Oceanographic Institution.

tide. Specimens of *Crassostrea virginicus, Mytilus edulis,* and *Modiolus modiolus* showed without exception interior temperatures within a few tenths of a degree of the air temperature. There seems no reason to doubt that the smaller snails and barnacles are in the same condition.

Ice could also be felt with the thermistor probe. These animals were alive and appeared normal when brought into the laboratory. From this it appeared reasonable that internal ice formation can take place without being fatal to the animal. It was next undertaken to determine the amount of ice formed at various temperatures.

METHOD

Water, on crystallizing to ice, gives off heat and also expands. These two properties have been separately employed in determining the amount of ice in biological material. The dilatometer as used by Gortner (1937) and others measures the expansion directly. The flotation method of Scholander *et al.* (1953) determines the specific gravity change which results from this expansion. Both of these techniques require that the animal be free of gas bubbles. This seemed impossible to determine in an animal living in a shell, so it was necessary to use a calorimetric method.

When a frozen animal is introduced into the calorimeter a certain number of calories of heat are absorbed to raise its temperature to some value above 0°. Part of this represents the heat of fusion of any ice which may have been present in the animal. The rest is the result of the heat capacity of the animal and its shell. The specific heats of these components are uncertain so it is impossible to calculate the latter value. However, in this work it is measured directly by finding the calories necessary to warm the animal through a temperature range in which there is no ice formation.

An ordinary wide-mouth Thermos bottle proved to be an efficient calorimeter vessel. A mercury thermometer through the stopper was read to .01° with a lens. By varying the amount of water in the calorimeter different sized animals could be studied efficiently. The freezer compartment of a home refrigerator was used to cool the animals. By adding additional insulation the temperature variation during the cycling of the refrigerator thermostat was less than 0.25° C. To minimize heat loss the animal was transferred to the calorimeter at the door of the refrigerator with cold tongs.

The calorimeter was calibrated by dropping weighed amounts of ice into it. Small cups were pressed from aluminum foil. These were filled with fresh water and frozen to a known temperature. The amount of heat absorbed in warming one from a temperature T_1 below 0° C. to a temperature T_2 above 0 is equal to:

$$C = M_w(T_1 \times .49 + T_2) + M_w \times 79.6 + M_{al} \times .21(T_1 + T_2)$$

where: C = gram calories
M_w = mass of water
M_{al} = mass of aluminum cup
.49 = average specific heat of ice
.21 = specific heat of aluminum.

The heat capacity of the calorimeter is then computed from

$$\text{heat capacity} = \frac{C}{T}\,\text{calories/degree}$$

where T is the temperature drop in the calorimeter vessel resulting from the introduction of the ice.

If the heat capacity of a specimen were constant with temperature a number of calories equal to $(T_2 + T_1)$ times its heat capacity would be required to warm it. All calories in excess of this could then be attributed to the change of state from ice to water. This is not strictly true since the specific heat of ice is half that of water. As more ice is formed the heat capacity of the animal is correspondingly lowered. This results in the correction shown in Figure 1. The rigorous equation of Ditman *et al.* (1942) is difficult to apply and in actual practice some of the terms are very small. The graphical method used here is believed to have an accuracy commensurate with the experimental technique.

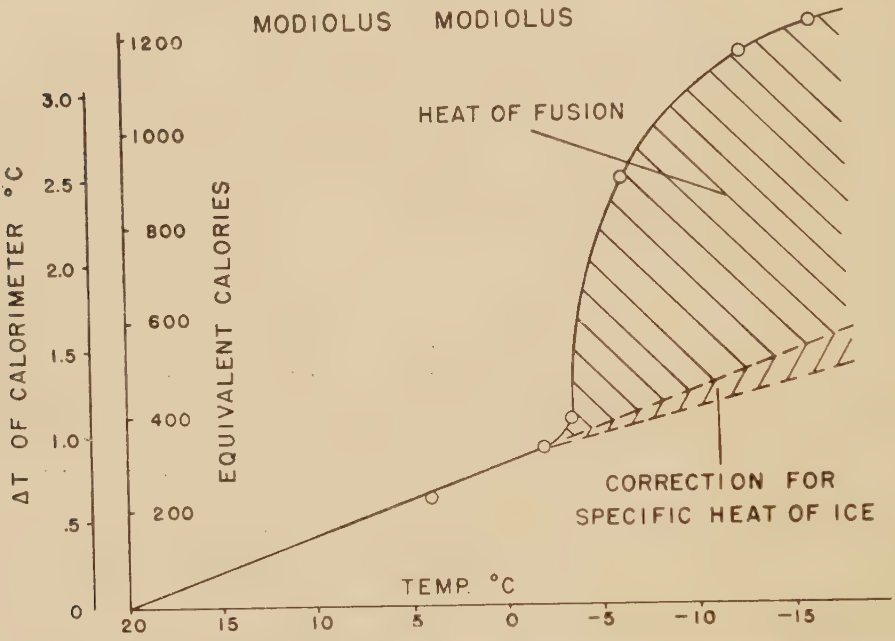

FIGURE 1. Graph showing ice formation in the mussel Modiolus modiolus. The shaded portion represents the calories used in the melting of ice. All points are from a single individual. The heat capacity of the animal changes as more ice is formed, resulting in the correction shown.

Ice determinations were made on animals frozen normally on the shore. They were placed directly in the calorimeter with a heavily gloved hand. Values obtained were essentially the same as for the animals frozen in the laboratory.

The bivalves were wedged open and all excess sea water forcibly shaken from them. They closed normally when the wedge was removed. They were then wrapped with a layer of self-vulcanizing rubber tape which provided a water-tight cover with a minimum of insulation. This cover allowed the animal to be removed from the calorimeter and refrozen at a different temperature without varying the amount of water in the shell.

In order to work with a single individual of the smaller species, such as Littorina, a method of micro calorimetry was worked out. The calorimeter vessel consisted of a round bulb on the end of a long thin-walled glass tube. Loose cotton insulation was packed around this. Such an arrangement was found to have a desirably small temperature drift. In a small calorimeter vessel the ratio of surface to volume becomes unfavorably large. It can be shown that most of the heat leakage is by way of conduction through the wall forming the opening to the chamber.

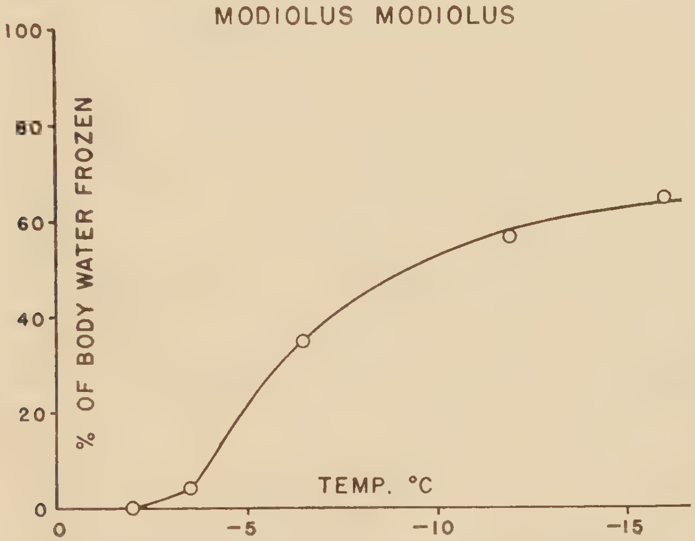

FIGURE 2. Graph showing the percentage of water as ice. The calories of the shaded portion of Figure 1 were converted to grams of ice and expressed as the percentage of the total water in the animal.

To reduce this the thinnest glass tube possible was used. The methods employed on larger systems, such as silvering and operating in a vacuum, do not appreciably improve a small calorimeter. The volume of the bulb varied from 10 to 25 cc. depending on the size of the specimen. The temperature was measured with a thermistor suspended in the water. The same method of calibrating with a weighted amount of ice was used.

RESULTS

Figure 1 is typical of the results obtained. It is a graph of the amount of heat necessary to warm the animal up to 20° C. after it has been equilibrated for several hours at some lower temperature. Since the specific heats of tissue, shell, etc. are not appreciably altered by temperature one might expect a linear relationship. The amount of heat should depend only on the temperature range if the heat capacity of the system is unaltered. However, below 0° a larger number of calories than expected is absorbed. It is this additional heat that is required to melt the ice in the animal. Its amount can be found from the curve at different temperatures and converted to grams of ice. Since the total body water is found at the end of the run it is known what fraction of this is frozen at the various temperatures. Figure 2 is the result of such a calculation from the data in Figure 1. All points on a curve such as the one in Figure 1 are measured on a single animal. The data were not considered if the animal was not alive and of normal appearance at the end of the run.

TABLE I

Percentage of water frozen at —15° C.

Species	% frozen at −15°
Mytilus edulis	62
Modiolus modiolus	65
Littorina littorea	59
Crassostrea virginicus	54
Littorina rudis	67

Table I gives the fractions of body water as ice at − 15° C. in the different species examined. Individual measurements were made on Modiolus and *L. littorea* at − 22° C., the lower limit of the refrigeration equipment. The fractions of body water frozen at this temperature were 71% and 76%, respectively. The animals survived several days exposure to this temperature. *Littorina rudis* was studied at Hebron in Labrador while on an expedition sponsored by the Arctic Institute of North America.

DISCUSSION

Bachmetjew (1899), Salt (1950), and others have claimed super cooling of animals as great as − 15 to − 20° C. However, they expressed the strong belief that freezing was fatal and seemed to reason inversely that when the animal was dead it was therefore frozen. Ditman *et al.*'s (1942) calorimetric work represents one of the few quantitative ice studies. It was necessary for them to use a number of insects simultaneously in the calorimeter. They reasoned that the appearance of more and more ice at lower temperatures was due to variability in the super cooling of the individuals. Their curves indicate 70% frozen body water for codling moth larvae at − 18°. This seems at variance with their conclusions of super cooling. This is not supplemented with measured lethal low temperatures although in a later paper Ditman shows complete survival of this species at this temperature.

The values in Table I show large amounts of ice at − 15° in all the forms that could stand freezing. The shape of the ice-temperature curve for the other species was the same as that in Figure 2. Some of the forms could stand a period at − 5° without ice formation. In no case, though, was this observed at − 7° or lower. Values of ice in the region of super cooling were obtained by cooling the animal to a lower temperature to start ice formation and then warming the animal. Super cooling of shore animals in nature only appears to occur down to −7° as a maximum.

As much as 75% of the water in the animals can be tied up as ice. It is interesting to speculate on the severity of the physiological stress represented by this sudden dehydration.

With the living processes in the protoplasm deprived of this water one might expect a slowing down of the metabolic rate. Lichens have been shown to respire at a rate related to their moisture content (Smyth, 1934; Neubauer, 1938). Scholander *et al.* (1953) have shown a precipitous drop in oxygen consumption concurrent with ice formation in a chironomid larva. This resulted in an apparent Q_{10} as high as 50 in this low temperature range.

In an animal that is 75% frozen the remaining brine concentration is 4 times the normal value. Actually some of the salts will probably have begun to precipitate out at this temperature and concentration. One might suspect many dire consequences at such a high salinity. Lovelock (1953) has published results which indicate that the high electrolyte concentration is the destructive factor in the freezing of red blood cells. The dehydration and high salinity appear to be factors the intertidal species can tolerate, at least at these low temperatures.

Ice is thought not to occur inside cells without damage (Chambers and Hale, 1932; Asahina *et al.*, 1954). It seems reasonable that such a finely organized structure as protoplasm could not stand the physical disruptions of intracellular ice. Apparently the cells are able to allow for a rapid exit of water and to stand the distortion of intercellular ice crystals. Meryman (1953) has shown this situation in slowly frozen rabbit liver. In the thawed tissue the water has migrated back into the cells and the appearance is once again normal. Siminovitch and Briggs (1952) have related frost hardiness in plants with an increased ability of the water to diffuse in and out of the cells. Asahina and collaborators have observed both extra- and intracellular freezing in insects. The latter was always fatal to the cells involved. Proof of such a situation in the frozen shore life can only come from histological examination.

The ice determinations here are reproducible within a range of ± 5%. Weighed amounts of ice could be measured with a 2% error. However, the large amounts of shell and wrapping hinder thermal equilibrium and require many calories for their warming. This forms a background above which ice determinations in such animals must be made.

In Figure 3 the freezing curve for a mussel is reproduced with one for sea water. This latter was obtained by treating a capsule of sea water in the same manner as the animals, *i.e.*, it was cooled to different temperatures and warmed in the calorimeter. No freezing curve for sea water could be found in the literature. The mussel contains significantly less ice than sea water at all temperatures. Part of this may be due to the lack of thermal equilibrium in the animal, particularly on the steep part of the curve. However, the many theories of bound water lend support to the idea that the disparity of these curves is real. To some extent the body fluids can be considered salt solutions and to this extent such a freezing curve would be expected. Any departure may well represent the participation of water in living processes other than as that of a simple solvent. Such a molecule as water with its high dipole moment can be held in low energy fashions unlike conventional bonding. This would compete with freezing which is itself a low energy per molecule process. When the physics of water in living systems is more thoroughly understood a closer approximation to the actual freezing curve can be theorized.

Attempts were made to freeze a large variety of molluscs, echinoderms, annelids, and arthropods which occur only below tide level. No animal was found to stand low temperatures and large internal ice formation that is not faced with these conditions in nature. The hardiness towards ice formation may be the principal reason allowing intertidal species to successfully invade the shore. Resistance to freezing runs parallel with the ability to withstand dehydration (Scarth, 1944; Siminovitch and Briggs, 1952; etc.). Both of these conditions are found in a situation of tidal exposure. The shore snails can be kept out of water for a period of weeks as can the mussels. However, all the forms frozen so far are encased in a shell and it is not certain how much natural dehydration they undergo independent of freezing.

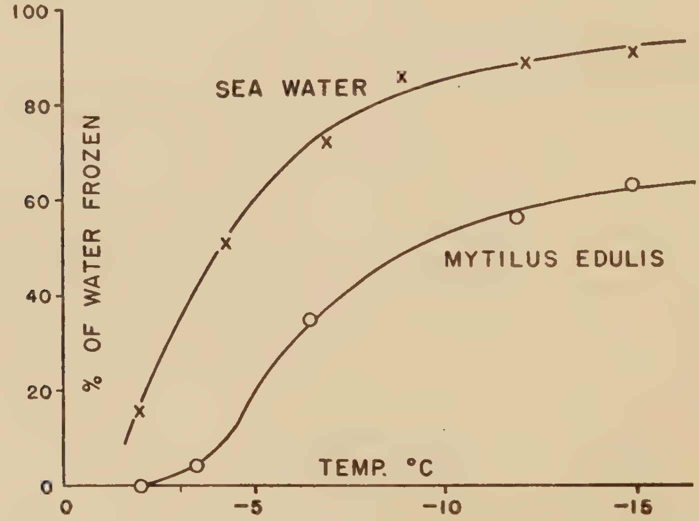

FIGURE 3. Graph of ice determined in the same fashion for a vial of sea water and a mussel. The difference is believed to represent unfreezable or bound water.

Finally, some observations were made in the Arctic that are interesting. In this region of permafrost the only protection from freezing afforded poikilotherms in the winter is in the sea. Hebron Fiord in Labrador has a year round bottom temperature of − 1.7° C. In spite of this the extensive bottom invertebrate fauna could not stand freezing. Here are animals that live and breed right up against the freezing barrier, and yet the particular adaptations of the shore life are absent. The only two plentiful intertidal forms were Mytilus and Littorina. Both of these displayed their usual resistance to freezing. Beds of Mytilus were noted which spend 6 to 8 months frozen solid in the ground ice at temperatures of − 20° C. and below! In the spring the Eskimos chip them out for food.

I am greatly indebted to Dr. Per Scholander for his continued interest and help-

ful advice during this work. My wife has also been of great assistance, particularly under the trying conditions of cold winter days on the shore.

SUMMARY

1. The temperature environment of shore life in the Woods Hole vicinity has been found to range as low as − 20° C. in the winter. *In situ* measurements have shown that no protection in the way of a micro climate is afforded most of this life.

2. A variety of intertidal forms has been frozen in nature and in the laboratory and their ice content measured. In live animals as much as 75% of the body water has been shown to be in the form of ice at temperatures regularly met in nature.

3. Some physiological consequences of this ice formation are considered.

LITERATURE CITED

ASAHINA, E., K. AOKI AND J. SHINOZAKI, 1954. The freezing process of frost-hardy caterpillars. *Bul. Entomological Research,* **45**: 329–339.

BACHMETJEW, P., 1899. Über die Temperatur der Insecten nach Beobachtungen in Bulgarien. *Zeitschr. wissen. Zool.,* **66**: 521–604.

CHAMBERS, R., AND H. P. HALE, 1932. The formation of ice in protoplasm. *Proc. Roy. Soc. London, Ser. B,* **110**: 336–352.

DITMAN, L. P., G. B. VOGT AND D. R. SMITH, 1942. The relation of unfreezable water to cold-hardiness of insects. *J. Economic Entomology,* **35**: 265–272.

GORTNER, R. A., 1937. Selected topics in colloid chemistry. Cornell Univ. Press, Ithaca.

LOVELOCK, J. E., 1953. The haemolysis of human red blood-cells by freezing and thawing. *Biochimica et Biophysica Acta,* **10**: 414–426.

LUYET, B. J., AND P. M. GEHENIO, 1940. Life and death at low temperatures. Biodynamica, Normandy, Missouri.

MERYMAN, H. T., 1953. Ice crystal formation in frozen tissues. Lecture and Review Series, Naval Medical Research Institute, No. 53–3: 25–48.

NEWBAUER, H. F., 1938. Zur Okologie von in Buchenkronen epiphytisch lebenden Flechten. *Beitrage Biol. Pflanzen,* **25**: 273–289.

SACHAROV, N. L., 1930. Studies in cold resistance of insects. *Ecology,* **11**: 505–517.

SALT, R. W., 1950. Time as a factor in the freezing of undercooled insects. *Canadian J. Res.,* **28**, sect. D. 285–291.

SCARTH, G. W., 1944. Cell physiological studies of frost resistance: a review. *New Phytologist,* **43**: 1–12.

SCHOLANDER, P. F., W. FLAGG, R. J. HOCK AND L. IRVING, 1953. Studies on the physiology of frozen plants and animals in the Arctic. *J. Cell. Comp. Physiol.,* **42**: supplement 1, 1–56.

SIMINOVITCH, D., AND D. R. BRIGGS, 1952. Studies on the chemistry of the living bark of the black locust in relation to its frost hardiness. *Plant Physiology,* **28**: 15–34.

SMYTH, E. S., 1934. A contribution to the physiology and ecology of *Peltigra canina* and *P. polydactyla. Ann. Bot.,* **48**: 267–270.

Contribution No. 783

The Commonwealth of Massachusetts

DEPARTMENT OF NATURAL RESOURCES
Arthur T. Lyman, Commissioner
DIVISION OF MARINE FISHERIES
Francis W. Sargent, Director

SEVENTH REPORT ON

INVESTIGATIONS OF THE SHELLFISHERIES OF MASSACHUSETTS

Prepared by the
WOODS HOLE OCEANOGRAPHIC INSTITUTION
In Accordance with Contract
July 1, 1954

PREFACE

The following report, prepared by Harry J. Turner, Jr., Biologist of the Woods Hole Oceanographic Institution, is a summary of the investigations of the shellfish resources of Massachusetts which were carried out in 1954 by the Woods Hole Oceanographic Institution under contract with the Division of Marine Fisheries, Massachusetts Department of Natural Resources.

The investigations were conducted under the leadership of Mr. Turner. Those participating were Stanley Scher, graduate assistant, David Casiles, captain of the R.V. ASTERIAS, and Peter Southerland. The work was greatly aided by counsel from Dr. David L. Belding, former Biologist for the Massachusetts Department of Fisheries and Game who is now a member of the staff of the Woods Hole Oceanographic Institution.

The Institution has worked in close cooperation with the U. S. Fish and Wildlife Service which is conducting investigations in Essex County and in other parts of New England under a Federal Appropriation for the improvement of the soft and hard clam fisheries. Members of the Institution served on the Committee of Clam Technicians sponsored by the Atlantic States Marine Fisheries Commission of which Massachusetts is a member.

The Woods Hole Oceanographic Institution wishes to express its appreciation to Mr. Francis W. Sargent, Director of the Division of Marine Fisheries, and to Mr. Charles L. Wheeler, Assistant Director and Biologist of the Division for their valuable suggestions and close cooperation.

Alfred C. Redfield
Associate Director
Woods Hole Oceanographic Institution

December 31
1954

SEVENTH REPORT ON INVESTIGATIONS OF THE SHELLFISHERIES OF MASSACHUSETTS *

BY
HARRY J. TURNER, JR.

INTRODUCTION

During the year 1954 the Woods Hole Oceanographic Institution continued investigations of the edible crab, *Cancer irroratus*, and conducted experiments on various aspects of the biology of certain commercial molluscs.. The investigation of the edible crab was conducted in Boston harbor for the purpose of completing the studies begun in 1953, when it was ascertained that the daily rate of capture of crabs was in part determined by the moulting cycle. The investigations carried out in 1954 were designed to determine how much of the adult population was actually taken during the fishing season. An extensive tagging program was undertaken which demonstrated that the fishery was so intense in 1954 that at least 20% of the mature male crab population was caught and that there is a high probability that the removal fraction may have exceeded 50%. Conclusive evidence was obtained that the adult edible crab exhibits no migratory pattern that might affect the fishery but there were indications that the taking of crabs slightly under the preferred size would be reflected in a reduction in the catch the following year.

A number of experiments were conducted on the feeding of the quahaug, *Venus mercenaria*. to determine what kinds of microscopic plants are suitable for food. These experiments were undertaken because the state of knowledge of the nutrition of all commercial molluscs is so inadequate that it is impossible to comply with frequent requests for analyses to determine if water contains sufficient food for shellfish. The quahaug was selected because of its ability to live and grow in confined waters. The results obtained were preliminary and too inconclusive to permit an extensive discussion at the present time. However, it was determined that the quahaug would take almost any small particle into its digestive tract, but siliceous diatoms and armored flagellates would pass through undigested. Small cells such as *Chlorella* and related forms, as well as naked flagellates were found to be digestable.

The biochemistry of nutrition of marine molluscs is an important subject that deals with the intricate methods by which the organisms utilize their food for growth and to produce energy for the various living processes. The literature is extensive and widespread, scattered through journals published in almost every language. Mr. Stanley Scher has summarized and correlated the important works that pertain to commercial molluscs and related species and compiled a bibliography as an aid to future investigations. Mr. Scher's review and appended bibliography is included in this report.

---

* Contribution No. 783 from The Woods Hole Oceanographic Institution.

The possibility that dissolved organic constituents of sea water may play an important role in the biology of marine organisms has been suggested by a number of workers. Wilson (1951) has determined that marine waters may contain an unknown factor which affects the setting and survival of marine invertebrates and Collier et al (1950) have described the activity of some soluble organic substance, probably a carbohydrate, that appears to stimulate pumping in oysters. However, the investigations of many of the organic constituents of seawater have been hindered by difficulties in detecting and identifying these various complex substances, in high dilution. Mr. Scher ran a number of preliminary experiments to devise a method of determining the sea water concentration of thiamin, a well known growth factor which may affect the existence and growth of commercial molluscs. Mr. Scher found that a thiamin-requiring mold could be used to provide a rough estimate by bioassay of the thiamin content of marine waters.

A conference was held in July with the Board of Directors of the Massachusetts Shellfish Officer's Association to discuss ways of aiding the members of the association in solving some of their immediate problems. The perennial problem of obtaining seed was discussed at length and the members of the association showed enthusiastic interest in the advances in artificial propagation by rearing shellfish larvae to the setting stage, a development of the Fish and Wildlife Service Laboratory at Milford, Connecticut. The current status of artificial propagation is discussed in this report with indications as to how it might satisfy the probable needs of the coastal towns of Massachusetts.

REFERENCES

COLLIER, A., RAY, S., and MAGNITSKY, W., 1950. A preliminary note on naturally occurring organic substances in sea water affecting the feeding of oysters. Science, V. 111

WILSON, DOUGLAS P., 1951. A biological difference between natural sea waters. J. Mar. Bio. Assn. U.K. V. 30

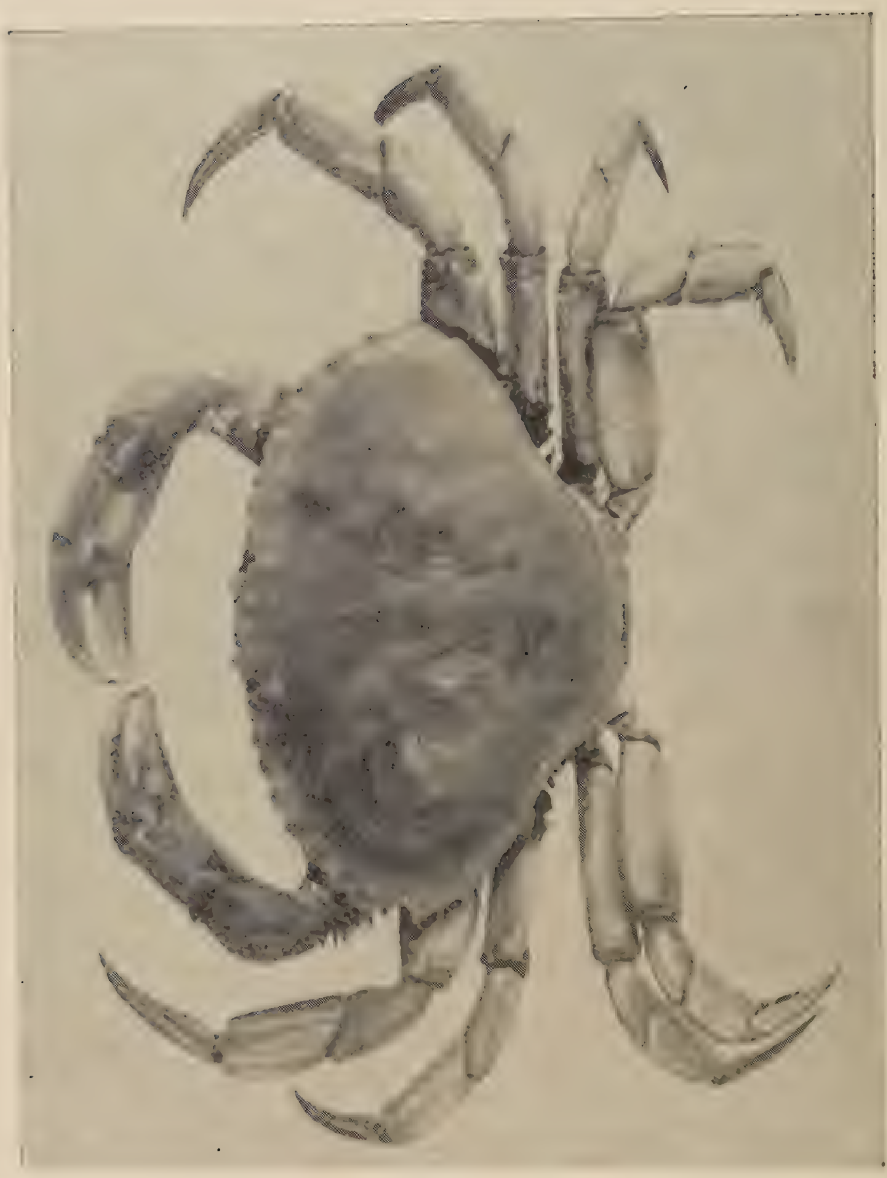

Figure 1. A mature male edible crab, *Cancer irroratus*.

THE EDIBLE CRAB FISHERY OF BOSTON HARBOR

INTRODUCTION

The edible crab, *Cancer irroratus* (Fig. 1) is the only marine crustacean other than the lobster that is available in quantity to the small boat fishermen of the Commonwealth of Massachusetts. The crab fishery is relatively small in comparison with many other fisheries of the Commonwealth but it provides either part or full time employment for several hundred persons, who fish for crabs or process and distribute crab products. The production of native crab meat reduces the dependency of local consumers on imported crab meat, and the exportation of live crabs to inland states provides a signficant revenue to certain of the coastal communities.

Cancer irroratus is found from Nova Scotia to Florida so that the entire coast line of Massachusetts is a potential fishing ground. The main part of the fishery is centered in Boston Harbor and various harbors along the southern coast of Cape Ann where small boats can operate in all kinds of weather, and the productive waters appear to support populations of crabs in high densities. Crabs taken in other parts of the coastal waters as an incidental part of the lobster catch are occasionally marketed when there is a local demand for them.

In Massachusetts, edible crabs are caught exclusively by means of traps which resemble lobster pots in many respects. A typical trap is a rectangular box-like structure approximately one foot high, two feet wide, and three feet long (see Fig. 2). The exact size varies according to preferences of the fishermen. The trap is constructed on an oak framework covered with unplaned laths, each spaced approximately one inch apart. The anterior third or "head" of the trap is provided with two funnel shapped entrances of heavy netting, one on each side. A second funnel of similar construction leads from the "head" into the "parlor" which constitutes the posterior two thirds of the trap. The top of the trap has a removable cover for the purpose of taking out the catch and replacing the bait. A number of bricks are fastened to the bottom by strips of lath to overcome the buoyancy of the trap and insure rapid sinking. The buoy line is fastened to a short bridle which is securely tied to the frame.

The crab trap differs from the conventional lobster pot in two respects. The twine funnels are tied in such a way that their small ends are flattened from top to bottom and elongated laterally to conform to the shape of the crabs. In addition several of the laths on each end of the trap are replaced with a solid board six inches wide through which one or more holes are drilled to permit the escape of small crabs. The escape holes vary from $1^1/_4$ to $1^5/_8$ inches in diameter according to the preferences of the fishermen. Some fishermen provide for the escape of small crabs through an extra wide space between the bottom two laths generally gauging the spacing by the width of the back

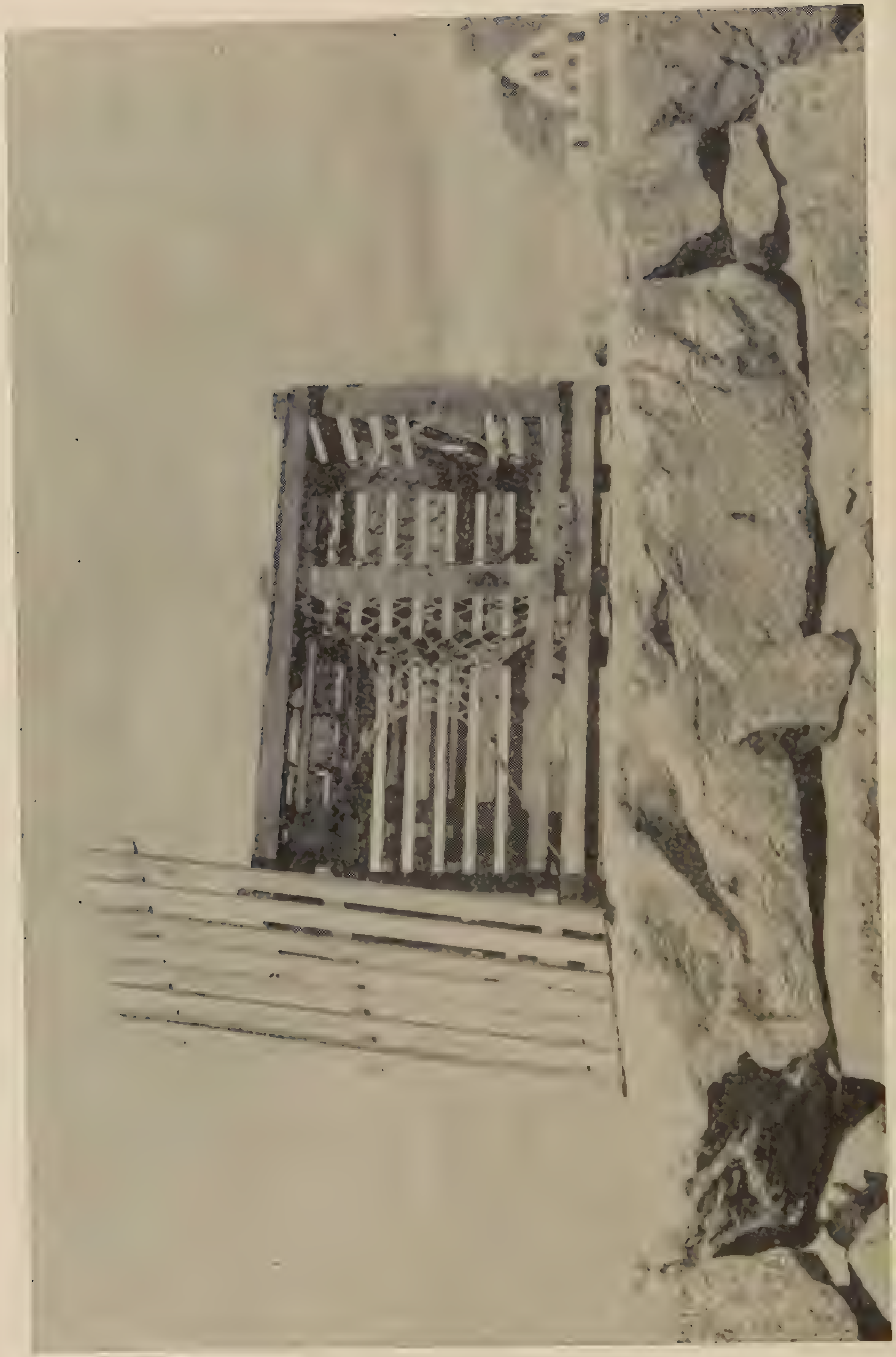

Figure 2. A typical crab trap with the cover removed showing the head chamber (right) and the parlor (left).

of a claw hammer which is approximately $1^{3}/_{8}$ inches. Others prefer to maintain narrow spacing because erosion of the strips may widen the spacings to permit the escape of marketable crabs.

Crab traps are baited in the head chamber with fresh fish heads or cuttings and are then set out in rows between aids to navigation or other reference points on muddy or sandy bottoms. Each fisherman tries to plan his operations so that he can make a complete circuit of his trap lines with a minimum of running time. The traps are set close together with only sufficient space to permit the hoisting of one trap without entangling the propellor of the boat with the buoy line of the next. The fishermen, two to a boat, generally leave at or soon after sunup and tend eighty to one hundred traps, returning with their catch in the early afternoon.

The crabs are brought to the dock in crates which are similar to the traps but without the openings and funnels. Many fishermen make crates out of old traps by removing the funnels and replacing the side laths. As each trap is hoisted to the side of the boat, the cover is removed and the catch is quickly culled into an open crate. There are three methods of culling which differ sufficiently to affect the composition of the catch. The first method is accomplished by simply picking out the large male crabs with gloved hands and throwing them into an open crate. The trap is then inverted over the side to release the females and small males. In the second method, the females and small males are culled out and thrown over the side. The trap is then inverted over an open crate which is placed on deck in such a position that the catch may be dumped into it with a minimum of effort and motion. In the third method, two crates are arranged on deck in such a way that one will receive the contents of the head and the other the contents of the parlor when a trap is inverted over them. Culling is accomplished by quickly moving all the large males into one chamber of the trap and the females and small males into the other. The trap is then inverted over the two crates, the useful part of the catch falling into one crate and the rejects into the other. The females and small males are released when convenient, usually during a run from the end of one line of traps to the beginning of another.

The first method is practiced primarily by fishermen supplying the live crab market or vendors of boiled whole crabs where large crabs are mandatory. It is disadvantageous to the fishermen in that large crabs are often missed when the traps are reasonably full. The other two methods were adopted by some fishermen to eliminate waste motion and speed up the culling. However, catches culled by these methods often contain a higher percentage of small males and an occasional female.

After the catch is culled the head is rebaited, the cover is replaced, and trap is dropped overboard as the boat gets underway to clear the buoy line. A crate $^{3}/_{4}$ full holds from 300 to 400 crabs. As each crate is filled to the $^{3}/_{4}$ mark, the cover is replaced and the crate is stacked on the after deck. In cool weather, all crabs are brought into the dock and those not needed for immediate processing or shipment are kept alive in the crates which are hung in the water at the side of the dock. During the spring and late fall the crabs will live several days in spite of the crowded condition. The survival time becomes progressively shorter as the water warms up in the summer making it necessary for the fishermen to hold their surplus crabs in crates submerged in the deeper cold waters of the fishing areas. Crabs caught on weekends when the crabmeat factories are closed are also held in this manner.

Live crabs are either sold locally or are shipped inland by rail as far as the middle west. They are generally sold by the piece instead of by weight but the market will only accept large crabs. Most of the catch is processed into crab meat in picking factories in Boston and Lynn. In preparation for picking, the crabs are first boiled in large wooden or stainless steel vats containing salt water heated by live steam blown into the vats below the surface. The length of the boiling time is of utmost importance. If the crabs are underdone the meat adheres to the shell, and if boiling is too prolonged the flesh becomes soft and mushy. The optimal time is determined for each batch by testing one or more crabs at one minute intervals after the first ten minutes. As soon as the test samples show that the crabs are in prime condition for picking, the steam is turned off and the crabs are removed with dip nets and placed in galvanized buckets with perforated bottoms to drain and cool. When crabs are needed immediately in the picking rooms, salt water hoses are played over the buckets to hasten the cooling process. More satisfactory results are obtained by allowing the crabs to cool slowly so that they can drain.

Crabmeat picking is done on a piecework basis, by women who receive a definite sum per pound of meat picked. Each picker is supplied with a heavy tile, hardwood stick, and a curved knife. A skillful picker tears the legs off 20 or 30 boiled crabs and sets the legless bodies to one side. She then places each leg on the tile and strikes the upper joint with the stick in such a way the shell splits lengthwise. The shell is then opened up with the knife and fingers, and the flake of meat is flipped into a plastic or metal container of half or one pound capacity. When the container is nearly full, the last layer of flakes is added with considerable care to give the package an attractive appearance. The meat of the pincer claws is also used, but unlike that of the blue crab, does not present a particularly neat appearance. Body meat, sometimes called "broken" is removed by inserting the knife in the leg holes and scooping it out. It is not as attractive as the solid flake meat in the legs, and does not bring as high a price. For this reason some companies pay their pickers less for picking body meat but the ease with which it can be removed compensates for the lower rate. As soon as a container is filled, it is weighed by the checker and the weight credited to the individual picker. Full containers are then packed in crushed ice to await delivery.

The various aspects of the edible crab industry are affected to some degree by the condition of the crabs as they are caught. The most desired raw product is a large, hard, full-meated crab. The practice of dealing in crabs by the piece instead of by weight makes it obligatory for dealers in live crabs to handle only those in prime condition. Customers will not buy small crabs or those with watery tissues, and only crabs with hard shells can survive shipment to distant points. However, the crabmeat factories are somewhat less affected by the condition of the crabs. Companies which depend on their own boats for their supply do not have the problem of making a direct payment for the raw product, and since meat-picking is financed on a piece-work basis, the only real requirement for successful operation is that crabs be available in quantity regardless of condition. However, excessive numbers of small crabs are undesirable because the pickers may discard many of them unless closely supervised.

SEASONAL ASPECTS OF THE CRAB FISHERY

The crab fishermen and dealers have noticed seasonal changes in the size and condition of the crabs. The male crab molts some time between November and March so that crabs caught during this period have relatively soft shells and the meat yield is poor. It has also been observed that crabs seem to be easily trapped in large numbers during the late winter and early spring with a progressive decline in the catch during the late spring, summer, and early fall. This peculiar situation has proved unfortunate for the industry, particularly the dealers in live crabs, because the crabs are most readily available when in poor condition, and the supply declines as the condition improves.

An attempt to ameliorate the situation was made in 1938 when legislation was enacted which imposed a closed season on crab fishing from January 1 to March 31. Certain participants in the industry felt that this closed season was advantageous and in 1951 they succeeded in sponsoring legislation to extend the closed season to include the months of December and April. This extension worked a hardship on certain other members of the crab industry who usually began operations in April and a request was made for a biological investigation to determine how the crab fishery might best be regulated.

INVESTIGATIONS DURING THE 1953 SEASON

The investigations conducted during the 1953 crab fishing season were designed to determine quantitatively the changes in the meat content of the crabs, the changes in the daily catch per trap, and the changes in the size composition of the catch. The preliminary results have been published previously (Turner 1953). A summary is included here together with an analysis of the changes in the size composition of the catch not previously reported.

An estimate of the preseason condition of the fishery was made by conducting two experimental fishing trips early in April. From these it was possible to determine what the daily catch per trap would have been if fishing had been permitted. The catch was then boiled and processed by employees of the crabmeat companies to determine the meat content. During the open season (May through November) estimates of the daily catch per trap were obtained by making trips with commercial fishermen and by interviewing others as the catch was landed. The meat content was determined at intervals from random samples of the catch which were picked separately according to standard procedure and the size composition was determined by measuring the carapace widths of large random samples.

The results that pertain directly to the crab industry are summarized in Table I.

TABLE I

	Daily catch per trap	Crabs per lb. meat	Average meat yield of daily catch per trap
April*	125-150	35-38	Nearly 4 lbs.
May	50-75	19-21	Over 3 lbs.
June	35-50	19-21	Over 2 lbs.
July	35-50	26**	Under 2 lbs.
Aug.	20-40	30**	About 1 lb.
Sept.	20-40	30**	About 1 lb.
Oct.	20-40	33**	Under 1 lb.
Nov.	30-50	40	About 1 lb.

* Experimental fishing

** Increase in small crabs in catch

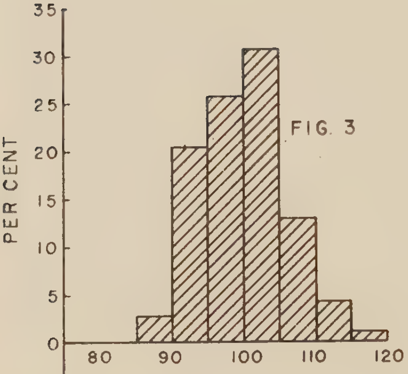
FIG. 3

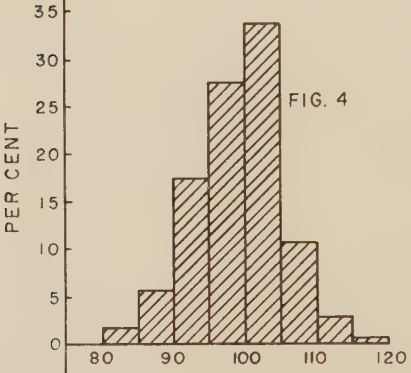
FIG. 4

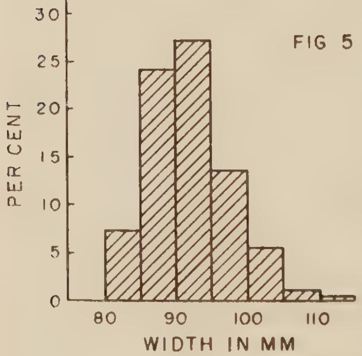
FIG 5

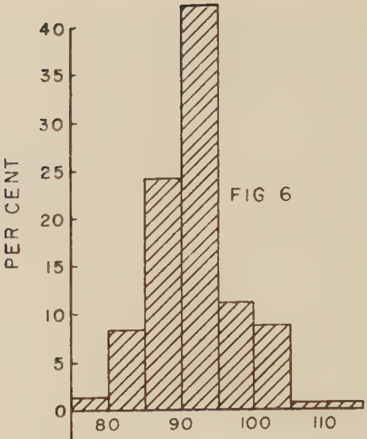
FIG 6

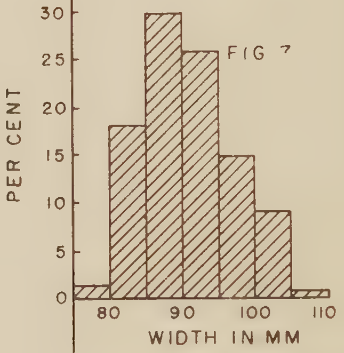
FIG 7

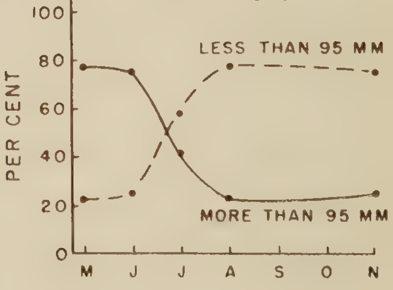
FIG 8

Figure 3 - 7. Graphs of the distributions of sizes of crabs in the 1953 commercial catch for the months of May (fig. 3), June (fig. 4), July (fig. 5), August (fig. 6), and November (fig. 7).

Figure 8. Graph of the changes in the composition of the commercial catch during the season of 1953.

The preseason experimental fishing trips showed that crabs were abundant and readily trapped during the month of April. Their meat content was poor, but numbers that would enter the traps offset this factor and the softness of the shells made it possible to pick them easily and rapidly.

When the season opened in May the daily catch per trap was only about half as great as that determined from the experimental fishing trips in April. This reduction is particularly significant because it could not have been caused by a depletion of the population by fishing. The change was believed to be due to a difference in response to baited traps of hard crabs that needed less food than the soft post-moult crab which would need extra amounts of food to fill out its watery tissues.

It is also apparent from Table I that the meat content per crab declined in July and remained at a low level for the remainder of the season in spite of the full meated condition of the individual crabs. This decline resulted from an increase in the relative numbers of small crabs as the season progressed. The size compositions of the crabs in the commercial catches during May and June shown in graphs, Figures 3 through 7 indicate little change during that period. In July, however, the percentage of crabs measuring more than 100mm in carapace width (approximately 4 inches) declined considerably and by August the average was reduced below 95mm ($3^3/_4$ inches). When the season closed at the end of November, the average size was even smaller, and the appearance of new post-moult crabs in the catch brought about a further reduction in the meat content per crab.

The trend in the changes in the size composition is shown in graph Figure 8 which summarizes the data given in graphs, Figures 3 through 7. From the commercial point of view, crabs less than 95mm ($3^3/_4$ inches) wide are undesirable. Dealers in live crabs find their customers unwilling to buy them and managers of crab meat factories complain that the meat pickers discard many of them. For these reasons a dividing line of 95mm has been used in the construction of Figure 8 which shows the ratios of the undersized crabs to the desirable sized crabs landed during the 1953 season. During May and June approximately 75% of the crabs landed were satisfactory for shipment or meat picking. During July the percentage of the larger size crabs fell to 40% and by August it declined to 25% where it remained for the rest of the season. It is thus evident that the industry was operating efficiently only during the first two months of the season and was depending on inferior raw material to sustain it through the late summer and fall. See Table 1.

THE TAGGING PROGRAM OF 1954

Changes in the catch such as have been described for the edible crab fishery during 1953 may be the result of a number of factors. Progressive decline in the catch per unit of effort is often indicative of a reduction of the total stocks by fishing. Other causative factors include seasonal changes in response to fishing equipment and migration of the stocks to other areas.

An extensive tagging program was carried out in 1954 in Boston Harbor to determine how much of the crab population was caught. An experimental fishing expedition was made in April as soon as the season opened to procure crabs for tagging and to compare the condition of the fishery with that of the previous year. The crabs were tagged with brightly colored poultry bands which were slipped around the bases of the pincher claws, with different colors used to indicate the various points where they were released. Equal numbers of tagged crabs were liberated in each of four different localities selected as representative centers of fishing intensity. All crabs were released at least 100 yards from the nearest trap line to permit them to disperse before being caught. The tagged crabs, all males, numbered 2550, half of which were originally caught by the expedition and the other half bought from the fishermen. The tagging operation occupied most of the month of April. Fishermen were informed of the operation and requested to retain tags found on the crabs in their catch and to report the date and location of the capture. The response was variable; some fishermen turning in complete data with each tag while others indicating the area in a very general way. In addition there was a considerable variation in the number of returns which was influenced by the methods of culling. Fishermen who culled by picking the male crabs directly from the traps made much higher returns than did those who culled out the females and inverted their traps over the crates. In either case it was evident that tagged crabs were seldom discovred after the original culling at the traps because they were then dumped en masse into the boiling vats where the hot water softened the plastic, releasing the tags to disappear down the drain holes. The operation was successful in establishing the minimal percentage of the crab population that was caught, and also in establishing the extent of the migrations of the crabs.

Five hundred and seventy-three tags were received by the end of the 1954 fishing season; this is 22.5% of the number of tagged crabs originally released. All tags returned with complete data were taken from crabs caught within two miles of the point of liberation and the distribution of the points of capture indicated random movements with no directional migrations. See Figure 9.

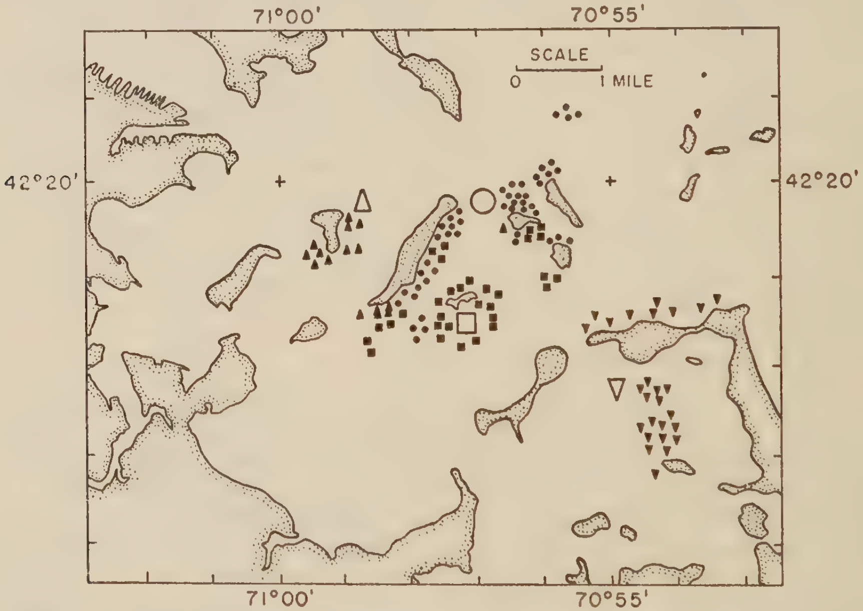

Figure 9. Map of Boston Harbor giving locations of the recaptures of tagged crabs. Large open figures (circle, square, upright triangle and inverted triangle) indicate places where tagged crabs were released. Small black figures indicate corresponding points of recapture.

These results indicate that the fishermen caught a little over 20% of the crabs available in Boston Harbor and that the crabs had no migratory habit during the fishing season that might affect the fishery.

The estimate of the fraction of the population that was caught (22.5%) requires some qualification, as it is a minimal figure derived from the tags that were actually returned. The variation in the number of returns from the different operating units suggests that this figure may be far too low because so many tags may have been missed during the culling process, or may not have been returned for other reasons. There is thus some justification for revising the estimate on the basis of data that is known to be reliable to derive a figure that may be termed the "probable catch".

Of the four major sources of tag returns, one turned in 305 tags with complete data as to the time and place of capture. The three other major sources together turned in only 103 tags, although each of these units was operating in essentially the same locality with as many traps as the first unit. If it is assumed that each of these three sources caught as many tagged crabs as the first one but missed them while culling, the total number actually caught would be about 1200. The addition of 165 tags returned by a lobsterman who was making a few trials near the crab grounds would raise the total to 1365. This gives a probable catch of a little over 50% of the population of marketable crabs. This probable catch is as high as can be derived from the available data. It does not take into account losses due to the rate of natural mortality, from losses of legs by the crabs, or from tags not turned in by incidental crab fishermen It is only justified to conclude that at least 20% of the marketable crabs in Boston Harbor were caught during the 1944 season, but probably as many as 50% were caught, and it is possible that the percentage was even higher.

THE CONDITION OF THE FISHERY IN 1954

The results of the experimental fishing expedition and observations made on commercial fishing boats indicated that crabs were both smaller and less than half as available in the 1954 season than they had been in 1953. The daily catch per trap averaged approximately 50 during April, declined steadily to 8-10 by the middle of July, and remained low for the remainder of the season. The distribution of sizes during April differed from that of the previous year by an increase in the number of smaller crabs. More than half the crabs were less than 95mm wide as is indicated in graph, Figure 10, and it took 45 crabs to produce a pound of meat. This decline was so serious that the fishermen had to increase the number of traps and many of them found the fishery so unprofitable that they shifted to lobstering before the end of the season.

The reduction in the daily catch per trap at the beginning of the 1954 season is of interest because it occurred at the time when crabs are most catchable, and is therefore indicative of a decrease in the numbers of crabs available. The composition of the catch during the last four months of the previous season suggests that the decline was in part caused by the taking of small crabs during that period. Efforts to determine the amount of growth after moulting were unsuccessful but Cleaver (1949) demonstrated that a related west-coast species, the Dungeness crab, grows approximately 20% in linear dimensions at each moult as it approaches maturity. This figure corresponds roughly with that observed for other species of crabs so it may be expected that the east-coast edible crab grows proportionately.

The average width during the last four months of the 1953 season was approximately 85mm, and three quarters of the crabs caught were less than 95mm as has been discussed previously. If these crabs had been permitted to moult one more time, the average width would have been increased to at least 100mm and the majority would have exceeded 95mm in width at the beginning of the 1954 season.

CONSERVATION PROBLEMS OF THE CRAB FISHERY

It has been shown that the adult male crabs of Boston Harbor form a local non-migratory population. The annual removal by the fishery is probably in excess of 50% of the standing crop. The fishery is thus comparable to the seasonal lobster fisheries of the Canadian Maritime Provinces and the West Coast Dungeness crab fishery. The high rate of removal of the adult male crabs is a desirable feature because it indicates that the resource is used efficiently. The protection of the females prevents any possibility of depletion of the breeding stock so that the future of the resource is assured.

There is evidence that the tendency to take small crabs in the latter months of the fishing season may reduce the numbers of large ones in the following season. It is suggested that these small crabs would reach a more desirable size if permitted one additional moult with the accompanying growth. Considerable success has been achieved in the Dungeness crab industry by imposing a minimal legal size limit so that the crabs may reach their full growth before being caught. Such a measure invariably works a hardship on the fishery during the first season when in force, but subsequent gains are advantageous if the rate of natural survival is high.

REFERENCES

Cleaver, Fred C., 1949. Preliminary results of the coastal crab (*Cancer magister*) investigation. Biological Rpt. No. 49A, Dept. of Fisheries, State of Washington.

Turner, Harry J. Jr., 1953. Sixth Report on Investigations of the Shellfisheries of Massachusetts. Div. Mar. Fish., Dept. Nat. Res., Commonwealth of Massachusetts.

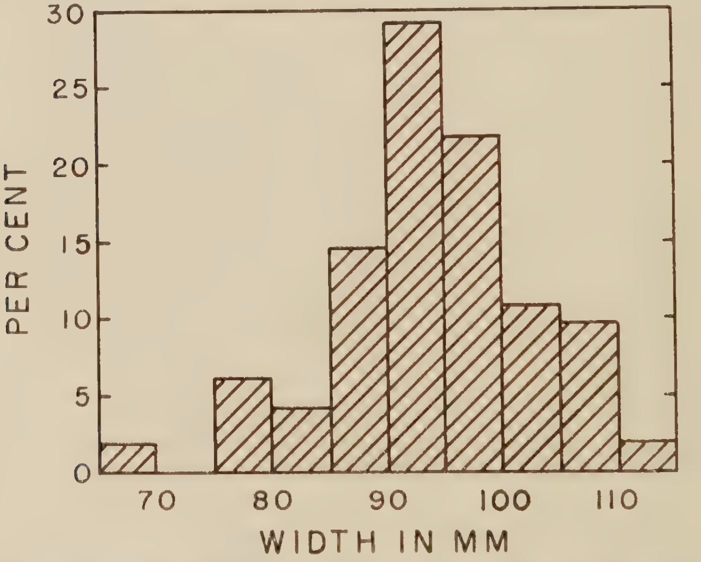

Figure 10. Graph of the distribution of sizes of crabs at the beginning of the 1954 season.

ARTIFICIAL PROPAGATION OF SHELLFISH SEED BY LARVACULTURE

One of the primary requirements for material improvement of coastal shellfish resources is the discovery of a reliable method of populating areas that fail to obtain natural sets at regular and frequent intervals. Until such a method is discovered the extension of public shellfish grounds or the development of private grants will continue to depend on the sporadic occurrence of localized natural sets which are dense enough to provide seed for distribution over wide areas at a reasonable cost. The uncertain manner in which sets of this kind occur in both time and place limits the effectiveness of shellfish improvement programs at the present time and even when such sets do occur there are seldom adequate financial or legal provisions to permit their full utilization. The problem is particularly acute in the case of the sand dwelling species such as clams and quahaugs because no successful method of preparing the ground to induce setting has ever been discovered. Even the oyster industry which has been operated on a system of private culture since antiquity still depends to a considerable degree on chance in obtaining seed. Solid collectors in the form of shells, concrete coated egg crates or limed tiles may or may not receive an adequate number of spat when placed in the water during the setting season.

Recent advances in the development of larvaculture made by Dr. Victor L. Loosanoff and his associates at the U.S. Fish and Wildlife Service Laboratory at Milford, Connecticut, have stimulated interest in the possibility of applying the method to the production of shellfish seed on a commercial scale. The success achieved at the Milford Laboratory in producing large numbers of juvenile quahaugs and other molluscs with limited facilities has made it appear that the entire seed problem could be solved by a larger installation designed to provide a continuous and reliable source of seed in commercial quantities. The quahaug which has been reported to be the easiest species to culture is of particular interest to the coastal communities of Massachusetts because it occurs naturally along the South Shore, and there are extensive areas along the North Shore where experimental plantings have grown but failed to propagate. Thus any facility that would provide a continual supply of seed in quantity would benefit the South Shore by augmenting the natural supply, and also provide a substitute for the dwindling supply of soft clams along the North Shore.

A number of questions must be investigated and a number of problems must be solved to provide information as to whether or not artificial propagation by larvaculture is practicable. The fundamental problem involves the question as to whether or not it would be possible to supply the demands of the entire coastline of Massachusetts from one or more plants that could be designed, built, and operated at a cost that would be economically feasible.

1. The needs of the coastal communities must be determined so that some estimate can be made of the required capacity of the plant.
2. The efficiency of the method must be considered to determine the probable output.

3. The biology of the species of shellfish under consideration needs thorough investigation to determine its survival under natural conditions and this to indicate what production would be required to compensate for mortality.
4. Finally, the cost of operations and the question of finance must be taken into consideration.

A recent survey (Turner 1948) has shown that there are at least 3000 intertidal and shallow water acres along the coast of Massachusetts. If it is assumed that half of this area (1500) acres is suitable for quahaugs, the ideal plan would be to manage it on a three-year rotating basis which is the average length of time required to grow little-necks. According to such a plan there would be 500 acres requiring seed each year. Each acre would support one million quahaugs and, if mortality were low, would yield 1,000 to 1,500 bushels of little-necks in three years. The required output of a propagation plant would thus have to be at least 500 million seed quahaugs per year.

The method of propagating quahaugs as reported by Loosanoff (1954) appear to be remarkably efficient in respect to the physical space requirements so that it is quite possible that 500 million quahaugs per year could be reared to metamorphosis in an installation of reasonable size. Large parent specimens are taken from the beds and conditioned for spawning in trays stacked one above the other to conserve space. Conditioning is accomplished by raising the temperature of the water a number of degrees each day to accelerate early development of the eggs and sperm so that the process is completed in a matter of weeks. Spawning is induced by thermal or chemical stimuli and the fertilized eggs are placed in 5 gallon earthenware containers full of sea water. As soon as the eggs develop into swimming larvae that require food, a calculated amount of microscopic algal suspension is added. Every two days the larvae are screened out with fine stainless steel sieves so that the water may be changed. With temperatures maintained at an optimal level setting is usually completed in two weeks. Each five gallon container may support several hundred thousand larvae, of which the majority may reach the setting stage under favorable conditions.

The spawned out breeding stock is unable to reproduce again for several months. Consequently the operation may be carried out only during the late winter, spring, and early summer if the breeders are taken from natural beds. However, Loosanoff and his associates have discovered that spawning may be inhibited by low temperatures so that breeding stock may be held in refrigerated water or in the cold water of Maine for conditioning and spawning at any time of the year. This development suggests that the required annual production could be met with far fewer facilities than would be necessary in a propagation plant operating seasonally.

Artificial propagation of any species of shellfish would be of little value unless the majority of the seed thus produced should survive after distribution. In the case of the soft clam Belding (1909) and the author (Turner 1953) have shown that mortality of natural sets may be as great as 99% before the legal length of 2 inches is attained. The quahaug with its heavy shells and strong adductor muscles is presumed to be more resistant to adverse conditions but Haskin (1952) has shown that the very young quahaug is so susceptible to the predations of the boring snail *Polynices* that elaborate methods of protection are necessary until the quahaug grows to be of considerable size. This indicates that there would have to be some provision for holding artificially propagated quahaugs in growing tanks or some other protected environment until they grew large enough to withstand the rigors of the natural environment. The optimal size for distribution would have to be determined and methods of holding the seed during the preliminary growth period would have to be devised so that they could be incorporated in the design of the propagation plant.

In spite of the remarkable success at the Milford Laboratory, the present methods of rearing larvae are not completely satisfactory. From time to time entire cultures die after a renewal of the water. The lethal water is identical with that which supports normal growth as far as can be determined by conventional analytical tests so there is no way of predicting when such catastrophes are likely to occur. A water supply that might frequently contain this lethal factor would seriously impair the efficiency of a propagation plant. In addition to the lethal water problem, Davis et al (1954) have described a fungus that attacks and kills growing larvae. This fungus is almost always found in a few individuals in any culture of larvae and at times it reaches epidemic proportions, spreading to and killing every larva in the culture in a short time. It is clear that the success of artificial propagation on a large scale depends on the identification of the lethal factor in the water supply and the development of methods of combating the fungus.

In the event that biological and technological problems of artificial propagation of shellfish are solved, the question of financing is a serious one. The operation would undoubtedly be costly because of the need of elaborate facilities and highly trained personnel and it would be necessary to determine if the ultimate benefits would justify the cost. In addition, the question arises as to how such a project could be financed in view of the free fishing tradition of the Commonwealth. The fisherman, who is the primary beneficiary of any shellfish improvement program is in no position to share materially in the cost of the program. His investment in the resources consists merely of his license fee which is an insignificant fraction of the value of his harvest. He, as an individual, is in constant competition with his fellow fishermen and thus has no assurance that any investment that he makes in the fish or shellfish will bring additional returns directly to him. The coastal cities and towns, however, benefit both directly and indirectly from improvement of the shellfish resources. Shellfishing provides a gainful occupation for many inhabitants and the exportation of a product produced locally is beneficial to the economy of the community as a whole. Progressive communities at the present time appropriate substantial sums for the improvement of their shellfish resources even though current methods are far from satisfactory. It is possible that the combined appropriations of all the coastal cities and towns of the Commonwealth might contribute substantially toward the maintenance and operation of a propagation plant if it could be shown that such a plant would be beneficial.

REFERENCES

BELDING, DAVID L., 1909. Report on the Mollusk Fisheries of Massachusetts. Boston.

DAVIS, H. C., LOOSANOFF, V. L., WESTON, W. H., and MARTIN, C., 1954. A fungus disease of clam and oyster larvae. Science V 120.

HASKIN, H. 1952. Personal communication.

LOOSANOFF, V. L., 1954. New Advances in the Study of Bivalve Larvae. American Scientist, V 42., No. 4.

TURNER, HARRY J. JR., 1953. Growth and Survival of Soft Clams in Densely Populated Areas. Sixth Report on Investigations of the Shellfisheries of Massachusetts. Div. Mar. Fish., Dept. Nat. Res. Commonwealth of Massachusetts.

A REVIEW OF THE NUTRITIONAL BIOCHEMISTRY OF MARINE POLECYPODS

BY

STANLEY SCHER

INTRODUCTION

The shellfish biologist has long studied the food requirements of pelecypods as whole organisms in an attempt to understand their nutrition. The current biochemical trend has been to investigate the component reactions which occur in the cells and tissues of the organisms, and to describe the physiological mechanisms in the language of chemistry and physics. Such information becomes significant when it is related to the activities of the organism as a whole. The present review will therefore attempt to summarize the biochemical aspects of pelecypod nutrition, and to integrate these findings with the known physiology of these animals.

Few modern discussions of nutritional biochemistry have been concerned with marine pelecypods. In a comparative study of animal physiology, Prosser (1) has considered the nutrition, and digestion of a number of invertebrate types, but his treatment of molluscan metabolism is cursory. Similarly Scher (2) briefly discusses the metabolism of molluscs, but most of the examples cited are derived from studies of cephalopods and gastropods rather than pelecypods. A review covering the nutrition of invertebrates by Kidder (3) has recently been published. This discussion is limited to those invertebrates vis. Protozoa, Nemathelminthes and Arthropods, which have been successfully grown in the absence of contaminating microorganisms.

Korringa (4) has also included some information of a biochemical nature in his description of the anaerobic life, egg development, spawning and respiration of the oyster, but nutritional metabolism is not considered extensively.

As most of the investigations in the biology and physiology of pelecypods have been confined to commercial species, the scope of any review which attempts to discuss them will be restricted to comparatively few forms. However, references will be made to related non-commercial species where such studies offer valuable contributions to the subject.

INORGANIC NUTRITION

Inorganic salts must be supplied to all biological forms for normal growth and function. In pelecypods these compounds may contribute to the formation of the shell, aid in the regulation of osmotic pressure, or help maintain the acid-base equilibrium. In addition, they may have specified roles in the metabolism of nutrients.

Mineral requirements of higher animals and plants have been investigated in great detail, but relatively few critical experiments have been conducted on marine pelecypods. Some definite requirements are known, but many are inferred or suspected without direct evidence.

A number of methods have been employed in the determination of specific requirements. Growth inhibition after depletion of a particular element may be observed after extended periods of cultivation in non-circulating sea water. Such conditions may be induced more rapidly by supplementing the culture medium with a non-metabolizable chelating agent such as ethylene-diamine tetraacetic acid. This compound forms complexes with metals in the following sequence: copper, cobalt, zinc, iron, manganese and magnesium (5). Activation of isolated enzyme systems by reactive chemical groups constitutes a second method of obtaining evidence of a more specific metabolic requirement. Although gross chemical analyses may indicate the presence of a variety of substances, the precise techniques of histo- and cytochemical localization provide more significant information. With such methods, the exact distribution of biologically important compounds can be determined within the cells and tissues of the organism.

The major elements which are generally required in substantial quantities include calcium, magnesium, sodium, potassium, phosphorus and sulphur.

Calcium has been shown to have metabolic functions in addition to formation of the molluscan shell. Dugal and others (6. 7) have reported that this element is used to buffer the weak non-volatic organic acids produced as a result of anaerobic glycolysis in *Venus mercenaria.* Humphrey (8) has shown that calcium is required by the succinoxidase system in adductor muscle homogenates of *Saxostrea.* The physiological importance of these enzyme systems will be discussed in the section devoted to the metabolism of carbohydrates.

Many of the fundamental catalytic reactions in carbohydrate metabolism are dependent upon the presence of magnesium as an activating ion. It has been shown to be one of the essential components of the glycolytic system in the oyster *S. commercialis* (9). The acid phosphomonoesterase in the posterior adductor muscle of *Mytilus edulis* is also stimulated by magnesium (10). Indeed nearly all transphosphorylation reactions involving Adenosine triphosphate (ATP) require this metal (11). The activating effect of magnesium is not completely specific, as manganese and other divalent ions can in some cases function in a similar way (12).

Sodium and potassium are found almost universally as the principal monovalent cations of extracellular and intracellular fluids respectively. In addition to their roles in osmotic regulation, they also serve as essential elements for metabolic reactions. Humphrey (13) has found that salts of sodium and potassium accelerate endogenous respiration in homogenates of *Gryphaea commercialis.* The effect of potassium or glycolysis in the muscle of *Saxostrea* has also been reported by Humphrey (9). The stimulatory effect of potassium on this system is probably related to its known activity in the ATP pyruvic transphosphorylation reaction.

The biochemical importance of phosphorus has been established in a variety of vital processes. Phosphates are intimately associated with the metabolism of all types of nutrients. It is bound to organic residues in the form of phospholipids, nucleotides, phosphoproteins, and phosphorylated sugars as well as a number of essential metabolic intermediates. Phosphate tends to form anhydrous linkages with other phosphates as in ATP. The latter functions in anaerobic glycolysis as a source of energy. In addition, primary and secondary phosphate contributes to the buffering mechanism. Bevelander (14, 15) has studied the relationship of phosphate metabolism to calcification in marine molluscs. He found that phosphorylation occurs as a result of the action of mantle phosphatase upon mantle mucous. The effect of inhibitors on phosphate uptake in excised gills of *Mytilus* has been investigated by Ronkin (16). Inhibition by cyanide, sulfide and iodoacetate was correlated with penetration into cells.

Sulphur is a constituent of a number of metabolically active molecules including some of the protein amino acids, vitamins, enzymes and hormones. Cysteine and glutathione, a tripeptide which contains a residue of the sulfur amino acid cysteine, have been shown to accelerate inactivation of catalase in *Mytilus* (17). These compounds also increase oxygen consumption in oyster spermatozoa (18). Humphrey (19) has studied the adenosine triphosphatase activity in myosins of *Mya arenaria* and other marine organisms. He found that cysteine activated the splitting of ATP. The effect of these compounds on different enzyme systems is probably due to their reducing activity which prevents oxidation of the sulfhydryl group of the enzyme. Thiamine, the sulphur containing vitamin, will be discussed in the section on growth factors.

With the improvement of analytical techniques, an increasing number of elements have been detected in molluscan tissues. However, the metabolic role of few of these metals has been established.

Rangnecker (20) has investigated the nature of the oxygen carrier in the blood of the mussel *Lamellidens.* An iron containing substance similar to hematin was detected. Other molluscs are known to utilize hemocyanin, a polypeptide linked to copper. Fox and Marks (21) have demonstrated the presence of the iron-dependent enzyme catalase in the California mussel. Iron containing cytochromes are discussed in relation to terminal oxidation in a subsequent section.

Although Galtsoff (22) assumes that seasonal fluctuations of manganese have physiological signficance in the oyster, Korringa (3) believes such accumulation can be observed with other ions such as mercury and that this phenomenon is not necessarily meaningful.

The presence of Vitamin B_{12} in soft and hard clams (23) indicates that cobalt, an essential constituent of cobalamin, may function in the synthesis of purines. The latter will be discussed in the section devoted to the metabolism of nitrogen compounds.

Stolkowski (24) has found that calcium carbonate precipitation in Gryphaea is related to the action of the zinc-catalyzed carbonic anhydrase.

ORGANIC NUTRITION

The diet of animals in general contains a vast array of complex, often non-diffusable organic molecules. These are usually in the form of carbohydrates, proteins, fats and vitamins. Food materials must be digested or converted into relatively simple compounds capable of permeating the cell membrane. Once within the cell they may be assimilated or utilized for energy. Since these metabolic reactions are generally catalyzed by enzyme systems, the latter must be considered in order to understand the nutritional process. As our present knowledge of pelecypod metabolism is incomplete, the available information will be interpreted on the basis of established biochemical concepts.

METABOLISM OF CARBON COMPOUNDS

It is convenient to divide metabolism of carbon compounds into several stages: 1. The initial degradation of the complex dietary carbohydrates, 2. The breakdown and synthesis of glycogen, 3. The tricarboxylic acid cycle, and 4. The terminal oxidative mechanism.

ENZYMATIC DEGRADATION OF DIETARY CARBOHYDRATES

Digestion of carbohydrates is initiated by the action of hydrolytic enzymes which are liberated by the crystalline style. Starch and glycogen, the principal reserve polysaccharides of plants and animals respectively, can be broken down by a step-wise procedure to disaccharides and ultimately to glucose or its esters. Mansour and others (25 - 28) have demonstrated the presence of amylase in a number of pelecypods, and glycogenase activity has been found in *Mytilus edulis diegensis* by Coe (26). A number of sucroclastic enzymes have been reported by Yonge (27). These split the trisaccharide raffinose, the disaccharides sucrose, maltose and lactose, as well as the glycosides salicin and amygdalin. He found that other polysaccharides such as inulin, pentosans and cellulose were not digested. In a review of cellulose and chitin digestion by invertebrates, Yonge (29) states that molluscan cellulase is confined to the wood-boring Teredinidae. However, Lavine (30) has reported cellulolytic activity in the clams *Mactra* and *Mya.* A summary of the enzymes which are known to function in the digestion of carbohydrates is given in Figure 1.

A SUMMARY OF CARBOHYDRATE DIGESTION

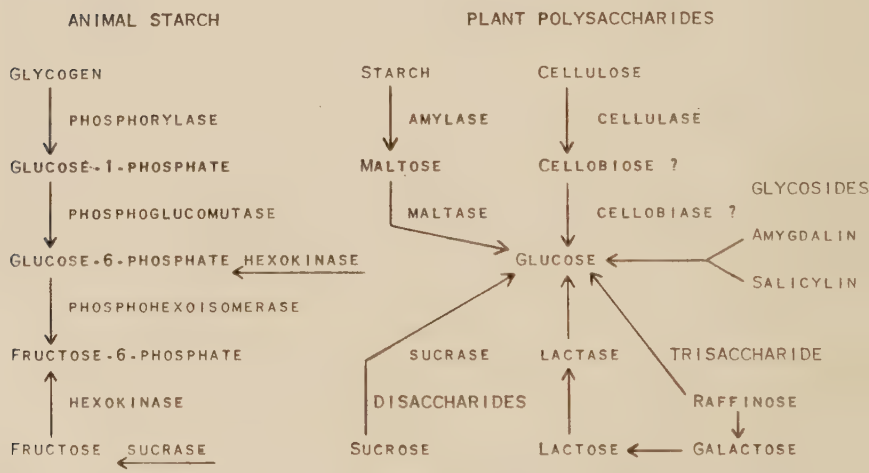
ANIMAL STARCH
PLANT POLYSACCHARIDES
GLYCOGEN
PHOSPHORYLASE
GLUCOSE-1-PHOSPHATE
PHOSPHOGLUCOMUTASE
GLUCOSE-6-PHOSPHATE
HEXOKINASE
PHOSPHOHEXOISOMERASE
FRUCTOSE-6-PHOSPHATE
HEXOKINASE
FRUCTOSE
SUCRASE
STARCH
AMYLASE
MALTOSE
MALTASE
CELLULOSE
CELLULASE
CELLOBIOSE ?
CELLOBIASE ?
GLUCOSE
GLYCOSIDES
AMYGDALIN
SALICYLIN
SUCRASE
DISACCHARIDES
SUCROSE
LACTASE
LACTOSE
TRISACCHARIDE
RAFFINOSE
GALACTOSE

Figure 1

GLYCOLYSIS AND GLYCOGENESIS

The breakdown and synthesis of glycogen can be considered as a single process in which the intermediate steps are generally reversible. Degradation of glucose or glycogen ultimately yields pyruvic and lactic acids, with the simultaneous production of energy. In the reverse process, simple organic acids can be employed in the formation of glycogen which can be stored for further use.

In 1926 Yonge (27) observed that the enzyme glycogenase, which initiates the degradation process, is inactivated when it is dialyzed. This indicated that the activity of this enzyme was dependent upon the presence of a cofactor of small molecular size. Several years later Cori (31) showed that inorganic phos-

A SUMMARY OF GLYCOLYSIS AND GLYCOGENISIS

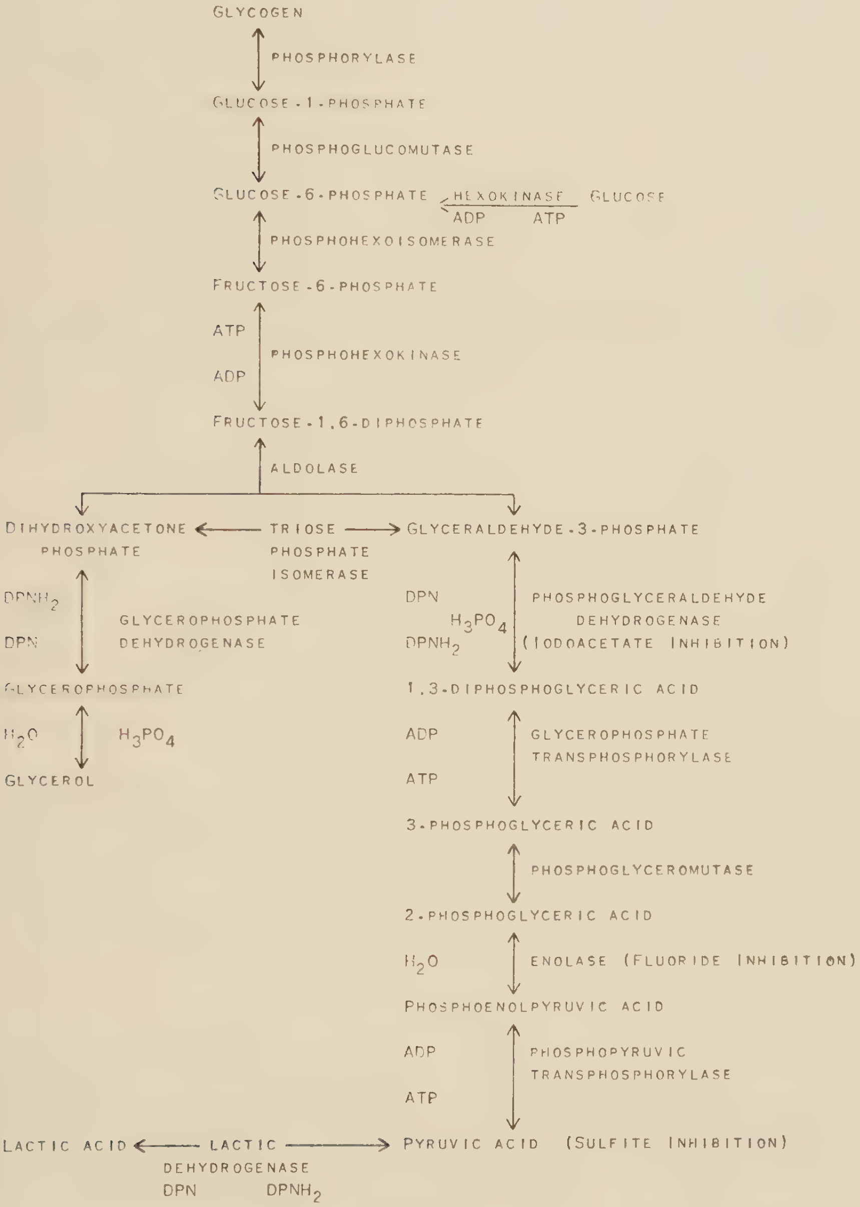
GLYCOGEN
PHOSPHORYLASE
GLUCOSE-1-PHOSPHATE
PHOSPHOGLUCOMUTASE
GLUCOSE-6-PHOSPHATE
HEXOKINASE
GLUCOSE
ADP
ATP
PHOSPHOHEXOISOMERASE
FRUCTOSE-6-PHOSPHATE
ATP
PHOSPHOHEXOKINASE
ADP
FRUCTOSE-1,6-DIPHOSPHATE
ALDOLASE
DIHYDROXYACETONE PHOSPHATE
TRIOSE PHOSPHATE ISOMERASE
GLYCERALDEHYDE-3-PHOSPHATE
DPNH2
DPN
GLYCEROPHOSPHATE DEHYDROGENASE
GLYCEROPHOSPHATE
H2O
H3PO4
GLYCEROL
DPN
H3PO4
DPNH2
PHOSPHOGLYCERALDEHYDE DEHYDROGENASE
(IODOACETATE INHIBITION)
1,3-DIPHOSPHOGLYCERIC ACID
ADP
ATP
GLYCEROPHOSPHATE TRANSPHOSPHORYLASE
3-PHOSPHOGLYCERIC ACID
PHOSPHOGLYCEROMUTASE
2-PHOSPHOGLYCERIC ACID
H2O
ENOLASE (FLUORIDE INHIBITION)
PHOSPHOENOLPYRUVIC ACID
ADP
ATP
PHOSPHOPYRUVIC TRANSPHOSPHORYLASE
PYRUVIC ACID
(SULFITE INHIBITION)
LACTIC ACID
LACTIC DEHYDROGENASE
DPN
DPNH2

Figure 2

phate was an obligatory participant in the breakdown of glycogen, and that a phosphorylated monosaccharide was formed in the reaction. It was later identified as glucose-1-phosphate.

Humphrey has investigated the utilization of monosaccharides in oyster muscle glycolysis. He found that fructose, glucose, galactose and mannose could not act as substrates for the reaction (9), but that glucose-1-phosphate, glucose-6-phosphate and fructose diphosphate could (32). However, Cleland reports (33) that in unfertilized oyster egg homogenates, glucose, and fructose stimulated respiration, but not galactose, arabinose or xylose. This would seem to indicate that hexokinase, the enzyme which phosphorylates hexose sugars such as glucose and fructose, is present in the eggs but not in the adult. It would be interesting to see if larval stages can utilize these sugars.

A study of the phosphatase reaction reveals that two enzymes are present. Roche et al (10) reports that one acid phosphomonoesterase functions best at pH 4.2 - 4.5 and is not activated by magnesium. The other is most active at pH 5.6 and is stimulated by this metal.

Glaister and Kerly (34) have observed that iodoacetate, sodium fluoride and sodium sulfite inhibit oxygen uptake in manometric experiments employing retractor muscle of *Mytilus edulis.* Inhibition effects are well known biochemical phenomena and can be interpreted as evidence that specific enzyme systems are being inactivated. With respect to the mode of action of iodoacetate, the enzyme glyceraldehyde phosphate dehydrogenase (triose phosphate dehydrogenase) which catalyzes the conversion of 3-phosphoglyceraldehyde to 1, 3-diphosphoglyceric acid, is strongly inhibited by iodoacetate ion. Similarly the reaction leading from 2-phosphoglyceric to phosphoenolpyruvic acid is catalyzed by a fluoride-sensative enzyme, enolase. Sulfite functions to trap pyruvic acid. When the mechanism for the reoxidation of reduced diphosphopyridine nucleotide ($DPNH_2$) is blocked, dihydroxy acetone phosphate is reduced by $DPNH_2$ in the presence of the enzyme glycerophosphate dehydrogenase to glycerophosphate. Under these conditions, the latter compound and pyruvic acid may be formed in equal amounts from fructose diphosphate. Hydrolysis of glycerophosphate results in the production of glycerol. Cleland (33) has found that both glycerophosphate and glycerol stimulate respiration of oyster egg homogenates.

That DPN is essential for the glycolytic system of the adductor muscle of *Saxostrea* has been demonstrated by Humphrey (9). He also observed inhibitory effects of fluoride and iodoacetate on pyruvic and lactic acid production. Presence of lactic acid in oysters had been previously reported by Kobayashi (35) and others (36). Intermediate compounds in the glycolytic cycle have been isolated as barium salts by Humphrey (32). The metabolic pathway of glycogen breakdown and synthesis is summarized in Figure 2.

THE TRICARBOXYLIC ACID CYCLE

The series of reactions which constitutes the Krebs, citric acid or tricarboxylic acid cycle is the metabolic pathway by which pyruvic acid produced in the glycolytic system is ultimately oxidized to carbon dioxide and water. During this aerobic process, energy is generated in the form of phosphate bonds. Products of protein and lipid degradation such as amino acids and acetate may also be oxidized through this pathway. The preparative metabolism of such intermediates will be discussed in a subsequent section.

Cleland (33) has studied the oxidative metabolism of unfertilized oyster eggs. In respiratory experiments, citrate, ketoglutarate, succinate, fumarate and malate were stimulatory to homogenates. The presence of malic oxidase and succinoxidase systems as well as the formation of high energy phosphate during respiration would seem to indicate a functional tricarboxylic acid cycle.

In this reaction sequence, acetate produced by decarboxylation of pyruvate generally condenses with oxaloacetate to form citrate. Cleland and Humphrey (18) have found that pyruvate and oxaloacetate stimulate respiration, but that acetate was either not effective or inhibitory. This initial thiamine-catalyzed decarboxylation and subsequent condensation is only partially understood and requires further study.

Humphrey (8) has observed the effect of metabolic inhibitors on the succinoxidase system in adductor muscle homogenates of *Saxostrea.* Competitive inhibition by malonate (a structural analog of succinate) was demonstrated, and respiration was stimulated by the addition of the substate. This phenomenon was also noticed by Cleland in homogenates of unfertilized oyster eggs. This investigator has also determined the distribution of the enzymes of the tricarboxylic acid cycle (37). Cytochemical separation of egg components in the ultracentrifuge indicates that they are concentrated in the protein, yolk and mitochondrial fractions. A summary of the tricarboxylic acid cycle is presented in Figure 3.

A SUMMARY OF THE TRICARBOXYLIC ACID CYCLE

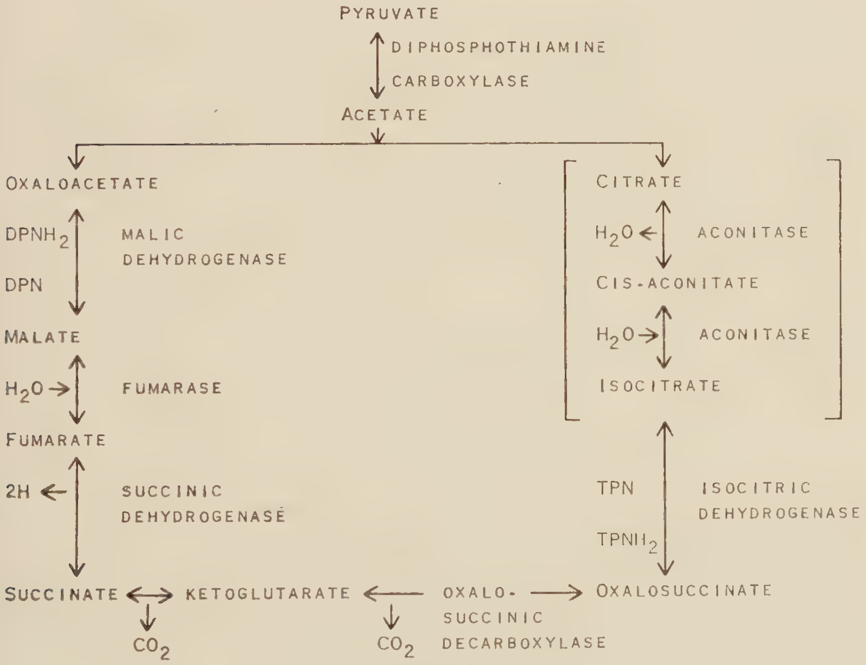
PYRUVATE
DIPHOSPHOTHIAMINE
CARBOXYLASE
ACETATE
OXALOACETATE
CITRATE
DPNH2
MALIC
DEHYDROGENASE
DPN
H2O
ACONITASE
CIS-ACONITATE
H2O
ACONITASE
MALATE
ISOCITRATE
H2O
FUMARASE
FUMARATE
2H
SUCCINIC
DEHYDROGENASE
TPN
ISOCITRIC
DEHYDROGENASE
TPNH2
SUCCINATE
KETOGLUTARATE
OXALO-
SUCCINIC
DECARBOXYLASE
OXALOSUCCINATE
CO2
CO2

Figure 3

TERMINAL OXIDATION

The series of steps by which hydrogen, produced as a result of dehydrogenation reactions in glycolysis and the tricarboxylic acid cycle, is transferred to oxygen, with the formation of water and concurrent liberation of energy will not be considered. The coenzymes which initiate the process, Diphosphopyridine nucleotide (DPN) and Flavin adenine dinucleotide (FAD) require the vitamins niacin and riboflavin respectively. By reversible reduction and oxidation, hydrogen is in turn transferred from DPN to FAD to the iron-dependent cytochromes. Water is ultimately formed through the action of cytochrome oxidase.

Cleland (33) and Humphrey (18) have studied this series of reactions in oysters. The former found that addition of DPN increased respiration. He also employed cyanide inhibition to show that respiration was mediated by a cytochrome-cytochrome oxidase system. The latter used methylene blue as an indicator to demonstrate that cytochrome increased oxygen uptake. Both DPN and cytochrome have been identified in tissue homogenates.

The effect of narcotics and other respiratory inhibitors on adductor muscle homogenates of *Saxostrea* has also been invesigated by Humphrey (38). Phenyl urethane, chloral hydrate salicylic acid, morphine, caffeine, barbitone, benzoic acid, salicylamid, and benzamid reduced oxygen consumption in these preparations. The steps involved in terminal oxidation are summarized in Figure 4.

TERMINAL OXIDATION

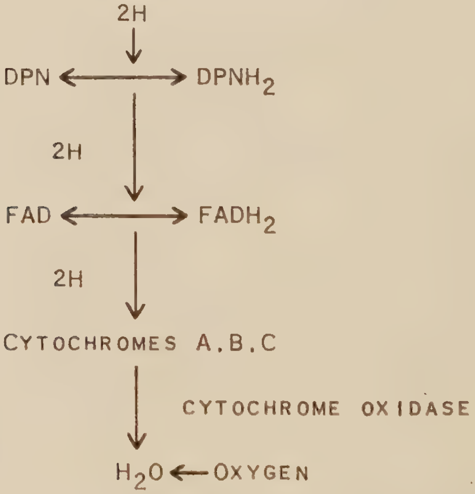

Figure 4

METABOLISM OF NITROGEN COMPOUNDS

The present knowledge of nitrogen metabolism in pelecypods is in general limited to the catabolic processes. Digestion of proteins and peptides, oxidative decomposition of amino acids and purines, and excretory mechanisms have been investigated, but little is known of synthetic phenomena.

ENZYMATIC DEGRADATION OF DIETARY NITROGEN COMPOUNDS

Tissue proteins derived from ingestion of plants or animals must be broken down to amino acids or other relatively simple nitrogen compounds before they can be utilized in the synthesis of new proteins or oxidized for energy. Proteolytic enzymes are required to catalyze the hydrolytic cleavage of peptide bonds which link the constituent amino acids to one another. In lamellibranchs, Yonge (39) considers such enzymes as primarily intracellular. Glycerol extracts of the digestive glands of *Mytilus, Ostrea* and *Mya* have been prepared by Rosen (40). Strong proteolytic activity was observed, and the endopeptidase cathepsin was identified. Mansour-Bek (41, 42) studied digestive enzymes in the gastric juice of *Tridacna* and other species. She demonstrated the presence of enzymes capable of degrading the natural protein fibrin, the polypeptide peptone, and the synthetic tri-and dipeptides leucylglycylglycine, leucylglycine and glycylglycine. Aqueous extracts of digestive diverticula prepared by Sawano (28) have been shown to contain proteolytic enzymes which digest casein and gelatin.

DECOMPOSITION OF METABOLIC NITROGEN COMPOUNDS

The nature of the amino acids present in pelecypods has been studied by Duchateau-Bosson et al (43). Fifteen non-protein amino acids were detected in tissues of *Mytilus* and *Ostrea*:

Glycine
* Proline
* Arginine
* Glutamic acid
Alanine
Aspartic acid
* Lysine
Threonine
Valine
Isoleucine
* Leucine
* Histidine
Methionine
* Phenyl alanine
* Tyrosine

Analysis of protein amino acids from marine molluscs by Zikeev (44) indicates tryptophane and asparagine (the amide of aspartic acid) and eight others noted above (*). Cysteine was not present in these samples.

Basic amino acids and other nitrogenous products of protein degradation have been reported in hot aqueous clam extracts. In addition to arginine and histidine, Sugino (45) reported taurine (a decarboxylation product of cysteic acid), betaine (the trimethyl derivative of glycine), trimethyl amine, the purines adenine and hypoxanthine, a guanidine derivative as well as a polypeptide containing lysine. Ataxopyrimidine, an organic acid with a basic nucleus, has also been found in clams (46).

Nitrogen compounds (derived from protein degradation) when present in excess of the organisms synthetic requirements may either be excreted as amino acids and purines, or deaminated by an amino oxidase. This type of enzyme attacks amino acids according to the following general equation:

Amino acid plus Oxygen gives Hydrogen peroxide plus
Imino acid which then gives Keto-acid plus Ammonia

Hydrogen peroxide produced as an intermediate in this reaction is decomposed to water and oxygen by the action of catalase (21).

Keto-acids formed by deamination may be oxidized by the tricarboxylic acid cycle. This would explain the stimulatory effect of aspartate and glutamate on respiration of unfertilized oyster egg homogenates observed by Cleland (33). Thus deamination may transform these amino acids to oxaloacetate and ketoglutarate, which are constituents of the oxidative cycle. Although glycine, alanine, leucine and tyrosine do not stimulate oyster eggs, glycine but not glutamate increases respiration of oyster spermatozoa. Apparently different enzymes are active in each of these preparations.

Blaschko and Hawkins have reported an amino acid oxidase present in *Mytilus* but absent in the fresh water mollusk *Anodonta.* This enzyme appears to be concerned with the synthesis of amino acids rather than their breakdown.

The function of arginine phosphate in invertebrate muscle is analogous to that of creative phosphate in vertebrate muscle. Kossel (11) demonstrated that basic proteins of cell nuclei (protamines and histones) yield large proportions of this amino acid on hydrolysis. Octopine, a derivative of arginine, is found in the muscle of scallops and other marine invertebrates. The nature and distribution of metabolic derivatives of arginine in invertebrate tissues has been investigated by Roche et al (49). They report that marine invertebrates in general contain no methyl guanidine, but may contain agmatine (a decarboxylation product of arginine), other monosubstituted guanidines such as guanidino-keto-valeric acid, and guanidino-butyric acid. Extracts of muscle, digestive tract and hepatopancreas of a number of molluscs have been shown to contain these acids (50). When arginine was added to a hepatopancreas preparation of *Mytilus,* it was converted to the first of these monosubstituted guanidines. Subsequent oxidative decarboxylation mediated by an amino oxidase resulted in the formation of guanidino-butyric acid (51). Thoai (52) concludes that arginine metabolism is essentially oxidative.

Initial degradation of nucleoproteins yields a protein and nucleic acid moiety. The protein fraction is further broken down to amino acids as described earlier, whereas the nucleic acid may be split to nucleotide units. These in turn may lose ammonia by the action of nucleotide deaminases to produce purine and pyrimidine nucleosides. Duchateau-Bosson et al (53) report that such enzymes are not present in invertebrates. Although purines may be excreted as such (54) Wolf and others (55, 56) have presented evidence that they can be oxidized. Adenase, guanase, and xanthine oxidase (57) have been detected in molluscs by Florkin et al (58). Adenine can therefore be deaminated to hypoxanthine, and then oxidized to xanthine and uric acid. Similarly, guanine may be deaminated to xanthine and subsequently oxidized to uric acid. In *Mytilus,* uricase can further oxidize uric acid to allantoin. Enzymatic hydrolysis by allantoinase converts allantoin to allantoic acid. Further hydrolysis results in the formation of urea, which is ultimately decomposed to ammonia and carbon dioxide by means of urease (59).

The metabolic fate of pyrimidines and their nucleotides derived from nucleic acids have not been investigated in marine pelecypods, however, enzymatic deamination has been demonstrated in other animal tissues.

Transmethylation (transfer of methyl groups) is employed in the production of metabolites and detoxication of noxious compounds. Thoai and Robin (60) have found that *Pecten* lacks a methylating enzyme, and cannot methylate guanidine-acetic acid. Methylation of this compound would result in the formation of creatine. Overall nitrogen metabolism is summarized in Figure 5.

METABOLISM OF LIPIDS

Comparatively little is known of the nutritional processes in marine pelecypods concerned with the metabolism of those biochemical substances which are soluble in organic solvents. Enzymatic breakdown of a number of fats, fatty acids, and their esters has been observed; and analytical studies indicate the

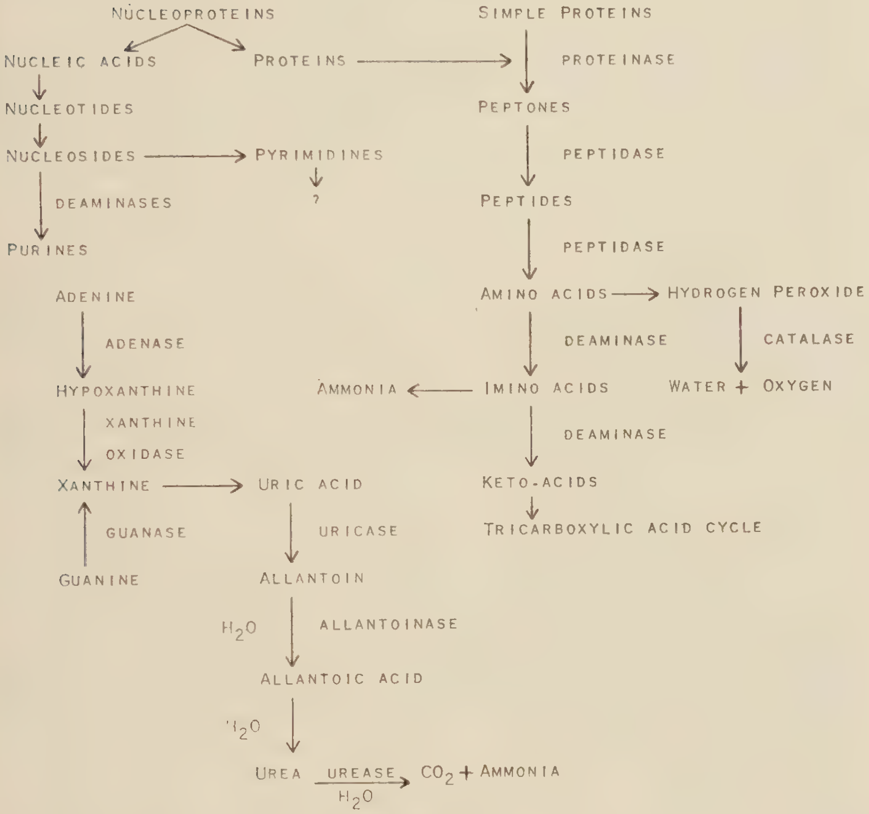
A SUMMARY OF NITROGEN METABOLISM

NUCLEOPROTEINS
NUCLEIC ACIDS
PROTEINS
NUCLEOTIDES
NUCLEOSIDES
PYRIMIDINES
?
DEAMINASES
PURINES
ADENINE
ADENASE
HYPOXANTHINE
XANTHINE OXIDASE
XANTHINE
GUANASE
GUANINE
URIC ACID
URICASE
ALLANTOIN
H2O
ALLANTOINASE
ALLANTOIC ACID
H2O
UREA
UREASE
H2O
CO2 + AMMONIA
SIMPLE PROTEINS
PROTEINASE
PEPTONES
PEPTIDASE
PEPTIDES
PEPTIDASE
AMINO ACIDS
HYDROGEN PEROXIDE
CATALASE
WATER + OXYGEN
DEAMINASE
AMMONIA
IMINO ACIDS
DEAMINASE
KETO-ACIDS
TRICARBOXYLIC ACID CYCLE

Figure 5

presence of a variety of phospholipids, sterols and carotenoids, but the mechanisms of lipid synthesis remain to be explained.

Degradation of dietary lipids by lipolytic enzymes or lipases have been invetsigated by Yonge (27, 39), Mansour (25), Mansour-Bek (61) and others. Enzymes found in gastric juice could split fats (free or as esters) (41), olive oil and tributyrin (42). Hydrolytic action by such enzymes results in the formation of glycerol and fatty acids. Sawano (28) has possibly demonstrated a butyrase in the crystalline style.

Fatty acids, namely, acetic, propionic, butyric and formic, when incorporated with oyster spermatozoa caused slight inhibition to their respiration (18). The phospholipid lecithin has no such effect on this preparation. Cleland (33) reports that respiration of unfertilized oyster egg homogenates was stimulated by butyrate, caproate, and lecithin, but not by acetate, propionate and acetoacetate. Higher fatty acids inhibited respiration even after ATP was added. Addition of tricarboxylic acid intermediates did not effect non-oxidation of such acids.

Mingo and others (62) have analyzed the fatty component of *Mytilus*. The report stearic and myristic acids in the solid fraction, culpanodonic and arachidonic acids in the liquid fraction, and the phospholipids lecithin, cephalin and sphingomyelin (63). Lanosterol, cholesterol as well as two forms of Vitamin D were noted in the unsaponifiable matter of this mussel. In other pelecypods the principal sterols have been shown to be other than cholesterol, namely, brassicasterol, meretristerol, conchasterol, ostreasterol and shakosterol (64).

The comparative biochemistry of carotenoids has been review by Goodwin (65) and Fox (66). Scheer (67) has presented evidence that xanthophylls play a positive role in the metabolism of *Mytilus californicus.* Activities of feeding as well as gametogenesis appear to be associated with increased destruction of pigment. Biochemical studies on the pearl oyster also indicate a relation between lipid content and spawning (68).

GROWTH FACTORS

In addition to their gross food requirements, heterotrophic organisms have been shown to need accessory factors in small amounts for normal growth. These substances have proved to be relatively simple organic compounds which generally function as coenzymes in vital catalytic systems. If such growth factors cannot be synthesized by the organism and must be supplied from an exogenous source, they can be considered as vitamins. Although no such requirement has been established for marine pelecypods, some of the better known vitamins have been detected in tissue extracts, others have been shown to be essential for specific enzymatic reactions, but only one has been studied extensively.

The unity of comparative biochemistry is shown by the universal requirement for thiamine. This water-soluble vitamin must be supplied to all animals which do not play host to thiamine-synthesizing microorganisms. Its role as coenzyme in the decarboxylation of pyruvic acid has been previously discussed with reference to carbohydrate metabolism. Thiamine as well as co-carboxylase (diphosphothiamine) have been reported in marine pelecypods. Keller's analysis (69) indicates the phosphorylated form but not free thiamine is present in the muscle of *Mytilus,* however, Goldbeck (70) and others have been able to find thiamine as such in oysters (71) as well as mussels (72). Interest in the thiamine-destroying enzyme found in shellfish and other aquatic forms has stimulated a number of fundamental studies on its biochemical nature and activity. The demonstration of reversibility of thiaminase is particularly significant with respect to nutritional metabolism. When pyrimidyl bases and thiazole were incubated with clam extracts containing this enzyme, thiamine was formed (73). This indicates that the clam can enzymatically synthesize Vitamin B_1 from these precursors.

The importance of niacin and riboflavin as functional components of Diphosphopyridine nucleotide and Flavinadenine dinucleotide has been presented in connection with terminal oxidation. Investigations by Humphrey (18) and Cleland (33) have demonstrated that DPN is required for glycolysis and that it stimulates respiration in oysters. Analyses by Hjarde et al (72) and other workers (71) indicate that both niacin and ribflavin are present in oysters and mussels.

The newest of the B Vitamins, Cobalamin, or Vitamin B_{12} has also been detected in soft and hard clams (23) as well as other molluscs (74). Although the function or functions of this cobalt-dependent vitamin is still being elucidated, it appears to be involved in the metabolism of nucleic acid and the formation of labile methyl compounds. This phase of pelecypod biochemistry has not been studied.

Posternak (75) has prepared a methyl inositol from the adductor muscle of *Mytilus* which has been named Mytilitol. Closely related cyclic polyhydroxy alcohols have been shown to exhibit vitamin-like activity in rats, however the status of these compounds as vitamins for other animals has been questioned.

The function of ascorbic acid as a reducing agent has not been linked with any specific metabolic process. Mussel catalase is inactivated by Vitamin C (17) and investigations on oysters and other shellfish indicate that the concentration varies with the organ analyzed.

Comparatively little is known of the metabolic functions of the fat soluble vitamins found in marine lamellibranchs. The Vitamin A content of mussels has been discussed by Scheunert (76). Goodwin (65) has considered the carotenoids which are asociated with vision and cites the work of Wald (77) and others. The occurance of several forms of Vitamin D has been reviewed by Bergmann (64) with respect to pelecypods. It is interesting that the provitamin D content of *Mytilus* and *Modiolus* has been found in such concentrations as to make commercial use of these forms feasible in vitamin preparations.

Investigations conducted at the New Jersey Agricultural Experimental Station have been reported (78) in which oysters were fed Vitamin D, to determine its effect on calcium metabolism. Preliminary results appear to be encouraging, but no detailed information has been supplied.

Finally this effect of administering a vitamin to promote shell growth brings to mind the carbohydrate factor which has been observed by Collier et al (79). The rate of feeding in oysters has been related to the concentration of a dissolved organic substance present in natural sea water.

The nutritional significance of dissolved organic substances in sea water which may function as growth factors for marine organisms has been discussed in preliminary reports submitted to the Woods Hole Oceanogrphic Institution by this author (80).

CONCLUSION

A great deal of factual data has accumulated since the techniques of the biochemist have been applied to the study of marine pelecypods. In the present review, an attempt has been made to arrange some of this information into a coherent plan of the mechanisms involved their nutrition. The metabolic processes have been considered as several sequential biochemical events. In addition, the author has tried to associate these phenomena with the physiological activity of the organism and its environment. It is hoped that this discussion will aid in the recognition of areas which require further study, and stimulate research in the nutritional problems which are fundamental to shellfish biology.

The author is indebted to H. J. Turner for critical reading of the manuscript. His comments and suggestions were invaluable to the final preparation of this review.

REFERENCES

1. Prosser, C. L., Ed., Comparative Animal Physiology, W. B. Saunders Co., Philadelphia (1950).
2. Scheer, B. T., Comparative Physiology, John Wiley, New York (1948).
3. Kidder, G. W., The Nutrition of Invertebrate Animals, in Biochemistry and Physiology of Nutrition, Ed. Bourne, G. H. and Kidder, G. W., 2 Academic Press, New York (1953).
4. Korringa, P., Quart. Rev. Biol., 27, 266-308, 339-365 (1952).
5. Irving, H. and Williams, R. J. P., Nature 162, 746 (1948).
6. Dugal, L. P., J. Cellular. Comp. Physiol. 13, 235-52 (1939).
7. Dugal, L. P. and Fourtier, G., Ann. ACFAS 7, 112 (1941).
8. Humphrey, G. F., J. Exptl. Biol. 24, 352-60 (1947).
9. Humphrey, G. F., Australian J. Exptl. Biol. Med. Sci. 22, 135-8 (1944).
10. Roche, J. et al, Bull. Soc. Chim. Biol. 34, 698-702 (1952).
11. Fruton, J. S. and Simmonds, S., General Biochemistry, John Wiley, New York (1953).
12. McElry, W. D. and Glass, B., Phosphorus Metabolism 1, John Hopkins Press. Baltimore (1951).
13. Humphrey, G. F., Australian J. Exptl. Biol, Med. Sci. 24, 261-7 (1946).
14. Bevelander, G. and Krimsky, F., Bermuda Biol. Sta. Ann. Report (1949).
15. Bevelander, G., Biol. Bull., 102, 9-15 (1952).
16. Ronkin, R. R., Proc. Soc. Exptl. Biol. Med. 73, 41 (1950).
17. Marks, G. W., J. Biol. Chem. 115, 299-314 (1936).
18. Humphrey, G. F., Australian J. Exptl. Biol. Med. Sci. 28, 1-13 (1950).
19. Humphrey, G. F., Physiol. Comparata et eocol. 1, 89-94 (1948).
20. Rangenecker, P. V., J. Univ. Bombay, Sect. B 21, Pt. 3, 88-9 (1952).
21. Fox, D. L. and Marks, G. W., Bull. Scripps Inst. Oceano., Univ. Calif. Tech. Series 3 (1934).
22. Galtsoff, P. S., Collect. Net. 16, 5 (1941).
    Galtsoff, P. S., Physiol. Zool. 15, 210-215 (1942).
23. Proctor, B. E. and Lang, D. A., Nature 168, 36-7 (1951).
24. Stolkowski, J., Ann. Inst. Oceanog. (Paris) 26, No. 1, 113 pp. (1951).
25. Mansour, K., Nature 157, 482 (1946).
26. Coe, W. R., J. Exptl. Zool., 99, 1-14 (1945).
27. Yonge, C. M., J. Marine Biol. Assoc. United Kingdom 14, 295 (1926).
28. Sawano, E., Sci. Rept. Tohoku Imp. Univ. IV 24, 327 (1949)
29. Yonge, C. M., Science Progress 32, 1 (1938).
30. Lavine, T. F., J. Cellular Comp. Physiol. 28, 183 (1946).
31. Cori, C. F., et al., J. Biol. Chem. 121, 465 (1937).
32. Humphrey, G. F., Australian J. Exptl. Biol. Med. Sci. 28, 151-60 (1950).
33. Cleland, K. W., Proc. Linnean Soc. N.S. Wales 75, 296-313 (1950).
34. Glaister, D. and Kerly, M., J. Physiol. (London) 87, 56-66 (1936).
35. Kobayashi, S., Sci. Rep., Tohoku Imp. Univ. IV 4, 193 (1929).
36. Dotterweich, H. and Elssner, E., Biol. Zentr. 55, 138 (1935).
37. Cleland, K. W., Australian J. Exptl. Biol. Med. Sci. 29, 35-45 (1951).
38. Humphrey, G. F., J. Mar. Biol. Assoc. United Kingdom 27, 304-12 (1948).
39. Yonge, C. M., Nature 157, 729 (1946).
40. Rosen, B., Arkiv Kemi 1, 205-11 (1949).
41. Mansour-Bek, J. J., Actualities biochim 10, 41-6 (1947).
42. Mansour-Bek, J. J., Enzymologia 12, 221-3 (1948).

43. Duchateau-Bosson, G., et al., Arch inter. physiol. 60, 124-5 (1952).
44. Zikeev, B. V., Chem. Zentr. II, 716 (1948).
45. Sugino, K., et al., J. Chem. Soc. Japan 72, 252-5 (1951).
46. Sasaki, T., Vitamins (Japan) 4, 416-19 (1951).
47. Blaschko, H., and Hawkins, J., Biochem. J. 52, 306-10 (1952).
48. Baldwin, E., Biol. Rev. 8, 74 (1933).
49. Roche, J., et al., Compt. rend. soc. biol. 146, 1899-1902 (1952).
50. Thoai, N. van, et al., Compt, rend. 235, 832-4 (1952).
51. Robin, Y., Bull. soc. chim. biol., 35, 285-8 (1953).
52. Thoai, N. van, et al., Biochim et Biophys. Acta 11, 403-11 (1953).
53. Duchateau-Bosson, G., et al., Bull. classe sci., Acad. roy. Belg. 27, 169-73 (1941).
54. Delaunay, H., Biol. Rev. 6, 265 (1931).
55. Wolf, E., Z. Vergleich. Physiol. 19, 1 (1933).
56. Grah, H., Zool. Jahrb., Abt. Allg. Zool. Physiol. 57, 355-379 (1937).
57. Florkin, M. and Duchateau-Bosson, G., Bull. classe sci. Acad. roy. Belg. 27, 174-8 (1941).
58. Florkin, M. and Frappez, Compt. rendus soc. biol. 134, 117 (1940).
59. Brunel, A., Compt. rend. 206, 858-60 (1938).
60. Thoai, H. van and Robin, Y., Compt. rend. 232, 452 (1951).
61. Mansour-Bek, J. J., Nature 158, 378 (1946).
62. Mingo, M.de, and Calles, J. A., Rev. real. acad. cienc. exact. fis. y nat. Madrid 40, 361-92 (1946).
63. Mingo, M.de and Espunaco, J. de la Serra. Rev. real. acad. cienc. exact. fis. y nat. Madrid 45, 263-323 (1951).
64. Bergmann, W., J. Marine Research (Sears Foundation) 8, 137 (1949).
65. Goodwin, T. W., Carotenoids, their comparative biochemistry, 176 Chem. Pub. Co., N.Y., N.Y. (1952).
66. Fox, D. L., Ann. Rev. Biochem. 16, 443 (1947).
67. Scheer, B. T., J. Biol. Chem. 136, 275-99 (1940).
68. Ashikaga, C., J. Agr. Chem. Soc., Japan 24, 436-8 (1950-51).
69. Keller, M., Boll. soc. ital. biol. sper. 16, 718-19 (1941).
70. Goldbeck, G. G., Com. Fisheries Rev. 9, #8, 13-21 (1947).
71. French, R. B. and Townsend, R. O., Florida Agr. Exptl. Sta. Bull. 482, 5-9 (1951).
72. Hjarde, W., et al., Nord. Med. 48, 123-5 (1952).
73. Fujita, A., et al., J. Biol. Chem. 196, 313 (1952).
74. Maxwell, B. E., J. Fisheries Res. Bd. Canada 9, 164-8 (1952).
75. Posternak, T., Helv. Chim. Acta. 27, 457-68 (1944).
76. Scheunert, A., Ernahrung 2, 128-31 (1937).
77. Wald, G., Am. J. Physiol. 133, 479 (1941).
78. Martin, W. H., N. J. Agr. Exptl. Sta., Ann. Rept. 1945-46, 7-109 (1947).
79. Collier, A., et al., Science 111, 151 (1950)
80. Scher, S., unpublished reports, Woods Hole Oceanographic Institution, Woods Hole, Mass. (1954).

Contribution No. 785

Särtryck ur Tellus nr 2, 1955.

The Acidity of Scandinavian Precipitation

By

EARL BARRETT, Institute of Meteorology, University of Stockholm and Woods Hole Oceanographic Institution[1]

GUNNAR BRODIN, Royal Agricultural College, Uppsala

(Manuscript received March 3, 1955.)

Abstract

Data on the pH of the total monthly precipitation at stations of a Swedish network for sampling and chemical analysis of precipitation and atmospheric aerosols during the year July 1953—June 1954 are presented and discussed, together with the pH data from the first two months of operation of a larger pan-Scandinavian net. It is found that well-defined regions of acidity and alkalinity relative to the pH of water in equilibrium with atmospheric carbon dioxide exist, and that these regions persist to such an extent that the monthly deviations from the pattern of the annual mean pH at each station are relatively small. The mean pH of the entire network shows a distinct annual cycle, with greatest acidity in winter and greatest alkalinity in late spring. Coastal stations unaffected by local pollution show persistently high acidity, while inland northern stations show equally persistent alkalinity. Some possible reasons for the observed distributions are considered.

Introduction

Although there is doubtless a considerable number of spot observations of the acid-alkaline balance of precipitation which have been made and reported in various journals during the past, there has been no effort (so far as is known to the writers) to systematize such observations and present them in a significant and readily-assimilable form. One can readily recognize two reasons for this; the first reason is that the observations had been made for the most part by workers who are not trained in the concepts and techniques of synoptic observations and analysis, while the second is that, even if the observers felt the desirability of a synoptic presentation, the necessary organized network of stations for the purpose did not exist. Within the last few years both of the obstacles have been overcome to some degree. A network of stations has been established in Sweden for the purpose of analyzing one-month samples of precipitation for the principal ionic constituents. This net, originally established for agricultural purposes by the Royal Agricultural College of Sweden, has been extended by degrees, until, at the time of writing, it provides excellent coverage of Sweden and moderate coverage of Norway, Denmark and Finland. This network and the sampling equipment have been described in previous papers (Egnér and Eriksson, 1955; Rossby and Egnér, 1955).

The second obstacle has been removed by the establishment of a co-operative program between the Agricultural College and the Meteorological Institute of the University of Stockholm. The junior author of this paper has had the responsibility for the collection and chemical analysis of the samples, while the senior author has undertaken the work of synoptic analysis and meteorological interpretation of the data.

---

[1] Contribution No. 785 from Woods Cole Oceanographic Institution.

The objective of the paper is to present the results of a preliminary survey of the spatial and temporal variation of the acid-alkaline balance of precipitation. It should be made clear at the outset that this paper will pose many problems and solve few, if any, of them. The atmosphere, considered as a chemical system, is so highly multivariate that it resembles a biological or sociological system in complexity; thus one cannot expect to find the simple logical connections between single causes and effects which one looks for in connection with well-isolated physical systems. The most that one may expect in the preliminary stages of study of such a complex system is to narrow down the field of investigation by looking for the highest correlations, and to subject these to more searching study with the aid, wherever possible, of theoretical models and idealized laboratory experiments. The objective of this paper is the modest one of displaying the data in synoptic form and laying a number of study topics before the attention of others, in the expectation that interest will be stimulated and answers to the questions will be sought by investigators at other institutions at the same time that they are being pursued in Stockholm.

Presentation of the Observations

Samples of rain and/or snow collected by a small heated rain-gauge draining into a plastic sampling bottle are taken during each entire month at all the stations of the network. The data considered in this paper were collected during the period July 1953 through June 1954. During this period the net consisted of 19 stations, all within Sweden and with a maximum density in the southern half of the country. Starting in November 1954 the net became pan-Scandinavian in scope and was increased to a total of 44 stations. The data for the first two months of expanded operations will also be included in the presentation, as they emphasize certain points which are not so clearly illustrated by the smaller net.

The acidity or alkalinity of the samples has been determined by measurement of the electrical potential generated by the galvanic cell using a glass electrode and calomel electrode, with the sample as the electrolyte (Beckman pH meter, model G). The data are reported as pH units, *i.e.*, the negative of the common logarithm of the molar concentration of hydrogen ions in the sample.

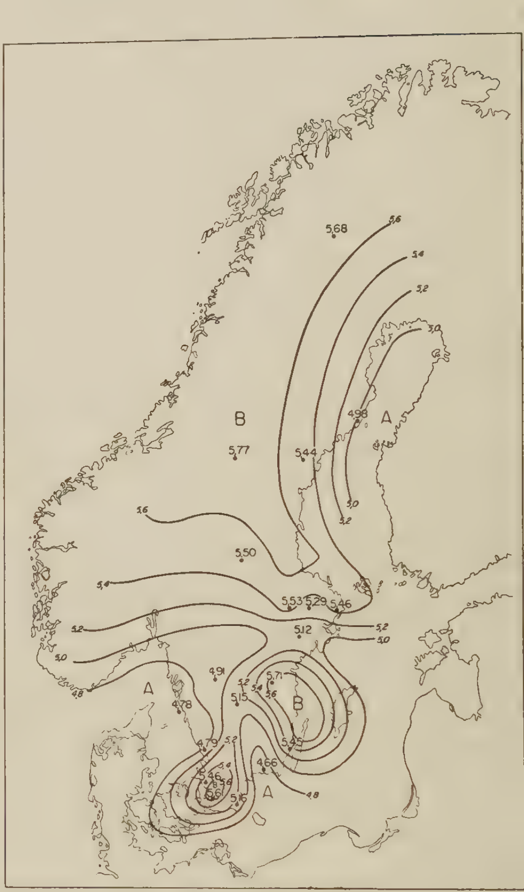

Fig. 1. Annual Mean pH of Precipitation, July 1953—June 1954.

It is customary in chemistry to take as neutral the pH value of 7.0 which is characteristic of ideally purified water at room temperature (25° C). However, the water in the atmosphere is in general not in this standard state of purity—in fact, it cannot possibly be Even if all soluble solid electrolytes and pollution could be kept out of the cloud water this water would always attempt to achieve equilibrium with the carbon dioxide pressure of the atmosphere. If one assumes that equilibrium is actually reached at the observed mean pressure of CO_2, the pH may be calculated from the known equilibrium constants to be 5.7 at 25° C. The variation with temperature is in the direct sense, although not linear

Since the samples are measured at room temperature, this value of 5.7 may be regarded as the neutral point for atmospheric water. This convention will be adopted in this paper. Thus pH values lower than 5.7 represent a net acidity for the sample, while values greater than 5.7 indicate a net alkalinity.

The monthly values for all stations have been entered on synoptic charts and isopleths of pH have been drawn for each month. In addition, two kinds of "mean" values have been computed. In calculating these, the pH numbers are converted to their negative antilogarithms (molar concentrations of hydrogen ion); these are then multiplied by the measured amount of the sample. The sum is formed and divided by the sum of the sample volumes; this concentration is then reconverted to a pH value. It is apparent that this procedure, analogous to the method of calculating the mean molecular weight of a mixture, gives the only physically significant mean; a simple arithmetic mean of the pH values is quite without significance because of the variation in precipitation in space and time and the inherently nonlinear nature of the pH unit.

The "mean" obtained by the weighting system described above represents the pH which would be measured by an instrument if all the samples being averaged were poured together into a common vessel and no CO_2 were allowed to escape from the solution; put in another way, it represents the strength of a solution of a completely ionized acid which would have brought the same amount of hydrogen ion per unit area to the ground as was brought by the rainfall. The fact that more alkaline samples would partly neutralize more acid ones if physically mixed is disregarded, since a measure of total acid rather than net acid is the quantity desired. It is clear that the monthly samples actually underestimate the total acid in cases where individual rains fluctuate in pH because of the loss of CO_2 when fractions of different pH combine; thus the pH figures for each month are really slightly too high if interpreted as a measure of total acid brought to the ground.

The mean, or effective, pH for the entire net (areal mean) for each month, and the mean for the year at each station have been calculated by the procedure described above.

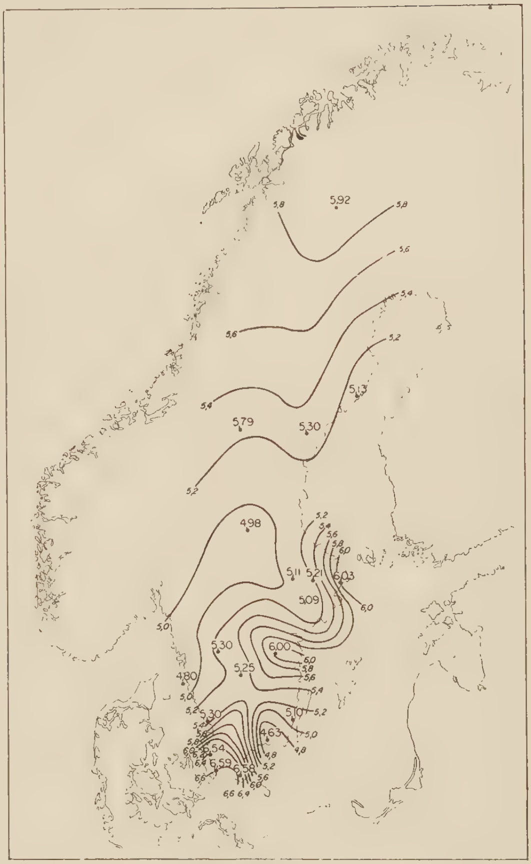

Fig. 2. pH of Precipitation, Sept. 1953.

Economy of page space does not permit the inclusion of the 15 charts which have been prepared. Figure 1 shows the distribution of the annual mean for each station for the year July 1953 to June 1954; this single chart displays most of the significant details which appear on the monthly charts. The two most atypical monthly charts are shown in Figs 2 and 3.

The principal features of the chart of Fig. 1 are: (a) the region of acid precipitation along the west coast; (b) the nearly neutral areas at the southwest tip of Sweden (Skåne) and along the southeast coast; (c) the acid tongue which separates these two neutral regions; (d) the acid region along the northeast (Bothnian) shore; (e) the large neutral or alkaline region covering the more elevated interior of Northern Sweden; (f) the acid "corridor" which joins the west-coast and Bothnian

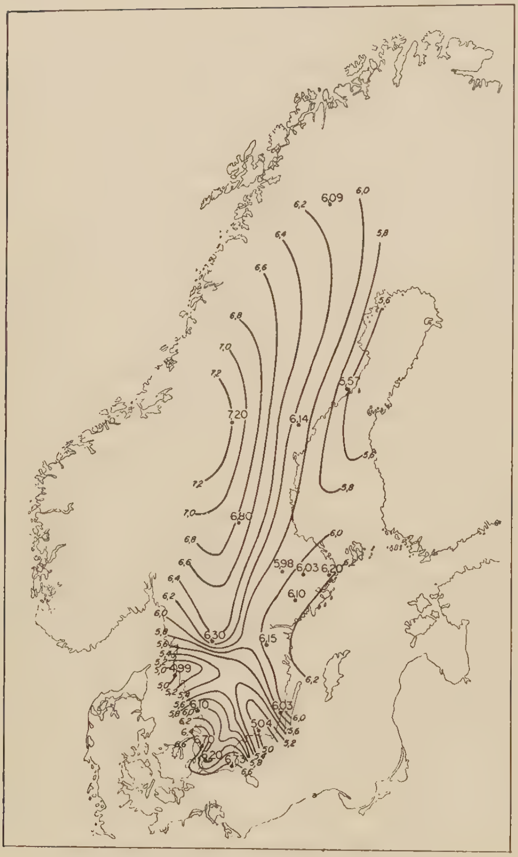

Fig. 3. pH of Precipitation, May 1954.

acid regions. This corridor shows a marked tendency to meander from month to month; in Fig. 2 it is shown displaced toward the northwest. When such a displacement occurs, a new region of alkalinity appears over the easternmost coastal region (Uppland). On other occasions the inland alkaline region extends southward to Uppland; the acid corridor then enters the Baltic farther south and the alkaline or neutral region of the south-east weakens strongly.

An examination of the monthly charts shows that the features discussed above are, in fact, semi-permanent features. The central values of pH fluctuate in magnitude from month to month and the positions of the centers shift slightly, but on the whole the pattern is remarkably persistent. The alkaline region of the northern interior (Norrland) does, however, show a distinct annual cycle; the pH is minimum there in late summer and is maximum in spring (compare Figs 2 and 3).

The monthly mean values for the entire network are shown plotted on the graph of Fig. 4. The solid curve applies to the values from the 19-station net for 1953—54, while the short dotted curve represents the means for the first two months of operation of the expanded 44 station net (November and December 1954). A distinct annual cycle is indicated, with a maximum of acidity (pH minimum) in the late fall and winter and a minimum acidity in the late spring. It is to be noted that, except for the month of May, the precipitation over Sweden as a whole is definitely more acid than the CO_2 equilibrium alone would permit; the neutral point is just reached in May. It is unfortunately true that the sampling in the alkaline north is sparse compared with the generally more acid south, so that allowance must be made for this in the interpretation; however, the curve would not be affected too strongly by the addition of more stations in the north because of the low winter precipitation there. The summer values would, however, be shifted upwards by the inclusion of more Norrland data. The two values for the new net (which has better northern coverage) show that the shift in the autumn means produced by doubling the number of stations is smaller than the month-to-month fluctuation.

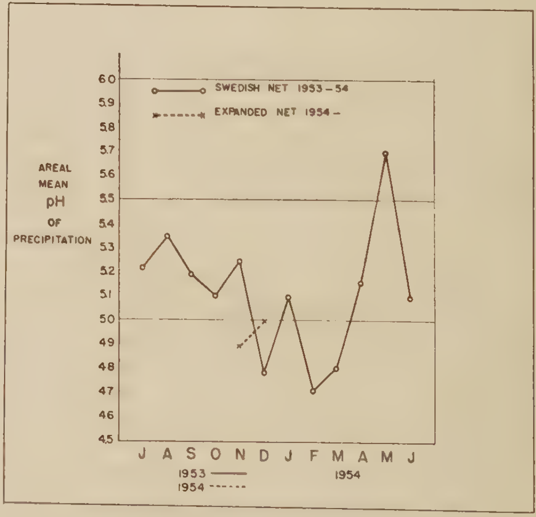

Fig. 4. Areal Mean of Precipitation pH vs. Time July 1953—June 1954 and Nov.—Dec. 1954.

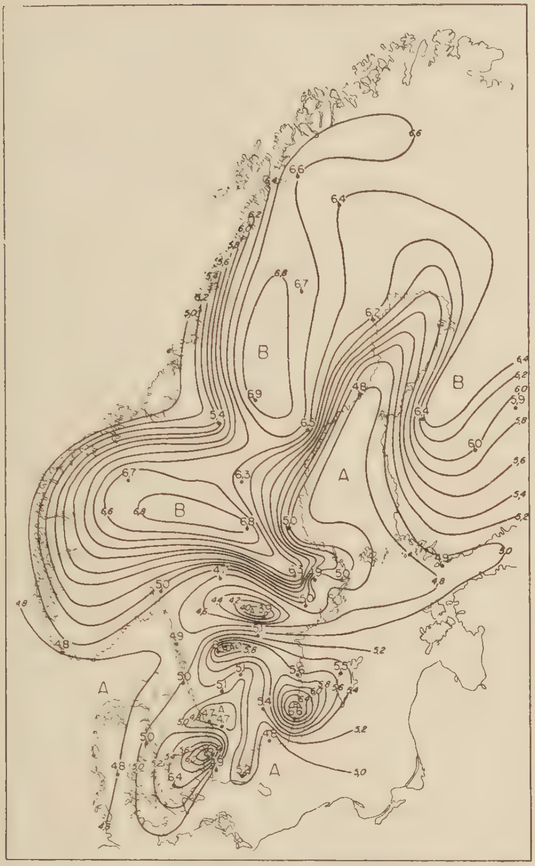

Fig. 5. pH of Precipitation—Expanded Network, November 1954.

Figs 5 and 6 show the pH distribution for the expanded network for the months of November and December 1954. It can be seen that the distribution is very much the same as for the smaller network; the acid character of most of the maritime regions and the alkaline character of the inland area are clearly illustrated. The acidity at the station in central Finland compared to the west Finnish station in the same latitude is, however, an anomalous feature.

Discussion

The data have shown that, on the whole, the precipitation over Sweden tends to be more acid than pure water in equilibrium with the carbon dioxide of the atmosphere. Furthermore, this excess acidity tends to be maximum at coastal stations and in the southern peninsula of Sweden, while the inland and northern regions tend to be neutral or slightly basic with respect to CO_2 equilibrium. The data from the larger network justify the extension of this picture to all of Scandinavia. The question of the source of the acid arises immediately. Examination of the anion analyses is not exceedingly helpful, since one cannot decide how much sulfate, for example, was collected as sulfuric acid and how much was picked up as neutral salts. One source which comes immediately to mind is combustion acids, primarily sulfuric acid, produced in densely populated and industrial regions. There is no particular difficulty in ascribing the acid tongue which enters Sweden from the south to this source, since the prevailing flow of air into this region is from the industrialized area of Central Europe during most rainy periods. The acid corridor across the southern peninsula of Sweden may also be attributed, at least in part, to such industrial acid. The acid region of the Sea and Bay of Bothnia may probably in part be due to the cellulose industries locates along the coasts in Norrland and Finland. One of the stations in the new network (Kvarntorp 1) is located in close proximity to a shale-oil plant; the pH values for this station are among the lowest recorded.

It appears difficult, on the other hand, to explain the high acidity of the precipitation on the south coast of Norway, the west coast of Sweden, the south coast of Finland and to some extent the coasts of the Sea and Bay of Bothnia as being caused by combustion products. It appears, therefore, that one must look to the sea itself as a source of acids. Provided that such a source can be found in the sea, the decreasing acidity with distance from the coast which is observed in areas free of pollution is readily explainable as a result of washing out of the acids by the precipitation, possibly coupled with addition of alkaline aerosols from the soil in snow-free months.

The next question is whether the sea can provide a source of volatile or easily-dispersed acid, and the chemical nature of this acid. Three possibilities immediately come to mind. The first of these is the possibility that organic acids which are products of biological activity may be concentrated in the thin surface film of the sea and dispersed from thence into the air by evaporation and/or the mechanical action of foaming and bubble breaking. This

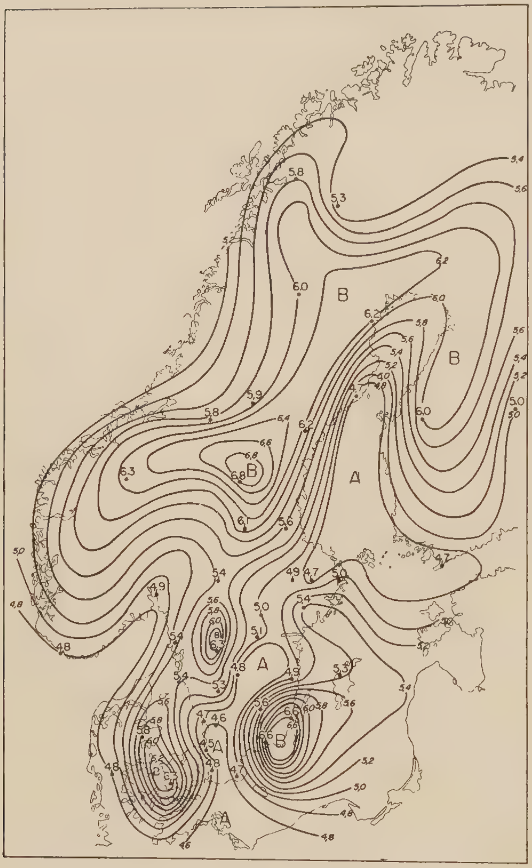

Fig. 6. pH of Precipitation—Expanded Network, December 1954.

possibility is amenable to experimental testing. Exactly the same argument applies to the hydrogen sulfide formed by biological action. This gas should be rather rapidly oxidized to SO_3 photocatalytically and by ozone, and would provide a supply of sulfuric acid. Unfortunately no data are apparently available on the rate of emission of H_2S from the sea, although it is known to occur. Presumably the gas is oxidized rather quickly, at least in daylight, and so the analyses of the air for sulfide would greatly underestimate the actual production. It remains to be determined whether or not this source strength is great enough to account for the observed acidity of the rainfall in coastal regions.

A third possible maritime source of acid may be sought in the ionic separation which has been observed to occur as a concomitant of the foaming of the sea surface (CAUER 1949, KÖHLER and BÅTH 1953). It is conceivable that the fine spray which ultimately becomes the source of many of the condensation nuclei is enriched in anions at the time of formation. This hypothesis is difficult to test, especially since the trapping and analysis of the smaller particles for anion-cation balance is no easy matter.

Although a decrease in acidity inland is to be expected as a result of the progressive washing-out of the (presumably maritime) acid contaminants as a precipitating air mass moves inland, it does not seem possible to account for pH values greater than about 5.7 in this way. In the mean, to be sure, the highest pH reported is 5.77 at Ås in central inland Sweden; however, the monthly values at the northern and inland stations are frequently above 6.0 and in a few cases above 7.0. It thus seems necessary to postulate the presence of alkaline aerosols of terrene origin. Examination of the concentrations of the various ions shows that many of these high pH values are associated with high calcium contents or a high ratio of calcium to sulfate; this suggests that aerosols of limestone are responsible for the alkalinity in the northern inland regions.

The two alkaline regions of Southern Sweden apparently result from a combination of pollution effects. The southeastern region coincides closely with the maximum area of surface limestone in Sweden; the Baltic islands of Gotland and Öland and the nearby Swedish coast possess considerable deposits of this mineral. The southwestern region, which also extends over eastern Denmark, is, in contrast to the area just mentioned, characterized by a high percentage of ammonium ions in most cases. The source of this ammonia is probably to be found in the extensive dairy farms of Denmark as a product of biological activity. However, a calcium pollution source exists at the southwest tip of Sweden in the form of a large cement factory; this point source frequently results in an anomalously high pH and calcium content at one or both of the two observing stations in this region. One may conclude, therefore, that the southwestern alkaline cell is clearly a result of human activity, in contrast to the southeastern cell and the northern inland.

The annual cycle of the network mean pH, Fig. 4, is interpretable as a combination of effects. The minimum in February-March coincides rather well with the time of maximum combustion of fuel. At the same time the prevailing air flow during rain periods is from the south. In May the situation is reversed; the combustion decreases and the prevailing air flow is from the north and northeast in connection with the blocking anticyclone over the British Isles and the North Sea. In summer the blocking breaks down and the rain-bearing air may arrive from any direction; the maritime and industrial acids which are brought in from southerly and westerly areas bring the pH down from the spring maximum of 5.7 to intermediate values of around 5.2.

It is admitted that the making of such generalizations on the basis of only one year's data is slightly presumptuous. The conclusions are therefore put forward as tentative suggestions, subject to later revision when several years of data have been accumulated.

It would be highly desirable to attempt to relate the pH of precipitation to the region of origin of the associated air mass and to the past history of the air mass. It is unfortunately impossible to accomplish this in an unambiguous way if one is constrained to use total monthly samples of precipitation. One may attempt to relate the pH distribution to the mean isobaric pattern for the month and so obtain characteristic charts of pH distributions associated with air flows from various directions. These may, however, be somewhat misleading, since the precipitation samples represent, for particular stations, only a fraction of the days in the month. Furthermore, it sometimes happens that all of the rainfall at the station occurs on one or two days with completely atypical flow patterns. The monthly mean pressure pattern can therefore only be used for correlation studies when an examination of the daily charts shows that most of the precipitation did indeed arrive with wind patterns closely resembling the mean flow. A more satisfactory approach (although much more laborious) is to calculate precipitation-wind roses for each station and, by a study of the daily synoptic charts, to estimate trajectories of the air for each rain day and each station. In this way the fraction of the total precipitation which derives from a particular source region may be computed for each station.

A much better approach to the problem of correlation of precipitation properties to air masses would be to equip some stations (in regions free of local pollution) with large-aperture precipitation collectors and to analyse the samples collected at such stations during a single rain period. This procedure is contemplated, and it is expected that more reliable correlations between precipitation chemical composition and air masses will be obtained thereby. In the meantime the monthly mean isobaric patterns provide the only readily calculable information for correlation studies, but they must be used with caution.

REFERENCES

Cauer, H., 1949: Ergebnisse Chemisch-meteorologischer Forschung. *Arch. f. Meteor., Geophys. u. Bioklimat.*, Ser. B, 1, 221—256.

Egnér, H., and Eriksson, E., 1955: Current data on the chemical composition of air and precipitation. *Tellus* 7, 134—139.

Köhler, H., and Båth, Markus, 1953: Quantitative chemical analysis of condensation nuclei from sea water. *Nova Acta Reg. Soc. Sci. Ups. Ser. IV, vol. 15, no.* 7.

Rossby, C.-G., and Egnér, H., 1955: On the chemical climate and its variation with the atmospheric circulation pattern. *Tellus* 7, 118—133.

PRINTED IN SWEDEN
ESSELTE, STHLM 55

Contribution No. 786

Reprinted from SCIENCE, December 16, 1955, Vol. 122, No. 3181, pages 1188–1189.

Calcium Uptake by a Coral

In the course of a series of experiments designed to test the usefulness of radioisotope tracers for the study of calcium deposition by corals, we have obtained some interesting data on the common Atlantic coral *Astrangea danae* (*1*). Pieces of living coral were placed in beakers one-third full of glass beads and containing 40 to 60 ml of sea water that had previously been filtered through No. 4 Whatman filter paper. Stirring and aeration were accomplished by means of jets of water-saturated air impinging on the surface. After the coral polyps became reextended, radioactive calcium-45 in neutralized sea water was added by pipette in amounts sufficient to give about 1000 counts per minute from 0.1-ml aliquots. All samples were spread to uniform area on copper planchets and counted at the same geometry with a 1.8-mg/cm² mica end-window Geiger-Müller tube. The high specific activity of the calcium-45 permitted very small additions of total calcium, never exceeding 0.1 µg/ml of the final solution, compared with about 400-µg/ml concentration in normal sea water.

At intervals, polyps were sampled by snipping off the distal half with fine scissors. These were blotted on filter paper, quickly weighed, dried on planchets, and counted. The counts were compared with those made on the sea water, aliquots being taken immediately before and after sampling the polyps. These data are summarized in Table 1, which covers polyps from six different colonies in two separate experiments.

Table 1. Calcium equilibrium between coral polyps and sea water. Counts given are means.

Time (hr)	Counts/min per µl water	Counts/min per mg fresh polyp	Polyps (No.)
6	10.0	9.3	5
11	10.9	9.0	6
23	10.0	7.0	2
31	9.6	9.3	3
50	9.4	8.7	4

Evidently isotope exchange equilibrium between the polyp-tissue calcium and outside sea-water calcium is reached in less than 6 hours. The exchangeable calcium of the tissues is apparently maintained at about 88 percent of the calcium concentration of the medium. Actually, this figure should be high, because the uncompensated errors from occluded sea water and from the slight differences in self-absorption in the counted samples both tend in that direction. The findings thus agree fairly well with Hosoi's (*2*) analytic data for tissue calcium in sea anemones (74.5, 72.8 and 66.3 percent of the concentration in medium, respectively, for three species).

Table 2. The calcium-45 content of sea-water samples after various times of contact with living and dead coral as compared with a sea-water control. All counts given are mean counts/min per µl of water.

Time (hr)	Living coral*	Dead coral†	Control†
1	10.4	3.5	3.2
11	10.6	3.3	3.5
23	11.0	3.2	3.8

* Mean of three experiments.

† Initial calcium-45 activity was one-third that added to the living coral.

In Table 2 the calcium-45 contents of sea-water samples after various times of contact with living coral colonies, or with dead corallum treated in various ways, are compared with blank series that consisted simply of sea-water samples stirred by air, in beakers. The temperature was maintained at 8° to 10°C by circulating sea water. At this temperature *Astrangea* does not appear to grow at all. The withdrawal of calcium-45 by isotopic exchange with the corallum was well below the 5 percent that could have been detected. No effect appeared to be produced by heavy feeding before an experiment, or even during an experiment. Tiny bits of ground fresh fish bone, when these occurred in the food mixture, attained radioactivities per unit volume of 10 to 20 times that of the medium.

The solutions in these experiments contained from 50 to 75 mg of $CaCO_3$, whereas the coral specimens represented 4 to 6 g of $CaCO_3$. It is evident, then, that isotopic exchange between corallum and medium involved only the free surface of the carbonate crystals and may consequently be assumed to have reached equilibrium rather quickly. This was unexpected, in view of the degree to which all our specimens of *Astrangea* have been riddled with boring sponges. It appears to promise that in experiments on rapidly calcifying reef corals, calcium-45 incorporated by exchange will be readily differentiable from that incorporated by active deposition; it also appears to promise that it will thus be possible to establish actual rates of deposition and to ascertain by what physiological factors the rates are controlled. One of us (T.F.G.) is embarking on such a study.

T. F. Goreau*
V. T. Bowen
Woods Hole Oceanographic Institution,
Woods Hole, Massachusetts

References and Notes

1. Contribution No. 786, Woods Hole Oceanographic Institution. This work was supported by Office of Naval Research contract Nonr 1238-(00). Calcium-45 was obtained from Oak Ridge National Laboratory on allocation from the U.S. Atomic Energy Commission. James McInnis of the Marine Biological Laboratory, Woods Hole, Mass., contributed the living coral.
2. K. Hosoi, *Science Repts. Tôhoku Univ. Fourth Ser.* 10, 377 (1935).

* Permanent address: Department of Physiology, University College of the West Indies, Mona, St. Andrew, Jamaica, British West Indies.

16 July 1955

Contribution No. 787

B R E V I O R A

Museum of Comparative Zoology

Cambridge, Mass. November 18, 1955 Number 49

THREE NEW SHARK RECORDS FROM THE GULF OF MEXICO

By Henry B. Bigelow, W. C. Schroeder and Stewart Springer[1]

The trawlings recently carried out by "Oregon" of the U. S. Fish and Wildlife Service in the Gulf of Mexico have yielded two specimens of *Etmopterus pusillus* (Lowe) 1839, one of *Centrophorus granulosus* (Bloch and Schneider) 1801, and one of *Dalatias licha* (Bonnaterre) 1788, sharks that had long been known in the eastern side of the Atlantic, but which had not been reported previously from the Gulf, though one specimen of *Dalatias* has been taken on the northern edge of Georges Bank.

As the Gulf of Mexico specimens of *E. pusillus* and of *C. granulosus* are the first of their kinds to be reported from the western side of the Atlantic or tributary waters, brief accounts follow to emphasize such of their diagnostic characters as may not be immediately apparent from the accompanying illustrations (Figs. 1, 2), and to justify our identifications of them.

Genus ETMOPTERUS Rafinesque 1810

Type species *Squalus spinax,* Linnaeus 1758

Whitley (1939, p. 266) has recently revived the genus *Acanthidium* Lowe 1839, type species *Centrina nigra* Lowe 1834 which, in 1839, Lowe renamed *Acanthidium pusillum,* thinking it separable generically from *Etmopterus* Rafinesque 1810, type species *Squalus spinax* Linnaeus 1758. But the differences in fin-characters cited by Whitley do not seem to us sufficient to justify this separation. And the specific name *niger* is preoccupied in *Etmopterus* by *nigrum* (Cloquet) 1820,[1] p. 93 and various subsequent authors, proposed as a substitute for *spinax* Linnaeus 1758.

---

[1] Contribution No. 787. Woods Hole Oceanographic Institution.

ETMOPTERUS PUSILLUS (Lowe) 1839

Study material. Male, 445 mm. long, U. S. Nat. Mus. No. 157835, and female of 458 mm., Mus. Comp. Zool. No. 39572, northern part of Gulf of Mexico, "Oregon" Station 1281, Lat. 29°13′ N., Long. 87°54′ W., in 250 fathoms. Also female 278 mm. long, Madeira (Mus. Comp. Zool. No. 1026), and female of 167 mm., off Equatorial West Africa, Lat. 6°08′ S., Long. 11°24′ E., Mus. Comp. Zool. No. 38002, received through the kindness of Dr. Max Poll.

The Gulf of Mexico specimens agree so closely with those with which we have compared them, from Madeira and from tropical West Africa that we have no hesitation in referring them to the same species.

The morphological feature the most sharply diagnostic for *pusillus,* among its genus-mates of the Equatorial and North Atlantic, of the Mediterranean and of the Gulf of Mexico, is that the denticles on the sides of its trunk are low, truncate, the great majority with concave crowns, but an occasional denticle flat, or perhaps even weakly convex, on a conspicuously 4-radiate base.[2] In these respects they contrast with the slender, bristle-like denticles of *E. spinax* (Linnaeus) 1758 and of *E. schultzi* (Bigelow, Schroeder and Springer 1953, fig. 9G), with the stouter, more thorn-like denticles of *E. hillianus* Poey 1861 (Bigelow and Schroeder 1948, p. 489, fig. 92B), of *E. polli* (Bigelow, Schroeder and Springer, 1953, fig. 7 C) and of *E. princeps* (see Bigelow, Schroeder and Springer, 1953, figs. 8 E, 8 F), and with the more conical claw-like denticles of *E. virens* (Bigelow, Schroeder and Springer 1953, fig. 10 D, E).

The color, also, of *E. pusillus* is distinctive. It recalls *E. princeps,* Collett 1904, of higher latitudes in both sides of the Atlantic, and *E. schultzi* Bigelow, Schroeder and Springer 1953, of the Gulf of Mexico, in the uniformly dark slaty to black

---

[1] Garman (1913, p. 223) credits the earliest use of *niger* in this connection to Gunner 1763, but we have not been in a position to verify this citation.

[2] Our earlier characterization of them as a whole (Bigelow, Schroeder and Springer 1953, p. 240) as "flat or weakly convex" was an evident misstatement.

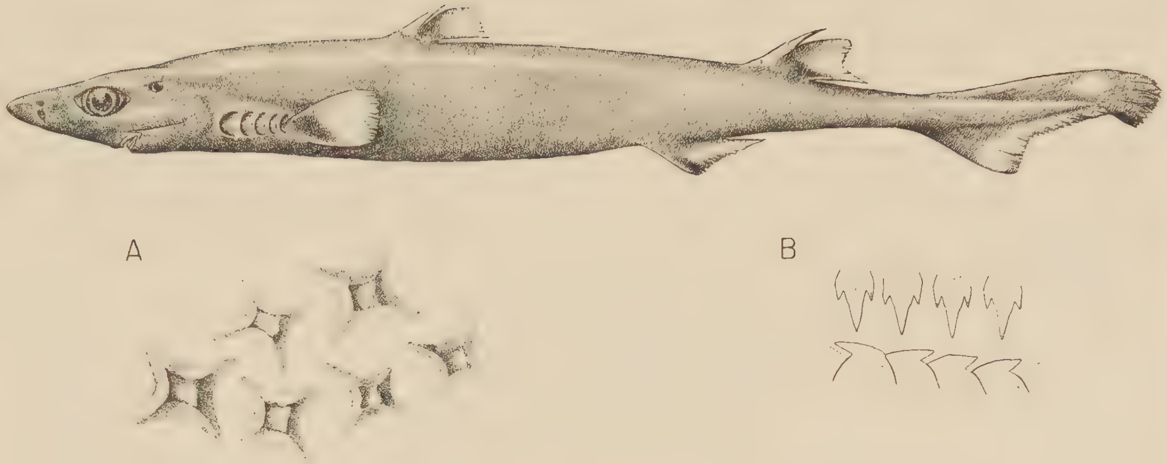

Fig. 1. *Etmopterus pusillus* (Lowe), 1839. Female, 458 mm. long, northern part of Gulf of Mexico. ''Oregon'' Sta. 1281, Mus. Comp. Zool. No. 39572. *A*, group of dermal denticles from below first dorsal fin, x about 40; *B*, upper and lower teeth at center of jaw, x about 5.

ish hue of its trunk not only below, but above as well (except for the pale intraocular spot mentioned below), and in the lack of definitely outlined paler and darker areas on its sides. But the outer part of its pectoral fins, with the rear part of its two dorsal fins are white and more translucent, which is not the case either in *princeps,* in *schultzi,* or in any other *Etmopterus* for that matter, that is known yet from the North Atlantic, from the Mediterranean, or from the Gulf of Mexico. This very conspicuous feature of *pusillus* is shown on Lowe's (1843, Pl. 6) original illustration of it (as *Acanthidium pusillum*) ; also on the colored illustration by Braganza (1904, Pl. 2, fig. 2, as *E. pusillus*).

Other features that in combination are diagnostic for *pusillus* are: that the upper margin of its caudal fin is only about as long as from the tip of the snout to the level of the second pair of gill openings; that the distance from the rear end of the bases of its pelvic fins to the origin of the lower side of its caudal fin is shorter than from the tip of the snout to the level of the first pair of gill openings; that the rear end of the base of its first dorsal fin is much nearer to a perpendicular at the axils of the pectoral fins than to a perpendicular at the origin of the pelvic fins; that the margins of its pectoral fins are not deeply fringed normally as they are in *E. schultzi* (Bigelow, Schroeder and Springer 1953, fig. 9 D) ; that the anterior edge of the first pair of gill openings is not concave enough to expose the tips of the gill-folds as it is in *E. princeps* (see Bigelow, Schroeder and Springer 1953, fig. 8 D) ; and that the upper surface of the head is marked between the eyes with a pale yellowish spot, as it is in *E. polli,* in *E. schultzi,* in *E. virens,* and in *E. spinax,* (where there is also a white spot "above the hind part of each orbit," Garman 1913, p. 224), but not in *E. princeps.*

Two species of *Etmopterus, schultzi* and *virens,* Bigelow, Schroeder and Springer 1953, had been known previously in the Gulf. The discovery of *pusillus* there now increases the local list to three. And a fourth member of the genus (*hillianus* Poey 1861) is to be expected there for it has been found widespread in Cuban waters and in the West Indian region, and has been recorded from as far to the northward as the offing of Chesapeake Bay.

E. pusillus, originally reported from Madeira, has since been recorded from various localities in the eastern side of the Atlantic between Equatorial West Africa (Lat. 6°08′S, see above) and the coast of Portugal, the Cape Verde Islands, the Canaries and the Azores. Earlier reports of it from the West Indian region, listed elsewhere (Bigelow and Schroeder 1948, p. 493), seem actually to have been based on *E. hillianus*.

The discovery that *pusillus* occurs in the Gulf of Mexico shows that its range parallels that of *Centrophorus granulosus* (p. 9), also that of *C. uyato* Rafinesque 1810, which had been known only from the Mediterranean and from the eastern side of the Atlantic in low and mid-latitudes until 1951-1952, when ''Oregon'' trawled 2 specimens of it in the Gulf (Bigelow, Schroeder and Springer, 1953, p. 227).

Tanaka (1912, pl. 22; p. 88) also, has referred to *pusillus* the Japanese shark that was earlier described and pictured by Pietschmann (1907, p. 395; 1908, p. 654, pl. 1, fig. 2, pl. 2, fig. 2) as *E. frontimaculatus*. But while the latter agrees with *pusillus* in the nature of its dermal denticles (Pietschmann, 1908, p. 657, text figs. 1, 2), it differs from *pusillus* in a more rearward position of the first dorsal fin (relative to the positions of the pectoral and pelvic fins), in a relatively longer interspace between the pelvic and caudal fins, and in color pattern, with the lower surface of its head, its belly, and a definitely outlined area above and anterior to each pelvic fin much darker than the upper part of its sides. A further difference is that the lower surface is as densely clothed with denticles as are the sides and back in *pusillus* whereas it is largely naked in the Japanese species.

Genus CENTROPHORUS Müller and Henle 1837

Type species *Squalus granulosus* Bloch and Schneider 1801

CENTROPHORUS GRANULOSUS (Bloch and Schneider) 1801

Study material. Female 922 mm. long from northern part of Gulf of Mexico, Lat. 29°15′N., Long. 88°18′W., ''Oregon'' Sta. 1246, 200-210 fathoms, U. S. Nat. Mus. No. 157833; also skin of a male, 855 mm. long, eastern Atlantic, exact locality not known, Mus. Comp. Zool. No. 662.

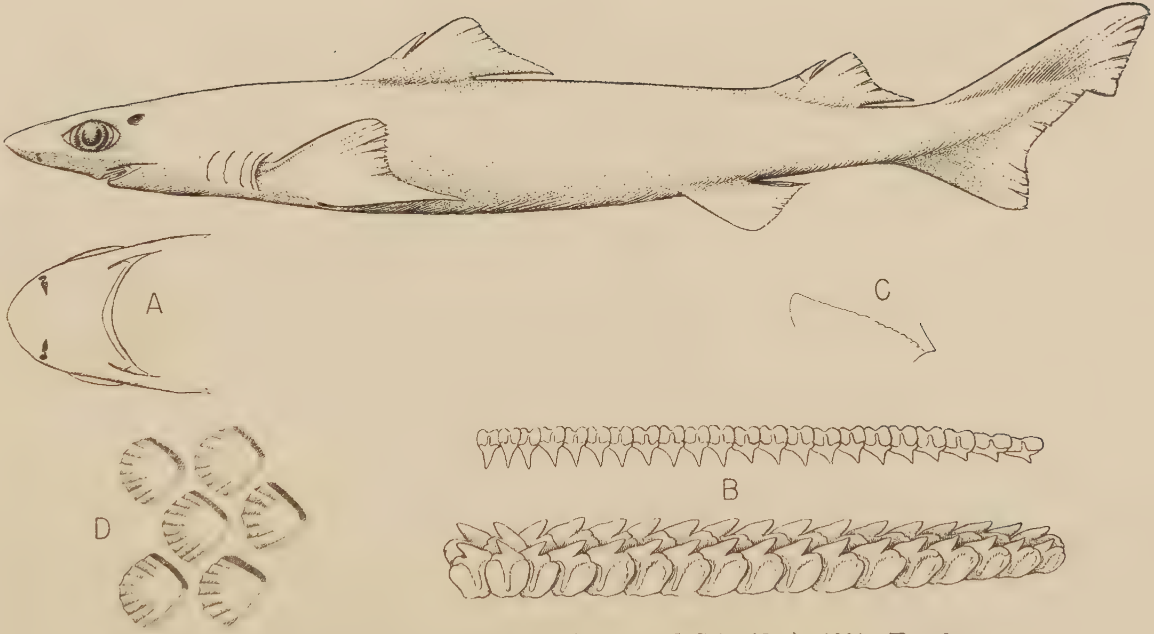

Fig. 2. *Centrophorus granulosus* (Bloch and Schneider), 1801. Female, 922 mm. long, northern part of Gulf of Mexico. ''Oregon'' Sta. 1246, U. S. Nat. Mus., No. 157833. *A*, lower surface of anterior part of head; *B*, upper and lower tooth band, left hand side of jaw, x about 1.7; *C*, cutting edge of 5th lower right hand tooth, x about 7, to show serrations; *D*, dermal denticles from side below first dorsal fin, x about 11.

The most evident diagnostic features that set apart *C. granulosus* (with *C. machiquensis* Maul 1955) from the other two species of its genus (*squamosus* Bonnaterre 1788 and *uyato* Rafinesque 1810) that are known from the North Atlantic province are: that the inner corner of its pectoral fins is greatly extended and narrowly pointed (Fig. 2); that the interspace between its two dorsal fins is longer than the head (to origin of pectoral fins) by a distance nearly as long as the eye; that the denticles on the sides of the body are low, block-like with the ridges on the outer surface converging rearward, closely spaced in quincuncial arrangement, but not overlapping (Fig. 2, *D*); and that the upper teeth are erect and nearly symmetrical all along the central part of the jaw (Fig. 2, B). In *granulosus* also, as in *squamosus,* the cutting edge of the lower teeth is partially serrate, but so finely so that this feature is visible only on careful examination under a lens (Fig. 2, *C*). In *uyato,* on the contrary, the lower teeth are smooth-edged, like the uppers.

Proportional dimensions, in per cent of total length, of female, 922 mm. long, northern part of Gulf of Mexico, U. S. Nat. Mus. No. 157833.

Trunk at origin of pectoral. Breadth 9.7, height 10.8.
Snout length in front of. Outer nostrils 2.8; mouth 9.1; eye 4.9
Eye. Horizontal diameter 4.9.
Mouth. Breadth 7.9.
Nostrils. Distance between inner ends 3.6.
Spiracles. Distance between inner ends 7.0.
Labial furrows, upper. Length 5.4; distance between inner ends 6.4.
Gill openings, lengths. 1st 2.6; 2nd 2.7; 3rd 2.8; 4th 3.0; 5th 3.3.
First dorsal fin. Vertical height 5.4; length of base 11.1; base rearward from anterior beginning of spine 8.5; diagonal from emergence of spine to rear end of base 7.1; free rear margin of fin 6.9.
Second dorsal fin. Vertical height 5.0; length of base 7.0; base rearward from anterior beginning of spine 5.7; diagonal from emergence of spine to rear end of base 5.4; free rear margin of fin 4.5.
Caudal fin. Upper margin 20.3; lower anterior margin 12.3.
Pectoral fin. Outer margin 12.9; inner margin 13.2; greatest width 7.6.

Distance from snout to. 1st gill opening 16.8; to origin of 1st dorsal spine 34.8; to origin of 2nd dorsal spine 69.2; upper caudal 79.7; pectoral 22.2; pelvics 58.7.

Interspace between. Anterior beginning 1st dorsal spine to 2nd dorsal spine 34.4; rear tip of 1st dorsal fin to rear tip of 2nd dorsal 29.5; 2nd dorsal and caudal 6.0; pelvics and caudal 13.4.

Distance from origin to origin of. Pectoral and pelvics 37.6; pelvics and caudal 18.1.

Head, to origin of pectoral fins, about 28 per cent of trunk to origin of upper side of caudal fin; snout moderately rounded, its length in front of snout about ⅓ of head to origin of pectorals; eye about 22 per cent as long as head; distance from level of front of eyes to tip of snout about as long as eye; spiracle about ¼ as long as eye, its anterior edge only slightly posterior to rear corner of eye. Nostrils a little less than ½ as long as distance between nostrils, approximately transverse, the outer ends posterior to level of tip of snout by a distance a little shorter than distance between nostrils. Anterior nasal flap short, narrowly triangular. Distance between nostrils a little less than ½ as great as from tip of snout to mouth. Mouth very low-arched, its gape when closed occupying about ⅘ of breadth of head at level of outer corners of mouth. Distance between inner ends of nasal furrows about 1.8 times as long as between nostrils. Longest gill opening (5th) is almost as long as distance between nostrils.

Teeth $\frac{40}{15\text{-}1\text{-}15}$, of shapes illustrated in Figure 2, *B;* uppers with the post-functional (outermost) row partly lost, followed by a nearly vertical functional row and then by an oblique backward pointing row that will be next in service; lowers with two rows visible from outside the mouth, one of which is functional, 16 teeth pointing to the right hand side, of which one is a median tooth, and 15 teeth pointing to the left hand side; cutting edge of some of the lowers with microscopically fine and somewhat irregular serrations (Fig. 2, *C*) but others merely somewhat irregular, a difference probably due to wear. Dermal denticles on sides of body sessile, block-like, sub-quadrate, with the more acute corner directed rearward, closely spaced in quincuncial pattern but not overlapping, the crown weakly convex or flat, its anterior ½ to ⅔ with (usually) 5-7 low ridges, converging rearward (Fig. 2, *D*), the outermost pair the longest.

Denticles at mid-level of side below first dorsal fin averaging about 0.9 mm. long.

Length of base of first dorsal fin, measured from point of emergence from skin of anterior side of first dorsal spine, about 1.3 times as long as base of second dorsal fin, similarly measured. Interspace between rear end of base of first dorsal and point of emergence of second dorsal spine longer than head (to origin of pectorals) by a distance about equal to length of eye and about 7½ times as long as between nostrils. Exposed portion of first dorsal spine about 1⅓ times as long as that of second spine, the second spine reaching about mid-way along the free anterior margin of the fin. Interspace between rear end of base of second dorsal fin and origin of upper side of caudal fin about as long as base of second dorsal fin measured from point of emergence, from skin, of anterior edge of second dorsal spine.

Upper edge of caudal fin about as long as from tip of snout to level of fourth pair of gill openings, its lower edge with obtuse subterminal notch and rounded lower anterior lobe. Interspace between origin of lower edge of caudal fin and rear ends of bases of pelvic fins about ⅗ as long as from tip of snout to level of 5th pair of gill openings. Origin of pelvic fins (in female) anterior to a perpendicular at emergence of anterior edge of second dorsal spine, by an amount about equal to interspace between origin of lower edge of caudal fin and rear ends of bases of pelvic fins. Pectorals with inner corner greatly extended and narrowly pointed, reaching rearward (when laid back) nearly to a perpendicular from rear base of first dorsal fin.

Sharks referable with certainty to *granulosus*, not to *uyato* which Rey (1928, p. 436) considered synonymous with it, had previously been recorded in the Mediterranean, off the coast of Portugal, and at Madeira (specimen in British Museum; Günther 1870, p. 421). The capture of a typical *granulosus* in the Gulf now shows that its Atlantic range parallels that of *C. uyato* Rafinesque 1810, which was recently found to occur in the Gulf (Bigelow, Schroeder and Springer 1953, p. 227). The third species of *Centrophorus* that is known from the Atlantic (*squamosus* Bonnaterre 1788) has so far been reported only off the coast of Portugal and northward to southwestern Iceland and the vicinity of the Faroes.

Pietschmann (1908, pp. 663-667) credits *granulosus* to Japan also, from his comparison of two Japanese specimens with *granulosus* from the Mediterranean. But the eventual decision, whether the northwestern Pacific *Centrophorus* of this general character is indeed indistinguishable from the Atlantic-Mediterranean *granulosus,* is best postponed until a larger number of specimens have been examined, critically, with this question in mind.

Genus DALATIAS Rafinesque 1810

DALATIAS LICHA (Bonnaterre) 1788

Study material. Female 845 mm. long from northern part of Gulf of Mexico, Lat. 28°25′N., Long. 86°02′W., "Oregon" Sta. 1275, 225 fathoms, U. S. Nat. Mus. No. 157834.

The specific identification of this specimen as *D. licha* is so evident, from its close agreement in bodily form, fin characters, teeth, and denticles with the Georges Bank specimen described and pictured previously (Bigelow and Schroeder 1948, p. 502, figs. 96, 97) that no further account seems called for here.

As the only previous record for this shark in the western Atlantic was this Georges Bank example, the capture of one in the northern part of the Gulf of Mexico widely expands its known range.

In the eastern side of the mid and north Atlantic the known range of *D. licha* extends from Equatorial West Africa (Rio de Oro) to the Irish Atlantic slope, including the Mediterranean. And it is doubtful whether the representatives of the genus that have been reported from South Africa, from the New Zealand-Australian region and from Japan can be separated specifically from *D. licha* of the Atlantic. (For discussion, see Bigelow and Schroeder 1948, p. 501).

REFERENCES

BIGELOW, HENRY B., and W. C. SCHROEDER
1948. Fishes of the Western North Atlantic. No. 1, Mem. Sears Foundation for Marine Research, Part 1, pp. 59-576, text figs. 6-105.

BIGELOW, HENRY B., W. C. SCHROEDER, and STEWART SPRINGER
1953. New and little known sharks from the Atlantic and from the Gulf of Mexico. Bull. Mus. Comp. Zool., vol. 109, no. 3, pp. 213-276, text figs. 1-10.

BLOCH, M. E., and I. G. SCHNEIDER
1801. Systema Ichthyologiae iconibus ex illustratum. lx + 584 pp.; 110 pls.; 2 vols.

BONNATERRE, P. J.
1788. Ichthyologie *in*: Tab. Encyc. Méthod. Trois règnes de la Nature. lvi + 215 pp., pls. A, B + 1-100. Paris.

BRAGANZA, CARLOS DE
1904. Esqualos obtidos nas Costas de Portugal. Resultados das Invest. Sci. . . . Yacht ''Amelia.'' Ichthyologia. II; 107 pp., 2 pls. Lisbon.

CLOQUET, HIPPOLYTE
1820. Le sagre, spinax niger. Dict. Sci. Nat., vol. 1, suppl., p. 93.

COLLETT, R.
1904. Diagnoses of four hitherto undescribed fishes from the depths south of the Faroe Islands. Videns. Selskabs Forhand. Christiania, 1904, no. 9, 7 pp.

GARMAN, SAMUEL
1913. The Plagiostomia. Mem. Mus. Comp. Zool., vol. 36, xiii + 515 pp., 77 pls.

GÜNTHER, ALBERT
1870. Catalogue of fishes of the British Museum, vol. 8, xxv + 549 pp.

JORDAN, D. S., and B. W. EVERMANN
1896. The fishes of North and Middle America. Bull. U. S. Nat. Mus. No. 47, Part 1, lx + 1240 pp.

LINNAEUS, C.
1758. Systema naturae, 10th Ed., vol. 1, 824 pp., Holmiae.

LOWE, R. T.
1834. A collection of fishes made in Madeira. Proc. Zool. Soc. London (1833), Part 1, 1834, pp. 142-144.
1839. A supplement to a synopsis of the fishes of Madeira. Proc. Zool. Soc. London, Part 7, 1839, pp. 76-92.
1843. A history of the fishes of Madeira . . . 196 pp., 27 pls., London.

MAUL, G. E.
1955. Five species of rare sharks new for Madeira. . . . Notul. Natur. Acad. Nat. Sci. Philadelphia, No. 279, 13 pp., 3 pls.

MÜLLER, JOHANNES, and F. G. J. HENLE
1837. Ueber die Gattungen der Haifische und Rochen . . . Arch. Naturgesch., Jahrg. 3, vol. 2, pp. 394-401, 434.

Pietschmann, Viktor

1907. Zwei neue Selachier aus Japan. Anz. Akad. Wiss. Wien. Vol. 44, pp. 394-396.

1908. Japanische Plagiostomen. Sitzber. Akad. Wiss. Wien, math. Nat. Kl., vol. 117, pt. 1, pp. 637-710, pls. 1, 2.

Poey, Felipe

1858-1861. Memorias sobre la historia natural de la isla de Cuba, vol. 2, 442 pp., 19 pls.

Rafinesque, Constantine Samuel

1810. Carratteri di alcuni nuovi generi e nuovi specie di animali e piante della Sicilia. pp. iv, 105, 20 pls. Palermo.

Rey, Luis Lozano

1928. Fauna Iberica. Peces. Vol. 1, 690 pp., 20 pls. Inst. Nac. Ciencias, Madrid.

Tanaka, Shigeho

1912. Figures and descriptions of the fishes of Japan. Vol. 5, pp. 71-86 + [1], pls. 21-25; vol. 6, pp. 87-108, pls. 26-30.

Whitley, Gilbert

1939. Studies in ichthyology no. 12. Rec. Australian Mus. Vol. 20, No. 4, pp. 264-277.

Contribution No. 788

Transactions, American Geophysical Union Volume 36, Number 4 August 1955

THE CIRCULATION OVER THE CONTINENTAL SHELF SOUTH OF CAPE HATTERAS

Dean F. Bumpus

(Contribution No. 788 from the Woods Hole Oceanographic Institution)

Abstract--South of Cape Hatteras, a southerly-flowing coastal current, such as is common to the northward, is a transient affair. Such a current, when present, is restricted to a very narrow portion of the continental shelf. The dynamic pressure gradient resulting from the combined effect of the runoff and the cross-shelf thermal gradient together with the prevailing wind and the frictional drag of the Florida Current provides for a northeasterly drift over a broad part of the Carolina continental shelf.

The waters of the continental shelf of the United States south of Cape Hatteras (Fig. 1) have received, until recently, exceedingly little attention compared with the shallow and slope waters to the north. Prior to 1948 the oceanographic data from this region comprised occasional observations by Bigelow, one section by ISELIN [1936], and current measurements by the U. S. Coast and Geodetic Survey alluded to by RUDE [1922] and reported by HAIGHT [1942].

The only discussion of the oceanography of the region lies in a recent summary by MARSHALL [1951], but that deals mostly with the waters of the sounds. Toumey in the Geological Survey of South Carolina for 1848 described 'an eddy current which washes the coast southwardly' [GULLIVER, 1899]. Backset eddies driven by the Florida Current have been considered as responsible for the cuspate form of the coast line by ABBE [1895], GULLIVER [1899], DAVIS [1912], and SHEPARD [1948]. RUDE [1922], on the basis of current measurements in the winter of 1915-16 and 1916-17, does not accept the theory of backset eddies. He found superimposed on the rotary tidal current 'a set with the local wind prevailing at the time of observation.' PARR [1933] noted the winter temperature barrier which occurs at Cape Hatteras. PIERCE [1953] demonstrated that the distribution of chaetognaths was directly related to the water masses in the area.

One of the characteristic features of the hydrography of continental shelf waters is a dynamic coastal current induced by the addition of fresh river runoff water at the coast. The southerly-flowing current along the eastern seaboard of the United States north of Cape Hatteras is an example. Part of this current manifests itself near the coast as a slow drift of three to 20 mi/day [MILLER, 1952], but most of the transport is near the 100-fm contour where it does not have to overcome bottom friction.

It has become evident from recently collected data south of Cape Hatteras that a southerly-flowing coastal current in that region does not always exist. Certainly, one can never exist along the 100-fm line inasmuch as the Florida Current lies just a few miles from the 100-fm line, and waters over the edge of the shelf are subject to the frictional drag of this great stream.

There appear to be several reasons why a dynamic coastal current is a transient affair in this region:

(1) Raleigh Bay and Onslow Bay receive no regular contribution of freshened water or southerly-flowing water from north of Cape Hatteras. Hence there is no continuity with the waters north of Cape Hatteras. As will be noted in (2) below, the fresh-water contribution from the rivers is small and mixed with sea water. If the runoff into this region were comparable to that of Chesapeake Bay, a coastal current would be assured of a healthy inception.

(2) River water contributions per unit length of coast line are on the average less than one half as great as for any other section of the coast (Table 1), It is apparent that the runoff per unit area for the Carolina region is not, on the average, significantly less than for the other regions, but the runoff per unit length of coast line between Cape Hatteras and the South Carolina border, that is, of the Pamlico, Neuse, and Cape Fear River basins, is very small, being 1.9 m^3/sec km, as compared with an average of 5.2 m^3/sec km for all the other sections of this coast. Further, the effluent from the rivers becomes well mixed with sea water in the estuaries and sounds so that the water entering the sea through the inlets is no longer very fresh. (Mixing in the Cape Fear River may not be as complete as in the other estuaries in the region.) For instance, salinities observed at Hatteras and Ocracoke Inlets ranged from 28.5 to 35.5 $^0/_{00}$ [ROELOFS and BUMPUS, 1953]; at Beau-

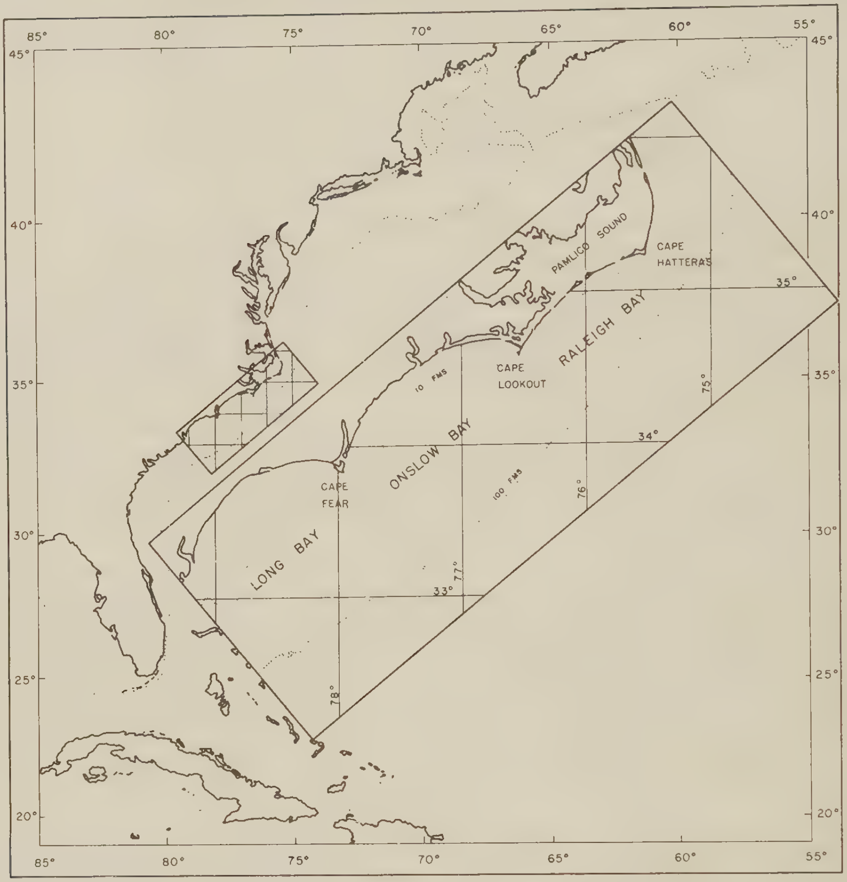

Fig. 1--Chart of east coast of the United States with inset indicating area under discussion

fort Inlet from 18 to 35.4 $^{o}/_{oo}$ [SUTCLIFFE, 1951], but generally greater than 32 $^{o}/_{oo}$. Lower salinities are always found at the mouths of the Hudson River, Delaware Bay, and Chesapeake Bay. As a result the salinity gradient is greater next to the coast off the northern shores than in Raleigh or Onslow Bays.

(3) The temperature gradient across the continental shelf during the winter months is more than sufficient to counteract the salinity effect on the pressure gradient during periods of average runoff, thus dynamically providing for a northerly set to the coastal waters.

(4) Owing to the geography of the coast line the southwesterly wind, which is the prevailing wind during many months of the year, blows parallel to the general direction of the coast south of Cape Hatteras, whereas from Hatteras to New York it is an offshore wind. This wind with a relatively long fetch at Long, Onslow, and Raleigh Bays serves to retard or deflect offshore any south flowing coastal current.

(5) Further, this southwest wind will pile up water on the south sides of the capes creating an hydraulic current which tends to flow offshore over the projecting bars. This hydraulic current will deflect offshore any southerly flowing coastal current approaching the cape on the lee side, and, through turbulence, will mix it with more saline water, thus preventing augmentation of the current from one river mouth to the next. (This opposition of currents at the cape tips may indeed provide the mechanism which helps to maintain the capes, inasmuch as the velocities may be reduced there and the heavier elements of the sediment loads dropped.)

(6) Finally, the proximate Florida Current produces a frictional drag on much of the water over the continental shelf, which drag a coastal current must overcome.

Table 1--Mean runoff data for several drainage basins along Atlantic Seaboard of the United States

Drainage basin	Runoff[a]	Drainage area[b]	Runoff	Coastline	Runoff
	m^3/sec km^2	km^2	m^3/sec	km	m^3/sec km
Hudson River	0.017	34618	588	135	4.35
Delaware River	0.019	36001	684	136	5.02
Chesapeake Bay	0.013	173979	2261	244	9.3
Albermarle Sound	0.012	43019	516	67	7.7
Pamlico to Cape Fear River	0.011	61981	682	352	1.9
Peedee, Savannah and Altamaha Rivers	0.012	198430	2380	485	4.9

[a] Based on U. S. Geological Survey Water-Supply Papers 1171 and 1172.
[b] Includes both gaged and ungaged areas.

Thus it appears that a southerly-flowing coastal current will not prevail during the winter months unless the runoff is exceptionally great. At other times of the year such a current will depend primarily on the amount of runoff and secondarily on the wind direction, force, and duration. The following observations are presented in support of this hypothesis.

Runoff data--The runoff for the period October, 1947, to September, 1953, and the occasions when the cruises were made to collect the hydrographic data are shown in Figure 2. We see that immediately prior to Reliance Cruises 4 and 6 the runoff had been four times greater than the mean but was diminishing rapidly. Prior to Caryn Cruise 7 and Albatross III Cruises 18-19 the runoff had been well above the mean for several months but had dropped to near mean values. Prior to Albatross III Cruises 30 and 32 runoff averaged less than the mean for several months. Prior to Caryn Cruise 64 runoff had been twice the mean but had since diminished. These runoff trends are reflected in the salinity distribution over the continental shelf and hence contribute to the distribution of the dynamic pressure gradient.

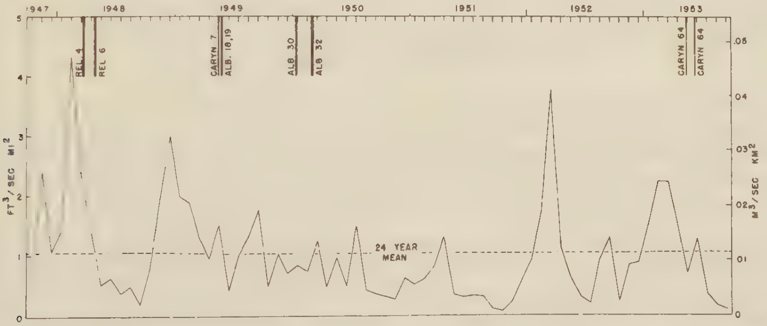

Fig. 2--Runoff for the period October, 1947, to September, 1953, from Pamlico, Neuse, and Cape Fear River basins, [U. S. GEOLOGICAL SURVEY [1952, 1953] and data kindly furnished by the District Engineer in North Carolina

Drift bottles--Two sets of drift bottles (with and without drags) were released in the North Carolina area, one set in January and the other in February and early March, 1950, Albatross III Cruises 30 and 32.

The first set comprised 816 bottles released at 51 positions, 16 bottles at each position. The 46 recoveries from 17 of the positions are shown in Figure 3. The second set comprised 490 bottles released at 49 stations, ten at each station. The 24 returns from 15 positions are shown in Figure 4.

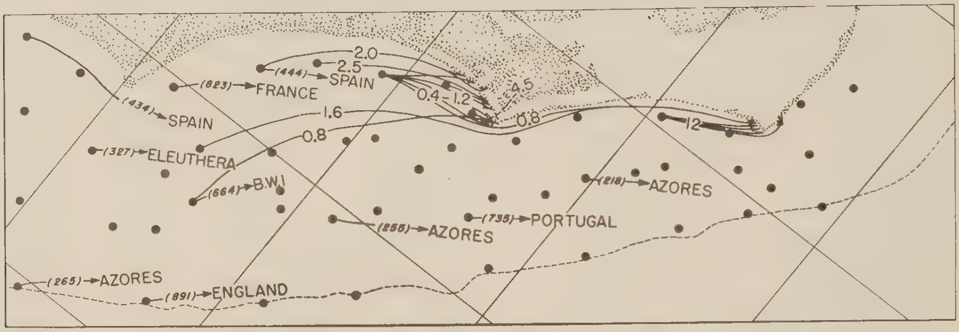
2.0
(444) → SPAIN
2.5
(823) → FRANCE
(434) → SPAIN
4.5
0.4-1.2
1.6
0.8
0.8
12
(327) → ELEUTHERA
(664) → B.W.I.
(218) → AZORES
(735) → PORTUGAL
(256) → AZORES
(265) → AZORES
(891) → ENGLAND

Fig. 3--Routes of drift bottles released January 9-13, 1950, Albatross III, Cruise 30; numbers indicate drift in miles per day; numbers in parentheses indicate days of drift

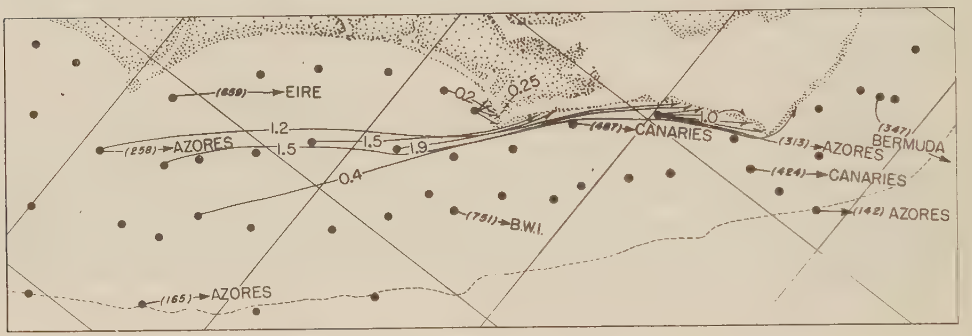
(659) → EIRE
0.2
0.25
1.2
1.0
(487) → CANARIES
(258) → AZORES
1.5
1.5
1.9
(313) → AZORES
(347) BERMUDA
0.4
(424) → CANARIES
(751) → B.W.I.
(142) AZORES
(165) → AZORES

Fig. 4--Routes of drift bottles released February 25 - March 4, 1950, Albatross III Cruise 32; numbers as noted under Fig. 3

These drift-bottle recoveries indicate a definite north-easterly movement of the surface coastal waters during January-March, amounting to from 0.2 to 12 mi/day. It is also apparent from the foreign returns and from the bottles conspicuous by their absence that the movement tends somewhat offshore rather than onshore. These drifts are compatible with that indicated by the hydrographic conditions for the same period, a period of less than mean runoff.

Two of MILLER's [1952] bottles, launched in the offing of Cape May in May 1951, stranded on the shores of Raleigh Bay, having moved southerly around Cape Hatteras presumably during the five days of easterly winds, June 15-20. These are the only bottles on record to have rounded the Cape in that direction or, for that matter, to have been recorded as moving southerly in this region.

Temperature, salinity, and density distribution--The temperature and salinity data were collected in the course of eight cruises: March 19-25, 1948, Reliance, Cruise 4; April 26-May 1, 1948 Reliance, Cruise 6; May 13-15, 1949, Caryn, Cruise 7; May 20-25, 1949, Albatross III, Cruises 18-19; January 8-13, 1950, Albatross III, Cruise 30; February 25-March 4, 1950, Albatross III, Cruise 32; May 13, 1953, Caryn, Cruise 64; and June 9-10, 1953, Caryn, Cruise 64.

Typical sections across Onslow Bay, Figures 5, 7, 9, 11, 13, 15, 17, and 18, diagram the distribution of temperature, salinity, and density in profile. The distribution of these same properties at the surface in Long, Onslow, and Raleigh Bays is illustrated in Figures 6, 8, 10, 12, 14, and 16. From the two sets of figures a general idea of the hydrography of the area may be obtained. The conditions peculiar to the several times of observation are summarized below.

January 8-13, 1950; Albatross III Cruise 30 (Fig. 5 and 6)--Strong horizontal temperature gradients but minimal vertical temperature gradients were characteristic of the shelf waters in January

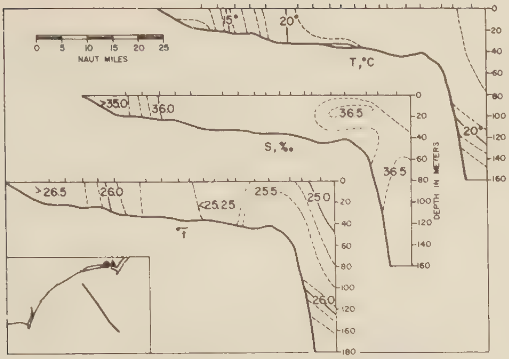

Fig. 5--Distribution of temperature, salinity, and density across a typical section in Onslow Bay, January, 1950, Albatross III, Cruise 30

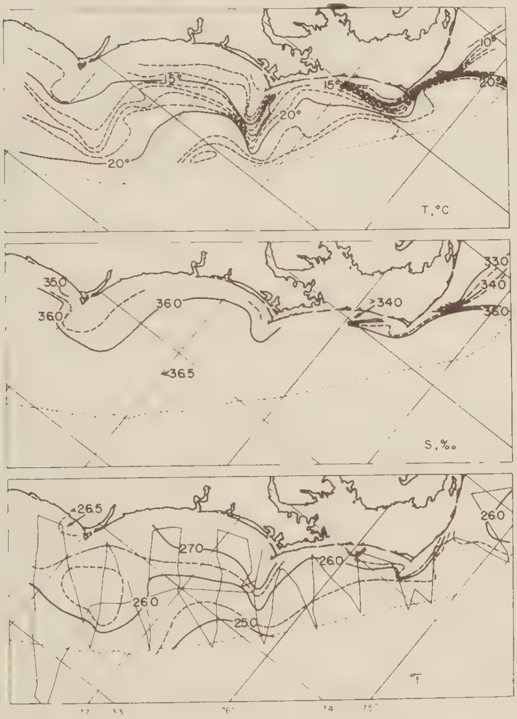
15°
15°
10°
20°
20°
T,°C
35.0
36.0
36.0
>34.0
33.0
34.0
36.0
<36.5
S,‰
<26.5
27.0
26.0
26.0
26.0
25.0
σT

Fig. 8--Distribution of surface temperature, salinity, and density on North Carolina shelf, February, 1950, Albatross III, Cruise 32

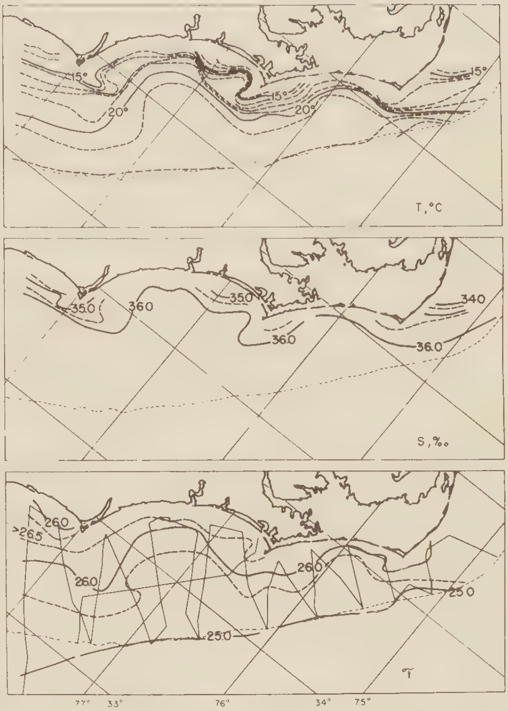
15°
20°
15°
20°
15°
T,°C
35.0
36.0
35.0
36.0
34.0
36.0
S,‰
26.0
>26.5
26.0
26.0
25.0
25.0
σT
77° 33°
76°
34° 75°

Fig. 6--Distribution of surface temperature, salinity, and density on North Carolina shelf, January, 1950, Albatross III, Cruise 30

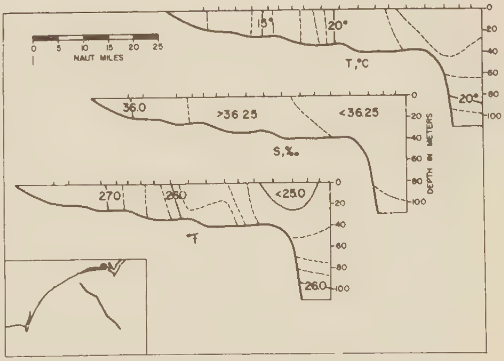

Fig. 7--Distribution of temperature, salinity, and density across a typical section in Onslow Bay, February, 1950, Albatross III, Cruise 32

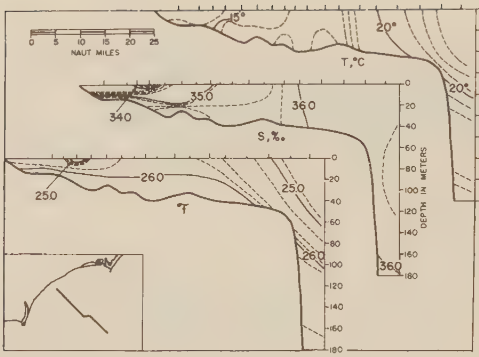

Fig. 9--Distribution of temperature, salinity, and density across a typical section in Onslow Bay, March, 1948, Reliance, Cruise 4

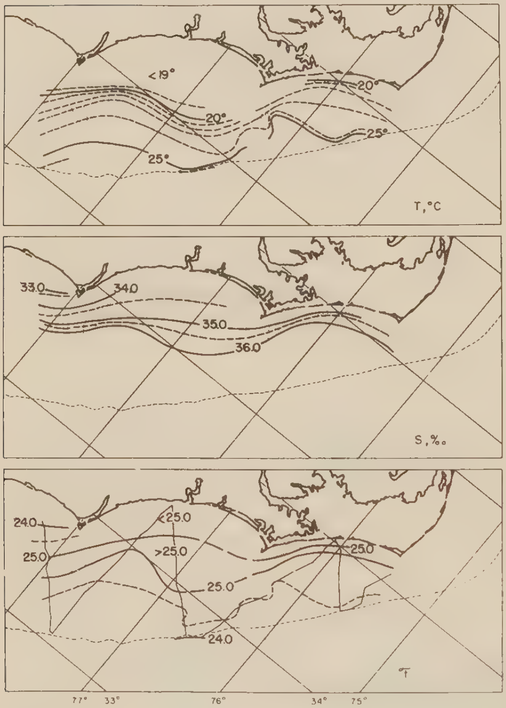
<19°
20°
20°
25°
25°
T,°C
33.0
34.0
35.0
36.0
S,‰
24.0
<25.0
25.0
>25.0
25.0
25.0
24.0
σT
77° 33°
76°
34° 75°

Fig. 12--Distribution of surface temperature, salinity, and density on North Carolina shelf, April, 1948, Reliance, Cruise 6

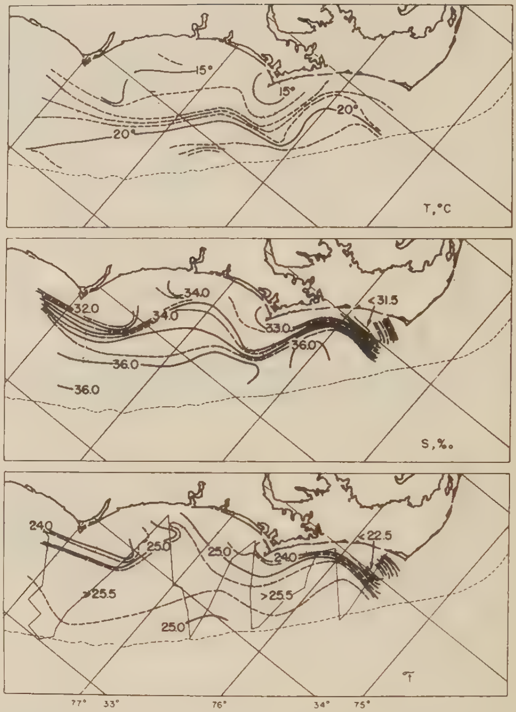
15°
15°
20°
20°
T,°C
34.0
32.0
34.0
<31.5
33.0
36.0
36.0
36.0
S,‰
24.0
25.0
25.0
<22.5
24.0
>25.5
>25.5
25.0
σT
77° 33°
76°
34° 75°

Fig. 10--Distribution of surface temperature, salinity, and density on North Carolina shelf, March, 1948, Reliance, Cruise 4

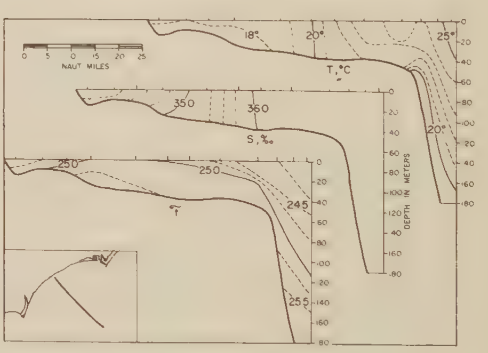

Fig. 11--Distribution of temperature, salinity and density across a typical section in Onslow Bay, April, 1948, Reliance, Cruise 6

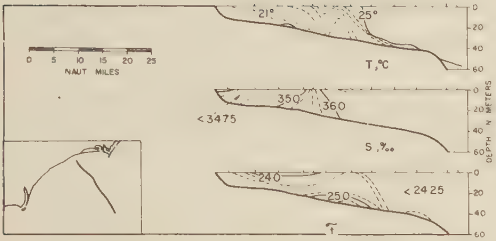

Fig. 13--Distribution of temperature, salinity, and density across a typical section in Onslow Bay, May, 1949, Caryn, Cruise 7

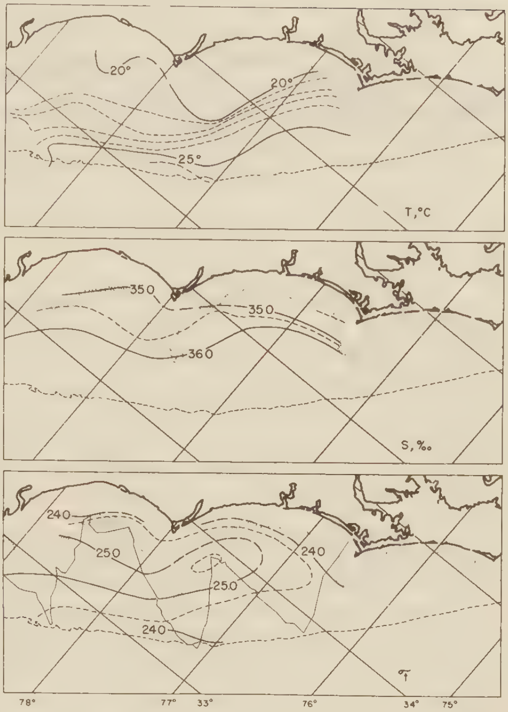
20°
20°
25°
T, °C
35.0
35.0
36.0
S, ‰
24.0
25.0
24.0
25.0
24.0
σT
78°
77°
33°
76°
34°
75°

Fig. 14--Distribution of surface temperature, salinity, and density on North Carolina shelf, May, 1949, Caryn, Cruise 7

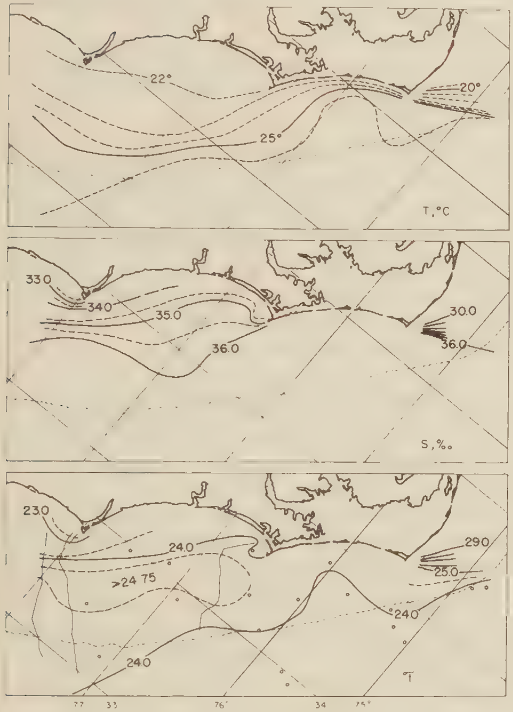
22°
20°
25°
T, °C
33.0
34.0
35.0
30.0
36.0
36.0
S, ‰
23.0
24.0
29.0
>24.75
25.0
24.0
24.0
σT
77
33
76
34
75°

Fig. 16--Distribution of surface temperature, salinity, and density on North Carolina shelf, May, 1949, Albatross III, Cruises 18-19.

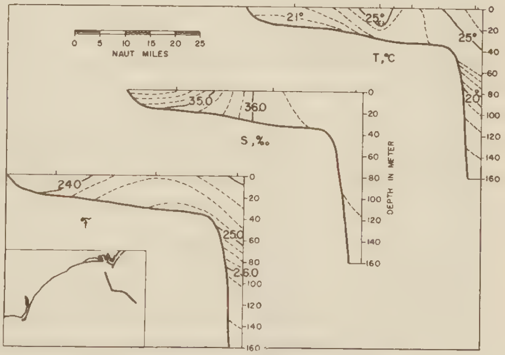

Fig. 15--Distribution of temperature, salinity, and density across a typical section in Onslow Bay, May, 1949, Albatross III, Cruises 18-19.

1950. The salinity distribution tended to be similar to the thermal structure although the relatively small runoff during the preceding weeks accounts for the absence of lowered salinity next to the coast. Water of salinity greater than 36 $^{0}/_{00}$ had penetrated at all depths well across the shelf to within ten miles of the coast on the average. Density decreased from the coast seaward in Onslow and Raleigh Bays. This was due to the temperature increase seaward and the insufficiency of freshened water next to the coast to counteract the temperature effect. Hence the

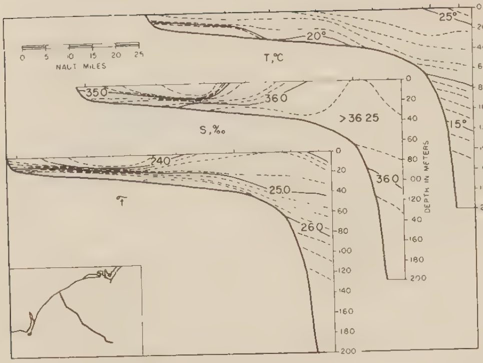

Fig. 17--Distribution of temperature, salinity, and density across a typical section in Onslow Bay, May, 1953, Caryn, Cruise 64

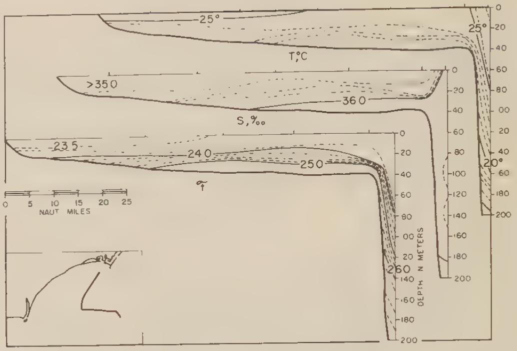

Fig. 18--Distribution of temperature, salinity, and density across a typical section in Onslow Bay, June, 1953, Caryn, Cruise 64

density structure suggests the absence of a countercurrent and a slow northerly drift all across the shelf. South of Cape Fear a southerly coastal drift is indicated. The northerly drift over the shelf was substantiated in the drift bottle experiment described above.

February 1950; Albatross III Cruise 32 (Fig. 7 and 8)--The temperature and salinity structure for this period was very similar to that observed during the previous month. The effect of lower than normal runoff allowed the intrusion of highly saline water even closer to the coast than earlier. The NNW wind which prevailed during the month appears to have pushed water from Pamlico Sound out through Hatteras and Ocracoke Inlets, freshening and cooling the water in their offings. Again the temperature effect on density produced a decrease in density with distance offshore at all depths, suggesting a northward drift of all the water over the shelf. The nascent coastal current south of Cape Fear was less well developed. The drift bottle experiment conducted during this cruise also gave supporting evidence for a northerly drift of all the shelf waters in this region.

March 19-25, 1948; Reliance Cruise 4 (Fig. 9 and 10)--In March, 1948, the temperature and salinity distribution differed from the January and February conditions of 1950 owing in part to the vernal warming, but chiefly to the preceding large runoff from the adjacent watershed. Water of salinity greater than 36 ‰ lay over the outer one-third of the shelf, the inner two-thirds being occupied by effluent water of less than 33.5 ‰ minimum in Onslow Bay and less than 31.5 ‰ minimum in Raleigh Bay. Temperature increased with depth as did salinity owing to the flooding of the colder effluent out over warmer more saline shelf water. These conditions combined to produce a slight vertical density gradient, maximum densities at all depths occurring over the central part of the shelf, with lowered densities offshore and still lower densitites inshore. These dynamic conditions should produce a weak southerly coastal current over the inner part of the shelf. The winds were predominantly NE during the preceding month and a half. The SW wind blowing at the time the observations were made in the northern part of Raleigh Bay served to move a thin layer of the Pamlico Sound water from Hatteras and Ocracoke Inlets offshore over more saline water.

April 26 - May 1, 1948; Reliance Cruise 6 (Fig. 11 and 12)--Although the observed salinity measurements were not as low in April as during the preceding month it is apparent that the previous large accumulation of water of low salinity and the continued greater than mean runoff was more uniformly distributed over the inner part of the shelf because of the prevailing southwest wind during April. Horizontal and vertical gradients were weaker than during the previous month. A slight horizontal density gradient prevailed throughout the area with the maximum at all depths over the center of the shelf in Onslow Bay, but closer inshore in Raleigh Bay. This indicates a weak southerly coastal current inshore of this low and a northerly drift offshore parallel to the Florida Current.

May 13-15, 1949; Caryn Cruise 7 (Fig. 13 and 14)--No observations were made in Raleigh Bay during Caryn Cruise 7 nor were those in Onslow Bay well distributed. They do serve, however, to demonstrate the tendency at this time for a thermocline to develop, although it was very weak over the inner one-third of the shelf. The intrusion of considerable runoff augmented the stability, although the vertical salinity gradient was weak. There appears from the density structure to be a weak southerly current although there may be a weaker northerly current inshore if it. The prevailing SW wind during the preceding month may have served to move the coastal current and attendant freshened water slightly offshore. The outer one-third of the shelf was occupied by virtually isothermal, isohaline Florida Current water.

May 20-25, 1949; Albatross III Cruises 18 and 19 (Fig. 15 and 16)--Little change in the vertical structure since the cruise a few days earlier is evidenced in these data. During this cruise, with somewhat better coverage of the area than, *Caryn* Cruise 7, Raleigh Bay was virtually flooded with highly saline water, $S > 36^{0}/_{00}$, whereas freshened water, $S < 35\ ^{0}/_{00}$, tended offshore in the southern part of Onslow Bay. A density high occurred over the central part of Onslow Bay with an appreciable gradient toward the shore, especially in the northern part of Long Bay. This suggests the development of a moderate southerly-flowing coastal current commencing in Onslow Bay, being augmented in Long Bay by the Cape Fear River.

May 13, 1953; Caryn Cruise 64 (Fig. 17)--A single section across the center of Onslow Bay provides data for May, 1953. The waters are slightly more stratified than on the 1949 cruises in May, apparently owing to the intrusion of cold, highly saline water across the shelf on the bottom. On this is superimposed freshened water from the relatively high runoff during March and April. The temperature and salinity distribution have tended to reinforce each other in the production of a rather stable density structure. The density distribution suggests a slight southerly coastal current down the center of Onslow Bay with a slight northerly countercurrent inshore. Such motions can only serve to further dilute the river effluent and weaken the coastal current. This appears to be borne out in the June, 1953, data.

June 9-10, 1953; Caryn Cruise 64 (Fig. 18)--One section across Onslow Bay and one across Raleigh Bay comprise the June 1953 data. Since May, 1953, the water had increased in temperature at all depths over the inner half of the Onslow Bay shelf. The decreased runoff since April together with rather complete mixing and dispersion of freshened water with shelf water are reflected in the increased salinity of the surface waters. The intrusion of water with a salinity greater than $36\ ^{0}/_{00}$ had receded. The temperature and salinity distribution have combined to continue to produce a rather stable density distribution. The coastal current had degenerated to a very weak affair.

From these examples of the hydrographic structure of the shelf waters in Onslow Bay it is apparent that the overall picture is much simpler than that over the shelf north of Cape Hatteras. The shallow depths, the short distance from the coast to the continental edge, and the swift Florida Current flowing along that edge permit the transfer of runoff through the area at a rather rapid rate. Winds and the rotary tidal currents in the shallow waters increase mixing and resist the development of strong density gradients.

Fresh-water content--Estimates of the fresh-water content on the continental shelf on the several occasions have been made by planimetering the areas between the isohalines on the salinity sections, Table 2. Sea water salinity was assumed to be $36.0\ ^{0}/_{00}$.

Table 2--*Fresh-water content of Carolina shelf waters*

Date	Cruise	Pct of total volume[a]			Fresh-water volume × $10^{10}m^3$			
		Raleigh	Onslow	Long	Raleigh	Onslow	Long	Total
Jan. 1950	*Albatross III*-30	0.14	0.10	0.20	0.030	0.047	0.034	0.111
Feb. 1950	*Albatross III*-32	0.02	0.10	0.11	0.004	0.051	0.019	0.074
Mar. 1948	*Reliance*-4	0.63	1.63	0.80	0.133	0.800	0.137	1.070
Apr. 1948	*Reliance*-6	0.19	1.09	0.97	0.041	0.534	0.166	0.740
May 1949	*Caryn*-7	- -	0.44	0.78	- -	0.214	0.134	- -
May 1949	*Albatross III*-18,19	0.00	0.75	1.28	0.000	0.368	0.220	0.588
May 1953	*Caryn*-64	- -	1.43	- -	- -	0.704	- -	- -
June 1953	*Caryn*-64	0.21	1.53	- -	0.044	0.751	- -	- -

[a] Total volume to 100-fm line: Raleigh Bay 21.15 × $10^{10}m^3$; Onslow Bay 49.11 × $10^{10}m^3$; northern part of Long Bay 17.16 × $10^{10}m^3$; grand total 87.42 × $10^{10}m^3$.

It is clear from Table 2 and is quantitatively indicated that the volume of fresh water contained in the waters over the North Carolina shelf varies from time to time by more than one order of magnitude. It is also clear that the fluctuations in fresh-water volume are associated with the gross sustained fluctuations in runoff. We have not been able to derive a satisfactory relationship between the fresh-water volume and the runoff for a short period.

We conclude that the removal of water from the Carolina shelf is not steady, but is perhaps modified by the wind systems and modulations in the flow of the adjacent Florida Current [VON ARX, and Others, 1954]. A southwest wind will deflect the freshened water offshore into the frictional drag of the Florida Current where it will be quickly removed. The Florida Current may encroach, either along the bottom where it displaces water at that depth and forces freshened water off at the surface, as was observed to occur on another part of *Caryn* Cruise 64, or it may move in bodily at all depths, sweeping coastal water out of the area, presumably to the north where it becomes part of the Gulf Stream or slope water.

Surface observations at Diamond Shoals Lightship over a period of nearly six years reveal large, and frequently sudden, fluctuations in the water temperature owing to the passage to an fro of the interface between the colder waters from north of Cape Hatteras and the waters of Raleigh Bay influenced by the Florida Current. Meander-like encroachments of the Florida Current onto the shelf and recessions from it appear to be one of the logical explanations for these fluctuations. Correlations with wind direction and force are patently unsatisfactory. Yet northeast storms are effective in driving Middle Atlantic coastal water southerly across Diamond Shoals.

Light winds which produce no great frictional effect and onshore winds will permit fresh water to accumulate on the shelf. These influences make it possible for fresh water to diminish with increasing runoff or to accumulate on the shelf with a falling runoff. But from the overall point of view high sustained runoff produces a large relative volume of fresh water on the shelf (that is, March, 1948) and a low sustained runoff yields a relatively low fresh-water volume.

Summary--The hydrography of the continental shelf off North Carolina, south of Cape Hatteras, is controlled by an environment which produces moderate horizontal gradients and weak to moderate vertical gradients in temperature and salinity. In winter water temperatures may range from 10°C at the coast to 22°C only 60 mi to the southeast. Salinity is as low as 18 $^{0}/_{00}$ in the sounds, bays, and rivers, and approximately 32 $^{0}/_{00}$ at the inlets, yet a salinity of 36 $^{0}/oo$ may occasionally be found within ten miles of the coast and never farther than 50 mi away. Gradient conditions are greatest in Raleigh Bay, less strong in Onslow Bay, and least in Long Bay, owing chiefly to the geography; that is, widening of the continental shelf toward the southwest. The seasonal progression of temperature and salinity distribution may frequently be modified by intrusions of the Florida Current over the continental shelf. This intrusion may be especially broad in Raleigh Bay.

Nontidal currents over the shelf may be so slow that they are barely detectable, yet just over the edge of the continental shelf the Florida Current ceaselessly flows at speeds greater than 150 cm/sec. Six reasons why a dynamic coastal current is a transient affair in this region are given. The nontidal currents over the inner parts of the shelf appear to result from the balance of forces at work, tending northerly in general but turning southerly when the pressure gradient is modified sufficiently by the runoff to counteract the thermal effect, or the frictional drag of the southerly winds or the Florida Current.

Acknowledgment--This research was sponsored by the Office of Naval Research under Contract N6onr-27701.

References

ABBE, C., JR., Remarks on the cuspate capes of the Carolinia coast, Proc. Boston Soc. Nat. Hist., v. 26, pp. 489-497, 1895.

DAVIS, W. M., Die erklärende Beschreibung der Landformen, pp. 475-476, Leipzig and Berlin, 1912.

GULLIVER, F. P., Shoreline topography, Proc. Amer. Acad. Arts Sci., v. 34, p.180, 1899.

HAIGHT, F. J., Coastal currents along the Atlantic Coast of the United States, U. S. Coast and Geod. Surv., Spec. Pub. 230, 77 pp., 1942.

ISELIN, C. O'D., A study of the circulation of the north Atlantic Ocean, Pap. in Phy. Ocean. and Met., v. 4, No. 4, 101 pp., 1936.

MARSHALL, N., Hydrography of North Carolina marine waters, Survey of Marine Fisheries of North Carolina, by H. F. Taylor and associates, pt. 1, pp. [illegible]-76, Univ. of North Carolina Press, Chapel Hill, 1951.

MILLER, A. R., A pattern of surface coastal circulation inferred from surface salinity-temperature data and drift bottle recoveries, WHOI Ref. 52-28, 14 pp., 1952 (unpublished manuscript).

PARR, A. E., A geographic-ecological analysis of the seasonal changes in temperature conditions in shallow water along the Atlantic coast of the United States, Bull., Bingham Oceanogr. Coll., v. 4, no. 3, pp. 1-90, 1933.

PIERCE, E. L., The chaetognaths over the continental shelf of North Carolina with attention to their relation to the hydrography of the area, J. Mar. Res., v. 12, pp. 75-92, 1953.

ROELOFFS, E. W. and D. F. BUMPUS, The hydrography of Pamlico Sound, Bull. Mar. Sci., Gulf and Caribbean, v. 3, no. 3, pp. 181-205, 1953.

RUDE, G. T., Shore changes at Cape Hatteras, An. Assn. Amer. Geog., v. 12, pp. 87-95, 1922.

SHEPARD, F. P., Submarine geology, Harper and Bros., New York, 1948.

SUTCLIFFE , W. H., JR., Qualitative and quantitative study of zooplankton at Beaufort, North Carolina, thesis Duke University, 1950.

U. S. GEOLOGICAL SURVEY, Surface water supply of the United States, 1950, pt. 2, South Atlantic Slope and Eastern Gulf of Mexico Basins, Water-Supply Pap. 1172, 1952.

U. S. GEOLOGICAL SURVEY, Surface water supply of the United States, 1950, pt. 1, North Atlantic Slope Basins, Water-Supply Pap. 1171, 1953.

VON ARX, W. S., D. F. BUMPUS, and W. S. RICHARDSON, Short-term fluctuations in the structure and transport of the Gulf Stream system, WHOI Ref. 54-76, 23 pp., 1954 (unpublished manuscript).

Woods Hole Oceanographic Institution,
Woods Hole, Mass.

(Communicated manuscript received December 9, 1954; open for formal discussion until January 1, 1956.)

Contribution No. 791

Deep-Sea Research, 1955, Vol. 3, pp. 82 to 87. Pergamon Press Ltd., London

A new theory of Caribbean bottom-water formation

L. V. WORTHINGTON

Abstract—A recent section across the Caribbean Sea shows that in the Caribbean deep water oxygen values have dropped 0·3 ml/l in the last twenty years, a loss closely corresponding to that in the North Atlantic deep water. Study of the surrounding Atlantic water suggests that the Caribbean deep water has not been renewed since the end of the eighteenth century, coincident with a cold climatic variation at high latitudes in the North Atlantic. It is further deduced that the Windward Passage was the sill over wnich this water originally came from the Atlantic, and that both the Jungfern and Windward Passage sills must be considerably shallower than DIETRICH's (1939) estimates.

SINCE 1933-1937, when the principal oceanographic surveys of the Caribbean Sea were carried out (PARR, 1937, 1938) changes have taken place which throw some doubt on the system of Caribbean bottom-water formation described by DIETRICH (1939), and in fact on the location and depth of the sill over which, in his view, this water flowed. In presenting new hypotheses on these matters the present author is at a great advantage over earlier authors in that they were limited to virtually synoptic data as far as the deep water is concerned, whereas he as access to observations made after a lapse of twenty years, when the changes which take place continually are thrown into bold relief.

The new data take the form of a hydrographic section which was made in the *Atlantis* in December, 1954. This section was planned in order to repeat one of PARR's sections which he made across the Caribbean Sea in March, 1933. The station positions of both these sections are plotted in Fig. 1. Before presenting the changes which have occurred, a brief description of the Caribbean deep water will be given together with DIETRICH's theory as to its formation.

In the Caribbean Basin the temperature diminishes with increasing depth to a minimum of 4·03° to 4·09° at about 2,250 m. Below this minimum the temperature rises slowly towards the bottom at a gradient slightly less than adiabatic. The water below the temperature minimum has a salinity of between 34·97‰ and 34·99‰ and can be regarded as a single water type. DIETRICH showed that the potential temperature of all the deep water varied between 3·81° and 3·85°, a value nearly 2° higher than that of the surrounding North Atlantic deep water. He considered that the Jungfern Passage was the deepest path of communication between the Caribbean and the Atlantic, and that Caribbean deep water flowed over this sill into the basin. Immediately outside the Jungfern Passage water with a potential temperature of 3·81° (the Caribbean minimum) was found at a depth of 1,600 m, and this was the sill depth he assumed, the colder Atlantic water below this level being cut off from the Caribbean Basin. None of DIETRICH's conclusions could be seriously disputed if the deep water in the Caribbean had remained unchanged.

The principal change which has taken place is the loss of oxygen in the deep water. SEIWELL (1938) gave average values of oxygen in the deep water for the whole

Caribbean Basin. These values are summarized below together with the averages for the recent section.

Table 1. *Oxygen concentration at various depths below the temperature minimum in the Caribbean Basin.*

Depth, m	*Dissolved oxygen, ml/l*		
	1933-4	1954	*Loss*
2,500	5·10	4·77	0·33
3,000	5·10	4·81	0·29
3,500	5·15	4·84	0·31
4,500	5·18	4·92	0·26
Average	5·13	4·83	0·30

The temperature changes which accompany this oxygen loss are extremely small as shown in Table 2.

Table 2. *The average temperatures at various depths from* Atlantis *stations* 1506-1514 *in* 1933 *and stations* 5235, 5257-5261 *in* 1954. *Figures in parenthesis are the number of observations.*

Depth, m	*Temperature, °C*		
	1933	1954	*Gain*
2,000	4·061 (9)	4·075 (6)	0·014
2,500	4·070 (5)	4·078 (6)	0·008
3,000	4·118 (5)	4·122 (5)	0·004
3,500	4·167 (3)	4·172 (5)	0·005

Below 3,500 m the data are insufficient for an average, but in no case does the temperature at any level vary by more than 0·01° between the years. Since the thermometers are only accurate to this amount, nothing can be said about the very deep water until sufficient new observations have been made elsewhere in the Basin. The small gains in temperature above the 3,000 m level do appear to be significant, and are evidently the result of eddy diffusion from higher levels.

The rate of oxygen consumption of 0·3 ml/l in twenty years (0·015 ml/l-year) has certain implications which bear discussion. If the temperature and salinity of a water type are known, its oxygen saturation point is also known. If the oxygen consumption rate in this water type has remained unchanged since the time of saturation, a date can be assigned to its last renewal by contact with the atmosphere. This method of dating is somewhat crude, and it is open to criticism in that the initial oxygen consumption due to the immediate oxidization of the organic matter in the water may be at a far higher rate than subsequently (REDFIELD, personal communication). A further objection is that the water may not have been fully saturated with oxygen by the process of its last renewal. If either of these objections is valid, a date of last renewal must be moved into the more recent past, so that the method at least sets a time limit before which the last renewal should not be supposed to have taken place, since there is no reason for thinking that the rate of consumption has become more rapid.

The deep-water consumption rate of 0·015 ml/l-year is identical to that estimated by WORTHINGTON (1954) for the North Atlantic deep water. His estimate was a fairly rough one due to the paucity of recent data. Now that numerous samples have been obtained from the depths of the Caribbean, which are filled with nearly homogeneous water, perhaps a consumption rate of this magnitude can be more widely relied upon. Doubtless the rate is not the same throughout the oceans, but varies with the locality, since the supply of organic matter from the upper layers will not remain constant in different areas.

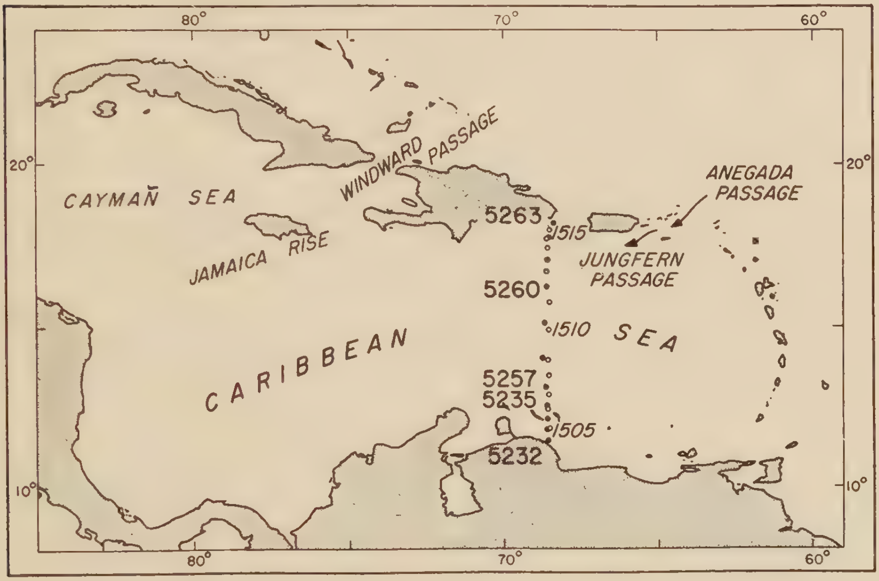

Fig. 1. The Caribbean and Cayman Seas, including the principal sills. Two *Atlantis* sections are plotted, one from 1933 and the other from 1954.

In his estimate of the age of the North Atlantic deep water WORTHINGTON used the following figures:

Average O_2 in 1930 = 5·8 ml/l. From SEIWELL's (1934) chart of O_2 at 2,500 m.

Average O_2 in 1950 = 5·5 ml/l. From *Atlantis* stations in the years 1947-1954. This gave the rate of 0·015 ml/l-year.

Saturation point of the water = 7·6 ml/l. It was assumed that the water had a temperature of 2° and a salinity of 34·9‰ at the time of its formation.

Subtracting 7·6-5·8 = 1·8 ml/l of oxygen consumed between the saturation date and 1930.

1·8 ml/l at 0·015 per year = 120 years prior to 1930.
= 1810.

A coherent dating system can be arrived at for the Caribbean and Cayman Seas by using this consumption rate, a system, moreover, which is consistent with what is known of the climatic variation at high latitudes. No recent observations have been obtained in the Cayman Sea, and it will have to be assumed that the rate of 0·015 ml/l holds true there. In the chronology which follows we are dealing with the history of a single water type: $T = 4{\cdot}0°$, $S = 34{\cdot}98‰$. The oxygen saturation-point of this water is 7·25 ml/l (using the potential temperature of 3·8°). The last renewal of this water in the North Atlantic is the latest date in the chronology, and the dates which are of the greatest concern are those at which the basins became isolated from each other and from the Atlantic. Dates are rounded off to the nearest decade; oxygen values are in ml/l.

1790 The 4·0° isotherm drops below the threshold at the Jamaica Rise. Deep water communication between the Cayman and Caribbean ceases. (O_2 in the Caribbean Sea in 1933 was 5·13 from Table 1, 7·25-5·13 = 2·12 consumed. At 0·015/yr = 142 years prior to 1933.)

1810 Last renewal of North Atlantic deep water (from WORTHINGTON).

1840 The 4·0° isotherm drops below the threshold at the Windward Passage. Deep water communication between the North Atlantic and the Cayman Sea ceases. (O_2 in the Cayman Sea in 1933 was 5·85, from SEIWELL, 1938. 7·25-5·85 = 1·40 consumed. At 0·015/yr = 93 years prior to 1933.)

1850 The 3·8° isotherm loses contact with the atmosphere at high latitudes. (O_2 of this water outside the Windward Passage was 5·95, from SEIWELL, 1938. 7·25-5·95 = 1·30 consumed. At 0·015/yr = 87 years prior to 1933.)

This chronology is strongly supported by climatological evidence. AHLMANN (1948) summed up a vast mass of data of many kinds (glaciological, eustatic, biological, etc.) which all confirm that a remarkably cold period centred around the end of the eighteenth century. This can be most clearly illustrated by the temperature data from Holland, which extended back to the beginning of the eighteenth century. AHLMANN's January and July average temperatures (30-year overlapping means) are reproduced here (Fig. 2). There is much glaciological evidence that this is not merely a local phenomenon. AHLMANN in fact suggests that the glaciers in the North Atlantic area reached their greatest point of advance since the Würm/Wisconsin ice age in the middle or late eighteenth century.

If this system of deep water formation is accepted, there is no further need for assuming that the Jungfern Passage is the sill for the Caribbean basin and thus for accepting the coincidence that the sill-depth waters flowing through the Jungfern and Windward Passages, which are 750 km distant from each other, differ by not as much as 0·01‰ in salinity and by only 0·04° in potential temperature. If the concept of the steady state is held to, it is impossible to supply the Caribbean Basin from any other source since, in 1933, at any rate, the same temperature minimum was found at greater depths in the Cayman than in the Caribbean Basin. The close similarity between the two water types on either side of the Jamaica Rise supports the conclusions that the Caribbean deep water was originally supplied from the Cayman Sea, and that the Windward Passage was the ultimate sill over which the water of both basins poured in from the Atlantic.

The isolation of the Cayman deep water from the Atlantic occurs at 1840 in this chronology, some years subsequent to the period of greatest cold at high latitudes. This occurrence can be attributed to the gradual weakening of the North Atlantic eddy. This weakening, according to the geostrophic equation, should be accompanied by a rise in the level of the thermocline at the centre of the eddy, and a drop in level around the edges. In 1954 the Woods Hole Oceanographic Institution undertook a new oceanographic survey of the western North Atlantic in repetition of the survey made between the years 1922-1934, principally by the research vessels *Dana* and *Atlantis*. While it would be premature to give detailed results until the new survey is nearer completion, there is abundant preliminary evidence that the eddy has weakened since that period. This evidence comes in many forms; among them are an average drop of 10 per cent in the computed volume transport of the Gulf Stream off Woods Hole, the further advance of the Mediterranean water into the Sargasso Sea, and on one section at least (Bermuda to Hispaniola) just such changes in the depth of the thermocline as are described above, and as would cause the 4° isotherm to drop even further below the sill depth at the Windward Passage. This weakening of the eddy is related to the amelioration of the Arctic climate.

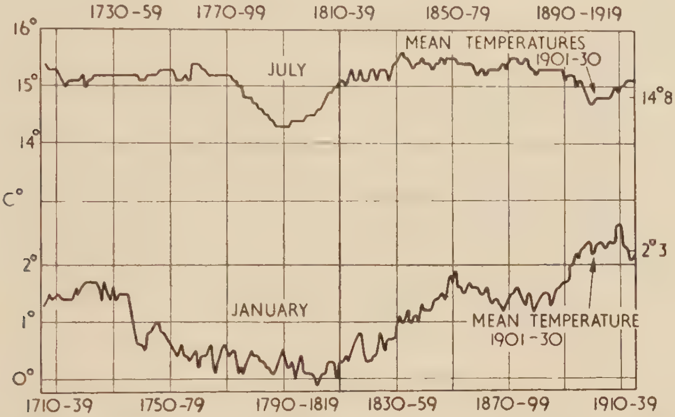

Fig. 2. January and July temperatures in Holland plotted in 30-year overlapping means. Reproduced from Ahlmann (1948).

It is implicit in the reconstruction of events presented here that the sill depths of both the Jungfern and Windward Passages must be considerably shallower than those assumed by Dietrich (both 1,600 m) in order to permit steady flow. No one has yet established by actual sounding the depth of any of the important sills which connect the various basins of the American Mediterranean Sea to each other and to the Atlantic.

If the Windward Passage were to be sounded thoroughly, a simple matter with the continuously recording sonic equipment available today, one could determine the amount that the 4° isotherm has subsided below the sill depth since the days when free communication took place between the Cayman deep water and the Atlantic. By such means as this, a beginning could be made towards estimating the

Contribution No. 794

Deep-Sea Research, 1955, Vol. 3, pp. 46 to 65. Pergamon Press Ltd., London.

On the fine-structure of the Gulf Stream front*

W. S. von Arx, D. F. Bumpus and W. S. Richardson

Detailed study of the water motion in the Gulf Stream has revealed a structure which, as far as one can tell, is best interpreted as a succession of short, overlapping segments which may be described as " shingles." Since shingling viewed from the gable end may have left- and right-hand symmetry with respect to the ridge pole, we may regard the shingle structure of the Gulf Stream as left-handed on the continental side looking down stream. Fuglister (1951), in his paper on the multiple currents of the Gulf Stream, was the first to suggest this possibility from consideration of temperature data alone. Since then the present authors (1953, 1954) have found evidence for both this and a similar but finer shingle structure through other kinds of observations from both ships and aircraft. Malkus and Johnson (1954) followed one filament of the large-scale shingle elements in a drifting ship. The field observations to be described here indicate that several different scales of shingling occur simultaneously. Individual filaments have been traced which range in length from perhaps 500 to 100 km or less. Associated with these are smaller shingles some tens of km long or a complex multiple-front system extended a like distance. The existence of shingles less than 10 km long has been suggested by direct visual observation of the sea surface from aircraft.

It appears at the moment that the individual current filaments are distinguishable by their temperature, velocity, water type, and an associated slope of the isotherms below the surface, which is generally sharpest somewhere near the mid-length of the segment and blends into the background at each end. It is our experience that the overlap of these filaments is sufficient, in most cases, for the succeeding filament downstream to be intercepted from the air by flying 90° to the left of the heading steered when the evidence for the first streamer vanished into the background.

THE LONGITUDINAL PATTERN AS SEEN FROM THE AIR

During 26-27 February, 1953, an attempt was made to fly along the length of the Gulf Stream front between Miami, Florida and 70°W longitude. On this flight, as during an earlier flight made in November, 1952 (Stommel *et al.*, 1953), the Stommel-Parson airborne radiation thermometer was used together with photographic (von Arx, 1953) and visual observations to determine the position of the frontal outcrop on the sea surface. The radiation thermometer consists of a Golay detector which, through optical means, alternately views the sea surface and a blackened body whose temperature is known. The signal from the detector is nulled by changing the temperature of the reference body so that its emission is equal to that arriving from the sea surface and the water vapour in the intervening atmosphere. The temperature of the reference body is regarded as representative of that of the sea surface. The course of the flight was determined partly by this temperature information, and partly by visible indications of the edge of the current, which include the contrast in water colour between Gulf Stream water and Slope water, the change in sea state across the frontal outcrop, the accumulated Sargassum and flotsam over the frontal convergence, and, in calm weather, characteristic patterns of slicks which tend to lie parallel with the front in Slope water. The aircraft was flown at an altitude of 1,500 ft. (under cloud base), and its position fixed by Loran at intervals of a few minutes when it was possible to follow the outcrop, and at crossings of the outcrop when a zigzag flight plan was employed. Fig. 1 shows the observed frontal outcrop.

---

* Contribution No. 794 of the Woods Hole Oceanographic Institution. This work was supported by the Office of Naval Research under Contracts N6onr-27701 (NR-083-004) and Nonr-769 (00) with the Woods Hole Oceanographic Institution.

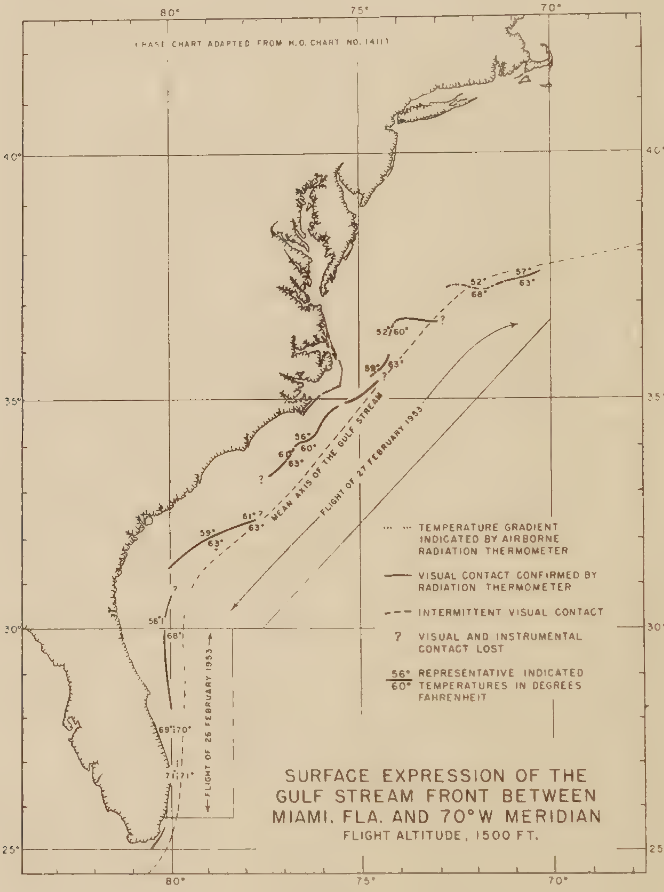
80°
75°
70°
(BASE CHART ADAPTED FROM H.O. CHART NO. 1411)
40°
35°
30°
25°
52° 57° 63° 68°
52/60°
59°/63°
56° 60° 63°
61° 63°
59° 63°
56°
68°
69° 70°
71° 71°
?
MEAN AXIS OF THE GULF STREAM
FLIGHT OF 27 FEBRUARY 1953
FLIGHT OF 26 FEBRUARY 1953
TEMPERATURE GRADIENT INDICATED BY AIRBORNE RADIATION THERMOMETER
VISUAL CONTACT CONFIRMED BY RADIATION THERMOMETER
INTERMITTENT VISUAL CONTACT
? VISUAL AND INSTRUMENTAL CONTACT LOST
56°/60° REPRESENTATIVE INDICATED TEMPERATURES IN DEGREES FAHRENHEIT
SURFACE EXPRESSION OF THE GULF STREAM FRONT BETWEEN MIAMI, FLA. AND 70°W MERIDIAN
FLIGHT ALTITUDE, 1500 FT.

Fig. 1.

In following each segment, one had the experience that the temperature contrast across the front, and the change of sea state and sea colour coincident with the temperature contrast, grew stronger and then fainter as observations were pursued down stream, until at last none of these clues were sufficiently pronounced to direct the aeroplane further. The course was then changed 90° left (as earlier experience directed) and in every case contact with the frontal outcrop was re-established. This fresh contact was usually strong, so that one can infer that the filament extended up stream some distance. Thus the pattern of filaments plotted in Fig. 1 does not show the overlap that was probably present. Visual observations from the aeroplane at this time indicated a fine shingle structure, usually left-handed, which interrupted the continuity of the frontal outcrop at intervals in the order of 10 km. When horizontal visibility was good, it was possible to fly across these individual irregularities without losing track of the larger scale features.

The relationship between the frontal position detected from ships and from aircraft has been studied to some extent. The aeroplane is capable of detecting only the superficial expressions of the frontal structure which, it is known, may differ in position from that of the steepest horizontal gradients of temperature at depths of 100 to 200 metres. Strack (1953) has shown that the discrepancy between the greatest temperature contrast at the surface and at 100 metres may be as much as 50 miles or more in summer, but much more closely correlated in winter. Therefore the evidence given by the radiation thermometer is probably most reliable geographically during the winter months, when this flight was made.

On 5th and 6th June, 1953 it was possible to observe the position of the frontal outcrop from the air at the same time that a ship on the sea surface below made observations of the horizontal transverse temperature gradient to a depth of 200 metres. On 5th June the frontal outcrop was sharp as seen from the air, and its position was found to be 5 miles shoreward of the position of the greatest temperature contrast at a depth of 200 metres as shown in Section W. On the following day the aeroplane was unable to find a front in the vicinity of the ship and, indeed, a traverse shown in Section Y across the Gulf Stream revealed no sharp temperature contrast in the upper 200 metre layer. These two observations are not sufficient to establish the identity of aerial and shipboard observations of the frontal position in all instances, but they suggest a correlation which, in the presence of other evidence, seems worthy of provisional acceptance.

SERIAL SECTIONS FROM SHIPBOARD

The shingle structures of the Gulf Stream are probably migratory and possibly ephemeral. It has not been possible as yet to make consecutive aerial observations that would show either the direction or speed of migration of these features or their changes with time. However, a succession of crossings of the Gulf Stream axis made with the R/V *Caryn* (Cruise 64) in the area shown in Fig. 2 show that the velocity and the temperature contrast of the currents change rapidly with time, even in the course of a single day. In all, 26 sections (A through Z) were made at right angles to the mean axis of the Gulf Stream in the offing of Onslow Bay. When everything was in good order, it was possible to sail the ship across the current at least twice and sometimes three times during a 24 hour interval. Steering with the aid of the GEK it was possible to compensate for downstream set and thus to keep the plane of observation nearly fixed in space. Three groups of 5 and one group of 9 consecutive sections were made during the period 16 May through 7th June, 1953. Observations included measurements of surface salinity (Fig. 3a), temperature to a depth of 200 metres by means of the bathythermograph (Fig. 3b, c, d), and of the surface velocity (Fig. 3 and Sections A-Z) by means of both the GEK and the Loran dead-reckoning method. The values recorded on Sections A-Z were obtained by GEK. The mode of Loran DR velocities was greater by a factor 1·46, the interquartile range being 1·41 to 1·55.

The results show that the surface motion is directed alternately on shore and off shore in the course of two or three weeks. A similar regime of motion in the sub-surface water has been inferred by BUMPUS (1955) and BUMPUS and PIERCE (1955) from hydrographic and biological evidence obtained on the continental shelf in the offing of Onslow and Raleigh Bays. Corresponding migrations of the temperature field, but an imperfectly related strengthening and weakening of the horizontal temperature contrast, are also evident. The successive sections are designated A through Z. The group A through I revealed a strong tendency to offshore surface motion with increasing horizontal temperature contrast at 200 metres. The horizontal temperature contrast was also strong in the group J through N when the current was essentially parallel to the coast, and increasing contrast is to be noted in the group Q through U when the current direction changed from slightly offshore to onshore. A weakening of horizontal temperature contrast is to be noted in the group V through Z when the current direction was shifting from parallel to the coast to offshore. If anything, these observations suggest that the temperature contrast may increase when the surface current has a strong onshore or offshore component, but even this relationship is not without exception.

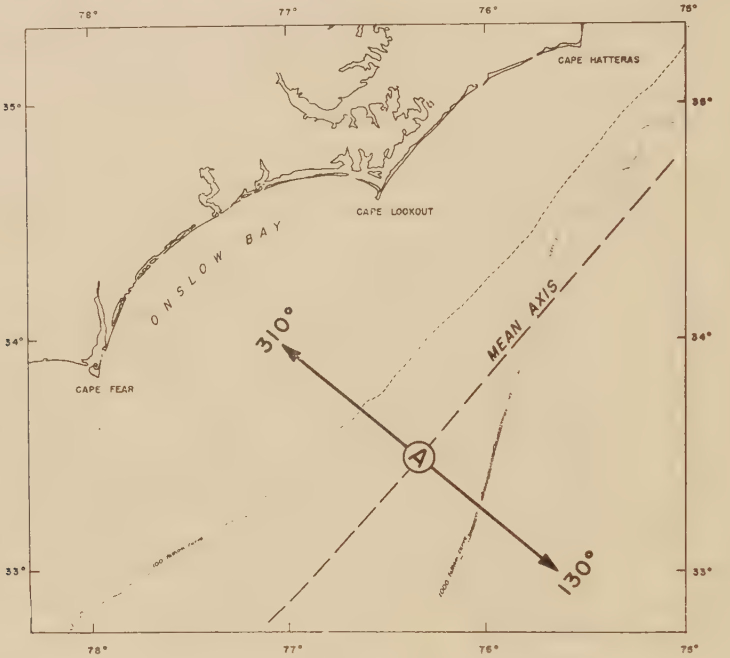

Fig. 2. Site of the serial sections made by R/V *Caryn*. The point A, marking the intersection of the line of traverse with the mean axis of the Gulf Stream, is indicated on Figs. 3a, b, c, d, and Sections A-Z.

The characteristic maximum surface velocities observed by GEK and Loran DR fluctuated between 1·5 and 3 m/sec. The rate of change of surface velocity was notable. It was found that the persistence of velocity at any point on the section

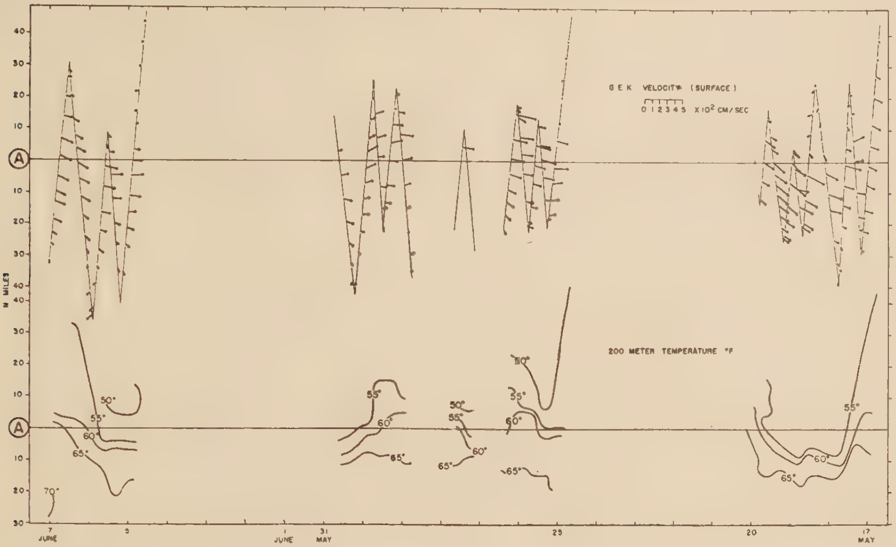
GEK VELOCITY (SURFACE)
0 1 2 3 4 5 X10² CM/SEC
200 METER TEMPERATURE °F
N MILES
40
30
20
10
A
10
20
30
40
50°
55°
60°
65°
70°
7 JUNE
9
1 JUNE
31 MAY
25
20
17 MAY

Fig. 3.

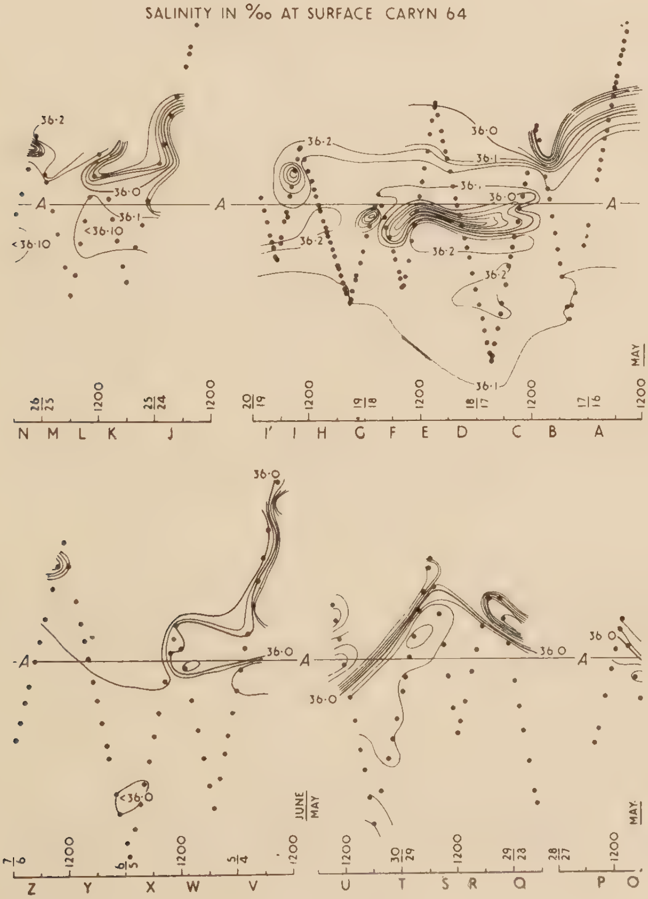
SALINITY IN ‰ AT SURFACE CARYN 64
36·2
36·0
36·1
<36·10
A
36·2
36·0
36·1
36·2
36·1
MAY
26/25
1200
25/24
1200
20/19
1200
19/18
1200
18/17
1200
17/16
1200
N M L K J
I' I H G F E D C B A
36·0
<36·0
36·0
36·0
36 0
36 O
A
7/6
1200
6/5
1200
5/4
1200
JUNE/MAY
1200
30/29
1200
29/28
28/27
1200
MAY
Z Y X W V
U T S R Q
P O

Fig. 3 (a).

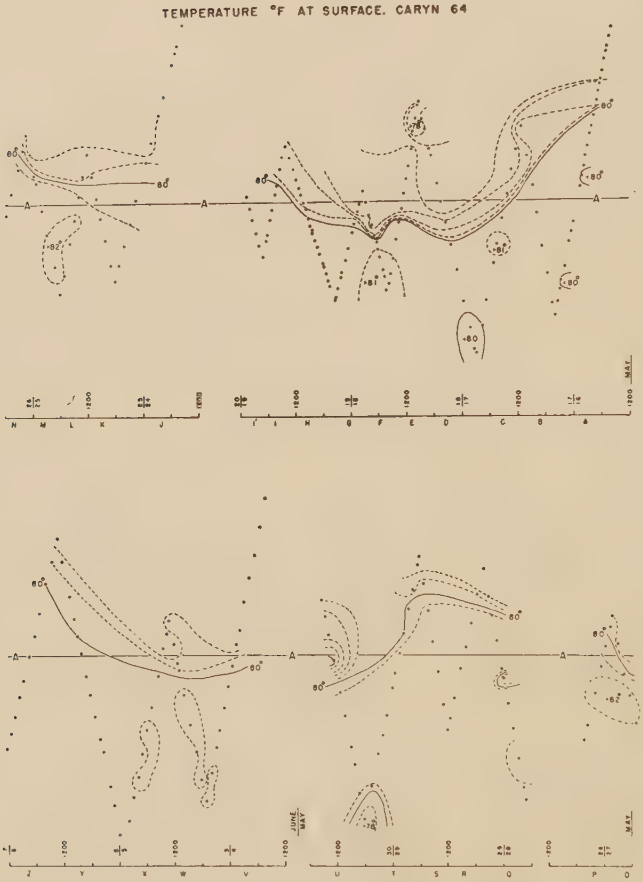
TEMPERATURE °F AT SURFACE. CARYN 64
80°
82
81
78
A
MAY
JUNE
1200
N M L K J
I' I H G F E D C B A
Z Y X W V
U T S R Q
P O

Fig. 3 (b).

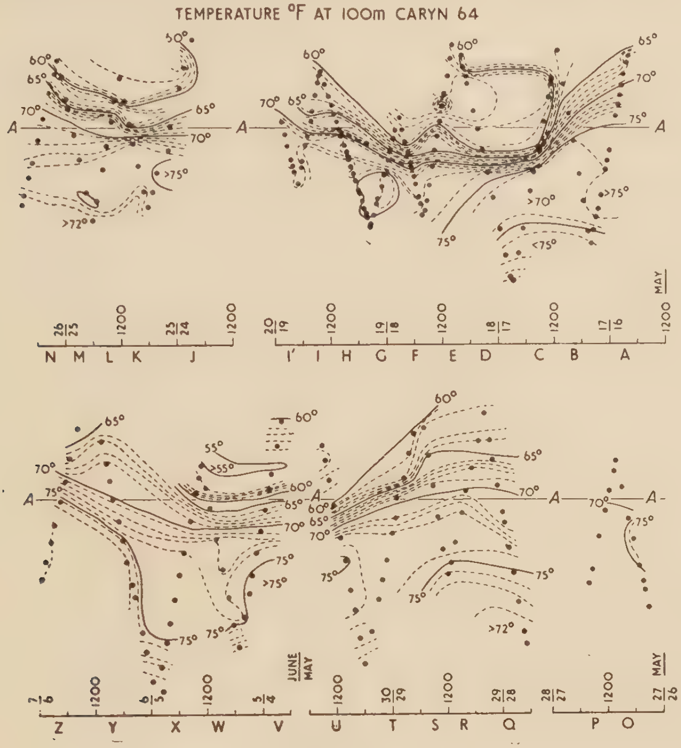
TEMPERATURE °F AT 100m CARYN 64

Fig. 3 (c).

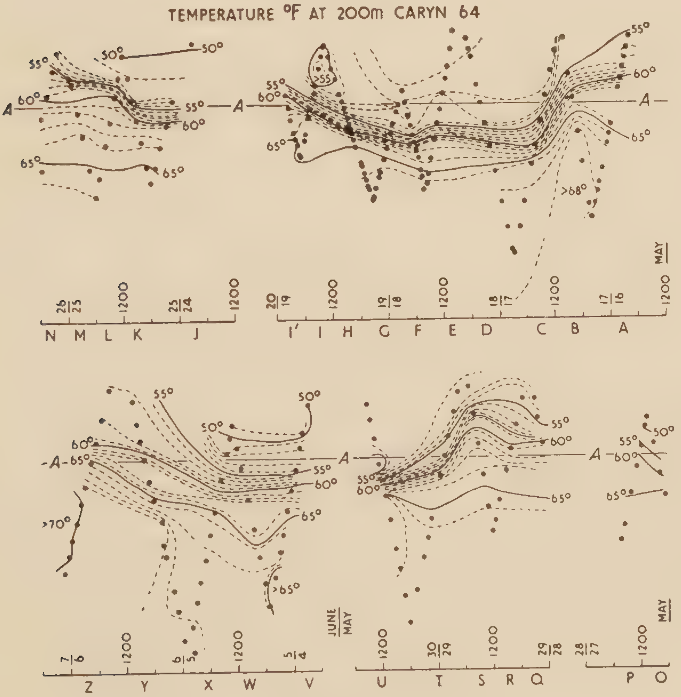
TEMPERATURE °F AT 200m CARYN 64

Fig. 3 (d).

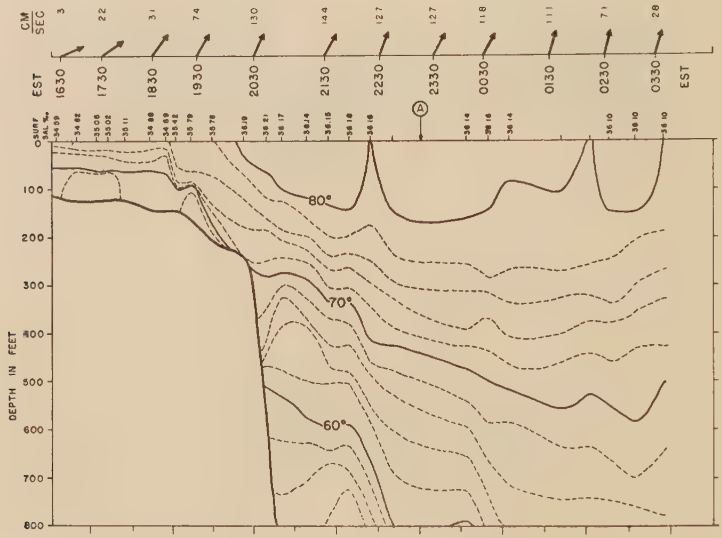

SECTION A → 130°T 1630 MAY 16-0400 MAY 17 1953

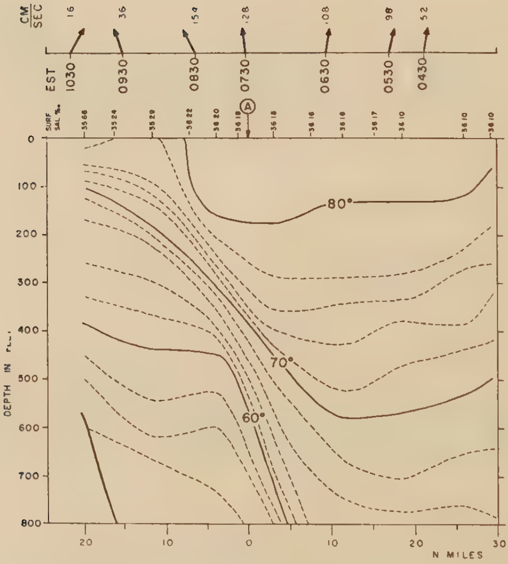

SECTION B →310° T 0400 MAY 17-1100 MAY 17 1953

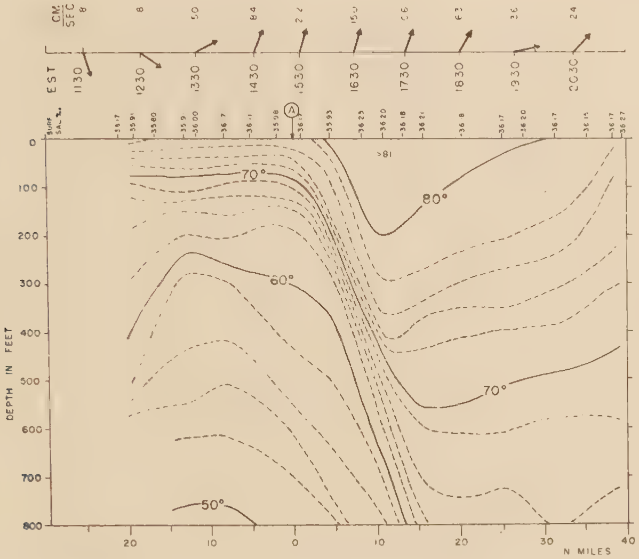

SECTION C ⟶130° T 1100 MAY 17 - 2100 MAY 17 1953

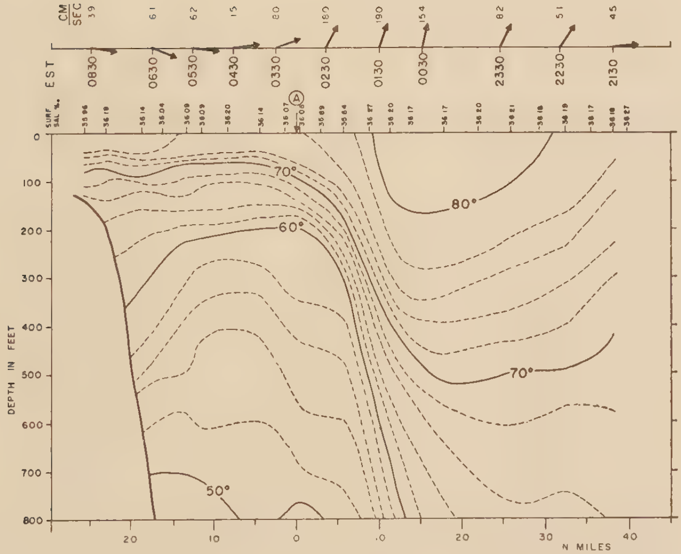

SECTION D ⟵310° T 2100 MAY 17 — 0900 MAY 18 1953

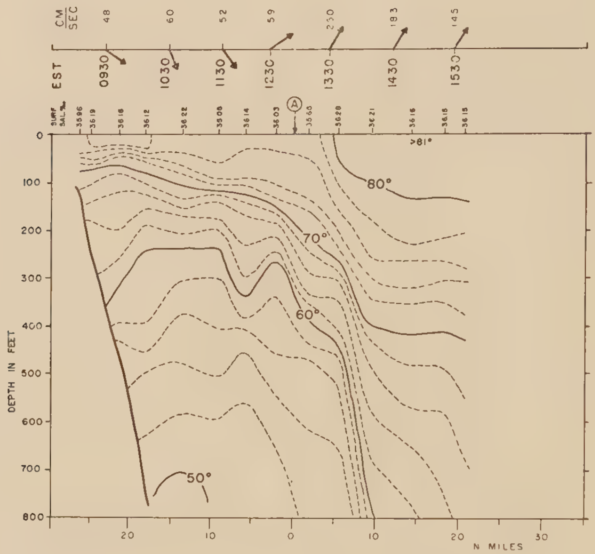

SECTION E → 130° T 0900 MAY 18 – 1600 MAY 18 1953

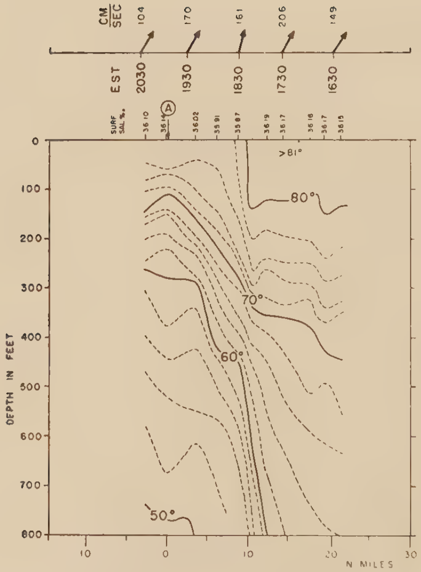

SECTION F → 310° T
1600 MAY 18 – 2100 MAY 18 1953

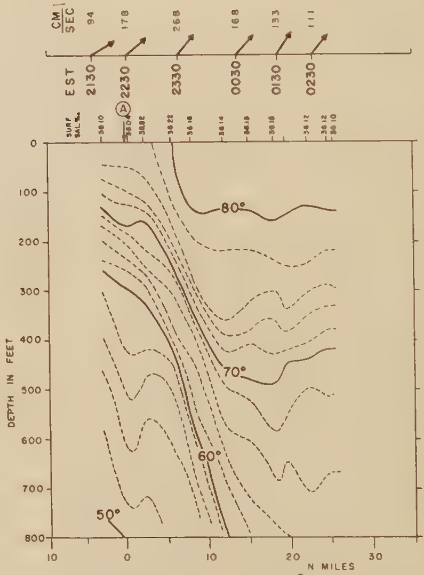

SECTION G → 130° T
2100 MAY, 18 – 0330 MAY 18 1953

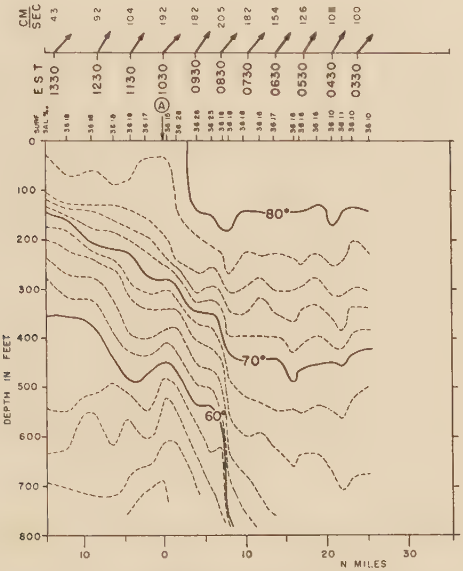

SECTION H ← 310° T
0330 MAY 19—1400 MAY 19 1953

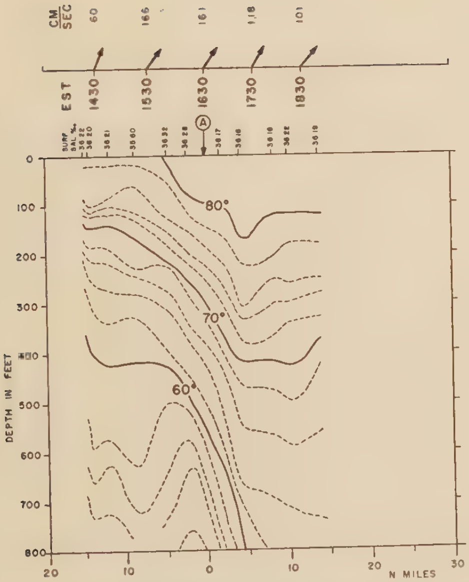

SECTION I → 130° T
1400 MAY 19—1900 MAY 19 1953

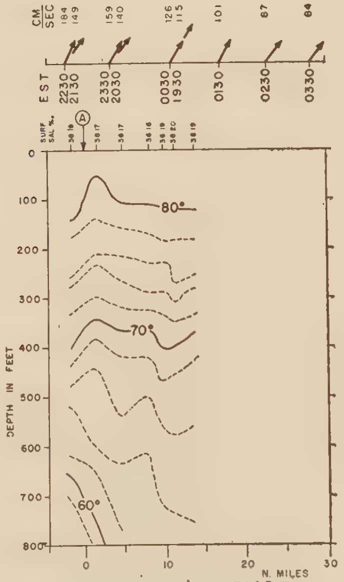

SECTION I′ ↔ 310° T
1900 MAY 19—0330 MAY 20 1953

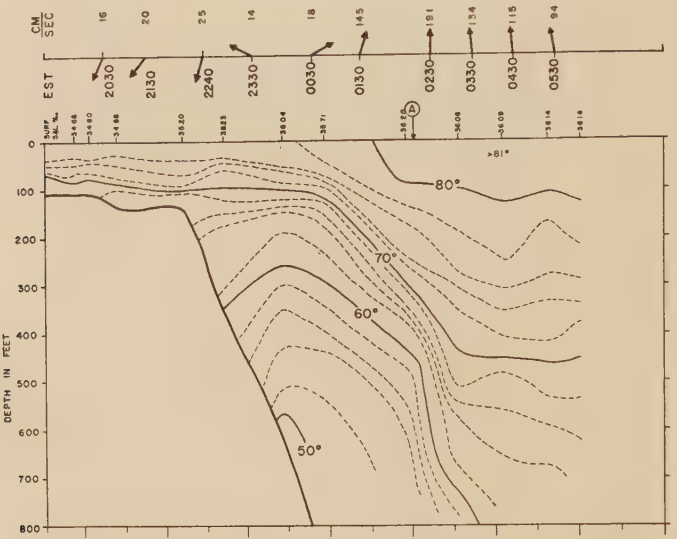

SECTION J → 130° T 1530 MAY 24 – 0600 MAY 25 1953

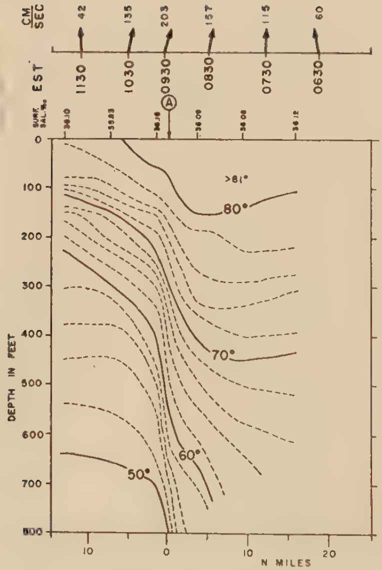

SECTION K → 310° T
0600 MAY 25 – 1200 MAY 25 1953

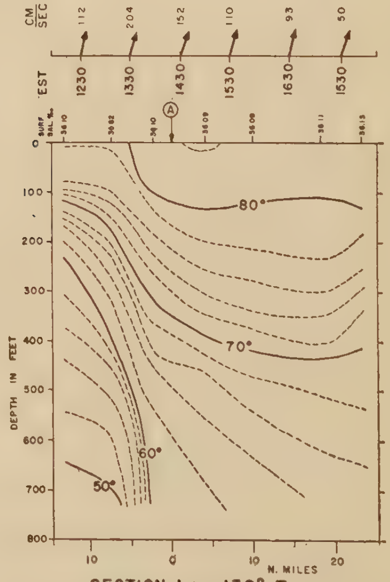

SECTION L → 130° T
1200 MAY 25 – 1800 MAY 25 1953

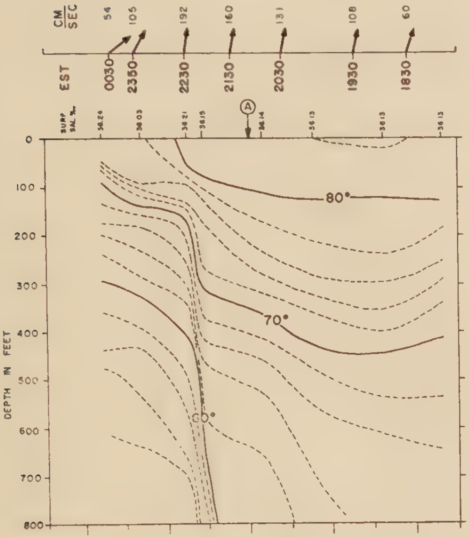

SECTION M ← 310° T
1800 MAY 25 – 0100 MAY 26 1953

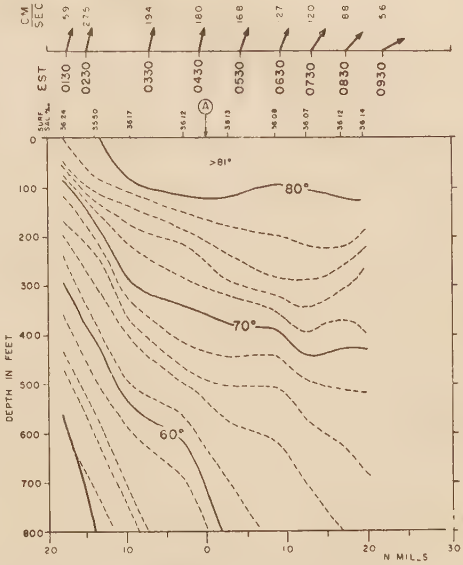

SECTION N → 130° T
0100 MAY 26 – 1000 MAY 26 1953

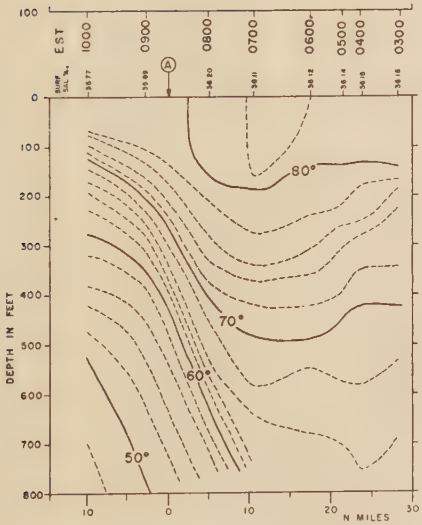

SECTION O ← 310° T
0300 MAY 27 – 1000 MAY 27 1953

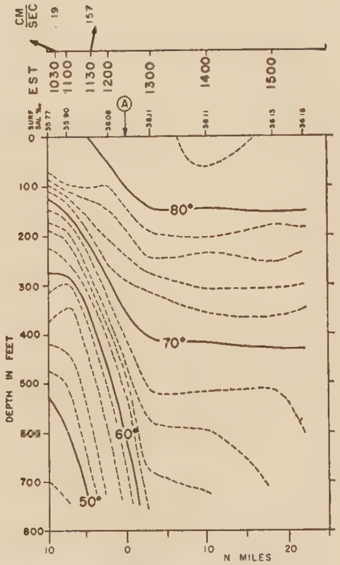

SECTION P → 130° T
1000 MAY 27 – 1700 MAY 27 1953

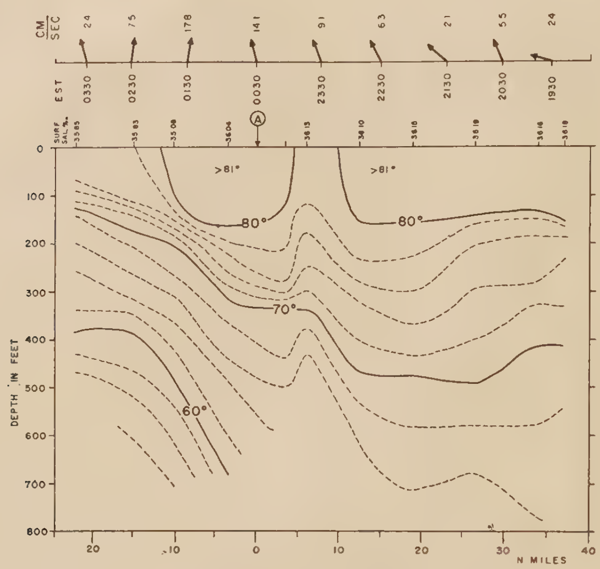

SECTION Q ⟵ 310° T
1700 MAY 28 — 0400 MAY 29 1953

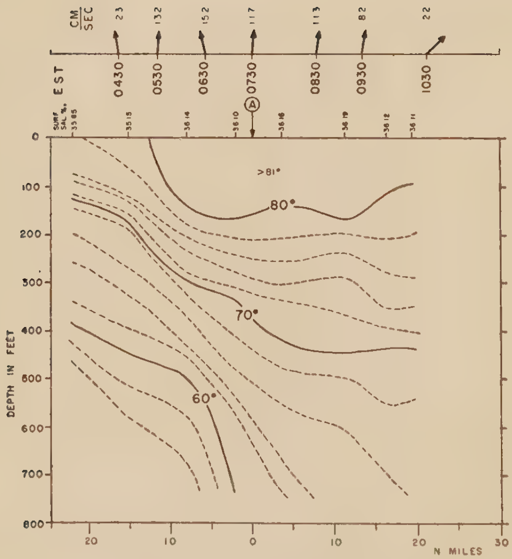

SECTION R ⟶ 130° T
0400 MAY 29 — 1100 MAY 29 1953

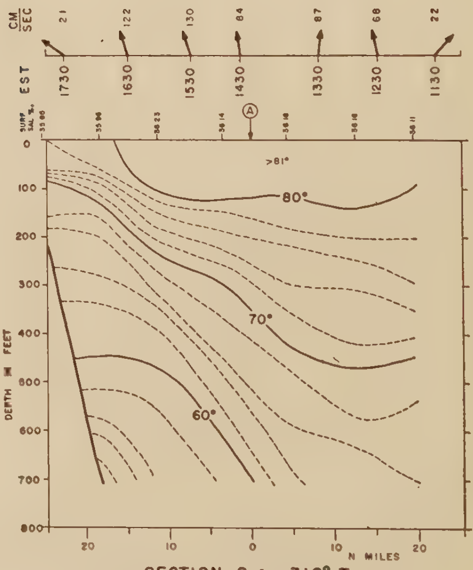

SECTION S ⟵ 310° T
1100 MAY 29 — 1800 MAY 29 1953

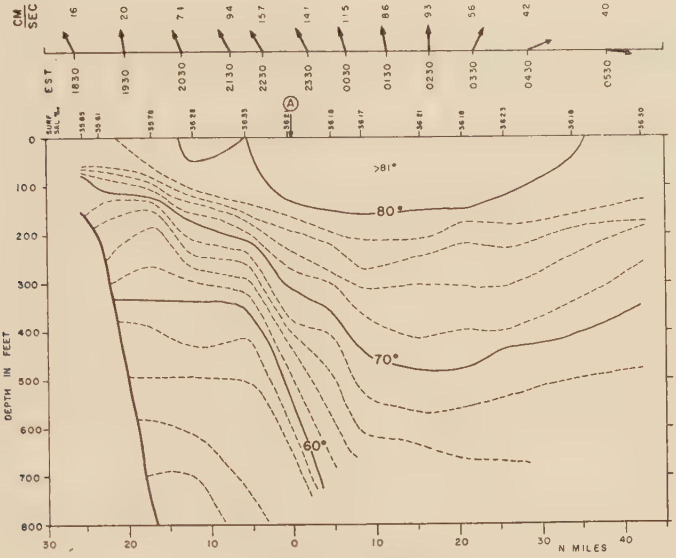

SECTION T ⟶ 130° T
1800 MAY 29 – 0600 MAY 30 1953

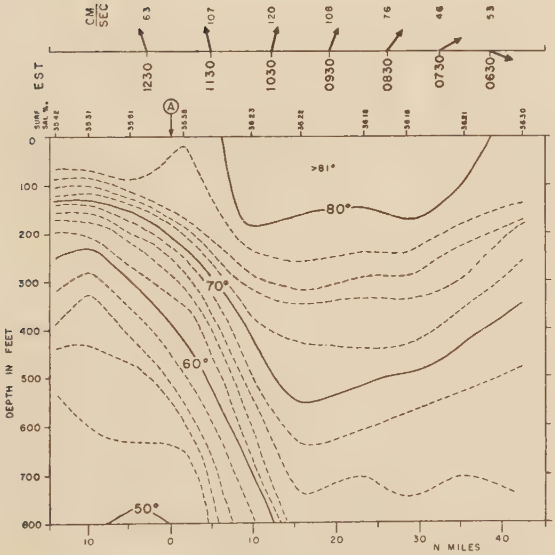

SECTION U ⟵ 310° T
0600 MAY 30 – 1500 MAY 30 1953

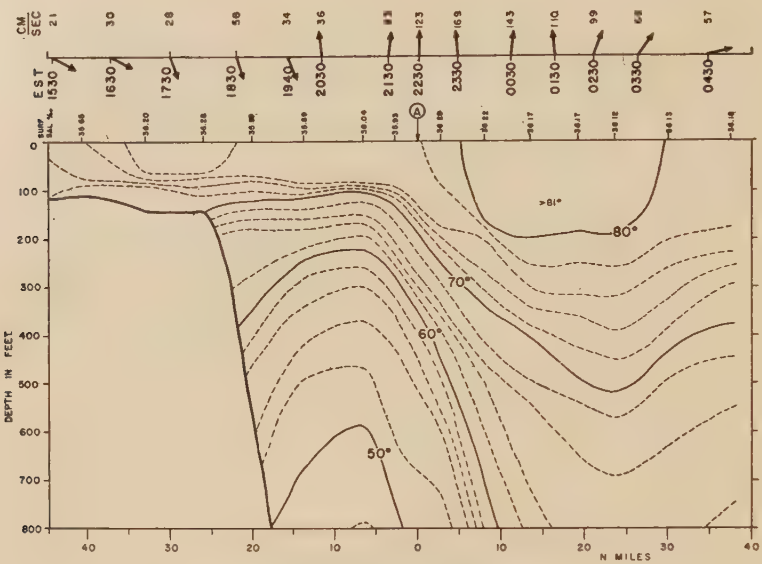

SECTION V ⟶ 130° T
1500 JUNE 4 — 0500 JUNE 5 1953

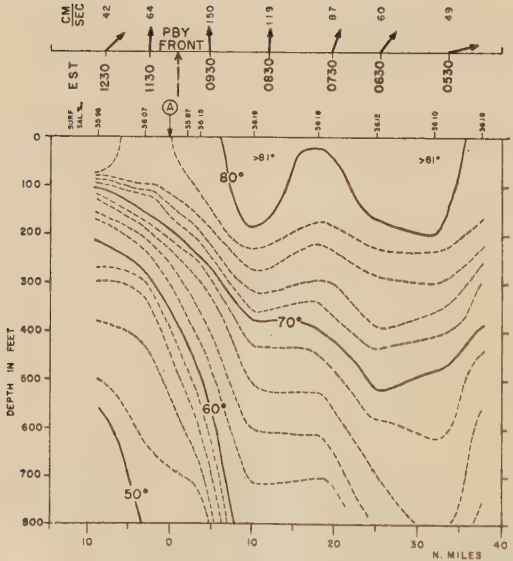

SECTION W ⟵ 310° T
0500 JUNE 5 — 1300 JUNE 1953

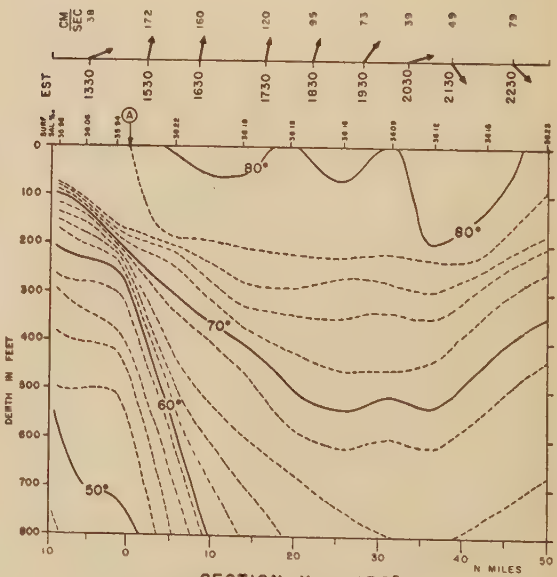

SECTION X ⟶ 130° T
1300 JUNE 5 — 2300 JUNE 5 1953

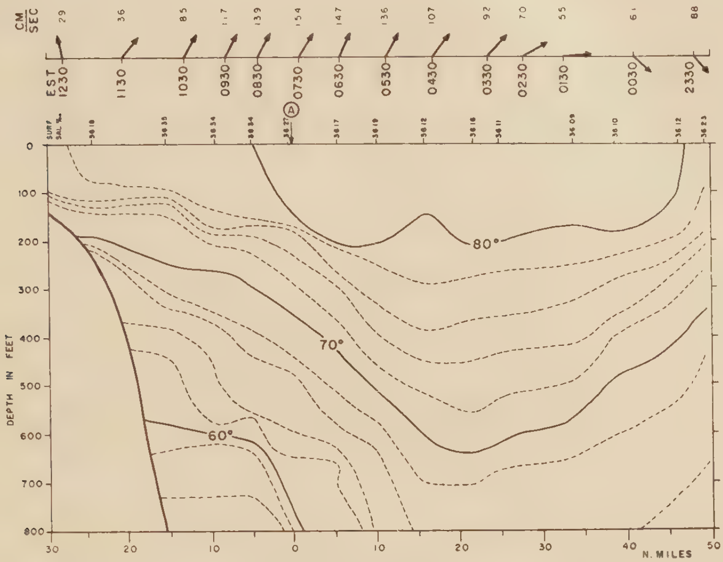

SECTION Y → 310° T
2300 JUNE 5 – 1300 JUNE 6 1953

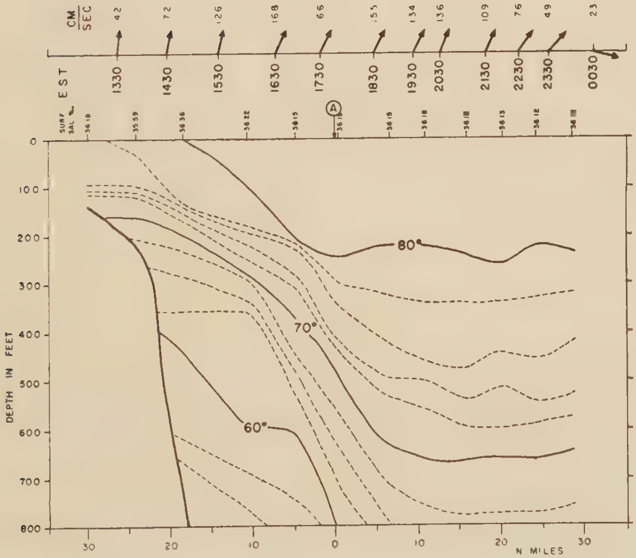

SECTION Z ⟶ 130° T
1300 JUNE 6 – 0100 JUNE 7 1953

was limited to 3 or 4 hours. The vectors shown in Fig. 3 were observed hourly, and one can see that in almost every case there was an appreciable change in current speed and direction within 2 hours of the turning point on successive sections. One can also see that within a matter of a day or two the character of surface motion could change from a diffluent to a confluent regime. The strongest currents appear to be associated with the strongest salinity contrasts, as might be expected, and it seems evident that, in addition to the normal gradient of salinity off the coastline, there are longitudinal irregularities associated with the current structure.

A POSSIBLE INTERPRETATION OF RESULTS

Pillsbury (1880) was probably the first to detect fluctuations in the flow of the Gulf Stream by direct measurements in the Straits of Florida and in the offing of Cape Hatteras. Parr (1937) reported similar fluctuations of salinity and temperature in the Straits of Florida, which he related to changes in the surface velocity observed with a taffrail log. Recently Wertheim (1954a, 1954b) has obtained electro-magnetic measurements of the fluctuations of volume transport through the Straits of Florida which vary by a factor of about 2. Murray (1952) and Wagner and Chew (1953) have also reported short-period fluctuations in the surface current from GEK observations in the offing of Miami.

The filamentary structure of the Gulf Stream suggested by Fuglister in 1951 seems to be borne out in subsequent observations by Malkus and Johnson and the present writers.

The characteristic velocities in the cores of Gulf Stream current filaments appear to be in the neighbourhood of $1\frac{1}{2}$ to 3 m/sec. During a 24 hour period a parcel of water moving within this range of speeds would cover a distance ranging from 130 to 260 km. This is roughly the range of length of the segments observed from the air, and the longest of them is not in disagreement with the lengths of the filaments plotted by Fuglister (1951, 1955), the interval between successive hot patches reported by Fuglister and Worthington (1951), and the length of drift obtained by Malkus and Johnson (1954). In view of this evidence, it is conceivable that each filament in the structure of the Gulf Stream may be in some way related to a day's discharge of water from the Gulf of Mexico. This discharge in turn may be related to the tidal sequence in the Gulf of Mexico which, it is well known from the works of Harris (1897, 1900) Endrös (1908), Wegemann (1908), Sterneck (1921), and Schureman (1940), is predominantly diurnal, being interrupted at fortnightly intervals by a short succession of weak semidiurnal tidal seiches. The diurnal tide in the Gulf of Mexico is essentially in phase at all points around its perimeter (Grace, 1932), which requires that there be a diurnal change in the volume of water in the Gulf when this tidal species predominates. Since the flow through the Straits of Florida is uni-directional, the increase in volume required for rise in the diurnal tide must be accomplished through a change in the rate of outflow through the Straits of Florida if the rate of inflow through the Yucatan Channel is constant.

To speculate further on this assumption : the flow through the Yucatan Channel and the Straits of Florida is given by Sverdrup (1942) as 26×10^6 m^3/sec, by Montgomery (1941) as between 26 to 30×10^6 m^3/sec, and by Parr (1937) as between 30 and 34×10^6 m^3/sec. The amplitude of the average diurnal tide in the Gulf of Mexico can be said to be ·4 metres and, its area $1{\cdot}3 \times 10^{12}$ m^2. Hence the volume that must enter to supply this rise in the diurnal tide is approximately 5×10^{11} m^3. If the average rate of inflow through the Yucatan Channel is 30×10^6 m^3/sec, the outflow through the Straits of Florida must be less than this figure in order for the tidal rise to occur. Assuming that the rate of rise is linear during a 12 hour period, approximately 10×10^6 m^3/sec must be contributed to effect the tidal rise, hence the flow through the Florida Straits must be this amount of short average, namely about 20×10^6 m^3/sec during the rise of diurnal tide ; and on the ebb the Straits of Florida must transport about 40×10^6 m^3/sec. Since the cross-sectional area of the Straits of Florida is not materially changed by the rise and fall of the diurnal tide, the mean velocity must change by something like a factor of 2 during the course of one diurnal tidal cycle. This requirement is not inconsistent with both the daily and weekly range of transport measured by WERTHEIM (1954a, 1954b). There are, however, other causes which may be invoked to explain the fluctuations of transport through the Straits of Florida, which will give the proper amplitude of variation at other than tidal frequencies due mainly to seasonal and synoptic changes in the wind field and pressure pattern of the atmosphere over the Gulf, Caribbean, and western North Atlantic areas.

At present there is no sound basis for relating the tidal sequence of any species to the short-period fluctuations of transport and velocity in the Gulf Stream. However, the coincidence of the range of variation of velocity and transport with the requirements of the tidal rise and fall is suggestive. The observations reported here offer evidence of fluctuations of considerable magnitude during the course of one day which, together with this and other evidence of longer period fluctuations, may be related to the shingle structure of the currents composing the Gulf Stream.

Acknowledgements—Most of the new field-work reported in this paper was made possible by funds supplied by the Office of Naval Research, under Contracts N6onr-27701 (NR-083-004) and Nonr-769 (00), which support is gratefully acknowledged.

We are indebted to members of a number of groups who have co-operated in these efforts, namely : the University of North Carolina Institute of Fisheries Research; the U.S. Fish and Wildlife Service, U.S. Fisheries Laboratory, Beaufort, North Carolina; U.S. Marine Corps Air Station, Cherry Point, North Carolina; U.S. Coast Guard Air Station, Elizabeth City, North Carolina; and University of Miami, Marine Laboratory, Coral Gables, Florida.

Woods Hole Oceanographic Institution, Woods Hole, Massachusetts.

REFERENCES

BUMPUS, D. F. (1955), The circulation over the continental shelf south of Cape Hatteras. *Trans. Amer. Geophys. Un.*, **36** (4) (in press).

BUMPUS, D. F. and PIERCE, E. L. (1955), The hydrography and the distribution of Chaetognaths over the continental shelf off North Carolina. *Pap. Mar. Biol. & Oceanogr., Suppl.* Deep-Sea Res. **3** : 92-109.

ENDRÖS, A. (1908), Vergleichende Zusammestellung der Hauptseichesperioden der bis jetzt unterzuchen Seen mit Anwendung auf verwandte Probleme. *Petermanns Mitteil.*, **54** : 86-88.

FUGLISTER, F. C. (1951), Multiple currents in the Gulf Stream System. *Tellus*, **3** (4) : 230-233.

FUGLISTER, F. C. (1955), Alternative analyses of current surveys. *Deep-Sea Res.*, **2** : 213-229.

FUGLISTER, F. C. and WORTHINGTON, L. V. (1951, Some results of a multiple ship survey of the Gulf Stream. *Tellus*, **3** (1) : 1-14.

Grace, S. F. (1932), The principal diurnal constituent of tidal motion in the Gulf of Mexico. *Mon. Not. R. Astron. Soc., Geophys. Suppl.*, **3** : 70-83.

Harris, R. A. (1897), Manual of Tides, I, *USC & GS Rept.* 357.

Harris, R. A. (1900), Manual of Tides, IV, A. *USC & GS Rept.* 661.

Malkus, W. V. R. and Johnson, K. (1954), A drift study of the Gulf Stream. *Woods Hole Oceanogr. Inst. Tech. Rept., Ref.* No. 54-67 (unpublished manuscript).

Montgomery, R. B. (1941), Transport of the Florida Current off Havana. *J. Mar. Res.*, **4** : 198-220.

Murray, Kenneth M. (1952), Short period fluctuations of the Florida Current from geomagnetic electrokinetograph observations. *Bull. Mar. Sci. Gulf and Carib.*, **2** (1) : 360-375.

Parr, Albert E. (1937), Report on hydrographic observations at a series of anchor stations across the Straits of Florida. *Bull. Bingham Oceanogr.* Coll., **6** (3) : 1-62.

Pillsbury, J. E. (1880), Current measurements in the Gulf of Mexico, Straits of Florida, and off Cape Hatteras. *Rept. Dir. U.S. Coast Survey.*

Schureman, Paul (1940), Manual of Harmonic Analysis and Prediction of Tides. *USC & GS Spec. Pub.* 98.

Sterneck, R. (1921), Die Gezeiten der Ozeane. *Sitz. Akad. Wis. Wein.* IIa, **130** : 363-371.

Stommel, Henry, von Arx, W. S., Parson, D. and Richardson, W. S. (1953), Rapid aerial survey of Gulf Stream with camera and radiation thermometer. *Science*, **117** (3049) : 639-640.

Strack, S. L. (1953), Surface temperature gradients as indicators of the position of the Gulf Stream. *Woods Hole Oceanogr. Inst. Tech. Rept., Ref.* 53-53 (unpublished manuscript).

Sverdrup, H. U., *et al.* (1942), The Oceans, Prentice-Hall, Inc., New York : 1087 pp.

von Arx, W. S. (1953), Cartographic principles applied to wide-field photography. *Photogr. Engineering*, **4** (2) : 60-73.

von Arx, W. S., Bumpus, D. F. and Richardson, W. S. (1954), Short term fluctuations in the structure and transport of the Gulf Stream System. *Woods Hole Oceanogr. Inst. Tech. Rept.*, 54-76 (unpublished manuscript).

von Arx, W. S. and Richardson, W. S. (1953), Aerial reconnaissance of the surface outcrop of the Gulf Stream front. *Woods Hole Oceanogr. Inst. Tech. Rept., Ref.* 53-24 (unpublished manuscript).

Wagner, L. P. and Chew, Frank (1953), Some results of the Florida Current survey. *Univ. of Miami Marine Lab. Tech. Rept.* 53.9, (unpublished manuscript).

Wegemann, G. (1908), Über secundäre Gezeitenwellen. *Ann. Hydroga., usw.* **36** : 532-541.

Wertheim, Gunther K. (1954a), Studies of the electric potential between Key West, Florida and Havana, Cuba. *Trans. Amer. Geophys. Un.*, **35** (6) : 872-882.

Wertheim, Gunther K. (1954b), Studies of the electric potential between Key West, Florida and Havana, Cuba. No. II. *Woods Hole Oceanogr. Inst. Tech. Rept., Ref.* 54-68 (unpublished manuscript).

Printed in Great Britain by The Salisbury Press Ltd., Publicity House, Wilton Road, Salisbury, Wilts. (93307)

Contribution No. 795

Reprinted from BIOLOGICAL BULLETIN, Vol. 109, No. 2, 328–334, October, 1955
Printed in U. S. A.

MICRO GASOMETRIC DETERMINATION OF DISSOLVED OXYGEN AND NITROGEN

P. F. SCHOLANDER, L. VAN DAM, C. LLOYD CLAFF AND J. W. KANWISHER
Woods Hole Oceanographic Institution, Marine Biological Laboratory, Woods Hole, Massachusetts, and Harvard Univ. Medical School, Boston, Massachusetts

MICRO GASOMETRIC DETERMINATION OF DISSOLVED OXYGEN AND NITROGEN[1]

P. F. SCHOLANDER, L. VAN DAM, C. LLOYD CLAFF AND J. W. KANWISHER

Woods Hole Oceanographic Institution, Marine Biological Laboratory, Woods Hole, Massachusetts, and Harvard Univ. Medical School, Boston, Massachusetts

For polluted water and many biological fluids the Winkler method for the determination of dissolved oxygen may easily become unreliable, or inapplicable. This difficulty can be avoided by using gasometric methods. We describe below such a method for the determination of oxygen (and nitrogen) in one cubic centimeter of water. It has been used extensively under field conditions to analyze, for instance, mud water in mangrove swamps (Scholander, Van Dam and Scholander, 1955), the sap in grape vines (Scholander, Love and Kanwisher, 1955), and the gases in icebergs (Scholander, Kanwisher and Nutt, 1955). The principle and apparatus are based on a micro method for the determination of carbon monoxide in blood (Scholander and Roughton, 1942).

PRINCIPLE

The water sample, followed by acid, is drawn anaerobically into an extraction syringe pipette, containing bicarbonate in the dead space. The dissolved gases escape into the large CO_2 gas phase generated by the reagents. The liquids are ejected, and the CO_2 is absorbed by strong KOH, leaving the extracted oxygen and nitrogen as a bubble which is moved into the capillary of the extractor. The gas bubble is transferred to a syringe analyzer, where the oxygen is absorbed.

APPARATUS

The apparatus consists of two parts: (1) combined water sampler and gas extractor, and (2) gas analyzer.

The extractor (Fig. 1B) consists of a 5-cc. syringe, with a fused capillary tip 5 cm. long, and of 0.7 mm. bore. It is provided with a releasable spring drag, made by passing a wire through a rubber cuff. The syringe is mounted on a wood or plastic base provided with a levelling screw, so that the tip of the capillary can be set to match the cup on the gas analyzer. The capillary tip can be closed with a rubber stopper which has a small hole slit at one end, and can also be provided with a glass cup for KOH (Fig. 1, D and E).

The gas analyzer (Fig. 1A) consists of a millimeter-graduated 0.6-mm. pre-

---

[1] Contribution Number 795 from the Woods Hole Oceanographic Institution. This work was supported by a grant from the National Science Foundation, and developed in part on the Blue Dolphin Labrador Expedition, 1954, under the auspices of the Arctic Institute of North America, Project Number ONR 138, with funds provided by the Office of Naval Research.

cision bore capillary, fused to a $3/16$-inch precision bore glass tubing, which acts as a barrel for a stainless steel plunger, terminating in an $8/40$ screw. The screw is engaged by a spring-loaded lever arm. The analyzer is temperature-stabilized by a plastic water jacket, fluted along the edges and resting on legs to keep it insulated from direct contact with hands and table.

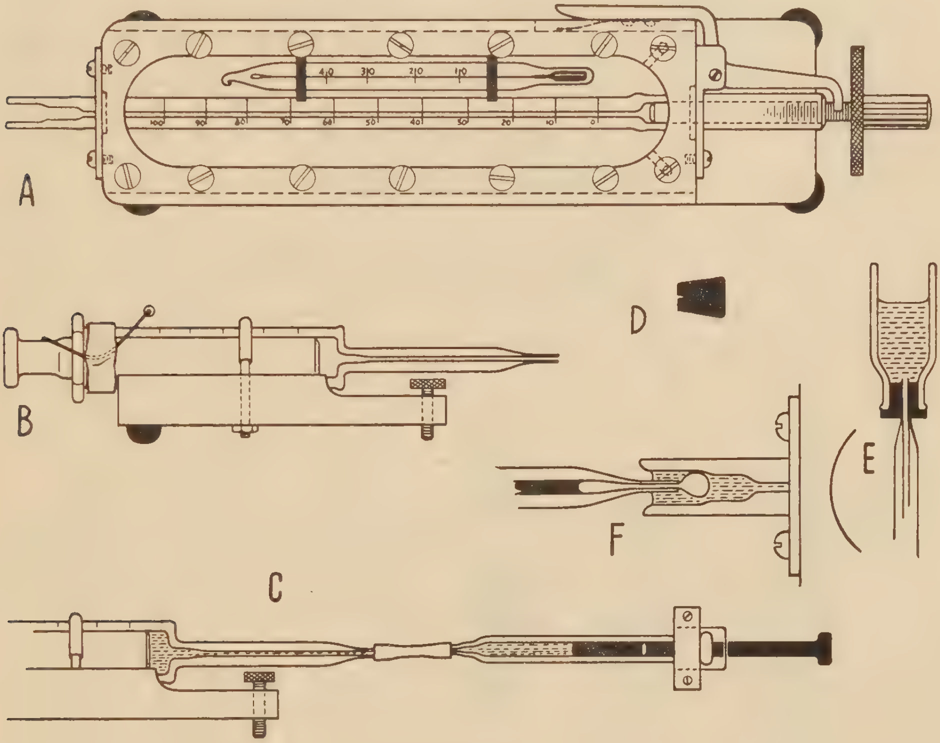

FIG. I

Figure 1. A, gas analyzer. B, extractor. C, transfer of water sample from syringe burette to extractor. D, rubber stopper for closing of extractor. E, KOH cup placed on extractor tip. F, transfer of extracted bubble to cup of gas analyzer.

Reagents

A. *For extracting gases from sample*

1. Carbonate solution: Dissolve 8 g. sodium citrate $Na_3C_6H_5O_7 \cdot 2H_2O$ and 5 g. K_2CO_3 in 20 cc. water.
2. Acid solution: Dissolve 10 g. citric acid and 3 g. sodium citrate in 20 cc. water.
3. Strong KOH solution: Add 100 g. KOH to 60 cc. water in a beaker.

Store (1) and (2) in Erlenmeyer flasks.

B. For gas analysis

1. Acid citrate: Dissolve 170 g. sodium citrate and 6 g. citric acid in 200 cc. water.
2. Alkaline citrate: Dissolve 70 g. sodium citrate and 5 g. KOH in 120 cc. water.
3. Oxygen absorber: Add 15 g. pyrogallol to 100 cc. 20% NaOH in a rubber-stoppered bottle and cover with a layer of paraffin oil 2 cm. thick. The pyrogallol is dissolved under the oil by stirring with a glass rod.
4. Acid rinsing solution: Add 1 cc. concentrated sulfuric acid to 500 cc. water and add 10 mg. potassium permanganate.

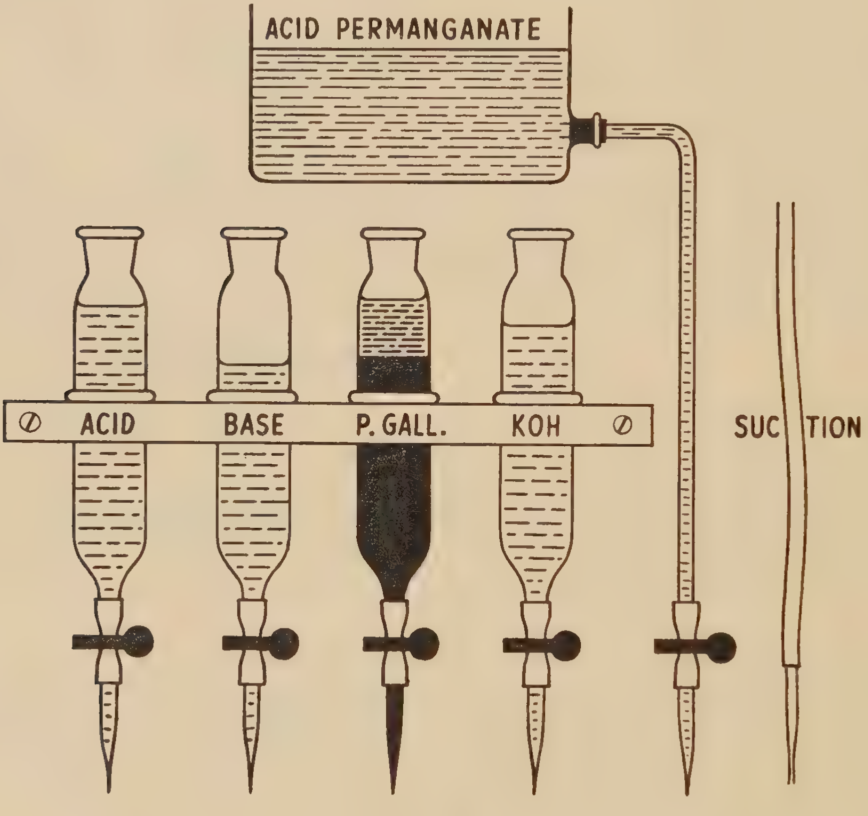

FIG. II

Figure 2. Rack for reagents and suction.

The reagents are stored as shown in Figure 2. Solutions A1 and A2 are highly concentrated in order to keep the gas solubility low. The salts crystallize out when cold, so it is often necessary to redissolve them by heating. The solutions are boiled when made up, to overcome the gas supersaturation that results from dissolving the salts.

Calibration

The capillary of the gas analyzer is most easily calibrated by means of a micrometer burette (Scholander, 1942a), with the tip above the bulb running horizontally. With the analyzer mounted horizontally on a stand, and the screw plunger removed, a stiff rubber connection is made between the water-filled cup of the capillary and the tip of the burette, being careful not to trap any air bubbles in the connection. The water is *slowly* and *evenly* moved back in the capillary by means of the micrometer, reading off partial as well as total calibration.

For accurate work it is best to draw the sample into an accurately calibrated syringe burette, with or without automatic stop, as in Figure 1C (Scholander, 1947), and from there deliver it into the extractor syringe. In many cases it will, however, suffice to measure the water sample directly into the extractor, which has been calibrated by delivering water from the one-cc. mark until the plunger touches bottom. During this operation the number on the plunger is kept facing up. The water is delivered into a cylindrical shell vial, about 1 × 3 cm., silicon-coated on the inside. The vial is handled only by forceps. The tall sides and absence of thermal convection effectively prevent evaporation loss during weighing (Scholander, Edwards and Irving, 1943). For repeated deliveries remove the water by means of suction.

Procedure

Collecting sample and extraction of gas

Pour the boiled acid and alkaline solutions (A1 and A2) into two 10-cc. beakers, which are kept covered. Rinse the extractor with water. Draw in ½ cc. of carbonate solution, discard this, and fill the dead space with the same, orienting the plunger with the number up. Either draw in the one-cc. water sample directly or push it in from the burette (Fig. 1C) through a short piece of rubber or plastic tubing. A long and thin-walled polyethylene tube is seriously pervious to gases and should not be used. Trapping of air bubbles must, of course, be scrupulously avoided. The extractor is now held vertically with the tip in the acid, and 0.2 cc. is carefully drawn in. This layers under the carbonate solution, and there is time to close the capillary tip with the rubber stopper before the CO_2 evolution begins. The loss of a few cubic millimeters of gas or liquid at this point is immaterial. With the plunger clip released, the extractor is shaken until CO_2 evolution stops, which with the proper strength of carbonate solution (A1) should be at a gas phase of about 4 cc. Shaking should be continued for two minutes, which is conveniently done by placing the extractor on a rotator. Holding the extractor tip down, the plunger is forced in to give a slight over pressure. The stopper is removed and the extracted water is allowed to run down into a finger bowl of water. Keeping the tip under water as a safety measure all of the syringe fluid is disposed of, leaving only a seal in the capillary. Turn the extractor tip up, readjusting the plunger so as to maintain the liquid seal in the capillary, and attach the KOH cup (Fig. 1E). Fill this half way up with strong KOH (A3). Expel into the KOH any air trapped in the capillary. Draw down the KOH over the CO_2 in the barrel, letting the plunger in as the CO_2 is absorbed. At the very last stage of the absorption, run the remaining bubble of oxygen and nitrogen up into the capillary, where it is safely protected from diffusion exchange until it is transferred to the analyzer.

Transfer and analysis of gas bubble

The analyzer is rinsed and the dead space plus the cup is filled with the alkaline citrate solution (B2). With the extractor and analyzer placed on the table, the extractor tip is introduced into the citrate which fills the cup of the analyzer, and the gas bubble is carefully transferred into the cup by gently twisting the extractor plunger in (Fig. 1F). The analyzer is held cup down, and the gas bubble is drawn into the capillary. With the cup up, the bubble is drawn down into the barrel, and then brought back very *slowly and evenly* into the capillary for a reading. Any abrupt movement of the meniscus leaves excess liquid on the sides of the capillary, and the volume of the bubble will be estimated too large. Enough of the citrate above the gas bubble is drawn off so that both menisci of the seal remain within the capillary during the reading. If the upper meniscus is in the cup, the gas volume reads significantly too large. The readings are made with a hand lens and with the analyzer resting on the table. The length of the bubble is checked by repeating the procedure, and the smallest reading is used (V_1). Oxygen is absorbed by slowly and steadily drawing one cupful of pyrogallol down over the bubble, with the instrument held cup up. The pyrogallol layers around the bubble in the barrel on top of the citrate. By this procedure fresh pyrogallol, in excess, runs over the bubble, which effectively prevents the formation of monoxide. The remaining nitrogen [2] bubble is slowly moved up into the capillary, and the volume is read with all three menisci in the capillary (V_2). Read the temperature of the analyzer.

After analysis, rinse the analyzer several times in water under the faucet, disconnecting the screw feed and removing the plunger. If the water supply is limited, rinsing with permanganate solution (B4) until this retains its color may be necessary.

CALCULATIONS

The oxygen contained in the sample equals $(V_1 - V_2 - C)$ $(F_s \times i) \times F_a$, where C is the blank correction for oxygen in the reagents, F_s is the factor reducing measured gas volumes to standard conditions (STPD), i is the factor for gas remaining in the liquid phase (near to 1.0075 when liquid volume/gas volume is $\frac{1}{4}$), and F_a is the calibration of the analyzer capillary. F_s is based on (1) a temperature corrected barometer reading, from which is subtracted the water vapor tension at the analyzer temperature, and (2) the temperature of the analyzer (Handbook of Chemistry and Physics, 1952, pp. 2130 ff. and 1910 ff.).

The nitrogen contained in the sample equals $(V_2 - C)$ $(F_s \times i) \times F_a$, where C is the blank correction for nitrogen in the reagents, F_s is the same as above, i is near to 1.004, and F_a is the same as above.

When the analysis is performed at a temperature between 15° and 30° C. the following empirical terms can be used, with less than 0.2% error, as substitutes for $(F_s \times i)$, namely, for oxygen $F_s \times i = 0.215\ B/t + 160$, and for nitrogen $F_s \times i = 0.214\ B/t + 160$, where B is the uncorrected barometric pressure in mm. Hg and t is the temperature of the analyzer in centigrade degrees.

---

[2] "Nitrogen" here includes the noble gases and other non-absorbable components, like methane, if such are present.

Determination of Reagent Blank C

Half a liter of water is boiled in an Erlenmeyer flask, provided with a cork through which a capillary glass siphon fits loosely. The free end of the siphon has a short piece of rubber tubing with a pinchcock. After half an hour of steady boiling, 10 cc. of the still boiling water are transferred anaerobically through the siphon to a 10-cc. syringe. This is closed with a fine bore rubber tube and glass plug and is cooled under the faucet. The gas-free water is quickly transferred from this into the extractor by means of a short and heavy-walled tubing. Air bubbles must be scrupulously avoided. The extraction and analysis proceed as described. Our blanks amount to 0.8 mm. for oxygen and 2.4 mm. for nitrogen.

Checks on Air-Equilibrated Water

Fifty cc. distilled water are rotated in a 500-cc. open bottle which is kept partly submerged in a water bath of room temperature. Bubbling of air through water results in an unknown degree of supersaturation and cannot be used in this connection. After a half hour's equilibration samples may be taken out. The dissolved oxygen in the sample equals

$$\frac{\alpha \times (B - b - w)}{760} \times 0.2094,$$

where α is the solubility coefficient, B is the read barometric pressure, b the temperature correction for the barometric reading, w the water vapor tension at the water bath temperature, and 0.2094 the oxygen fraction in the air.

Accuracy

The method has been tested on air-equilibrated water as described above. Out of 21 consecutive oxygen analyses 16 were within ± 1% of the theoretical value, 4 were within ± 2%. The average for 20 determinations was 100.1%.

In the same series, 17 nitrogen determinations were within ± 1% of the value given in the Handbook of Chemistry and Physics (1952), and 3 were within + 2%. The average of 20 determinations was 100.6%.

Use of the Instrument for Straight Gas Analysis

For simple gas analysis the analyzer is charged with the acid citrate solution (B1), and a gas bubble is deposited in the cup, using a syringe technique as described by Scholander, Claff, Teng and Walters (1951), or a mercury pipette (Scholander, 1942b). Thanks to the smooth screw control and the water jacket, an accuracy of ± 0.2% or better can easily be obtained for CO_2, O_2, and nitrogen. At high carbon dioxide concentrations (20% or more) a slight loss of CO_2 must be expected, unless the sample is drawn into a mercury pipette and delivered into mercury which fills the analyzer cup (cp. Scholander, 1942b).

We are much indebted to Mr. J. D. Graham, Department of Physiology, University of Pennsylvania, for suggesting the precision bore tubing for the barrel and for much advice in the development of the apparatus. We also wish to acknowledge the craftsmanship of Mr. J. L. Allen at the instrument shop of the Woods Hole Oceanographic Institution, who built the first models, and of Image Transfer Inc. of Randolph, Massachusetts, which engineered the final models.

LITERATURE CITED

Handbook of Chemistry and Physics, 1952. 34th Edition. Chemical Rubber Publ. Co., Cleveland.

Scholander, P. F., 1942a. Microburette. *Science,* **95**: 177–178.

Scholander, P. F., 1942b. A micro-gas-analyzer. *Rev. Sci. Instruments,* **13**: 264–266.

Scholander, P. F., 1947. Simple syringe burette. *Science,* **105**: 581.

Scholander, P. F., C. L. Claff, C. T. Teng and V. Walters, 1951. Nitrogen tension in the swimbladder of marine fishes in relation to the depth. *Biol. Bull.,* **101**: 178–193.

Scholander, P. F., L. van Dam and S. I. Scholander, 1955. Gas exchange in the roots of mangroves. *Amer. J. Bot.,* **42**: 92–98.

Scholander, P. F., G. A. Edwards and L. Irving, 1943. Improved micrometer burette. *J. Biol. Chem.,* **148**: 495–500.

Scholander, P. F., J. W. Kanwisher and D. C. Nutt, 1955. Gases in icebergs. *Science,* in press.

Scholander, P. F., W. E. Love and J. W. Kanwisher, 1955. The rise of sap in tall grapevines. *Plant Physiol.,* **30**: 93–104.

Scholander, P. F., and F. J. W. Roughton, 1942. A simple microgasometric method of estimating carbon monoxide in blood. *J. Industrial Hygiene Toxicology,* **24**: 218–221.

Contribution No. 796

Deep-Sea Research, 1955, Vol. 3, pp. 88 to 90. Pergamon Press Ltd., London.

Lateral eddy viscosity in the Gulf Stream system

HENRY STOMMEL

(*Received* 16 *August*, 1955)

RECENTLY (FOFONOFF, 1954 ; STOMMEL, 1955) attention has been called to the inertial properties of the Gulf Stream. A new inertial boundary layer theory of the Gulf Stream (Morgan, 1955 ; Charney, 1955) has been offered as an alternative to the earlier (MUNK, 1950) viscous boundary layer theory. In his original attempt to fit the viscous theory to the Gulf Stream, MUNK (1950) chose a representative width of 200 km, which led to a coefficient of lateral eddy viscosity of 5×10^7 cm^2 sec^{-1}. The recent detailed cross-sections by WORTHINGTON (1954) indicate an instantaneous width of less than 100 km, corresponding to coefficients of lateral eddy viscosity of somewhat less than 5×10^6 cm^2 sec^{-1}. In this case, however, the inertial terms are no longer negligible, even in the viscous boundary layer theory, and the inertial boundary layer theory seems to give a good representation with vanishing friction. It has become important, therefore, to make an independent measurement of the lateral eddy viscosity on a scale appropriate to the instantaneous width of the Gulf Stream, in order to decide whether the inertial or the viscous boundary layer theory is the better description of the dynamics of the Stream.

The literature does not contain current measurements at any place in the Stream, well removed from the coast, sufficiently detailed to permit computation of lateral Reynolds stresses, but I have found, in the original log books of Pillsbury, deposited in the archives of the U.S. Coast and Geodetic Survey, 633 consecutive surface current measurements made at fifteen minute intervals during a week-long anchor station of the *Blake* in 200 fathoms, 8 miles off Fowey Rocks in the Florida Straits. This is the region of strong cyclonic shear (about 10^{-4} sec^{-1}) to the west of the axis of maximum velocity.

The computed eastward u and northward v components (magnetic) of the measured velocities are plotted in Fig. 1, and also the product uv. Since the mean Stream is very nearly due north, the turbulent flux of momentum per unit area F to the eastward is approximately $\rho\,(\overline{uv} - \bar{u}\,\bar{v})$, where the bar signifies a time mean over a large number of observations.

The probable errors of measurement can only be guessed at, after all these years (the measurements were made in 1885). Details of how the measurements were made may be found in PILLSBURY'S summary paper (1890). On the basis of current practice we may suppose that the probable error in direction of a single measurement is $\pm \frac{1}{4}$ points ($\pm$ 3 degrees), and that the probable error of the speed measurement (current pole) is $\pm$ 0·1 knots. Because the current is always so nearly northward, the error in u is mostly due to errors in direction, and that in v mostly due to errors in speed. Both probable errors amount to about $\pm$ 0·1 knots. The probable error of each product uv is taken as $\pm$ 0·2 square knots. The probable error of various means of n observations is taken as $(n)^{-\frac{1}{2}}$ that of individual errors, and the value of F/ρ for all 633 observations is $-$ 0·034 $\pm$ 0·016 square knots. When one plots the consecutive values of uv, as in Fig. 1, he sees that there is a tendency for large persistence from one time to another ; values of same sign tend to occur in blocks of 2 to 16 hours' duration. This suggests the possibility of large sampling errors in the above computations. As a check, the first 592 observations have been divided

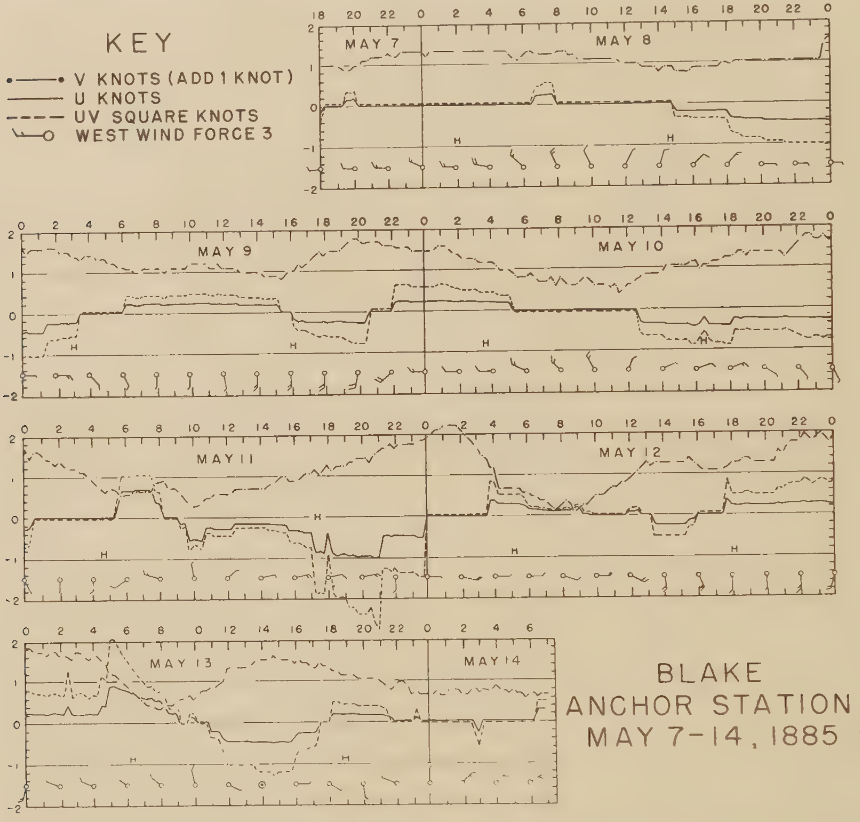

Fig. 1. Eastward (u) and northward (v) components of the surface velocity as observed every fifteen minutes starting at 1800 LCT, 7 May, 1885, by the *Blake*, Lt. J. E. Pillsbury commanding, eight miles off Fowey Rocks in the Florida Current. The product uv is also shown. The time of high water (tide) observed at Fowey Rocks is marked by H. The winds as recorded in the *Blake* log are also indicated according to standard symbols. A different origin is used for v. Units of u and v are knots, for uv, (knots)^2.

into four equal sub-groups, and values of F/ρ computed separately ; and an additional group of 306 independent observations of a later date is also exhibited in Table 1. A comparison of these variously computed values of F/ρ suggests that the sampling error is negligible, that the computed values of F/ρ tend to cluster about a point slightly less than zero, but almost within the range of error. Corresponding values of the lateral eddy coefficient $(F/\rho)/(\partial\bar{v}/\partial x)$, using $\partial v/\partial x = 10^{-4}$ sec^{-1}, are also tabulated. We see at once that they are much less than the large values quoted above in connection with the viscous boundary layer theory of the Gulf Stream. Thus, although we have made a very bad determination of the actual eddy coefficient in the Florida Current off Miami, we can say that it is probably less than one fifth the minimum value required by the viscous theory, and that the inertial theory is a better description of the instantaneous Stream in the Florida Straits.

During the week of observation about 700 km of water flowed past the point of observation, so that any eddy-like features with dimensions less than the width of the Stream should be included in the average, unless they are extremely elongated.

Table I. Velocity components, cross-products, Reynolds stresses, and eddy viscosities computed for various samples of the data in the Florida Straits.

Date and time of beginning	*No. Obs.* n	$\bar{u}$ *east knots*	$\bar{v}$ *north knots*	$\overline{uv}$ *(knots)*^{2}	$F/\rho = \overline{uv} - \bar{u}\,\bar{v}$ *(knots)*^{2}		*Coeff. Eddy viscosity* $cm^2\ sec^{-1}$
1885 A.D.							
May 7, 1800 *LCT*	633	− 0.0228	2·1176	− 0·0825	− 0·034	± 0·016	$9\,(\pm 5) \times 10^5$
Sub-groups							
May 7, 1800	148	− 0·0953	2·008	− 0·2160	− 0·025	± 0·034	
May 9, 0600	148	0·0063	2·112	0·0147	0·014	± 0·034	
May 10, 1900	148	− 0·1618	2·086	− 0·4019	− 0·064	± 0·034	
May 12, 0800	148	0·1038	2·204	0·1999	− 0·029	± 0·034	
Independent Series							
May 24, 1700	306	− 0·2223	2·133	− 0·4819	− 0·007	± 0·024	$2\,(\pm 6) \times 10^5$

It should be emphasized that comparable measurements are not available in the regions of cyclonic and anticyclonic shear off Cape Hatteras in the truly " free " Stream, and that therefore the choice between viscous and inertial theory for the Stream as a whole is not settled. The present results do give indication of what we may expect to find, however, and may act as a guide as to how the observations ought to be made.

The very high value of eddy diffusivity (Stommel, 1951), which I computed in an analysis of downstream spreading-out of the envelope of fourteen surveys of the inshore edge of the Gulf Stream, was $2{\cdot}3 \times 10^8$ cm^2 sec^{-1}. I now suspect that this estimate may have been a misinterpretation of the data : the wavy meander-like structures in the instantaneous Stream do not necessarily produce a net cross-stream transport of properties. The frequency of occurrence of detached eddies is not known; and no reliable estimate of cross-stream transport can really be made from the data I used. In any case the scale of turbulence associated with this very high value is too great to permit its use as a process involved in the formation of the instantaneous filament-like Gulf Stream : indeed, this " Gross-Austausch " appears to be produced by the instability and decay of the instantaneous Stream.

Contribution No. 796 from the Woods Hole Oceanographic Institution

REFERENCES

Charney, J. G. (1955), *The Gulf Stream as an inertial Boundary Layer.* (In press).

Fofonoff, N. P. (1954), Steady flow in a frictionless homogeneous ocean. *J. Mar. Res.* **13**, (3), 254-262.

Morgan, G. W. (in press).

Munk, W. H. (1950), On the wind-driven ocean circulation. *J. Meteorol.* **7**, 79.

Pillsbury, J. E. (1890), The Gulf Stream. *Rep. of the Superintendent, U.S. Coast and Geodetic Survey, App.* **10**, pp. 459-620.

Stommel, Henry (1951), Determination of the lateral eddy diffusivity in the climatological mean Gulf Stream. *Tellus*, **3**, 43.

Stommel, Henry (1955), Discussion during the Woods Hole Convocation, 1954. *J. Mar. Res.* 14. (in press).

Worthington, L. V. (1954), Three detailed cross-sections of the Gulf Stream. *Tellus*, **6**, 116.

Printed in Great Britain by The Salisbury Press Ltd., Publicity House, Wilton Road Salisbury, Wilts. (93311)

Contribution No. 802

ANNOTATED REFERENCES CONCERNING THE EFFECTS OF MAN-MADE SOUNDS ON THE MOVEMENTS OF FISHES

by

JAMES M. MOULTON
Department of Biology, Bowdoin College,
Brunswick, Maine

and

RICHARD H. BACKUS
Woods Hole Oceanographic Institution,
Woods Hole, Massachusetts

FISHERIES CIRCULAR NO. 17

DEPARTMENT OF SEA AND SHORE FISHERIES
Vickery-Hill Building
Augusta, Maine

October 1955

ANNOTATED REFERENCES CONCERNING THE EFFECTS OF MAN-MADE SOUNDS ON THE MOVEMENTS OF FISHES

JAMES M. MOULTON AND RICHARD H. BACKUS*

INTRODUCTION

No method as yet devised of introducing sound into natural waters has consistently altered the movements of fishes. Several considerations summarized here suggest that in the future sound may prove useful in this connection, success awaiting demonstration of the appropriate method. Commercial fishermen, industrialists drawing fresh water from rivers, and fisheries biologists aiming at conservation and control of an important resource have been particularly concerned with experiments in this direction. It is primarily as an aid to planning new experiments and to determining the applicability of sound to fisheries problems that this material has been prepared.

The transmission of sound through water is extremely efficient (Kinsler and Frey, 1950), its radius of perception being far greater than that of any other stimulus demonstrated to influence fish behavior. There is no problem in transmitting sounds loud enough for fishes to hear, to judge from those species which have been studied (Griffin, 1950, Table 3; Poggendorf, 1952; Kleerekoper and Chagnon, 1953). Further, the directionality of sound may be partly controlled (Kinsler and Frey, 1950).

Fishes hear through the mechanism of an inner ear. In addition, they possibly perceive low frequency vibrations through a system of canals on the body, the lateral line system. The lowest frequencies to which fishes are sensitive may be perceived through isolated sensory receptors in the skin (von Frisch, 1938). As has been shown in the case of a catfish, the inner ear may respond to sounds as high as 13,000 cycles per second (Stetter, 1929), a figure approaching the upper limit of adult human hearing. It is probable that the upper frequency limit of hearing in the herring family is even higher (Griffin, 1950; Moulton, unpublished).

That sounds are significant to some fishes is certain. The presence of an inner ear is in itself supporting evidence. Many species of fishes produce calls; a given species may produce one call at times of emergency, another during breeding (Moulton, unpublished). The calling of at least one species may be incited and suppressed by appropriate signals (Moulton, 1955). In some species, only the males possess a calling mechanism (Marshall, 1954, p. 260).

Several species of fishes, under natural conditions as well as in the laboratory, are startled to increased activity by noises as they are by other stimuli. But as they do to several other stimuli (Brett and MacKinnon, 1954; Hubbs and Rechnitzer, 1952; Loukashkin and Grant, 1954), individual fish rapidly adapt themselves to sounds initially causing marked reactions, whether these sounds be intermittent, warble tones, or constant signals, and whether they be of single or multiple frequencies (Burner and Moore, 1953). It is possible that the orientation of a fish school to a sound source differs from the reactions of individual members (Moulton, unpublished). It has been with relatively few individuals of non-schooling species that most experiments have been performed.

The principal evidence of fish hearing lies in the results of conditioning experiments (von Frisch, 1938). In these experiments, fishes have been conditioned to respond consistently to signals, and it is possible that it will be through new applications of this method that sound will be most useful in influencing the movements of fishes. Meanwhile, it has been demonstrated that conditioned fish may be attracted to (Kleerekoper and Chagnon, 1953) or repelled from (Griffin, 1950) a sound source, depending on the nature of the unconditioned stimulus.

---

* Contribution No. 802 from the Woods Hole Oceanographic Institution.

There is considerable ground then for anticipation that the utilization of sound in controlling the movements of fishes in nature awaits only appropriate methods of application. In the following annotations, the nature of the sounds produced and the method of application are summarized to the extent that the original work permits.

ANNOTATED REFERENCES

Anonymous 1948 Aquatic resources of the Ryukyu area. Report No. 117, Natural Resources Section, General Headquarters, Supreme Commander for the Allied Powers, Tokyo, reproduced as Fishery Leaflet 333, USFW Serv., February, 1948.

Two applications of sound to a marine fishery are described, both used in connection with gill nets. One of these employs a sound tub, "a wooden barrel with a wooden handle fastened across the open top. Weights are hung from the handle. When the waves move the floating tub, the weights hit the sides of the barrel and make considerable noise. Sound tubs are effective in driving fishes out of their hiding places into the net." The other application employs scare ropes which are used in the Ryukyuan drive-in-net fishery, as well as in conjunction with gill nets. In the case of the former, which serves as illustration, individual fishermen swim in toward the net, pulling the ropes which are about 45 meters in length. Iron rings or a large stone at the lower end of each rope are dragged over the reef, scaring fishes from their crevices into the net. In another method, the scare ropes are hung directly from the net lines. White cloth or leaves tied to the ropes at 1 or 1½ meter intervals are felt to contribute to the effectiveness of these scare ropes.

Burner, C. J., and H. L. Moore, 1953. Attempts to guide small fish with underwater sound. USFW Serv. Special Scientific Report: Fisheries No. 111.

Experiments were performed on two species of trout *(Salmo gairdneri* and *S. trutta),* as an approach to the possible guiding of salmon fingerlings in the Columbia River by the use of sound. A long wire and frame trough (100′ x 3′ x 3′) built in a pond was divided by nine gates into ten sections each ten feet in length. The gates could be opened or closed simultaneously. After a given test or control run, the gates were closed and the fish in each section counted to see whether a given sound produced at one end or side, or in the center of the trough might have altered the distribution of the fish. A variety of sound sources was used. Frequencies were projected into the trough varying from 60 cps to 70 kc at sound pressure levels probably in all cases well within the sensitivity range of species of fishes that have been tested. While there were significant differences in the distribution of the fish in the various sections of the trough after sound trials and after controls in some cases, no observations of the behavior of the fish indicated that sound stimuli were responsible for the differences. There was some indication that the fish adapted to the sounds employed.

Griffin, D. R., 1950. Underwater sounds and the orientation of marine animals, a preliminary survey. Proj. NR 162-429, t. o. 9, between ONR and Cornell University, Tech. Report No. 3.

An excellent review of the problems connected with fish hearing, with comment on possible relations of sound to fish behavior. Largely concerned with the physiology of fish hearing, it presents some evidence that at least one species of fish orients to the echo of its own call.

Hubbs, C. L., and A. B. Rechnitzer, 1952. Report on experiments designed to determine effects of underwater explosions on fish life. Calif. Fish and Game, **38:** 333-366.

Sound engendered by a variety of explosives were not considered in this report, but the paper is of interest in connection with Parker's (1911) earlier tests of the effects of explosive sounds on the movements of fishes. The authors found that explosives discharged within similar areas on subsequent days (23 and 24 May, 1950) caused mortalities within these areas on both days as indicated by collections of killed fish. Eight blasts on 23 May secured 3357 fishes while five on 24 May secured only 121 fishes. It was felt that the decreased catch for 24 May was due to the high kill of the 23rd. The kills of the 23rd on successive blasts showed a marked reduction of recoveries immediately following the first blast, from 2134 to 359, then successive kills of 369, 80, 117, 12, and 286. Of the 121 fish collected 24 May, 74% were silversides (atherinids), free-swimmers as contrasted with bottom dwellers. The authors' remarks do not include consideration of a possible influence of sound as being related to the results.

Kerr, James E., 1953. Studies on fish preservation at the Contra Costa steam plant of the Pacific Gas and Electric Company. Fish Bull. No. 92, State of Calif., Dept. of Fish and Game: 1-66.

A variety of sound sources not specified were used in attempts to divert anadramous fishes, especially striped bass *(Roccus saxatilis)* and king salmon *(Oncorhynchus tshawytscha),* from the water intake of a steam plant on the San Joaquin River at Antioch, California. The devices tried included "a steel barge, in which a large air hammer had been so mounted that it kept up a constant tattoo on the metal hull. The barge was anchored at the intake structure, . . ."* No effective results were obtained from any of the devices tried.

Kleerekoper, H., and E. C. Chagnon, 1953. Hearing in fish, with special reference to *Semotilus atromaculatus atromaculatus* (Mitchill). J. Fish. Res. Bd. Can., 11: 130-152.

A report on the results of experiments on the hearing of the creek chub accompanies a review of the literature on fish hearing. The methods of measuring frequencies and sound intensities produced are not described. The aspect of the work most significant to the present report is the observation that fish conditioned to respond to sound with food presentation as the unconditioned stimulus, swam toward the sound source, possibly along crests of greatest sound intensity. When presented with two sources of sound at a single frequency but different intensities, the conditioned fish moved toward the source of higher intensity. These observations suggest the value of more detailed study of the paths of fishes within a sound field. Moorhouse's observations on movement of the surf perch *(Cymatogaster aggregatus)* to the sound source after conditioning are not related by the authors to their own observations.

Miyake, Iwao, 1952. Observations on sound production and response in tuna. Part IV of Reaction of tunas and other fishes to stimuli. USFW Serv. Special Scientific Report: Fisheries No. 91: 59-68.

---

* Letter from John Radovich, Assistant Chief, Marine Fisheries Branch, Calif. Dept. of Fish and Game, January 20, 1955.

Negative results characterized attempts to influence the behavior of yellowfin by sound in a concrete tank and pool. Frequencies from 100 cps to 70 kc were presented in variable fashion. Equipment consisted of a Hewlett-Packard audio oscillator, Model OAY Sound Measuring Equipment, Model OCP-1 Sonar Test Equipment, and NEL Underwater Sound Monitoring Equipment. There was some possibility that a yellowfin oriented toward the sound of exhaust from a motor boat and toward a 200 cps signal. Acoustical conditions of the experiments are not specified. The usual criterion of reaction was whether the fish was located in an area in which a given sound was 'audible' or in one in which the sound was 'not audible'. Startle reactions were not reported.

Moorhouse, V. H. K., 1933. Reactions of fish to noise. Contr. to Can. Biol. and Fish., N. S. **7:** 465-475.

Four different sound sources, a tapper, an electric bell, a buzzer and a motor horn were submerged individually in a galvanized box within aquaria and pens, and intermittently sounded to test the reactions of eight marine species to sound: a surf perch *(Cymatogaster aggregatus)*, two sculpins *(Oligocottus maculosus* and *Leptocottus armatus)*, three flounders *(Platichthys stellatus, Lepidopsetta bilineata,* and *Parophrys vetulus)*, a rock cod *(Sebastodes caurinus)*, and a dogfish *(Squalus suckleyi)*. Only the surf perch showed consistent reactions, and these only to the motor horn, moving to the opposite end of the tank and diving deep. On conditioning with food as the unconditioned stimulus, the surf perch were attracted to the sound source after eight trials, but after forty trials rose to the opposite end of the tank where food was always presented. After conditioning to the horn, a variety of stimuli brought the fish to the surface. The surf perch were also conditioned to dive at the sound of a bell with darkness as the unconditioned stimulus.

Parker, G. H., 1911. Effects of explosive sounds, such as those produced by motor boats and guns, upon fishes. U. S. Bur. Fish. Document No. 752: 1-9.

The sounds of a motor boat failed to alter the behavior of killifish *(Fundulus heteroclitus)*, scup *(Stenotomus chrysops)*, kingfish *(Menticirrhus saxatilis)*, and mackerel *(Scomber scombrus)*. Cunners *(Tautogolabrus adspersus)* ceased feeding while the running boat stood six feet away from baited lines. Bluefish *(Pomatomus saltatrix)* ceased feeding on close passage of the boat. The sounds of the boat used were of low intensity to an underwater observer regardless of whether exhaust was discharged into the water or air. Caged *Fundulus* were only momentarily startled by discharge of a shotgun near the cage, whether feeding or swimming about, the sound of the discharge resembling a faint pop to an underwater observer. The response was elicited when the shotgun was fired up to 200 feet from the cage. Up to 30 feet from a 6-lb. howitzer firing a powder charge on a vessel, the same momentary response was observed. At 2000′ there was no response to the firing of the howitzer.

Parker, G. H., 1912. Sound as a directing influence in the movements of fishes. Bull. Bur. Fish., 30: 97-104.

The distribution of nine species of fishes in a wooden tank (50 cm. x 60 cm. x 100 cm.), after allowing a 4300 gm. iron ball to strike against one end and then the other of the outside of the tank, was studied. The tautog *(Tautoga onitis)*, scup *(Stenotomus chrysops)*, kingfish *(Manticirrhus saxatilis)* and puffer *(Spheroides maculatus)* tended to concentrate in the end of the tank away from the sound source. Two species of sea robin *(Prionotus carolinus* and *Prionotus strigatus)* tended to concentrate at the end toward the sound source. Three other species, two of the killifishes *(Fundulus heteroclitus* and *F. Majalis)* and the cunner *(Tautogolabrus adspersus)* sank to the bottom in random distribution on striking of the ball. It was noted in the case of the scup that within twenty minutes after three applications of the sound source during a ten-minute interval, the fish had returned to random distribution. Of those species orienting toward one end or the other of the tank, the strongest response was in the case of the tautog, when 66% of 2500 possible orientations were to the end of the tank opposite the sound source. The orientation of the sea robins toward the sound sources occurred in 56% of 2500 possibilities.

Radovich, John, Assistant Chief, Marine Fisheries Branch, Calif. Dept. Fish and Game, Letter to Moulton of 20 January 1955.

" . . . In the Spring of 1951 an electrically operated noise making device was tested at an irrigation canal on Mill Creek, Tehama County. This canal, which has a flow of from 40 to 50 c. f. s. attracts many small down-stream migrant salmon. The noisemaker was first used at this location in conjunction with an electric fish screen, and later was tested by itself. Small salmon (30 to 60 mm. in length) disregarded both the electric screen together with the sound device, and the sound device alone."

" . . . For many years fishermen have located schools on dark nights by observing the bioluminescence they created. When the bioluminescence is very poor, the fishermen frequently "light up" the schools by pounding on the deck with a large wooden mallet. We have used a similar technique and have located schools by detonating a small explosive charge in the water. The effect is that, for an instant, schools several hundred yards away may be seen. It would appear that a sudden noise startles the fish, however it does not necessarily drive them away. A steady noise, or one with a uniform pulse, seems to have little effect on them."

EXPERIMENTS WITH ECHO-SOUNDERS:

Cushing, D. H., and I. D. Richardson 1955. Echo sounding experiments on fish. Fishery Investigations, Ministry of Agric. and Fisheries, Ser. II, **18** (4): 1-34.

Each of three echo sounders (10, 14 and 30 kc) was directed at 100 live perch in a cage of shrimp netting. The fish could be seen from the surface. No modification of behavior was noted during operation of the echo sounders, confirming the observations of Schärfe (1951).

Dow, Robert L., Director of Research. Maine State Department of Sea and Shore Fisheries, Augusta. Letters to Moulton of 20 January 1953 and 17, 18 August 1955.

Experiments performed by Leslie W. Scattergood and R. L. Dow at the U. S. Fish and Wildlife Service Station at Boothbay Harbor in 1952 included observations on the behavior of herring *(Clupea harengus)* in tanks during operation of Bendix and Fathometer echo-sounders. Observations and photographs showed a lack of influence of the devices tested upon the herring under conditions of the experiments. Both instruments transmitted signals of 50 kc. into tanks measuring from 11′ ¼″ x 2′ 8¾″ x 2′ 6″ to 11′ 8½″ x 2′ 3½″ ID, the water standing at approximately 2′ in depth. The approximately 250 fish used in a typical series of experiments had been held for three months prior to the experiments.

Hodgson, W. C., 1950. Echo-sounding and the pelagic fisheries. Fishery Investigations, Ministry Agric. and Fisheries. Ser. II, **17** (4): 1-25.

Although this paper makes no direct reference to the behavior of fishes as related to the operation of an echo-sounder, the following quotation may pertain, since marine animals other than fishes (porpoises) are said to desert the vicinity of a vessel rapidly when its echo-sounder is turned on.* "The main point to stress (in searching for schools of fish) first of all, is that the sounder *must* be kept running continuously while the ship is in an area where the presence of fish is suspected. Many skippers of herring drifters content themselves by taking an occasional sounding, and if no fish are present they switch off the machine and try again later. Such a practice leads to failure."

Radovich, John. Letter to Moulton of 20 January 1955.

"On the ocean we have had some experiences which may interest you. Our survey vessel *M. V. Yellowfin* is equipped with two fathometers, one of which is a recording Fathometer, and a Sea Scanar. We have never noticed any effect on fish by these instruments." This same general opinion is conveyed in a letter from Mason Case, Assistant Manager, Fishermen's Cooperative Association of San Pedro, California, also dated January 20, 1955. Radovich's letter continues: "We have traced the movement of schools with our Fathometers from depths of about 120 feet up to the surface, and have observed fish move in from about 300 feet away with our Sea Scanar. We have not noticed any difference in the length of time this movement takes with the equipment on or off."

Scharfe, J., 1951. Zur Frage der Fischscheuchung durch Lotschall. Fischereiwelt, **3** (2): 30. (As cited by Cushing and Richardson).

An echo sounder had no effect on the behavior of *Cyprinus carpio, Perca fluviatilis, Tinca tinca, Ameiurus nebulosus, Cobitis fossilis,* and *Coregonus wartmanni.*

Skoglund, G., 1953. Skrämmer ekolod fisken? (Does the echo sounder frighten fish?) Ostkusten, **25** (6): 14.

Herring 10 to 12 inches in length contained in a box (4.9′ x 4.1′) suspended in the sea and in an aquarium (7′ x 3.6′ x 1.8′) were exposed to a 30 kc sound from a commercial type echo sounder at distances varying from 82 to 3.3 feet. No reactions to the sound were noted.

---

* Letter from Radovich to Moulton, 20 January 1955.

References Cited and Annotated

Anonymous 1948. Aquatic resources of the Ryukyu area. Report No. 117, Natural Resources Section, General Headquarters, Supreme Commander for the Allied Powers, Tokyo, reproduced as Fishery Leaflet 333, USFW Serv., February, 1949.

Brett, J. R., and D. MacKinnon 1954. Some aspects of olfactory perception in migrating adult coho and spring salmon. J. Fish. Res. Bd. Canada, *11*: 310 - 318.

Burner, C. J., and H. L. Moore 1953. Attempts to guide small fish with underwater sound. USFW Serv., Spec. Sci. Rep.: Fish. No. 111.

Cushing, D. H., and I. D. Richardson 1955. Echo sounding experiments on fish. Fishery Investigations, Ministry of Agric. and Fisheries, Ser. 11, *18* (4): 1 - 34.

Dow, Robert L. Letters to Moulton of 20 January 1953 and 17, 18 August, 1955.

Griffin, D. R. 1950. Underwater sounds and the orientation of marine animals, a preliminary survey. Proj. NR 162 - 429, t. o. 9, between ONR and Cornell University, Tech. Report No. 3.

Hodgson, W. C. 1950. Echo-sounding and the pelagic fisheries. Fishery Investigations, Ministry Agric. and Fisheries. Ser. 11, 17 (4): 1-25.

Hubbs, C. L., and A. B. Rechnitzer 1952. Report on experiments designed to determine effects of underwater explosions on fish life. Calif. Fish and Game, *38*: 333 - 366.

Kerr, James E. 1953. Studies on fish preservation at the Contra Costa plant of the Pacific Gas and Electric Company. Fish Bull. No. 92, State of Calif., Dept. of Fish and Game: 1 - 66.

Kinsler, L. E., and A. R. Frey. Fundamentals of Acoustics. John Wiley and Sons, Inc., New York. 1950. Chapter 15, " Underwater acoustics ".

Kleerekoper, H., and E. C. Chagnon 1953. Hearing in fish, with special reference to *Semotilus atromaculatus atromaculatus* (Mitchill). J. Fish Res. Bd. Can., *11*: 130 - 152.

Loukashkin, A., and N. Grant 1954. Further studies of the behavior of the Pacific sardine (*Sardinops caerulea*) in an electrical field. Proc. Calif. Acad. Sci., Ser. 4, *28*: 323 - 337.

Marshall, N. B. Aspects of Deep Sea Biology. Hutchinson's. London. 1954. p. 260.

Miyake, Iwao 1952. Observations on sound production and response in tuna. Part IV of Reaction of tunas and other fishes to stimuli. USFW Serv., Spec. Sci. Rep.: Fish. No. 91: 59 - 68.

Moorhouse, V.H.K. 1933. Reactions of fish to noise. Contr. to Can. Biol. and Fish., N. S. 7: 465 - 475.

Moulton, J. M. 1955. The eliciting and suppressing of a marine biological sound. (Abstr.) Bull. Ecol. Soc. Amer., *36*: 80.

Moulton, J. M. Unpublished.

Parker, G. H. 1911. Effects of explosive sounds, such as those produced by motor boats and guns, upon fishes. U. S. Bur. Fish. Document No. 752: 1 - 9.

Parker, G. H. 1912. Sound as a directing influence in the movements of fishes. Bull. Bur. Fish., *30*: 97 - 104.

Poggendorf, D. 1952. Die absoluten Horschwellen des Zwergwelses (*Amiurus nebulosus*) und Beitrage zur Physik des weberschen Apparates des Ostariophysen. Zeitschr. f. vergl. Physiol., 9: 339 - 477.

Radovich, J. Letter to Moulton of January 20, 1955.

Scharfe, J. 1951. Zur Frage der Fischscheuchung durch Lotschall. Fischereiwelt, 3 (2): 30.

Skoglund, G. 1953. Skrammer ekolod fisken? (Does the echo sounder frighten fish?) Ostkusten, 25 (6): 14.

Stetter, H. 1929. Untersuchungen uber den Gehorsinn der Fische, besonders von *Phoxinus Laevis* L. und *Amiurus nebulosus* Raf. Zeitschr. f. vergl. Physiol., 9: 339 - 477.

von Frisch, K. 1938. The sense of hearing in fish. Nature, *141*: 8 - 11.

Contribution No. 806

Reprinted from SCIENCE, October 21, 1955, Vol. 122, No. 3173, pages 748–751.

Oceanographic Instrumentation

Allyn C. Vine

Oceanography as a science is still small enough so that physicists, biologists, chemists, geologists, and others who concentrate on the marine aspects of the profession are usually called oceanographers, particularly if they go to sea. Because it is a borderline field, the instrument requirements are as diverse as the problems; and because work on a ship is so different from work in a conventional laboratory, the instruments often develop along unconventional lines. In a short paper it is impractical to go into detail, or even to give fair coverage to all oceanographic instruments. Instead, I shall emphasize oceanographic problems, techniques, and instrument development, of which I have reasonable knowledge.

Sverdrup, Fleming, and Johnson have covered instruments in use up to 1940 in considerable detail (*1*). In 1952, the National Research Council and the Office of Naval Research sponsored a 3-day symposium on oceanographic instrumentation (*2*) that covered the present field of oceanographic instrumentation. Since each of the 12 papers had several discussants, the instrument problems were considered from different points of view, and much of the prevalent philosophy behind instrument development emerged in printed form. From the numerous references in these two sources, one can get fairly complete and up-to-date information.

Perhaps a brief description of some of the more significant characteristics of the ocean from the standpoint of a research worker or designer of instruments would be helpful. The fact that the ocean covers 70 percent of the earth is well known, but its division into surprisingly well-defined areas of continental shelves, oceanic basins, and deep trenches, somewhat comparable to the plains, plateaus, and mountain ranges on land, is less well known. In actual practice, this means that oceanographic instruments that are sensitive to, or dependent on, pressure are usually built and used for one of the following maximum depths: (i) 10 meters for harbors and coastlines and for wave measurements, (ii) 200 meters for the continental shelf and the wind-stirred layer, (iii) 6000 meters for most of the open ocean, and (iv) 10,000 meters for the deep trenches.

Thus, oceanographic ships carry 5 to 6 miles of steel cable on their winches, and most deep-sea instrumentation must operate at water pressures of 600 kilograms per square centimeter (8500 pounds per square inch). In deep water

---

Mr. Vine is on the staff of the Woods Hole Oceanographic Institution, Woods Hole, Mass. This paper is a condensation of a discussion entitled "Oceanographic instrumentation" that was given at the AAAS Gordon Research Conference on Instrumentation at Colby Junior College on 28 July 1955.

the weight of the wire comes so close to the strength of the cable that tapered cables are often required for the great depths. Studying the depths or the bottom of the ocean can, with some justification, be compared to studying the continents from a balloon or aircraft at night at a height of 2 miles.

Water temperatures in the ocean vary from about −1°C to about 30°C. The salinity can vary from nearly 40 parts per 1000 in the Red Sea to nearly fresh off the mouth of the Amazon. However, in the open sea the salinity seldom varies more than 2 parts from 35 parts per 1000.

Physically, the ocean seems homogeneous only to those who do not investigate it closely. Patches, streaks, and transients keep appearing as detailed observations are made. Biologically, many fish are in schools, and plankton concentration varies with depth and location. Observations made within a given similar area or time often must be made very precisely. Investigations aimed at studying the transition zones must be more numerous and emphasize qualitative features.

Research Vessel

Perhaps the most important instrument of all is the research vessel itself. Away from the dock it becomes not only a laboratory but a home and a way of life. The type of problem tackled and the quantity and precision of data obtained are determined to a large extent by the ability of the ship to go somewhere and get a job done, particularly in adverse weather. Shipboard research quickly convinces one of the importance of teamwork, and being considered a good shipmate is high praise. Equipment breakdowns at sea without adequate repair facilities bring out or show the lack of resourcefulness. Laboratory space is often cramped and inefficient. Yet a good research vessel has an undeniable laboratory atmosphere about it, because it represents our most effective large-scale contact with the ocean. Although both research ships and land-based laboratories are required in oceanography, the question of which should be regarded as the service facility for the other is debatable.

An efficient vessel is so important in oceanography that much consideration has been given recently to the design of a truly modern research vessel with increased maneuverability, larger and more convenient laboratory space, relative freedom from roll, and greater versatility. There has been a steady output of new laboratories, accelerating machines, and so forth, for research on land, but there has been no equivalent, sustained emphasis or building program to develop more versatile and capable research vessels for the study of the ocean. A research vessel is as specialized as a yacht, merchantman, or a warship, and converting one to the other can give only a partially adequate vessel.

Aircraft are being used more and more in oceanography and offer great possibilities for observation and the collection of data. It seems almost certain that the airplane will be used in direct proportion to the number of good oceanographic instruments designed for aircraft use.

The wider thinking and use of buoys to supplement ship or aircraft in the collection of data are also broadening the field of techniques and desirable instrumentation. A ship can plant or herd quite a number of buoys and thus increase its area of coverage. Buoys that float even at the bottom of the ocean have also been used to replace wires or cables and can carry instruments down to and back from the deepest parts of the ocean. This technique permits deep-water research to be done from a ship without a winch and also permits the equipment to stay on the bottom for a considerable length of time.

Temperature and Salinity Measurements

Because of the relative ease in measuring temperature in comparison with measuring salinity, density, or current, temperature has remained important, not only as an end in itself, but also as an indicator of other changes. It is presumed that temperature measurements will continue to be one of the most powerful and versatile ways to figure out our oceanographic puzzle.

During the years, we have gradually accumulated enough temperature measurements to obtain a rough over-all picture of the northern Atlantic and Pacific that is reasonably descriptive for large-scale phenomena. We are unable, however, to describe in a detailed way how thermal exchanges take place or accurately to predict small-scale oceanographic features.

Most of the water in the ocean is nearly isothermal and, at most, only a few degrees above freezing. However, except for the polar regions, in the winter the upper few hundred meters of the water column is warmed, and the result is a thermocline with a consequent density gradient that tends to isolate surface water from deep water. The high degree of vertical stability in the ocean is of great importance and is intimately tied up with the circulation of the ocean. The temperature gradients of the upper 100 or 200 meters of water may change with the seasons. If gradients are present at greater depths, they are referred to as the permanent thermocline.

Near the surface, large temperature changes can occur in a small depth difference, for example, as much as 10°C in 10 meters. At depth, the situation is reversed, and the temperature change may be as little as 0.1°C in 1000 meters. These important facts must be considered before one starts to build an all-purpose thermometer.

The Richter reversing thermometer is a mercury thermometer, which was developed in the 19th century, that, when upended, preserves the temperature reading at the moment of reversal to within about 0.01°C. This thermometer is mounted on a Nansen sampling bottle of about 1-liter capacity that closes off a sample of water when it is upended. From the sample the oxygen or salinity content of the water can be determined. A suitably spaced series of bottles and thermometers are placed on the wire and are tripped by an ingenious series of messengers that slide down the wire. The thermometers are usually used in pairs. The protected types are inside a pressure-proof glass case and read the true temperature of the water. The unprotected ones have the slightly compressible glass mercury bulb exposed to sea pressure; they read high by about 1°C per 100 meters of depth. This pressure coefficient of temperature thus furnishes a precise depth gage. The Nansen bottle-reversing thermometer combination has many limitations, but it is such a trouble-free and accurate device that it will surely be in use for a long time.

The bathythermograph, designed and improved just before World War II, was a significant step in making observations from a ship underway, and as a result there are several hundred thousand continuous temperature-depth traces for the top 50 to 250 meters over much of the ocean. The bathythermograph (BT) is a small, commercially available, torpedo-shaped instrument, with its mechanism exposed to sea water, that records on a smoked microscope slide. The speed of thermal response is only 0.8 seconds for a 90-percent response, and the precision is good to about 2 percent in depth and 0.1°C in temperature, depending somewhat on the instrument, the operator, and the usage. In operation, it is dropped overboard and the 3/32-inch steel cable is paid out faster than the ship is moving. When depth is reached, the operator stops the winch, the BT rises nearly to the surface, and the operator then hoists the BT back to the ship and aboard.

A more recent instrument, the STD, continuously measures the temperature, electric conductivity, and depth and automatically computes the salinity of the water from the temperature-conductivity-salinity relationships and records temperature, salinity, and depth. This instrument has been of value in studying inshore and estuarine waters, but it needs another order of precision to be used on most offshore problems where changes tend to be smaller. The fact that the STD continuously computes and records a desired variable makes it a prototype instrument of unusual interest.

The study of thermal microstructure and the vertical distribution of temperature in the sediments under the bottom are new and interesting fields that are beginning to receive attention. Infrared measurements of surface temperatures from aircraft show great promise of delineating gross features, such as the edge of the Gulf Stream, with a detail and speed that was not possible before.

Current Measurements

The circulation of the ocean is sufficiently complex and interesting to bring out a full array of ideas and instruments. Many current measurements are made as they were hundreds of years ago (and as the jet stream was recently discovered in the upper atmosphere) by recording errors in dead reckoning. This amounts to the navigator noting that his ship did not go where he thought it was going. If good navigation or loran is available, this ship-set method is not as crude as one might suppose.

The drift method has been elaborated by setting out and following drifting buoys that transmit radio signals that can be homed on from the land or a ship. The motion of water far below the surface has been observed by following surface buoys that are secured by thin piano wire to deep-sea anchors made of aviator's parachutes and located at the depths of interest. Where offshore navigation is inadequate, buoys have been anchored to the bottom by piano wire even in several miles of water and have served as fixed references for making local current measurements or local bathymetric surveys.

Many propeller-type current meters have been built and several types are in frequent use. Perhaps the most novel current meter has been the GEK (Geomagnetic Electro Kinetograph), which, in effect, measures with a potentiometer the difference in voltage induced in a wire towed behind a ship and the voltage induced in the ocean as it flows through the earth's vertical magnetic field. The voltage difference is of the order of 1 millivolt per knot of current for spacing of 100 meters between the silver-silver chloride electrodes and is independent of the ship's velocity. The instrument is also known as the Jog Log, because the navigator is asked to make frequent three-sided rectangular jogs from the ship's base course in order to obtain two components of the current and to redetermine the electric zero of the instrument. In spite of certain theoretical and practical limitations, particularly in shoal water, the GEK has quickly become a basic and widely used oceanographic instrument.

Acoustic Measurements

Because the ocean is so much more transparent to acoustic waves than to electromagnetic waves, sound is a principal means of studying the ocean with both active and passive sonar gear. The echo sounder is the most widely used acoustic instrument. At sea it has been used successfully in studying the daily vertical migration of organisms as well as the depth of the water, and in shallow water it sometimes shows the depths of thin sediments. Geophysical seismic exploration techniques have been used at sea for nearly two decades and have produced quantitative and exciting data about geologic structures under the ocean. Explosives are a favorite sound source for acoustics work, because they are such convenient high-energy, broadband sources. The use of broad-band sources and frequency analysis on the signal often gives clues regarding the creature or geologic layer being studied.

One of the most exciting new uses for sound is in telemetering scientific data to the surface as it is being taken. Not only does this permit more data to be taken, but it also permits the scientists to study changes and transients in a less haphazard and survey manner. Acoustic beacons also provide a way of locating or following surface or subsurface buoys or of using a bottomed beacon as a local fixed point for a bathymetric survey.

Underwater Photography

In harbors the visibility may drop to a fraction of a meter. The visibility in the open sea is comparable to a thick fog and may range between 10 and 80 meters. Good pictures can be taken at about one-third to one-half of this distance. Although this limits photography or vision, it permits clear underwater pictures to be taken over a larger area than can usually be illuminated with artificial light. Numerous bottom photographs have been taken at depths up to several thousand meters. The problems of underwater photography are not primarily optical ones; rather, they are the mechanics and techniques required to handle the gear and to keep the camera at the right range from and pointed toward the target. The lens focus is set at three-fourths of the distance that it would be in air, and the amount of illumination is increased. Flashbulbs and electronic light sources have both been used with success. The easiest photographic subject to get is the bottom, because the picture can be taken in a downward direction, with the distance established when a weight on a known length of string touches bottom.

Underwater television is in its infancy, but it should do much to increase our knowledge of the ocean bottom and marine life at shallow depths.

Bathymetry

The development of piano wire in the 19th century permitted, for the first time, the making of a reasonable number of soundings in the open ocean. The invention in this century of the echo sounder, which electrically times and records a sound wave going to the bottom and back, has permitted continuous depth profiles to be made from ships underway. The great submerged ranges and deep trenches showed up very quickly, but only in the last few years have echo sounders been developed to give depths to, say, 1 meter out of 5000. This type of precision has been obtained by making the timing circuit and recorder precise to better than 1 millisecond, as in facsimile recorders that are used for transmitting weather maps. As usual in science, newer and more accurate data continue to open up new problems. The added precision is never a hindrance, and often it is essential in order to tell whether the ocean bottom is really flat, like parts of Kansas, or rolling, like parts of new England. In addition, it has shown that little ridges or valleys exist in broad plain areas, which might otherwise have been thought to be instrumental error. The finite width of the acoustic beam below the ship has some advantages and some disadvantages. The recording shows the closest bottom, whether it is exactly under the ship or not. Because of this, the records sometimes need greater interpretation, but also there is more there to interpret. The full potentialities of the echo sounder and its many variations have not yet been fully recognized or widely exploited.

Pressure Vessels and Materials

It is often possible to make instruments that do not need pressure-proof cases. A surprising number of commercial items, such as small photoflashbulbs, work well under pressure. Some subminiature vacuum tubes and electronic parts will stand depths of thousands of meters when they are housed in an oil-filled flexible container. Automobile and flashlight batteries operate satisfactorily at the bottom of the ocean if external insulation is provided. Smoked glass, waxed paper, or soft metal plates are water resistant and can be scribed with very light pressures.

Glass, bronze, stainless steel, aluminum, plastics, and ordinary steel have all been used successfully as pressure vessels, with the choice being dependent on weight, handling problems, availability, and cost. For the thicker instrument cases of cylindrical form, one can consider the ratio of the wall thickness to the radius of the tube to be the same as the ratio of the external pressure to the desired maximum working stress of the material. It is also possible to make pressure vessels of glass or aluminum that can go to a depth of several miles and still be light enough to be buoyant. Corrosion problems can be minimized by proper choice of materials, design clearances, and "elbow grease."

Oddly enough, oceanographers are seldom bothered more by leaks at great depth than they are at shallow depths. This is because, when designing for great depths, they usually take pains to design seals properly. Modern electronic equipment is amazingly trouble free if given reasonable care.

Conclusion

Many instrument problems, such as navigation, the collection of bottom samples, the measurement of gravity at sea, the design of unattended instruments, towed electric cables, marine meteorology, marine biology, and the study of radioactive waste disposal, are just as interesting and essential as those to which space has been devoted. Also, it has not been possible to discuss here the many oceanographic instruments in the shore laboratory that are needed to supplement seagoing work. This omission is only partly excusable on the grounds that they tend to be more like conventional instruments.

I hope that this article (*3*) gives some idea of the scope of oceanographic instruments. It should be apparent that most instrumentation should be simple, rugged, and reliable. However, for exploratory work, serious scientists use the best instruments available. In most cases, the designer has to be shipmates with his creation before it can be called an instrument. The designer and user must work as a team, because simple measurements and precise thinking usually result in a greater scientific product than precise measurements and simple thinking. Rather than dwell on the relative merits of theory versus measurement, I hope that instrument designers, experimentalists, and theoreticians will each do their work aggressively and well.

References and Notes

1. H. U. Sverdrup, R. H. Fleming, N. W. Johnson, *The Oceans* (Prentice-Hall, New York, 1942).
2. *Natl. Research Council Natl. Acad. Sci.* (*U.S.*) *Publ. No. 309, Oceanographic Instrumentation.*
3. Contribution No. 806 from the Woods Hole Oceanographic Institution.

Contribution No. 807

Reprinted from JOURNAL OF APPLIED PHYSIOLOGY
Vol. 8, No. 3, November, 1955
Printed in U.S.A.

Counter-Current Vascular Heat Exchange in the Fins of Whales[1]

P. F. SCHOLANDER AND WILLIAM E. SCHEVILL. *From the Woods Hole Oceanographic Institution, Woods Hole, Massachusetts*

IT MAY BE a source of wonder that whales swimming about in the icy waters of the polar seas can maintain a normal mammalian body temperature. What prevents them from being chilled to death from heat loss through their large thin fins?[2] These are well enough vascularized to justify the question (fig. 1). One may conjecture that a whale may be so well insulated by its blubber that it needs such large surfaces to dissipate its heat. On the other hand, if heat conservation is at a premium, there must be some mechanism whereby the fins can be circulated without losing much heat to the water. One may point to two circulatory factors which would reduce the heat loss from the fin: *a*) slow rate of blood flow and, *b*) precooling of the arterial blood by veins before it enters the fin.

Bazett and his coworkers (1) found that in man the brachial artery could lose as much as 3°C/decimeter to the two *venae comitantes*. This simple counter-current exchange system is a mere rudiment compared to the multichannelled arteriovenous blood vascular bundles which we find at the base of the extremities in a variety of aquatic and terrestrial mammals and birds. These long recognized structures have most recently been studied by Wislocki (2), Wislocki and Straus (3) and Fawcett (4).

The function of these bundles has long been a mystery. No matter what else they do, they must exchange heat between the arteries and veins, and it has been pointed out that they very likely play an important role in the preservation and regulation of the body heat of many mammals and birds (5).

In the present study we describe a conspicuous arteriovenous counter-current system in the fins and flukes of whales, which we interpret as organs for heat preservation.

MATERIAL

Two species of porpoises have been studied: *Lagenorhynchus acutus:* dorsal fin, tail-fluke, and flipper of an adult female collected 50 miles east of Cape Cod; *Tursiops truncatus:* dorsal fin and tail-fluke of a 4-month-old calf from Florida, supplied through the courtesy of the Marineland Research Laboratory.

Lagenorhynchus is a genus of fairly high latitudes, the southern limit of *L. acutus* being about latitude 41°N. on the New England coast and about 55°N. in the British Isles. It has been caught at least as far north as latitude 64°N. in west Greenland and Norwegian waters. *Tursiops* is found in lower latitudes, *T. truncatus* overlapping slightly with *L. acutus* and occurring south into the tropics.

DESCRIPTION

Figure 2 illustrates the vascular supply at the base of the dorsal, pectoral and caudal fins. It may be seen that all major arteries are located centrally within a trabeculate venous channel. This results in two concentric conduits, with the warm one inside. In addition to the circumarterial venous channels there are separate superficial veins, as seen in figure 2. The circumarterial venous channels are conspicuously thin walled compared to the simple veins, as may be seen in figure 3. When an artery was perfused with saline, the solution returned through both of these venous systems.

INTERPRETATION

Based on the anatomical findings and on the perfusion experiments, we interpret the artery-within-vein arrangement as a heat-conserving counter-current system, as schematically presented in fig. 4. In such an arrangement the warm arterial blood is cooled by the venous blood which has been chilled in the fin. The result is a steep proximodistal temperature drop from the body into the appendage. The heat of the arterial blood does not reach the fin, but is short-circuited back into the body in the venous system. Body heat is therefore conserved at the expense of keeping the appendage cold. There is reason to believe that the analogous blood vascular bundle in the proxi-

---

Received for publication July 21, 1955.

[1] Contribution Number 807 from the Woods Hole Oceanographic Institution.

[2] In 'fin' we include the structures more specifically called flippers (pectoral fins), flukes (caudal fins) and dorsal fin.

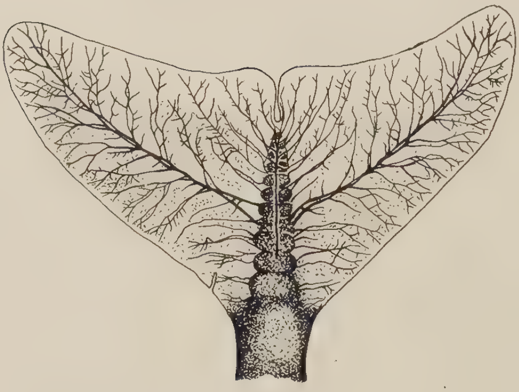

FIG. 1. Arterial supply to the flukes in the common porpoise (*Phocoena phocoena*), drawn from an x-ray picture by Braun (6).

mal part of the extremities of sloths serves a similar function, inasmuch as these animals can barely keep warm even in their warm environment (5). Cold extremities have been described in many arctic mammals and birds as important factors for conservation of body heat (7), but to what extent arteriovenous counter-current structures are present in these animals is not known.

The efficiency of heat exchange in a system like that diagrammed in figure 4 is related to the blood flow. The slower the flow, the more nearly identical will be the arterial and venous temperatures along the system, and the more efficient will be the heat conservation. At high rates of flow, warm blood will reach the periphery and cool venous blood will penetrate into the body.[3]

It was shown by perfusion experiments on the detached fins that the arterial blood may return via the concentric veins, and/or through the separate superficial veins. As pointed out above, the concentric vein channels are very thin walled and weak compared to the thick-walled superficial veins (fig. 3). One may interpret these anatomical facts in the following way. If the animal needs maximal heat conservation, blood circulation through the fins should be slow, and the venous return should preferentially take place through the counter-current veins. But a slow rate of blood flow would need only weak venous walls, as actually found. If, on the other hand, the animal needed maximal cooling, as during exercise in relatively warm water, this would be most effectively accomplished by a high rate of blood flow through the fins, with venous return through the superficial veins and the least possible flow through the concentric veins. This would require the strong and thick walls of the superficial veins. One may even see the likelihood of a semiautomatic regulatory function in the concentric system, for when the artery is swelled by increased blood flow, the concentric veins will be more or less obliterated,

---

[3] The theory for a multichannel counter-current system has been elaborated in connection with the swimbladder in deep sea fishes (8).

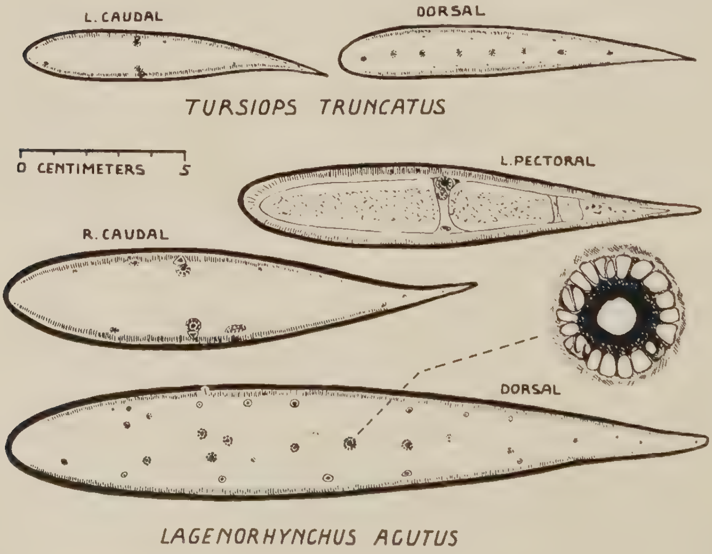

FIG. 2. Sections near base of fins and flukes of two species of porpoises. Each artery is surrounded by a multiple venous channel. Simple veins are near the skin (only the larger ones are indicated).

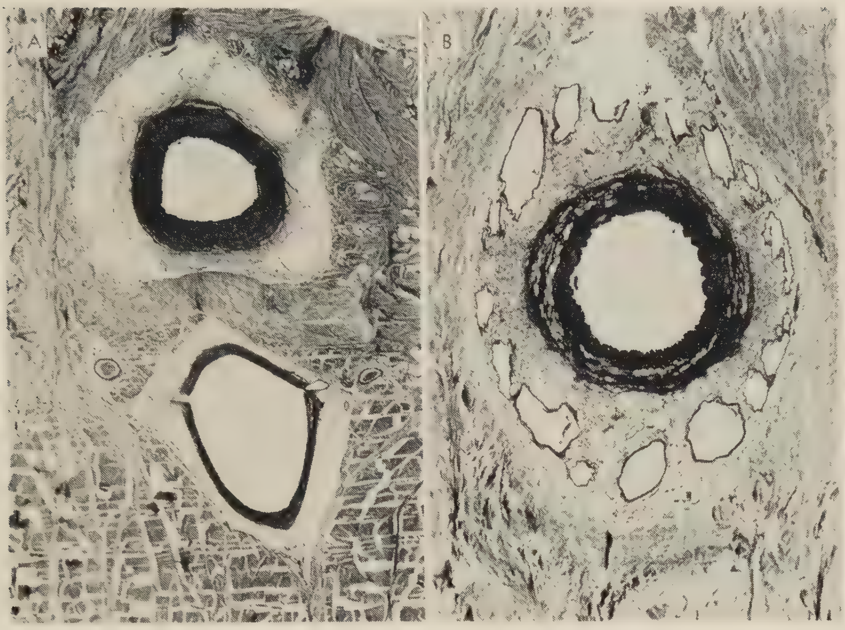

Fig. 3. Sections from *Tursiops truncatus*. (Courtesy of the Department of Anatomy, Harvard Medical School.) *A*. From tail-fluke. Upper: artery surrounded by thin-walled venous channels. Lower: superficial single thick-walled vein in the hypodermis. (× 9) *B*. From dorsal fin. Artery surrounded by thin-walled venous channels (× 12)

but will remain open when the diameter of the artery is reduced during decreased blood flow. Thus the anatomical findings fit logically into the simplest possible scheme of heat regulation in the fins.

There are a few observations available indicative of heat regulation in the fins of porpoises. Tomilin (9) made some observations on an east Siberian 'white-sided dolphin' on deck, and found that the fins could vary between 25° and 33.5°C, while the body varied only 0.5°. Schevill observed that the flukes in a Florida *Tursiops* out of water became about 10° warmer than the body surface itself. In both of these cases the animals were probably resisting overheating. On the other hand, Scholander (5) has recorded cold flippers in water-borne common porpoises (*Phocoena*).

The concentric counter-current system of an artery within a vein appears to be a peculiarly cetacean arrangement, and we have seen it only in the fins, flippers and flukes of these animals.[4] This is an impressive example of bioengineering, which, together with other factors, adapts these homeotherms for a successful existence in a heat-hungry environment.

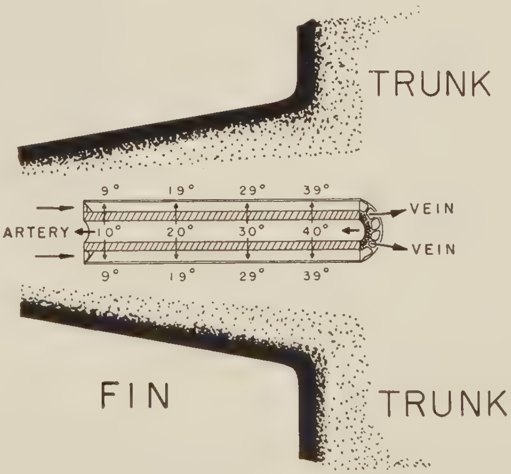

Fig. 4. Schematic diagram of hypothetical temperature gradients in a concentric counter-current system.

SUMMARY

The vascular supply to the fins and flukes of two species of porpoises, *Lagenorhynchus acutus* and *Tursiops truncatus*, is described. All major arteries entering the fins and flukes

---

[4] The present material is from odontocetes, but these structures have also been noted by Scholander in the tail flukes of a mysticete (fin whale).

are surrounded by a trabeculate venous channel. The arteries drain into these, but also into superficial simple veins. The artery within the venous channel is interpreted as a heat-conserving counter-current exchange system. The heat regulatory aspects of the two venous systems are discussed.

We wish to express our appreciation to Dr. F. G. Wood, Jr., and the Marineland Research Laboratory, Marineland, Fla., for providing the material of *Tursiops truncatus*, and to Dr. G. B. Wislocki of the Dept. of Anatomy, Harvard Medical School, Boston, Mass., for providing the histological sections and photographs.

REFERENCES

1. Bazett, H. C., L. Love, M. Newton, L. Eisenberg, R. Day and R. Forster II. *J. Appl. Physiol.* 1: 3, 1948.
2. Wislocki, G. B. *J. Morphol.* 46: 317, 1928.
3. Wislocki, G. B. and W. L. Straus, Jr. *Bull. Mus. Comp. Zool. Harvard* 74: 1, 1932.
4. Fawcett, D. W. *J. Morphol.* 71: 105, 1942.
5. Scholander, P. F. *Evolution* 9: 15, 1955.
6. Braun, M. *Zool. Anz.* 29: 145–149, 1905.
7. Irving, L. and J. Krog. *J. Appl. Physiol.* 7: 355, 1955.
8. Scholander, P. F. *Biol. Bull.* 107: 260, 1954.
9. Tomilin, A. G. *Rybnoe Khozaistvo* 26: 50, 1950. (In Russian.)

Contribution No. 808

PHYSIOLOGIA PLANTARUM, VOL. 8. 1955

The Interaction of Photosynthesis and Respiration and Its Importance for the Determination of ^{14}C-Discrimination in Photosynthesis

By

E. STEEMANN NIELSEN

Royal Danish School of Pharmacy, Botanical Department

(Contribution No. 808 from the Woods Hole Oceanographic Institution)
(Received August 1, 1955)

1. Introduction

Van Norman and Brown in 1952 published the results of some admirable experiments with the green alga Chlorella according to which $^{13}CO_2$ is assimilated at a rate 2 per cent lower than $^{12}CO_2$, but $^{14}CO_2$ at a rate 14 per cent lower than $^{12}CO_2$. The statement about $^{13}CO_2$ was in perfect agreement both with previous investigations (3 per cent according to Nier and Gulbransen 1939) and with what is theoretically to be expected. The statement about $^{14}CO_2$ agrees well with the only previous measurements of $^{14}CO_2$ discrimination by Weigl and coworkers 1949, 1951, although these measurements were criticized by van Norman and Brown. Theoretically, however, the assimilation rate of $^{14}CO_2$, as compared with the rates of $^{12}CO_2$ and $^{13}CO_2$, seems rather astonishing. A discrimination of $^{14}CO_2$ against $^{12}CO_2$ of about 4 per cent, the double value of that for $^{13}CO_2$, would have seemed more likely.

If the discrimination mentioned is to be measured it is necessary to know whether respiration and photosynthesis are going on independently of each other. In order to investigate this, experiments were made by van Norman and Brown using oxygen tracers and a recording mass-spectograph. No influence of light was found on the rate of respiration as measured by the uptake of $^{18}O_2$ from the outside medium. These results were considered a proof that respiration and photosynthesis are going on independently of each other although the two authors mention that because O_2-uptake and O_2-release are independent in light this must not necessarily be the same for CO_2.

The scientists working with radiocarbon dating have presented first class measurements of the specific activity of ^{14}C in recent wood. Unfortunately we have no reliable measurements of the specific activity of ^{14}C in the atmospheric air and presumably it is too late now to make such determinations because of the experiments with H-bombs.

In freshwater some few determinations of the ^{14}C-content in the submerged plants as compared with the content in the CO_2-system of the water has been made by Deevey et al. 1954. They seem to indicate that that ^{14}C-discrimination in photosynthesis under natural static conditions in water is only slight.

In the present article the high discrimination apparently found in the experiments made by van Norman and Brown will be recomputed. It will further be shown that the photosynthetic and the respiratory mechanisms do not work independently of each other although the O_2-metabolism apparently indicates this to be so.

When describing the ^{14}C-method for measuring organic productivity in the sea — Steemann Nielsen 1952 — it was already rendered probable that CO_2-uptake by photosynthesis and CO_2-release by respiration do not take independently of each other. It was therefore pointed out that the ^{14}C-method cannot be used for measuring the rate of photosynthesis at low light intensities where the rate of respiration is the same or lower as the rate of photosynthesis.

An example may be mentioned. In an experiment with Chlorella pyrenoidosa the same rate of photosynthesis (gross production) was found at 7,000 lux when using either the ^{14}C-method or an oxygen method (Winkler analyses) if the photosynthetic quotient was put at 1.2. At 300 lux, which was just below the compensation point, the ^{14}C-method, however, gave a value (gross production) which was only 31 per cent of the value obtained by using the oxygen method. If the rate of respiration is higher than the rate of photosynthesis, the intermixing of the two processes has thus a considerable influence on the measurements of photosynthesis with the ^{14}C technique.

At high light intensities a correction for the measurements of gross production by the ^{14}C-method was introduced corresponding with 40 per cent of the rate of respiration and thus about 4 per cent of the maximum rate of photosynthesis which normally was found to be about 10 times the rate of respiration. As will be shown below, the correction should rather be put at 6 per cent.

2. Experiments on the Release by Respiration of $^{14}CO_2$ Previously Assimilated

One of the easiest ways of investigating the intermixing of CO_2-release due to respiration and CO_2-uptake due to photosynthesis seems to be by measuring in the light and in the dark the release of ^{14}C previously assimilated. If according to van Norman and Brown's measurements with oxygen tracers it is a priori assumed that the rate of respiration is the same in the light and in the dark, any decrease in the release of ^{14}C must be due to some interaction either between CO_2-uptake and CO_2-release or between respiration and photosynthesis. The real reason for such an interaction may, however, be searched for in several instances, such as:

1. A preferable assimilation inside the cells of CO_2 produced by respiration. CO_2 from the outside is to diffuse into the cells before being assimilated by the photosynthetic apparatus, whereas such a diffusing is not necessary for respiratory CO_2 produced inside the cell.
2. A preferable use for respiration of organic matter just produced by photosynthesis.
3. An intermixing of respiration and photosynthesis due to joint pools of intermediates in the two processes.
4. O_2-consumption as measured according to the uptake of tracer oxygen in light is not due exclusively to oxidation of hydrogen produced during the decomposition of organic matter but also in an appreciable extent to oxidation of hydrogen produced from water during the photochemical partial processes in photosynthesis.
5. The mechanism of respiration differs in the light and in the dark.
6. The carboxylation in photosynthesis may demand HCO_3^- which also may be released in respiration instead of CO_2. In spite of carbonic anhydrase the process $CO_2+H_2O \rightleftarrows H_2CO_3$ is not momentary. A preferable uptake of $CO_2(HCO_3^-)$ produced by respiration could therefore be expected.

Of these 6 possibilities the first will in the present article be shown not to be the normal cause of the intermixing of CO_2-release and CO_2-uptake in light. According to work done by Calvin's group in Berkeley (cp. e.g. Calvin and Massini 1952) it seems further unlikely that organic matter just produced by photosynthesis is preferably used for respiration or that joint pools of intermediates are of decisive importance in this respect.

One of the main experiments will now be described. Cells from a 3 days old fast-growing culture of Chlorella pyrenoidosa (Warburg strain) were transferred to a medium, pH 8.2, containing a total amount of $^{14}CO_2$ in the medium corresponding to 7.5×10^6 counts per minute. After 2 hours at 8,000 lux 20° C., during which period about 25 per cent of the ^{14}C was assimilated, the algae were centrifuged in the dark and washed twice with

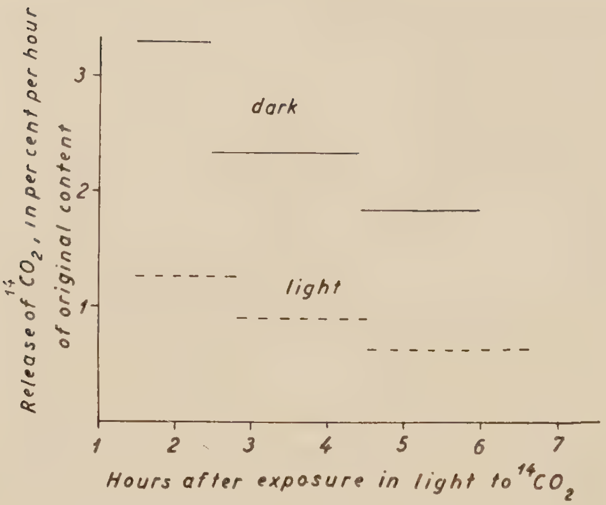

Figure 1. *The release of previously assimilated $^{14}CO_2$ in the light and in the dark. Chlorella.*

a bicarbonate buffer containing 0.03 per cent free CO_2. The algae were then transferred to a fresh medium and kept in the dark at 20° C. for 1 1/2 hours before the experiments proper were started.

One of the reasons why these experiments were not started at once was that $^{14}CO_2$ found in the cells due to previous dark fixation during the first hour in the dark to a high degree interchanged with the normal CO_2 in the outside medium, as no $^{14}CO_2$ was present in the outside medium. As the loss of tracer due to this process at the beginning may be as high or even higher than the loss due to respiration, some time must elapse before the influence of light on the $^{14}CO_2$ produced by respiration can be investigated.

Another reason for not starting the experiments immediately after the uptake of tracer carbon is finished, is that the rate of respiration in the dark for some time after a change in pH may be rather different from the normal one. Such a change is necessary in some special experiments. In light, on the other hand, transitory differences in the metabolism of Chlorella due to a shift in pH seem to be of very short duration only (Steemann Nielsen 1955). This complication can of course be totally avoided by making the whole experiment at the same pH. As this, however, was not the case in the preliminary experiment concerning the influence of light on the release of previously assimilated ^{14}C published by Steemann Nielsen 1953, no stress can be laid on the absolute value given there, although the result in principle agrees very well with the results of later experiments.

After the 1 1/2 hours mentioned the Chlorella suspension was centrifuged, washed, and centrifuged again. The cells were then suspended in 100 ml of the medium and distributed to 2 bottles with glass stoppers each containing

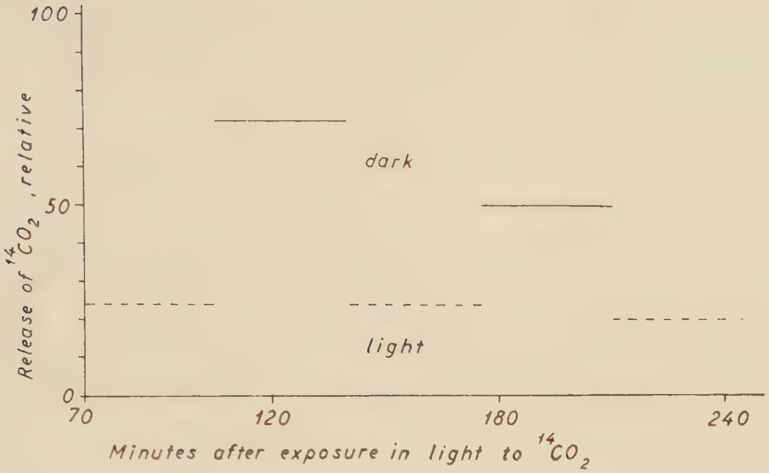

Figure 2. *The release of previously assimilated $^{14}CO_2$ in the light and in the dark. Myriophyllum.*

50 ml, one of which was put in the dark and one in the light of about 8,000 lux.

After about 1 hour, 3 and 5 hours, 10 ml of each bottle were filtered through a millipore filter. The activity of the $^{14}CO_2$ in the filtrate was determined according to Steemann Nielsen 1952: the CO_2 was precipitated as $BaCO_3$.

In Figure 1 the $^{14}CO_2$-release in the light and in the dark is given during the times indicated as per cent released by hour of the amount found in the algae at the start of the proper experiments. In light from 3.3 to 1.8 per cent per hour was released, in dark from 1.3 to 0.6 per cent. It is thus seen that tracer-carbon during the whole experiment was given off in the light at a rate of 33—40 per cent of the rate in the dark. During the five hours the release of $^{14}CO_2$, both in the light and in the dark, decreased by about 50 per cent.

In order to investigate whether the different behaviour of the $^{14}CO_2$ production in light and dark should be caused by a preferable assimilation in photosynthesis of interior CO_2 produced by respiration, some similar experiments lasting for about 1 ½ hours were made at a concentration of free CO_2 150 times as high as in the experiment presented in Figure 1 (4.5 per cent). The light intensity was so low (500 lux) that the rate of photosynthesis just equalled the rate of respiration. A similar difference between the release of $^{14}CO_2$ in light and dark was, however, found. In one experiment about 50 per cent of the $^{14}CO_2$ given off in the dark was given off in the light in another at about 30 per cent, in a third at about 50 per cent. No preferable uptake in respiration of interiorly produced oxygen was found in the light by van Norman and Brown. The idea of preferable uptake of respiratory CO_2 due to diffusion may thus be rejected as being the main cause of the different rate of $^{14}CO_2$ released in the light and in the dark.

Other plant species seem to behave like Chlorella. In Figure 2 is thus shown a series of experiments at 20° C. with a submerged specimen of the phanerogamic aquatic Myriophyllum amphibium from a river on Cape Cod, Mass., U.S.A. After photosynthesis in a medium containing $^{14}CO_2$ for 2 hours, during which time 25 per cent of the tracer was assimilated, the plant was washed in the dark in water without $^{14}CO_2$ for 70 minutes. It was subsequently placed alternately in the light (8,000 lux) and in the dark for 35 minute periods. The concentration of free CO_2 was 0.6 per cent, pH about 5. No ^{14}C was originally found in the carbon-dioxide system of the water.

The plant specimen was fastened to a perforated celluloid plate inside a closed cuvette, which was placed on a rotating disc in a water bath. As the plate was shorter than the cuvette, an effective stirring was produced inside the cuvette (about details cp. Steemann Nielsen 1942). The release of $^{14}CO_2$ during the experiment was measured in the same way as in the Chlorella experiments. $^{14}CO_2$ was given off in the light at a rate of about 40 per cent of the rate in the dark.

If all experiments are taken as a whole, it can be stated that in light only from 30—50 per cent of the labelled CO_2 given off due to the respiration in the dark is released in the light. An average of 60 per cent of the respiratory CO_2 is thus in light identical with CO_2 taking part in photosynthesis. The background of this behaviour is most likely to be found in one of the three possibilities stated as Nos. 4—6 on p. 947 or there may be still another reason.

If the rate of respiration is 10 per cent of the rate of photosynthesis which is normally found at a high light intensity, the rate of photosynthesis (real assimilation) as measured through the assimilation of the tracer carbon is $100-\frac{10\times60}{100}=94$ per cent of the real value. A correction must therefore be made if the ^{14}C-technique is used for measuring gross production. The correction 6 (6.4) per cent (4 per cent according to Steemann Nielsen 1952) is of course only correct if the rate of respiration is 10 per cent of the rate of photosynthesis at the high light intensity at which the measurements are made. If the rate of respiration is 20 per cent the correction for the measurements made with the ^{14}C technique should be 14 per cent. When the standard correction 6 per cent is used in this case the computed photosynthesis rate is 8 per cent too low. If the rate of respiration is $^1/_4$ of the rate of photosynthesis at a high light intensity (an extreme quotient which in plankton algae in nature only on rare occasions will be approached, see Steemann Nielsen and Al Kholy in press) the measurements by the ^{14}C-technique corrected in the standard way are 13 per cent too low.

3. ^{14}C-Discrimination in Photosynthesis

As mentioned in the introduction, $^{14}CO_2$ according to van Norman and Brown 1952 is assimilated during photosynthesis at a rate 14 per cent lower than $^{12}CO_2$, whereas $^{13}CO_2$ is only assimilated at a rate 2 per cent lower. The measurements were made with the use of a recording mass spectrograph. They are of a technically very high standard.

It must, however, be mentioned that in these experiments the discrimination of ^{13}C was measured under static conditions, the ^{14}C-discrimination under kinetic conditions. $^{14}CO_2$ was first introduced into the Chlorella culture at the start of the experiment, whereas no enrichment was done of $^{13}CO_2$ relative to $^{12}CO_2$. In measuring ^{13}C-discrimination it is therefore neither necessary to take any dark uptake into account nor to consider any possible interaction between photosynthesis and respiration. Both circumstances have to be considered when dealing with $^{14}CO_2$.

Let us first consider the dark uptake of $^{14}CO_2$. Van Norman and Brown supposed that the uptake of $^{14}CO_2$ due to isotope interchange was the same during the first 35 minutes in light as during the previous 35 minutes in the dark and they made their correction according to this supposition. This is not, however, correct.

Figure 3 shows a typical curve illustrating the dependence of dark interchange of $^{14}CO_2$ on time. During the first 35 minutes the rate is at least twice the rate during the subsequent 35 minutes. For some reason or other the dark interchange of $^{14}CO_2$ was extremely high in van Norman and Brown's experiment — about 5 times as high as normally found in a first class culture of Chlorella. It is therefore of real importance for the determination of the isotope discrimination if the correction made is twice the correction really to be done. If the authors had used the correct correction, ^{14}C-discrimination would in this way have been 10 instead of 14 per cent. A value of 10 per cent must, however, still be considered too high.

The interaction of photosynthesis and respiration shown in section 2 is the other important factor to be considered if a recalculation of the ^{14}C-discrimination in photosynthesis on the basis of van Norman and Brown's data has to be made. The rate of respiration was about 8 per cent of the rate of photosynthesis (total assimilation) according to Fig. 3 in the article mentioned. If it is assumed that 60 per cent of the respiratory CO_2 is identical with CO_2

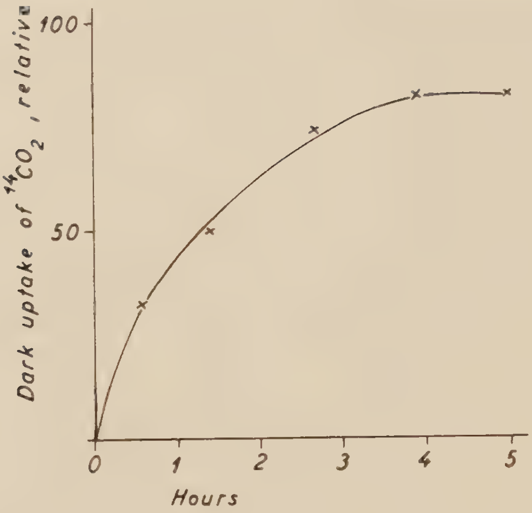

Figure 3. *Dark uptake of $^{14}CO_2$ in Chlorella.*

assimilated during photosynthesis this means that only $100-\frac{8\times60}{100}=95$ per cent of $^{14}CO_2$ is assimilated. In stead of being 10 per cent the ^{14}C-discrimination in photosynthesis is thus only about 5 per cent. This value is theoretically in perfect agreement with the value for ^{13}C as measured by van Norman and Brown. and by Nier and Gulbransen. It is also in good agreement with Deevey's measurements regarding specific activity of ^{14}C in the CO_2 of lake water and in the submerged plants from the same locality.

Summary

Although oxygen metabolism shows no interaction of photosynthesis and respiration, CO_2 metabolism shows such an interaction amounting to about 50—70 per cent of the respiratory rate.

It is shown that the main cause of the interaction is not found in a preferable assimilation of respiratory CO_2 due to the shorter distance for diffusion as compared with CO_2 from the outside medium. Instead some other possible explanations of the fact are presented.

The ^{14}C-discrimination in photosynthesis is recalculated on the basis of the measurements by van Norman and Brown 1952. Besides taking the interaction of photosynthesis and respiration into account, it is at the same time necessary to recalculate the influence of isotopic interchange independent of photosynthesis. The authors mentioned supposed the dark assimilation of

$^{14}CO_2$ to be constant during the first 70 minutes. This is not, however, correct. Taking all evidence into account the discrimination of ^{14}C as compared with ^{12}C is about 5 per cent.

References

Calvin, M. and Massini, P.: The Path of Carbon in Photosynthesis (XX. The Steady State). — Experientia 8: 445. 1952.

Deevey, E. S., Gross, M. S., Hutchinson, G. E. and Kraybill, H. L.: The Natural C^{14}Contents of Materials from Hard-Water Lakes. — Proceed. Nat. Acad. Science. 40: 285. 1954.

Nier, A. O. and Gulbransen, E. A.: Variations in the Relative Abundance of the Carbon Isotopes. — J. Amer. Chem. Soc. 61: 697. 1939.

van Norman, R. W. and Brown, A. H.: The Relative Rates of Photosynthetic Assimilation of Isotopic Forms of Carbon Dioxide. — Plant. Physiol. 27: 691. 1952.

Steemann Nielsen, E.: Der Mechanismus der Photosynthese. — Versuche mit Fucus serratus und anderen Submersen. — Dansk Bot. Ark. 11, nr. 2: 1. 1942.

— The Use of Radio-active Carbon (C^{14}) for measuring Organic Production in the Sea. — Journ. du Conseil Intern. l'Explor. de la Mer. 18: 117. 1952.

— Carbon Dioxide Concentration, Respiration during Photosynthesis and Maximum Yield of Photosynthesis. — Physiol. Plant. 6: 316. 1953.

— Carbon Dioxide as Carbon Source and Narcotic in Photosynthesis and Growth of Chlorella pyrenoidosa. — Ibidem 8: 317. 1955.

— and Al Kholy, A. A.: The Use of the ^{14}C-Technique in Measuring Photosynthesis under Condition of Deficiency in P or N. — In press.

Weigl, J. W. and Calvin, M.: An Isotope Effect in Photosynthesis. — Journ. Chem. Phys. 17: 210. 1949.

— Warrington, P. M. and Calvin, M.: The Relation of photosynthesis to Respiration. — J. Amer. Chem. Soc. 73: 5058. 1951.

Contribution No. 817

Copyrighted, 1955, by the Society of Motion Picture and Television Engineers, Inc

Cameras and Lights for Underwater Use*

By HAROLD E. EDGERTON
and LLOYD D. HOADLEY

The design of underwater automatic and controlled cameras is discussed. A camera of linear design uses a 4-in. (ID) cylinder and a standard 100-ft roll of 35mm film, exposing 800 frames of double 35mm size. Electronic flash is used for illumination, either synchronized with a shutter when external light is present, or without a shutter in darkness. Simplified calculations are given in chart form for cylinders and end plates with external pressure. A few experimental points are given.

Photography is one of the most powerful methods of taking observational data on the geology and on the marine life in the open sea and on the conditions at the bottom. Almost everyone who is interested in any phase of oceanography at some time desires photographic records to study, or to illustrate his findings or to educate other people. As a result many attempts have been made to obtain underwater photographs. Selected references follow at the end of this article.

Flash lighting, both expendable and electrical, seems to be the most desirable source of illumination for underwater photography. Many recent experimenters have used the electronic flash illumination system, since it permits the production of a large number of pictures per camera lowering. The camera described in this article requires electronic flash to illuminate the 800 exposures that can be made on a standard 100-ft length of 35mm film.

Several types of cameras are required for the various kinds of photographic records that are desired. This paper describes the design of a camera that can readily be adapted to almost any type of photography that requires an automatic recycling mechanism.

Camera Casing Design

Many underwater cameras have been designed by putting a watertight case around a standard camera. The case must be designed to withstand the hydrostatic pressures for the desired depths. For each 32 ft of lowering, the pressure increases by 1 atm; that is, the pressure in pounds per square inch is approximately equal to the depth in feet divided by 2.2. At 1-mile depth the pressure is about 2500 psi. The deepest known spot in the sea is about 36,000 ft, requiring a case that will withstand a pressure of about 17,000 psi.

Two alternatives are open to the camera designer: (1) a casing that will withstand the pressure; and (2) a casing that is automatically filled with air (or liquid) at the right pressure as the camera is lowered into the sea. For the latter type, a thin-walled case can be used. Cousteau uses this second system with high-pressure air on his hand-held motion-picture and still cameras, employing the same demand regulator as used in his Aqualung diving equipment. The liquid-filled camera case design is very inviting but introduces complications for the details of operation of lenses, film, batteries, motors, etc.

Pressure-withstanding camera cases of spherical shape are very desirable from a stress standpoint, but packaging of the internal mechanism is awkward. It is also difficult to provide the access holes for windows and doors.

The next most desirable shape, from stress and construction standpoints, is the cylinder, which is the shape used in the designs shown in this paper. Cylindrical pipes and tubes are available in many standard sizes in many metals and other materials, such as glass.

Since conventional cameras are not easily adaptable to the cylindrical shape, an in-line camera design was evolved about the standard (No. 10) 100-ft 35mm motion-picture reel. Figure 1 shows the way in which the camera parts are lined

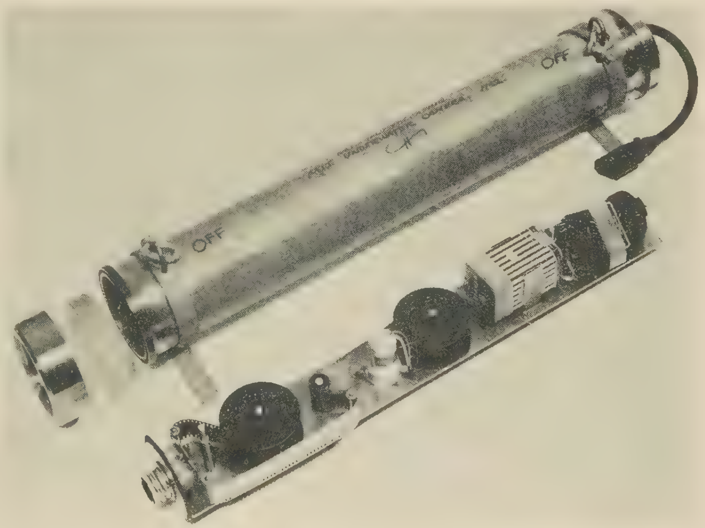

Fig. 1. Camera case with camera chassis removed from the pressure case. The reels hold 100 ft of 35mm film. An agastat was used for timing on this model.

Presented on April 21, 1955, at the Society's Convention at Chicago by Harold E. Edgerton, Dept. of Electrical Engineering, Massachusetts Institute of Technology, Cambridge 39, Mass., and Lloyd D. Hoadley, Woods Hole Oceanographic Institution, Woods Hole, Mass.
(This paper was received on February 28, 1955.)

* CONTRIBUTION NO. 817 FROM THE WOODS HOLE OCEANOGRAPHIC INSTITUTION.

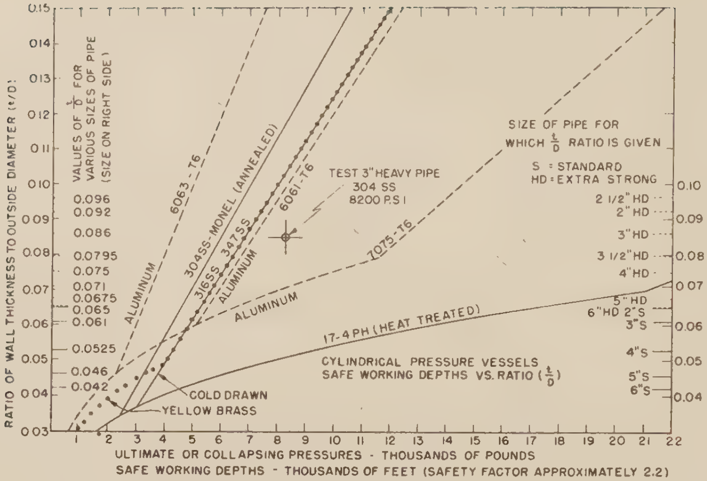

Fig. 2. Maximum pressure or depth of long cylinders as a function of the ratio of wall thickness to diameter.

up on a chassis that slips into the cylindrical housing. A 4-in. diameter is required for the film reel.

Actually, a 4-in. hole is slightly tight for the standard 100-ft reel. Some troubles were experienced in the field by film-motion stoppage at depths where the distortion of the case caused the reels to bind against the side of the case. This difficulty was solved by reducing the outside diameter of the reels in a lathe.

Figure 2 is a graph for cylindrical pressure vessels of various metals showing the maximum or collapsing pressures and the safe working depths plotted against the t/D ratio (wall thickness to outside diameter). These curves are for cylinders whose effective length is greater than six times the outside diameter; they were obtained by combining the formulas of Timoshenko, Carmen and Love and were modified by experimental data both in the laboratory and at sea.

The cylinder for the case shown in Fig. 3 is made of standard 4-in. iron pipe size, Type 304 stainless-steel pipe. The square plates welded to the tube are to facilitate mounting of the window and end-cap, and also to reduce the effective length/OD ratio, which gives a slight increase in the maximum pressure, and to provide better and more versatile mounting methods.

Figure 4 gives maximum pressures and safeworking pressures vs. the t/D ratio for various end closures. From this it can be seen that a 1-in. thick window with a 4-in. diameter (t/D = 0.25) will break at about 2500 psi, or approximately 1 mile. In order to use a 1-in. thick window (the maximum stock thickness of plate-glass) for greater depths and to equal the strength of the case, a stainless-steel insert or ring with a $1\frac{1}{2}$-in. effective diameter is used (t/D = 0.6667, maximum P = 17,000 theoretical); see Fig. 3. Three test points show considerable deviation from theory. See Fig. 4 for $1\frac{1}{4}$- and $1\frac{1}{2}$-in. window data.

Although regular plate-glass, which is almost optically flat, has a slight greenish tint and is not the strongest material available, it has proved to be the most satisfactory window material. Herculite, a hardened plate-glass, has strengths as much as four and five times as great as that of regular plate-glass. The slight waviness that may be introduced in the hardening process makes the seating difficult and gives highly unpredictable pressure results. These results vary from the calculated values for Herculite to values lower than for ordinary plate-glass.

Fused ground quartz has been used to gain optical qualities in special cases, but for general work the slight gain does not outweigh the cost ratio. There is no gain in strength.

End-caps are generally made of the same metal as the tube (case) and are generally thicker than the minimum to facilitate easy opening, loading and closing, and to provide ample material for the electrical connections and fittings.

Standard "O" ring seals are used on the windows and caps to provide a water- and pressure-tight unit. Single "O" rings are used for safe working pressures up to 10,000 psi. For greater pressures, double or triple rings, or double rings with leather or Teflon back-up rings are recommended. These are used for pressures up to 20,000 psi, although they usually require radial grooves similar to piston-ring grooves, and necessitate a longer tube for a given inside length.

Camera Design

Figure 1 illustrates how the various mechanical components have been mounted in line on a metal strip. The mercury switch has proved to be a most convenient method of switching while at sea. This method permits the camera to be loaded, sealed and left on the deck in the "off" position awaiting the moment of lowering, thus keeping the interior dry and clean.

Open cameras at sea can become filled with warm, humid air. As a result, when the cameras are lowered into the cold sea, the moisture condenses on the inside

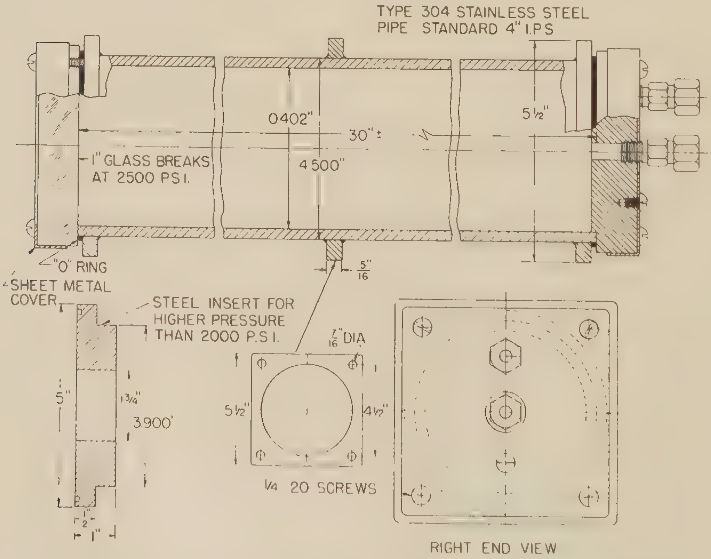

TYPE 304 STAINLESS STEEL PIPE STANDARD 4" I.P.S
0.402"
30" ±
5½"
4.500"
1" GLASS BREAKS AT 2500 PSI.
"O" RING
SHEET METAL COVER
5/16"
STEEL INSERT FOR HIGHER PRESSURE THAN 2000 P.S.I.
7/16" DIA
5"
1¾"
3.900'
5½"
4½"
1/4 20 SCREWS
1/2"
1"
RIGHT END VIEW

Fig. 3. Camera case, as made of 4-in. I.P.S. stainless steel with optical window and electrical connections.

of the glass window, destroying the photographic quality. Every effort must be made to keep the inside dry. For example, the camera could be flushed with dry gas before being sealed.

When a camera comes up from the sea and is cold, it should not be opened, since a layer of moisture will immediately condense over the entire interior. It is advisable to wait until the camera has warmed up, to prevent the condensation.

The film transportation has been accomplished by using two "O" rings as belts from a motor to the sprocket shaft and to the take-up reel shaft. One main sprocket is used to meter the film. A microswitch, operated by a cam on this sprocket shaft, can be used in a variety of ways, such as stopping the film motion after a frame has advanced, or flashing an electronic flash lamp at the proper moment. The take-up reel shaft is driven by a loose "O" ring belt that slips as the film builds up on the reel. The motor and attached gear reductions are attached as a unit to the camera plate. Several gear and voltage combinations can be selected from catalog combinations of the Hansen Manufacturing Co. of Princeton, Ind. The 4.5-rpm 6-v motor runs the film at a 10 to 15-sec interval/frame, which is satisfactory for many underwater assignments. At this rate the 100-ft reel is run through in about 3 hr.

Since there is no provision or necessity for focusing the camera, owing to space limitations, the optical parts have been put on an assembly that can be removed by taking out two screws. Then a ground glass can be put at the film position and the optics adjusted for maximum resolution with an enlarging eyepiece. Figure 5 shows this gate assembly with the magnifier in place over the ground glass.

Leica-type threads are used on the camera, so that Leica lenses of different focal lengths can be used.

When a shutter is required, a special Wollensak shutter with an "X" synchronizing contact can be used with a Heiland solenoid control (see Fig. 6). This special shutter has an extra arm that is connected mechanically to the shutter-blade operating ring. A spring returns the shutter to its closed position, following a pulse on the solenoid. The camera shutter can be operated from the exterior by pushbutton. Examples of such operation are cameras for use with the Bathyscaphe and with television viewing. The shutter is required for the applications to prevent exposure due to continuous lights needed for viewing. The pushbutton control enables the observer to click the photograph at the right moment, using synchronized electronic flash lighting to expose the film.

Electrical connections are brought through the cases or end-cap in gland-type fittings, as made by the Conax Mfg. Co. of 4515 Main St., Buffalo, N.Y. A

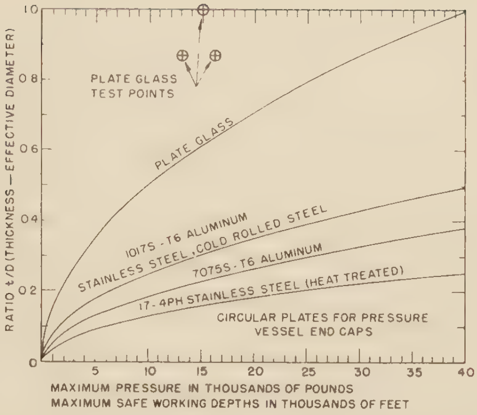

Fig. 4. Maximum pressure or depth of flat end-caps for cylinders, as a function of thickness to diameter.

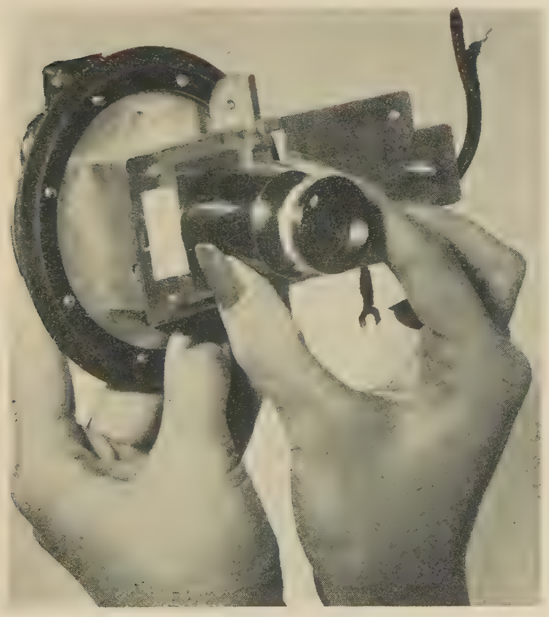

Fig. 5. Placement of a ground glass on the camera gate for alignment and focus, using an enlarging eyepiece. The front elements of the camera are separable from the camera by the removal of two screws and electrical connections.

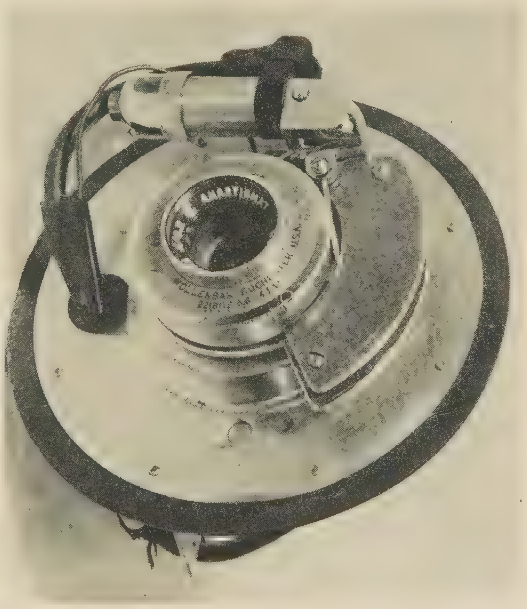

Fig. 6. Pulse-operated shutter with "X" synchronizing contact. The solenoid connects directly to an arm on the shutter ring. Leica-type threads are used back of the shutter, so that other lens combinations without a shutter can be used.

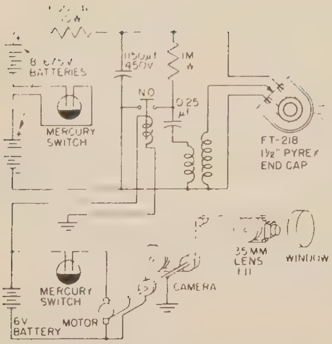

Fig. 7. Wiring diagram of a continuously recycling camera that flashes a dry-battery powered flashtube. The lamp unit is shown as Fig. 9.

solid wire with plastic insulation works very well. The use of stranded wire in the gland may result in a leak through the space between the strands if the rubber wire insulation does not completely seal.

Watertight molded plugs, made by the Joy Co., Henry W. Oliver Bldg., Pittsburgh 22, Pa., have molded ends which do not leak under pressure. Their single-prong type, 1B125F and 1B125M, and the double-prong type, 2E125F and 2E125M, have been used successfully.

Pyrex end-caps and other glass plumbing supplies of several sizes, as manufactured by the Corning Glass Works of Corning, N.Y., serve very well as covers for the flashtubes and as containers. Since the rubber gasket seldom has time to regain its original thickness or shape when the camera reaches the surface and the water pressure is released, the end-cap will be left loose. It is therefore important to use thin rubber or neoprene gaskets and to use springs under the hold-down bolts, so that leaks will not occur.

All cases should be pressure-tested with sustained pressures of 150% to 175% of the maximum expected working pressures. One must not yield to the temptation to "pop" test a case, since flaws in material or machinery may show up only under sustained stress, owing to "creep" characteristics of materials near the maximum yield stresses. Once the window has been sealed and tested it must be left undisturbed, since even the slightest piece of foreign material (dirt, chips, etc.) between the window and seat can cause premature failures. All access to the camera case should be via the metal end-cap.

On serious expeditions where a leak may occur at sea at a great distance from a base of supplies, it is very important to be prepared with spare cameras. Another precaution is to keep spare parts, such as lenses, motors, and microswitches. These are the only parts that are damaged by water. With the designs shown in this paper, a flooded camera can again be put into action quickly by changing the above-mentioned components and washing down the mechanical parts with fresh water.

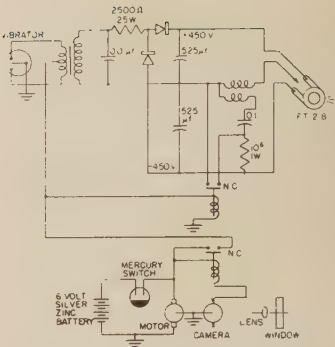

Fig. 8. Wiring diagram of a continuously recycling camera that operates both camera and flashlamp from a wet battery (6-v d-c).

Optical Correctors

When a conventional lens is used behind a plane window in an underwater camera, the image suffers distortion, especially at the edges of the frame.

James Baker has designed a two-glass corrector, which mounts back of a 35mm focal length lens. One of these was used on a camera that is now in service on Cousteau's ship, the "Calypso."

Another corrector has been designed by Thorndike (see bibliography). This is also a two-glass element, but it is placed in the water, in front of the lens and window. A corrector of this type

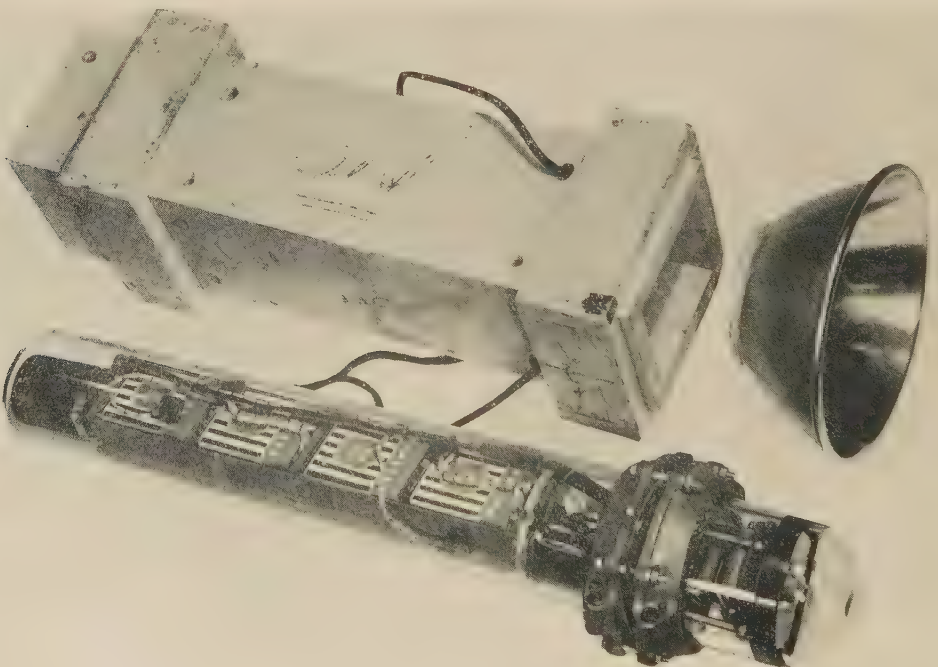

Fig. 9. Pyrex glass-encased flash unit of the dry-battery type with circuit similar to that shown in Fig. 7.

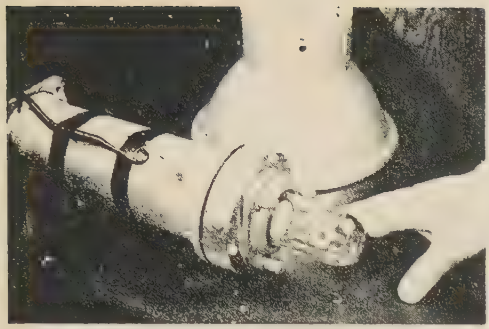

Fig. 10. Light-producing end of a 200-wsec flash unit in 3-in. heavy pipe of Type 304 stainless steel, as used on the Bathyscaphe with 24-v input.

was used on the camera installed on the exterior of the French Bathyscaphe, FNRS 3.

Electronic Flash

The flash equipment consists of standard commonly used components that are selected mainly for packaging in the cylindrical pressure cases. One major decision in the design is the type of battery to use. Both high-voltage dry batteries (see circuit Fig. 7), and wet batteries (see Fig. 8) have been used. On some occasions the wet batteries of the silver-zinc type have been employed because of the smaller volume of the battery for a given amount of wattseconds of energy storage.

Figure 9 shows a photograph of a device whose diagram is given in Fig. 7. The glass case is protected by the wood cover. Notice that the reflector is external.

The flash output varies from 50 to 200 wsec for the various units that have been used. The FT-218 (General Electric Co.) flashtube has been used at 450 v. although rated 900 v, by selecting tubes and by using a vigorous starting pulse.

When more powerful flashes are needed, multiple lighting units are supplied. For example, the French Bathyscaphe, FNRS 3, has four flash units of 200-wsec input that operate from a 24-v battery in the body of the sphere. The wiring circuit of the lamps is similar to the one shown as Fig. 8. Notice that both power and synchronism control come into the lamp case in a single wire, since the ground is common.

The case consists of 3-in. heavy pipe (iron pipe size) stainless-steel, Type 304, with a 1-in. thick end-cap. A test to destruction required 8200 psi (see test point on Fig. 2). The safe operational use was limited to 6000 psi, which corresponds to the pressures experienced by the Bathyscaphe. The light-producing end of this arrangement is shown in Fig. 10. The FT-218 tube is protected by a $1\frac{1}{2}$-in. pyrex end-cap that is modified by grinding the cast surface flat. Note the springs under the screws to maintain gasket pressure when the unit comes up from the depths. The gasket does not return to its initial thickness, because of the high pressure. The pyrex end-caps have been tested with 10,000 psi.

An experimental camera case is now being built following the designs described in this paper. The camera case will be tested to 17,000 psi. or possibly 20,000. The specifications for the deep model are:

Material: Centrifugally cast 17-4PH stainless steel, heat-treated after machining.
Inside diameter: 4.05 in.
Wall thickness: $\frac{3}{8}$-in. t/D = 0.078 max. 24,000 psi.
End-cap: 1-in. t/D = 0.25 max. 40,000 psi.
Windows: $1\frac{1}{4}$-in. thick glass.
Window diameter: $1\frac{1}{2}$-in. diameter over $1\frac{1}{2}$-in. thick steel plate.
Window: t/D = 0.833 max. 27,000 psi (theoretical), tests showed 15,000 and 16,250 psi.

Figure 12 shows the above case and the camera that goes with it.

Cameras in Use

(1) Used at W.H.O.I., summer of 1952, on the "Bear." At Honolulu by the U.S. Fish & Wildlife Service, 1952. Now at

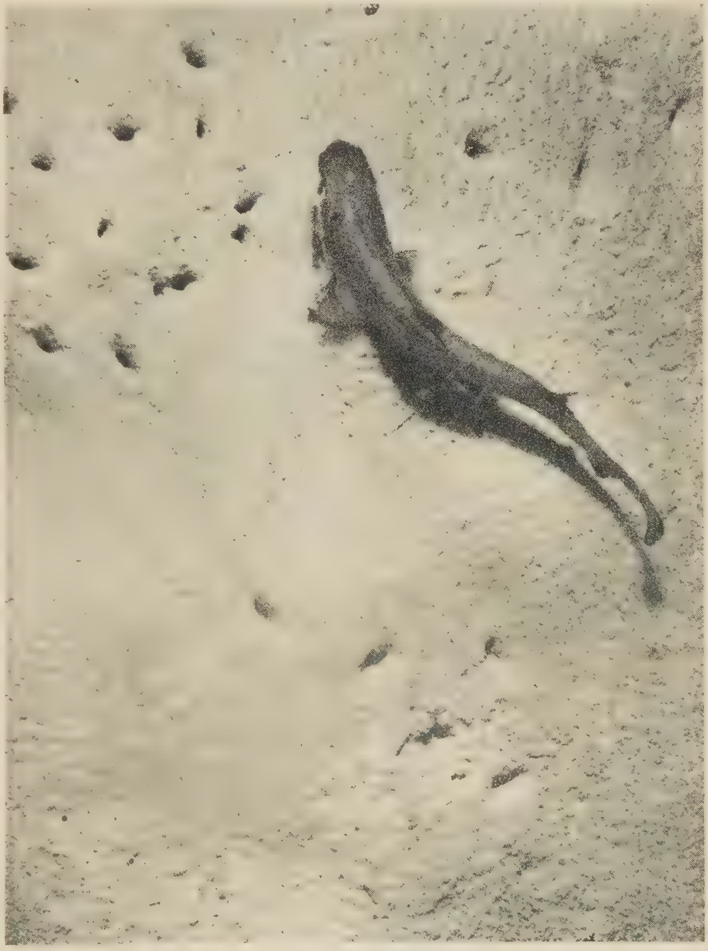

Fig. 11. The bottom of the sea at $\frac{1}{2}$-mile depth in the Mediterranean, showing a small fish and holes in the mud. A pulsed sonar transmitter was used to indicate the position of the camera and the sea-bottom by a mercury switch, which turned the sonar off upon contact.

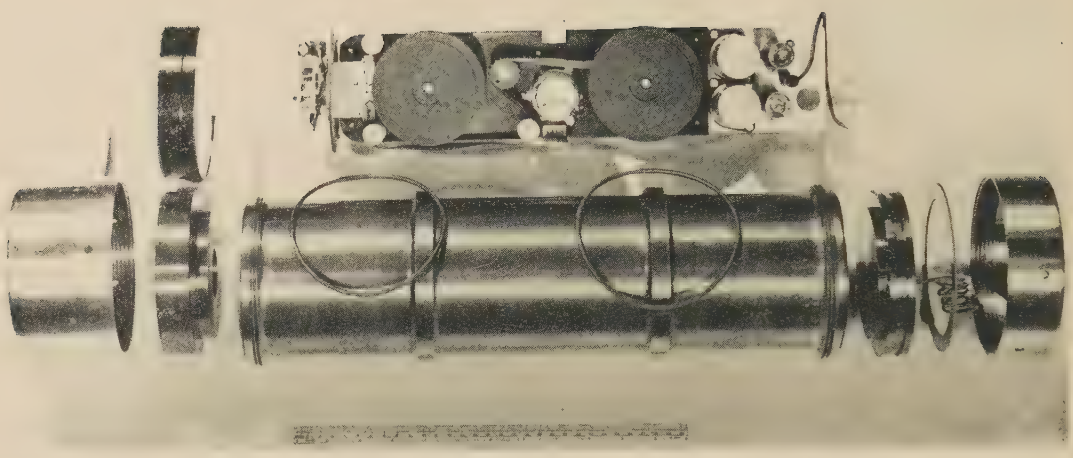

Fig. 12. A 35mm camera with 100 ft of film for the French Bathyscaphe FNRS 3. Cast 17-4PH metal cylinder with $\frac{3}{8}$-in. wall and a $1\frac{1}{4}$-in. plate-glass window was used.

W.H.O.I. on D.S.L. (Deep Scattering Layer) work; depth 2000 ft.

(2) Used by Cousteau and Edgerton on the "Calypso," summer of 1953, on D.S.L. photography in the Mediterranean off French coast; depth 2000 ft.

(3) Silhouette model used by Cousteau and Edgerton on the "Calypso," 1953, in the Mediterranean; depth 1000 ft. Used by W.H.O.I., summer 1954; now at M.I.T.

(4) In use at University of Miami, Fla., by Smith on D.S.L. and bottom photography; depth 2000 ft.

(5) Improved model used on "Calypso," summer 1954, with sonar bottom indicator; depth 6000 ft.

(6) Now in use on exterior of Bathyscaphe for pushbutton photography; depth 2000 m; Toulon, France.

(7) Now at W.H.O.I., modified with surface pushbutton control for D.S.L., with sonar viewer.

(8) Built as spare for "Calypso" effort, in case of camera loss at sea; now at M.I.T.

(9) and (10) Under construction at M.I.T. for the Bathyscaphe, with casings to withstand 4000-m depths.

Acknowledgments

Technical assistance and cooperation by Wollensak Optical Co., Sprague Electric Co., Mallory Electric Co., Hansen Motor Co., Conax Mfg. Co., General Electric Co., International Carbon Co., Wagn H. Hargbol, Precision Optics Laboratory, Parker Appliance Co., Edward M. Thorndike, James Baker, Joseph Vitka, Edo Corp., and W. G. White, Inc., are hereby gratefully acknowledged.

This project was supported by the National Geographic Society, the Woods Hole Oceanographic Institution, The Massachusetts Institute of Technology and Edgerton, Germeshausen and Grier, Inc. The Research Laboratory of Electronics' machine shop at M.I.T. constructed the cameras and greatly assisted in their design, in particular John Keefe, the foreman.

References

1. Maurice Ewing, Allyn Vine and J. L. Worzel, "Photography of the ocean bottom," *J. Opt. Soc. Am.*, *36:* 307–321, 1946.
2. E. Newton Harvey and Edward R. Baylor, "Deep sea photography," *J. Marine Research* (*Sears Foundation*), *VII:* No. 1, 10–16, Apr. 1948.
3. J. B. Collins, "Underwater photography," *Phot. J.* (*London*), *90B:* 24–31, Jan.–Feb. 1950.
4. K. O. Emery, "Submarine photography with the Benthograph," *Sci. Monthly*, *55:* No. 1, 1, July 1952.
5. E. M. Thorndike, "A wide-angle, underwater camera lens," *J. Opt. Soc. Am.*, *40:* 823, 1950.
6. G. Shumway, R. F. Dill and H. S. Kierstead, "The USNEL Deep-Sea Camera," *Rept. No. 388, U.S. Navy Electronics Lab.*, San Diego, Calif.
7. E. M. Thorndike, Tech. Rept. No. 5 CU-24-53-NObsr, Geology, Nov. 1953, (Optical Corrector).
8. E. R. Cross, *Underwater Photography and Television*, Exposition Press, Inc., New York, 1954.
9. H. Schenck and Henry Kendall, *Underwater Photography*, Cornell Maritime Press, Cambridge, Md., 1954.
10. H. E. Edgerton, "Photographing the sea's dark underworld," *Nat. Geog. Mag.*, April 1955, p. 523.

Contribution No. 822

Reprinted from PLANT PHYSIOLOGY, Vol. 30, No. 6, November, 1955, pages 560–561.

PRINTED IN U.S.A.

HYDROSTATIC PRESSURE IN COCONUTS[1, 2]

P. F. SCHOLANDER[3]

WOODS HOLE OCEANOGRAPHIC INSTITUTION
AND
LERNER MARINE LABORATORY, BIMINI, BAHAMAS

David Fairchild in "Garden Islands of the Great East" (3) gives a vivid description of the natives of Java and the Philippines climbing wine palms 60 feet high and harvesting every day a bamboo container full of the sugary sap which drips from the bruised and cut stems of the inflorescences. The coconut palm also yields enough sap from the cut flower stems to support an important palm sugar industry (2). As the pressure in the transpiration stream of the palm stem is very likely low, and possibly under cohesive tension, some local process must develop in the cut flower stem which steps up this pressure to make it possible for sap to drip out 20 meters above the ground.

It is described as quite an art to get a successful flow of sap from the coconut palm, but a large supply of free liquid is readily available inside the coconuts, and one might wonder what the pressure of this liquid would be. During a visit to the Lerner Marine Laboratory in Bimini, Bahamas, an opportunity arose to find out. A green, unripe coconut was taken into the laboratory, and a syringe needle pushed into the cavity. When the needle was pulled out a fine jet of sap shot out of the puncture hole with such a force that it hit the ceiling. This occasioned some studies of the pressure relations of the coconut milk in respect to the size of the nut, its height above ground, and the osmotic potential of the milk. By comparing these values one may venture to make certain guesses as to the nature of the mechanism responsible for the pressure build-up in the nuts.

It was established that young nuts in the same inflorescence, i.e, of the same age and of selected size, had similar pressures whether measured in situ or freshly detached. No liquid leaked from the cut petiole. The pressure was measured in the laboratory with a tuberculin syringe full of water and containing

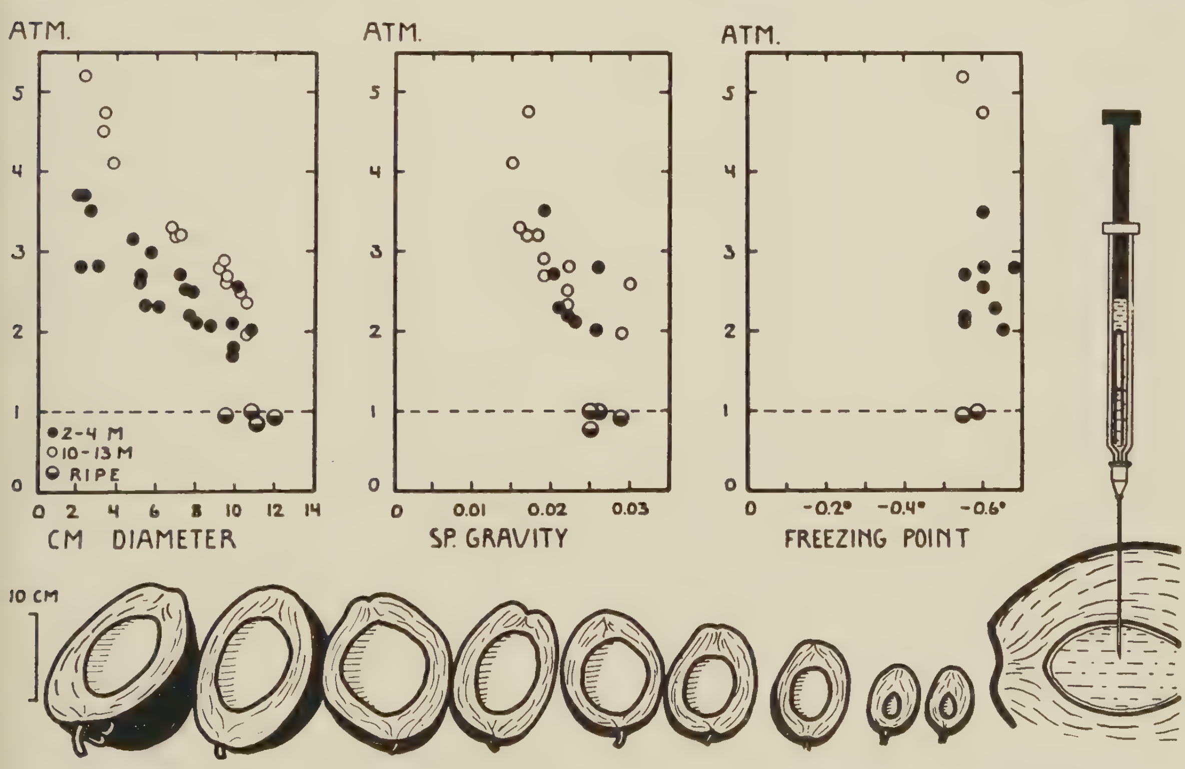

FIG. 1. *Top.* Liquid pressure in coconut cavity versus (a) largest diameter of cavity, (b) specific gravity of milk, (c) freezing point of milk. *Bottom.* Size range of nuts used, after photograph. *Right.* Method for pressure measurements. Capillary manometer inside syringe barrel.

---

[1] Received July 14, 1955.

[2] Contribution No. 822 from the Woods Hole Oceanographic Institution.

[3] Present address: Institute of Zoophysiology, University of Oslo, Blindern, Norway.

a small air-filled capillary manometer open at one end (fig 1). The length of the air column in the capillary was measured on the syringe scale (V_1), and the position of the plunger was noted. The needle was pushed into the cavity of the nut and unplugged by forcing the plunger in slightly. The plunger was immediately returned to its original position and held there while the gas volume in the manometer tube was measured (V_2). The hydrostatic pressure was calculated as V_1/V_2 in atmospheres. The pressure dropped slowly, especially in the smallest nuts, due to a slight leak along the needle. The figures are hence minimum values, but undoubtedly quite near to the true values. In ripe, hard-shelled nuts it was necessary to drill through the husk and hard outer shell before introducing the needle.

Freezing point determinations were performed by observing the melting and freezing of a few microscopic ice crystals present in a large excess of sap, according to a modification of the method described by Pounder and Masson (4).

Specific gravity of the coconut sap was determined by weighing in a pycnometer.

In young green nuts the hydrostatic pressure increases with decreasing size (fig 1). The nuts which were taken from two tall palms 10 and 13 meters above ground had higher pressures in all sizes than were found in nuts taken from lower palms at 2 to 4 meters. The values ranged from 2 atmospheres in the biggest green nuts to over 5 atmospheres in the smallest. Only ripe nuts contained a gas phase, usually somewhat below atmospheric pressure, suggesting the possibility that part of the milk had been absorbed and that gas had diffused in to take its place.

The freezing point of the coconut milk was between $-0.55°$ and $-0.68°$ C, with an average osmotic potential of 7 atmospheres. This was not correlated with milk pressure, specific gravity, height above ground, or size (age) of the nuts (fig 1).

The specific gravity of the coconut milk varied between 1.015 and 1.030, with the lowest values in the sap which was under the highest pressure (fig 1). This correlation undoubtedly is secondary to the fact that the sap gets slightly more concentrated as the nuts grow older (1). Compared to the very watery coconut milk, the palm sugar sap dripping from the cut flower stems has been found to be some three times more concentrated, with a specific gravity averaging 1.07 (2).

There is an inverse relation between the size of the nut cavity and the internal pressure. This is not very surprising on the basis of structural stress considerations, for the maximum pressure which a hollow sphere can stand for a given wall strength is inversely proportional to the diameter.

Coconuts growing on the same tree are equally high above the ground and ultimately derive water from the same source, namely, the transpiration stream in the palm trunk, which for all the nuts may be assumed to present the same osmotic potential. The coconuts were all found to have essentially the same osmotic potential in the milk. With all these factors constant, if the nuts were simple osmometers, they should have the same hydrostatic pressure. But this was found to be related to the nut size and varied from 5 atmospheres in the small nuts to 2 atmospheres in the large ones. Some of these isosmotic nuts did therefore maintain an osmotic unbalance of at least 3 atmospheres, i.e, the hydrostatic pressure in the nuts is not produced by a simple process of osmosis. The fact that the hydrostatic pressure in isosmotic nuts was higher in tall palms than in low, points in the same direction. One may furthermore observe that it seems dubious that an osmotic "pull" of 7 atmospheres by the coconut milk would be enough to produce a pressure of 5 atmospheres in the nuts, against: a hydrostatic pull of 13 meters plus whatever cohesive and osmotic "pull" there may be in the sap of the palm stem.

One may therefore conclude that there must be some active "secretory" process capable of regulating the pressure in the coconut against an osmotic gradient of several atmospheres. As detached nuts do not bleed through the stalk, it seems likely that the pressure regulation is located within the nut.

LITERATURE CITED

1. Chandrasena, J. P. C. The chemistry of the products of *Cocos nucifera*. II. Biochem. Jour. **27**: 3–4. 1933.
2. Copeland, E. B. The Coconut, 3rd ed, rev. Pp. 1–233. Macmillan and Co., Ltd., London 1931.
3. Fairchild, D. Garden Islands of the Great East. Pp. 1–239. Charles Scribner's Sons, New York 1943.
4. Pounder, F. E. and Masson, I. Thermal analysis and its application to the dinitrobenzenes. Jour. Chem. Soc. 1934: 1357–1360. 1934.

Report for the year 1955

THE
WOODS HOLE OCEANOGRAPHIC INSTITUTION

REPORT FOR THE YEAR
1955

1956

TABLE OF CONTENTS

PAGE

I. Trustees as of December 31, 1955 4

II. Members of the Corporation, as of December 31, 1955 . 5

III. Research Staff 7

IV. Director's Report 10

V. Treasurer's Report 37

Appendix 44

ARNAUD C. MARTS

President of the Corporation, 1950–1955

"He has given unstintingly of time and effort. His judgment, ability, and leadership have strengthened the Institution and brought it greatly increased recognition and support." (*Excerpt from Board of Trustees' Resolution of August 11, 1955.*)

I. TRUSTEES

(As of December 31, 1955)

Honorary Trustees

Henry B. Bigelow, Museum of Comparative Zoology, Cambridge 38, Mass.
Marion Eppley, 510 Park Avenue, New York, N.Y.
Alexander Forbes, 610 Harland Street, Milton, Mass.

To serve until 1959

J. S. Coles, Bowdoin College, Brunswick, Maine.
Carl H. Eckart, Scripps Institution of Oceanography, La Jolla, Cal.
Ross G. Harrison, Osborn Zoological Laboratory, Yale University, New Haven, Conn.
Milford R. Lawrence, Siders Pond Road, Falmouth, Mass.
Harlow Shapley, Harvard College Observatory, Cambridge, Mass.
Francis C. Welch, 73 Tremont Street, Boston, Mass.

To serve until 1958

Charles Francis Adams, Jr., Raytheon Manufacturing Company, 138 River Street, Waltham 54, Mass.
Horace S. Ford, 77 Massachusetts Avenue, Cambridge 39, Mass.
Arnaud C. Marts, 521 Fifth Avenue, New York, N.Y.
Albert E. Parr, American Museum of Natural History, Central Park West at 79th Street, New York, N.Y.
Athelstan F. Spilhaus, Institute of Technology, University of Minnesota, Minneapolis 14, Minn.
Selman A. Waksman, Institute of Microbiology, Rutgers University, New Brunswick, N.J.

To serve until 1957

Eric G. Ball, Department of Biological Chemistry, Harvard Medical School, Boston, Mass.
L. O. Colbert, 4408 29th Street, N.W., Washington, D.C.
Frank A. Howard, 30 Rockefeller Plaza, New York, N.Y.
Columbus O'D. Iselin, Woods Hole Oceanographic Institution, Woods Hole, Mass.
Raymond Stevens, c/o Arthur D. Little, Inc., 30 Memorial Drive, Cambridge, Mass.
E. Bright Wilson, Jr., Department of Chemistry, Harvard University, Cambridge 38, Mass.

To serve until 1956

Detlev W. Bronk, The Rockefeller Institute of Medical Research, 66th Street and York Avenue, New York 21, N.Y.
Daniel Merriman, Bingham Oceanographic Laboratory, Yale University, New Haven, Conn.
Alfred C. Redfield, Woods Hole Oceanographic Institution, Woods Hole, Mass.
Lawrason Riggs, Riggs, Ferris and Geer, Room 1201, 74 Trinity Place, New York 6, N.Y.
Henry L. Shattuck, 10 Milk Street, Boston, Mass.
Gerard Swope, Jr., c/o International General Electric Co., 570 Lexington Avenue, New York, N.Y.

Ex Officio

Edwin D. Brooks, Jr., P.O. Box 1135, Boston 3, Mass.
Mary Sears, Woods Hole Oceanographic Institution, Woods Hole, Mass.
Edward H. Smith, Woods Hole Oceanographic Institution, Woods Hole, Mass.

OFFICERS

Raymond Stevens, President of the Corporation, c/o Arthur D. Little, Inc., 30 Memorial Drive, Cambridge, Mass.
Henry B. Bigelow, Chairman of the Board of Trustees, c/o Museum of Comparative Zoology, Cambridge 38, Mass.
Edwin D. Brooks, Jr., Treasurer, P.O. Box 1135, Boston 3, Mass.
Mary Sears, Clerk of the Corporation, Woods Hole Oceanographic Institution, Woods Hole, Mass.

II. MEMBERS OF THE CORPORATION

Charles Francis Adams, Jr., Raytheon Manufacturing Company, 138 River Street, Waltham 54, Mass.
Oliver Ames III, North Easton, Mass.
Philip Armstrong, Medical Center of Syracuse, State University of New York, Syracuse, N.Y.
Eric G. Ball, Harvard Medical School, Shattuck Street, Boston, Mass.
Henry B. Bigelow, Museum of Comparative Zoology, Cambridge 38, Mass.
Lindsay Bradford, 215 East 72nd Street, New York, N.Y.
Detlev W. Bronk, The Rockefeller Institute of Medical Research, 66th Street and York Avenue, New York 21, N.Y.
Edwin D. Brooks, Jr., P.O. Box 1135, Boston 3, Mass.
C. Lloyd Claff, Single Cell Research Foundation, Inc., 5 Van Beal Road, Randolph, Mass.
L. O. Colbert, 4408 29th Street, N.W., Washington, D. C.
Kenneth S. Cole, National Institute of Health, Bethesda 14, Md.
J. S. Coles, Bowdoin College, Brunswick, Maine.
Henry B. DuPont, Wilmington, Del.
Ferdinand Eberstadt, 39 Broadway, New York 6, N. Y.
Carl H. Eckart, Scripps Institution of Oceanography, La Jolla, Cal.
Harrison P. Eddy, c/o Metcalf & Eddy, 1300 Statler Building, Boston, Mass.
Marion Eppley, 510 Park Avenue, New York, N.Y.
Alexander Forbes, 610 Harland Street, Milton, Mass.
Horace S. Ford, 77 Massachusetts Avenue, Cambridge 39, Mass.
John A. Gifford, 14 Wall Street, New York 5, N.Y.
Ross G. Harrison, Osborn Zoological Laboratory, Yale University, New Haven, Conn.
Hudson Hoagland, Worcester Foundation for Experimental Biology, 222 Maple Avenue, Shrewsbury, Mass.
Frank A. Howard, 30 Rockefeller Plaza, New York, N.Y.
Columbus O'D. Iselin, Woods Hole Oceanographic Institution, Woods Hole, Mass.
August B. Kinzel, Union Carbide and Carbon Corporation, 30 East 42nd Street, New York 17, N. Y.
Milford R. Lawrence, Siders Pond Road, Falmouth, Mass.
Lamar R. Leahy, 910 Park Avenue, New York, N.Y.
Alfred L. Loomis, Room 2420, 14 Wall Street, New York, N.Y.
Arnaud C. Marts, 521 Fifth Avenue, New York, N.Y.
Robert E. McConnell, 230 Park Avenue, New York, N. Y.
Noel B. McLean, Edo Corporation, College Point 56, N.Y.
Daniel Merriman, Bingham Oceanographic Laboratory, Yale University, New Haven, Conn.
Henry S. Morgan, 2 Wall Street, New York, N.Y.
Frank A. Pace, General Dynamics Corporation, 445 Park Avenue, New York 22, N.Y.
Albert E. Parr, American Museum of Natural History, Central Park West at 79th Street, New York, N.Y.
Alfred C. Redfield, Woods Hole Oceanographic Institution, Woods Hole, Mass.
Lawrason Riggs, Riggs, Ferris and Geer, Room 1201, 74 Trinity Place, New York 6, N.Y.
George H. Richards, 68 William Street, New York, N.Y.
Francis C. Ryder, Massachusetts Institute of Technology, Cambridge 39, Mass.
Mary Sears, Woods Hole Oceanographic Institution, Woods Hole, Mass.

Athelstan F. Spilhaus, Institute of Technology, University of Minnesota, Minneapolis 14, Minn.
Lyman Spitzer, Jr., Princeton University Observatory, 14 Prospect Avenue, Princeton, N.J.
Harlow Shapley, Harvard College Observatory, Cambridge, Mass.
Henry L. Shattuck, 10 Milk Street, Boston, Mass.
Edward H. Smith, Woods Hole Oceanographic Institution, Woods Hole, Mass.
Raymond Stevens, c/o Arthur D. Little, Inc., 30 Memorial Drive, Cambridge, Mass.
Julius A. Stratton, Office of the Vice President and Provost, Massachusetts Institute of Technology, Cambridge 39, Mass.
Gerard Swope, Jr., c/o International General Electric Co., 570 Lexington Avenue, New York, N.Y.
J. H. Van Vleck, Lyman 332, Harvard University, Cambridge 38, Mass.
Selman A. Waksman, Institute of Microbiology, New Brunswick, N.J.
Thomas J. Watson, Jr., International Business Machines Corporation, 590 Madison Avenue, New York 22, N. Y.
Francis C. Welch, 73 Tremont Street, Boston, Mass.
E. Bright Wilson, Jr., Department of Chemistry, Harvard University, Cambridge 38, Mass.

III. RESEARCH STAFF

(As of December 31, 1955)

Director

Edward H. Smith

Senior Scientists

Columbus O'D. Iselin, Associate Professor of Physical Oceanography, Harvard University and Research Oceanographer, Museum of Comparative Zoology; Senior Oceanographer.

Bostwick H. Ketchum, Senior Oceanographer.

Alfred C. Redfield, Professor of Physiology, Harvard University; Senior Oceanographer.

Scientists

Vaughan T. Bowen, Geochemist.

Dean F. Bumpus, Oceanographer.

Andrew F. Bunker, Meteorologist.

George L. Clarke, Associate Professor of Zoology, Harvard University; Marine Biologist.

Willard Dow, Electronics Engineer.

Frederick C. Fuglister, Physical Oceanographer.

John B. Hersey, Physical Oceanographer.

Joanne S. Malkus, Meteorologist.

Willem V. R. Malkus, Physical Oceanographer.

Charles B. Officer, Jr., Geophysicist.

Francis A. Richards, Chemical Oceanographer.

William S. Richardson, Physical Chemist.

Carl-G. Rossby, Director, Institute of Meteorology, University of Stockholm; Meteorologist.

Harold E. Sawyer, Research Engineer.

William C. Schroeder, Associate Curator of Fishes, Museum of Comparative Zoology, Harvard University; Ichthyologist.

Mary Sears, Planktonologist.

Henry M. Stommel, Physical Oceanographer.

Harry J. Turner, Jr., Marine Biologist.

Allyn C. Vine, Physical Oceanographer.

William S. von Arx, Physicial Oceanographer.

Alfred H. Woodcock, Oceanographer.

Research Associates

William D. Athearn, Research Associate in Geology.

Richard H. Backus, Research Associate in Marine Biology.

Duncan C. Blanchard, Research Associate in Meteorology.

Robert H. Brockhurst, Research Associate in Physics.

John G. Bruce, Jr., Research Associate in Physics.

Elizabeth T. Bunce, Research Associate in Physics.

Joseph Chase, Research Associate in Meteorology.

JOSEPH H. CONNELL, Research Associate in Marine Biology.
ALAN J. FALLER, Research Associate in Meteorology.
HARLOW G. FARMER, JR., Research Associate in Hydraulics.
DAVID H. FRANTZ, JR., Research Associate in Engineering.
HENRY R. JOHNSON, Research Associate in Underwater Acoustics.
JOHN W. KANWISHER, Research Associate in Biophysics.
SYDNEY T. KNOTT, JR., Research Associate in Engineering.
ROBERT A. LUFBURROW, Research Associate in Physics.
WILBUR MARKS, Research Associate in Physical Oceanography.
FRANK J. MATHER III, Research Associate in Oceanography.
WILLIAM G. METCALF, Research Associate in Physical Oceanography.
ARTHUR R. MILLER, Research Associate in Physical Oceanography.
DAVID M. OWEN, Research Associate in Underwater Photography.
F. CLAUDE RONNE, Research Associate in Photography.
JOHN H. RYTHER, Research Associate in Marine Biology.
HOWARD L. SANDERS, Research Associate in Marine Biology.
KARL E. SCHLEICHER, Research Associate in Physics.
HERBERT SMALL, Research Associate in Electronics.
ALLARD T. SPENCER, Research Associate in Engineering.
RALPH F. VACCARO, Research Associate in Microbiology.
ROBERT G. WALDEN, Research Associate in Electronics.
GEOFFREY G. WHITNEY, JR., Research Associate in Physical Oceanography.
L. VALENTINE WORTHINGTON, Research Associate in Physical Oceanography.
RALPH F. WYRICK, Research Associate in Underwater Acoustics.
JOHN W. ZEIGLER, Research Associate in Marine Geology.

Associate Scientists

ARNOLD B. ARONS, Professor of Physics, Amherst College; Associate in Physical Oceanography.

JOHN C. AYERS, Assistant Professor of Oceanography, Department of Conservation, Cornell University; Associate in Marine Biology.

DAVID L. BELDING, Professor of Bacteriology and Experimental Pathology (Emeritus), Boston University; Consultant, U. S. Fish and Wildlife Service; Associate in Marine Biology.

HENRY B. BIGELOW, Professor of Zoology (Emeritus), Harvard University and Research Oceanographer, Museum of Comparative Zoology; Associate in Oceanography.

CORNELIA L. CAREY, Associate Professor in Botany (retired), Barnard College; Associate in Marine Bacteriology.

L. A. EARLSTON DOE, Associate in PHYSICAL OCEANOGRAPHY.

WILLIAM MAURICE EWING, Professor of Geology, Columbia University; Director, Lamont Geological Observatory; Associate in Geophysics.

CHARLES J. FISH, Professor of Marine Biology, University of Rhode Island and Director, Narragansett Marine Laboratory; Associate in Marine Biology.

BERNHARD HAURWITZ, Professor of Meteorology and Chairman of the Department of Meteorology and Oceanography, New York University; Associate in Meteorology.

LOUIS W. HUTCHINS, Associate in Marine Biology.

BENJAMIN B. LEAVITT, Assistant Professor of Biological Sciences, University of Florida; Associate in Marine Biology.

RAYMOND B. MONTGOMERY, Associate Professor of Oceanography, Chesapeake Bay Institute, Johns Hopkins University; Associate in Physical Oceanography.

HILARY B. MOORE, Associate Professor in Marine Biology and Assistant Director, Marine Laboratory, University of Miami; Associate in Marine Biology.

James M. Moulton, Assistant Professor of Biology, Bowdoin College; Associate in Marine Biology.

Jerome Namias, Chief, Extended Forecast Section, U. S. Weather Bureau, Associate in Meteorology.

Daniel R. Norton, Chemist, Sprague Electric Company, North Adams, Mass.; Associate in Chemical Oceanography.

Mary Alys Plunkett, Associate Professor of Chemistry, Vassar College; Associate in Chemistry.

Roy L. Rather, Jr., Associate in Underwater Acoustics.

Gordon A. Riley, Associate Professor of Marine Biology, Yale University; Associate in Marine Physiology.

Helen M. Roberts, Assistant Professor of Mathematics, University of Connecticut; Associate in Mathematics.

Marshall Schalk, Assistant Professor of Geology and Geography, Smith College; Associate in Geology.

Irving I. Schell, Department of Physics, Tufts College; Associate in Meteorology.

William E. Schevill, Research Associate in Zoology, Museum of Comparative Zoology; Associate in Oceanography.

Per F. Scholander, Professor of Zoophysiology, University of Oslo; Associate in Physiology.

George T. Scott, Professor of Zoology, Oberlin College; Associate in Physiology.

Paul F. Smith, Electronics Engineer, Rockefeller Institute for Medical Research; Associate in Physical Oceanography.

Floyd M. Soule, Principal Senior Oceanographer, U. S. Coast Guard; Associate in Physical Oceanography.

Athelstan F. Spilhaus, Dean, Institute of Technology, University of Minnesota; Associate in Physical Oceanography.

Thomas T. Sugihara, Assistant Professor of Chemistry, Clark University; Associate in Geochemistry.

Parker D. Trask, Research Engineer, University of California; Associate in Submarine Geology.

Edmond E. Watson, Professor of Physics, Queen's University, Kingston, Ontario; Associate in Physical Oceanography.

Raymond Wexler, Research Meteorologist, Harvard University and Massachusetts Institute of Technology; Associate in Meteorology.

George P. Woollard, Professor of Engineering Geology and Geophysics, University of Wisconsin; Associate in Geophysics.

ADMINISTRATIVE STAFF

Edward H. Smith, Director
Alfred C. Redfield, Associate Director.
Ronald A. Veeder, Assistant to the Director.
Jan Hahn, Public Information.
John McGilvray, Business Manager.
Norman T. Allen, Administrator.
Harvey MacKillop, Controller.
John F. Pike, Port Captain.
Delmar R. Jenkins, Purchasing Agent.
Otis E. Hunt, Laboratory Services.

IV. DIRECTOR'S REPORT

Introduction

When one chronicles the important events of a year's work at an Institution such as ours, one often asks the question, how do the achievements of one year compare with the number and value of those of other years? Are we maintaining the rate of progress, and what, if anything, distinguishes the year 1955 from 1954, or from that of earlier years? What will 1956 yield in new discoveries as our ships bring home their collections of data and the laboratory conducts further experiments, practical and theoretical.

One barometer of the activity of an oceanographic institution is the number of days at sea of its research ships and the days in which its aircraft have been airborne. In this respect 1955 compares well with the others. Atlantis spent 234 days at sea, Bear 147, Caryn 75, and the Institution's one research airplane was in flight some portion of each one of 114 days.

Another index of activity is the number of scientific papers which have been published during the course of the year. The total in 1955 of 72 exceeds by over 20 per cent that of 1954, and is nearly double the number of 1953 or 1952.

Oceanography, dealing as it does with varied processes on a vast scale in nature, provides the scientist with an endless fund of interesting problems to solve. The subjects for investigation seem infinite, as the building blocks of today form the larger structures of tomorrow. This report records briefly the effort of one institution, in one year of research, as it strives to add more and more information to Man's store of knowledge of the sea.

Among the scientific tasks of 1955 which have engaged our attention are:

(*a*) The Atlantis Marine Geological Expedition to Peru, 1955
(*b*) Continued acoustical investigations of the ocean
(*c*) Inauguration of long-range statistical studies of East Coast shelf waters
(*d*) Continued field investigations of the western North Atlantic deep-water
(*e*) Investigation of sea level changes accompanying severe gales and hurricanes
(*f*) Continued theoretical studies of oceanic circulation.

A specific event, which over the years is bound to be reflected in future sea operations of the Institution, was the acquisition of, and title to, the ex-Coast Guard Cutter Crawford. A further report is contained in the section devoted to vessels. Leading to this transaction, and also of equal if not greater significance, was the recognition of the Institution by the Office of Education of the U. S. Department of Health, Education, and Welfare, as an accredited institution of higher education.

The financial status of the Institution continued to show satisfactory improvement as is evidenced by the Treasurer's report. The level of both income and expense witnessed an increase during the year, as the costs of salary increases and the new retirement plan, to mention two major items, became offset partially by new contracts with Government agencies both military and civilian. It was pleasing to note, furthermore, the additional support during the year from private sources, the most substantial of which came from the Associates of the Woods Hole Oceanographic Institution. More extended remarks on the subject of the Associates is contained in the section devoted to acknowledgments.

Research

So far as the circulation problem is concerned, during the past year advances have been made on several fronts, and we have begun to consider seriously the challenges and opportunities that will soon be presented to us by the International Geophysical Year. Although the oceanographic field work probably will not officially begin until November 1957, it may well be advisable to initiate some earlier exploratory work.

As now planned, the emphasis during I. G. V. is to be on learning more exactly the rates of circulation in the deeper waters of the South Atlantic. As a first step we have been re-examining the pertinent existing North Atlantic data and the ATLANTIS has been in the process of securing more very deep sections and reoccupying old ones.

Mr. Stommel and Mr. Fuglister have recently been studying intensively the very complete north-south section from Nova Scotia to Venezuela occupied last year by Mr. Worthington. The problem is to locate the most probable depth of no motion. They have tried various mathematical tricks and are gaining considerable insight as to why these do not produce the desired result. This is the fundamental problem that must be cracked before we can go to the South Atlantic with any assurance that we can interpret the new observations more convincingly than the Germans were able to do roughly thirty years ago.

The geostrophic equation alone, no matter how complete the temperature and salinity data, does not enable one to calculate the deep transport with any certainty of arriving at a reliable result. Although the deep velocities are probably low, such huge quantities of water are involved that enormous transports can be found or the direction of motion can change, depending on the starting point of the calculations. We evidently need additional information and the question is: just where in the system should this be obtained and what are the most practical sorts of new observations that might be secured?

From Mr. Worthington's standpoint the new deep sections are very satisfactory indeed, for they continue to show a steady and uniform loss of dissolved oxygen from the deep water over wide areas of the North Atlantic and Caribbean. The fact that his results indicate that the deep water is so much younger than claimed by those using the Carbon-14 techniques does not particularly worry him, for he has thousands of observations and as yet the Carbon-14 people have only a few of which they feel reasonably certain. In the end, of course, this discrepancy must be cleared up and preferably before the start of the International Geophysical Year. The carbon measurements indicate that the water increases in age with depth, the oxygen values show a rather uniform and much younger water mass everywhere below 2500 meters, and the text books say that the oldest water should be located well above the bottom. There have been many lively discussions on these matters during recent months. Mr. David Frantz has been busy developing new instruments which we hope can help to settle the problem one way or another.

Mr. Stommel spent most of the winter at The Institute for Advanced Study at Princeton working on various new mathematical models of ocean circulation and especially he was successful in interesting Dr. Charney, Dr. Veronis and others there to do likewise. Mr. Stommel and Dr. Veronis developed a theory of the response of the ocean to transient wind systems and have submitted it to the *Journal of Marine Research.* It is hoped that this theory will shed light on the dynamics of the ocean circulation in a way that will be helpful, and perhaps critical, in formulating plans for sea-level observations during the International Geophysical Year. Dr. Walter Munk of the Scripps Institution of Oceanography and Mr. Stommel have been corresponding about these matters.

Mr. Stommel's visit to the Institute also played a part in stimulating Dr. Jule G. Charney's new inertial boundary-layer theory of the Gulf Stream, a marked departure from the viscous boundary-layer theory of Munk, and it seems that this new theory has more physical plausibility than the old one. In addition, through collaboration with Mr. Stommel, Dr. George Morgan of Brown University re-examined the basic theoretical structure of our understanding of the wind-driven circulation, in particular the role of internal friction, stratification, and inertial terms. Dr. Morgan has also contributed some alternative formulations of the inertial boundary-layer Gulf Stream theory.

During the period January 1–April 1, Mr. Hodgson was in Bermuda tending the thermometric cable. We now have 13 months of half-hourly temperature readings near the top of the main thermocline. It seems evident from these data that during the winter stormy period there are large internal waves traveling away from the storm centers at about 200 km/day. From a practical point of view these internal waves may be of importance in detecting the presence of hurricanes in the area between the Cape Verde Islands and the Windward Islands. Present plans are to maintain operation of the Bermuda cable in order to get more precise information concerning the disturbances set up in the main thermocline by isolated storms.

As part of his doctorate thesis at Massachusetts Institute of Technology Dr. von Arx successfully modeled the wind-driven circulation of the southern hemisphere oceans, using the seven-foot diameter flat basin. With the help of Mr. Faller and others he has also cleaned up a good deal of the theory of rotating hydraulic models. Due to limitations of funds he was forced to reconsider the design of the driving mechanism for the 24-foot rotating basin and this turned out to be fortunate, for he conceived a most clever and effective way of gaining absolutely steady rotation with no need for heavy bearings or a complex control of the driving motor's speed. The new system, which is basically a fluid clutch, is so much cheaper to construct that we were able to go ahead immediately and the large basin will soon be in operation. Incidentally, this most ingenious device seems to have important applications in astronomy, for it is capable of forming parabolic reflectors of almost any size.

The planning of a new, long-range program in coastal circulation is well advanced. The central core of continuing observations will be financed by funds supplied by the Fish and Wildlife Service through the Saltonstall-Kennedy Bill, but it is also expected that other parts of our over-all program can be modified so as to contribute additional support. Mr. Bumpus is organizing the new observational program. Assisted by Mr. Day he has also been working on the coastal currents south of Cape Hatteras.

Basically the problem is to find out under what circumstances coastal circulation is sufficiently changed so as to modify the environmental factors to a degree that is significant in the commercial fisheries. In coastal circulation the main energy source comes from the inflow of river water. How much does this have to vary before the current system is markedly disturbed? How much do the winds and the climate have to change to do likewise? A new paper by Dr. Ketchum on the cross-continental shelf mixing coefficients, provides a fine starting point to this problem, as well as do the new 400-day temperature recorders and current meters developed by Mr. Frantz. We are most hopeful of making a significant contribution to fisheries biology during the next few years.

Wave research continues to be active. Mr. Marks is reaching the end of the analysis of the RTSK observations secured more than a year ago. So far he has mainly been studying pitch and roll separately but recently he has begun to take up coupled motions. He has also spent considerable time working on the excellent wave pictures secured on Project SWOP when two airplanes obtained some stereo-pairs of a large area of the sea surface with waves 12 to 14 feet high. Mr. Farmer has been working on means of measuring the high-frequency end of the wave spectrum in preparation for a joint operation with representatives of the Naval Research Laboratory which was carried out off Bermuda in October. We have installed the British ship-borne wave recorder in the ATLANTIS, and this for the first time will give us reliable data on the opposite end of the wave spectrum.

Dr. Richardson has completed the development of a new tool for the study of near-surface physical phenomena. He has equipped a powered dory so that it can be operated as a drone, either from a plane or from a ship. He has given it sensitive, near-surface thermal probes. The dory both records and telemeters the incoming information. In this way we hope to explore convection cells, slicks, convergences, and other small-scale surface phenomena without the disturbing influence of a large hull.

The visit of Dr. Gifford Ewing last summer from Scripps has stimulated interest in the near-surface mechanisms whereby the sea takes up energy from the winds. We suspect that at least half a dozen effects are involved, some well established and some only dimly seen. Dr. Ewing has for some years been observing the surface of the Pacific from a plane and has studied especially the manner in which internal waves produce slicks. We hope that through his visit a more effective observational program of near-surface phenomena can be evolved.

Dr. Malkus and his wife remained in Europe until December. Their time was most profitably spent. During the autumn Mr. Ronne joined Dr. Joanne Malkus at the meteorological laboratory of the Imperial College in order to lend his special skills in photography to some laboratory studies of convective motions.

Mr. Woodcock and Mr. Blanchard have been busy with the extensive cloud data secured last winter at Hawaii. It will be remembered that this was a large-scale, cooperative assault on the physics of warm clouds. It will be some time before all the results are fully digested.

Mr. Bunker has continued to interest himself in the diffusion of heat and momentum into the lower atmosphere and its effects upon large-scale phenomena. The years spent in developing the PBY aircraft as a calibrated meteorological tool are now paying off in observations of heat flow and stress obtained over the open ocean. In the early part of the year numerous flights were made over the Atlantic Ocean between the mainland and the island of Bermuda. While many of these observations are still being reduced, the few already studied are giving valuable information concerning the method of transport of heat by convective parcels in the region below the cloud level. These observations are serving as a check on the existing theories of heat flow and indicate new approaches to the study.

Mr. Ballenzweig, who joined the project for the year that Dr. Malkus was on leave of absence at Imperial College, has been working on the larger scale aspects of the heat flow problem over the ocean. His first study was of the modification of the air ahead of and behind cold fronts as they moved out from the continent over the waters of the Atlantic. One fact brought out by this study is that the local heating of the air by the warm waters in the vicinity of the Gulf Stream are of minor importance in producing Type A cyclogenesis which reaches its maximum in this area.

Under the terms of one of the contracts between the Woods Hole Oceanographic Institution and the Office of Naval Research, a continuing program of cooperation has been established between the Woods Hole Oceanographic Institution and the Institute of Meteorology of the University of Stockholm. This program is directed by Professor Carl-G. Rossby who divides his time between the two institutions.

The work of the Stockholm group is concentrated on problems of numerical weather prediction by means of high-speed computers. This should ultimately lead to a technique for the prediction of wind stresses at the sea surface. In addition, work is now in progress on the development of a method for the prediction of storm tides along the North Sea coast (in cooperation with the Deutsches Hydrographisches Institut) and on the general theory of the dynamics of currents (air or ocean). One group of investigators at the Stockholm institute are now making detailed studies of the composition of atmospheric precipitation. These studies have raised important questions concerning the nature of the physical-chemical processes taking place in the surface layers of the ocean and may thus necessitate even closer research cooperations between the two institutions.

A new contract, with Dr. Arnold Arons as principal investigator, has recently been concluded with the Division of Biology and Medicine of the Atomic Energy Commission. Motivated by questions regarding physical processes and water motions taking place in the ocean depths (questions which have long been formulated but which are rapidly becoming more urgent and pressing because of speculation regarding deep ocean disposal of high-level radioactive wastes), this project will undertake fundamental research along lines which have not hitherto been pursued at the Institution.

The first stage of the work is now getting under way with Professor Bruce

Benson of Amherst College preparing to perform a systematic mass spectroscopic study of dissolved gases in ocean water. The Nier-type mass spectrometer, constructed in the Amherst College physics department, has been made available for this program. With the perfection of the technique and the eventual hiring of a full-time technician to run analyses, it is hoped to make the instrument available to other groups at the Institution as well. By a systematic study of isotope contents and fractionations in samples from different geographical locations and various depths, it is hoped to learn more about the time and space histories of various water masses.

Preliminary studies are also being made of certain instrumental problems such as the development of a scintillation counter for use in making *in situ* studies of radioactive background and for eventual general use in underwater tracer experiments, etc.

Dr. Officer and his associates are hard at work on the analysis of the refraction profiles secured last winter in the West Indian region. Such steady progress has been made in submarine geophysical techniques during recent years that there is little doubt that many new and exciting discoveries will come out of the study of last winter's extensive data, but it is too early to try to predict what these may be. Dr. Officer has accepted a promising position at the Rice Institute. Fortunately he will have considerable time for research during the winter and plans to return here next summer.

Dr. Hersey has had a very busy winter and spring. Not only has he had the responsibility of keeping our own acoustical research program on an even keel, but also as Chairman of the Navy's committee on deep ocean sound propagation he has had considerable influence on the national program in underwater acoustical research.

Mr. Zeigler has completed a paper on the recently discovered chain of sea mounts extending southeastward from Georges Bank. We hope very much that we can obtain permission for this to be declassified. He and Mr. Athearn have also been working up the Georges Banks' long cores obtained last summer. These are throwing much light on the recent geological history of this area. Additional material will be gained next summer as more permanent radar platforms are erected.

Mr. Zeigler will continue Mr. Stetson's study of the changes in the outer beaches of Cape Cod. Supplementary measurements on Martha's Vineyard have recently been undertaken. A parallel investigation on Arctic beaches is now in its second summer at Point Barrow, Alaska, under the direction of Dr. Marshall Schalk.

Each year the Institution endeavors to carry out at least one major sea expedition aimed at one of the five recognized fields of oceanographic activity. In 1955 this refers to "The Atlantis Marine Geological Expedition to Peru and Chile, 1955" which explored the deep trenches that parallel the west coast of South America between Talara, Ecuador, in 5° south latitude, to 80 miles south of Antofagasta, Chile, in 25° south. Mr. Henry C. Stetson was the Chief Scientist on board the ATLANTIS until his unfortunate death at sea on December 3rd when the remainder of the cruise was carried out under the direction of Dr. Parker D. Trask. The primary object of the expedition was the collection of sediment cores, a total of 100 being secured along twelve profiles running normal to the coast distances as much as 90 miles offshore. The area, which had had little previous marine geological attention prior to our survey, is probably one of the most interesting regions in the world of recent and existing tectonic activity. Continuous soundings throughout the ATLANTIS' track with the precision echo-sounder recorder developed at the Institution by Mr. Sydney T. Knott, Jr., and others, testifies to the extremely rugged submarine topography. For example a trench 500 miles in length, three miles in width, and 25,000 feet deep, the walls of which rose 1,500 feet in one-fourth of a mile, was recorded on the fathometer trace. Balancing this deep escarpment towers the Andes to 20,000 feet above the sea less than 125 miles distance. The study of the data and the preparation of the scientific results for publication will require at least two years.

This is by no means a complete account of our physical and geological program, and it tends to give too optimistic a picture. We continue to uncover many more problems than we solve. The operation of our vessels drains off too much of the free funds. The income available for the development of instruments is entirely inadequate in view of the magnitude of the problems we are trying to solve and the limitations of the classical tools of physical oceanography. There is general awareness of these problems in the Office of Naval Research, but the factors resulting in "project research" are the stronger. We must resist this trend in every way that we can so that our staff can exercise imagination and enterprise, and not be too much influenced by budgetary considerations.

The cruise of the ATLANTIS to the Caribbean during the winter provided an opportunity for Dr. F. A. Richards and Mr. R. F. Vaccaro to examine the chemical conditions in the Cariaco Trench. This is a depression in the continental shelf of northern Venezuela, more than 1300 meters in depth, separated from the Caribbean by a sill with depths of about 120 meters. Unlike other similar depressions in the ocean floor the Cariaco Trench proves to be entirely stagnant, and the condition of the water approaches that found in the Black Sea and other smaller enclosed inland seas and bays. Dr. Richards obtained valuable information on the quantities of organic matter which have decomposed in this basin, quantities which proved to be about 50 per cent more than found in the deep Atlantic, though much less than found in the Black Sea. A comparison of the productivity of the surface water of the Cariaco Trench determined by Dr. Ryther on this cruise with the accumulation of organic derivations at depth indicates that the water has remained *in situ* for at least 100 years. The Cariaco Trench should prove to be a valuable laboratory in which to study the processes of decomposition which take place in the deep sea. The constancy of the bottom temperature would make this a good place to measure the rate of heat transfer through continental rock, using the methods which have been employed for such measurements in the deep ocean.

With Grace (Creitz) Fraser, Dr. Richards has continued investigations of chlorophyll and other plankton pigments, relating their occurrence to nutrient supply and age in cultures and to phyllogenetic groups and environmental conditions in natural populations. A paper describing improvements in the method for determining plankton pigments is now in press.

A study of oxygen-density relationships in the Caribbean and Gulf of Mexico has been undertaken by Miss Betty Ann Morse and Dr. Richards. The method appears to differentiate between Caribbean and Gulf of Mexico water emerging from the Straits of Florida.

On this same cruise Dr. Ryther found that the addition of the nutrients nitrogen and phosphorus to the nutrient poor surface waters increased the productivity of the water. The carbon 14 method of determining productivity gave lower values than the oxygen method for the nutrient poor water, but the enriched samples gave better agreement. This suggests that the nutrient deficiency explanation of the discrepancy between the two methods is applicable to oceanic conditions. Observations on the relationship between the rate of photosynthesis and light intensity have made it possible to calculate the relative rate of photosynthesis at various depths in the ocean. Measurement at sea of the transparency of the water and of photosynthesis at one light intensity can be translated to the total production of the entire water column.

Dr. Bowen has continued his studies of the neutron activation analysis of the rare earth content of sea water. Analysis of surface water samples has given significant counting rates on extracts but indicates that larger samples will have to be prepared in order to permit radiochemical identification of the fission products. A study of the production of organic phosphorus compounds by plankton algae in culture has been initiated. It is hoped that identification of these phosphorus compounds will be of value in interpreting the ecological cycle of phosphorus in the sea.

Many years ago the Institution pioneered in the study of the penetration of light into the ocean through Dr. George L. Clarke's efforts. Recently this matter has received new interest as the result of the precise information being obtained by acoustical methods on the vertical migration of plankton in response to the daily variation in sunlight. Dr. Clarke has recently developed a new photometer employing a photomultiplier cell which is sensitive to light one thousand billionth as intense as sunlight. The instrument was tested from the Marine Laboratory of the University of Miami during the early winter. It measured sunlight to the greatest depths obtained, 1900 feet, and detected moonlight down to 1700 feet. Not only were the flashes of light produced by luminescent animals recorded for the first time but at extreme depths at night a general background of weak illumination was observed which is believed to be due to the combined effects of myriads of luminescent organisms.

During June Dr. N. G. Jerlov of the University of Göteborg, Sweden, an expert on submarine illumination, visited the Institution for two weeks. On the occasion of his visit a very profitable series of conferences were held at which the physical and biological problems relating to light penetration into the sea were discussed. Dr. James Snodgrass of the Scripps Institution of Oceanography and Dr. Hilary B. Moore of the University of Miami participated with Dr. Jerlov and members of the staff in these discussions.

The Institution's study of the hydrography of Lake Maracaibo being made for the Creole Petroleum Corporation has been completed. A final item in the investigation was an examination of the chemical composition of the bottom sediments of the Lake. The results throw additional light on the importance of the oxygen content of the water, and on the rate of sedimentation in the entrapment of organic matter in sedimentary deposits, and thus on the initial processes leading to the formation of petroleum. Mr. L. A. Earlston Doe, an associate on our staff, has been appointed Oceanographer by the Creole Petroleum Corporation and will continue the studies we have been making of Lake Maracaibo.

The hurricanes which visited Woods Hole last year called attention forcefully to oceanographic phenomena which have received little systematic attention; namely, the effects of such storms on sea levels. Dr. A. C. Redfield had collected some data on the storms of 1938 and 1944, and immediately after the current storms he and Mr. A. R. Miller gather such information as they could on the water levels developed by them. Because of the dense population of the shores affected, more detailed information now exists on the inundations caused by the New England storms than are available for any other parts of the world. A report summarizing their findings has been prepared at the request of the U. S. Weather Bureau and has been circulated for the use of weather forecasters during the present season. Mr.

Miller is continuing studies of the effects of wind on water levels under a contract with the Weather Bureau while Dr. Redfield has served as a consultant to both the Weather Bureau and the Beach Erosion Board in connection with their hurricane problems.

Dr. B. H. Ketchum has prepared a valuable paper on the circulation of the water on the continental shelf between Cape Cod and Cape Hatteras. By employing methods developed for studying the circulation of estuaries, in which the river water is used as a tracer, he has found that although the net movement of water along the coast is southward as a definite coastal current, a large part of the fresh water introduced by the rivers escapes directly to the outer sea by lateral mixing processes. This fresh water is replaced by saltier oceanic water to such an extent that the water of the coastal current actually becomes more saline as it progresses in spite of the continued addition of river water. With Dr. Richards he has continued the study of the distribution of plant nutrients in the equatorial Atlantic. They have developed a method to differentiate between the accumulations of local origin and those transported into the region. Collections of total phosphorus samples have been made on several recent cruises and have been analyzed by Mr. Nathaniel Corwin. The description of the distribution is now fairly complete for the western North Atlantic Ocean.

Mr. William C. Schroeder has written a report of the results of the exploration of the continental slope for fishes, which has engaged his attention during recent years. It will be recalled that these expeditions which have extended from Nova Scotia to the offing of Cape Charles have not only brought to light information on the distribution of many species of scientific interest, but have also led to the discovery of potential fishery resources for the redfish, red crab, and lobster.

Mr. Frank J. Mather III participated in a cruise of the Fish and Wildlife Service in the Gulf of Mexico and western Caribbean Sea to determine the effectiveness of long-line fishing in those waters. It was discovered that the Atlantic big-eye tuna, formerly known only from east of the Azores, occurred in the Caribbean Sea and that the true albacore, the most valuable of all the tunas, was present in fair abundance. Mr. Mather has been granted a leave of absence to enable him to make fishery studies for the government of the Virgin Islands. During his absence the program of studies on the migration of tuna will continue under the guidance of Mr. William C. Schroeder.

Dr. Richard H. Backus, with Mr. Stewart Springer of the Fish and Wildlife Service, has prepared a paper on the natural history of the white-tipped shark. This fish is ubiquitous in the warm waters of the ocean beyond the 100-fathom contour and is perhaps one of the most abundant species of shark in the sea. With Mr. Malcolm S. Gordon he has published a valuable report on the fishes of Labrador.

Dr. Scholander and Dr. William E. Schevill have written a very interesting account of the vascular arrangements which prevent excessive heat loss from the fins of whales when in cold water.

Dr. Scholander and Dr. John W. Kanwisher visited Hebron, Labrador, in March in order to supplement the studies made the preceding summer on the resistance of fish and other marine organisms to freezing. Dr. Kanwisher took part in an extensive cruise of the R. V. HORIZON of the Scripps Institution of Oceanography to the tropical Pacific during the fall in order to make physiological studies of oceanic animals.

It is to be regreted greatly that Dr. Scholander has given up his position at the Institution to become Professor of Zoophysiology at the newly-founded Zoophysiology Institute, University of Oslo. Dr. Levie Van Dam has resigned his position as Research Associate in Physiology to become associated with the Academy of Natural Sciences in Philadelphia and to serve as Chief Biologist at the Philadelphia Aquarium.

Mr. H. J. Turner's report to the Commonwealth of Massachusetts on work done on shellfisheries this year contains a final account of his studies on the rock crab fishery of Boston Harbor. Of particular interest are the results of experiments in which large numbers of marked crabs were recovered after release, which show that this crab, unlike some others, does not indulge in extensive migrations. The study as a whole provides the Commonwealth with valuable information for use in regulating this fishery.

On June 22–23 a conference was held in the Laboratory of Oceanography on the Disposal of Radioactive Wastes at Sea. This conference, arranged by Professor C. E. Renn of Johns Hopkins University as a follow-up on a similar meeting last summer, brought together representatives of this and other oceanographic institutions, of the Atomic Energy Commission, and of other agencies concerned with evaluating the problem of sea disposal of the wastes expected to result from the industrial development of atomic power.

A collection of scientific papers, prepared under the editorship of Dr. Mary Sears, was published in honor of Professor Henry B. Bigelow. The volume contains contributions from Dr. Bigelow's many scientific associates and students, not only at Harvard and at Woods Hole but throughout the scientific world. It has been published as a supplement to the current volume of *Deep-Sea Research.* Because of his close association with the Woods Hole Oceanographic Institution, from its founding to the present day, it is planned to distribute copies of this volume as Part II of *Collected Reprints* of the Institution for 1955.

Among the biologists who have worked at the Institution during the present year the following may be mentioned:

Dr. Benjamin B. Leavitt, Associate Professor at the University of Florida, who studied the zooplankton associated with the scattering layer; Dr. Milton A. Miller, Associate Professor at the University of California at Davis, who is examining the isopods collected from navigation buoys during the wartime fouling surveys; Dr. James B. Moulton, Assistant Professor at Bowdoin College, who investigated the acoustical responses of fish; Dr. Emil Witschi, Professor of Zoology at State University of Iowa, who is studying the auditory mechanisms of aquatic vertebrates; Dr. Mary A. Plunkett, Associate Professor of Chemistry at Vassar College, who is examining the chemical composition of marine sediments; Dr. Leon S. Ciereszko, Associate Professor of Chemistry at University of Oklahoma, who is interested in the organic substances present in marine animals; and Dr. Colm O'h Eocha of University College, Galway, who is interested in the pigments of the red algae.

Mr. Joseph H. Connell and Dr. Howard L. Sanders joined the staff as Research Fellows in Biology in September.

During the autumn Dr. John C. Ayers of Cornell University spent a sabbatical leave at the Institution. He has written a very valuable paper on the application of the methods of dynamic oceanography to the circulation of fresh-water lakes.

Publications

Seventy-two papers bearing contribution numbers have been published in 1955.

	Contr. No.
Scott, G. T. and H. R. Haywood, 1955. Sodium and potassium regulations in *Ulva lactuca* and *Valonia macrophysa*. In: Electrolytes in Biological Systems, 35–64, 21 text figs.	597
Gealy, Betty Lee, 1955. Topography of the continental slope in northwest Gulf of Mexico. *Bull. Geol. Soc., Amer.*, 66(2): 203–237, 7 text figs., 2 fold-ins.	650
Soule, F. M., A. J. Bush and J. E. Murray, 1955. Physical oceanography of the Grand Banks and the Labrador Sea in 1953. *U. S. Coast Guard Bull.*, 39: 45–138, 43 text figs.	675
Richards, F. A., and A. C. Redfield, 1955. Oxygen-density relationships in the western North Atlantic. *Deep-Sea Res.*, 2(3): 182–199, 14 text figs.	688
Malkus, J. S., and R. S. Scorer, 1955. The erosion of cumulus towers. *J. Meteorol.*, 12(1): 43–57, 10 text figs.	706
Scholander, P. F., W. E. Love and J. W. Kanwisher, 1955. The rise of sap in tall grape vines. *Plant Physiol.*, 30(2): 93–104.	709
Scholander, P. F., L. Van Dam and S. I. Scholander, 1955. Gas exchange in the roots of mangroves. *Amer. J. Bot.*, 42(1): 92–98, 13 text figs.	710

	Contr. No.
Ryther, J. H., 1955. Ecology of autotrophic marine dinoflagellates with reference to red water conditions. In: Luminescence of Biological Systems, F. H. Johnson, Edit., A.A.A.S., 387–414, 5 text figs.	712
Officer, C. B., 1955. Southwest Pacific crustal structure. *Trans. Amer. Geophys. Union*, 36(3): 449–459, 11 text figs.	724
Wilson, K. G., and A. B. Arons, 1955. Osmotic pressures of sea water solutions computed from experimental vapor pressure lowering. *J. Mar. Res.*, 14(2): 195–198	725
Malkus, J. S., 1955. On the formation and structure of downdrafts in cumulus clouds. *J. Meteorol.*, 12(4): 350–354, 3 text figs.	726
Malkus, J. S., 1955. The effect of a large island upon the trade-wind air stream. *Q.J.R. Meteorol. Soc.*, 81(350): 538–550	727
Dow, Willard, 1955. Underwater telemetering. *Deep-Sea Res.*, 2(2): 145–151, 9 text figs.	729
Officer, C. B., 1955. A deep-sea seismic profile. *Geophysics*, 20(4): 270–282	731
Bigelow, H. B., and W. C. Schroeder, 1955. Occurrence off the middle and north Atlantic United States of the offshore hake *Merluccius albidus* (Mitchill) 1818 and of the blue whiting *Gadus* (*Micromesistius*) *poutassou* (Risso) 1826. *Bull. Mus. Comp. Zool., Harvard Coll.*, 113(2): 205–226	732
Ryther, J. H., 1955. The ratio of photosynthesis to respiration in marine plankton algae and its effect upon the measurement of productivity. *Deep-Sea Res.*, 2(2): 134–139, 2 text figs.	733
Chase, Joseph, 1955. Winds and temperature in relation to the brood-strength of Georges Bank haddock. *J. du Cons.*, 21(1): 17–24	735
Creitz, Grace I., and F. A. Richards, 1955. The estimation and characterization of plankton populations by pigment analysis. III. A note on the use of "millipore" membrane filters in the estimation of plankton pigments. *J. Mar. Res.*, 14(3): 211–216	736
Fish, C. J., 1955. Preliminary observations on the biology of Boreo-Arctic and subtropical oceanic zooplankton populations. *Symp. Mar. & Fresh-Water Plankton, Indo-Pacific, Bangkok, Jan. 25–26, 1954- FAO-UNESCO:* 3–9	737
Metcalf, W. G., 1955. On the formation of bottom water in the Norwegian Basin. *Trans. Amer. Geophys. Union*, 36(4): 596–600, 2 text figs.	739
Bunker, A. F., 1955. Turbulence and shearing stresses measured over the North Atlantic Ocean by an airplane-acceleration technique. *J. Meteorol.*, 12(5): 445–455	740
Marks, Wilbur and F. C. Ronne, 1955. Aerial stereo-photography and ocean waves. *Photogrammetric Eng.* (Mar.): 107–110, 3 text figs.	741
Gordon, M. S., 1955. Summer ecology of oceanic birds off southern New England. *The Auk*, 72: 138–147, 1 text fig.	742
Officer, C. B., 1955. Geologic interpretation of a series of seismic reflection profiles from Bermuda to the continental margins. *Deep-Sea Res.*, 2(4): 253–260, 4 text figs.	743

	Contr. No.
Kanwisher, J. W., and Gordon Volkmann, 1955. A scattering layer observation. *Science*, 121(3134): 108–109, 1 text fig.	744
Farmer, H. G., W. Marks, R. G. Walden and G. G. Whitney, Jr., 1955. A technique for ocean wave measurements. *Proc. First Conf., Ships and Waves, Oct. 1954, Counc. Wave Res. and Soc., Naval Arch. and Mar. Eng.*, 11–12, figs.	746
Blanchard, D. C., 1955. Electrified droplets from the bursting of bubbles at the air-water interface. *Nature*, 175(4451): 334–336, 2 text figs.	747
Fuglister, F. C., 1955. Alternative analyses of current surveys. *Deep-Sea Res.*, 2(3): 213–229, 5 text figs.	749
Voss, G. L., 1955. The Cephalopoda obtained by the Harvard-Havana Expedition off the coast of Cuba in 1938–39. *Bull. Mar. Sci., Gulf and Caribbean*, 5(2): 81–115, 4 text figs.	750
Essapian, F. S., 1955. Speed-induced skin folds in the bottle-nosed porpoise, *Tursiops truncatus*. *Breviora*, No. 43: 4 pp., 9 pls.	751
Barlow, J. P., 1955. Physical and biological processes determining the distribution of zooplankton in a tidal estuary. *Biol. Bull.*, 109(2): 211–225.	753
Scholander, P. F., 1955. Evolution of climatic adaptation in homeotherms. *Evolution*, 9(1): 15–26, 5 text figs.	755
Moore, H. B., 1955. Variations in temperature and light response within a plankton population. *Biol.Bull.*, 108(2): 175–181, 4 text figs.	756
Woodcock, A. H., and W. A. Mordy, 1955. Salt nuclei, wind and daily rainfall in Hawaii. *Tellus*, 7(3): 291–300.	757
Soule, F. M., and J. E. Murray, 1955. Physical oceanography of the Grand Banks and Labrador Sea in 1954. *U. S. Coast Guard Bull.* 40: 79–168	758
Ketchum, B. H., N. Corwin and D. J. Keen, 1955. The significance of organic phosphorus determinations in ocean waters. *Deep-Sea Res.*, 2(3): 172–181, 3 text figs.	759
Bumpus, D. F., and E. L. Pierce, 1955. Hydrography and the distribution of chaetognaths over the continental shelf of North Carolina. *Pap. Mar. Biol. and Oceanogr., Deep Sea Res., Suppl.* to Vol 3: 92–109.	760
Woodcock, A. H., 1955. Bursting bubbles and air pollution. *Sewage and Industrial Wastes*, 27(10): 1189–1192.	761
Riley, G. A., 1955. Review of the oceanography of Long Island Sound. *Pap. Mar. Biol. and Oceanogr., Deep-Sea Res., Suppl.* to Vol 3: 224–238	762
Waterman, T. H., 1955. Polarization of scattered sunlight in deep water. *Pap. Mar. Biol. and Oceanogr., Deep-Sea Res., Suppl.* to Vol. 3: 426–434	763
Thorndike, E. M., 1955. Hydroscopes. *Trans. Amer. Geophys. Union*, 36(3): 470–472	767
Woodcock, A. H., and D. C. Blanchard, 1955. Tests of the sea-salt hypothesis of rain formation. *Tellus* 7(4): 437–448.	768
Rossby, C.-G., and H. Egnér, 1955. On the chemical climate and its variation with the atmospheric circulation pattern. *Tellus* 7(1): 118–133, 16 text figs.	770

	Contr. No.
Machlup, Stefan, and J. B. Hersey, 1955. Analysis of sound-scattering observations from non-uniform distributions of scatterers in the ocean. *Deep-Sea Res.*, 3(1): 1–22	771
Ketchum, B. H., 1955. Distribution of coliform bacteria and other pollutants in tidal estuaries. *Sewage and Industrial Wastes*, 27(11): 1288–1296	772
Scholander, S. I., 1955. Land birds over the western North Atlantic. *The Auk* 72: 225–239	773
Ketchum, B. H., and D. J. Keen 1955. The accumulation of river water over the continental shelf between Cape Cod and Chesapeake Bay. *Pap. Mar. Biol. and Oceanogr.*, *Deep-Sea Res.*, *Suppl.* to Vol. 3: 346–357	775
Redfield, A. C., 1955. The hydrography of the Gulf of Venezuela. *Pap. Mar. Biol. and Oceanogr.*, *Deep-Sea Res.* *Suppl.* to Vol. 3: 115–133	776
Turner, H. J., Jr., 1955. How clam drills capture razor clams. *The Nautilus* 69(1): 20–22	777
Kanwisher, J. W., 1955. Freezing in intertidal animals. *Biol. Bull.* 109(1): 56–63, 3 text figs.	778
Turner, R. D., 1955. Scaphopods of the *Atlantis* dredgings in the western Atlantic with a catalogue of the scaphopod types in the Museum of Comparative Zoology. *Pap. Mar. Biol. and Oceanogr.*, *Deep-Sea Res.*, *Suppl.* to Vol. 3: 309–320	779
Steemann Nielsen, E., 1955. The production of antibiotics by plankton algae and its effect upon bacterial activities in the sea. *Pap. Mar. Biol. and Oceanogr.*, *Deep-Sea Res.*, *Suppl.* to Vol 3: 281–286	780
Edmondson, W. T., 1955 Factors affecting productivity in fertilized salt water *Pap. Mar. Biol. and Oceanogr.*, *Deep-Sea Res.*, *Suppl.* to Vol. 3: 451–464	781
Stetson, H. C., 1955. Patterns of deposition at the continental margin. *Pap. Mar. Biol. and Oceanogr.*, *Deep-Sea Res.*, *Suppl.* to Vol. 3: 298–308	782
Turner, H. J., Jr. and Stanley Scher, 1954. Seventh report on investigations of the shellfisheries of Massachusetts. *Comm. Mass.*, *Dept. Nat. Res.*, *Div. Mar. Fish.*, 35 pp.	783
Barrett, E., and G. Brodin, 1955. The acidity of Scandinavian precipitation. *Tellus*, 7(2): 251–257, 6 text figs.	785
Goreau, T. F., and V. T. Bowen, 1955. Calcium uptake by a coral. *Science*, 122(3181): 1188–1189	786
Bigelow, H. B., W. C. Schroeder and Stewart Springer, 1955. Three new shark records from the Gulf of Mexico. *Breviora*, No. 49: 12 pp.	787
Bumpus, D. F., 1955. The circulation over the continental shelf south of Cape Hatteras. *Trans Amer. Geophys. Union*, 36(4): 601–611, 18 text figs.	788
Griffin, D. R., 1955. Hearing and acoustic orientation in marine animals. *Pap. Mar. Biol. and Oceanogr.*, *Deep-Sea Res.*, *Suppl.* to Vol. 3: 406–417	789
Schroeder, W. C., 1955. Report on the results of exploratory otter-trawling along the continental shelf and slope between Nova Scotia and Virginia during the summers of 1952 and 1953. *Pap. Mar. Biol. and Oceanogr.*, *Deep-Sea Res.*, *Suppl.* to Vol. 3: 358–372	790

	Contr. No.
Worthington, L. V., 1955. A new theory of Caribbean bottom-water formation. *Deep-Sea Res.*, 3(1): 82–87	791
Iselin, C. O'D., 1955. Coastal currents and fisheries. *Pap. Mar. Biol. and Oceanogr., Deep-Sea Res., Suppl.* to Vol 3: 474–478	792
Von Arx, W. S., D. F. Bumpus and W. S. Richardson, 1955. On the fine-structure of the Gulf Stream front. *Deep-Sea Res.*, 3(1): 46–65	794
Scholander, P. F., L. Van Dam, C. Lloyd Claff and J. W. Kanwisher, 1955. Micro gasometric determination of dissolved oxygen and nitrogen. *Biol. Bull.*, 109(2): 328–334	795
Stommel, Henry, 1955. Lateral eddy viscosity in the Gulf Stream system *Deep-Sea Res.*, 3(1): 88–90	796
Moulton, J. M., and R. H. Backus, 1955. Annotated references concerning the effects of man-made sounds on the movements of fishes. *Dept. Sea and Shore Fish., Maine, Fish. Circular*, No. 17: 7 pp.	802
Vine, A. C., 1955. Oceanographic instrumentation. *Science*, 122(3173): 748–751.	806
Scholander, P. F., and W. E. Schevill, 1955. Counter-current vascular heat exchange in the fins of whales. *J. Appl. Physiol.*, 8(3): 279–282, 4 text figs.	807
Steemann Nielsen, E., 1955. The interaction of photosynthesis and respiration and its importance for the determination of 14 C discrimination in photosynthesis. *Physiol. Plant.*, 8: 945–953	808
Edgerton, H. E., and L. D. Hoadley, 1955. Cameras and lights for underwater use. *J. Soc. Motion Picture and Television Eng.*, 64: 345–350	817
Scholander, P. F., 1955. Hydrostatic pressure in coconuts. *Plant Physiol.*, 30(6): 560–561	822

Several semi-popular scientific articles have appeared in periodicals under the authorship of members of the staff. To list a few from among these:

> Stommel, Henry M., Anatomy of the Atlantic Ocean. *Scientific American*, January 1955, Vol. 192, No. 1, pp. 30–36.
>
> Stetson, Henry C., The Continental Shelf. *Scientific American*, March 1955, Vol. 192, No. 3, pp. 82–86.

The pamphlet Oceanus has been published by the Institution quarterly throughout the year to keep the Associates in touch with the activities and research at Woods Hole. Although numerous requests have been received for subscription privileges, it is desired, at least for the present, to keep Oceanus primarily for the Associates and for their continued interest in our scientific studies of the sea.

After a lapse of more than a decade the practice of issuing an Annual Announcement by the Institution was resumed. Among other features the Announcement, which was distributed to the principal colleges and universities, informed them of the opportunities for students to gain a practical training and education in oceanographic research.

The Authors' Index listing all Contributions of the Institution, first published in 1950, is being re-issued to include all papers through 1955. It is cross-indexed by subjects to facilitate reference.

Vessels and Airplanes

Winter-time operations in northern waters can accomplish little with our small and weak-powered ships. One of the strong reasons advocating the construction of modern seaworthy oceanographic ships is the need of winter-time observations.

Following the practice of recent years, the field work was shifted south when ATLANTIS and CARYN sailed the middle of January on a two and one-half months geophysical reconnaissance of the island arc of the Caribbean Sea. A series of seismic profiles were made as ATLANTIS and CARYN alternated in shot and listening positions until the completion of the survey in March when they parted company off St. Thomas.

The ATLANTIS, developing a reflection profile north of the Greater Antilles, proceeded to Charleston, South Carolina, out of which port she operated with BEAR until entering Munro's Yard, Boston, the first week in May.

Again ATLANTIS was at sea at the end of June recording wave observations off the island of Bermuda. The end of the year found her cruising the west coast of South America engaged in a two months marine geological expedition. This was ATLANTIS' debut in the Pacific. During the year she was at sea a total of 234 days.

The CARYN, on parting company with ATLANTIS in March, returned home to Woods Hole arriving on April 15th. Due largely to the stringency of boat operating funds the CARYN was decommissioned at the Institution's waterfront pier, where she remained for the balance of the year. The fact that she had always been marginal with respect to her limitations on space, speed, and cruising radius, caused the further retention of CARYN to be questionable. She was offered for sale but the year's end witnessed her still at the dock with no purchaser in view.

The BEAR departed Woods Hole on 31 January to join the Hudson Laboratory's ship ALLEGHANY and to work out of Guantanamo with a submarine on acoustical studies. From there she proceeded to Charleston, South Carolina, in company with the VEMA, and then joined ATLANTIS returning with her to Woods Hole the first week in May. For the remainder of the year BEAR made short trips out and into Woods Hole, first to assist in surveying bottom sites on Georges Bank and later to engage in many sound transmission studies south of Martha's Vineyard. The BEAR, with her relatively spacious main deck for electronic equipment, has proved a useful, short cruising craft for the Institution.

The PBY airplane also proved its worth as an oceanographic tool. Operations were interrupted in February and March by the need to replace PBY-6A 46683 with a rebuilt airplane of the same type, number 64107, but a full schedule ensued thereafter for the remainder of the year. Among the missions carried out mention is made of several flights to photograph the changing outline of ocean beaches on which project studies are being conducted. Airborne radiation surveys of the Gulf Stream, low-level turbulence meteorological observations of coastal air masses, and other dynamic studies were some of the varied and interesting field operations. From August until the middle of October the airplane was especially active in conducting an extensive magnetometer reconnaissance of the West Indies-Caribbean area, and thence the entire coastal United States from Texas to Maine.

The smaller Stinson airplane was used on short flights in connection with sea-salt nuclei field investigations. In order to carry out this work special equipment is installed similar to the larger observational PBY.

ASTERIAS, the smallest of our fleet, was employed on short trips out of Woods Hole. The ASTERIAS would be used more by the staff were it available at a lower per diem cost. The high cost tends to discourage its use and this unfortunately in turn raises the price.

The need to replace our vessels with those especially designed for oceanographic field service has witnessed certain limited progress this year. Members of the Staff have participated in the deliberations of a steering committee organized by the Office of Naval Research; preliminary drawings and a general description have been prepared. As the year ends it is rumored that the Navy is including funds for more detailed design studies in its annual ship construction appropriation for an oceanographic research ship.

Plant

The Institution's property in land and buildings has received usual care and maintenance. The stringency of funds, however, experienced during a part of this year reduced somewhat expenditures on alterations and improvements.

No new property was added during the year but there is, however, an awareness noted to provide for the future growth of the Institution by taking advantage of real estate opportunities whenever they may appear. The Scientific Advisory Committee in its report to the Board of Trustees recommended the appointment of a Special Committee on Long Range Growth, and the Chairman, Mr. Milford R. Lawrence, made the first report to the

Trustees at their Annual Meeting in August, 1955. Certain sites were suggested as being advantageous for the Institution to acquire but no action was taken other than to request the committee to continue its investigations.

The East Boston water-front property of the Institution, which was reported last year as a donation by the General Foods Corporation, was offered for sale at a reduced price in order to attract a buyer. The valuation of $276,000 established on the property for taxation purposes by the City of Boston was reduced to $168,000 and this action assisted to facilitate in the sale of a small parcel to the New Street Realty Company in December for the sum of $5,000.

Last year a report was made of the damage inflicted to our water-front property by Hurricane Carol, August 31st. During the winter of 1955, while the vessels were absent in the south, repair of the pier was accomplished. The cost, totaling somewhat less than $25,000, covered not only the actual hurricane damage but included additional repairs necessitated by deterioration over the years. The small pier extending from the west sea wall was enlarged to provide safer berthing accommodations for small craft.

The hurricane damage to our structures on the land at Nonamessett Island leased for the storage of explosives, was repaired with the exception of the small pier still being worked on as the year ended.

Speaking of hurricanes, we became quite conscious of them — Connie on August 10–13; Diane on August 15–18; and Ione on September 17–20. Earlier in the season a hurricane bill indicating the precautions to be taken prior to, and on arrival of, a hurricane was distributed to the personnel. As a result of the three threatening hurricanes, much valuable time was lost from regular pursuits, both in the securing of our plant property and in the removal of our ships to safer harbors.

In the main laboratory building the oil heating furnaces were refitted to gas installation,— the anticipated saving in fuel costs amounting to approximately one-half that of the oil-type burners.

The former grocery store, a part of the so-called "Hall property" across the street from our main building, is now utilized as a storage for equipment and supplies. It serves as a more convenient place than the "barn" on the rear of our village property which is used for dead storage and heavier equipment.

The cafeteria at Challenger House remained closed throughout the year except for the reception and lunch provided for the Trustees on August 11.

Personnel

At their twenty-sixth Annual Meeting the Members of the Corporation re-elected the following Trustees to serve until 1959; namely,

James S. Coles
Carl H. Eckart
Ross G. Harrison
Milford R. Lawrence
Harlow Shapley
Francis C. Welch

At the Trustees' Meeting, which followed immediately that of the Corporation, the resignation of Dr. Arnaud C. Marts as President of the Corporation was accepted with much regret. Mr. Raymond Stevens, whose name was placed in nomination, was elected unanimously and by acclamation as President of the Corporation. The following was entered upon the record:

> "Resolved that the Board of Trustees of the Woods Hole Oceanographic Institution at this their 26th Annual Meeting make formal recognition of their great appreciation for the service rendered the Institution by Arnaud C. Marts as President from August 1950 to August 1955. Throughout this period, when other demands on him have been abnormally heavy, he has given unstintingly of time and effort. His judgment, ability and leadership have strengthened the Institution and brought it greatly increased recognition and support. The Trustees wish to record the affection and respect he has inspired and in forwarding a copy of this resolution to him convey their good wishes."

The Board re-elected Dr. Henry B. Bigelow as Chairman of the Board, and the following were elected as new members of the Corporation:

C. Lloyd Claff
Kenneth S. Cole
Henry B. duPont
Hudson Hoagland
Augustus B. Kinzel
Julius A. Stratton
J. H. Van Vleck
Thomas J. Watson, Jr.

The Research Staff in 1955 numbered 217. As of July 1, 1955 the persons associated with the Institution were tabulated as follows:

	1954		*1955*	
Research Staff				
Full time:				
Scientists and Technicians:				
At Woods Hole	94		86	
Off Campus	21		17	
Secretaries and Clerks	7		7	
Part time:				
At Woods Hole	44		43	
Off Campus	37		37	
Fellowship Holders	20		21	
Visiting Investigators	6	229	6	217*
Supporting Personnel				
Administrative:				
Department Heads and Assistants	10		11	
Secretaries and Clerks	12		12	
General Maintenance and Service Personnel	63		52	
Crews of Vessels	47	132	41	116
Grand Total		361		333

* Includes 90 Staff Appointees

It is with pleasure that we record the names of the following persons to the Research Staff for a period of one year from September 1:

William D. Athearn	Research Associate in Geology
Joseph H. Connell	Research Associate in Marine Biology
Alan J. Faller	Research Associate in Meteorology
James M. Moulton	Associate in Marine Biology
Mary Alys Plunkett	Associate in Chemistry
Howard L. Sanders	Research Associate in Marine Biology

During the year we accepted with regret the resignations of Dr. Per F. Scholander, Dr. Levie Van Dam, Mr. Earl W. Barrett, Mr. E. M. Ballenzweig, and Mr. Gunther K. Wertheim. Dr. Scholander has accepted an honorary appointment as Associate in Physiology on the Institution's Staff.

Reappointments for one- and three-year terms, as authorized by the Board of Trustees, were made to all Staff Members whose terms expired on September 1.

Death came unexpectedly December 3, 1955 to one of the members of the original Staff of the Institution, Mr. Henry C. Stetson, Submarine Geologist, while he was at sea off the coast of Chile serving as Chief Scientist on board the Research Vessel ATLANTIS. Under an early agreement with Harvard University Mr. Stetson's services were shared with this Institution, — an arrangement which resulted over the years in a most productive scientific career. His passing is grieved by his colleagues and removes from the Institution a scientist who stood high in the field of submarine geology.

Captain Arvid Karlson, a veteran seaman, who for many years sailed as mate on the ATLANTIS and more recently served as master of the CARYN, passed away on October 18, 1955. He represented one of those we call "of the old school" whose seamanship was expert. In accordance with his wishes his last remains were put to rest at sea in the presence of the full crew of the ATLANTIS.

Various members of the Staff made trips abroad during the year. Dr. J. B. Hersey visited England May 29 to June 13 to attend a conference on underwater sound. Following these meetings Dr. Hersey visited several of the Royal Naval Establishments where sea acoustics are being studied. During August 1 to 9 he attended a sound propagation committee meeting held at Greenock, Scotland.

Drs. Edward H. Smith and Columbus O'D. Iselin attended a meeting of a Working Group on Oceanography, a subcommittee of the Special Committee of the International Geophysical Year, in Brussels, Belgium, on September 8 to 10.

Mr. Allyn C. Vine gave a paper at a Regional Symposium on Physical

Oceanography held at Tokyo, Japan, on October 19 to 22 under the auspices of the United Nations Economic and Scientific Congress Organization.

Dr. Willem V. R. Malkus and Joanne S. Malkus returned early in December after spending a year abroad. The wife lectured and studied at the Imperial College of Science in London and the husband continued his research at the National Institute of Oceanography near London. Both of these scientists gave several technical papers before various royal societies in England during their profitable visit.

Dr. Gifford C. Ewing, Assistant Research Oceanographer, Scripps Institution of Oceanography, was appointed the Woods Hole Oceanographic Associates' Lecturer for 1955. Following an interesting series of illustrated lectures to the Staff on the usefulness of aerial reconnaissance in interpreting the physical processes in the upper mixed layer of the ocean, Dr. Ewing participated in certain phases of the Institution's research, particularly that of aerial sea observations.

The following were awarded grants or fellowships during the year:

Bermuda Biological Station for Research
Lawrence K. Coachman
Albert P. Crary
George M. Creswell
Harold Edgerton
Gifford C. Ewing
Helen B. Fink
Bernhard Haurwitz
Peter Hughes
Robert B. Hulsman
Benjamin B. Leavitt
Conrad Malicoat
Milton A. Miller
Robert L. Miller
Raymond B. Montgomery
James R. Moore III
James M. Moulton
John R. Nicholson
Colm 'Oh Eocha
Waldemar Ohle
Carl H. Oppenheimer
Roderic B. Park
Gordon A. Riley
Raymond G. Stevens
Eugene J. Tynan
W. A. van Bergeijk
George Veronis
Bernard Vonnegut
Gilbert L. Voss
Bruce A. Warren
E-an Zen

This year marked the inauguration by the Institution of a fellowship program supported by the Associates. An appropriation is set aside annually from the endowed income of the Institution and from contributions of the Woods Hole Oceanographic Associates to provide grants and fellowships for properly qualified students and visiting investigators. Each holder of a fellowship will be expected to submit a written report on his work at the expiration of his appointment. No application for a second term will be accepted unless this report be considered satisfactory.

The persons whose names follow were members of the Institution (additional to those otherwise listed) for a period of six months or more during the calendar year 1955.

RESEARCH ASSISTANTS, ENGINEERS, AND TECHNICIANS

Anderson, Nellie E.
Baldwin, Elizabeth E.
Ballenzweig, Emmanuel M.
Barstow, Elmer M.
Bennett, Paul E.
Bergstrom, Stanley W.
Berry, Audrey W.
Bradshaw, Alvin L.
Cain, Henry A.
Campbell, Sybil A.
Cangiamila, Angelo
Carter, Alwyn L.
Chute, Edward H.
Colburn, Barbara A.
Corwin, Nathaniel
Day, C. Godfrey
Dingwell, Paul E.
Dunkle, William M., Jr.
Edwards, Melville E.
Edwards, Richard S.
Fee, Frances M.
Fraser, Grace C.
Fraser, John G.
Hayes, Carlyle R.
Hoadley, Lloyd D.
Hodgson, Sloat F.
Kahler, Yolande A.
Lavin, Delia M.
Moss, William M.
Morehouse, Clayton B.
Pasley, Gale G., Jr.
Poole, Stanley E.
Purinton, Charles S.
Raiche, Shirley A.
Rose, John C.
Rutstein, Milton S.
Schroeder, Elizabeth H.
Shearer, Barbara J.
Shultz, William S.
Soderland, Eloise M.
Thayer, Lawrence A.
Thayer, Mary C.
Torphy, Shannon R.
Vaccaro, Martha W.
Wilkins, Charles H.
Witzell, Warren E.

TECHNICAL CLERKS AND SECRETARIES

Allen, Ethel B.
Barbour, Rose L.
Bergstrom, Eileen S.
Bradley, Mabel D.
Casiles, Ann E.
Dow, Evelyn
English, Jean
Glaeser, Florence E.
Mellor, Florence K.
Ortolani, Mary
Ostiguy, Betty P.
Phillips, Helen F.
Rogers, M. Dorothy
Scharff, Margaret
Souza, Cecelia
Thatcher, Beverly J.
Vest, Dolores R.
Wilson, Esther N.

ADMINISTRATIVE AND SECRETARIAL PERSONNEL

Backus, Jeanne M.
Behrens, Henry G.
Broadbent, Madeline P.
Bryant, Edwin T.
Camper, Barbara B.
Casiles, Phyllis M.
Crocker, Marion W.
Ferris, Alice H.
Ferris, George A.
Griffin, T. S. Perry
Hatzikon, Kaleroy L.
Lopes, Mary D.
Sandblom, John D.
Young, Anita W.

TECHNICAL SERVICES PERSONNEL

Bailey, Frank A.
Blake, Forrest W.
Bodman, Ralph H.
Bowman, Warren O.
Brigham, Robert K.
Day, Robert L.
Dimmock, Richard H.
Eldridge, Stanley N.
Feldman, Joel
Fisher, Stanley O.
Gallagher, Gloria S.
Gallagher, William F.
Gaskell, Fred
Gifford, James E.
Grant, Carlton
Hodgkins, Harry L.
Howland, Myron P., Jr.
Morrison, Kenneth
Penniman, Norman
Perry, Allison E.
Rennie, Thomas D.
Shanahan, Hugh J., Jr.
Spooner, Charles E.
Stimpson, John W.
Weeks, Robert G.
Wing, Carleton R.

MAINTENANCE, HOUSING AND CUSTODIAL PERSONNEL

Backus, Harold
Christian, John A.
Condon, J. William
Fielden, Frederick E.
Salthouse, James
Solberg, Otto
Souza, Matthew R.
Sparks, Elizabeth C.
Stansfield, Richard
Tometich, Louis J.
Turner, Catherine
Wilde, Phillips B.
Woodward, Fred C., Jr.
York, Javan D.

OFFICERS AND CREWS OF VESSELS, BOATS, AND AIRCRAFT

Backus, Cyril
Bisaillon, Ralph
Bray, W. Scott
Bumer, John G.
Cabral, John V.
Callan, Thomas P.
Casiles, David F.
Cavanaugh, James J.
Colburn, Arthur D., Jr.
Cook, Hans
Copestick, Louis B.
Coughlin, Brooks W.
Day, Joseph V.
Fournier, Richard A.
Gingrass, Norman
Graffam, Robert
Howarth, Walter G.
Howe, Paul M.
Howland, Paul C.
Hurwitz, Robert K.
Karlson, Arvid (deceased)
Lambert, Joseph L.
Leslie, John E.
Mackey, Malcolm R.
Matthews, Francis S.
McCann, Clement L., Jr.
Mysona, Eugene J.
Nailor, David A.
Pierce, Samuel F.
Roderick, Milton
Rose, Lawrence
Salthouse, James E.
Seibert, Harry H.
Shields, William J.
Smith, John J.
Speight, Carl W.
Sutherland, Peter A.
Tucker, William G.
Williams, David H.

The Retirement Plan which was established in 1954 covered a total of 117 employees at the end of 1955, 24 of them having come into the Plan at the latter time. The Retirement Committee which administers the Plan lost one member, Evangeline T. Wilkins, through resignation and the Executive Committee elected Mary Ortolani to fill the vacancy. The other members are Dean F. Bumpus, Stanley O. Fisher, John McGilvray, and John F. Pike.

Acknowledgments

Again this year it is desired to record the support and consideration extended in the form of contracts in behalf of the Institution's research program by the U. S. Navy Department's Office of Naval Research, Bureau of Ships, Bureau of Aeronautics, Bureau of Ordnance, Hydrographic Office, and other agencies. We also have two small contracts with the U. S. Air Force.

During the year contracts were initiated with the following civilian agencies of the Federal Government, viz., U. S. Weather Bureau and the Atomic Energy Commission.

The Commonwealth of Massachusetts, Division of Marine Fisheries, renewed its grant to the Institution in support of shell fish investigations of state waters.

Due appreciation is also made to the following for their cooperation and support of the Institution's program in education and research:

Atlantic Tuna Club
Bendix Aviation Corporation
Benjamin Fund
Creole Petroleum Corporation
Edo Foundation
Esso Research and Enginefring Company
James Foundation of New York, Inc.
Life Saving Benevolent Association of New York
Robert Earll McConnell Foundation
National Science Foundation
Research Corporation
Rockefeller Brothers Fund
Rockefeller Foundation
Shell Companies Foundation
Socony Mobil Oil Company, Inc.

In making acknowledgment to the several organizations which are assisting with the support of the research and education in oceanography, none stands higher than the Associates of the Woods Hole Oceanographic Institution. During the past two and one-half years this group, which had its inception in the Woods Hole summer colony, now includes several of the largest industrial corporations of the country.

The past year has witnessed the support of the Associates in the following projects of the Institution: (a) a spectrographic study of sea-water samples collected world-wide, tracing the physical and chemical changes produced by the cycle of evaporation and precipitation and return to the ocean; (b) the establishment of an annual summer lectureship to bring a distinguished visiting scientist to Woods Hole; (c) the establishment of a series of doctoral fellowships in the earth sciences; (d) the partial underwriting of an ocean geophysical expedition to the island arc of the West Indies, (e) financial participation in a pelagic game fish tagging cruise to the Caribbean Sea, and (f) similarly sponsored "The Atlantis" Marine Geological Expedition to Peru and Chile, 1955.

The Associates of the Woods Hole Oceanographic Institution held their Third Annual Dinner April 19 at the New York Yacht Club at which time they were addressed by Mr. Robert H. Simpson of the U. S. Weather Bureau on the subject of hurricanes.

The annual meeting of the Associates was held in connection with the Open House day of the Institution August 8th. Several changes in the officers took place with Mr. Gerard Swope, Jr. becoming Chairman of the Board, Mr. Noel B. McLean, President, and Mr. John A. Gifford continuing as secretary. Mr. Charles F. Adams, Jr. accepted the Chairmanship of the Corporate Committee. At the end of the year the organization recorded a total enrollment of 142 Individual Members and 26 Corporation Members. The support which the Associates are giving to the advancement of the

Institution's research and educational programs has in a few short years become substantial indeed.

The Endowment Committee of the Institution appointed a few years ago in an effort to form a tangible force to encourage donations and bequests to the capital endowment of the Institution regretted to report no contributions for the year.

V. TREASURER'S REPORT

THE accounts for the year 1955 have been audited by Lybrand, Ross Bros. & Montgomery.

The book value of endowment funds, including cash and advance to current funds, at December 31, 1955 was $3,135,361, of which $715,941 represents the accumulated net gains from sales of investments, and $2,419,420 represents the original value of endowment funds. The market value of endowment assets on the same date was $4,554,396. Schedule D shows an analysis by major groups of securities of the endowment investments, and the income received therefrom.

The income received on endowment assets, including interest charged on the advance to current funds was $158,743 for the year ending December 31, 1955, compared with $149,255 for the calendar year 1954. This income represents a return on the endowment investments of 3.5% on the year-end market value, 5.1% on the book value, and 6.6% on the original value of the endowment.

The executive committee, upon the recommendation of the finance committee, voted to allocate for 1955 operating expenses from the endowment income 5.3% of the original book value of the endowment, which amounted to $128,229. The balance of endowment income, $30,514, was transferred to the income and salary stabilization reserve. The rate was the same as voted in 1954.

The advance to current funds from endowment funds was reduced from $175,000 to $50,000 during the year. Interest on this advance at 2¼% is credited to endowment income and charged to current expense.

Deferred charges amounting to $59,153 represent expenditures for the benefit of future years. A proportionate part of these charges will be added to current costs, or other appropriate accounts, as the benefits accrue.

The details of unexpended balances of gifts and grants for research are shown in Schedule C; in addition, contributions of the Woods Hole Oceanographic Associates as yet not specifically allocated amount to $32,296.

The Institution's 1955 contribution to the new Woods Hole Oceanographic Institution Employees Retirement Plan and Trust amounted to $52,698 and appears on the balance sheet as a current liability as of December 31, 1955. The amount so constituted is held in a separate trust fund administered by three trustees. The balance remaining in the old retirement fund, which is in the custody of the Treasurer, amounted to $61,713 as at December 31, 1955.

During the year we received from the individual and corporate members of the Woods Hole Oceanographic Associates a total of $32,160, and $33,200 was allocated to lectureships, fellowships, and various research projects.

On the following pages you will find the auditor's certificate, balance sheet and income statement, with the supporting schedules. Schedules A and B show details of direct costs of research activity, general and administrative expenses, and expenses of plant operation. Schedule C gives a summary of gifts and receipts for research, and Schedule D a summary of the endowment investments. It is interesting to note that for each dollar spent 77.3 cents were spent for direct costs of research activity, 16.7 cents for general and administration expenses and 6.0 cents for plant operation and miscellaneous. It is also interesting that total administrative salaries amounted to only 7.2 cents of each dollar of total expense.

BALANCE SHEET

As at December 31, 1955

ASSETS

Endowment Fund Assets:		
Investment securities (Schedule D):		
Bonds (market quotations $1,851,275)		$1,855,499
Stocks (market quotations $2,579,873)		1,156,614
		3,012,113
Cash		73,248
Advance to current funds		50,000
		3,135,361
Plant Assets (note A):		
Laboratory plant and equipment		$524,014
Vessels and equipment		364,983
Other property		161,541
		1,050,538
Current Fund Assets:		
Cash		102,049
Accounts receivable:		
U. S. Government	$9,049	
Tax abatement	15,451	
Other	4,998	29,498
Unbilled costs on research contracts:		
U. S. Government	224,521	
Other	5,471	229,992
Supply inventories		22,299
Deferred charges (note B)		59,153
		442,991
		$4,628,890

LIABILITIES

Endowment Funds:		
Unrestricted		$2,000,000
For upkeep of plant		419,420
Accumulated net gain on sale of investments		715,941
		3,135,361
Funds Invested in Plant		1,050,538
Current Liabilities and Funds:		
Accounts payable and accrued expenses		42,836
Contribution payable to employees' retirement plan and trust		52,698
Advance from endowment funds		50,000
Unexpended balances of gifts and grants:		
For research (Schedule C)		40,362
Oceanographic Associates		32,296
General Fund:		
General plant and equipment reserve	$158,450	
Income and salary stabilization reserve	75,173	
(Deficit)	(8,824)	224,799
		442,991
		$4,628,890

Notes: A — Since 1945 the Institution has provided for depreciation of plant assets other than vessels at annual rates of 2% on buildings and 5% to 33⅓% on equipment, carrying the amounts to general plant and equipment reserve.

B — Real estate received as a gift in 1954 and held for sale at December 31, 1955 is not included in assets; it will be added to current fund assets when sold at the net amount of the proceeds from sale. Deferred charges include $12,580 net expenses in connection with this property.

STATEMENT OF INCOME, OPERATING EXPENSES AND UNAPPROPRIATED GENERAL FUND

For the Year Ended December 31, 1955

Income:		
Reimbursement of sponsored research activity:		
For direct costs		$1,272,164
For indirect costs		403,849
		1,676,013
Endowment income after amortization of bond premiums (Schedule D)	$158,743	
Less amount added to income and salary stabilization reserve	30,514	128,229
Miscellaneous		1,448
Total income availed of		1,805,690
Operating Expenses:		
Direct costs of research activity (Schedule A):		
Salaries and wages		700,977
Vessel operations		345,996
Materials and services		267,168
Travel		92,704
		1,406,845
Indirect costs:		
General and administration (Schedule B)	304,995	
Plant operation (Schedule B)	105,736	
Miscellaneous	3,187	413,918
Total operating expenses		1,820,763
Excess of Operating Expenses		15,073
Additions to plant from current funds:		
Books and equipment purchased	11,862	
Less equipment charged to general plant and equipment reserve	4,862	7,000
		22,073
Unappropriated General Fund, January 1, 1955		13,249
Deficit in Unappropriated General Fund, December 31, 1955		$8,824

SCHEDULE A

DIRECT COSTS OF RESEARCH ACTIVITY

For the Year Ended December 31, 1955

	Salaries and Wages	Vessel Operations	Materials and Services	Travel	Total
U.S. GOVERNMENT CONTRACTS	$581,667	$308,744	$204,882	$79,220	$1,174,513
OTHER SPONSORED RESEARCH	44,028	14,000	34,427	5,196	97,651
Total direct costs of sponsored research ...	625,695	322,744	239,309	84,416	1,272,164
INSTITUTION RESEARCH......	75,282	23,252	27,859*	8,288	134,681
Total direct costs of research.............	$700,977	$345,996	$267,168	$92,704	$1,406,845

* Includes $20,531 grants and fellowships.

SCHEDULE B

GENERAL AND ADMINISTRATION EXPENSES AND EXPENSES FOR PLANT OPERATION

For the Year Ended December 31, 1955

GENERAL AND ADMINISTRATION

GENERAL EXPENSES:		
Staff benefits:		
Contributions to retirement plan............................		$52,698
Social security taxes..		18,014
		70,712
Shop services..		52,995
Housing, net..		1,973
ADMINISTRATION EXPENSES:		
Salaries and wages....................................	$131,365	
Insurance, travel, supplies and other....................	47,950	179,315
		$304,995

PLANT OPERATION

SALARIES AND WAGES..		$43,151
PROVISION FOR DEPRECIATION (credited to general plant and equipment reserve)..		22,578
OTHER REPAIR COSTS..	$27,813	
HEAT, LIGHT AND POWER....................................	18,523	
OTHER..	3,671	50,007
		115,736
Less repairs charged to general plant and equipment reserve.........		10,000
		$105,736

Schedule C

SUMMARY OF GIFTS AND RECEIPTS FOR RESEARCH

Year Ended December 31, 1955

	Unexpended Balance January 1, 1955	Received	Expended		Other Charges or (Credits)	Unexpended Balance December 31, 1955
			Direct Costs	Indirect Costs		
American Bureau of Shipping		$2,000	$941	$616		$443
American Society of Limnology and Oceanography		706	560	146		
Arctic Institute of North America:						
Buoyancy control in fish		1,037	789	248		
Freezing of living tissue		2,500	107	1		2,392
Barataria Bay model	$130		85			45
Bermuda Biological Station for Research		536	531	5		
Boat Lemming		113	94	19		
Bigelow volume		2,748				2,748
Commonwealth of Massachusetts	9,111	20,000	9,550	5,358		14,203
Creole Petroleum Corporation		2,651	1,141	717	$793 (1)	
Esso Research and Engineering Company		5,300	1,796	1,144	147 (1)	2,213
Manufacture, sale, and calibration of instruments		3,241	8,452	3,947	(9,158) (2)	
Massachusetts Institute of Technology		600	565			35
Motion picture on oceanography		19,559	19,559			
Munitalp Foundation	5,800				5,800 (3)	
National Science Foundation:						
Biological and chemical productivity		2,444	2,125	319		
Buoyancy control in fish		3,127	2,574	553		
Measurement of light in the sea		8,500	2,652	398		5,450
Nitrification in sea water		6,900	4,532	680		1,688
Penetration of light	1,083		822	261		
Properties of chlorophyll	2,486	2,000	3,429	514		543
Oceanographic Associates:						
Deuterium studies	4,358		3,588	366		404
Peruvian expedition		15,000	7,443	2,079		5,478
Other		18,200	18,200			
Research Corporation	1,406		12		(826) (4)	2,220
Rockefeller Foundation:						
Marine physiology	5,450		5,450			
Meteorological research	1,042		1,042			
Socony-Vacuum Laboratories		2,500				2,500
U.S. Coast Guard Oceanographic Unit		1,655	1,612	519	(476) (1)	
	$30,866	$121,317	$97,651	$17,890	($3,720)	$40,362

---

(1) Credited or (charged) to income.

(2) Equipment and calibration services charged to other projects.

(3) Payments to designated award recipients.

(4) Receipts from sales.

Schedule D

SUMMARY OF INVESTMENTS

As at December 31, 1955

	Book Amount	% of Total	Market Quotation	% of Total	Income
BONDS:					
U.S. Government..........	$492,340	16.34	$479,920	10.83	$11,193
Railroad..................	499,924	16.60	507,919	11.46	19,737
Public utility..............	192,201	6.38	183,075	4.13	8,932
Industrial.................	332,497	11.04	342,375	7.73	8,692
Financial and investment...	338,537	11.24	337,986	7.63	7.847
Total bonds..........	1,855,499	61.60	1,851,275	41.78	$56,401
STOCKS:					
Preferred.................	323,843	10.75	371,101	8.37	$16,904
Common:					
Public utility...........	274,370	9.11	455,638	10.28	$19,192
Industrial..............	417,491	13.86	1,475,718	33.31	52,271
Miscellaneous	140,910	4.68	277,416	6.26	11,609
Total common stocks	832,771	27.65	2,208,772	49.85	83,072
Total stocks.........	1,156,614	38.40	2,579,873	58.22	99,976
Total investments....	$3,012,113	100.00	$4,431,148	100.00	156,377
INTEREST ON ADVANCE TO CURRENT FUNDS CHARGED TO MISCELLANEOUS OPERATING EXPENSE..........					2,366
TOTAL ENDOWMENT FUND INCOME..........					$158,743

WOODS HOLE OCEANOGRAPHIC INSTITUTION
WOODS HOLE, MASSACHUSETTS

We have examined the balance sheet of Woods Hole Oceanographic Institution as at December 31, 1955 and the related statement of income, operating expenses and unappropriated general fund for the year then ended. Our examination was made in accordance with generally accepted auditing standards, and accordingly included such tests of the accounting records and such other auditing procedures as we considered necessary in the circumstances.

In our opinion, the accompanying financial statements present fairly the position of Woods Hole Oceanographic Institution at December 31, 1955 and the results of its operations for the year then ended, on a basis consistent with that of the preceding year.

LYBRAND, ROSS BROS. & MONTGOMERY

Boston, Massachusetts
May 15, 1956

APPENDIX

ATLANTIS

Cruise No.	Depart	Arrive	From	To	Days	Chief Scientist—Remarks
213	19 Jan.	23 Jan.	Woods Hole	Bermuda	5	H. Johnson
	28 Jan.	2 Feb.	Bermuda	St. Thomas	6	H. Johnson
	5 Feb.	15 Feb.	St. Thomas	Martinique	11	C. Officer
	18 Feb.	20 Feb.	Martinique	Barbados	3	C. Officer
	20 Feb.	28 Feb.	Barbados	Trinidad	9	C. Officer
	3 Mar.	13 Mar.	Trinidad	Roosevelt Rds.	11	C. Officer
	14 Mar.	15 Mar.	Roosevelt Rds.	St. Croix	2	C. Officer
	15 Mar.	23 Mar.	St. Croix	St. Thomas	9	H. Johnson
	28 Mar.	3 Apr.	St. Thomas	Charleston	7	H. Johnson
	7 Apr.	8 Apr.	Charleston	Charleston	2	H. Johnson
	9 Apr.	10 Apr.	Charleston	Charleston	2	H. Johnson
	13 Apr.	21 Apr.	Charleston	Charleston	9	H. Johnson
	23 Apr.	5 May	Charleston	Woods Hole	13	R. Edwards
214	7 May	7 May	Woods Hole	Boston	1	To Boston for annual
	24 May	24 May	Boston	Woods Hole	1	drydocking
215	7 June	14 June	Woods Hole	Bermuda	8	V. Worthington
	16 June	23 June	Bermuda	Nassau	8	V. Worthington
	26 June	6 July	Nassau	Woods Hole	11	V. Worthington
216	17 July	23 July	Woods Hole	Woods Hole	7	W. Dow–G. Clarke
217	28 July	1 Aug.	Woods Hole	Bermuda	5	F. Fuglister
	3 Aug.	22 Aug.	Bermuda	Bermuda	20	F. Fuglister
	25 Aug.	28 Aug.	Bermuda	Woods Hole	4	F. Fuglister
218	30 Aug.	30 Aug.	Woods Hole	Boston	1	To shipyard for
	16 Sept.	16 Sept.	Boston	Woods Hole	1	engine overhaul
219	22 Sept.	27 Sept.	Woods Hole	Woods Hole	6	W. Dow
220	3 Oct.	6 Oct.	Woods Hole	Bermuda	4	H. Farmer
	9 Oct.	15 Oct.	Bermuda	Bermuda	7	H. Farmer
	17 Oct.	18 Oct.	Bermuda	Bermuda	2	H. Farmer
	19 Oct.	21 Oct.	Bermuda	Bermuda	3	H. Farmer
	22 Oct.	26 Oct.	Bermuda	Bermuda	5	H. Farmer
	29 Oct.	29 Oct.	Bermuda	Bermuda	1	J. Hahn
221	29 Oct.	5 Nov.	Bermuda	Cristobal	7	Passage to Panama Canal
	6 Nov.	6 Nov.	Cristobal	Balboa	1	Transit of Panama Canal
	9 Nov.	9 Nov.	Balboa	Balboa	1	J. Zeigler
	9 Nov.	14 Nov.	Balboa	Talara	6	J. Zeigler
	15 Nov.	23 Nov.	Talara	Callao	9	H. Stetson
	25 Nov.	3 Dec.	Callao	Antofagasta	9	H. Stetson
	6 Dec.	11 Dec.	Antofagasta	Antofagasta	6	P. Trask
	13 Dec.	19 Dec.	Antofagasta	Callao	7	P. Trask
	26 Dec.	29 Dec.	Callao	Talara	4	R. Lufburrow
			Total		234	

CARYN

Cruise No.	Depart	Arrive	From	To	Days	Chief Scientist—Remarks
89	19 Jan.	23 Jan.	Woods Hole	Bermuda	5	J. Ewing
	28 Jan.	2 Feb.	Bermuda	St. Thomas	6	J. Ewing
	5 Feb.	15 Feb.	St. Thomas	Martinique	11	H. Johnson
	18 Feb.	20 Feb.	Martinique	Barbados	3	H. Johnson
	20 Feb.	28 Feb.	Barbados	Trinidad	9	H. Johnson
	3 Mar.	13 Mar.	Trinidad	Roosevelt Rds.	11	H. Johnson
	14 Mar.	15 Mar.	Roosevelt Rds.	St. Croix	2	H. Johnson
	15 Mar.	23 Mar.	St. Croix	St. Thomas	9	H. Johnson
90	31 Mar.	8 Apr.	St. Thomas	Charleston	9	J. Hahn
	10 Apr.	15 Apr.	Charleston	Woods Hole	6	J. Hahn
91	21 Apr.	21 Apr.	Woods Hole	Woods Hole	1	To embark editors at New Bedford and return W. H.
92	9 Aug.	10 Aug.	Woods Hole	Boston	2	Hurricane precaution
	24 Aug.	24 Aug.	Boston	Woods Hole	1	Return passage
		Total			75	

* On voyage No. 91, Hahn, Athearn and Fuglister were on board demonstrating equipment.

BEAR

Cruise No.	Depart	Arrive	From	To	Days	Chief Scientist — Remarks
112	14 Jan.	14 Jan.	Boston	Woods Hole	1	Return from shipyard
113	31 Jan.	5 Feb.	Woods Hole	Bermuda	6	Passage to Bermuda for oil then to St. Thomas to pick up scientists
	10 Feb.	14 Feb.	Bermuda	St. Thomas	5	
	15 Feb.	18 Feb.	St. Thomas	St. Thomas	4	J. Hersey
	21 Feb.	26 Feb.	St. Thomas	Mayaguez, P.R.	6	J. Hersey
	28 Feb.	11 Mar.	Mayaguez, P.R.	Charleston	12	J. Hersey
	14 Mar.	21 Mar.	Charleston	Charleston	8	R. Wyrick
	23 Mar.	3 Apr.	Charleston	Charleston	12	R. Wyrick
	7 Apr.	8 Apr.	Charleston	Charleston	2	J. Hersey
	9 Apr.	10 Apr.	Charleston	Charleston	2	J. Hersey
	13 Apr.	21 Apr.	Charleston	Charleston	9	J. Hersey
	23 Apr.	4 May	Charleston	Woods Hole	12	J. Hersey
114	16 June	16 June	Woods Hole	Woods Hole	1	W. Richardson
115	17 June	17 June	Woods Hole	Woods Hole	1	L. Hoadley
116	20 June	22 June	Woods Hole	Woods Hole	3	J. Zeigler
117	28 June	1 July	Woods Hole	Woods Hole	4	W. Richardson
118	7 July	16 July	Woods Hole	Woods Hole	10	J. Zeigler
119	21 July	21 July	Woods Hole	Woods Hole	1	J. Zeigler
120	22 July	22 July	Woods Hole	Woods Hole	1	R. Walden
121	25 July	29 July	Woods Hole	Woods Hole	5	J. Zeigler
122	1 Aug.	3 Aug.	Woods Hole	Woods Hole	3	J. Zeigler
123	8 Aug.	8 Aug.	Woods Hole	Woods Hole	1	L. Thayer
124	8 Aug.	10 Aug.	Woods Hole	Boston	3	D. Bumpus
	14 Aug.	14 Aug.	Boston	Woods Hole	1	D. Bumpus
	14 Aug.	17 Aug.	Woods Hole	Woods Hole	3	D. Bumpus
	18 Aug.	22 Aug.	Woods Hole	Woods Hole	5	D. Bumpus
125	6 Sept.	10 Sept.	Woods Hole	Woods Hole	5	G. Clarke
126	12 Sept.	12 Sept.	Woods Hole	Woods Hole	1	D. Grey
127	14 Sept.	14 Sept.	Woods Hole	Woods Hole	1	D. Grey
128	11 Oct.	14 Oct.	Woods Hole	Woods Hole	4	R. Backus
129	18 Oct.	18 Oct.	Woods Hole	Woods Hole	1	Gyro calibration
130	24 Oct.	24 Oct.	Woods Hole	Woods Hole	1	J. Hahn
131	26 Oct.	27 Oct.	Woods Hole	Cape May, N.J.	2	To pick up Crawford to tow to Woods Hole
	31 Oct.	2 Nov.	Cape May, N.J.	Woods Hole	3	
132	15 Nov.	19 Nov.	Woods Hole	Woods Hole	5	R. Backus
133	6 Dec.	6 Dec.	Woods Hole	Woods Hole	1	S. Knott
134	14 Dec.	14 Dec.	Woods Hole	Woods Hole	1	To Vineyard Sound to pick up recording buoy
135	15 Dec.	15 Dec.	Woods Hole	New Bedford	1	To shipyard
			Total		147	

PBY–6A BUNO 46683

Flight No.	Dates	From	To	Days	Chief Scientist—Remarks
181–187	3 Jan.–18 Jan.	Otis — local		7	
188	18 Jan.	Otis	Bermuda		Bunker
	20 Jan.	Bermuda	Bermuda		Bunker
	22 Jan.	Bermuda	Otis	3	Bunker
189	25 Jan.	Otis	Pensacola		Airworthiness check
	26 Jan.	Pensacola	Pensacola		
	4 Feb.	Pensacola	Otis	3	Ferry to Otis
190	24 Feb.	Otis – local		1	To Quonset for maintenance
191	25 Feb.	Otis — local		1	To Quonset for maintenance
192	19 Mar.	Otis	NAS Columbus		Ferry flight to return
	20 Mar.	NAS Columbus	NAS St. Louis		PBY-6A 46683 for storage
	22 Mar.	NAS St. Louis	Wichita, Kan.		
	23 Mar.	Wichita	El Paso, Tex.		
	24 Mar.	El Paso	Litchfield Park Arizona	5	

PBY–6A BUNO 64107

Flight No.	Dates	From	To	Days	Chief Scientist—Remarks
1	30 Mar.	Pensacola	Otis	1	Ferry flight
2	31 Mar.	Otis	Quonset	1	For acceptance check
3	8 April.	Quonset	Otis	1	Ferry flight
4–33	11 Apr.–18 July	Otis — local		30	
34	19 July	Otis	Daytona		W. Schevill
	21 July	Daytona	Otis	2	
35	22 July	Otis	Quonset	1	120-hour check
36	16 Aug.	Quonset	Quonset	1	Test hop
37	17 Aug.	Quonset	Otis	1	Return Ferry
38	20 Aug.	Otis — local		1	Brigham-Davidson
39	21 Aug.	Otis	Atlantic City		First leg of magnetometer flight. Davidson, Chief Scientist
	22 Aug.	Atlantic City	Cherry Point		
	23 Aug.	Cherry Point	Jacksonville		
	24 Aug.	Jacksonville	Miami		
	26 Aug.	Miami	San Juan		
	28 Aug.	San Juan	San Juan		
	29 Aug.	San Juan	San Juan		
	1 Sept.	San Juan	San Juan		
	2 Sept.	San Juan	Antigua		
	4 Sept.	Antigua	Antigua		
	5 Sept.	Antigua	Trinidad		

PBY–6A BUNO 64107 (*Continued*)

Flight No.	Dates	From	To	Days	Chief Scientist—Remarks
39 (cont)	6 Sept.	Trinidad	Trinidad		Davidson (Cont.)
	8 Sept.	Trinidad	St. Lucia		
	9 Sept.	St. Lucia	Barbados		
	11 Sept.	Barbados	Antigua		
	12 Sept.	Antigua	Antigua		
	13 Sept.	Antigua	San Juan		
	16 Sept.	San Juan	San Juan		
	17 Sept.	San Juan	San Juan		
	18 Sept.	San Juan	Curacao		
	19 Sept.	Curacao	Haiti and Guantanamo		
	20 Sept.	Guantanamo	Havana		
	21 Sept.	Havana	Corpus Christi		
	24 Sept.	Corpus Christi	Harlingen AFB, Texas		
	25 Sept.	Harlingen	Houston		
	26 Sept.	Houston	Pensacola		
	27 Sept.	Pensacola	Pensacola		
	8 Oct.	Pensacola	Mobile, Ala.		
	9 Oct.	Mobile	Tampa, Fla.		
	10 Oct.	Tampa	Cherry Point		
	11 Oct.	Cherry Point	Otis AFB		
	14 Oct.	Otis — local			To Bar Harbor area
	17 Oct.	Otis — local		33	To New Jersey area — final tow
40	20 Oct.	Otis	Bermuda		Fraser
	21 Oct.	Bermuda	Otis	2	
41	25 Oct.	Otis — local		1	Brigham
42	28 Oct.	Otis	Bermuda		Fraser
	29 Oct.	Bermuda	Otis		
	1 Nov.	Otis	Bermuda		
	2 Nov.	Bermuda	Bermuda		
	3 Nov.	Bermuda	Otis	5	
43–49	12 Nov.–1 Dec.	Otis — local		7	
50	5 Dec.	Otis	Bermuda		Bunker
	7 Dec.	Bermuda	Otis	2	
51	10 Dec.	Boston	Norfolk		Gulf Stream Survey
	11 Dec.	Norfolk	Pensacola		To Pensacola for check
	22 Dec.	Pensacola	Pensacola		Test flight
	23 Dec.	Pensacola	Otis	4	Ferry flight
52	30 Dec.	Otis — local		1	To Quonset for parts
		Total	. . . .	114	

List of Contributions

LIST OF CONTRIBUTIONS

FROM THE WOODS HOLE OCEANOGRAPHIC INSTITUTION

See Author Index in *Collected Reprints* 1950 for a complete list up to that year.

No. 366. Bostwick H. Ketchum. Plankton Algae and their Biological Significance. In: Manual of Phycology — an Introduction to the Algae and their Biology, Ch. 17, pp. 335–346. Gilbert M. Smith, Editor. Published by The Chronica Botanica Co., Waltham, Mass. 1951.

No. 401. W. S. Butcher. A New Species of *Nonion* (Foraminifera) from the Woods Hole Region. *Contr. Cushman Lab. Foram. Res.*, Vol. 24, (1), No. 308, pp. 21–23. 1948.

No. 402. Edward S. Deevey, Jr. On the Date of the Last Rise of Sea Level in Southern New England, with Remarks on the Grassy Island Site. *Amer. Jour. Sci.*, Vol. 246, pp. 329–352. 1948.

No. 403. Charles M. Weiss. The Abnormal Development of Tunicates Attached to Glass Surfaces Adjacent to Antifouling Paints. *Ecology*, Vol. 29, No. 2, pp. 215–218. 1948.

No. 404. Charles M. Weiss. The Seasonal Occurrence of Sedentary Marine Organisms in Biscayne Bay, Florida. *Ecology*, Vol. 29, No. 2, pp. 153–172. 1948.

No. 405. R. B. Montgomery. Vertical Eddy Flux of Heat in the Atmosphere. *Jour. Meteorology*, Vol. 5, No. 6, pp. 265–274. 1948.

No. 406. Hilary B. Moore. The Zooplankton of the Upper Waters of the Bermuda Area of the North Atlantic. *Sears Found., Jour. Mar. Res.*, Vol. 12, Art. 2, pp. 1–97. 1949. (Not included in *Collected Reprints.*)

No. 407. H. R. Seiwell. Evaluation of Sea-Surface Roughness from Underwater-Pressure Recordings. *Trans. Amer. Geophys. Union*, Vol. 29, No. 2, pp. 197–201. 1948.

No. 408. Henry Stommel. The Westward Intensification of Wind-Driven Ocean Currents. *Trans. Amer. Geophys. Union*, Vol. 29, No. 2, pp. 202–206. 1948.

No. 409. Sidney C. Hsiao. The Simple Micromethod for Rapid Extraction of Lipids. *Science*, Vol. 107, No. 2766, pp. 24–25. 1948.

No. 410. Austin H. Clark. Some Interesting Starfishes and Brittle-Stars Dredged by the *Atlantis* in the Mid-Atlantic. *Jour. Wash. Acad. Sci.*, Vol. 38, No. 2, pp. 75–78. 1948.

No. 411. Alfred C. Redfield and Charles M. Weiss. The Resistance of Metallic Silver to Marine Fouling. *Biol. Bull.*, Vol. 94, No. 1, pp. 25–28. 1948.

No. 412. J. B. Hersey and H. B. Moore. Progress Report on Scattering Layer Observations in the Atlantic Ocean. *Trans. Amer. Geophys. Union*, Vol. 29, No. 3, pp. 341–354. 1948.

No. 413. Gardner Emmons. Vertical Distributions of Temperature and Humidity over the Ocean between Nantucket and New Jersey. *Papers in Physical Oceanography and Meteorology*, Vol. 10, No. 3, pp. 1–89. 1947.

No. 414. W. T. Edmondson and Yvette H. Edmondson. Measurements of Production in Fertilized Salt-Water. *Sears Found., Jour. Mar. Res.*, Vol. 6, No. 3, pp. 228–245. 1947.

No. 415. J. Lamar Worzel and Maurice Ewing. Propagation of Sound in the Ocean: Explosion Sounds in Shallow Water. *Mem. Geol. Soc. Amer.*, 27, pp. i–vi, 1–53. 1948.

C. L. Pekeris. Propagation of Sound in the Ocean: Theory of Propagation of Explosive Sound in Shallow Water. *Mem. Geol. Soc. Amer.*, 27, pp. i–viii, 1–117. 1948.

Maurice Ewing and J. Lamar Worzel. Propagation of Sound in the Ocean: Long-Range Sound Transmission. *Mem. Geol. Soc. Amer.*, 27, pp. i–v, 1–35. 1948. (Not included in *Collected Reprints.*)

No. 416. Sidney Cornell. The Collapse of Long Cylindrical Shells under External Pressure. *Soc. Exper. Stress Analysis*, Vol. 6, No. 1, pp. 111–114. 1948.

No. 417. Alfred H. Woodcock. The Swimming of Dolphins. *Nature*, Vol. 161, p. 602. 1948.

No. 418. J. M. Richardson, A. B. Arons and R. R. Halverson. Hydrodynamic Properties of Sea Water at the Front of a Shock Wave. *Jour. Chem. Physics*, Vol. 15, No. 11, pp. 785–794. 1947.

No. 419. Bostwick H. Ketchum and Jean Keen. Unusual Phosphorus Concentrations in the Florida "Red Tide" Sea Water. *Sears Found., Jour. Mar. Res.*, Vol. 7, No. 1, pp. 17–21. 1948.

No. 420. C. A. Barnes, D. F. Bumpus and John Lyman. Ocean Circulation in Marshall Islands Area. *Trans. Amer. Geophys. Union*, Vol. 29, No. 6, pp. 871–876. 1948.

No. 421. William S. von Arx. The Circulation Systems of Bikini and Rongelap Lagoons. *Trans. Amer. Geophys. Union*, Vol. 29, No. 6, pp. 861–870. 1948. Revised and published as *Geol. Survey Prof. Pap.* No. 260-b. In: Bikini and nearby Atolls. Pt. 2, Oceanography (Physical), pp. 265–273. 1954.

No. 422. William L. Ford. Radiological and Salinity Relationships in the Water at Bikini Atoll. *Trans. Amer. Geophys. Union*, Vol. 30, No. 1, pp. 46–54. 1949.

No. 423. R. B. Montgomery. Ivory's Psychrometric Formula and the Concepts of Equivalent Temperature and Wet-Bulb Temperature. *Jour. Meteorology*, Vol. 5, No. 3, pp. 113–115. 1948.

No. 424. Parker D. Trask, Fred B Phleger, Jr., and Henry C. Stetson. Recent Changes in Sedimentation in the Gulf of Mexico. *Science*, Vol. 106, No. 2759, pp. 460–461. 1947.

No. 425. George L. Clarke and David W. Bishop. The Nutritional Value of Marine Zooplankton with a Consideration of its Use as an Emergency Food. *Ecology*, Vol. 29, No. 1, pp. 54–71. 1948.

No. 426. J. Lamar Worzel. Ocean Bottom Sampler for Ships Under Way. *Geophysics*, Vol. 13, No. 3, pp. 452–456. 1948.

No. 427. Clinton M. Osborn. Factors Influencing the Growth of Integumentary Pigment in Fishes. I. The Role of Light. *Proc. Soc. Exper. Biol. and Med.*, Vol. 67, pp. 440–445. 1948.

No. 428. A. W. Jacobson. An Instrument for Recording Continuously the Salinity, Temperature, and Depth of Sea Water. *Trans. Amer. Inst. Elec. Eng.*, Vol. 67, pp. 1–9. 1948.

No. 429. Fred B Phleger, Jr. Foraminifera of a Submarine Core from the Caribbean Sea. *Kungl. Vet.-o. Vittern. Samh. Handl.*, F. 6, Ser. B, Bd. 5, No. 14, pp. 1–9. 1948.

No. 430. A. B. Arons, J. P. Slifko and A. Carter. Secondary Pressure Pulses due to gas Globe Oscillation in Underwater Explosions. I. Experimental Data. *Jour. Acoust. Soc. Amer.*, Vol. 20, No. 3, pp. 271–276. 1948.

No. 431. A. B. Arons. Secondary Pressure Pulses due to Gas Globe Oscillation in Underwater Explosions. II. Selection of Adiabatic Parameters in the Theory of Oscillation. *Jour. Acoust. Soc. Amer.*, Vol. 20, No. 3, pp. 277–282. 1948.

No. 432. Talbot H. Waterman. Studies on Deep-Sea Angler-Fishes (Ceratioidea). III. The Comparative Anatomy of *Gigantactis longicirra* Waterman. *Jour. Morphology*, Vol. 82, No. 2, pp. 81–149. 1948.

No. 433. L. N. Liebermann. Reflection of Sound from Coastal Sea Bottoms. *Jour. Acoust. Soc. Amer.*, Vol. 20, No. 3, pp. 305–309. 1948.

No. 434. Charles M. Weiss. Seasonal and Annual Variations in the Attachment and Survival of Barnacle Cyprids. *Biol. Bull.*, Vol. 94, No. 3, pp. 236–243. 1948.

No. 435. H. R. Seiwell. Sea Surface Roughness Measurements in Theory and Practice. *Annals N. Y. Acad. Sci.*, Vol. 51, Art. 3, pp. 483–501. 1949.

No. 436. H. R. Seiwell. Results of Research on Surface Waves of the Western North Atlantic. I. Investigation of Bottom Pressure Fluctuations and Surface Waves. II. Results of Sea Roughness Determinations in the Vicinity of Woods Hole, Massachusetts and Bermuda. *Papers in Physical Oceanography and Meteorology*, Vol. 10, No. 4, pp. 1–56. 1948.

No. 437. A. B. Arons and R. H. Cole. Design and Use of Piezoelectric Gauges for Measurement of Large Transient Pressures. *Review of Sci. Instruments*, Vol. 21, No. 1, pp. 31–38. 1950.

No. 438. Arthur A. Klebba. Details of Shore-Based Wave Recorder and Ocean Wave Analyzer. *Annals N. Y. Acad. Sci.*, Vol. 51, Art. 3, pp. 533–544. 1949.

No. 439. Athelstan F. Spilhaus. Drop Size, Intensity and Radar Echo of Rain. *Jour. Meteorology*, Vol. 5, No. 4, pp. 161–164. 1948.

No. 440. Athelstan F. Spilhaus and Arthur R. Miller. The Sea Sampler. *Sears Found., Jour. Mar. Res.*, Vol. 7, No. 3, pp. 370–385. 1948.

No. 441. Gordon A. Riley and Samy Gorgy. Quantitative Studies of Summer Plankton Populations of the Western North Atlantic. *Sears Found., Jour. Mar. Res.*, Vol. 7, No. 2, pp. 100–121. 1948.

No. 442. Alfred C. Redfield. The Exchange of Oxygen across the Sea Surface. *Sears Found., Jour. Mar. Res.*, Vol. 7, No. 3, pp. 347–361. 1948.

No. 443. Patricia A. Langwell. Inhomogeneities of Turbulence, Temperature, and Moisture in the West Indies Trade-wind Region. *Jour. Meteorology*, Vol. 5, No. 5, pp. 243–246. 1948.

No. 444. Fred B. Phleger, Jr. Origin and Deposition of Deep Sea Sediments. *Trans. Amer. Geophys. Union*, Vol. 30, No. 2, pp. 180–182. 1949.

No. 445. B. Haurwitz. The Effect of Ocean Currents on Internal Waves. *Sears Found., Jour. Mar. Res.*, Vol. 7, No. 3, pp. 217–228. 1948.

No. 446. Bostwick H. Ketchum, Cornelia L. Carey and Margaret Briggs. Preliminary Studies on the Viability and Dispersal of Coliform Bacteria in the Sea. *In* Limnological Aspects of Water Supply and Waste Disposal. Ed. F. R. Moulton and and Florence Hitzel. *Publ. Amer. Assoc. Adv. Sci.*, pp. 64–73. 1949.

No. 447. Henry B. Bigelow and William C. Schroeder. New Genera and Species of Batoid Fishes. *Sears Found., Jour. Mar. Res.*, Vol. 7, No. 3, pp. 543–566. 1948.

No. 448. Hilary B. Moore. A Camera for Producing One-Dimensional Reduction in Narrow Records. *Sears Found., Jour. Mar. Res.*, Vol. 8, No. 1, pp. 21–23. 1949.

No. 449. A. B. Arons and D. R. Yennie. Energy Partition in Underwater Explosion Phenomena. *Rev. Modern Physics*, Vol. 20, No. 3, pp. 519–536. 1948. (Not included in *Collected Reprints*.)

No. 450. J. B. Hersey and Maurice Ewing. Seismic Reflections from beneath the Ocean Floor. *Trans. Amer. Geophys. Union*, Vol. 30, No. 1, pp. 5–14. 1949.

No. 451. C. O'D. Iselin and Frederick C. Fuglister. Some Recent Developments in the Study of the Gulf Stream. *Sears Found., Jour. Mar. Res.*, Vol. 7, No. 3, pp. 317–329. 1948.

No. 452. Norris W. Rakestraw and Dayton E. Carritt. Some Seasonal Chemical Changes in the Open Ocean. *Sears Found., Jour. Mar. Res.*, Vol. 7, No. 3, pp. 362–369. 1948.

No. 453. Henry Stommel. The Theory of the Electric Field Induced in Deep Ocean Currents. *Sears Found., Jour. Mar. Res.*, Vol. 7, No. 3, pp. 386–392. 1948.

No. 454. Parker D. Trask. Oceanography and Geosynclines. *Sears Found., Jour. Mar. Res.*, Vol. 7, No. 3, pp. 679–685. 1948.

No. 455. L. N. Liebermann. Reflection of Underwater Sound from the Sea Surface. *Jour. Acoust. Soc. Amer.*, Vol. 20, No. 4, pp. 498–503. 1948.

No. 456. Lewis F. Richardson and Henry Stommel. Note on Eddy Diffusion in the Sea. *Jour. Meteorology*, Vol. 5, No. 5, pp. 238–240. 1948.

No. 457. Joanne Starr Malkus. Effects of Wind Shear on Some Aspects of Convection. *Trans. Amer. Geophys. Union*, Vol. 30, No. 1, pp. 19–25. 1949.

No. 458. Alfred H. Woodcock and Mary M. Gifford. Sampling Atmospheric Sea-Salt Nuclei over the Ocean. *Sears Found., Jour. Mar. Res.*, Vol. 8, No. 2, pp. 177–197. 1949.

No. 459. William L. Ford. The Field Use of a Salinity-Temperature-Depth Recorder. *Sears Found., Jour. Mar. Res.*, Vol. 8, No. 1, pp. 84–96. 1949.

No. 460. William E. Schevill and Barbara Lawrence. Underwater Listening to the White Porpoise (*Delphinapterus leucas*). *Science*, Vol. 109, No. 2824, pp. 143–144. 1949.

No. 461. H. R. Seiwell and George P. Wadsworth. A New Development in Ocean Wave Research. *Science*, Vol. 109, No. 2829, pp. 271–274. 1949.

No. 462. Harry J. Turner, Jr., John C. Ayers and Charles L. Wheeler. Report on Investigations of the Propagation of the Soft-Shell Clam, *Mya arenaria*. *Com. Mass., Dept. Cons., Div. Mar. Fish.*, pp. 1–61. 1948.

No. 463. Floyd M. Soule and E. R. Challender. Discussion of some of the Effects of Winds on Ice Distribution in the Vicinity of the Grand Banks and the Labrador Shelf. *U. S. Coast Guard Bull.*, No. 33, pp. 59–61. 1949.

No. 464. Gordon A. Riley, Henry Stommel and D. F. Bumpus. Quantitative Ecology of the Plankton of the Western North Atlantic. *Bull. Bingham Oceanographic Coll.*, Vol. 12, Art. 3, pp. 1–169. 1949. (Not included in *Collected Reprints*.)

No. 465. A. F. Bunker, B. Haurwitz, J. S. Malkus and H. Stommel. Vertical Distribution of Temperature and Humidity over the Caribbean Sea. *Papers in Physical Oceanography and Meteorology*, Vol. 11, No. 1, pp. 1–82. 1949.

No. 466. David M. Pratt. Experiments in the Fertilization of a Salt Water Pond. *Sears Found., Jour. Mar. Res.*, Vol. 8, No. 1, pp. 36–59. 1949.

No. 467. Floyd M. Soule, H. H. Carter and L. A. Cheney. Oceanography of the Grand Banks Region and Labrador Sea, 1948. *U. S. Coast Guard Bull.*, No. 34, pp. 67–118. 1950.

No. 468. Richard A. Craig. Vertical Eddy Transfer of Heat and Water Vapor in Stable Air. *Jour. Meteorology*, Vol. 6, No. 2, pp. 123–133. 1949.

No. 469. Henry Stommel. Trajectories of Small Bodies Sinking Slowly through Convection Cells. *Sears Found., Jour. Mar. Res.*, Vol. 8, No. 1, pp. 24–29. 1949.

No. 470. Henry W. Menard, Jr. Synthesis of Sand Mixtures. *Jour. Sed. Petrology*, Vol. 19, No. 2, pp. 71–77. 1949.

No. 471. Austin H. Clark. Echinoderms from the Mid-Atlantic Dredged by the *Atlantis* in the Summer of 1948. *Jour. Wash. Acad. Sci.*, Vol. 39, No. 11, pp. 371–377. 1949.

No. 472. Gordon A. Riley and Ruth Von Arx. Theoretical Analysis of Seasonal Changes in the Phytoplankton of Husan Harbor, Korea. *Sears Found., Jour. Mar. Res.*, Vol. 8, No. 1, pp. 60–72. 1949.

No. 473. Bostwick H. Ketchum, Lois Lillick and Alfred C. Redfield. The Growth and Optimum Yields of Unicellular Algae in Mass. Culture. *Jour. Cell. and Comp. Physiol.*, Vol. 33, No. 3, pp. 267–279. 1949.

No. 474. Bostwick H. Ketchum and Alfred C. Redfield. Some Physical and Chemical Characteristics of Algae Grown in Mass. Culture. *Jour. Cell. and Comp. Physiol.*, Vol. 33, No. 3, pp. 281–299. 1949.

No. 475. Joanne Starr Malkus. Cumulus, Thermals and Wind. *Soaring*, Vol. 13, Nos. 9–10, pp. 6–9, 12. 1949.

No. 476. Henry W. Menard. Transportation of Sediment by Bubbles. *Jour. Sed. Petrology*, Vol. 20, No. 2, pp. 98–106. 1950.

No. 477. B. Haurwitz. Internal Waves of Tidal Character. *Trans. Amer. Geophys. Union*, Vol. 31, No. 1, pp. 47–52. 1950.

No. 478. Richard A. Craig and R. B. Montgomery. Evaporation (Measured) from Ocean into Hydrostatically Stable Air. *Jour. Meteorology*, Vol. 6, No. 6, pp. 426-427. 1949.

No. 479. Athelstan F. Spilhaus, A. Ehrlich and Arthur R .Miller. Hydrostatic Instability in the Ocean. *Trans. Amer. Geophys. Union*, Vol. 31, No. 2, pp. 213–215. 1950.

No. 480. Maurice Ewing, J. L. Worzel, N. C. Steenland and Frank Press. Geophysical Investigations in the Emerged and Submerged Atlantic Coastal Plain. Part V: Woods Hole, New York, and Cape May Sections. *Bull. Geol. Soc. Amer.*, Vol. 61, pp. 877–892. 1950.

No. 481. Mary Sears. Notes on Siphonophores. I. Siphonophores from the Marshall Islands. *Sears Found., Jour. Mar. Res.*, Vol. 9, No. 1, pp. 1–16. 1950.

No. 482. R. B. Montgomery. The Taylor Diagram (Temperature against Vapor Pressure) for Air Mixtures. *Arch. Meteorol. Geoph. u. Bioklim.*, Ser. A: Meteorol. und Geoph., Band II, Heft 2–3, pp. 163–183. 1950.

No. 483. Maurice Ewing, J. L. Worzel, J. B. Hersey, Frank Press and G. R. Hamilton. Seismic Refraction Measurements in the Atlantic Ocean Basin. (Part I). *Bull. Seismol. Soc. Amer.*, Vol. 40, No. 3, pp. 233–242. 1950.

No. 484. Fred B. Phleger. The Foraminifera. *In* The Boylston Street Fishweir II. *Papers Robert S. Peabody Found. Archaeol.*, Vol. 4, No. 1, pp. 99–108. 1949.

No. 485. Fred B. Phleger. Submarine Geology and Pleistocene Research. A Review by the Members of the Committee on Interrelations of Pleistocene Research, National Research Council. 8. Submarine Geology and Pleistocene Research. *Bull. Geol. Soc. Amer.*, Vol. 60, pp. 1457–1461. 1949.

No. 486. H. R. Seiwell. The Principles of Time Series Analyses Applied to Ocean Wave Data. *Proc. Nat. Acad. Sci.*, Vol. 35, No. 9, pp. 518–528. 1949.

No. 487. Henry C. Stetson. The Sediments and Stratigraphy of the East Coast Continental Margin: Georges Bank to Norfolk Canyon. *Papers in Physical Oceanography and Meteorology*, Vol. 11, No. 2, pp. 1–60. 1949.

No. 488. Martin J. Pollak. Notes on Determining the Depths of Sampling in Serial Oceanographic Observations. *Sears Found., Jour. Mar. Res.*, Vol. 9, No. 1, pp. 17–20. 1950.

No. 489. Alfred H. Woodcock. Subsurface Pelagic Sargassum. *Sears Found., Jour. Mar. Res.*, Vol. 9, No. 2, pp. 77–92. 1950.

No. 490. A. B. Arons and D. R. Yennie. Phase Distortion of Acoustic Pulses Obliquely Reflected from a Medium of Higher Sound Velocity. *Jour. Acoust. Soc. Amer.*, Vol. 22, No. 2, pp. 231–237. 1950.

No. 491. Rushdi Said. Foraminifera of Narragansett Bay. *Contr. Cushman Found. Foram. Res.*, Vol. 2, (3), pp. 75–86. 1951.

No. 492. William L. Ford. Seagoing Photoelectric Colorimeter. *Analytical Chemistry*, Vol. 22, No. 11, pp. 1431–1435. 1950.

No. 493. Henry W. Menard. Current-Ripple Profiles and their Development. *Jour. Geology*, Vol. 58, No. 2, pp. 152–153. 1950.

No. 494. Jack L. Hough. Pleistocene Lithology of Antarctic Ocean-Bottom Sediments. *Jour. Geology*, Vol. 58, No. 3, pp. 254–260. 1950.

No. 495. Martin J. Pollak. The Water Structure in the Brownson Deep. *Trans. Amer. Geophys. Union*, Vol. 31, No. 3, pp. 393–397. 1950.

No. 496. Henry Stommel. Horizontal Diffusion Due to Oceanic Turbulence. *Sears Found., Jour. Mar. Res.*, Vol. 8, No. 3, pp. 199–225. 1949.

No. 497. David M. Pratt. Experimental Study of the Phosphorus Cycle in Fertilized Salt Water. *Sears Found., Jour. Mar. Res.*, Vol. 9, No. 1, pp. 29–54. 1950.

No. 498. Ivan Tolstoy and Maurice Ewing. North Atlantic Hydrography and the Mid-Atlantic Ridge. *Bull. Geol. Soc. Amer.*, Vol. 60, pp. 1527–1540. 1949.

No. 499. William S. von Arx. An Electromagnetic Method for Measuring the Velocities of Ocean Currents from a Ship Under Way. *Papers in Physical Oceanography and Meteorology*, Vol. 11, No. 3, pp. 1–62. 1950.

No. 500. Floyd M. Soule and C. A. Barnes. Physical Oceanography of the Ice Patrol Area in 1941. *U. S. Coast Guard Bull.*, No. 31, pp. 1–62. 1950.

No. 501. Alfred H. Woodcock. Condensation Nuclei and Precipitation. *Jour. Meteorology*, Vol. 7, No. 2, pp. 161–162. 1950.

No. 502. Andrew F. Bunker. Fluctuations of the Vertical Component of the Wind Associated with the Outflow of Cold Air from a Thunderstorm. *Bull. Amer. Meteorol. Soc.*, Vol. 31, No. 5, pp. 178–180. 1950.

No. 503. Henry Stommel. The Gulf Stream. A Brief History of the Ideas Concerning Its Cause. *The Scientific Monthly*, Vol. 70, No. 4, pp. 242–253. 1950.

No. 504. H. R. Seiwell. A New Mechanical Autocorrelator. *Review of Sci. Instruments*, Vol. 21, No. 5, pp. 481–484. 1950.

No. 505. H. R. Seiwell. Problems in Statistical Analyses of Geophysical Time Series. *Science*, Vol. 112, No. 2905, pp. 243–246. 1950.

No. 506. Ralph F. Vaccaro, Margaret P. Briggs, Cornelia L. Carey and Bostwick H. Ketchum. Viability of *Escherichia coli* in Sea Water. *Amer. Jour. Public Health*, Vol. 40, No. 10, pp. 1257–1266. 1950.

No. 507. Fred B. Phleger and William R. Walton. Ecology of Marsh and Bay Foraminifera, Barnstable, Mass. *Amer. Jour. Sci.*, Vol. 248, pp. 274–294. 1950.

No. 508. Jan Hahn. Some Aspects of Deep Sea Underwater Photography. *Jour. Photo. Soc. Amer.*, Sect. B. Phot. Sci. Tech., Vol. 16, No. 6, pp. 27–29. 1950.

No. 509. William S. von Arx. Some Current Meters Designed for Suspension from an Anchored Ship. *Sears Found., Jour. Mar. Res.*, Vol. 9, No. 2, pp. 93–99. 1950.

No. 510. Harry J. Turner, Jr. Report on Investigations of Methods of Improving the Shellfish Resources of Massachusetts. *Com. Mass., Dept. Cons., Div. Mar. Fish.*, pp. 1–22. 1949. (Included in *Collected Reprints* for 1950.)

No. 511. Henry B. Bigelow and William C. Schroeder. New and Little Known Cartilaginous Fishes from the Atlantic. *Bull. Mus. Comp. Zool.*, Vol. 103, No. 7, pp. 385–408. 1950.

No. 512. Henry W. Menard. Sediment Movement in Relation to Current Velocity. *Jour. Sed. Petrology*, Vol. 20, No. 3, pp. 148–160. 1950.

No. 513. B. Haurwitz and H. A. Panofsky. Stability and Meandering of the Gulf Stream. *Trans. Amer. Geoph. Union*, Vol. 31, No. 5, pp. 723–731. 1950.

No. 514. Alfred C. Redfield. Some Applications of Oceanography to Engineering Problems. *Jour. Boston Soc. Civil Eng.*, Vol. 37, No. 3, pp. 275–295. 1950.

No. 515. Bostwick H. Ketchum. Hydrographic Factors Involved in the Dispersion of Pollutants Introduced into Tidal Waters. *Jour. Boston Soc. Civil Eng.*, Vol. 37, No. 3, pp. 296–314. 1950.

No. 516. Bostwick H. Ketchum. The Exchanges of Fresh and Salt Waters in Tidal Estuaries. *Sears Found.*, *Jour. Mar. Res.*, Vol. 10, No. 1, pp. 18–38. 1951.

No. 517. Alfred H. Woodcock. Impact Deposition of Atmospheric Sea Salts on a Test Plate. *Amer. Soc. for Testing Materials*, Vol. 50, pp. 1151–1166. 1950.

No. 518. Arthur R. Miller. A Study of Mixing Processes over the Edge of the Continental Shelf. *Sears Found.*, *Jour. Mar. Res.*, Vol. 9, No. 2, pp. 145–160. 1950.

No. 519. Vern O. Knudsen, Alfred C. Redfield, Roger Revelle, and Robert R. Shrock. Education and Training for Oceanographers. *Science*, Vol. 111, No. 2895, pp. 700–703. 1950.

No. 520. George L. Clarke. Conservation and the Productivity of the Sea. *The Gamma Alpha Record*, Vol. 40, No. 4, pp. 95–101. 1950.

No. 521. H. R. Seiwell. Ocean Wave Analyses. In: Symposium on Applications of Autocorrelation Analysis to Physical Problems, Woods Hole, Massachusetts, 13–14 June 1949, *Office of Naval Research*, NAVEXOS-P-735, pp. 74–79. 1950.

No. 522. Alfred H. Woodcock and A. F. McBride. Wave-riding Dolphins. *Jour. Exper. Biol.*, Vol. 28, No. 2, pp. 215–217. 1951.

No. 523. John Northrop and Bruce C. Heezen. An Outcrop of Eocene Sediment on the Continental Slope. *Jour. Geology*, Vol. 59, No. 4, pp. 396–399. 1951.

No. 524. Henry Stommel. An Example of Thermal Convection. *Trans. Amer. Geophys. Union*, Vol. 31, No. 4, pp. 553–554. 1950.

No. 525. Alfred C. Redfield. Hemocyanin. In: Copper Metabolism, A Symposium on Animal, Plant and Soil Relationships, W. D. McElroy and B. Glass, Editors, Johns Hopkins University Press, pp. 174–190. 1950.

No. 526. William S. von Arx. Dead Reckoning by Surface Current Observation. *Jour. Inst. Navigation* (London), Vol. 4, No. 2, pp. 117–125. 1951.

No. 527. Patricia A. Langwell. Forced Convection Cell Circulation in Clear Air. *Trans. Amer. Geophys. Union*, Vol. 32, No. 1, pp. 7–14. 1951.

No. 528. Alfred H. Woodcock. Sea Salt in a Tropical Storm. *Jour. Meteorology*, Vol. 7, No. 6, pp. 397–401. 1950.

No. 529. Alfred C. Redfield. The Analysis of Tidal Phenomena in Narrow Embayments. *Papers in Physical Oceanography and Meteorology*, Vol. 11, No. 4, pp. 1–36. 1950.

No. 530. G. L. Clarke and D. F. Bumpus. The Plankton Sampler — An Instrument for Quantitative Plankton Investigations. *Amer. Soc. Limnol. and Oceanogr.*, Spec. Publ. No. 5 (revised), pp. 1–8. 1950.

No. 531. H. R. Seiwell. Experimental Correlogram Analyses of Artificial Time Series (with Special Reference to Analyses of Oceanographic Data). In: Proc. Second Berkeley Symposium on Mathematical Statistics and Probability, Univ. Calif. Press, pp. 639–666. 1951. (Published posthumously.)

No. 532. Henry Stommel. An Elementary Explanation of Why Ocean Currents are Strongest in the West. *Bull. Amer. Meteorol. Soc.*, Vol. 32, No. 1, pp. 21–23. 1951.

No. 533. Henry Stommel. Entrainment of Air into a Cumulus Cloud II. *Jour. Meteorol.*, Vol. 8, No. 2, pp. 127–129. 1951.

No. 534. Joanne Starr Malkus, Andrew F. Bunker and Kenneth McCasland. A Formation of Pileus-like Veil Clouds over Cape Cod, Massachusetts. *Bull. Amer. Meteorol. Soc.*, Vol. 32, No. 2, pp. 61–66. 1951.

No. 535. Hilary B. Moore. The Relation between the Scattering Layer and the Euphausiacea. *Biol. Bull.*, Vol. 99, No. 2, pp. 181–212. 1950.

No. 536. Bostwick H. Ketchum. The Flushing of Tidal Estuaries. *Sewage and Industrial Wastes*, Vol. 23, No. 2, pp. 198–209. 1951.

No. 537. Henry Stommel. Streaks of Natural Water Surfaces. In: International Symposium on Atmospheric Turbulence in the Boundary Layer. Mass. Inst. Tech., 4–8 June, 1951. *Geophys. Res. Pap., Air Force Cambridge Research Center*, No. 19, pp. 145–154. 1952.

No. 538. Henry Stommel. Streaks on Natural Water Surfaces. *Weather*, Vol. 6, No. 3, pp. 72–74. 1951.

No. 539. Edward S. Castle. Electrical Control of Marine Fouling. *Ind. Eng. Chem.*, Vol. 43, No. 4, pp. 901–904. 1951.

No. 540. Rushdi Said. Organic Origin of some Calcareous Sediments from the Red Sea. *Science*, Vol. 113, No. 2940, pp. 517–518. 1951.

No. 541. Rushdi Said. Preliminary Note on the Spectroscopic Distribution of Elements in the Shells of some Recent Calcareous Foraminifera. *Contr. Cushman Found. Foram. Res.*, Vol. 2, Pt. 1, pp. 11–13. 1951.

No. 542. Gordon A. Riley. Oxygen, Phosphate and Nitrate in the Atlantic Ocean. *Bull. Bingham Oceanographic Coll.*, Vol. 13, Art. 1, pp. 1–126. 1951. (Not included in *Collected Reprints*.)

No. 543. J. Lamar Worzel and Maurice Ewing. Gravity Measurements at Sea, 1947. *Trans. Amer. Geophys. Union*, Vol. 31, No. 6, pp. 917–923. 1950.

No. 544. Arnold B. Arons and Henry Stommel. A Mixing-length Theory of Tidal Flushing. *Trans. Amer. Geophys. Union*, Vol. 32, No. 3, pp. 419–421. 1951.

No. 545. Arthur A. Klebba and Henry Stommel. A Simple Demonstration of Coriolis Force. *Amer. Jour. Physics*, Vol. 19, No. 4, p. 247. 1951.

No. 546. Henry W. Menard and A. J. Boucot. Experiments on the Movement of Shells by Water. *Amer. Jour. Sci.*, Vol. 249, No. 2, pp. 131–151. 1951.

No. 547. E. W. Roelofs and D. F. Bumpus. The Hydrography of Pamlico Sound. *Bull. Mar. Sci. Gulf and Caribbean*, Vol 3, No. 3, pp. 181–205. 1953.

No. 548. Frederick C. Fuglister and L. V. Worthington. Some Results of a Multiple Ship Survey of the Gulf Stream. *Tellus*, Vol. 3, No. 1, pp. 1–14. 1951.

No. 549. Bostwick H. Ketchum, Alfred C. Redfield and John C. Ayers. The Oceanography of the New York Bight. *Papers in Physical Oceanography and Meteorology*, Vol. 12, No. 1, pp. 1–46. 1951.

No. 550. Floyd M. Soule. Physical Oceanography of the Grand Banks Region, the Labrador Sea and Davis Strait in 1949. *U. S. Coast Guard Bull.*, No. 35, pp. 49–116. 1951.

No. 551. Floyd M. Soule. Physical Oceanography of the Grand Banks Region and the Labrador Sea in 1950. *U. S. Coast Guard Bull.*, No. 36, pp. 61–127. 1951.

No. 552. Henry Stommel. Determination of the Lateral Eddy Diffusivity in the Climatological Mean Gulf Stream. *Tellus*, Vol. 3, No. 1, p. 43. 1951.

No. 553. Henry Stommel and Alfred H. Woodcock. Diurnal Heating of the Surface of the Gulf of Mexico in the Spring of 1942. *Trans. Amer. Geophys. Union*, Vol. 32, No. 4, pp. 565–571. 1951.

No. 554. Henry B. Bigelow and William C. Schroeder. A New Genus and Species of Anacanthobatid Skate from the Gulf of Mexico. *Journ. Wash. Acad. Sci.*, Vol. 41, No. 3, pp. 110–113. 1951.

No. 555. Henry B. Bigelow and William C. Schroeder. Three New Skates and a New Chimaerid Fish from the Gulf of Mexico. *Journ. Wash. Acad. Sci.*, Vol. 41, No. 12, pp. 383–392. 1951.

No. 556. Martin J. Pollak. The Sources of the Deep Water of the Eastern Mediterranean Sea. *Sears Found., Jour. Mar. Res.*, Vol. 10, No. 1, pp. 128–152. 1951.

No. 557. Frederick C. Fuglister. Annual Variations in Current Speeds in the Gulf Stream System. *Sears Found., Jour. Mar. Res.*, Vol. 10, No. 1, pp. 119–127. 1951.

No. 558. Donald Parson and Andrew F. Bunker. A Recording Computer for the Direct Measurement of the Turbulent Heat Exchange in the Atmosphere. In: International Symposium on Atmospheric Turbulence in the Boundary Layer. Mass. Inst. Tech., 4–8 June, 1951. *Geophys. Res. Pap., Air Force Cambridge Research Center*, No. 19, pp. 369–379. 1952.

No. 559. Ivan Tolstoy. Submarine Topography in the North Atlantic. *Bull. Geol. Soc. Amer.*, Vol. 62, No. 5, pp. 441–450. 1951.

No. 560. Hilary B. Moore. The Seasonal Distribution of Oceanic Birds in the Western North Atlantic. *Bull. Mar. Sci. Gulf and Caribbean*, Vol. 1, No. 1, pp. 1–14. 1951.

No. 561. Bostwick H. Ketchum, John C. Ayers and Ralph F. Vaccaro. Processes Contributing to the Decrease of Coliform Bacteria in a Tidal Estuary. *Ecology*, Vol. 33, No. 2, pp. 247–258. 1952.

No. 562. J. B. Hersey, H. R. Johnson and L. C. Davis. Recent Findings about the Deep Scattering Layer. *Sears Found., Jour. Mar. Res.*, Vol. 11, No. 1, pp. 1–9. 1952.

No. 563. Alfred H. Woodcock. Atmospheric Salt Particles and Raindrops. *Jour. Meteorol.*, Vol. 9, No. 3, pp. 200–212. 1952.

No. 564. Harry J. Turner, Jr., David B. Sawyer, Carl N. Shuster, Jr., and Julius A. Posgay. Third Report on Investigations of Methods of Improving the Shellfish Resources of Massachusetts. *Com. Mass., Dept. Cons., Div. Mar. Fish.*, pp. 1–31. 1951.

No. 565. Fred B. Phleger. Ecology of Foraminifera, Northwest Gulf of Mexico. Part I. Foraminifera Distribution. *Mem. Geol. Soc. Amer.*, No. 46, pp. 1–88. 1951. (Not included in *Collected Reprints.*)

No. 566. Fred B. Phleger and Frances L. Parker. Ecology of Foraminifera, Northwest Gulf of Mexico. Part II. Foraminifera Species. *Mem. Geol. Soc. Amer.*, No. 46, pp. 1–64. 1951. (Not included in *Collected Reprints.*)

No. 567. Bostwick H. Ketchum and William L. Ford. Rate of Dispersion in the Wake of a Barge at Sea. *Trans. Amer. Geophys. Union*, Vol. 33, No. 5, pp. 680–684. 1952.

No. 568. Patricia A. Langwell. The Onset of Rain from Cumuli. *Jour. Meteorol.*, Vol. 8, No. 5, pp. 354–356. 1951.

No. 569. Stefan Machlup. A Theoretical Model for Sound Scattering by Marine Crustaceans. *Jour. Acoust. Soc. Amer.*, Vol. 24, No. 3, pp. 290–293. 1952.

No. 570. Henry B. Bigelow and William C. Schroeder. Fishes of the Western North Atlantic. Sawfishes, Guitarfishes, Skates and Rays. *Mem. Sears Found. Mar. Res.*, No. 1, Pt. 2, Ch. 1, pp. 1–514. 1953. (Not included in *Collected Reprints*.)

No. 571. Henry B. Bigelow and William C. Schroeder. Fishes of the Western North Atlantic. Chimaeroids. *Mem. Sears. Found. Mar. Res.*, No. 1, Pt. 2, Ch. 2, pp. 515–562. Index to Chs. 1 and 2, pp. 563–588. 1953. (Not included in *Collected Reprints*.)

No. 572. Andrew F. Bunker. Recognition of the Presence of Convective Currents within a Nonsaturated Turbulent Layer of the Atmosphere. In: International Symposium on Atmospheric Turbulence in the Boundary Layer. Mass. Inst. Tech., 4–8 June, 1951. *Geophys. Res. Pap., Air Force Cambridge Research Center*, No. 19, pp. 309–322. 1952.

No. 573. John Northrop. Ocean-bottom Photographs of the Neritic and Bathyal Environment South of Cape Cod, Massachusetts. *Bull. Geol. Soc. Amer.*, Vol. 62, No. 12, pp. 1381–1384. 1951.

No. 574. I. I. Schell. Stability and Mutual Compensation of Relationships with the Iceberg Severity off Newfoundland. *Trans. Amer. Geophys. Union*, Vol. 33, No. 1, pp. 27–31. 1952.

No. 575. D. B. Ericson, Maurice Ewing and Bruce C. Heezen. Deep-sea Sands and Submarine Canyons. *Bull. Geol. Soc. Amer.*, Vol. 62, No. 8, pp. 961–965. 1951.

No. 576. R. B. Montgomery. The Present Position of the Study of Exchange across the Ocean-Atmosphere Interface. In: International Symposium on Atmospheric Turbulence in the Boundary Layer. Mass. Inst. Tech., 4–8 June, 1951. *Geophys. Res. Pap., Air Force Cambridge Research Center*, No. 19, pp. 131–140. 1952.

No. 577. Gordon A. Riley. Parameters of Turbulence in the Sea. *Sears Found., Jour. Mar. Res.*, Vol. 10, No. 3, pp. 247–256. 1951.

No. 578. Gordon A. Riley. Hydrography of the Long Island and Block Island Sounds. *Bull. Bingham Oceanographic Coll.*, Vol. 13, Art. 3, pp. 5–39. 1952.

No. 579. Gordon A. Riley. Phytoplankton of Block Island Sound, 1949. *Bull. Bingham Oceanographic Coll.*, Vol. 13, Art. 3, pp. 40–64. 1952.

No. 580. Woods Hole Oceanographic Institution. Marine Fouling and its Prevention. U. S. Naval Inst., Annapolis, Md. 388 pp. 1952. (Not included in *Collected Reprints*.)

No. 581. Hilary B. Moore. Physical Factors Affecting the Distribution of Euphausids in the North Atlantic. *Bull. Mar. Sci. Gulf and Caribbean*, Vol. 1, No. 4, pp. 278–305. 1952.

No. 582. Henry A. Kierstead. Bottom Pressure Fluctuations due to Standing Waves in a Deep, Two-Layer Ocean. *Trans. Amer. Geophys. Union*, Vol. 33, No. 3, pp. 390–396. 1952.

No. 583. J. B. Hersey, Charles B. Officer, H. R. Johnson, and S. Bergstrom. Seismic Refraction Observations North of the Brownson Deep. *Bull. Seismol. Soc. Amer.*, Vol. 42, No. 4, pp. 291–306. 1952.

No. 584. Frederick C. Fuglister. Multiple Currents in the Gulf Stream System. *Tellus*, Vol. 3, No. 4, pp. 230–233. 1951.

No. 585. Gerald B. Collins. Factors Influencing the Orientation of Migrating Anadromous Fishes. Fish and Wildlife Service, Vol. 52, *Fish. Bull.* 73, pp. 375–396. 1952.

No. 586. Alfred C. Redfield and Lionel A. Walford. A Study of the Disposal of Chemical Waste at Sea. Report of the Committee for Investigation of Waste Disposal. *Nat. Res. Council*, Publ. 201, 49 pp. 1951.

No. 587. Henry Stommel and Harlow G. Farmer. Control of Salinity in an Estuary by a Transition. *Sears Found., Jour. Mar. Res.*, Vol. 12, No. 1, pp. 13–20. 1953.

No. 588. Rushdi Said. Foraminifera of Great Pond, East Falmouth, Massachusetts. *Contr. Cushman Found. Foram. Res.*, Vol. 4, Pt. 1, pp. 7–14. 1953.

No. 589. Frances L. Parker. Foraminifera Species off Portsmouth, New Hampshire. *Bull. Mus. Comp. Zool.*, Vol. 106, No. 9, pp. 391–423. 1952.

No. 590. Frances L. Parker. Foraminiferal Distribution in the Long Island Sound-Buzzards Bay Area. *Bull. Mus. Comp. Zool.*, Vol. 106, No. 10, pp. 427–473. 1952.

No. 591. Fred B. Phleger. Foraminifera Ecology off Portsmouth, New Hampshire. *Bull. Mus. Comp. Zool.*, Vol. 106, No. 8, pp. 315–390. 1952.

No. 592. Henry B. Bigelow and William C. Schroeder. Fishes of the Gulf of Maine. Fish and Wildlife Service, Vol. 53, *Fish. Bull.* 74, pp. i–viii, 1–577. 1953. (Not included in *Collected Reprints.*)

No. 593. Bostwick H. Ketchum and D. Jean Keen. The Exchanges of Fresh and Salt Waters in the Bay of Fundy and in Passamaquoddy Bay. *Jour. Fish. Res. Bd. Canada*, Vol. 10, No. 3, pp. 97–124. 1953.

No. 594. I. I. Schell. The Problem of the Iceberg Population in Baffin Bay and Davis Strait and Advance Estimate of the Berg Count off Newfoundland. *Jour. Glaciology*, Vol. 2, No. 11, pp. 58–59. 1952.

No. 595. Joanne Starr Malkus. Recent Advances in the Study of Convective Clouds and their Interaction with the Environment. *Tellus*, Vol. 4, No. 2, pp. 71–87. 1952.

No. 596. Henry B. Bigelow, William C. Schroeder and Stewart Springer. New and Little Known Sharks from the Atlantic and from the Gulf of Mexico. *Bull. Mus. Comp. Zool.*, Vol. 109, No. 3, pp. 213–276. 1953.

No. 597. George T. Scott and Hugh R. Haywood. Sodium and Potassium Regulation in *Ulva lactuca* and *Valonia macrophysa*. In: Electrolytes in Biological Systems, pp. 35–64. 1955.

No. 598. Bostwick H. Ketchum. Relation between Circulation and Planktonic Populations in Estuaries, *Ecology*, Vol. 35, No. 2, pp. 191–200. 1954.

No. 599. Frank J. Mather, III. Three Species of Fishes, Genus *Seriola*, in the Waters of Cape Cod and Vicinity. *Copeia*, No. 3, pp. 209–210. 1952.

No. 600. Jeffries Wyman, Jr., P. F. Scholander, G. A. Edwards and L. Irving. On the Stability of Gas Bubbles in Sea Water. *Sears Found., Jour. Mar. Res.*, Vol. 11, No. 1, pp. 47–62. 1952.

No. 601. Floyd M. Soule, P. S. Branson and R. P. Dinsmore. Physical Oceanography of the Grand Banks Region and the Labrador Sea in 1951. *U. S. Coast Guard Bull.*, No. 37, pp. 17–85. 1952.

No. 602. Mary Sears. Notes on Siphonophores. 2. A Revision of the Abylinae. *Bull. Mus. Comp. Zool.*, Vol. 109, No. 1, pp. 1–119. 1953. (Not included in *Collected Reprints.*)

No. 603. I. I. Schell. On the Role of the Ice off Iceland in the Decadal Air Temperatures of Iceland, and some other Areas. *Jour. du Conseil*, Vol. 18, No. 1, pp. 11–36. 1952.

No. 604. D. B. Ericson, Maurice Ewing and Bruce C. Heezen. Turbidity Currents and Sediments in the North Atlantic. *Bull. Amer. Assoc. Petrol. Geol.*, Vol. 36, No. 3, pp. 489–511. 1952.

No. 605. Andrew F. Bunker. On the Determination of Moisture Gradients from Radiosonde Records. *Bull. Amer. Meteorol. Soc.*, Vol. 34, No. 9, pp. 406–409. 1953.

No. 606. Frank J. Mather, III and Howard A. Schuck. Additional Notes on the Distribution of the Blackfin Tuna (*Parathunnus atlanticus*). *Copeia*, No. 4, p. 267. 1952.

No. 607. Mary Sears. Notes on Siphonophores. 3. *Nectopyramis spinosa* n. sp. *Breviora*, No. 3, pp. 1–4. 1952.

No. 608. W. V. R. Malkus and M. E. Stern. Determination of Ocean Transports and Velocities by Electromagnetic Effects. *Sears Found., Jour. Mar. Res.*, Vol. 11, No. 2, pp. 97–105. 1952.

No. 609. Joanne Starr Malkus. The Slopes of Cumulus Clouds in Relation to External Wind Shear. *Quart. Jour. Roy. Meteor. Soc.*, Vol. 78, No. 338, pp. 530–542. 1952.

No. 610. Henry B. Bigelow and William C. Schroeder. A New Species of the Cyclostome Genus *Paramyxine* from the Gulf of Mexico. *Breviora*, No. 8, pp. 1–10. 1952.

No. 611. Frank J. Mather, III. Sport Fishes of the Vicinity of the Gulf of Honduras, certain Caribbean Islands, and Carmen, Mexico. *Proc. Gulf and Caribbean Fish. Inst.*, pp. 118–129. 1952.

No. 612. C. O'D. Iselin. The Gulf Stream System. *Proc. Amer. Philos. Soc.*, Vol. 96, No. 6, pp. 660–662. 1952.

No. 613. Frederick B. Laidlaw. The History of the Prevention of Fouling. *U. S. Naval Inst. Proc.*, Vol. 78, No. 7, Whole No. 593, pp. 768–779. 1952.

No. 614. Gary Felsenfeld. The Binding of Copper by Hemocyanin. *Jour. Cell. and Comp. Physiol.*, Vol. 43, No. 1, pp. 23–38. 1954.

No. 615. Harry J. Turner, Jr. Fourth Report on Investigations of the Shellfisheries of Massachusetts. *Com. Mass., Dept. Cons., Div. Mar. Fish.*, pp. 1–21. 1951.

No. 616. Henry Stommel and Harlow G. Farmer. Abrupt Change in Width in Two-Layer Open Channel Flow. *Sears Found., Jour. Mar. Res.*, Vol. 11, No. 2, pp. 205–214. 1952.

No. 617. Joanne Starr Malkus and Andrew F. Bunker. Observational Studies of the Air Flow over Nantucket Island during the Summer of 1950. *Papers in Physical Oceanography and Meteorology*, Vol. 12, No. 2, pp. 1–50. 1952.

No. 618. Andrew F. Bunker. Measurements of the Vertical Water Vapor Transport and Distribution within Unstable Atmospheric Ground Layers and the Turbulent Mass Exchange Coefficient. *Papers in Physical Oceanography and Meteorology*, Vol. 12, No. 3, pp. 1–42. 1952.

No. 619. William L. Ford and A. R. Miller. The Surface Layer of the Gulf Stream and Adjacent Waters. *Sears Found., Jour. Mar. Res.*, Vol. 11, No. 3, pp. 267–280. 1952.

No. 620. Willem V. R. Malkus. The Heat Transport and Spectrum of Thermal Turbulence. *Proc. Roy. Soc.*, A, Vol. 225, pp. 196–212. 1954. (Not included in *Collected Reprints.*)

No. 621. William S. von Arx. Notes on the Surface Velocity Profile and Horizontal Shear across the Width of the Gulf Stream. *Tellus*, Vol. 4, No. 3, pp. 211–214. 1952.

No. 622. William S. von Arx. A Laboratory Study of the Wind-driven Ocean Circulation. *Tellus*, Vol. 4, No. 4, pp. 311–318. 1952.

No. 623. Helen S. Vishniac and S. W. Watson. The Steroid Requirements of *Labyrinthula vitellina* var. *pacifica*. *Jour. Gen. Microbiol.*, Vol. 8, No. 2, pp. 248–255. 1953.

No. 624. Joanne Starr Malkus and Melvin E. Stern. The Flow of a Stable Atmosphere over a Heated Island, Part I. *Jour. Meteorology*, Vol. 10, No. 1, pp. 30–41. 1953.

No. 625. Melvin E. Stern and Joanne Starr Malkus. The Flow of a Stable Atmosphere over a Heated Island, Part II. *Jour. Meteorology*, Vol. 10, No. 2, pp. 105–120. 1953.

No. 626. William E. Schevill. On the Nomenclature of the Pacific Gray Whale. *Breviora*, No. 7, pp. 1–3. 1952.

No. 627. Alfred C. Redfield. The Flushing of Harbors and other Hydrodynamic Problems in Coastal Waters. In: *Hydrodynamics in Modern Technology*, Mass. Inst. Tech., pp. 127–135, December 1951.

No. 628. L. V. Worthington. Oceanographic Results of Project Skijump I and Skijump II in the Polar Sea, 1951–1952. *Trans. Amer. Geophys. Union*, Vol. 34, No. 4, pp. 543–551. 1953.

No. 629. Charles B. Officer, Jr. The Refraction Arrival in Water Covered Areas. *Geophysics*, Vol. 18, No. 4, pp. 805–819. 1953.

No. 630. Harry J. Turner, Jr. The Drilling Mechanism of the Naticidae. *Ecology*, Vol. 34, No. 1, pp. 222–223. 1953.

No. 631. Andrew F. Bunker. Diffusion, Entrainment and Frictional Drag Associated with Non-Saturated, Buoyant Air Parcels rising through a Turbulent Air Mass. *Jour. Meteorology*, Vol. 10, No. 3, pp. 212–218. 1953.

No. 632. P. F. Scholander and L. van Dam. Composition of the Swimbladder Gas in Deep Sea Fishes. *Biol. Bull.*, Vol 104, No. 1, pp. 75–86. 1953.

No. 633. L. van Dam and P. F. Scholander. Concentration of Hemoglobin in the Blood of Deep Sea Fishes. *Jour. Cell. and Comp. Physiol.*, Vol. 41, No. 3, pp. 522–524. 1953.

No. 634. Willem V. R. Malkus. A Recording Bathypitotmeter. *Sears Found., Jour. Mar. Res.*, Vol. 12, No. 1, pp. 51–59. 1953.

No. 635. A. B. Arons and C. F. Kientzler. Vapor Pressure of Sea Salt Solutions. *Trans. Amer. Geophys. Union*, Vol. 35, No. 5, pp. 722–728. 1954.

No. 636. Alfred C. Redfield. Interference Phenomena in the Tides of the Woods Hole Region. *Sears Found., Jour. Mar. Res.*, Vol. 12, No. 1, pp. 121–140. 1953.

No. 637. Floyd M. Soule. Physical Oceanography of the Grand Banks Region and the Labrador Sea in 1952. *U. S. Coast Guard Bull.*, No. 38, pp. 31–100. 1953.

No. 638. Harlow G. Farmer and George W. Morgan. The Salt Wedge. *Proc. Third Conf. on Coastal Engineering*, Cambridge, Mass., October 1952, pp. 54–64. 1953.

No. 639. J. R. D. Francis. A Note on the Velocity Distribution and Bottom Stress in a Wind-Driven Water Current System. *Sears Found., Jour. Mar. Res.*, Vol. 12, No. 1, pp. 93–98. 1953.

No. 640. Henry Stommel. Computation of Pollution in a Vertically Mixed Estuary *Sewage and Industrial Wastes*, Vol. 25, No. 9, pp. 1065–1071. 1953.

No. 641. Jack L. Hough. Pleistocene Climatic Record in a Pacific Ocean Core Sample. *Jour. Geology*, Vol. 61, No. 3, pp. 252–262. 1953.

No. 642. Bostwick H. Ketchum. Circulation in Estuaries. *Proc. Third Conf. on Coastal Engineering*, Cambridge, Mass., October 1952, pp. 65–76. 1953.

No. 643. A. H. Woodcock. Salt Nuclei in Marine Air as a Function of Altitude and Wind Force. *Jour. Meteorology*, Vol. 10, No. 5, pp. 362–371. 1953.

No. 644. Henry Stommel, W. S. von Arx, D. Parson and W. S. Richardson. Rapid Aerial Survey of Gulf Stream with Camera and Radiation Thermometer. *Science*, Vol. 117, No. 3049, pp. 639–640. 1953.

No. 645. Henry Stommel. Examples of the Possible Role of Inertia and Stratification in the Dynamics of the Gulf Stream System. *Sears Found., Jour. Mar. Res.*, Vol. 12, No. 2, pp. 184–195. 1953.

No. 646. Henry C. Stetson. The Sediments of the Western Gulf of Mexico. Part I. The Continental Terrace of the Western Gulf of Mexico: its Surface Sediments, Origin and Development. *Papers in Physical Oceanography and Meteorology*, Vol. 12, No. 4, pp. 1–45. 1953.

No. 647. Parker D. Trask. The Sediments of the Western Gulf of Mexico. Part II. Chemical Studies of Sediments of the Western Gulf of Mexico. *Papers in Physical Oceanography and Meteorology*, Vol. 12, No. 4, pp. 47–120. 1953.

No. 648. William E. Schevill and Barbara Lawrence. Auditory Response of a Bottlenosed Porpoise, *Tursiops truncatus*, to Frequencies above 100 kc. *Jour. Exper. Zool.*, Vol. 124, No. 1, pp. 147–165. 1953.

No. 649. William S. von Arx. Cartographic Principles Applied to Wide-Field Photography. *Photogr. Engineering*, Vol. 4, No. 2, pp. 60–73. 1953.

No. 650. Betty Lee Gealy. Topography of the Continental Slope in Northwest Gulf of Mexico. *Bull. Geol. Soc. Amer.*, Vol. 66, No. 2, pp. 203–227. 1955.

No. 651. Frank J. Mather III and C. Godfrey Day. Observations of Pelagic Fishes of the Tropical Atlantic. *Copeia*, No. 3, pp. 179–188. 1954.

No. 652. Joseph Chase. A Comparison of Certain North Atlantic Wind, Tide Gauge and Current Data. *Sears Found., Jour. Mar. Res.*, Vol. 13, No. 1, pp. 22–31. 1954.

No. 653. Barbara Lawrence and William E. Schevill. *Tursiops* as an Experimental Subject. *Jour. Mammalogy*, Vol. 35, No. 2, pp. 225–232. 1954.

No. 654. William E. Schevill. Sight Records of the Gray Grampus, *Grampus griseus* (Cuvier). *Jour. Mammalogy*, Vol. 35, No. 1, pp. 123–124. 1954.

No. 655. Henry Stommel. The Role of Density Currents in Estuaries. *Proc. Minnesota Int. Hydraulics Conv.*, Sept. 1–4, 1953, pp. 305–312. 1953.

No. 656. Harry J. Turner, Jr. Fifth Report on Investigations of the Shellfisheries of Massachusetts. *Com. Mass., Dept. Cons., Div. Mar. Fish.*, pp. 1–37. 1952.

No. 657. Henry B. Bigelow and William C. Schroeder. A New Family, a New Genus, and Two New Species of Batoid Fishes from the Gulf of Mexico. *Breviora*, No. 24, 16 pp. 1954.

No. 658. Duncan C. Blanchard. Raindrop Size-Distribution in Hawaiian Rains. *Jour. Meteorology*, Vol. 10, No. 6, pp. 457–473. 1953.

No. 659. Duncan C. Blanchard. A Simple Recording Technique for Determining Raindrop Size and Time of Occurrence of Rain Showers. *Trans. Amer. Geophys. Union*, Vol. 34, No. 4, pp. 534–538. 1953.

No. 660. A. H. Woodcock. Hawaii as a Cloud Physics Laboratory. *Pacific Science*, Vol. 7, No. 4, pp. 522–524. 1953.

No. 661. Daniel R. Norton, Mary A. Plunkett and Francis A. Richards. Spectrophotometric Determination of Uric Acid and Some Redeterminations of its Solubility, *Analytical Chemistry*, Vol. 26, No. 3, pp. 454–457. 1954.

No. 662. C. B. Officer, Jr. and Maurice Ewing. Geophysical Investigations in the Emerged and Submerged Atlantic Coastal Plain. *Bull. Geol. Soc. Amer.*, Vol. 65, pp. 653–670. 1954.

No. 663. William E. Schevill and Barbara Lawrence. High-Frequency Auditory Response of a Bottlenosed Porpoise, *Tursiops truncatus* (Montagu). *Jour. Acoust. Soc. Amer.*, Vol. 25, No. 5, pp. 1016–1017. 1953.

No. 664. R. B. Montgomery. Analysis of a Hugh M. Smith Oceanographic Section from Honolulu Southward across the Equator. *Sears Found., Journ. Mar. Res.*, Vol. 13, No. 1, pp. 67–75. 1954.

No. 665. C. H. Keith and A. B. Arons. The Growth of Sea-Salt Particles by Condensation of Atmospheric Water Vapor. *Jour. Meteorology*, Vol. 11, No. 3, pp. 173–184. 1954.

No. 667. Joanne Starr Malkus. Some Results of a Trade-Cumulus Cloud Investigation. *Jour. Meteorology*, Vol. 11, No. 3, pp. 220–237. 1954.

No. 668. F. C. Fuglister. Average Temperature and Salinity at a Depth of 200 Meters in the North Atlantic. *Tellus*, Vol. 6, No. 1, pp. 46–58. 1954.

No. 669. Hilary B. Moore, Harding Owre, Everett C. Jones and T. Dow. Plankton of the Florida Current. III. The Control of the Vertical Distribution of Zooplankton in the Daytime by Light and Temperature. *Bull. Mar. Sci. Gulf and Caribbean*, Vol. 3, No. 2, pp. 83–95. 1953.

No. 670. Willem V. R. Malkus. Discrete Transitions in Turbulent Convection. *Proc. Roy. Soc.*, A, Vol. 225, pp. 185–195. 1954. (Not included in *Collected Reprints.*)

No. 671. Mary Sears. Notes on the Peruvian Coastal Current. 1. An Introduction to the Ecology of Pisco Bay. *Deep-Sea Research*, Vol. 1, pp. 141–169. (Also published as: Notas sobre la Corriente Costanera del Peru. 1. Introduccion a la Ecologia de la Bahia de Pisco. *Bol. Cient. Cia. Admora. Guano*, Lima, Peru, Vol. 1, No. 2, pp. 133–179). 1954.

No. 672. Ralph F. Wyrick. Observations on the Movements of the Pacific Gray Whale *Eschrichtius glaucus* (Cope). *Journ. Mammalogy*, Vol. 35, No. 4, pp. 596–598. 1954.

No. 673. A. H. Woodcock, C. F. Kientzler, A. B. Arons and D. C. Blanchard. Giant Condensation Nuclei from Bursting Bubbles. *Nature*, Vol. 172, No. 4390, pp. 1144–1145. 1953.

No. 674. Harry J. Turner, Jr. An Improved Method of Staining the External Organelles of Hypotrichs. *Jour. Protozoology*, Vol. 1, No. 1, pp. 18–19. 1954.

No. 675. Floyd M. Soule, A. J. Bush and J. E. Murray. Physical Oceanography of the Grand Banks Region and the Laborador Sea in 1953. *U. S. Coast Guard Bull.*, No. 39, pp. 45–138. 1955.

No. 676. J. B. Hersey and R. H. Backus. New Evidence that Migrating Gas Bubbles, Probably the Swimbladders of Fish, are Largely Responsible for Scattering Layers on the Continental Rise South of New England. *Deep-Sea Research*, Vol. 1, pp. 190–191. 1954.

No. 677. Ilmo Hela, Hilary B. Moore and Harding Owre. Seasonal Changes in the Surface Water Masses and in their Plankton in the Bermuda Area. *Bull. Mar. Sci. Gulf and Caribbean*, Vol. 3, No. 3, pp. 157–167. 1953.

No. 678. B. Haurwitz. The Occurrence of Internal Tides in the Ocean. *Arch. Meteorol. Geoph. u. Bioklim.*, Ser. A, Meteorol. und Geoph., Band 7, pp. 406–424. 1954.

No. 679. Gunther K. Wertheim. Studies of the Electric Potential between Key West, Florida, and Havana, Cuba. *Trans. Amer. Geophys. Union*, Vol. 35, No. 6, pp. 872–882. 1954.

No. 680. John C. Ayers. A Method for Rendering Wood Resistant to Marine Borers. *Bull. Mar. Sci. Gulf and Caribbean*, Vol. 3, No. 4, pp. 297–304. 1954.

No. 683. R. F. Vaccaro and J. H. Ryther. The Bactericidal Effects of Sunlight in Relation to "Light" and "Dark" Bottle Photosynthesis Experiments. *Jour. du Conseil*, Vol. 20, No. 1, pp. 18–24. 1954.

No. 684. J. H. Ryther and R. F. Vaccaro. A Comparison of the Oxygen and 14C Methods of Measuring Marine Photosynthesis. *Jour. du Conseil*, Vol. 20, No. 1, pp. 25–34. 1954.

No. 685. John H. Ryther. The Ecology of Phytoplankton Blooms in Moriches Bay and Great South Bay, Long Island, New York. *Biol. Bull.*, Vol. 106, No. 2, pp. 198–209. 1954.

No. 686. E. E. Watson. An Experiment to Determine the Hydrodynamic Forces on a Cable Inclined to the Direction of Flow. *Sears Found., Jour. Mar. Res.*, Vol. 12, No. 3, pp. 245–248. 1953.

No. 687. Bostwick H. Ketchum. Mineral Nutrition of Phytoplankton. *Ann. Rev. Plant Physiol.*, Vol. 5, pp. 55–74. 1954.

No. 688. Francis A. Richards and Alfred C. Redfield. Oxygen-Density Relationships in the Western North Atlantic. *Deep-Sea Research*, Vol. 2, pp. 182–199. 1955.

No. 689. William S. von Arx. Measurements of the Oceanic Circulation in Temperate and Tropical Latitudes. In: Oceanographic Instrumentation. *National Research Council Publ.*, No. 309, pp. 13–35. 1954.

No. 690. M. S. Longuet-Higgins, M. E. Stern and Henry Stommel. The Electrical Field Induced by Ocean Currents and Waves, with Applications to the Method of Towed Electrodes. *Papers in Physical Oceanography and Meteorology*, Vol. 13, No. 1, pp. 1–37. 1954.

No. 691. C. F. Kientzler, A. B. Arons, D. C. Blanchard and A. H. Woodcock. Photographic Investigation of the Projection of Droplets by Bubbles Bursting at a Water Surface. *Tellus*, Vol. 6, No. 1, pp. 1–7. 1954.

No. 692. Henry B. Bigelow and William C. Schroeder. Deep Water Elasmobranchs and Chimaeroids from the Northwestern Atlantic Slope. *Bull. Mus. Comp. Zool.*, Vol. 112, No. 2, pp. 37–87. 1954.

No. 693. Henry Stommel. Exploratory Measurements of Electrical Potential Differences between Widely Spaced Points in the North Atlantic Ocean. *Arch. Meteorol., Geoph. u. Bioklim.*, Ser. A, Meteorol. und Geoph., Band 7, pp. 292–304. 1954.

No. 694. L. V. Worthington. Three Detailed Cross-Sections of the Gulf Stream. *Tellus*, Vol. 6, No. 2, pp. 116–123. 1954.

No. 695. Francis A. Richards and Alfred C. Redfield. A Correlation between the Oxygen Content of Sea Water and the Organic Content of Marine Sediments. *Deep-Sea Research*, Vol. 1, pp. 279–281. 1954.

No. 696. Allyn C. Vine. Oceanographic Instruments for Measuring Temperature. In: Oceanographic Instrumentation. *National Research Council Publ.*, No. 309, pp. 55–69. 1954.

No. 697. J. B. Hersey. Acoustic Instrumentation as a Tool in Oceanography. In: Oceanographic Instrumentation. *National Research Council Publ.*, No. 309, pp. 101–122. 1954.

No. 698. A. B. Arons. Underwater Explosion Shock Wave Parameters at Large Distances from the Charge. *Jour. Acoust. Soc. Amer.*, Vol. 26, No. 3, pp. 343–346. 1954.

No. 699. P. F. Scholander and L. Van Dam. Secretion of Gases against High Pressures in the Swimbladder of Deep Sea Fishes. I. Oxygen Dissociation in Blood. *Biol. Bull.*, Vol. 107, No. 2, pp. 247–259. 1954.

No. 700. P. F. Scholander. Secretion of Gases against High Pressures in the Swimbladder of Deep Sea Fishes. II. The Rete Mirabile. *Biol. Bull.*, Vol. 107, No. 2, pp. 260–277. 1954.

No. 701. R. B. Montgomery. Convection of Heat. *Arch. Meteorol., Geoph. u. Bioklim.*, Ser. A, Meteorol. und Geoph., Band 7, pp. 125–132. 1954.

No. 702. Frank J. Mather III. Northerly Occurrences of Warm Water Fishes in the Western Atlantic. *Copeia*, No. 4, pp. 292–293. 1954.

No. 703. C. W. Newton. Analysis and Data Problems in Relation to Numerical Prediction. *Bull. Amer. Meteorol. Soc.*, Vol. 35, No. 7, pp. 287–294. 1954.

No. 704. George L. Clarke. Elements of Ecology. John Wiley & Sons, Inc., New York. 534 pp. (Not included in *Collected Reprints*.)

No. 705. L. Van Dam. On the Respiration in Scallops (Lamellibranchiata). *Biol. Bull.*, Vol. 107, No. 2, pp. 192–202. 1954.

No. 706. Joanne Starr Malkus and R. S. Scorer. The Erosion of Cumulus Towers. *Jour. Meteorol.*, Vol. 12, No. 1, pp. 43–57. 1955.

No. 707. Athelstan F. Spilhaus. Sea and Air Resources. *Geogr. Rev.*, Vol. 44, No. 3, pp. 346–351. 1954.

No. 708. Charles J. Fish and Mary Curtis Cobb. Noxious Marine Animals of the Central and Western Pacific Ocean. Fish and Wildlife Service, *Research Report* 36, 45 pp., 1954.

No. 709. P. F. Scholander, Warner E. Love and John W. Kanwisher. The Rise of Sap in Tall Grapevines. *Plant Physiol.*, Vol. 30, No. 2, pp. 93–104. 1955. (Not included in *Collected Reprints*.)

No. 710. P. F. Scholander, L. Van Dam and Susan I. Scholander. Gas Exchange in the Roots of Mangroves. *Amer. Jour. Bot.*, Vol. 42, No. 1, pp. 92–98. 1955.

No. 711. Duncan C. Blanchard. A Simple Method for the Production of Homogeneous Water Drops down to 1 Micron Radius. *Jour. Colloid Sci.*, Vol. 9, No. 4, pp. 321–328. 1954.

No. 712. John H. Ryther. Ecology of Autotrophic Marine Dinoflagellates with Refence to Red Water Conditions. In: The Luminescence of Biological Systems, F. H. Johnson, Edit., Publ. by Amer. Assoc. Adv. Sci., Washington, pp. 387–414. 1955.

No. 713. Henry Stommel. Serial Observations of Drift Currents in the Central North Atlantic Ocean. *Tellus*, Vol. 6, No. 3, pp. 203–214. 1954.

No. 715. Harry J. Turner, Jr. and J. Arthur Posgay. Sixth Report on Investigations of the Shellfisheries of Massachusetts. *Com. Mass.*, *Dept. Nat. Res.*, *Div. Mar. Fish.*, pp. 1–74. 1953.

No. 716. Joanne Starr Malkus and Claude Ronne. On the Structure of Some Cumulonimbus Clouds which Penetrated the High Tropical Troposphere. *Tellus*, Vol. 6, No. 4, pp. 351–366. 1954.

No. 717. L. V. Worthington. A Preliminary Note on the Time Scale in North Atlantic Circulation. *Deep-Sea Research*. Vol. 1, pp. 244–251. 1954.

No. 718. Arthur R. Miller. Some Suggestions for more precise Loran Navigation. *Navigation*, Vol. 3, Nos. 1 and 2, pp. 23–29. 1951. (Included in *Collected Reprints* for 1953.)

No. 719. Henry B. Bigelow and Isabel Pérez Farfante. Fishes of the Western North Atlantic. Lancelets. *Mem. Sears Found. Mar. Res.*, No. 1, Pt. 1, Ch. 1, pp. 1–28. 1948. (Not included in *Collected Reprints*.)

No. 720. Henry B. Bigelow and William C. Schroeder. Fishes of the Western North Atlantic. Cyclostomes. *Mem. Sears Found. Mar. Res.*, No. 1, Pt. 1, Ch. 2, pp. 29–58. 1948. (Not included in *Collected Reprints*.)

No. 721. Henry B. Bigelow and William C. Schroeder. Fishes of the Western North Atlantic. Sharks. *Mem. Sears Found. Mar. Res.*, No. 1, Pt. 1, Ch. 3, pp. 59–576. 1948. (Not included in *Collected Reprints*.)

No. 722. Arthur H. Clarke, Jr. Some Mollusks from the Continental Slope of Northeastern North America. *Breviora*, No. 40, 11 pp. 1954.

No. 723. C. W. Newton. Frontogenesis and Frontolysis as a Three-Dimensional Process. *Jour. Meteorology*, Vol. 11, No. 6, pp. 449–461. 1954.

No. 724. Charles B. Officer. Southwest Pacific Crustal Structure. *Trans. Amer. Geophys. Union*, Vol. 36, No. 3, pp. 449–459. 1955.

No. 725. K. G. Wilson and A. B. Arons. Osmotic Pressures of Sea Water Solutions Computed from Experimental Vapor Pressure Lowering. *Sears Found., Jour. Mar. Res.*, Vol. 14, No. 2, pp. 195–198. 1955.

No. 726. Joanne Starr Malkus. On the Formation and Structure of Downdrafts in Cumulus Clouds. *Jour. Meteorol.*, Vol. 12, No. 4, pp. 350–354. 1955.

No. 727. Joanne Starr Malkus. The Effects of a Large Island upon the Trade-Wind Air Stream. *Quart. Jour. Roy. Meteor. Soc.*, Vol. 81, No. 350, pp. 538–550. 1955.

No. 728. Paul Ferris Smith. Further Measurements of the Sound Scattering Properties of Several Marine Organisms. *Deep-Sea Research*, Vol. 2, pp. 71–79. 1954.

No. 729. Willard Dow. Underwater Telemetering. *Deep-Sea Research*, Vol. 2, pp. 145–151 (erroneously dated 1954). 1955.

No. 730. John H. Ryther. Inhibitory Effects of Phytoplankton upon the Feeding of *Daphnia magna* with Reference to Growth, Reproduction, and Survival. *Ecology*, Vol. 35, No. 4, pp. 522–533. 1954.

No. 731. Charles B. Officer. A Deep-Sea Seismic Reflection Profile. *Geophysics*, Vol. 20, No. 2, pp. 270–282. 1955.

No. 732. Henry B. Bigelow and William C. Schroeder. Occurrence off the Middle and North Atlantic United States of the Offshore Hake *Merluccius albidus* (Mitchill) 1818, and of the Blue Whiting *Gadus (Micromesistius) poutassou* (Risso) 1826. *Bull. Mus. Comp. Zool.*, Vol. 113, No. 2, pp. 205–226. 1955.

No. 733. John H. Ryther. The Ratio of Photosynthesis to Respiration in Marine Plankton Algae and its Effect upon the Measurement of Productivity. *Deep-Sea Research*, Vol. 2, pp. 134–139 (erroneously dated 1954). 1955.

No. 734. Duncan C. Blanchard. Bursting of Bubbles at an Air-Water Interface. *Nature*, Vol. 173, p. 1048. 1954.

No. 735. Joseph Chase. Winds and Temperatures in Relation to the Brood-Strength of Georges Bank Haddock. *Jour. du Conseil*, Vol 21, No. 1, pp. 17–24. 1955.

No. 736. Grace I. Creitz and Francis A. Richards. The Estimation and Characterization of Plankton Populations by Pigment Analysis. III. A Note on the use of "Millipore" Membrane Filters in the Estimation of Plankton Pigments. *Sears Found., Jour. Mar. Res.*, Vol. 14, No. 3, pp. 211–216. 1955.

No. 737. Charles J. Fish. Preliminary Observations on the Biology of Boreo-Arctic and Subtropical Oceanic Zooplankton Populations. In: Symposium on Marine and Fresh-Water Plankton in the Indo-Pacific, Bangkok, Jan. 25–26, 1954, FAO-UNESCO, Sect. 1, No. 1, pp. 1–7, 1955. (Not included in *Collected Reprints*.)

No. 739. William G. Metcalf. On the Formation of Bottom Water in the Norwegian Basin. *Trans. Amer. Geophys. Union*, Vol. 36, No. 4, pp. 596–600. 1955.

No. 740. Andrew F. Bunker. Turbulence and Shearing Stresses Measured over the North Atlantic Ocean by an Airplane-Acceleration Technique. *Jour. Meteorol.*, Vol 12, No. 5, pp. 445–455. 1955.

No. 741. Wilbur Marks and F. Claude Ronne. Aerial Stereo-Photography and Ocean Waves. *Photogr. Engineering*, March 1955, pp. 107–110. 1955.

No. 742. Malcolm S. Gordon. Summer Ecology of Oceanic Birds off Southern New England. *The Auk*, Vol 72, pp. 138–147. 1955.

No. 743. Charles B. Officer. Geologic Interpretation of a Series of Seismic Reflection Profiles from Bermuda to the Continental Margins. *Deep-Sea Research*, Vol. 2, pp. 253–260. 1955.

No. 744. J. W. Kanwisher and Gordon Volkmann. A Scattering Layer Observation. *Science*, Vol. 121, No. 3134, pp. 108–109. 1955.

No. 746. H. G. Farmer, W. Marks, R. G. Walden and G. G. Whitney, Jr. A Technique for Ocean Wave Measurements. In: Proc. First Conf., Ships and Waves, Oct. 1954, Counc. Wave Res. and Soc. Naval Arch. and Mar. Eng., pp. 11–32. 1955.

No. 747. Duncan C. Blanchard. Electrified Droplets from the Bursting of Bubbles at an Air-Sea Water Interface. *Nature*, Vol. 175, No. 4451, pp. 334–336. 1955.

No. 749. F. C. FUGLISTER. Alternative Analyses of Current Surveys. *Deep-Sea Research*, Vol. 2, pp. 213–229. 1955.

No. 750. GILBERT L. VOSS. The Cephalopoda Obtained by the Harvard-Havana Expedition off the Coast of Cuba in 1938–39. *Bull, Mar. Sci., Gulf and Caribbean*, Vol. 5, No. 2, pp. 81–115. 1955.

No. 751. FRANK S. ESSAPIAN. Speed-Induced Skin Folds in the Bottle-Nosed Porpoise, *Tursiops truncatus*. *Breviora*, No. 43, 4 pp., 9 Pls. 1955.

No. 753. JOHN P. BARLOW. Physical and Biological Processes Determining the Distribution of Zooplankton in a Tidal Estuary. *Biol. Bull.*, Vol. 109, No. 2, pp. 211–225. 1955.

No. 755. P. F. SCHOLANDER. Evolution of Climatic Adaptation in Homeotherms. *Evolution*, Vol. 9, No. 1, pp. 15–26. 1955.

No. 756. HILARY B. MOORE. Variations in Temperature and Light Response within a Plankton Population. *Biol. Bull.*, Vol. 108, No. 2, pp. 175–181. 1955.

No. 757. A. H. WOODCOCK and W. A. MORDY. Salt Nuclei, Wind and Daily Rainfall in Hawaii. *Tellus*, Vol. 7, No. 3, pp. 291–300. 1955.

No. 758. FLOYD M. SOULE and J. E. MURRAY. Physical Oceanography of the Grand Banks Region and the Laborador Sea in 1954. *U. S. Coast Guard Bull.*, No. 40, pp. 79–168. 1955.

No. 759. BOSTWICK H. KETCHUM, NATHANIEL CORWIN and D. JEAN KEEN. The Significance of Organic Phosphorus Determinations in Ocean Waters. *Deep-Sea Research*, Vol. 2, pp. 172–181. 1955.

No. 760. DEAN F. BUMPUS and E. LOWE PIERCE. The Hydrography and the Distribution of Chaetognaths over the Continental Shelf off North Carolina. Pap. Mar. Biol. and Oceanogr., *Deep-Sea Research*, Suppl. to Vol. 3, pp. 92–109. 1955. (Included in *Collected Reprints* for 1955, Part II.)

No. 761. A. H. WOODCOCK. Bursting Bubbles and Air Pollution. *Sewage and Industrial Wastes*, Vol. 27, No. 10, pp. 1189–1192. 1955.

No. 762. GORDON A. RILEY. Review of the Oceanography of Long Island Sound. Pap. Mar. Biol. and Oceanogr., *Deep-Sea Research*, Suppl. to Vol. 3, pp. 224–238. 1955. (Included in *Collected Reprints* for 1955, Part II.)

No. 763. TALBOT H. WATERMAN. Polarization of Scattered Sunlight in Deep Water. Pap. Mar. Biol. and Oceanogr., *Deep-Sea Research*, Suppl. to Vol. 3, pp. 426–434. 1955. (Included in *Collected Reprints* for 1955, Part II.)

No. 767. EDWARD M. THORNDIKE. Hydroscopes. *Trans. Amer. Geophys. Union*, Vol. 36, No. 3, pp. 470–472. 1955.

No. 768. A. H. WOODCOCK and D. C. BLANCHARD. Tests of the Salt-Nuclei Hypothesis of Rain Formation. *Tellus*, Vol. 7, No. 4, pp. 437–448. 1955.

No. 770. C.-G. ROSSBY and H. EGNÉR. On the Chemical Climate and its Variation with Atmospheric Circulation Pattern. *Tellus*, Vol. 7, No. 1, pp. 118–133. 1955.

No. 771. STEFAN MACHLUP and J. B. HERSEY. Analysis of Sound-Scattering Observations from Non-Uniform Distributions of Scatterers in the Ocean. *Deep-Sea Research*, Vol. 3, pp. 1–22. 1955.

No. 772. Bostwick H. Ketchum. Distribution of Coliform Bacteria and other Pollutants in Tidal Estuaries. *Sewage and Industrial Wastes*, Vol. 27, No. 11, pp. 1288–1296. 1955.

No. 773. Susan I. Scholander. Land Birds over the Western North Atlantic. *The Auk*, Vol. 72, pp. 225–239. 1955.

No. 775. Bostwick H. Ketchum and D. Jean Keen. The Accumulation of River Water over the Continental Shelf between Cape Cod and Chesapeake Bay. Pap. Mar. Biol. and Oceanogr., *Deep-Sea Research*, Suppl. to Vol. 3, pp. 346–357. 1955. (Included in *Collected Reprints* for 1955, Part II.)

No. 776. Alfred C. Redfield. The Hydrography of the Gulf of Venezuela. Pap. Mar. Biol. and Oceanogr., *Deep-Sea Research*, Suppl. to Vol. 3, pp. 115–133. 1955. (Included in *Collected Reprints* for 1955, Part II.)

No. 777. Harry J. Turner, Jr. How Clam Drills Capture Razor Clams. *The Nautilus*, Vol. 69, No. 1, pp. 20–22. 1955.

No. 778. J. W. Kanwisher. Freezing in Intertidal Animals. *Biol. Bull.*, Vol. 109, No. 1, pp. 56–63. 1955.

No. 779. Ruth D. Turner. Scaphopods of the *Atlantis* Dredgings in the Western Atlantic with a Catalogue of the Scaphopod Types in the Museum of Comparative Zoology. Pap. Mar. Biol. and Oceanogr., *Deep-Sea Research*, Suppl. to Vol. 3, pp. 309–320. 1955. (Included in *Collected Reprints* for 1955, Part II.)

No. 780. E. Steemann Nielsen. The Production of Antibiotics by Plankton Algae and its Effect upon Bacterial Activities in the Sea. Pap. Mar. Biol. and Oceanogr., *Deep-Sea Research*, Suppl. to Vol. 3, pp. 281–286. 1955. (Included in *Collected Reprints* for 1955, Part II.)

No. 781. W. T. Edmondson. Factors Affecting Productivity in Fertilized Water. Pap. Mar. Biol. and Oceanogr., *Deep-Sea Research*, Suppl. to Vol. 3, pp. 451–464. 1955. (Included in *Collected Reprints* for 1955, Part II.)

No. 782. Henry C. Stetson. Patterns of Deposition at the Continental Margin. Pap. Mar. Biol. and Oceanogr., *Deep-Sea Research*, Suppl. to Vol. 3, pp. 298–308. 1955. (Included in *Collected Reprints* for 1955, Part II.)

No. 783. Harry J. Turner, Jr. and Stanley Scher. Seventh Report on Investigations of the Shellfisheries of Massachusetts. *Com. Mass., Dept. Nat. Res., Div. Mar. Fish.*, 35 pp. 1954.

No. 785. Earl Barrett and Gunnar Brodin. The Acidity of Scandinavian Precipitation. *Tellus*, Vol. 7, No. 2, pp. 251–257. 1955.

No. 786. T. F. Goreau and V. T. Bowen. Calcium Uptake by a Coral. *Science*, Vol. 122, No. 3181, pp. 1188–1189. 1955.

No. 787. Henry B. Bigelow, William C. Schroeder and Stewart Springer. Three New Shark Records from the Gulf of Mexico. *Breviora*, No. 49, 12 pp. 1955.

No. 788. Dean F. Bumpus. The Circulation over the Continental Shelf South of Cape Hatteras. *Trans. Amer. Geophys. Union*, Vol. 36, No. 4, pp. 601–611. 1955.

No. 789. Donald R. Griffin. Hearing and Acoustic Orientation in Marine Animals. Pap. Mar. Biol. and Oceanogr., *Deep-Sea Research*, Suppl. to Vol. 3, pp. 406–417. 1955. (Included in *Collected Reprints* for 1955, Part II.)

No. 790. William C. Schroeder. Report on the Results of Exploratory Otter-Trawling along the Continental Shelf and Slope between Nova Scotia and Virginia during the Summers of 1952 and 1953. Pap. Mar. Biol. and Oceanogr., *Deep-Sea Research*, Suppl. to Vol. 3, pp. 358–372. 1955. (Included in *Collected Reprints* for 1955, Part II.)

No. 791. L. V. Worthington. A New Theory of Caribbean Bottom-Water Formation. *Deep-Sea Research*, Vol. 3, pp. 82–87. 1955.

No. 792. C. O'D. Iselin. Coastal Currents and the Fisheries. Pap. Mar. Biol. and Oceanogr., *Deep-Sea Research*, Suppl. to Vol. 3, pp. 474–478. 1955. (Included in *Collected Reprints* for 1955, Part II.)

No. 794. William S. Von Arx and W. S. Richardson. On the Fine-Structure of the Gulf Stream Front. *Deep-Sea Research*, Vol. 3, pp. 46–65. 1955.

No. 795. P. F. Scholander, L. Van Dam, C. Lloyd Claff and J. W. Kanwisher. Micro Gasometric Determination of Dissolved Oxygen and Nitrogen. *Biol. Bull.*, Vol. 109, No. 2, pp. 328–334. 1955.

No. 796. Henry Stommel. Lateral Eddy Viscosity in the Gulf Stream System. *Deep-Sea Research*, Vol. 3, pp. 88–90, 1955.

No. 802. James M. Moulton and Richard H. Backus. Annotated References Concerning the Effects of Man-Made Sounds on the Movements of Fishes. *Dept. Sea and Shore Fish.*, Augusta, Maine, Fish. Circ. No. 17, 8 pp. 1955.

No. 806. Allyn C. Vine. Oceanographic Instrumentation. *Science*, Vol. 122, No. 3173, pp. 748–751. 1955.

No. 807. P. F. Scholander and William E. Schevill. Counter-Current Vascular Heat Exchange in the Fins of Whales. *Jour. Appl. Physiol.*, Vol. 8, No. 3, pp. 279–282. 1955.

No. 808. E. Steemann Nielsen. The Interaction of Photosynthesis and Respiration and its Importance for the Determination of ^{14}C-Discrimination in Photosynthesis. *Physiologia Plantarum*, Vol. 8, pp. 945–953. 1955.

No. 817. Harold E. Edgerton and Lloyd D. Hoadley. Cameras and Lights for Underwater Use. *Jour. Soc. Motion Pic. and Tel. Eng.*, Vol. 64, pp. 345–350. 1955.

No. 822. P. F. Scholander. Hydrostatic Pressure in Coconuts. *Plant Physiol.*, Vol. 30, No. 6, pp. 560–561. 1955.